



Low-Hazardous Air Pollutant (HAP)/Volatile Organic Compound (VOC)-Compliant Resins for Military Applications: Final Report

**by John La Scala, Steven Boyd, Kevin Andrews, Terese Glodek,
Caroline Lochner, Philip Myers, Felecia Levine, Daniel De Bonis,
Robert Hayes, James Sands, Maureen Foley, Roger Crane,
Nicholas Shevchenko, Steven Andersen, John Gillespie, Jr., David Fudge,
Kyle Brand, Michael Starks, Jorge Gomes, Lawrence Coulter,
Kenneth Patterson, Dane Morgan, Frank Bruce, Xing Geng, Steven Smith,
and Giuseppe Palmese**

ARL-TR-6036

July 2012

NOTICES

Disclaimers

The findings in this report are not to be construed as an official Department of the Army position unless so designated by other authorized documents.

Citation of manufacturer's or trade names does not constitute an official endorsement or approval of the use thereof.

Destroy this report when it is no longer needed. Do not return it to the originator.

Army Research Laboratory

Aberdeen Proving Ground, MD 21005-5069

ARL-TR-6036**July 2012**

Low-Hazardous Air Pollutant (HAP)/Volatile Organic Compound (VOC)-Compliant Resins for Military Applications: Final Report

**John La Scala, Steven Boyd, Kevin Andrews, Terese Glodek,
Caroline Lochner, Philip Myers, Felecia Levine, Daniel De Bonis,
Robert Hayes, and James Sands
Weapons and Materials Research Directorate, ARL**

**Maureen Foley and Roger Crane
Naval Surface Warfare Center, Carderock Division**

**Nicholas Shevchenko, Steven Andersen, John Gillespie, Jr.,
David Fudge, and Kyle Brand
University of Delaware**

**Michael Starks and Jorge Gomes
Red River Army Depot**

**Lawrence Coulter, Kenneth Patterson, Dane Morgan, and Frank Bruce
U.S. Air Force Research Laboratory**

**Xing Geng, Steven Smith, and Giuseppe Palmese
Drexel University**

REPORT DOCUMENTATION PAGE			Form Approved OMB No. 0704-0188		
<p>Public reporting burden for this collection of information is estimated to average 1 hour per response, including the time for reviewing instructions, searching existing data sources, gathering and maintaining the data needed, and completing and reviewing the collection information. Send comments regarding this burden estimate or any other aspect of this collection of information, including suggestions for reducing the burden, to Department of Defense, Washington Headquarters Services, Directorate for Information Operations and Reports (0704-0188), 1215 Jefferson Davis Highway, Suite 1204, Arlington, VA 22202-4302. Respondents should be aware that notwithstanding any other provision of law, no person shall be subject to any penalty for failing to comply with a collection of information if it does not display a currently valid OMB control number.</p> <p>PLEASE DO NOT RETURN YOUR FORM TO THE ABOVE ADDRESS.</p>					
1. REPORT DATE (DD-MM-YYYY) July 2012		2. REPORT TYPE Final		3. DATES COVERED (From - To) January 2006–March 2010	
4. TITLE AND SUBTITLE Low-Hazardous Air Pollutant (HAP)/Volatile Organic Compound (VOC)-Compliant Resins for Military Applications: Final Report			5a. CONTRACT NUMBER		
			5b. GRANT NUMBER		
			5c. PROGRAM ELEMENT NUMBER		
6. AUTHOR(S) John La Scala, Steven Boyd, Kevin Andrews, Terese Glodek, Caroline Lochner, Philip Myers, Felecia Levine, Daniel De Bonis, Robert Hayes, James Sands, Maureen Foley, * Roger Crane, * Nicholas Shevchenko, † Steven Andersen, † John Gillespie, Jr., † David Fudge, † Kyle Brand, † Michael Starks, † Jorge Gomes, † Lawrence Coulter, † Kenneth Patterson, † Dane Morgan, † Frank Bruce, † Xing Geng, ** Steven Smith, ** and Giuseppe Palmese **			5d. PROJECT NUMBER WP-0617		
			5e. TASK NUMBER		
			5f. WORK UNIT NUMBER		
7. PERFORMING ORGANIZATION NAME(S) AND ADDRESS(ES) U.S. Army Research Laboratory ATTN: RDRL-WMM-C Aberdeen Proving Ground, MD 21005-5069			8. PERFORMING ORGANIZATION REPORT NUMBER ARL-TR-6036		
9. SPONSORING/MONITORING AGENCY NAME(S) AND ADDRESS(ES) Environmental Security Technology Certification Program 901 North Stuart Street, Suite 303, Arlington, VA 22203			10. SPONSOR/MONITOR'S ACRONYM(S) ESTCP		
			11. SPONSOR/MONITOR'S REPORT NUMBER(S)		
12. DISTRIBUTION/AVAILABILITY STATEMENT Approved for public release; distribution is unlimited.					
13. SUPPLEMENTARY NOTES * Naval Surface Warfare Center, 9500 MacArthur Blvd., West Bethesda, MD 20817 † University of Delaware, 202 Composite Manufacturing Science Laboratory, Academy St., Newark, DE 19716 ‡ Red River Army Depot, U.S. Army TACOM, AMSTA-RR-OM, Texarkana, TX 75507-5000 § U.S. Air Force Research Laboratory, Advanced Composite Office, 5851 F Ave., Bldg. 849, Room B-46, Hill AFB, UT 84056 ** Drexel University, Department of Chemical and Biological Engineering, 3141 Chestnut St., Philadelphia, PA 19104					
14. ABSTRACT Liquid resins used for molding composite structures are a significant source of hazardous air pollutant (HAP) emissions. One method of reducing styrene emissions from vinyl ester (VE) resins is to replace some or all of the styrene with fatty acid–based monomers. This patented technology allows for the formulation of high-performance composite resins with no more than 25 weight-percent styrene, which is a 25%–50% reduction in HAP emissions vs. commercial VE resins. This work validated the commercially produced low-HAP vinyl ester resins from Applied Pleramics, Inc., for use in U.S. Department of Defense composite structures. Tests have shown that the established resin formulations met the property requirements, including viscosity, glass transition temperature, modulus, strength, short beam shear strength, fracture toughness, and weatherability. The Army has demonstrated and validated the use of the high-mobility multipurpose wheeled vehicle transmission container, M35A3 hood, and M939 hood under laboratory testing and field conditions. The Air Force has demonstrated the production of an F-22 canopy cover, T-38 dorsal cover, and rapid prototyping splash molds. Mine countermeasure rudders were successfully demonstrated at the production level and validated at the laboratory level. An economic analysis has shown that these resins will cost an additional \$0.1–\$1.20/lb (depending on manufacturing scale) more than baseline resins. However, these resins reduce life-cycle costs by more than \$1.20/lb, making them economically feasible.					
15. SUBJECT TERMS composites, resins, vinyl esters					
16. SECURITY CLASSIFICATION OF:			17. LIMITATION OF ABSTRACT UU	18. NUMBER OF PAGES 1004	19a. NAME OF RESPONSIBLE PERSON John La Scala
a. REPORT Unclassified	b. ABSTRACT Unclassified	c. THIS PAGE Unclassified			19b. TELEPHONE NUMBER (Include area code) (410) 306-0687

Contents

List of Figures	vii
List of Tables	xiii
Acknowledgments	xvii
Executive Summary	xix
1. Introduction	1
1.1 Background	1
1.2 Objective of the Demonstration	3
1.3 Regulatory Drivers	5
2. Demonstration Technology	6
2.1 Low-HAP Resin Technology Description	6
2.1.1 Bimodal Blends of Vinyl Ester Monomers	7
2.1.2 Fatty Acid Monomers	8
2.2 Technology Development	12
2.2.1 Fatty Acid Vinyl Ester Resin Development	12
2.2.2 Composite Demonstration Articles	17
2.3 Advantages and Limitations of the Technology	18
3. Performance Objectives	19
3.1 Resin Quality Control	28
4. Site/Platform Description	30
4.1 Test Platforms/Facilities	30
4.1.1 Replacement Parts for Army Tactical Vehicles	30
4.1.2 Marines Ballistic Helmet Hardtop for HMMWV	35
4.1.3 Composite Parts for Air Force Applications	36
4.1.4 Navy Composite Rudder	40
4.2 Present Operations	42
4.3 Site-Related Permits and Regulations	42

4.3.1	Environmental Checklist	42
4.3.2	Other Regulatory Issues	42
4.3.3	End-User/Original Equipment Manufacturer Issues	43
5.	Test Design	44
5.1	JTP Testing and Laboratory Experimentation.....	44
5.1.1	Testing and Evaluation Plan.....	44
5.1.2	MFA and FAVE Resin Manufacture.....	46
5.1.3	JTP MFA and Resin Batch Testing.....	46
5.1.4	Neat Resin Testing	51
5.1.5	Composite Panel Testing.....	53
5.1.6	Fatigue Testing	56
5.1.7	Environmental and Chemical Aging	58
5.2	Composite Part Validation Testing	61
5.2.1	Composite Part Demonstration	61
5.2.2	HMMWV Hardtop Demonstration/Validation Testing	61
5.2.3	Army Vehicle Hoods Demonstration/Validation Testing	62
5.2.4	Army HMMWV Transmission Container Demonstration/Validation Testing ..	64
5.2.5	Air Force T-38 Dorsal Cover Demonstration/Validation Testing.....	72
5.2.6	Air Force F-22 Canopy Cover Demonstration/Validation Testing.....	72
5.2.7	Air Force Splash Molds Demonstration/Validation Testing	72
5.2.8	Navy MCM Rudder Demonstration/Validation Testing	72
6.	Performance Assessment	73
6.1	JTP Results and Laboratory Results.....	73
6.1.1	JTP MFA Monomer Assessment	73
6.1.2	Resin Formulations.....	77
6.1.3	Resin JTP Results	85
6.1.4	Resin Properties.....	93
6.1.5	Composite Panel Testing Results	102
6.2	Demonstration/Validation Results	130
6.2.1	T-38 Dorsal Cover.....	130
6.2.2	F-22 Canopy Cover	132
6.2.3	Splash Molds	145
6.2.4	Air Force Demonstration/Validation Summary	150
6.2.5	Navy MCM Composite Rudder	151
6.2.6	HMMWV Transmission Container	180
6.2.7	M35A3 Hood.....	192

6.2.8	M939 Hood.....	199
6.2.9	Marines HMMWV Hardtop	201
7.	Cost Assessment	203
7.1	Cost Model and Composite Production.....	203
7.1.1	Cost Model	203
7.1.2	Selecting the Resin System	203
7.1.3	Manufacturing the Composites	204
7.1.4	Vacuum Assisted Resin Transfer Molding	205
7.1.5	Application Manufacturing	205
7.1.6	Styrene Emissions	206
7.1.7	Cost Model/Assumptions	207
7.2	Drexel Cost Analysis and Comparison	211
7.2.1	Cost Avoidance	211
7.2.2	Estimated MFA Price	211
7.2.2	Estimated FAVE Price	211
7.3	CTC Cost Analysis and Comparison.....	213
7.3.1	Resin Cost Estimation	213
7.3.2	Material Costs by Application.....	221
7.3.3	Engineering Controls.....	223
7.3.4	Cost Comparison	226
7.4	Environmental Impact	232
7.4.1	Preparation of Incumbent Resin (Derakane 8084)	233
7.4.2	Preparation of Replacement Resin (FAVE-L-25S).....	233
7.5	LCA Conclusions	235
8.	Implementation Issues	236
9.	References	238
	Appendix A. Points of Contact	243
	Appendix B. ATC Validation of HMMWV Transmission Container	245
	Appendix C. Resin Formulation	289
	Appendix D. Gel Time Results	401

Appendix E. Publications	435
Appendix F. Air Force Composite Testing	485
Appendix G. Navy Resin Testing	491
Appendix H. Army and Marines Composite Panel Testing Results	597
Appendix I. Navy Composite Rudder Demonstration and Validation Report	655
Appendix J. Sioux Manufacturing Corp. Report	687
Appendix K. Concurrent Technology Corporation Life Cycle Analysis	709
Appendix L. Drexel MFA Production and Cost Report	761
List of Symbols, Abbreviations, and Acronyms	975
Distribution List	978

List of Figures

Figure 1. Current and future uses of composite materials in the military include the high-mobility multipurpose wheeled vehicle (HMMWV), Navy DDX, and Crusader.	1
Figure 2. This program demonstrated/validated low-HAP VE resin composites for (a) HMMWV ballistic hardtop and (b) a HMMWV transmission container; 1–2 types of composite replacement hoods including (c) M939, (d) M35A3, or (e) HMMWV; and (f) MCM rudder, (g) T-38 dorsal cover, and (h) F-22 canopy cover.	4
Figure 3. Volatile emissions are liberated during all stages of composite production.	6
Figure 4. Methods to reduce VOC/HAP emissions in thermosetting resins.	7
Figure 5. Photographs of (a) the unpainted composite hood affixed on an M35A3 truck and (b) the underside view of the low VOC/HAP hood painted with MIL-DTL-64159 low VOC water-dispersible CARC. The blue stripes in (b) are PVC foam stiffeners that are fabricated into the part.	9
Figure 6. Photographs of (a) the hat-stiffened structure and (b) the hat region of a composite prepared by NSWCCD using the low-VOC/HAP VE resin developed by ARL/Drexel.	10
Figure 7. Design schematic to decide which resin modification was used for any of the demonstrations.	11
Figure 8. Schematic illustration of composite manufacture process.	12
Figure 9. Riveted hood of M35 results in fast corrosion failure of the hood.	31
Figure 10. Part design for M35A3 hood.	32
Figure 11. Part design for the HMMWV hood.	32
Figure 12. Part design for HMMWV transmission container.	33
Figure 13. The Amtech ballistic hardtop mounted on HMMWV.	35
Figure 14. Damage that occurs with current UPE-based dorsal covers for T-38.	37
Figure 15. Part design for T-38 dorsal cover.	38
Figure 16. Photographs of cavitation damage on metallic straight rudder and metallic twisted rudder, which occur at lower speeds than the composite counterparts.	40
Figure 17. Demonstratoin/validation process design for FAVE resins used in DOD composite applications.	45
Figure 18. Graphical representation of the styrene weight-percent loss over a 20-day period for both Derakane 8084 and 441–400 epoxy VE resins.	51
Figure 19. Illustration of sine waveform cycle.	57
Figure 20. Preparation of composite armor targets (left) and final armor target after trimming (right).	62
Figure 21. Center loading (left) and front loading (right) of M35A3 hood in test frame for static and cyclic testing.	63

Figure 22. Flexural loading showing driver side (left) and passenger side (right) loading of M35A3 hood in test frame for static and cyclic loading.....	63
Figure 23. Photograph of setup for edgewise drop test.	65
Figure 24. Photograph of setup for cornerwise drop test.	66
Figure 25. Photographs of the tip over test.	66
Figure 26. Photographs of the impact test.	67
Figure 27. Photograph of the flatwise drop test.	68
Figure 28. Photographs depicting the stacking test.	68
Figure 29. Photograph showing the concentrated load resistance test.....	69
Figure 30. Vibration setup for the FAVE transmission container (left) and response accelerometer inside the container to measure the vibration response of the container (right).	70
Figure 31. Loose cargo (shock) test setup.	71
Figure 32. Schematic structures of Novolac VE, bisphenol A VE, styrene, MLau, and MOct. ..	79
Figure 33. Gel time as a function of 2,4-P content for Derakane 8084 and FAVE-O-25S at 70 °F using 0.3 weight-percent CoNap and 2 weight-percent Trigonox.	96
Figure 34. Viscosity of commercial and FAVE resins at 25 °C.	98
Figure 35. Dry glass transition temperature of commercial and FAVE resins.....	99
Figure 36. Wet glass transition temperature of commercial and FAVE neat resins.....	99
Figure 37. Hot/wet T_g of MFA modified VEs compared with commercial ones.	100
Figure 38. Flexural modulus of commercial and FAVE neat resins.....	101
Figure 39. Flexural strength of commercial and FAVE neat resins.	101
Figure 40. The fracture toughness of the commercial and FAVE neat resins.	102
Figure 41. Residual flexural strength of resins after 10,000 cycles.....	103
Figure 42. Residual elasticity modulus of resins after 10,000 cycles.....	104
Figure 43. Fatigue life vs. strength for flexural loading conditions. The black line represents Derakane 411-350, and the white is 10% bio-rubber toughened.....	104
Figure 44. Fatigue life vs. elasticity modulus for flexural loading conditions. The black line represents Derakane 411-350, and the white is 10% bio-rubber toughened.....	105
Figure 45. Flexural strength of commercial and FAVE composites showing baseline (no aging), JP8 aging, and xenon weathering.	106
Figure 46. Flexural stiffness of commercial and FAVE composites showing baseline (no aging), JP8 aging, and xenon weathering.	106
Figure 47. SBS strength of commercial and FAVE composites showing baseline (no aging), JP8 aging, xenon weathering, and freeze-thaw-soak cycle aging.....	107
Figure 48. Flexural properties for Navy composites subject to simulated saltwater immersion aging.....	108

Figure 49. Flexural properties for Air Force composites subject to MEK immersion aging.	109
Figure 50. Dry and wet glass transition temperatures for commercial and FAVE composites. .	110
Figure 51. Glass transition temperatures (dry) for commercial and FAVE composites showing baseline (no aging), JP8 aging, freeze-thaw-soak aging, and MEK aging.....	110
Figure 52. Tensile strength results.	113
Figure 53. Tensile modulus results.	114
Figure 54. Compressive strength results.	115
Figure 55. Compressive modulus results.	115
Figure 56. Shear strength results.....	116
Figure 57. Mode I interlaminar toughness results.	118
Figure 58. Mode I interlaminar toughness results effect of post cure.	118
Figure 59. Mode I interlaminar toughness results for carbon fiber reinforced VE systems.	119
Figure 60. Percent weight gain vs. exposure time for FAVE-L composite samples at 50 °C and 80% relative humidity.	124
Figure 61. DMA results for the FAVE-L-20S resin material.	127
Figure 62. Dorsal cover tool with fiber pack ready to be infused.....	130
Figure 63. Failed attempt to infuse T-38 dorsal cover with FAVE-L.	131
Figure 64. F-22 canopy covered with Teflon tape.....	132
Figure 65. Application of gel coat on F-22 canopy.	133
Figure 66. Canopy cover splash curing.....	134
Figure 67. Application of rib stiffeners on splash.....	134
Figure 68. Final F-22 canopy splash mold.....	135
Figure 69. Layup of glass and tooling dough for F-22 canopy master.	136
Figure 70. Final canopy master.....	137
Figure 71. Application of offset with foam block on master tool.....	137
Figure 72. Application of modeling clay to master tool.	138
Figure 73. Final canopy cover master tool.....	139
Figure 74. Layup of glass fabric fiber pack for canopy cover infusion.	140
Figure 75. Setup of infusion lines for canopy cover infusion.....	140
Figure 76. FAVE-L-25S resin preparation for canopy cover infusion.	141
Figure 77. Resin infusion of F-22 canopy cover.....	142
Figure 78. F-22 canopy cover with foam interface strips.	142
Figure 79. Final F-22 canopy cover being fit tested on an F-22.....	143
Figure 80. Final F-22 canopy cover next to an F-22 canopy.	144
Figure 81. Splash mold resin flow test.....	145

Figure 82. Application of gel coat on part surface.....	146
Figure 83. Glass cloth placed on part surface.	147
Figure 84. Splash being vacuum bagged and set up for infusion.	148
Figure 85. Splash mold after removal from aircraft surface.	148
Figure 86. Final splash mold with edges trimmed.	149
Figure 87. Flow study results indicating movement of flow front with time denoted in minutes for three different panel types.	153
Figure 88. Fabrication of MCM composite hub.	155
Figure 89. Foaming and shear ties fabrication of MCM rudder.	157
Figure 90. MCM rudder 1—infusion 1.....	159
Figure 91. MCM rudder 1—infusion 2.....	161
Figure 92. Completed MCM rudder 1.	162
Figure 93. Unloading MCM rudder 1 from fabrication fixturing.....	164
Figure 94. MCM rudder 2—foaming and shear tie fabrication.	165
Figure 95. MCM rudder 2—glass wrapping.....	166
Figure 96. MCM rudder 2—caul plate locations.	166
Figure 97. MCM rudder 2—infusion 1.....	168
Figure 98. MCM rudder 2 after infusion 1.	169
Figure 99. MCM rudder 2—infusion 2.....	170
Figure 100. MCM rudder 2 after infusion 2.	172
Figure 101. MCM rudder 2—locations of face sheet samples.	173
Figure 102. MCM rudder 2—locations of rudder cross sections.....	174
Figure 103. MCM rudder 2—leading edge near caul plate.	175
Figure 104. MCM rudder 2—leading edge away from caul plate.....	176
Figure 105. MCM rudder 2—shear ties and caul plate area.	177
Figure 106. MCM rudder 2—corner of tip and trailing edge.	178
Figure 107. MCM rudder 2—middle of trailing edge.	179
Figure 108. Photographs of the completed laboratory demonstrated HMMWV transmission composite container.	181
Figure 109. Images showing (a) vacuum-bagged box and (b) infusion of FAVE-L-25S-RDX resin into the HMMWV transmission container.....	182
Figure 110. Infused and cured (a) bottom and (b) top of the HMMWV transmission container that used FAVE-L-25S resin.....	183
Figure 111. Image showing (a) bottom and (b) top of FAVE HMMWV transmission with outer hardware.	183
Figure 112. Bottom of FAVE HMMWV transmission container with internal hardware.	184

Figure 113. Assembled FAVE HMMWV transmission container demonstration.	184
Figure 114. Results from impact resistance test.	186
Figure 115. Results after impact test showing deformation of the aluminum internal brackets.	186
Figure 116. Vibration response of the Derakane 8084 container (left) and FAVE-L-25S- RDX container (right).	187
Figure 117. Status of the Derakane 8084 (left) and FAVE-L-25S-RDX (right) containers after loose cargo testing.	187
Figure 118. Photograph showing that the D-ring separated from the clasp during vibration testing.	188
Figure 119. Photograph showing the broken wooden feet after loose cargo testing.	188
Figure 120. Transmission loaded into the baseline (Derakane 8084) and low-HAP FAVE containers.	189
Figure 121. Derakane 8084 composite showing external damage after field test.	190
Figure 122. FAVE-L-25S-RDX composite showing external damage after field test.	190
Figure 123. Evidence of internal damage for Derakane 8084 transmission container after field test.	191
Figure 124. Evidence of internal damage for FAVE-L-25S-RDX transmission container after field test.	191
Figure 125. M35A3 hood after vacuum bagging (left) and at the moment of resin infusion (right).	193
Figure 126. M35A3 hood after 10-min (left) and 19-min (right) resin infusion using FAVE- L-HT-RDX.	194
Figure 127. M35A3 hood after 51-min resin infusion using FAVE-L-HT-RDX.	194
Figure 128. FAVE-L-HT-RDX M35A3 hood manufactured by SMC.	195
Figure 129. Load deflection curves for center top loading (left) and center front (right) for FAVE-L-HT-RDX M35A3 hood.	196
Figure 130. Load deflection curve for driver corner (left) passenger corner lift (right) for FAVE-L-HT-RDX M35A3 hood.	196
Figure 131. Load deflection curve for driver corner (left) passenger corner lift (right) for FAVE-L-HT-RDX M35A3 hood after cyclic handle loading.	197
Figure 132. Load deflection curve for top center (left) front center (right) for FAVE-L-HT- RDX M35A3 hood after cyclic handle loading.	197
Figure 133. Impact damage to the FAVE-L-HT-RDX M35A3 hood as a result of drops on or near stiffeners.	198
Figure 134. Impact damage to the FAVE-L-HT-RDX M35A3 hood as a result of drops on corners.	198
Figure 135. Photographs showing bagging, infusion, and demonstration of M939 hood using FAVE-O-HT.	199

Figure 136. Photographs of the top (left) and underside (right) of the M939 hood using FAVE-O-HT-RDX resin.....	200
Figure 137. Photographs of the front (left) and passenger side (right) of the M939 hood using Hetron 980/35 resin mounted on a M939 frame and the FAVE-L-HT resin (bottom) on the M939 frame.....	200
Figure 138. The 4-ply panel was tested against NIJ IIIa (44 magnum) equivalent (top photos), and 12-ply panel was tested against NIJ III (7.62 M80 ball) equivalent.	202
Figure 139. Schematic illustration of composite manufacturing process.	204
Figure 140. Illustration of VARTM (38).	205
Figure 141. Monomer synthesis steps.....	216
Figure 142. Adwest's RETOX dual chamber RTO system requirements (54).	224
Figure 143. Aspects of the product life cycle compared for the two resin systems.	232
Figure 144. Derakane 8084 process flow diagram.	233
Figure 145. FAVE-L-25S process flow diagram.	234
Figure 146. Methacrylated lauric acid process flow diagram.....	234
Figure 147. Derakane 441-400 process flow diagram.	235

List of Tables

Table 1. Common performance and testing requirements for the FAVE monomer.....	19
Table 2. Common performance and testing requirements for the FAVE resin.	20
Table 3. Performance objectives for Army hoods with appropriate fabric reinforcement for application.....	21
Table 4. Performance objectives for HMMWV transmission container with appropriate fabric reinforcement for application.	23
Table 5. Performance objectives for Marines HMMWV hardtop.	25
Table 6. Performance objectives for Air Force T-38 dorsal cover, splash molds, and F-22 canopy cover.	26
Table 7. Performance objectives for Navy composite rudder.....	27
Table 8. Acid number criteria for MFA and low-HAP resins.	47
Table 9. Viscosity criteria for MFA and low-HAP resins.	47
Table 10. FTIR criteria for MFA and low-HAP resins.....	48
Table 11. NMR criteria for MFA and low-HAP resins.	49
Table 12. SEC criteria for MFA and low-HAP resins.	50
Table 13. Gel time criteria for MFA and low-HAP resins.	51
Table 14. Proposed applications for commercial VE and FAVE composites in the military.	54
Table 15. Relevant aging testing per application and proposed FAVE composite replacement.	58
Table 16. Composite layup, approximate thickness, and estimated fiber and matrix volume fraction for studied commercial VE and FAVE composites.	59
Table 17. Initial reaction conditions for MFA monomers to determine ideal production reaction conditions.	73
Table 18. Batch testing results of initial production batches of MFA.	74
Table 19. Target reactant concentrations for the production of MFA monomers.	74
Table 20. Deviation of reactant contents for the production of MFA.	74
Table 21. Acid number of MFA monomers.....	75
Table 22. Viscosity of MFA monomers.	76
Table 23. NMR results of MFA monomers.	77
Table 24. Basic resin formulations.	80
Table 25. The formulations for the resin variants of FAVE-L and the neat resin properties. In bold are the optimum properties and highlighted in green are the optimum formulations.	81

Table 26. The formulations for the resin variants of FAVE-O and the neat resin properties. In bold are the optimum properties and highlighted in green are the optimum formulations.	81
Table 27. The formulations for the resin variants of FAVE-L-25S and the neat resin properties. In bold are the optimum properties and highlighted in green are the optimum formulations.	82
Table 28. The formulations for the resin variants of FAVE-O-25S and the neat resin properties. In bold are the optimum properties and highlighted in green are the optimum formulations.	82
Table 29. The formulations for the resin variants of FAVE-L-HT and FAVE-O-HT and the neat resin properties. In bold are the optimum properties and highlighted in green are the optimum formulations.	83
Table 30. The formulations for the resin variants of toughened FAVE-L/O and the neat resin properties. In bold are the optimum properties.	83
Table 31. The formulations for the resin variants of toughened FAVE-L/O-25S and the neat resin properties. In bold are the optimum properties.	84
Table 32. Deviation in component concentrations of FAVE-L/O and FAVE-L/O-25S according to API mix sheets.	85
Table 33. Deviation in component concentrations of FAVE-L/O-HT according to API mix sheets.	86
Table 34. NMR batch testing results of FAVE resins.	87
Table 35. Acid number titration results of FAVE batches.	88
Table 36. Styrene weight-percent content in FAVE resins measured using as evaporative losses in TGA experiment.	89
Table 37. FAVE batch viscosity.	91
Table 38. Gel time for each batch of FAVE resins with 0.2 weight-percent CoNap and 1 weight-percent Trigonox at 72 °F.	92
Table 39. Modulus at 30 °C and T_g of API batch samples as measured using DMA.	93
Table 40. Gel time for selected FAVE resins with 0.2 weight-percent CoNap and 1 weight-percent Trigonox as a function of storage time.	94
Table 41. Effect of temperature on the gel time of FAVE-L.	95
Table 42. The effect of Trigonox content on gel time of FAVE-L at 72°F.	95
Table 43. The effect of CoNap content on gel time of FAVE-L at 72 °F.	95
Table 44. The effect of hydroquinone content on gel time of FAVE-L at 72 °F.	96
Table 45. Properties of the commercial resins used in this work.	97
Table 46. The properties of Air Force composite coupons.	111
Table 47. Summary of density measurements (ASTM D 792).	112
Table 48. Summary of constituent material measurements (ASTM D 3171).	112
Table 49. ASTM D 638 tension test results.	113

Table 50. ASTM D 695 compression test results.	114
Table 51. Shear test results (ASTM D 2344).....	116
Table 52. Mode I interlaminar toughness results (RTD) (glass fabric SW1810).	117
Table 53. Mode I interlaminar toughness results (RTD) (carbon fiber fabric T700 FOE size, plain weave, 9 oz/sq yd).....	119
Table 54. Panel identification and fiber orientation.....	120
Table 55. Summary of density measurements (ASTM D 792).	121
Table 56. Summary of constituent material measurements (ASTM D 3171).	121
Table 57. ASTM D 638 tension test results.	122
Table 58. ASTM D 695 compression test results.	122
Table 59. ASTM D 5379 v-notch shear test results.....	123
Table 60. ASTM D 638 tension test results (RTD and elevated temperature wet).	124
Table 61. ASTM D 695 compression test results.	125
Table 62. Shear test results.	125
Table 63. Mode I interlaminar toughness results.....	126
Table 64. Glass transition temperature results as determined by the dynamic mechanical thermal analysis test for the FAVE-L-20S resin.....	127
Table 65. Glass transition temperature results as determined by the dynamic mechanical thermal analysis test for a variety of resin systems.....	128
Table 66. Panel testing results of FAVE-HT resin systems for hardtop and transmission container applications.	129
Table 67. Panel testing results of FAVE-HT resin systems for hood applications.....	129
Table 68. Time vs. distance chart collected from the infusion of the flat panel.	145
Table 69. Gel time study—trial A.....	151
Table 70. Gel time study—trial B.....	151
Table 71. Gel time study—trial C.....	152
Table 72. Panel identification and fiber orientation.....	152
Table 73. Viscosity of resin systems.....	154
Table 74. Core drill samples thicknesses from rudder faces.	173
Table 75. Neat resin properties as measured by SMC of the resins used for the HMMWV transmission container.	181
Table 76. HMMWV validation test results.....	185
Table 77. Neat resin properties as tested by SMC for resins for Army truck hood applications (M35A3 and M939).....	192
Table 78. The validation results for the FAVE-O-HT-RDX and Hetron 980/35 M939 hoods.	201
Table 79. Incumbent and replacement resin for selected composite military applications.	204

Table 80. Projected scale of operations for various demonstrations.	206
Table 81. Styrene emissions from manufacturing composite applications.....	207
Table 82. Cost avoidance in the high emissions factor case for FAVE resins in place of commercial resins.	208
Table 83. Cost avoidance in the low emissions factor case for FAVE resins in place of commercial resins.	208
Table 84. The estimated cost of MFA in 2008.	212
Table 85. Estimated price of FAVE resins for a small manufacturer.	212
Table 86. Estimated price of FAVE resins for a large manufacturer.....	213
Table 87. Cost of incumbent VE resins.	214
Table 88. Cost of replacement FAVE resin components.....	215
Table 89. Prices quoted by API for MLau and MOct.....	216
Table 90. Estimated breakdown of current costs for small resin manufacturer to produce 55- gal batch of monomers.....	217
Table 91. Prices quoted by API for FAVE resins.....	218
Table 92. Estimated breakdown of costs to produce 55 gal of resins for small resin manufacturer.	220
Table 93. FAVE resin costs for large resin manufacturer.	221
Table 94. Material requirements for VARTM production of VE resins.....	222
Table 95. Total material cost for incumbent and replacement resins with no engineering controls.....	222
Table 96. Price quotes obtained for RTOs.....	224
Table 97. RTO capital and operating costs spread over a 15-year economic lifetime.	225
Table 98. Worst case total estimated cost per part with resin prices from small manufacturer.	227
Table 99. Realistic scenario total estimated cost per part with resin prices from small manufacturer.	228
Table 100. Worst case total estimated cost / part with resin prices from large manufacturer.	229
Table 101. Realistic scenario total estimated cost/part with resin prices from large manufacturer.	230
Table 102. RTO usage price increase for FAVE resins.....	231

Acknowledgments

The authors would like to thank the Environmental Security Technology Certification Program for funding this effort. We would also like to thank Strategic and Environmental Research and Development Program (SERDP) PP-1271 for development of the technology necessary for this demonstration/validation project and the Environmental Quality Basic Research Development Program and the Tactical Vehicles Program at the University of Delaware for leveraged support. The authors would like to thank the contractors at Applied Poleramics, Inc., for preparing the methacrylated fatty acids and fatty acid vinyl esters. Thank you also to the composite manufactures at Sioux Manufacturing Corp. and Structural Composites, Inc. The authors also thank the engineers and technicians at U.S. Army Aberdeen Test Center and Red River Army Depot for their work in validating the high-mobility, multipurpose, wheeled vehicle transmission container. We thank Steven Smith from Drexel and the staff at Concurrent Technologies Corporation for their help with the life cycle analysis. We also thank Drexel undergraduate students Nicole Galante, Colleen Mackey, Michael Matt, and Thomas Salerno for their work in assessing the manufacture and economics of methacrylated fatty acid on a continuous scale. Lastly, we thank all of the scientists, engineers, technicians, and support staff that aided with this project at the U.S. Army Research Laboratory, U.S. Naval Surface Warfare Carderock Division, Center for Composite Materials, Drexel University, Red River Army Depot, and Hill Air Force Base.

INTENTIONALLY LEFT BLANK.

Executive Summary

Composite materials are used in the U.S. Department of Defense (DOD) because of their low weight and excellent properties, enabling the production of lighter weight and stronger vehicles, ships, and structures. Programs have been initiated to replace metallic components of the high-mobility, multipurpose, wheeled vehicle (HMMWV) and other U.S. Army vehicles and naval ships with composite parts. However, fabrication of composite materials can produce large amounts of volatile organic compound (VOC) and hazardous air pollutant (HAP) emissions.

The U.S. Army Research Laboratory (ARL)/Drexel have developed low-HAP fatty acid vinyl ester (FAVE) resin systems that would allow DOD facilities to continue manufacturing vinyl ester (VE) resins using current practices and facilities while reducing pollution and health risks. These resins reduce HAP content in composite resins by using fatty acid monomers as styrene replacements and using bimodal molecular weight distributions of VE monomers to maintain high performance while using low styrene/HAP contents.

The objectives of this program are threefold as follows: (1) demonstrate/validate the processing and performance of low VOC/HAP resins developed by ARL/Drexel as a viable alternative to current VE and unsaturated polyester (UPE) systems used in the DOD; (2) quantify the impact of these resins on facility-wide HAP emissions at selected facilities and DOD contract manufacturing sites, and demonstrate compliance with proposed military National Emissions Standard for Hazardous Air Pollutants (NESHAP) and existing composites NESHAP through monitoring and record-keeping; and (3) demonstrate cost-savings potential for transitioning to low-VOC/HAP VE and UPE resins relative to using standard commercial resins or implementing facility modifications.

The FAVE resin technology was demonstrated/validated on a variety of weapons platforms. For the Army, composite materials for tactical vehicles (M35A3 hood, M939 hood, and HMMWV transmission box) were demonstrated. For the Marines, low FAVE was used to demonstrate a ballistic HMMWV hardtop that currently uses high-VOC/HAP VE resins. For the U.S. Air Force, these low-HAP resins were used to replace current resins used in a composite dorsal cover for the T-38, F-22 canopy cover, and splash molds. This resin was also used to replace VE resins currently used for the composite rudder on mine countermeasure (MCM) ships and current and future class of destroyers (DDG and DDX, respectively).

The first aspect of the demonstration was for a company to scale up the manufacture of the methacrylated fatty acid (MFA) monomers used to partly replace styrene in FAVE. Applied Poleramics, Inc. (API), of Benicia, CA, was contracted to do this. API demonstrated the successful manufacture of two MFA monomers at 5 gal and 55 gal—methacrylated lauric acid (MLau) and methacrylated octanoic acid (MOct). These resins were validated at ARL and Drexel

through a variety of tests outlined in the joint testing protocol (JTP). Although there were some initial production issues, these were rectified with simple steps resulting in a simple manufacturing method to produce these materials effectively and reproducibly.

FAVE resin formulations were developed by ARL/Drexel. This was done by blending MFA with various commercial VE resins to produce formulations with properties similar to current resins. A variety of resin formulations were prepared in this manner and were then transitioned to API for production.

API was also contracted to produce the FAVE resins. They did so according to the direction of ARL/Drexel by blending the MFA with commercial VEs. Various formulations were detailed by ARL/Drexel to produce different viscosities, glass transition temperatures, and toughness. The manufacture of these resins was validated by ARL/Drexel according to the joint test protocol. There were some production issues in the first year and a half of the project. These stemmed mainly from loss of styrene through the plastic containers used to ship the resin. This was rectified by using metal containers instead of plastic. Afterward, the resins consistently passed JTP.

Preparation of MFA and FAVE resins has been transitioned to a larger company, Dixie Chemicals, Inc. This company will scale-up these resins and provide them to commercial and DOD markets in the near future.

ARL/Drexel validated composite panels prepared using the resins developed by API and the fibers used in each of the demonstrations. ARL/Drexel did standard mechanical testing, as well as accelerated aging and fatigue of these materials. The results indicated that the FAVE performed very similarly to commercial resins but had improved fatigue and weathering properties.

A FAVE resin formulation was demonstrated/validated on three U.S. Air Force platforms. The resin was validated initially using viscosity and panel testing. Demonstration parts were then prepared successfully. The demonstration parts were then validated and showed that the FAVE resin performed similarly to the commercial VE resins used in these applications.

A FAVE resin formulation was successfully demonstrated/validated on the MCM rudder. The resin was tested initially using viscosity flow studies and composite panel coupon testing. The results of the FAVE resins were similar to that of commercial VE resins used by the U.S. Navy. The FAVE was then used to manufacture two composite rudders at Structural Composites, Inc. The composite part was manufactured successfully, and the manufacturer was satisfied with the use of this resin in a production environment. One of the rudders was cross-sectioned and was found to have excellent fiber wet out and few defects. The second rudder was kept on hand to potentially validate its use on the MCM once approval is granted by the Navy.

A couple of FAVE resins were tested for the Marines HMMWV hardtop application. Composite panels were prepared and tested using standard composite testing procedures. The results

indicated similar performance for the FAVE composites relative to commercial composites. In addition, ballistic panels were prepared to show that the FAVE performed in a manner superior to that of current commercial resins.

FAVE resin was demonstrated/validated for composite hoods applications (M35A3 and M939). Composites panels were prepared and tested and again showed similar performance of the FAVE vs. the commercial resins. Composite demonstration parts were prepared in the laboratory to prove that the FAVE resin could successfully be used for this application. Composites were then prepared at Sioux Manufacturing Corp. (SMC) to validate the resin processing and to prepare parts for validation testing. SMC was satisfied with the processability of the resins and successfully produced the composite hoods alongside hoods using commercial resins. These manufactured parts were then validated on a test frame at the Center for Composite Materials (CCM) at the University of Delaware. The results from the test-frame experiments showed identical performance of the FAVE composite hoods vs. the commercial resins, and the FAVE composites passed all required specifications. The composite hoods were tested form, fit, and function at Red River Army Depot (RRAD) and were shown to pass all requirements.

FAVE resin was demonstrated/validated for HMMWV transmission container application. Composites panels were prepared and tested and again showed similar performance of the FAVE vs. the commercial resins. Composite demonstration parts were prepared in the laboratory to prove that the FAVE resin could successfully be used for this application. Composites parts were then prepared at SMC to validate the resin processing and to prepare parts for validation testing. SMC was satisfied with the processability of the resins and successfully produced the composite hoods alongside hoods using commercial resins. These manufactured parts were then validated using tests specified in the technical data package for these parts. The results showed identical performance of the FAVE composite hoods vs. the commercial resins, and the FAVE composites passed all required specifications. The composite containers were tested at the U.S. Army Aberdeen Test Center for shock and vibration testing according to specifications for shipping containers. The results indicated that the FAVE passed all requirements. RRAD validated the FAVE and commercial resin containers by shipping the containers around the depot for a period of 3 months. The results again showed very similar behavior for the FAVE and commercial resins. However, both the RRAD and ATC testing indicated some issues with the design of the HMMWV transmission container, such as the strap hooks are positioned too low to the bottom of the container, the wooden feet tend to break, and the aluminum hardware that bolts to the transmission can break at the bolts connecting the hardware to the composite container. Those aspects were redesigned, but the tests make the FAVE resin a qualified resin for this application.

Life-cycle analysis (LCA) of the FAVE resins was performed by two independent groups. The results showed in all cases that the FAVE resins were more expensive per pound of resin than the commercial resins. However, when considering costs associated with emissions capture, FAVE resins become more competitive. In general, production of composites tended to favor the use of

FAVE resins, such as in the Army demonstrations. However, smaller scale uses, such as the Navy and Air Force demonstrations, favored the commercial resins.

Overall, the FAVE resins met the performance requirements for all of the demonstration platforms and were thus validated successfully. The LCA shows that the FAVE resins can be competitive when considering total production costs. Thus, it is recommended that FAVE resins be considered for use in all large scale uses of VE resin polymer matrix composites in the military and are potentially considered in moderate use applications as well.

1. Introduction

1.1 Background

Polymer matrix composites (PMCs) are materials made by combining a polymer with another class of materials, such as a ceramic. In general, the intention of making polymer-composites is to have low-weight, high-performance materials that are superior in a number of ways to the individual components. Fiberglass automobile bodies and tennis racquets are examples of the combination of polymers with glass fibers. Composite materials are used in the U.S. Department of Defense (DOD) because of their low weight and excellent properties, enabling the production of lighter weight and stronger vehicles, ships, and structures. Programs have been initiated to replace metallic components of the high-mobility multipurpose wheeled vehicle (HMMWV) and other U.S. Army vehicles and naval ships with composite parts (figure 1). Future classes of vehicles and ships will use significantly higher amounts of composite materials, making these vehicles lighter, faster, and more maneuverable. However, aspects of these technologies have an adverse effect on the environment. Fabrication of composite materials can produce large amounts of volatile organic compound (VOC) and hazardous air pollutant (HAP) emissions. Sources of pollution from these materials include disposal of hazardous polymer ingredients, solvents used for viscosity reduction, gases evolved during and after processing, and disposal of contaminated scrap materials (*1*).

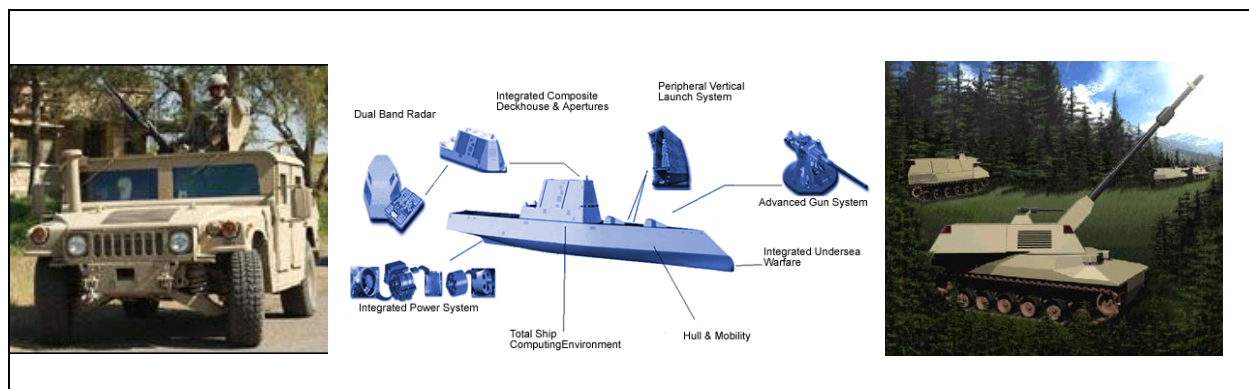


Figure 1. Current and future uses of composite materials in the military include the high-mobility multipurpose wheeled vehicle (HMMWV), Navy DDX, and Crusader.

Reactive diluents in vinyl ester (VE) and unsaturated polyester (UPE) resins, such as styrene and methyl methacrylate, are used to reduce the resin viscosity to enable liquid molding. However, these diluents are VOCs and HAPs. Typical commercial resins contain 40–60 weight-percent styrene. There are some low-HAP varieties that contain as little as 33 weight-percent styrene, such as Derakane 441-400. However, the viscosity and fracture properties of such resins are poor.

An obvious solution to reducing VOC/HAP emissions from composite resins is to simply reduce the reactive diluent content. There are a number of problems with this approach. First, the resin viscosity increases exponentially as the diluent content is decreased, making it difficult to use liquid molding techniques to produce the composite part. High viscosity is why thermoplastic materials, such as polycarbonate, cannot be used to a large extent in composite manufacture. In addition, properties such as the strength and toughness decrease significantly as the diluent content is reduced. Lastly, reducing the styrene content increases the cost of the resins because VE/UPE monomers typically cost approximately double the amount of inexpensive diluents like styrene.

Various petroleum-based monomers with volatilities lower than that of styrene have been used as styrene replacements, such as vinyl toluene (2). However, these styrene replacements still produce significant emissions and are therefore still regulated by the U.S. Environmental Protection Agency (EPA) (3). In addition, few monomers yield resins with performance comparable to styrene-based resins, and even fewer can match the low cost of styrene.

Vapor suppressants have been used to reduce emissions from VE resins. These suppressants are typically a surfactant or paraffin wax that segregates to the air interface and reduces the styrene evaporation rate (4). Unfortunately, these suppressants also tend to segregate to the resin-fiber interface, which decreases fiber-matrix adhesion and the mechanical properties of the composite.

Another possible solution is to trap the VOC/HAP emissions during resin processing, composite production, and painting applications. These trapping devices need to absorb most of the VOC/HAP emissions and then efficiently remove the emissions from the air before exhausting to the atmosphere. Trapping devices fail in two major aspects. First, their use is not feasible in the production of large-scale structures or in field repair. Large-scale structures are typically fabricated outside or in covered shelters, and building a device to trap a significant portion of the emissions is cost prohibitive. Secondly, although these devices remove the VOCs/HAPs from the atmosphere, the workers are still subject to the emissions and the health risks they pose. The resins developed by ARL/Drexel reduce VOC/HAP emissions while maintaining good resin and materials performance and are therefore ideal solutions to this problem. However, incorporating these resins into current military platforms requires technology demonstration/validation, which is the purpose of this proposal.

VE resins and UPEs resins are being used in various military platforms and are being evaluated for use in additional platforms. VE composites are excellent candidates for making parts for tactical vehicles, planes, and radome structures. Their low weight and high performance translates into better fuel economy and greater durability relative to metal parts. Furthermore, VE and UPE repair resins are regularly used by the military. Bondo* and other such repair resins are used to repair dents and other damage to maintain durability, survivability, and reduce overall

* Bondo is a registered trademark of 3M Company.

cost associated with various platforms, including tactical vehicles. Unfortunately, the current resins used for the applications no longer meet EPA regulations. Because the use of these resins is integral to the development of a lighter, faster, and more maneuverable military, it is imperative to develop low-VOC/HAP resins for the military applications.

ARL/Drexel have developed low-HAP VE and UPE resin systems that would allow DOD facilities to continue manufacturing VE resins using current practices and facilities while reducing pollution and health risks. These resins reduce HAP content in composite resins by using fatty acid monomers as styrene replacements and using bimodal molecular weight distributions of VE monomers to maintain high performance while using low styrene/HAP contents.

1.2 Objective of the Demonstration

The objectives of this program were threefold as follows: (1) demonstrate/validate the processing and performance of low-VOC/HAP resins developed by ARL/Drexel as a viable alternative to current VE and UPE systems used in the DOD; (2) quantify the impact of these resins on facility-wide HAP emissions at selected facilities and DOD contract manufacturing sites, and demonstrate compliance with proposed military NESHAP and existing composites NESHAP through monitoring and record-keeping; and (3) demonstrate cost-savings potential for transitioning to low-VOC/HAP VE and UPE resins relative to using standard commercial resins or implementing facility modifications. Once these objectives have been met, ARL will use its contacts to produce these resins commercially for the military and industry and will include these resins in technical data packages for the Army, Marines, Air Force, and Navy. Furthermore, the results from this work were published and presented at technical conferences to increase awareness of this technology.

This project seeks to expand the use of the low-VOC/HAP materials developed in U.S. Strategic Environmental Research and Development Program (SERDP) PP-1271 into the Army, Marines, Air Force, and Navy (figure 2). For the Army, composite materials for tactical vehicles (M35A3 hood, HMMWV hood, or HMMWV transmission box) were demonstrated. For the Marines, low-VOC/HAP VE was used to manufacture and demonstrate a ballistic HMMWV hardtop that currently uses high-VOC/HAP VE resins. For the Air Force, these low-HAP resins were be used to replace current resins used in a composite dorsal cover for the T-38. This resin was also be used to replace VE resins currently used for the composite rudder on mine countermeasure (MCM) ships and current and future classes of destroyers (DDG and DDX, respectively). However, the DOD does very little composite manufacture. Most composite parts are provided to the DOD through contracting industry. On the other hand, the DOD does some composite repair at facilities, such as Red River Army Depot (RRAD). Therefore, this proposed Environmental Security Technology Certification Program (ESTCP) work did not only validate the use of low-VOC/HAP resins at DOD-contracted industry for military vehicle body parts but also validated their use at DOD repair facilities.



Figure 2. This program demonstrated/validated low-HAP VE resin composites for (a) HMMWV ballistic hardtop and (b) a HMMWV transmission container; 1–2 types of composite replacement hoods including (c) M939, (d) M35A3, or (e) HMMWV; and (f) MCM rudder, (g) T-38 dorsal cover, and (h) F-22 canopy cover.

ARL/Drexel focused on optimizing the resin for a particular application. Applied Poleramics, Inc., (API) produced the low-VOC/HAP resins to be used throughout this work. The University of Delaware Center for Composite Materials (CCM) and ARL design, fabricate, and test composite panels for Army, Marines, and Navy applications. The U.S. Air Force Research Laboratory at Hill Air Force Base (AFB) fabricates and tests these composites for Air Force applications. RRAD, ARL/APG, and the Advanced Composites Office (ACO) at Hill AFB validated these low-VOC/HAP composites. Structural Composites, Inc., (SCI) demonstrated the composite rudder in conjunction with the U.S. Naval Surface Warfare Center Carderock (NSWCCD). SCI and Sioux Manufacturing Corp. (SMC) were used to produce the low-VOC/HAP composite parts on a larger scale for the DOD.

These demonstrations showed that ARL/Drexel low-HAP resins can be used to replace commercial VE and UPE resins. As such, composite performance was maintained, life-cycle cost was maintained, and HAP content was significantly lowered below National Emissions Standards for Hazardous Air Pollutants (NESHAP) regulations relative to commercial resins.

1.3 Regulatory Drivers

Reactive diluents in VE and UPE resins, such as styrene and methyl methacrylate, are used to reduce the resin viscosity to enable liquid molding. However, these diluents are VOCs and HAPs. HAPs were defined by the 1990 Clean Air Act Amendments (section 112) as chemicals that must have emissions limits. These chemicals have adverse health effects, including headache, fatigue, depression, irritation, and cancer, and they are damaging to the environment. VOCs evaporate at substantial rates at room temperature (RT) and could potentially produce smog-promoting ozone, as well as long-term and acute health effects. VOC/HAPs are emitted during all phases of composite fabrication (figure 3). Emissions occur during the mixing of diluents, catalysts, and initiators into the system. Composite parts typically have very large surface to volume ratios, which allows up to 20% loss of diluent content during the molding stage. The elevated temperatures generated during cure increase the vapor pressure of diluent and thus increase the rate of VOC emission. Unfortunately, even after cure during the lifetime of the part, VOC emissions can be substantial. Up to 40% of the styrene in VE resins is unreacted after cure (5). These unreacted monomers evaporate as VOCs, giving the composite an unpleasant odor, and they can leach out into the water supply during the lifetime of the part. A study has shown that although the composites industry only consumes 9% of the styrene, it produces 79% of the styrene emissions (4). For these reasons, by means of the Clean Air Act, the EPA has enacted the Reinforced Plastic Composites NESHAP to limit styrene emissions from composite manufacturing (3). This legislation could have a significant impact on the use of composite materials in military and commercial applications unless methods for mitigating VOC/HAP emissions during composite processing, curing, and fielding of the composite part are developed. Current high-performance resins typically contain ~40–50 weight-percent HAP content. The new regulations require the HAP content to be effectively ~30 weight-percent,

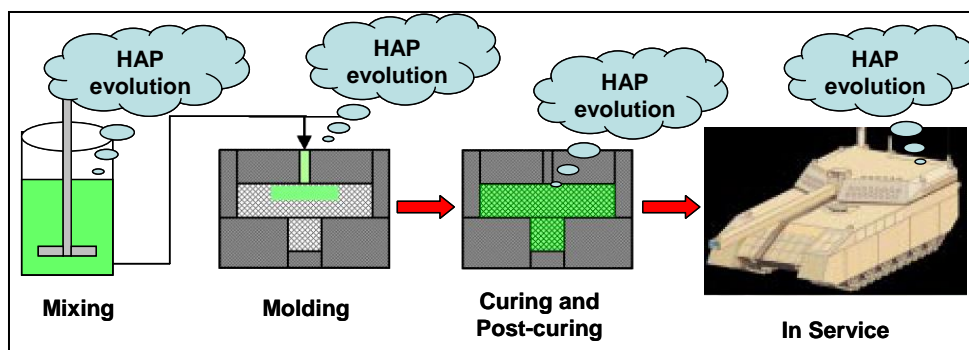


Figure 3. Volatile emissions are liberated during all stages of composite production.

resulting in emissions reduction of ~8000 tons per year. Although some commercial resins have as little as 30 weight-percent HAP content, these resins suffer from poor properties.

Through implementation of the Clean Air Act and Clean Water Act, the EPA has established regulations limiting the amount of VOCs, HAPs, and heavy metals that can be used in composite materials. The regulation requires facility wide emissions limits as of 2008, which make compliance through low emissions materials desirable. Although there are commercial resin systems that meet the current NESHAP requirements for individual DOD facilities, these resins have poor performance and processability. Therefore, DOD facilities would need to implement add-on control devices to capture volatile emissions from composite processing in order to use the high-performance commercial resins. Considering the number of current and future DOD sites using composite resins, the cost of implementing these add-on facilities is prohibitive (6). The alternatives would be to use more expensive epoxy resins (approximately three times more expensive) or to reduce the usage of composites in the DOD, making it difficult to realize the initiative to make a lighter, faster, and more maneuverable military.

2. Demonstration Technology

2.1 Low-HAP Resin Technology Description

Typical commercial VE and UPE resins contain 40–60 weight-percent styrene or other reactive diluent. These resins are not NESHAP compliant. Commercial industry has developed low-HAP resins, such as Derakane 441-400 and Reichhold Hydrex 100-LV, which are low-HAP content and are NESHAP compliant for most composite fabrication applications. However, the fracture toughness and viscosities of these resins are poor and unacceptable for most military use. ARL/Drexel has developed two solutions for making NESHAP compliant resins with excellent resin and polymer performance—fatty acid vinyl ester/unsaturated polyester (FAVE/UPE) and bimodal vinyl ester (BMVE) (figure 4). The FAVE/UPE resin uses fatty acid

monomers (7) as a reactive diluent to replace all but ~20 weight-percent of the styrene HAP in the VE or UPE resin (8). The BMVE resin uses a mixture of low- and high-molecular-weight VE monomers (i.e., bimodal) to reduce resin viscosity and improve fracture performance while using only 28–38 weight-percent styrene (9). The solutions, which are in the process of being patented (7, 10), are depicted in figure 4 and involve replacing conventional reactive diluents with plant-oil-derived monomers and altering the molecular structure of the cross-linking agent to reduce the styrene content in these resins.

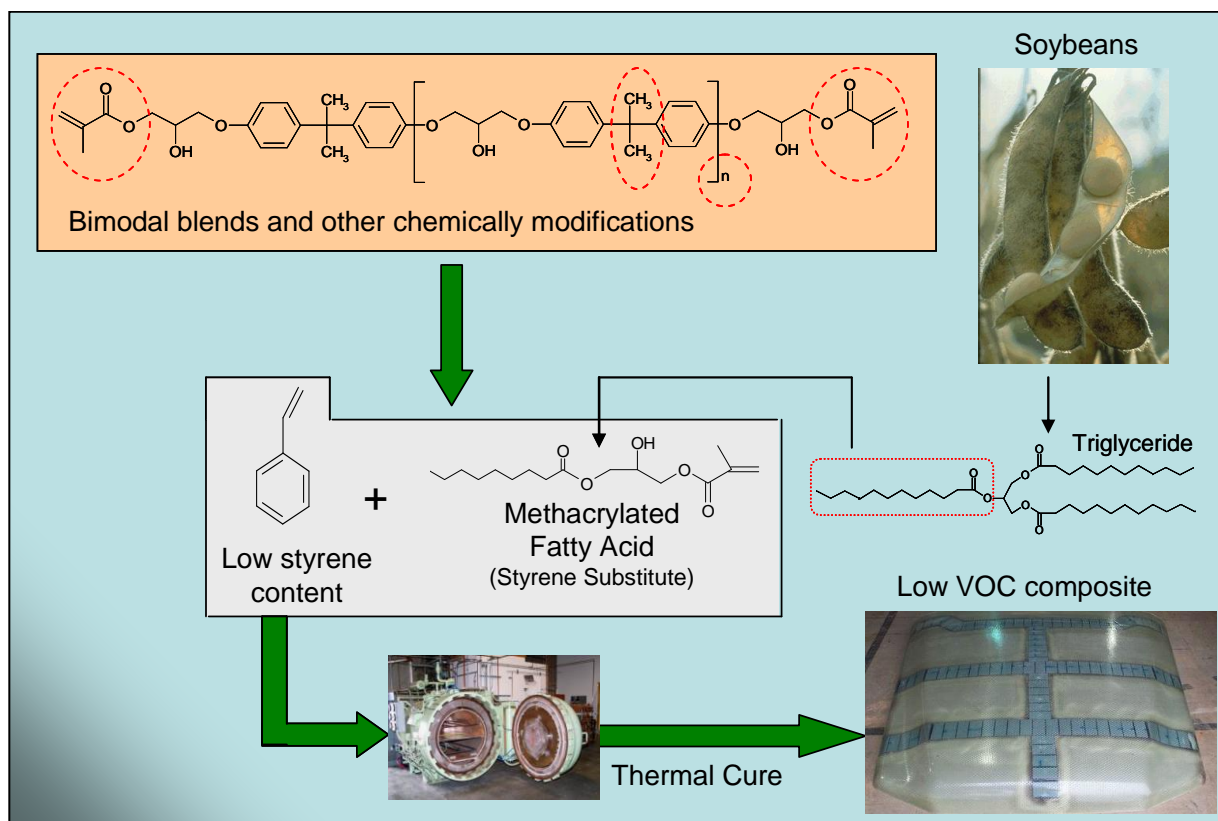


Figure 4. Methods to reduce VOC/HAP emissions in thermosetting resins.

2.1.1 Bimodal Blends of Vinyl Ester Monomers

Altering the molecular structure of VE monomers can be used to affect the polymer properties and reduce the styrene content in these resins. Simply reducing or increasing the molecular weight of VE monomers does not provide a means for both decreasing styrene emissions and maintaining resin and polymer properties. Low-molecular-weight VE monomers have low viscosities but also have poor fracture properties because of their high cross-link densities. High-molecular-weight VE monomers yield resins with high fracture properties because of reduced cross-link density (i.e., matrix toughening), but have high resin viscosities. On the other hand, a mixture of low- and high-molecular-weight VE monomers (i.e., bimodal blend) can be used to maintain low resin viscosities and low styrene contents while achieving high fracture toughness (9).

Experimental results showed that the styrene content of these bimodal blends can be reduced while still maintaining low enough viscosity for composite liquid molding applications (9, 11). The viscosity was found to be dependent on the number average molecular weight of the bimodal blends of VE monomers. As a result, the styrene content can be decreased to as low as 28–38 weight-percent while maintaining low resin viscosities of 500 cP or less. Although not a severe reduction in styrene content, this does amount to ~20% reduction in VOC/HAP emissions relative to commercial resins. The modulus and strength were the same as that of commercial resins for the neat resin but superior for the bimodal composites (11). Furthermore, bimodal blends substantially improved the toughness relative to commercial resins. Therefore, the concept of bimodal blends of VE monomers can be used not only to reduce VOC/HAP emissions (12) but also to improve the composite properties.

2.1.2 Fatty Acid Monomers

Triglycerides are the main component of oils derived from plant and animal sources. Triglycerides are three fatty acids connected by a glycerol center (figure 4). Triglycerides are simply broken down into fatty acids using industrial processes, such as saponification. A number of synthetic routes have been established by ARL/Drexel for making fatty acid-based monomers (7). The methacrylated fatty acid (MFA) monomer has proven to be the best fatty acid monomer for composite production. MFA monomers are produced through a simple addition reaction of the carboxylic acid of fatty acids with the epoxide group of glycidyl methacrylate to form a single product within a few hours at temperatures ranging from room temperature to 80 °C. Each MFA contains one terminal polymerizable unsaturation site per molecule. In this way, the fatty acid monomers act as chain extenders, analogous to styrene, in VE resins. The resulting monomers have fairly high molecular weight and are non-volatile, making them excellent alternatives to styrene in liquid molding resins. Furthermore, these monomers promote global sustainability because they are made using a renewable resource. Numerous fatty acids have been used to make MFA monomers. The molecular structures of the fatty acids used do have an effect on the polymer and resin properties. The resin viscosity decreases and polymer properties increase as fatty acid chain length decrease (8), but cost is also a factor. Methacrylated lauric acid monomers represent a balance of these factors, as they have good resin and polymer properties and low cost. Due to the low cost of fatty acids and the simple modifications to produce fatty acid monomers, these monomers are inexpensive, with an estimated cost only slightly above that of styrene. Although plant oils have been used to make polymers for years, the use of fatty acid monomers as reactive diluents is a novel concept (7).

Ideally, all of the styrene in VE and UPE resins could be replaced with fatty acid-based monomers; however, the resulting resin and polymer properties are poor relative to commercial resins. Therefore, rather than completely replacing styrene with fatty acid monomers, styrene was partially replaced with the fatty acid monomers. Styrene contents ranging from 10 weight-percent to 20 weight-percent (55%–78% reduction in VOC/HAP content relative to commercial resins) were used resulting in good resin and polymer properties. The resin viscosities were far

below the threshold for liquid molding processes (1000 cP) and have been successfully used to produce defect-free composite parts at high production rates (13, 14). The glass transition temperature was similar to commercial resins ($>120^{\circ}\text{C}$), and the toughness was twice that of commercial resins. On the other hand, the stiffness and strength were a bit lower than that of commercial resins, while still having moduli over 3 GPa and strength over 100 MPa. In addition, part shrinkage was reduced by more than 50% relative to commercial resins, helping to maintain dimensional stability. Thermo gravimetric analysis results showed that the fatty acid monomers are not volatile, and resins formulated with these monomers produce only styrene emissions. Therefore, these MFA monomers do indeed reduce the VOC/HAP content in composite resins.

A number of composite materials were made using VE resins with both styrene and fatty acid monomers as the reactive diluents. The strength and moduli of the fatty acid-based composites were not significantly different from that of the commercial resins (14) even though the neat resin properties were slightly inferior, indicating improved fiber-matrix adhesion in fatty acid-based composites. To prove that these resins can be used to produce large-scale structures, a composite hood for an M35A3 truck (figure 5) was fabricated using a low-VOC/HAP resin containing 15 weight-percent fatty acid monomers and only 20 weight-percent styrene (13). The resin infused very quickly for such a large structure (7- \times 7-ft) and cured well to produce a fine composite structure. Furthermore, NSWCCD successfully demonstrated that these resins can be used to make large scale parts, including a representative hat-stiffened structure that was used for the Composite Advanced Sail Program and DDX (figure 6). Therefore, successful low-VOC/HAP resins are not merely a concept but instead are reality. Overall, the properties of both the FAVE and BMVE resin systems solutions are similar to that of commercial resin systems, while having much lower VOC/HAP contents that qualify for exemption under NESHAP rules.

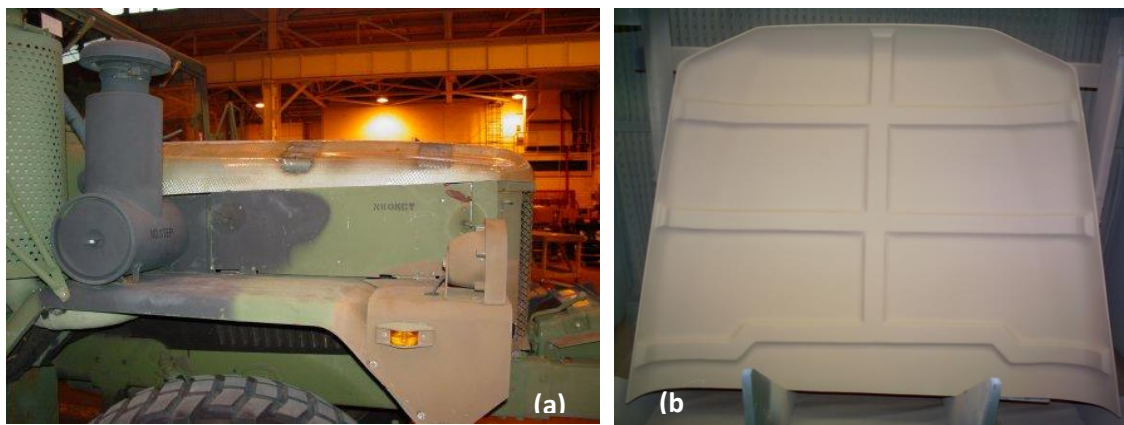


Figure 5. Photographs of (a) the unpainted composite hood affixed on an M35A3 truck and (b) the underside view of the low VOC/HAP hood painted with MIL-DTL-64159 low VOC water-dispersible CARC. The blue stripes in (b) are PVC foam stiffeners that are fabricated into the part.



Figure 6. Photographs of (a) the hat-stiffened structure and (b) the hat region of a composite prepared by NSWCCD using the low-VOC/HAP VE resin developed by ARL/Drexel.

Overall, there some key design criteria for the resins depending on the required properties and performance of the fabricated composites. First, there are the following two different technologies that can be used to reduce HAP emissions from composite resins:

- fatty acid monomers and
- bimodal VEs.

There are also a number of other technologies that can be used to modify the performance of these technologies as follows:

- VE type (bisphenol A vs. Novolac),
- fatty acid chain length (lauric acid vs. octanoic acid), and
- resin component ratio.

Figure 7 was used to decide which resin design is used to meet the required composite performance. The FAVE resin based on lauric acid (FAVE-L) was used initially as the standard resin for all applications. However, for cases where this resin did not meet the required performance, first, shorter fatty acids (FAVE-O – octanoic acid-based resins) were used. When higher performance was still required, FAVE-L-25S or FAVE-O-25S resins with 25 weight-percent styrene were evaluated. Also, novolac VEs were used to replace or partially replace the bisphenol VEs (FAVE-LN—the N indicates that the resin is Novolac-based rather than bisphenol-based). If higher performance is still required, both shorter chain fatty acids and Novolac VEs were used together (FAVE-ON). Lastly, bimodal VEs could have been used if the fatty acid technology did not have the correct performance, but this was not the case. The reason for initially starting with the fatty acid technology is twofold—(1) the FAVE resins have far lower HAP content then the bimodal resins (~20 weight-percent vs. ~30 weight-percent) and (2) the FAVE resins are far easier for our commercial manufacturer to prepare relative to the BMVE. In all of these variations, the resin mix ratio can be adjusted. We decided initially to use FAVE resins with 65 weight-percent VE monomer, 15 weight-percent fatty acid, and 20 weight-percent styrene. Properties can be further improved by using resins with 65 weight-percent

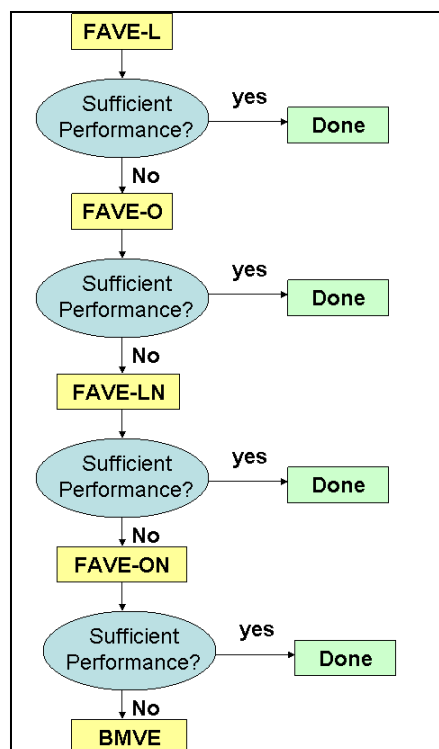


Figure 7. Design schematic to decide which resin modification was used for any of the demonstrations.

VE monomer, 10 weight-percent fatty acid (FA), and 25 weight-percent styrene. This resin would still have far lower HAPs than low-HAP commercial resins.

Figure 8 is an illustration of the process required to make and field a composite part. Initially, the monomers are synthesized usually by a commercial resin producer and/or chemical companies. The components are then blended by the resin producer. Catalyst, initiator, free-radical inhibitors, and other additives are mixed in by the resin user shortly before composite infusion. The fibers are layed-up in the proper orientation. Then, the resin is injected into the mold and allowed to cure. The sample is then to be de-molded. Postcure at elevated temperatures is optional depending on the required performance. The part is then sanded and polished to give a class A surface for painting. Finally, the painted part is used to replace worn parts on the weapons platform.

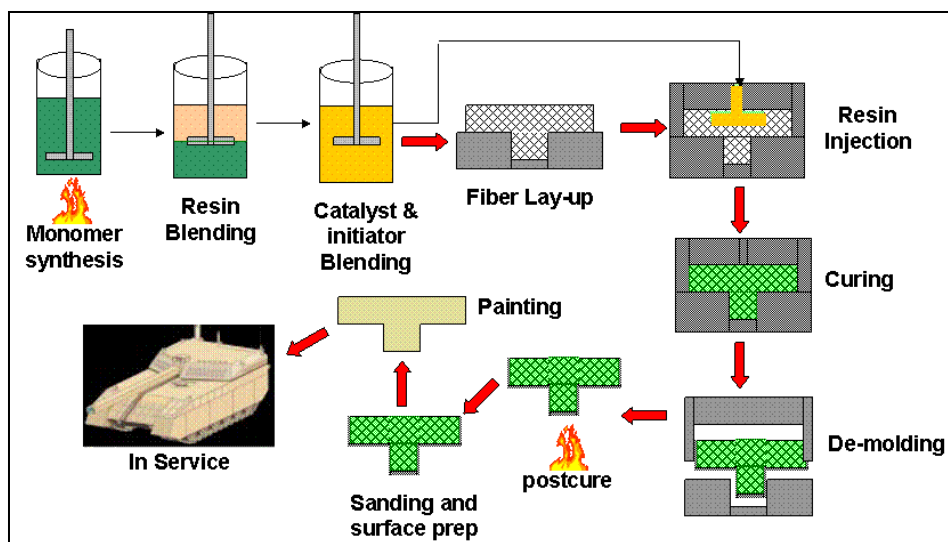


Figure 8. Schematic illustration of composite manufacture process.

2.2 Technology Development

2.2.1 Fatty Acid Vinyl Ester Resin Development

Much of the ARL/Drexel low-HAP resins chemistry optimization and testing was conducted under SERDP project PP-1271, “Low-Cost and High-Impact Environmental Solutions for Military Composite Structures.” Most of that testing was performed by ARL and Drexel University, but some testing was performed by NSWCCD. Testing and properties can be found in the following articles, reports, and patent applications that were performed during SERDP WP-1271 or ESTCP 0617:

- La Scala, J. J.; Orlicki, J. A.; Jain, R.; Ulven, C. A.; Palmese, G. R.; Vaidya, U. K.; Sands, J. M. Emission Modeling of Styrene From Vinyl Ester Resins With Low Hazardous Air Pollutant Contents, *Clean Tech Environ Policy* **2009**, *11*, 283–292.
- Palmese, G. R.; La Scala, J. J.; Sands, J. M. Fatty Acid Monomers to Reduce Emissions and Toughen Polymers. U.S. Patent 7,525,909, 28 April 2009.
- Palmese, G. R.; La Scala, J. J.; Sands, J. M. Multimodal Vinyl Ester Resins. Australian Patent 2005250354, 11 June 2009.
- Palmese, G. R.; La Scala, J. J.; Sands, J. M. Composite Repair Resins Containing Minimal Hazardous Air Pollutants and Volatile Organic Compounds. U.S. Patent Application 11/689,191, 11 June 2009.
- Palmese, G. R.; La Scala, J. J.; Sands, J. M. Multimodal Vinyl Ester Resins. U.S. Patent 7,449,525, 11 November 2008.

- Glodek, T. E.; Boyd, S. E.; McAninch, I. M.; LaScala, J. J. Properties and Performance of Fire Resistant Eco-Composites Using Polyhedral Oligomeric Silsesquioxane (POSS) Fire Retardants. *Comp. Sci. and Tech.* **2008**, 68, 2994–3001.
- La Scala, J. J.; Logan, M. S.; Sands, J. M.; Palmese, G. R. Composites Based on Bimodal Vinyl Ester Resins with Low Hazardous Air Pollutant Contents. *Comp. Sci. and Tech.* **2008**, 68, 1869–1876.
- Boyd, S. E.; La Scala, J. J.; Palmese, G. R. Molecular Relaxation Behavior of Fatty Acid-Based Vinyl Ester Resins. *J. Appl. Polym. Sci.* **2008**, 108, 3495–3506.
- Palmese, G. R.; La Scala, J. J.; Sands, J. M. Multimodal Vinyl Ester Resin. European Patent Application 05804814.1–2109, 25 September 2008.
- La Scala, J. J.; Jeyarajasingam, A.; Logan, M. S.; Winston, C.; Myers, P.; Sands, J. M.; Palmese, G. R. Fatty Acid-Based Vinyl Ester Composites With Low Hazardous Air Pollutant Contents. *J. Biobased Matl. and Bioenergy* **2007**, 1, 409–416.
- La Scala, J. J.; Glodek, T.; Lochner, C.; Geng, X.; Quabili, A.; Patterson, K.; Bruce, F.; Bartling, E.; Johnson, C.; Myers, P.; Boyd, S.; Andersen, S.; Coulter, L.; Crane, R.; Gillespie, J., Jr.; Sands, J. M.; Starks, M.; Gomez, J.; Palmese, G. R. *Demonstration of Military Composites With Low Hazardous Air Pollutant Content*; ARL-RP-185; U.S. Army Research Laboratory: Aberdeen Proving Ground, MD, July 2007.
- La Scala, J. J.; Levine, F.; Myers, P.; Sands, J. M.; Andersen, S.; Gillespie, J., Jr.; Patterson, K.; Coulter, L.; Crane, R.; Starks, M.; Gomez, J.; Geng, X.; Palmese, G. R. Demonstration of Military Composites with Low Hazardous Pollutant Contents. *Proceedings of the 52nd International SAMPE Symposium and Exhibition*, Baltimore, MD, May 2007.
- Can, E.; La Scala, J. J.; Sands, J. M.; Palmese, G. R. The Synthesis of 9-10 Dibromo Stearic Acid Glycidyl Methacrylate and Its Use in Vinyl Ester Resins. *J. Appl. Polym. Sci.* **2007**, 106, 3833–3842.
- La Scala, J. J.; et al. Environmentally Friendly Composite Materials Based on Fatty Acid Monomers, *EM* **2007**.
- Geng, X. J.; La Scala, J. J.; Sands, M.; Palmese, G. R. High Performance Fatty Acid-Based Vinyl Ester Resin for Liquid Molding. *Proceedings of the 52nd International SAMPE Symposium and Exhibition*, Baltimore, MD, May 2007.
- La Scala, J. J.; Levine, F.; Myers, P.; Sands, J. M.; Andersen, S.; Gillespie, J., Jr.; Patterson, K.; Coulter, L.; Crane, R.; Starks, M.; Gomez, J.; Geng, X.; Palmese, G. R. Demonstration of Military Composites with Low Hazardous Pollutant Contents. *Proceedings of the 2006 Army Science Conference*, Orlando, FL, November 2006.

- La Scala, J. J.; Ulven, C.; Orlicki, J. A.; Jain, R.; Palmese, G. R.; Vaidya, U.; Sands, J. M. Emission Modeling of Styrene from Vinyl Ester Resins. *Clean Technology and Environmental Policy* **2006**, 9, 265–279.
- La Scala, J. J.; Jeyarajasingam, A.; Winston, C.; Sands, J. M.; Palmese, G. R. *Predicting The Viscosity of Low VOC Vinyl Ester Resins*; ARL-TR-3681; U.S. Army Research Laboratory: Aberdeen Proving Ground, MD, December 2005.
- La Scala, J. J.; Orlicki, J. A.; Winston, C.; Robinette, E. J.; Jeyarajasingam, A.; Lee, J.; Dey, T.; Cavan, C.; Baer, J.; Brown, J.; DeSchepper, D.; McKnight, S. H.; Ulven, C. A.; Jain, R.; Kamath, P.; Sahu, A.; Crane, R. M.; Vaidya, U. K.; Palmese, G. R.; Sands, J. M. *Low-Cost and High-Impact Environmental Solutions for Military Composite Structures, Final Report*; SERDP PP-1271; U.S. Strategic Environmental and Development Program: Arlington, VA, December 2005.
- La Scala, J. J.; Orlicki, J. A.; Winston, C.; Robinette, E. J.; Jeyarajasingam, A.; Lee, J.; Dey, T.; Cavan, C.; Baer, J.; Brown, J.; DeSchepper, D.; McKnight, S. H.; Ulven, C. A.; Jain, R.; Kamath, P.; Sahu, A.; Crane, R. M.; Vaidya, U. K.; Palmese, G. R.; Sands, J. M. *Low-Cost and High-Impact Environmental Solutions for Military Composite Structures*; Annual SERDP Report; U.S. Strategic Environmental and Development Program: Arlington, VA, December 2005.
- La Scala, J. J.; Orlicki, J. A.; Winston, C.; Robinette, E. J.; Sands, J. M.; Palmese, G. R. The Use of Bimodal Blends of Vinyl Ester Monomers to Improve Resin Processing and Toughen Polymer Properties. *Polymer*, **2005**, 46, 2908–2921.
- La Scala, J. J.; Sands, J. M.; Palmese, G. R. Clearing the Air: Army Composites Research Reduces Harmful Emissions. *The AMPTIAC Quarterly* **2004**, 8, 118–125.
- La Scala, J. J.; Sands, J. M.; Orlicki, J. A.; Robinette, E. J.; Palmese, G. R. Fatty Acid-Based Monomers as Styrene Replacements for Liquid Molding Resins. *Polymer* **2004**, 45, 7729–7737.
- Palmese, G. R.; La Scala, J. J.; Sands, J. M. Fatty Acid Monomers to Reduce Emissions and Toughen Polymers. U.S. Patent Application DREX-1014US, 6 May 2005.
- Palmese, G. R.; La Scala, J. J.; Sands, J. M. Multimodal Vinyl Ester Resin. PCT Application DREX-1036WO, 6 May 2005.
- La Scala, J. J.; Jeyarajasingam, A.; Winston, C.; Sands, J. M.; Palmese, G. R. *Predicting the Viscosity of Low VOC Vinyl Ester Resins*; ARL-TR-3681; U.S. Army Research Laboratory: Aberdeen Proving Ground, MD, December 2005.

- La Scala, J. J.; Orlicki, J. A.; Winston, C.; Robinette, E. J.; Sands, J. M.; Palmese, G. R. *The Use of Bimodal Blends of Vinyl Ester Monomers to Improve Resin Processing and Toughen Polymer Properties*; ARL-RP-95; U.S. Army Research Laboratory: Aberdeen Proving Ground, MD, May 2005.
- La Scala, J. J.; Sands, J. M.; Orlicki, J. A.; Robinette, E. J.; Palmese, G. R. *Fatty Acid-Based Monomers as Styrene Replacements for Liquid Molding Resins*; ARL-RP-94; U.S. Army Research Laboratory: Aberdeen Proving Ground, MD, May 2005.
- La Scala, J. J.; Robinette, E. J.; Palmese, G. R.; Sands, J. M.; Orlicki, J. A.; Bratcher, M. S. *Successful Initial Development of Styrene Substitutes and Suppressants for Vinyl Ester Resin Formulations*; ARL-TR-3023; U.S. Army Research Laboratory: Aberdeen Proving Ground, MD, August 2003.
- Ulven, C.; Sands, J. M.; Vaidya, U. K. *Emission and Mechanical Evaluations of Vinyl Ester Resin Systems*; ARL-TR-2930; U.S. Army Research Laboratory: Aberdeen Proving Ground, MD, March 2003.
- Gillespie, J., Jr. Accelerated Insertion of Lightweight Materials into Military Vehicles. *Proceedings of the 3rd Annual Lightweight Materials for Defense*, Arlington, VA, 28 February–2 March 2005.
- Andersen, S.; Gillespie, J., Jr.; Haque, J.; Heider, D.; Shevchenko, N.; Siers, R.; Sands, J. Overview of the Composite Body Parts Replacement Program. *Proceedings of the Defense Manufacturing Conference 2004*, Las Vegas, NV, 29 November–2 December 2004.
- Gillespie, J. Jr.; Heider, D.; Shevchenko, N.; Sands, J.; Siers, R.; Florence, J. An Overview of the Composites Replacement Parts Program for Military Tactical Wheeled Vehicles. *Proceedings of the American Society for Composites 18th Technical Conference*, Gainesville, FL, 20–22 October 2003.

Overall, the testing described in the above publications rigorously measured numerous aspects of these materials, including the four essential properties and benchmarks for this work as follows: (1) resin viscosity, (2) neat resin properties, (3) composite properties, and (4) HAP emissions. These publications are summarized in the following paragraphs.

Three means of reducing the styrene emissions were proposed. First, styrene emissions can be reduced by using a bimodal blend of VE monomers. Second, some or all of the styrene monomer in VE and UPE resins can be replaced with low-volatile petroleum or fatty acid-based monomers. Lastly, the use of a self-assembling vapor barrier using surface-active dendritic polymers to suppress styrene emissions was investigated.

Characterization techniques, including Fourier transform infrared spectroscopy (FTIR) and size exclusion chromatography (SEC), show that VE monomers with narrow molecular weight distributions and bimodal blends of these monomers have been successfully prepared. These bimodal blends have low resin viscosities and high fracture and thermal properties. Furthermore, these bimodal blends can be used to reduce the VOC emissions from VEs by ~20%.

Out of all the petroleum-based comonomers studied as styrene replacements, cyclohexyl methacrylate has been shown to be the most successful because its VE resins have low vapor pressure, good thermo-mechanical, and acceptable viscosities. A number of synthetic procedures have been developed to produce fatty acid-based monomers. These monomers are inexpensive, have very low volatilities, and have improved global sustainability. Results have shown that low-molecular-weight and saturated fatty acid monomers yield resins with the lowest viscosities and highest thermo-mechanical properties. However, thermal cure of fatty acid-based VEs resulted in polymers with properties inferior to those of commercial resins. Electron beam cure was used to increase the performance of fatty acid-based VEs. In addition, fatty acid monomers can be blended with styrene to reduce the styrene content in VE resins while maintaining good thermo-mechanical, fracture, and rheological properties relative to commercial VE resins. The VOC emissions are reduced by 50%–78% in these blends of VE, fatty acid monomers, and styrene.

Composites have been prepared from these low-VOC resins. The properties of fiberglass-reinforced composites were similar or superior for these newly developed low-VOC formulations relative to commercial resins. Furthermore, large-scale composite structures have been fabricated successfully using standard resin infusion techniques.

A macro-thermogravimetric analyzer was developed to measure the styrene emissions from VE resins because the results from more conventional techniques, such as desorption gas chromatography and micro-thermogravimetric analyzer, had low reproducibility due to the small masses involved. Emissions studies from the bimodal blends of VE monomers and commercial VE resins display a characteristic elbow where the initial emission rate of styrene suddenly drops to a much lower emission rate. The position of this elbow moved to higher volatile content remaining as the number average molecular weight of the VE monomers increased. The initial rate of emission was only dependent on the styrene content in the resin. However, overall emissions were reduced by increasing the molecular weight of the VEs used, as in the bimodal blends. Overall, this technique shows that bimodal blends of VEs and fatty acid-based VEs reduce emissions significantly relative to commercial resins.

Commercial dendritic polymers and triglycerides were investigated in their ability to form a self-assembling vapor barrier to suppress styrene emissions. These dendritic polymers were successfully modified with fluorine groups and vinyl functionality to induce surface migration to reduce styrene emissions and to allow them to react into the polymer network. Although these resins do reduce styrene emissions, their effect is small and takes a long time to reduce

emissions. In fact, commercial styrene suppressants also fail for this long time scale for styrene emissions reductions, but these additives reduce styrene emissions to a much greater degree at that point.

Overall, the program has been successful at identifying critical DOD environmental needs, developing practical solutions to these requirements, and developing candidate resins for reducing VOC emissions from VE resins for military applications. Future work must still be done to validate the ability of these resins to produce high-performance, large-scale materials for the DOD.

VE resins are not easily produced at small scales. In addition, we were unable to partner with large-scale resin manufacturers in this effort. As a result, bimodal VE resins could not be feasibly prepared in this work for demonstration/validation. As a result, all of the work focuses on fatty acid VE resins. As was shown, this compromise also had some effect on the performance of the fatty acid VEs, but that was able to be overcome.

2.2.2 Composite Demonstration Articles

The ACO has performed lamina tests on VE and epoxies to examine the vacuum-assisted resin transfer molding (VARTM) process for the T-38 dorsal cover in the following reference:

- Bartling, E. T-38 Dorsal Cover Resin Infusion. U.S. Air Force Presentation, Hill Air Force Base, UT, June 2005.

Tensile per American Society for Testing and Materials (ASTM) D 3039, compression per ASTM D6691, and shear per ASTM D 5379 have been done. The six types of reinforcement fibers cloths with example processes were tested. Fiber volume was also examined. This testing was done in winter 2005, and these results can be supplied as needed. The VARTM manufacturing process was successful and yielded a good potential replacement part for the T-38 (15).

The CCM has rigorously tested VE composites for Army tactical vehicles and Marines HMMWV hardtop applications in the following references:

- Gillespie, J., Jr. Accelerated Insertion of Lightweight Materials into Military Vehicles. *Proceedings of the 3rd Annual Lightweight Materials for Defense*, Arlington, VA, 28 February–2 March 2005.
- Andersen, S.; Gillespie, J. W., Jr.; Haque, J.; Heider, D.; Shevchenko, N.; Siers, R.; Sands, J. Overview of the Composite Body Parts Replacement Program. *Proceedings of the Defense Manufacturing Conference 2004*, Las Vegas, NV, 29 November–2 December 2004.
- Gillespie, J. Jr.; Heider, D.; Shevchenko, N.; Sands, J.; Siers, R.; Florence, J. An Overview of the Composites Replacement Parts Program for Military Tactical Wheeled Vehicles. *Proceedings of the American Society for Composites 18th Technical Conference*, Gainesville, FL, October 20–22, 2003.

Technical data packages have been written for the M35A3. A far superior HMMWV hood was created for Army applications than the current as supported by various testing. This HMMWV hood has been produced by TPI Composites and is qualified, available, and eligible as a replacement part for HMMWV.

NSWCCD has characterized the properties of the composite system for MCM composite rudder applications as follows:

- Griffiths, B. Rudder Gets New Twist With Composites. *Composites Technology* **2006**, 60–62.
- Crane, R. *Low HAP/VOC Compliant Resins for Navy Composite Rudder Application*; Naval Surface Warfare Center Carderock Division, West Bethesda, MD, March 2006.

The results indicate a large benefit with using either composite material or both materials or a twisted rudder design. Furthermore, the MCM composite rudder has been in the field for over 5 years with no sign of wearing and has received the praise of Navy officers and program managers.

2.3 Advantages and Limitations of the Technology

The main advantage of the ARL/Drexel low-HAP resins is their low-HAP content while maintaining low resin viscosity, and high fracture properties. For the FAVE resin, low part shrinkage and partly renewable chemical make-up is also an advantage. Cost and thermal properties are likely to be the primary draw-backs to the FAVE resin, especially when produced at smaller scales. FAVE-O resins and those using Novolac VEs improve the thermal properties, but also increase the cost. Therefore, it is possible that these resins will not be able to replace commercial resins for composite parts that must meet high temperature requirements. Cost and difficulty with resin production are the main disadvantages to the BMVE resin. However, cost should not be a factor for the BMVE resins when it is produced at a commercial scale.

There are several factors that can impact the start-up and recurring cost of the ARL/Drexel low-HAP resins. The main cost driver is that the FAVE and BMVE resins were produced on a small scale relative to that of commercial composite resins. Larger scale machinery, chemical reactants, etc., would lower the cost. This could easily occur if a large resin supplier licensed and produced this technology. The cost of the glycidyl methacrylate, one of the reactants used to produce the fatty acid monomers, is currently high due to high petroleum costs and has a strong effect on resin cost. The fatty acid type also affects the cost. Shorter fatty acids, such as octanoic acid, are more expensive than longer acids, such as lauric acid. Novolac resins are more expensive than bisphenol A-based VE resins. Therefore, the required use of either of these higher-performance resins affects the cost.

The DOD will not have to invest any capital costs for these resins. Resin producers will make these resins as drop-in replacements for commercial VE and UPE resins. The resin cost per pound may be more for the low-HAP resins, but life-cycle analysis shows that they are

competitive based on cradle-to-grave cost differences. Part of this cost is associated with monitoring emissions, capital, and operating expenses associated with capture and scrubbing equipment to remove emissions from the air. These low-HAP resins should not require capture and scrubbing equipment but require costs for monitoring emissions. Traditional VEs should require these capital and operating expenses. However, the cost for these is not well established but is calculated in section 7.0. Additionally, the cost associated with fines and facility shutdown has also not been determined.

Performance could be affected by the quality of the fatty acids used to produce the resins, proper mix ratios of reactants, and proper mix ratios of the blend components. Quality control was established during this project to ensure these are a non-factor. Shelf life has a strong effect on resin performance after ~9–12 months. However, testing has shown that these resins have a superior shelf life relative to commercial resins. Unfortunately, we had not previously done ample studies on these low-HAP resins to examine the effect of UV radiation and moisture on performance. These factors were measured during this demonstration.

3. Performance Objectives

There are numerous performance objectives for this project. The initial performance objective is to demonstrate the scale-up of the MFA monomers (table 1) and low-HAP resins (table 2). The low-HAP resin was then demonstrated/validated for applications in Army hood applications (table 3), the HMMWV transmission container (table 4), the Marines HMMWV hardtop (table 5), the Air Force T-38 dorsal cover, the F-22 canopy cover, the splash mold (table 6), and the Navy composite rudder (table 7).

Table 1. Common performance and testing requirements for the FAVE monomer.

Performance Requirement	Data Requirement	Success Criteria	Results
Acid number	ASTM D 1980-87	Acid number <20	Acid number <20
Viscosity at 25 °C	Viscometer, rheometer	Viscosity <80 cP at 25 °C (MLau) Viscosity <70 cP at 25 °C (MOct)	Viscosity <80 cP at 25 °C (MLau) Viscosity <70 cP at 25 °C (MOct)
Unreacted epoxy	FTIR, nuclear magnetic resonance spectroscopy (NMR)	No epoxy present	None detected
Correct reactant ratios	NMR	Methacrylate to FA ratio of 1:1 (+0.05, -0.1)	Ratio ranged from 1.05:1 to 1:0.9

Note: NMR = nuclear magnetic resonance spectroscopy.

Table 2. Common performance and testing requirements for the FAVE resin.

Performance Requirement	Data Requirement	Success Criteria	Results
Acid number	ASTM D 1980-87	Acid number <5	Acid number <5
Viscosity at 25 °C	Viscometer, rheometer	Viscosity <1000 cP at 25 °C	Viscosity <1000 cP
Unreacted epoxy	FTIR, NMR	No epoxy present	None detected
Correct reactant ratios	NMR	Methacrylate to FA ratio of 1:1 (+0.05, -0.1)	Ratio ranged from 1.05:1 to 1:0.9
Correct VE MW	NMR, SEC	VE MW <700 g/mol (bisphenol A) VE MW <900 g/mol (Novolac)	Bisphenol VE MW <700 g/mol
Correct component ratios	NMR, SEC	VE to MFA to styrene ratio should be $\pm 5\%$ based on desired formulation	VE: MFA: Sty. ratios were within 5% of specified
Gel time	ASTM D 2471-99	Variable gel time from 10 min to 5 h	Gel times ranged from 5 min to 5 h
Production scale-ability of low-HAP resins	Production scale-ability of low-HAP resins	Pass individual tests described in joint testing protocol	Simple production. Production is scalable. Passed JTP tests.

Table 3. Performance objectives for Army hoods with appropriate fabric reinforcement for application.

Type of Performance Objective	Primary Performance Criteria	Expected Performance (Metric)	Actual Performance
Quantitative	Dry T _g through DMA test	>250 °F	289 °F
Quantitative	Wet T _g through DMA test	>225 °F	271 °F
Quantitative	Flexural strength at RT (ASTM D 790)	≥55 ksi	62 ksi
Quantitative	Flexural strength at 250 °F (ASTM D 790)	≥30 ksi	37 ksi
Quantitative	Flexural modulus at RT (ASTM D 790)	≥3.7 Msi	3.8 Msi
Quantitative	Flexural modulus at 250 °F (ASTM D 790)	≥3.0 Msi	3.1 Msi
Quantitative	Short beam shear (SBS) strength at RT (ASTM D 2344)	≥4.5 ksi	4.6 ksi
Quantitative	SBS strength at 250 °F (ASTM D 2344)	≥3.0 ksi	3.3 ksi
Quantitative	Top center loading - HMMWV hood - M35A3 hood - M939 hood	≤0.5-in deflection ≤0.5-in deflection ≤0.5-in deflection	Not performed 0.1 in 0.11 in
Qualitative	Top center loading - M939 hood - M35A3 hood - M939 hood	No damage No damage No damage	Not performed No damage No damage
Quantitative	Top front loading - HMMWV hood - M35A3 hood - M939 hood	≤0.5-in deflection ≤0.5-in deflection ≤0.5-in deflection	Not performed 0.04 in 0.03 in
Qualitative	Top front loading - M939 hood - M35A3 hood - M939 hood	No damage No damage No damage	Not performed No damage No damage
Quantitative	Driver/passenger flexural static lifts - HMMWV hood - M35A3 hood - M939 hood	>50 lb for 0.375 in >50 lb for 0.375 in >50 lb for 0.375 in	Not performed 0.015 in at 50 lb 0.2 in at 50 lb
Qualitative	Driver/passenger flexural static lifts - HMMWV hood - M35A3 hood - M939 hood	≤cosmetic damage ≤cosmetic damage ≤cosmetic damage	Not performed Cosmetic damage Cosmetic damage
Qualitative	Impact resistance - HMMWV hood - M35A3 hood - M939 hood	≤cosmetic damage ≤cosmetic damage ≤cosmetic damage	Not performed Cosmetic damage Cosmetic damage

Table 3. Performance objectives for Army hoods with appropriate fabric reinforcement for application (continued).

Type of Performance Objective	Primary Performance Criteria	Expected Performance (Metric)	Actual Performance
Qualitative	Cyclic hood testing – top center loading - HMMWV hood - M939 hood - M35A3 hood	No damage No damage No damage	Not performed No damage No damage
Qualitative	Cyclic hood testing – passenger and driver corners - HMMWV hood - M939 hood - M35A3 hood	No damage No damage No damage	Not performed No damage No damage
Quantitative	Top center loading after cyclic testing - HMMWV hood - M35A3 hood - M939 hood	≤0.5-in deflection ≤0.5-in deflection ≤0.5-in deflection	Not performed 0.1 in 0.11 in
Qualitative	Top center loading after cyclic testing - M939 hood - M35A3 hood - M939 hood	No damage No damage No damage	Not performed No damage No damage
Quantitative	Top front loading after cyclic testing - HMMWV hood - M35A3 hood - M939 hood	≤0.5-in deflection ≤0.5-in deflection ≤0.5-in deflection	Not performed 0.04 in 0.03 in
Qualitative	Top front loading after cyclic testing - M939 hood - M35A3 hood - M939 hood	No damage No damage No damage	Not performed No damage No damage
Quantitative	Driver/passenger flexural static lifts after cyclic testing - HMMWV hood - M35A3 hood - M939 hood	>50 lb for 0.375 in >50 lb for 0.375 in >50 lb for 0.375 in	Not performed 0.015” at 50 lb 0.2” at 50 lb
Qualitative	Driver/passenger flexural static lifts after cyclic testing - HMMWV hood - M35A3 hood - M939 hood	≤cosmetic damage ≤cosmetic damage ≤cosmetic damage	Not performed Cosmetic damage Cosmetic damage
Qualitative	Resin fills part in allotted time - HMMWV hood - M939 hood - M35A3 hood	Fabricator approval Fabricator approval Fabricator approval	Not performed Resin filled part Resin filled part
Qualitative	Resin gels in correct amount of time for hood - HMMWV hood - M939 hood - M35A3 hood	Fabricator approval Fabricator approval Fabricator approval	Not performed Appropriate gel time Appropriate gel time

Table 3. Performance objectives for Army hoods with appropriate fabric reinforcement for application (continued).

Type of Performance Objective	Primary Performance Criteria	Expected Performance (Metric)	Actual Performance
Qualitative	Resin fully wets fibers for hood - HMMWV hood - M939 hood - M35A3 hood	Fabricator approval Fabricator approval Fabricator approval	Not performed Resin fully wet fibers Resin fully wet fibers
Qualitative	Field test hood - HMMWV hood - M939 hood - M35A3 hood	Depot approval Depot approval Depot approval	Not performed Good performance Good performance

Table 4. Performance objectives for HMMWV transmission container with appropriate fabric reinforcement for application.

Type of Performance Objective	Primary Performance Criteria	Expected Performance (Metric)	Actual Performance
Quantitative	Dry T _g through DMA test	>200 °F	257 °F
Quantitative	Wet T _g through DMA test	>180 °F	239 °F
Quantitative	Flexural strength at RT (ASTM D 790)	≥55 ksi	69 ksi
Quantitative	Flexural modulus at RT (ASTM D 790)	≥3.7 Msi	3.8 Msi
Quantitative	SBS strength at RT (ASTM D 2344)	≥4.5 ksi	5.0 ksi
Qualitative	Resin fills part in allotted time	Fabricator comments and approval	Resin filled part in allotted time. Resin performed well according to fabricators.
Qualitative	Resin gels in correct amount of time	Fabricator comments and approval	Resin gel time was controllable from short to long times. Resin performed well according to fabricators.
Qualitative	Resin fully wets fibers	Fabricator comments and approval	Resin fully wet fibers. Resin performed well according to fabricators.
Qualitative	Field test of container	User comments	Good performance.
Qualitative	Edgewise drop, before and after fielding	No permanent deformation, separation of reinforcements or cracks observed	No permanent deformation, separation of reinforcements or cracks observed.
Qualitative	Cornerwise drop, before and after fielding	No permanent deformation, separation of reinforcements or cracks observed	No permanent deformation, separation of reinforcements or cracks observed.

Table 4. Performance objectives for HMMWV transmission container with appropriate fabric reinforcement for application (continued).

Type of Performance Objective	Primary Performance Criteria	Expected Performance (Metric)	Actual Performance
Qualitative	Tip over, before and after fielding	No permanent deformation, separation of reinforcements or cracks observed	No permanent deformation, separation of reinforcements or cracks observed.
Qualitative	Trans. container external pressure	≤ 0.22 in deformation $\leq 0.09\%$ in plane strain	Passed.
Qualitative	Impact, before and after fielding	No permanent deformation, separation of reinforcements or cracks observed in the container composite structure	No permanent deformation, separation of reinforcements or cracks observed in the container composite structure.
Qualitative	Flatwise drop, before and after fielding	No permanent deformation, separation of reinforcements or cracks observed	No permanent deformation, separation of reinforcements or cracks observed.
Qualitative	Stacking, before and after fielding	No slippage was observed and the fork truck was able to perform this task	No slippage was observed and the fork truck was able to perform this task.
Qualitative	Concentrated load resistance, before and after fielding	No permanent deformation, separation of reinforcements or cracks observed	No permanent deformation, separation of reinforcements or cracks observed.
Qualitative	Impact resistance, before and after fielding	Insignificant/minor cracking of the resin; no permanent deformation	Insignificant/minor cracking of the resin. No permanent deformation.
Qualitative	Field test, before and after fielding	Depot inspector comments	Field tests showed good performance of resin and similar to that of baseline resin.
Qualitative	Tip over, before and after fielding	No permanent deformation, separation of reinforcements or cracks observed	No permanent deformation, separation of reinforcements or cracks observed.
Qualitative	Trans. container external pressure	≤ 0.22 in deformation $\leq 0.09\%$ in plane strain	Passed.

Table 5. Performance objectives for Marines HMMWV hardtop.

Type of Performance Objective	Primary Performance Criteria	Expected Performance (Metric)	Actual Performance
Quantitative	Dry T _g through DMA test	>250 °F	257 °F
Quantitative	Wet T _g through DMA test	>200 °F	239 °F
Quantitative	4 point bend static sandwich testing (ASTM D 6272-98)	≥9000 lbs	12,000 lb
Quantitative	4 point bend fatigue sandwich testing (ASTM D 6272-98) at 5000 lb, R = 0.1 at 1 Hz	≥500,000 cycles	Test stopped at 500,100 cycles
Quantitative	SBS static sandwich testing (ASTM D 2344)	≥2 ksi	3 ksi
Quantitative	SBS fatigue sandwich testing (ASTM D 2344) at 1.1 ksi at R = 0.1 at 1 Hz	≥500,000 cycles	Test stopped at 500,100 cycles
Qualitative	Ballistic coupon testing	V50 Level IIIa at ~4 psf V50 Level III at ~12 psf V50 Level III in sandwich configuration with HJ1 phenolic core – total AD ~10.5 psf	Passed Passed Not Tested
Qualitative	Hardtop 3000-mile off-road test	Depot inspector comments	Testing not performed.
Qualitative	Resin fills part in allotted time	Fabricator comments and approval	Resin filled part in allotted time. Resin performed well according to fabricators.
Qualitative	Resin gels in correct amount of time	Fabricator comments and approval	Resin gel time was controllable from short to long times. Resin performed well according to fabricators.
Qualitative	Resin fully wets fibers	Fabricator comments and approval	Resin fully wet fibers. Resin performed well according to fabricators.
Qualitative	Fatigue testing	Similar or better than incumbent resin	Superior performance relative to incumbent.

Table 6. Performance objectives for Air Force T-38 dorsal cover, splash molds, and F-22 canopy cover.

Type of Performance Objective	Primary Performance Criteria	Expected Performance (Metric)	Actual Performance
Qualitative	Resin fills part in allotted time	Fabricator comments and approval	Resin filled part in allotted time. Resin performed well according to fabricators.
Qualitative	Resin gels in correct amount of time	Fabricator comments and approval	Resin gel time was controllable from short to long times. Resin performed well according to fabricators.
Qualitative	Resin fully wets fibers	Fabricator comments and approval	Resin fully wet fibers. ACO approved resin.
Qualitative	Flight test	Depot inspector comments and approval	Flight test did not occur.
Qualitative	Flight test	Rigid structure that maintains shape at fielding temperatures	Passed.

Table 7. Performance objectives for Navy composite rudder.

Type of Performance Objective	Primary Performance Criteria	Expected Performance (Metric)	Actual Performance
Quantitative	Wet T _g through DMA test	>100 °C	>110 °C
Quantitative	Water absorption	<5 weight-percent	<0.4 weight-percent
Quantitative	SBS strength at RT (ASTM D 2344)	≥5.3 ksi	7.2 ksi
Quantitative	SBS strength at RT – wet (ASTM D 2344)	≥5.3 ksi	6.2 ksi
Quantitative	Tensile modulus at RT (ASTM D 638) - 0° - 90°	≥2.7 Msi ≥1.9 Msi	4.6 Msi 3.2 Msi
Quantitative	Tensile strength at RT (ASTM D 638) - 0° - 90°	≥52 ksi ≥37 ksi	89 ksi 55 ksi
Quantitative	Tensile modulus at RT – wet (ASTM D 638)	≥2.6 Msi	4.8 Msi
Quantitative	Tensile strength at RT – wet (ASTM D 638)	≥40 ksi	85 ksi
Quantitative	Compressive modulus at RT (ASTM D 695) - 0° - 90°	≥2.7 Msi ≥2.3 Msi	4.5 Msi 3.7 Msi
Quantitative	Compressive strength at RT (ASTM D 695) - 0° - 90°	≥42 ksi ≥38 ksi	83 ksi 44 ksi
Quantitative	Compressive modulus at RT – wet (ASTM D 695)	≥2.0 Msi	5.0 Msi
Quantitative	Compressive strength at RT – wet (ASTM D 695)	≥41 ksi	45 ksi
Qualitative	Field test	Depot inspector comments	Part not yet fielded.
Qualitative	Resin fills part in allotted time	Fabricator comments and approval	Resin infused part in allotted time. Resin performed well according to fabricators.
Qualitative	Resin gels in correct amount of time	Fabricator comments and approval	Resin gel time was controllable from short to long times. Resin performed well according to fabricators.
Qualitative	Resin fully wets fibers	Fabricator comments and approval	Resin fully wet fibers. Resin performed well according to fabricators.

3.1 Resin Quality Control

It is possible that the MFA monomers are not completely reacted after the scaled-up process. Also, incorrect mix ratios of reactants or components can be used to create resins with incorrect formulations. As a result, quality control of these resins is necessary to validate the scale-up of these resins and to assure uniformity of the resins from batch to batch for other DOD composite demonstrations.

Because of the simplicity of the FAVE reaction and the much greater potential to reduce HAPs, the FAVE-L resin is the base resin that was tested for all DOD applications. However, the FAVE-O, FAVE-L-25S, FAVE-O-25S, FAVE-L-HT, and FAVE-O-HT resins were utilized for the given DOD applications.

The quality control of resin scale-up was tested using a set of five tests, as described in the JTP. ASTM D 1980 was used to access the acid number of MFA monomers and resins. This test determined whether there is too much free acid remaining in the system, which indicated incomplete conversion of the reactants into the MFA and VE monomers. FTIR testing was used to determine the presence of unreacted epoxy groups. Unreacted epoxy groups indicate incomplete conversion of the reactants in the MFA and VE monomers. NMR was used to determine various chemical aspects of the resins. First, the quantity of unreacted epoxy groups was measured. The ratio of methacrylate groups to VE or MFA monomers was quantified. Also, the molar ratio of VE to styrene in BMVE resins or VE/MFA/styrene in FAVE was quantified. Lastly, a rheometer was used to measure this viscosity of the MFA monomers and resins at 25 °C. Too high of a viscosity indicates side reactions occurred that degrade the resin properties and processability. SEC was used to determine the content of high molecular weight species in the MFA monomers, FAVE resins, and BMVE resins.

The engineering requirements for which the tests in this joint testing protocol (JTP) were chosen are the following:

- Monomer acid number – high acid number indicates incomplete reaction.
- Resin acid number – high acid number indicates incomplete reaction.
- Monomer viscosity – high resin viscosity indicates side-reactions occurred that degrade the monomer and resin properties.
- Resin viscosity – high resin viscosity hurts the ability to process the resin and form a good composite.
- No unreacted epoxy – unreacted epoxy indicates the MFA or BMVE reaction was not run to completion. This degrades resin performance and increases toxicity of the MFA resin.
- Correct reactant ratios – a methacrylate to fatty acid ratio of 1:1 is desired for complete reaction and optimum resin properties.

- Correct VE MW – low molecular weight VEs are desired to reduce resin viscosity.
- Correct VE/MFA/styrene ratio – resins formulations have been established with optimum properties. Changing the formulation affects the properties.
- Gel time – ability to vary the gel time from as short as 15 min to as long as 4 h.

Objectives for the HMMWV hood, M35A3 hood, and M939 hood are to meet or exceed all relevant performance parameters of the material system without an increase in weight. Because both the M35A3 and M939 hoods were validated, the HMMWV hood was not demonstrated in this work. However, the validation results for the FAVE resin show that FAVE should be valid for HMMWV hood applications.

In the static load experiments, a 250-lb weight was placed over a 3- × 3-in area at the center and front center of the hood to simulate a soldier standing on the hood. The 250-lb load applied to the outside surface over a maximum 10- × 10-in area. The load was applied at the center and front areas of the hood. The deflection was measured at the point of application of the load but on the opposite surface. Plot of load vs. deflection was obtained. The hood is required to deflect no more than 0.25 in at -50 °F and 0.5 in at 250 °F and sustain no damage. The durability requirement is for the hood to resist all damage from a 250-lb force downward at the center of the hood followed by 100,000 cycles at 1 cps to simulate a cyclic soldier load on the hood for the lifetime of the vehicle. Upon completion, a plot of load vs. deflection was obtained. The flexural properties must be such that an upward force of 50 lbf at the right and left corners will not cause any damage to the part and will not result in >0.5 in deflection. An upward load was applied at the corner lift handles. The center latch was engaged, and both right and left sides were tested (separately). Displacement of the hood corner above the fixture was measured. Plots of load vs. deflection were obtained. The lifting load will not exceed 100 lb. The structure must withstand cyclic corner loads. Upward loads of 50 lb were applied at the corner lift handles with the center latch engaged. The loads were applied in alternating fashion (right then left) over an 8-h period at 10 cycles per minute. Upon completion, plots of load vs. deflection were obtained. These tests simulate a lifetime of lifting the corners of the hood. The impact resistance was quantified by dropping a 2-lb, 2 3/8-in-diameter chrome-plated steel ball from 6 ft onto the hood. The ball was dropped on six different locations to ensure toughness across the structure, as only insignificant cosmetic damage is considered acceptable. The hood must also be able to be manufactured via VARTM, and thus there are processing requirements. The hood also must fit the truck once fabricated. In addition, some basic properties must be achieved in composite laminate coupons.

The HMMWV transmission container must be able to withstand the damage associated with shipping. Thus, fully loaded containers were tested under field trials and using lab validation scenarios that would be experienced in fielding environments. These include dropping the container from a height, stacking the containers, dropping items onto the container, and tipping

over the container. In addition, some basic properties must be achieved in composite laminate coupons.

Objectives for the Amtech HMMWV ballistic hardtop are to meet or exceed all relevant performance parameters of the material system without an increase in weight. It should be noted that the 3000-mile durability test and the ballistics performance of the sandwich coupon were not performed. This is because testing done on other platforms and coupons validated the part without need for these tests.

The APG ballistics range was utilized to determine V50 numbers for the composites used for Army and especially Marines applications. The samples must meet V50 level IIIa at ~4 psf, V50 level III at ~12 psf, and V50 level III in sandwich configuration with HJ1 phenolic core—total AD ~10.5 psf. Because the durability testing was not done, fatigue testing results were added to the matrix to ensure adequate fatigue performance of the resin. In addition, some basic properties must be achieved in composite laminate coupons.

The Air Force parts must be processable resins with moderate property requirements. They must be able to form rigid parts that maintain their performance in ambient conditions.

Resins used for Navy rudders must have properties to enable them to work at high shears, where potentially high local temperatures are achieved. The composites must also perform well in wet environments. The resins must be processable to form a large composite part.

4. Site/Platform Description

4.1 Test Platforms/Facilities

4.1.1 Replacement Parts for Army Tactical Vehicles

The tactical vehicle parts targeted in this project impact the HMMWV platform and M35A3 platform. Damage of the HMMWV transmissions during shipment is a large issue for depots in the U.S. and overseas. RRAD has experience with fixing and replacing transmissions and is a potential customer for the transmission box. The CCM designed and validated the box, showing that it can sustain moderate impacts without being damaged (16). The SMC hoods for the HMMWV are always cracking and in need of replacement. Again, RRAD is heavily involved in replacing and repairing these hoods. A more durable hood, such as the vacuum-infused hood using low-HAP VE resins, would be a more durable replacement. The M35A3 metallic hoods have to be repaired for corrosion issues on a regular basis (17). Replacing the metallic hoods with a composite hood would reduce the logistical burden on Army depots, such as RRAD. The CCM designed and demonstrated both the VARTM HMMWV hood and M35A3 hood (18, 17). The current composite replacement M35A3 hood is also ~25% cheaper than the equivalent steel hood but with significantly greater performance and 40% less weight (17).

The CCM developed composite replacement hoods for the M35 truck and M939, along with SMC (17). A few years ago, during a recap/reset, the M35 received a new drive train. Unfortunately, the new power train did not fit within the existing hood (17). As a result, the steel hood was cut into two separate pieces and a spacer piece placed in between and a steel strip was placed at the back of the hood to fit the new engine. The four pieces were riveted together. Unfortunately, this leads to high corrosion rates of the hood, requiring a lot of maintenance work (figure 9). Sheet molding compound hoods fracture very easily and are not meant to take the loads soldiers would put on them by standing and jumping on them (17). Thus, the CCM vacuum-infused M35A3 hood and HMMWV hood to solve the problems associated with the previous hood designs and have excellent performance (17, 18). Both hoods use VE or epoxy resin as the matrix and meet all load, cyclic loading, flexural, thermal, and impact properties. The M35A3 hood uses 18-lb resin, with an estimated production of 8000 units over a 10-year period (17).



Figure 9. Riveted hood of M35 results in fast corrosion failure of the hood.

The part designs for the M35A3 hood demonstration are illustrated in figure 10 (17). The M939 is a very similar design, but it must fit to a different contour and in particular have longer sides (16). Both hoods used a single ply of 96-oz E-glass fibers with 2- x3-in PVC foam stiffeners. There was a 2-in-wide border band of an additional 24-oz plies placed along the edge and where the hood is hinged to the truck to reinforce these areas.

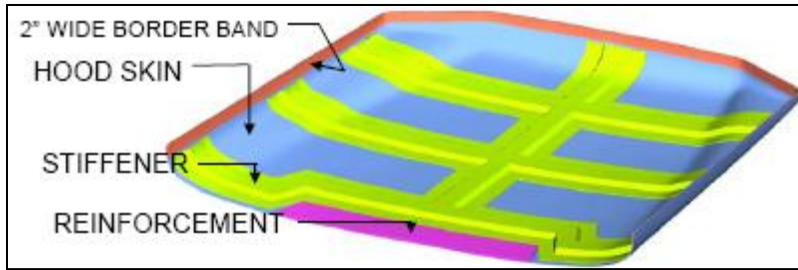


Figure 10. Part design for M35A3 hood.

The CCM designed replacement HMMWV hoods with TPI Composites. The existing SMC HMMWV hoods fracture and fatigue very quickly due to soldiers standing and jumping on them while in battle, or doing surveillance, or maintenance (18). Thus, the CCM vacuum designed and vacuum infused the HMMWV hood to solve the problems associated with the previous hood designs and to have excellent performance (18). Both hoods use VE or epoxy resin as the matrix and meet all load, cyclic loading, flexural, thermal, and impact properties. The HMMWV hood uses 20-lb resin with an expected production of 1800/month.

Figure 11 shows the part design for the HMMWV hood (18). The HMMWV hood is made from a three-dimensional (3-D) preform. The composite hood is molded using this preform. After resin cure, a separately molded stiffener network is bonded to the preform part. The bulk of the HMMWV hood is about as thick as the M35A3 hood, and both use E-glass fiber reinforcement.



Figure 11. Part design for the HMMWV hood.

HMMWV transmissions are shipped into theatre using foam and cardboard shipping containers. Due to the poor structural properties of these shipping materials, the transmissions are often damaged during shipping (16). In most cases, the transmissions are return-shipped from theatre on base wood pallets, which further exposes them to significant damage. RRAD has explored the use of metal shipping containers, but corrosion issues and the maintenance required makes

this route unfeasible. The CCM has recently developed a VE-based shipping container to meet all of the packaging requirements to prevent transmission damage during shipment (16). These containers meet high strength, impact, and thermal requirements. These containers use 35-lb resin each, with an estimated production of 5000 units (16).

The original HMMWV transmission container part design is illustrated in figure 12 (16). A modified version was developed during the course of the project and is pictured elsewhere. The container weighs 140 lb empty and 305 lb loaded with the transmission. Outer dimensions are 43 5/8-in length \times 30 5/8-in width \times 28 7/8-in height (16). These parts are molded in only two steps, with the lid being made independently of the base. The transmission container also used E-glass fiber reinforcement.

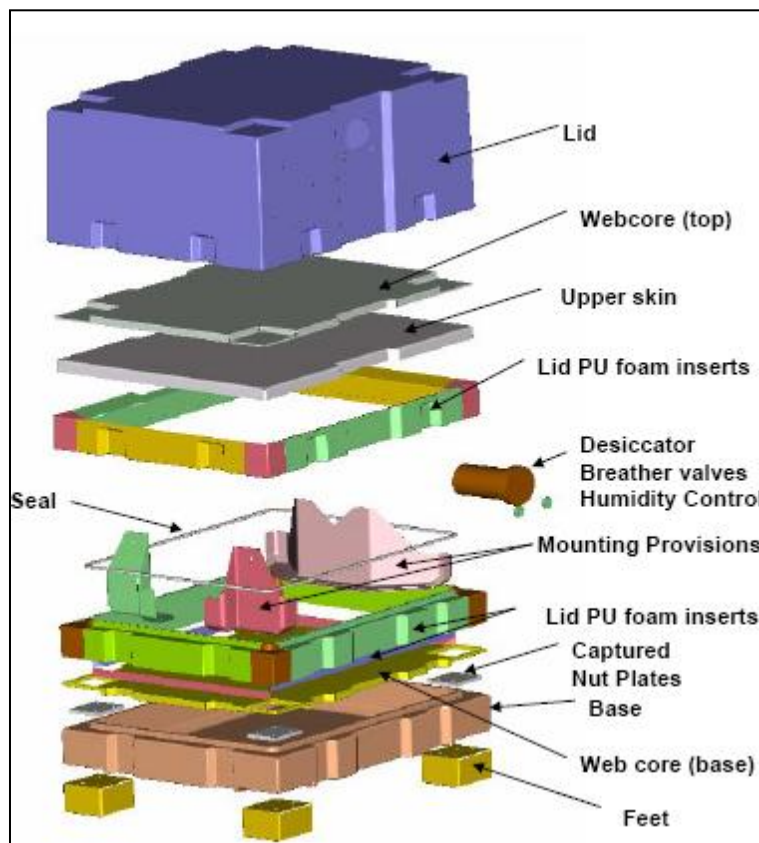


Figure 12. Part design for HMMWV transmission container.

The CCM, located in Newark, DE, has been an international leader in composites science and engineering research, education, and industrial collaboration for 30 years. Founded in 1974, CCM was one of the first centers at the university and is currently one of nine research centers in the College of Engineering. CCM attracts faculty and students from the Departments of Chemical Engineering, Materials Science and Engineering, Civil and Environmental Engineering, Electrical and Computer Engineering, and Mechanical Engineering, as well as from the Departments of Mathematics, Physics and Astronomy, and Chemistry and Biochemistry in

the College of Arts and Science and from the Accounting and MIS Department within the College of Business and Economics. Since 1986, CCM's programs and initiatives have been designated "Centers of Excellence" six times by the National Science Foundation (NSF) and the DOD.

CCM's research philosophy encourages faculty, post-docs, professionals, and students from different science and engineering disciplines to work in a collaborative environment to meet the research needs of our sponsors. Six research thrust areas describe Center interdisciplinary research in composites. The Center's researchers conduct world-class research in each of these areas but also work in research teams at the interface between these disciplines to design and optimize new materials and processes that deliver performance and affordability. The Center's unique manufacturing science laboratory provides facilities for synthesis of new materials, chemical and mechanical characterization from the nanoscale to large-scale structures, computation, design, and re-engineering and manufacturing work-cells on existing and next-generation processes that are ready for transition to our sponsors.

The three Centers of Excellence and other funding sources provide significant leverage to the Center's industrial sponsors. Companies of all sizes currently benefit from our commitment to technology transfer, which provides them with new ideas, new technologies, problem-solving capabilities, and access to potential employees with the capability to make immediate contributions.

Red River Army Depot (RRAD), located 18 miles west of Texarkana in the northeast corner of Texas, is one of our nation's largest defense depots in terms of people and workload, with a combined population of almost 2822 employees, including tenants. The workforce on the Red River complex is drawn from throughout the Four States region as follows: Texas, Arkansas, Oklahoma, and Louisiana.

The depot's enormous maintenance mission includes the repair, rebuild, overhaul, and conversion of tactical wheeled vehicles, as well as the Army's light tracked combat vehicle fleet, including the Bradley Fighting Vehicle System, the Multiple Launch Rocket System, and their associated secondary items. Vehicles depart the depot's modernized maintenance facility in "like new" condition. Among our technical resources, RRAD has the capability to design, fabricate, and manufacture a wide range of intricate items, ranging from specialty parts to unique prototype vehicles needed by its customers.

In recent years, RRAD has been recognized as a leader in developing and implementing quality-based processes into daily activities, as encouraged by the National Performance Review for all Federal activities. With its largely blue-collar workforce, the depot was a recipient of the National Partnership Award for 1996, reflecting the growth and involvement of the union-management partnership in effect at the base. Red River was also named one of 13 winners of the Army Communities of Excellence Award (ACOE) in 1996 and ACOE Runner-Up in 1998. RRAD earned a Quality Improvement Prototype Award from the National Performance Review

in 1995. The awards are part of an ongoing quality journey at Red River intended to maintain the depot's position as a competitive industrial complex excelling in quality products and services to our customers.

The mission of RRAD is as follows:

- Conduct (light) ground combat and tactical systems sustainment maintenance operations, air defense systems certification, and related support services worldwide for the U.S. armed forces and Allied/friendly nations.
- Train and employ the Army's emerging component repair companies.
- Provide essential base support services to Red River Industrial Complex missions.
- Be an active and viable partner in Bowie County, the Greater Texarkana community, and the Four States area at large.

4.1.2 Marines Ballistic Helmet Hardtop for HMMWV

The Marines have been using a non-ballistic HMMWV hardtop for communications platforms that was developed with the Amtech Corporation (figure 13). Amtech has over 15 years of production experience with this part. However, there was a need for added ballistic protection and a new process method (16). Along with Amtech, the CCM developed and demonstrated a ballistic helmet HMMWV hardtop (16). The part exceeds all ballistic and structural requirements and has a relatively low cost (16). The CCM also improved the process design by making it a vacuum infusion process to reduce emissions (16). However, the part originally used Derakane 8084 as the matrix resin, which is a toughened VE containing 40 weight-percent styrene (16). Because this resin does not meet NESHAP requirements, this would be an excellent demonstration of the environmentally friendly FAVE and/or BMVE technology. Furthermore, because of the high toughness of these low-VOC replacements and good properties, we expect successful development of this low-VOC/HAP HMMWV ballistic hardtop. The Marines and Army communication platforms are the targeted application. The weight of resin used per part is 220 lb, with an anticipated production of 40/month for 8800 lb resin/month.



Figure 13. The Amtech ballistic hardtop mounted on HMMWV.

HMMWV is a widely used platform in the Army and Marines. Amtech sells their HMMWV hardtops to the military for communications and other applications. These hardtops do an excellent job of electromagnetic interference (EMI) shielding while keeping the vehicle non-descript to keep it from being a primary target for enemy fire. Unfortunately, traditional HMMWV hardtop designs did not protect well against small-arms fire and needed to have add-on armor kits attached when used in dangerous situations. This increased the weight on the HMMWV, limiting its effectiveness. The HMMWV helmet hardtop provides small-arms ballistics protection while still giving excellent EMI shielding character. Furthermore, the overall structure is lighter than armored hardtop designs for HMMWV with communication equipment.

4.1.3 Composite Parts for Air Force Applications

The T-38 is a legacy aircraft used for training purposes at Hill AFB. The problems with dorsal cover for this platform arose during an avionics upgrade that converts 400 aircraft to T-38 “C” model (15). The upgrade includes “glass cockpit” and adds GPS capability with a GPS antenna attached to the dorsal cover. During installation of the GPS antenna, many of the dorsal covers were found to be damaged (figure 14). Some minor damage is repairable, but some covers have damage that is beyond repair, so these covers need to be replaced (15). Spare cover supply was exhausted; no covers can be ordered because they are no longer manufactured, and no tooling was available for new manufacture. Being a legacy aircraft, there were no available replacement parts. As a result, the Hill AFB Air Logistics Center was spending more time than desired in fixing and replacing dorsal covers. Furthermore, polyester composites used to make the dorsal covers were molded through a hand layup, which would result in high emissions during composite fabrication if replicated.

During the initial start of Systems Project Office (SPO) assistance in the 2003 timeframe, the ACO designed and procured tooling for use during repair. To relieve an immediate shortage, the ACO repaired three covers that were damaged beyond field repair limits. The T-38 SPO needed to start up new procurement effort for additional parts. The current drawing for the cover specifies polyester/fiberglass/phenolic honeycomb and hand fabrication. Configuration control of the existing covers is questionable, as there appear to be covers in use made from epoxy, as well as polyesters. This lack of configuration control means it is difficult to adequately baseline the properties of existing covers.

One approach for replacement parts is to perform a new build with autoclave/pre-preg/honeycomb and utilize current inventory materials for F-16 fiberglass pre-preg/film adhesive/honeycomb and autoclave processing. The use of F-16 qualified materials would shorten the acceptance of new material systems on the T-38. The ACO repair tooling would be used. However, this approach was determined to be too costly. Therefore, the ACO proposed a new approach using VARTM utilizing similar materials to the original—glass fabrics, room temperature processing with polyester, VE, or epoxy resins. The tooling that was made for repair is easily usable for the VARTM process.

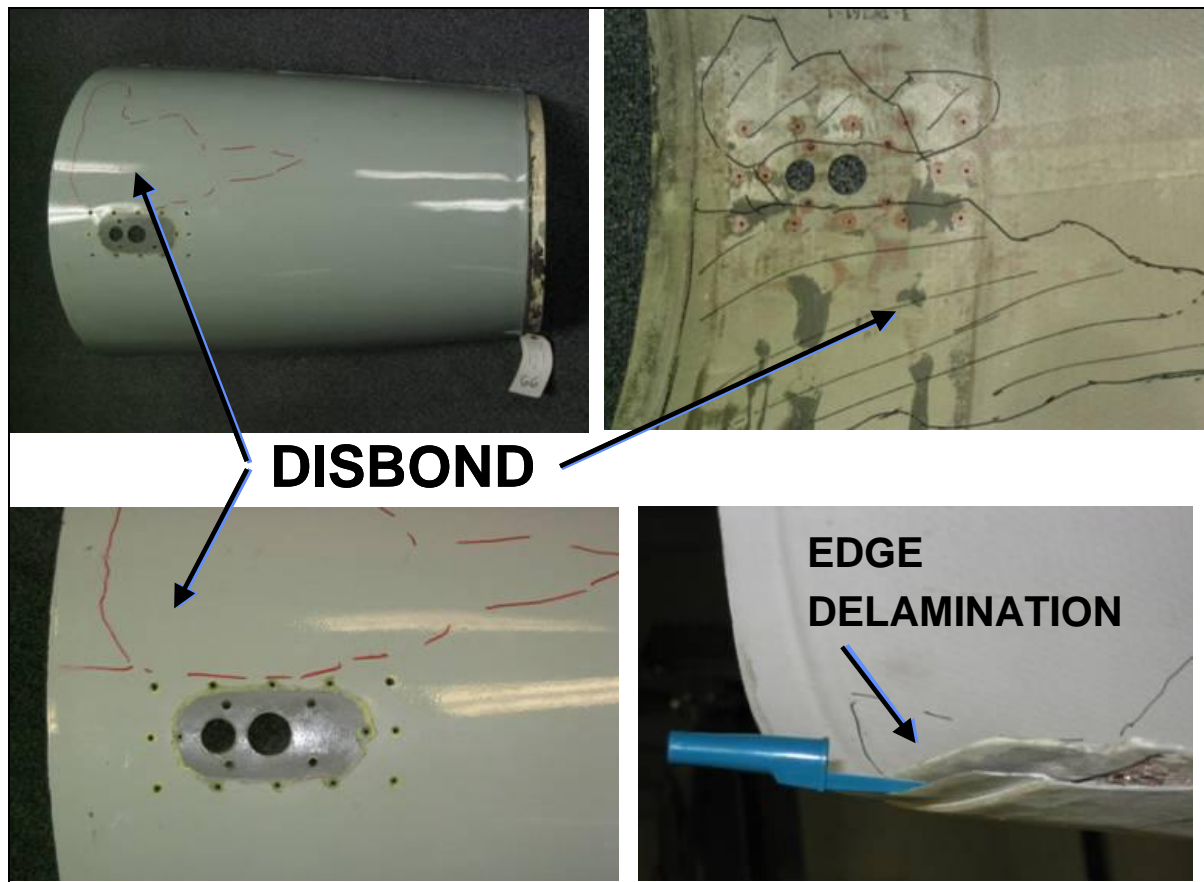


Figure 14. Damage that occurs with current UPE-based dorsal covers for T-38.

The part design for the T-38 dorsal cover is shown in figure 15. A few types of E-glass fiber are used for this piece as follows: E-BX 1200-10, Style 7781 satin weave, Vector ply stitched biaxial, E-BX 1700-5, Style 120 satin weave, warp 60, fill 58, 3.16 oz/yd². Some Kevlar reinforcement is used for the edges as follows: Style 353 crowfoot warp 17 fill 17, 5-oz/yd Aramid. Lantor SORIC XF1004 infusible core material is used in the core alone. This proposed VARTM dorsal cover was accepted by the SPO by 2010. Most validation of this part was done through composite panel testing, including modulus, strength, and interlaminar shear strength measurements. In addition, the full composite part was fabricated and flight tested.

The ACO also demonstrated/validated the FAVE resins for other repair applications. These included the F-22 canopy cover and splash molds. These applications are additional demonstration/validation platforms that were not originally proposed or discussed in the technical demonstration plans.

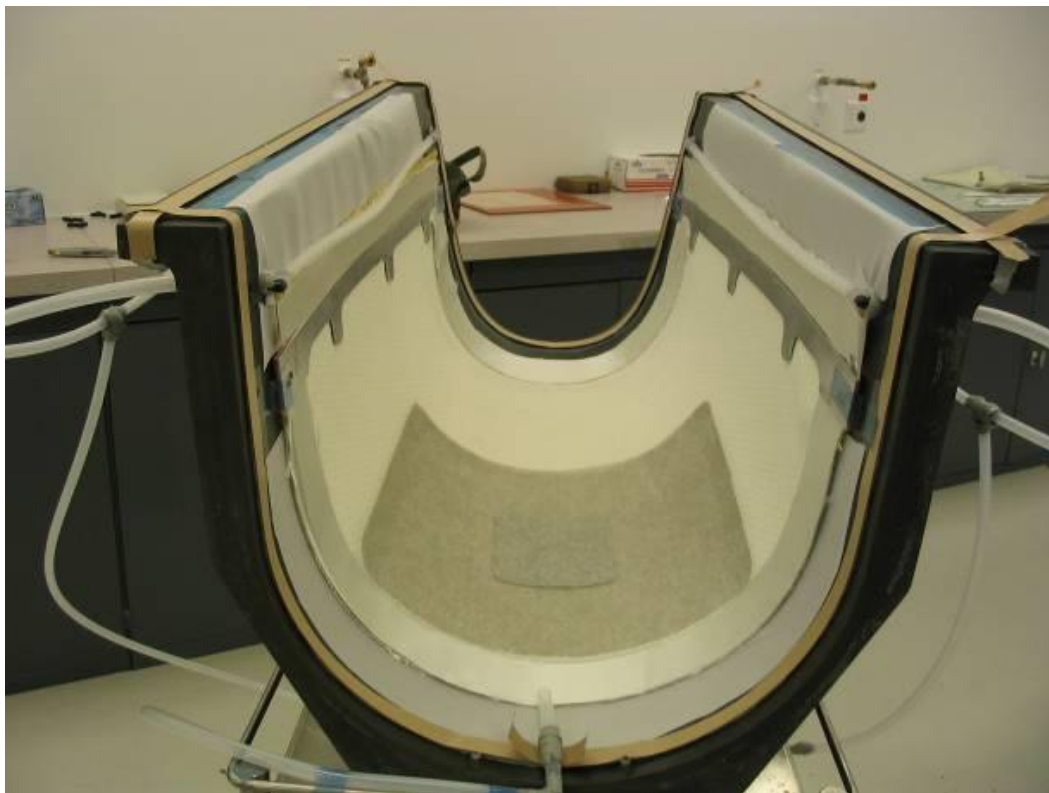


Figure 15. Part design for T-38 dorsal cover.

The Air Force F-22 program office came to the ACO and requested that this office design and build a prototype of an F-22 canopy cover. The program office requested the canopy cover prototype because the aircraft has to deal with various rugged environments throughout the world, which damage the canopy. The F-22 canopy is made up of multiple materials stacked in layers, which gives the jet the capability of being undetectable by enemy radar. These layers are very thin films and coatings that are very sensitive to any outside influence. These layers can be damaged by the elements and prevent the aircraft from being able to maintain maximum stealth capacity. Since the F-22 relies very heavily on its ability to be undetectable by radar, any degradation in this capability could significantly decrease mission effectiveness. Currently, the program office's biggest concern is the hazardous weather that comes with the jets being stationed at Elmendorf AFB, AK. Elmendorf AFB, in the city of Anchorage, AK, sees extreme cold weather conditions. These extreme cold weather conditions include ice, hail, strong winds, rain, sleet, and snow. These extreme weather conditions wreak havoc on the very thin, sensitive coatings of the canopy cover. Ice, the biggest concern, proves to be a problem when aircraft maintainers attempt to remove ice buildup from the canopy. The de-icing solution used on the rest of the aircraft to remove the ice also damages the coatings on the canopy. When the aircraft maintainers attempt to scrape the ice off the canopy, it damages the coatings as well. Intense heat could be used to melt the ice, but it is a long process in sub-zero weather, and if too much heat is concentrated on any one area of the canopy, it could damage the coatings on that area.

The F-22 program office thought the best way to protect the canopy was to place a cover on it, which would act as a barrier from the outside elements.

The ACO was approached by the C-5 program office at Warner Robins AFB and asked to develop a process for a rapid splash molding tooling system. This process was required to create a splash tool from any area of the aircraft, which could then be used to create a repair part. When an aircraft is damaged, a repair must be fashioned to get it back on flying status. Currently, the Warner Robins maintenance workers are using a hand layup technique to create the splash tool for the repair, which takes several days to a couple of weeks. When one aircraft is damaged, they have to create a splash tool off a non-damaged aircraft. This process grounds the non-damaged aircraft until the splash is made. This grounding of a flight-capable aircraft for such extended periods of time has a severe negative impact on the operational capability of the flying unit.

The impact to operational capability spurred the need for a quicker splash tooling process in order to get both aircraft back on flying status much quicker. Some of the areas on which the splash must be made, underneath a wing or on a vertical tail, can be very difficult for a hand layup process due to the effects of gravity pulling the fiber pack away from the surface. The hand layup method currently used by the maintainers involves placing 2–3 plies (layers) covered with resin on at a time, letting them cure, and repeating the process until they get the desired tool thickness (usually 20–30 plies). It can take a whole day for each of these 2–3 ply sections to fully cure and be ready for the application of the next section. This cure time causes the entire process to be very slow and inefficient. A quicker process would not only save maintenance time but allow the aircraft to fly more missions.

The ACO decided to explore producing molds using a VARTM process. This method is very beneficial due to its quick manufacturing time, good fiber compaction, and better fiber to resin ratio, which leads to increased mechanical properties and reduced weight. The ACO would design and develop a process and build a demonstration splash tool to show the effectiveness of the VARTM process.

The ACO was established at the Sacramento Air Logistics Center, McClellan AFB, CA, on July 25, 1983, at the direction of Headquarters U.S. Air Force. We are now an operating location of the U.S. Air Force Research Laboratory, Materials and Manufacturing Directorate, Wright-Patterson Air Force Base, located at the Ogden Air Logistics Center, (OO-ALC), Hill Air Force Base, UT.

The objectives of the ACO are the following:

- To establish a capability within the Air Force to apply advanced composites technology to the solution of aerospace and ground vehicle structural/service life problems.

- To transfer the knowledge and expertise in the use of advanced composites and the maintenance of existing advanced composite structures to Air Logistics Centers and operational commands throughout the Air Force. In this role, ACO is required to continually survey industry and academia to efficiently exploit advanced technology.

4.1.4 Navy Composite Rudder

NSWCCD developed the composite rudder as a solution to the cavitation problems that quickly cause severe damage to metallic rudders (figure 16). The far smoother composite design allows for much higher speeds before cavitation occurs. Furthermore, removal of paint during cavitation in metal systems accelerates corrosion rates to compound the problem, while this is not the case for composites systems that have negligible corrosion rates.



Figure 16. Photographs of cavitation damage on metallic straight rudder and metallic twisted rudder, which occur at lower speeds than the composite counterparts.

The composite twisted rudder (CTR) was designed to minimize cavitation/erosion problems associated with standard rudders (19) (figure 16). This rudder designs allow for even higher speeds before cavitation occurs (20). However, the twisted design is difficult to fabricate in steel, and the composite version weighs significantly less (20). The intent for this low-HAP rudder is to use it on DDG 103–109. If this rudder is successful for DDG, a similar design and the same materials will be used for future classes of ships. The seven DDG ships each have two rudders per ship. The composite laminate for each rudder weighs ~6000 lb including foam core, steel sub-structure, and rudder stock. The composite laminate for DDX (a future class of ship that was cancelled) rudder was projected to weigh ~10,000 lb.

The technology for manufacturing composite rudders to date has been targeted specifically at MCM ship applications. Cost analysis performed has shown that the acquisition cost of the composite rudder is potentially less than that of the traditional nickel-aluminum-bronze rudder. However, the benefits of composite rudders go far beyond cost factor. The 50% reduction in rudder weight that has been achieved (from 5772 lb to 2820 lb) impacts the trim of the vessel,

which allows for removal of unnecessary ballast from the bow and facilitates water drainage which, in the past, has had a deleterious effect upon the wooden deck structure. Furthermore, reduced weight also translates into reduced fuel consumption. Reduction in metal components further reduces not only the magnetic signature but also the electrical signature, which is of utmost importance to the survivability of an MCM.

Although the structural demonstration for this effort was a rudder for an MCM, of which there is a limited production run, success with the installation and demonstration of the structural performance of this system could provide the Navy with an alternative environmentally friendly resin system for similar applications. This resin could then be simply transitioned to DDG rudders and future DDX rudders. DDG and DDX applications are significantly larger than the MCM rudder and could have a larger environmental impact if the conventional resin system is utilized.

The two MCM rudders were installed on the Pioneer (MCM-9) for at-sea evaluation. The program office is targeting replacement of the nickel aluminum bronze rudders on the other 13 MCMs. This has not occurred due to funding issues. PMS 490, John Edwards, reported that “the composite rudder on MCM-9 is looking good after 5+ years on the ship.” He would like all MCM class rudders to be the same composite design. Steel cannot be used for this application since the rudder must be nonferrous for magnetic signature concerns.

The part design for the MCM composite rudder entails an elegant wrapping process around the central hub. The fiber used is E-glass 5SW 1810 fabric.

The NSWCCD consists of ~3800 scientists, engineers, and support personnel working in more than 40 disciplines ranging from fundamental science to applied/in-service engineering. We are the Navy’s experts for maritime technology. Headquartered in West Bethesda, MD, the division houses world-class facilities and laboratories. A major operating site in Philadelphia is recognized as the center for naval machinery. The division also conducts research and development at several remote sites across the country.

As a major component of the Naval Sea Systems Command, the Carderock Division provides cradle-to-grave support for its technical products over an enormous range of scientific areas related to surface and undersea platforms. The division addresses the full spectrum of applied maritime science and technology, from the theoretical and conceptual beginnings through design and acquisition to implementation and follow-on engineering. This includes all technical aspects of improving the performance of ships, submarines, military water craft, and unmanned vehicles, as well as research for military logistics systems. In addition, the division is uniquely chartered by Congress to support America’s maritime industry.

The mission of the Carderock Division is to provide the following:

- Research, development, test and evaluation, fleet support, and in-service engineering for surface and undersea vehicle hull, mechanical, and electrical (HM&E) systems and propulsors,
- logistics research and development, and
- support to the Maritime Administration and maritime industry.

4.2 Present Operations

The low-HAP VE resins are intended to replace high-HAP VE resins used or considered for use on Army tactical vehicles, the Marines helmet hardtop, the T-38 dorsal cover, F-22 canopy cover, splash molds, and the MCM composite rudder currently used or being proposed for use. SMC composites for HMMWV hoods are currently being used, have poor performance, and produce large amounts of styrene HAP during production. The VARTM HMMWV hood is in production from TPI Composites (in an expanded-capacity vehicle HMMWV variant) but still contains a high HAP content in the resin. The M35A3 and M939 composite hoods are being produced by Sioux Manufacturing Corporation but use a high-cost epoxy resin for these parts. The HMMWV transmission container is not currently in production from any company, but the original CCM design specifies a high-HAP VE resin. The original T-38 dorsal replacement cover is a hand layup UPE resin, glass-reinforced composite. The resin is a high-HAP UPE, but this part is no longer produced. Therefore, current parts are repaired by machining and hand tooling. The VARTM T-38 dorsal cover recently designed by the ACO uses a high-HAP VE resin. If not for the FAVE resins, high-HAP resins would likely be used for the production of F-22 canopy covers and splash molds. The MCM composite rudder was produced by Structural Composites, Inc., for a single MCM ship. The resin used is a high-HAP VE resin.

4.3 Site-Related Permits and Regulations

4.3.1 Environmental Checklist

These low-HAP composite resins are very similar to commercial composite resins. API, CCM, RRAD, the U.S. Air Force (AF), NSWCCD, Drexel, and ARL currently use commercial VE resins. As a result, most aspects of working with these resins were not affected. All sites added the FAVE resins to their approved materials list before implementation. The use of these resins, as with all operational chemicals, was governed by each site's pollution compliance permit and policy. The FAVE resins still contain HAPs and therefore are regulated under the Reinforced Plastics Composites NESHAP. However, since this NESHAP does not currently apply to existing facilities and military installations, it has no direct implications.

4.3.2 Other Regulatory Issues

Production of the FAVE resin at API or other resin suppliers requires the reactant glycidyl methacrylate, which is toxic. Facilities that produce this resin require toxicity clearances. Production of BMVE resin at API or other resin suppliers requires the use of methacrylic acid,

which is a highly corrosive material and also requires clearances and special equipment for the company manufacturing this resin. Besides the NESHAPs and possibly the Defense Land Systems for Miscellaneous Equipment, there are no other known regulations that apply to these materials.

4.3.3 End-User/Original Equipment Manufacturer Issues

The end users of these low-HAP composite resins include the Army depots, Air Force depots, Navy shipbuilding companies, and original equipment manufacturers (OEMs) for the DOD. More specifically, RRAD is interested in using this resin to make composites for repair and replacement parts of Army tactical vehicles. NSWCCD is interested validating this resin for rudder applications and would make this the approved resin for Navy manufacturing companies, such as SCI. OO-ALC would use this resin to repair and make replacement parts for legacy systems, such as the T-38. Other interested parties include the EPA for environmental reasons; contact information is as follows:

- Mr. Michael Kosusko, EPA, ph: 919-541-2734, kosusko.mike@epa.gov.

In addition, people are interested in this resin for naval applications; contact information is as follows:

- Mr. Ian Hawkins, NADEP Jacksonville, ph: 904-542-4516 x139, ian.hawkins@navy.mil.

These demonstrations should show all interested parties whether these low-HAP resins can truly be used as drop-in replacements for commercial resins while maintaining high performance and low cost. The rigorous property and performance testing as well as cost analysis should adequately validate this technology.

This effort did not scale-up resin production to large commercial scale. However, we were actively pursuing companies to license this technology. Scale-up issues were addressed in this demonstration and should show its simplicity. However, it is unlikely that commercially available materials were available at large scales at the end of this demonstration. This demonstration has convinced resin suppliers that there is a market for this resin, and thus Dixie Chemicals has licensed this technology for commercial resin production. However, until Dixie proves that there is substantial commercial market for this resin, it will not produce the resin in significant quantities.

The technology was customized for this demonstration in a manner similar to commercial composite resins. Most composite resins have a standard inexpensive version of their resin and variations that give better mechanical or higher thermal properties. Our demonstration did the same and aided in commercialization of the technology. This demonstration involved working with various OEMs, including CCM, Sioux Manufacturing, and Structural Composites, Inc. These demonstrations allowed these companies to gain firsthand experience with the resin and allowed them to decide for themselves whether the resin is a good, environmentally friendly

alternative to their current resins. The technology met their specifications and thus should ensure that technical data packages for the parts include these low-HAP resins as qualified products. In addition, the military partners will do what they can to change specifications mandating the use of this resin.

5. Test Design

5.1 JTP Testing and Laboratory Experimentation

5.1.1 Testing and Evaluation Plan

For Army applications, once adequate data have been generated by the initial screening tests, the data are used to down-select the demonstration articles and resin to be used for further study. For the other applications, basic resin and some composite testing was done to determine whether the FAVE-L resin has sufficient performance. If not, other resin systems were used (figure 7). All demonstrations continued with a combination of analysis (based on the measured properties and properties that were developed in the second stage of testing) and processing trials of both subcomponents and/or full-scale articles. For the ballistic hardtop, subcomponents were built to check and validate the properties rather than building the full-scale article due to the cost of the materials and tooling. In the case of the other demonstrations, infusion trials were performed on smaller parts before making the full-scale part.

The process trials were used to ensure that the process is scalable using the low-HAP resins. These process trial articles were used for full-scale testing to validate the performance of the resin. The testing performed was determined by the choice of the demonstration components. Vehicle hoods were tested initially on the same fixture used at CCM for validation of the hoods developed under the body parts program. This included ball drop and impact tests, flexural loading simulating a soldier on the hood surface (both static and fatigue), flexural loading of the corners of the hood or lifting of the hood to open/close, and in the case of the HMMWV hood, simulated quasi-static crash testing. For the transmission container, stacking loading, drop testing, and impact testing were performed. The full-scale composite rudder and dorsal cover were not tested using any machinery. Instead, they were field tested, and their performance was compared to standard resin systems.

Data collected were used to compare the performance of the new resins to the current materials used in these applications. This assessment included the appropriate cost studies to validate the assumptions and approach used in the proposal to develop the cost-benefit analysis.

The experiment design was the same for the Army, Marines, Navy, and Air Force demonstrations. Figure 17 illustrates the experimental design. Resin was produced by API. Drexel and ARL performed quality control experiments to ensure the resins produced meet the

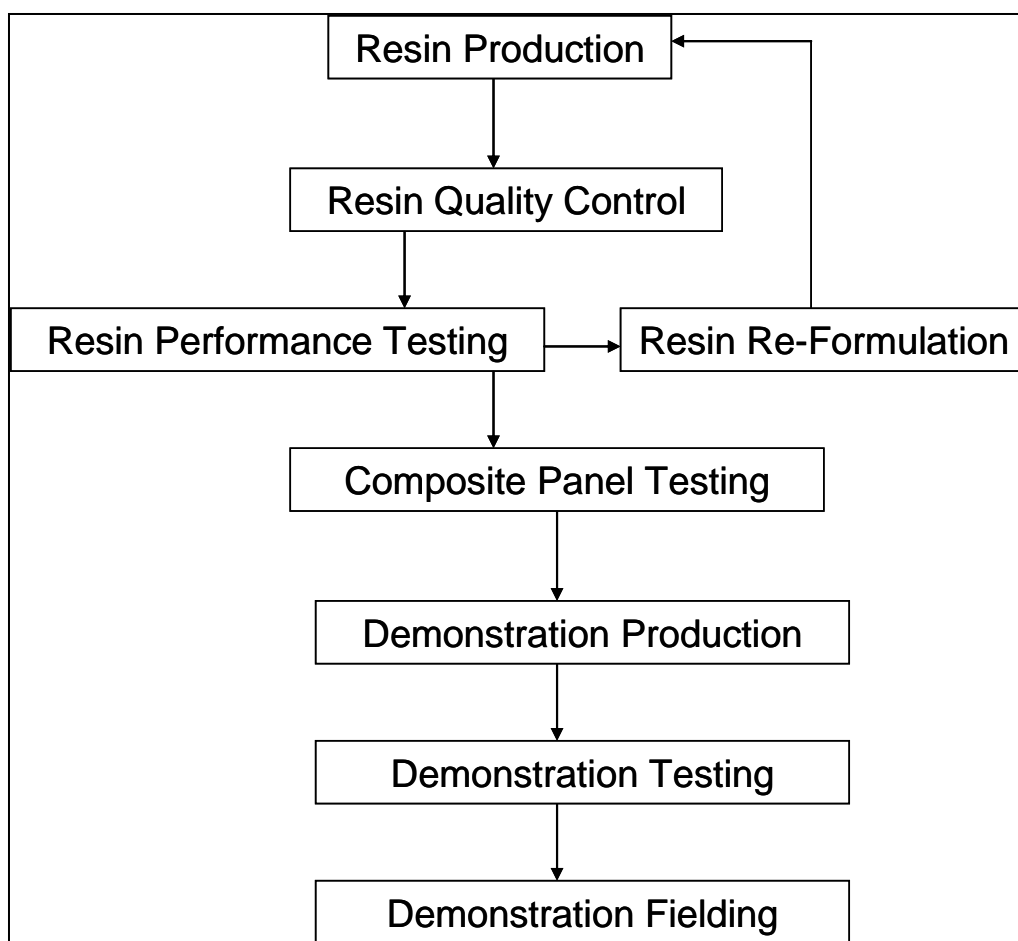


Figure 17. Demonstrator/validation process design for FAVE resins used in DOD composite applications.

required specifications. These tests involve ASTM acid number testing, rheometer viscosity testing, and NMR/FTIR chemical analysis. Furthermore, basic resin properties were measured using dynamic mechanical analysis (DMA) and Instron mechanical tests. If the properties were not high enough for a given application, resin variables were adjusted. These resin variables included using different VE type (novolac vs. bisphenol A), different fatty acid chain length, and different resin composition (VE/MFA/styrene ratios).

For a given resin chemistry, composite panels were prepared and tested. Initially, infusion trials were done to ensure good resin flow and adequate gel time. After that, various ASTM testing was performed on the composite panels to ensure the properties are similar to commercial resin-based composites. If not, the resin formulation was adjusted, and additional composite testing was run to ensure compliance. Most of the variables in terms of resin and composite performance were set at this point.

After successful composite panel trials, demonstration articles were fabricated based on the ideal resin composition previously found for the particular demonstration article. Resin infusion was

observed during fabrication of the demonstrations. In the case of the Army demonstration, various testing of the completed part will ensue using a specially designed testing apparatus. The Army and other demonstration articles were fielded. Inspection of the parts after fielding was done using DOD personnel and the PIs of this project.

5.1.2 MFA and FAVE Resin Manufacture

There are two manufacturing elements regarding FAVE resin manufacture—MFA manufacture and resin blending. Both elements were performed by API under the guidance of ARL/Drexel. The manufacture of MFA must be able to be simply performed by API at the scale of 1–55 gal. The reactants and additives must be able to be blended effectively, easily, and reproducibly. The blending of the resin components (MFA, commercial VE resins, and pure VE monomers) must be able to be done effectively, easily, and reproducibly. As API is not batch testing each resin, their observations were strictly qualitative. They will (in particular) comment on poor mixing of components, difficulty in reaction control (temperature, viscosity), difficulty in blending components, and poor mixing of resin components.

5.1.3 JTP MFA and Resin Batch Testing

Each batch of MFA and resin manufactured by API was batch tested by ARL/Drexel. The quality control of resin scale-up was tested using a set of five tests, as described in the JTP. ASTM D 1980 was used to access the acid number of MFA monomers and resins. This test will determine if there is too much free acid remaining in the system, which would indicate incomplete conversion of the reactants into the MFA and VE monomers. FTIR testing as described in La Scala et al. (8) was used to determine the presence of unreacted epoxy groups. Unreacted epoxy groups indicate incomplete conversion of the reactants in the MFA and VE monomers. NMR as described in La Scala et al. (9) was used to determine various chemical aspects of the resins. First, the quantity of unreacted epoxy groups was measured. The ratio of methacrylate groups to VE or MFA monomers was quantified. Also, the molar ratio of VE to styrene in BMVE resins or VE/MFA/styrene in FAVE was quantified. A rheometer was used to measure this viscosity of the MFA monomers and low-HAP resins at 25 °C (8, 9). Too high of a viscosity indicates side reactions occurred that degrade the resin properties and processability. SEC as described in La Scala et al. (9) was used to determine the content of high molecular weight species in the MFA monomers, FAVE resins, and BMVE resins. Lastly, the gel time of the resin was adjusted from 15 min to 4 h by varying the initiator, catalyst, and inhibitor contents. Being able to adequately adjust the gel time is important for creating parts of different sizes.

5.1.3.1 Acid Number Testing. Acid number titration was used during the course of the reaction to measure the amount of free (unreacted) acid in the VE system. The acid number tests were performed in accordance with ASTM D 1980-87. Approximately 1 g of the sample is dissolved in 5 g of acetone. Three drops of 0.5 weight-percent phenolphthalein in 50% ethanol is added to

the mixture to determine the neutralization point. The solution is then titrated with 0.5 N of sodium hydroxide until the solution remains slightly pink in color for 30 s. The acid number is

$$\text{Acid number} = V N \text{ MW}_{\text{NaOH}}/m, \quad (1)$$

where V is the volume in milliliters of NaOH solution used, N is the normality of the NaOH solution, and m is the VE mass in grams. Table 8 lists the testing and acceptance criteria.

Table 8. Acid number criteria for MFA and low-HAP resins.

Number and Type of Specimens per Candidate Alternative	1
Trials per Specimen (if needed)	1
Experimental Control Specimens	1 per batch of 0.5 N NaOH – acid number of known VE sample
Acceptance Criteria	Acid number <20 (MFA monomers) Acid number <5 (MFA resins) Acid number <15 (BMVE resins)

5.1.3.2 Viscosity. This test was designed to measure the viscosity, or resistance to flow of the monomer or resin at a particular temperature. The viscosities of the resins were measured using a Brookfield digital viscometer in Couette geometry (i.e., concentric cylinders) or a TA Instruments AR2000 rheometer in steady shear flow experiments. For the Brookfield viscometer, ~8 ml of the sample is placed into the sample holder. Spindle 21 is used in all cases because of its large diameter of 1.5 cm, which allows the measurement of the low viscosity samples. Because this viscometer provides more reliable numbers when the torque applied is near the middle of the instrument's range, the shear rate is varied, depending on the sample viscosity, to do this. As a result, the rotation rate is typically varied from 2.5 to 100 rpm, depending on the sample viscosity. All samples are run at 25 °C. For the TA rheometer, an ~1-mL sample is placed in between parallel plates with a gap spacing of 1000 µm. The temperature is equilibrated at 25 °C, and the shear rate is increased from 1 to 3000 s⁻¹ and then decreased back to 1 s⁻¹, and 10 measurements were taken per decade. At a given shear rate, the shear stress is measured every 2 s. The shear rate and viscosity are recorded when the shear rate stabilizes to within 5% tolerance for three consecutive points. The viscosity is recorded for the range where viscosity is independent of shear rate. Table 9 lists the testing and acceptance criteria.

Table 9. Viscosity criteria for MFA and low-HAP resins.

Number and Type of Specimens per Candidate Alternative	1
Trials per Specimen (if needed)	1
Experimental Control Specimens	1 silicone viscosity standard sample every 30 days to ensure consistency of data
Acceptance Criteria	Viscosity <80 cP (MLau) Viscosity <70 cP (MOct) Viscosity <1000 cP (FAVE and BMVE)

5.1.3.3 Fourier Transform Infrared Spectroscopy. This test was designed to determine if there is unreacted epoxy in the monomers or resins. Unreacted epoxy indicates the reaction is not complete or side-reactions occurred. Either one will degrade the resin performance. Furthermore, unreacted glycidyl methacrylate (GM) in the MFA monomer increases the toxicity of the resin. FTIR and near-IR were used to measure the concentration of unreacted epoxides and attached methacrylate groups. A Thermo Nicolet Nexus 670 FTIR was used in absorbance mode, taking 16 scans per spectrum with a resolution of 4 cm^{-1} . The raw FTIR spectra of completely reacted monomers shows that the peaks representing the epoxide groups (6066 , 4530 , and 917 cm^{-1}) are no longer visible after reaction, and methacrylate groups (6160 and 942 cm^{-1}) are present in the resin (21, 22). Interference with other peaks prevents determining the extent of reaction over 95% conversion. These results indicate whether the epoxide groups react to near completion with methacrylic acid. Table 10 lists the testing and acceptance criteria.

Table 10. FTIR criteria for MFA and low-HAP resins.

Number and Type of Specimens per Candidate Alternative	1
Trials per Specimen (if needed)	1
Experimental Control Specimens	None are necessary
Acceptance Criteria	No epoxide groups present

5.1.3.4 Nuclear Magnetic Resonance Spectroscopy. This test is designed to determine if there is unreacted epoxy in the monomers or resins, the molecular weight of the VE monomer, the reactant ratios in the MFA monomers, and the component ratios in the resin. Unreacted epoxy indicates the reaction is not complete or side-reactions occurred.

NMR was run on the prepared VEs and commercial VE resins to verify the extent of methacrylation, styrene content, epoxide content, VE molecular weight, and component ratios. A Bruker 600 MHz spectrometer with spectral window of $\pm 2000\text{ Hz}$, 16 scans at 293 K, and 90° pulse width was used. The method used to analyze the VE is described in the literature (5, 9). The internal standards for VE are the four methylene protons and the six methyl protons of the methacrylate groups per VE. The area per proton for these standards should be in agreement.

The value of n for the VE was calculated based on the area of the $5n+10$ isopropyl protons, the $8n+8$ phenyl protons, or the $6n+6$ DGEBA methyl protons. These values of n resulting from all three standards should always be within 3% error. In addition, the calculated values of n should always be within experimental error of the values calculated using epoxy titration. The styrene content is calculated by measuring the relative area of the styrene methylene protons (5.2 and 5.8 ppm) to the internal standards. The extent of methacrylation is determined by measuring the height of the three epoxide peaks at 3.33, 2.88, and 2.73 ppm relative to the heights of the phenyl protons and the DGEBA methyl protons before and after methacrylation. Epoxide peaks appear at 2.6–3.3 ppm. The ratio of GM methyl methacrylate groups (three protons at 1.9 ppm, one

proton at 5.5, and one proton at 6.1 ppm) to fatty acid groups (three at 0.9 ppm, two at 1.6 ppm, and two at 2.3 ppm) should be 1 to 1. Table 11 lists the testing and acceptance criteria.

Table 11. NMR criteria for MFA and low-HAP resins.

Number and Type of Specimens per Candidate Alternative	1
Trials per Specimen (if needed)	1
Experimental Control Specimens	None are necessary
Acceptance Criteria (Unreacted Epoxy)	No epoxide groups present
Acceptance Criteria (VE MW)	VE MW <700 g/mol (bisphenol A) VE MW <900 g/mol (Novolac) VE MW <800 g/mol (BMVE)
Acceptance Criteria (MFA Reactant Ratios)	Methacrylate to FA ratio of 1:1 (+0.05, -0.1)
Acceptance Criteria (FAVE Component Ratios)	VE to MFA to styrene ratio should be $\pm 5\%$ based on desired formulation
Acceptance Criteria (BMVE Component Ratios)	VE to styrene ratio should be $\pm 5\%$ based on desired formulation

5.1.3.5 Size Exclusion Chromatography. This test is designed to determine the molecular weight of VE monomers and component ratios in the VE resins. SEC was run on styrene and the VE resins to determine VE molecular weight and styrene content in the bimodal blends. A Waters 515 gel permeation chromatography (GPC) is used with two 30-cm-long, 7.5-mm-diameter, 5- μ m-styrene-divinyl benzene columns in series. The columns were equilibrated and run at 45 °C using tetrahydrofuran (THF) (Aldrich) as the elution solvent at a flow rate of 1 mL/min. The column effluent was monitored by two detectors operating at 25 °C—a Waters 2410 refractive index detector and a Waters 2487 dual absorbance detector operating at 270 and 254 nm (absorbed by phenyl rings). Samples were prepared by dissolving 2 mg of sample in 1-mL THF.

Because high molecular weight species cannot diffuse into the packing, they elute first from the column, while lower molecular weight species elute later (23, 24). Therefore, the molecular weights can be determined from the peak elution time. To measure the molecular weights of VE resins using SEC, the molecular weight as a function of retention time was calibrated using Epon resin samples (9). The number average molecular weight of the Epon 100XF resins is known through epoxy titration results. The calibration curve relating peak retention time to Epon molecular weight was constructed and used to calculate the number average molecular weights of the VE peaks. For the bimodal blends, the relative areas of the peaks and the two different number average molecular weights were used to simply calculate the number average (M_n) and weight average molecular weights (M_w) (equations 2 and 3) as follows:

$$M_n = \frac{n_{high}M_{high} + n_{low}M_{low}}{n_{high} + n_{low}}, \quad (2)$$

and

$$M_w = \frac{n_{high}M_{high}^2 + n_{low}M_{low}^2}{n_{high}M_{high} + n_{low}M_{low}}. \quad (3)$$

where the subscripts *high* and *low* refer to the high and low VE molecular weight species/peak, respectively, *M* is the molecular weight as determined by the Epon calibration, and *n* is the number of moles. In addition, previous work has shown that if a significant amount of epoxy homopolymerization occurred, a broad peak appearing at 10 min and lower elution times would appear (24). Table 12 lists the testing and acceptance criteria.

Table 12. SEC criteria for MFA and low-HAP resins.

Number and Type of Specimens per Candidate Alternative	2
Trials per Specimen (if needed)	1
Experimental Control Specimens	None are necessary
Acceptance Criteria (Unreacted Epoxy)	No epoxide groups present
Acceptance Criteria (VE MW)	VE MW <700 g/mol (bisphenol A) VE MW <900 g/mol (Novolac) VE MW <800 g/mol (BMVE)
Acceptance Criteria (FAVE Component Ratios)	VE to MFA to styrene ratio should be $\pm 5\%$ based on desired formulation
Acceptance Criteria (BMVE Component Ratios)	VE to styrene ratio should be $\pm 5\%$ based on desired formulation

5.1.3.6 Gel Time. This test is designed to determine the working time of the resin before it solidifies into a gelatinous solid that no longer flows, and therefore cannot further wet fiber reinforcement in composites. Samples were prepared according to ASTM 2471-99.

Samples are prepared by pouring 10 g of resin into a 30-mL screw-cap scintillation vial. Initiator breakdown was catalyzed using 0.1 weight-percent cobalt naphthenate and 1 weight-percent Trigonox to cure the samples. Various samples were prepared using various contents of these initiator, catalysts, and inhibitor. In all cases, inhibitor was added first. After mixing, catalyst was added. The samples were tested at an ambient temperature of 72 °F. The 10-g sample of resin was maintained at this temperature until gelation. The sample was probed every 15 s with an applicator stick in the center of the material. When the resin no longer flowed to fill in the void left by the applicator stick, the sample was considered gelled. The gel time was the duration of time that elapsed between mixing in of initiator until gelation occurs. Table 13 lists the testing and acceptance criteria.

Table 13. Gel time criteria for MFA and low-HAP resins.

Number and Type of Specimens per Candidate Alternative	2
Trials per Specimen (if needed)	1
Experimental Control Specimens	Commercial Derakane 441-400
Acceptance Criteria (Fast Gel Time)	Gel time ≤ 15 h
Acceptance Criteria (Slow Gel Time)	Gel time ≥ 4 h

5.1.4 Neat Resin Testing

Neat resin properties were assessed in a variety of laboratory tests to ensure quality of the resin prior to making composite parts. The FAVE resins should have properties similar to the incumbent resins. This testing is applicable to all demonstration/validation platforms.

5.1.4.1 Styrene Content by Evaporative Weight Loss – Macro-Scale. Approximately 10 g of each resin were mixed in a closed container with 10 g of MFA. MLau was added to prevent the epoxy resin from forming a surface skin that would limit the evaporation of styrene. The combined mixture was then poured into an open beaker and allowed to evaporate in a vented hood for 15 days. They were then moved to a 45 °C oven to evaporate for an additional 5 days. Beakers were periodically weighed, and evaporative loss was calculated. All evaporative loss was attributed to loss of styrene from the Derakane portion of the mixture. The styrene weight-percent loss was calculated based using equation 4 as follows:

$$\frac{\text{Evaporative Mass Loss}}{\text{Original Derakane Mass}} \times 100 = \text{Styrene Weight \% Loss} \quad (4)$$

Figure 18 shows the weight loss for baseline samples. The overall weight loss levels off in ~2 weeks, and the overall styrene content matches the known amount in the commercial VE resin. Therefore, this method is acceptable for measuring the styrene weight loss.

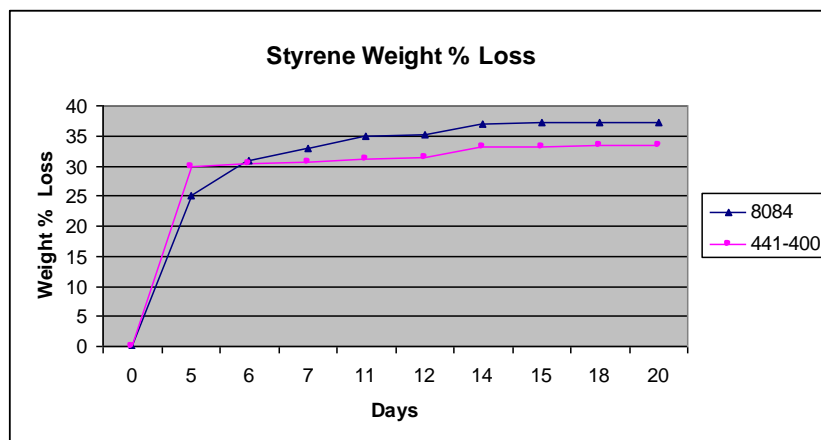


Figure 18. Graphical representation of the styrene weight-percent loss over a 20-day period for both Derakane 8084 and 441–400 epoxy VE resins.

5.1.4.2 Resin Viscosity. The resin viscosity was measured as described above for measuring the MFA viscosity. Target viscosity was <1000 cP for all resins.

5.1.4.3 Gel Time Variance of FAVE. The ability of the gel time to be varied from very short to very long was measured by using a variety of initiator package components and concentrations and temperatures. The gel times were then measured as previously described.

5.1.4.4 Resin Cure. All resins were initiated using methyl ethyl ketone peroxide (MEKP) and a 4:1 ratio of 6% cobalt naphthenate (CoNap) and N,N-dimethylaniline (N,N-DMA) as a catalyst to promote room temperature cure. Hydroquinone (HQ) inhibitor is used to increase the gel time. The exact amount of initiator, catalyst, and inhibitor concentrations used depend on the desired gel time. All resins were allowed to cure at room temperature for 16 h. Various samples will also be post cured at 130 °C for 3 h.

5.1.4.5 Dynamic Mechanical Property Testing. The thermo-mechanical properties of VEs were measured using DMA. Rectangular samples with approximate dimensions of 25- × 9- × 3-mm were tested using a TA Instruments 2980 DMA in single cantilever geometry. The samples are tested at 1 Hz with a deflection of 15 µm while ramping the temperature from 30 to 200 °C at a rate of 2 °C/min. Two temperature ramp experiments are run for each sample. The first ramp completely post-cures the polymer.

The temperature at which the peak in the loss modulus occurs in the fully post-cured polymer is considered the glass transition temperature of the material (25). The experimental error in T_g is ± 3 °C. The point at which the modulus in the rubbery plateau begins to increase with increasing temperature is used to calculate the molecular weight between cross-links, M_c . The theory of rubber elasticity is used to calculate M_c (equation 5) as follows:

$$E = 3RT\rho/M_c, \quad (5)$$

where E is the rubbery modulus, R is the ideal gas constant, T is the absolute temperature, and ρ is the sample density (26, 27). Rubber elasticity applies to polymers with low cross-link densities and would not be expected to give completely accurate cross-link density measurements for highly cross-linked VE systems. However, the calculated numbers are on the correct order of magnitude based on cross-link density calculations and provide a means for comparing and quantifying whether one sample is more cross-linked than another.

Samples were tested dry and wet. Dry samples were tested after curing/post curing the DMA samples. Wet samples were prepared by placing the samples in water or in a controlled humidity environment until the sample is saturated (weight stays constant with further exposure time). Samples in water were placed in water at room temperature for weeks. Samples were also placed in 95 °C water for 24 h to more quickly achieve a saturated sample. Both methods resulted in similar water uptake and similar wet DMA properties.

Wet samples for Navy applications were prepared by saturating polymer samples in water at 30 °C for 2 weeks. The samples were removed and their surface was dried for testing. The samples were placed in an 80% humidity box until testing. Wet T_g testing for Army applications involves maintaining the polymer samples for 2 weeks at 60% relative humidity prior to testing.

5.1.4.6 Flexural Testing. Flexural tests, in accordance with ASTM 790M, were performed to determine the modulus of elasticity and flexural strength. The samples will have approximate dimensions of 10- × 80- × 64-mm and were measured prior to testing. The samples were tested flat-wise on a support span, resulting in a support-to-depth ratio of 16. All tests were performed at ambient conditions. The samples were tested using an Instron at a crosshead speed of 0.17 mm/min. The flexural modulus, elongation at failure, and flexural strength were calculated according to the ASTM standard.

5.1.4.7 Fracture Toughness Testing. Three-point single-edge notch bend (SENB) specimens were used for fracture toughness measurements. ASTM 5045-93 specifies that approximate sample dimensions of 2.00 × 0.50 × 0.25 in should be used to assure plain strain conditions. A notch was placed in the samples equal to half the sample depth. The actual sample dimensions were measured after testing so that the notch length could be accurately measured. A sharp razor blade was used to initiate a crack at the base of the notch. The samples were tested using an Instron 4505 or equivalent in flexural mode at a crosshead speed of 0.05 in/min. An un-notched sample was run in the same manner twice during the course of the experiment to account for system compliance, loading pin penetration, and sample compression. All tests were performed at ambient conditions, which were ~22 °C and 40% relative humidity. When tests were completed, the fracture specimens were examined for signs of plastic deformation. If plastic deformation was apparent, the sample was not used in the reported results.

5.1.5 Composite Panel Testing

5.1.5.1 Composite Resins and Fibers for Panels and Demonstration Articles. Selection of the fiber and resin systems for a particular DOD application is summarized in table 14. Various Army applications focus on Hetron 980/35 (higher T_g with 35 weight-percent styrene) and Derakane 8084 (a rubber-toughened resin with improved fracture toughness properties and 40 weight-percent styrene) with Mahogany 24 oz/yd² E-glass, 5 × 4, woven roving and 3TEX, Inc., 96 oz/yd² 3WEAVE E-glass with 2022 silane sizing (P3W-GE044). Bio-resin replacements for the Derakane resins include FAVE-L/O-25S (manufactured with methacrylated lauric or octanoic acid with 25 weight-percent styrene) and FAVE-L/O-HT (a novolac-based VE for higher temperature performance). The Marine HMMWV hardtop utilizes 3TEX, Inc., 54 oz/yd² 3WEAVE E-glass with 2022 silane sizing (P3W-GE045) with Derakane 8084 and FAVE-O-25S. The Air Force application for the T-38 dorsal cover and F-22 canopy cover utilize both Fibre Glast Developments Corp. Style 120 3 oz/yd² E-glass satin weave and Style 7781 9 oz/yd² E-glass satin weave fabric with Hexion Specialty Chemicals 781-2140 (with 47 weight-percent styrene). The Navy application for the composite rudder currently uses Fiber Glass Industries

18 oz/yd² unidirectional E-glass fiber tows with a stitched mat backing and Interplastic Corp. CoREZYN Corve 8100 (with 50 weight-percent styrene) with the proposed replacement resin FAVE-L-25S (manufactured with methacrylated lauric acid with 25 weight-percent styrene).

Table 14. Proposed applications for commercial VE and FAVE composites in the military.

Application	Fabric	Resin	Resin Replacement
Amtech helmet hardtop	3-TEX 100-oz S2-glass and 24-oz S2-glass	Derakane 8084	FAVE-L-25S/O-25S
HMMWV hood	3-D E-glass	Hetron 980-35	FAVE-L-HT/O-HT
M35A3 and M939 hood	3-TEX 96-oz E-glass	Hetron 980-35 (VE) or Huntsman 8605 (epoxy)	FAVE-L-HT/O-HT
Transmission container	3-TEX 54-oz E-glass	Derakane 8084	FAVE-L-25S/O-25S
T-38 dorsal cover and F-22 canopy cover	Fibre Glast Developments Corp. 120 3-oz E-glass and Style 7781 E-glass 9 oz	Hexion 781-2140	FAVE-L-25S/O-25S
Rudders	Fiber Glass Ind. 18-oz E-glass	Corezyn Corve 8100 and Derakane 510A-40	FAVE-L-25S

Rectangular composite panels were prepared for all tests using samples that conform to the layup (type, number of plies, and thickness) (e.g., M35A3 hood and HMMWV hardtop) they are being used to validate unless otherwise noted (see “Composite Demo” section). In some cases, such as the HMMWV hardtop where the configuration varies across the dimensions of the part, only panels with the geometries of the critical areas are made. The exact dimensions of each sample will conform to the ASTM or testing specifications according to the sample thickness. The three potential Army demos use only E-glass reinforcement, so all panels are tested with these fibers only using sample thicknesses equal to that of the M35A3 hood, which is about 0.25 in thick. Panels for Marines demonstration testing were 1 in thick. The panels were ~1/8 in thick for Air Force applications. For Navy applications, two panel thicknesses were made—3/8 and 3/4 in thick.

Composite panel properties were assessed in a variety of laboratory tests to ensure quality of the composite prior to making demonstration parts. The FAVE composites should have properties similar to the incumbent resins. This testing is applicable to all demonstration/validation platforms.

5.1.5.2 Infusion Trials. As composite panels are being made for testing, the flow of resin through these panels was studied. Time for infusion was measured and compared to standard resins. In addition, the duration for gelation to occur (i.e., amount of time available for the resin to flow through and fill the part) was measured. Therefore, gel time was measured during the infusion trials and compared to the desired gel time. Variances were noted and initiator/

catalyst/inhibitor content was adjusted to account for the difference. In addition, panels were examined for good fiber wet out. Essentially, all of the individual fibers that make up each tow should be coated with resin.

5.1.5.3 Dynamic Mechanical Property Testing. The thermo-mechanical properties of composite samples were measured using DMA. Rectangular samples with approximate dimensions of 25- × 9- × 3-mm were cut from the composite and tested using a TA Instruments 2980 DMA in single cantilever geometry. The samples are tested at 1 Hz with a deflection of 15 μm while ramping the temperature from 30 to 200 °C at a rate of 2 °C/min. Two temperature ramp experiments are run for each sample.

Wet samples for Navy applications were prepared by saturating composite samples in water at 30 °C for at least 2 weeks. The samples were removed and their surface thoroughly dried for testing. The samples were placed in an environmental chamber at 160 °F and 85% humidity. The samples were massed periodically until no mass change occurs. At that point, the sample is ready for testing. Wet T_g testing for Army applications involves maintaining the composite samples for 2 weeks at 60% relative humidity prior to testing.

5.1.5.4 Three-Point Bend Flexural Property Testing. In order to evaluate flexural properties, a three-point bending test following ASTM D 790-92 guidelines was performed for Army, Marines, and Navy demonstrations. The dimensions used for the testing were a depth range of ~0.125–0.150 in, a width of 1 in, and a l/d ratio of 32 to 1, as recommended by ASTM. The crosshead rate used is 0.33 in/min.

5.1.5.5 Tensile Property Testing. In order to evaluate tensile properties, a tensile test following ASTM D 638 guidelines was performed. This test is used to determine the tensile modulus (stiffness) and strength of the material.

5.1.5.6 Compressive Property Testing. In order to evaluate compressive properties for AF composites, a compressive test following ASTM D 695 guidelines was performed. The compressive test determined the compressive modulus and strength of the material.

5.1.5.7 Short Beam Shear/Interlaminar Shear Property Testing. The interlaminar strength of each composite system was tested following ASTM D 2344-84 for all demonstrations. It is important to point out that as stated in the ASTM standard, because of the variety of failure modes that can occur in this specimen, it is not generally possible to relate the SBS strength to any other material property. However, failures are normally dominated by interlaminar properties, and the test can be used for comparative testing of composite materials, provided that failures occur consistently within the same mode. Each specimen was subjected to a three-point bend, where the crosshead was lowered at a rate of 0.05 in/min until interlaminar failure occurs. Samples for Marines applications were 1-in-thick, dictating that the span of these tests should be 3 in, with an overall length of 6 in and a width of 1.5 in. Ten samples were tested for each

composite. Elevated temperature testing is performed in an environmental chamber compatible with Instron mechanical testing.

5.1.5.8 Four-Point Bend Static Sandwich Testing. The four-point bend static sandwich test was used to assess bending strength and modulus via ASTM D 6272-98. Samples tested were 16×4 in wide \times ~ 1 in thick. The fatigue properties were also measured using the same size specimens. The samples were fatigued at 5000 lb with $R = 0.1$ at 1 Hz.

5.1.5.9 Fiber Fraction and Void Content. The fiber, resin, and void fractions of the composites were measured using ASTM 2584. Resin and void content are measured by burning a composite sample at 565°C and measuring the mass loss. The fibers will not burn at that temperature, thereby giving a measure of the resin fraction. The fiber fraction was measured using equation 6 as follows:

$$V_f = \frac{d}{n_{plies} * \rho_f^a / \rho_f}, \quad (6)$$

where d is the sample thickness, n_{plies} is the number of plies of fiber, ρ_f is the fiber density, and ρ_f^a is the aerial density of the fiber plies. For glass fabric, the aerial density is $\rho_f = 2550 \text{ kg/m}^3$. The aerial density is usually supplied by the manufacturer but can be experimentally determined by dividing the mass of a ply by its area. Based on the expected fiber fraction and measured resin content, the void fraction can be determined.

5.1.6 Fatigue Testing

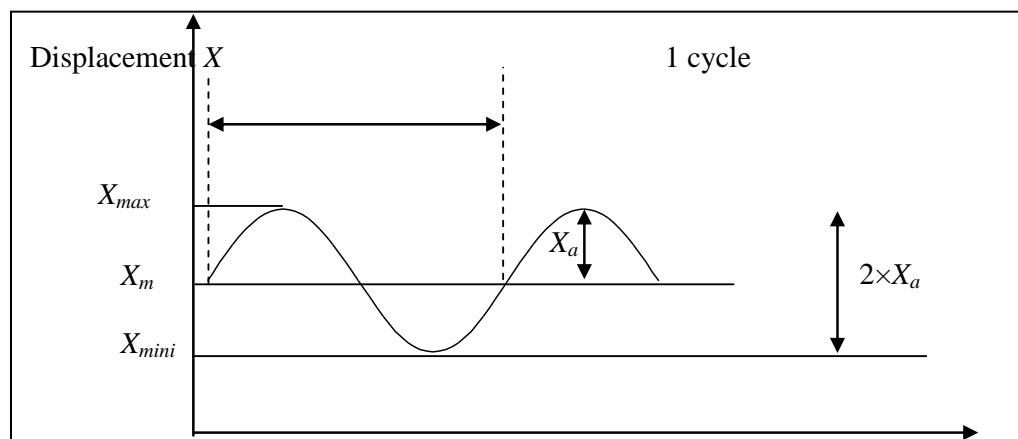
In principle, a fatigue test can be designed by exerting repetitive stress on the sample until the occurrence of failure. Normally, a full $S-N$ diagram (i.e., applied stress vs. the number of cycles applied prior to failure) can be recorded. The repetitive stress can be designed in three waveforms—sine, triangular, and square. It showed there was no difference for longer lives. Parameters like test frequency, mean condition, and applied amplitude, or alternatively minimum and maximum values, are also needed to be considered in association with corresponding waveforms.

Mechanical properties can be obtained mainly by two different categories of tests—flexural tests and axial tests. Correspondingly, in fatigue test design, displacement and load or strain control was applied, respectively. In this current case, the displacement control aiming to evaluate the flexural properties of polymer composites was utilized.

Several artifacts may affect the results of the fatigue test of polymer composites when using displacement control. Of them, one issue worthy of mentioning is rate dependence effects, which may induce self-generated heating. For polymer composites, rate dependence of the material properties themselves in the absence of the temperature effects is another concern.

Static three-point flexural tests were conducted following the ASTM D 790 for three-point bending. Five tests for each sample were given to determine the loading parameters for the fatigue tests.

As pointed out, there is no standard for the flexural fatigue testing of unidirectional carbon-fiber-reinforced polymer composites. The relevant parameters are illustrated in figure 19. All tests were performed using an Instron 8872 servo-hydraulic test machine.



Note: X_{max} = maximum displacement, X_{min} = minimum displacement, X_{mean} = mean value, and X_a = amplitude.

Figure 19. Illustration of sine waveform cycle.

In this design, the maximum displacement values were determined in correspondence to the maximum load of 80%, 60%, and 40% of the load value obtained by the static flexural tests. The stress ratios R , a ratio of minimum and maximum load ($\text{load}_{\min}/\text{load}_{\max}$), are critical parameters that have an influence on the fatigue behavior. Different R value scenarios can be identified in the International Organization for Standards ISO 13003. The range of the R value for the flexural fatigue test can be 0–1. The popular one is 0.1. In this case, R value close to 0 is applied. However, slight contact of load cell with sample is maintained by choosing the minimum load as 2 lbf in order to fix the position of specimen. The corresponding displacement can thus be determined based on this strategy.

In addition, 10,000 cycle tests were performed at a frequency of 1 Hz in order to minimize adiabatic heating effects, as well as the time and cost of undertaking a fatigue program. After the fatigue tests, static flexural tests were given to each specimen to determine the residual flexural strength and elasticity modulus. Consequently, the comparison of two samples under same conditions can be given. In this case, two specimens were tested for each design, and the values were averaged for the final results.

On the other hand, fatigue life was determined for flexural loading conditions. In the experiment design, R value close to 0.5 was applied. Moreover, the tests were conducted at a frequency of 4 Hz to reduce the test time. The 40% of the initial flexural load was applied to each test. After predetermined cycles, the residual flexural performance was measured.

5.1.7 Environmental and Chemical Aging

Environmental and chemical aging procedures conducted on the various composites were determined based on the anticipated exposure to environmental and chemical agents over the working lifetime of the composite parts (as summarized in table 15). None of the actual aging tests are exact applications of a standard test but rather are based on standard testing methods listed in test method standard MIL-STD-810F (environmental engineering considerations and laboratory tests) and consultation with ESTCP program partners. Duration and intensity of the exposure were chosen to demonstrate some decrease in mechanical and thermal properties over the period of aging. Environmental aging was performed on all commercial and FAVE composites and included wet T_g , freeze/thaw cycling, and xenon arc lamp weathering. Chemical aging included exposure to various chemical agents (method 504: Contamination by Fluids), which were selected as a hydro-carbon fuel (JP-8), a solvent (methyl ethyl ketone), and salt water exposure for the Navy composites exclusively.

Table 15. Relevant aging testing per application and proposed FAVE composite replacement.

Applications	Composites	Resin	Replacement Resin	Aging Tests	
HMMWV Transmission Container (ARMY)	Mahogany 24 oz E-glass/ Derakane 8084	Derakane 8084	FAVE-O-25S	Wet Tg Freeze/Thaw	Xenon Weathering Chemical-JP8
HMMWV Hood (ARMY)	24 oz/Derakane 441-400	Hetron 980/35	FAVE-O-25S	Not Tested	
M35A3 Hood (ARMY)	3TEX 3D weave 96 oz/Derakane 441-400	Hetron 980/35 (VE) or Huntsman 8605 (epoxy)	FAVE-O-HT	Wet Tg Freeze/Thaw	Xenon Weathering Chemical-JP8
Amtech HMMWV Hardtop (MARINES)	3TEX 3D weave 54 oz/Derakane 8084	Derakane 8084	FAVE-O-25S	Wet Tg Freeze/Thaw	Xenon Weathering Chemical-JP8
T-38 Dorsal Cover (AIR FORCE)	FibreGlast Style 120 3 oz E-glass/Hexion 781-2140	Hexion 781-2140	FAVE-O-25S	Wet Tg Freeze/Thaw	Xenon Weathering Chemical-MEK
T-38 Dorsal Cover (AIR FORCE)	FibreGlast Style 7781 9 oz E-glass/Hexion 781-2140	Hexion 781-2140	FAVE-O-25S	Wet Tg Freeze/Thaw	Xenon Weathering Chemical-MEK
MCM Rudder (NAVY)	Fiber Glass Ind. 18 oz E-glass uni stitch mat/Corve 8100	CoREZYN Corve 8100 and Derakane 510A-40	FAVE-L-25S	Wet Tg Freeze/Thaw	Simulated Salt water solution

5.1.7.1 Composite Layup. Composite panels were manufactured for all 12 composites using VARTM to provide samples for testing. The chemical cure package used included Condea Servo (CoNap) as a catalyst, Akzo Nobel TrigonoX 239A anti-foaming organic peroxide as an initiator, and EMD N,N – dimethylaniline and Avocado Research Chemicals Ltd. 2,4 – Pentanedione, 99% as an inhibitor. Gel time studies were performed for each resin using various weight-percentages of these chemicals to arrive at a gel time of ~1 h or less. Composite panels were laid up to a thickness required by the thickness to width and span ratios set forth in ASTM D 790 – 03 (standard test method for flexural properties of reinforced plastics) and ASTM D 2344/D 2344M – 00 (standard test method for the SBS strength of PMCs) and for all the composites did not exceed 4 mm. The layups and approximate thicknesses of the individual composites are listed in table 16.

Table 16. Composite layup, approximate thickness, and estimated fiber and matrix volume fraction for studied commercial VE and FAVE composites.

Composite	Lay-up	Thickness (mm)	V _f (%)	V _m (%)
3 oz/Hexion	32-ply; warp	~3.5	40.6	59.4
3 oz/FAVE-O-25S	32-ply; warp	~3.8	39.6	60.4
9 oz/Hexion	[0/90] _{3S}	~2.7	50.7	49.3
9 oz/FAVE-O-25S	[0/90] _{3S}	~2.6	59.8	40.2
18 oz/Corve 8100	[0/90] _S	~3.5	46.3	53.7
18 oz/FAVE-L-25S	[0/90] _S	~3.5	47.1	52.9
24 oz/Derakane 8084	[0/90/0] _S	~3.9	53.0	47.0
24 oz/FAVE-O-25S	[0/90/0] _S	~3.9	50.0	50.0
54 oz/Derakane 8084	2-ply; warp	~3	51.5	48.5
54 oz/FAVE-O-25S	2-ply; warp	~3	49.0	51.0
96 oz/Derakane 441-400	Single ply	~2.7	48.6	51.4
96 oz/FAVE-O-HT	Single ply	~2.7	47.9	52.1

5.1.7.2 Determination of Wet and Dry Glass Transition Temperatures. The Army HMMWV, M35A3, and M939 hoods, in addition to the Marine Amtech HMMWV hardtop, are all subject to dry and wet T_g requirements. To determine the wet T_g for the composites, DMA samples were cut for each composite and soaked in distilled, deionized water filtered using a Barnstead B-pure water purification unit for days until subsequent weighing of the samples demonstrated no further mass increase. The samples were then tested in a TA Instruments DMA Q800 with a dual cantilever geometry at 1 Hz; the T_g was determined from the peak of the loss modulus curve vs. temperature. Two temperature ramp runs were conducted on the wet T_g samples to ensure that the dry T_g values were recoverable.

5.1.7.3 Cyclic Freeze and Thawing Tests. Freeze/thaw aging was conducted on DMA and SBS samples of all composites to assess possible effects of cyclic water sorption and freezing on the SBS properties. Typically with water sorption, a degradation of composite strength and stiffness is observed due to the diffusion of water into the glass fiber and its retention at the fiber/matrix interface. Subsequent cycles of water sorption on freezing should weaken the interfacial bonds and inhibit optimum shear transfer between fiber and matrix under loading. Approximately 15 cycles of freezing and thawing were conducted—24 h of freezing at -24°C and 24 h of thawing and water immersion in deionized water. After the freeze/thaw cycles were completed, the samples were dried or thawed and tested for T_g and SBS strength.

5.1.7.4 Xenon Arc Lamp Weathering. All composites were subject to weathering tests to simulate real exposure conditions that may be encountered upon mission-critical deployments. A xenon lamp weathering instrument was selected because the xenon arc lamp radiation output most closely simulates average actual sunlight exposure in the ultraviolet (UV) and visible region (300–2450 nm). An ATLAS Ci5000 weatherometer was used to subject all composites to a cycle of radiation exposure of $\sim 1.1 \text{ kW/m}^2$ for 20 h and darkness for 4 h at a constant temperature of 49°C and constant relative humidity of 50%. The cycle of radiation exposure is consistent with guidelines recommend in ASTM practices G 151-00, G 155-04a, and was adapted from a suggested cycle of exposure put forth in military standard MIL-STD-810F, method 505.4 (Solar Radiation), procedure II. Composite panels from both commercial and FAVE matrix resins were cut to $\sim 200 \times 150 \text{ mm}$ and weathered for 62 cycles. Before and after photographs of the panels were taken in polarized light to detect color change and possible internal stress fringes. After aging was completed, each panel was cut into samples for DMA and mechanical testing.

5.1.7.5 Chemical Aging. All composites except the Navy composites, 18-oz fabric with either Corve 8100 or FAVE-L-25S, were exposed to hydrocarbon turbine fuel JP-8 (MIL-DTL-83133F) according to military standard MIL-STD-810F, method 504 (Contamination by Fluids). JP-8, of course, is the military standard fuel utilized by all services in multiple combat vehicles. The procedure suggested therein for prolonged exposure was extended from 3 days to a duration of 1 week to ensure any possible effect of the JP-8 contamination on the thermal and mechanical properties would be observed. DMA, SBS, and flexural samples were cut from the bulk composite and soaked in a bath of JP-8 at ambient temperature for 1 week and then drained for several days. Drained and fully dried samples were then tested.

All of the Air Force composites, the 3- and 9-oz fabrics with either Hexion 781-2140 or FAVE-O-25S matrices, were exposed to the solvent methyl ethyl ketone (MEK) because it is a widely used industry solvent and a likely re-agent that these composites would come in contact with as they are processed and fielded. The exact procedure discussed for JP-8 exposure was used, making special note of before and after exposure color changes and leeching into the solvent bath. Drained and fully dried samples were then tested.

The Navy composites, 18-oz fabric with either Corve 8100 or FAVE-L-25S, were exposed to a simulated seawater bath to gage possible corrosion effects on mechanical properties. Cut composite samples were soaked for ~1 month in a solution of 1 L of VWR distilled water to 40 g of Sigma Aldrich Sea Salts (S9883). Samples were then dried and tested.

5.1.7.6 Mechanical Testing of Weathered Composites. DMA testing was used to determine the glass transition temperature T_g and storage and loss modulus. Basic mechanical performance was assessed through flexural strength and SBS testing.

5.2 Composite Part Validation Testing

5.2.1 Composite Part Demonstration

5.2.1.1 Infusion Trials. It is imperative for all demonstrations that the composites structures are able to be formed by VARTM using the new low-HAP resin. In particular, the time required for fiber wet out was noted and compared to the time required for commercial resins. Secondly, the ability of the resin to gel when desired was noted compared to neat resin cure samples. Lastly, the fiber wet out was noted and is expected to be similar to that of commercial resins. In many cases, smaller composite samples were tested prior to infusion testing of the full part.

Demonstration of the M35A3 hood, M939 hood, and HMMWV transmission containers was performed at SMC between January 2008 and January 2009. Two hoods of each type were fabricated, and four HMMWV transmission containers were fabricated. Demonstration of the MCM composite rudders was performed by SCI, of Melbourne, FL, and took place between November 2008 and February 2009. Two rudders were prepared, both using the FAVE-L-25S resin. The composite parts were compared to previous composites prepared by SCI.

5.2.1.2 Observations by Part Manufacturer. Assessment of the resin's performance for infusing the part and the appearance and feel of the final part was qualitatively assessed by the part manufacturer.

5.2.2 HMMWV Hardtop Demonstration/Validation Testing

The Amtech hardtop has a few key material performance requirements that may be critical when changing resin systems. Potential issues were screened by doing Sandwich Testing – 4 Point Bend (ASTM D 6272) and SBS testing (ASTM D 2344), as previously described. In addition, ballistic properties will need to be measured, as previously described. Lastly, the part was required to endure a 3000-mile road test to ensure the resin meets specifications.

5.2.2.1 Ballistics Testing. The APG ballistics range was utilized to determine V50 numbers for the composites used for Army and especially Marines applications. The samples must meet V50 Level IIIa at ~4psf, V50 level III at ~12 psf, and V50 level III in sandwich configuration with HJ1 phenolic core – total AD ~10.5 psf.

Two armor panels (figure 20) were created for each resin formulation, for a total of 10 composite panels. The final size of all armor panels was 24×24 inches, so infused parts were $\sim 27 \times 27$ inches in order to trim the samples to remove edge effects. One panel for each formulation was four layers of the 100-oz 3-Tex 3-D weave fabric layered cross-ply. The other panel is 12 layers of the 100-oz fabric layered cross-ply. The FAVE-O-HT panels are cured at room temperature and post cured at 130°C , while the FAVE-L-25S panels are post cured at 125°C . For comparison purposes, FCS2 Epoxy was cured at 65°C and post cured at 130°C . The VE 8084 composites were cured at room temperature and post cured at 120°C .



Figure 20. Preparation of composite armor targets (left) and final armor target after trimming (right).

5.2.3 Army Vehicle Hoods Demonstration/Validation Testing

For the truck hood, the ability of this structure to withstand static load, cyclic load, high service temperatures, and impact was demonstrated to simulate the forces the structure would be exposed to in the field. A custom-designed and built test fixture at the CCM (previously used to test the HMMWV and M35A3 hood designs) was used to validate the hood's performance. The testing was performed on an M35A3 and M939 hood prepared from FAVE-L-HT, 8605 Huntsman Epoxy, and Hetron 980/35.

The validation testing experiments were performed at the CCM in Newark, DE, from June 2008 to April 2009 at room temperature. In the static load experiments, a 250-lb weight was placed over a 3×3 -in area at the center and front center of the hood to simulate a soldier standing on the hood (figure 21). The 250-lb load applied to the outside surface over a maximum 10×10 -in area. The load was applied at the center and front areas of the hood. The deflection was measured at the point of application of the load but on the opposite surface. Plot of load vs. deflection was obtained. The hood is required to deflect no more than 0.25 in at -50°F and 0.5 in at 250°F and sustain no damage. The durability requirement is for the hood to resist all damage from a 250-lb force downward at the center of the hood, followed by 100,000 cycles at 1 cps to simulate a cyclic soldier load on the hood for the lifetime of the vehicle. Upon completion, a plot of load vs. deflection was obtained. The flexural properties must be such that when an upward force of 50 lbf at the right and left corners will not cause any damage to the part

and not result in greater than 0.5-in deflection (figure 22). An upward load was applied at the corner lift handles. The center latch was engaged, and both right and left sides were tested (separately). Displacement of the hood corner above the fixture was measured. Plots of load vs. deflection were obtained. The lifting load will not exceed 100 lb. The structure must withstand cyclic corner loads. Upward loads of 50 lb were applied at the corner lift handles with the center latch engaged. The loads were applied in alternating fashion (right then left) over an 8-h period at 10 cycles per minute. Upon completion, plots of load vs. deflection were obtained. These tests simulate a lifetime of lifting the corners of the hood. The impact resistance was quantified by dropping a 2-lb chrome-plated steel ball with 2 3/8-in-diameter from 6 feet onto the hood. The ball was dropped on six different locations to ensure toughness across the structure, as only insignificant cosmetic damage is considered acceptable.

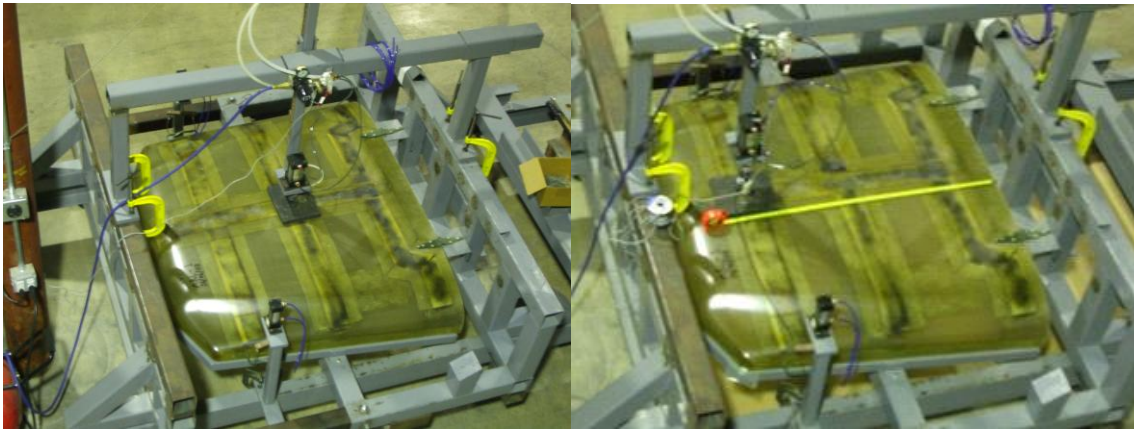


Figure 21. Center loading (left) and front loading (right) of M35A3 hood in test frame for static and cyclic testing.



Figure 22. Flexural loading showing driver side (left) and passenger side (right) loading of M35A3 hood in test frame for static and cyclic loading.

Army vehicle hoods were also tested for form, fit, and function at RRAD during March 2009. The testing was performed on an M35A3 and M939 hood prepared from FAVE-L-HT, 8605 Huntsman Epoxy, and Hetron 980/35. RRAD attached each of these hoods to the respective vehicle and examined the form, fit, and function. Essentially, how well the hood fit on the truck was observed. The load bearing capacity of the hood was assessed by the operator walking and jumping on the hood.

5.2.4 Army HMMWV Transmission Container Demonstration/Validation Testing

5.2.4.1 CCM Validation Testing. The properties of the HMMWV transmission containers were measured in the CCM using established procedures. The procedures are a part of a developing technical data package but are not yet approved; as such, there is no current specification number. The testing was performed on FAVE-L-25S and FAVE-O-25S relative to the incumbent resin, Derakane 8084.

Edgewise Drop Test

The procedure for the edgewise drop test is as follows:

The packed container (with appropriate HMMWV transmission) shall be supported at one end of its base on a wood sill or block, 15 cm in height, and placed at right angles to the skid. Each of the bottom edges of the packed container shall be elevated and allowed to drop freely onto a metal surface. The opposite end of the container shall be raised and allowed to drop freely from heights of 30, 60, and 90 cm successively onto a concrete or metal surface.

The test shall be applied to each end of the container. If the size of the container and the location of the center of gravity are such that drop tests cannot be made from all of the prescribed heights, the greatest attainable height shall be the height for succeeding drops until a total of three drops have been accomplished.

Drops were completed for three different heights as follows:

- Short edge drop heights: 18-, 29.5-, and 37 in.
- Long edge drop heights: 18- and 26 in twice.

Figure 23 is a photograph of the setup for the edgewise drop test.



Figure 23. Photograph of setup for edgewise drop test.

Cornerwise Drop Test

The procedure for the cornerwise drop test is as follows:

The packed container shall be supported at one corner of its base on a block, 15 cm in height. A block, 30 cm in height, shall be placed under the other corner of the same end of the container. Each of the bottom corners of the packed container shall be elevated and allowed to drop onto a metal surface. The lowest point of the opposite end of the container shall then be raised and allowed to fall freely from heights of 30, 60, and 90 cm successively onto a concrete or metal surface. If the size of the container and the location of the center of gravity are such that drop tests cannot be performed from all of the prescribed heights, the greatest attainable height shall be the height for succeeding drops until three drops have been accomplished. This test shall be applied on two diagonal corners at the bottom of the container.

Drops were completed for three different heights as follows:

- Drop heights for short edge supported: 18-, 29.5 -, and 34 in.
- Drop heights for long edge supported: 18- and 22 in twice.

Figure 24 is a photograph of the setup for the edgewise drop test.



Figure 24. Photograph of setup for cornerwise drop test.

Tip Over Test

The procedure for the tip over test is as follows:

The packed container shall be slowly tipped to the side until it falls freely and solely by its own weight to the floor. After righting the container, the test shall be repeated on the opposite side. Figure 25 depicts the tip over test.



Figure 25. Photographs of the tip over test.

Impact Test

The procedure for the impact test is as follows:

An impact test shall be applied to each end of the packed container. The container shall be suspended, as a pendulum, at the end of four or more cables. The cables shall be of sufficient length to prevent any interference or binding. A flat, vertical, stationary masonry or metal barrier, with a thickness of not more than 5 cm of wood between the barrier and container, shall

be provided for the container to strike against. The suspended container shall be raised vertically to a height that will allow the lowest point of the container (while swinging through the arc of the pendulum) to clear the floor. While the suspended container is resting lightly against the barrier and prior to pulling back for the impact, the center of balance shall be marked (if not stenciled on the container) as a measuring reference point. This mark shall be placed at the lowest point on the container shell. The suspended container shall be pulled back with a straight, even pull until a height of 46 cm plus the aforementioned floor clearance is reached. This measurement shall be taken from the measuring reference point on the container to the floor. At this point, the container shall be released in a manner to allow a smooth, even travel to the barrier.

The suspended container was pulled back to a height of 46 cm above its rest position. The container was then released and allowed to impact a steel barrier with 1-in-thick wood covering. Figure 26 depicts the impact test.



Figure 26. Photographs of the impact test.

Flatwise Drop Test

The packed container was raised with its base parallel to the floor and allowed to fall freely from heights of 15 and 30 cm. Figure 27 is a photograph of the test.



Figure 27. Photograph of the flatwise drop test.

Stacking Test

The stacking test shall be performed using a forklift truck to place the unloaded base on the cover in a normal stacking position. The stacked arrangement shall then be tilted 15° from the horizontal in two mutually perpendicular planes. Test pass criteria are as follows:

- Any slippage in excess of stacking provisions, (e.g., between male and female mating surfaces) constitutes failure.
- Inability of the forklift to effect a stable arrangement constitutes failure.

The stacking test was performed using a forklift truck to place the container upon another.

The stacked arrangement was then be tilted 15° from the horizontal in two mutually perpendicular planes. The test was performed twice, in one test with the FAVE container on the bottom and the other with it on top. Figure 28 shows photographs depicting the stacking test.



Figure 28. Photographs depicting the stacking test.

Concentrated Load Resistance

The container shall be placed on its bottom on a flat, level, rigid floor. A load W shall be applied to the top of the container in a manner simulating the effect of similar containers being stacked on top. Parameters are as follows:

- $W = P \times (16-H)/H$.
- P = weight of the loaded container.
- H = height of the container, in feet.
- Test duration shall be for a total of 16 h.

Test pass criteria:

- No permanent deformation, cracking, or any damage that would impair the functional performance of the container.

A load of 1800 lb was applied to the top of the container in a manner simulating the effect of similar containers being stacked. Test duration exceeded 16 h for each configuration (FAVE container on top or on bottom). Figure 29 is of photographs depicting the concentrated load resistance test.



Figure 29. Photograph showing the concentrated load resistance test.

Impact Resistance

The impact test shall be conducted at room temperature. The 2-lb steel ball will be dropped on the container and will undergo a 6-in drop. Impact will occur at the following locations:

- on flat surface,
- on small radius surface, and
- on large radius surface.

Test pass criteria are as follows:

- no permanent deformation,
- no separation of reinforcements, and
- no cracks allowed.

5.2.4.2 Shock and Vibration Testing of the HMMWV Shipping Containers. Shock and vibration testing of shipping containers is required in accordance with MIL-STD-810G and A-A-52486. Testing was performed by ATC in August 2009 on transmission containers fabricated by Sioux Manufacturing Corp. using the FAVE-L-25S resin and the Derakane 8084 incumbent resin. The details of the testing procedure are listed in appendix B. In summary, endurance testing subjected the containers to vibration at their most prominent resonant frequency (figure 30).

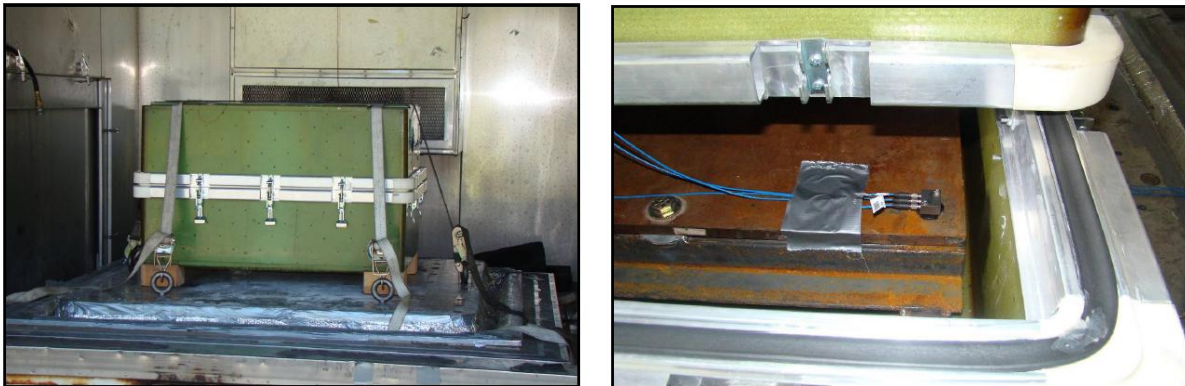


Figure 30. Vibration setup for the FAVE transmission container (left) and response accelerometer inside the container to measure the vibration response of the container (right).

Loose cargo testing (shock) simulated service conditions for when the containers would be transported by vehicle (figure 31). Vibration testing was completed with a representative weight installed in each container. The payload was secured in accordance with the operator's manual and with guidance from on-site customer representatives.



Figure 31. Loose cargo (shock) test setup.

The status of the transmission containers was documented regularly throughout the demonstration/validation through observations and photographs. The status of the transmission containers after the demonstration/validation was evaluated by observations, photographs, and a re-test of the drop tests, impact tests, stacking test, and load/impact resistances.

5.2.4.3 Field Testing of the HMMWV Containers. The test is a field trial in which the containers loaded with actual transmissions are handled and transported on vehicles. RRAD was responsible for the reconstruction/rehabilitation of the HMMWV and other military trucks. Therefore, this activity mimicked real situations.

The demonstration/validation took place over 3 months from June 2009 to September 2009. The containers were loaded with a standard HMMWV transmission. RRAD tested two variants of the transmission container, one made with commercially available VE resin (Derakane 8084) and one made from an experimental FAVE-L-25S. Monthly, the HMMWV transmission was unloaded, and a different transmission was loaded. Both containers were loaded and unloaded from transport trucks daily. Both containers were always loaded onto the same truck. The exact positioning of the each container on the truck was not always the same, but there was no systematic difference in treatment/positioning of each container. In fact, RRAD treated the test articles as they would the cardboard and wood crates that are currently used, the difference being that the composite transmission container is easily reusable. Normal rough handling and full use of lift rings, tie-down accessories, and latches was performed. We specifically told the users at RRAD that no one should fear breaking the test item, as long as they document how it broke. Re-settable shock sensors were placed at various places on the inside and outside of the container to determine whether extensive shocks were received.

The status of the transmission containers and shock sensors were documented regularly throughout the demonstration/validation through observations and photographs. The status of the transmission containers after the demonstration/validation was evaluated by observations, photographs, and a re-test of the drop tests, impact tests, stacking test, and load/impact resistances.

5.2.5 Air Force T-38 Dorsal Cover Demonstration/Validation Testing

Processability is the primary test to qualify a resin for this application after composite panel validation testing. Composite performance would otherwise be assessed in in-flight testing, which was not performed for this demonstration platform. The composite part was demonstrated/validated in January 2006. FAVE-L was the resin used and compared to the incumbent Hexion 781-2140.

5.2.6 Air Force F-22 Canopy Cover Demonstration/Validation Testing

Processability is the primary test to qualify a resin for this application after composite panel validation testing. Dimensional stability of the canopy cover is also extremely important, such that the final part adequately fits the F-22 canopy as expected. Thus, the ability of the canopy cover to fit the canopy was evaluated through observations. The composite part was demonstrated/validated in June 2008. FAVE-L was the resin used and compared to the incumbent Hexion 781-2140.

5.2.7 Air Force Splash Molds Demonstration/Validation Testing

Processability is the primary test to qualify a resin for this application after composite panel validation testing. Dimensional stability of the splash molds is also extremely important, such that the final part adequately fits part being molded. Thus, the dimensional stability was evaluated through observations. The composite part was demonstrated/validated in May 2009. FAVE-L was the resin used and compared to the incumbent Hexion 781-2140.

5.2.8 Navy MCM Rudder Demonstration/Validation Testing

Processability is a primary test to qualify a resin for this application after composite panel validation testing. The ability to flow across the part and wet out the part before gelation is extremely important. In addition, the part was sectioned to ensure good wetting of the fibers in the toes and in all areas of the part. FAVE-L-25S was the only resin validated. The resin was validated at SCI between November 2008 and February 2009, while the structure was validated at NSWCCD from March 2009 through June 2009.

6. Performance Assessment

6.1 JTP Results and Laboratory Results

6.1.1 JTP MFA Monomer Assessment

All batches of MFA monomers were assessed according to the JTP protocol outlines in section 5.1. Initial testing was done to determine a methodology to efficiently and reproducibly manufacture these monomers at API. Afterward, these monomers were prepared in batches, and each batch was used in a number of resin batches.

6.1.1.1 MFA Production. MFA monomers were prepared by API for demonstration/validation studies. Because the monomers were being produced at the 5-gal scale rather than then lab scale of ~500 mL, testing was initially performed to determine an optimum reaction procedure at this scale. Eight batches of monomers were prepared to determine the ideal reaction conditions (table 17). Each batch had slightly different molar ratios of FA to GM and different weight-percent catalyst. Also, two different catalysts were tested. API catalyst consisted of 75% triphenylphosphine and 25% triphenyl antimony and was compared to AMC-2, which was used successfully in lab testing (13).

Table 17. Initial reaction conditions for MFA monomers to determine ideal production reaction conditions.

Batch	MFA	FA:GM Ratio	Catalyst	Cat. Wt%	Reaction T (°C)	Duration (h)	Final Reaction T (°C)	Duration (h)
1	MLau	1.010	AMC-2	0.53	46	24		
2	MLau	1.019	API #1	0.57	46	24		
3	MLau	1.038	API #2	1.12	46	24		
4	MLau	1.010	AMC-2	0.53	46	24	71	4
5	MLau	1.011	API #1	0.57	46	24	71	4
6	MOct	1.022	AMC-2	0.48	46	24		
7	MOct	1.022	AMC-2	0.48	46	24	71	4
8	MOct	1.019	API #1	0.50	46	24	71	4

The results of batch testing of the monomers according to the JTP clearly showed that some formulations were better than others. Table 18 lists the viscosity as measured by both ARL and API and amount of epoxy qualitatively measured using FTIR and quantified using NMR. The results indicate that the AMC-2 catalyst was better than the API catalyst and the high temperature step appears to be unnecessary but not harmful to the product. Thus, it was decided that MFA monomers were to be prepared using the weight ratios of reactants as described in table 19 and reacted at a temperature of 46 °C for 24 h in a 5-gal bucket.

Table 18. Batch testing results of initial production batches of MFA.

Batch	MFA	FTIR results	NMR Results		API Viscosity		ARL Viscosity		High Temp	
			Epoxy/FA	at 25oC (cP)	at 20oC (cP)	Step	Catalyst	Result		
1	MLau	no epoxy	0	58	89	N	AMC-2, 0.5%	Good		
2	MLau	Epoxy	0.1	46.5	62	N	API, 0.5%	Not Acceptable		
3	MLau	small epoxy	0.05	49.5	64	N	API, 1%	Not Acceptable		
4	MLau	no epoxy	0	73.5	85	Y	AMC-2, 0.5%	Good		
5	MLau	small epoxy	0.03	44.5	40	Y	API, 0.5%	Not Acceptable		
6	MOct	no epoxy	0	39.5	54	N	AMC-2, 0.5%	Good		
7	MOct	no epoxy	0	45	49	Y	AMC-2, 0.5%	Good		
8	MOct	no epoxy	0	57.5	64	Y	API, 0.5%	high viscosity		

Table 19. Target reactant concentrations for the production of MFA monomers.

Reactant	MLau (weight-percent)	MOct (weight-percent)
Lauric acid (C-12)	58.7	
Octanoic acid (C-8)	—	50.6
GMA	41.3	49.4
Aerojet AMC-2 catalyst	0.5	0.5

6.1.1.2 MFA Batch Testing. Table 20 lists the monomer batch sheet information from API for each batch of MFA prepared in this work after the eight trial batches. The results show low deviations in the monomer reactants, all of which are lower than the maximum tolerable amounts of 1% FA, 1% GM, and 5% AMC-2.

Table 20. Deviation of reactant contents for the production of MFA.

MFA	Date	Deviation (%)		
		FA	GM	AMC-2
MLau	May 2006	0.00	0.00	-4.00
MLau	September 2006	-0.17	0.24	0.40
MLau	February 2007	0.17	-0.24	0.60
MLau	May 2007	0.00	0.00	-2.60
MLau	October 2007	-0.17	0.24	-3.00
MLau	December 2007	0.17	-0.24	1.00
MLau	June 2008	-0.10	0.17	1.00
MLau	March 2009	0.10	-0.17	-0.50
MOct	May 2006	0.20	-0.20	1.00
MOct	September 2006	0.00	0.00	-1.00
MOct	February 2007	-0.20	0.20	-4.00
MOct	May 2007	0.00	0.00	0.40
MOct	July 2007	0.00	0.00	0.60
MOct	September 2007	0.20	-0.20	-2.60
MOct	October 2007	0.40	0.20	-3.00
MOct	June 2008	-0.20	0.20	-0.60
MOct	March 2009	0.10	-0.10	0.80

Table 21 lists the acid number for each of these MFA monomers. All batches had acid numbers that were within the specified range.

Table 21. Acid number of MFA monomers.

MFA	Date of Sample	Acid No.	Acceptable Acid No. Range
MLau	May 2006	17.5	10–20
MLau	September 2006	16.0	10–20
MLau	February 2007	15.5	10–20
MLau	May 2007	16.0	10–20
MLau	September 2007	15.0	10–20
MLau	October 2007	14.5	10–20
MLau	December 2007	18.7	10–20
MLau	June 2008	14.0	10–20
MLau	March 2009	13.0	10–20
MOct	May 2006	16.0	10–20
MOct	September 2006	16.5	10–20
MOct	February 2007	15.0	10–20
MOct	May 2007	15.5	10–20
MOct	July 2007	16.5	10–20
MOct	September 2007	16.0	10–20
MOct	October 2007	12.8	10–20
MOct	June 2008	13.0	10–20
MOct	March 2009	13.2	10–20

The viscosities of the MFA monomers were measured and are listed in table 22. The first couple of batches had viscosity problems. In the first case, the reason was known, as the reaction was run too long. The reaction procedure was modified to improve the results.

Table 22. Viscosity of MFA monomers.

MFA	Date of Sample	Viscosity (cP)	Acceptable Viscosity (cP)	Comments
MLau	May 2006	114	<80	Reacted too long
MLau	June 2006	88	<80	—
MLau	September 2006	75	<80	—
MLau	February 2007	70	<80	—
MLau	May 2007	75	<80	—
MLau	September 2007	72	<80	—
MLau	October 2007	75	<80	—
MLau	December 2007	70	<80	—
MLau	June 2008	70	<80	—
MLau	March 2009	70	<80	—
MOct	May 2006	74	<70	Reacted too long
MOct	September 2006	40	<70	—
MOct	February 2007	45	<70	—
MOct	May 2007	50	<70	—
MOct	July 2007	55	<70	—
MOct	September 2007	45	<70	—
MOct	October 2007	40	<70	—
MOct	June 2008	40	<70	—
MOct	March 2009	40	<70	—

FTIR of each MFA batch was also performed. For all batches, the epoxide peak from the glycidyl methacrylate product was gone after reaction, indicating complete reaction of the glycidyl methacrylate. Thus, FTIR qualitatively showed good performance of each batch and was not sensitive enough to ensure high quality from batch to batch.

SEC results were used to indicate whether polymerization occurred during reaction or high contents of unreacted species remained. Like FTIR, all the results were similar and indicated no polymerization and similar and low amounts of remaining unreacted compounds.

NMR was used to assess the fatty acid backbone ratio to methacrylate ratio in the monomer. The results are shown in table 23. The results clearly show acceptable FA/GM range, although it was slightly higher during the first few batches and became lower over the course of time as a result of improvements in the MFA preparation process.

Table 23. NMR results of MFA monomers.

MFA	Date of Sample	FA: GM Ratio	Acceptable FA/GM Ratio Range
MLau	May 2006	1.06	1.1–0.95
MLau	September 2006	1.05	1.1–0.95
MLau	February 2007	1.04	1.1–0.95
MLau	May 2007	1.05	1.1–0.95
MLau	September 2007	1.04	1.1–0.95
MLau	October 2007	1.03	1.1–0.95
MLau	December 2007	1.03	1.1–0.95
MLau	June 2008	1.04	1.1–0.95
MLau	March 2009	1.03	1.1–0.95
MOct	May 2006	1.05	1.1–0.95
MOct	September 2006	1.07	1.1–0.95
MOct	February 2007	1.06	1.1–0.95
MOct	May 2007	1.05	1.1–0.95
MOct	July 2007	1.05	1.1–0.95
MOct	September 2007	1.04	1.1–0.95
MOct	October 2007	1.05	1.1–0.95
MOct	June 2008	1.04	1.1–0.95
MOct	March 2009	1.04	1.1–0.95

6.1.2 Resin Formulations

6.1.2.1 Introduction. During SERDP PP-1271, it was determined that resins containing 65% VE, 20–25% styrene, and 15–10% MFA were optimum resin formulations. However, these resins used contained VE 828, a non-commercial VE monomer. All resins used in this work must be commercially available or able to be manufactured for this project. It was determined a priori that the production of VE monomers, such as VE 828, would be too difficult.

To solve these issues, commercial resins were going to be blended with MFAs to produce the FAVE resins. Derakane 441-400 was a good starting candidate because of the moderate molecular weight of its VE monomers (~700 g/mol) and low styrene content (33 weight-percent) (9, 28). To formulate the FAVE with the correct amount of VE, styrene, and MFA, pure VE monomer would have to be added to the batch. Again, commercial production of VE 828 was not going to be considered. Fortunately, there exist commercial VE monomers, Sartomer CN151 (29) and Cytec RDX26936 (30), that are similar to VE 828.

Another alternative was also determined during the course of this project—Arapol 914 (31). This VE contains 20% styrene but is otherwise very similar to VE 828. As an added benefit, because it is already mixed with styrene, it is very simple to mix this product with other chemicals. This is unlike VE 828, CN151, and RDX26936, all which require heating to ~70 °C

and extensive mixing to ensure homogenization. As a result, no resins used in this work were manufactured in significant quantities using these VEs as the sole source of VE monomers. However, laboratory samples were prepared using pure VE monomers as the sole source of cross-linkers.

To achieve high temperature properties, commercial VE resins use Novolac VEs, such as in Derakane 470HT-400 (32), instead of bisphenol A VEs. Thus, to make high temperature formulations, we used Derakane 470HT-400 to manufacture these resins. However, there is no supplier of pure Novolac VE monomers. Thus, the FAVE high temperature formulations are a blend of Novolac VE (from Derakane 470HT-400) and bisphenol A VE (from CN-151, RDX26936, or Arapol 914). Derakane 470HT-400 contains 33 weight-percent styrene (32).

To achieve toughened properties analogous to Derakane 8084 (33), some laboratory FAVE formulations were prepared using Derakane 8084 as a basis. Derakane 8084 uses a Carboxy-terminated butadiene rubber modified VE cross-linker to achieve high toughness but with reduced T_g . This VE monomer is not supplied commercially without styrene. Thus, toughened FAVE formulations were based Derakane 8084 and blended with standard bisphenol A VE (from CN-151, RDX26936, or Arapol 914). Derakane 8084 contains 40 weight-percent styrene (33).

As a result of all of these possible ways to formulate a given resin, there are a number of variants for each type of formulation. Selection of the optimum variant is based on two criteria, which have been found to be the important criteria for these types of VE resins—viscosity and glass transition temperature. Viscosity is especially important in FAVE resins because reduced styrene content generally means higher viscosity, reducing the ability to vacuum infuse these resins. T_g is important because it determines the operating temperature range of the resulting part.

6.1.2.2 Resin Formulations and Variants. Each resin formula used the components listed in figure 32. Novolac VE provides the highest thermal properties but also tends to be more brittle. MFA monomers tend to reduce T_g and have higher viscosities than styrene but result in resins with reduced HAP content.

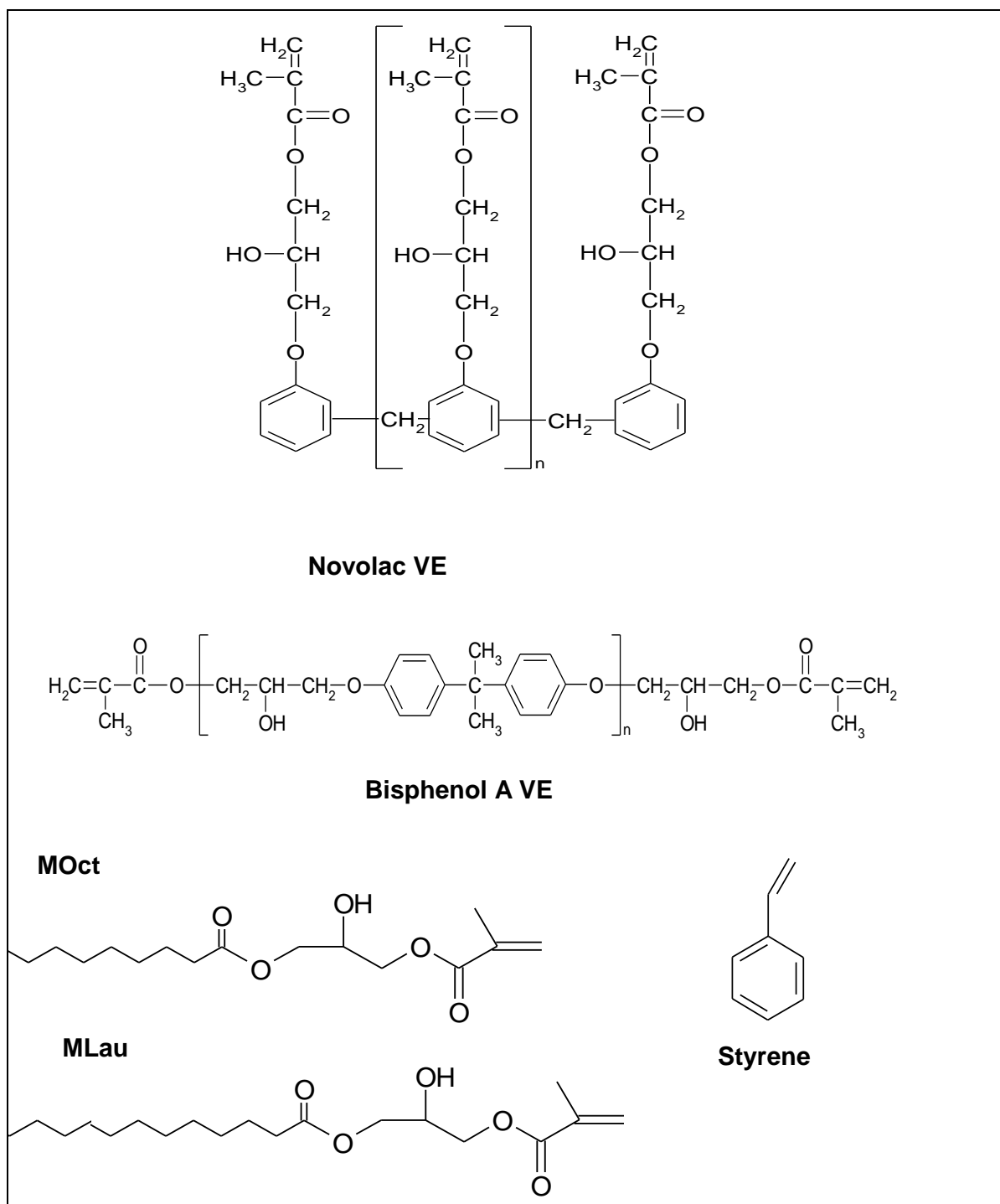


Figure 32. Schematic structures of Novolac VE, bisphenol A VE, styrene, MLau, and MOct.

There are a number of base formulations that were determined a priori (table 24). In particular, these are the FAVE-L/O and FAVE-L/O-25S. The HT formulations were defined only after it was determined that the -25S formulations did not meet the properties required for the Army hood applications. That development is discussed in appendix C. The basic formulations using 65 weight-percent bisphenol A VEs only contained 20 weight-percent styrene and 15 weight-percent MFA (FAVE-L or FAVE-O) or 25 weight-percent styrene and 10 weight-percent MFA (FAVE-L-25S and FAVE-O-25S). The basic formulations containing a total of 65 weight-percent Novolac and bisphenol A VE with 25 weight-percent styrene and 10 weight-percent MFA are FAVE-L-HT and FAVE-O-HT.

Table 24. Basic resin formulations.

Basic Formulation	Bisphenol VE (weight-percent)	Bis. A/Novolac VE (weight-percent)	MLau (weight-percent)	MOct (weight-percent)	Styrene (weight-percent)
FAVE-L	65	—	15	—	20
FAVE-O	65	—	—	15	20
FAVE-L-25S	65	—	10	—	25
FAVE-O-25S	65	—	—	10	25
FAVE-L-HT	—	65	10	—	25
FAVE-O-HT	—	65	—	10	25

Resin variants were created for each formula depending on basis of the resin (e.g., Arapol 914 or Derakane 441-400) and the pure VE monomer used (e.g., CN-151 and RDX26936). Appendix C shows the work that was done to determine some of those resin variants of interest. The formulation variants are listed in tables 25–31. The initial formulations for FAVE-L/O and FAVE-L/O-25S used Derakane 441-400 and CN-151 and were given the base name. The variants that used different components to make the same formulation were given extensions to signify the variant. For example, -RDX resins were formulated with Derakane 441-400 and RDX26936. The -A1 resins used Arapol only as the VE component, while -A2 resins used Arapol 914 and Derakane 441-400. The -VE formulation used only pure VE (RDX26936) for comparison purposes only and was never manufactured at a significant scale. The -T resins are toughened resin formulations containing Derakane 8084 as a basis for the resin. These were not used in this demonstration/validation program but were developed nonetheless in case they were necessary to meet performance requirements. The development of these toughened resins is discussed in appendix C.

Table 25. The formulations for the resin variants of FAVE-L and the neat resin properties. In bold are the optimum properties and highlighted in green are the optimum formulations.

Component	FAVE-L	FAVE-L-RDX	FAVE-L-A1	FAVE-L-A2	FAVE-L-VE
Derakane 441-400 (%)	60.6	60.6	—	23.1	—
Arapol 914 (%)	—	—	81.0	61.9	—
CN151 (%)	24.4	—	—	—	—
RDX26936 (%)	—	24.4	—	—	65.0
Styrene added (%)	—	—	4.0	—	20.0
MLau (%)	15.0	15.0	15.0	15.0	15.0
Viscosity at 25 °C (cP)	900	850	600	650	600
Tg dry (°C)	102	106	120	114	118
Tg wet (°C)	91	95	110	107	110
Flex mod. (GPa)	2.7	2.7	2.7	2.7	2.7
Flex str. (MPa)	120	120	120	120	120
G _{IC} (J/m ²)	150	220	190	200	170

Table 26. The formulations for the resin variants of FAVE-O and the neat resin properties. In bold are the optimum properties and highlighted in green are the optimum formulations.

Component	FAVE-O	FAVE-O-RDX	FAVE-O-A1	FAVE-O-A2	FAVE-O-VE
Derakane 441-400 (%)	60.6	60.6	—	23.1	—
Arapol 914 (%)	—	—	81.0	61.9	—
CN151 (%)	24.4	—	—	—	—
RDX26936 (%)	—	24.4	—	—	65.0
Styrene added (%)	—	—	4.0	—	20.0
MOct (%)	15.0	15.0	15.0	15.0	15.0
Viscosity at 25 °C (cP)	850	800	680	730	690
Tg dry (°C)	101	105	122	116	120
Tg wet (°C)	91	95	111	109	108
Flex mod. (GPa)	2.7	2.7	2.7	2.7	2.7
Flex str. (MPa)	120	120	120	120	120
G _{IC} (J/m ²)	140	220	180	190	160

Table 27. The formulations for the resin variants of FAVE-L-25S and the neat resin properties. In bold are the optimum properties and highlighted in green are the optimum formulations.

Component	FAVE-L-25S	FAVE-L-25S-RDX	FAVE-L-25S-A1	FAVE-L-25S-A2	FAVE-L-25S-VE
Derakane 441-400 (%)	75.8	75.8		54.0	—
Arapol 914 (%)	—	—	81.0	36.0	—
CN151 (%)	14.2	—	—	—	—
RDX26936 (%)	—	14.2	—	—	65.0
Styrene added (%)	—	—	9.0	—	25.0
MLau (%)	10.0	10.0	10.0	10.0	10.0
Viscosity at 25 °C (cP)	550	550	360	455	350
Tg dry (°C)	111	118	125	120	125
Tg wet (°C)	101	110	115	111	114
Flex mod. (GPa)	2.9	2.9	2.9	2.9	2.9
Flex str. (MPa)	125	125	125	125	125
G _{IC} (J/m ²)	120	200	170	180	150

Table 28. The formulations for the resin variants of FAVE-O-25S and the neat resin properties. In bold are the optimum properties and highlighted in green are the optimum formulations.

Component	FAVE-O-25S	FAVE-O-25S-RDX	FAVE-O-25S-A1	FAVE-O-25S-A2	FAVE-O-25S-VE
Derakane 441-400 (%)	75.8	75.8	—	54.0	—
Arapol 914 (%)	—	—	81.0	36.0	—
CN151 (%)	14.2	—	—	—	—
RDX26936 (%)	—	14.2	—	—	65.0
Styrene added (%)	—	—	9.0	—	25.0
MOct (%)	10.0	10.0	10.0	10.0	10.0
Viscosity at 25 °C (cP)	550	470	350	475	360
Tg dry (°C)	115	119	128	121	128
Tg wet (°C)	104	110	119	111	120
Flex mod. (GPa)	2.9	2.9	2.9	2.9	2.9
Flex str. (MPa)	125	125	125	125	125
G _{IC} (J/m ²)	120	190	165	180	140

Table 29. The formulations for the resin variants of FAVE-L-HT and FAVE-O-HT and the neat resin properties.
In bold are the optimum properties and highlighted in green are the optimum formulations.

Component	FAVE-L-HT	FAVE-O-HT	FAVE-L-HT-RDX	FAVE-O-HT-RDX	FAVE-L-HT-A2	FAVE-O-HT-A2
Derakane 470HT-400 (%)	75.8	75.8	75.8	75.8	54.0	54.0
Arapol 914 (%)	—	—	—	—	36.0	36.0
CN151 (%)	14.2	14.2	—	—	—	—
RDX26936 (%)	—	—	14.2	14.2	—	—
Styrene added	—	—	—	—	—	—
MLau (%)	10.0	—	10.0	—	10.0	—
MOct (%)	—	10.0	—	10.0	—	10.0
Viscosity at 25 °C (cP)	560	530	560	530	535	515
Tg dry (°C)	140	141	143	144	144	144
Tg wet (°C)	130	131	133	135	132	135
Flex mod. (GPa)	2.8	2.8	2.8	2.8	2.8	2.8
Flex str. (MPa)	110	110	110	110	110	110
G _{IC} (J/m ²)	85	80	85	85	95	95

Table 30. The formulations for the resin variants of toughened FAVE-L/O and the neat resin properties.
In bold are the optimum properties.

Component	FAVE-L-T1	FAVE-O-T1	FAVE-L-T2	FAVE-O-T2
Derakane 8084 (%)	50.0	50.0	15.0	15.0
Arapol 914 (%)	—	—	70.0	70.0
RDX26936 (%)	35.0	35.0	—	—
Styrene added	—	—	—	—
MLau (%)	15.0	—	15.0	—
MOct (%)	—	15.0	—	15.0
Viscosity at 25 °C (cP)	—	—	—	—
Tg dry (°C)	102	105	111	113
Tg wet (°C)	101	101	113	115
Flex mod. (GPa)	2.7	2.7	2.8	2.8
Flex str. (MPa)	110	110	115	115
G _{IC} (J/m ²)	450	420	300	300

Table 31. The formulations for the resin variants of toughened FAVE-L/O-25S and the neat resin properties. In bold are the optimum properties.

Component	FAVE-L-25S-T1	FAVE-O-25S-T1	FAVE-L-25S-T2	FAVE-O-25S-T2
Derakane 8084 (%)	62.5	62.5	55.0	55.0
Arapol 914 (%)	—	—	35.0	35.0
RDX26936 (%)	27.5	27.5	—	—
Styrene added	—	—	—	—
MLau (%)	10.0	—	10.0	—
MOct (%)	—	10.0	—	10.0
Viscosity at 25 °C (cP)	—	—	—	—
T _g dry (°C)	114	115	125	127
T _g wet (°C)	101	101	113	115
Flex mod. (GPa)	2.6	2.6	2.7	2.7
Flex str. (MPa)	105	105	115	115
G _{IC} (J/m ²)	350	330	250	250

Each table clearly shows one or two variants that are ideal for each resin formulation, and some are clearly inferior. In general, the -A1 variant proved to be the ideal formulation, having optimized most properties in addition to having the simplest processing. In the case of the high temperature formulations, the FAVE-O-HT-A2 proved to be the ideal formulation. However, the properties were only slightly greater than that of FAVE-L-HT-A2 or FAVE-L-HT-RDX. Yet, as was shown, the cost of the MOct is significantly more than that of the MLau. Thus, FAVE-L-HT-A2 is likely the ideal formulation. However, most of these variants, including the -A1 and -A2, were not realized until after the project had begun. Thus, the initial variants prepared are not the ideal choice. However, these ideal variants were produced towards the middle and end of the project for the actual demonstration/validation trials.

6.1.2.3 Resin Formulation Conclusions. A number of conclusions can be made regarding non-toughened FAVE resin formulations as follows:

1. FAVE resin formulations can be prepared in a variety of ways using a variety of components.
2. RDX26936 exhibits superior performance to CN151 in terms of cure behavior and performances.
3. Arapol 914 resins A1 variants had the highest T_g and lowest viscosity while also eliminating the need to mix viscous VE monomers into low-viscosity components.

6.1.3 Resin JTP Results

6.1.3.1 Resin Preparation. FAVE resins were prepared by API using the formulas described in tables 18–23. Because CN-151 and RDX26936 are very viscous, the resin had to be heated to 70 °C to reduce the viscosity enough to allow it to flow to be able to easily remove it from the can. The CN-151 or RDX26936 is then added to the other resin components in a bucket or drum. The bucket or drum is then roll-mixed for up to a week to ensure homogeneity of the resin. For resin formulations containing components other than CN-151 or RDX26936, the components are added to a bucket or drum and roll mixed for 2 h to ensure homogeneity. The mix sheets as given by API generally show slight deviations from the desired formulas (tables 32 and 33). Clearly, resins that used CN-151 had the highest mix sheet deviation. RDX26936 had a much lower deviation from CN-151, likely due to improvements in processing, allowing for better metering out of components. Resins using Arapol had the lowest deviation as a result of the lower viscosity of Arapol, making pouring and weighing out this component much easier.

Table 32. Deviation in component concentrations of FAVE-L/O and FAVE-L/O-25S according to API mix sheets.

Resin	Date	Deviation (%)				
		441-400	Arapol 914	CN151	RDX26936	MFA
FAVE-L	May 2006	−0.24	—	0.83	—	−0.39
FAVE-L	July 2006	−0.50	—	0.93	—	0.50
FAVE-L	March 2007	0.02	—	0.11	—	−0.24
FAVE-L	May 2007	−0.04	—	0.05	—	0.06
FAVE-O	May 2006	−0.04	—	0.05	—	0.06
FAVE-O	July 2006	0.00	—	0.09	—	−0.15
FAVE-L-25S	July 2006	−0.14	—	0.90	—	−0.24
FAVE-L-25S	August 2007	−0.27	—	1.65	—	−0.33
FAVE-L-25S	September 2007	−0.27	—	1.65	—	−0.33
FAVE-L-25S	December 2007	−0.36	—	2.08	—	−0.24
FAVE-L-25S-RDX	February 2008	−0.10	—	—	0.50	−0.15
FAVE-L-25S-RDX	July 2008	0.15	—	—	−0.10	0.20
FAVE-L-25S-A2	December 2008	−0.03	0.03	—	—	−0.01
FAVE-L-25S-A2	April 2009	−0.02	0.01	—	—	−0.01
FAVE-O-25S	August 2006	0.05	—	−0.51	—	0.35
FAVE-O-25S	February 2007	0.12	—	0.00	—	−0.91
FAVE-O-25S	July 2007	0.13	—	−1.03	—	0.49
FAVE-O-25S	September 2007	0.05	—	−0.41	—	0.24
FAVE-O-25S	November 2007	0.06	—	−0.32	—	0.00
FAVE-O-25S	December 2007	0.07	—	−0.02	—	−0.54
FAVE-O-25S-RDX	February 2008	−0.12	—	—	0.40	−0.20
FAVE-O-25S-RDX	June 2008	−0.01	—	—	0.30	−0.05
FAVE-O-25S-A2	December 2008	0.01	−0.05	—	—	0.02
FAVE-O-25S-A2	April 2009	−0.03	0.05	—	—	−0.02

Table 33. Deviation in component concentrations of FAVE-L/O-HT according to API mix sheets.

Resin	Date	Deviation (%)				
		470HT-400	Arapol 914	CN151	RDX26936	MFA
FAVE-O-HT	February 2007	-0.17	—	0.76	—	0.19
FAVE-O-HT	July 2007	0.05	—	-0.41	—	0.24
FAVE-O-HT-RDX	September 2007	0.03	—	—	0.17	-0.49
FAVE-O-HT-RDX	January 2008	0.05	—	—	-0.10	0.07
FAVE-O-HT-A2	May 2008	-0.01	0.03	—	—	-0.05
FAVE-O-HT-A2	September 2008	0.03	-0.03	—	—	0.01
FAVE-L-HT-RDX	May 2008	0.10	—	—	-0.25	0.15
FAVE-L-HT-A2	October 2008	-0.08	0.05	—	—	0.00
FAVE-L-HT-A2	March 2009	-0.07	0.04	—	—	-0.01

6.1.3.2 Resin Batch Testing. Batch testing of each resin batch was performed according to the JTP. The batch testing included chemical analysis through FTIR, SEC, NMR, and acid number titration and physical property measurements, including viscosity and DMA property measurement.

FTIR results of all FAVE resins were qualitative in nature. The results all confirmed the presence of styrene (910 cm^{-1}) and VE and MFA methacrylate peaks (942 cm^{-1}). SEC results were also used qualitatively. These results did not show the presence of any peaks at low retention times, indicating undesired polymerization before use. Thus, based on these results, no degradation of the resins was observed during the normal course of use and storage of these resins.

NMR results were used to quantify the amount of VE, styrene, and MFA. Furthermore, NMR was used to determine the molecular weight of the VE monomers in FAVE-L, FAVE-O, and FAVE-L-25S, and FAVE-O-25S resins. NMR cannot quantify the molecular weight of Novoloc VE, thus preventing this measurement for FAVE-L-HT and FAVE-O-HT.

The results of NMR analysis are tabulated in table 34. The results clearly show that initial formulations have a few red values (indicating values outside of specifications). Initial batches were packaged in plastic containers. Styrene is able to diffuse out of these containers and reduces the amount of styrene in the resin. This problem was clearly solved, as later batches all much more closely met the specification for styrene content.

Table 34. NMR batch testing results of FAVE resins.

Resin	Date of Sample	Experimental Values			Expected Values		
		VE MW (g/mol)	Styrene Content (wt%)	MFA (wt%)	VE MW (g/mol)	Styrene Content (wt%)	MFA (wt%)
FAVE-L	May 2006	634	19.1	15.1	644	20.0	15.0
FAVE-L	July 2006	654	19.6	15.3	644	20.0	15.0
FAVE-L	March 2007	645	18.5	15.4	644	20.0	15.0
FAVE-L	May 2007	645	18.4	15.1	644	20.0	15.0
FAVE-O	May 2006	644	19.8	15.1	644	20.0	15.0
FAVE-O	July 2006	645	18.1	15.5	644	20.0	15.0
FAVE-L-25S	August 2007	670	23.9	10.3	666	25.0	10.0
FAVE-L-25S	September 2007	660	25.0	10.5	666	25.0	10.0
FAVE-L-25S	December 2007	652	23.8	10.4	666	25.0	10.0
FAVE-L-25S	January 2008	658	24.9	10.5	666	25.0	10.0
FAVE-L-25S-RDX	February 2008	655	24.7	10.2	666	25.0	10.0
FAVE-L-25S-RDX	July 2008	675	24.8	10.3	666	25.0	10.0
FAVE-L-25S-A2	December 2008	680	24.9	10.2	670	25.0	10.0
FAVE-L-25S-A2	April 2009	675	24.9	10.1	670	25.0	10.0
FAVE-O-25S	August 2006	675	23.5	10.5	666	25.0	10.0
FAVE-O-25S	February 2007	665	24.3	10.4	666	25.0	10.0
FAVE-O-25S	July 2007	670	22.6	12.5	666	25.0	10.0
FAVE-O-25S	September 2007	672	24.1	10.6	666	25.0	10.0
FAVE-O-25S	November 2007	658	24.9	10.3	666	25.0	10.0
FAVE-O-25S	December 2007	659	24.8	10.4	666	25.0	10.0
FAVE-O-25S-RDX	February 2008	672	25.0	10.5	666	25.0	10.0
FAVE-O-25S-RDX	June 2008	658	24.8	10.4	666	25.0	10.0
FAVE-O-25S-A2	December 2008	680	25.1	10.1	670	25.0	10.0
FAVE-O-25S-A2	April 2009	653	25.0	10.0	670	25.0	10.0
FAVE-O-HT	February 2007	—	24.1	10.1	—	25.0	10.0
FAVE-O-HT	July 2007	—	23.8	10.2	—	25.0	10.0
FAVE-O-HT-RDX	September 2007	—	24.2	10.1	—	25.0	10.0
FAVE-O-HT-RDX	January 2008	—	24.8	10.0	—	25.0	10.0
FAVE-O-HT-A2	May 2008	—	24.9	10.1	—	25.0	10.0
FAVE-O-HT-A2	September 2008	—	24.8	10.3	—	25.0	10.0
FAVE-L-HT-RDX	May 2008	—	24.7	9.9	—	25.0	10.0
FAVE-L-HT-A2	October 2008	—	25.0	10.2	—	25.0	10.0
FAVE-L-HT-A2	March 2009	—	25.0	10.1	—	25.0	10.0

Acid number titration determined the amount of free acid in the resin, mostly a result of residual FA in the MFA, although some of the acid is due to remaining methacrylic acid from the commercial production of VE monomers. Acid number titration results (table 35) showed that all batches passed the acid number specifications.

Table 35. Acid number titration results of FAVE batches.

Resin	Date of Sample	Acid No.	Acid No. Range
FAVE-L	May 2006	8.8	5–10
FAVE-L	July 2006	8.0	5–10
FAVE-L	March 2007	7.0	5–10
FAVE-L	May 2007	6.8	5–10
FAVE-O	May 2006	9.0	5–10
FAVE-O	July 2006	7.9	5–10
FAVE-L-25S	August 2007	7.0	5–10
FAVE-L-25S	September 2007	7.0	5–10
FAVE-L-25S	December 2007	6.6	5–10
FAVE-L-25S	January 2008	5.9	5–10
FAVE-L-25S-RDX	February 2008	5.8	5–10
FAVE-L-25S-RDX	July 2008	6.0	5–10
FAVE-L-25S-A2	December 2008	5.8	5–10
FAVE-L-25S-A2	April 2009	5.9	5–10
FAVE-O-25S	August 2006	7.5	5–10
FAVE-O-25S	February 2007	7.2	5–10
FAVE-O-25S	July 2007	6.7	5–10
FAVE-O-25S	September 2007	6.7	5–10
FAVE-O-25S	November 2007	6.8	5–10
FAVE-O-25S	December 2007	6.8	5–10
FAVE-O-25S-RDX	February 2008	5.9	5–10
FAVE-O-25S-RDX	June 2008	5.8	5–10
FAVE-O-25S-A2	December 2008	6.1	5–10
FAVE-O-25S-A2	April 2009	5.9	5–10
FAVE-O-HT	February 2007	14.8	10–20
FAVE-O-HT	July 2007	14.8	10–20
FAVE-O-HT-RDX	September 2007	15.4	10–20
FAVE-O-HT-RDX	January 2008	15.2	10–20
FAVE-O-HT-A2	May 2008	15.1	10–20
FAVE-O-HT-A2	September 2008	14.9	10–20
FAVE-L-HT-RDX	May 2008	15.0	10–20
FAVE-L-HT-A2	October 2008	15.0	10–20
FAVE-L-HT-A2	March 2009	14.4	10–20

Styrene evaporative measurements were performed on many batches of resin (table 36). This test was not originally part of the JTP but was determined that it should be because of its accurate measurement of styrene concentration. As a result, the first few batches of resin were not tested, but all later batches were tested. The results show that the initial batches had low styrene contents, causing the higher viscosities that were observed for the users. Switching to metal containers reduced the styrene losses in these samples, resulting in higher quality FAVE resins that conformed better to JTP specifications.

Table 36. Styrene weight-percent content in FAVE resins measured using as evaporative losses in TGA experiment.

Resin	Date of Sample	Styrene Weight-Percent
FAVE-L	May 2006	NA
FAVE-L	July 2006	NA
FAVE-L	March 2007	18
FAVE-L	May 2007	17
FAVE-O	May 2006	NA
FAVE-O	July 2006	NA
FAVE-L-25S	August 2007	23
FAVE-L-25S	September 2007	22.5
FAVE-L-25S	December 2007	23
FAVE-L-25S	January 2008	23.5
FAVE-L-25S-RDX	February 2008	24.5
FAVE-L-25S-RDX	July 2008	24.7
FAVE-L-25S-A2	December 2008	24.8
FAVE-L-25S-A2	April 2009	24.7
FAVE-O-25S	August 2006	NA
FAVE-O-25S	February 2007	NA
FAVE-O-25S	July 2007	22.9
FAVE-O-25S	September 2007	23.4
FAVE-O-25S	November 2007	24.1
FAVE-O-25S	December 2007	24
FAVE-O-25S-RDX	February 2008	24.5
FAVE-O-25S-RDX	June 2008	24.8
FAVE-O-25S-A2	December 2008	24.8
FAVE-O-25S-A2	April 2009	24.7
FAVE-O-HT	February 2007	NA
FAVE-O-HT	July 2007	23.6
FAVE-O-HT-RDX	September 2007	24.2
FAVE-O-HT-RDX	January 2008	24.5
FAVE-O-HT-A2	May 2008	24.7
FAVE-O-HT-A2	September 2008	24.7
FAVE-L-HT-RDX	May 2008	24.6
FAVE-L-HT-A2	October 2008	24.7
FAVE-L-HT-A2	March 2009	24.9

Note: NA = not available.

Viscosity measurements were run on each FAVE batch (table 37). Viscosity results clearly showed that the initial batches had viscosity issues while later batches did not. Again, this is due to switching the resin storage method from plastic to metal containers. After this switch, the resin viscosities were reduced considerably and met the specifications with ease. Resins using MLau as a reactive diluent have slightly higher viscosities than resins using MOct. Increasing styrene content reduced the viscosity of the resin as expected because styrene is the least viscous component. FAVE-HT resins (25 weight-percent styrene) have slightly higher viscosities than FAVE-25S resins because of the higher viscosity of novolac VE relative to bisphenol A VE monomers. Furthermore, Arapol 914-based variants had lower viscosities relative to the other varieties of that same resin. Thus, the use of Arapol 914 is beneficial to the performance of FAVE resins.

For batch testing, gel time of FAVE resins was characterized using a consistent content of CoNap (0.2 weight-percent) and Trigonox (1 weight-percent) and an ambient temperature of 72 °F. The gel time was measured for each batch. The gel times are listed in table 38. The results show that gel time remained consistent from batch to batch. The results also showed that as the molar concentration of cross-linker content increased, the gel time decreased. The commercial resins had higher gel times for this same reason relative to similar FAVE resins. The Derakane 470HT-400 had a higher gel time than the Derakane 441-400, probably due to additional inhibitor.

Basic DMA results were recorded for cured polymer samples from each of the API FAVE batches (table 39). The results showed good consistency from batch to batch of the same resin formulation. In all cases, the switch from CN-151 to RDX26936 resulted in a 3–5 °C increase in T_g . Switching from RDX26936/Derakane 441-400 blend to an Arapol 914/Derakane 441-400 blend had no significant effects on the basic resin properties.

Table 37. FAVE batch viscosity.

Resin	Date of Sample	Viscosity (cP)	Acceptable Viscosity at 25 °C (cP)
FAVE-L	May 2006	1200	<1000
FAVE-L	June 2006	910	<1000
FAVE-L	July 2006	1120	<1000
FAVE-L	March 2007	1550	<1000
FAVE-L	May 2007	850	<1000
FAVE-O	May 2006	1200	<1000
FAVE-O	July 2006	990	<1000
FAVE-L-25S	August 2007	740	<800
FAVE-L-25S	September 2007	1030	<800
FAVE-L-25S	December 2007	550	<800
FAVE-L-25S	January 2008	460	<800
FAVE-L-25S-RDX	February 2008	480	<800
FAVE-L-25S-RDX	July 2008	490	<800
FAVE-L-25S-A2	December 2008	450	<800
FAVE-L-25S-A2	April 2009	460	<800
FAVE-O-25S	August 2006	710	<800
FAVE-O-25S	February 2007	690	<800
FAVE-O-25S	July 2007	800	<800
FAVE-O-25S	September 2007	1025	<800
FAVE-O-25S	November 2007	650	<800
FAVE-O-25S	December 2007	790	<800
FAVE-O-25S-RDX	February 2008	450	<800
FAVE-O-25S-RDX	June 2008	490	<800
FAVE-O-25S-A2	December 2008	480	<800
FAVE-O-25S-A2	April 2009	470	<800
FAVE-O-HT	February 2007	950	<1000
FAVE-O-HT	July 2007	1030	<1000
FAVE-O-HT-RDX	September 2007	940	<1000
FAVE-O-HT-RDX	January 2008	530	<1000
FAVE-O-HT-A2	May 2008	520	<1000
FAVE-O-HT-A2	September 2008	510	<1000
FAVE-L-HT-RDX	May 2008	560	<1000
FAVE-L-HT-A2	October 2008	530	<1000
FAVE-L-HT-A2	March 2009	540	<1000

Table 38. Gel time for each batch of FAVE resins with 0.2 weight-percent CoNap and 1 weight-percent Trigonox at 72 °F.

Resin	Date of Sample	Gel Time (min)
FAVE-L	May 2006	15
FAVE-L	June 2006	14
FAVE-L	July 2006	16
FAVE-L	March 2007	15
FAVE-L	May 2007	14
FAVE-O	May 2006	14
FAVE-O	July 2006	14
FAVE-L-25S	August 2007	24
FAVE-L-25S	September 2007	23
FAVE-L-25S	December 2007	22
FAVE-L-25S	January 2008	23
FAVE-L-25S-RDX	February 2008	22
FAVE-L-25S-RDX	July 2008	23
FAVE-L-25S-A2	December 2008	23
FAVE-L-25S-A2	April 2009	22
FAVE-O-25S	August 2006	18
FAVE-O-25S	February 2007	17
FAVE-O-25S	July 2007	15
FAVE-O-25S	September 2007	16
FAVE-O-25S	November 2007	16
FAVE-O-25S	December 2007	17
FAVE-O-25S-RDX	February 2008	16
FAVE-O-25S-RDX	June 2008	16
FAVE-O-25S-A2	December 2008	16
FAVE-O-25S-A2	April 2009	16
FAVE-O-HT	February 2007	30
FAVE-O-HT	July 2007	31
FAVE-O-HT-RDX	September 2007	31
FAVE-O-HT-RDX	January 2008	30
FAVE-O-HT-A2	May 2008	29
FAVE-O-HT-A2	September 2008	31
FAVE-L-HT-RDX	May 2008	31
FAVE-L-HT-A2	October 2008	31
FAVE-L-HT-A2	March 2009	30
Derakane 441-400	May 2007	29
Derakane 470HT-400	May 2007	40

Table 39. Modulus at 30 °C and T_g of API batch samples as measured using DMA.

Resin	Date of Sample	T _g (°C)	E' at 30° C (GPa)
FAVE-L	May 2006	102	2.6
FAVE-L	July 2006	101	2.7
FAVE-L	March 2007	107	2.7
FAVE-L	May 2007	104	2.7
FAVE-O	May 2006	106	2.7
FAVE-O	July 2006	107	2.6
FAVE-L-25S	August 2007	112	2.8
FAVE-L-25S	September 2007	111	2.8
FAVE-L-25S	December 2007	114	2.7
FAVE-L-25S	January 2008	110	2.8
FAVE-L-25S-RDX	February 2008	117	2.8
FAVE-L-25S-RDX	July 2008	118	2.9
FAVE-L-25S-A2	December 2008	118	2.8
FAVE-L-25S-A2	April 2009	117	2.9
FAVE-O-25S	August 2006	115	2.8
FAVE-O-25S	February 2007	114	2.7
FAVE-O-25S	July 2007	116	2.7
FAVE-O-25S	September 2007	115	2.8
FAVE-O-25S	November 2007	116	2.7
FAVE-O-25S	December 2007	115	2.8
FAVE-O-25S-RDX	February 2008	118	2.9
FAVE-O-25S-RDX	June 2008	119	2.8
FAVE-O-25S-A2	December 2008	118	2.9
FAVE-O-25S-A2	April 2009	118	2.7
FAVE-O-HT	February 2007	130	2.8
FAVE-O-HT	July 2007	131	2.7
FAVE-O-HT-RDX	September 2007	134	2.8
FAVE-O-HT-RDX	January 2008	135	2.8
FAVE-O-HT-A2	May 2008	134	2.8
FAVE-O-HT-A2	September 2008	134	2.8
FAVE-L-HT-RDX	May 2008	133	2.7
FAVE-L-HT-A2	October 2008	134	2.9
FAVE-L-HT-A2	March 2009	133	2.8

6.1.4 Resin Properties

6.1.4.1 Gel Time Adjustability. Gel time is a function of temperature and the concentration of the components in the initiator package. Gel time adjustability is important to be able to tune the working time of the resin for the particular part being fabricated. The initiator package includes the catalyst (CoNap), promoter (N,N-DMA), inhibitor (2,4-pentanedione [2,4-P] or hydroquinone) and initiator (Trigonox or MEKP). Ambient temperature and initiator package

component concentrations were varied systematically to show their effect on gel time. The results below show the effect of each of these variables on gel time.

The gel time of select batches were measured as a function storage time to determine stability of the FAVE resin. Table 40 shows that the gel time decreased slightly over time but for the most part remained fairly consistent over the period of 1 year for these resins, indicating good shelf life.

Table 40. Gel time for selected FAVE resins with 0.2 weight-percent CoNap and 1 weight-percent Trigonox as a function of storage time.

Resin	Date of Sample	Storage Time (months)	Gel Time (min)
FAVE-L-25S-RDX	February 2008	0	22
FAVE-L-25S-RDX	February 2008	3	22
FAVE-L-25S-RDX	February 2008	6	21
FAVE-L-25S-RDX	February 2008	9	21
FAVE-L-25S-RDX	February 2008	12	20
FAVE-L-HT-A2	May 2008	0	29
FAVE-L-HT-A2	May 2008	3	28
FAVE-L-HT-A2	May 2008	6	29
FAVE-L-HT-A2	May 2008	9	27
FAVE-L-HT-A2	May 2008	12	27

Table 41 shows the effect of temperature on gel time for constant concentrations of inhibitor packages. Clearly, the gel time decreased as ambient temperature increased. The table also shows that gel time decreased as CoNap or Trigonox content increased, which was expected since higher concentration of initiator and catalyst should result in more free-radical initiation sites.

The concentration of components also affects the gel time and can be used to adjust the gel time to desired working time (tables 42–44). The gel time results show clear trends that increasing the 2,4-pentanedione (2,4-P) inhibitor increased the gel time. The promoter (N,N-DMA), catalyst (CoNap), and Trigonox each result in a decreased gel time as their concentration increases. Furthermore, very short (<15 min) and long (>2 h) gel times were clearly achievable.

Table 41. Effect of temperature on the gel time of FAVE-L.

Temperature (°F)	Trigonox Content (weight-percent)	Cobalt Naphthenate (weight-percent)	N,N-DMA (weight-percent)	Hydroquinone (ppm)	2,4-P (weight-percent)	Gel Times (min)
71.6	1	0.14	0	100	0	262
80.6	1	0.14	0	100	0	212.5
89.6	1	0.16	0	100	0	39
71.6	1.5	0.14	0	100	0	117.5
89.6	1.5	0.14	0	100	0	40
71.6	1	0.39	0	100	0	87
80.6	1	0.37	0	100	0	55
71.6	1.5	0.37	0	100	0	44.5
80.6	1.5	0.38	0	100	0	32
71.6	1	0.51	0	100	0	42
80.6	1	0.50	0	100	0	35
89.6	1	0.51	0	100	0	23
71.6	1.5	0.50	0	100	0	36
80.6	1.5	0.50	0	100	0	30
89.6	1.5	0.51	0	100	0	17

Table 42. The effect of Trigonox content on gel time of FAVE-L at 72°F.

Trigonox Content (weight-percent)	Cobalt Naphthenate (weight-percent)	N,N-DMA (weight-percent)	Hydroquinone (ppm)	2,4-P (weight-percent)	Gel Times (min)
1	0.14	0	100	0	262
1.5	0.14	0	100	0	117.5
1	0.39	0	100	0	55
1.5	0.37	0	100	0	44.5
1	0.51	0	100	0	42
1.5	0.50	0	100	0	36

Table 43. The effect of CoNap content on gel time of FAVE-L at 72 °F.

Cobalt Naphthenate (weight-percent)	Trigonox Content (weight-percent)	N,N-DMA (weight-percent)	Hydroquinone (ppm)	2,4-P (weight-percent)	Gel Times (min)
0.09	1	0	100	0	313
0.14	1	0	100	0	262
0.30	1	0	100	0	72.5
0.39	1	0	100	0	55
0.51	1	0	100	0	42
0.10	1.5	0	100	0	404
0.14	1.5	0	100	0	117.5
0.50	1.5	0	100	0	36
0.37	1.5	0	100	0	44.5
0.25	1.5	0	100	0	64

Table 44. The effect of hydroquinone content on gel time of FAVE-L at 72 °F.

Hydroquinone (ppm)	Trigonox Content (weight-percent)	CoNap (weight-percent)	N,N-DMA (weight-percent)	2,4-P (weight-percent)	Gel Times (min)
100	1	0.14	0	0	262
200	1	0.17	0	0	128.5
100	1	0.30	0	0	72.5
200	1	0.27	0	0	99
100	1	0.39	0	0	55
200	1	0.38	0	0	80.5
100	1	0.51	0	0	42
200	1	0.50	0	0	47.5

The gel time of FAVE-O-25S was compared to that of Derakane 8084 using the same catalyst (0.3 weight-percent CoNap) and initiator content (2 weight-percent Trigonox) measured at 70 °F (figure 33). The results show similar trends, but the FAVE resin cured much faster for the same initiator package. This is a result of the higher crosslinker content in FAVE-O-25S and possibly due to additional inhibitor in the Derakane 8084 added by the manufacturer during preparation.

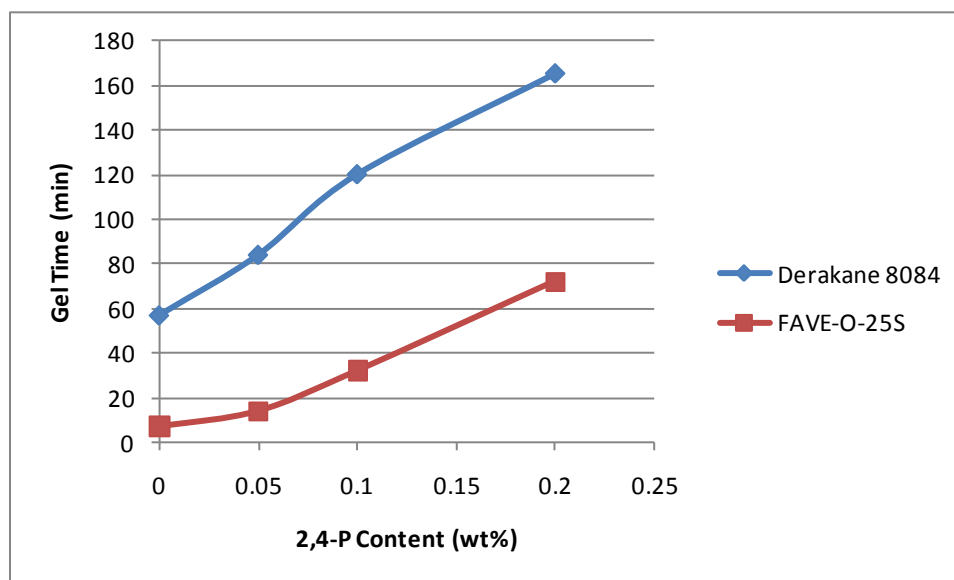


Figure 33. Gel time as a function of 2,4-P content for Derakane 8084 and FAVE-O-25S at 70 °F using 0.3 weight-percent CoNap and 2 weight-percent Trigonox.

Both MEKP and Trigonox were used throughout this demonstration/validation program. The gel times of resins using the same concentrations of these initiators results in slightly different gel times.

Appendix D shows that the desired amount of initiator package is the minimum content to achieve the proper working time. The initiator does cause a noticeable plasticization of the resin, thereby reducing the T_g . Appendix D also contains other gel time testing results.

Various other concentrations of initiators, catalysts, promoters, and inhibitors were used. Overall, the results clearly show that the gel time of FAVE resins can be varied from as long as a few hours to as short as a few minutes. Furthermore, the viscosity of VE resins, including the FAVE resins, is fairly constant until the gel time. At the gel time, the viscosity of the resins increases rapidly. Thus, the processing of FAVE resins should only depend on the initial viscosity and not the gel time, as this will be adjustable for liquid molding of any composite part.

6.1.4.2 Commercial Neat Resin Properties. The neat resin properties of the commercial resins are shown in table 45. The properties of the commercial resins are good with a combination of low viscosity and fairly high thermal properties.

Table 45. Properties of the commercial resins used in this work.

Resin	Viscosity (cP)	T_g Dry ($^{\circ}$ C)	T_g Wet ($^{\circ}$ C)	Flex Modulus (MPa)	Flex Str (GPa)	G_{IC} (J/m ²)
Corve 8100	200	128	119	3.0	125	150
Hexion 781-2140	300	130	121	3.0	130	160
Derakane 8084	600	115	103	2.8	120	650
Derakane 441-400	550	142	128	3.1	120	100
Hetron 980/35	500	130	119	3.0	120	150
Huntsman 8605	550	158	140	2.6	120	200

6.1.4.3 Neat Resin Viscosity. The neat resin viscosity at 25 $^{\circ}$ C for the commercial and FAVE resins, including all variants, is shown in figure 34. The results show that some FAVE formulations have much higher viscosities than the commercial resins. In particular, FAVE-L and FAVE-O have the highest viscosities. Some of the variants, in particular the -A1 and -A2 variants, have viscosities that are similar to those of some of the commercial resins. The FAVE-L/O-25S and FAVE-L/O-HT had moderate viscosities that were comparable to those of some of the higher viscosity commercial resins. However, the results clearly show that some of the commercial resins with high styrene contents like the Corve 8100 and Hexion 781-2140 have significantly lower viscosities than all of the FAVE resins. The reason for this is the MFA monomers have a much higher viscosity (~50–70 cP) relative to styrene (<1 cP).

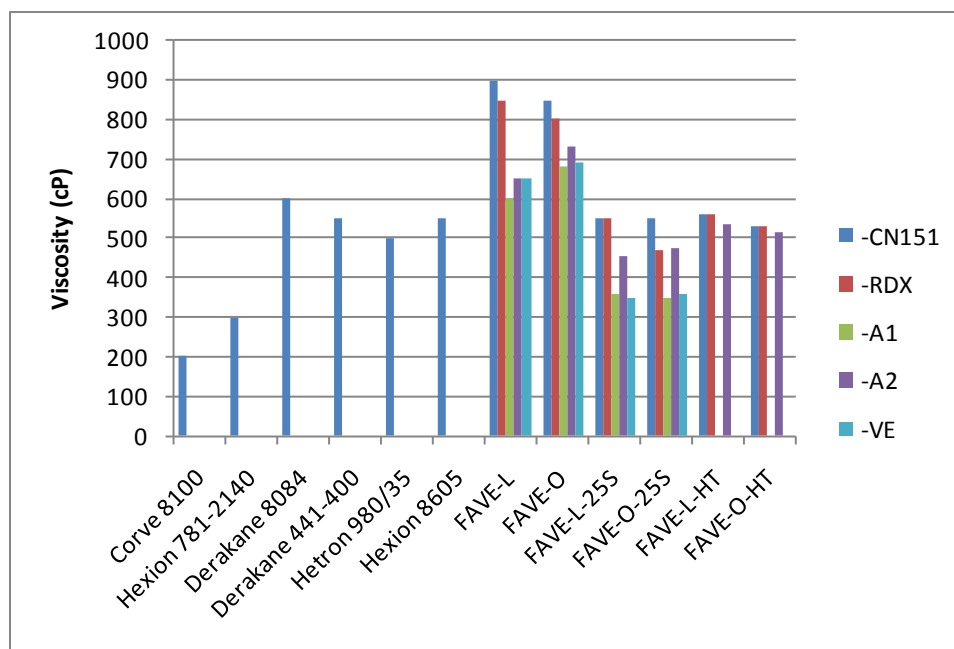


Figure 34. Viscosity of commercial and FAVE resins at 25 °C.

6.1.4.4 Neat Resin Glass Transition Temperature. The glass transition temperature was measured for the various commercial and FAVE resin formulations (figure 35). Like the viscosity, the glass transition temperature of the FAVE-L and FAVE-O are considerably worse (lower) than that of the commercial resins. The variants do have significantly better performance but still have considerably lower T_g . Variants of the FAVE-L/O-25S have T_g similar to that of most of the commercial resins. In fact, the FAVE-L/O-HT resins have T_g higher than that of all the commercial resins except the epoxy (Huntsman 8605).

The wet glass transition temperature, measured after saturation with water, is shown in figure 36. The results are similar to those of the dry T_g , but in general, the FAVE resins had a smaller reduction in T_g when wet relative to the commercial resins. T_g reduction for FAVE resins was generally <10 °C, while the commercial resins had T_g reductions >10 °C. This result is likely due to the higher crosslink density of the FAVE resins (8, 13). Frequency dependence of the T_g is presented in appendix E.

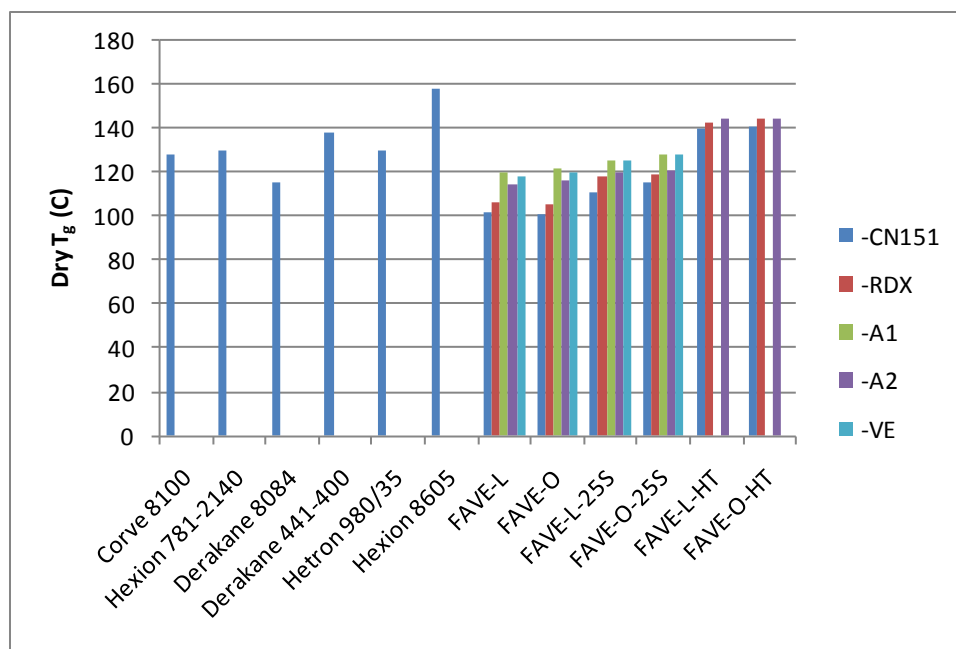


Figure 35. Dry glass transition temperature of commercial and FAVE resins.

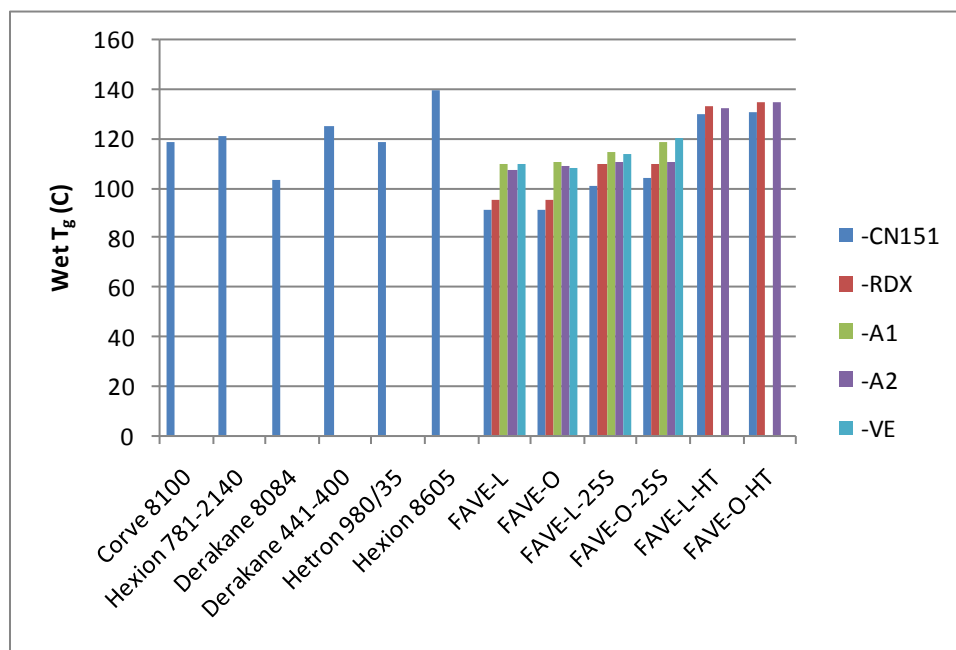


Figure 36. Wet glass transition temperature of commercial and FAVE neat resins.

Water Susceptibility of MFA Modified Vinyl Ester Resins

Water was detrimental to the T_g of resins as the role of plasticizer. Particularly for those resin systems containing hydrophilic components, the outcomes are even worse. Accordingly, wet T_g is defined as the measured T_g of a resin sample after conditioning in water or moisture environment for a designated period of time. The protocol for this measurement was designed by ARL with details described in the report of ARL-RP-184 (appendix E). Hot/wet T_g of low-VOC resins was measured, along with the commercial ones for a comparison. The results showed that the low-VOC resins exhibit similar water resistance to those commercial ones with high styrene content, which constitutes another merit of the developed low-VOC VE resin.

Water Resistance Evaluation of Low-VOC Vinyl Esters

Based on this testing method, the wet T_g of MFA modified low-VOC VEs was evaluated, along with the commercial ones for a comparison. According to the hot/wet T_g values presented in figure 37, it can be deduced that although the MFA does absorb some water, the MFA modified VEs exhibit comparable water resistance capability to commercial high styrene content VE resins.

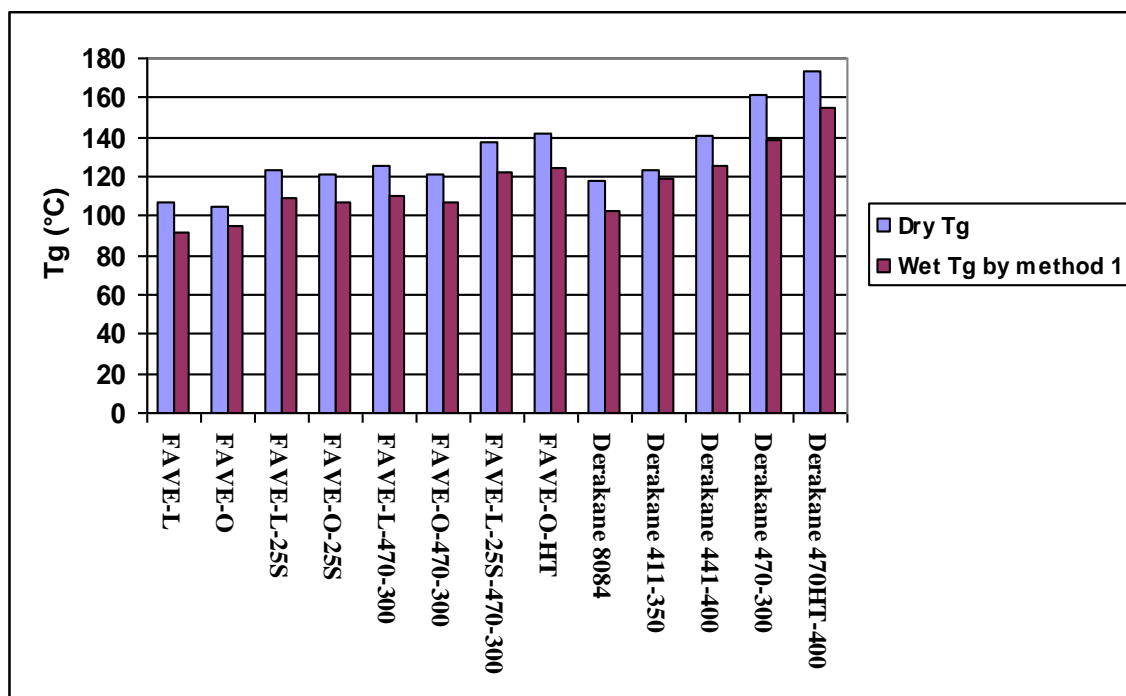


Figure 37. Hot/wet T_g of MFA modified VEs compared with commercial ones.

6.1.4.5 Neat Resin Flexural Properties. The flexural modulus (figure 38) and strength (figure 39) of the FAVE and commercial resins were measured. Except for the Derakane 8084, the differences in moduli are not significant. Derakane 8084 has a lower modulus because of the toughened nature of that resin. The flexural strengths are also very similar and are not significantly different for the most part.

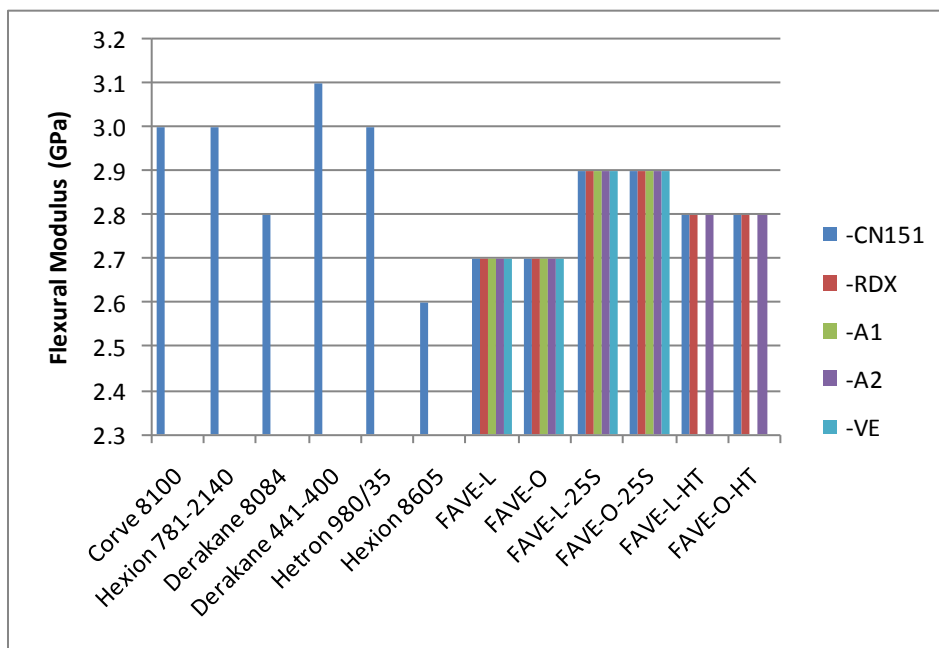


Figure 38. Flexural modulus of commercial and FAVE neat resins.

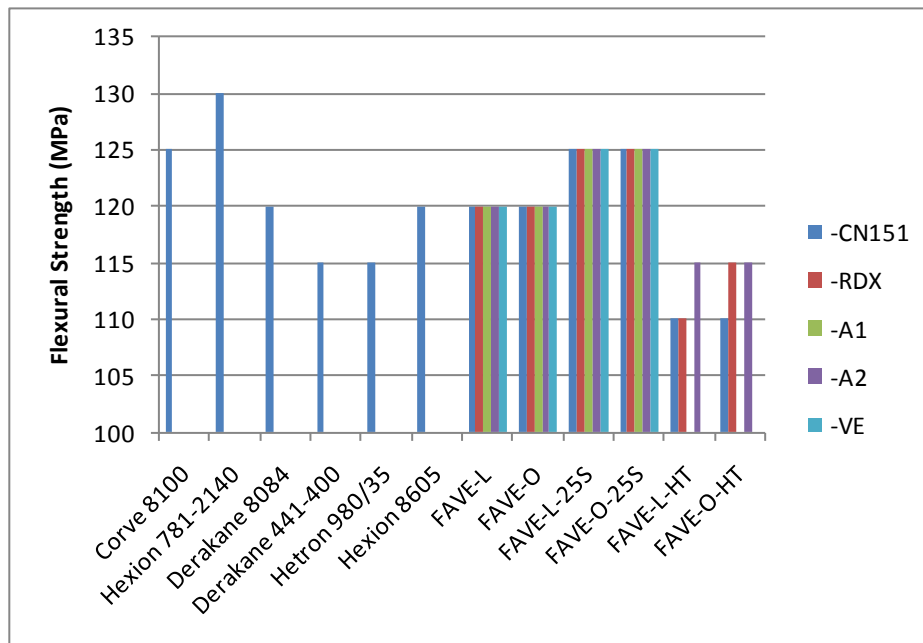


Figure 39. Flexural strength of commercial and FAVE neat resins.

6.1.4.6 Neat Resin Fracture Toughness. The fracture toughness of the commercial and FAVE resins is shown in figure 40. Clearly, the Derakane 8084 has the highest fracture toughness. Otherwise, the FAVE-L/O and FAVE-L/O-25S resins have similar or better fracture toughness relative to the commercial resins. The FAVE-L/O-HT resins have lower fracture toughness than the other FAVE resins because of the brittle novolac nature of the resin.

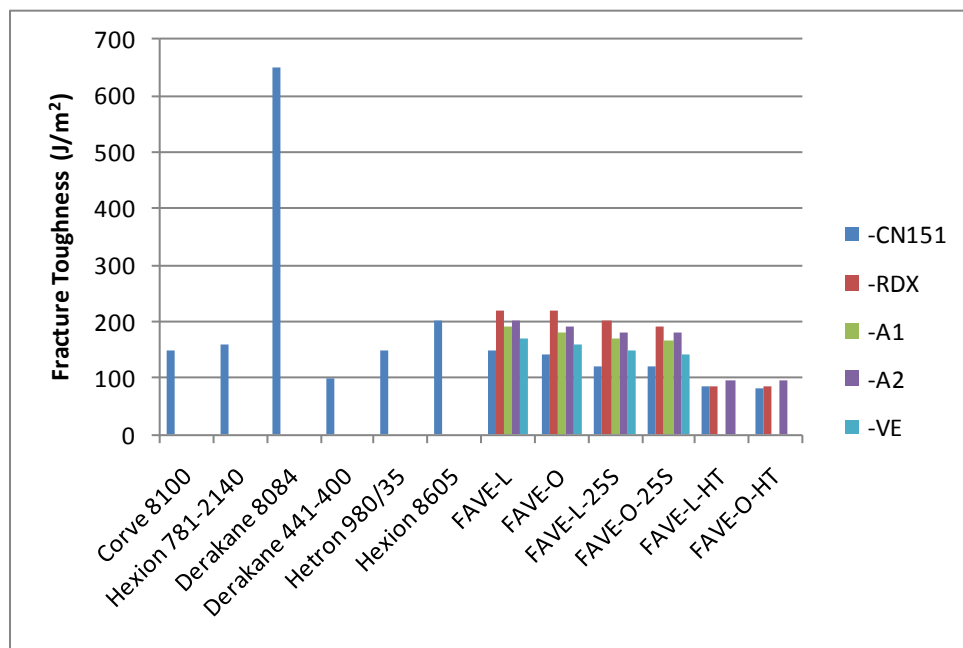


Figure 40. The fracture toughness of the commercial and FAVE neat resins.

6.1.5 Composite Panel Testing Results

6.1.5.1 Fatigue Behavior of Low-VOC Vinyl Ester Resins. The repetitive loading of a composite material causes degradation due to the accumulation of discrete micro-damage (e.g., fiber fractures, fiber/matrix debonds, and matrix cracks) or macro-crack propagation, aided in some by an aggressive environment, including moisture. Therefore, a fatigue test has to be carried out to assess the resistance of a material to repetitive loading. One important benefit from this test is to ensure that the fatigue life is greater than required, and/or the replacement life is identified. Accordingly, a fatigue test is of great importance for engineers in designing novel materials.

The purpose of this study is to compare the fatigue behavior of the developed low-VOC VE resin with that of the commercial ones. FAVE-O-25S was used as a model resin to this end. Its fatigue behavior was evaluated based on the procedure designed by ARL as illustrated in the following part. The results show that FAVE-O-25S exhibits comparable fatigue behavior to that of the commercial resin of Hexion.

As illustrated by figures 41 and 42, FAVE-O-25S possesses similar flexural behavior to that of Hexion, with flexural strength as 530 and 550 MPa, respectively, and elasticity modulus as 19 and 18 GPa, respectively. After a dynamic fatigue test wherein force in a sine wave mode with maximum value equals to 80%, 60%, and 40% of flexural strength of each resin system was loaded on each sample and continued for 10,000 cycles, both flexural strength and elasticity moduli for these two resin systems exhibit a declining trend with the increase of cycling load on samples. Moreover, this trend is duplicated for both resin systems, indicating a similar fatigue behavior presented by two resins, with a minor exception when the cycling load is equivalent to 40% of flexural strength. In the case of load equivalent to 40% of flexural strength, after 10,000 cycles, FAVE-O-25S exhibited lower value in both flexural strength and elasticity modulus. Since only one data point was given to each test condition, this deviation may also be attributed to the experimental error.

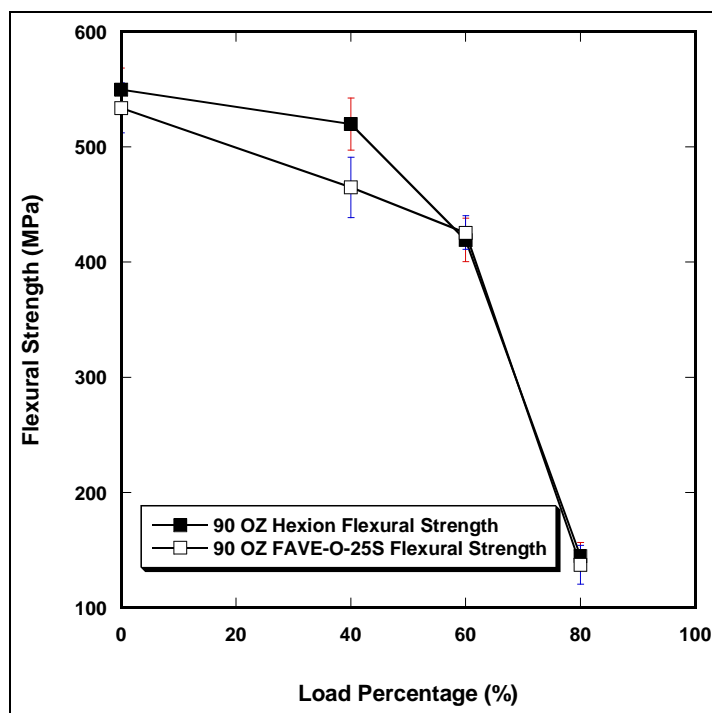


Figure 41. Residual flexural strength of resins after 10,000 cycles.

The fatigue life is plotted as a function of residual strength and elasticity modulus for flexural tests in figures 43 and 44, respectively. The flexural performance of pure Derakane 411-350 resin exhibits decreasing trend with increasing cycles and fails completely after 250,000 cycles. On the other hand, for the 10% BR toughened resin, the flexural performance is fully retained under the same test conditions. Even though the strength of the bio-rubber samples is lower before fatigue, for 100,000–350,000 cycles, the bio-rubber has significantly higher strength. The constant performance of the biorubber samples is under investigation, but is likely a result of toughening that blunts or prevents the formation of microcracks.

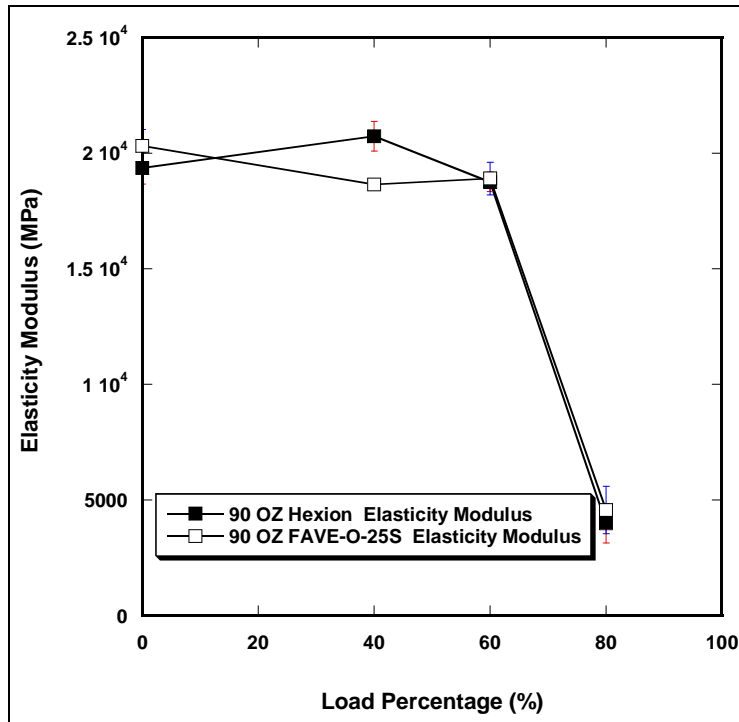


Figure 42. Residual elasticity modulus of resins after 10,000 cycles.

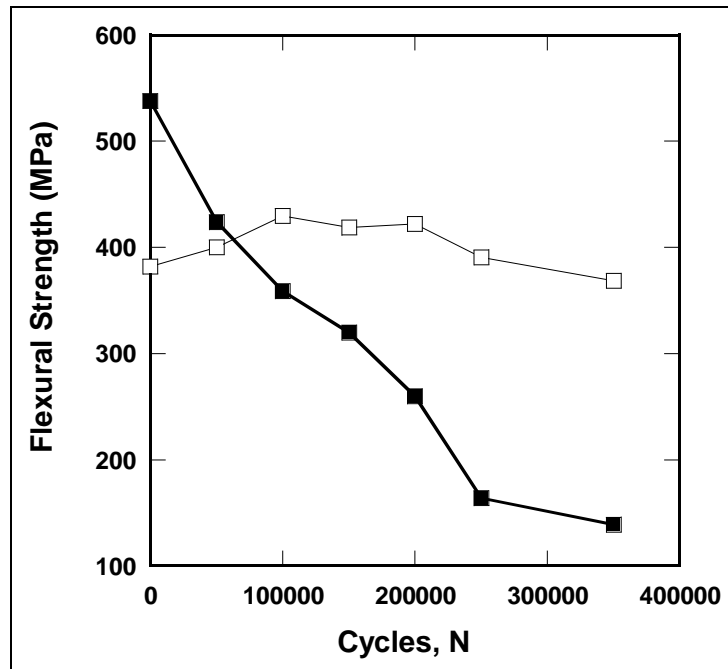


Figure 43. Fatigue life vs. strength for flexural loading conditions. The black line represents Derakane 411-350, and the white is 10% bio-rubber toughened.

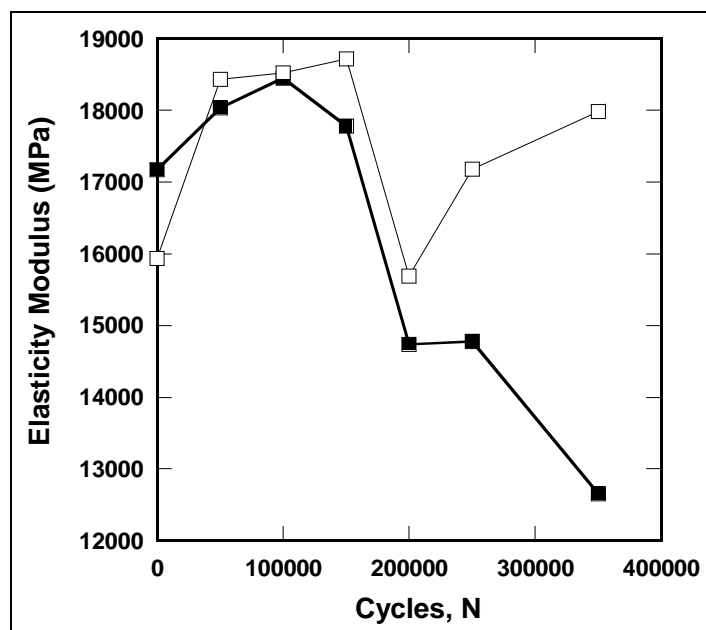


Figure 44. Fatigue life vs. elasticity modulus for flexural loading conditions. The black line represents Derakane 411-350, and the white is 10% bio-rubber toughened.

6.1.5.2 Environmental and Chemical Aging. Environmental and chemical aging procedures conducted on the various composites were determined based on the anticipated exposure to environmental and chemical agents over the working lifetime of the composite parts (as summarized in table 9). None of the actual aging tests are exact applications of a standard test but rather are based on standard testing methods listed in test method standard MIL-STD-810F (environmental engineering considerations and laboratory tests) and consultation with ESTCP program partners. Duration and intensity of the exposure was chosen so as to demonstrate some decrease in mechanical and thermal properties over the period of aging. Environmental aging was performed on all commercial and FAVE composites and included wet T_g , freeze/thaw cycling and xenon arc lamp weathering. Chemical aging included exposure to various chemical agents (method 504: Contamination by Fluids), which were selected as a hydro-carbon fuel (JP-8), a solvent (methyl ethyl ketone), and salt water exposure for the Navy composites, exclusively.

Flexural Properties

The flexural properties are shown in figures 45 and 46. The results are presented such that multiple resins using the same fibers are next to each other. The results show baseline results tested at room temperature and after JP-8 and xenon weathering. In general, none of the weathering resulted in significant reduction in properties. It should be noted that the high flexural stiffness for 96-oz/Derakane 441-400 is not believed to be correct. Furthermore, the composites using FAVE resins performed similarly before weathering and after weathering relative to composites using commercial resins.

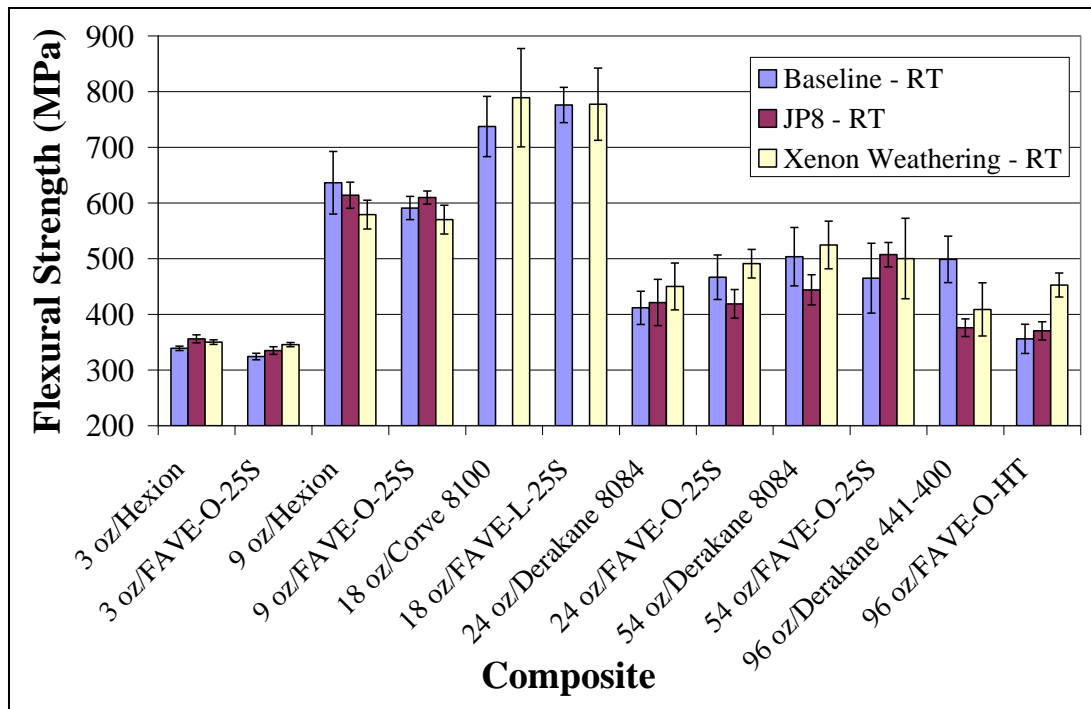


Figure 45. Flexural strength of commercial and FAVE composites showing baseline (no aging), JP8 aging, and xenon weathering.

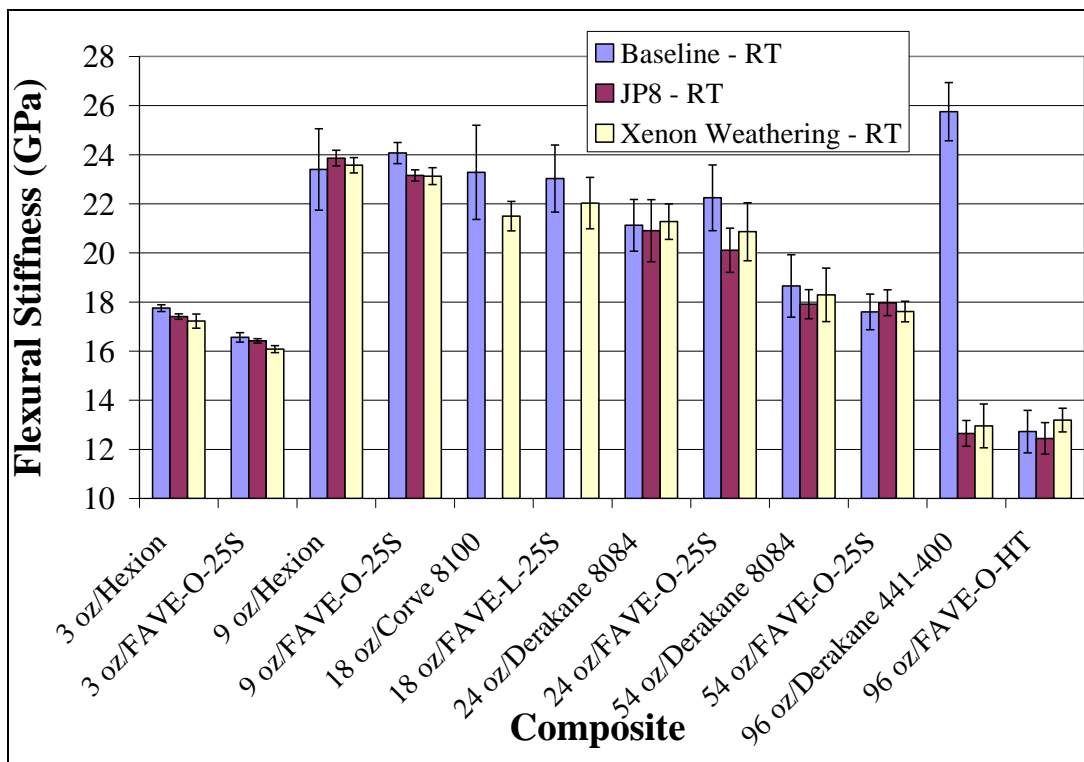


Figure 46. Flexural stiffness of commercial and FAVE composites showing baseline (no aging), JP8 aging, and xenon weathering.

Short Beam Shear Properties

SBS properties were affected to some degree by chemical exposure or weathering (figure 47). In particular, freeze/thaw cycles clearly reduced the SBS strength of most composites. In fact, freeze/thaw of 9-oz/Hexion 780-2140 resulted in halving the SBS strength. Xenon weathering most significantly affected the properties of the 54-oz fiberglass for both the FAVE and commercial resin and is thus more likely an issue with the fiber rather than the resin. For the most part, the composites using FAVE resins performed similarly before weathering and after weathering relative to composites using commercial resins.

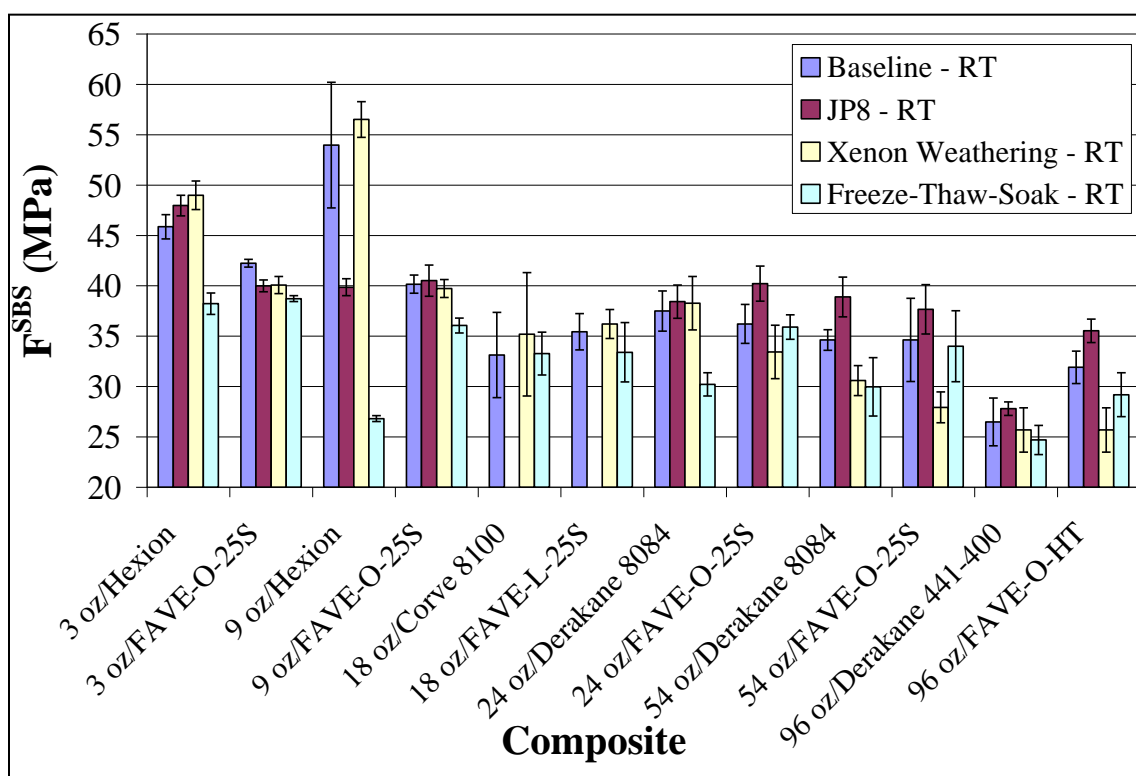


Figure 47. SBS strength of commercial and FAVE composites showing baseline (no aging), JP8 aging, xenon weathering, and freeze-thaw-soak cycle aging.

Saltwater immersion tests were performed on the Navy composites, as this would be the only application where the composite would be continually exposed to saltwater. The flexural strength and stiffness and SBS strengths are shown in figure 48. The results show that a composite made with FAVE resin performs similarly to that of the incumbent resin. When comparing to figures 45–47, saltwater immersion caused little reduction in properties of the composite.

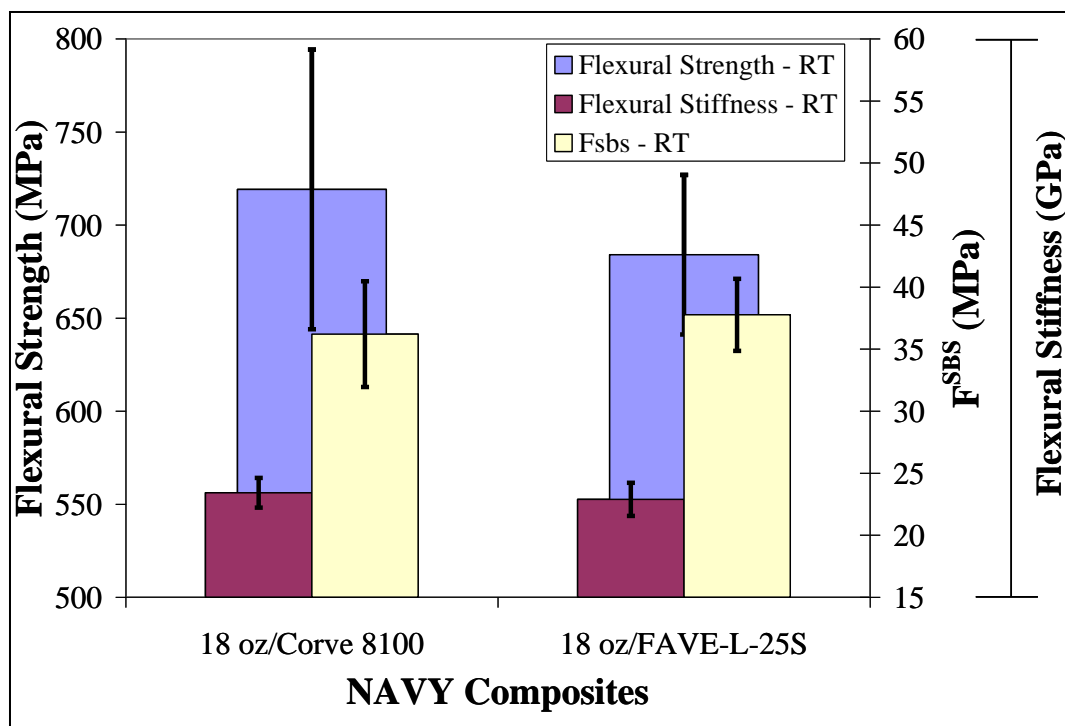


Figure 48. Flexural properties for Navy composites subject to simulated saltwater immersion aging.

Immersion in MEK had its largest effect on composites using the fine-weave fiberglass in the aircraft structures. Figure 49 shows the properties for Air Force composite panels subjected to MEK immersion. Comparing this to figures 45–47 shows that the composites made with the commercial Hexion resin had significantly reduced stiffness, flexural strength, and SBS strength after exposure. However, the composites made using the FAVE resin retained their properties. Previous results clearly showed that FAVE resins have little to no styrene remaining after cure, while VE/styrene has as much as 40% unreacted styrene. Thus, the changes shown in figure 49 are likely the effect of MEK extracting free-styrene from the Hexion composite, whereas the MEK is unable to extract significant quantities of material in the FAVE.

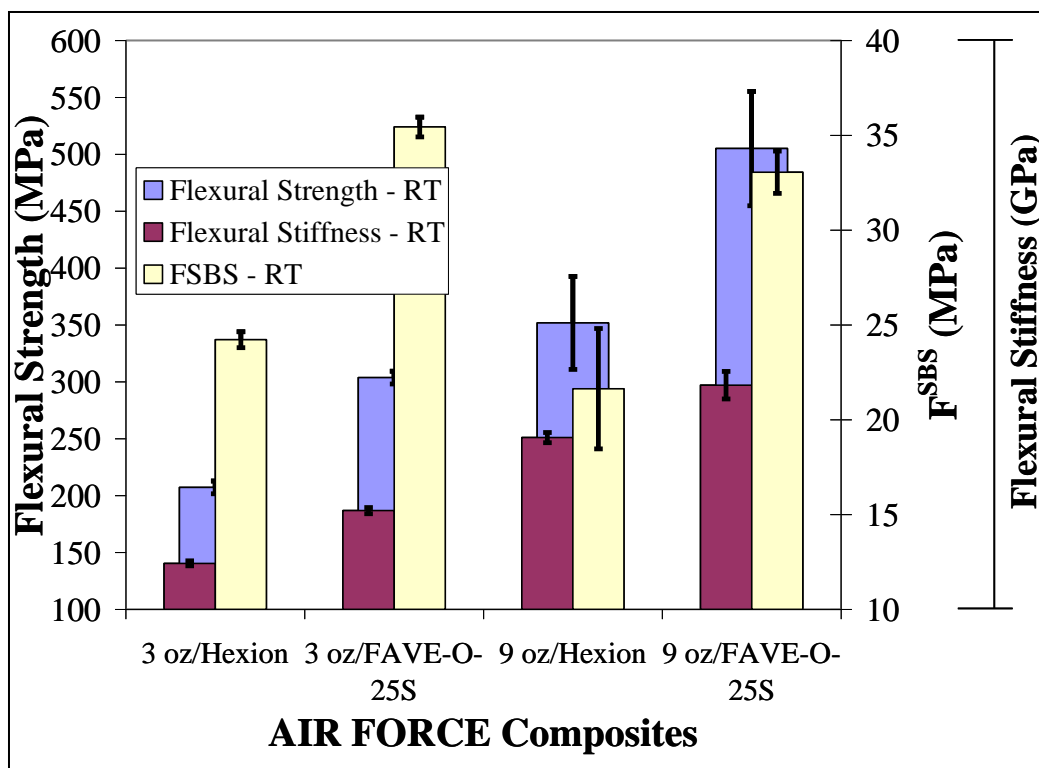


Figure 49. Flexural properties for Air Force composites subject to MEK immersion aging.

The T_g was measured as a function of weathering. Figure 50 shows the effect of water on these composites. Clearly, the wet T_g for all of the composites is reduced by water immersion. The range of T_g reduction is from 1 to 10 °C. However, when the sample is dried by heating the sample in the dynamic mechanical analyzer (second run), the T_g increased to higher than that of the original T_g . This is due to additional postcure and the washing out of unreacted plasticizer components. Again, the results show similar properties of FAVE composites relative to composites made using commercial resins. Figure 51 again shows little effect of xenon or JP-8 weathering. Freeze/thaw reduced T_g similarly to standard water immersion. MEK immersion again significantly reduced the T_g of the composites using the 3- and 9-oz fibers with the Hexion resin. Similar composites made using the FAVE resins were affected to a much lesser degree.

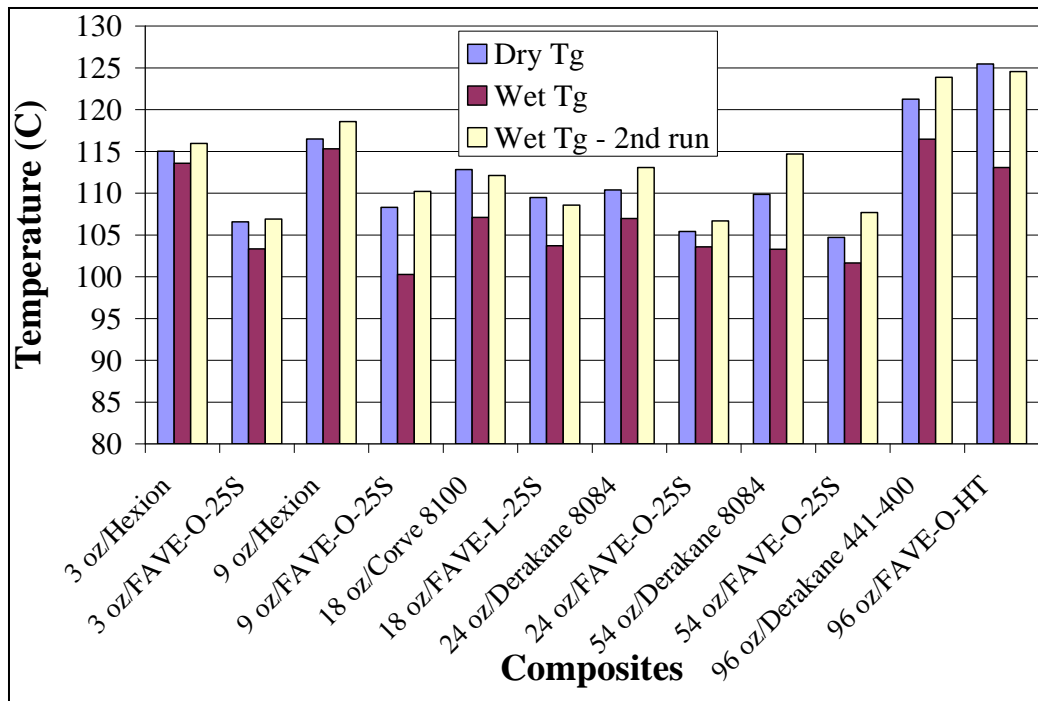


Figure 50. Dry and wet glass transition temperatures for commercial and FAVE composites.

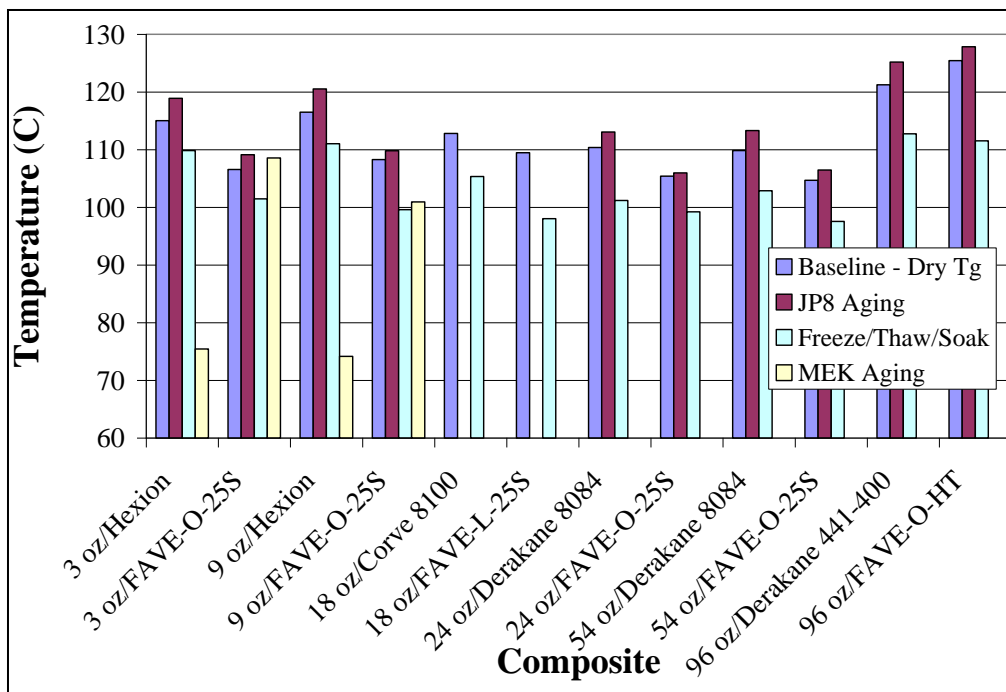


Figure 51. Glass transition temperatures (dry) for commercial and FAVE composites showing baseline (no aging), JP8 aging, freeze-thaw-soak aging, and MEK aging.

6.1.5.3 Air Force Composite Panel Testing Results. Air Force composite panel testing results are shown in appendix F. The results indicate that composites made using the FAVE resins (FAVE-L, FAVE-L-25S, and FAVE-O-25S) behaved similarly relative to composites made using the Hexion resin (table 46). It should be noted that T_g was measured using Differential Scanning Calorimetry at a ramp of 20 °C/min according to the ASTM standard, resulting in a higher T_g than was determined using DMA. Nonetheless, the trends are the same, as they show the FAVE-L had the lowest T_g , the FAVE-L-25S/-O-25S had moderate T_g 's, and the Hexion composite had the highest T_g .

Table 46. The properties of Air Force composite coupons.

Property	FAVE-L	FAVE-O-25S	FAVE-L-25S	Hexion 781-2140
Tensile strength (ksi)	32.4 ± 1.5	33.5 ± 1.5	33.9 ± 1.5	35 ± 1.5
Tensile modulus (ksi)	2601 ± 100	2503 ± 100	2513 ± 100	2641 ± 100
Compressive strength (ksi)	17.6 ± 1.5	18.4 ± 1.5	20.6 ± 1.5	21.1 ± 1.5
Compressive modulus (ksi)	3309 ± 150	3503 ± 175	3380 ± 150	3596 ± 200
SBS strength (ksi)	17.8 ± 1.5	18.1 ± 1.5	20.6 ± 1.5	17.7 ± 1.5
T_g (°C)	139.9	—	—	145.9

6.1.5.4 Navy Composite Panel Testing Results. The following test plan was developed to characterize the room temperature dry (RTD) properties of glass fiber reinforced FAVE-L-25S, Derakane 510A, and CORVE 8100 composite systems. The Derakane 510A resin was tested so as to provide baseline materials properties for a non-low-VOC resin system currently in use in Navy applications. The CORVE 8100 was also tested, as it is the current resin system used in the MCM rudder application. The test plan consisted of physical attribute characterization, such as fiber volume fraction and density and mechanical testing, to determine the tensile, compressive, shear, and toughness properties. Initial studies also looked at the gel time for different formulations and also the flow rate through the fabricated panels.

The density of both the neat resin and composite pieces taken from each panel was tested according to the guidelines of ASTM D 792. The results are summarized in table 47. The results show fairly consistent composite panel densities for the 8-ply composite panel regardless of ply layout.

Table 47. Summary of density measurements (ASTM D 792).

Panel	Type	Density (g/cm ³)
—	Neat resin FAVE-L-25S	1.17 ± 0.002
—	Neat resin Derakane 510A	1.35 ± 0.008
—	Neat resin CORVE 8100	1.14
070801	Composite FAVE-L-25S	1.84 ± 0.003
070903	Composite Derakane 510A	1.91 ± 0.005
080304	Composite CORVE 8100	1.83 ± 0.002

The fiber, resin, and void fraction were determined using the burnout method described in ASTM D 3171. An E-glass fiber density was assumed to be 2.59 g/cm³ for these calculations.* The results of these tests are shown in table 48. Detailed specimen level results are shown in appendix G.

Table 48. Summary of constituent material measurements (ASTM D 3171).

Panel	Type	% Fiber Volume Fraction	% Resin Volume Fraction	% Void Volume Fraction
070801	Composite FAVE-L-25S	47.9 ± 0.2	51.5 ± 0.3	0.6 ± 0.2
070903	Composite Derakane 510A	47.0 ± 0.4	51.7 ± 0.4	1.30 ± 0.06
080304	Composite CORVE 8100	49.6 ± 0.2	49.6 ± 0.2	0.82 ± 0.03

Tension Testing

The tension tests were performed in the same manner as in the previous FAVE-L-20S section. The results of test are shown in table 49, and figures 52 and 53. Detailed specimen-level results are included in appendix G. The results indicate the FAVE-L-20S, FAVE-L-25S, and Derakane 510A composite systems all appear to exhibit similar tensile strengths and tensile modulus within the uncertainty of the test. The CORVE 8100 composite appears to have a slightly higher tensile strength and modulus.

*Fiber Glass Industries (www.fiberglassindustries.com).

Table 49. ASTM D 638 tension test results.

Panel ID	Type	Tensile Strength (ksi)	Elastic Modulus ^a (Msi)
061001	Composite FAVE-L-20S (0°)	89.9 ± 3.9	4.8 ± 0.07
070801	Composite FAVE-L-25S (0°)	88.6 ± 5.8	4.6 ± 0.3
070903	Composite Derakane 510A (0°)	86.0 ± 3.9	4.6 ± 0.2
08304	Composite CORVE 8100 (0°) (90°)	103.2 ± 4.1	5.1 ± 0.4
		15.6 ± 0.6	2.1 ± 0.1

^aRange of 1000 to 3000 in/in.

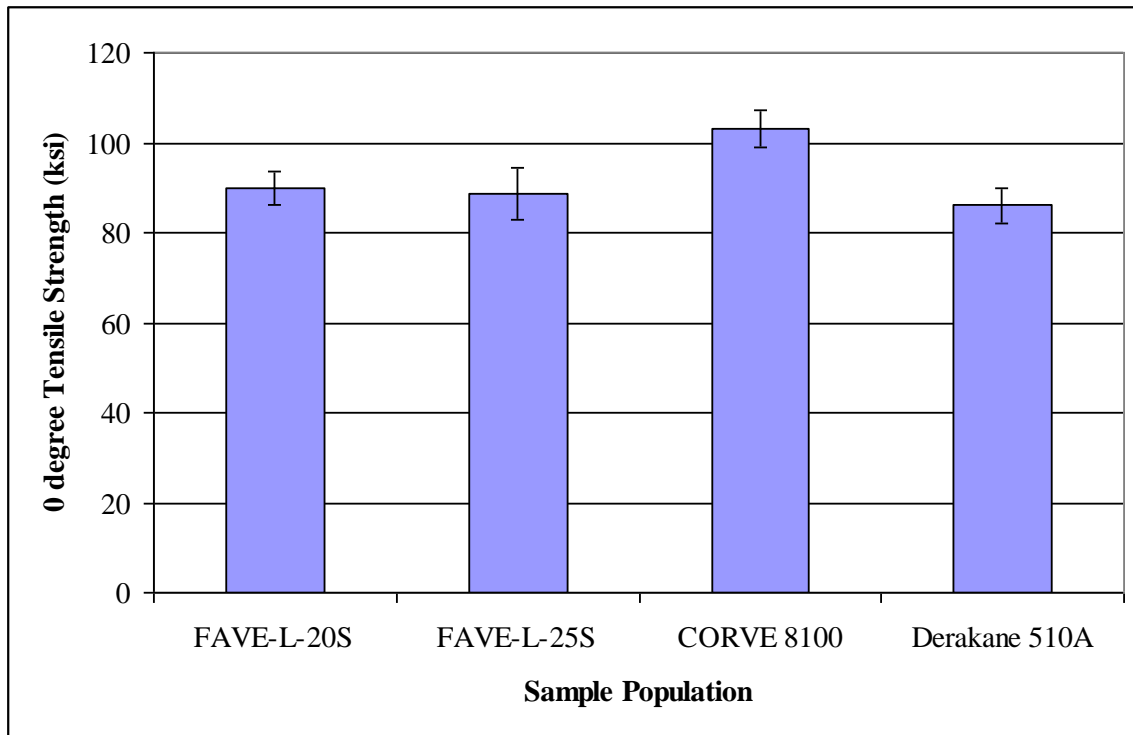


Figure 52. Tensile strength results.

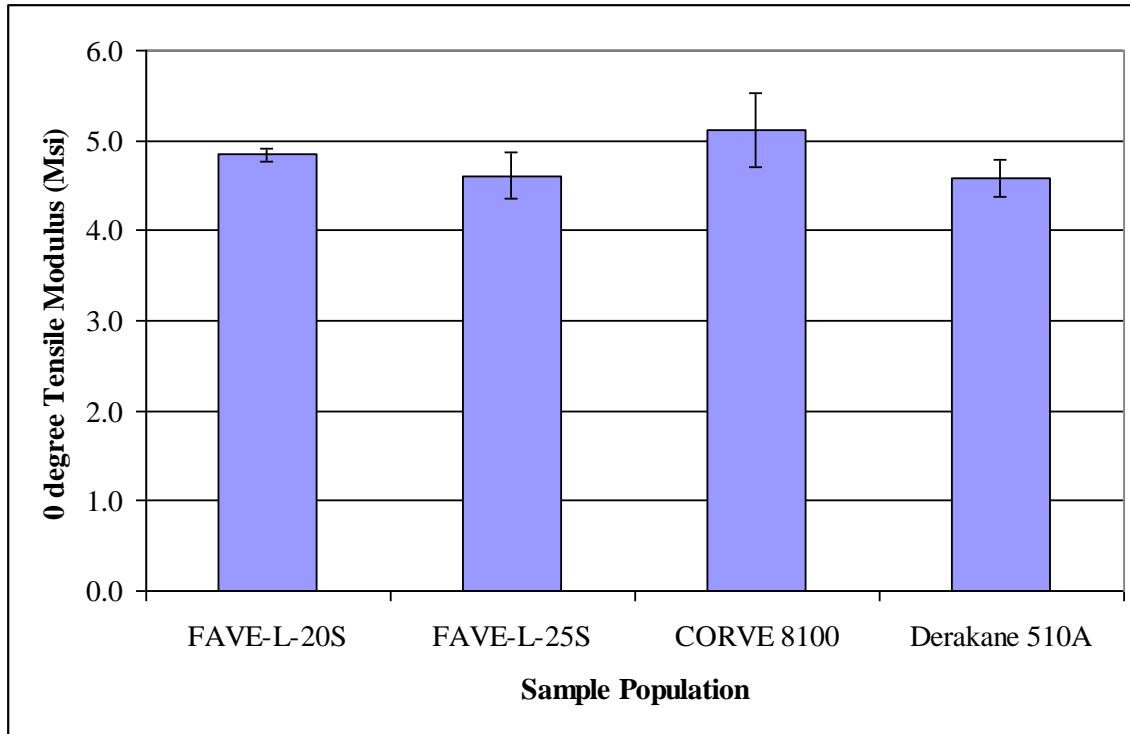


Figure 53. Tensile modulus results.

Compression Testing

The compression tests were performed in the same manner as the FAVE-L-20S in the previous section. The results of test are shown in table 50 and figures 54 and 55. Detailed specimen-level results are included in appendix G. The results indicate that the FAVE-L-25S, Derakane 510A, and CORVE 8100 composite systems exhibit significantly higher compressive strengths than the FAVE-L-20S. All three resin systems exhibit comparable compressive moduli. The FAVE-L-25S exhibits a higher strength but a lower modulus than the current 8100 MCM rudder material.

Table 50. ASTM D 695 compression test results.

Panel ID	Type	Compressive Strength (ksi)	Elastic Modulus ^a (Msi)
061001	Composite FAVE-L-20S (0°)	53.6 ± 6.0	5.03 ± 0.3
070801	Composite FAVE-L-25S (0°)	83.0 ± 2.2	4.52 ± 0.2
070903	Composite Derakane 510A (0°)	79.3 ± 4.0	4.5 ± 0.2
08304	Composite CORVE 8100 (0°) (90°)	63.1 ± 4.4	5.1 ± 0.6
		21.8 ± 0.6	1.8 ± 0.1

^aRange of 1000 to 3000 in/in.

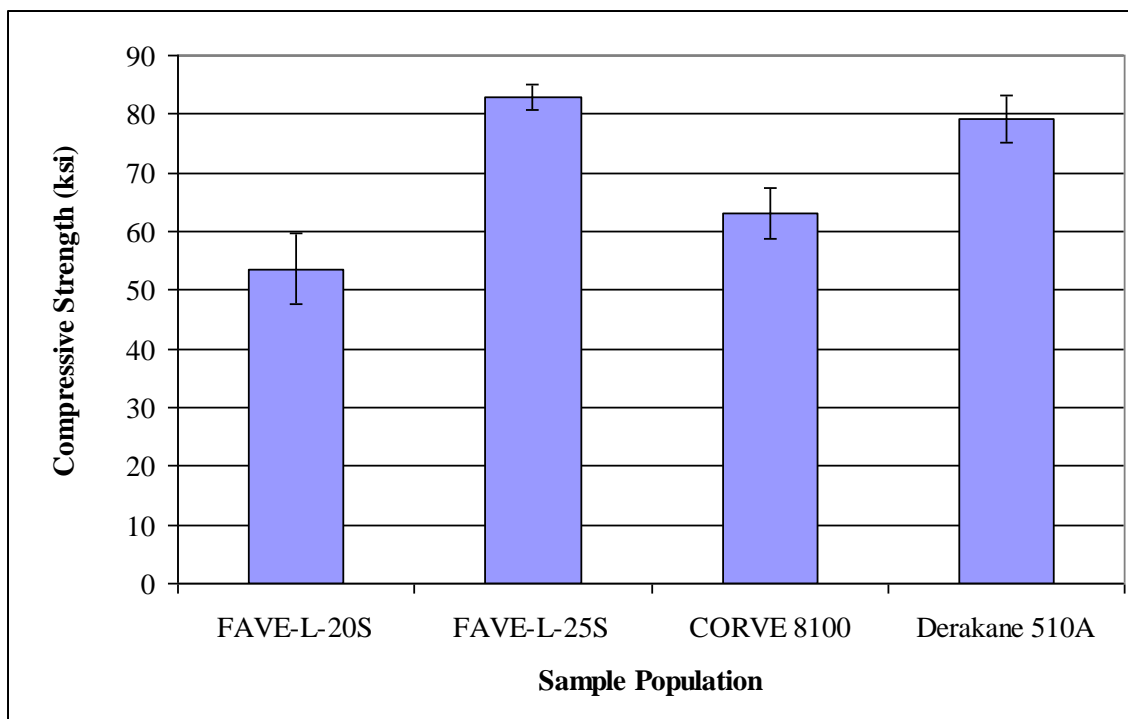


Figure 54. Compressive strength results.

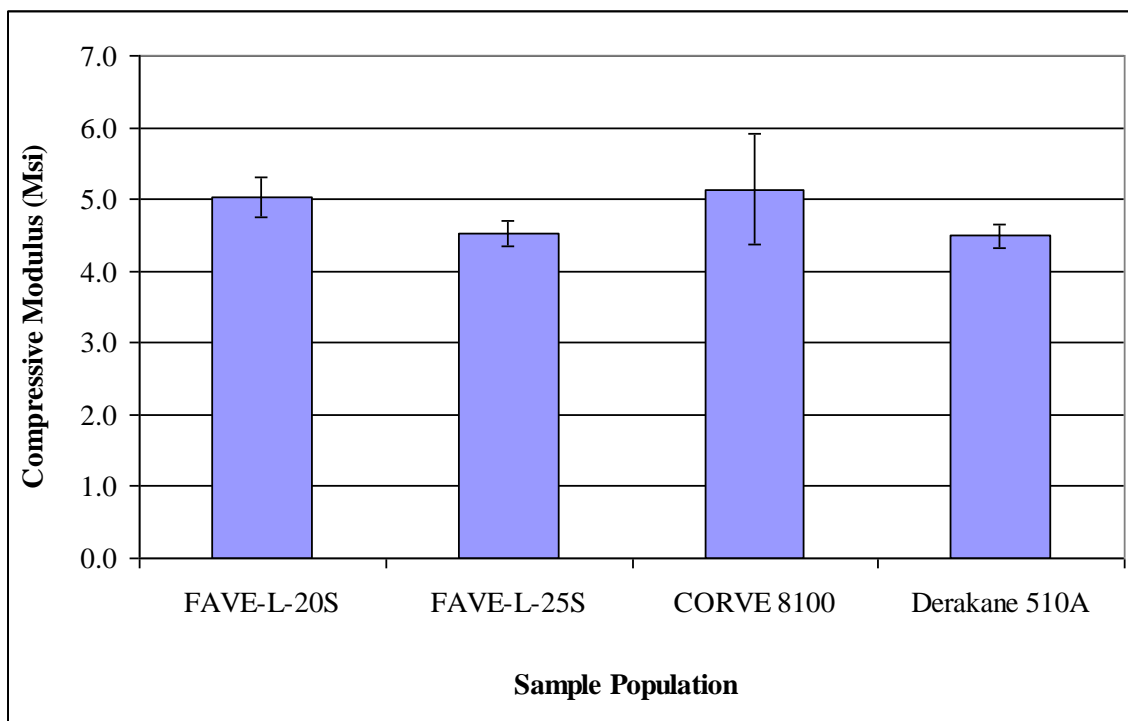


Figure 55. Compressive modulus results.

Shear Testing

The shear tests were performed according to ASTM D 2344 (Short Beam Shear). The results of test are shown in table 51 and figure 56. Detailed specimen-level results are included in appendix G. The results indicate the FAVE-L-20S and FAVE-L-25S appear to have slightly higher SBS strengths than the CORVE 8100 and Derakane 510A composite systems.

Table 51. Shear test results (ASTM D 2344).

Panel ID	Type	Shear Strength (ksi)
070201	Composite FAVE-L-20S (0°)	7.1 ± 0.3
070801	Composite FAVE-L-25S (0°)	7.2 ± 0.03
070903	Composite Derakane 510A (0°)	6.2 ± 0.03
08304	Composite CORVE 8100 (0°) (90°)	6.5 ± 0.1 4.0 ± 0.2

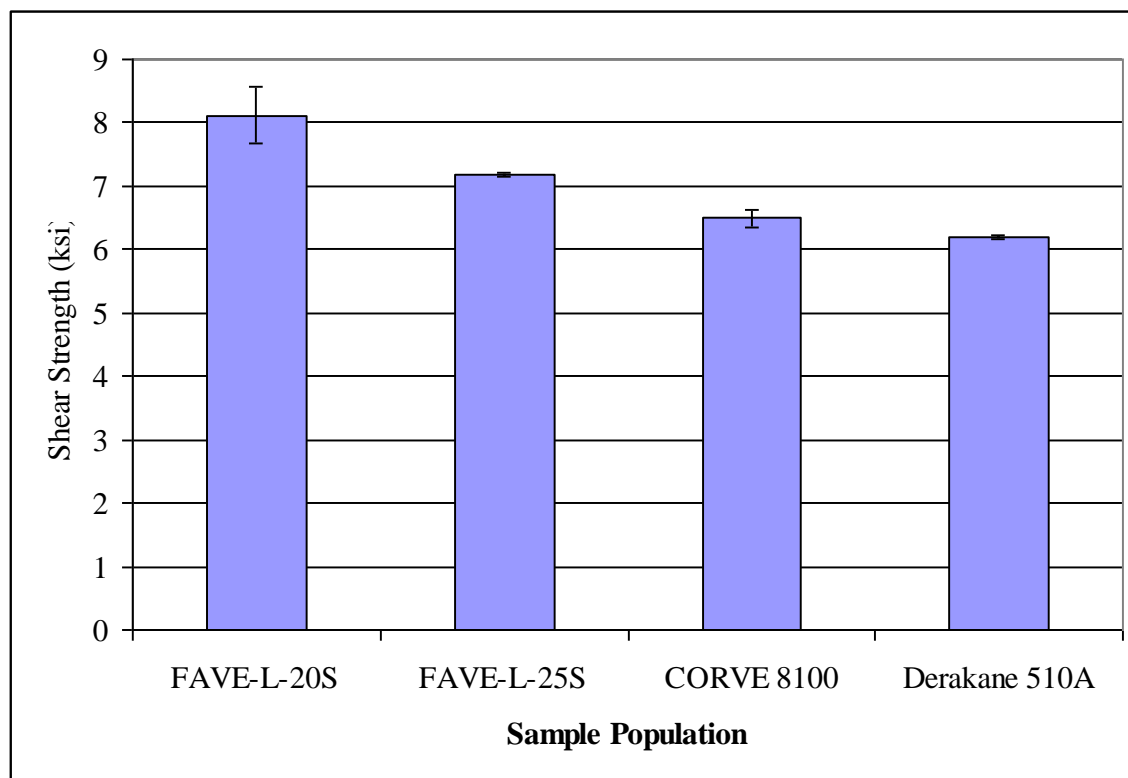


Figure 56. Shear strength results.

Mode I Interlaminar Fracture Toughness Testing

Specimens were prepared and tested as in the previous FAVE-L-20S section. The results of the tests are summarized in table 52 and figures 57 and 58. The onset of the G_{Ic} was defined as when the crack gage indicated that the crack started to open. The propagation value is taken as the G_{Ic} value after 0.25 in of crack growth. Since these specimens appear to exhibit an increasing G_{Ic} as the crack propagates and then flattens out after 1 in of crack growth, as shown in figure 57, a steady-state G_{Ic} value was determined by averaging the G_{Ic} values from 1 to 1.6 in of crack growth. The results indicate that the FAVE-L-25S composite exhibits similar room temperature dry toughness properties across the board (onset, propagation, and steady state) as the FAVE-L-20S. The Derakane 510A and CORVE 8100 composites exhibited close to double the toughness of the FAVE systems across the board. The effect of post cure of 4 h at 160 °F was also investigated to see if this raised the toughness values. The results indicate that there was no change in the toughness within the scatter of the test after the post cure.

Table 52. Mode I interlaminar toughness results (RTD) (glass fabric SW1810).

Panel ID	Type	G_{Ic} (in-lb/in ²)		
		Onset	Propagation	Steady State
070201	Composite FAVE-L-20S	0.56 ± 0.24	1.63 ± 0.23	3.11 ± 0.10
070801	Composite FAVE-L-25S	0.62 ± 0.16	1.57 ± 0.24	3.68 ± 0.25
070801	Composite FAVE-L-25S (post cured)	0.29 ± 0.05	1.45 ± 0.24	3.47 ± 0.92
070903	Composite 510A	1.15 ± 0.29	3.01 ± 0.59	6.70 ± 0.60
070903	Composite 510A (post cured)	1.27 ± 0.16	3.40 ± 0.47	6.88 ± 0.39
080304	Composite 8100	0.38 ± 0.20	2.76 ± 0.12	6.02 ± 0.37
080304	Composite 8100 (post cured)	0.20 ± 0.15	2.99 ± 0.47	6.38 ± 0.60

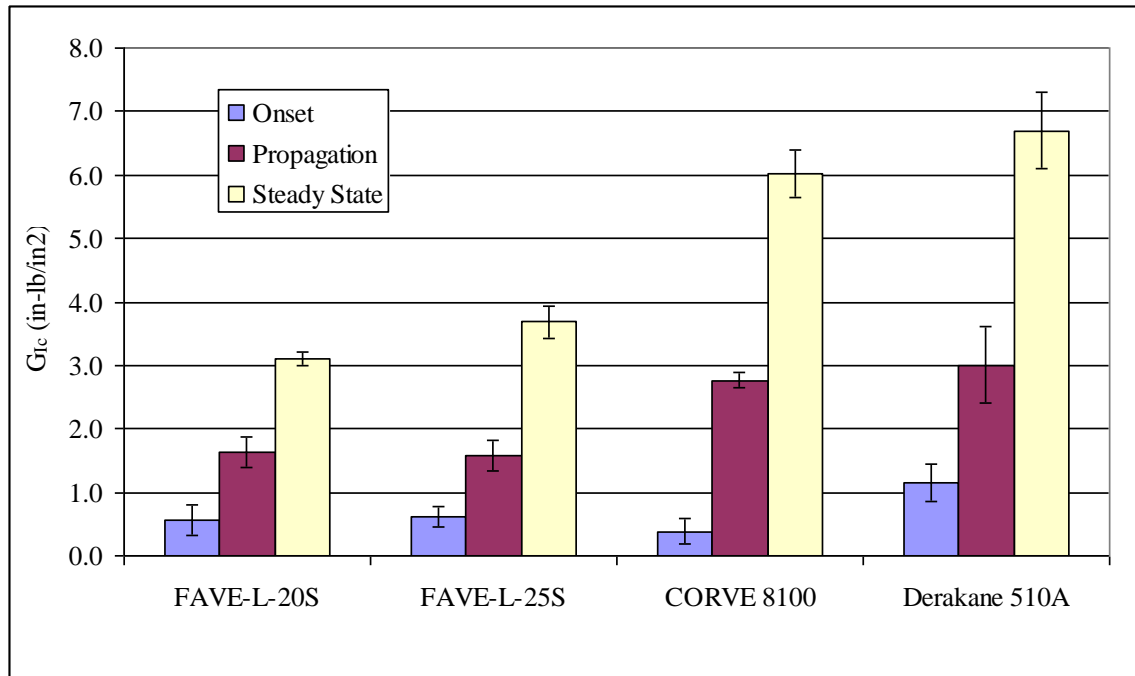


Figure 57. Mode I interlaminar toughness results.

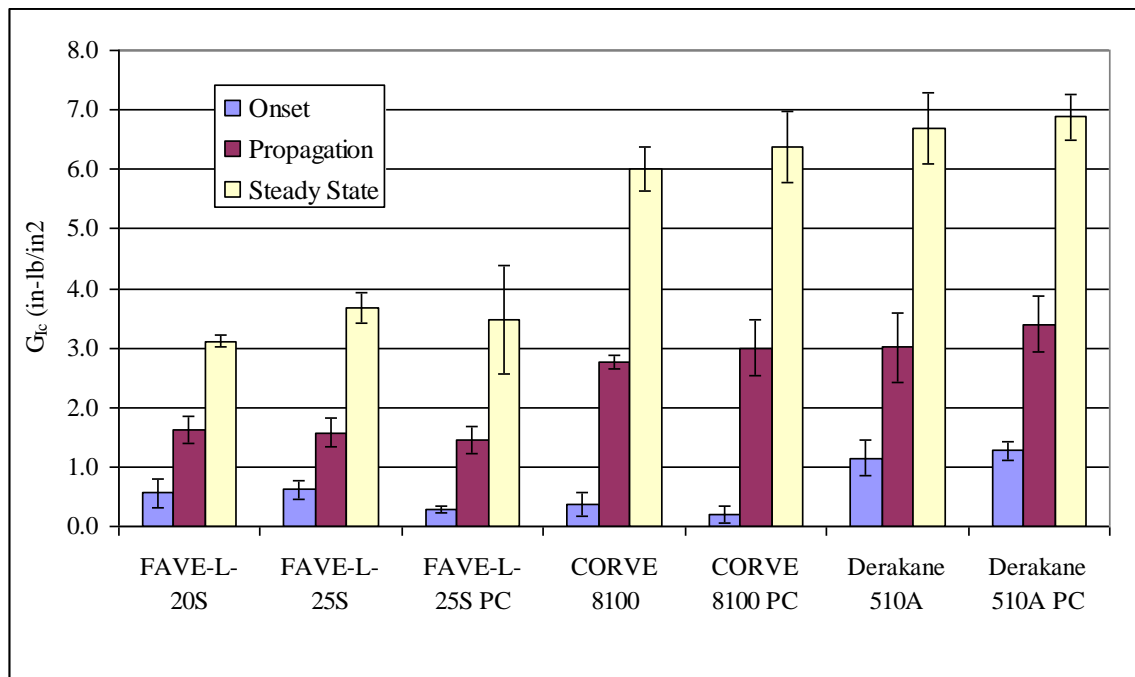


Figure 58. Mode I interlaminar toughness results effect of post cure.

Carbon Fiber Mode I Interlaminar Fracture Toughness Testing

A series of tests were also performed by infusing the FAVE-L-25S, 510A, and West Systems Epoxy into a T700 FOE size, 9-oz/sq yd plain weave carbon fiber woven roving to determine if the FAVE-L-25S might exhibit any better bonding to carbon fiber than the baseline 510A used in Navy designs. The results indicated that the FAVE-L-25S exhibited significantly lower G_{Ic} values than the 510A and the West Systems Epoxy, as shown in table 53 and figure 59.

Table 53. Mode I interlaminar toughness results (RTD) (carbon fiber fabric T700 FOE size, plain weave, 9 oz/sq yd).

Panel ID	Type	G_{Ic} (in-lb/in ²)		
		Onset	Propagation	Steady State
080305	Composite FAVE-L-25S with carbon fabric	0.14 ± 0.007	0.91 ± 0.18	1.76 ± 0.20
080401	Composite 510A with carbon fiber fabric	1.16 ± 0.37	2.77 ± 0.67	4.49 ± 0.60
080502	Composite West Systems 117LV with carbon fiber fabric	0.29 ± 0.23	2.4 ± 0.38	4.07 ± 0.34

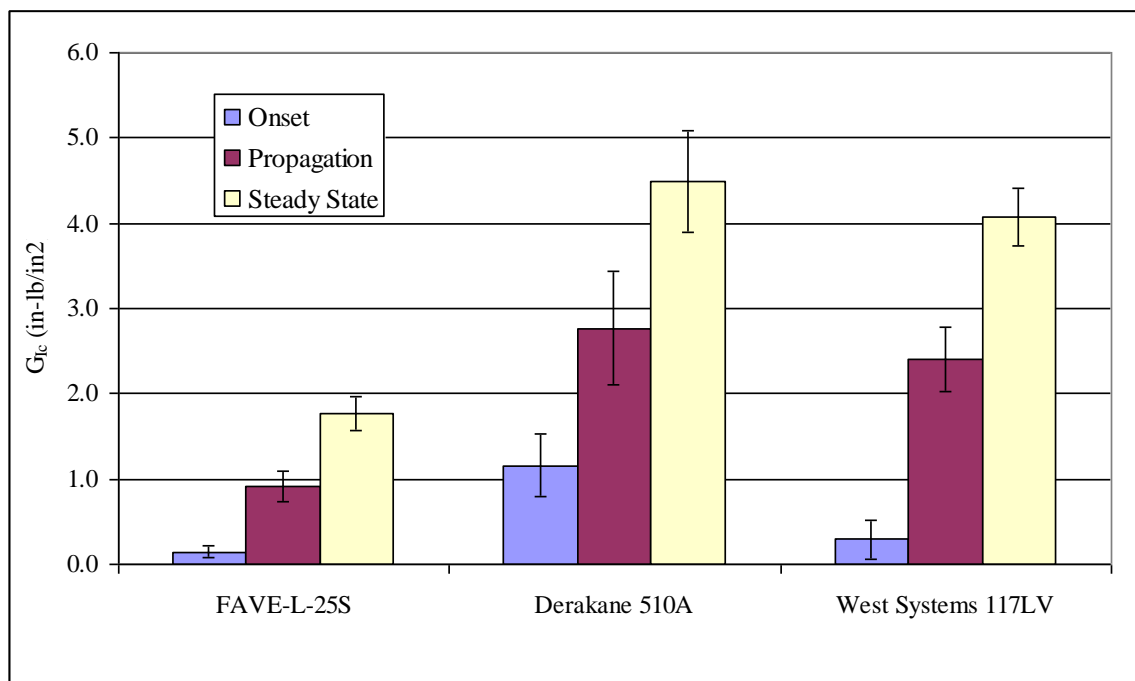


Figure 59. Mode I interlaminar toughness results for carbon fiber reinforced VE systems.

FAVE-L Additional Panel Testing

The following additional panel testing results were performed on FAVE-L. These tests completed the requirements for 0° and 90° testing. Based on the superior performance in virtually every way, NSWCCD felt there was no need to complete these tests for FAVE-L-25S.

Four panels were fabricated at NSWCCD for evaluation of the FAVE-L-20s resin system (table 54). These panels were made using standard VARTM techniques and the resin and fabric. A summary of the fiber orientation of the four different panels is shown in table 48.

Table 54. Panel identification and fiber orientation.

Panel	Layup	Denoted
061001	[0] ₁₀	Uni
061002	[0/+45/90/-45] _s	Quasi
061201	[0/90] _{4s}	Cross-ply
070201	[0] ₈	Uni

Panel Fabrication

Panel fabrication is as follows:

1. Resin: FAVE-L-20S (fatty acid vinyl ester, –L [methacrylate lauric acid])
65 weight-percent bisphenol A vinyl ester
20% styrene
15 weight-percent methacrylate lauric acid
2. Formulation: 97.25-weight-percent FAVE-L-20S Resin
2.0 weight-percent methyl ethyl ketone peroxide (MEKP) (Cadox L-50a)
0.3 weight-percent cobalt naphthenate 6% (CoNap6%)
0.25 weight-percent 2,4-pentanedione (2,4-P)
0.2 weight-percent dimethylaniline (N,N-DMA)
3. Fabric: SW1810 Uni/Mat fabric from Fiber Glass Industries—Nominally 18 oz/yd² unidirectional E-glass fibers stitched to 10 oz/yd² binder-free chopped strand mat (similar architecture to twisted rudder program).

Density and Void Content

The density of both the neat resin and composite pieces taken from each panel was tested according to the guidelines of ASTM D 792. The results are summarized in table 55. The results show fairly consistent composite panel densities for the 8-ply composite panel regardless of ply layup. The quasi panel exhibited a slightly higher density than the unidirectional or cross-ply panels.

Table 55. Summary of density measurements (ASTM D 792).

Panel	Type	Density (g/cm ³)
—	Neat resin	1.167 ± 0.002
061001	Uni	1.838 ± 0.021
061002	Quasi	1.854 ± 0.003
061201	Cross-ply	1.847 ± 0.009
070201	Uni	1.849 ± 0.015

The fiber, resin, and void fraction were determined using the burnout method described in ASTM D 3171. An E-glass fiber density was assumed to be 2.59 g/cm³ for these calculations.* The results of these tests are shown in table 56.

Table 56. Summary of constituent material measurements (ASTM D 3171).

Panel	Type	% Fiber Volume Fraction	% Resin Volume Fraction	% Void Volume Fraction
061001	Uni	47.74 ± 1.33	51.60 ± 1.19	0.65 ± 0.15
061002	Quasi	48.74 ± 0.09	50.72 ± 0.03	0.54 ± 0.12
061201	Cross-ply	48.11 ± 0.47	51.53 ± 0.27	0.35 ± 0.20

Tension Testing

Samples were prepared using standard machining techniques to ASTM D 638 Type III specimen dimensions. Two sets of specimens were prepared. One set had the outer plies of the composite oriented in the 0° direction along the axis of the specimen, while the other had set the outer plies oriented in the 90° direction perpendicular or transverse to the axis of the specimen. The average of three measurements was used to determine the width and thickness of the samples in the gage length of the specimen. Vishay strain gages of type CEA-06-125WT-350, gage factor 2.15, were attached to the center of the gage length to allow for the calculation of the elastic modulus and Poisson's ratio. Specimens were tested using a Southwark-Emery 60-kip load frame with a 60-kip load cell. Samples were loaded at a rate of 0.2 in/min. Prior to testing, the grips were vertically aligned using a stock metal piece. This was found to be the best method to ensure that the grips remained aligned during testing due to the large amount of play that is present in the load train system of the machine. The results are shown in table 57.

* Fiber Glass Industries (www.fiberglassindustries.com).

Table 57. ASTM D 638 tension test results.

Panel ID	Type	Tensile Strength (ksi)		Elastic Modulus ^a (Msi)		Poisson's Ratio ^a (ν)	
		0°	90°	0°	90°	0°	90°
061001	Uni	89.93 ± 3.88	11.37 ± 0.73	4.84 ± 0.07	1.18 ± 0.19	0.307 ± 0.014	0.112 ± 0.025
061002	Quasi	39.92 ± 0.48	41.92 ± 2.47	2.69 ± 0.03	2.92 ± 0.24	0.325 ± 0.018	0.319 ± 0.02
061201	Cross-ply	53.20 ± 3.29	55.41 ± 1.83	3.28 ± 0.14	3.17 ± 0.27	0.176 ± 0.018	0.185 ± 0.021

^aRange of 1000 to 3000 in/in.

Compression Testing

Samples were prepared using standard machining techniques to ASTM D 695 specimen dimensions. Two sets of specimens were prepared. One set had the outer plies of the composite oriented in the 0° direction along the axis of the specimen, while the other had set the outer plies oriented in the 90° direction perpendicular or transverse to the axis of the specimen. The average of three measurements was used to determine the width and thickness of the samples in the gage length of the specimen. Vishay strain gages of type CEA-06-062UW-350 were attached to the center of the gage length to allow for the calculation of the elastic modulus. Specimens were tested using a Southwark-Emery 60-kip load frame with a 60-kip load cell. Samples were loaded at a rate of 0.05 in/min. The results are shown in table 58.

Table 58. ASTM D 695 compression test results.

Panel ID	Type	Compressive Strength (ksi)		Elastic Modulus ^a (Msi)	
		0°	90°	0°	90°
061001	Uni	53.64 ± 5.99	21.14 ± 0.76	5.03 ± 0.28	2.55 ± 0.65
061002	Quasi	37.95 ± 1.35	35.34 ± 1.27	3.06 ± 0.08	3.71 ± 0.36
061201	Cross-ply	37.02 ± 3.67	43.83 ± 0.95	3.71 ± 0.18	3.74 ± 0.81

^aRange of 1000 to 3000 in/in.

Shear Testing

Samples were prepared using standard machining techniques to ASTM D 5379 v-notch shear specimen dimensions. One set of specimens was prepared with the outer plies of the composite oriented in the 0° direction along the length of the specimen. The average of three dimensions

was used to determine the width and thickness of the samples in the gage length of the specimen. Vishay strain gages of type CEA-06-062WT-350 were attached at the center of the specimen as described in ASTM D 5379 to allow for the calculation of the shear modulus. Specimens were tested using a Southwark-Emery 60-kip load frame with a 60-kip load cell. Samples were loaded at a rate of 0.05 in/min. The results are shown in table 59.

Table 59. ASTM D 5379 v-notch shear test results.

Panel ID	Type	Shear Modulus ^a (Msi)	Ultimate Shear Strain (in/in)	Shear Strength (ksi)		
				@ 0.2% offset	@ 5% Strain	Ultimate
		0°	0°	0°	0°	0°
061001	Uni	0.79 ± 0.10	0.059 ± 0.010	8.12 ± 0.44	14.36 ± 1.67	15.15 ± 0.96
061002	Quasi	1.07 ± 0.13	0.026 ± 0.002	15.41 ± 3.96	—	20.21 ± 1.15
061201	Cross-ply	0.82 ± 0.13	0.082 ± 0.021	8.59 ± 1.43	16.40 ± 0.53	17.30 ± 0.78

^aRange of 1000 to 4000 in/in.

Environmental Conditioning

Twenty-one samples underwent environmental exposure at 50 °C and 80% relative humidity. These included samples to perform tension and compression (as outlined in the previous sections) and also SBS (ASTM D 2344) and interlaminar toughness (ASTM D 5528). Samples were weighed at prescribed intervals to monitor the percent moisture uptake over time. After the percent moisture has reached the equilibrium state defined by ASTM D 5229, the samples were tested to determine the effect of temperature and moisture on the composite material. The percent weight gain of the samples over time is included as a reference in figure 60. The varying volume/surface area of the different samples appears to contribute to a difference in the percent weight gain of each different sample type. The slight drop in the moisture uptake curve at 38.5 h was due to loss of humidity chamber conditions. After 140 days of exposure, the samples appeared to reach an equilibrium saturation level. Samples taken from the same panel (070201) that have been aged at room temperature were also tested at the same time for direct comparison.

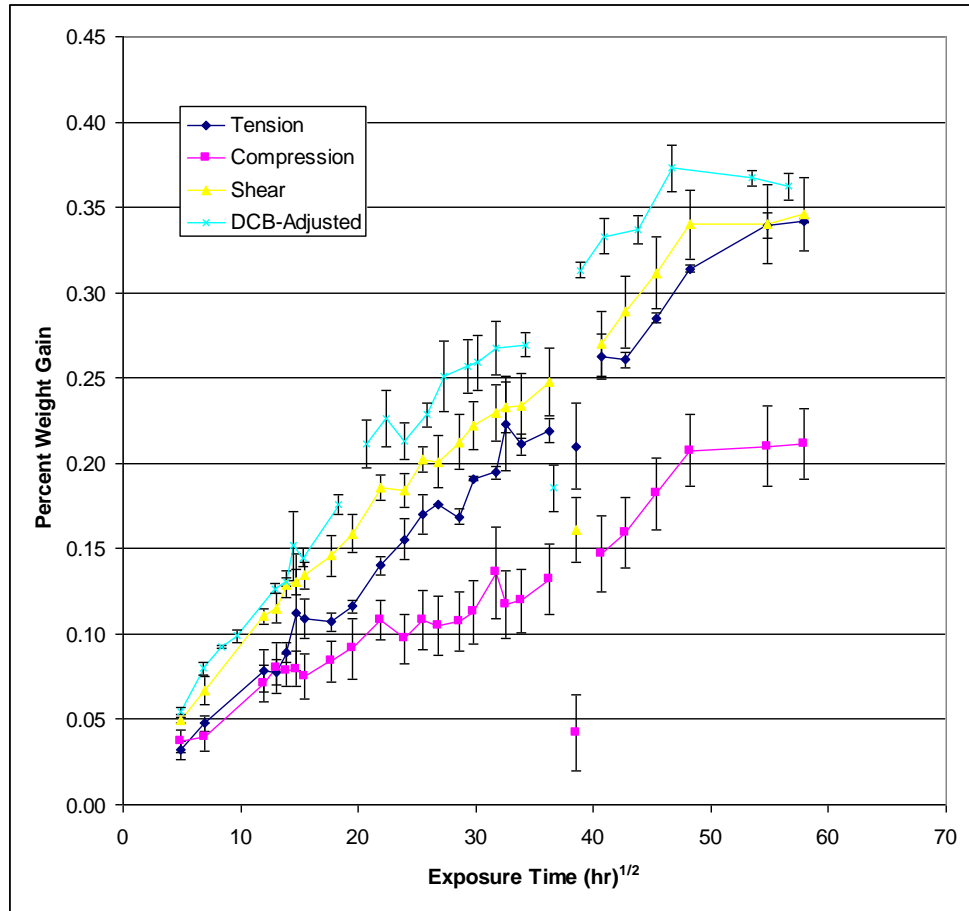


Figure 60. Percent weight gain vs. exposure time for FAVE-L composite samples at 50 °C and 80% relative humidity.

Tension Testing After Environmental Conditioning

The tension tests were performed in the same manner as in the previous section. The results of the room temperature dry and elevated temperature wet test specimens that were taken from the same panel are shown in table 60. The results indicate a small decrease in average tensile strength (5%) after the elevated temperature wet exposure. This level of change is just above the coefficient of variation of the sample population of 4%. There was no noticeable change in the tensile modulus after the elevated temperature wet exposure.

Table 60. ASTM D 638 tension test results (RTD and elevated temperature wet).

Panel ID	Type	Conditioning	Tensile Strength (ksi)	Elastic Modulus ^a (Msi)
061001	Uni	As-manufactured	89.9 ± 3.9	4.8 ± 0.1
070201	Uni	RTD	89.1 ± 3.8	5.0 ± 0.1
070201	Uni	Elevated temperature wet	85.1 ± 3.6	4.8 ± 0.3

^aRange of 1000 to 3000 in/in.

Compression Testing After Environmental Conditioning

The compression tests were performed in the same manner as in the previous section. The results of the room temperature dry and elevated temperature wet test specimens that were taken from the same panel are shown in table 61. The results indicate that there was no significant change in the compressive strength or modulus after the elevated temperature wet exposure.

Table 61. ASTM D 695 compression test results.

Panel ID	Type	Conditioning	Compressive Strength (ksi)	Elastic Modulus^a (Msi)
061001	Uni	As-manufactured	53.6 ± 6.0	5.0 ± 0.3
070201	Uni	Room temperature dry	47.5 ± 6.1	5.0 ± 0.3
070201	Uni	Elevated temperature wet	44.8 ± 7.0	5.0 ± 0.1

^aRange of 1000 to 3000 in/in.

Shear Testing After Environmental Conditioning

Samples were prepared using standard machining techniques to ASTM D 2344 SBS specimen dimensions. One set of specimens was prepared with the outer plies of the composite oriented in the 0° direction along the length of the specimen. The average of three dimensions was used to determine the width and thickness of the samples in the gage length of the specimen. Specimens were tested using a Southwark-Emery 60-kip load frame with a 60-kip load cell.

Samples were loaded at a rate of 0.05 in/min using a three-point bend type fixture with a span to depth ratio of 4. This type of test was selected for use over the v-notch test due to the ease of machining and the v-notch non-ideal failure of composites with off-axis fibers. The results of the room temperature dry and elevated temperature wet test specimens that were taken from the same panel are shown in table 62. The results indicate that there was a 12% decrease in SBS strength after the elevated temperature wet exposure.

Table 62. Shear test results.

Panel ID	Type	Conditioning	Shear Strength (ksi)
061001	Uni	As-manufactured	8.1 ± 0.4 (ASTM D 5379)
070201	Uni	Room temperature dry	7.1 ± 0.3 (ASTM D 2344)
070201	Uni	Elevated temperature wet	6.2 ± 0.4 (ASTM D 2344)

Mode I Interlaminar Fracture Toughness Testing After Environmental Conditioning

Samples were prepared using standard machining techniques to ASTM D 5528 specimen dimensions. One set of specimens was prepared with the outer plies of the composite oriented in the 0° direction along the length of the specimen. Piano hinges were attached to the composite specimens using epoxy adhesive. Crack gauges of type TK-09-CPS05-001 by Vishay Measurements were attached to the side of the specimen to monitor the crack advancement. The average of three dimensions was used to determine the width and thickness of the samples of the specimen. Specimens were tested using an Instron 4202 load frame with a 2000-lb load cell at a rate of 0.2 in/min. The use of crack gauges has been seen to automate the testing process and to eliminate the ambiguity of the operator visual noting the crack tip displacement. The results of the room temperature dry and elevated temperature wet test specimens that were taken from the same panel are shown in the following table and figures. Three different G_{Ic} values are reported. The onset is defined as when the crack gage shows the onset of crack tip displacement. The non-linear offset is defined as the G_{Ic} value calculated when the load vs. displacement curve is no longer linear. Finally, the propagation value is the G_{Ic} value after 0.25 in of crack tip displacement. These three values have been defined and used in the past in Navy programs (34). The results (table 63) indicate that there was a slight increase in all the G_{Ic} values after the elevated temperature wet exposure compared to the room temperature dry specimens.

Table 63. Mode I interlaminar toughness results.

Panel ID	Type	Conditioning	G_{Ic} (in-lb/in ²)		
			Onset	Propagation	Steady State
070201	Uni	Room temperature dry	0.56 ± 0.24	1.63 ± 0.23	3.11 ± 0.10
070201	Uni	Elevated temperature wet	0.98 ± 0.21	2.25 ± 0.36	3.76 ± 0.65

Thermal Property Characterization – Dynamic Mechanical Analysis:

A dynamic mechanical analysis was performed on a neat resin sample of the FAVE-L-20S resin using a TA Instruments DMA. The sample was run in the single cantilever bending mode at a frequency of 1 Hz. The temperature ramp rate was set to 2 °C/min from 30° to 150°C. The results, shown in figure 61, were analyzed according to ASTM E 1640, and the T_g values are shown in table 64.

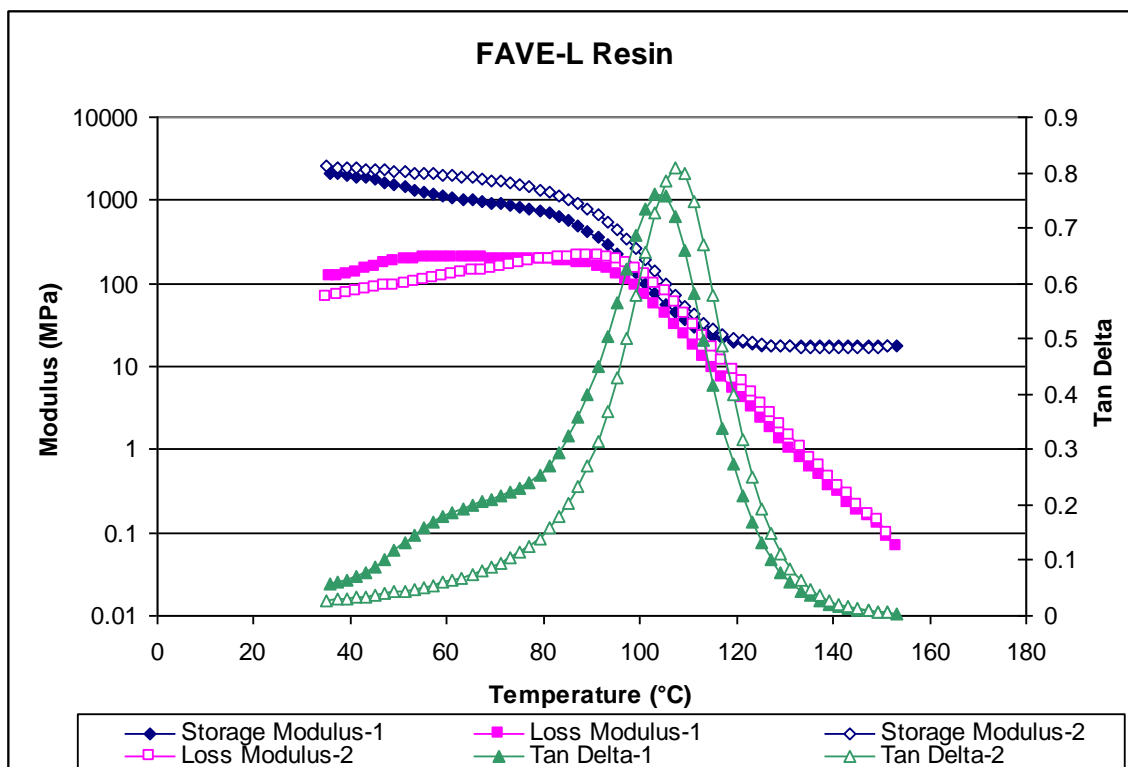


Figure 61. DMA results for the FAVE-L-20S resin material.

Table 64. Glass transition temperature results as determined by the dynamic mechanical thermal analysis test for the FAVE-L-20S resin.

FAVE-L-20S	Glass Transition Temperature, T_g (°C), as Determined by		
	Extrapolated Onset of Change of the Storage Modulus ^a	Peak of Loss Modulus	Peak of Tan Delta Curve
1st heating	78.9	—	105
2nd heating	73.8	89.2	107

^aTypical Navy design criteria.

The FAVE-L-20S resin system was originally selected for characterization based on the published data on the T_g of the system being >100 °C. Using DMA and the extrapolated onset of the change of the storage modulus, since the T_g is below 80 °C, it was determined that another formulation of the FAVE product line should be considered. Several additional samples were received from ARL for consideration. These were the FAVE-L-25S and FAVE-O-25S, which contain slightly more styrene at 25 weight-percent. Similar DMA tests were run on these samples, as well as baseline samples of the Ashland Derakane 510A and 8084, as well as the Interplastic CoRezyn CORVE 8100, which are commercially available VEs that are being used in Navy applications. The results of the DMA scans are summarized in table 65.

Table 65. Glass transition temperature results as determined by the dynamic mechanical thermal analysis test for a variety of resin systems.

		Glass Transition Temperature, T _g (°C), as Determined by		
		Extrapolated Onset of Change of the Storage Modulus ^a	Peak of Loss Modulus	Peak of Tan Delta Curve
FAVE-L-20S	1st heating	78.9	—	105
	2nd heating	73.8	89.2	107
FAVE-L-25S	1st heating	84.2	98.2	114
	2nd heating	96.2	106	122
FAVE-O-25S	1st heating	82.4	100	116
	2nd heating	94.4	110	124
Derakane 510A	1st heating	101	114	128
	2nd heating	111	124	136
Derakane 8084	1st heating	73.0	80.2	118
	2nd heating	85.0	110	130
CORVE 8100	1st heating	108	110	122
	2nd heating	112	114	126

^aTypical Navy design criteria.

The DMA results indicated that the FAVE-L-25S would be a good low-VOC resin system to evaluate further since it would be comparable to a resin system that has temperature properties that fall between the Derakane 8084 and Derakane 510A resin systems. It is a little lower in T_g than the current CORVE 8100 resin system currently used in the MCM rudder application. The FAVE-O-25S also would fit into this category, but it is predicted to more expensive to produce than the FAVE-L-25S.

Laboratory Testing Conclusions

A variety of tests were performed in support of this several year ESTCP low-HAP/VOC composite resin system. Several different low-VOC resins were evaluated, and a final down selection of the FAVE-L-25S was made. Extensive materials testing and processing studies were performed and compared to other typical Navy VE resin systems. In general, the system was able to be processed using standard VARTM practices with formulation variations allowing for short and long infusion times. The quality of the composites parts with the FAVE-L-25S was similar in density, fiber volume fraction, and void content as the Derakane 510A and CORVE 8100 resin systems. The glass transition temperature of the FAVE-L-25S is lower than the Derakane 510A and CORVE 8100 and closer to the Derakane 8084 resin. Composites made with the Derakane 510A, CORVE 8100, and FAVE-L-25S all exhibited similar mechanical properties (tensile, compressive, and shear). However, the FAVE-L-25S exhibited significantly lower Mode I interlaminar fracture toughness than the Derakane 510A and CORVE 8100 materials. This appeared to be the case whether or not the part was post cured and occurred with both glass and carbon fiber composites. In general, this FAVE-L-25S resin appears promising

and might be considered for future composite applications where a low-HAP/VOC system is required and the interlaminar fracture toughness is not critical to the design.

6.1.5.5 Composite Panels Relevant to HHMWV Hardtop and HHMWV Transmission

Container. Four-point bending and SBS tests at room temperature were performed to determine whether the FAVE resins meet stiffness and strength requirements for the HHMWV hardtop and HHMWV transmission container (table 66). The results showed that the first batch of FAVE-O-25S did not perform as well as the second batch. This improvement was a direct result of using RDX26936 instead of CN151 in the formulation. Nonetheless, both formulations met the property specifications. Unexpectedly, the FAVE-L-25S-RDX outperformed the FAVE-O-25S-RDX. Overall, the results indicate that FAVE-L/O-25S resins will likely meet the performance requirements for Army hoods. Appendix H lists composite panel testing for Army and Marines applications.

Table 66. Panel testing results of FAVE-HT resin systems for hardtop and transmission container applications.

Property	FAVE-O-25S (Batch 1)	FAVE-O-25S-RDX (Batch 2)	FAVE-L-25S- RDX	Requirement
4-point bend modulus at RT (Msi)	3.70	3.80	3.85	3.7
4-point bend strength (RT) (ksi)	62.0	68.4	70.0	55
SBS at RT (ksi)	4.80	4.95	5.10	4.5

6.1.5.6 Composite Panels Relevant to Army Hoods. Four-point bending and SBS tests at room temperature and 250 °F were performed to determine whether the FAVE resins meet stiffness and strength requirements at normal and elevated temperatures (table 67). The results showed that the first batch of FAVE-O-HT did not meet most property requirements. However, when using the FAVE-O-HT-RDX, most properties met the requirements, and only one property was questionable. This improvement was a direct result of using RDX26936 instead of CN151 in the formulation. Unexpectedly, the FAVE-L-HT-RDX outperformed both FAVE-O-HT variants. Overall, the results indicate that FAVE-HT resins will likely meet the performance requirements for Army hoods.

Table 67. Panel testing results of FAVE-HT resin systems for hood applications.

Property	FAVE-O-HT (Batch 1)	FAVE-O-HT-RDX (Batch 2)	FAVE-L-HT- RDX	Requirement
4-point bend modulus at RT (Msi)	3.67	3.76	3.81	3.7
4-point bend modulus at 250 °F (Msi)	2.69	3.0	3.2	3.0
4-point bend strength (RT) (ksi)	56.6	62.0	62.3	55
4-point bend strength at 250 °F (ksi)	29.3	36.2	37.3	30
SBS at RT (ksi)	3.7	4.08	4.60	4.5
SBS at 250 °F (ksi)	2.9	3.2	3.3	3.0

6.2 Demonstration/Validation Results

6.2.1 T-38 Dorsal Cover

6.2.1.1 Viscosity Flow Studies. The flow of FAVE resins was compared to that of the Hexion 781-2140 incumbent resin. This was performed by preparing connected or identical rectangular fiber layups and infusing FAVE resin into one layup and the Hexion resin into the other. The results clearly showed that the FAVE-L resin was much more viscous than the Hexion resin, and took significantly longer to infuse the part.

6.2.1.2 Validation Process. The tooling and fiber reinforcement pack was set up per the developed VARTM process for the Hexion resin system (figure 62). The Army FAVE-L resin system was substituted for the Hexion Specialty Chemicals, Inc.'s VE resin system. All other variables remained the same to isolate the effects of the reduced styrene diluents.



Figure 62. Dorsal cover tool with fiber pack ready to be infused.

6.2.1.3 Issues Encountered. The major issue with the FAVE-L resin was that the viscosity does not match the commercial resin that is diluted with the styrene monomer. This resulted in a lower inflow rate and a longer processing time to infuse the fiber pack. The infusion of the part per process specifications was unsuccessful due to the higher viscosity of the FAVE-L resin system. The FAVE-L resin gelled (cured to a rapid jump in viscosity) before the fiber pack was completely infused as can be seen in figure 63.

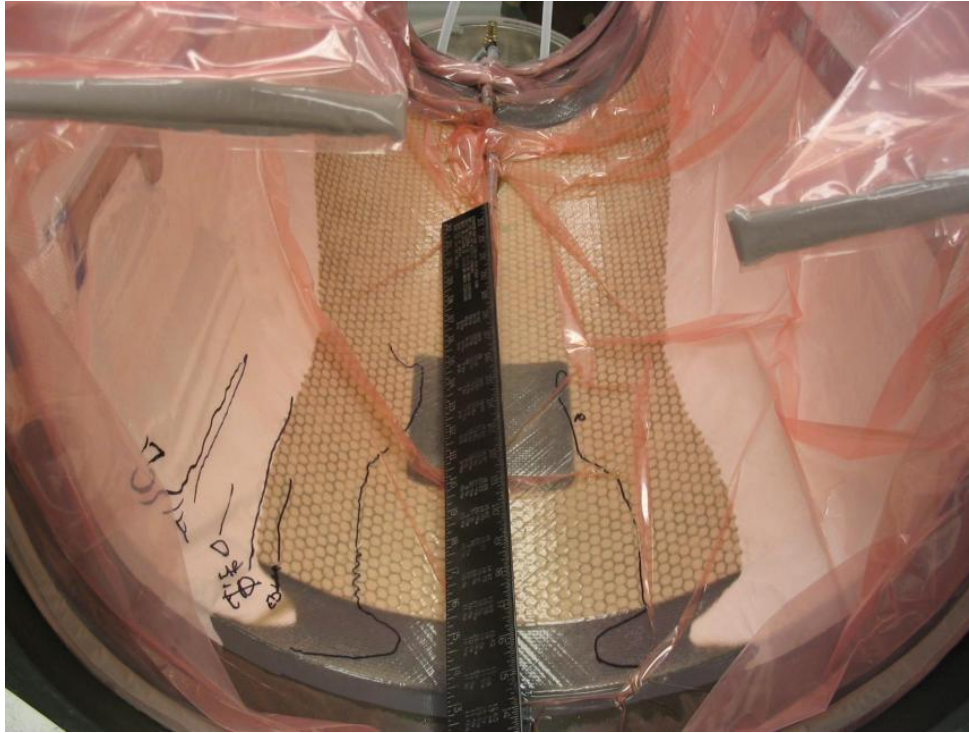


Figure 63. Failed attempt to infuse T-38 dorsal cover with FAVE-L.

6.2.1.4 Validation Results. Since the infusion of the part following the set process specifications was unsuccessful, the FAVE-L resin did not meet the standards set for the validation testing. The FAVE-L resin with a higher viscosity cannot be directly substituted for the commercially available styrene-diluted Hexion resin systems, currently called out in the process documents. In order to use this FAVE-L resin system for this part, a change in the manufacturing process would be needed. Alternatively, a lower viscosity resin such as the FAVE-L-25S could be used.

6.2.1.5 Conclusion. Moving from a commercially available VE resin to a reduced styrene resin system with different viscosity profiles will require process changes to produce parts. These process changes could require requalification of existing products built using original equipment manufacturers (OEM) qualified processes. This is a very time consuming and expensive process. It is not in the Air Force's best interest to pursue a manufacturing process change to requalify the T-38 dorsal cover using the ESTCP resin. Additionally, during the validation process, the Air Force requested bids from contractors to produce the dorsal cover using the old method. This request was answered by a contractor and more T-38 dorsal covers were produced. Although these dorsal covers will most likely face the same problem as the originals, cracking and delamination, the AF currently does not have the need to manufacture new parts.

6.2.2 F-22 Canopy Cover

In order to meet the set requirement of being able to manufacture this part in <1 day, we decided to use a VARTM process. A wet layup process could be used, but it would be a much longer process, requiring more people and material, which could possibly extend the manufacturing time to several days if the whole part was not cured at the same time. Other disadvantages of the wet layup method include poor compaction of the fibers, causing air filled pockets or voids, and a high resin to fiber ratio, leading to increased weight with decreased strength. For these reasons, it was decided that using the VARTM process would produce a better part and be more cost effective in meeting our set criteria. We decided to use the FAVE-L-25S resin system for this part. We determined that this prototype part would be a good avenue to test the ARL resin system and determine its ability to compete with equivalent VE resin systems in a large-scale part. The process for building this part consisted of a splash, tool, master tool, and final part. Each one of the separate parts had its own separate process that was explained.

6.2.2.1 Splash Tool Process. In order to create the canopy cover, the first part in the process was to create a splash, or copy, of the actual canopy. The Air Force let the ACO borrow an F-22 canopy that was to be sent to the Air and Space Museum at Wright-Patterson AFB, OH. Using this canopy, the ACO created a splash, or an exact replica, of the top surface of the canopy. First, the canopy was completely covered with Teflon^{*}-coated tape (figure 64). This allowed us to protect the canopy while giving us a non-stick surface to layup the glass.



Figure 64. F-22 canopy covered with Teflon tape.

^{*}Teflon is a registered trademark of DuPont.

After the canopy was covered with Teflon tape, two layers of gel coat were applied (figure 65). These gel coat layers acted as a smooth transition barrier between the replica surface and the reinforcement glass fibers. They also allow for sanding and touch up without damaging the underlining fibers. The first layer of gel coat was allowed to cure to a tacky state before applying the second layer.



Figure 65. Application of gel coat on F-22 canopy.

After the gel coat layers were applied, 10 layers of fiberglass were applied. These layers were applied by wetting out 2- x4-in sheets of 7500 fiberglass cloth with urethane tooling resin. These wet out sheets of glass were then placed on top of the gel coat layers and allowed to cure (figure 66).

On top of the last layer of glass, a layer of polyester peel ply was applied. This peel ply when ripped off after the part had been cured to give the top surface a rough texture more preferable for bonding additional layers of reinforcement or paint. To strengthen the splash and give it added stiffness, additional rib structures were bonded onto the top surface (figure 67). These rib structures were made out of foam strips, tooling dough and 7500 glass reinforcement. They were applied in the same fashion as the rest of the splash. The foam was cut into stiffener shapes and glued onto the surface. Tooling dough was then applied, followed by three layers of 7500 glass reinforcement.



Figure 66. Canopy cover splash curing.



Figure 67. Application of rib stiffeners on splash.

After all layers and rib structure were applied, the splash was given 7 days at room temperature to fully cure. Once cured, the splash was pulled off the canopy and turned upside down so that a master could be made. The inner surface of the splash held the exact representation of the top surface of the canopy (figure 68). There were areas on the inner surface of the splash that had been damaged from the removal of the splash from the canopy. These areas were sanded down, filled with resin, and then sanded flush to the rest of the surface. Once the touch up on the surface was finished, the final splash was completed and ready for the master to be made from it.



Figure 68. Final F-22 canopy splash mold.

6.2.2.2 Canopy Master. The next step in the process was to create a male canopy master. This master would have the top (working) surface the same shape as the canopy itself. This allowed us to have a surface to work on without a fear of damaging the actual canopy. The first step in preparing the master was to thoroughly clean the surface of the splash. This was done by wiping the surface with tech wipes and acetone. Before beginning the layup process, the splash was covered with a very thin layer of release coating called Zyvax Watershield. This layer of release film allowed the clean removal of the master from the splash. After the release layer was applied, two layers of gel coat, PTM&W 1105 epoxy surface coat, were applied. This gel coat acted as a smooth surface and a barrier for the underlying fiberglass. After the gel coat layer was applied and allowed to tack, we placed the first two layers of wet out glass inside of the splash. The master was made up of fiberglass and a core of tooling dough, creating a sandwich structure (figure 69). The 7500 glass cloth was cut into 2- × 4-in pieces and hand wet out using PTM&W 2050 laminating resin. After the glass was applied, the two part tooling dough was properly

mixed, and resin was added to the mixture to make it more workable. Then, a layer of tooling dough was applied on top of the glass, followed by two more layers of fiberglass cloth. This created a sandwich structure, with the fiberglass being the face sheets and the tooling dough acting as the core.



Figure 69. Layup of glass and tooling dough for F-22 canopy master.

Polyester peel ply was then added on top of the last layer of fiberglass. The master was allowed to cure, and then the peel ply was ripped off to create a better bonding surface. In order to stiffen the structure and give it mounting points to set on a stand, wood beams were bonded to the inside of the master. These wood beams were bonded to the inside of the master using tooling dough and fiberglass reinforcement. Once the tooling dough and fiberglass had time to cure, the master was removed from the splash, resulting in a surface having the exact same shape as the original canopy itself. This surface was used to create the offset needed for the creation of a master tool (figure 70) on which the canopy cover would be made.

6.2.2.3 Master Tool. After completing the canopy master, we were ready to proceed to producing the master tool, upon which the canopy cover would be built. The first step in creating the master tool was to create the offset required for the canopy cover. This offset was needed because the canopy cover is not allowed to touch the surface of the canopy or it will damage the coatings. To start the offset, hundreds of 2- in cubes were cut out of Dow pink insulation Styrofoam* (figure 71).

*Styrofoam is a registered trademark of the Dow Chemical Company.



Figure 70. Final canopy master.



Figure 71. Application of offset with foam block on master tool.

These foam cubes were then hot glued to the canopy cover. This created an even 2-in offset throughout the entire surface of the canopy cover. A hot wire was then used to taper the foam, from 2 to 1/2 in at the bottom edge of the tool. This was done in order to have an area where the canopy cover would be able to interface with the skirt of the F-22 canopy and be securely fastened. Once all the foam was placed on the master and tapered down at the ends, a layer of 7500 fiberglass cloth was layed up over the top of the foam. The glass cloth was cut into 2- x 4-ft sheets hand wet out with PTM&W laminating epoxy resin. Then, the glass was placed on top of the foam and smoothed out to make a nice even surface to work with. On top of the glass, a layer of polyester peel ply was also applied. The fiberglass was given time to cure, and then the polyester peel ply was removed, which created a nice even surface free from resin flash (excess cured resin fragments). Fifty to 75 lb of Kleen Modeling Clay, soft and medium hardness, was then spread evenly on top of the cured fiberglass (figure 72). Heat was applied to the clay, a small section at a time, and smoothed down with a metal scraper. The heat allowed the clay to become very soft and pliable, which made it much easier to work with.



Figure 72. Application of modeling clay to master tool.

Once the clay was smoothed down to the desired surface finish and curvature, it was allowed to cool down to gain its original hardness. On top of the clay, 2–3 layers of PTM&W PA0801 paste wax mold release were applied. These layers of wax allowed a non-stick surface on which the cover could be built and, more importantly, removed with ease. Once the wax was applied, the master tool was complete (figure 73).



Figure 73. Final canopy cover master tool.

6.2.2.4 Canopy Cover. Once the master tool was completed, the canopy cover was ready to be fabricated. Instead of a hand layup technique used on the master tool and canopy master, we decided to use a VARTM technique when creating the canopy cover. This technique gave us greater strength, lighter weight, and the ability to create the cover in a short period of time. The first step was to layup our fiber pack. The fiber pack consists of all the material that the end product, the canopy cover, will consist of. Our fiber pack was designed to be a sandwich structure consisting of glass and an infusion media, HIFLUX-90, which doubled as a core. HIFLUX-90, made by Polynova, is unique because it allows for the distribution of resin during the infusion process while at the same time staying in the fiber pack and acting as a core material. Our fiber pack had the layup scheme of two plies of 7500 glass, two plies of 181 glass, HIFLUX-90 core, two plies of 181 glass, and two plies of 7500 glass. Each ply of glass was cut to shape and placed on the canopy cover master tool in the order mentioned (figure 74).

These glass fibers were placed on the tool as dry fabric and were not wet out with resin. To keep the fibers from sliding around or off the master tool, they were sprayed with Airtech tackifier adhesive. This adhesive kept the fiber packs from becoming misaligned during the infusion process. After the fiber pack was layed up and fully secured to the master tool, a vacuum bag was placed around the part. The vacuum bag was secured and sealed to the edge of the part with double-sided tacky tape. We placed our infusion lines inside the vacuum bag (figure 75).



Figure 74. Layup of glass fabric fiber pack for canopy cover infusion.

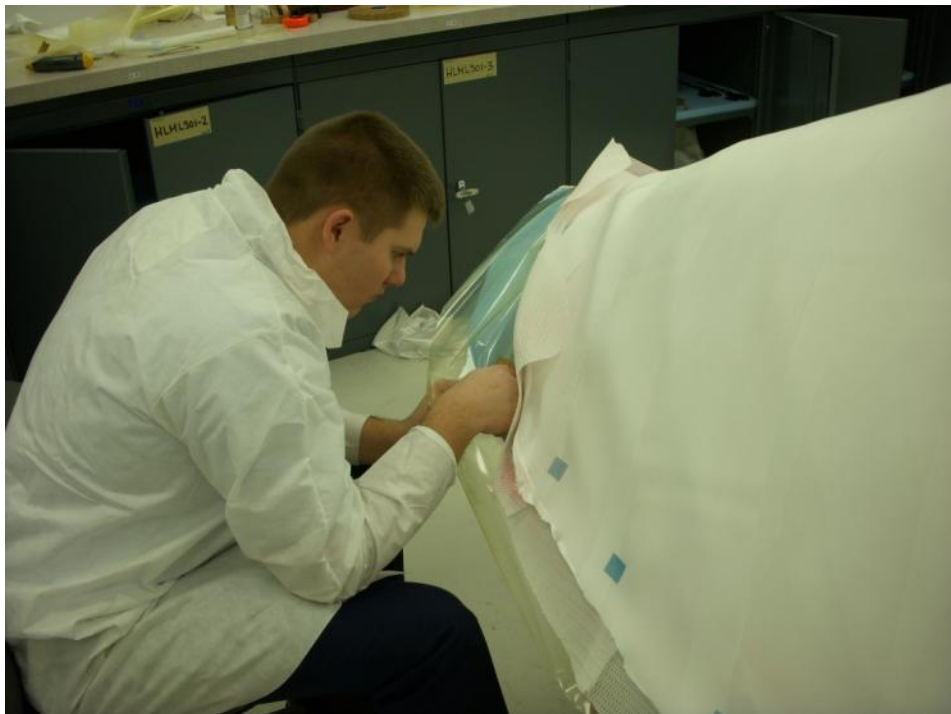


Figure 75. Setup of infusion lines for canopy cover infusion.

These infusion lines, spiral-wrapped polyethylene tubing, allowed the resin to flow to the entire fiber pack. At one end of the infusion lines, solid polyethylene tubing was added and continued into a resin trap bucket. This bucket is where we drew our vacuum, and it also allowed us to catch any excess resin flowing through the lines before it was able to enter the vacuum lines. At the other end of the infusion lines, solid polyethylene tubing was connected to the spiral-wrapped tubing. This solid tubing ran to our infusion bucket, which was the source of our resin used to infuse the part. Once the bagging and infusion lines were in place, we drew vacuum on the part. We used a vacuum pump to draw out all of the air within the vacuum bag, around our part, and allowed to atmospheric pressure to compact the fiber pack. We tested our vacuum integrity with a vacuum gage and fixed any leaks present. Once the vacuum integrity reached an acceptable level (a drop of <1 in Hg/minute), the part was ready to be infused. Before the infusion could begin, we needed to prepare the FAVE-L-25S resin (figure 76).



Figure 76. FAVE-L-25S resin preparation for canopy cover infusion.

The VE FAVE L-25S resin system was used (created by ARL), which contains only 25% styrene. The weight of our dry fiber pack was ~ 8000 g, so we estimated that we would need a net resin weight of 10,000 g, taking into account the excess used in the tubing. To promote the resin, we added 0.1% by weight of cobalt naphthenate and mixed thoroughly. As an activator, we added 1% by weight of Trigonox 239 and mixed thoroughly. This percentage of promoter and activator gave us an estimated 1-h gel time (time before the resin increases in viscosity and ceases to flow). Once the resin was mixed, we allowed the infusion process to start. The bucket of resin was placed at one end of the infusion line, and the atmospheric pressure pushed the resin through the fiber pack (figure 77) until the entire fiber pack was fully infused. Total infusion time took 45 min.



Figure 77. Resin infusion of F-22 canopy cover.

Once cured, the canopy cover was painted. On the bottom inside edge of the canopy cover, 2-in-wide and 1/2-in-thick strips of foam were glued to create a non-damaging interface between the canopy cover and the canopy skirt (figure 78). We were able to fit test the canopy cover on F-22 aircraft at Hill AFB, UT, and Elmendorf AFB, AK (figure 79). Both fit tests were successful.



Figure 78. F-22 canopy cover with foam interface strips.



Figure 79. Final F-22 canopy cover being fit tested on an F-22.

6.2.2.5 Issues Encountered. There were no major issues encountered during the process. The FAVE-L-25S resin performed very well, and we were able to fully infuse the canopy cover. The fit testings at both Hill AFB and Elmendorf AFB were successful.

6.2.2.6 Validation Results. By performing permeability tests on the FAVE-L-25S resin, we were able to design an infusion system that would ensure complete wet out before gelation of the resin. With this system, we were able to successfully infuse the canopy cover (figure 80) with the FAVE-L-25S resin system, using our designed process on the first attempt. No process changes had to be made to accommodate the FAVE-L-25S resin system, and it compared equally to other commercial VE resin systems used for infusion. The part was able to meet the criteria of being manufactured in less than a day. It also had the strength and stiffness requirements for two maintenance workers to transport, install, and uninstall the cover. This part validates that the FAVE-L-25S resin system can be used successfully to perform a VARTM infusion of a large-scale part.



Figure 80. Final F-22 canopy cover next to an F-22 canopy.

6.2.2.7 Conclusion. The F-22 system program office was very impressed with the demonstration of the F-22 canopy cover prototype. There were discussions about including port holes and tubing systems so that the cover could accept hot air and heat the canopy and cockpit while protecting it at the same time. Unfortunately, the canopy cover program ended in the prototype development phase due to the changing needs of the F-22 program office. New hangers were built at Elmendorf AFB, who was the primary customer for the canopy cover. These hangers allowed the jets to be parked inside a temperature-controlled building instead of on the flight line, which eliminated the need to have a protective cover for the canopy. With the need gone, the canopy cover program hit a dead end in the prototype development phase. However, this was a very successful validation of the performance of the FAVE-L-25S resin system compared to equivalent VE resin systems, which use very high styrene contents to decrease viscosity. It proved that the FAVE-L-25S resin system could be used to successfully infuse a very large part without having a large styrene content to decrease the viscosity. If this need ever arises again, the FAVE-L-25S resin system would be a prime candidate for the F-22 canopy cover.

6.2.3 Splash Molds

6.2.3.1 Laboratory Validation Testing. The ACO decided to perform the demonstration splash tool on the underside of a T-38 horizontal stabilizer. Before building the demonstration splash, the ACO tested the flow properties of the FAVE-L-25S resin in the fiber pack by building a flat panel. The flat panel, measuring 13 × 50 in, had the layup scheme of 10 plies of 7500 glass, HIFLUX-90, and 10 more plies of 7500 glass. The HIFLUX-90 would act as both the core and infusion media. After setting up the fiber pack and drawing a vacuum, we successfully infused the part up to a distance of 35 in (on a 13-in-wide part) with a total time of 1 h and 8 min before the resin became too viscous to flow (figure 81 and table 68). The weight of the fiber pack was 1400 g, and the amount of resin used was 1500 g. From the total resin weight, 0.15% of cobalt naphthenate was used as the promoter, and 1.0% of MEKP was used as the activator. After successfully infusing the flat panel and gathering the data from the test, we decided to press forward with the infusion of the demonstration rapid splash tool.

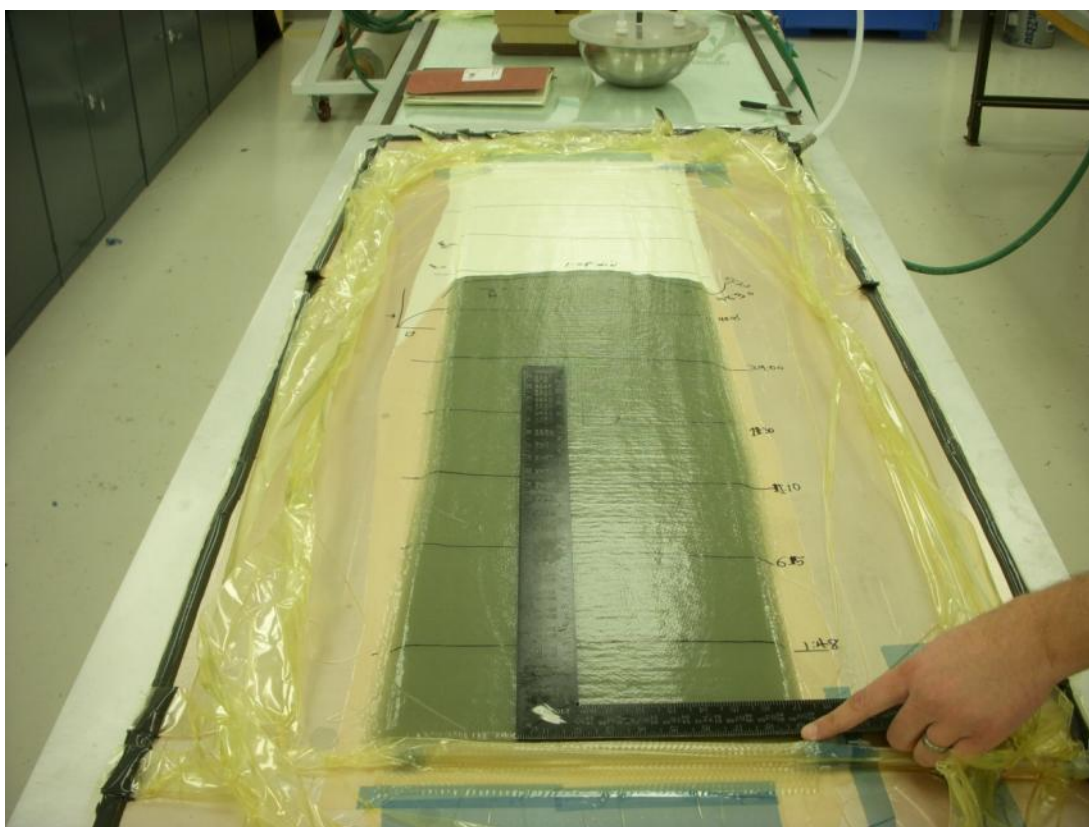


Figure 81. Splash mold resin flow test.

Table 68. Time vs. distance chart collected from the infusion of the flat panel.

Distance	5 in	10 in	15 in	20 in	25 in	30 in	33 in	34 in	35 in
Time (min: s)	1:48	6:15	11:10	18:30	29:00	40:45	48:30	55:20	60:08

The surface of the T-38 horizontal stabilizer was thoroughly cleaned, and all the fabric for the splash tool was cut. The splash tool had the same layup schedule of the test panel, 20 plies of 7500 glass with a core of HIFLUX-90 sandwiched in the middle. Once the surface was cleaned and materials cut, we placed Teflon-backed tape, Airtech's ToolTec, on the surface where we wanted the splash mold. A single layer of tacky tape was then placed around the edge of the Teflon tape for later use as the seal for the vacuum bag. Next, a gel coat layer was rolled on and allowed to reach tacky state (figure 82).

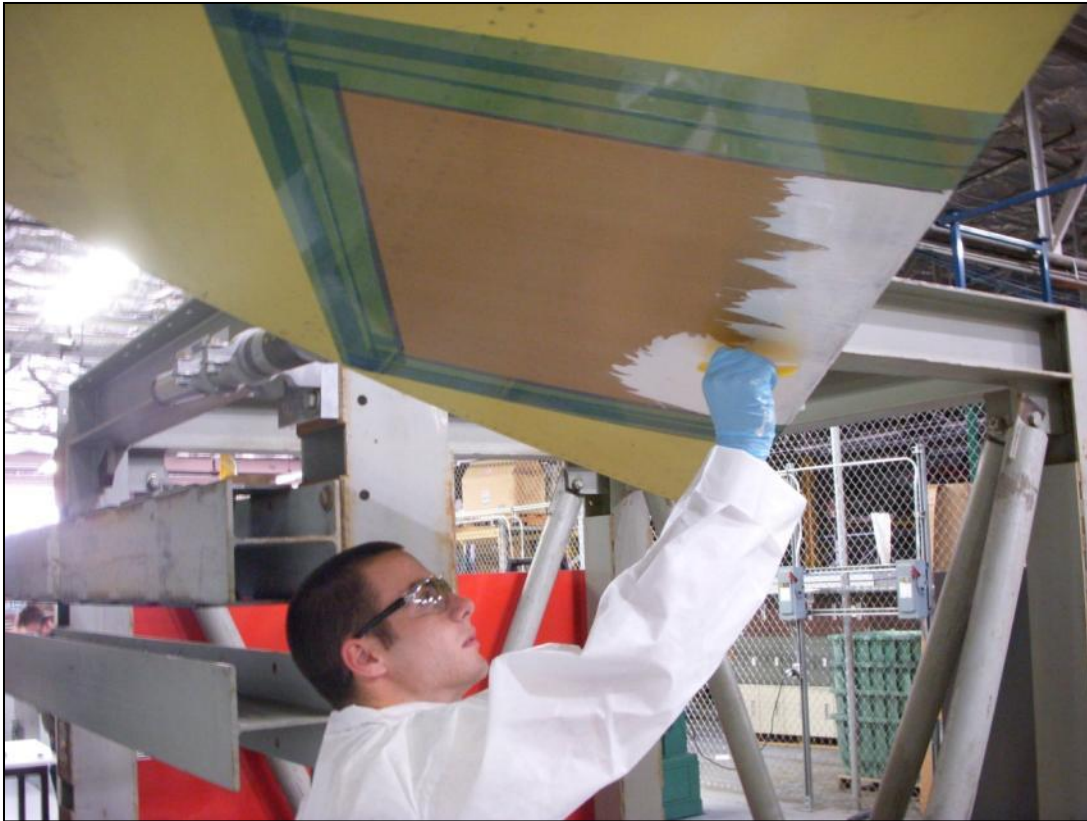


Figure 82. Application of gel coat on part surface.

The fabric was then placed on the surface of the stabilizer on top of the layer of gel coat. Infuzene tackifier spray adhesive was used to stick the layers of fabric together. Since the splash mold process was performed on the underside surface of the stabilizer, it was necessary to use an adhesive to keep the fabric from falling off until the vacuum bag could be installed and a vacuum maintained. The three plies of glass were adhered together, on a table, and then placed on the surface of the stabilizer (figure 83). This process was repeated until all plies of glass were placed on the surface of the stabilizer.



Figure 83. Glass cloth placed on part surface.

After all the plies were on the surface, a single ply of polyester peel ply was placed as the top layer. This peel ply would allow the splash mold to be easily removed from the vacuum bag and create a nice clean surface free of resin splash. Along one edge of the part, a spiral-cut polyethylene resin feed line was placed in a folded peel ply pocket and taped in place. On the opposite and highest edge, the vacuum line (also of spiral-cut polyethylene) was connected to solid line and connected to a vacuum pot. The pot serves to protect the pump from ingesting curing matrix material by providing a catch pot. The catch pot was plumbed to the vacuum pump so vacuum could be drawn through the lines. Figure 84 shows the splash being vacuum bagged and set up for infusion.

Once all the fabric was placed on the surface, the part was covered and sealed with a nylon vacuum bag. Vacuum was drawn on the part, and the infusion process was started after the resin was ready. The 2000 g of FAVE-L-25S resin was used to infuse the part. From the total resin weight, 0.15% of cobalt naphthenate was used as the promoter, and 1.0% of MEKP was used as the activator. It took 30 min to fully infuse the part and 60 min for the part to gel. After infusion, the part was allowed to cure at room temperature for 24 h and then removed from the surface of the horizontal stabilizer (figure 85). The part was cleaned up and inspected for cracks or surface abnormalities. No cracks or abnormalities were found.



Figure 84. Splash being vacuum bagged and set up for infusion.



Figure 85. Splash mold after removal from aircraft surface.

6.2.3.2 Issues Encountered. There were no issues encountered when using the FAVE-L-25S resin to infuse the rapid splash mold. The resin performed adequately compared to other resins with similar viscosity. The slightly higher viscosity of the FAVE-L-25S resin, due to the lack of styrene, did not have a negative effect on the infusion of the part. The splash mold made with the FAVE-L-25S resin maintained surface shape and was able to hold vacuum integrity in order to successfully create a repair part.

6.2.3.3 Validation Results. The FAVE-L-25S resin was validated during the rapid splash molding process against the criteria the ACO specified for the program. The resin was able to be successfully infused against the surface of the aircraft to create a splash with the size and thickness required (figure 86). After fabrication, it was able to hold vacuum in order to create a repair part off of the splash tool. During the process, no cracks or abnormalities appeared in the surface of the splash tool made by the FAVE-L-25S resin system. The FAVE-L-25S resin performed adequately compared to higher styrene content VE resin systems.

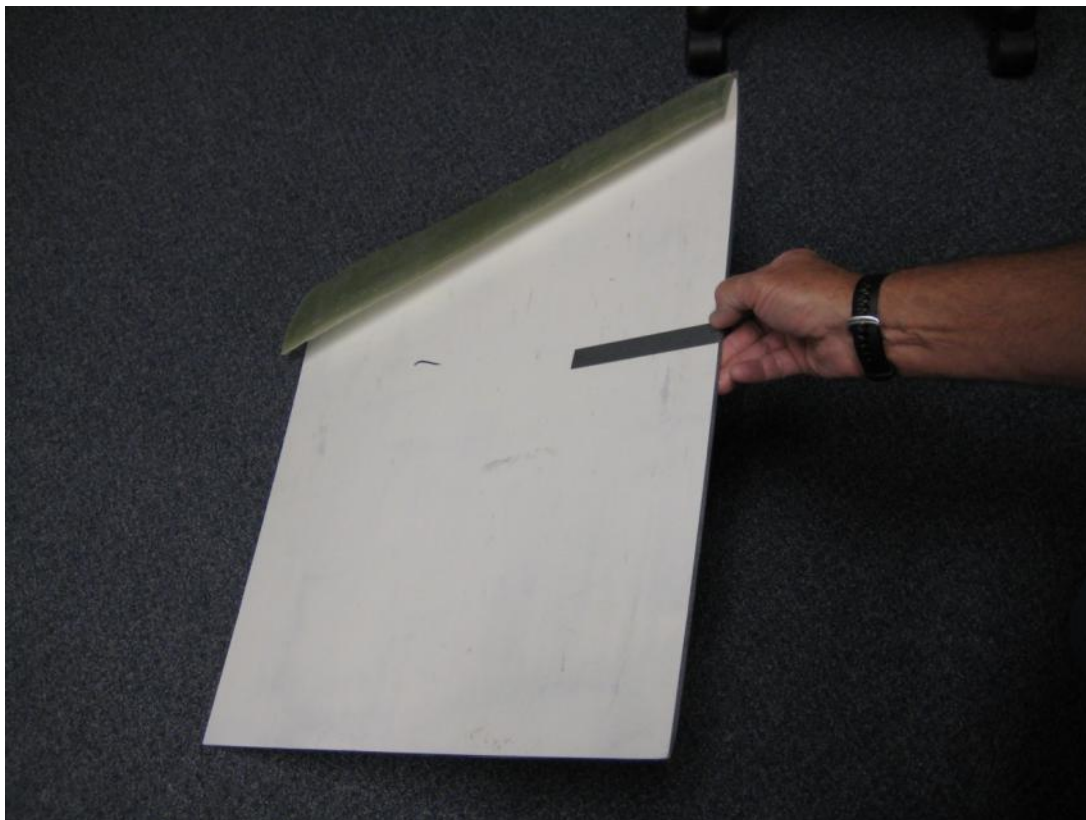


Figure 86. Final splash mold with edges trimmed.

6.2.3.4 Conclusion. The FAVE-L-25S resin system was able to successfully infuse the first trial demonstration rapid splash tool. The demonstration tool showed that this resin system could match that of commercial resin systems with the current selected process. The process for the rapid splash tooling system will most likely undergo changes as the process development continues. As changes to the mold making process change, the FAVE-L-25S resin system was reevaluated to assess whether it continues to meet the rapid splash tooling system requirements. The FAVE-L-25S resin system is a candidate resin system that was compared to commercial VE systems as well as epoxy resin systems. During the first demonstration of the rapid splash tooling process, the ACO was very pleased with the performance of the FAVE-L-25S resin system. Making the health of its workers a top priority, the Air Force is interested in any way to reduce potential risk. This fact alone makes the FAVE-L-25S resin system an excellent candidate system for use in the rapid splash tooling process.

6.2.4 Air Force Demonstration/Validation Summary

The ACO was very impressed with the performance of the FAVE-L-25S resin system. For the F-22 canopy cover and rapid splash tooling system, the FAVE-L-25S resin system met or exceeded the requirements set for the system. For these two parts, the system performed as well as a commercially available VE resin systems. Being able to eliminate a portion of the hazardous chemical, styrene, is very beneficial to the health and safety of Air Force maintainers and manufacturers. With ever-evolving health and safety standards, the reduction of styrene content in commercial resin systems was necessary. The reduction in the styrene content of resin systems does have an adverse effect on viscosity of the resin system. Since styrene is used to lower the viscosity in resin systems, reducing the amount of styrene tends to increase the viscosity. We saw a problem with this in the T-38 dorsal cover part. The FAVE-L resin system could not directly replace the commercial resin system used because the viscosity of that particular resin was too high. The high viscosity would not allow a proper infusion of the part using the existing fiber layup and process specifications. Process specifications could be changed to accommodate the resin system but would require an extensive validation process not practical for the Air Force. Thus, a lower-viscosity resin system such as the FAVE-L-25S could be used for the T-38 dorsal cover and probably would have been successful. The increase in viscosity is a disadvantage in the resin system but is low enough to still perform successful vacuum infusion in many cases. It should be examined and tested further to be used as a substitute material for parts and as the original material of any new parts on the way to being manufactured. The potential of a decreased risk to our workers and the overall reduction of harmful emissions necessitates that this resin system should be further investigated for use on current and future aircraft parts.

6.2.5 Navy MCM Composite Rudder

A more detailed report of the demonstration/validation results can be found in appendix I.

6.2.5.1 Processing

Gel Time Study

A series of tests were performed with the FAVE-L-25S resin system prior to the infusion of panels to determine the appropriate formulation for the desired gel time. A 5-h gel time would be desired for manufacturing of large-scale parts, whereas a slightly shorter gel time would be desirable for small-scale laboratory parts. An initial test was performed with the same formulation as the FAVE-L-20S resin system but with the Trigonox 239A catalyst, and this yielded a gel time of 6 h, with the samples still tacky to the touch. Some variations on this formulation were attempted, as shown in table 69, but this only resulted in longer gel times. The catalyst was then switched back to the Cadox L-50 MEKP material for trial B, as shown in table 70. In general, this yielded approximately the same gel times, with the samples a little less tacky to the touch. Finally, the N,N-dimethylacetamide (DMAA) component was switched to N,N-DMA, which had been used in the past in VE formulations. This resulted in formulations that fully cured and were not tacky to the touch once cured. Formulations for a short-term (~1 h) and longer-term (4–5 h) gel time were tested. The trial denoted 2C was used for panel fabrication for characterization purposes, and the trial 1C is recommended for large part fabrication (table 71).

Table 69. Gel time study—trial A.

Fave-L-25S	Trial					
	(weight-percent)					
Component	1A	2A	3A	4A	5A	6A
CoNap	0.3	0.3	0.3	0.3	0.25	0.3
2,4 P	0.25	0.25	0.3	0.3	0.3	—
N,N-DMA	0.2	—	—	—	—	—
Trigonox	2.0	2.0	2.0	1.5	1.0	1.5
Gel time	6 h ^a	Overnight ^a	Overnight ^a	Overnight ^a	Overnight ^a	20 min ^a

^aSamples tacky to touch once cured.

Table 70. Gel time study—trial B.

Fave-L-25S	Trial				
	(weight-percent)				
Component	1B	2B	3B	4B	5B
CoNap	0.3	0.3	0.3	0.3	0.25
2,4 P	0.25	0.25	0.3	0.3	0.3
DMAA	0.2	—	—	—	—
Cadox L-50a	2.0	2.0	2.0	2.0	1.5
Gel time	7 hr ^a	2.5 hr ^a	10 + hr ^a	10+ hr ^a	10+ hr ^a

^aSamples less tacky to touch once cured than first set of trials.

Table 71. Gel time study—trial C.

Fave-L-25S	Trial (weight-percent)	
Component	1C	2C
CoNap	0.3	0.3
2,4 P	0.25	0.1
N,N-DMA	0.2	0.2
Cadox L-50a	1.5	1.5
Gel time	4–5 h	50 min

Panel Fabrication

A total of two panels were fabricated at NSWCCD for evaluation of the FAVE-L-25S and Derakane 510A resin systems. These panels were made using standard VARTM techniques with the same fabric as in the previous section and the resin, as shown in table 72.

Table 72. Panel identification and fiber orientation.

Panel	Layup	Resin/Formulation	
070801	[0] ₈	FAVE-L-25S	0.3% CoNap 0.1% 2,4 P 0.2% N,N-DMA 1.5% Cadox L-50
070902	[0/90] ₄	FAVE-L-25S	0.3% CoNap 0.1% 2,4 P 0.2% N,N-DMA 1.5% Cadox L-50
070903	[0] ₈	Derakane 510A	0.25% CoNap 0.1% 2,4 P 1.25% Trig 239A
080304	[0] ₁₀	CORVE 8100	0.1% CoNap 1.25% Cadox L-50

Flow/Viscosity Study

As the panels shown in table 72 were being infused, an outline of the infusion flow front was drawn on the bag at specified time intervals. Photographs were taken at the end of the infusion and a flow front with time graph was constructed for each of the panels, as shown in figure 87.

The flow study results indicated that the FAVE-L-25 S resin appears to infuse at a much slower rate than the Derakane 510A resin in a unidirectional panel (43 vs. 20 min). The addition of 90° plies appears to aid in speeding up the flow front by decreasing the infusion time from 43 to 35 min. A brief check of the resin viscosities with a Model RV Brookfield viscometer yielded higher than expected viscosities for the FAVE-L resin systems, as shown in table 73. It should be noted that these viscosities measured were for the original FAVE-L-25S and not the variants (e.g., -A2, -RDX) that had reduced viscosity and improved performance.

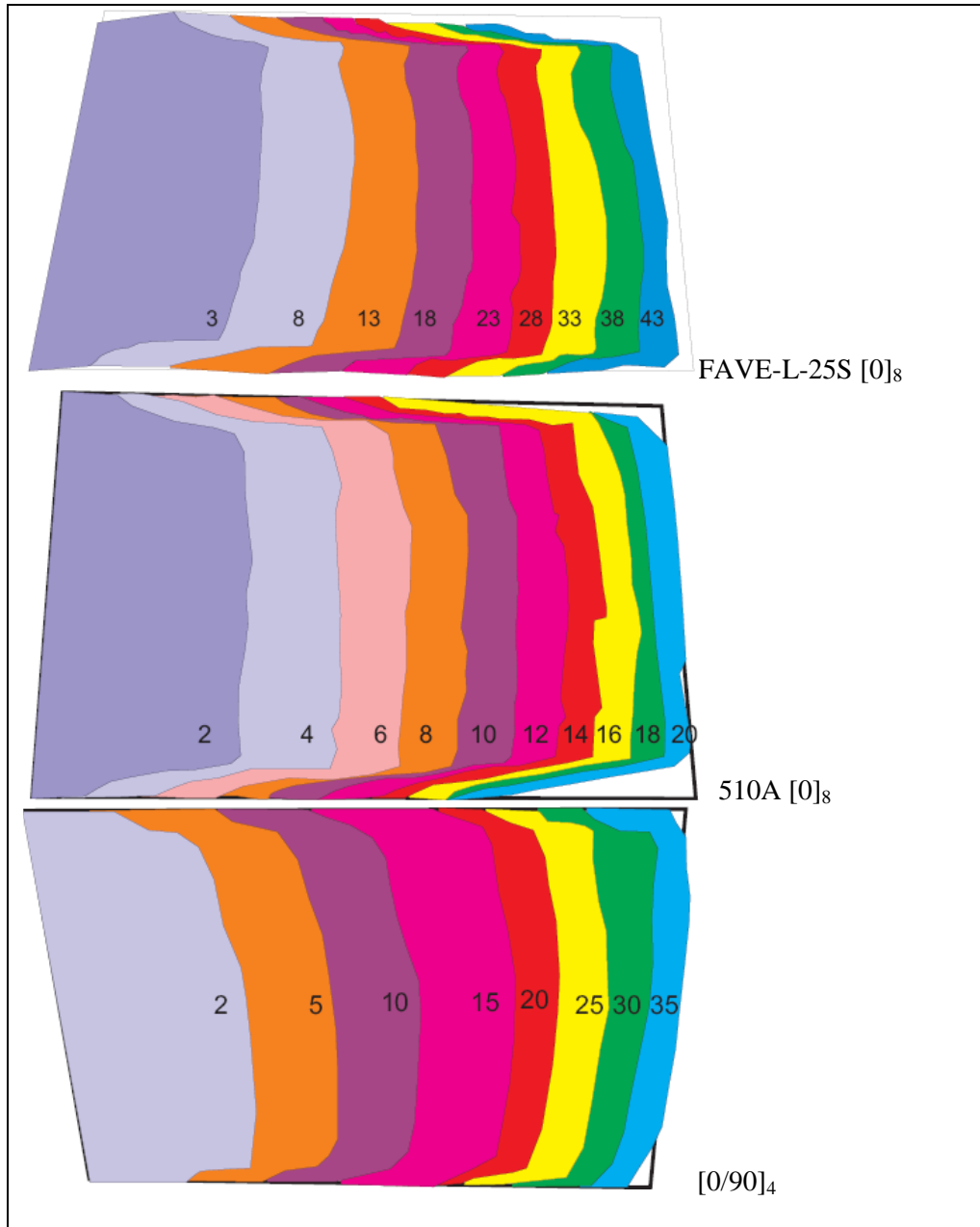


Figure 87. Flow study results indicating movement of flow front with time denoted in minutes for three different panel types.

Table 73. Viscosity of resin systems.

Type	Viscosity (cP)
FAVE-L-20S	1992 ± 11
FAVE-L-25S	1171 ± 99
Derakane 510A	520 ± 0
Corve 8100	100 ^a

^aInterplastic data sheet value.

6.2.5.2 Rudder Demonstration/Validation. Two MCM rudder demonstration articles were fabricated by Structural Composites, Inc. The main difference between the two rudders was that the first rudder had a fabricated representative composite hub, whereas the second rudder was only foam filled and did not contain a hub. The second rudder would be used for evaluation of the process by performing destructive evaluation, whereas the first rudder would be held intact for potential further testing. In addition, a SIDER non-destructive test was performed to confirm the quality of the part.

Fabrication Process

The MCM rudder for this demonstration process was made using the same glass fiber reinforcement and fiber layup as with the DDG51 composite twisted rudder (CTR). The SW1810 Uni/Mat fabric from Fiber Glass Industries is 18 oz/yd² unidirectional E-glass fibers stitched to a 10 oz/yd² binder-free chopped strand mat. The main fabrication process difference was that these rudders were fabricated using a two-step infusion process rather than the single stage resin recirculation process that was used to fabricate the in-service MCM rudders. It was found as a result of the DDG51 CTR program (34) that the risk to a program is substantially reduced by the use of a multi-step infusion process for thick section composite parts by allowing the possibility of repair after each infusion step. The five layers of fabric were laid up on the part for each infusion step using an alternating 0/90° layup with the mat side placed against the part.

Rudder 1 Fabrication

Structural Composites decided to fabricate a composite hub for this rudder. Initial inquiries into the cost of a metallic bronze hub were in excess of \$50k, which was well outside the boundaries of this demonstration. The hub was constructed using the metallic version as a guideline and also taking into account the hub and flange design of the DDG51 CTR. The hub was made in several stages with the circular hub formed around a steel cylinder. The flanges were fabricated separately and then secondarily bonded to the main hub. Figure 88 shows a series of photos that were taken of the composite hub fabrication process.



MCM Rudder Tooling



Infused Hub Stiffener



E-Glass Wrapped Cylinder



Infused E-glass Hub



Foam cut outs for Flange Fabrication



Foam Overwrapped with E-Glass



Flange Infusion



Composite Hub Assembly

Figure 88. Fabrication of MCM composite hub.

After the hub was manufactured, the part was placed into the foaming mold, and a two-part polyurethane foam was blown into place. As part of this process demonstration, risk reduction trials for the DDG51 class rudder composite manufacturing process were evaluated where possible. One of these trials involved the fabrication of vertical shear ties located near the tip of the rudder. In the case of the CTR, there were issues ensuring that the full thickness of the shear ties was fully and uniformly infused. Therefore, for this demonstration, a new process was evaluated to make the cutouts in the foam required for the placement of the shear ties. In this case, a wooden preform was molded into the foam at the desired shear tie location. Once the foaming was complete, the wooden preforms were removed, leaving a uniform cut out in the foam for the insertion of the fabric that was used to make the shear tie. As was shown in the destructive evaluation portion of the second rudder, this method yielded very uniform shear ties with minimal (if any) voids.

After the foaming was complete, the glass preform shear ties were installed into the foam in the desired locations and then infused. Figure 89 shows pictures of the foaming and shear tie fabrication process. It should be noted that the orange/pinkish color on the foam is fairing compound that was used to fill in the surface holes. The rudder was then placed on the assembly stand, and the glass fiber was wrapped to the required layup. To reduce the risk to the program, half of the required layers were infused at a time.

The first infusion for rudder 1 was witnessed by Roger Crane (code 655). One of the key issues in the VARTM process is the control of the vacuum bag seal. It is extremely important that there are very minimal (if any) leaks in the bag seal to ensure that no air is pulled into the part during the manufacturing stage. As parts get larger, it becomes more and more difficult to find leaks in the seams. Generally, a leak down test was performed prior to infusion, the requirement being that the vacuum pressure in the bag cannot drop more than 1 in of mercury over 15 min. If this requirement is not met, then the bag seal is inspected again to determine where the leak is originating and is repaired.

Structural Composites, Inc., uses a unique combination of vacuum bagging materials in the infusions. The resin distribution media is fairly open, allowing very fast movement of the resin along the surface of the part. The distribution media used in this application is also very stiff and has sharp edges where it has been trimmed. It is believed that these sharp edges might have contributed to issues with vacuum leaks developing during the infusion process. It was determined in the DDG51 CTR program through a peel ply study (35) that a heat-scoured peel ply provides the best surface for secondary bonding. Several infusion lines are used in this vertical infusion. The initial two ports are located at the base of the rudder as it sits on the infusion platform. Once flow is past the next line of infusion, the next set of inlet ports is opened. All lines are kept open until the resin gels in the buckets. In some instances, if a leak appears in the part, an additional inlet/outlet port may be quickly added to minimize the effect of the leak. In this infusion, the trailing edge tip of the rudder was the last to infuse.



Foam Form with Embedded Flanges from the Composite Hub Present



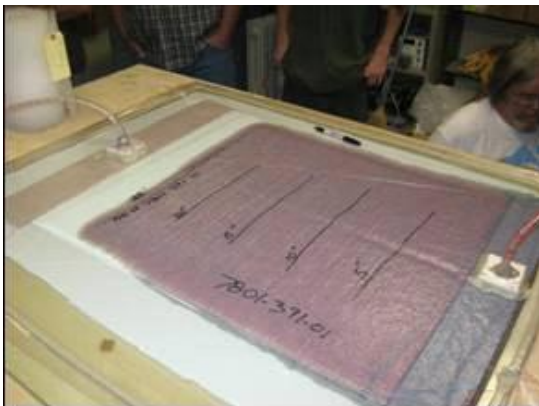
Foam Form with Embedded Flanges from the Composite Hub Present



Vertical Shear Ties Inserted into Slots



Shear Ties in Place with Flange Overwraps



Infusion of Vertical Shear Ties



Infusion of Horizontal Flanges

Figure 89. Foaming and shear ties fabrication of MCM rudder.



Figure 89. Foaming and shear ties fabrication of MCM rudder (continued).

The first infusion yielded a good outer face sheet laminate. This infusion is shown in figure 90. The whiteness of the part is due to surface scrapes from removing the white heat scoured peel ply. It was found that this peel ply would tear as it was being removed from the part, which necessitated removing the peel ply in smaller pieces using mechanical assistance. A significant effort in both time and labor was required to remove the vacuum bag and distribution media for the first layer infusion. In subsequent infusion, an additional layer of Super Release Blue peel ply was used over the heat scoured peel ply to aid in the removal of the bag and distribution media.

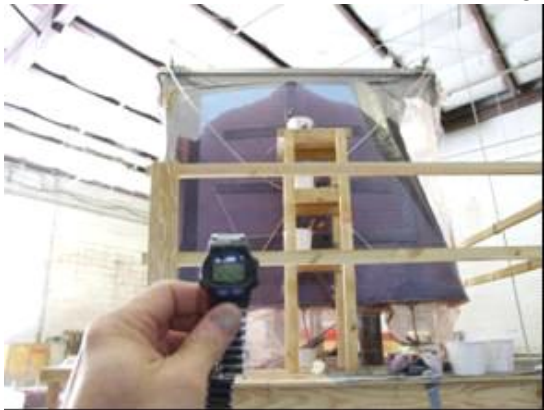
A similar process was performed with the second infusion of rudder 1. Figure 91 shows the progression of the infusion up the MCM rudder from the base to the tip. This infusion (and all subsequent face sheet) infusions were witnessed by Maureen Foley (code 655). Structural Composites decided to wrap the rudder with pallet wrap prior to placing the vacuum bag over the part. It was hoped that by holding the glass fabric more tightly in place prior to application of the vacuum, it would minimize the wrinkling on the leading edge. After infusion, (figure 92) it was seen that wrinkling still occurred on the leading edge. In this case, the overlaps in the pallet wrap layers caused areas of excess resin pockets to form along the faces of the rudder, as well as the root of the rudder. After the infusion, the rudder was carefully removed from the assembly stand that was also used as an infusion station (figure 93).



MCM Rudder Before Infusion One



MCM During Infusion One



MCM Rudder Towards End of Infusion

Figure 90. MCM rudder 1—infusion 1.



Figure 90. MCM rudder 1—infusion 1 (continued).

In general, the face sheet infusions took ~1 h to infuse through the vertical height of the rudder. Initially, there was concern that the nominally higher viscosity of the FAVE-L-25S resin (400 cps) compared to the CORVE 8100 resin (100 cps) would cause problems with the infusion, but the infusions were fairly well behaved. The only manufacturing concern with the FAVE-L-25S was that it did not appear to have a very stable gel time with a given mix ratio. Before each infusion, a gel time test was performed, and the mix ratio varied accordingly to meet the desired 1–1.5 h gel time. During the infusion, the mix ratio of the buckets mixed later in the infusion contains higher amounts of catalyst so that they would gel at approximately the same time as the first buckets that were mixed.

Rudder 2 Fabrication

The second rudder that was fabricated under this demonstration project did not have a composite hub. Instead, it simply had a steel cylinder to which several pieces of steel were welded on to provide a flange-type support. The purpose of the flange was simply to ensure that the steel cylinder would not rotate within the foam, ensuring that the glass wrapping process could take place.



Start 1315



1402



1412



1412



1414



1415



1417 Infusion Complete



1418 Infusion Complete

Figure 91. MCM rudder 1—infusion 2.



Figure 92. Completed MCM rudder 1.



Figure 92. Completed MCM rudder 1 (continued).

Figure 94 shows some additional steps of the fabrication process. Initially, the full foam preform was molded and faired as needed. The vertical shear tie foam area was removed and wooden preform installed for the second foaming step, which yielded uniform shear tie slots. The vertical shear ties were installed and infused, as with rudder 1.



Figure 93. Unloading MCM rudder 1 from fabrication fixturing.

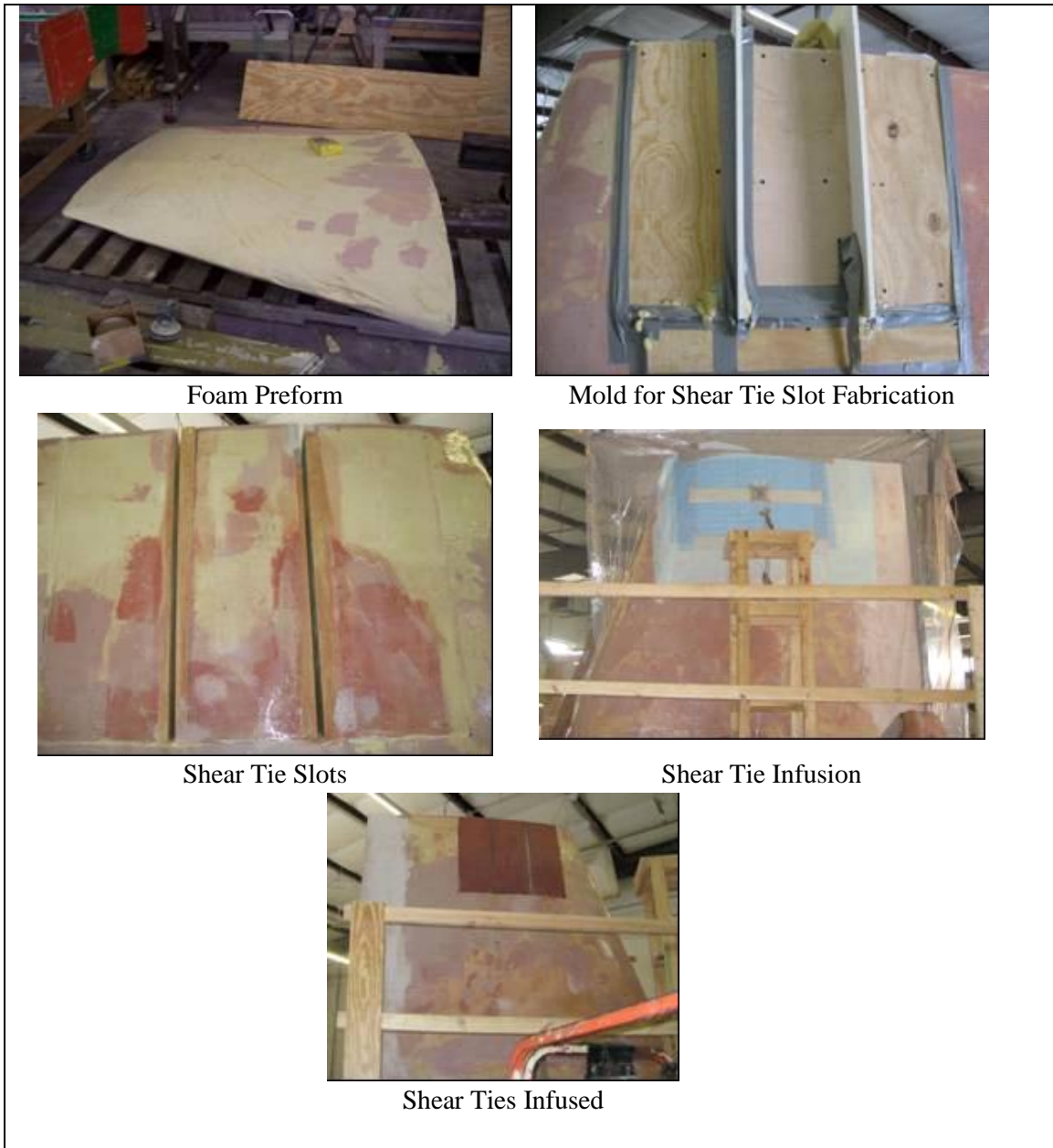


Figure 94. MCM rudder 2—foaming and shear tie fabrication.

Figure 95 shows part of the glass wrapping process. The SW1810 is wrapped around the rudder using a fixture that was developed under a previous program. The mat side of the glass fabric was placed against the foam in alternating 0/90 layers for a total layup of (0/90/0/90/0) for each infusion.



Figure 95. MCM rudder 2—glass wrapping.

During the infusions of rudder 2, two caul plates were evaluated to determine if their use would minimize the wrinkling of the glass fabric around the edges of the rudder. Glass fiber-reinforced caul plates were fabricated using the MCM molds and placed on the middle of the tip of the rudder and about one-fourth of the way down from the root on the leading edge. Figure 96 shows the caul plates installed with the distribution media prior to the installation of the vacuum bag.

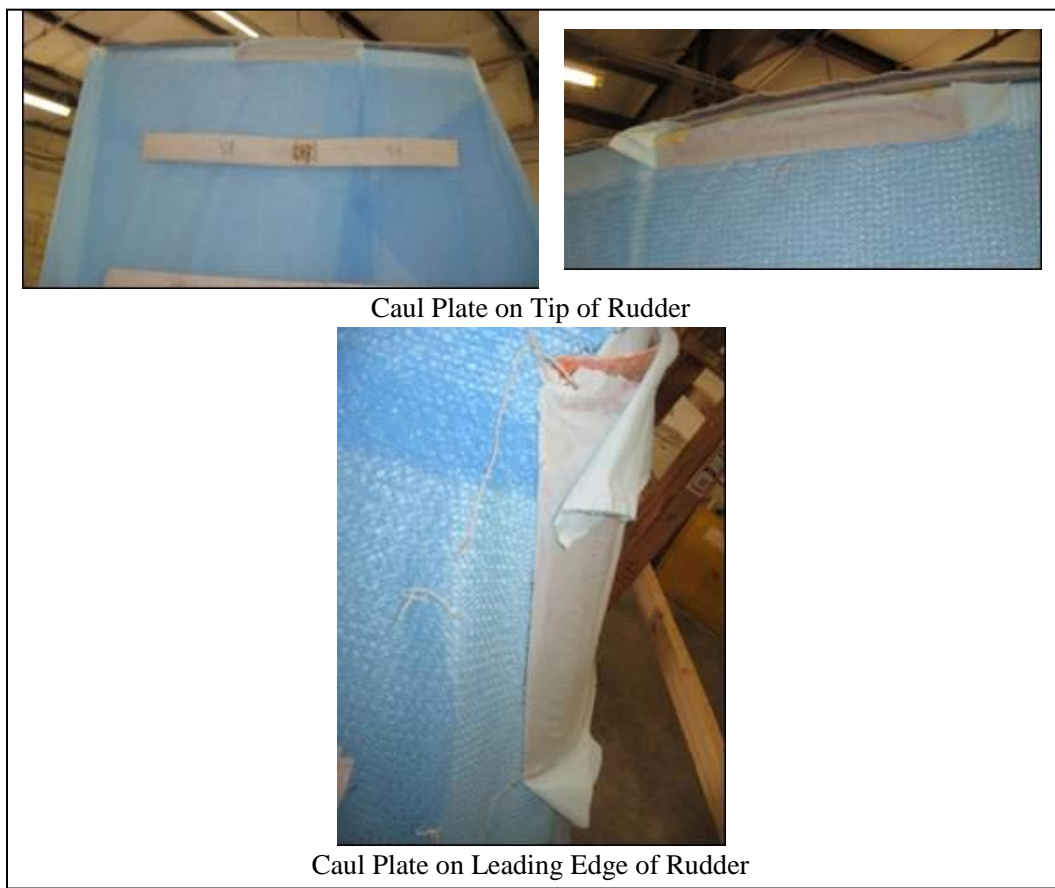


Figure 96. MCM rudder 2—caul plate locations.

A progression of the MCM rudder 2, infusion 1 can be seen in figure 97. As with the previous infusions, the infusion time was ~1 h. Figure 98 shows different views of the MCM rudder 2 after the first infusion. The results are similar to the previous infusions. In the areas where the caul plate was used, it appeared that wrinkling was prevented in the glass fabric in the immediate area. However, the use of the caul plate caused the wrinkle to move to an area not covered by the caul plate. On one side of the rudder, there was a large black inclusion, as circled in red in figure 98. Upon further inspection, this was found to be a piece of vacuum tape that was not removed before the next infusion. This incidence was somewhat indicative of the kinds of manufacturing defects can occur when quality checks are not adhered to on the production floor.



1307



1315



1323



1329



1330



1333



1338



1358

Figure 97. MCM rudder 2—infusion 1.



Side 1



Side 2



Area on Tip where Caul Plate was Used



Near Root



Leading Edge (Large Inclusion circled in Red)



Figure 98. MCM rudder 2 after infusion 1.

A progression of the MCM rudder 2, infusion 2 can be seen in figure 99. As with the previous infusions, the infusion time was ~1 h. Figure 100 shows different views of the MCM rudder 2 after the second infusion. The results are similar to the previous infusions. In the areas where the caul plate was used, it appeared that it did prevent wrinkling in the glass fabric in the immediate area, but the wrinkle moved to an area not covered by the caul plate. A destructive analysis was performed in these areas to confirm these findings.

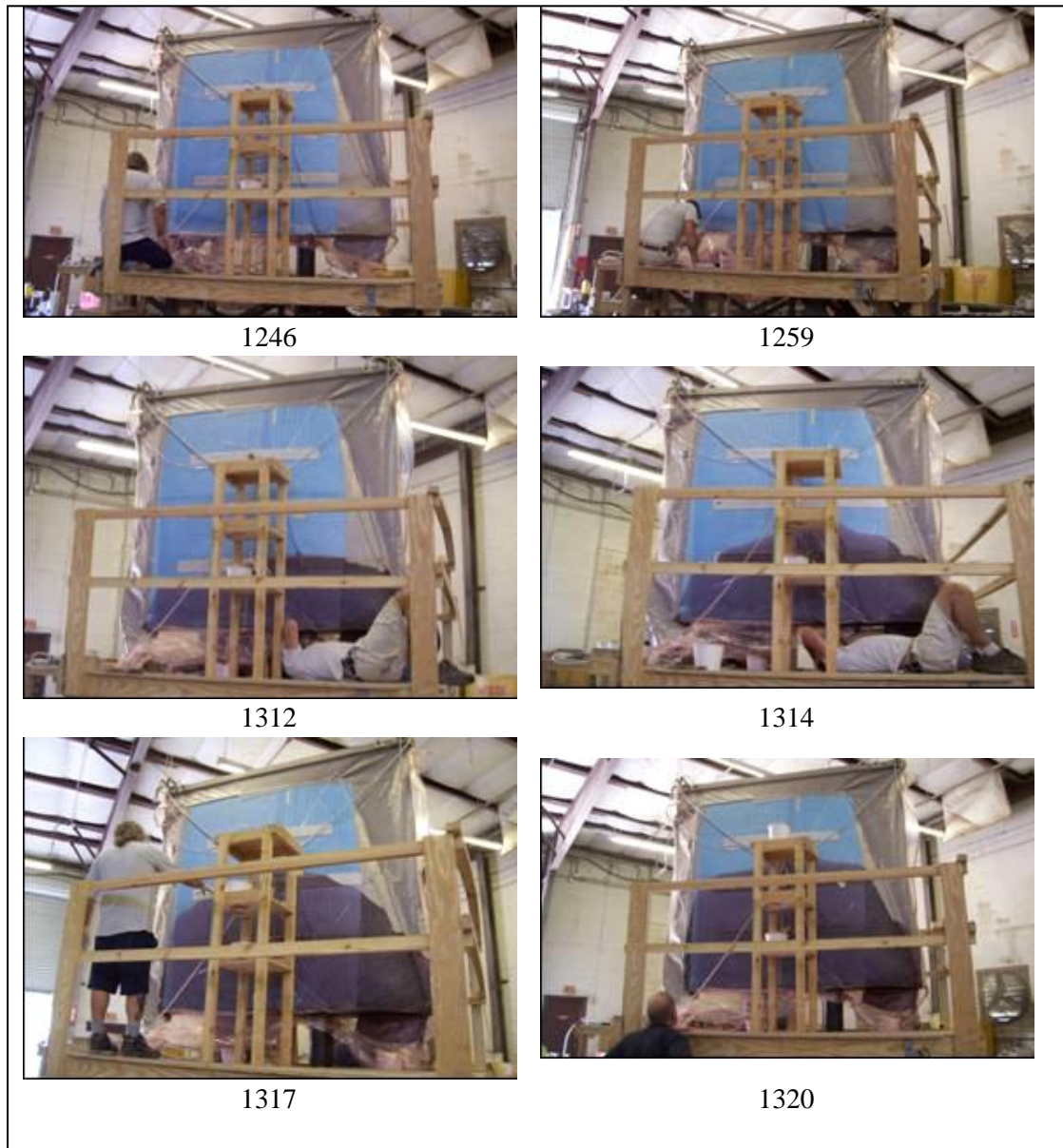


Figure 99. MCM rudder 2—infusion 2.

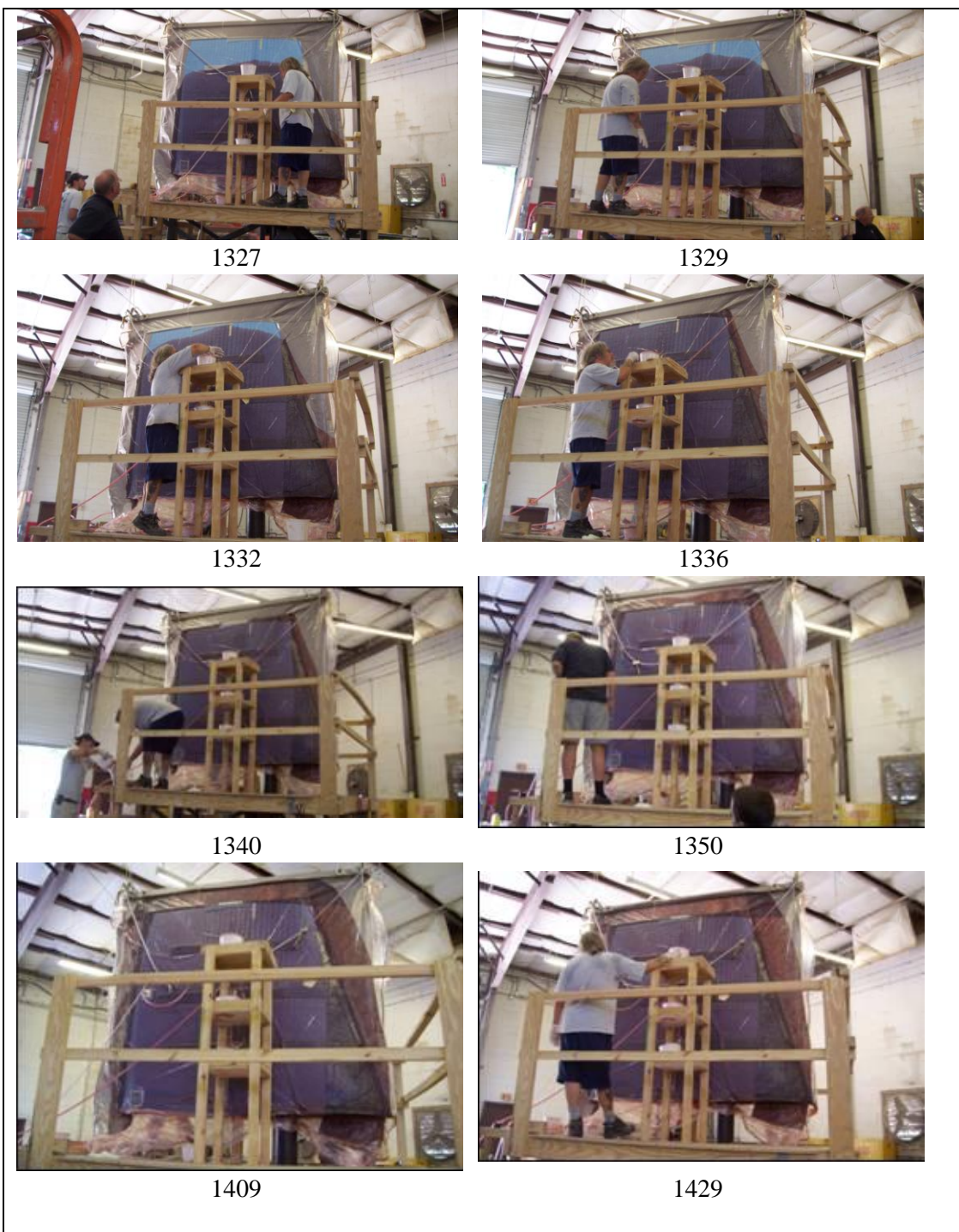


Figure 99. MCM rudder 2—infusion 2 (continued).

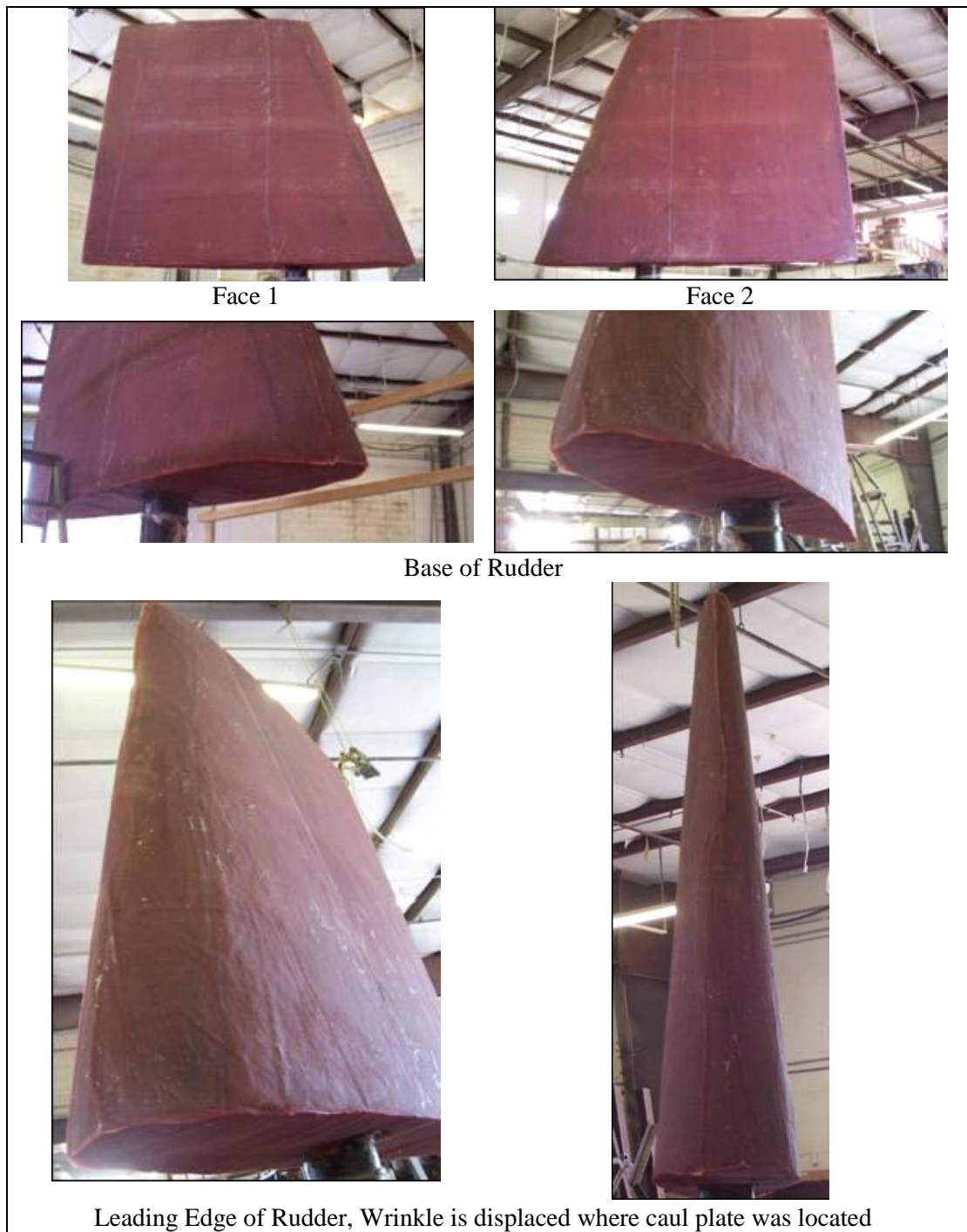


Figure 100. MCM rudder 2 after infusion 2.

Destructive Evaluation of Rudder 2

Face Sheet Core Samples

Four samples were extracted using a core drill from each face of the rudder to determine an average face sheet thickness. Figure 101 shows photos of the two faces with the locations marked where the samples were removed. The results are shown in table 74. The results show fairly good agreement from one face to another on thickness of the face sheet material. The average of samples does not include the B samples, which were taken in the area of the vertical shear ties and therefore have an additional thickness due to the shear tie overwraps.

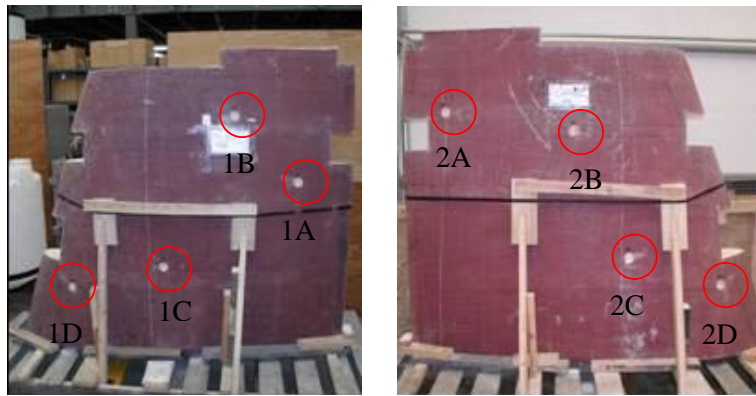


Figure 101. MCM rudder 2—locations of face sheet samples.

Table 74. Core drill samples thicknesses from rudder faces.

Sample	Face 1 (in)	Face 2 (in)
A	0.3755	0.3790
B	0.5010	0.5205
C	0.3600	0.3495
D	0.4105	0.4115
Average \pm st. dev.	0.382 ± 0.026	0.380 ± 0.031

Rudder Cross Sections

Around the edges of rudder 2, large pieces of composite were removed so that a detailed analysis could be performed on the cross section of the composite (figure 102). Two locations were removed on the leading edge—one in the area of caul plate use (LEC) and the other away from the caul plate location (LE). Similarly, two pieces from the tip of the rudder were removed for inspection—one through the two shear ties and caul plate area (TC) and the other at the corner of the tip and trailing edge (TTE). The remaining piece was removed from the middle of the trailing edge (TE). All sides of the composites pieces that were removed were polished using standard polishing techniques so that an overall snapshot of the quality of the composite part, such as fiber ply alignment and void/resin/fiber ratio, could be obtained.

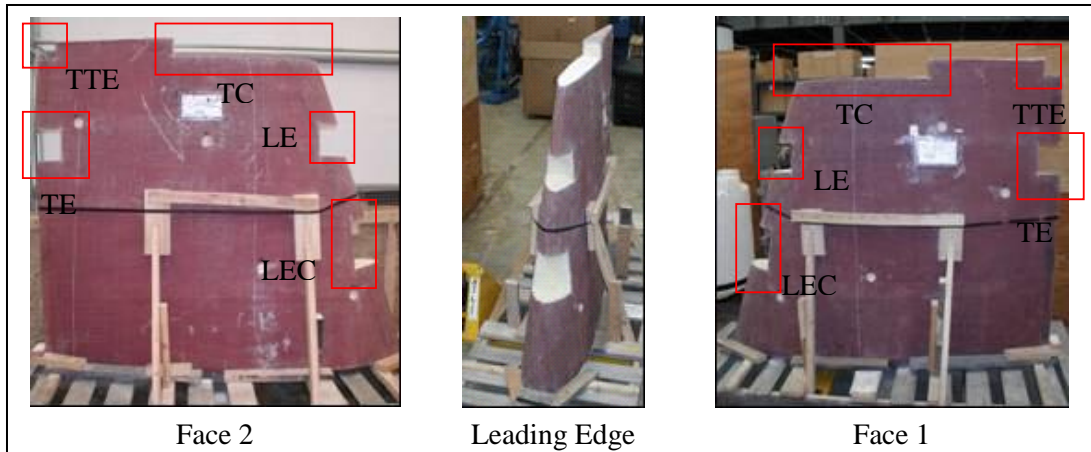


Figure 102. MCM rudder 2—locations of rudder cross sections.

Leading Edge – Caul Plate Area (LEC)

A large piece of composite was removed on the leading edge in the area where the caul plate was in place during the two infusions. All edges of the part were polished, and results are shown in figure 103. Results indicate that the caul plate appeared to shift the wrinkling from the leading edge to the edge of the caul plate.

Leading Edge – Away from Caul Plate Area (LE)

A large piece of composite was removed on the leading edge in an area away from the caul plate. All edges of the part were polished, and results are shown in figure 104. Results indicate that there was a substantial amount of wrinkling along the leading edge due to non-uniform compression of the glass fabric plies during the application of vacuum. These types of wrinkles are expected with this manufacturing process and were also evident in the CTR. As compared to the results in the previous section, the wrinkles in this part were much more pronounced than the ones in the caul plate area.

Tip – Shear Ties and Caul Plate Area (TC)

A large piece of composite was removed on the tip of the rudder that included an area though the two shear ties. All edges of the part were polished, and results are shown in figure 105. Results indicate a fairly uniform cross section within the shear ties, with minimal (if any) voids. The layer of distribution media (blue) left in the part can be seen in the resin-rich layer in the center of the shear tie. While the composite areas look very uniform, the foam regions are less than homogeneous. In general, the foam is used to fill up the space and not required to take any load. It is uncertain whether the voids in the foam region are critical. While the new technique to fabricate consistent shear ties appears to have worked, there has been some degradation in the quality of the foam in the areas around the shear ties.

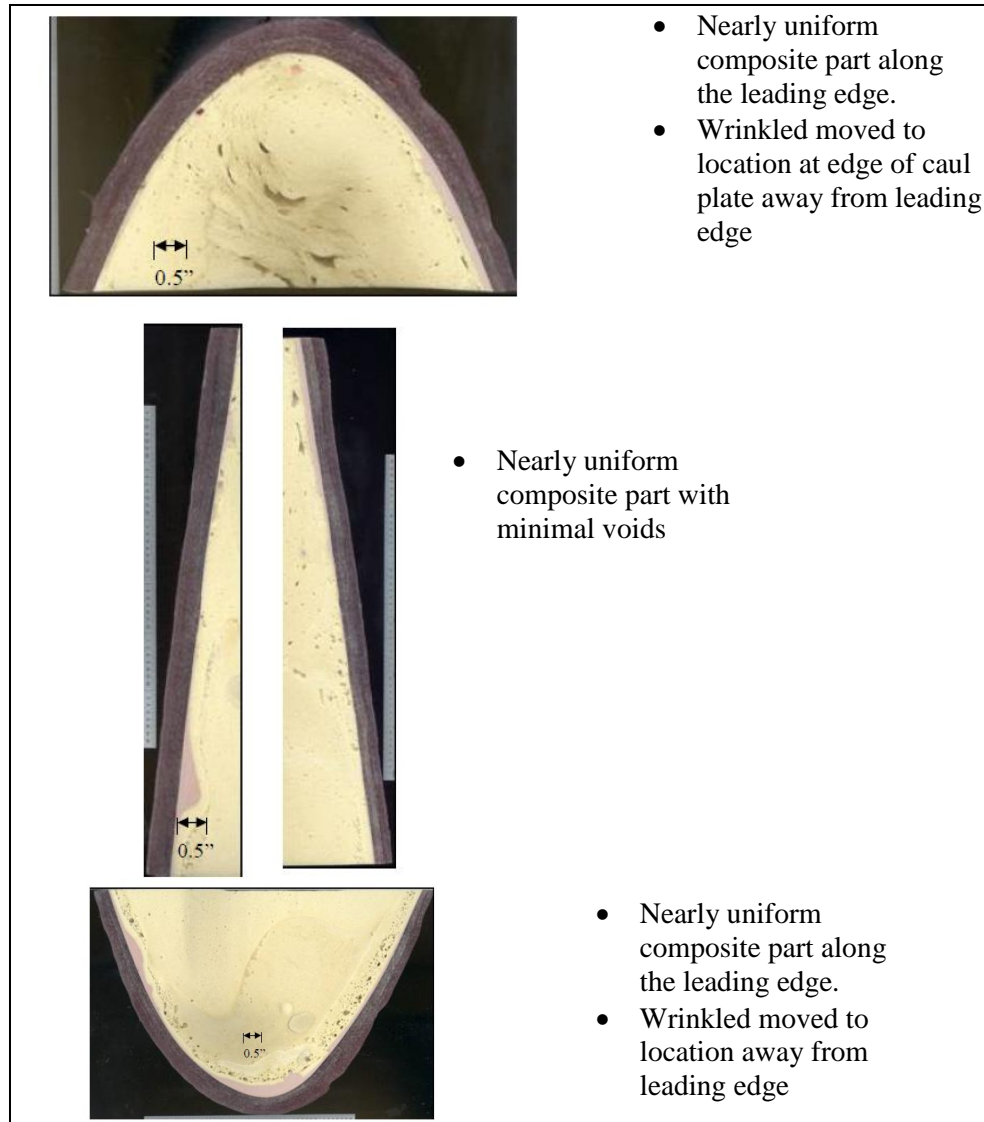


Figure 103. MCM rudder 2—leading edge near caul plate.

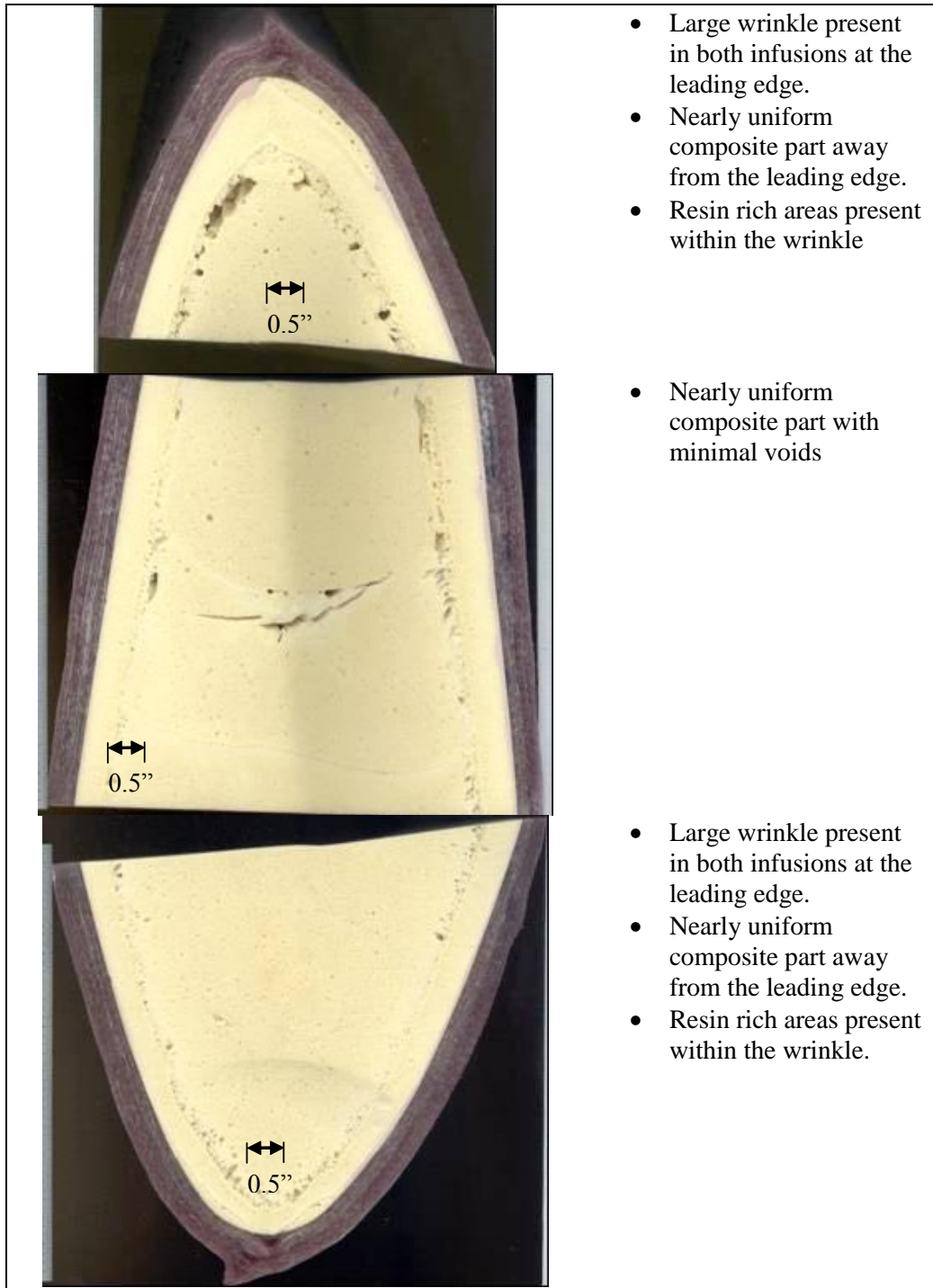


Figure 104. MCM rudder 2—leading edge away from caul plate.

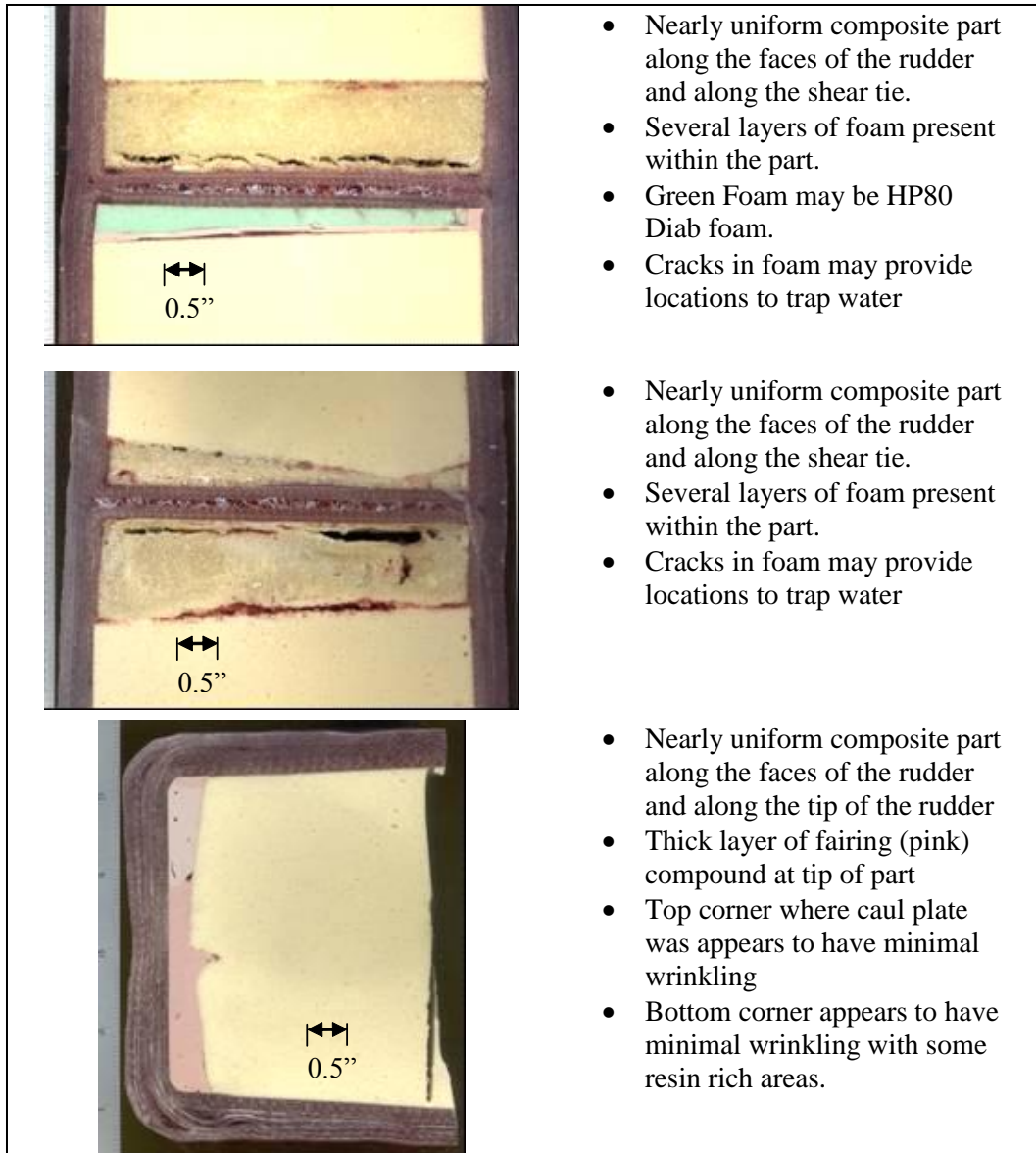


Figure 105. MCM rudder 2—shear ties and caul plate area.

The cross section of the part where the caul plate was located shows a uniform composite sample with continuous plies going around one of the sides of the tip. The other side, which did not have the caul plate, showed some minimal wrinkling with some resin-rich areas.

Corner of Tip and Trailing Edge (TTE)

A large piece of composite was removed from the corner of the rudder at the tip and leading edge. All edges of the part were polished, and results are shown in figure 106. The trailing edge side of the part showed fairly uniform glass layers going around the trailing edge. In contrast, the tip side of the part exhibited significant wrinkling of the layers, especially in the second infusion.

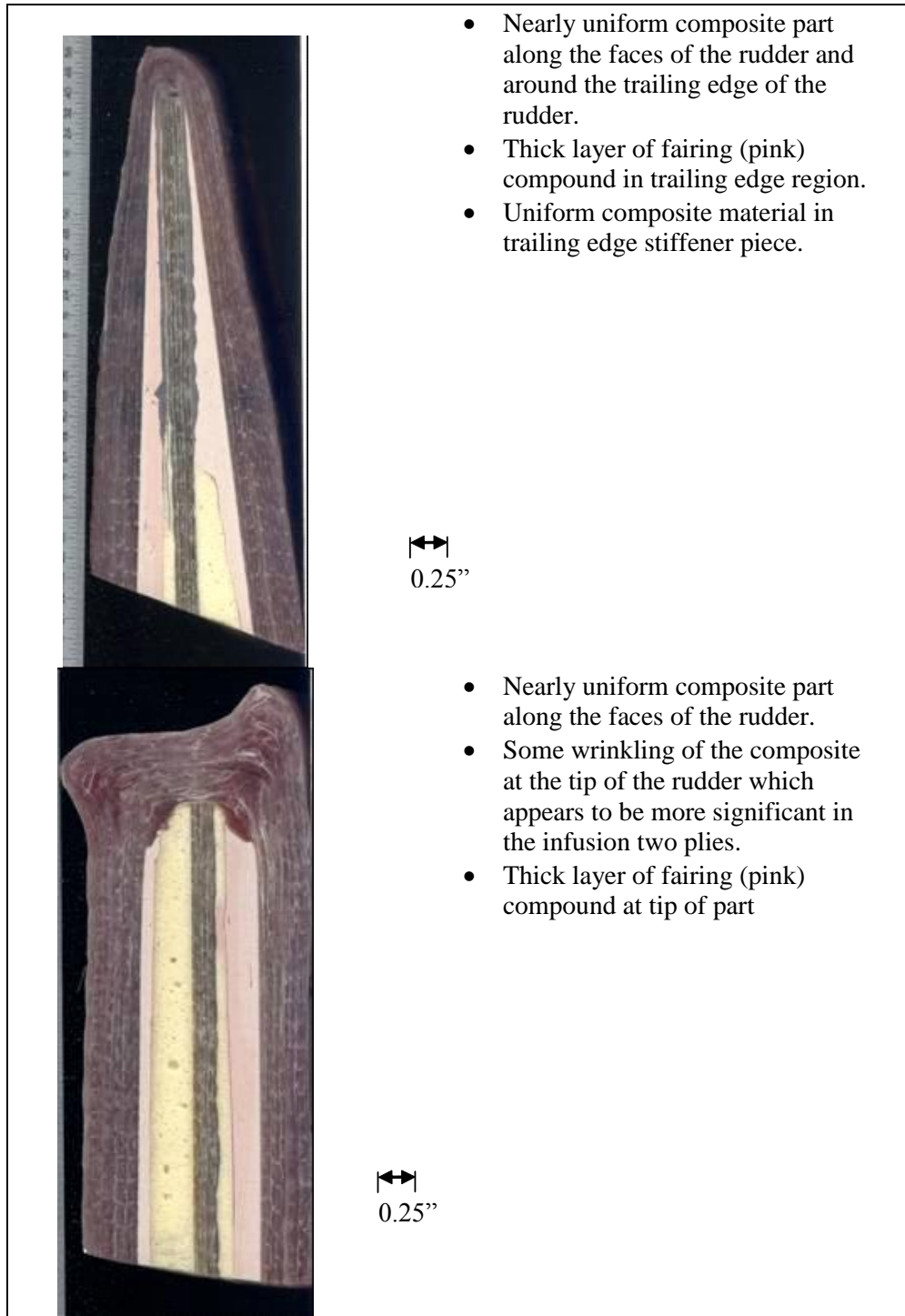


Figure 106. MCM rudder 2—corner of tip and trailing edge.

Middle of the Trailing Edge (TE)

A large piece of composite was removed from the middle of the trailing edge of the rudder. All edges of the part were polished, and results are shown in figure 107. The results indicate that the glass layers appear to be continuous and uniform around the trailing edge with minimal (if any) wrinkling.

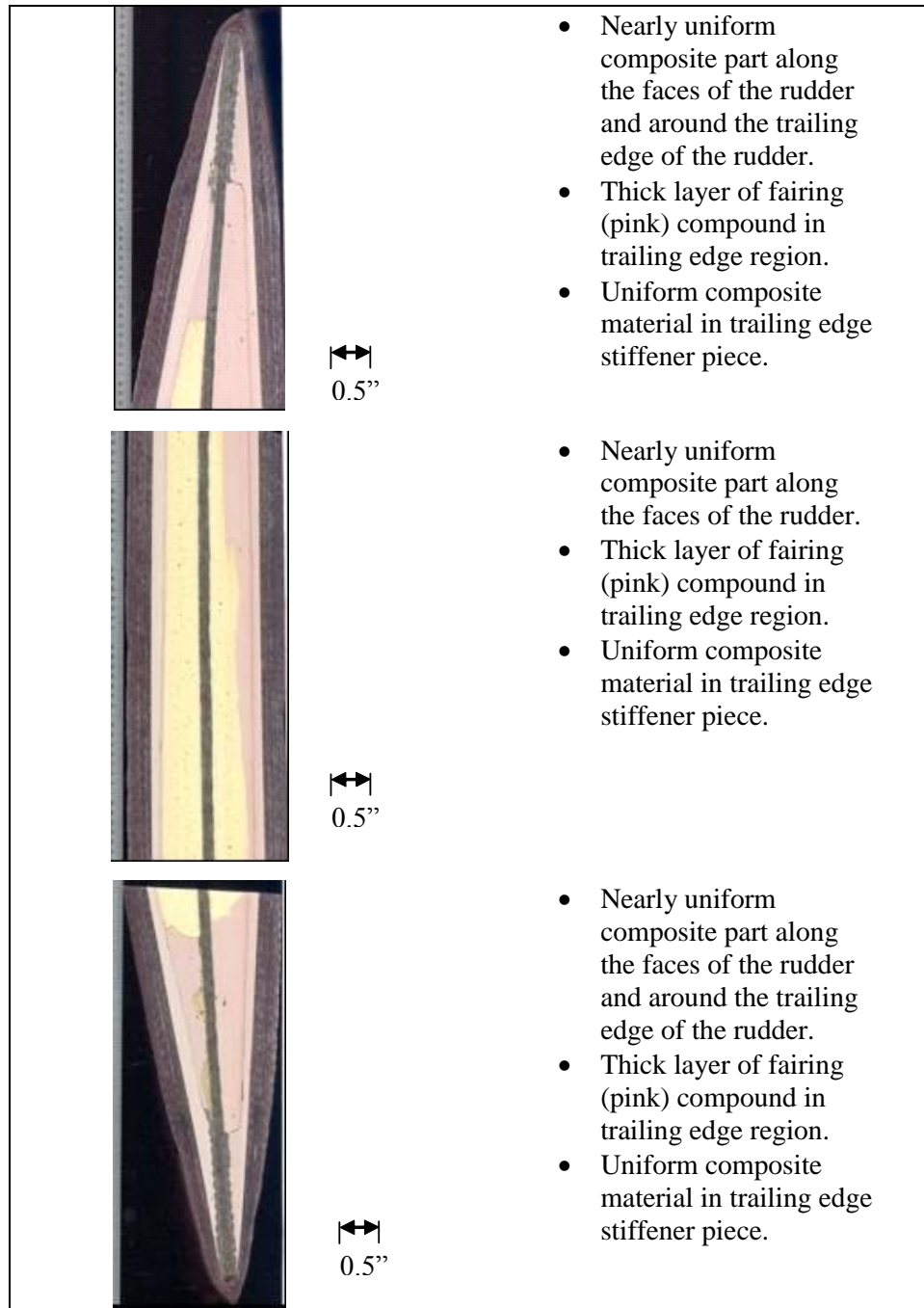


Figure 107. MCM rudder 2—middle of trailing edge.

6.2.5.3 MCM Rudder Conclusions. The FAVE-L-25S low-HAP/VOC resin system was used to fabricate two full-scale MCM rudder demonstration articles. The resin system was able to be processed using the standard marine-grade VARTM materials and techniques to fabricate good quality composite parts. The higher viscosity of the FAVE-L-25S compared to the baseline resin system (CORVE 8100) did not appear to adversely affect the manufacturability of the part. The FAVE-L-25S did appear to be slightly more affected by changes over time and of processing conditions than other commercially available resin systems, which required closer monitoring using gel time tests prior to infusion and adjustments to the mixing ratios as the part was being infused. Several manufacturing processes were evaluated under this program for risk reduction of the DDG51 CTR manufacturing. The new method for the manufacturing and placement of the shear tie structure appears to be very successful. In addition, there was a moderate improvement in the wrinkling on the leading edge and tip with the use of caul plates.

6.2.6 HMMWV Transmission Container

6.2.6.1 Laboratory Demonstration. A HMMWV transmission container was fabricated in the CCM laboratory. This was done for a few reasons. First, we wanted to make sure the FAVE resin used could infuse the part to ensure the resin had the appropriate viscosity and could infuse the part, including the nearly right angle corners. Secondly, it was the second demonstration piece to be made, and the first one after the failed T-38 dorsal cover. Therefore, we wanted to ensure the container could be infused with representatives from all groups involved with this project. Only a partial demonstration product was produced. The container produced was simply one-half of the composite box. No hardware was installed.

The major steps in box production are as follows:

1. cut 3TEX plies,
2. cut and drill foam,
3. layup plies and foam,
4. bag part,
5. mix resin, CoNap, and Trigonox and infuse with FAVE-O-25S, and
6. post-cure part.

It should be noted that FAVE-O-25S was used for this demonstration article (figure 108). The composite was infused with 30 min. Good fiber wet out was achieved overall with only one relatively dry spot that is likely an issue due to composite layup and not the resin. There was some bridging of resin occurred around the corners due to the fit of the foam. Overall, the lab demonstration part was successful. Thus, we proceeded with the demonstration at SMC.

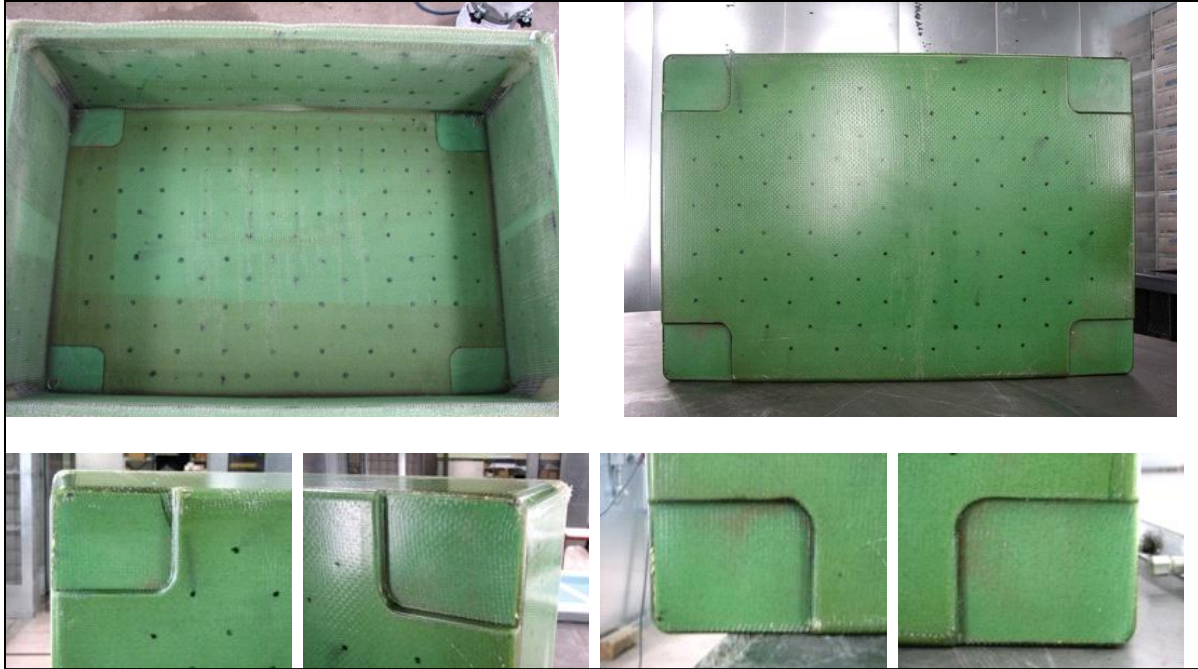


Figure 108. Photographs of the completed laboratory demonstrated HMMWV transmission composite container.

6.2.6.2 Sioux Manufacturing Demonstration. Shown in table 75 is a comparison of the three resins employed in this study as measured by SMC. The results show that the FAVE resin has similar properties to that of the commercial resins and should be adequate for this application. It should be noted that the resin variant used by SMC was the FAVE-L-25-RDX. The report from SMC can be found in appendix J.

Table 75. Neat resin properties as measured by SMC of the resins used for the HMMWV transmission container.

Resin	Density (g/mL)	Viscosity (cP)	Flexural Strength (MPa)	Flexural Modulus (GPa)	Glass Transition Temperature (°C)
FAVE-L-25S	1.07	550	110	3.2	120
Derakane 8084	1.14	360	130	3.3	115

SMC utilized the procedures developed for the CCM effort in the fabrication of the HMMWV transmission container. The major steps in box production are as follows:

1. Cut 3TEX plies,
2. cut and drill foam,
3. layup plies and foam,

4. bag part,
5. mix resin, CoNap, and MEKP and infuse with FAVE-L-25S-RDX or Derakane 8084 VE resin,
6. post-cure part,
7. cut holes for hardware,
8. add hardware,
9. trim top of box,
10. cut aluminum rails,
11. attach rails to box,
12. cut metal for internal cradle, and
13. assemble cradle.

Sioux Manufacturing produced four containers for the purposes of this work. Two containers used the FAVE-L-25S resin, while two containers used the incumbent Derakane 8084 resin. The box was layed up using the fiberglass and foam. The box was then vacuum bagged (figure 109A). After leak checks were performed and corrected, the resin was infused (figure 109B). No difficulties were encountered during the infusion process. According to SMC, resin infused as well or better than incumbent resins. Resin required only 30 min for infusion, indicating good flow of the resin through the part. In addition, there were no obvious defects or dry spots, including corners, edges, and other potential problem areas.

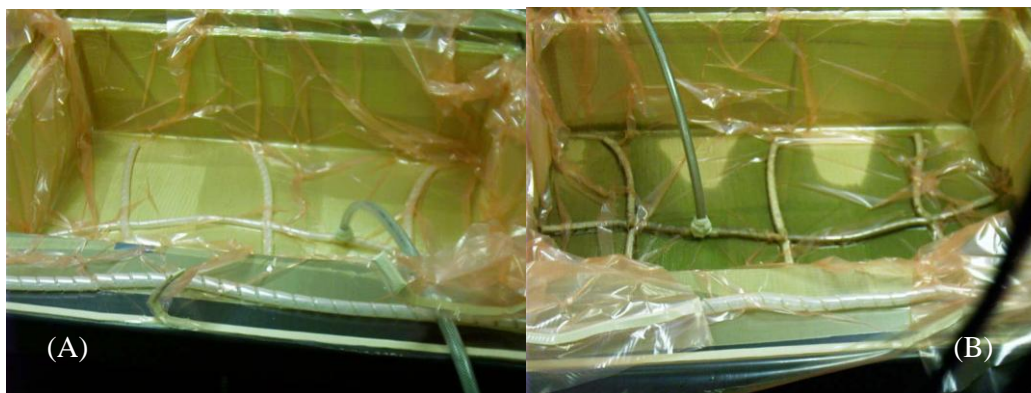


Figure 109. Images showing (a) vacuum-bagged box and (b) infusion of FAVE-L-25S-RDX resin into the HMMWV transmission container.

After infusion, the part cured overnight to produce the part shown in figure 110. It should be noted that this part is identical to the top (partial view to the right in the figure). The top and bottom are differentiated after production. Figure 110a shows the wooden feet drilled into the bottom half of the transmission container. The brass desiccant port is added to the top half, as shown in figure 110b. The outer hardware is added to top and bottom to secure the two halves of the container together and to be properly secured to a vehicle for transport (figure 111). The clasps are steel, but the rest of the outer hardware is aluminum. The aluminum internal hardware is then added to the bottom to be able to secure a transmission within the container (figure 112). Figure 113 shows the assembled container.



Figure 110. Infused and cured (a) bottom and (b) top of the HMMWV transmission container that used FAVE-L-25S resin.



Figure 111. Image showing (a) bottom and (b) top of FAVE HMMWV transmission with outer hardware.



Figure 112. Bottom of FAVE HMMWV transmission container with internal hardware.



Figure 113. Assembled FAVE HMMWV transmission container demonstration.

The final FAVE HMMWV transmission containers had the same overall quality as the Derakane 8084 containers. Both resins processed very similarly as well. Thus, according to SMC, the FAVE resin is a viable alternative to the Derakane 8084.

6.2.6.3 Laboratory Validation. The results of the laboratory validation testing of the HMMWV container are shown in table 76. The results show that the FAVE-L25S-RDX performed as well as the Derakane 8084 container. Photographs of the containers after most testing showed no visible damage and are thus not shown below. Only impact resistance testing showed some visible deformation, as shown in figure 114. The three impacts labeled in the picture did not show any permanent deformation. Minor cracking of the composite matrix resin was observed, but this is noted to be insignificant. The results also show that both composites passed the requirements for the HMMWV transmission container. After the impact test (swinging into the wall), deformation of the brackets to which the transmission is bolted was observed (figure 115). This is recognized as an aspect of the overall construction that needs to be redesigned and improved.

Table 76. HMMWV validation test results.

Test	Summary of Test Results for HMMWV Containers Made Using Derakane 8084 and FAVE-L-25S Resins	
	Derakane 8084	FAVE-L-25S
Edgewise Drop	No permanent deformation, separation of reinforcements, or cracks observed.	No permanent deformation, separation of reinforcements, or cracks observed.
Cornerwise Drop	No permanent deformation, separation of reinforcements, or cracks observed.	No permanent deformation, separation of reinforcements, or cracks observed.
Tip Over	No permanent deformation, separation of reinforcements, or cracks observed.	No permanent deformation, separation of reinforcements, or cracks observed.
Impact	No permanent deformation, separation of reinforcements, or cracks observed in the container composite structure.	No permanent deformation, separation of reinforcements, or cracks observed in the container composite structure.
	Deformation of the brackets to which the transmission is bolted was observed.	Deformation of the brackets to which the transmission is bolted was observed.
Flatwise Drop	No permanent deformation, separation of reinforcements, or cracks observed.	No permanent deformation, separation of reinforcements, or cracks observed.
Stacking	No slippage was observed, and the fork truck was able to perform this task.	No slippage was observed, and the fork truck was able to perform this task.
Concentrated Load Resistance	No permanent deformation, separation of reinforcements, or cracks observed.	No permanent deformation, separation of reinforcements, or cracks observed.
Impact Resistance	Insignificant/minor cracking of the resin. No permanent deformation.	Insignificant/minor cracking of the resin. No permanent deformation.

Note: Green indicates passing results, and yellow indicates questionable results.

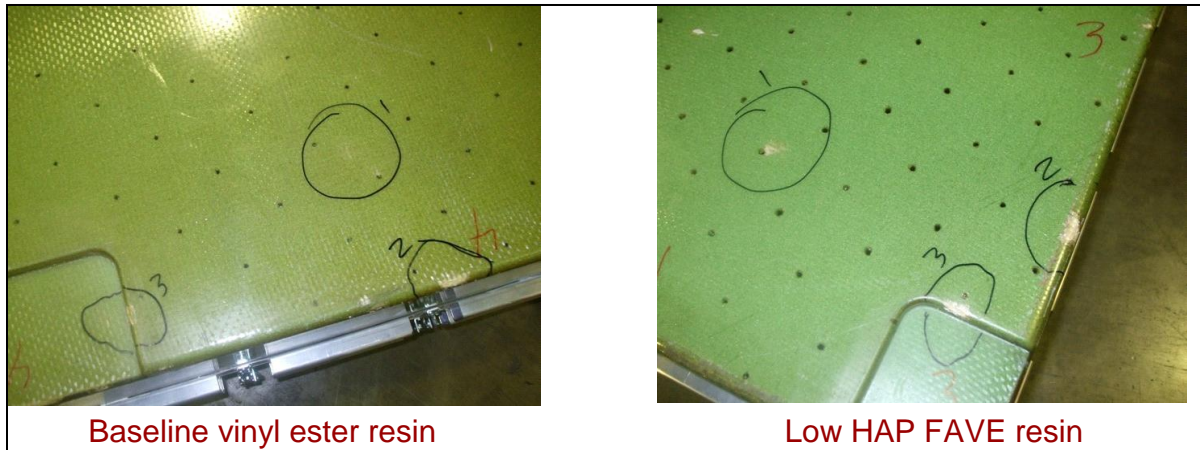


Figure 114. Results from impact resistance test.



Figure 115. Results after impact test showing deformation of the aluminum internal brackets.

6.2.6.4 Shock and Loose Cargo Testing. Shock and vibration (loose cargo testing) was performed at ATC on the transmission containers made using the FAVE-L-25S and the Derakane 8084. The results are shown in appendix B. The results indicated no significant difference between the two resins. There were slight differences in the vibration profiles between the Derakane 8084 container and the FAVE container (figure 116). It was concluded that these differences were due to slightly different weight distribution of the mass added to each container. Figure 117 shows that the status of the two containers after loose cargo testing was similar. The composite structural integrity in both cases was good.

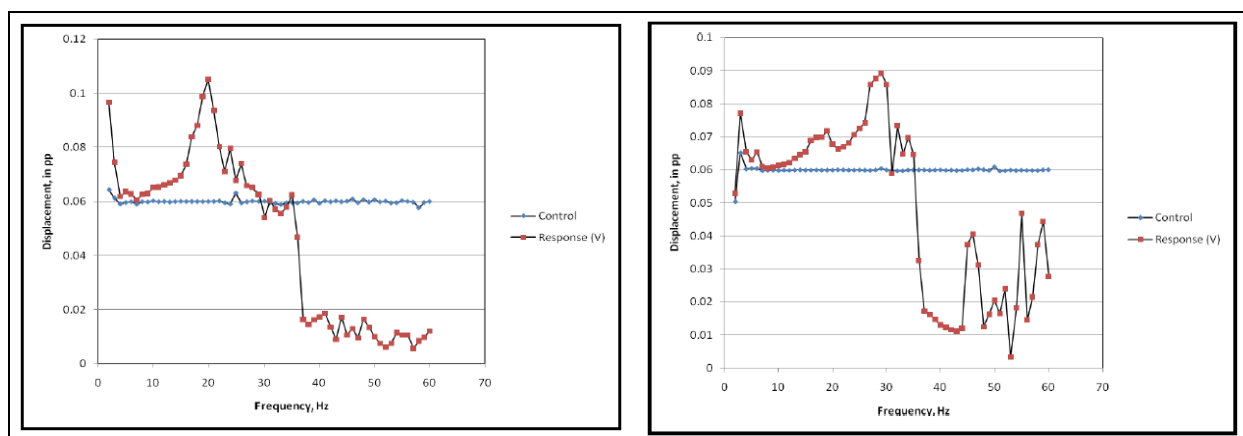


Figure 116. Vibration response of the Derakane 8084 container (left) and FAVE-L-25S-RDX container (right).

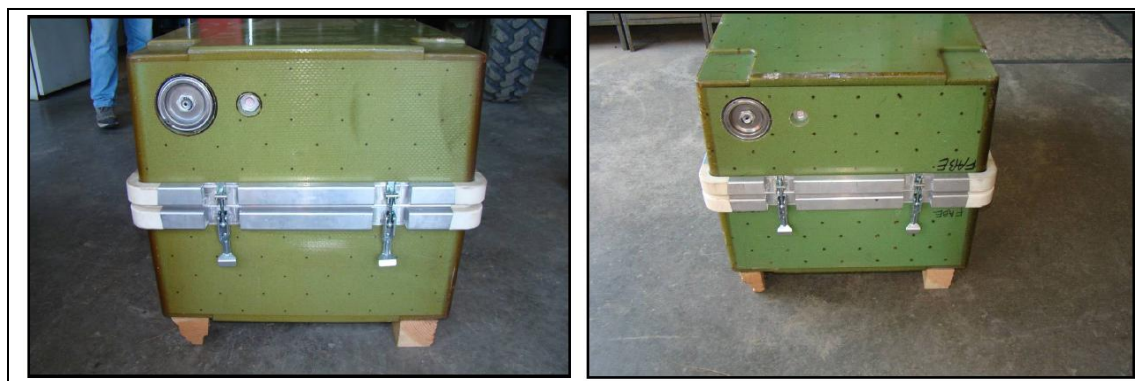


Figure 117. Status of the Derakane 8084 (left) and FAVE-L-25S-RDX (right) containers after loose cargo testing.

However, a few aspects of the composite design were found to be insufficient. First, the hooks used for strapping down the box are located too low on the box and should be raised to at least half the height of the part. Possibly as a result, the D-ring separated from the clasp during the vibration testing (figure 118). In addition, the wooden feet broke during the loose cargo testing (figure 119). Also, the aluminum hardware in the interior of the box is damaged and disbonds from the box easily. These aspects were taken into account in a redesign of the box. Nonetheless, the results clearly show the FAVE resin should be used in this application with comparable performance to the baseline, while reducing HAP emissions during production.



Figure 118. Photograph showing that the D-ring separated from the clasp during vibration testing.



Figure 119. Photograph showing the broken wooden feet after loose cargo testing.

6.2.6.5 Field Trial Validation. RRAD field tested the HMMWV transmission containers. Prior to doing so, they documented the status of the containers. Figure 120 shows the initial status of the containers.

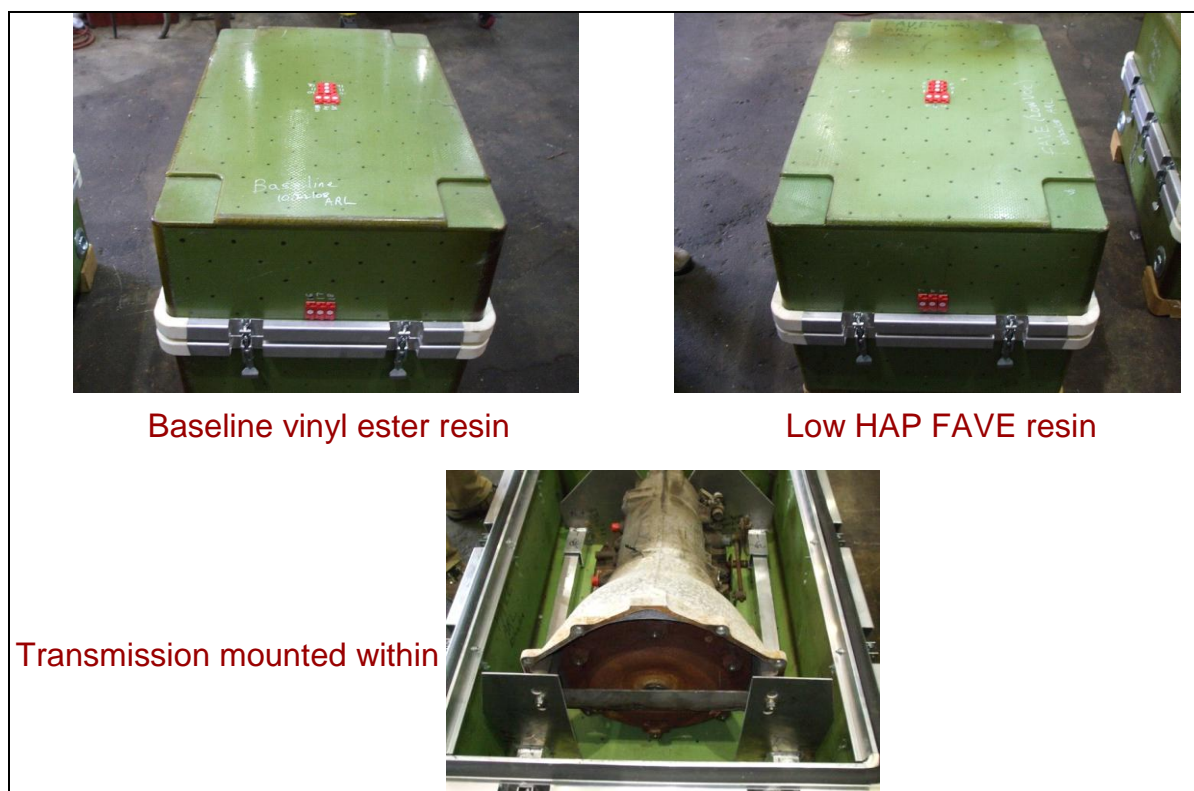


Figure 120. Transmission loaded into the baseline (Derakane 8084) and low-HAP FAVE containers.

Both the FAVE-L-25S-RDX and Derakane 8084 composite containers experienced similar damage as a result of their similar exposure (figures 121–124). First, both containers showed discoloration on the top surface as a result of sunlight exposure. There was less discoloration in the FAVE-L-25S composite because of its lower aromatic content. However, discoloration is not a real problem, as these containers would be painted with chemical-agent-resistant coating prior to actual use. Both experienced similar scrapes and gouges, but none penetrated the composite. Thus, the composite itself performed quite well. Some of the latches bent as a result of the rough handling. The feet were severely damaged for both composites, showing an obvious flaw in the design of the container. Chunks of wood are missing and deep cracking is noted. Most likely, the feet will have to be replaced with a material with better long term durability. These results coincide well with the loose cargo testing results. Transmission fluid leaked into both containers, but no leakage occurred outside the container, showing good performance of the container. Lastly, as for the validation testing, the aluminum brackets bent significantly during testing but still fastened the transmission in place. However, this mounting hardware is no longer usable. Thus, redesign of this aspect is required.



Figure 121. Derakane 8084 composite showing external damage after field test.



Figure 122. FAVE-L-25S-RDX composite showing external damage after field test.



Figure 123. Evidence of internal damage for Derakane 8084 transmission container after field test.

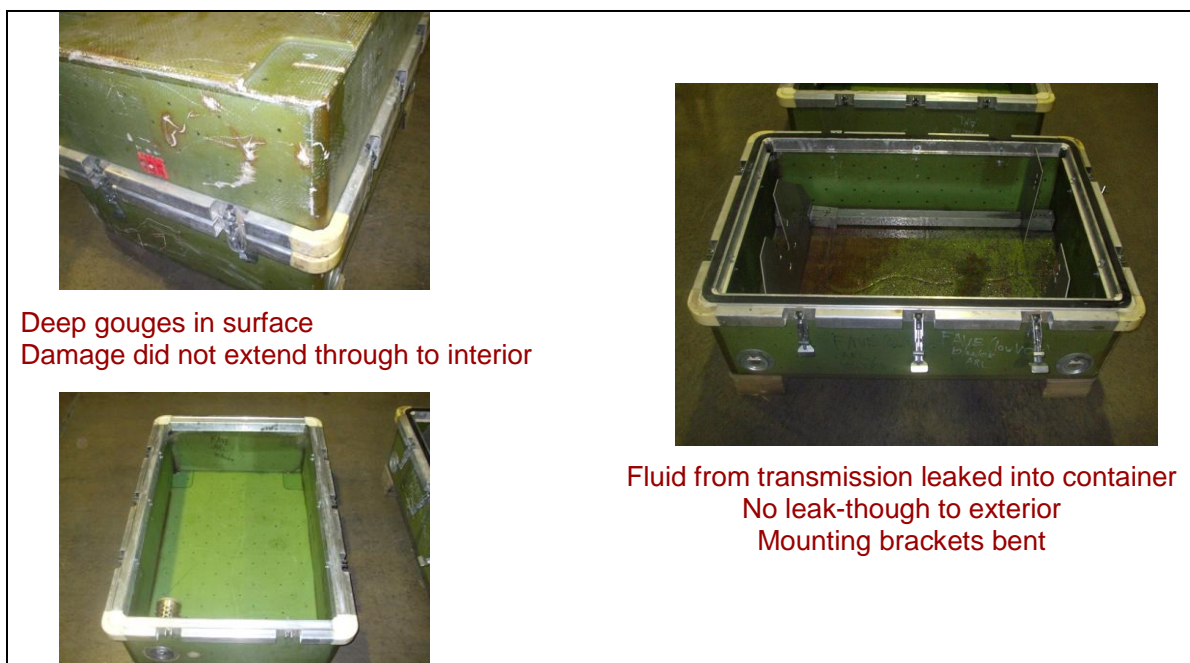


Figure 124. Evidence of internal damage for FAVE-L-25S-RDX transmission container after field test.

6.2.6.6 Laboratory Validation of Containers After Loose Cargo Testing and RRAD Field Trials. All four HMMWV containers were revalidated in the laboratory testing after loose cargo testing at ATC and field testing at RRAD. As a result of the damage to the containers, certain tests could not be performed, such as the stacking test. However, all of the other tests were performed. The results were the same as before fielding, with passing marks for the composite containers for both resin formulations.

6.2.6.7 HMMWV Transmission Container Conclusions. The FAVE resin infused as well as the incumbent Derakane 8084 VE resin. The laboratory panel testing, laboratory validation testing, RRAD field testing, vibration testing, and loose cargo testing showed similar performance of the FAVE composite relative to the commercial resin composite. Thus, the FAVE-L-25S is sufficient for the HMMWV transmission container application.

6.2.7 M35A3 Hood

6.2.7.1 Sioux Manufacturing Demonstration. Shown in table 77 is a comparison of the three resins employed in this study as measured by SMC. The results show that the FAVE resin has similar properties to that of the commercial resins and should be adequate for this application. It should be noted that the resin variant used by SMC was the FAVE-L-HT-RDX. The report from SMC can be found in appendix J.

Table 77. Neat resin properties as tested by SMC for resins for Army truck hood applications (M35A3 and M939).

Resin	Density (g/mL)	Viscosity (cP)	Flexural Strength (MPa)	Flexural Modulus (GPa)	Glass Transition Temperature (°C)
FAVE-L-HT	1.07	575	110	3.3	120
Vantico (Hexion) 8605	1.14	360	130	2.8	165
Hetron 980/35	1.14	350	120	3.3	130

SMC utilized the procedures developed for the UN/CCM effort in the fabrication of the ARL hood and container. The major steps in hood production are as follows:

1. Cut 3TEX 96-oz main ply.
2. Layup plies and stiffeners (stiffeners consisting of a foam core and wrapping ply are purchased pre-cut).
3. Place additional reinforcement plies over the stiffeners and along the perimeter of the hood.
4. Bag part.

5. Mix resin, CoNap, and MEKP and infuse with FAVEL VE resin or Vantico 8605 epoxy resin.
6. Post-cure part.
7. Trim hood in router.
8. Drill holes for hardware.
9. Bond safety latch and handles.

Sioux Manufacturing produced four hoods for the purposes of this work. Two hoods used the FAVE-L-HT-RDX resin, while two hoods used the incumbent Huntsman 8605 resin.

The hood was layed up using the fiberglass and PVC foam stiffeners. The hood was then vacuum bagged (figure 125). After leak checks were performed and corrected, the resin was infused (figure 125). No difficulties were encountered during the infusion process, as can be seen in figure 126. According to SMC, resin infused as well or better than incumbent resins. The FAVE resin required only 51 min for infusion, indicating good flow of the resin through the part (figure 127). In addition, there were no obvious defects or dry spots, including corners, edges, and other potential problem areas, as shown by the final part (figure 128).

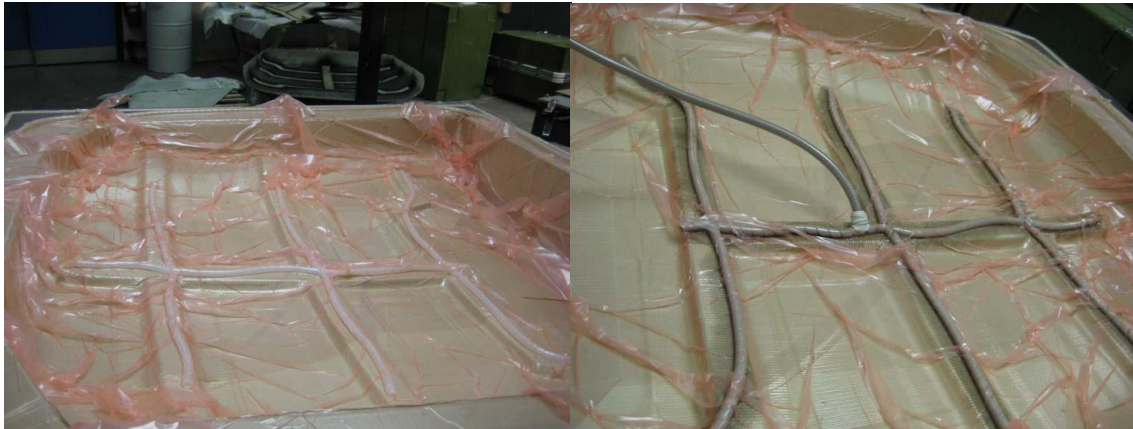


Figure 125. M35A3 hood after vacuum bagging (left) and at the moment of resin infusion (right).

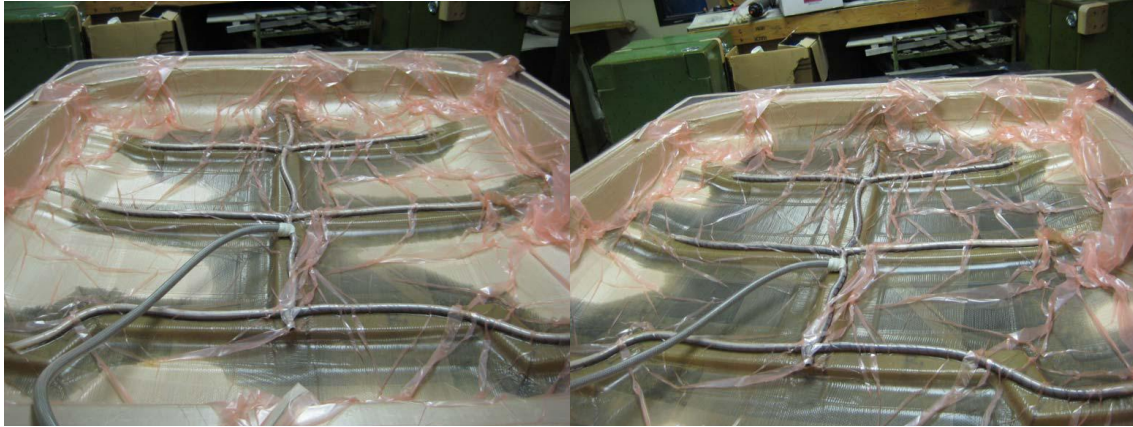


Figure 126. M35A3 hood after 10-min (left) and 19-min (right) resin infusion using FAVE-L-HT-RDX.



Figure 127. M35A3 hood after 51-min resin infusion using FAVE-L-HT-RDX.



Figure 128. FAVE-L-HT-RDX M35A3 hood manufactured by SMC.

6.2.7.2 Laboratory Validation. The M35A3 hood was validated using the CCM test fixture. The FAVE-L-HT-RDX passed the center top loading specifications (figure 129) and performed nearly identically to that of the commercial resins. There was no permanent deformation, no separation of reinforcements from the hood, and no cracks. Overall, the composite performed quite well with having an elastic deflection of 0.10 in at 250 lb, which is much less than the 0.50 in allowed and even passed the requirement of <0.25 in of deflection at -50°F . The Huntsman 8605 had a higher deflection of 0.15 in at 250 lb as a result of its slightly lower modulus and probably slight differences in the stiffener placement/integrity in the hood. FAVE-L-HT-RDX also passed the center front loading test (figure 129). There was no permanent deformation, no separation of reinforcements from the hood, and no cracks. Furthermore, the elastic deflection of 0.04 in at 250 lb was much less than 0.50 in allowed and even passed the requirement of <0.25 in of deflection at -50°F . The elastic deflection was nearly identical for the Huntsman 8605 of 0.05 in at 250 lb. Thus, the FAVE-L-HT-RDX passed the center and top loading requirements and performed similarly or better than that of the incumbent resin.

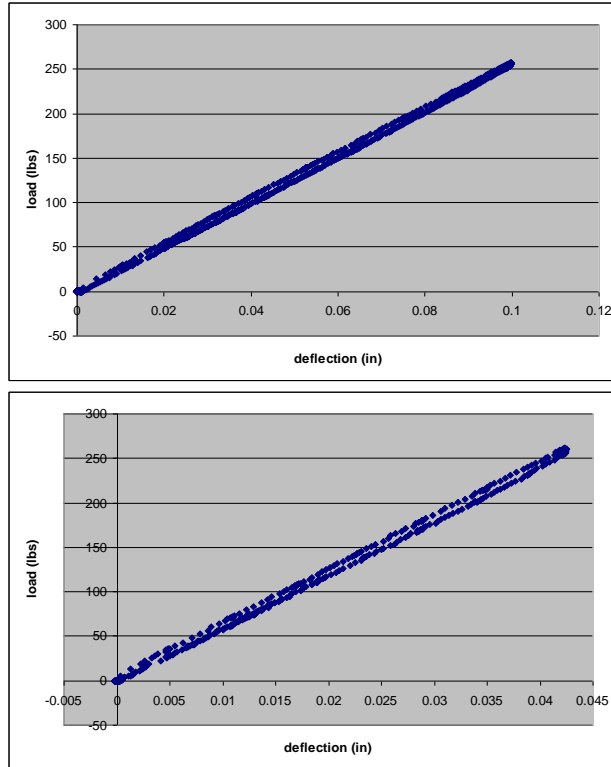


Figure 129. Load deflection curves for center top loading (left) and center front (right) for FAVE-L-HT-RDX M35A3 hood.

The FAVE-L-HT-RDX also passed the flexural results, including driver corner and passenger corner static lifts (figure 130). In both cases, there was no permanent deformation, no separation of reinforcements from the hood, and no cracks. The elastic deflection for the driver side was 0.16 in at 85 lb, while the passenger side was 0.12 in. For the Huntsman 8605, the driver deflection was 0.18 in, and the passenger side was 0.15 in. The full lifting load was <100 lb as specified, and the amount of load required to lift the hood to >0.375 in was 50 lb as specified for both resin systems and both testing locations.

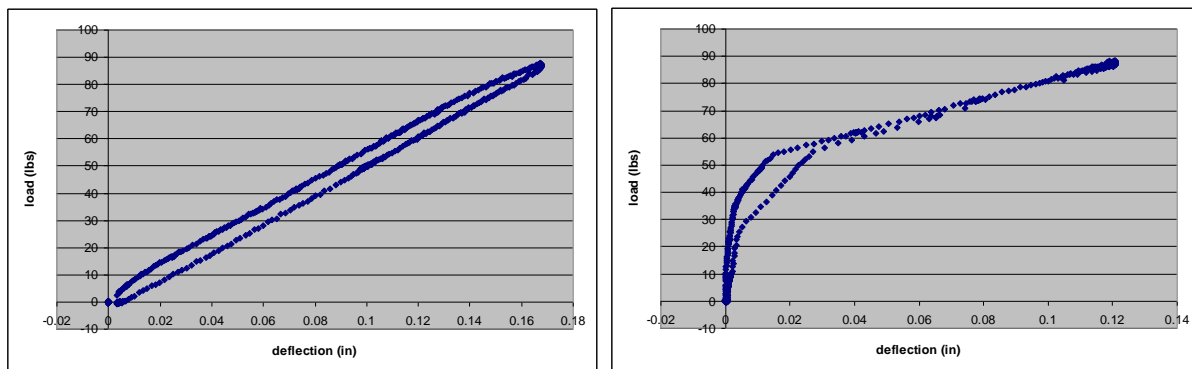


Figure 130. Load deflection curve for driver corner (left) passenger corner lift (right) for FAVE-L-HT-RDX M35A3 hood.

Cyclic handle loading was performed. Even after the cyclic loading, there was no permanent deformation, no separation of reinforcements from the hood, no cracks, and no broken fibers visible on areas where the hood contacts the fixture. The load deflection curves after cyclic testing were very similar to prior to cyclic testing (figure 131). Furthermore, the deflections at 85 lb were identical to their values prior to cyclic testing for both resin systems and both testing locations. Thus, this cyclic fatigue had no negative effect on resin or composite performance.

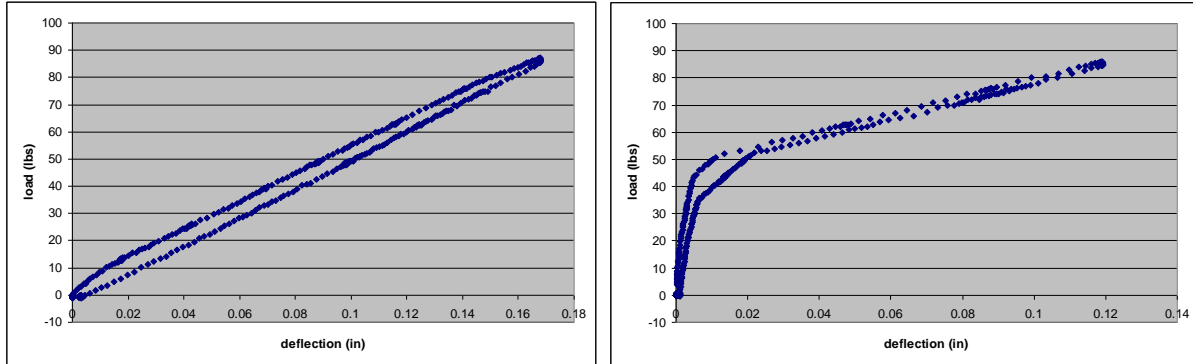


Figure 131. Load deflection curve for driver corner (left) passenger corner lift (right) for FAVE-L-HT-RDX M35A3 hood after cyclic handle loading.

Cyclic center and front loading were also performed. As before, there was no permanent deformation, no separation of reinforcements from the hood, no cracks, and no broken fibers visible on areas where the hood contacts the fixture. The load deflection curves after cyclic loading are shown in figure 132. The elastic deflection was the same as before cyclic loading for both resin systems and both testing locations, again indicating that this cyclic loading did not affect the performance of the resin or composite.

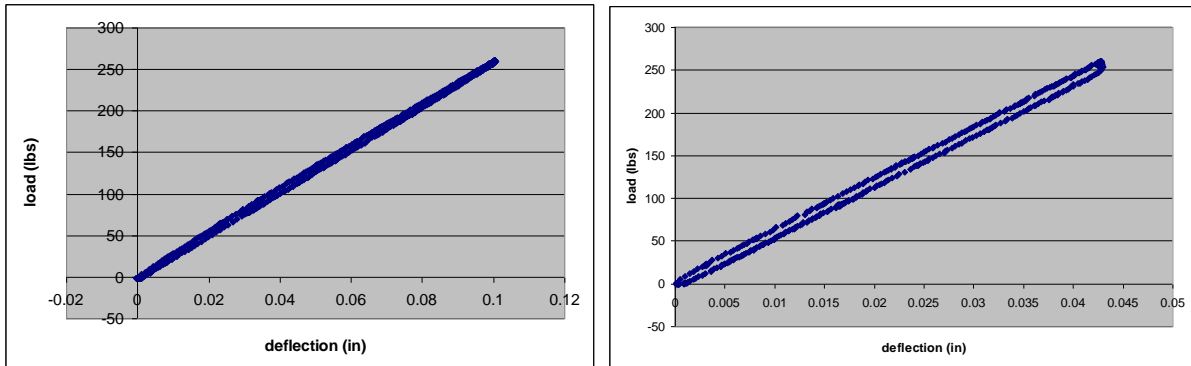


Figure 132. Load deflection curve for top center (left) front center (right) for FAVE-L-HT-RDX M35A3 hood after cyclic handle loading.

Impact damage to the composites was superficial, leaving a mark but creating no real damage to the structure. Figure 133 shows the damage done to the structure on or near the stiffeners, while figure 134 shows the damage on the corners. Overall, there was no permanent deformation, no separation of reinforcements from the hood, and no cracks, and thus the hood passed the specifications. The damage for the Huntsman 8605 composite was similar.

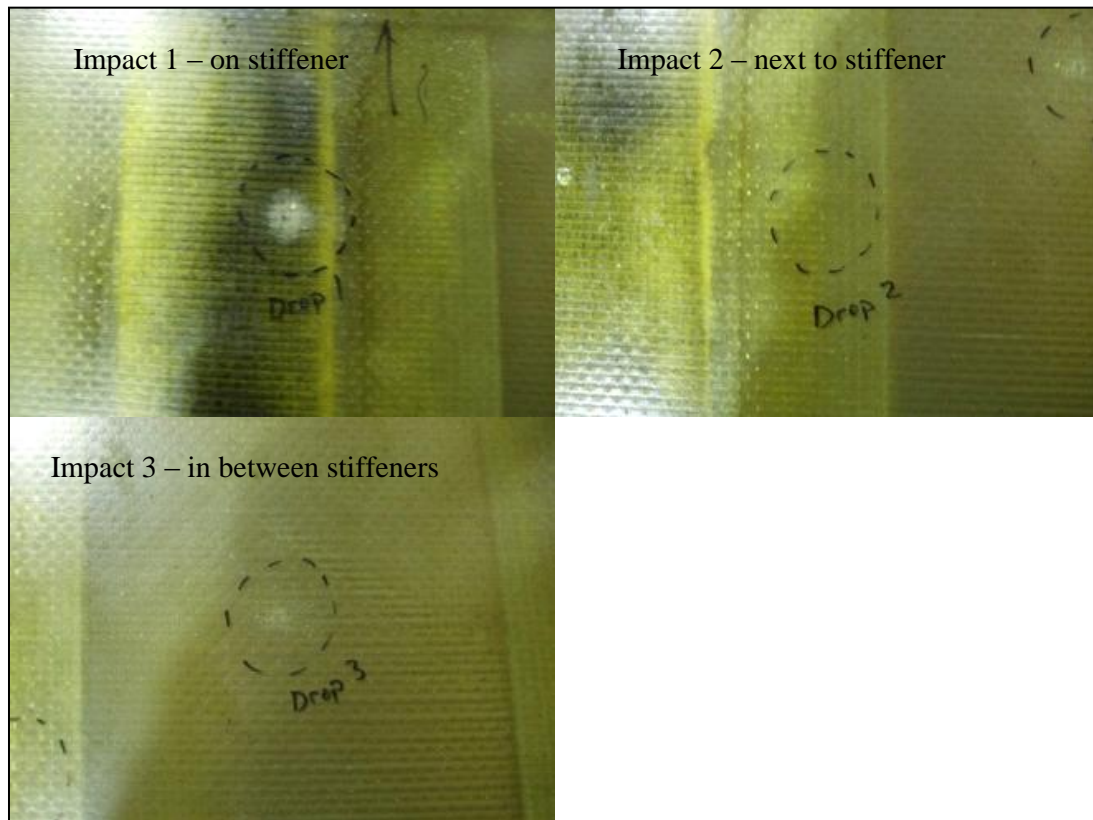


Figure 133. Impact damage to the FAVE-L-HT-RDX M35A3 hood as a result of drops on or near stiffeners.

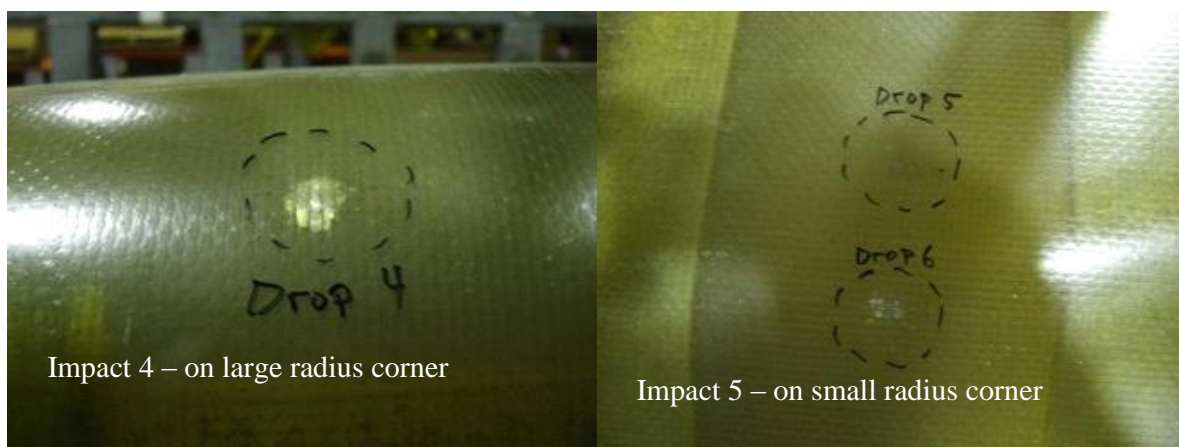


Figure 134. Impact damage to the FAVE-L-HT-RDX M35A3 hood as a result of drops on corners.

6.2.7.3 Field Trial Validation. The M35A3 hood was validated at RRAD for form, fit, and function. RRAD was able to simply attach these hoods to M35A3 trucks. The resulting hood hit very well, having sufficient clearance with the engine block and fitting onto the truck body well and was able to withstand the forces of people standing and jumping onto the hood.

6.2.7.4 M35A3 Demonstration/Validation Conclusions. The lab panel testing results, demonstration results from SMC, an independent company, and the validation results from CCM and RRAD show that the FAVE-L-HT-RDX has excellent performance for the M35A3 application. The FAVE composites met all specifications and performed as well as the commercial incumbent resins.

6.2.8 M939 Hood

6.2.8.1 M939 Demonstration. Two M939 hoods were prepared at the CCM. One used the FAVE-O-HT-RDX. The other used the incumbent Hetron 980/35. The hoods (figure 135) were manufactured very similarly to that of the M35A3. The FAVE resin performed well and was able to be infused in <1 h. The final part was fully wetted out and had no apparent defects (figure 136). Furthermore, the parts fit well onto the M939 frame (figure 137), indicating good form, fit, and function.

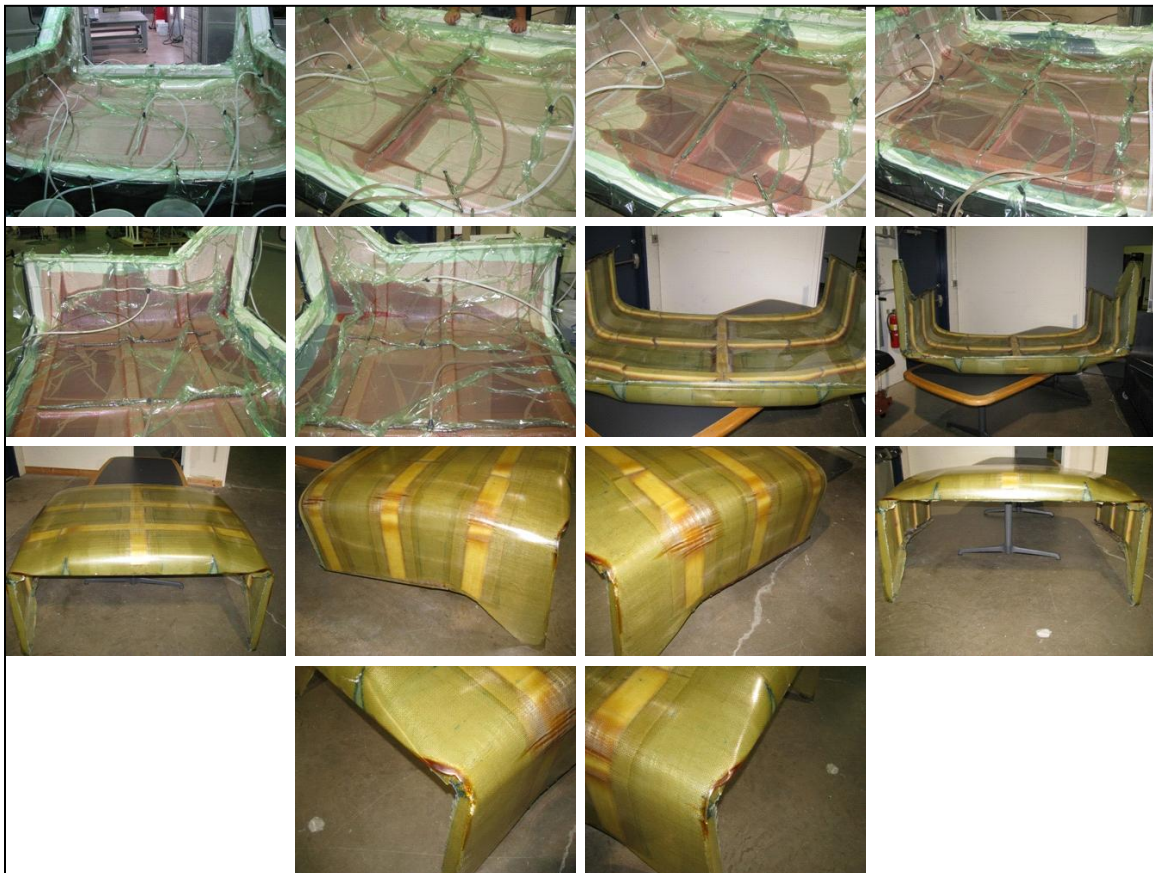


Figure 135. Photographs showing bagging, infusion, and demonstration of M939 hood using FAVE-O-HT.



Figure 136. Photographs of the top (left) and underside (right) of the M939 hood using FAVE-O-HT-RDX resin.



Figure 137. Photographs of the front (left) and passenger side (right) of the M939 hood using Hetron 980/35 resin mounted on a M939 frame and the FAVE-L-HT resin (bottom) on the M939 frame.

6.2.8.2 Laboratory Validation. The M939 hoods were validated in an identical manner to that of the M35A3 hoods. The static and dynamic center and top loading were assessed. There was no permanent deformation, no separation of reinforcements from the hood, no cracks, and no broken fibers visible on areas where the hood contacts the fixture for either the baseline or low-HAP hood. Table 78 summarizes the results and shows that the FAVE-O-HT performed as well as the Hetron 980/35.

Table 78. The validation results for the FAVE-O-HT-RDX and Hetron 980/35 M939 hoods.

Test	Hetron 980/35	FAVE-O-HT-RDX	Specification
Top center loading	0.12 in at 250 lb	0.11 in at 250 lb	<0.5 in at 250 lb
Top front loading	0.04 in at 250 lb	0.03 in at 250 lb	<0.5 in at 250 lb
Top center after cyclic loading	0.12 in at 250 lb	0.11 in at 250 lb	<0.5 in at 250 lb
Top front after cyclic loading	0.04 in at 250 lb	0.03 in at 250 lb	<0.5 in at 250 lb
Driver corner lift	0.21 in at 50 lb	0.20 in at 50 lb	>50 lb to deflect ≥ 0.5 in
Passenger corner lift	0.23 in at 50 lb	0.22 in at 50 lb	>50 lb to deflect ≥ 0.5 in
Driver corner lift after cyclic loading	0.21 in at 50 lb	0.20 in at 50 lb	>50 lb to deflect ≥ 0.5 in
Passenger corner lift after cyclic loading	0.23 in at 50 lb	0.22 in at 50 lb	>50 lb to deflect ≥ 0.5 in
Impact testing	Superficial damage only	Superficial damage only	Superficial damage only

6.2.8.3 M939 Conclusions. The FAVE-O-HT-RDX composite performed nearly identically to the Hetron 980/35 hood M939. Thus, FAVE-O-HT-RDX is an acceptable resin for M939 composite hoods.

Based on this and the similarity of their composite and neat resin properties, we expect the FAVE-O-HT-RDX and FAVE-L-HT-RDX to both be able to be used for the M35A3 hood, M939 hood, and likely various other composite hoods for DOD applications.

6.2.9 Marines HMMWV Hardtop

6.2.9.1 Ballistic Testing. Ballistic resistance of the composites is a necessary performance criterion of the HMMWV hardtop. For this application, FAVE-L-25S, FAVE-O-25S, and FAVE-O-HT were the selected resin systems as a result of the need for a low-viscosity resin. The ballistic resistance of the FAVE resin systems was compared to that of a ballistic epoxy resin and a toughened VE. The epoxy resin used was API FCS2 resin, which is a blend of API SC-15 and SC-79. The VE resin used was VE 8084.

The four-ply panel was tested against NIJ IIIa (44 magnum) equivalent. The 12-ply panel was tested against NIJ III (7.62 M80 ball) equivalent. The results (figure 138) clearly showed that all three FAVE resins outperformed the Derakane 8084 and performed similarly to the FCS2 epoxy resin. Overall, there was a smaller delamination zone, as seen by the target face view and similar levels of delamination when viewed from the side.

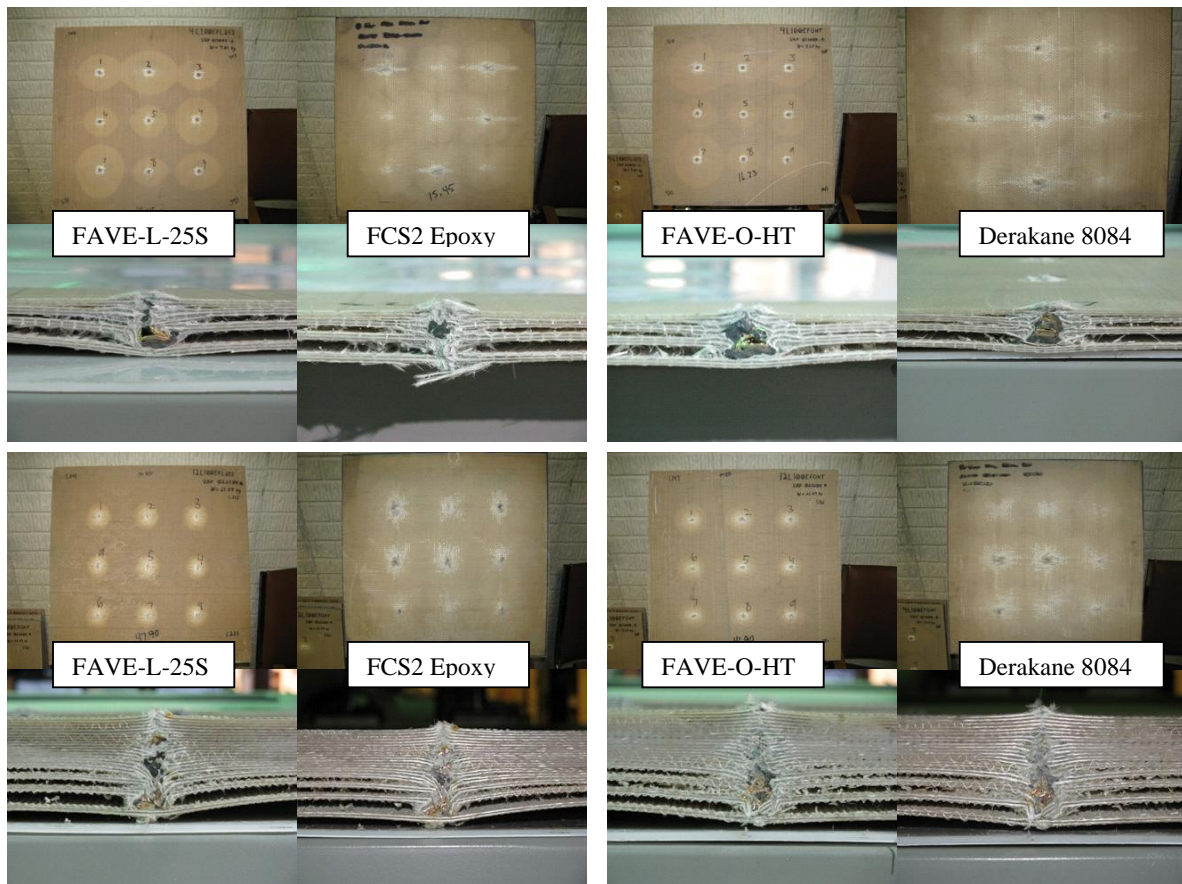


Figure 138. The 4-ply panel was tested against NIJ IIIa (44 magnum) equivalent (top photos), and 12-ply panel was tested against NIJ III (7.62 M80 ball) equivalent.

6.2.9.2 HMMWV Hardtop Conclusions. Fatigue testing and the loose cargo testing done for the HMMWV transmission container using the FAVE-L-25S resin showed that FAVE-L-25S would be a good resin choice for the HMMWV hardtop.

6.2.9.3 Demonstration/Validation Summary and Conclusions. The FAVE resins were successfully demonstrated for the HMMWV hardtop, HMMWV transmission container, M35A3 hood, M939 hood, F-22 canopy cover, and splash molds. The FAVE-L resin was not successful for the T-38 dorsal cover because of its high viscosity. Based on the performance of the FAVE-L-25S with the other demonstration articles, we expect that FAVE-L-25S would have been successfully demonstrated and validated for the T-38 dorsal cover. All of the FAVE resins were successfully validated for every application except the T-38. Furthermore, the processing of the FAVE-L-25S or FAVE-L/O-HT was found to be equivalent to that of the commercial resins, and the properties were also generally equivalent (some were reduced, but others were greater, but all properties met the required specifications) to those of commercial resins. However, the FAVE resins had significantly less styrene and thus are more environmentally friendly and would allow manufacturers and the DOD to be better able to meet NESHAP regulations. Published journal articles and reports that focused on aspects of this demonstration/validation testing are provided

in appendix E. Furthermore, partially as a result of this effort, the MFA and FAVE resin technologies have been licensed by Dixie Chemicals, which is in the process of scaling up and selling these products to industry and the DOD.

7. Cost Assessment

Two separate cost estimates were performed—one by Steven Smith of Drexel University and the other by Concurrent Technologies Corp. (CTC) (appendix K). Appendix L is a student report on the production and manufacturing costs associated with manufacturing MFA and agrees well with the analysis done by CTC and Steven Smith.

7.1 Cost Model and Composite Production

7.1.1 Cost Model

In this LCCA, the follow two courses of action have been explored for VE resins: (1) continue using incumbent VE resins, which are assumed to require composite manufacturers to install and use pollution control equipment, or (2) adopt replacement FAVE resins, which are assumed to not require pollution controls. Both options are expected to increase the costs for a composites manufacturer and consequently the DOD's costs to purchase the composite products. Since VARTM is considered by the EPA to be a closed molding process, it is unknown what, if any, requirements must be met to ensure compliance under the NESHAP rule. As a compliance evaluation is out of the scope of this project, it is assumed that these two scenarios are required to ensure compliance with the Reinforced Plastic Composites NESHAP rule.

A cost effectiveness analysis (CEA) was performed to evaluate which of these options is more cost effective at meeting the goal of maintaining tactical vehicle performance while also meeting NESHAP requirements. CEA was used to compare the relative costs and outcomes of the two courses of action. It can be assumed that the outcomes of the two approaches are similar; that is, tactical vehicle performance is maintained and NESHAP requirements are met. Only the costs that differ between the two courses of actions are included in the analysis. A 15-year study period was used. Annual production volumes are assumed to stay constant over the 15 years.

7.1.2 Selecting the Resin System

The low-HAP/VOC FAVE resin systems are being considered for six military applications. Table 79 lists the composite systems currently used for each application, as well as the proposed replacement resins. Four commercial VE resin systems are currently used for these applications. Ashland Inc.'s Derakane 8084 is used to produce the HMMWV transmission container and Amtech HMMWV hardtop. Ashland Inc.'s Hetron 980/35 is used to produce the M939 hood and M35A3 hood. Hexion Specialty Chemical's Hexion 781-2140 is used to produce the T-38 dorsal cover. Interplastic Corporation's Corezyn Corve 8100 is used to produce Navy rudders,

Table 79. Incumbent and replacement resin for selected composite military applications.

Application	Service	Incumbent Resin	Replacement Resin
HMMWV transmission container	Army	Derakane 8084	FAVE-L-25S or FAVE-O-25S
M939 hood	Army	Hetron 980/35 or Huntsman RenInfusion 8605/Ren 8605	FAVE-L-HT or FAVE-O-HT
M35A3 hood	Army	Hetron 980/35 or Huntsman RenInfusion 8605/Ren 8605	FAVE-L-HT or FAVE-O-HT
Amtech HMMWV hardtop	Marines	Derakane 8084	FAVE-L-HT, FAVE-O-HT, or FAVE-L-25S
T-38 dorsal cover	Air Force	Hexion 781-2140	FAVE-L-25S
MCM rudder	Navy	Corve 8100	FAVE-L-25S

such as the MCM rudder. FAVE-L-25S or FAVE-O-25S is the targeted replacement resin for the HMMWV transmission container. FAVE-L-25S is the targeted replacement for the T-38 dorsal cover and MCM rudder applications. To obtain the necessary heat distortion temperatures, FAVE-O-HT or FAVE-L-HT must be used for the M939 hood, M35A3 hood, and Amtech HMMWV hardtop. FAVE-L-25S is also being considered for the Amtech HMMWV hardtop. An epoxy resin, Huntsman Advanced Materials' RenInfusion 8605/Ren 8605, is also being considered for use in the M35A3 and M939 applications. The FAVE resins comprised all of the variants in this cost analysis.

7.1.3 Manufacturing the Composites

The process for manufacturing composites is illustrated in figure 139. If a FAVE replacement resin is to be used, then the process begins with MFA monomer synthesis. This mixture is stirred and gently heated at a controlled temperature for about four hours. The MFA monomer is then blended with the other materials to make the resin (see formulations in tables 25–31). The synthesis and blending steps (blue box) are not required for the current VE resins.

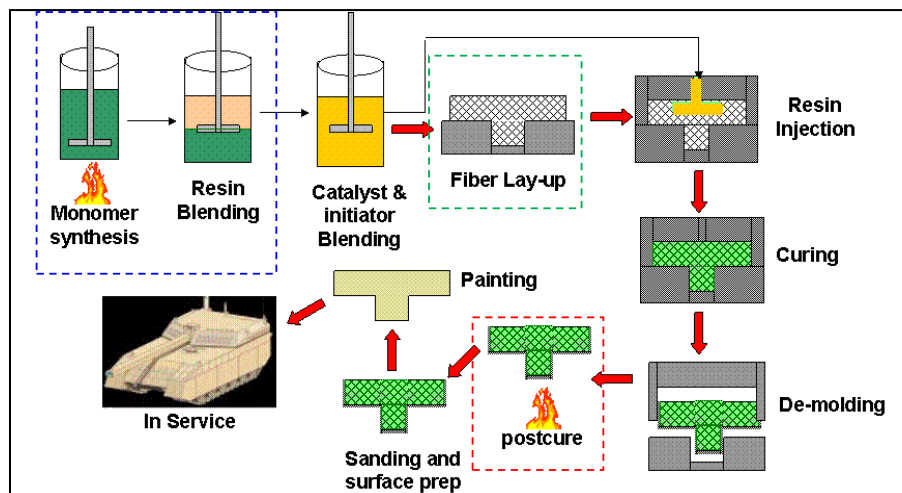


Figure 139. Schematic illustration of composite manufacturing process.

While the rest of the steps vary for different applications, they are the same regardless of whether the current VE or a replacement FAVE is used. The resin is blended with a catalyst (cobalt naphthenate) and initiator (Trigonox 239 or methyl ethyl ketone peroxide), regardless of whether an incumbent or replacement resin is used. Following the catalyst and initiator blending step, the prepared resin is injected into the mold, cured, de-molded, sanded, and painted. Except for the MCM rudder, it is unlikely that the resin parts were post cured.

Overall, the FAVE resins were drop-in replacements for commercial VE resins. Consequently, composite manufactures will not require any process changes when switching to the FAVE resins.

7.1.4 Vacuum Assisted Resin Transfer Molding

There are various composite molding processes that are used to manufacture composite structures. The molding process evaluated in this analysis is VARTM. VARTM is an infusion process where a vacuum draws a resin into a one-sided mold (36). First, dry fabric or a preform is laid up on one-sided tooling and covered with a vacuum bag. The air is evacuated by a vacuum pump, and then liquid resin from an external reservoir is drawn into the mold by the vacuum. A vacuum is created between the preform and the vacuum bag, which allows for an even thickness mold. After the molded part is cured, which can be several hours for a large part, the structure is opened, and the molded part is released. VARTM is considered by the EPA to be a closed molding process (37). This process is illustrated in figure 140.



Figure 140. Illustration of VARTM (38).

7.1.5 Application Manufacturing

The various applications listed in table 73 are made by small to medium-sized composites manufacturers scattered through the United States, often near DOD installations. The size of the parts and the production volume vary widely, as seen from information provided by ARL in table 80.

Table 80. Projected scale of operations for various demonstrations.

Application	Total Mass Per Part (lb)	Resin Mass Per Part (lb)	Estimated Production (per year)	Total Resin Weight (lb/year)	Styrene Reduction Through Low-HAP Resins (lb/year)	Location
M35A3 hood	52	18	100	1800	~450	Fort Totten, ND
M939 hood	60	20	5000	100,000	~25,000	Fort Totten, ND
HMMWV transmission container	110	35	500	17,500	~4000	Fort Totten, ND
HMMWV hardtop	1400	220	480	100,000	~25,000	Wapato, WA
T-38 dorsal cover	10	4	40	160	~80	Hill AFB, UT
Composite rudder for MCM	1400	190	5	960	240	Annapolis, MD

The F-22 canopy cover and splash molds were not considered in this analysis. However, we expect their production rates and resin quantities to be similar to that of the T-38 dorsal cover. Therefore, we consider a specific analysis of these demonstration platforms to be unnecessary. However, the sum of all of the AF platforms increases the production rate and could change the LCA. Therefore, the effects of summing these applications was discussed later in this section.

7.1.6 Styrene Emissions

The styrene emissions from the manufacturing of these parts can be estimated based on the amount of styrene in the part and the accepted styrene emission factor. The styrene content varies from 35%–50% depending on the resin, but an average value of 40% styrene was used throughout the calculations. According to EPA’s AP-42 emission factor for resin for a closed molding process, 1%–3% of the starting monomer is emitted (37). The highest value in the range was used in the calculations as a conservative estimate. Table 81 shows the anticipated styrene emission rate for a hypothetical composites manufacturer near Fort Totten, ND, that only manufactures the M35A3 hood, the M939 hood, and the HMMWV transmission container using the VARTM method. It is assumed no other parts are made in the facility and the total annual production is 5600 pieces per year (based on estimated production in table 74). It is assumed the facility operates two 8-h shifts per day, 5 days per week, 51 weeks per year, for a total of 4080 h per year. An average styrene emission rate was calculated to be 0.35 lb styrene per hour by dividing the annual styrene emissions by the operating hours.

Table 81. Styrene emissions from manufacturing composite applications.

Part	Resin/Part (lb)	Styrene/Part (lb)	Styrene Emissions/Part (lb)	Annual Production (Pieces)	Annual Styrene Emissions (lb)
M35A3 hood	18	7.2	0.22	100	22
M939 hood	20	8	0.24	5000	1200
HMMWV transmission container	35	14	0.42	500	210
Total	—	—	0.88	5600	1432
Total annual operating hours					4080
Average styrene emission rate					0.35

7.1.7 Cost Model/Assumptions

7.1.7.1 Drexel Cost Model/Assumption. The economic and environmental analysis of the application case studies for the project were researched and developed using the technical information base that was used to prepare the maximum achievable control technology rules for the NESHAP (3). This technical information base was begun in 1997 and was completed with the final rulemaking in 2004. The techniques, tools, and information flowed directly from the technical evaluation methods that the composites industry currently uses for permitting and compliance evaluation. This technical information base is supported by a number of references (3, 39–47). In addition, the authors of the evaluation methods were contacted to discuss suitability for this application.

The manufacturing cases provided by the project were the HMMWV hood, HMMWV hardtop, and the HMMWV transmission container. The basis of the defender challenger study is as follows:

1. Defender is the current low-HAP resin plus emissions controls.
2. Challenger is new resin system.
3. Manufacturing applications are hoods, hardtops, etc.
4. Resin use rate is 100–175 thousand pounds per year.
5. Defender compliance emissions control is CATOX with natural gas fuel.
6. Sensitivity case—production in one site, 390 thousand pounds per year.
7. Sensitivity case—purchase of carbon offsets for greenhouse gases in defender pollution control system.

The applications were force ranked by increasing order of annual resin use. Base resin was assumed to be Derakane 8084 as the current “defender.” The pounds/year of Derakane are converted to tons per year (TPY) to match the regulatory basis of calculation. The column labeled EF is the “emissions factor,” developed and calculated from the rule-making database (tables 82 and 83). The EF is dependent on many factors, and the technical rule-making documents were used to determine the appropriate EF for the manufacturing application.

Table 82. Cost avoidance in the high emissions factor case for FAVE resins in place of commercial resins.

Application	Resin Use Resin #/yr	TPY resin DeraKane 8084	EF #/ton 180	Exhaust CFM	CATOX CAPEX\$	CATOX TAC\$	Cost/ton Emission	Cost \$/lb resin
HMMWV Hood	100000	50	4.5	10200	\$920,000	\$280,000	62222	2.80
HMMWV Hardtop	100000	50	4.5	10200	\$920,000	\$280,000	62222	2.80
HMMWV TC	175000	88	7.9	17800	\$1,200,000	\$380,000	48254	2.17
M35A3 Hood	14400	7	0.6	1500	\$570,000	\$160,000	246914	11.11
One Site	389400	195	17.5	40000	\$2,100,000	\$680,000	38806	1.75
Application	Greenhouse Gases Produced, TPY		Priority Pollutants Produced, TPY		Carbon offset cost \$/yr	Offset Cost Per # Resin	Total Cost Avoided per # resin	
HMMWV Hood	2400		9		\$76,800	0.77	3.57	
HMMWV Hardtop	2400		9		\$76,800	0.77	3.57	
HMMWV TC	3200		12		\$102,400	0.59	2.76	
M35A3 Hood	1400		5		\$44,800	3.11	14.22	
One Site	5800		22		\$185,600	0.48	2.22	

Table 83. Cost avoidance in the low emissions factor case for FAVE resins in place of commercial resins.

Application	Resin Use Resin #/yr	TPY resin DeraKane 8084	EF #/ton 100	Exhaust CFM	CATOX CAPEX\$	CATOX TAC\$	Cost/ton Emission	Cost \$/lb resin
HMMWV Hood	100000	50	2.5	5700	\$740,000	\$215,000	86000	2.15
HMMWV Hardtop	100000	50	2.5	5700	\$740,000	\$215,000	86000	2.15
HMMWV TC	175000	88	4.4	9900	\$910,000	\$270,000	61714	1.54
M35A3 Hood	14400	7	0.4	800	small	small	na	na
One Site	389400	195	9.7	22000	\$1,400,000	\$440,000	45198	1.13
Application	Greenhouse Gases Produced, TPY		Priority Pollutants Produced, TPY		Carbon offset cost \$/yr	Offset Cost Per # Resin	Total Cost Avoided per # resin	
HMMWV Hood	1800		7		\$57,600	0.58	2.73	
HMMWV Hardtop	1800		7		\$57,600	0.58	2.73	
HMMWV TC	2300		9		\$73,600	0.42	1.96	
M35A3 Hood	na		na					
One Site	3700		14		\$118,400	0.30	1.43	

For the defender, the initial costs are the purchase and installation of a catalytic oxidation system to control HAP to meet the NESHAP. Then, the systems must be operated during production at full rate and at low rate when production is not occurring to maintain thermal stability and reduce startup/shutdown costs. The yearly operating costs were estimated from the technical database, and costs were updated to 2007. Table 82 lists the costs that were calculated. The total annual cost (TAC) for the system is the sum of the annual operating cost plus the capital recovery factor to provide a 10% return on initial capital investment. The TAC was then divided by the resin rate to provide the estimate of additional cost per pound for the defender. This additional cost is the cost to be avoided by installing the challenger (new) technology. Investment and operating costs of catalytic oxidation are driven by the scale (rate) of exhaust airflow from the workspace. Using the control technology cost models that are the basis of the rule making, this model updated with costs in 2007 dollars shows initial capital costs for the Regenerative Catalytic Oxidizer (RCO) (CATOX) to be \$0.9–\$1.2 million for the applications. In the TAC\$ column, this refers to the total annual cost, including recovery of capital. So, the TAC\$ are divided by total resin use to get a measure of the “avoided cost” of “end of pipe” treatment vs. adjusting the formulation. This number in column current cost of \$2.17–\$2.80/lb is the challenger advantage margin. Using the price of Derakane 8084 and adding \$1.50–\$2.50/lb extra cost provides an estimate of the price point that the new resin must be below to justify using the new technology.

In the last two columns of the table, we show additional greenhouse gasses produced by the installation of RCO and the additional production of priority pollutants from RCO. These environmental effects are avoided by implementing the low-HAP resins. The cost of carbon offsets was estimated using the current market prices from active markets in the European Union, as the U.S. does not have a large market today. Converted to dollars, each U.S. ton of carbon offset costs about \$32/ton.

7.1.7.2 CTC Cost Model/Assumptions. When determining which cost model would give the appropriate results for this analysis, it was determined a custom analysis was necessary. The models traditionally used by CTC, environmental cost analysis methodology (ECAM) and pollution prevention (P2) finance, are not relevant because ARL/DOD is not making an investment but rather purchasing products from companies that may have to make this investment. Therefore, a project specific cost model was created in Excel* by the project team.

The annualized costs for regenerative thermal oxidizer (RTO) equipment, labor, and utilities (see section 7.3.3) were divided by the annual RTO throughput to calculate a cost per pound for operating the RTO. To perform these calculations, several assumptions were made. These are summarized as follows:

*Excel is a registered trademark of Microsoft.

1. RTO capital cost:

- Assume an RTO is the best solution for ensuring compliance with NESHAP rule.
- Assume a 2000-ft³/min unit is the correct size for this scenario.
- Assume the EPA's indirect cost formula correctly captures these costs.
- Assume an economic life of 15 year for the RTO.

2. RTO Maintenance:

- Assume a burdened labor rate of \$65/h for a technician.
- Assume RTO consumable materials total \$1000 annually.
- Assume RTO maintenance requirements total 41 h of labor annually.

3. Utilities for the RTO:

- Assume an average electricity rate of \$0.11/kWh, based on inquiries near Fort Totten, ND; Wapato, WA; Hill AFB, UT; and Annapolis, MD.
- Assume an average natural gas rate of \$6.50/dekatherm, based on inquiries near Fort Totten, ND; Wapato, WA; Hill AFB, UT; and Annapolis, MD.
- Assume the RTO must keep running 24 h/day, every day, regardless of the production schedule. Many air permits require RTOs to stay at a certain temperature to meet the required VOC destruction efficiency, and they do not respond quickly to temperature fluctuations.

4. Production:

- Assume the production estimates in table 80 are reliable estimates.
- For the worst case scenario, assume only one line of production is routed to the RTO.
- For the more realistic scenario, assume all Fort Totten parts (for Army vehicles) are made in one facility. Assume that all three product lines go to the same RTO and no other products go to the RTO.
- Assume the Fort Totten facility example is representative for all applications, even those with very small annual production estimates. Assume the cost per pound increase from RTO usage can be applied to all applications.

5. Environmental, Health, and Safety Compliance:

- Assume that the annual costs for preparing Toxics Release Inventory (TRI) reports are the same for both VE and replacement resins. For the Fort Totten facility example, the reporting threshold for processing styrene (10,000 lb per year) is exceeded for both the incumbent and replacement FAVE resins.

- Assume that no TRI reporting is required for an epoxy resin. According to the EPA, the annual burden for completing a TRI report for one chemical is \$630. If this cost were divided by an average annual production rate (assume 5000 parts per year), the cost savings for an epoxy resin for not completing a TRI report is ~\$0.13 per part.
- Assume that a baseline industrial hygiene survey and personal air sampling must be performed for facilities using incumbent resins and for facilities using replacement FAVE resins.

7.2 Drexel Cost Analysis and Comparison

7.2.1 Cost Avoidance

Based on the production rates of the parts and amount of styrene emitted, the cost of capturing the emissions using thermal oxidizers was calculated. Table 76 focuses on the high emissions factor (EF) case (major polluter), while table 77 focuses on the low emissions factor case (minor polluter). The results are listed in the cases where a production site produces only the single part or sums them all into a single site. The likelihood is that the single site was more realistic to a typical composite manufacturer. The results state that using the FAVE resins instead of the commercial incumbent VE would have a cost avoidance of \$1.75/lb (high EF) or \$1.13/lb (low EF) of resin for the cost of thermal oxidizers and would decrease the cost of greenhouse gases (not required by U.S. law) by \$2.22/lb (high EF) or \$1.43/lb (low EF).

7.2.2 Estimated MFA Price

Table 84 gives the estimated cost of the MFA monomers. This accounted for the price of fatty acids, glycidyl methacrylate, catalyst, and capital costs and operating costs for running the reactors. Additionally, a 25% markup was added to the cost for profit purposes. The results suggest that the price of MLau should range between \$1.23–\$2.45/lb, and the price of MOct should range between \$1.28–\$2.85/lb. The large range in cost is mainly due to variability in the cost of glycidyl methacrylate. The MLau is slightly less expensive, and based on the properties, it is the more likely candidate for implementation. Both MFAs cost considerably more than styrene (~\$0.7/lb).

7.2.2 Estimated FAVE Price

The cost/price of the FAVE resin is a function of economy of scale. The FAVE production will cost small manufacturers considerably more money per pound of resin than larger companies. Thus, the cost of FAVE was determined for both the small manufacturer (table 85) and large manufacturer (table 86) cases. The results are dependent on the cost of commercial VE resins and MFA used to manufacture the FAVE, and thus there is variability in the price. For the small manufacturer case, the resin cost varies from \$2.65–\$4.38/lb. In the conservative case (low EF), the cost avoidance for FAVE resins is \$1.13/lb. In this case, FAVE-L-25S, FAVE-O-25S, FAVE-L-HT, and FAVE-O-HT would likely have a reduced overall cost base. The FAVE-L would be borderline, and the FAVE-O would likely have slightly increased costs. For large

manufacturers, the resin cost varies from \$2.01–\$3.61/lb. This analysis shows that the FAVE resins should only cost slightly more than that of commercial resins. Again, using the conservative cost avoidance \$1.13/lb, every FAVE formulation would have a reduced overall cost.

Table 84. The estimated cost of MFA in 2008.

Raw Material	Percent (wt%)	Min Cost (\$/lb)	Max Cost (\$/lb)	Min Cost (\$/lb)	Max Cost (\$/lb)
MLau					
GM	41.29%	\$1.38	\$3.00	\$0.57	\$1.24
Lauric Acid	58.21%	\$0.33	\$0.65	\$0.19	\$0.38
AMC-2 catalyst	0.50%	\$32.67	\$32.67	\$0.16	\$0.16
MLau Cost =				\$0.93	\$1.78
Annual Capital				\$0.04	\$0.10
Waste				\$0.00	\$0.03
Operating				\$0.02	\$0.05
Price (25% markup) =				\$1.23	\$2.45
MOct					
GM	41.29%	\$1.38	\$3.00	\$0.57	\$1.24
Octanoic Acid	58.21%	\$0.40	\$1.20	\$0.23	\$0.70
AMC-2 catalyst	0.50%	\$32.67	\$32.67	\$0.16	\$0.16
MOct Cost =				\$0.97	\$2.10
Annual Capital				\$0.04	\$0.10
Waste				\$0.00	\$0.03
Operating				\$0.02	\$0.05
Price (25% Markup) =				\$1.28	\$2.85

Table 85. Estimated price of FAVE resins for a small manufacturer.

Component	Min Cost (\$/lb)	Max Cost (\$/lb)	Component Percent					
			FAVE-L	FAVE-O	FAVE-L-25S	FAVE-O-25S	FAVE-L-HT	FAVE-O-HT
Derakane 441-400	\$2.00	\$3.00	60.60%	60.60%	75.76%	75.76%		
Derakane 470HT-400	\$2.50	\$3.50					75.76%	75.76%
RDX 26936 VE	\$4.00	\$5.00	24.40%	24.40%	14.24%	14.24%	14.24%	14.24%
Mlau	\$1.23	\$2.45	15.00%		10.00%		10.00%	
Moct	\$1.28	\$2.85		15.00%		10.00%		10.00%
Minimum Cost			\$2.37	\$2.38	\$2.21	\$2.21	\$2.59	\$2.59
Minimum Price (20% Markup)			\$2.85	\$2.86	\$2.65	\$2.66	\$3.10	\$3.11
Price Difference vs Baseline			\$0.85	\$0.86	\$0.65	\$0.66	\$0.60	\$0.61
Maximum Cost			\$3.41	\$3.47	\$3.23	\$3.27	\$3.61	\$3.65
Maximum Price (20% Markup)			\$4.09	\$4.16	\$3.88	\$3.92	\$4.33	\$4.38
Price Difference vs Baseline			\$1.09	\$1.16	\$0.88	\$0.92	\$0.83	\$0.88

Table 86. Estimated price of FAVE resins for a large manufacturer.

Component	Min Cost (\$/lb)	Max Cost (\$/lb)	Component Percent					
			FAVE-L	FAVE-O	FAVE-L-25S	FAVE-O-25S	FAVE-L-HT	FAVE-O-HT
Bisphenol A VE	\$2.64	\$3.99	65.00%	65.00%	65.00%	65.00%		
Novalac VE	\$3.39	\$4.73					65.00%	65.00%
Styrene	\$0.70	\$1.00	20.00%	20.00%	25.00%	25.00%	25.00%	25.00%
Mlau	\$1.23	\$2.45	15.00%		10.00%		10.00%	
Moct	\$1.28	\$2.85		15.00%		10.00%		10.00%
Minumum Price			\$2.04	\$2.05	\$2.01	\$2.02	\$2.50	\$2.50
Prrice Difference vs Baseline			\$0.04	\$0.05	\$0.01	\$0.02	\$0.00	\$0.00
Maximum Price			\$3.16	\$3.22	\$3.09	\$3.13	\$3.57	\$3.61
Prrice Difference vs Baseline			\$0.16	\$0.22	\$0.09	\$0.13	\$0.07	\$0.11

7.3 CTC Cost Analysis and Comparison

7.3.1 Resin Cost Estimation

Many factors contribute to the total cost of using a new material. These include the costs of developing and producing the alternative material, forming components, maintaining equipment, assembling components on tactical vehicles, complying with environmental and safety regulations, and disposing of waste. The actual cost incurred depends on raw material and energy prices, production methods, labor rates, and regulatory requirements, which depend on market conditions, production volumes, and other factors. Cost estimates for the incumbent and replacement resins are developed based on data collected from manufacturers, distributors, and ARL, as well as many underlying assumptions. The cost estimation procedure, input data, underlying assumptions, and results for each of the resin systems are described and presented in subsequent sections.

It is relatively straightforward to calculate costs for raw materials, energy, and labor, as detailed in this section of this report. But without realistic figures for facility rent and maintenance, overhead labor, equipment costs, etc., it is difficult to estimate hidden costs often grouped together as “other.” Profit estimates, often treated like another fixed cost, are also factored into a product’s price. There are many different methods for pricing a product to cover both costs and profit, ranging from cost-plus pricing to competitive pricing to markup pricing (48). For small businesses selling resin to low-volume users (such as hobbyists or small research groups), the markup on the materials can be as high as 100% or more (49). Even industry experts cannot predict or explain the pricing strategy for resins. A conversation with Mr. Keith Johnson, a subject matter expert with over 30 years in the resin industry, revealed that resin pricing depends on current market prices, and (profit) margins vary by manufacturer (50). In an earlier conversation between ARL and Mr. Johnson, a 35% markup for resin was discussed as a typical resin pricing strategy, but Mr. Johnson refuted this value in a more recent conversation with the project team (50).

It is generally accepted that prices will decrease with increasing production volume as costs are spread out over a larger quantity of products. Based on resin price inquiries during the Subtask 2 portion of this project, as well as conversations with ARL, it appears as though the markup on

resin costs does not drop off sharply with increasing volume. Instead, the prices change only slightly with increasing volume, if at all, implying a minimal markup of resin costs. By this logic, resin markup is probably not very high for the market, and it is unlikely that a medium to large size resin manufacturer would have a very high markup in its resin prices.

More concrete evidence of resin markup can be found in the U.S. Census Bureau's Annual Survey of Manufactures for Plastics Material and Resin Manufacturing (North American Industry Classification System code 325211) (51). For the year 2006 (the most recent year available), if the "Value of Product Shipments" is divided by the "Total Cost of Materials," the result is the ratio 1.45.* According to the definition of the term "Value of Product Shipments," this item covers the received or receivable net selling values (in other words, sales). The term "Total Cost of Materials" refers to direct charges actually paid or payable for items consumed or put into production during the year, including freight charges, the cost of materials, and fuel consumed. Therefore, 1.45 represents the sales to cost of materials ratio and can be used to calculate the sale price of a resin or determine the markup that is factored into a price of a resin. The EPA used this approach to compute the market prices of reinforced plastics composites (RPCs) in the Economic Impact Analysis of the Final Reinforced Plastics NESHAP (3). To find the markup percentage, divide the markup value (the difference between the sales and the cost) by the total cost. According to the 2006 U.S. Census data for the resin industry, the markup is 45%. This figure was used as the final markup estimate in all of the resin pricing estimations.

7.3.1.1 Incumbent VE Resins. The incumbent VE resins can be readily purchased in a blended form ready for molding. The purchase price for each incumbent resin currently used in the tactical vehicle applications was obtained from the manufacturer or one of its distributors. Because this is a comparison study and both incumbent and replacement resins would be shipped to the same composite manufacturing location, shipping costs were quoted in price per pound for for a drum (55 gal) of each product. These prices, as well as the data sources and dates, are listed in table 87.

Table 87. Cost of incumbent VE resins.

Resin	Price/lb	Source
Derakane 8084	\$3.43	Ashland (October 2008, verified February 2009)
Hetron 980/35	\$2.36	Ashland Specialty Chemicals (February 2009)
Huntsman RenInfusion 8605 / Ren 8605	\$13.27	Freeman Composites (February 2009)
Hexion 781-2140	\$2.49	Hexion Specialty Chemicals (October 2008, verified February 2009)
CoRezyn Corve 8100	\$2.00	Interplastic (February 2009)

* The 2006 value of product shipments = \$78,410,325,000, and the 2006 total cost of materials = \$54,017,672,000.

For certain chemicals, the price quoted depended upon the quantity that would be ordered, with larger volumes fetching cheaper prices. For these situations, the least expensive prices were assumed in anticipation of large-scale production. For the Hetron 980, the higher price was used because it was assumed that the quantity ordered for resin production would be <40,000 lb. The prices for all chemicals, including the incumbent resins, are located in appendix K.

7.3.1.2 Replacement FAVE Resin Components. The replacement FAVE resins currently serve a niche market and are not as readily available as the incumbent VE resins. ARL has purchased both the blended replacement resins, which were ready for molding, as well as the components of replacement resins, which ARL blended into resin prior to molding. The blended FAVE resins have been acquired from one supplier at a low volume. If the replacement resins are adopted for use in tactical vehicles, it is expected that composites manufacturers will purchase higher volumes ready for molding. Since material prices are volume dependent, this would likely reduce the purchase price of the blended replacement resins.

ARL obtained costs for the replacement FAVE resin components in 2006. As part of this task, the U.S. National Defense Center for Energy and Environment acquired current prices from manufacturers or one of their distributors. As with the incumbent resins, the prices were quoted in price per pound for a drum (55 gal) of each product with no shipping costs. The 2006 and updated prices, as well as the data sources and dates, are listed in table 88. Ashland Specialty Chemicals would not provide a price for Arapol 914 since the product is not currently sold commercially. For this analysis, ARL's price for Arapol was used. All other updated prices were between 0% and 83% higher than the prices obtained by ARL in 2006. These differences demonstrate how prices can change with time, as well as the difficulty in estimating the future material cost. The updated prices are used in the remainder of the analysis.

Table 88. Cost of replacement FAVE resin components.

Resin	2006 Price/lb	Updated Price/lb	Source	Change
Lauric Acid	\$0.65	\$0.65	Twin Rivers (April 2009)	0%
Octanoic Acid	\$1.20	\$2.19	Acme-Hardesty Co. (April 2009)	83%
Glycidyl methacrylate	\$2.75	\$3.50	NOF America Corporation (January 2009)	27%
AMC-2 catalyst	\$32.20	\$36.62	AMPAC Fine Chemicals (October 2008)	14%
Derakane 441-400	\$2.50	\$3.07	Ashland (October 2008, verified February 2009)	23%
Arapol 914	NA	\$3.29	Price quoted to ARL	NA
Derakane 470HT-400	\$3.00	\$3.95	Ashland (October 2008, verified February 2009)	32%

Note: NA = not available.

7.3.1.3 Methacrylated Fatty Acid Monomers. The MFA monomer production process was discussed with API, the small resin blender in Benicia, CA, used by ARL (52). In addition, API quoted the prices provided in table 89 for volumes of 5 and 55 gal. The information gleaned from API is used here to estimate the current price breakdown for MLau and MOct. Future prices are then estimated based on increased production volumes. API uses the same process, shown in figure 141, to synthesize both MLau and MOct. Here, the costs are categorized as material, labor, and energy. Other costs not itemized in the tables are costs for equipment, tooling, maintenance, overhead labor, building and capital, and profit.

Table 89. Prices quoted by API for MLau and MOct.

Monomer	5-Gal Price/lb	55-Gal Price/lb
MLau	\$8.40	\$7.00
MOct	\$8.40	\$7.00

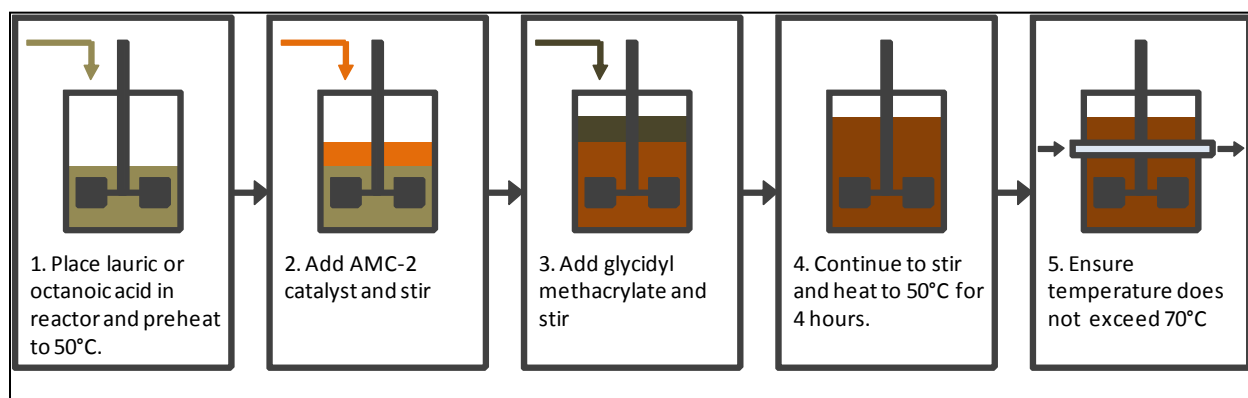


Figure 141. Monomer synthesis steps.

The costs to produce 55 gal of MLau and MOct by a small resin blender are estimated in table 90. The material costs are derived using monomer formulas provided by ARL and the component costs from table 88. The labor costs were derived from production information provided by API. According to API, for a small resin blending operation, very little labor is required to blend the raw materials into an MFA monomer. To make a 55-gal drum batch, about 1/2 h is required to pour the ingredients into a drum, seal it, and place it on a drum roller for mixing. A generic, fully burdened rate of \$65/hr was assumed for a technician.

The energy requirements for producing a 55-gal batch were also obtained from a discussion with API. According to API, it is not necessary to preheat the lauric or octanoic acid prior to blending, as long as the mixing tank is placed in a warm room. Even octanoic acid, which is a solid at temperatures below 63 °F, melts readily in a warm temperature and melts completely during the exothermic reaction that occurs when other materials are added. Therefore, there are no energy inputs required for heating the mixture. Temperature control, to prevent overheating

Table 90. Estimated breakdown of current costs for small resin manufacturer to produce 55-gal batch of monomers.

Cost Category			MLau (Batch = 438 lb)		MOct (Batch = 452 lb)	
	Component	Cost/lb	Weight- Percent	Cost/lb	Weight- Percent	Cost/lb
Materials	Lauric acid	\$0.65	58.5%	\$0.38	—	—
	Octanoic acid	\$2.19	—	—	50.4%	\$1.10
	Glycidyl methacrylate	\$3.50	41.5%	\$1.45	49.6%	\$1.74
	AMC-2 catalyst	\$36.62	0.5%	\$0.18	0.5%	\$0.18
	Total	—	—	\$2.01	□	\$3.02
Labor	Process	Labor	Time	Cost/lb	Time	Cost/lb
	Material handling	\$65/h	0.5 h	\$0.07	0.5 h	\$0.07
	Total	—	—	\$0.07	—	\$0.07
Energy	Process	Cost/ kWh	kWh	Cost/lb	kWh	Cost/lb
	Stirring	\$0.14	5.22	\$0.002	5.22	\$0.002
	Heating	\$0.14	NA	—	NA	—
	Total	—	—	\$0.002	—	\$0.002
Total for materials, labor, and energy	—	—	—	\$2.09	—	\$3.10
Cost with 35% markup	—	—	—	\$2.82	—	\$4.19
Materials with 45% markup	—	—	—	\$2.91	—	\$4.38
Cost with 100% markup	—	—	—	\$4.18	—	\$6.20
Price quoted by API	—	—	—	\$7.00	—	\$7.00

during the exothermic reaction, could be achieved by placing the mixing tank in a cool water bath. No costs were assumed for the water.

After the raw materials are poured into a drum, the drum is sealed and placed on a drum roller for 6–8 hr. An average size drum roller has a 1-hp engine. Using an average electricity rate for Benicia, CA (the location of the current resin blender), and the electricity cost for blending a batch of monomer on a drum roller for 7 h totals \$0.73. In table 84, the sum of the raw materials, labor, and energy costs was multiplied by various markup percentages to estimate the other costs. These costs would include equipment, tooling, maintenance, overhead labor, and building and capital costs, as well as the manufacturer's profit. To prevent double counting

some costs, the 45% markup is applied to the sum of materials cost only, not the cost with energy and labor factored into the calculations. This is based on data descriptions from the U.S. Census Bureau data. The prices charged by API for MLau and MOct appear to be greater than the 100% markup of all costs. When questioned, API would not reveal their pricing strategy, citing only market prices and competition as determining factors. The markup in this report was assumed to be 45%. Based on this analysis, the price of MLau was estimated to be \$2.91/lb, and the price of MOct was estimated to be \$4.38/lb.

7.3.1.4 Fatty Acid Vinyl Ester Resins. The FAVE resin production process was discussed with API. In addition, API quoted the prices provided in table 91 for 5-gal volumes. No prices were quoted for larger volumes because API had not yet made larger volumes of the resins. The information gathered from API is used to estimate the current price breakdown for FAVE resins. Future prices are then estimated based on increased production volumes. A variety of costs are incurred during this process. Here, they are categorized as material, labor, and energy costs. Other costs not itemized in the tables are costs for equipment, tooling, maintenance, overhead labor, building and capital, and profit.

Table 91. Prices quoted by API for FAVE resins.

Resin	5-Gal Price/lb
FAVE-L-25S	\$6.25
FAVE-O-25S	\$6.25
FAVE-L-HT	NA
FAVE-O-HT	NA

Note: NA = not available.

The costs to produce 55 gal of the FAVE resins are estimated in tables 92 and 93. Table 92 shows the estimated costs for a small resin manufacturer to produce the various resins. The material costs are derived using resin formulas provided by ARL and the material costs from table 88. It was assumed that the small resin manufacturer must purchase the Derakane resins at market price. The labor costs were derived from production information provided by API. According to API, for a small resin blending operation, very little labor is required to blend the monomer and other raw materials into a resin. To make a 55-gal drum batch, about 1/2 h is assumed to pour the ingredients into a drum and mix it gently by hand, although API indicated that even less time is required for this step. A generic fully burdened rate of \$65/h was assumed for a technician. According to API, no additional energy costs were necessary for heating or mixing the resin.

To estimate the costs to produce the FAVE resins, it was assumed that the resins were blended by the same company and in the same location as the MLau and MOct monomers. Consequently, shipping costs were not considered. Furthermore, by assuming the monomer manufacturer also blends the resins, then raw material costs are assumed for all components, rather than a marked-up price for the monomers. This assumption was supported by Keith Johnson, who said that one markup is often applied to all raw materials, regardless of their source. Likewise, labor and energy costs for making the monomers are listed again for the resin blending costs, so that table 92 provides a complete cost for making the resin that includes all costs for making the monomers. The sum of the raw materials, labor, and energy costs was multiplied by various markup percentages to estimate the other costs. These costs would include equipment, tooling, maintenance, overhead labor, and building and capital costs, as well as the

manufacturer's profit. In accordance with the sales to cost of materials ratio using the US Census Bureau data, the 45% markup is applied to the sum of materials cost only, to prevent double counting some costs. The markup for our purposes was assumed to be 45%.

Table 93 shows the estimated costs for a large resin manufacturer, such as Ashland Chemical, to produce the various resins. Because the Derakane resin and Arapol production costs are not available, the market or sales price is used for these materials. It is assumed that a 45% markup is already factored into the sales price. Likewise, the MFA monomer prices are listed with the 45% markup included. It is assumed that all labor, energy, profit, and other costs are already factored into sales price, including the costs associated with blending of the FAVE resins. The total costs, including profit, to produce FAVE resins for a large manufacturer are presented as the total in table 93.

Table 92. Estimated breakdown of costs to produce 55 gal of resins for small resin manufacturer.

Cost Category			FAVE-L-25S (Batch = 491 lb)		FAVE-O-25S (Batch = 493 lb)		FAVE-L-HT (Batch = 488 lb)		FAVE-O-HT (Batch = 490 lb)	
	Component	Cost/lb	Weight- Percent	Cost/lb	Weight- Percent	Cost/lb	Weight- Percent	Cost/lb	Weight- Percent	Cost/lb
Materials	Derakane 441-400	\$3.07	54%	\$1.66	54%	\$1.66	—	—	—	—
	Derakane 470HT-400	\$3.95	—	—	—	—	73%	\$2.88	73%	\$2.88
	Arapol 914	\$3.29	36%	\$1.18	36%	\$1.18	17%	\$0.56	17%	\$0.56
	MLau	\$2.01	10%	\$0.20	—	—	10%	\$0.20		
	MOct	\$3.02	—	—	10%	0.30			10%	\$0.30
	Total	—	—	\$3.04		\$3.14		\$3.64		\$3.74
Labor	Process	Labor	Time	Cost/lb	Time	Cost/lb	Time	Cost/lb	Time	Cost/lb
	Material Handling	\$65/h	1 h	\$0.13	1 h	\$0.13	1 h	\$0.13	1 h	\$0.13
	Total	—	—	\$0.13	—	\$0.13	—	\$0.13		\$0.13
Energy	Process	Cost/ kWh	kWh	Cost/lb	kWh	Cost/lb	kWh	Cost/lb	kWh	Cost/lb
	Stirring	\$0.14	5.22	\$0.002	5.22	\$0.002	5.22	\$0.002	5.22	\$0.002
	Heating	\$0.14	NA	—	NA	NA	NA	NA	NA	—
	Total	—	—	\$0.002	—	\$0.002	—	\$0.002	—	\$0.002
Total for materials, labor, and energy	—	—	—	\$3.17	—	\$3.27	—	\$3.77	—	\$3.87
Cost with 35% markup	—	—	—	\$4.29	—	\$4.42	—	\$5.09	—	\$5.23
Materials with 45% markup	—	—	—	\$4.41	—	\$4.55	—	\$5.28	—	\$5.43
Price quoted by API	—	—	—	\$6.25	—	\$6.25	—	—	—	—

Table 93. FAVE resin costs for large resin manufacturer.

Materials		FAVE-L-25S		FAVE-O-25S		FAVE-L-HT		FAVE-O-HT	
Component	Cost/lb	Weight-Percent	Cost/lb	Weight-Percent	Cost/lb	Weight-Percent	Cost/lb	Weight-Percent	Cost/lb
Derakane 441-400	\$3.07	54%	\$1.66	54%	\$1.66	—	—	—	—
Derakane 470HT-400	\$3.95	—	—	—	—	73%	\$2.88	73%	\$2.88
Arapol 914	\$3.29	36%	\$1.18	36%	\$1.18	17%	\$0.56	17%	\$0.56
MLau with 45% markup	\$2.91	10%	\$0.29	—	—	10%	\$0.29	—	—
MOct with 45% markup	\$4.38	—	—	10%	\$0.44	—	—	10%	\$0.44
Total	—	—	\$3.13	—	\$3.28	—	\$3.73	—	\$3.88

As the fatty acid monomers and FAVE resins move from research, development, test, and evaluation to production, the production processes will likely be more automated, and alternative methods for producing the materials may be explored. If they are adopted in large-scale commercial applications, additional economies of scale (as well as competition in the marketplace) may be realized. It is difficult to estimate how this progression would impact the cost of FAVE resins. Material prices can be expected to decrease until they reach a value equal to the cost of production plus some profit at high volumes (49). The FAVE resin prices calculated for this report range from \$3.13–\$4.41/lb for FAVE-L-25S, \$3.28–\$4.55/lb for FAVE-O-25S, \$3.73–\$5.28/lb for FAVE-L-HT, and \$3.88–\$5.43/lb for FAVE-O-HT.

7.3.2 Material Costs by Application

A variety of material losses can occur during part production. The losses currently occurring during VARTM production using the incumbent VE resins and the resulting material requirements are provided in table 94. This information was provided by ARL. Similar losses can be expected for the FAVE resins.

Table 94. Material requirements for VARTM production of VE resins.

Part	Mass (lb)	Trim Loss (%)	Waste (%)	Total Material Requirement (lb)
HMMWV transmission container	35	0	5	36.75
M939 hood	20	5	5	22
M35A3 hood	18	5	5	19.8
HMMWV hardtop	220	5	5	242
T-38 dorsal cover	4	7	5	4.48
MCM rudder	190	0	5	199.5

Using the monomer and resin price calculations detailed in tables 90, 92, and 93 and the resin mass per part information obtained from ARL, the resin cost per part was calculated using resin prices from both small- and large-scale manufacturers (table 95). The resin price per pound and the corresponding price per part (for each application) are provided for the incumbent VE resin (shaded in gray) and the proposed replacement resin (no shading). For the small resin manufacturer, the FAVE resin costs with 45% markup were used in this table.

Table 95. Total material cost for incumbent and replacement resins with no engineering controls.

Application	Resin Used Per Part (lb)	Resin	Cost/lb Small Mfr. (\$)	Cost/Part Small Mfr. (\$)	Cost/lb Large Mfr. (\$)	Resin Cost/Part Large Mfr. (\$)
HMMWV transmission container	36.75	Derakane 8084	3.43	126.05	3.43	126.05
		FAVE-L-25S	4.41	162.07	3.13	115.03
		FAVE-O-25S	4.55	167.21	3.28	120.54
M939 hood	22	Hetron 980/35	2.46	54.12	2.46	54.12
		Huntsman RenInfusion 8605/Ren 8605	13.27	291.94	13.27	291.94
		FAVE-L-HT	5.28	116.16	3.73	82.06
		FAVE-O-HT	5.43	119.46	3.88	85.36
M35A3 hood	19.8	Hetron 980/35	2.46	48.71	2.46	48.71
		Huntsman RenInfusion 8605/Ren 8605	13.27	262.75	13.27	262.75
		FAVE-L-HT	5.28	104.54	3.73	73.85
		FAVE-O-HT	5.43	107.51	3.88	76.82
Amtech HMMWV hardtop	242	Derakane 8084	3.43	830.06	3.43	830.06
		FAVE-L-25S	4.41	1,067.22	3.13	757.46
		FAVE-L-HT	5.28	1,277.76	5.28	1,277.76
		FAVE-O-HT	5.43	1,314.06	5.43	1,314.06
T-38 dorsal cover	4.48	Hexion 781-2140	2.49	11.16	2.49	11.16
		FAVE-L-25S	4.41	19.76	3.13	14.02
MCM rudder	199.5	CoRezyn Corve 8100	2.00	399.00	2.00	399.00
		FAVE-L-25S	4.41	879.80	3.13	624.44

Note: The shaded areas indicate the incumbent VE resin information.

7.3.3 Engineering Controls

In light of the Reinforced Plastic Composites NESHAP that took effect in April 2006, it is assumed (based on information from ARL) that composite manufacturers employing VARTM technology are required to implement add-on control devices to capture volatile emissions from conventional styrene-based commercial resins. Furthermore, it is assumed that the replacement FAVE resins with a styrene content reduced by 15 weight-percent are exempt from the control device requirement.

Various air pollution control devices were studied, and it was determined that an RTO would be the most beneficial technology for composites manufacturing. The RTO eliminates the VOC emissions through high-temperature catalytic oxidization and subsequently releases carbon dioxide and water vapor as a result. The high temperatures necessary for RTO operation are achieved initially by burning natural gas, but energy from the hot exhaust air is recuperated to heat the process air coming into the RTO. This allows for added efficiency and inherent energy savings (53). Most RTOs are rated for 95% energy recovery. The following schematic in figure 142 details the air flow within an RTO.

Price quotes for RTOs were obtained from multiple vendors for sizes ranging from 25,000 to 35,000 ft³/min because this seemed to be the appropriate size RTO for a small- to medium-sized composites manufacturer. As additional research was conducted and process calculations were performed, these sizes proved to be much too large for small- to medium-sized composites manufacturers using the VARTM process. Based on the styrene emissions calculations using an EPA emission factor (see section 7.1.6 of this report), the RTO size was reduced to a 2000-ft³/min unit. (See table 96 for a listing of RTO sizes and prices researched during this process.)

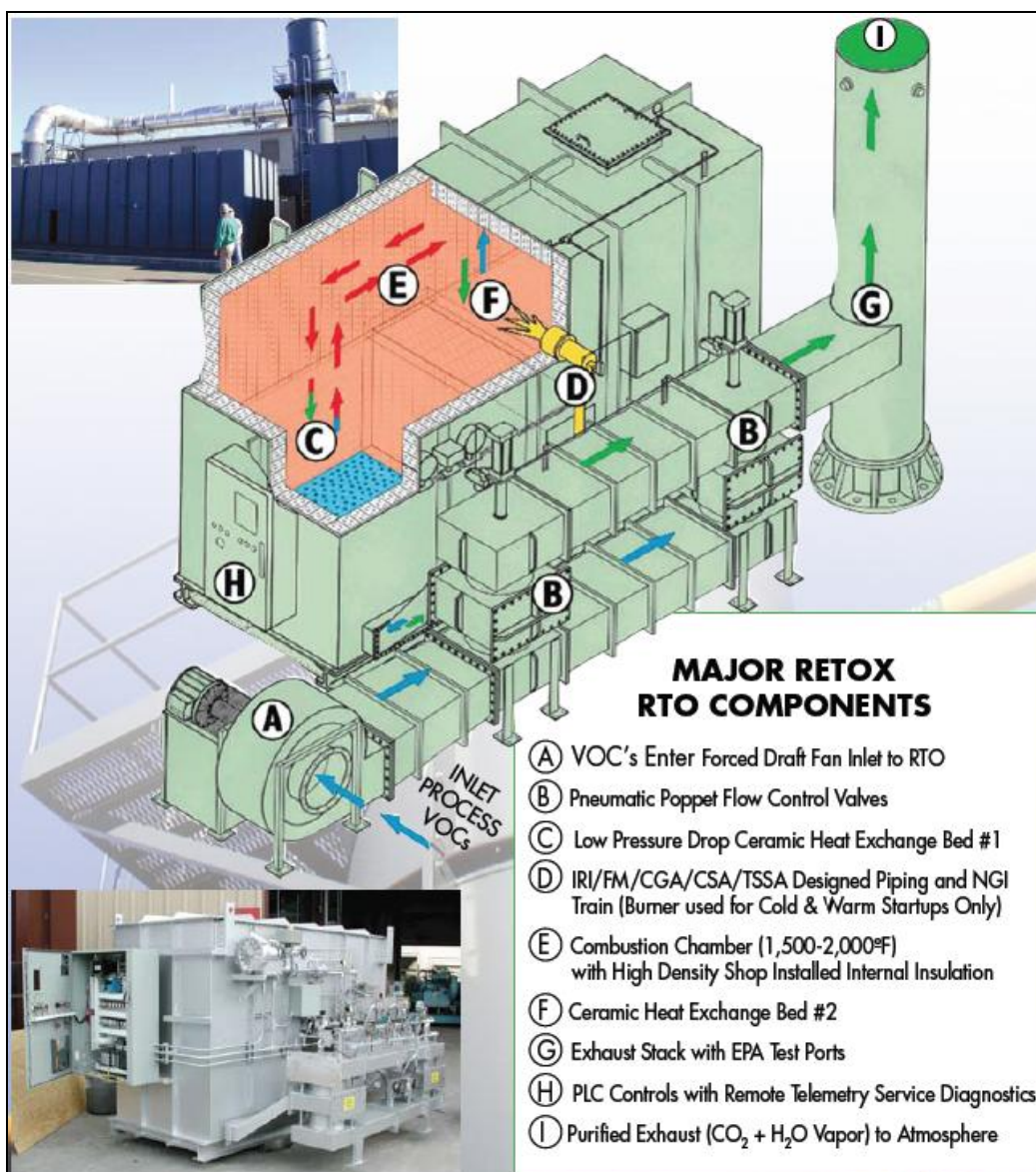


Figure 142. Adwest's RETOX dual chamber RTO system requirements (54).

Table 96. Price quotes obtained for RTOs.

RTO Manufacturer	RTO Size	Price (Including all Equipment, Freight, and Installation)
Adwest Technologies, Inc.	25,000 ft ³ /min	\$439,800 (does not include freight)
Adwest Technologies, Inc.	6,5000 ft ³ /min	\$211,800 (does not include freight)
Tellkamp Systems, Inc.	35,000 ft ³ /min	\$585,000
Tellkamp Systems, Inc.	2,000 ft ³ /min	\$265,000
Ship and Shore ^a	25,000 ft ³ /min	\$361,676 (does not include freight)

^aPrice estimate obtained from Bedford Materials. Bedford Materials purchased a 25,000 ft³/min from Ship and Shore for a similar price. Bedford Materials noticed that Ship and Shore's quote was about 20% less than the quote for the comparable Adwest RTO.

From the calculations in table 81, an average styrene emission rate was calculated to be 0.35 lb styrene per hour going to an RTO. As a conservative estimate, this figure was rounded up to 2.0 lb/h to size an RTO for this hypothetical facility. For a small- to medium-sized composite manufacturer that emits an average of 2 lb of styrene per hour, a 2000-ft³/min RTO would provide ample destruction efficiency for this process. A price quote of \$265,000 for the 2000-ft³/min unit was received from Tellkamp Systems, Inc., in April 2009. This price includes the installation and shipping to a facility in northern California. An additional price quote was received from Adwest Technologies, Inc., for a comparable 6500-ft³/min unit for \$211,800, including all equipment and installation but not shipping. The higher priced unit was used in subsequent calculations because it appeared to be a more complete price quote for a more appropriately sized RTO.

The annualized RTO costs are summarized in table 97. The total capital investment for the RTO is a sum of the direct and indirect costs. The direct costs were obtained from vendor quotes and include any auxiliary equipment, instrumentation, installation, and freight. The indirect costs can be estimated from the EPA's Air Pollution Control Cost Manual (55). According to the formula, the indirect costs, which include engineering, construction and field expenses, contractor fees, start-up costs, performance tests, and contingencies, can be estimated by multiplying the direct costs by 0.31. The total capital investment for the RTO was divided over 15 years, the assumed lifetime of the RTO.

Table 97. RTO capital and operating costs spread over a 15-year economic lifetime.

Annualized RTO Costs			
	Cost Category	Total Cost	Annualized Cost
RTO capital costs	RTO direct cost (incl. freight and installation)	\$265,000	\$17,666.67
	RTO indirect cost (engineering, contractor fees, start-up, etc.)	\$82,150	\$5,476.67
	Total	\$347,150	\$23,143.33
RTO maintenance (labor and parts)	Cost Category	Unit	Annualized Cost
	Perform visual inspection 2–3 h/month	30 h/year	\$1950.00
	Lubrications/replace gaskets, bearings, belts, etc. 10–12 h/year	11 h/year	\$715.00
	Maintenance materials	\$1000	\$1000.00
	Total		\$3665.00
RTO energy usage	Cost Category	Unit	Annualized Cost
	Electricity to run 10-hp fan on RTO for 24-h/7-day operation	\$0.77/h	\$6745.20
	Natural gas for RTO for 24-h/7-day operation	\$1.22/h	\$10,687.20
	Total		\$17,432.40
Total Annual Costs to use RTO			\$44,240.73

Other costs associated with RTO operation, such as operating energy costs and annual preventative maintenance costs, were also factored into the total cost to use the RTO. According to the Tellkamp Systems sales engineer, most RTOs would require a few minutes of daily visual inspections (totaling 2–3 h/month) and an annual shutdown period (10–12 h/year) to perform lubrications and replace bearings, belts, gaskets, or other parts in need of repair. Maintenance costs for consumable parts would be ~\$1000 per year.

The energy costs for the 2000-ft³/min RTO were calculated to be \$1.99/h, assuming 24-h operation of the RTO to maintain the proper temperature required for the permitted VOC destruction efficiency. Assuming an average electricity rate of \$0.11/kWh for a 10-hp fan, the electricity costs for the RTO total \$0.77/h. Assuming a 2-lb/h styrene input to the RTO (which could be hard to maintain at a constant rate and would therefore require additional natural gas to supplement the VOC input and maintain the RTO temperature), the natural gas cost would be \$1.22/h for a rate of \$6.50 per dekatherm. These operating costs were also factored into the total RTO cost in table 97.

7.3.4 Cost Comparison

In order to complete a cost analysis and comparison, it was necessary to determine the incremental variable costs associated with using a pollution control device. The annualized costs for RTO equipment, labor, and utilities (see table 97) were divided by the annual RTO throughput to calculate a cost per pound for operating the RTO. Once calculated, these costs were compared to the prices of the replacement FAVE resins.

A cost comparison was performed on both the cost per pound and cost per part for each of the products listed in tables 98–101. The incremental costs for RTO usage were calculated using a worst case scenario (with only one line of production routed to the RTO) and a more realistic scenario (with three production lines routed to the RTO). Tables 98 and 99 show the costs using resin prices from a small resin manufacturer, and tables 94 and 95 show the costs using resin prices from a large resin manufacturer.

For the worst case scenario, it was assumed that only one line of production is routed to the RTO. Obviously, it would be cost prohibitive to operate in this manner, and the costs reflect this unrealistic scenario. It is highly unlikely that a composite manufacturer would operate a pollution control device so far under its capacity. Only the applications that are heavy and/or are produced in high volume show a reasonable cost. The detailed calculations for these prices can be found in the spreadsheets in appendix K.

Table 98. Worst case total estimated cost per part with resin prices from small manufacturer.

Application	Resin	RTO Maintenance Labor and Parts (\$/lb)	RTO Purchase (\$/lb)	RTO Utilities (\$/lb)	Material (\$/lb)	Total (\$/lb)	Total Cost/Part
HMMWV transmission container	Derakane 8084	\$0.20	\$1.26	\$0.95	\$3.43	\$5.84	\$214.53
	FAVE-L-25S	—	—	—	—	\$4.41	\$162.07
	FAVE-O-25S	—	—	—	—	\$4.55	\$167.21
M939 hood	Hetron 980/35	\$0.03	\$0.21	\$0.16	\$2.46	\$2.86	\$62.97
	Huntsman RenInfusion 8605/Ren 8605	—	—	—	—	\$13.27	\$291.94
	FAVE-L-HT	—	—	—	—	\$5.28	\$116.16
	FAVE-O-HT	—	—	—	—	\$5.43	\$119.46
M35A3 hood	Hetron 980/35	\$1.85	\$11.69	\$8.80	\$2.46	\$24.80	\$491.12
	Huntsman RenInfusion 8605/Ren 8605	—	—	—	—	\$13.27	\$262.75
	FAVE-L-HT	—	—	—	—	\$5.28	\$104.54
	FAVE-O-HT	—	—	—	—	\$5.43	\$107.51
Amtech HMMWV hardtop	Derakane 8084	\$0.03	\$0.20	\$0.15	\$3.43	\$3.81	\$922.23
	FAVE-L-25S	—	—	—	—	\$4.41	\$1067.22
	FAVE-L-HT	—	—	—	—	\$5.28	\$1277.76
	FAVE-O-HT	—	—	—	—	\$5.43	\$1314.06
T-38 dorsal cover	Hexion 781- 2140	\$20.45	\$129.15	\$97.28	\$2.49	\$249.37	\$1117.17
	FAVE-L-25S	—	—	—	—	\$4.41	\$19.76
MCM rudder	CoRezyn Corve 8100	\$2.67	\$23.20	\$17.48	\$2.00	\$45.35	\$9047.15
	FAVE-L-25S	—	—	—	—	\$4.41	\$879.80

Note: The shaded areas indicate the incumbent VE resin information.

Table 99. Realistic scenario total estimated cost per part with resin prices from small manufacturer.

Application	Resin	RTO Maintenance Labor and Parts (\$/lb)	RTO Purchase (\$/lb)	Utilities (\$/lb)	Material (\$/lb)	Total (\$/lb)	Total Cost/Part
HMMWV transmission container	Derakane 8084	\$0.03	\$0.18	\$0.13	\$3.43	\$3.77	\$138.52
	FAVE-L-25S	—	—	—	—	\$4.41	\$162.07
	FAVE-O-25S	—	—	—	—	\$4.55	\$167.21
M939 hood	Hetron 980/35	\$0.03	\$0.18	\$0.13	\$2.46	\$2.80	\$61.59
	Huntsman RenInfusion 8605/Ren 8605	—	—	—	—	\$13.27	\$291.94
	FAVE-L-HT	—	—	—	—	\$5.28	\$116.16
	FAVE-O-HT	—	—	—	—	\$5.43	\$119.46
M35A3 hood	Hetron 980/35	\$0.03	\$0.18	\$0.13	\$2.46	\$2.80	\$55.43
	Huntsman RenInfusion 8605/Ren 8605	—	—	—	—	\$13.27	\$262.75
	FAVE-L-HT	—	—	—	—	\$5.28	\$104.54
	FAVE-O-HT	—	—	—	—	\$5.43	\$107.51
Amtech HMMWV hardtop	Derakane 8084	\$0.03	\$0.18	\$0.13	\$3.43	\$3.77	\$912.34
	FAVE-L-25S	—	—	—	—	\$4.41	\$1067.22
	FAVE-L-HT	—	—	—	—	\$5.28	\$1277.76
	FAVE-O-HT	—	—	—	—	\$5.43	\$1314.06
T-38 dorsal cover	Hexion 781- 2140	\$0.03	\$0.18	\$0.13	\$2.49	\$2.83	\$12.68
	FAVE-L-25S	—	—	—	—	\$4.41	\$19.76
MCM rudder	CoRezyn Corve 8100	\$0.03	\$0.18	\$0.13	\$2.00	\$2.34	\$466.83
	FAVE-L-25S	—	—	—	—	\$4.41	\$879.80

Note: The shaded areas indicate the incumbent VE resin information.

Table 100. Worst case total estimated cost / part with resin prices from large manufacturer.

Application	Resin	RTO Maintenance Labor and Parts (\$/lb)	RTO Purchase (\$/lb)	Utilities (\$/lb)	Material (\$/lb)	Total (\$/lb)	Total Cost/Part
HMMWV transmission container	Derakane 8084	\$0.20	\$1.26	\$0.95	\$3.43	\$5.84	\$214.53
	FAVE-L-25S	—	—	—	—	\$3.13	\$115.03
	FAVE-O-25S	—	—	—	—	\$3.28	\$120.54
M939 hood	Hetron 980/35	\$0.03	\$0.21	\$0.16	\$2.46	\$2.86	\$62.97
	Huntsman RenInfusion 8605/Ren 8605	—	—	—	—	\$13.27	\$291.94
	FAVE-L-HT	—	—	—	—	\$3.73	\$82.06
	FAVE-O-HT	—	—	—	—	\$3.88	\$85.36
M35A3 hood	Hetron 980/35	\$1.85	\$11.69	\$8.80	\$2.46	\$24.80	\$491.12
	Huntsman RenInfusion 8605/Ren 8605	—	—	—	—	\$13.27	\$262.75
	FAVE-L-HT	—	—	—	—	\$3.73	\$73.85
	FAVE-O-HT	—	—	—	—	\$3.88	\$76.82
Amtech HMMWV hardtop	Derakane 8084	\$0.03	\$0.20	\$0.15	\$3.43	\$3.81	\$922.23
	FAVE-L-25S	—	—	—	—	\$3.13	\$757.46
	FAVE-L-HT	—	—	—	—	\$3.73	\$902.66
	FAVE-O-HT	—	—	—	—	\$3.88	\$938.96
T-38 dorsal cover	Hexion 781- 2140	\$20.45	\$129.15	\$97.28	\$2.49	\$249.37	\$1117.17
	FAVE-L-25S	—	—	—	—	\$3.13	\$14.02
MCM rudder	CoRezyn Corve 8100	\$2.67	\$23.20	\$17.48	\$2.00	\$45.35	\$9047.15
	FAVE-L-25S	—	—	—	—	\$3.13	\$624.44

Note: The shaded areas indicate the incumbent VE resin information.

Table 101. Realistic scenario total estimated cost/part with resin prices from large manufacturer.

Application	Resin	RTO Maintenance Labor and Parts (\$/lb)	RTO Purchase (\$/lb)	Utilities (\$/lb)	Material (\$/lb)	Total (\$/lb)	Total Cost/Part
HMMWV transmission container	Derakane 8084	\$0.03	\$0.18	\$0.13	\$3.43	\$3.77	\$138.52
	FAVE-L-25S	—	—	—	—	\$3.13	\$115.03
	FAVE-O-25S	—	—	—	—	\$3.28	\$120.54
M939 hood	Hetron 980/35	\$0.03	\$0.18	\$0.13	\$2.46	\$2.80	\$61.59
	Huntsman RenInfusion 8605/Ren 8605	—	—	—	—	\$13.27	\$291.94
	FAVE-L-HT	—	—	—	—	\$3.73	\$82.06
	FAVE-O-HT	—	—	—	—	\$3.88	\$85.36
M35A3 hood	Hetron 980/35	\$0.03	\$0.18	\$0.13	\$2.46	\$2.80	\$55.43
	Huntsman RenInfusion 8605/Ren 8605	—	—	—	—	\$13.27	\$262.75
	FAVE-L-HT	—	—	—	—	\$3.73	\$73.85
	FAVE-O-HT	—	—	—	—	\$3.88	\$76.82
Amtech HMMWV hardtop	Derakane 8084	\$0.03	\$0.18	\$0.13	\$3.43	\$3.77	\$912.34
	FAVE-L-25S	—	—	—	—	\$3.13	\$757.46
	FAVE-L-HT	—	—	—	—	\$3.73	\$902.66
	FAVE-O-HT	—	—	—	—	\$3.88	\$938.96
T-38 dorsal cover	Hexion 781- 2140	\$0.03	\$0.18	\$0.13	\$2.49	\$2.83	\$12.68
	FAVE-L-25S	—	—	—	—	\$3.13	\$14.02
MCM rudder	CoRezyn Corve 8100	\$0.03	\$0.18	\$0.13	\$2.00	\$2.34	\$466.83
	FAVE-L-25S	—	—	—	—	\$3.13	\$624.44

Note: The shaded areas indicate the incumbent VE resin information.

For the more realistic scenario, it was assumed all Fort Totten parts (for Army vehicles) are made in one facility, and all three product lines go to the same RTO. It was further assumed that no other products go to the RTO. The calculations were completed for the HMMWV transmission container, the M939 hood, and the M35A3 hood, and these incremental variable costs per pound were then applied to the other applications. It was assumed that the Fort Totten facility example is representative for all applications, even those with very small annual production estimates. The cost per pound increase from RTO usage, \$0.34/lb regardless of the resin, was then applied to all applications.

This incremental cost increase for RTO usage was compared to the information found in the EPA's "Economic Impact Analysis of Final Reinforced Plastics" NESHAP (59). In this NESHAP, the compliance costs and market price changes resulting from the NESHAP regulation are summarized for the year 1997 (59). For the recommended alternative, the mean incremental variable compliance cost across all industries is \$0.06/lb, with a maximum value increase of \$1.08/lb (3). For the land transportation industry, the incremental cost was expected to increase to \$0.05/lb as a mean and \$0.20/lb maximum.

The cost analysis provided in this report assumes that all cost increases would be directly translated to the composites manufacturer and thus the DOD. According to the EPA's economic impact analysis (EIA), the increased cost of production due to the regulation is expected to slightly increase the price of composites and marginally reduce their production/consumption from baseline levels (3). However, according to the EIA, the price impacts are attenuated by the existence of a perfect substitute for the regulated RPC products, such as a part made out of a different material. Therefore, the incremental cost associated with RTO usage could indeed be closer to the EPA's \$0.20/lb value for land transportation RPC products.

Finally, an RTO usage incremental cost can be calculated in the event that FAVE resin composite parts also use an RTO for air pollution control. For this scenario, one can assume a facility in which many different composites parts are being manufactured using a variety of processes, such as open molding, VARTM, etc., and all of the emissions from these processes are being routed to the RTO. If one of these production lines replaced its incumbent resin with a FAVE resin, it is unlikely it would discontinue the RTO treatment of those emissions. In other words, the emissions from this process would still be routed to the RTO and, as a result, some of the FAVE resins would incur some of the RTO costs. One way to estimate the costs for this scenario would be to create a ratio of the FAVE resin styrene content to the incumbent resin styrene content and multiply this by the \$0.34/lb increase for the RTO usage; this is estimated in table 102. The styrene content of all FAVE resins is 25%. The cost per pound for a particular resin in this table would then be added to the FAVE resin cost per pound that is replacing this resin.

Table 102. RTO usage price increase for FAVE resins.

Resin	Styrene Content (%)	Ratio of FAVE Resin Styrene Content to Incumbent Resin Styrene Content	Cost Per Pound (\$)
Derakane 8084	40	0.625	0.21
Hetron 980/35	35	0.714	0.24
Hexion 781-2140	46	0.543	0.18
CoRezyn Corve 8100	49.5	0.505	0.17

7.4 Environmental Impact

Materials, energy, water, and other inputs are required to extract, process, and transport raw materials and to manufacture, transport, use, and retire composite structures used in military applications. In addition to consuming resources, these activities result in environmental discharges and generate waste. These aspects of the incumbent and replacement resins are not captured in the CEA provided above. Life cycle analysis (LCA) is an analytical process for quantifying the inputs and outputs for each life cycle stage and assessing the total environmental impact of a product. Consequential LCA is used to identify significant differences in the environmental burdens of using one product instead of another. In the following diagrams, consequential LCA is used to evaluate the environmental implications of substituting one of the replacement FAVE resin systems (i.e., FAVE-L-25S) for one of the incumbent VE resin systems (i.e., Derakane 8084). Figure 143 shows the product life cycle associated with using these resin systems in structural composites. The FAVE resins were drop-in replacements for commercial VE resins. The resource extraction and resin blending stages were different for both resin systems. During an LCA, all of the inputs and outputs associated with these stages are evaluated. No process changes are expected in the composite molding, use, or retirement stages. Since the styrene emissions during these stages depend on the composition of the composite, they would be evaluated.

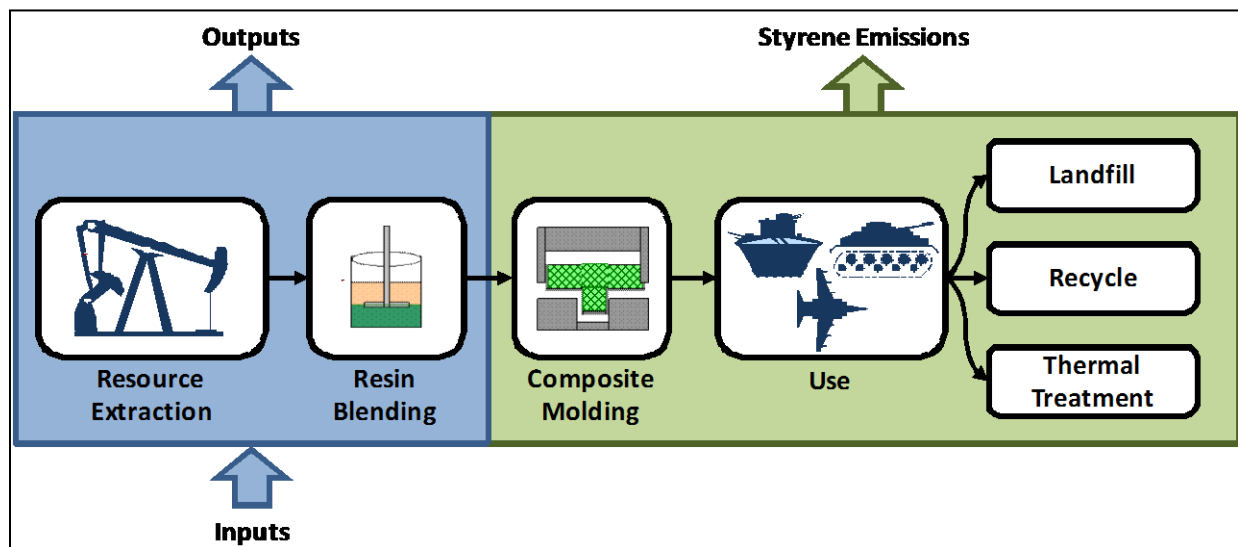


Figure 143. Aspects of the product life cycle compared for the two resin systems.

To identify the cradle-to-gate flows from preparing the incumbent and replacement resin, process flow diagrams were developed based on technical literature and reference books (56, 57). Since little detailed information is available from the resin producers, processes that have the greatest industrial performance were assumed. Several of the operations included in the process flow diagrams produce co-products. However, only the chemicals used in producing the incumbent

and replacement resins are shown. If an LCA were to be performed, the next step would be to quantify the inputs and outputs associated with preparing each material or chemical shown in the process flow diagrams.

7.4.1 Preparation of Incumbent Resin (Derakane 8084)

Derakane 8084 is an elastomer-modified bisphenol A epoxy VE. It is 60 weight-percent bisphenol A and 40 weight-percent styrene, with an unknown percentage of the non-styrene portion being an elastomer for toughening (58). The assumed process flow diagram for producing Derakane 8084 is shown in figure 144.

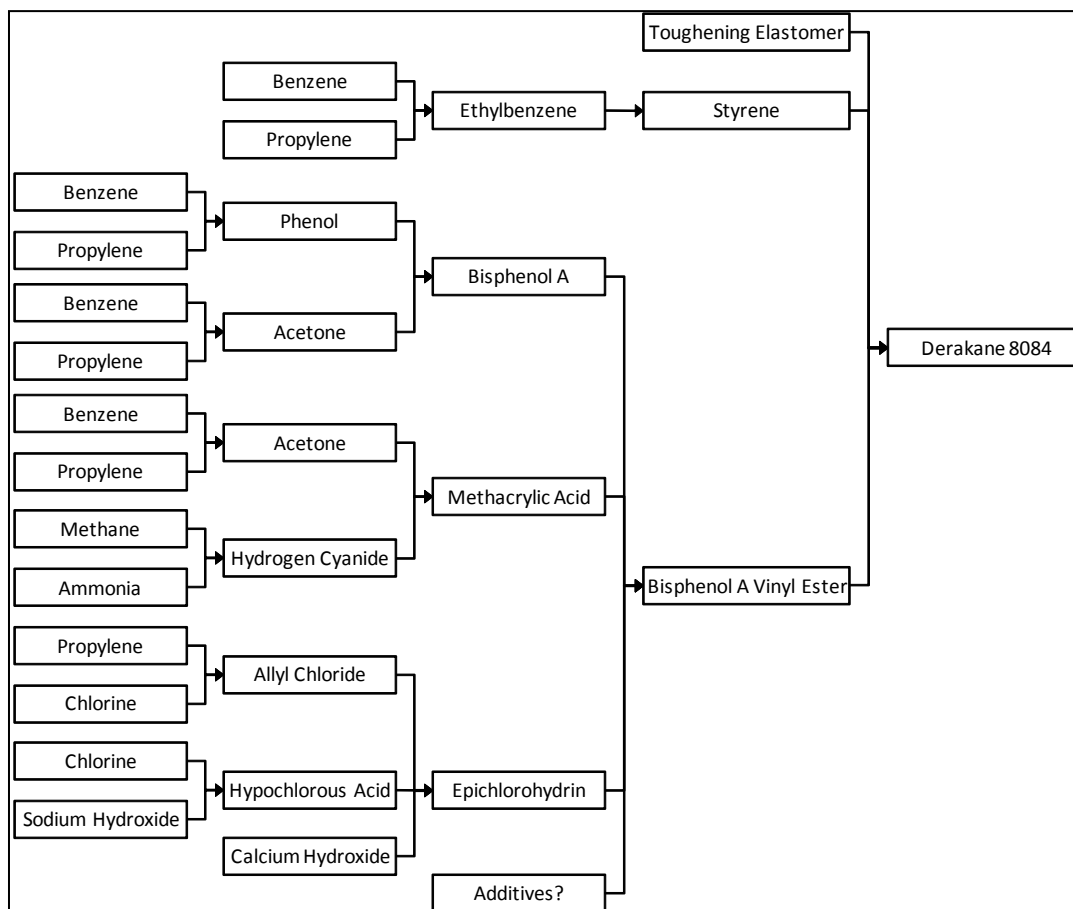


Figure 144. Derakane 8084 process flow diagram.

7.4.2 Preparation of Replacement Resin (FAVE-L-25S)

The replacement resin FAVE-L-25S has many of the same ingredients as the Derakane 8084, but a portion of the styrene is replaced with an MFA monomer that contains plant-derived ingredients. The assumed process flow diagram for the FAVE-L-25S replacement resin is shown in figure 145.

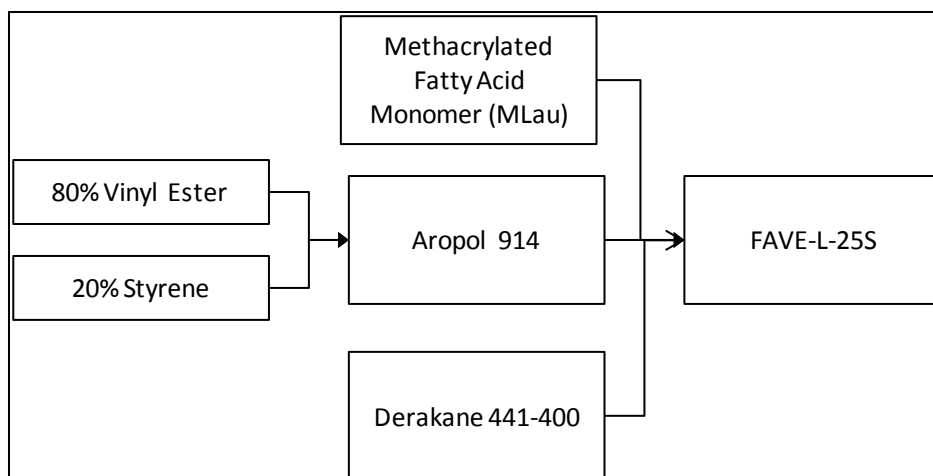


Figure 145. FAVE-L-25S process flow diagram.

The MLau monomer and Derakane 441-400 can be dissected further into their own process flow diagrams. The assumed process flow diagram for the MLau monomer is shown in figure 146.

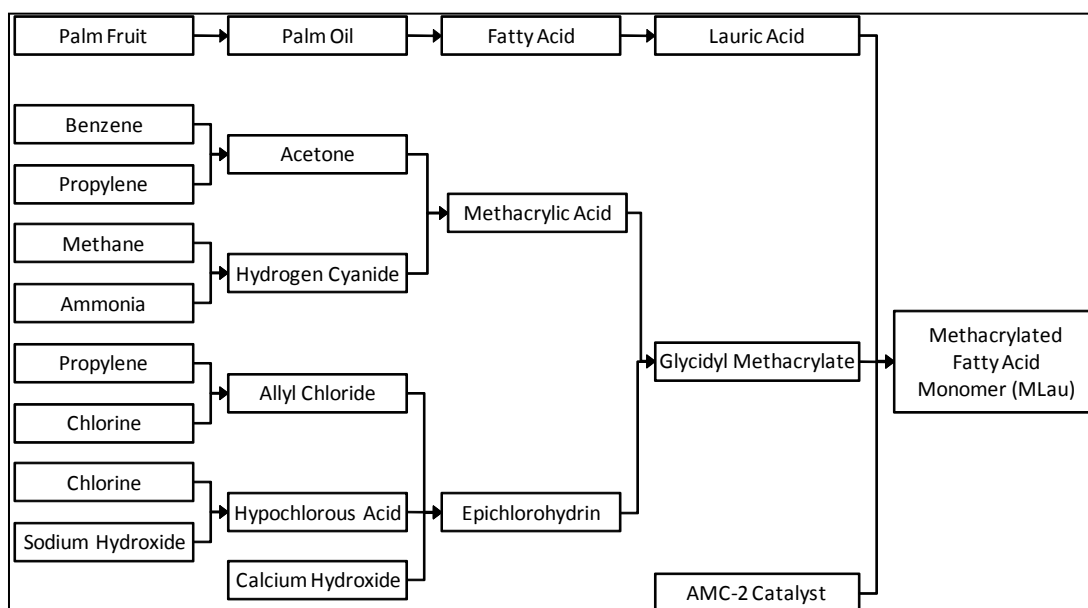


Figure 146. Methacrylated lauric acid process flow diagram.

Derakane 441-400, the VE portion of the FAVE-L-25S replacement resin, is also a bisphenol-A epoxy VE but without the elastomer-modified component. It is 67 weight-percent bisphenol A and 33 weight-percent styrene. The assumed process flow diagram for producing Derakane 441-400 is shown in figure 147.

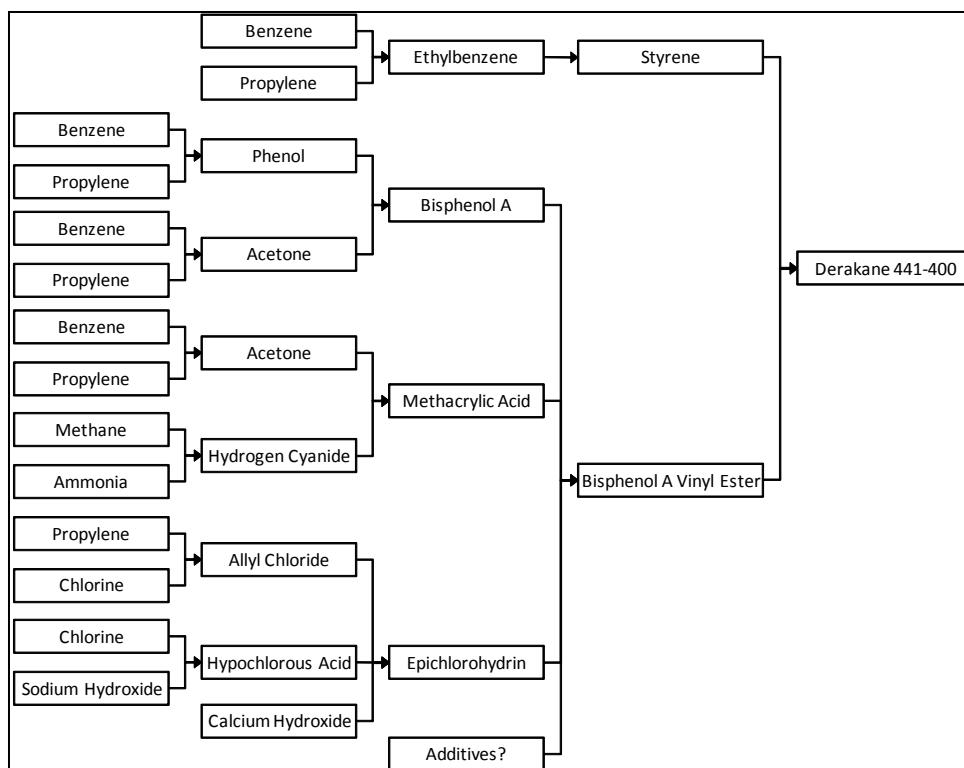


Figure 147. Derakane 441-400 process flow diagram.

7.5 LCA Conclusions

This life cycle cost analysis details the costs of implementing FAVE resins vs. using standard VE resins combined with facility modifications to meet NESHAP requirements. The data in tables 92–95 summarize the anticipated life cycle costs on a per pound and per part basis. The worst-case scenarios (tables 92 and 94) show costs that are so unrealistic that this scenario should not be considered further. Only the applications that are heavy (such as the HMMWV hardtop) and/or are produced in high volume (such as the M939 hood) show a reasonable cost. It is highly unlikely a composite manufacturer would operate a pollution control device so far under its capacity. As detailed in table 93 (for resin prices from a small manufacturer), for every application, the cost per pound and cost per part are less for the incumbent resin using pollution control equipment than for the replacement FAVE resin. The incremental cost with RTO usage amounts to pennies per pound. It should be noted that this cost analysis assumes all costs are translated directly to the consumer. As discussed in the EPA’s EIA, however, some of these costs are likely to be absorbed by the composites manufacturers. A close look at the calculations shows a sensitivity to RTO throughput, but it is likely that composites manufacturers would maximize the number of parts going to the RTO.

Upon reviewing the final costs among the different resin formulations, it is obvious that the epoxy resins remain the most expensive option. Even with the reduced burden of environmental reporting, the epoxy resin costs are two to four times higher than any other resin. For the Hetron,

Hexion, and CoRezyn incumbent resins, the costs with the RTO usage included are still significantly less than the replacement FAVE resins costs if the resins were produced by a small manufacturer. For the Derakane 8084, it is possible that the FAVE resin prices could be competitive. As shown in table 93, if the markup on the FAVE resin prices were reduced to a 19% margin (instead of 45%), the FAVE resin prices would be similar to the costs of Derakane 8084 with incremental costs of RTO usage included.

If the FAVE resins were manufactured on a large scale by a company such as Ashland Chemical (table 95), the FAVE prices would be competitive with some incumbent resin prices. The FAVE-L-25S and the FAVE-O-25S are less expensive than the Derakane 8084 by 17% and 13%, respectively. The FAVE-L-HT and the FAVE-O-HT are both about 35% more than the Hetron 980 and nearly identical in price to the Derakane 8084. Even the least expensive FAVE resin, the FAVE-L-25S, is more expensive than the Hexion and CoRezyn incumbent resins, probably due to the higher styrene content in these resins. A less expensive resin may be more economical in the FAVE resin formula than Derakane 441-400 or Derakane 470HT-400. If determined to be comparable in quality and performance to the Derakane products, the Hetron 980/35 should be considered for use in the FAVE resin formulas since all of these products contain ~35% styrene.

Not included in this cost analysis is the environmental LCA of the different resin formulations. An LCA would quantify the inputs and outputs for each life cycle stage and assess the total environmental impact of a product. A consequential LCA is recommended to identify significant differences in the environmental burdens of using one product instead of another.

8. Implementation Issues

There are a number of implementation issues with the FAVE resin technology. These issues range from resin production to composite approval to specific resin approval. We are actively dealing with these issues, some of which were easily overcome, while others are more difficult.

The production of FAVE resins is in transition. Dixie Chemicals, Inc., has recently licensed the MFA and FAVE technology from Drexel University. As a result of this, API is no longer allowed to manufacture the MFA of FAVE, except at the behest of Dixie Chemicals. Dixie Chemicals is in the process of scaling up the MFA technology and is looking for industrial partners (Ashland, etc.) to manufacture the FAVE resin. Until these steps are accomplished, the production of the resin was limited. Although mass production of FAVE by Dixie Chemicals or its partners cannot be guaranteed, there is a good chance that it will be produced in a 1- to 3-year timeframe.

Demonstration/validation of the HMMWV transmission container showed that the design of the container must be modified to meet Army specifications. The required changes are low risk. In particular, the failure of the wooden feet for this container indicates the need for more expensive feet. In turn, this will make the container more expensive and could limit its demand. Regardless, RRAD was very happy with the performance of container, which they considered far superior to past solutions. Thus, overall, we expect the risk of this implementation issue to be low.

Since the start of this project, the M35A3 truck has been discontinued from military use. Therefore, implementation of the M35A3 truck hood will not happen. Nonetheless, other hoods, such as the M939, have a need for composite solutions that could be implemented using FAVE resins. However, implementation of these other hoods, including the M939, will take a while because there are no approved technical data packages for these parts. These technical data packages are in the approval process, but past experience has shown that this will take 2–3 years. The risk of implementing the FAVE resins for Army truck hood applications is low but was delayed.

The T-38 dorsal cover application is being supported by a military contractor on an as-needed basis. Despite that, it is possible that they will use the FAVE resin for this application. However, they are currently using UPE resins because of their lower cost and will not likely switch to the more expensive FAVE resins for this application. The splash molds are controlled by the ACO. The ACO was satisfied with the performance of the FAVE resins and thus will use these resins when they are available for this application. The ACO was also satisfied with the use of the FAVE resins for the F-22 canopy cover. Again, they will use the FAVE resins when they are made available again. Furthermore, the ACO will use the FAVE resins for all relevant VE applications because of the good performance of these resins.

The MCM composite rudder performed well according to NSWCCD and Structural Composites. However, the rudder was prepared in a manner different from the previous rudder, as it used a composite internals rather than bronze internals. This decreased the cost of the part significantly. Nonetheless, the new design must be approved. Furthermore, although the FAVE resin performed well, some properties were different from the commercial resin. As a result, the new design and resin would have to be qualified. Implementation of new parts on Navy ships is a long process. Although we expect the resin/composite meets the performance needs, we expect the implementation delays to be significant (~5 years). Furthermore, LCA did not favor the more expensive resins. Manufacture of these resins through a larger company that could possibly drive the price even lower would increase implementation probability. Thus, the risk associated with implementation of the FAVE resins on MCM and other rudders is high.

9. References

1. Sands, J. M.; Fink, B. K.; McKnight, S. H.; Newton, C. H.; Gillespie, J., Jr.; Palmese, G. R. *Clean Products and Processing* **2001**, 2.
2. Smeal, T. W.; Brownell, G. L. U.S. Patent 5,292,841, 1994.
3. Environmental Protection Agency. *Federal Register* **2003**, 68.
4. Lacovara, B. *Reducing Emissions with Styrene Suppressants*; Composite Formulators Association, 1999.
5. Ziaee, S.; Palmese, G. R. Effects of Temperature on Cure Kinetics and Mechanical Properties of Vinyl-Ester Resins. *J. Polym. Sci. B: Polym. Phys* **1999**, 37.
6. Vallone, J. *NESHAP Requirements Assessment for Miscellaneous Coatings, Adhesives, Sealers, Etc.*; Final Report to ARL, Sustainable Painting Operations for the Total Army. Concurrent Technologies Corp.: Johnstown, PA, September, 2004.
7. Palmese, G. R.; La Scala, J. J.; Sands, J. M. Fatty Acid Monomers to Reduce Emissions and Toughen Polymers. U.S. Patent 7,525,909, 28 April 2009.
8. La Scala, J. J.; Sands, J. M.; Orlicki, J. A.; Robinette, E. J.; Palmese, G. R. Fatty Acid-Based Monomers as Styrene Replacements for Liquid Molding Resins. *Polymer* **2004**, 45.
9. La Scala, J. J.; Orlicki, J. A.; Winston, C.; Robinette, E. J.; Sands, J. M.; Palmese, G. R. The Use of Bimodal Blends of Vinyl Ester Monomers to Improve Resin Processing and Toughen Polymer Properties. *Polymer* **2005**, 46.
10. Palmese, G. R.; La Scala, J. J.; Sands, J. M. Multimodal Vinyl Ester Resins. U.S. Patent 7,449,525, 11 November 2008.
11. La Scala, J. J.; Logan, M. S.; Sands, J. M.; Palmese, G. R. Composites Based on Bimodal Vinyl Ester Resins With Low Hazardous Air Pollutant Contents. *Comp. Sci. and Tech.* **2008**, 68, 1869–1876.
12. La Scala, J. J.; Orlicki, J. A.; Jain, R.; Ulven, C. A.; Palmese, G. R.; Vaidya, U. K.; Sands, J. M. Emission modeling of Styrene from Vinyl Ester Resins With Low Hazardous Air Pollutant Contents. *Clean Tech Environ Policy*, **2009**, 11, 283–292.

13. La Scala, J. J.; Orlicki, J. A.; Winston, C.; Robinette, E. J.; Jeyarajasingam, A.; Lee, J.; Dey, T.; Cavan, C.; Baer, J.; Brown, J.; DeSchepper, D.; McKnight, S. H.; Ulven, C. A.; Jain, R.; Kamath, P.; Sahu, A.; Crane, R. M.; Vaidya, U. K.; Palmese, G. R.; Sands, J. M. *Low-Cost and High-Impact Environmental Solutions for Military Composite Structures, Final Report*; SERDP PP-1271; U.S. Army Research Laboratory: Aberdeen Proving Ground, MD, December 2005.
14. La Scala, J. J.; Jeyarajasingam, A.; Logan, M. S.; Winston, C.; Myers, P.; Sands, J. M.; Palmese, G. R. Fatty Acid-Based Vinyl Ester Composites with Low Hazardous Air Pollutant Contents. *J. Biobased Matl. and Bioenergy* **2007**, *1*, 409–416.
15. Bartling, E. T-38 Dorsal Cover Resin Infusion, Air Force Presentation, June 2005.
16. Gillespie, J., Jr. Accelerated Insertion of Lightweight Materials into Military Vehicles. *Proceedings of the 3rd Annual Lightweight Materials for Defense*, Arlington, VA, 28 February–2 March 2005.
17. Gillespie, J., Jr.; Heider, D.; Shevchenko, N.; Sands, J.; Siers, R.; Florence, J. An Overview of the Composites Replacement Parts Program for Military Tactical Wheeled Vehicles. *Proceedings of the American Society for Composites Eighteenth Technical Conference*, Gainesville, FL, 2003.
18. Andersen, S.; Gillespie, J., Jr.; Haque, J.; Heider, D.; Shevchenko, N.; Siers, R.; Sands, J. Overview of the Composite Body Parts Replacement Program. *Proceedings of the Defense Manufacturing Conference*, Las Vegas, NV, 2004.
19. Roger, C. *Low HAP/VOC Compliant Resins for Navy Composite Rudder Application*; Naval Surface Warfare Center, Carderock Division, West Bethesda, MD, March 2006.
20. Griffiths, B. Rudder Gets New Twist With Composites; *Composite Technology* **2006**, 60–62.
21. Brill, R. P.; Palmese, G. R. Investigation of Vinyl-Ester - Styrene Bulk Copolymerization Cure Kinetics Using Fourier Transform Infrared Spectroscopy. *J. Appl. Polym. Sci.* **2000**, *76*, 1572–1582.
22. Pouchert, C. J., Ed. *The Aldrich Library of Infrared Spectra*; 3rd ed.; Aldrich Chemical Co.: Milwaukee, WI, 1981.
23. Garcia, A. A.; Bonen, M. R.; Ramirez, V. J.; Sadaka, M.; Vuppu, A. *Bioseparation Process Science*; Blackwell Science, Inc.: Malden, MA, 1999, pp 181–183.
24. Khot, S. N. Synthesis and Application of Triglyceride Based Polymers. Ph.D. Dissertation, University of Delaware, Newark, DE, 2001.

25. Nielsen, L. E.; Landel, R. F. *Mechanical Properties of Polymers and Composites*; Marcel Dekker: New York, NY, 1994, pp 140–142.
26. Palmese, G. R.; McCullough, R. L. Effect of Epoxy-Amine Stoichiometry on Cured Resin Material Properties. *J. Appl. Polym. Sci.* **1992**, *46* (10):1863–1873.
27. Flory, P. J. *Principles of Polymer Chemistry*; Cornell University Press: Ithaca, NY, pp. 432–493.
28. Ashland, Inc. Technical Data Sheet for Derakane 441-400; Dublin, OH, 2005.
29. Sartomer. Technical Data Sheet for Sartomer CN151; Exton, PA, 1999.
30. Cytec Industries, Inc. Technical Data Sheet for Cytec RDX26936; Woodland Park, NJ, 2007.
31. Ashland, Inc. Technical Data Sheet for Arapol 914; Dublin, OH, 2008.
32. Ashland, Inc. Technical Data Sheet for Derakane 470-400HT; Dublin, OH, 2005.
33. Ashland, Inc. Technical Data Sheet for Derakane 8084; Dublin, OH, 2005.
34. Structural Composites, Inc. Composite Twisted Rudder Manufacturing Guide; contract no. N00014-06-D-0045; Melbourne, FL, June 2008.
35. Foley, M. E.; Dapp, T. L.; Kim, J. S.; Crane, R. *The Effect of Peel Ply and Surface Preparations on Secondary Bonding in VARTM Applications*; NSWCCD-65-TR-2009/36; Naval Surface Warfare Center, Carderock Division, West Bethesda, MD, March 2009.
36. Mallick, P. K.; Newman, S. *Composite Materials Technology*; Hanser Publishers: New York, 1990.
37. U.S. Environmental Protection Agency Technology Transfer Network. Clearinghouse for Inventories and Emission Factors, AP-42 Section 4.4 Polyester Resin Plastics Products Fabrication; Washington, DC, February 2007.
38. VARTM. http://www.an-cor.com/images/laminating_methods/vartm.jpg (accessed December 2011).
39. Haberlein, R. A. Feasibility and Cost of the Capture and Control of Hazardous Air Pollutant Emissions from the Open Molding of Reinforced Plastic Composites. EECS, April 2000 (in Maximum Achievable Control Technology docket).
40. Lacovara, R.; et al. Composite Industry Facility Examples: Effect of Pollution Prevention Implementation; Composite Fabricators Association; April 2000 (in MACT docket).
41. Lipiro, D. J. Non-Economic Impacts on the Reinforced Plastic Composites Industry of Emission Control by Oxidation Systems; ECRM Inc.; April 2000 (in MACT docket).

42. Lipiro, D.J. Emission Control vs. Pollution Prevention for Open Molding of Composites: Incremental Benefits and Impacts; ECRM Inc.; May 2000 (in MACT docket).
43. Environomics, Inc. MACT for Reinforced Plastics Composites: Affordability at Facilities with 100–250 TPY of HAP Emissions That Are Owned by Large Businesses; Washington, DC, 2000
44. U.S. Energy Information Administration Web site. Emissions of Greenhouse Gases Report, December 2009. <http://www.eia.gov/oiaf/1605/ggrpt/carbon.html> (accessed May 2012).
45. Intergovernmental Panel on Climate Change. Revised 1996 IPCC Guidelines for National Greenhouse Gas Inventories: Reference Manual; Geneva, Switzerland, 1996.
46. Conti, J.; Sweetnam, G. U.S. Energy Information Administration Web site. Documentation for Emissions of Greenhouse Gases in the United States 2005, October 2007; [http://www.eia.gov/oiaf/1605/ggrpt/documentation/pdf/0638\(2005\).pdf](http://www.eia.gov/oiaf/1605/ggrpt/documentation/pdf/0638(2005).pdf) (accessed May 2012).
47. U.S. Energy Information Administration Web site. Annual Energy Outlook 2011, April 2011. http://www.eia.gov/forecasts/aeo/chapter_executive_summary.cfm (accessed May 2012).
48. Entrepreneur Magazine. Pricing a Product. <http://www.entrepreneur.com/encyclopedia/term/82380.html> (accessed December 2011).
49. Boyer, J. M. Compilation of a Materials Cost Database for a WEB-Based Composites Cost Estimator, B. S. Ph.D. Thesis, Massachusetts Institute of Technology, Cambridge, MA, June 2001.
50. Johnson, K. Preforms, LLC. Telephone conversation, 4 May 2009.
51. U.S. Census Bureau. 2006 Annual Survey of Manufacturers. <http://www.census.gov/mcd/asm-as1.html>.
52. Moulton, R. Applied Polyamics, Inc., Benicia, CA. Telephone conversation, March 2009.
53. Anguil Environmental. Regenerative Thermal Oxidizer. <http://www.anguil.com/prregthe.php>.
54. Adwest Technologies, Inc. 2009 RETOX RTO Portfolio Brochure, Anaheim, CA, 2009.
55. U.S. Environmental Protection Agency. EPA Air Pollution Control Cost Manual; 6th ed.; Washington, DC, January 2002.
56. *Kirk-Othmer Encyclopedia of Chemical Technology*, 5th ed.; John Wiley & Sons, Inc.: Hoboken, NJ, 2007.
57. Speight, J. G. *Chemical and Process Design Handbook*; McGraw-Hill: New York, 2002.

58. Boyd, S. E.; La Scala, J. J.; Palmese, G. R. Molecular Relaxation Behavior of Fatty Acid-Based Vinyl Ester Resins. *J. Applied Polymer Science* **2008**, *108* (6), 3495–3506.
59. U.S. Environmental Protection Agency. *Economic Impact Analysis of Final Reinforced Plastics: Final Report*; Research Triangle Park, NC, August 2002.

Appendix A. Points of Contact

Contact information for the participants in this work has been omitted.

INTENTIONALLY LEFT BLANK.

Appendix B. ATC Validation of HMMWV Transmission Container

This appendix appears in its original form, without editorial change.

Appendix B

ATC Validation of HMMWV Transmission Container



U.S. ARMY ABERDEEN TEST CENTER

AD NO. _____
ATEC PROJECT NO. 2009-DT-ATC-ARLSP-E4867
REPORT NO. ATC-10144

Final Report

Shock and Vibration Test

Composite High Mobility Multipurpose Wheeled Vehicle (HMMWV) Transmission Container

November 2009



Joseph Rybak
Support Equipment Division, Warfighter Directorate
U.S. Aberdeen Test Center
Aberdeen Proving Ground, MD 21005-5055

Prepared for:
U.S. Army Research Laboratory
Aberdeen Proving Ground, MD 21005

U.S. Army Developmental Test Command
Aberdeen Proving Ground, MD 21005-5055

Distribution limited to U.S. Government Agencies only; Test and Evaluation;
November 2009. Other requests for this document must be referred to U.S. Army
Research Laboratory, ATTN: RDRL-WMM-C.

DISPOSITION INSTRUCTIONS

Destroy this document when no longer needed. Do not return to the originator.

The use of trade names in this document does not constitute an official endorsement or approval of the use of such commercial hardware or software. This document may not be cited for purposes of advertisement.



REPLY TO
ATTENTION OF

DEPARTMENT OF THE ARMY
US ARMY ABERDEEN TEST CENTER
400 COLLERAN ROAD
ABERDEEN PROVING GROUND, MARYLAND 21005-5059

TEDT-AT-WFE

25 NOV 2009

MEMORANDUM FOR Commander, US Army Developmental Test Command, 314 Longs
Corner Road, Aberdeen Proving Ground, MD 21005

SUBJECT: Final Report of the Shock and Vibration Test of the Composite High Mobility
Multipurpose Wheeled Vehicle (HMMWV) Transmission Container, ATEC Project
No. 2009-DT-ATC-ARLSP-E4867

1. The Final Report has been approved by this test center and is submitted for your information and retention.
2. The point of contact for this office is Mr. Joseph Rybak, TEDT-AT-WFE, 410-278-2881.

FOR THE COMMANDER:


JOHN B. RUHL
Director, Warfighter Directorate

SEE DISTRIBUTION LIST

REPORT DOCUMENTATION PAGE				<i>Form Approved</i> <i>OMB No. 0704-0188</i>	
<small>The public reporting burden for this collection of information is estimated to average 1 hour per response, including the time for reviewing instructions, searching existing data sources, gathering and maintaining the data needed, and completing and reviewing the collection of information. Send comments regarding this burden estimate or any other aspect of this collection of information, including suggestions for reducing the burden, to the Department of Defense, Executive Services and Communications Directorate (0704-0188). Respondents should be aware that notwithstanding any other provision of law, no person shall be subject to any penalty for failing to comply with a collection of information if it does not display a currently valid OMB control number.</small>					
PLEASE DO NOT RETURN YOUR FORM TO THE ABOVE ORGANIZATION.					
1. REPORT DATE (DD-MM-YYYY) November 2009		2. REPORT TYPE Final		3. DATES COVERED (From - To)	
4. TITLE AND SUBTITLE Final Report of the Shock and Vibration Test of the Composite High Mobility Multipurpose Wheeled Vehicle (HMMWV) Transmission Containe				5a. CONTRACT NUMBER	
				5b. GRANT NUMBER	
				5c. PROGRAM ELEMENT NUMBER	
6. AUTHOR(S) Joseph Rybak				5d. PROJECT NUMBER 2009-DT-ATC-ARLSP-E4867	
				5e. TASK NUMBER	
				5f. WORK UNIT NUMBER	
7. PERFORMING ORGANIZATION NAME(S) AND ADDRESS(ES) Commander U.S. Army Aberdeen Test Center ATTN: TEDT-AT-WFE Aberdeen Proving Ground, MD 21005-5059				8. PERFORMING ORGANIZATION REPORT NUMBER ATC-10144	
9. SPONSORING/MONITORING AGENCY NAME(S) AND ADDRESS(ES) U.S. Army Research Laboratory Aberdeen Proving Ground, MD 21005				10. SPONSOR/MONITOR'S ACRONYM(S) ARL	
				11. SPONSOR/MONITOR'S REPORT NUMBER(S) Same as Item 8	
12. DISTRIBUTION/AVAILABILITY STATEMENT Distribution limited to U.S. Government Agencies only; Test and Evaluation; November 2009. Other requests for this document must be referred to U.S. Army Research Laboratory, ATTN: RDRL-WMM-C.					
13. SUPPLEMENTARY NOTES					
14. ABSTRACT The composite high mobility multipurpose wheeled vehicle (HMMWV) transmission containers are two different reusable cases intended for the shipping and storage of HMMWV transmissions. One container was made using a low hazardous air pollutant (HAP) composite resin, while the other container was made using a standard composite resin. Testing was conducted to compare the shock and vibration durability of the two containers.					
15. SUBJECT TERMS					
16. SECURITY CLASSIFICATION OF: a. REPORT Unclassified			17. LIMITATION OF ABSTRACT	18. NUMBER OF PAGES	19a. NAME OF RESPONSIBLE PERSON Joseph Rybak
b. ABSTRACT Unclassified					19b. TELEPHONE NUMBER (Include area code) 410-278-2881
c. THIS PAGE Unclassified					

Reset

TABLE OF CONTENTS

Note: To use the hyperlinks in this report, click on the [blue, underlined text](#). To return to the previous position, click on the Previous Page View arrow available in the Page Navigation section of the toolbar.

PAGE

SECTION 1. EXECUTIVE DIGEST

1.1	SYSTEM DESCRIPTION	1-1
1.2	SUMMARY	1-1

SECTION 2. SUBTESTS

2.1	INITIAL INSPECTION	2.1-1
2.2	SHOCK AND VIBRATION	2.2-1
2.3	FINAL INSPECTION	2.3-1

SECTION 3. APPENDIXES

A	TEST CRITERIA	A - 1
B	TEST DATA	B - 1
C	REFERENCES	C - 1
D	ABBREVIATIONS	D - 1
E	DISTRIBUTION LIST	E - 1

SECTION 1. EXECUTIVE DIGEST

1.1 SYSTEM DESCRIPTION

The composite high mobility multipurpose wheeled vehicle (HMMWV) transmission containers (fig. 1-1) are two different reusable cases intended for the shipping and storage of HMMWV transmissions, and were designed by the University of Delaware Center for Composite Materials in conjunction with the U.S. Army Research Laboratory (ARL). One container was made using a low hazardous air pollutant (HAP) composite resin, while the other container was made using a standard composite resin. ARL requested the University of Delaware Center for Composite Materials evaluate and compare the durability of the two cases for potential military use.



Figure 1-1. Composite HMMWV transmission container.

1.2 SUMMARY

a. Test Authority. On 10 August 2009, U.S. Army Developmental Test Command (DTC) authorized U.S. Army Aberdeen Test Center (ATC), Aberdeen Proving Ground (APG), Maryland, to plan, conduct, and report a comparison shock and vibration test of the two composite HMMWV transmission containers. This was done through the establishment of a U.S. Army Test and Evaluation Command (ATEC) project (App C, [ref 1](#)).

b. Test Concept.

(1) ARL provided two different composite HMMWV transmission containers, one low HAP resin case and one standard resin case, to ATC for durability comparison.

(2) ATC provided the facilities, prime movers, and all personnel necessary for testing.

- c. A summary of the test results is presented in Table 1-1.

TABLE 1-1. SUMMARY OF RESULTS

SUBTEST	COMPLIANCE	REMARKS/ANALYSIS
Initial Inspection (para 2.1)	Met	Both containers were supplied complete, damage free, functional, and ready for planned testing.
Shock and Vibration (para 2.2)	Met	The composite HMMWV transmission containers could withstand shock and vibration testing without damage or permanent deformation; however, the wooden feet mounted on the bottom of each case split and separated as a result of testing.
Final Inspection (para 2.3)	Met	All equipment received was accounted and condition documented prior to its return to test sponsor.

SECTION 2. SUBTESTS

2.1 INITIAL INSPECTION

2.1.1 Objective

The objective of this test was to ensure that the composite HMMWV transmission containers were complete, undamaged, and mission ready prior to testing.

2.1.2 Criterion Compliance and Data Analysis

TABLE 2.1-1. CRITERION COMPLIANCE AND DATA ANALYSIS

CRITERION		REMARKS/ANALYSIS
APP A, ITEM NO.	COMPLIANCE	
1 – Initial Inspection	Met	Both the low HAP resin container and the standard resin container were in serviceable condition upon arrival.

2.1.3 Test Procedures and Findings

a. Characteristic photographs of each composite HMMWV transmission container is provided in Appendix B, [Figures B-2.1-1 and B-2.1-2](#).

b. The system was inventoried. All components required for operation were on-hand and serviceable. The results of the inventory are presented in [Table B-2.1-1](#).

c. All components were weighed on a calibrated platform scale ([table B-2.1-2](#)). The weight data are presented in [Table B-2.1-3](#). The weight of the standard resin composite container versus the low HAP resin composite container differed by 2.3 percent.

d. Each unit was visually inspected and there were no shipping or handling damages.

e. A representative payload was provided in place of an actual HMMWV transmission for use in testing. The payload was secured in the container using eight 3/8-in. fasteners ([fig. B-2.1-3](#)). The payload consisted of a steel plate welded to two lengths of steel box tubing. There were drilled holes in the tubing to accept the 3/8-in. studs protruding through the bottom of the case. Representative photographs of the fastening system and payload are shown in [Figures B-2.1-4 and B-2.1-5](#).

2.2 SHOCK AND VIBRATION

2.2.1 Objective

The objective of this test was to determine if each of the composite HMMWV transmission containers were able to withstand the impact forces encountered during shipment without visible damage.

2.2.2 Criteria Compliance and Analysis

TABLE 2.2-1. CRITERIA COMPLIANCE AND DATA ANALYSIS

CRITERION		REMARKS
APP A, ITEM NO.	COMPLIANCE	
2 – Vibration Endurance	Met	Both composite HMMWV transmission containers could withstand endurance vibration testing at their resonant frequency without damage or permanent deformation, visible signs of structural damage, misalignment, or any other irregularities.
3 – Loose Cargo Vibration	Met	The composite HMMWV transmission containers did not suffer any damage or permanent deformation, visible signs of structural damage or misalignment; however, the wooden feet mounted on the bottom of each case split and separated as a result of testing.

2.2.3 Test Procedure and Findings

a. General. Test procedures were derived from MIL-STD-810G ([ref 2](#)) and A-A-52486 ([ref 3](#)). Exploratory vibration testing was conducted to determine any resonant frequencies of the composite HMMWV transmission containers.

(1) Endurance testing subjected the containers to vibration at their most prominent resonant frequency.

(2) Loose cargo testing simulated service conditions for when the containers would be transported by vehicle.

(3) All vibration testing was completed with a representative weight installed in each container. The payload was secured in accordance with the Operator's Manual (OM) and with guidance from on-site customer representatives.

b. Instrumentation. Each payload was instrumented with one triaxial accelerometer to determine any resonant frequencies. The accelerometer location is shown in [Figure B-2.2-1](#). Unholtz-Dickie TA460W400 shaker-amplifier systems with 178-kN (40,000-lb. force) exciters were used for all testing. Control of these systems was accomplished using Unholtz-Dickie VWIN-II Vibration Test Systems ([fig. B-2.2-2](#)). One calibrated control accelerometer (± 3.5 -percent charge sensitivity) was used and positioned near the center of the adapter plate. The calibration information for all of the items used for this test is listed in Table 2.2-2.

TABLE 2.2-2. CALIBRATION INFORMATION

ITEM	MANUFACTURER	MODEL NUMBER	SERIAL NUMBER	CALIBRATION DUE DATE
Accelerometer	Endevco	7704-50	FK05	16-Mar-2011
Accelerometer	PCB	356A71	89821	14 Feb 2010
Charge amplifier	Unholtz-Dickie	122P	9717	22 Aug 2010
Charge amplifier	Unholtz-Dickie	122P	10021	16 Sep 2010
Charge amplifier	Unholtz-Dickie	122P	10019	22 Aug 2010
Charge amplifier	Unholtz-Dickie	122P	9705	12 Dec 2009
Vibration controller	Unholtz-Dickie	VWIN-II	119084	22 Oct 2009

c. Exploratory Vibration and Endurance.

(1) Exploratory vibration and fatigue testing was conducted in accordance with A-A-52486, paragraphs 2a (resonance vibration frequency) and 2b (resonance vibration fatigue). The containers were tested one at a time.

(2) Each composite HMMWV transmission container was secured on the vibration table using four 2-in. ratcheting tie-down straps. The standard resin container was secured using the four D-rings on the lower portion of the container, as shown in [Figures B-2.2-3 through B-2.2-6](#). In testing the low HAP resin container, four straps were used over the top of the container to secure it, as shown in [Figures B-2.2-7 through B-2.2-10](#). When securing the low HAP resin container to the table, one of the four D-rings separated from the clasp as a result of tension on the strap ([fig. B-2.2-11](#)). The D-rings on the lower portion of the container are too low to be useful as a good tie-down provision. Locating the D-rings on the lid of the case in the future is recommended.

(3) The table was vibrated at frequencies from 2 to 60 Hz, at a table vibratory double amplitude of 0.06 ± 0.002 in. in the "z" axis (vertical) only. The change in frequency was made in discrete frequency intervals of 1 Hz, and each frequency was maintained for approximately 15 seconds. Plots of the displacement versus frequency for the standard resin and low HAP resin containers are presented in [Figures B-2.2-12 and B-2.2-13](#), respectively. Off axis response was negligible.

(4) After the completion of the discrete frequency test, the ratio of the response channel in the vertical axis to the control channel was examined for each container ([fig. B-2.2-14 and B-2.2-15](#)). For the standard resin container, 20 Hz was selected as the frequency at which the fatigue test would be conducted. For the low HAP resin container, 29 Hz was the frequency selected. The difference in resonant frequency response between the two cases was most likely attributable to the tie-down method.

(5) The payloaded case was vibrated for 21 minutes at the frequency selected in the previous paragraph. Fatigue test profiles are presented in [Figures B-2.2-16 and B-2.2-17](#). After the conclusion of testing, the composite HMMWV transmission containers were inspected to determine if any physical damage, permanent deformation, compromise, buckling, delamination, seal separation, or structural failure of any part had occurred. There was no apparent damage to either container as a result of the vibration test.

d. Shock Test.

(1) Shock testing was conducted in accordance with MIL-STD-810G, Test Method 514.5, Annex C, para 2.2, Loose Cargo. A separate test was conducted on each of the two composite HMMWV transmission containers.

(2) Each composite HMMWV transmission case was positioned on the steel bed of the LAB-12000 package tester. Wooden retaining fence sections were placed around the perimeter of the container to prevent it from falling off the table. The fence sections were positioned to provide a free space of approximately 1 in. on all sides and ends of the case. The setup is shown in [Figure B-2.2-18 and B-2.2-19](#).

(3) The package tester was operated, shafts in phase, in a circular motion with a constant displacement of 1 in., double amplitude (DA), at a speed of 300 rpm, producing a table acceleration of 1.3 g. The package tester was operated in one 20-minute increment. The laboratory test represented 150 mi of loose cargo transport in a tactical wheeled vehicle.

(4) At the conclusion of testing, the composite HMMWV transmission cases were visually inspected to determine if any physical damage, permanent deformation, compromise, buckling, delamination, seal separation, or structural failure of any part had occurred. The visual inspection was successful; however, the wooden feet of both containers split as a result of the loose cargo test ([fig. B-2.2-20 through B-2.2-26](#)). There was no apparent damage to any of the composite material under test.

2.3 FINAL INSPECTION

2.3.1 Objectives

The objective of this test was to account for and to document the condition of the composite HMMWV transmission containers and components at the completion of testing.

2.3.2 Criterion Compliance and Data Analysis

TABLE 2.3-1. CRITERION COMPLIANCE AND DATA ANALYSIS

CRITERION		REMARKS/ANALYSIS
APP A, ITEM NO.	COMPLIANCE	
4 - Final inspection	Met	The equipment received was accounted for prior to shipment.

2.3.3 Test Procedures and Findings

- a. All test items and supporting equipment were inventoried, and all were accounted for.
- b. A visual inspection was conducted on each composite HMMWV transmission container to determine if physical damage, permanent deformation, delamination, seal separation, buckling of the cargo system, or structural failure in any part had occurred. No previously unreported damage was found. The conditions of each container post-test are shown in [Figures B-2.3-1 through B-2.3-16](#).
- c. All test items and support equipment were returned to the manufacturer.

SECTION 3. APPENDIXES
APPENDIX A. TEST CRITERIA

ITEM	APPLICABLE SOURCE	TEST CRITERION	SUBTEST	REMARKS
1	Test Agency devised, DTC approved	The composite HMMWV transmission case must be in serviceable condition upon arrival to ATC without damage or defects that inhibit test initiation.	2.1	Met. Both the low HAP container and the standard resin container were in serviceable condition upon arrival.
2	Test Agency devised, DTC approved	The composite HMMWV transmission case must be able to withstand endurance vibration testing at its resonant frequency without damage or permanent deformation. The composite HMMWV transmission case must show no visible signs of structural damage, misalignment or any other irregularities.	2.2	Met. Both composite HMMWV transmission containers could withstand endurance vibration testing at their resonant frequency without damage or permanent deformation, visible signs of structural damage, misalignment, or any other irregularities.
3	Test Agency devised, DTC approved	The composite HMMWV transmission case must be able to withstand the impact forces encountered in loose cargo vibration testing without damage or permanent deformation. The composite HMMWV transmission case must show no visible signs of structural damage, misalignment or any other irregularities.	2.2	Met. The composite HMMWV transmission containers did not suffer any damage or permanent deformation, visible signs of structural damage or misalignment; however, the wooden feet mounted on the bottom of each case split and separated as a result of testing.
4	Test Agency devised, DTC approved	All equipment received shall be accounted for prior to its return to test sponsor.	2.3	Met. The equipment received was accounted for prior to shipment.

APPENDIX B. TEST DATA

	<u>PAGE</u>
1 <u>INITIAL INSPECTION</u>	B-2.1-1
2 <u>SHOCK AND VIBRATION</u>	B-2.2-1
3 <u>FINAL INSPECTION</u>	B-2.3-1



Figure B-2.1-1. Composite HMMWV transmission case: standard resin (note light color).



Figure B-2.1-2. Composite HMMWV transmission case: low HAP resin (note dark color).

TABLE B-2.1-1. INVENTORY

QUANTITY	ITEM
1	Standard Composite Resin HMMWV Transmission Case
1	Low HAP Composite Resin HMMWV Transmission Case
1	Payload

TABLE B-2.1-2. INSTRUMENTATION

ITEM	MANUFACTURER	NUMBER		CALIBRATION DUE DATE, 2010	PERIOD, yr
		MODEL	SERIAL		
Scale	Ohaus Corporation	CD-11	0067446-6MF	15 June	1

TABLE B-2.1-3. WEIGHTS

ITEM	WEIGHT (lb)
Standard Composite Resin HMMWV Transmission Case (empty)	126.90
Low HAP Composite Resin HMMWV Transmission Case (empty)	129.90
Payload	175.45



Figure B-2.1-3. Payload installed in composite HMMWV transmission case.



Figure B-2.1-4. Composite HMMWV transmission case, payload mounting system.

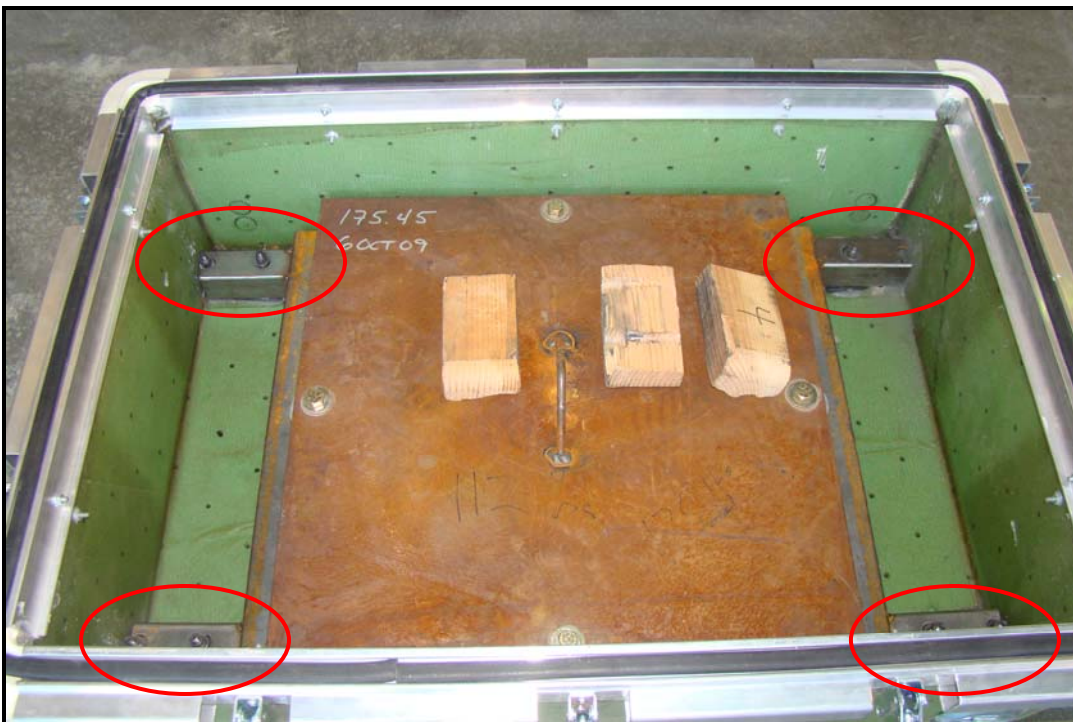


Figure B-2.1-5. Composite HMMWV transmission case, mounting hardware (eight total).



Figure B-2.2-1. Response accelerometer location inside container.

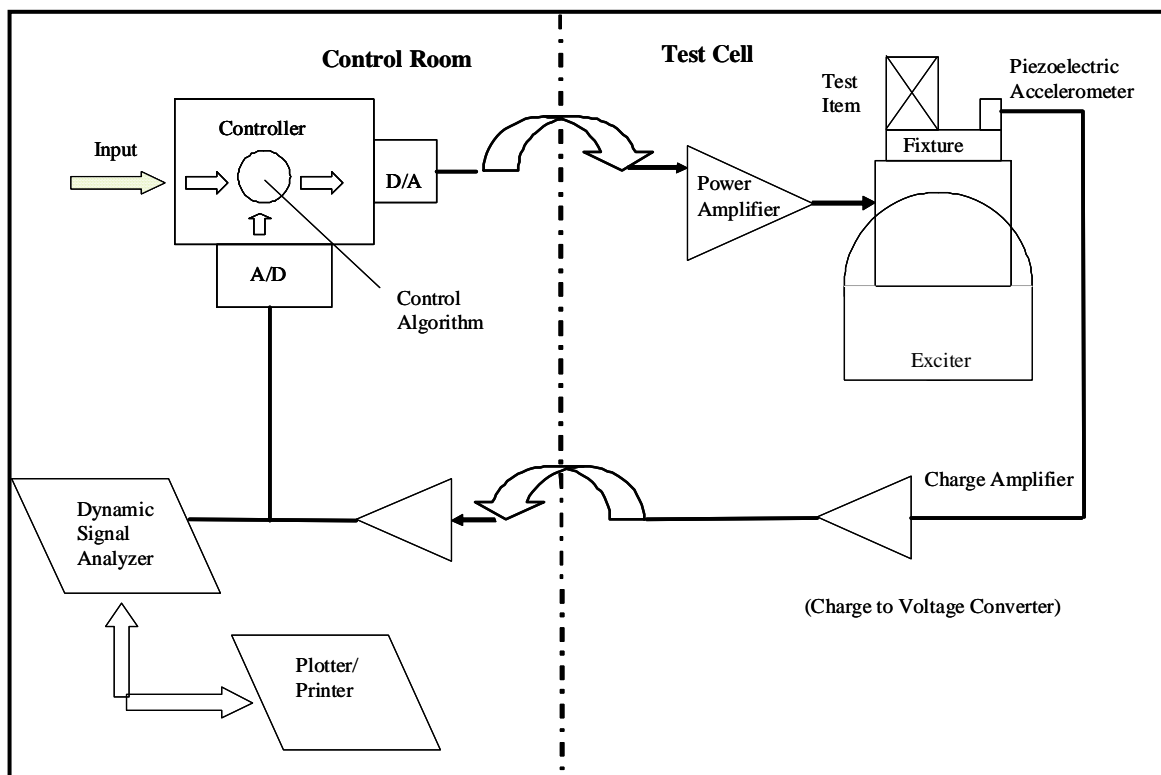


Figure B-2.2-2. Simplified block diagram of Vibration Control System.



Figure B-2.2-3. Vibration test setup (front), standard resin container.



Figure B-2.2-4. Vibration test setup (right), standard resin container.



Figure B-2.2-5. Vibration test setup (left), standard resin container.



Figure B-2.2-6. Vibration test setup (rear), standard resin container.

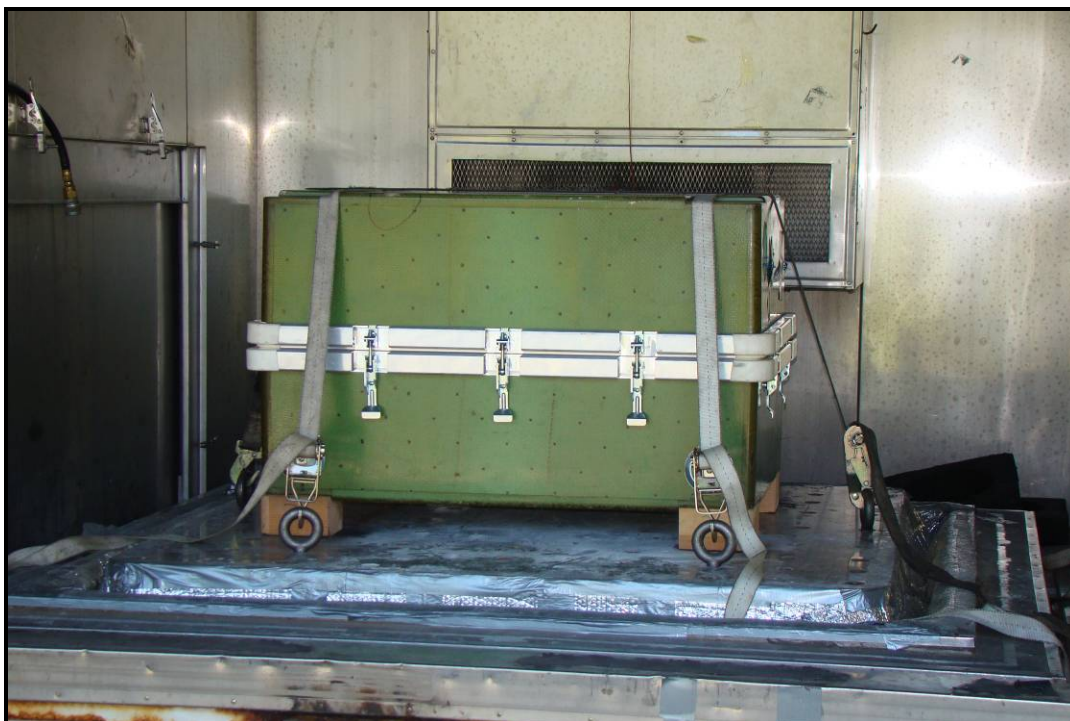


Figure B-2.2-7. Vibration test setup (front), low HAP resin container.



Figure B-2.2-8. Vibration test setup (right), low HAP resin container.



Figure B-2.2-9. Vibration test setup (left), low HAP resin container.



Figure B-2.2-10. Vibration test setup (rear), low HAP resin container.

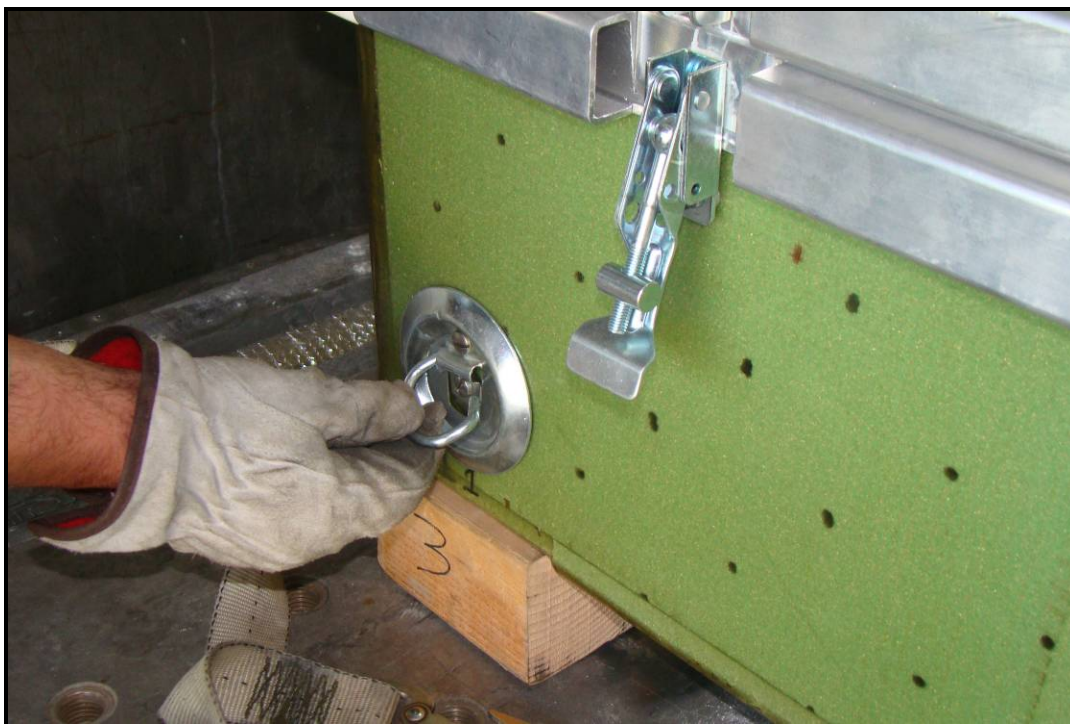


Figure B-2.2-11. D-Ring separated from clasp, low HAP resin container.

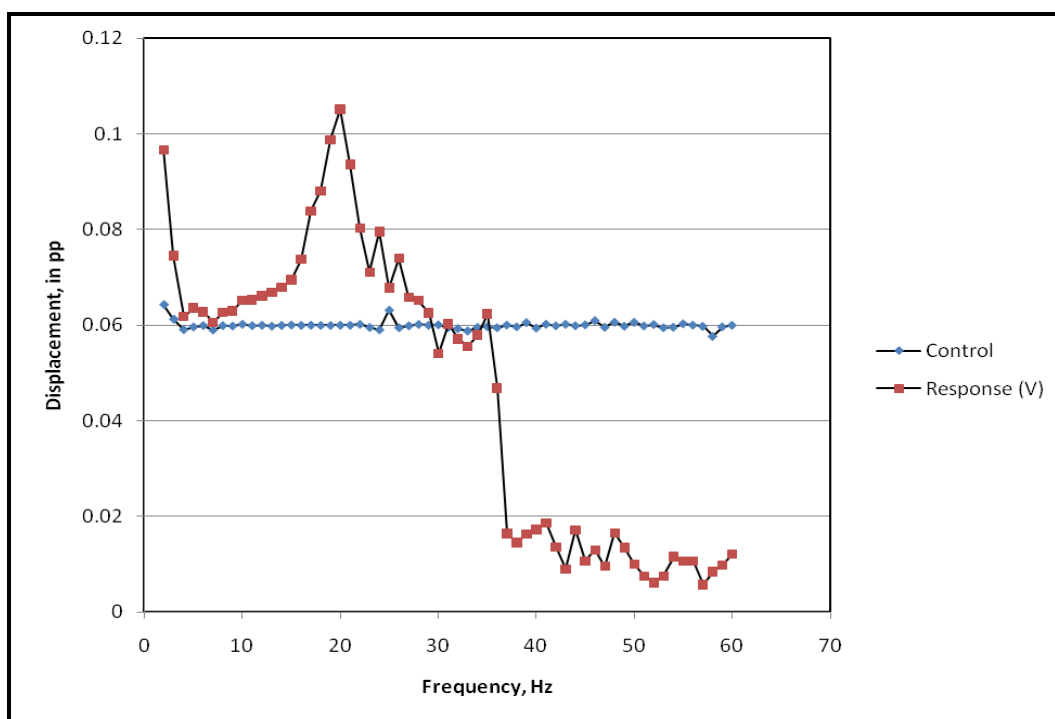


Figure B-2.2-12. Exploratory vibration results, standard resin container.

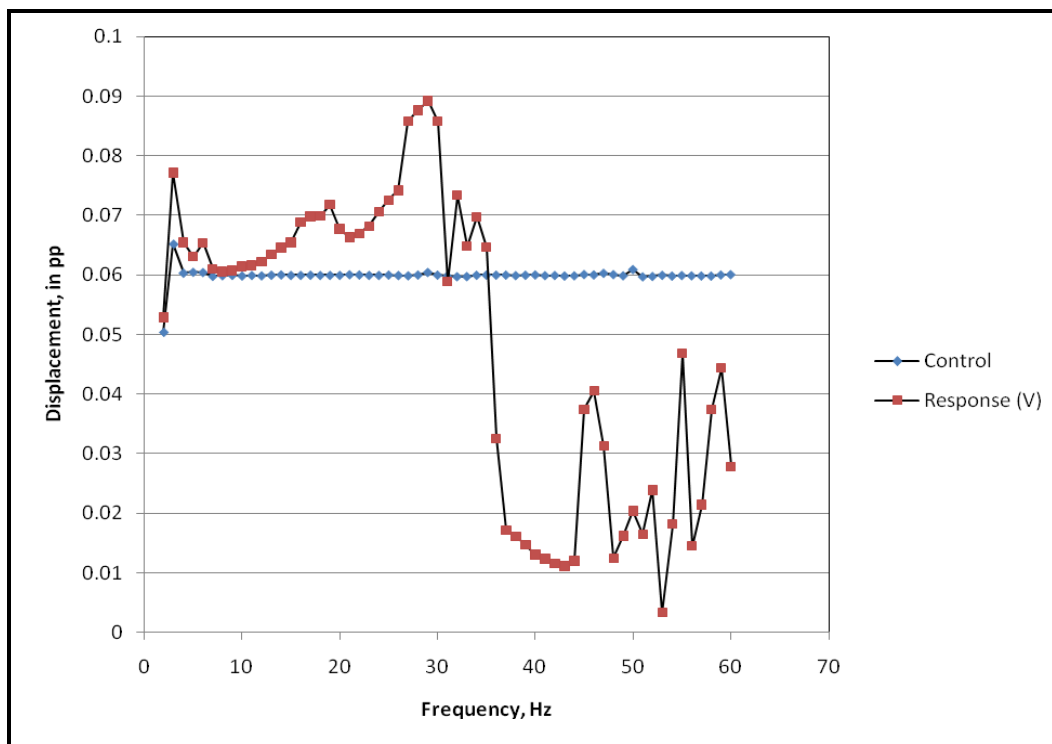


Figure B-2.2-13. Exploratory vibration results, low HAP resin container.

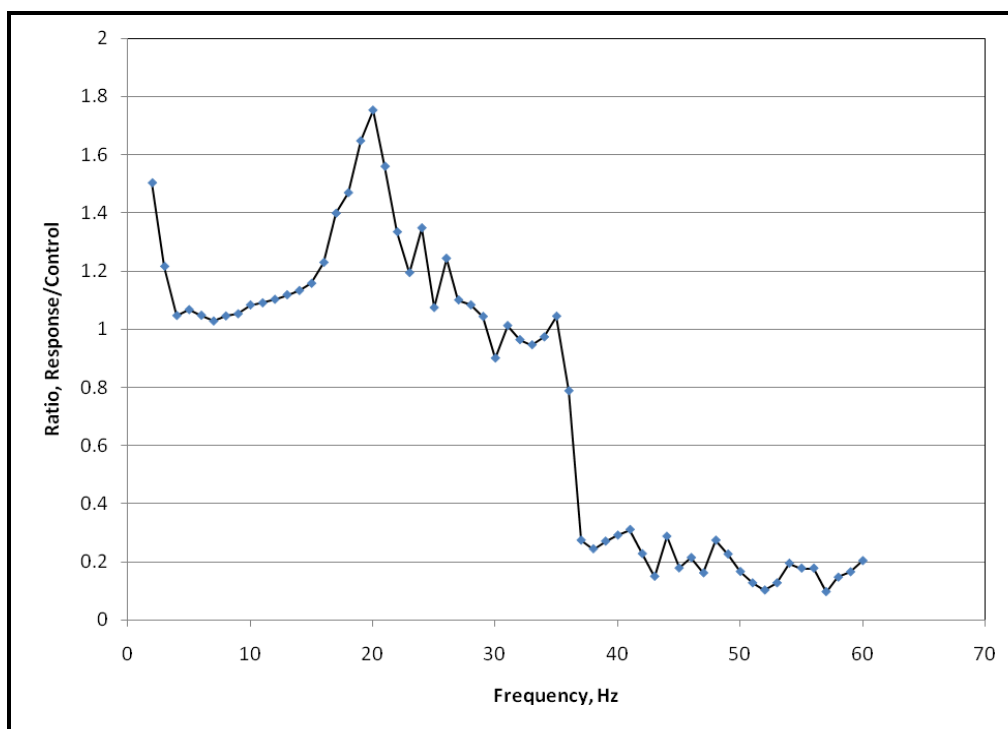


Figure B-2.2-14. Control/response ratio, standard resin container.

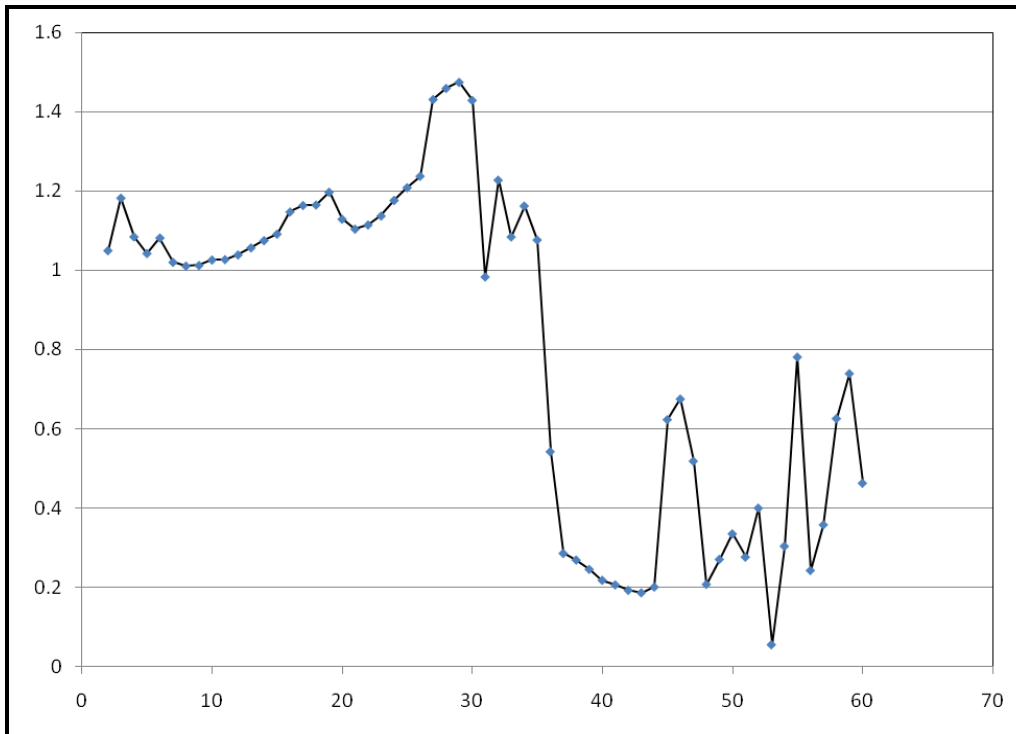


Figure B-2.2-15. Control/response ratio, low HAP resin container.

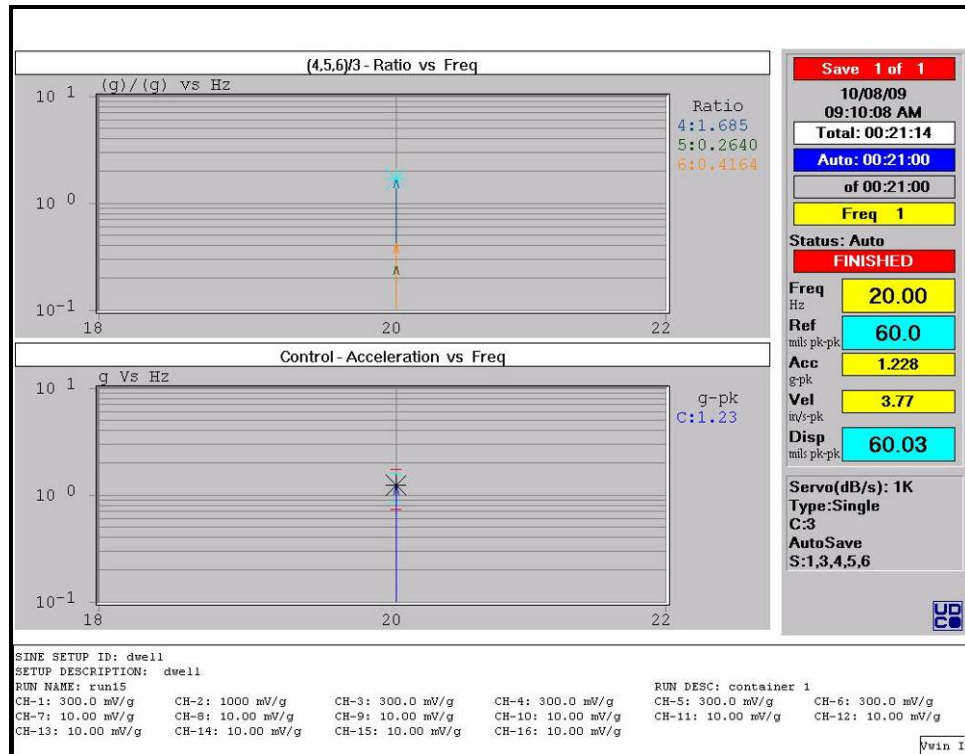


Figure B-2.2-16. Fatigue profile, standard resin container.

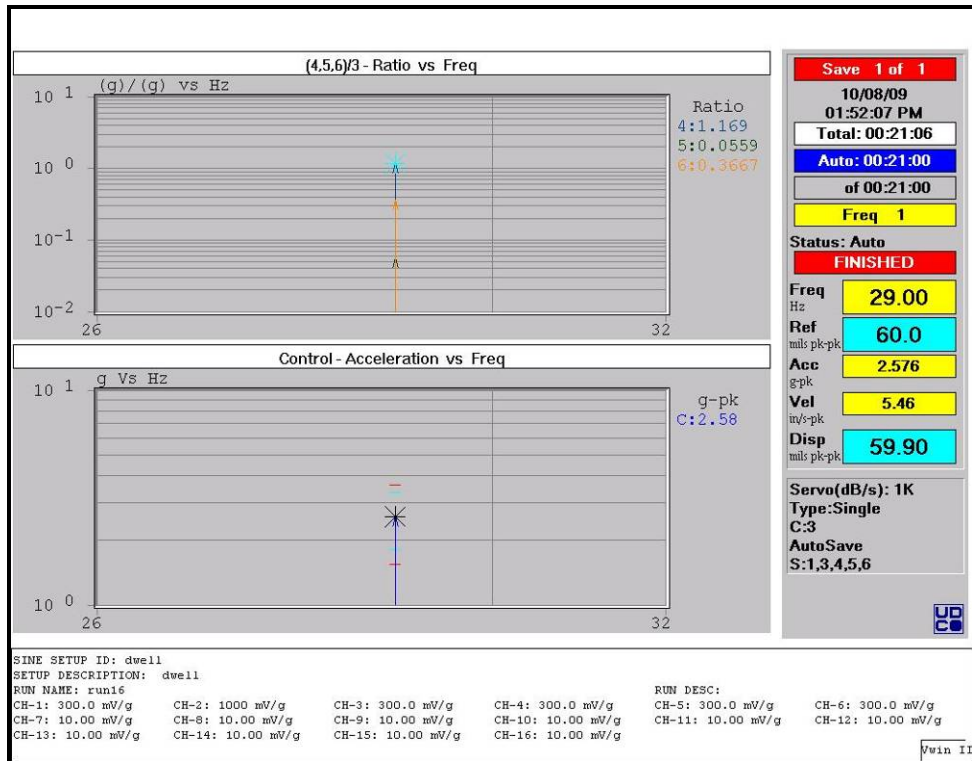


Figure B-2.2-17. Fatigue profile, low HAP resin container.



Figure B-2.2-18. Shock test bed.



Figure B-2.2-19. Loose Cargo test setup.



Figure B-2.2-20. Split wooden blocks following Loose Cargo test, standard resin container.



Figure B-2.2-21. Split wooden blocks following Loose Cargo test, standard resin container.



Figure B-2.2-22. Split wooden blocks following Loose Cargo test, standard resin container.



Figure B-2.2-23. Split wooden blocks following Loose Cargo test, low HAP resin container.



Figure B-2.2-24. Bottom corner following Loose Cargo test, container 2.



Figure B-2.2-25. Bottom corner following Loose Cargo test, container 2.



Figure B-2.2-26. Split wooden blocks following Loose Cargo test, low HAP resin container.



Figure B-2.3-1. Composite HMMWV transmission container: standard resin (front).



Figure B-2.3-2. Composite HMMWV transmission container: standard resin (right).



Figure B-2.3-3. Composite HMMWV transmission container: standard resin (left).



Figure B-2.3-4. Composite HMMWV transmission container: standard resin (rear).



Figure B-2.3-5. Composite HMMWV transmission container: standard resin (top).



Figure B-2.3-6. Composite HMMWV transmission container: standard resin (bottom).



Figure B-2.3-7. Composite HMMWV transmission container: standard resin (inside lid).

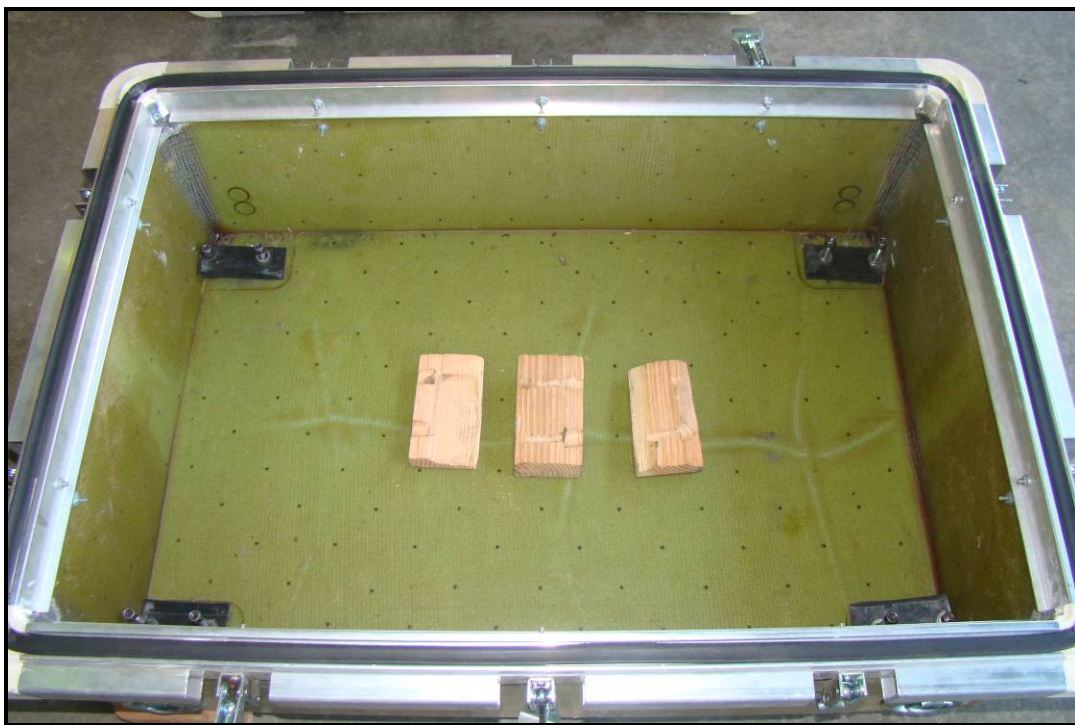


Figure B-2.3-8. Composite HMMWV transmission container: standard resin (inside bottom).



Figure B-2.3-9. Composite HMMWV transmission container: low HAP resin (front).



Figure B-2.3-10. Composite HMMWV transmission container: low HAP resin (right).



Figure B-2.3-11. Composite HMMWV transmission container: low HAP resin (left).



Figure B-2.3-12. Composite HMMWV transmission container: low HAP resin (rear).



Figure B-2.3-13. Composite HMMWV transmission container: low HAP resin (top).



Figure B-2.3-14. Composite HMMWV transmission container: low HAP resin (bottom).



Figure B-2.3-15. Composite HMMWV transmission container: low HAP resin (inside lid).



Figure B-2.3-16. Composite HMMWV transmission container: low HAP resin (inside bottom).

APPENDIX C. REFERENCES

1. ADSS project established, ATEC, TEDT-TMT, 10 August 2009, subject: Composite HMMWV Transmission Shock and Vibration Testing, ATEC Project No. 2009-DT-ATC-ARLSP-E4867
2. MIL-STD-810G, Department of Defense Test Method Standard Environmental Engineering Considerations and Laboratory Tests, 31 October 2008.
3. A-A-52486, Commercial Item Description; Mount, Shipping Container, Resilient: Shock and Vibration Testing, 18 January 1994

APPENDIX D. ABBREVIATIONS

APG	= Aberdeen Proving Ground
ARL	= U.S. Army Research Laboratory
ATC	= Aberdeen Test Center.
ATEC	= U.S. Army Test and Evaluation Command
DTC	= Developmental Test Command
HAP	= hazardous air pollutant
HMMWV	= high mobility multipurpose wheeled vehicle
OM	= Operator's Manual

APPENDIX E. DISTRIBUTION LIST

Note: A copy of the report will be posted on the Versatile Information Systems Integrated On-Line (VISION) Digital Library (VDL), <https://vdlis.atc.army.mil>. In addition, CD-ROM/electronic copies only will be sent to the recipients listed below.

<u>Addressee</u>	<u>Test Plans</u>	<u>Final Reports</u>
Commander U.S. Army Developmental Test Command ATTN: TEDT-TMT (Mr. Gregory Brewer) Aberdeen Proving Ground, MD 21005-5055	1	1
Department of the Army U.S. Army Research Laboratory ATTN: RDRL-WMM-C (John La Scala, Ph.D) Building 4600 Aberdeen Proving Ground, MD 21005	1	1
Nicholas Shevchenko Center for Composite Materials University of Delaware Newark, DE 19716	1	1
Commander U.S. Army Aberdeen Test Center ATTN: TEDT-AT-WFE (Mr. Joseph Rybak) TEDT-AT-PO/WFE (Kristina Kriss) Aberdeen Proving Ground, MD 21005-5059	1 1	1 1

Secondary distribution will be controlled by U.S. Army Research Laboratory,
ATTN: RDRL-WMM-C.

INTENTIONALLY LEFT BLANK.

Appendix C. Resin Formulation

This appendix appears in its original form, without editorial change.

Appendix C

Resin Formulation

Investigation of Sensitivity of VE Resins to Oxygen in Air

1. INTRODUCTION

This report summarizes the results achieved during a period from Aug.15 to Oct.31. The most important observation is that CN151, which is used in old formulation, is more sensitive to the oxygen in air. The direct consequence of this behavior reflected in ultimate performance of resin is illustrated in this study. Accordingly, the replacement, which is RDX26939, was investigated regarding to its cure behavior, performance. The results show that RDX 26939 is a successful replacement of CN151 in terms of its fast cure and high Tg performance. Correspondingly; the formulations providing a range of Tgs were designed with their processing properties examined as well. Besides these, toughening study was commenced and preliminary results were obtained.

2. RESULTS

2.1 Cure behavior of monomers

Cure behavior of Der470HT-400 was investigated in terms of its cure time and final Tg, along with other resins as VE 828 (synthesized in lab), CN151, RDX 26939 with 33% styrene respectively. The results are shown in Figures 1 to 7, and the results are also summarized in Table 1.

2.1.1 Der470HT-400

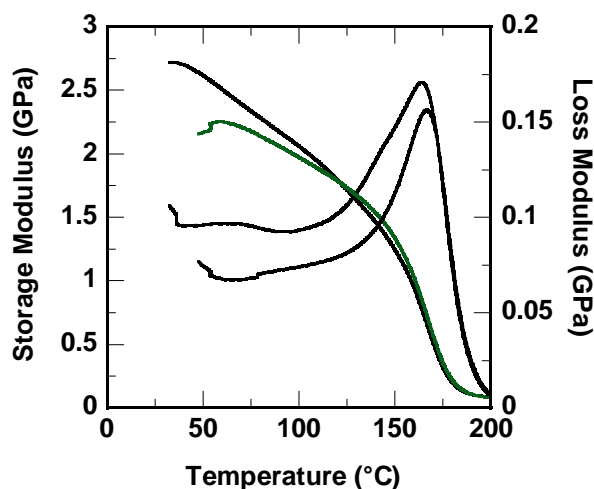


Figure 1 DMA spectra for the commercial Der470HT-400 resin. Tg of 1st run is 164°C, Tg of 2nd run is 167°C. Sample experienced a very fast cure. The cured sample was given DMA test directly.

2.1.2 VE 828 (synthesized in lab) with 33% styrene

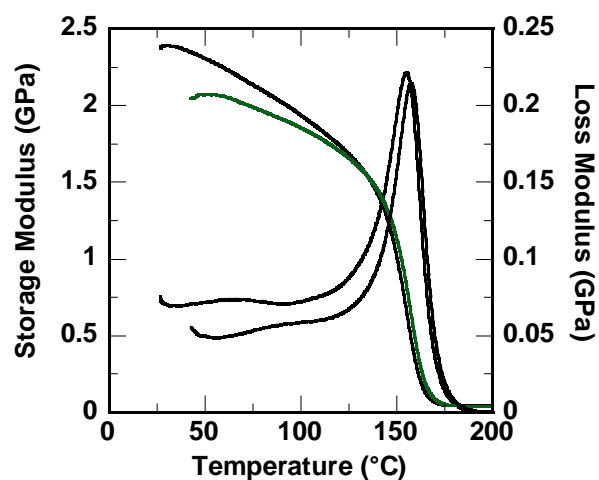


Figure 2 DMA spectra for VE828 (synthesized in lab) with 33% Styrene. Tg of 1st run is 155°C, Tg of 2nd run is 158°C. After room temperature cure for two days, the surface is sticky, and then the sample was put in oven at 90°C for 10 minutes.

2.1.3 CN 151 with 33% styrene

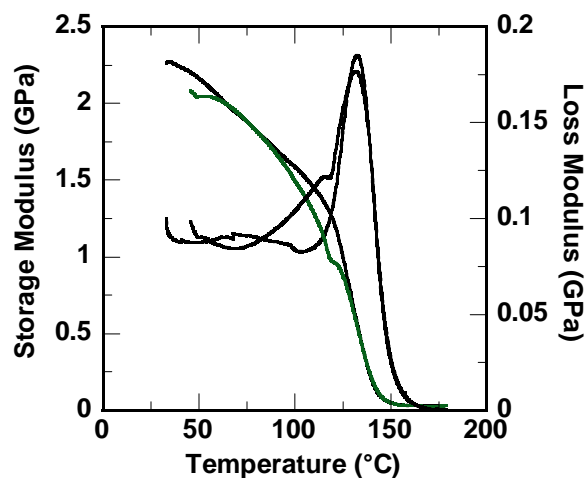


Figure 3 DMA spectra for CN151 with 33% Styrene. Tg of 1st run is 132°C, Tg of 2nd run is 132°C. After room temperature cure for two days, the surface is liquid, after staying in oven at 90°C for 4 hours, the surface is still very viscous. Fully cure indicating by the hardening of surface was realized after several days heating.

2.1.4 CN 151 with 33% styrene cure by different methodology

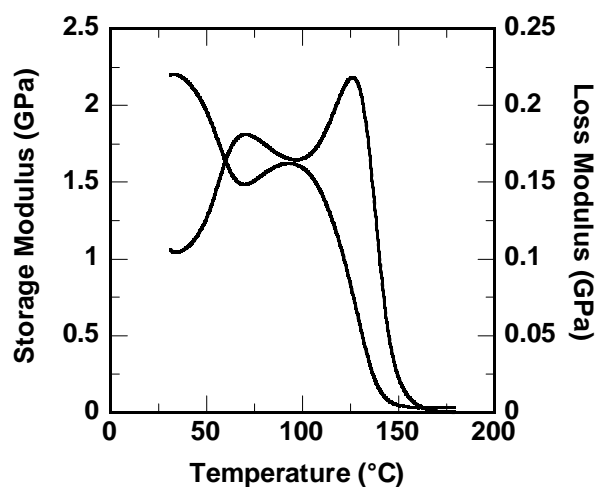


Figure 4 DMA spectra for sample of CN151 with 33% Styrene with different cure history. The first run shows two separate peaks with Tg as 68°C and 126°C respectively. After room temperature cure for 7 days, there exists a layer of liquid in the surface of sample. This liquid layer was wiped out. The residual sample portion was given a DMA scan.

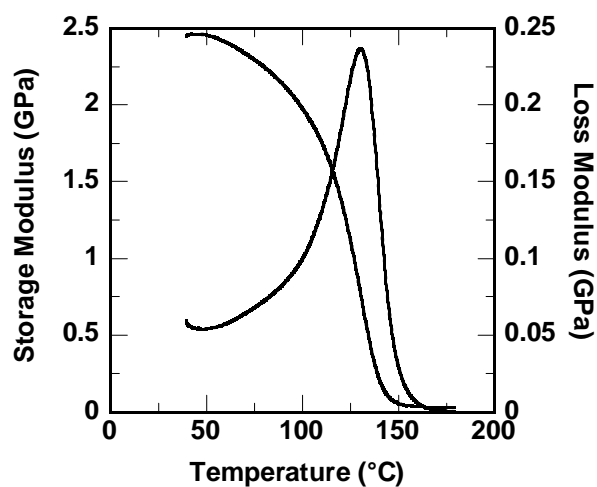


Figure 5 DMA spectra for sample of CN151 with 33% Styrene with different cure history. One Tg peak of 130°C was shown up in the second run, which is slightly lower than the value given in figure 3.

2.1.5 RDX 26939 with 33% St

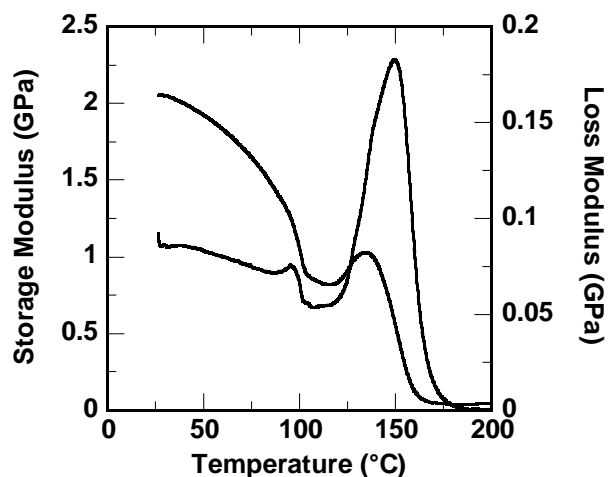


Figure 6 DMA spectrum of sample of RDX 26939 with 33% Styrene. Tg peak of 149°C shows up in the first run. The sample was cured at room temperature. After three days, the surface was still tacky. 10 minutes heating in oven of 90°C was given to sample subsequently.

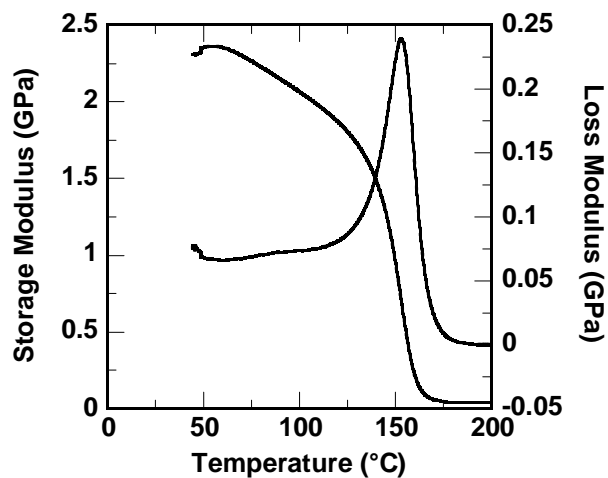


Figure 7 DMA spectrum of sample of RDX 26939 with 33% Styrene. Tg of 153°C shows up in the first run. The sample was cured at room temperature. After three days, the surface was still tacky. 10 minutes heating in oven of 90°C was given to sample subsequently.

Table 1 Cure behavior for different monomers

Resin system	Cure procedure	gel time	Tg 1 st run (°C)	Tg 2 nd run (°C)
Der470HT-400	RT	Very fast	164	167
VE828+33% St	RT(2days)+ 90°C(10minutes)	less fast, sticky surface	155	158
CN151+33% St -1	RT(2days)+ 90°C(several days)	Very slow, viscous surface	132	132
CN151+33% St -2	RT 7days	Very slow, liquid surface	68 126	130
RDX23969+33%St	RT 5days + 90°C(10minutes)	less fast, sticky surface	149	153
CN151	RT(2days)+90°C	slowest	NA	NA

2.2 Cure behavior of resins after replacing CN151 with RDX 26939

The significance of replacing CN151 with RDX 26939 is illustrated in this part of study, as shown in figures from 8 to 15.

2.2.1 FAVE-O resin

1) with CN151

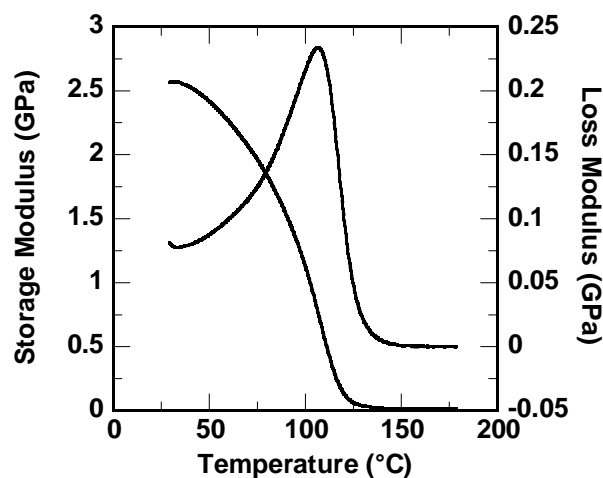


Figure 8 DMA spectrum of sample of FAVE-O (batch 2# received on 8.16.06 from John). In the first run, one single Tg peak of 107°C is shown up. The sample was cured at room temperature. After two days, the surface was sticky. The sticky layer was wiped out by acetone.

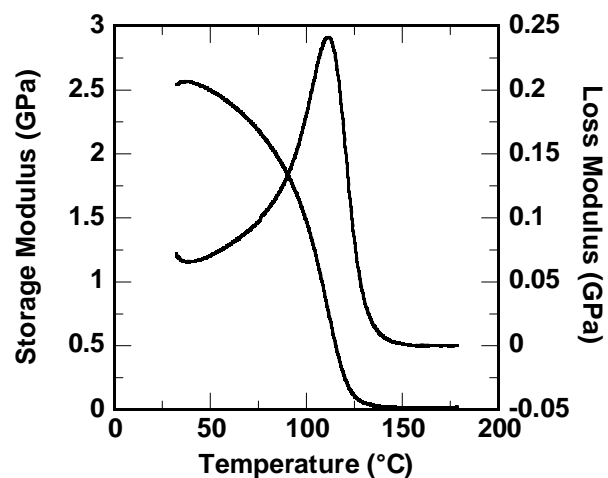


Figure 9 DMA spectrum of sample of FAVE-O (batch 2# received on 8.16.06 from John). In the second run, Tg peak of 111°C is shown up. The sample was cured at room temperature. After two days, the surface was sticky. The sticky layer was wiped out by acetone.

2) with RDX

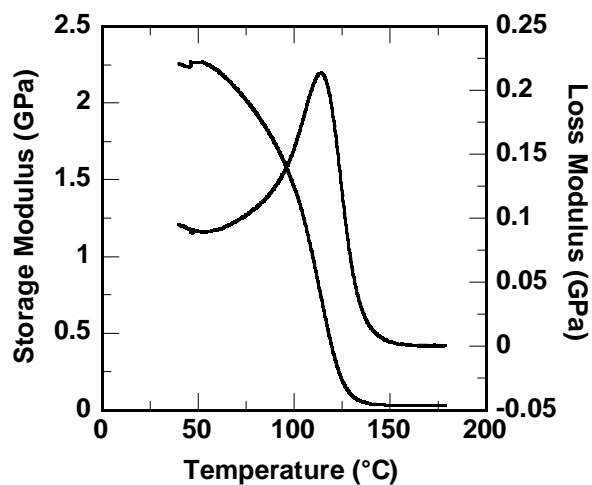


Figure 10 DMA spectrum of sample of FAVE-O with RDX26939 replacing CN151. In the first run, one single Tg peak of 114°C is shown up. The sample was cured at room temperature. After 4 days, the surface was tacky and when touching, could leave the impression of finger, which is a little bit serious than sample of RDX 26939 with 33% Styrene.

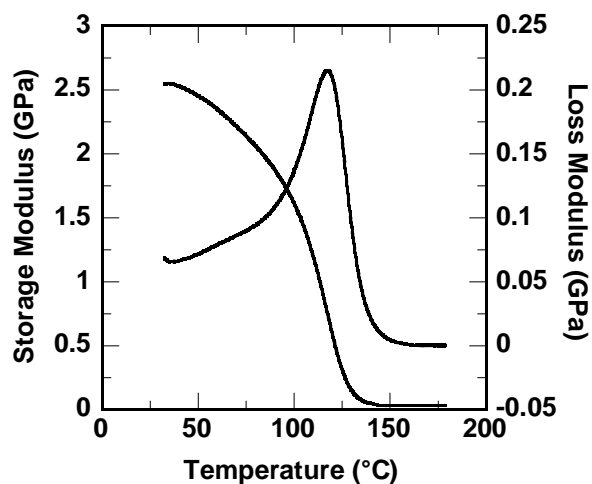


Figure 11 DMA spectrum of sample of FAVE-O with RDX26939 replacing CN151. In the second run, Tg peak of 118°C is shown up, which is 7°C higher than that of FAVE-O with CN151.

2.2.2 Der470 HT-400 formulation with Tg of 147°C

1) with CN151

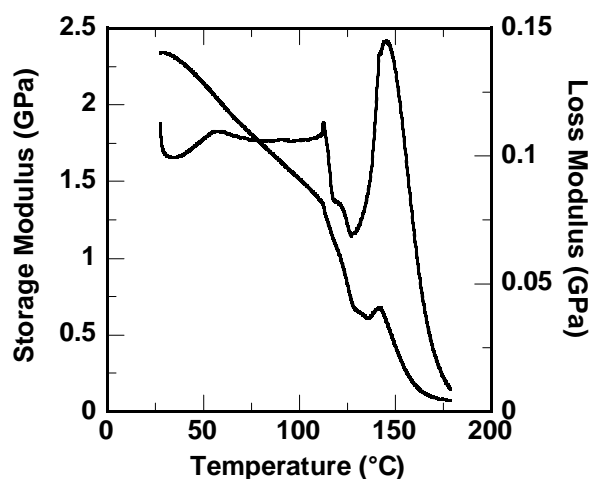


Figure 12 DMA spectrum of sample of Der470HT-400/CN151/MOOct (75.8-14.2-10). In the first run, more like two peaks, with high Tg peak of 145°C given. The sample was cured at room temperature for 24 hours and hard surface was achieved. The hardened sample was used for DMA test directly.

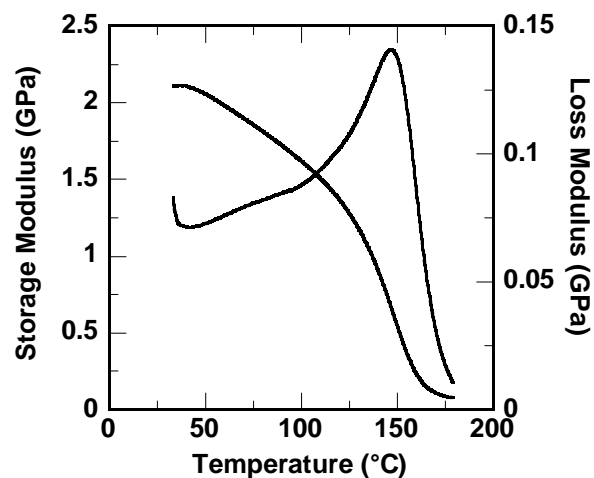


Figure 13 DMA spectrum of sample of Der470HT-400/CN151/MOOct (75.8-14.2-10). In the second run, Tg of 147°C is given.

2) with RDX

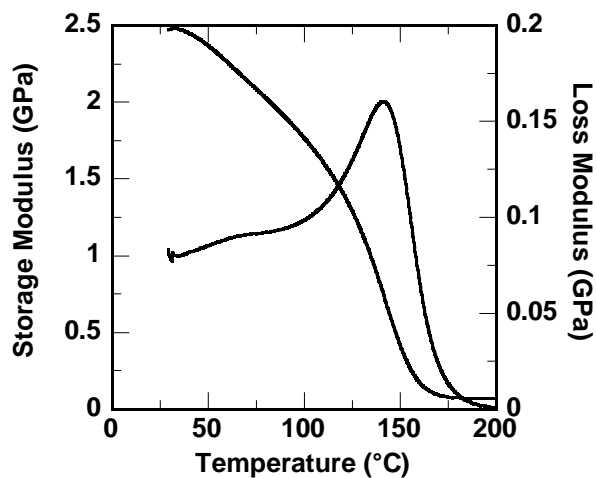


Figure 14 DMA spectrum of sample of Der470HT-400/RDX 26939/MOOct (75.8-14.2-10). In the first run, one single Tg peak of 141°C is given. The sample was cured at room temperature for 24 hours and hard surface was achieved. The hardened sample was used for DMA test directly.

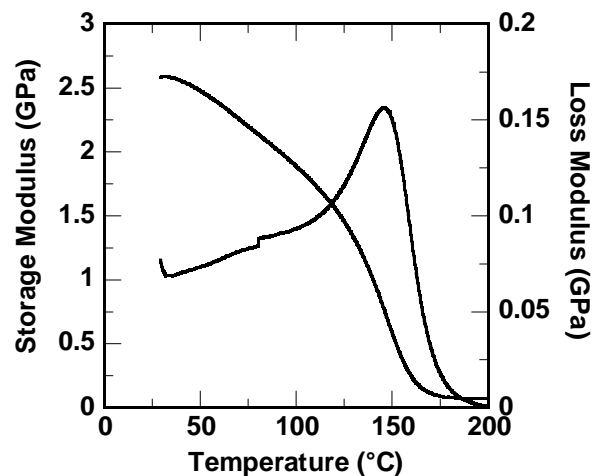


Figure 15 DMA spectrum of sample of Der470HT-400/RDX26939/MOOct (75.8-14.2-10). In the second run, Tg of 146°C is given. The reproducibility of resin is much increased.

Table 2 Cure behavior for different resin systems with RDX and CN151 respectively

Resin system	Cure procedure	gel time	Tg 1 st run (°C)	Tg 2 nd run (°C)
FAVE-O with CN151	RT 2days, remove the sticky surface	slow, sticky surface	107	111
FAVE-O with RDX26939	RT(4days)+ 90°C(1~2minute)	Less fast, a little bit sticky surface	114	118
Der470 HT-400 /CN151/MOOct (75.8-14.2-10)	RT 24 hours	fast, hard surface	145	147
Der470 HT-400 /RDX26939/MOOct (75.8-14.2-10)	RT 24 hours	fast, hard surface	141	146

2.4 Influence of catalyst concentration on cure behavior

The concentration of catalyst used in these systems was doubled in order to eliminate the influence of the oxygen on the cure behavior of resin systems. The results are displayed as figures from 16 to 19.

1) CN151 with 33% St

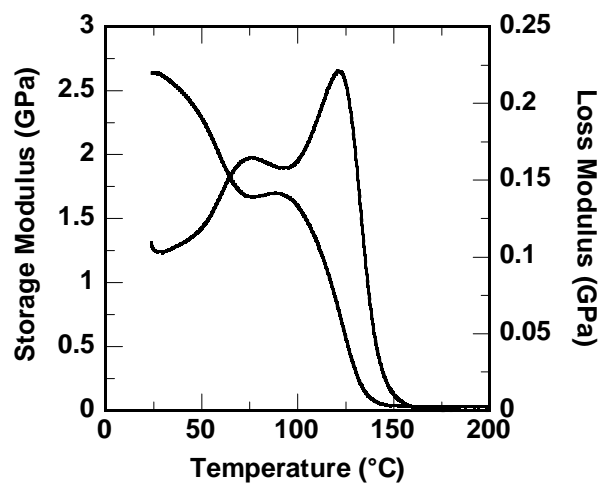


Figure 16 DMA spectra for sample of CN151 with 33% Styrene with double amount of Trignox 239 and Cobolt Naphthenate. The first run shows two separate peaks with Tg as 72°C and 122°C respectively. After room temperature cure for 7 days, the surface is hard.

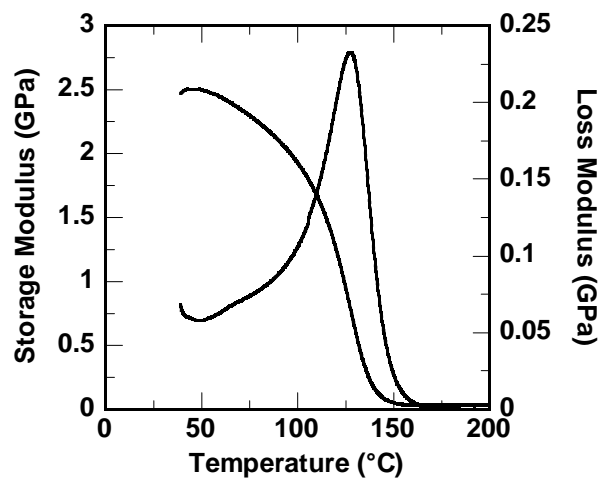


Figure 17 DMA spectra for sample of CN151 with 33% Styrene with double amount of Trignox 239 and Cobolt Naphthenate. The second run gives Tg of 127°C.

2) FAVE-O (batch #2 received 8.16.06 from John)

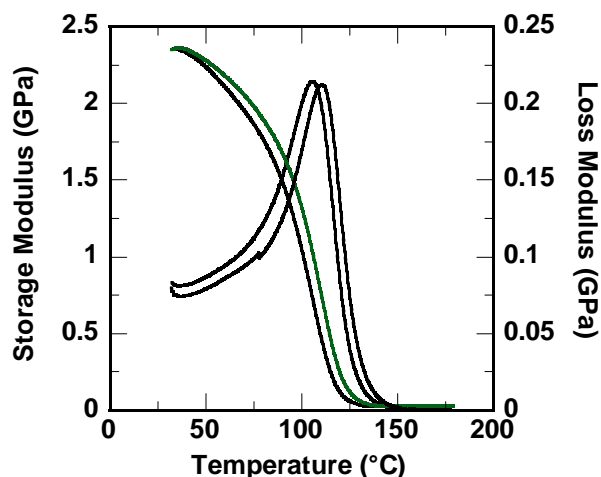


Figure 18 DMA spectrum of sample of FAVE-O (batch 2# received on 8.16.06 from John) cured with double amount of Trignox 239 and Cobolt Naphthenate. Tgs of 105°C and 111°C are assigned to the first run and second run respectively. The sample was cured at room temperature, at beginning, obviously exothermal effect was perceived. After 30 hours cure, the surface is sticky in comparison with the layer of FAVE-O with original amount catalyst, which is still in liquid state. The sticky layer was wiped out by acetone and DMA was then employed.

3) Der 470HT-400/RDX26939/MOOct (Tg of 147°C)

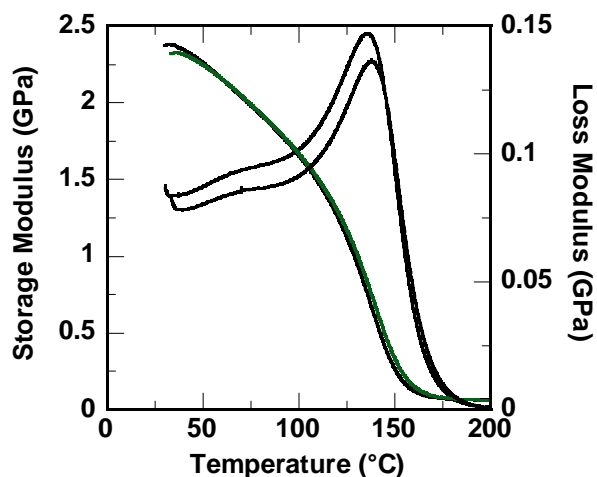


Figure 19 DMA spectrum of sample of Der470HT-400/RDX26939/MOOct (75.8-14.2-10) cured with double amount of Trignox 239 and Cobolt Naphthenate. Tgs of 136°C and 139°C are assigned to the first run and second run respectively. The sample was cured at room temperature, at beginning, obviously exothermal effect was perceived. After 20 hours cure, the sample with hard surface was used for DMA scan.

2.4 Optimum formulation design

This part work includes designing a range of Tgs by varying the weight fraction of the components aiming to detect the optimum formulation that providing Tg of 140°C as well as good processibility with the maximum amount of St replacing by MFA. The results are summarized in Tables from 3 to 6. Theoretical calculation was based on the Fox equation with Tgs of VE828, CN151 and RDX26939 as 194°C, 150°C and 185°C respectively. All the monomer Tg are also calculated based on Fox equation according to the previous results.

Table 3 Optimizing Der470HT-400 based high Tg formulation with VE828 as co-component

No	Formulation	Components WF	VE828 WF	Tg 1 st run(°C)	Tg 2 nd run(°C)	Tg of Der 470-400
1	Der 470HT-400/VE828/MOct 60-30-10	VE:70% MOct:10% St:20%	29.4%	143	147	174
2	Der 470HT-400/VE828/MOct 61-24-15	VE:65% MOct:15% St:20%	24.4%	131	138	187
3	Der 470HT-400/VE828/MOct 76-14-10	VE:65% MOct:10% St:25%	14.2%	146	147	178
4	Der 470HT-400/VE828/MOct 76-9-15	VE:60% MOct:15% St:25%	9.2%	132	136	185
5	Der 470HT-400/VE828/MOct 72.7-13.3-14	VE:60% MOct:14% St:24%	13.3%	134	135	178
6	Der 470HT-400/VE828/MOct 69.7-16.3-14	VE:60% MOct:14% St:23%	16.3%	135	136	179
7	Der 470HT-400/VE828/MOct 69.7-17.3-13	VE:60% MOct:13% St:23%	17.3%	137	140	180

Table 4 Supplement of the formulations with increasing amount of VE 828

No	Formulation	Components WF	VE828 WF	Tg 1 st run(°C)	Tg 2 nd run(°C)	Tg of Der 470-400
8	Der 470HT-400/VE828/MOct 49.5-40.5-10	VE:70% MOct:10% St:16.5%	40.5%	135	143	161
9	Der 470HT-400/VE828/MOct 57.75-35.25-10	VE:65% MOct:15% St:19.25%	35.25%	142	146	171
10	Der 470HT-400/VE828/MOct 62.5-27.5-10	VE:65% MOct:10% St:20.8%	27.5%	140	143	167

Table 5 Double check the reproducibility of the designed formulations by the use of CN151

No	Formulation	Components WF	CN151 WF	Tg 2 nd run(°C)	Tg of Der 470-400
1	Der 470-400/CN151/MOct 60-30-10	VE:70% MOct:10% St:20%	29.4%	138 138	178 178
2	Der 470-400/CN151/MOct 61-24-15	VE:65% MOct:15% St:20%	24.4%	132	193
3	Der 470-400/CN151/MOct 76-14-10	VE:65% MOct:10% St:25%	14.2%	132 147	163 186
4	Der 470-400/CN151/MOct 76-9-15	VE:60% MOct:15% St:25%	9.2%	136	190
5	Der 470-400/CN151/MOct 72.7-13.3-14	VE:60% MOct:14% St:24%	13.3%	135	186
6	Der 470-400/VE828/MOct 69.7-16.3-14	VE:60% MOct:14% St:23%	16.3%	137	191
7	Der 470-400/VE828/MOct 69.7-17.3-13	VE:60% MOct:13% St:23%	17.3%	135 136 137	183 185 187

Table 6 Processing performance indicated by viscosity

Resin	26~27(°C)	30(°C)	Shelf time
Der 441-400	620	448	
Der 470-300	660	496	
Der 8084	600	460	
Der 470-400	--	292	8.11.2006
Der 411-350		308	
FAVE-H	900	656	
FAVE-L	960	664	
Design 1(VE828)		780	8.17.2006
Design 2(VE828)		540	8.17.2006
Design 3(VE828)		388	8.17.2006
Design 4(VE828)		296	8.17.2006

2.5 Toughening study

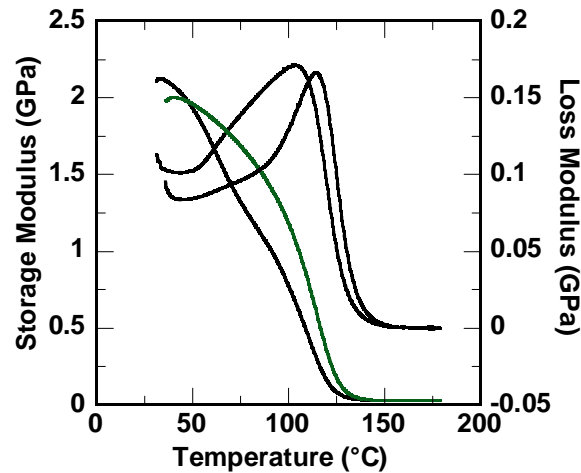


Figure 20 DMA spectrum of sample of Der8084/VE828 (synthesized in lab)/MOct (62.5-27.5-10). Tgs of 105°C and 115°C are assigned to the first run and second run respectively. The sample was cured at room temperature for 5 days before DMA scan.

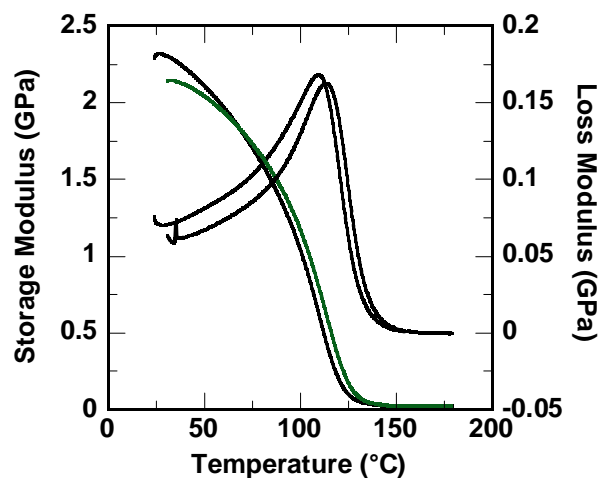


Figure 21 DMA spectrum of sample of Der8084/RDX26939/MOOct (62.5-27.5-10). Tgs of 109°C and 113°C are assigned to the first run and second run respectively. The sample was cured at room temperature, after 48 hours cure, the surface is a little bit tacky. The sample was put in oven at 100°C for 10 minutes before DMA scan.

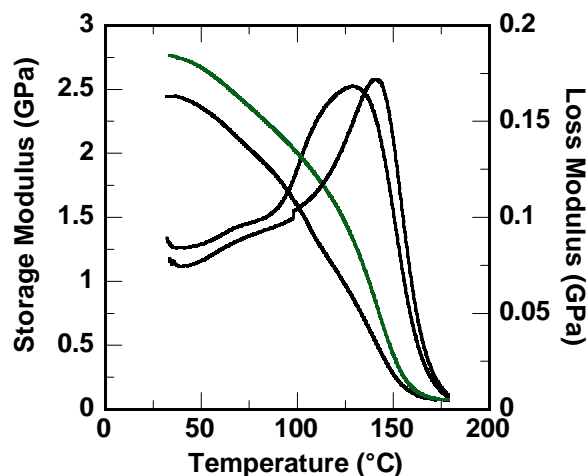


Figure 22 DMA spectrum of sample of Der470HT-400/RDX26939/MOOct (75.8-14.2-10). There exists a broad peak in the first run. Second run gives Tg of 141°C. 50g resin was cured in the mold with approximate dimensions as 15''×5'' ×0.5''. The mold was covered by aluminum foil after infusing resin. After 24 hours cure, the hardened sample was put in oven at 100°C for 2 hours before DMA scan.

3. DISCUSSIONS

3.1 Inhibition of oxygen in vinyl ester cure

As well known, oxygen can be an inhibitor for free radical polymerization through combining free radical to form peroxide, which results in termination of

polymerization and reduce the cure speed significantly. It was reported that the reaction rate of free radicals with oxygen is 105 times of that with monomers, thus even trace amount of oxygen in reaction system should also be given enough attention. Usually, the influence of oxygen is confined to the surface of resin reaction system, and similar observations are obtained in this study as well. Resins like FAVE-O and RDX26939 with 33% St exhibits a retarded cure in surface. Strange thing however, is the CN151 with 33% St, as shown in Figure 4. After the removal of the liquid surface layer, there are two separate Tg peaks in the first DMA scan compared one peak of other resins-even if it maybe broad, which means there are two distinct phases in one sample. In another word, the bulk resin of CN151 with 33% can also be affected by the oxygen. This phenomenon maybe explained as followed: there are some extra amount of additives existing in the commercial CN151 resins, for example inhibitor, which leading to the relative low reaction rate compared to the diffusion rate of oxygen thus permitting oxygen permeate to some depth of level and forming a transition region-lower Tg region, while for other resin systems, after adding the catalyst, the reaction proceed fast which leaves only surface layer influenced by oxygen. Also for CN151, extra amount of peroxide and some other defects will be formed under the influence of oxygen and hence result in the 20°C loss in Tg. This can be verified by the following facts: 1) pure CN151 put in oven at 90°C for 4 hours, the surface is much more viscous than CN151 with 33% St. The addition of 33% styrene decrease the concentration of inhibitors while adding more active centers; 2) Tg sequence of three systems: VE828 (lab made) with 33%St> RDX26939 with 33% St > CN151 with 33% St. The corresponding simple model based on this observation can then be suggested as followed:

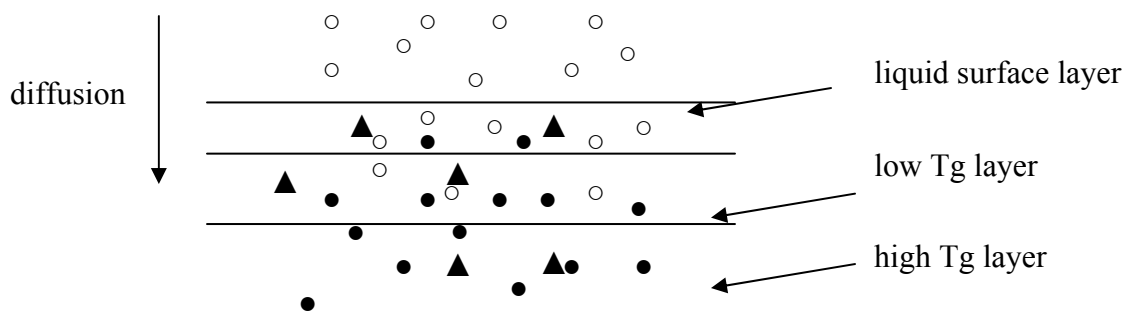


Figure 23 Model suggested for the cure of CN151 with 33% St. ● – free radical; ○- oxygen; ▲-inhibitor in CN151

3.2 Role of Der470HT-400

It was found that high Tg resin systems comprised of Der 470HT-400 exhibited a fast cure compared to other low Tg resin systems like FAVE-O and Der 8084. Moreover, even with similar Tg, Der470HT-400 resin comparing with VE828 and RDX26939 with

33% St respectively, the cure of Der470HT-400 resin proceed much faster. Possible explanation is that the novolac epoxy vinyl ester monomer that constituting Der470HT-400 possesses more functions than other monomers, which will lead to the more active centers in surface and diminish the influence of oxygen. On the other hand, the formed high crosslinked polymer layer may retard the diffusion of oxygen. However, for the fully cured Der470HT-400 resin, the Tg is 167°C, which is much lower than it supposed to be (195°C as claimed by company) compared to other resins like VE 828. The reason could also be attributed to the additives in the commercial Der470HT-400 resin, with the same behavior as CN151.

The deterioration in Tg caused by CN151 is diminished in Der470HT-400 resin systems compared to FAVE-O, particularly those with less amount of CN151, as illustrated by Table 3 and Table 5. With the increase of amount of CN151, as in formulation 1 and 2, this deterioration is also prominent, reflected by 6~9°C Tg loss.

Another interesting phenomenon is, as can be seen in Table 4 and 5, with the increase of weight fraction of VE 828 in the formulation from 9.2% to 40.5%, there is a decrease trend of the calculated Tg of Der470HT-400, which is from 185° C to 161°C (neglecting the lucky value of 187°C). In another word, in large amount of VE828, Tg of Der470HT-400 calculated by Fox equation is lower than 167°C whereas in small amount of VE828, the Tg of Der470HT-400 is more close to 195°C, which is claimed by the company. The two possible explanations are: 1) with the increase amount of VE 828, the active centers in unit area decreased, and the system is more easily subject to the influence of oxygen, and 2) on the contrary angle, with the more amount of Der470HT-400 in the system, the contribution of VE 828 to the final Tg is diminished, in another word, the lower value than 194°C should be used in calculation.

Similarly, the higher Tg value of Der470HT-400 obtained by using CN151 systems is because the influence of oxygen on CN151 is counteracted by the Der470HT-400, accordingly, higher Tg value than 150°C should be used in Fox equation calculating. In the meantime, same trend also exists in the CN151 systems, that with the high amount of CN151, the calculated Tg of Der470HT-400 is decreased.

3.3 Influence of the catalyst concentration on the cure behavior

The catalyst concentration was doubled in this study in order to eliminate the influence of oxygen on the cure behavior. As expected, the cure speed was improved, especially for the CN151 with 33% St, accompanied by the significant exothermal effect in the initial stage. However, except for Fave-O (John sample), other formulation will exhibit a Tg loss in a more or less extent. One possible reason could be due to the more residual Cobolt Naphthenate. While the change in morphology could be another reason. Thus, the further investigation on the competing of different species of double bond under oxygen in the cure system and its related kinetics may give the answer for this.

3.4 Effect of cure conditions on the final Tg

For FAVE-O sample, Yong also gave it a DMA run. As shown in Figure 24, in the first run, Tg of only 58°C was obtained. The low Tg is due to the insufficient cure time at room temperature. However, after thermal scan, Tg of 114°C was achieved which is 3°C higher than that given by normal cure procedure.

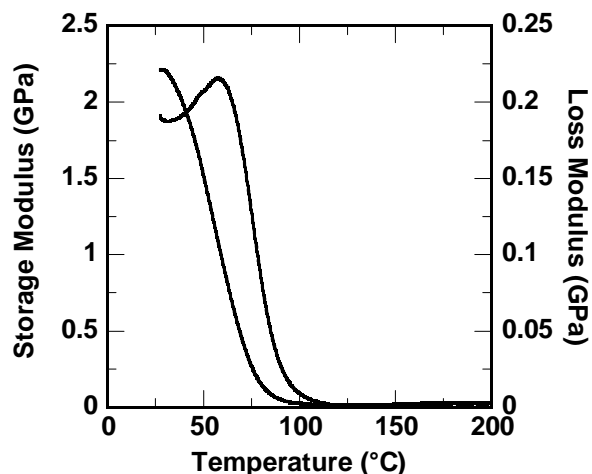


Figure 24 DMA spectrum of sample of FAVE-O (batch 2# received on 8.16.06 from John) given by Yongho. In the first run, one single Tg peak of only 58°C is shown up indicating the insufficient cure of resin due to the short cure time.

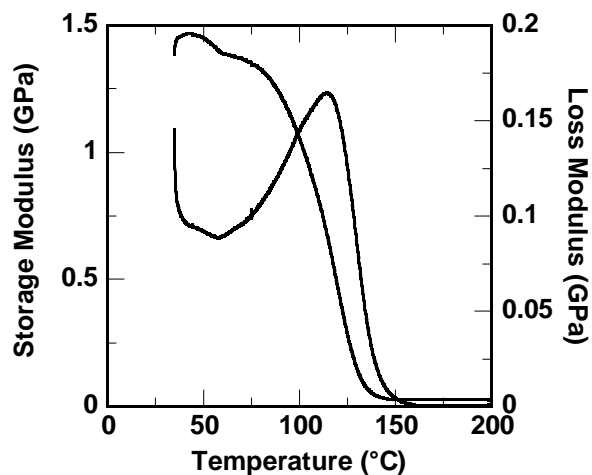


Figure 25 DMA spectrum of sample of FAVE-O (batch 2# received on 8.16.06 from John) given by Yongho. In the second run, Tg of 114°C was given.

The influence of cure conditions on the final performance was also exemplified by the toughening study sample. As seen in Figure 22, for a large amount of resin with large surface area, along with high concentration of oxygen, room temperature cure is not sufficient, even with 100°C cure for 2 hours, the Tg peak is also very broad indicating

insufficient cure. And consequently, after fully cure, the Tg is 141°C, which is much lower than it is expected to be, which is 147°C.

4. MAIN CONCLUSIONS

According to the previous results and discussions, several conclusions can be given as followed:

- 1) RDX 26939 exhibit superior performance to CN151 in terms of cure behavior and performances.
- 2) Der470HT-400 possesses several merits such as improving the cure speed, improving the oxygen sensitivity, and moreover, improving the final Tg.
- 3) Oxygen need to be removed during processing, particularly for the air bulbs trapped by the high viscous resin systems.
- 4) Optimum formulations based on Der470HT-400 and RDX26939 providing good performance and good processibility were designed and demonstrated.

Some thoughts ...

First, since we are talking about Free radicals, it is important to note the initiator conditions (either % of total and mix, or something). Without this information, the references to tacky surfaces are somewhat incomplete. Also if all samples are prepared using a common cure process, initiator concentration/ratio, etc., that can all be referred to up front. I don't recall seeing this info in the report, however.

Second, the multiple DMAs is nice. I see significant differences between the methods. However, there seems to be some issue with some of the DMA traces. If they are just a result of grip failures, etc., we should note that in the captions, so as to not consider these oddities in our evaluation.

Next, I think a table or DOE would be useful here to understand what design space we are exploring and to understand what the final properties vs initial conditions, post-cure, etc are. I think the content is all present (minus initiator details), but it is hard to grab and consider quickly. Is it possible to create a table for summary. The tables that you did provide are helpful to review the results, but I would also like to see the DOE (design of experiments) to see what is still incomplete, or what additional results may be forth-coming. From this report, it is hard to say what is left to do, and what else in process.

Commenting on the results, I think we need to address the "tacky" surface issue. I know it is related to oxygen passivation at the surface, but how is it mitigated, and what things can be done to achieve good surfaces, without resorting to formulating from derakane resins (470's seemed fine). I think we should gain in understanding of that phenomenon reasonably. John La Scala may have additional thoughts.

Hope this helps. Keep putting out the reports, though. It is a great way to see the progress and the topics that are being addressed at present.

Lastly, I don't think we want these types of internal reports submitted from a ".yahoo" location. I recognize the value of working from home, but .yahoo is an unrestricted open source domain. We should really consider it a very last resort for any reports on development works. Once it is in the ether, it is impossible to control the flow of information, so putting this kind of development information on public servers is probably not in the best interest of the technology.

Fracture surfaces of a series of FAVE-L resins with varying amounts of styrene were imaged using a JEOL JSM 6460LV scanning electron microscope with an accelerating voltage of 20 kV. All samples were cured for 24 hours at room temperature using 1.5wt% Trigonox 239A and 0.375wt% cobalt naphthenate, and then post cured 2 hours at 120°C. The fracture surfaces were generated by machining a notch in the sample, then breaking it in a similar fashion to the SENB fracture test (ASTM D 5045). Samples were cleaned using isopropanol and were then coated with gold using a Hummer XP sputterer (Anatech LTD, Alexandria VA).

The series included: pure methacrylated lauric acid and FAVE-L based resins containing 0, 10, 20 and 30 % styrene, as described in Table 1.

All samples showed ridges and signs of plastic deformation near the edge of crack initiation, though the amount decreased with increasing styrene concentration. Figure 1 shows the difference near the crack initiation of MLau, FAVE-L-10S, and FAVE-L-30S.

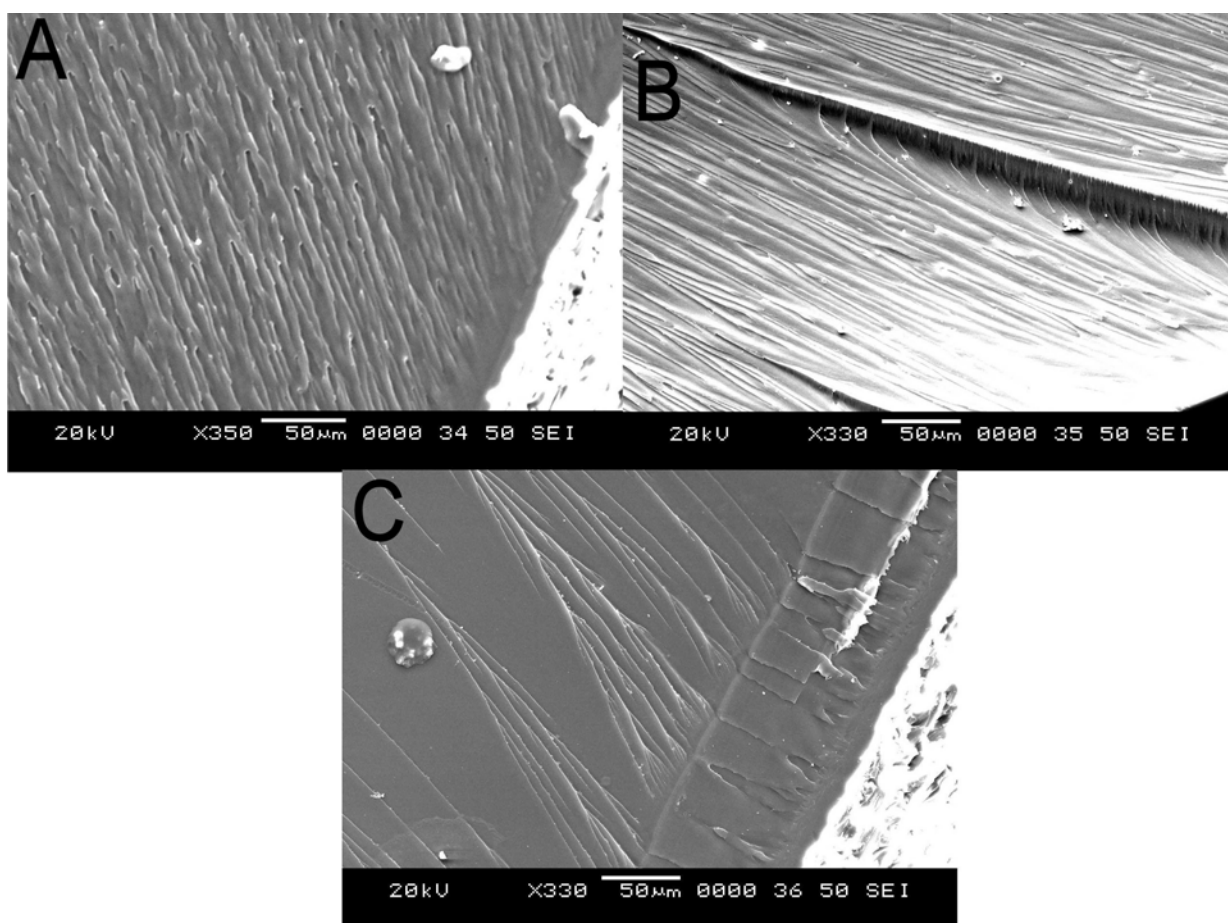


Figure 1: Near the crack initiation edge of A) MLau, B) FAVE-L-10S, and C) FAVE-L-30S

Similarly further away from the crack's leading edge, the plastic deformation was less for those samples containing more styrene. In approximately the middle of the fracture

surface, the sample containing the most styrene had the smoothest fracture surface. Figure 2D shows that the ridges of deformation end, leaving a smooth surface behind. The other samples continue (Figure 2A-C) to show plastic deformation.

Table 1: Formulation of fracture surfaces

	VE (%)	Styrene (%)	MLau (%)
FAVE-L-0S	65	0	35
FAVE-L-10S	65	10	25
FAVE-L	65	20	15
FAVE-L-30S	65	30	5
MLau	0	0	100

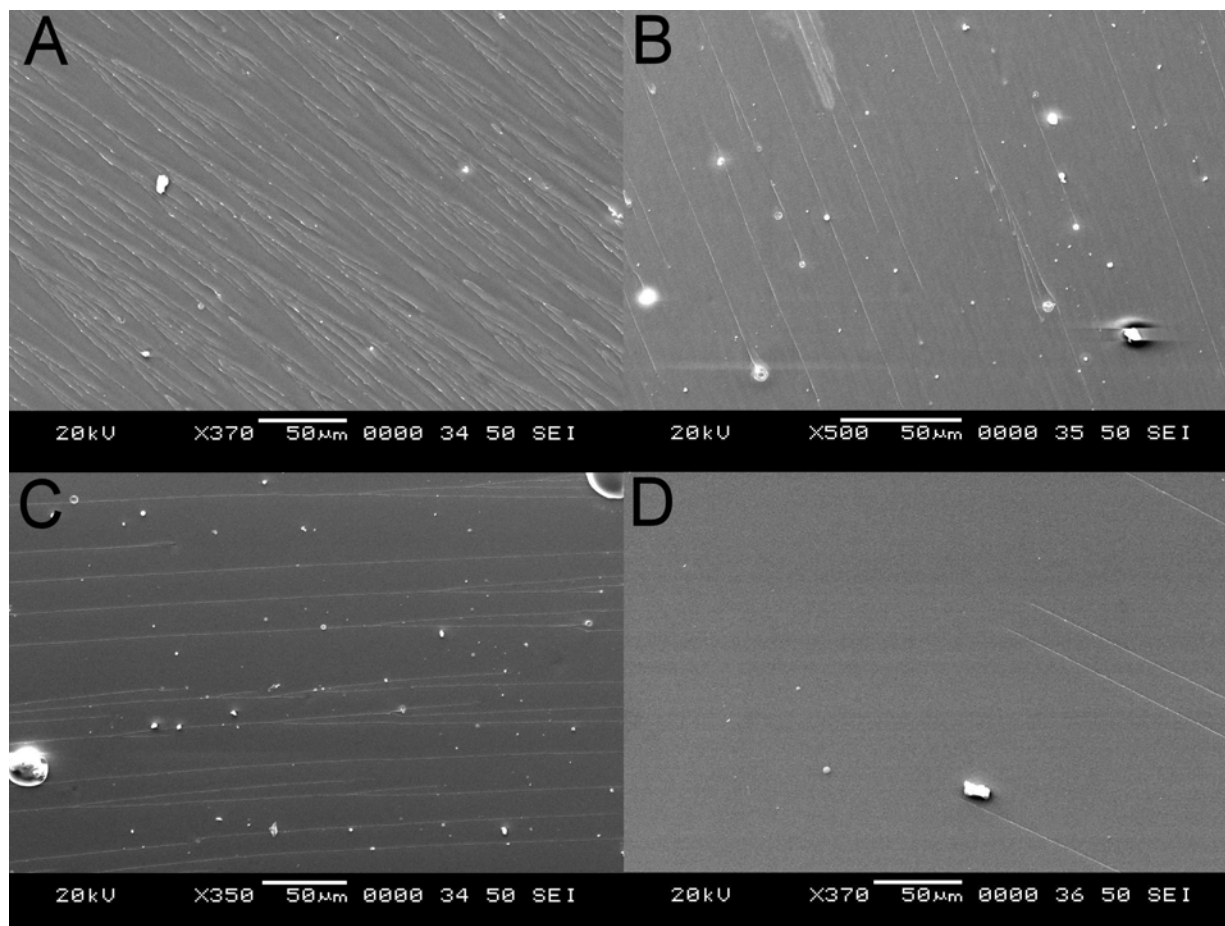


Figure 2: Approximately the middle of the fracture surface for A) MLau, B) FAVE-L-10S, C) FAVE-L, and D) FAVE-L-30S. The crack propagation is from lower right to upper left, or right to left. The large bright objects are dust particles.

Development of Low VOC High Performance Vinyl Ester Resins for Liquid Molding Applications

Final Report

Period of Performance: 7/1/06-12/20/08

Final Performance Report

Period of Performance: 8/1/07-12/20/08

1.0 Objectives

The objective of this work is to develop a low volatile organic compound (VOC) high performance vinyl ester resins for liquid molding applications by using methacylated fatty acids (MFA) to partially replace the styrene contained in the commercial vinyl ester (VE) resins. Success in addressing this objective requires a mechanistically model to provide a qualitative understanding of the relationships among the processing variables and their effects on the performance. In order to obtain such an understanding to develop a rational means for designing the desired resin systems, our study focuses on three major tasks.

- (1) Designing an optimum formulation possessing high dry/wet T_g , low styrene content, and good processibility. This entails the following considerations: (i) selection of appropriate styrene diluted commercial multi-functionalized vinyl ester resins as base materials providing high temperature resistance and good compatibility with MFA; (ii) utilization of commercial difunctional vinyl ester as subsidiary materials to improve the processibility and to compensate for the T_g loss when using MFA to replace the styrene contained in the commercial VE resins; (iii) conduction of hydrothermal experiment to evaluate the wet T_g of the resin system to meet the requirements of DoD. In particular, Fox equation was employed as an empirical model to optimize the T_g of the designed resin systems while maintaining low styrene content.
- (2) Toughening the obtained high wet/dry T_g resin system to meet the requirements of a variety of applications such as structural materials. Success in fulfilling this task relies on the good understanding of the toughening mechanism of liquid rubber modified VE resin systems. Traditional petroleum-based liquid rubbers were selected to carry out numerous studies to this end. Further investigation on the toughening of the FAVE-O-HT resin system was performed in order to obtain improved resin systems with fracture toughness comparable to the commercial vinyl ester of Derakane 8084 whose fracture toughness is as high as 680 J/m².
- (3) In order to gain a good understanding of the cure behavior of designed resin systems under processing conditions, a kinetic model that correlates processing variables with the conversion of C=C of VE resins was developed. The scientific challenge of this work was to develop a simple and accurate technique capable of real-time *in-situ* characterizing conversions of functional groups at varying temperatures.

2.0 Summary of Program Accomplishments

1. A vinyl ester resin system featuring low content of styrene and high dry/wet T_g was developed in this work in order to meet the requirements of DoD. This newly developed resin was named FAVE-O-HT. A more detailed report was given in the report of ARL-RP-184. Our accomplishments in this area can be summarized as follows.
 - A low VOC vinyl ester resin with T_g as high as 147°C was obtained by using methacrylated octanoic acid (MOct) to partially replace the styrene contained in the commercial vinyl ester resin-Derakane 470HT. As a consequence, styrene content was reduced from 33% to 25%. The obtained resin was named FAVE-O-HT.
 - FAVE-O-HT possesses low viscosity (392 cp @ 30°C) which is suitable for liquid molding applications.
 - Hydrothermal experiments show that the glass transition temperature of the obtained resin systems are susceptible to water or moisture resulting in 20°C loss in T_g after the saturation of water. Wet T_g as high as 122°C was obtained with FAVE-O-HT which meets the requirements of DoD.
 - Apart from the role of lowering VOC, MOct as a replacement for styrene can improve the fracture toughness of the resin system. As a result, the G_{Ic} value increased almost by a factor of two: from 56 J/m² for Derakane 470HT to 102 J/m² for FAVE-O-HT.
 - Further increase in fracture toughness was obtained by incorporating liquid rubber into the resin formulations while maintaining the glass transition temperature requirements. A maximum toughening effect was obtained by using 9 wt % vinyl terminated poly(butadiene-*co*-acrylonitrile) (VTBN) as a modifier. In this case, G_{Ic} as high as 167 J/m² was obtained with T_g maintaining same level.
 - Even though G_{Ic} of FAVE-O-HT is still lower than that of the commercial toughened vinyl ester resin Derakane 8084 (680 J/m²), the high T_g (147°C vs. 118°C) and low styrene content (25% vs. 40%) makes it to be a competitive one in the market.
2. Extensive studies were carried out to investigate the potential of other modifiers to further improve the fracture toughness of the FAVE-O-HT including polyurethane

elastomers, epoxidized soybean oil and its derivatives. Problems associated with these modifiers include poor compatibility and incomplete phase separation. Both of these resulted in poor toughening effect and significant T_g loss. An approach to toughen MFA modified vinyl ester resins by directly mixing with Derakane was also investigated.

- Multifunctional polyurethane elastomer (Eb264) with a molecular weight of ~2000 g/mol was selected as a modifier to toughen the FAVE-O-HT. Multifunctions incorporate Eb264 elastomer molecules into the resin network and limit the rubber phase separation. The insufficient phase separation leads to the significant loss in T_g for modified vinyl resins.
- Using epoxidized soybean oil (ESO) and acrylated soybean oil (AESO) to toughen FAVE-O-HT has the same problem of incomplete phase separation. Significant loss in T_g was also observed. A new liquid rubber toughener was thus developed to toughen the FAVE-O-HT resin.
- Significantly improved fracture toughness was obtained using newly developed liquid rubber as toughener. The glass transition temperature was highly retained. Additionally, the low viscosity associated with such liquid rubber offered processibility ease and depression of styrene content. For FAVE-O-HT resin toughened by this liquid rubber, G_{Ic} of 256 J/m² and T_g of 144°C were obtained. In the mean time, the styrene content was reduced to 22%.
- A simple toughening approach for low VOC vinyl esters by the addition of Derakane 8084 was also investigated. The results indicate that Fox equation can be used to predict both the T_g and G_{Ic} of the modified resin systems.

3. Processibility and water resistance of low VOC vinyl ester resins

- MFA exhibits higher viscosity than styrene due to the strong intermolecular association as a result of hydrogen bonding. This brings about processing problem and limits the applications of MFA in replacing styrene in some vinyl ester resins. The viscosity of MFA can be lowered by heating to eliminate the hydrogen bonding effects. This was demonstrated by MLau which showed a dramatic declination with the increase of temperature from 25°C to 70°C which provides the processing ease similar to styrene.
- Exothermal effects during cure may affect the performance of resin by altering the polymerization behavior and hence ultimate network structure or by introducing residual thermal stress. Exothermal effects of MFA modified vinyl ester resins were evaluated by DSC along with commercial resins. Less

exothermal effects associated with MFA modified resin systems were demonstrated.

- Hydrothermal experiments were conducted to numerous MFA modified vinyl esters to evaluate the water resistance of such resins based on the protocol designed by us. Compared with commercial vinyl ester resins, MFA modified samples exhibited a comparable water resistance ability.
4. Study was performed to determine the validity and practicality of near infrared (NIR) spectroscopic techniques for measurement of C=C conversion in vinyl ester resins during cure processing. Because glass is virtually transparent in the NIR spectrum, it was used in this technique as a sample holder with two ends sealed to prevent the evaporation of VE resins. Conversion measurements by NIR and mid-IR (MIR) were compared using VE 828 as a model compound. For the accurate peak height measurement, a deconvolution method based on software program was developed accordingly. The results showed conversion values obtained by NIR are in good agreement with those obtained by MIR technique. The nondestructive analysis of conversion by NIR offers advantages of convenience, practical specimen dimensions and precision compared with standard MIR analytical procedures. Investigation on the cure kinetics of FAVE-O-25S based on the developed NIR technique was performed subsequently.
- The newly developed technique is characterized with low cost, easily handling, error eliminating, and so forth.
 - A devolution method is explored to analyze the peak height associated with the double bonds of VE and styrene in NIR spectra. The results obtained by the developed NIR technique are in good agreement with those from MIR indicating the validity of the deconvolution method. The reactivity ratios of styrene (r_s) were 0.17 and 0.23 from the NIR and MIR respectively and those of vinyl ester (r_{ve}) were 0.30 and 0.21 from the NIR and MIR method respectively. The reactivity ratios of two monomers indicate that a pseudo-alternate copolymer was formed after cure. The rate constant showed a direct dependence on concentration; increasing as styrene concentration decreased. The rate constant and reaction constants obtained from the two techniques were about the same for resin systems containing 50 wt % and 40 wt % styrene, respectively.
 - Cure kinetics of FAVE-O-25s was studied. Conversion, reaction rate constants and reaction order were obtained at four different temperatures using the NIR technique developed in the proceeding study. Activation energy

of VE double bond and styrene double bond is 57.9 kJ and 52.1 kJ respectively.

4.0 Details of Accomplishments and New Findings for 8-1-07 to 12-20-08

4.1 Toughening FAVE-O-HT Resin

Summary

The task of developing low VOC high hot/wet T_g VE resin systems that meets the requirements of DoD was ended up with the exploration of FAVE-O-HT resin system wherein MOct was used to modify commercial Derakane 470HT resin. FAVE-O-HT resin is a low VOC VE resin developed by us for high temperature applications. The typical formulation comprises 75.8 wt% Derakane 470 HT, 14.2 wt% VE 828, 10 wt% VE828, and 25 wt% Styrene. The hot T_g of the derived resin is 147°C and the wet T_g is 124°C. However, the fracture toughness (G_{Ic}) is 102 J/m², which is insufficient for many applications demanding high deformation ability and is incomparable to the commercial toughened vinyl ester resin-Derakane 8084. Toughening such resin system is thus highly demanded.

The purpose of this investigation is to toughen this resin system for use in more applications. A toughening study was carried out using petroleum-based liquid rubbers, polyurethane elastomer, epoxidized soybean oil and its derivatives in order to improve the fracture toughness. Poor toughening effects associated with these toughening agents were obtained as the result of insufficient phase separation. This shortcoming was overcome by developing a novel liquid rubber. This rubber modifier provided good processibility, improved toughening effects and had good T_g retention capability. As a result, toughened FAVE-O-HT resin with high temperature performance and good processibility was developed for liquid molding applications.

Toughening by ETBN and VTBN The study was first carried out based on the traditional petroleum-based liquid rubbers, VTBN and ETBN, which are the abbreviated names for vinyl terminate poly (butadiene-*co*-acrylonitrile) and epoxy terminated poly (butadiene-*co*-acrylonitrile) respectively. Due to the poor miscibility of VTBN and ETBN with FAVE-O-HT resin, carboxyl terminated poly (butadiene-*co*-acrylonitrile) (CTBN) with high content of acrylonitrile (26% compared to 18% of VTBN and ETBN) was used accordingly. The results are summarized in Table 1 along with the fracture toughness of other commercial VE resins for a comparison.

Table 1. Fracture toughness (G_{Ic}) of liquid rubber modified and commercial VE resins

VE Resins	T_g (°C)	G_{Ic} (J/m ²)	St content (wt %)
Derakane 8084	118	680 ± 160	40
Derakane 470-HT	173	56 ± 18	33
FAVE-O-HT	145	102 ± 53	25
2.5 wt % ETBN FAVE-O-HT	145	135 ± 24	26.25
4.5 wt % ETBN FAVE-O-HT	151	141 ± 23	27.25
5 wt % VTBN FAVE-O-HT	146	--	23.75
9 wt % VTBN FAVE-O-HT	147	167 ± 31	22.75
10 wt % CTBN FAVE-O-HT	136	--	22.5
10 wt % BR FAVE-O-HT	144	251 ± 43	22.5

It can be seen from Table 1 that VTBN and ETBN did not impart significant toughness enhancement to FAVE-O-HT whereas CTBN resulted in a slight loss in T_g .

The highly retained T_g s associated with resin systems, with ETBN and VTBN as modifiers, are the result of rubber phase precipitation from the polymer matrix. Complete rubber phase separation from the polymer resin matrix is crucial to the good toughening effects and high T_g retention. This finding formed the basis of designing a novel liquid rubber for improved toughening effects. Based on this idea, efforts were made by using modifiers including polyurethane, epoxidized soybean oil and its derivatives.

Toughening by Polyurethane Elastomer It is believed that polyurethane (PU) elastomers can be employed to improve the fracture toughness of certain polymer resins. To apply this idea to the toughening FAVE-O-HT, several commercial PU elastomers were investigated. These PUs include aliphatic PU and aromatic PU. For retaining T_g maximally, a multifunctional PU was used. Ebecryl 264 (Eb264) is an aliphatic urethane triacrylate diluted 15% by weight with the reactive diluent 1,6-hexanediol diacrylated (HDODA). The MW of PU is about 2000 g/mol. However, significant T_g loss was detected in the experiments, as illustrated in Table 2. This is because Ebecryl 264 has a very low T_g of 42°C, and the multi-unsaturated function may prevent the phase separation of rubber phase from the polymer matrix to a great extent. Moreover, the MW of Ebecryl 264 is relatively low compared to that of liquid rubber ranging from 3000 to 4000 g/mol, which is detrimental to the phase separation as well.

Table 2. The formulation and the corresponding T_g values of modified resin systems using Ebecryl 264 as modifier.

Sample No.	Derakane HT	VE828 (RDX 26936)	MOct	Ebecryl 264	T_g
1	68	13	9	10	125
2	64.4	12.1	8.5	15	119

Toughening by epoxidized soybean oil and its derivatives 10 wt % ESO and AESO were used to toughen the FAVE-O-HT resin. T_g retention was measured as a criterion to evaluate the toughening effects. These results are helpful to understand the design strategy of the novel liquid rubber. The understanding derived from this study was then applied to the rational development of the novel liquid rubber.

Dynamic mechanical analysis was performed on AESO and ESO modified FAVE-O-HT resin to evaluate the T_g retention and phase separation. These results provide information about the insufficient toughening effects associated with ESO as well as the influence of multi-functionality associated with AESO on the toughening effects.

DMA plot of 10 wt % ESO modified FAVE-O-HT was shown in Figure 1. The T_g based on the loss modulus peak is 140°C, which is 7°C lower than the pure resin. Two bumps in the loss modulus curve prior to the advancement of the dominate glass transition peak, located at 70°C and 115°C respectively, indicate phase separation. The broad glass transition region indicates that the rubber phase did not separate from the polymer matrix completely. Figure 2 presents the DMA plot of 15 wt % ESO modified resin system, the much broadened transition region and lowered T_g indicate that the phase separation was deteriorated and more rubber was trapped in the polymer matrix.

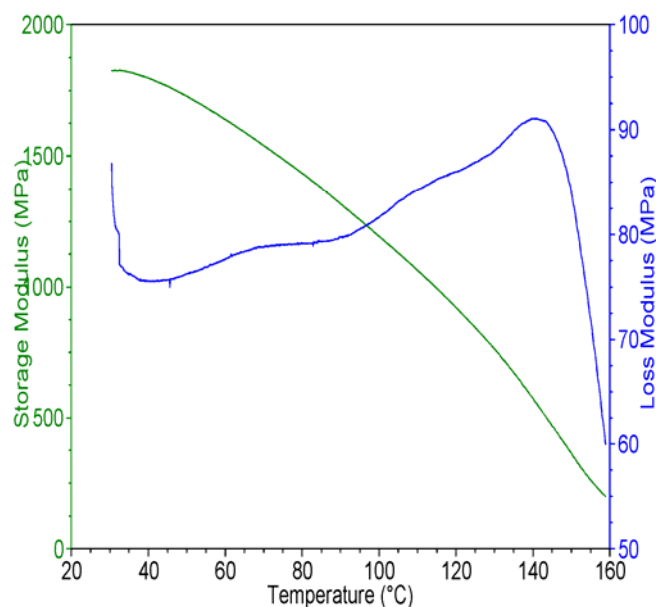


Figure 1. DMA spectrum of 10 wt % ESO modified FAVE-O-HT. T_g of 140°C was discerned based on the peak of loss modulus.

The incomplete phase separation associated with ESO in toughening FAVE-O-HT resin is thought to be due to the low MW of ESO. The phase separation of rubber can also be limited by the interaction between rubber phase and resin matrix, e.g., chemical reaction, physical bonding, etc. This was demonstrated by using AESO, an acrylated ESO with multi-functionality, to modify the FAVE-O-HT.

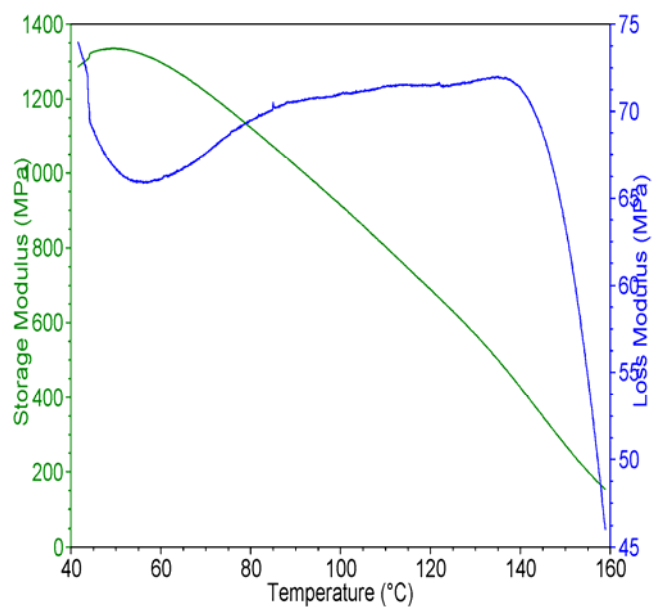


Figure 2. DMA spectrum of 15 wt % ESO modified FAVE-O-HT. T_g of 135°C was discerned based on the peak of loss modulus.

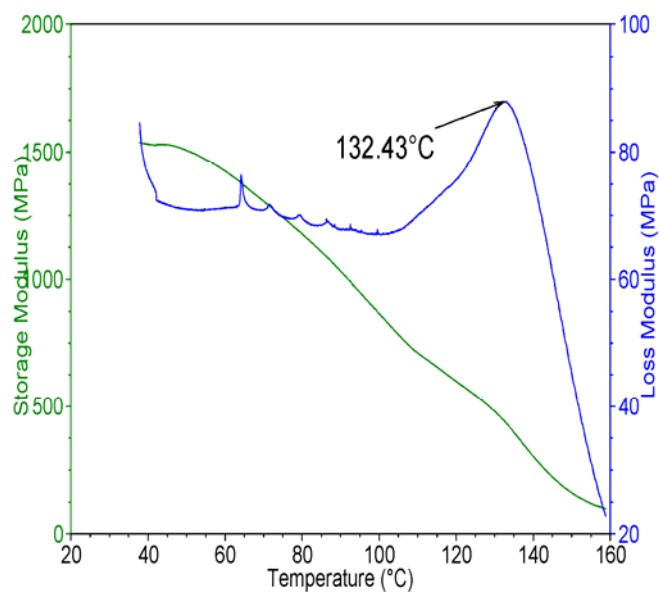


Figure 3. DMA spectrum of 15 wt % AESO modified FAVE-O-HT. T_g of 132°C was discerned based on the peak of loss modulus.

Figure 3 shows the DMA plot of 15 wt % AESO modified FAVE-O-HT. The single transition peak with low peak temperature of loss modulus is the indication of the incorporation of the rubber to the polymer structure. The low T_g associated with the obtained resin system is due to the low T_g of poly-AESO. Rubber phase, in this case, was trapped to the polymer matrix which resulted in the low glass transition temperature.

Subsequently, a novel liquid rubber to toughen FAVE-O-HT was developed in order for appropriate toughening and maintaining glass transition temperature requirements. Detailed information will be described in another report. The glass transition temperature retention was demonstrated by DMA analysis.

LR1 is the one with lower MW whereas LR2 is the one with larger MW. Using same concentration of these two liquid rubbers as modifiers to toughen FAVE-O-HT resin, DMA plots for different modifiers are given in Figure 4 and Figure 5, respectively.

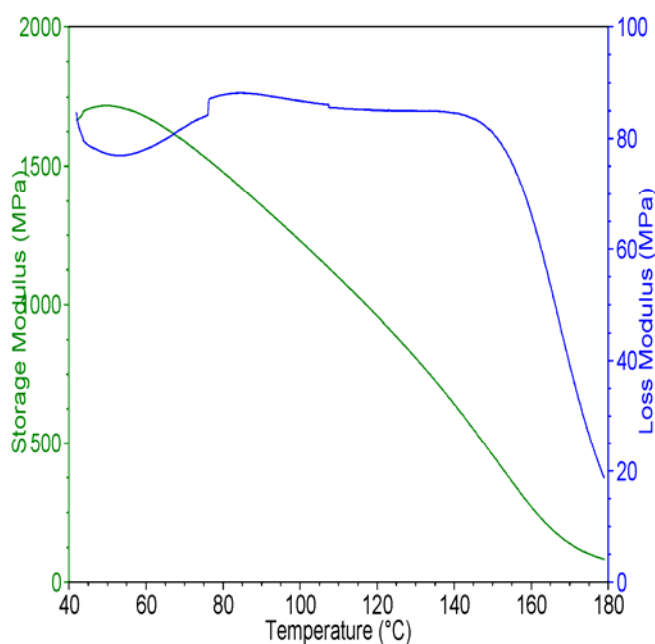


Figure 4. DMA spectrum of 10 wt % LR1 modified FAVE-O-HT.

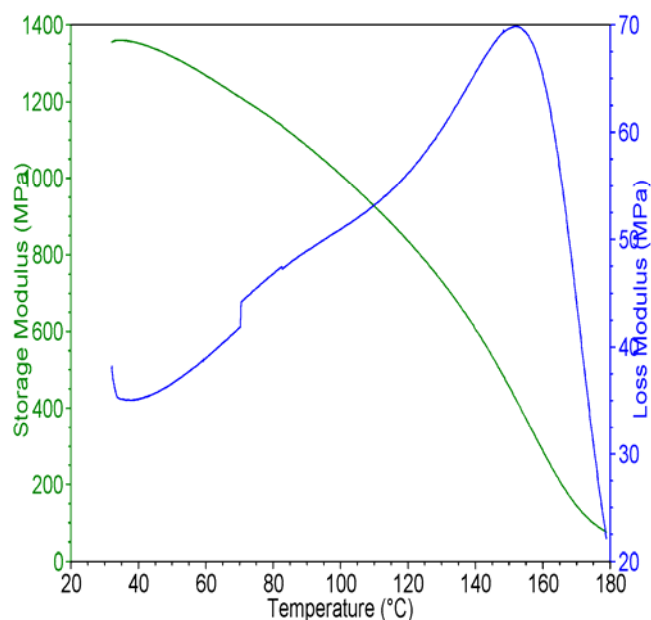


Figure 5. DMA spectrum of 10 wt % LR2 modified FAVE-O-HT. T_g of 150°C is shown by the loss modulus temperature peak.

It can be seen from the plots, the resin system with the higher MW liquid rubber as toughener exhibited a higher T_g and clear single glass transition region whereas the one with lower MW as toughener showed a broad glass transition region and lower T_g indicating high amount of rubber modifier was trapped in the polymer resin matrix. This result partially validates our hypothesis that T_g retention is the result of rubber phase separation from the polymer matrix which is highly dependent on the MW of rubber phase relative to the polymer matrix. Particularly, resin modified with LR2 showed an even higher T_g than pure resin itself. One possible reason is the separated rubber phase absorbed a certain amount of MFA due to chemical similarity which resulted in the lower concentration of MFA, compared to the pure resin system and hence the enhanced T_g . This result constitutes another salient feature of developed liquid rubber in that it may enhance the final T_g of the modified resin by trapping low T_g constituents.

The shortcoming associated with the developed liquid rubber in toughening resin was that the cured resin system lacked plasticity and looked chalky. Further modification was thus given to the liquid rubber. The details regarding this modification are summarized in a separate report. The developed toughener was used to modify the FAVE-O-HT resin. DMA plots given in Figure 6 illustrate the good T_g retention capability associated with this newly developed rubber modifier. The fracture toughness of the modified FAVE-O-HT is 251 J/m². Based on Table 1, the

rubber modified FAVE-O-HT resin system shows comparable performance to the commercial ones like Derakane 8084.

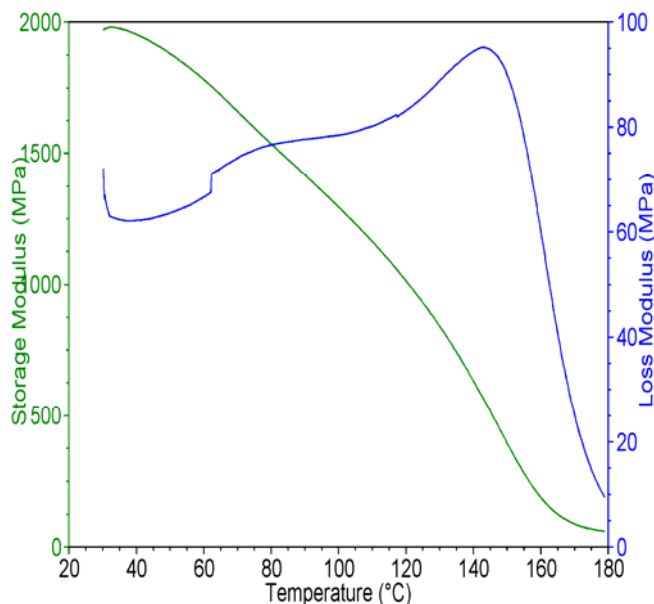


Figure 6. DMA spectrum of 10 wt % developed liquid rubber toughened FAVE-O-HT. T_g of 144°C is shown by the loss modulus temperature peak.

4.2 Toughening Low VOC VE resins by Directly Mixing with Derakane 8084

Summary

The purpose of this investigation is to develop a simple approach to toughen the designed low VOC vinyl esters to meet the application requirements. Derakane 8084 resin is an elastomer-modified epoxy vinyl ester designed to offer increased adhesive strength, superior resistance to abrasion and severe mechanical stress, while giving greater toughness and elongation. The great disadvantage associated with this resin is its high styrene content, which is as high as 40%. On the other hand, the MFA modified low VOC vinyl esters exhibit poor fracture toughness which limits their applications as structural materials. Blending Derakane 8084 directly with low VOC resins as a means to achieve high toughness and low styrene content was investigated using FAVE-L and FAVE-L-25S as model compounds. The effectiveness of this method was evaluated by comparing T_g and G_{Ic} of the resin systems before and after blending. Styrene content constitutes another indicative of the blending effects. The results showed that blending with Derakane 8084 can significantly improve the fracture toughness of the low VOC resins

while maintaining the T_g requirements. Furthermore, the obtained improved resin systems possessed low styrene content compared to the Derakane 8084 that can be potentially used for applications demanding low VOC emission.

Toughening FAVE-L and FAVE-L-25S by blending with Derakane 8084 FAVE-L-25S is a low VOC resin system obtained by using methacrylated lauric acid to partially replace the styrene contained in Derakane 441-400 resin. According to the toughening results summarized in Table 3, blending with Derakane 8084 at 50 wt %, the modified FAVE-L-25S exhibits T_g as high as 118°C and a G_{Ic} value of 321 J/m². Compared to Derakane 8084, although the G_{Ic} value is reduced by half, the styrene content is reduced as well from 40% to 32.5%.

FAVE-L is a vinyl ester resin obtained by a similar approach to FAVE-L-25S with even lower styrene content as low as 20%. The additional advantage of this resin is its much improved fracture toughness with G_{Ic} as high as 298 J/m². After mixing with Derakane 8084 at 50 wt %, a low VOC resin system was obtained with desirable fracture toughness and comparable T_g to FAVE-L-25S.

A further effort to reduce styrene content to 25% was made but this benefit was counteracted by the extremely low fracture toughness. Nevertheless, using Derakane 8084 to directly blend with the low VOC resin system is a simple way to obtain low VOC high performance resins. An interesting observation is that both the T_g and G_{Ic} value of modified resins seemly can be predicted based on the weighted average rule as demonstrated by FAVE-L and FAVE-L-25S resin systems.

Table 3. Toughening results of low VOC resins mixing with Derakane 8084

Resins	T_g (°C)	G_{Ic} (J/m²)	St content (wt %)
FAVE-L	107	298±53	20
FAVE-L-25S	115	93±26	25
Derakane 8084	118	680±160	40
50% FAVE-L with 50% Derakane 8084	113	473±116	30
50% FAVE-L-25S with 50% Derakane 8084	118	321±78	32.5
62.5% Derakane 8084 27.5% RDX 10% MOct	114	168±35	25

4.3 Exothermal Effects of Low VOC Resins

Summary

The exothermal effects in the cure of resin systems may affect the performance of products by altering the polymerization behavior or inducing residual thermal stress. Accordingly, the exothermal effects of low VOC vinyl esters were investigated in this study in comparison with the commercial ones. Preliminary results show that the heat release of low VOC resins is not as dramatic as that of the commercial ones due to the low concentration of unsaturated functionality associated with the low VOC vinyl ester resins.

Heat release amount of low VOC vinyl ester resins in comparison with commercial ones Table 4 presents the heat release data during the cure of the representative low VOC resin systems and comparison with commercial resins. For an intuitive feeling of the relative extent of exothermal effects of the resin systems, the heat release data are plotted in Figure 7 as a function of resin species. Compared with commercial resins with high styrene content, it can be concluded that the MFA modified ones exhibit less exothermal effects, which is beneficial to the good performance of final products.

Table 4. Heat release during cure of vinyl ester resin systems

VE resins	FAVE-L	FAVE-O	FAVE-O-25S	FAVE-O-HT	Derakane 411-350	Derakane 441-400
Heat release (J/g)	286.6	290.8	310.3	324.7	362.7	327.7

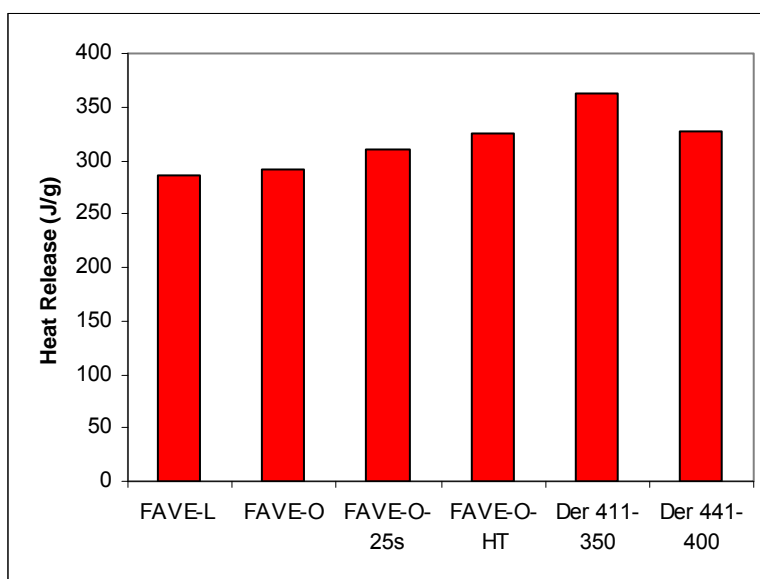


Figure 7. Comparison of the exothermal effects of different vinyl esters.

4.4 Water Susceptibility of MFA Modified Vinyl Ester Resins

Summary

Water will be detrimental to the T_g of resins as the role of plasticizer. Particularly for those resin systems containing hydrophilic components, the outcomes are even worse. Accordingly, wet T_g is defined as the measured T_g of a resin sample after conditioning in water or moisture environment for a designated period of time. The protocol for this measurement was designed by us with details described in the report of ARL-RP-184. Hot/wet T_g of low VOC resins were measured along with the commercial ones for a comparison. The results showed that the low

VOC resins exhibit similar water resistance to those commercial ones with high styrene content which constitutes another merit of the developed low VOC vinyl ester resin.

Water resistance evaluation of low VOC vinyl esters Based on this testing method, the wet T_g of MFA modified low VOC vinyl esters were evaluated along with the commercial ones for a comparison.

According to the hot/wet T_g values presented in Figure 8, it can be deduced that although the MFA are hydrophilic materials, the MFA modified vinyl esters exhibit comparable water resistance capability to commercial high styrene content VE resins.

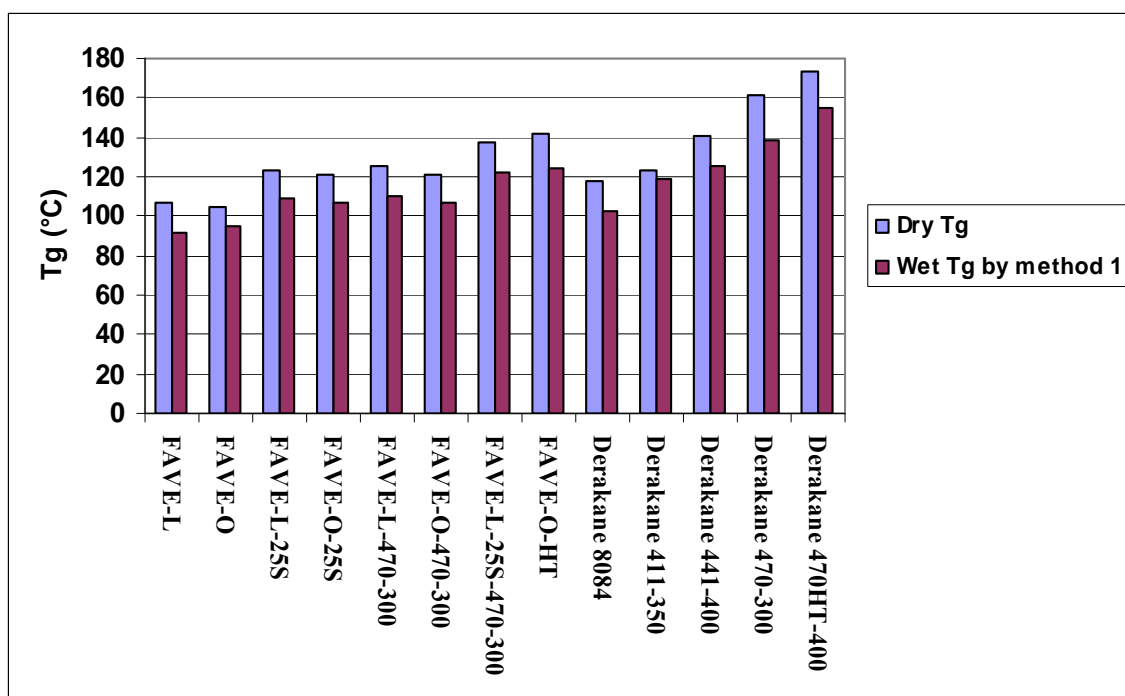


Figure 8. Hot/wet T_g of MFA modified vinyl esters compared with commercial ones

4.5 Fatigue Behavior of Low VOC Vinyl Ester Resins

Summary

The repetitive loading of a composite material causes degradation due to the accumulation of discrete micro-damage (e.g., fiber fractures, fiber/matrix debonds, matrix cracks) or macro-crack propagation, aided in some caused by an aggressive environment, including moisture. Therefore, a fatigue test has to be carried out to assess the resistance of a material to repetitive loading. One important benefit from this test is to ensure that the fatigue life is greater than required, and/or the replacement life is identified. Accordingly, a fatigue test is of great importance for engineers in designing novel materials.

The purpose of this study is to compare the fatigue behavior of the developed low VOC vinyl ester resin with that of the commercial ones. FAVE-O-25S was used as a model resin to this end. Its fatigue behavior was evaluated based on the procedure designed by us as illustrated in the following part. The results show that FAVE-O-25S exhibit comparable fatigue behavior to that of the commercial resin of Hexion.

Experimental design for the fatigue test In principle, a fatigue test can be designed by exerting repetitive stress on the sample until the occurrence of failure. Normally, a full *S-N* diagram (i.e., applied stress versus the number of cycles applied prior to failure) can be recorded. The repetitive stress can be designed in three waveforms, namely sine, triangular and square. It showed there was no difference for longer lives. Parameters like test frequency, mean condition and applied amplitude, or alternatively minimum and maximum values are also needed to be considered in association with corresponding waveforms.

Mechanical properties can be obtained mainly by two different categories of tests, flexural tests and axial tests. Correspondingly, in fatigue test design, displacement and load or strain control will be applied respectively.

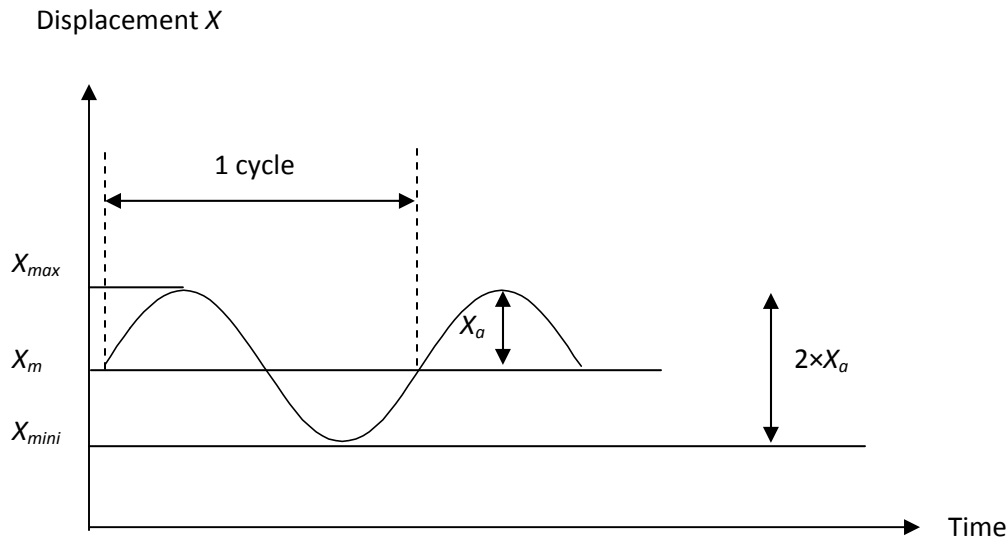
In this current case, the displacement control aiming to evaluate the flexural properties of polymer composites was utilized. The detailed information will be described in the next section.

Several artefacts may affect the results of the fatigue test of polymer composites when using displacement control. Of them, one issue worthy of mentioning is rate dependence effects, which may induce self-generated heating. For polymer composites, rate dependence of the material properties themselves in the absence of the temperature effects is another concern.

In this study, the aforementioned displacement control was employed to test the fatigue performance of two polymer resin based composites, 90 oz Hexion and 90 oz FAVE-O-25S, and the comparison of these two materials was given accordingly.

Static flexural tests were conducted following the ASTM D790 for three-point bending. Six tests for each sample were given to determine the loading parameters for the fatigue tests.

As pointed out, there is no standard for the flexural fatigue testing of unidirectional carbon fiber reinforced polymer composites. Therefore, in this case, we designed the fatigue test. The relevant parameters are illustrated in Figure 9. All tests were performed using an Instron 8872 servo-hydraulic test machine.



X_{max} : maximum displacement, X_{min} : minimum displacement, X_{mean} : mean value, X_a : amplitude.

Figure 9. Illustration of sine waveform cycle

In this design, the maximum displacement values were determined in correspondence to the maximum load of 80%, 60%, and 40% of the load value obtained by the static flexural tests. The stress ratio R , a ratio of minimum and maximum load ($\text{load}_{\min}/\text{load}_{\max}$), is a critical parameter that has an influence on the fatigue behavior. Different R values scenarios can be identified as in the ISO standard ISO 13003. The range of the R value for the flexural fatigue test can be $0 \sim 1$. The popular one is 0.1. In this case, R value close to 0 is applied. However, slight contact of load cell with the sample is maintained by choosing the minimum load as 1.7 lbf in order to fix the position of the specimen. The corresponding displacement can thus be determined based on this strategy.

In addition, 10,000 cycles tests were performed at a frequency of 1Hz in order to minimize adiabatic heating effects as well as to the time and cost of undertaking a fatigue program. After

the fatigue tests, static flexural tests were given to each specimen to determine the residual flexural strength and elasticity modulus. Consequently, the comparison of two samples under same conditions can be obtained.

Fatigue behavior of FAVE-O-25S compared with Hexion As illustrated by Figure 10 and Figure 11, FAVE-O-25S possesses similar flexural behavior to that of Hexion, with flexural strength as 530 MPa and 550 MPa respectively and elasticity modulus as 19 GPa and 18 GPa respectively. After a dynamic fatigue test, wherein force in a sine wave mode with maximum value equals to 80%, 60%, and 40% of flexural strength of each resin system were loaded on each sample and continued for 10,000 cycles, both flexural strength and elasticity modulus for these two resin systems exhibit a declining trend with the increase of cycling load on samples. Moreover, this trend is duplicated for both resin systems indicating a similar fatigue behavior presented by two resins, however, with a minor exception when the cycling load is equivalent to 40% of flexural strength. In the case of load equivalent to 40% of flexural strength, after 10,000 cycles, FAVE-O-25S exhibited lower value in both flexural strength and elasticity modulus. Since only one data point was given to each test condition, this deviation may also be attributed to the experimental error.

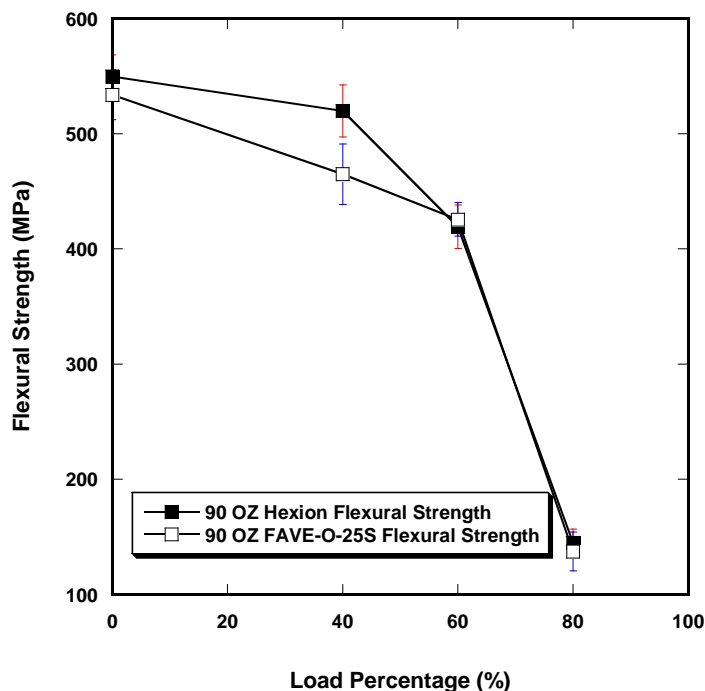


Figure 10. Residual flexural strength of resins after 10,000 cycles.

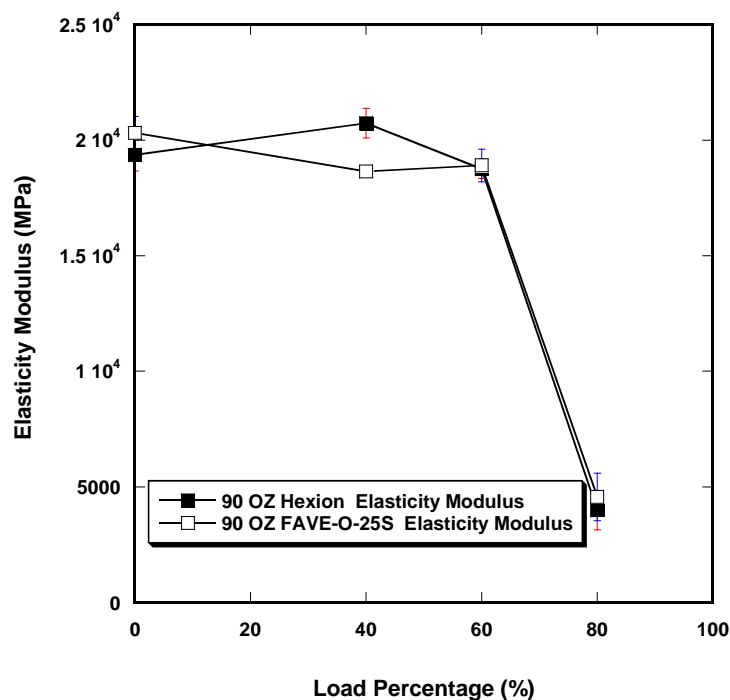


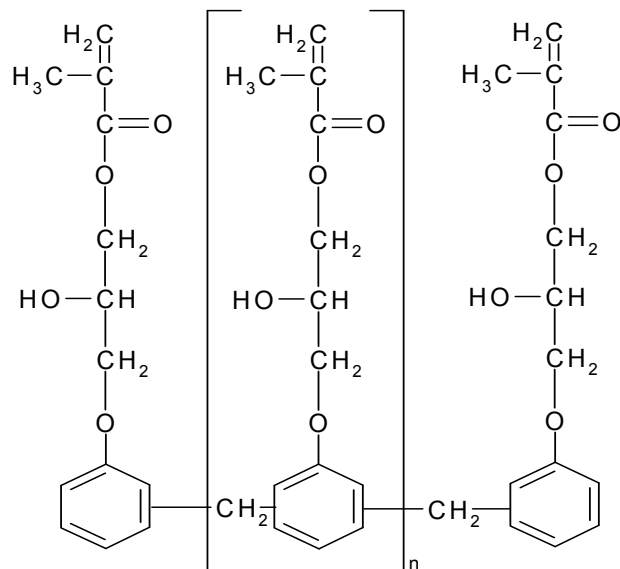
Figure 11. Residual elasticity modulus of resins after 10,000 cycles

4.6 Comparison of MOct and Styrene as Reactive Diluents in Achieving High T_g VE Resins

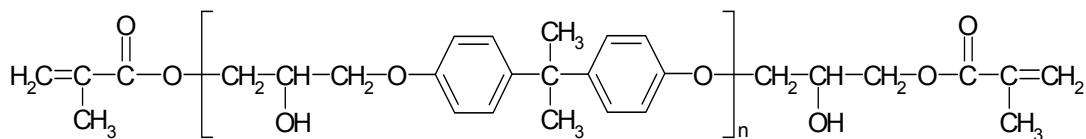
Summary

Multi-functionality vinyl ester resins are useful in obtaining high T_g resin systems due to their capabilities in forming high crosslink density network structures. In the preceding study, a high T_g low VOC FAVE-O-HT resin system was developed by using MOct to modify the commercial multi-functionality Derakane 470HT resin and this work was reported in detail in ARL-RP-184. However, the high T_g capability of a multi-functionality vinyl ester is often limited by the vitrification effect and the formation of structural defects during cure. This was illustrated in our study by comparing the dynamic mechanical behaviors of VE828 and VE160 (with structure shown in Figure 12), which possess bi-functionality and multi-functionality respectively, cured at different temperatures. The results showed that VE 160 exhibited similar T_g to VE 828 irrespective of the number of functionality. Using reactive diluents to aid in the cure of multi-functionality vinyl esters is a common strategy to realize their high T_g potentials by overcoming vitrification effect and by affecting network structure formation. The effectiveness of a reactive diluent, accordingly, is related to several variables, such as compatibility, reactivity, T_g and so forth. The major objective of this study is to compare the capability of MOct and styrene in

aiding in the network formation of VE160 in order for a rational method to develop low VOC high T_g vinyl ester resins. Resin systems comprising VE160 with varying amount of MOct and styrene were thus prepared. A study on the dynamic mechanical behaviors of such resin systems provided insight into the relationship between structure and performance and this information was helpful in determining the appropriate processing conditions for the cure processing and design of the optimum formulation for the maximized properties, as well as the information for the proper applications of the designed resin system. The deviation of the measured T_g s of designed formulations from the ones predicted by Fox equation was investigated regarding the variables like reactivity and compatibility in order to illustrate the effects of these factors on the T_g of the resulting resin systems. The results indicate that the potential of multi-functionality resin in the pursuit of high glass transition temperature can be realized by (a) curing at elevated temperature to improve monomer conversion by overcoming the vitrification problem, (b) improving the resin monomer conversion by introducing reactive diluents, (c) the certain amount of MOct in combination with styrene aiding in the cure of multi-functionality vinyl ester will not subject to the loss of T_g due to the synergistic effect, which is essential to the development of low VOC high T_g vinyl ester resins.



VE 160 n=0.5 MW: 650



VE 828 n=0.1 MW: 544

Figure 12. Schematic structures of VE 160 and VE828

Influence of Cure Temperature on the Dynamic Mechanical Behavior of Bi- and Multi-functional VE 828 and VE160 Neat Resins The storage and loss moduli, E' and E'' , of the VE 160 and VE 828 resins cured at two different temperatures, 50°C and 140°C respectively, are shown in Figure 13. It is apparent that at room temperature, VE160 resin cured at 50°C exhibits lower storage modulus of ~2.7 GPa than other three cases, which exhibit equal moduli of ~3GPa. At high temperatures exceeding 200°C, elevating cure temperature to 140°C exerts two opposite influences on the storage moduli of two resins; for VE160, the modulus increases whereas for VE828, the modulus decreases. According to rubber elasticity, VE828 cured at 140°C has a lower crosslink density and VE160 cured at 140°C has a higher crosslink density.

Moreover, it can be seen from Figure 13 that the glass transition region, reflected by the E'' peak, is very broad for the VE160 cured under two temperatures. Additionally, the E'' peak becomes even broader at the elevated cure temperature of 140°C. The broadness of the peak makes the T_g of VE160 neat resin indiscernible though a rough estimation of 140~150°C can be made. VE828 resin exhibits a much narrowed E'' peak and the peak becomes even sharper when curing at higher temperature accompanied with the increase in peak height. Like VE160, increasing cure temperature does show an appreciable T_g improvement for VE828 as well, which is around 150°C as reflected in E'' peak.

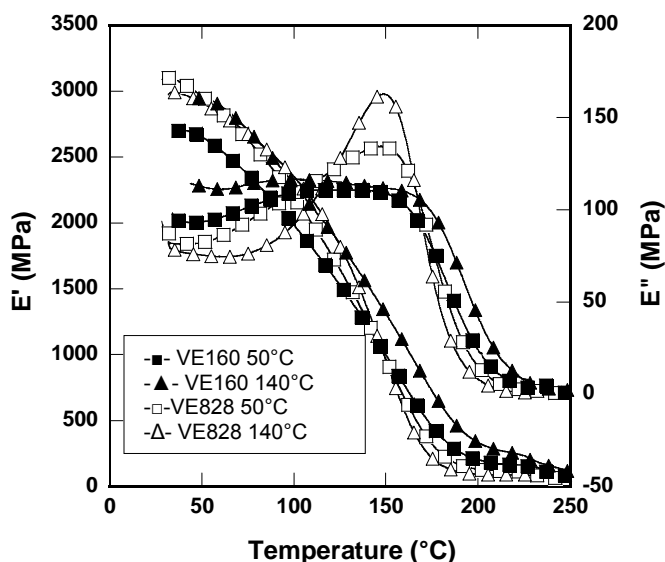


Figure 13. DMA plots for VE160 and VE828 neat resin cures at 50°C and 140°C respectively. Broad E'' peak and low storage modulus (E') are the two indicators of low monomer conversion.

The correlations between cure temperature and T_g as well as the corresponding network structure just described can be clearly illustrated by $\tan \delta$ curves as shown in Figure 14. Based on the peak position in $\tan \delta$, the T_g s of VE 828 cured at 50 °C and 140°C are 177 °C and 172 °C, respectively, and the T_g s of VE 160 under same cure conditions are 182 °C and 187 °C, respectively. Cure at 140 °C shifts the $\tan \delta$ peak by 5 °C for both VE 828 and VE 160 but in an opposite direction. The increase in crosslink density, which usually results in the increase of T_g , is accompanied with the observations that the $\tan \delta$ broadens and decreases in height. As demonstrated in Figure 14, VE160 exhibits much lower peak height and increased peak breadth compared with VE828, and correspondingly, higher crosslink density and higher T_g .

Additionally, cure at 140°C results in a noticeable decrease in peak height and hence an increase in T_g for VE160, whereas for VE828, there shows an inverse change.

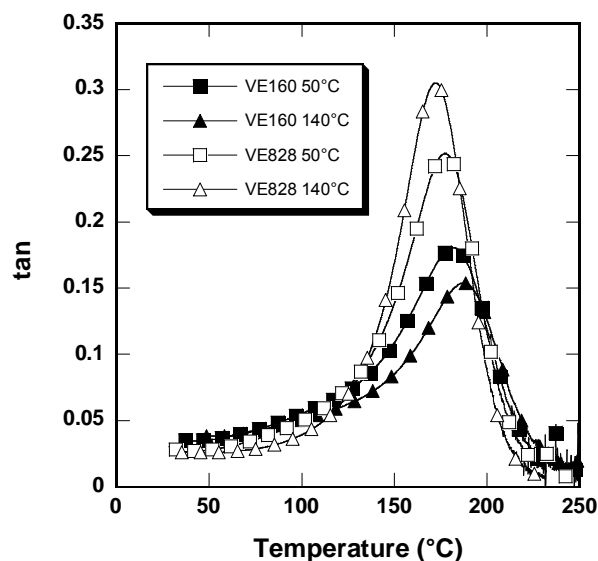


Figure 14. Damping peak ($\tan \delta$) of VE160 neat resin cure at 50°C and 140°C respectively. Lower peak height and broadened peak implies higher crosslink density.

T_g s, as indicated by the peak in E'' for both VE828 and VE160 are lower than expected, especially for VE 160 which possesses multi-functionalities. It is believed that the lower T_g is the result of incomplete reaction caused by vitrification effect and/or ‘topological restraint’, where reactive groups are spatially isolated from other reactive groups in the network. The dynamic mechanical behavior described is a combination of two factors, crosslink density and plasticization. The more functionalities associated with VE160 improves the crosslink density as demonstrated in Figure 14. The broader peak in E'' of VE160 is attributed to the broader MW distribution and worse network structure of the cured VE160 implying VE160 with more functionalities suffer from vitrification effect in a greater extent. The addition of even small amounts of plasticizer to polymers has been known to drastically broaden the transition from glassy to rubbery and reduce the overall modulus. Meanwhile, the plasticizer will introduce free volume and enable the network to deform more easily. As a consequence, the T_g is greatly reduced. The incomplete structures in both VE828 and VE160 act in the same manner as a plasticizer and reduce the T_g s drastically, which happened to VE160 more substantially leading to the similar T_g to VE828. For VE828, curing at higher temperature leads to higher conversion but lower crosslink density and hence lower T_g . This shows that besides the monomer

conversion, structure of network also play a very important role in governing the T_g of the cured resin.

Influence of Styrene and MOct on the Dynamic Mechanical Behavior of VE Resins Increasing cure temperature and adding reactive diluents are the two common methods employed to overcome the vitrification effects by changing the aggregation state of resin monomer and diluting the viscosity of resin system. As demonstrated in the preceding section, increasing cure temperature does not exhibit noticeable influence on the cure of such VE resins. Accordingly, in the following sections, the influence of reactive diluents of styrene and MOct are investigated by examination of the dynamic mechanical behavior of the mixtures comprised of VE160, VE828 respectively with varying amount of reactive diluents.

The loss moduli, E'' , of the VE 160 and VE 828 resins with different amounts of styrene, are shown in Figure 15 and 16, respectively. A minor relaxation occurs in the range of 50-100 °C, implying separated network structure formed. The dominate glass transitions, corresponding to T_g , for VE resins diluted with styrene becomes much narrower. The E'' peak values of various combinations, are summarized in Table 5, ranging from 140 °C to 160°C. As shown in Figure 17, in the current styrene content range, the dependency of E'' peak value on styrene content for VE 160 appears to be fairly linear, inversely proportional to the amount of styrene present. Whereas for VE 828, there exists a maximum peak value at a styrene content of 35%.

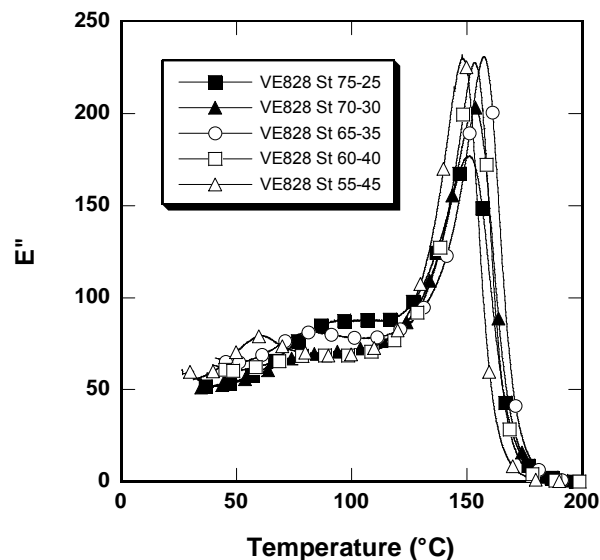


Figure 15. Loss modulus (E'') of VE systems comprised of VE828 and varying amount of styrene cure at room temperature. Much narrowed E'' peaks reveal that the VE828 conversion is higher improved in the presence of styrene, along with the T_g indicated by the peak in E'' .

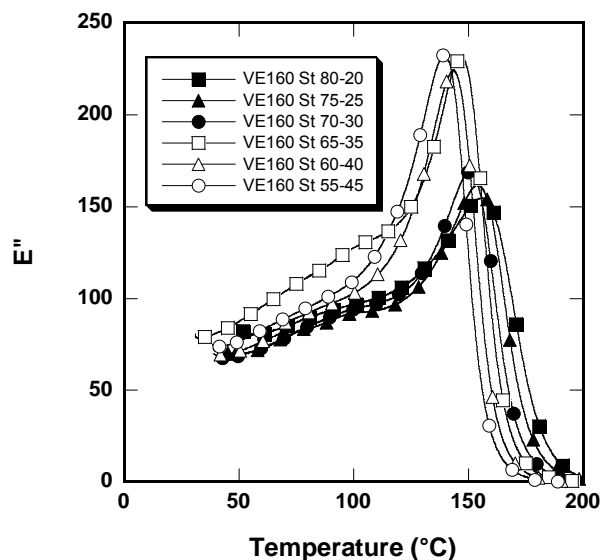


Figure 16. Loss modulus (E'') of VE systems comprised of VE160 and varying amount of styrene cure at room temperature. Much narrowed E'' peaks reveal that the VE160 conversion is higher improved in the presence of styrene, along with the T_g indicated by the peak in E'' .

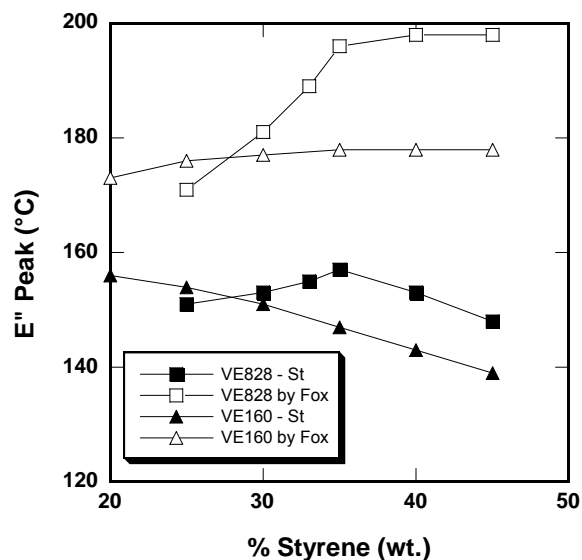


Figure 17. Peak temperatures for E'' for various compositions of VE828 and VE160 with styrene copolymer and the derived maximally attainable T_g s (E'' peak) of VE 828 and VE160 by Fox equation.

For a comparison, the loss moduli, E'', of the VE160 with different amounts of MOct, are shown in Figure 18. With MOct replacing styrene, the transition peaks becomes broader and T_g of the same composition exhibits a lower value as shown in Table 5.

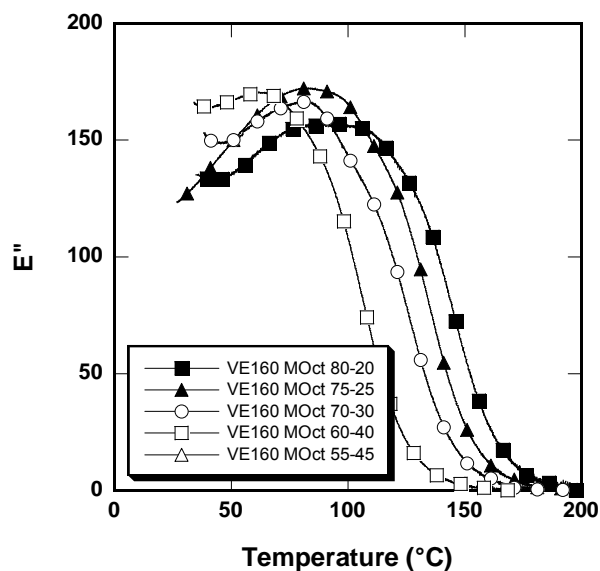


Figure 18. Loss modulus (E'') of VE systems comprised of VE160 and varying amount of MOct cure at room temperature.

Table 5. Peaks in E'' and tan δ , corresponding to T_g , for compositions of VE160 and reactive diluent copolymers and maximally attainable T_g (E'' peak) of VE160 by Fox equation.

VE/diluents ratio	E'' peak (°C)	tan δ peak (°C)	Maximally attainable Tg (E'') by Fox equation (°C)
VE828-St 100/0	148^a 149^b	172^a 177^b	148
VE828-St 75/25	151	163	171
VE828-St 70/30	153	164	181
VE828-St 67/33	155	165	189
VE828-St 65/35	157	167	196
VE828-St 60/40	153	163	198
VE828-St 55/45	148	158	198
VE160-St 100/0	140~150	182^a 187^b	
VE160-St 80/20	156	172	173
VE160-St 75/25	154	168	176
VE160-St 70/30	151	164	177
VE160-St 65/35	147	159	178
VE160-St 60/40	143	156	178
VE160-St 55/45	139	152	178
VE160-MOOct 80/20	96	148	144
VE160-MOOct 75/25	86	139	144
VE160-MOOct 70/30	83	130	158
VE160-MOOct 60/40	66	113	165
VE160-MOOct 55/45	56	105	163

Fox relation can be considered to characterize in a very rough approximation the additive behavior of the glass transition temperature of the one-phasic two component polymeric systems. Its mathematical expression is given as Equation 1.

$$\frac{1}{T_g} = \frac{w_1}{T_{g1}} + \frac{w_2}{T_{g2}} \quad 1$$

Where w_1 , w_2 are weight fractions of each component, T_{g1} , T_{g2} are glass transition temperatures of each component in K.

To clarify the influences of reactive diluents on the dynamic mechanical behavior of VE160, presumed E'' peak temperature of VE160 were calculated by Fox equation based on the dominate E'' peak of VE160-diluent systems, which can be, on the other hand, regarded as the maximally attainable T_g of VE160 in each composition under current cure conditions. The calculated T_g s are summarized in Table 5 as well. The derived T_g s against the reactive diluent content are plotted and shown in Figure 21. It can be seen that the derived T_g s of VE160 increases significantly with the addition of styrene in view of 140~150°C of T_g of neat resins, implying the increased conversion of VE160 monomers in the presence of styrene. Increasing amount of styrene does not show a significant influence on the VE160 T_g in the current content range. The lowest T_g with styrene content of 20% is 173 °C and the maximum T_g is 178 °C when the styrene content exceeds 35%. Whereas with MOct as reactive diluent, at low content of 20%~25%, the calculated T_g of VE160 is 144°C, which is similar to the T_g of neat resin and 30°C lower than that from VE160-St at same content. Increasing MOct amounts improve the T_g value of VE160 derived from Fox equation significantly, from 144°C to 165°C, corresponding to MOct content of 20% and 40% respectively. The discrepancy in the T_g s of VE160 associated with two diluents may be attributed to the difference in the solubility and/or mobility associated with two diluents, which result in the difference capability of diluents in overcoming vitrification effect. In other words, higher conversion of VE160 can be realized only in the higher amount of MOct due to the lower solubility and mobility of MOct. Meanwhile, styrene characterized with smaller molecular size and higher mobility may overcome 'topological restraint' associated with VE160 network more easily.

Tan δ graph of the aforementioned VE-diluent systems are shown in Figure 19 and Figure 20 respectively. It can be seen the lower styrene content copolymers have a higher crosslink density. This happens to VE160-MOOct systems as well but in a less appreciable manner. Additionally, the peak heights, corresponding to crosslink density, shows a pronounced correlation with the temperature where peaks occur, corresponding to the T_g , indicating higher crosslink density leads to higher T_g . A linear dependency of T_g on composition, decreasing with the amount of styrene and MOct present in the system, is illustrated in Figure 21. One important observation is the VE160-MOOct systems possess higher crosslink density compared to VE160-St reflected by lower tan δ peak height as well as increased peak broadness. The higher crosslink density associated with VE160-MOOct may be due to the diminishing of the network heterogeneity which is very prominent with the VE-St system.

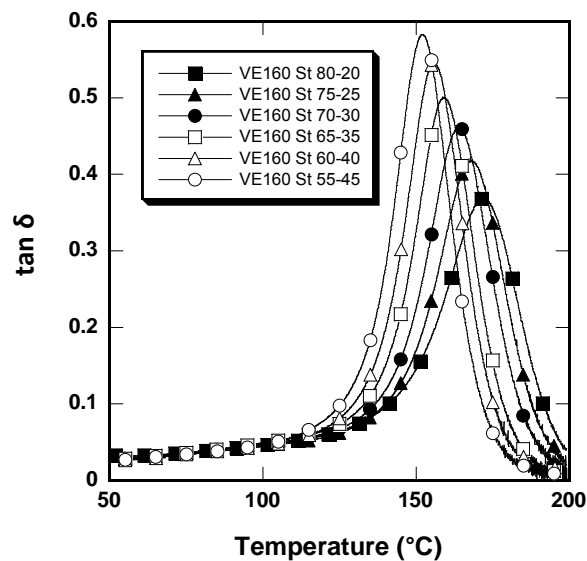


Figure 19. Damping peak ($\tan \delta$) of compositions of VE160 with varying amount of styrene. Increasing styrene amount increases the peak height consistently.

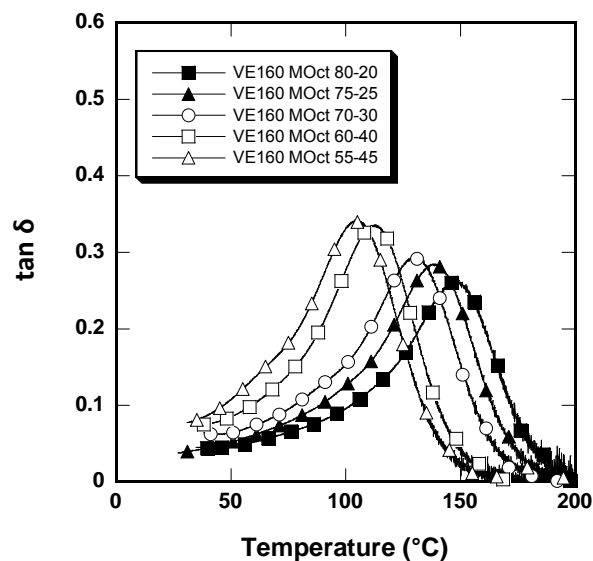


Figure 20. Damping peak ($\tan \delta$) of compositions of VE160 with varying amount of MOct. Similar peak height trend with respect to diluent amount exists. The overall peak height of VE160-MOOct is lower than that of VE160-St, indicating the higher network crosslink density in the presence of MOct.

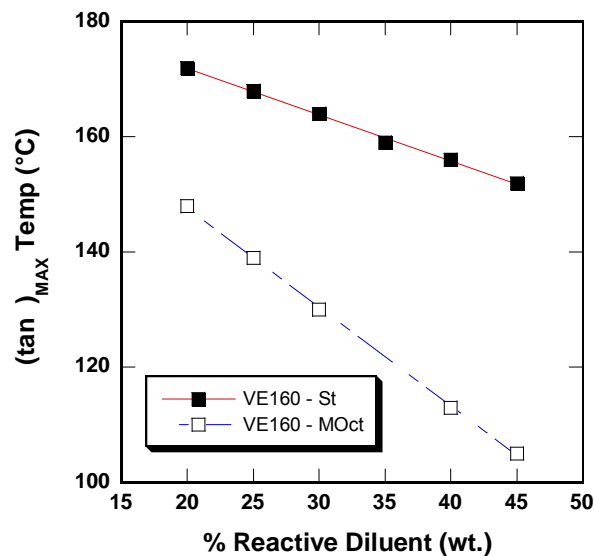


Figure 21 Peak in $\tan \delta$ as a function of reactive diluents content

For mimic the low VOC resins, systems of VE160-St, with weight ratio 70/30 and 65/35 respectively, were thus modified by replacing styrene with a varying amount of MOct. The detailed compositions are summarized in Table 6, along with the temperatures where E'' peak and $\tan \delta$ peak occurs, as well as the maximally attainable T_g s of VE160 derived from each composition by Fox equation.

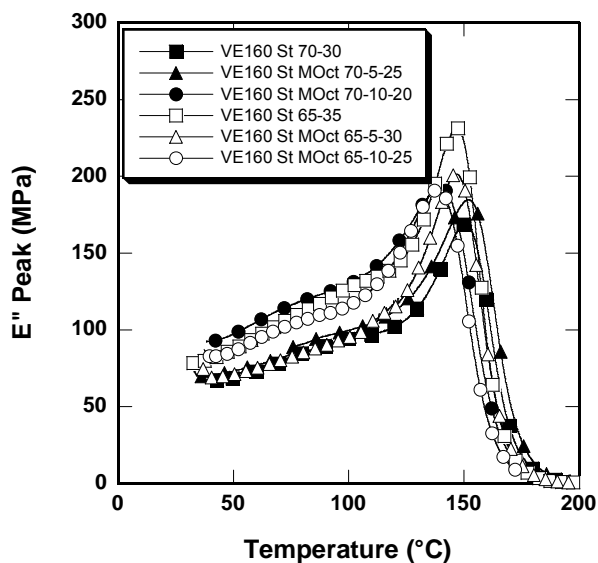


Figure 22. Loss modulus (E'') of VE systems comprised of VE160 and varying amount of MOct and styrene cure at room temperature.

Table 6. Peaks in E'' and $\tan \delta$, corresponding to T_g , for compositions of ternary VE resin systems comprised of VE160, styrene and MOct as well as maximally attainable T_g (E'' peak) of VE160 by Fox equation

VE/diluents ratio	E'' peak ($^{\circ}\text{C}$)	$\tan \delta$ peak ($^{\circ}\text{C}$)	Maximally attainable T_g (E'') of VE160 by Fox equation ($^{\circ}\text{C}$)
VE160-St 70-30	151	164	177
VE160-St-MOOct 70-25-5	152	165	198
VE160-St-MOOct 70-20-10	140	156	197
VE160-St 65/35	147	159	178
VE160-St-MOOct 65-30-5	147	159	198
VE160-St-MOOct 65-25-10	139	154	204

It can be seen from Figure 22 clearly that an addition of a small amount of MOct (5%) to the binary VE160-St resin systems does not impart the reduction in T_g though a extremely low T_g of -20°C is associated with MOct. Moreover, with the addition of MOct, the maximally attainable T_g of VE160 is highly improved, from 177°C to 204°C , indicating a synergistic effect arise from the concurrent use of styrene and MOct to modify VE160 resin which leads to higher conversion of monomers and improved network structure. The improvement in crosslinking density after adding of 5% MOct is reflected in the marked decrease in the $\tan \delta$ peak height as illustrated in Figure 23. Moreover, the peak height will experience another slight decrease with further addition of another 5% of MOct.

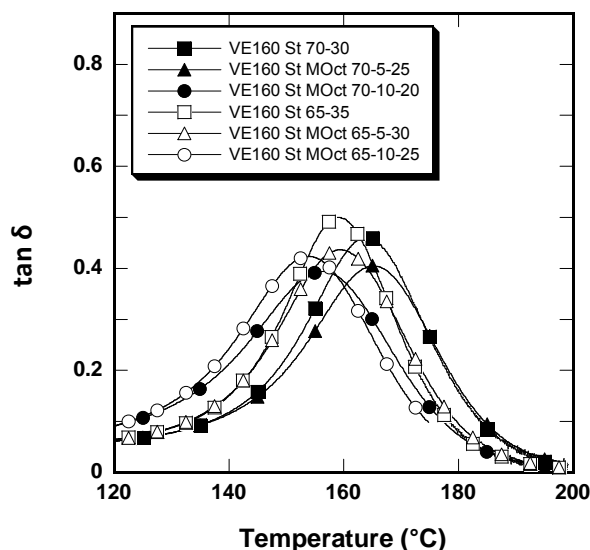


Figure 23. Damping peaks ($\tan \delta$) of ternary VE160 resin systems together with those of the binary counterparts. Apparently, with the addition of MOct, the crosslinking density of network increased.

T_g Predication of Low VOC VE Formulations Aided by Fox Equation To mimic the situations of designing low VOC high T_g VE formulations based on commercial resins, DGEBA type and Novolac type of VE, namely VE 828 and VE160 respectively, were mixed with styrene and MOct according to the compositions given in Table 7. Fox equation is employed to predict the T_g of designed resin systems based on the T_g of monomer components. As shown previously, the T_g of VE160 is designated as 200°C after averaging the obtained maximally attainable T_g in the presence of MOct and styrene. T_g of VE828 is 192°C based on the proceeding study. It can be seen that the predicated T_g match favorably with the measured T_g , designated as the temperature where E'' peak occurs.

Table 7. E'' peaks, corresponding to T_g , of quaternary VE resin system comprised of VE160, VE828, styrene, and MOct as well as the predicated T_g s for each composition by Fox equation

VE/diluents ratio	Theoretical T_g based on E'' peak by Fox equation (°C)	Measured E'' peak of resins (°C)
VE160-VE828-St-MOct	151	152

40-30-25-5		
VE160-VE828-St-MOct	140	140
40-30-20-10		
VE160-VE828-St-MOct	150	150
30-40-25-5		
VE160-VE828-St-MOct	139	140
30-40-20-10		

4.7 Development of Near FTIR Technique for Measuring Cure Kinetics of Vinyl Ester Resin

Summary

Studying the cure kinetics of vinyl ester resins is critical in determining the appropriate processing variables for the cure of improved VE resin systems. The extensively used method nowadays is mid-FTIR (MIR) which has some disadvantages including expensive tooling, difficulty in keeping sample thickness uniform and inability to prevent evaporation of styrene, especially at elevated temperatures. It was shown in this study that the near infrared (NIR) region can be used successfully for studying cure kinetics of VE resin systems. Additionally, cheap glass tubes can be used in this technique to prevent evaporation of styrene monomer by sealing both ends. However, the shortcoming associated with this technique is the overlapping of the two functionality peaks of vinyl ester and styrene appearing at 6164 cm^{-1} and 6134 cm^{-1} respectively that prevent accurately measuring the peak heights. The purpose of this study is to develop an effective method to deconvolute the two overlapping peaks using peak-fitting software. The created symmetrical data provides a constant baseline for the peaks to be fitted upon. The validity of this method was demonstrated by comparing the results with those obtained from MIR technique. Resulting conversion data was almost identical with a slight increase in deviation as the styrene concentration decreased. Reactivity ratios, reaction rate constant and reaction order were calculated from the fractional conversion data. The reactivity ratios of styrene (r_s) were 0.17 and 0.23 from the NIR and MIR respectively and those of vinyl ester (r_{ve}) were 0.30 and 0.21 from the NIR and MIR method respectively. The reactivity ratios of two monomers indicate that a pseudo-alternate copolymer was formed after cure. The rate constant showed a direct dependence on concentration; increasing as styrene concentration decreased. The rate constant and reaction constants obtained from the two techniques were about the same for resin systems containing 50 wt % and 40 wt % styrene, respectively. Subsequently, cure kinetics of FAVE-O-25s was studied. Conversion, reaction rate constants and reaction order were obtained at four different temperatures using the NIR technique developed in the proceeding

study. Activation energy of VE double bond and styrene double bond is 57.9 kJ and 52.1 kJ respectively.

Development of NIR technique The region of $14,000\text{ cm}^{-1}$ to $4,000\text{ cm}^{-1}$ is referred to as the near infrared (NIR) region. The NIR spectrum is composed mainly of absorptions based on bonds containing hydrogen atoms (C–H, O–H, N–H). The NIR combination bands are particularly useful sources of chemical information since unresolved overlapping absorptions in the mid-IR can often be distinguished in this region. Because of the low absorptivities over the NIR frequency range, relatively thick specimen pathlengths (typically 1–10 mm) are required for adequate transmission mode spectra. The particular groups of interest in this study are the C=C of VE at 6164 cm^{-1} as well as the C=C of styrene at 6134 cm^{-1} . The sample setup for this method differs slightly from that of MIR technique. Specifically, the sample is placed into a 3mm outer diameter glass tube that is then placed in the sample holder as shown in Figure 24.

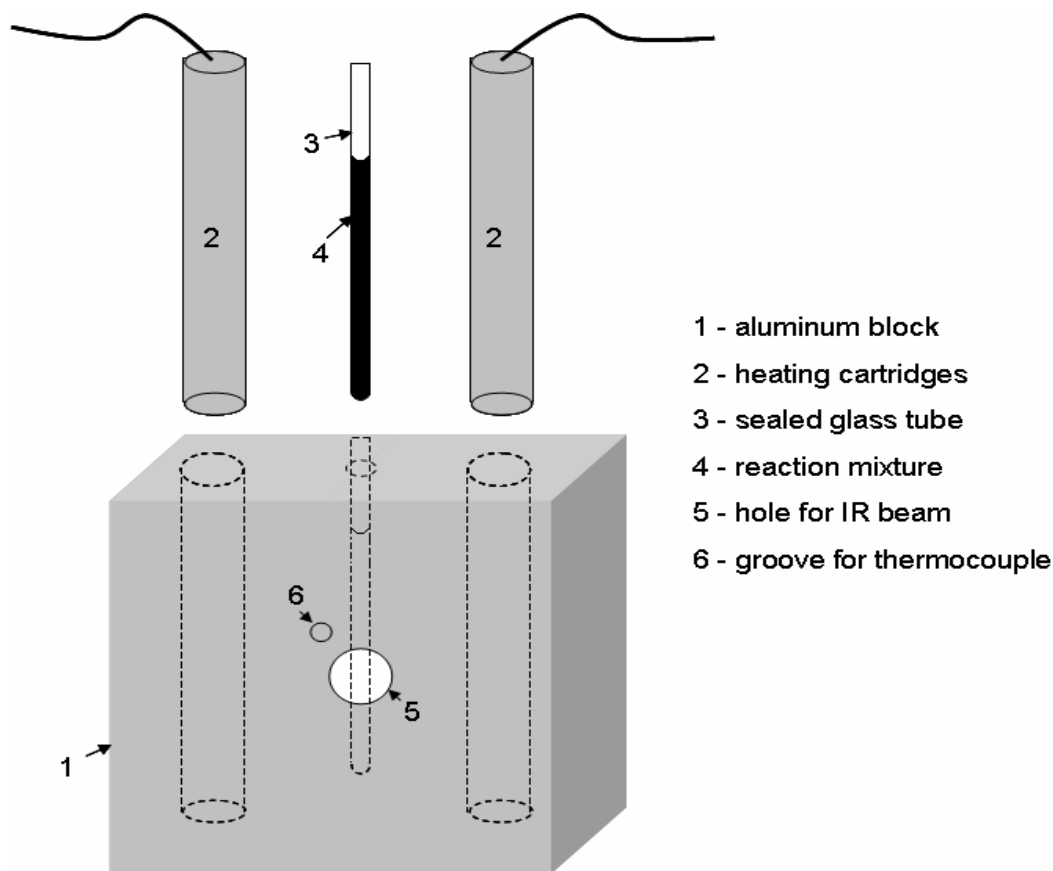


Figure 24. NIR sample holder setup

A typical Near IR spectrum of VE828 diluted in 30% styrene is shown in Figure 25. The peaks at 6164 cm^{-1} and 6134 cm^{-1} were used to follow the reaction of VE C=C with styrene C=C.

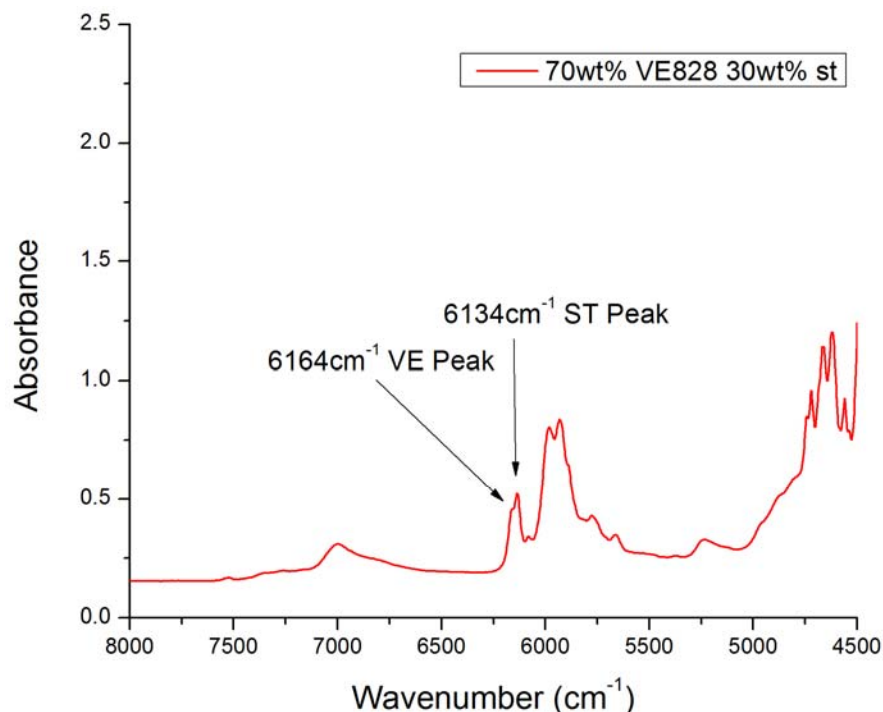


Figure 25. Spectrum of 70 wt % VE828 and 30 wt % styrene from Near IR Region

A typical MIR Spectrum of VE828 diluted in 30% styrene is shown in Figure 26 for a comparison. The peaks at 944 cm^{-1} and 910 cm^{-1} are attributed to VE C=C and styrene C=C respectively. Omnic® measuring tool was used to measure the peak heights. The baseline for the 944 cm^{-1} was selected from approximately 970 cm^{-1} to 920 cm^{-1} . The baseline selected for the 910 cm^{-1} peak was from approximately 920 cm^{-1} to 886 cm^{-1} . Reference peaks at 830 cm^{-1} for the 944 cm^{-1} peak and 700 cm^{-1} for the styrene 910 cm^{-1} peak were used as internal standards which correspond to bending of aromatic carbon hydrogen bonds within VE and styrene respectively.

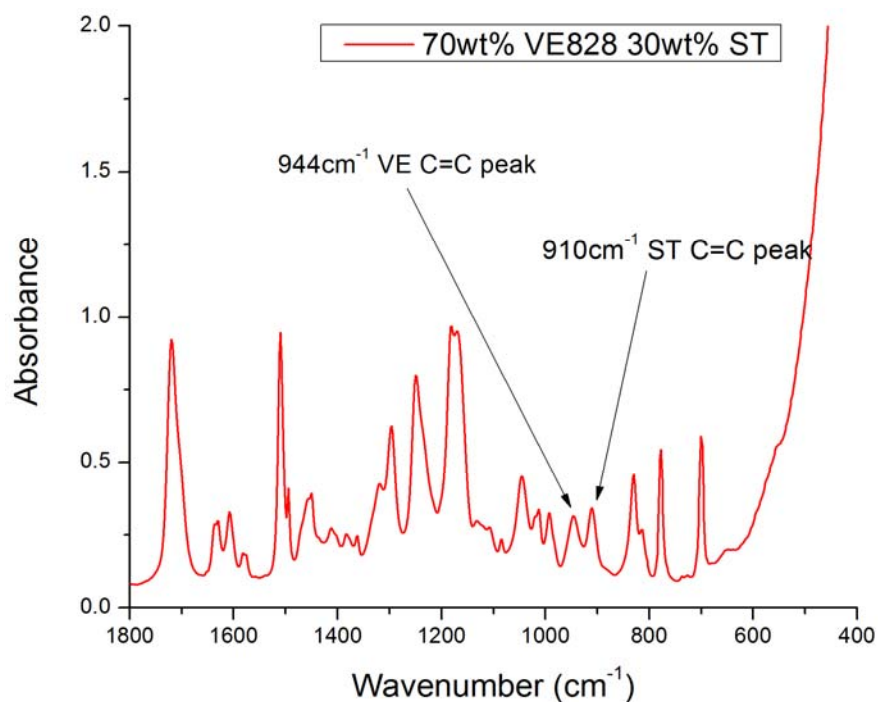


Figure 26. Spectrum of 70 wt % VE828 and 30 wt % styrene from MIR Region

For NIR spectrum, to solve the peak height measuring problem arising from the interruption of peak at 5978 cm^{-1} and the overlap of the peaks of styrene and vinyl ester, Origin 8 service release 4 peak fitting software was used to deconvolute the peaks. The spectrum from approximately 6270 cm^{-1} to approximately 5978 cm^{-1} was used. The peak at 5978 cm^{-1} was used as a point of symmetry to obtain the following spectrum in Figure 27. Data gathered from the spectrometer was exported as a CVS text file that can be opened in excel® in order to create the symmetrical data on the other half of the spectrum prior to be imported into Origin.

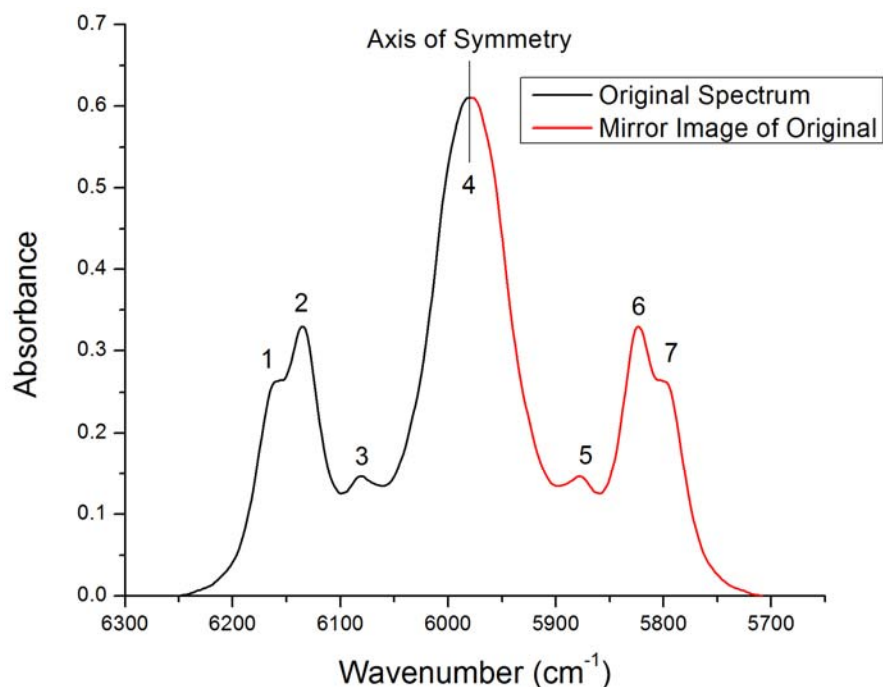


Figure 27. Manipulation of Near IR data Before Peak Fitting

Peaks were numbered from left to right. Peaks 1 and 7 correspond to the C=C of VE resin, peaks 2 and 6 correspond the styrene double bond peaks.

Origin has a built-in peak analyzer that was used to carry out the deconvolution. Upon selecting the goal of fitting peaks, there are 4 steps that the peak analyzer goes through. They included baseline mode, baseline treatment, find peaks and finally fit peaks. The baseline mode that was used was a constant Y value that is subtracted from the data that would shift the base of the spectrum to zero. During the baseline treatment stage this constant number is subtracted from the data. The third step in the process selects the number of peaks and their centers location within the spectrum being evaluated. Figure 28 is the menu for the peak analyzer during this stage and the associated preview window of the spectrum being fitted.

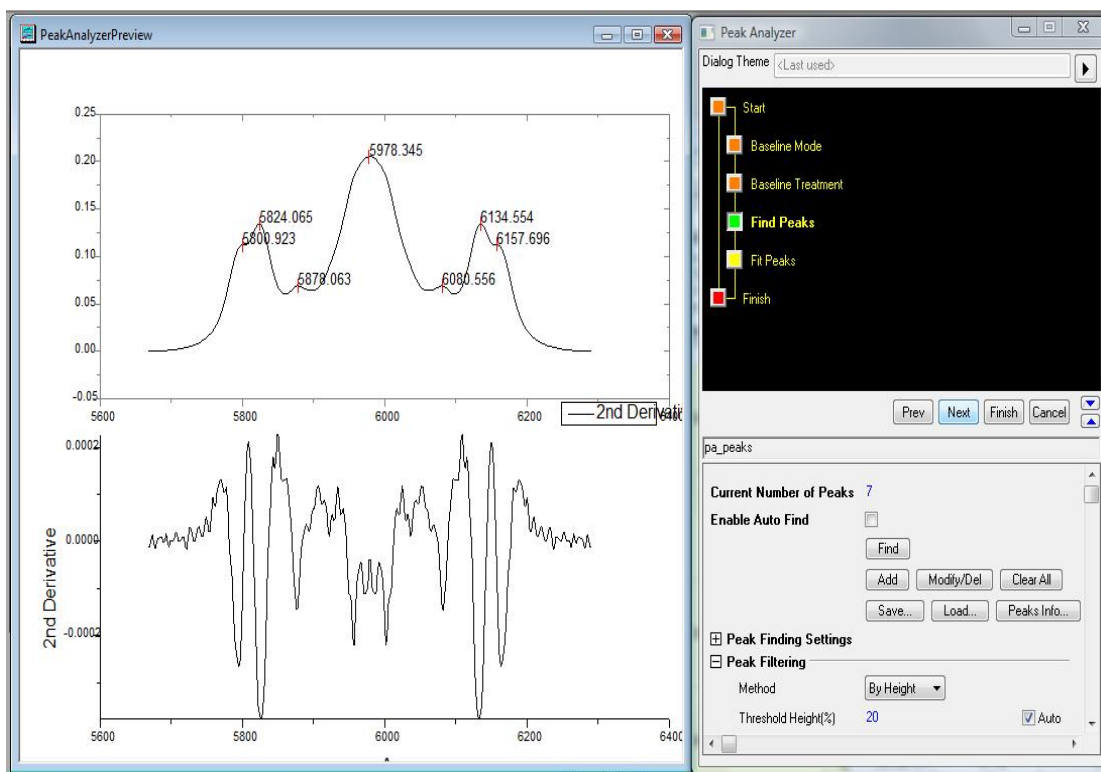


Figure 28. Peak fitting menu and preview window from Origin 8

The Find button was used to find peak centers of 2 through 6 automatically, while peaks 1 and 7 were manually added. The second derivative was used to approximate the position of peak center for 1 and 7. Once the correct number of peaks and their centers are selected then the fitting process can begin. This step utilizes the Fit Control menu to set and adjust various parameters. This menu is shown below in Figure 29.

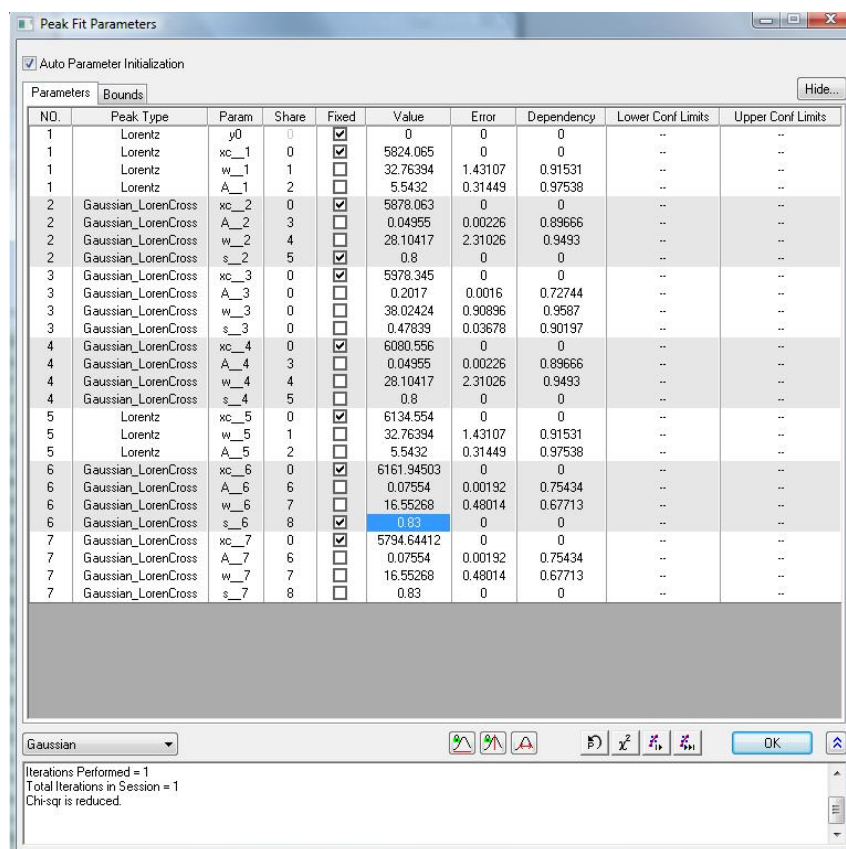


Figure 29. Fit Control Menu from Origin 8

The first parameter that can be changed is the peak type located in the second column. There is a list of built in functions that one can select. The actual selection for each peak type will be discussed in further detail in the next section. The most common functions used to fit FTIR spectra are the Gaussian function and the Lorentz function or a combination of the two functions. This combination function, or Gaussian Lorentz Cross (GLC) function, was selected for peaks 1, 3, 4, 5, 7 and the Lorentz function was determined to be the best function for the styrene peaks 2 and 6. The selection for the function chosen for each peak is discussed later.

The next column lists the parameters that define the peak. X_c refers to the peak center, w is the width at half the peak height commonly referred to as Full Width at half Max (FWHF), A is either Area as is the case with the Lorentz Function or amplitude as is the case with the GLC Function. The “s” parameter is a special parameter for the GLC Function that is between zero and one. The closer to zero the number is the more Gaussian the shape will be and the closer to one the number is the more Lorentz in shape the peak will be.

The next column labeled “share” allows different peaks to share the same value for certain parameters. This is useful when identical peaks exist. In this case there are three pairs of identical peaks; peaks 1 and 7, Peaks 2 and 6, and peaks 3 and 5. By specifying these shared parameters it aides a more precise, accurate and speed of fitting.

The column labeled “fixed” allows the particular parameter value to be locked and will not change from the specified value during the iterations. All the centers that were determined in the previous step were locked into place so that there was no shifting of peak centers. Several other parameters were also locked. The “s” parameter for peak 1 and 7 was fixed at a value of 0.83 and the width and amplitude parameters for peak 3 and 5 were fixed and manually adjusted.

The column labeled “value” displays the current value the parameter or the initial guess if coming directly from the find peaks step. It is here that one can change values and initial guesses. Problems with the analyzer converging on an answer can be solved by changing initial guesses and values within this column. Most initial guess values were left unchanged, however, in order to aid in software converging, initial values for width of peaks 1 and 7 and peaks 3 and 4 were entered corresponding to a value of 12 and 20 respectively. The “s” parameter for peaks 3 and 5 was fixed and an initial value of 0.8 was used in order to aid the initial convergence of the software. After the software was converged, the “s” parameter on peaks 3 and 5 was then unfixed and the height and width parameters were both fixed and manually adjusted as need to fit the spectrum. The final fit for a mixture of 70% VE828 and 30% styrene is shown in Figure 30.

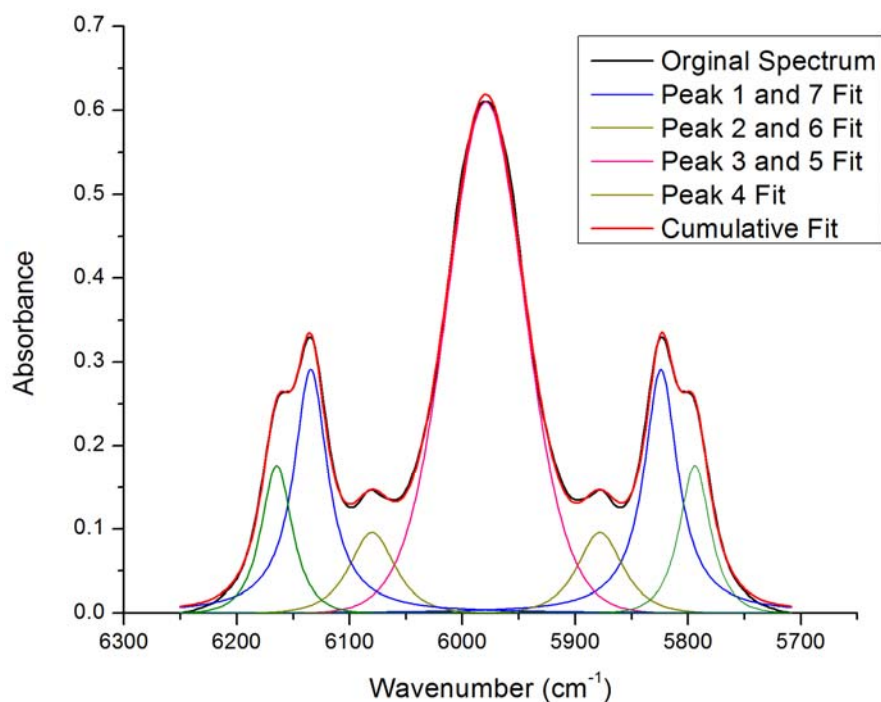


Figure 30. Peak fitting results for 70 wt %VE828 30 wt % styrene.

Peak function determination There are several fitting functions available in origin that can be used to model various peak shapes. The most common functions are the Gaussian or normal distribution function, the lorentz or Cauchy distribution, and the Gaussian Lorentz Cross (GLC). To determine the best fitting function for each peak, a pure VE828 spectrum and a pure styrene spectrum was analyzed and fitted separately using these three functions. Several different combinations of functions were tested to find the best fitting function for the respective peak. Figure 31 and Figure 32 show the two possible options, with one option only using Gaussian and Lorentz Functions and second variation including the GLC function with the Gaussian and Lorentz Functions. The fitting of pure VE828 is shown in Figure 31 using a Gaussian function on peaks 1 and 5 and Lorentz function for peaks 2, 3, and 4. Figure 32 shows the best fit using GLC Function for all three peaks.

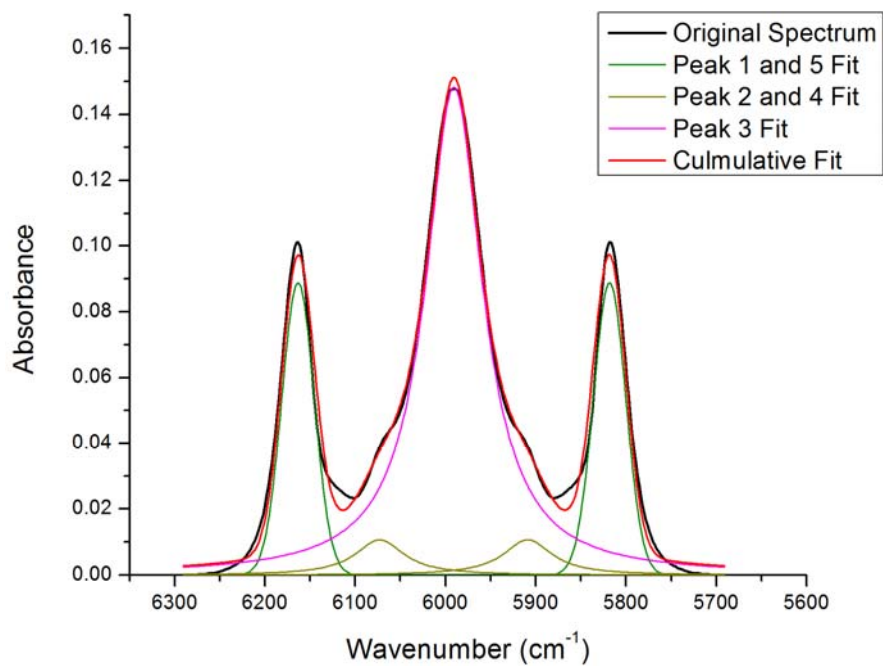


Figure 31. VE828 6164 cm^{-1} peak fitted with Gaussian function

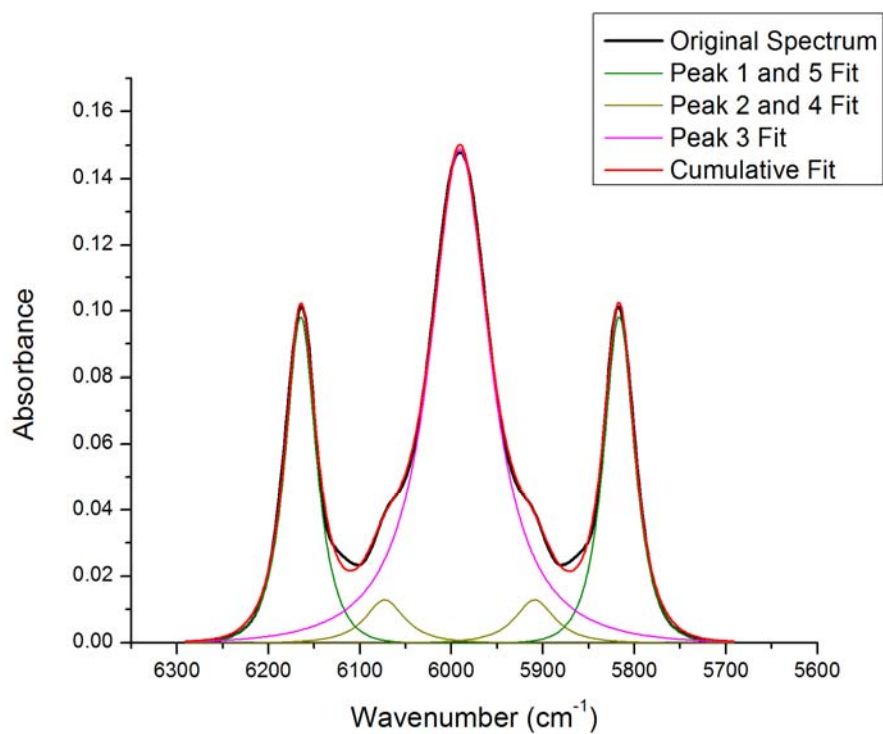


Figure 32. VE828 6164 cm^{-1} peak fitted with GLC function

The styrene peak has two adjacent peaks, one at 6081 cm^{-1} and the other at 5975 cm^{-1} , which makes it difficult to find an accurate base line. Using 5975 cm^{-1} as an axis of symmetry the resulting five peaks were analyzed using Gaussian, Lorentz, and GLC fitting functions. A spectrum using the Gaussian fitting function can be seen in Figure 33.

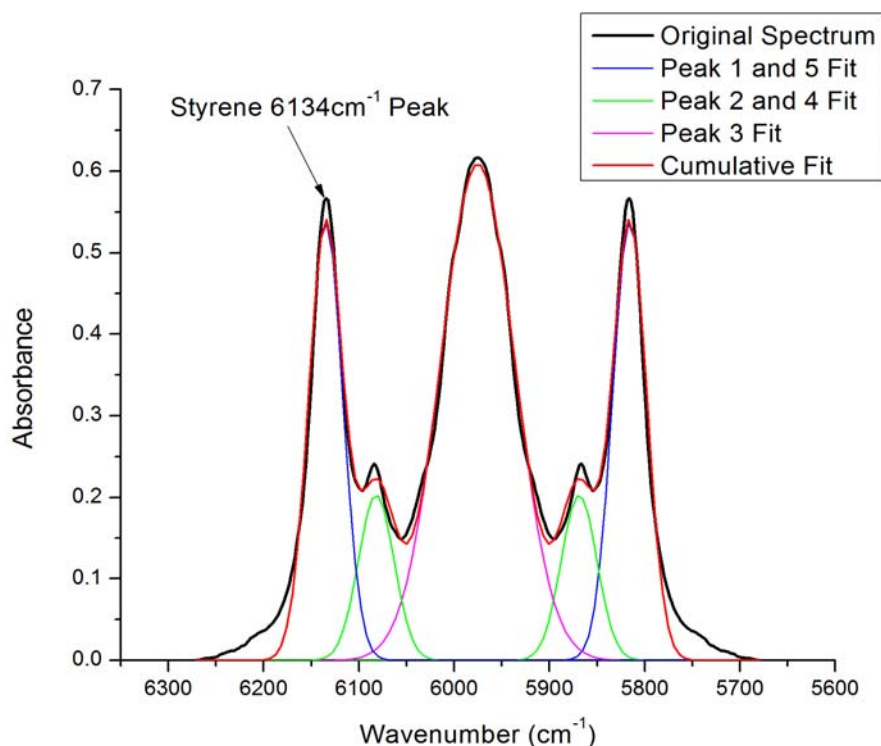


Figure 33. VE828 6134 cm^{-1} peak fitted with GLC function

The best combination for the best fit was using Lorentzian on the styrene peak at 6134 cm^{-1} and using GLC function on the 6081 cm^{-1} peak and 5975 cm^{-1} peak. The resulting fit is shown in Figure 34.

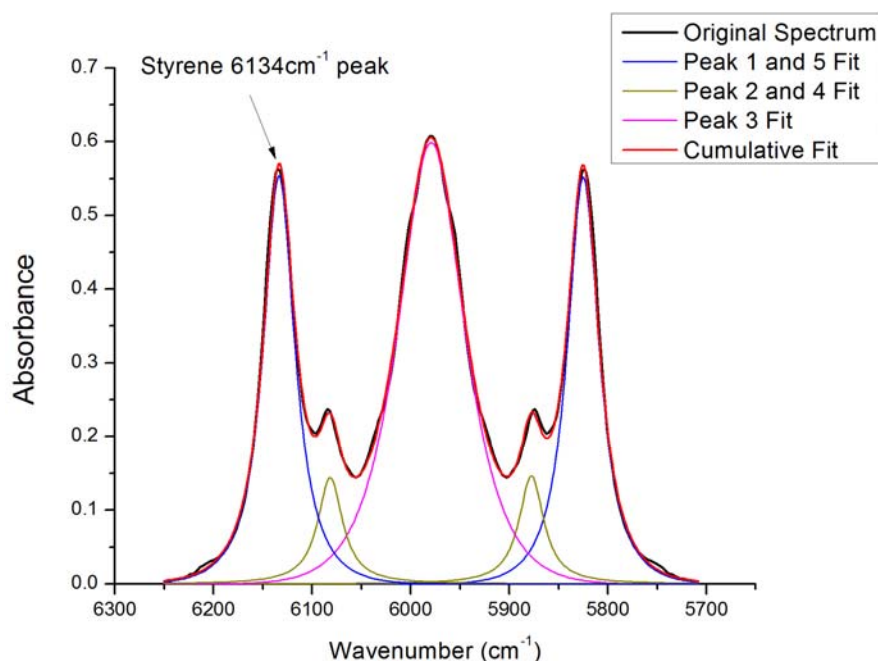


Figure 34. Styrene 6134cm⁻¹ peak fitted with Lorentz function and 6081 cm⁻¹ and 5975 cm⁻¹ peaks fitted with GLC Function

Determining the best functions for fitting each peak is important to ensure the accurate value for each peak height. Taking area from one peak will influence the area and heights from neighboring peaks. The final peak function selected for peaks 1, 3, 4, 5, and 7 of the VE828/styrene systems is the GLC function. The Lorentz function was determined to be the best fit for the styrene C=C peak at 6134 cm⁻¹.

Calibration curves Further validation and accuracy of the method was evaluated by running a set of samples of known concentrations and measuring the peak height ratio of styrene C=C to vinyl ester C=C. Taking a ratio of the two peak heights allows for a more accurate comparison of the fitted data. The premise for the usefulness of developing a calibration curve for both the MIR region and NIR region can be linked to beer's law of $A = \epsilon lc$. By taking the ratio of absorbance of the styrene (st) to VE C=C peak we obtain equation 2.

$$\frac{A_{st}}{A_{ve}} = \frac{\epsilon_{st}lc_{st}}{\epsilon_{ve}lc_{ve}} \quad 2$$

Since l is the same for a particular sample they cancel out and concentration is related to weight by $c_{st} = \frac{w_{st}}{V}$ where V is volume. Since volume is the same, it cancels out and weight of VE resin is related to the weight of styrene by $w_{ve}=1-w_{st}$ resulting in equation 3

$$\frac{A_{st}}{A_{ve}} = \frac{\epsilon_{st} w_{st}}{\epsilon_{ve} (1 - w_{st})} \quad 3$$

Graphing the weight ratio to the absorbance ratio should result in a linear line with the ratio of $\frac{\epsilon_{st}}{\epsilon_{ve}}$ being the slope of the line going through the origin. Figure 35 shows the calibration data obtained from two runs using the Near IR technique collected about one month apart using the same samples and data collected using the MIR technique. The initial NIR runs were conducted using an aperture setting of 4.

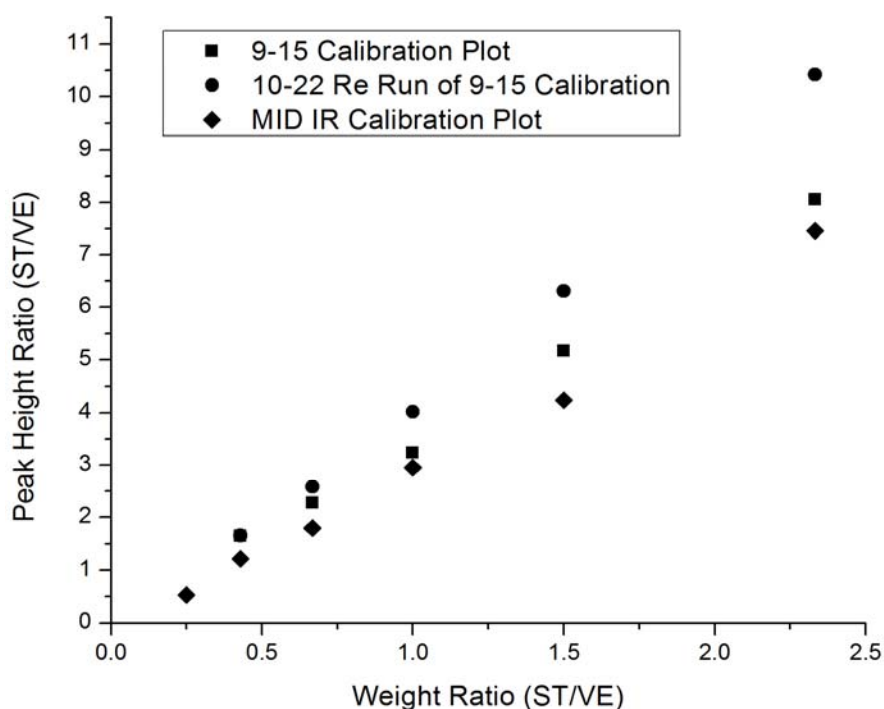


Figure 35. Calibration data using known concentrations of VE828 and styrene obtained from NIR and MIR regions

The initial run using NIR and MIR resulted in a line with a slope of 3.44 and 2.89 respectively. Taking into account the hidden peaks under the vinyl peak in the MIR of 944 cm^{-1} yields a slope of 3.05. When the NIR samples were rerun a slope of 4.41 was obtained. The difference between the two samplings was determined to be spectrometer alignment. While both runs were collected using the same settings, it was determined that the initial run was misaligned accounting for a lower range of absorbance than the second run where the spectrometer was fully aligned with the light source. The difference of these two spectra can be seen in Figure 36. Further investigation into this discrepancy is conducted in section of aperture effects.

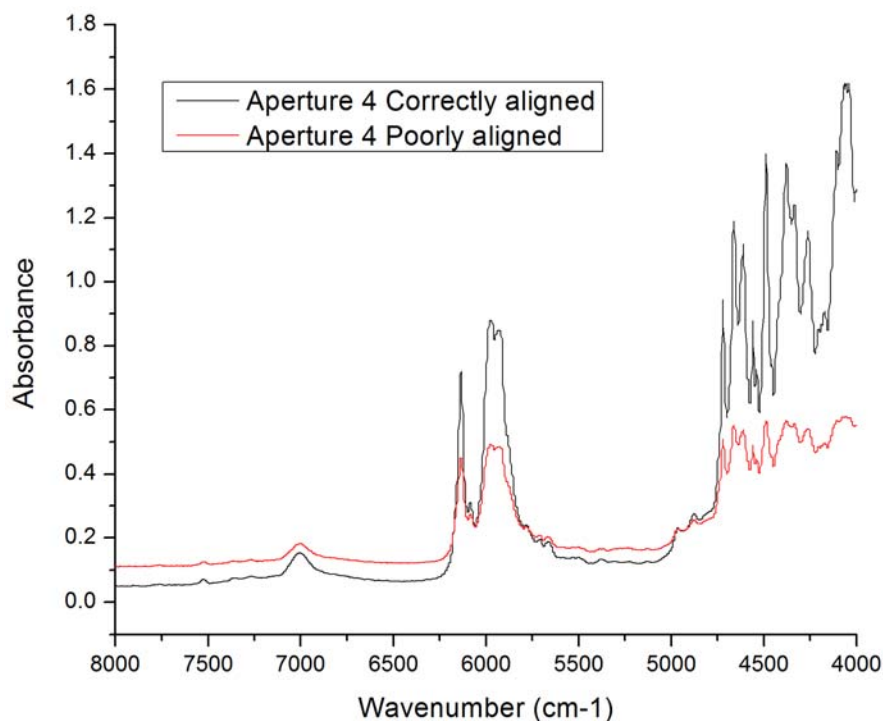


Figure 36. Sample spectra of xx wt % VE828 and yy wt % styrene showing good alignment and poor alignment conditions

A correlation between the ratio of peak area in Mid IR region and that obtained from the NIR technique were also examined, however no correlation was present. The resulting calibration data is shown in Figure 37. Therefore, peak height was used rather than peak area to calculate conversion.

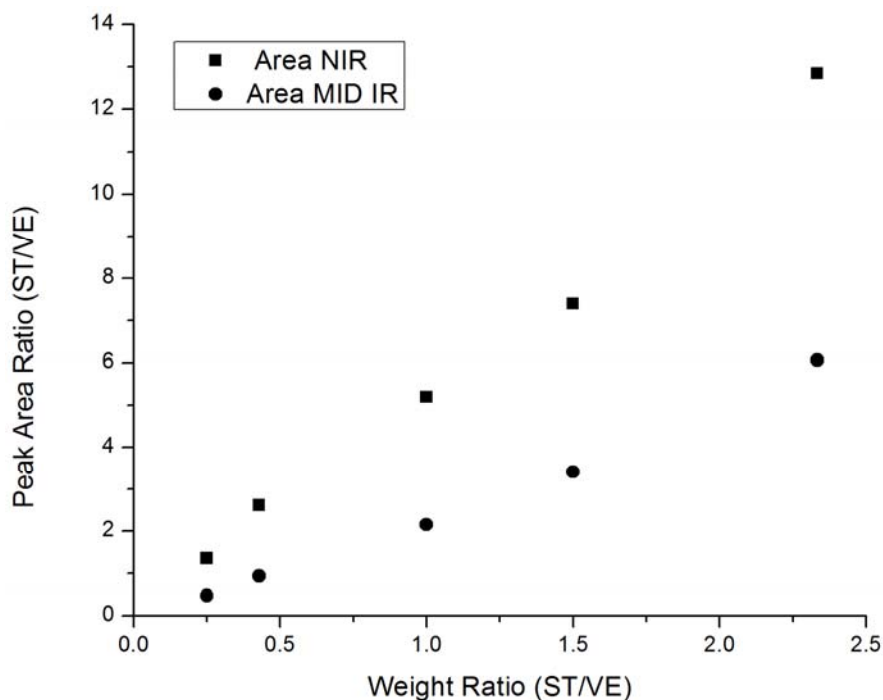


Figure 37. Plot of area ratio of ST/VE peaks comparing NIR and MIR regions

Aperture effects The alignment issue in essence has to do with how much light passes through the sample before entering the detector. The effects of which appear to have a large influence on the resulting deconvolution of the data, especially at higher concentrations of styrene. By adjusting the aperture setting while the FTIR is correctly aligned can simulate this behavior in a controlled manner. Several runs of the calibration samples were run and the results are displayed in Figure 38. As the aperture increases the slope of the resulting calibration curve decreases. The slope stopped changing once the aperture reached 50 and above, and the resulting spectrum did not change as the result of reaching a saturation of light transmittance through the sample. The resulting slope for an aperture setting of 50 and 69 was 3.15 and 3.13 respectively. Using an aperture setting below 50 would introduce variability into the results, particularly when concentrations of styrene are above 50 wt %. Using an aperture setting above 50 would expand the application range of this technique. If an aperture setting below 50 is to be used, one would either be required to limit styrene concentration to 50% and below or use a calibration curve for the particular aperture setting. An aperture setting of 69 was chosen to eliminate variability in the spectra collected and improve the consistency of the technique.

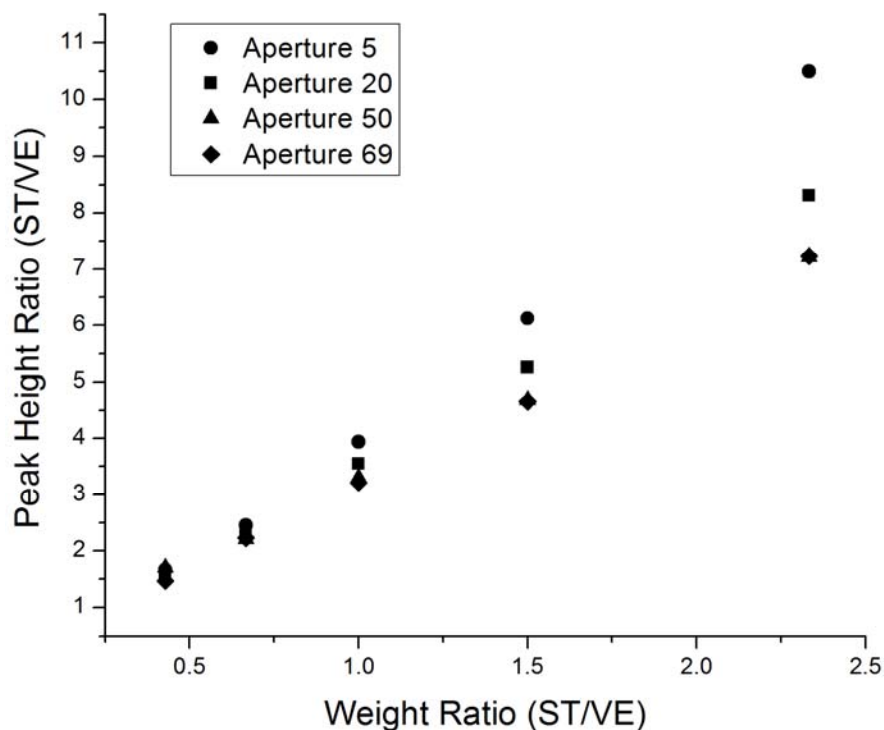


Figure 38. Calibration plot taken at four different aperture settings

Application range of the developed NIR technique The purpose of a kinetics study for vinyl ester is to ensure the cure of monomers proceed as complete as possible under proper conditions in order for the maximum performance. During the curing of VE resin systems, not only does the ratio of two corresponding peak heights change, but the ratio of them to the neighboring peaks does also, particularly for the 5978 cm^{-1} peak. The question addressed accordingly is that if this developed method is able to apply to the whole course of reaction, especially to the late stage of reaction where the intensity of absorbance is weak due to the small amount of chemical moiety. To simulate the changes of peak intensities during reaction a solvent THF was used at three concentrations of 50%, 70% and 90%, respectively. A calibration curve using known values was deconvoluted and the results are shown in Figure 39.

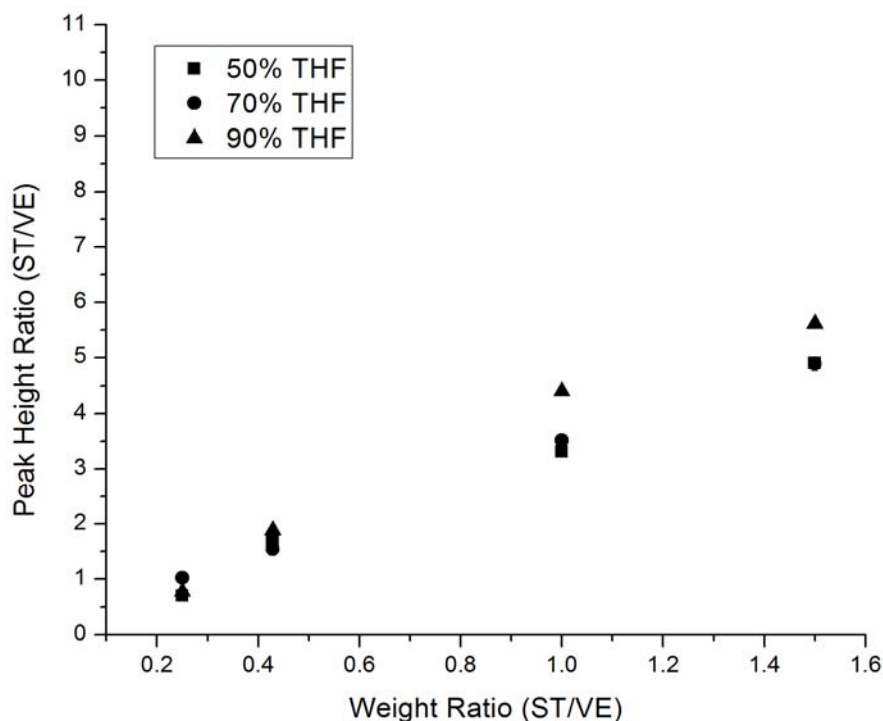


Figure 39. Calibration plots of VE828 and styrene diluted in 50 wt %, 70 wt % and 90 wt % THF.

The results show that there exists a linear relationship between the peak height ratios obtained from NIR technique and the actual weight ratios of two monomers with a slight deviation for mixtures with weight ratios of styrene to VE above 1 and THF concentration of 90%. It may thus be deduced that the developed NIR technique can be applied satisfactorily to monitor the reaction of vinyl ester resin systems during the whole course of reaction for the weight ratio of styrene to vinyl ester below 1 whereas for the weight ratio above 1, in the late stage of reaction, the weight ratio value derived from corresponding peak heights in NIR region is slightly higher than it supposed to be meaning a coefficient is needed in this case.

Using Developed Near IR Technique to Study Cure Kinetics of Model VE 828 Resin

Fractional conversion Three different concentrations of 70 wt %, 60 wt % and 50 wt % VE828 diluted in styrene were prepared. These experiments were conducted at room temperature of approximately 21°C to 24°C depending on time of day. Runs were conducted using the NIR technique and the MIR technique to compare the results accuracy. A representative

deconvolution of the initial and final spectrum of resin system containing 60% VE828 40% styrene using Origin is shown in Figure 40 and Figure 41.

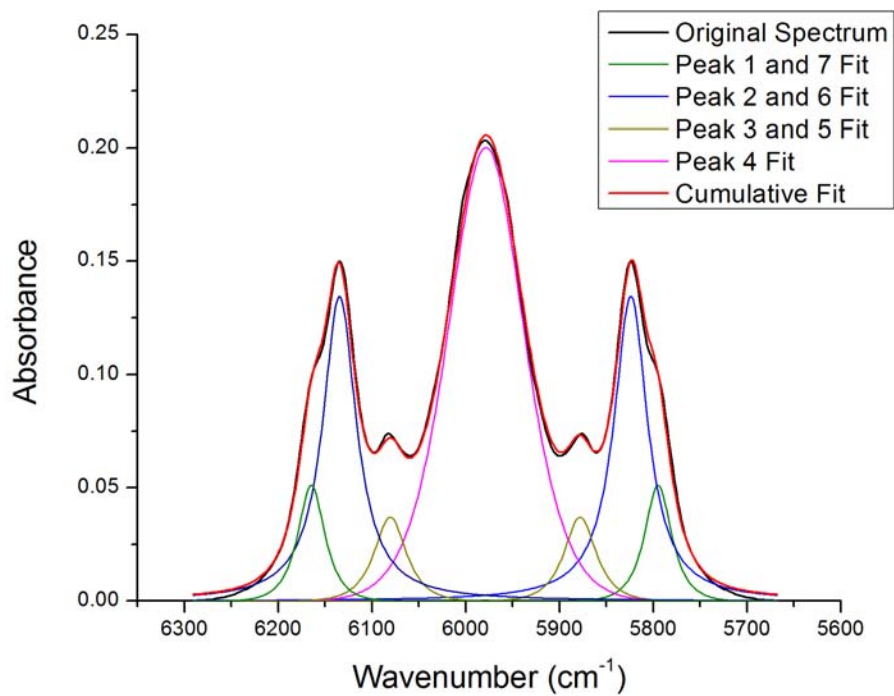


Figure 40. Peak fitting for 60 wt % VE828 40 wt % styrene at time $t = 0$ min

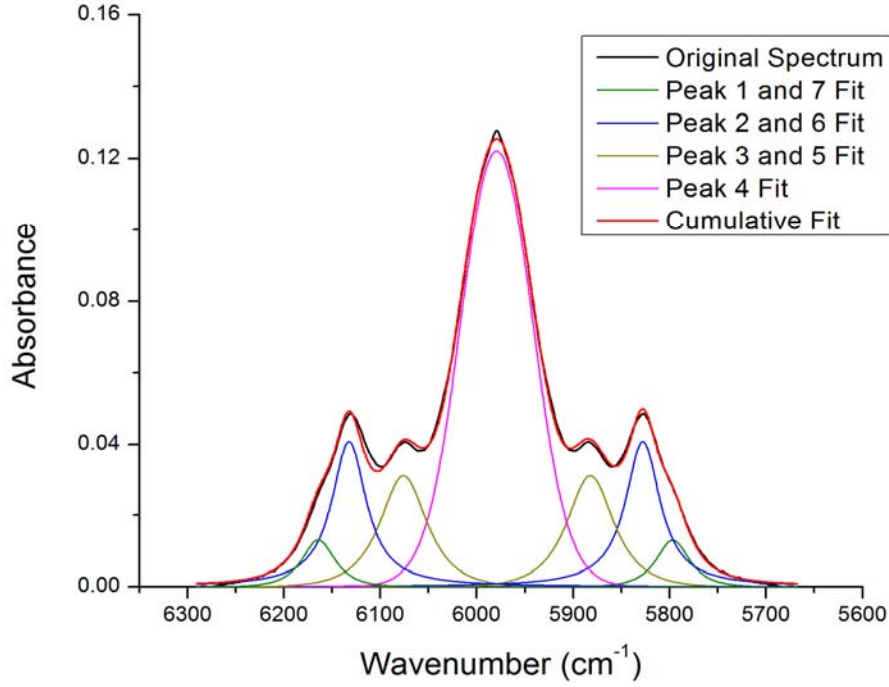


Figure 41. Peak fitting for 60 wt % VE828 40 wt % styrene at time $t = 301$ min

Peak heights were taken directly from Origin's Peak Characterization Report. The resulting absorbencies were used to calculate the normalized conversion based on equation 4a and 4b which are derived from Beer's law.

$$\alpha_{st} = 1 - \frac{ABS(t)_{6134cm^{-1}}}{ABS(t=0)_{6134cm^{-1}}} \quad 4a$$

$$\alpha_{ve} = 1 - \frac{ABS(t)_{6164cm^{-1}}}{ABS(t=0)_{6164cm^{-1}}} \quad 4b$$

Reference peaks at 830 cm^{-1} and 700 cm^{-1} were used as internal standards in the MIR technique. The equations used to calculate the normalized conversions are listed in equation 5a and 5b.

$$\alpha_{st} = 1 - \frac{ABS(t)_{910cm^{-1}}}{ABS(t=0)_{910cm^{-1}}} \cdot \left(\frac{ABS(t=0)_{700cm^{-1}}}{ABS(t)_{700cm^{-1}}} \right) \quad 5a$$

$$\alpha_{ve} = 1 - \frac{ABS(t)_{944cm^{-1}}}{ABS(t=0)_{944cm^{-1}}} \cdot \left(\frac{ABS(t=0)_{830cm^{-1}}}{ABS(t)_{830cm^{-1}}} \right) \quad 5b$$

The data collected for the three different concentrations are shown in Figures 42 through Figure 47.

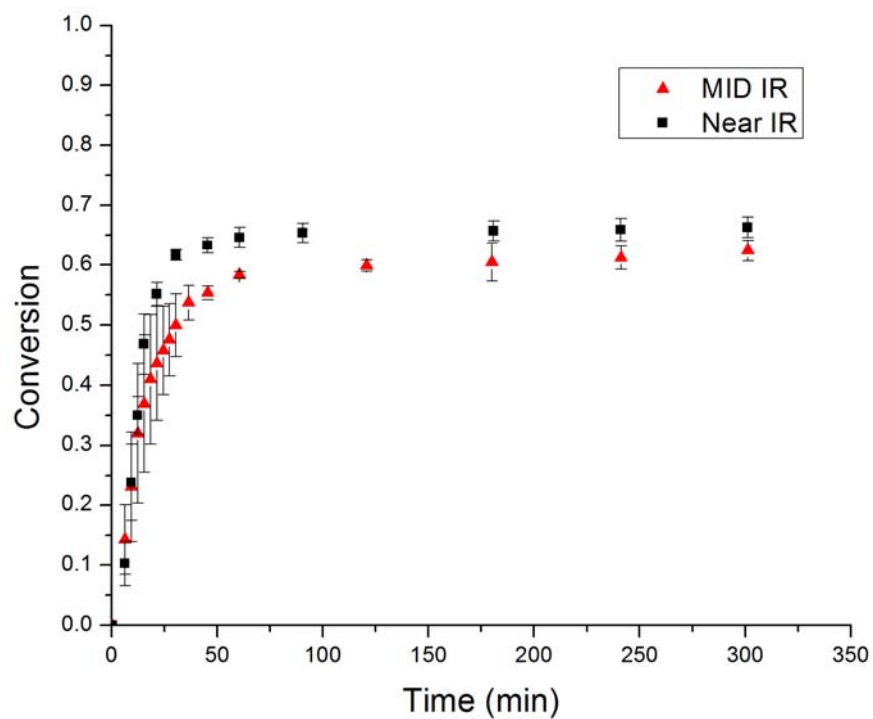


Figure 42. C=C conversion for resin system containing 70 wt % VE828 and 30 wt % styrene.

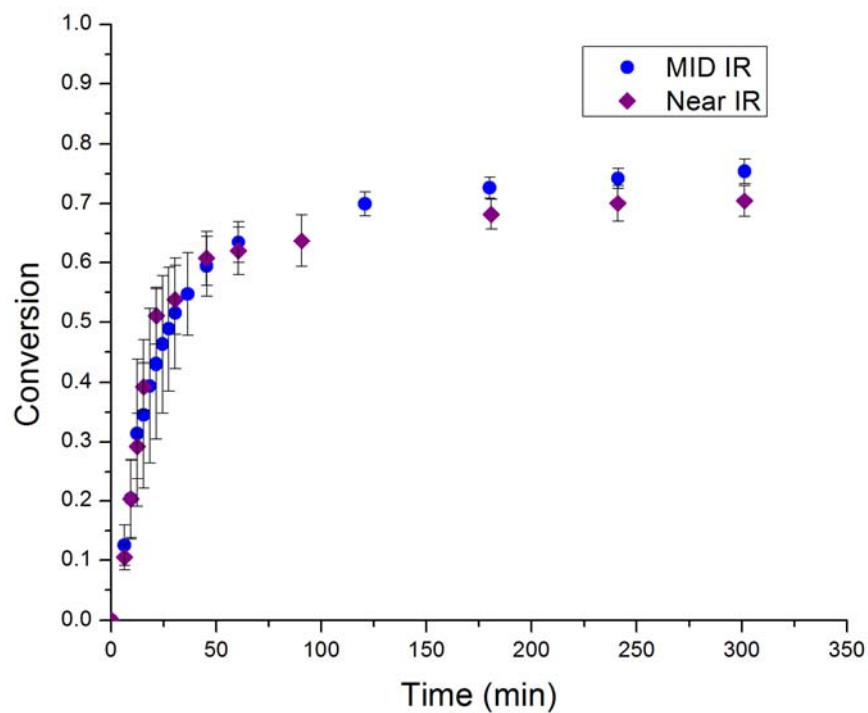


Figure 43. Styrene C=C conversion for 70 wt % VE828 and 30 wt % styrene.

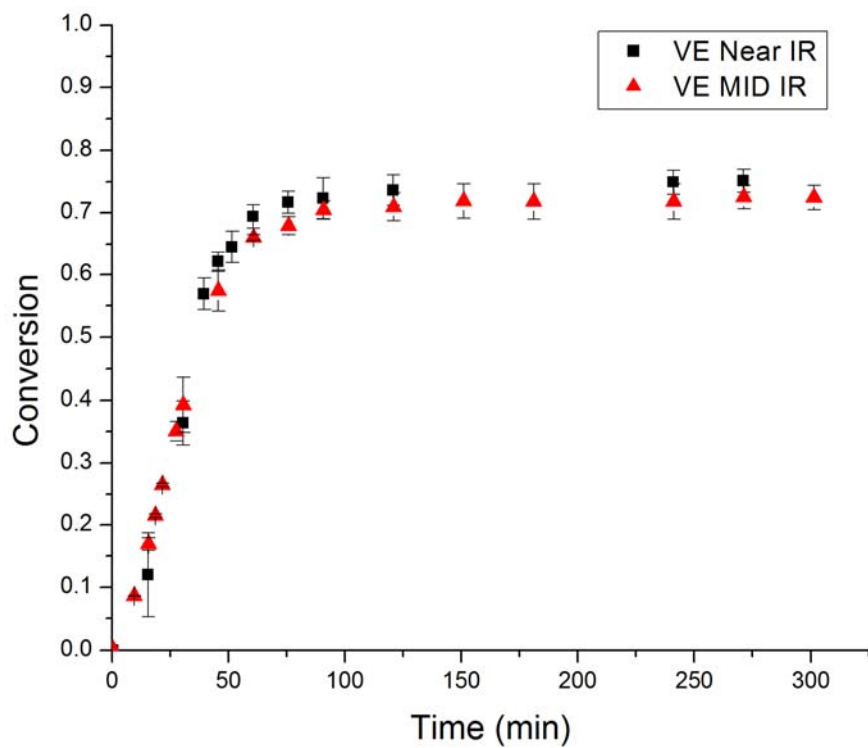


Figure 44. VE C=C conversion for mixture of 60 wt % VE828 40 wt % styrene.

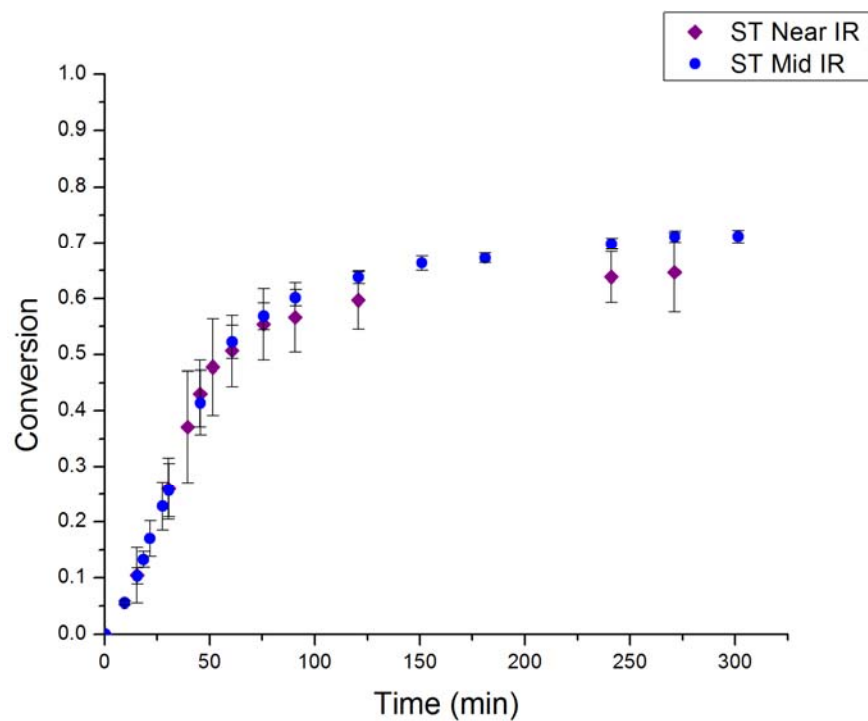


Figure 45. Styrene C=C conversion for mixture of 60 wt % VE828 40 wt % Styrene.

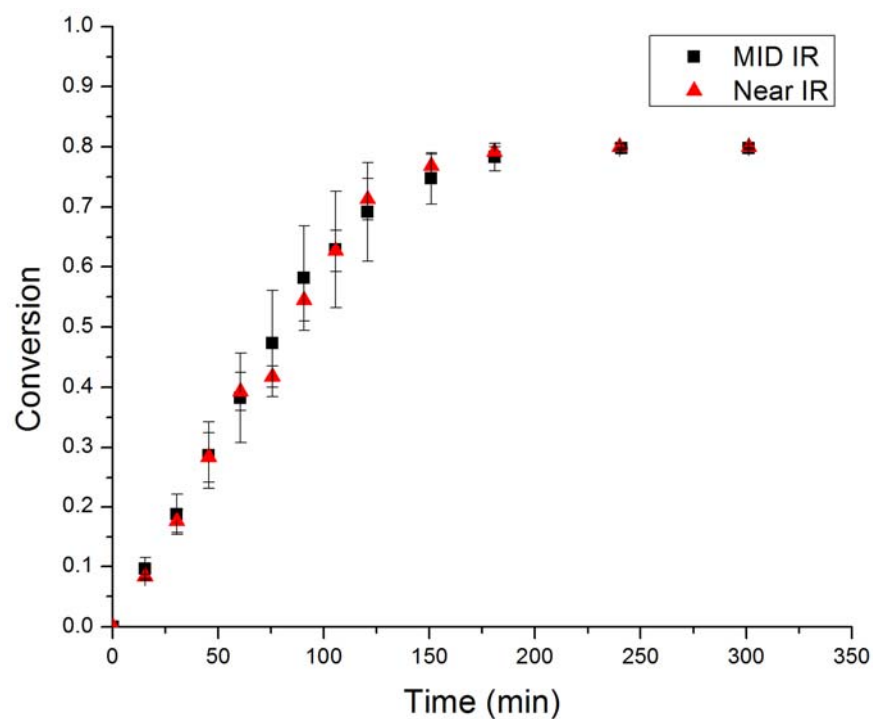


Figure 46. VE C=C conversion for mixture of 50 wt % VE828 50 wt % styrene.

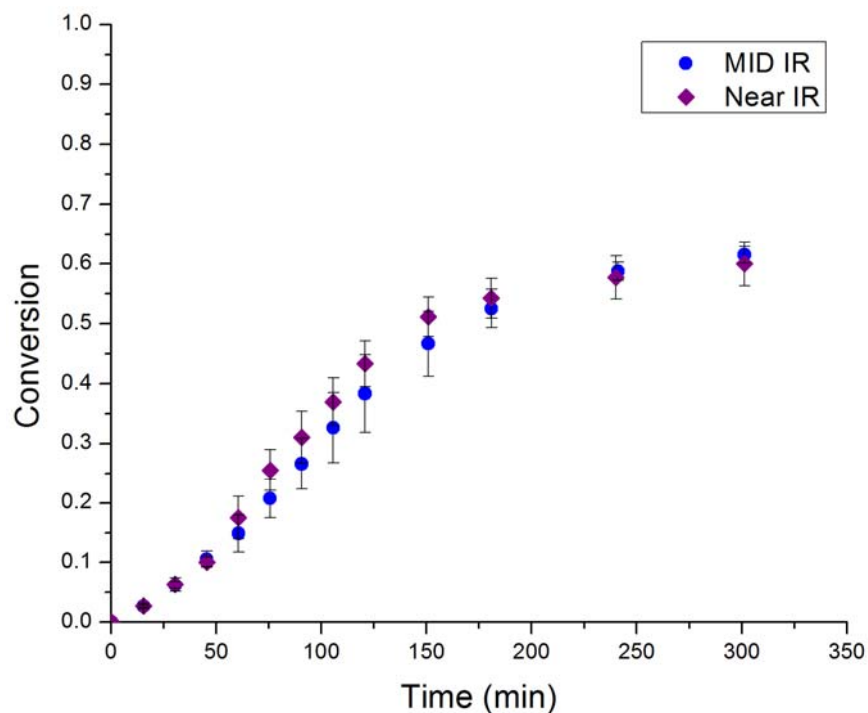


Figure 47. Styrene C=C conversion for mixture of 50 wt % VE828 50 wt % styrene.

The results are very encouraging. The graphs show the general trend for an autocatalytic reaction. An initial rapid rate of conversion followed by a slowing and leveling off of conversion is illustrated as the result of formation of polymer gel that reduces the molecule mobility. At styrene concentrations of 30 wt %, 40 wt %, and 50 wt % the results from two methods are in a good agreement. The final conversions are listed in Table 8. The agreement is best for resin system containing 50 wt % styrene where the VE C=C conversion was identical and the styrene C=C conversion was about 1% difference. The biggest discrepancy in styrene C=C conversion is with systems containing 40 wt % and 30 wt % styrene showing difference of 6% and 5% respectively. There is a clear trend that the styrene conversion increases as the VE concentration increases, while the VE C=C conversion decreases with increasing in VE concentration. This may be attributed to the decrease in mobility of the VE resin as the concentration of styrene decreases.

Table 8. Final conversion of VE828 C=C at styrene concentrations of 30 wt %, 40 wt % and 50 wt % from NIR and MIR methods

Styrene Concentration	30 wt %		40 wt %		50 wt %	
	VE	ST	VE	ST	VE	ST
NIR	0.66 ± 0.017	0.70 ± 0.026	0.75 ± 0.019	0.65 ± 0.071	0.8 ± 0.005	0.60 ± 0.037
MIR	0.62 ± 0.017	0.75 ± 0.020	0.72 ± 0.020	0.71 ± 0.011	0.8 ± 0.001	0.61 ± 0.014

There is an interesting trend with the experiment error as well. The standard deviation of data was generally large during the initial phase of reaction and was declining towards the end. This may be attributed to the fluctuation in temperature. The initial phase of the cure is highly sensitive to minor changes in temperature. Room temperature fluctuates from day to day as well as time of day. While most of these runs were within one or two degrees of each other, that much of a difference has a big effect during the initial reaction phase. Additionally the error associated with the NIR is much less than those obtained from the MIR data which constitutes another merit of NIR technique.

Autocatalytic Kinetic Model Kinetic modeling is possible from the conversion data obtain from FTIR experiments. Due to the formation of radicals in this free radical polymerization reaction, an autocatalytic model has been successfully used to obtain kinetic parameters. The basic equation that has been used for low temperature cure is listed in equation 6.

$$\frac{d\alpha}{dt} = (k_1 + k_2\alpha^m)(\alpha_{\max} - \alpha)^{2-m} \quad 6$$

This equation, however, is not useful for analyzing FTIR data as it is derived from DSC technique. A modified integrated form of this equation has been developed and is listed below as equation 7.

$$\alpha = \frac{\alpha_{\max} [kt\alpha_{\max}(1-m)]^{\frac{1}{1-m}}}{1 + [kt\alpha_{\max}(1-m)]^{\frac{1}{1-m}}} \quad 7$$

Where α is conversion, k is the reaction rate constant, α_{\max} is the maximum conversion and m is the reaction order. These parameters are very useful in understanding the rates of the particular mechanisms within this reaction. The data collected from the FTIR experiments were analyzed using Origin's nonlinear fitting tool. The resulting parameters are listed in Table 9.

Again, interesting trends can be seen from this kinetic data. The rate constant, k , increases as styrene concentration decreases. The impact of this is evident from the decrease in cure time needed for higher concentrations of VE resins. In other words, the polymer cures faster at lower concentrations of styrene. However, lower concentration of styrene is insufficient to overcome the vitrification problem associated with cure of VE which leads to lower conversion of VE.

Table 9. Kinetic parameters for VE828 for 30 wt %, 40 wt % and 50 wt % styrene from NIR and MIR technique cured at 21°C.

VE concentration		70%		60%		50%	
		VE	ST	VE	ST	VE	ST
k (min-1)	NIR	0.34	0.17	0.15	0.10	0.04	0.05
	MIR	0.22	0.11	0.12	0.07	0.05	0.04
m	NIR	0.62	0.41	0.68	0.54	0.56	0.62
	MIR	0.41	0.31	0.59	0.51	0.56	0.60
α_{\max}	NIR	0.66	0.70	0.75	0.65	0.80	0.60
	MIR	0.62	0.75	0.72	0.71	0.80	0.61

Reactivity Ratios Reactivity ratios are useful in providing the composition of the copolymer formed. A reactivity ratio less than one means that the species is less like to react with a species of its own kind, while a reactivity ratio greater than 1 means that the species is more like to react with another of its kind. The reactivity ratios can be calculated using equation 8.

$$r_s = \left[\frac{d[S]/d[Ve]}{([S]/[Ve])^2} \right] r_{ve} + \left[\frac{d[S]/d[Ve]-1}{([S]/[Ve])} \right] \quad 8$$

Where r_s is the reactivity ratio for styrene C=C and r_{ve} is the reactivity ratio for the VE C=C. $\frac{[S]}{[Ve]}$ is the molar ratio and $\frac{d[S]}{d[Ve]}$ is the rate of change in molar concentration. $\frac{d[S]}{d[Ve]}$ is obtained from the initial linear portion of a plot of conversion of styrene versus VE double bond conversion. Plotting equation 8 for each concentration yields a point where the three lines intersect. This point of intersection determines r_s and r_{ve} . The plots for data obtained from NIR and MIR are shown below in Figure 48 and Figure 49.

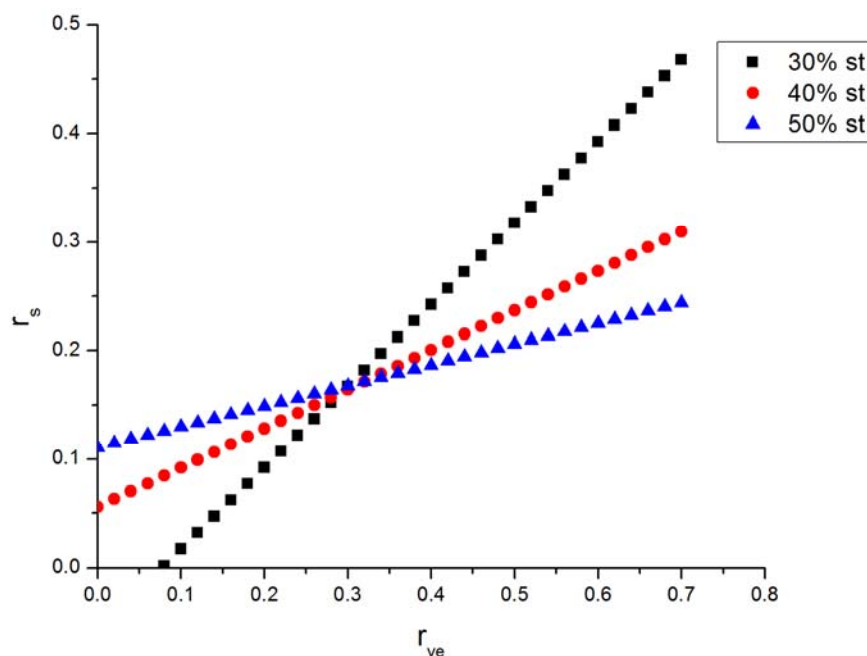


Figure 48. Plot of r_s versus r_{ve} for VE828 for 30 wt %, 40 wt %, and 50 wt % styrene from NIR data.

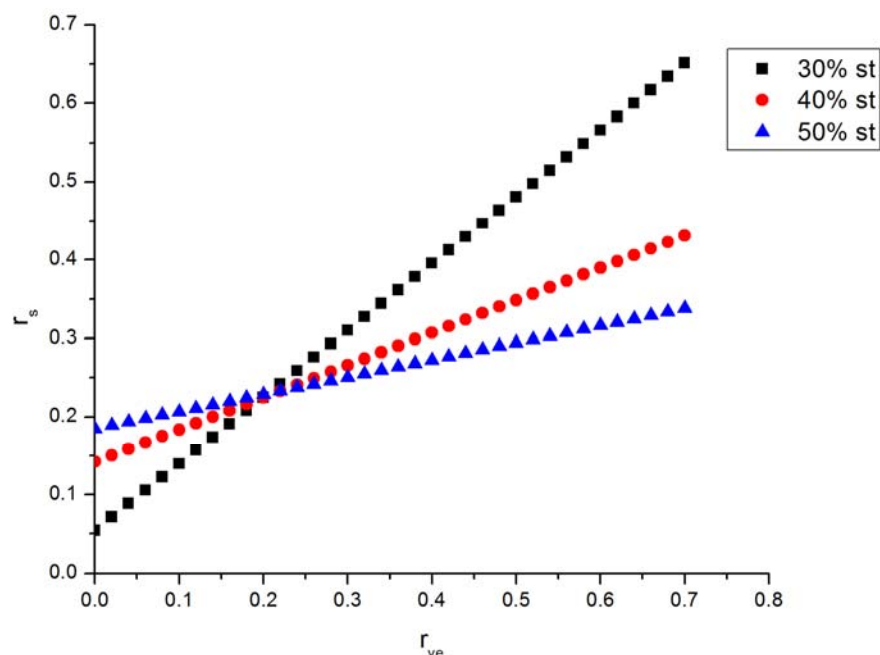


Figure 49. Plot of r_s versus r_{ve} for VE828 for 30 wt %, 40 wt %, and 50 wt % styrene from MIR data.

The values for r_s and r_{ve} obtained from the NIR data are 0.17 and 0.30 respectively. The values obtained from the MIR data for r_s and r_{ve} are 0.23 and 0.21 respectively. This indicates that the styrene and VE are more likely to react with each other than they are with species of their own leading to a generally alternating pattern.

Using Developed Near IR Technique to Study Cure Kinetics of Low VOC FAVE-O-25s

Fractional Conversion In this study, FAVE-O-25S was investigated regarding its cure kinetics using the developed NIR technique. Two runs were carried out at each of the four temperatures of 35°C, 45°C, 55°C and 66°C. Figure 50 and 51 shows the conversion of the VE and styrene C=C respectively, which was calculated using equations 4a and 4b.

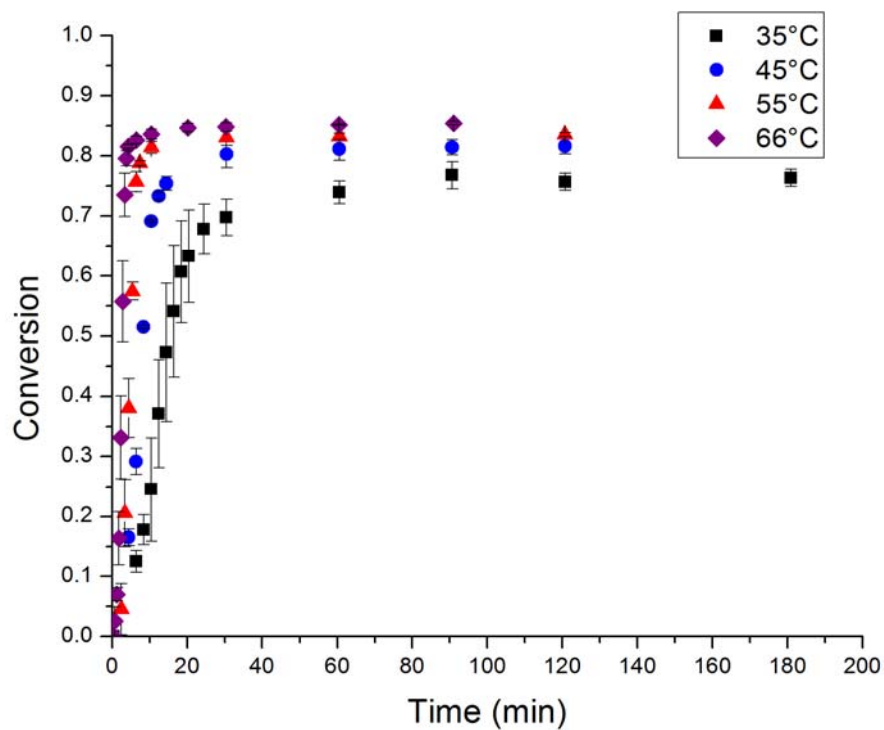


Figure 50. VE C=C conversion for FAVE-O-25s at 35°C, 45°C, 55°C.

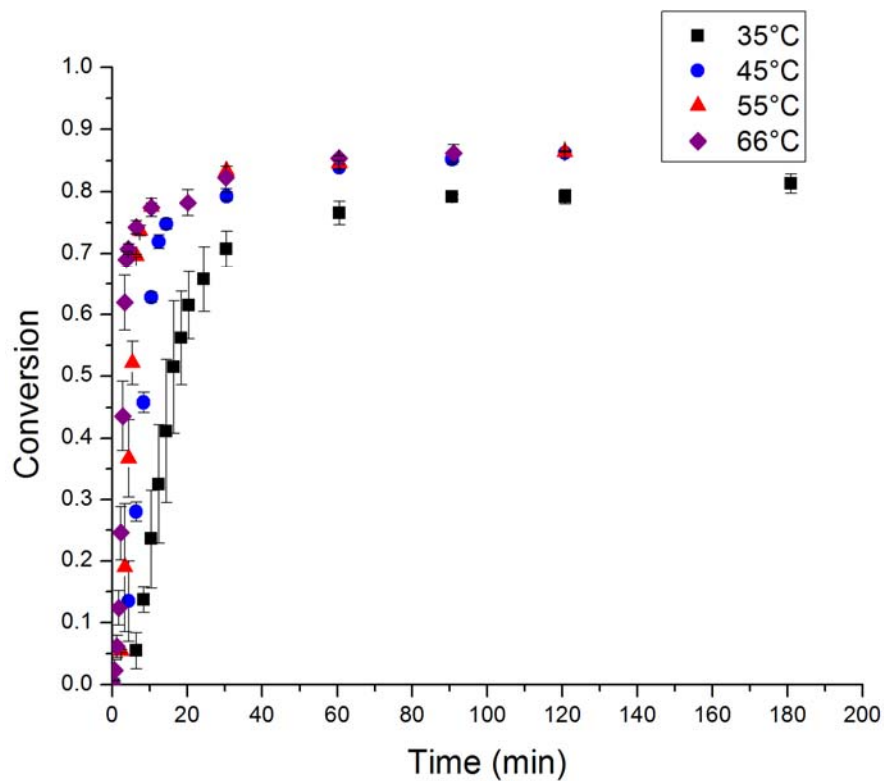


Figure 51. Styrene C=C conversion for FAVE-O-25S at 35°C, 45°C and 55°C.

The results were then analyzed using the autocatalytic model given in equation 7. The results are shown in Table 10. The rate constant, k , is higher for the VE C=C indicating VE C=C reacted faster than styrene C=C. This is maintained until the late stage of reaction where the VE C=C conversion slows down significantly while the styrene conversion continues and reaches a slightly higher fractional conversion than the VE C=C. This is believed to be due to the small molecular size of styrene suffering from less serious vitrification problem than VE. Also, it can be seen that the higher the temperature the faster the polymer cures and higher conversion of both styrene and VE double bond. For each increase of 10 degrees the rate constant nearly doubles. The reaction order, m , is about the same for a given temperature and slightly increases as temperature increase.

Table 10. Kinetic parameters for FAVE-O-25s run at 35°C, 45°C, 55°C and 65°C from NIR method

Temperature		35°C	45°C	55°C	66°C
k (min-1)	VE	0.32	0.64	1.32	2.48
	ST	0.25	0.47	0.94	1.56
m	VE	0.67	0.73	0.8	0.81
	ST	0.65	0.69	0.74	0.73
α_{\max}	VE	0.76	0.82	0.83	0.85
	ST	0.81	0.86	0.87	0.86

Activation Energy The reaction rate constant is temperature dependant. This temperature dependence is given by the popular Arrhenius equation shown in equation 9.

$$k = Ae^{-\frac{E_a}{RT}} \quad 9$$

A is the pre-exponential factor, E_a is the activation energy (J), R is the universal gas constant $\left(\frac{J}{mol \cdot K}\right)$ and T is temperature (K). Obtaining k at several different temperatures allows one to plot $\ln(k)$ versus $1/T$ to obtain a linear line which will have a slope of E_a/R and the y intercept will be $\ln(A)$, the pre exponential factor. This is plotted in Figure 52 with the corresponding fit.

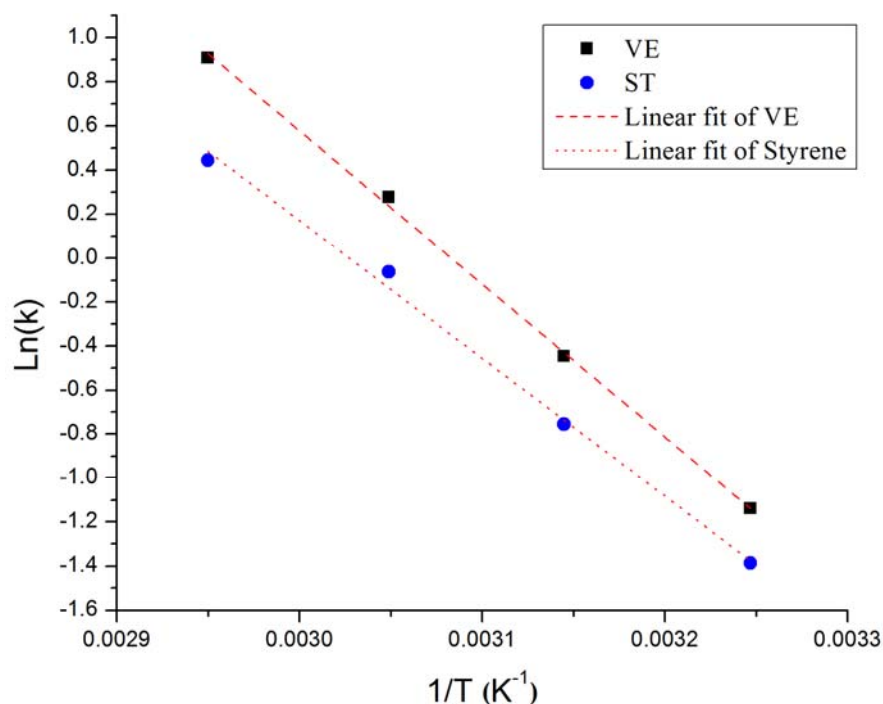


Figure 52. Slope of $\ln(k)$ versus the $1/T$, used to obtain activation energy and pre-exponential factor

A value of 57.9 kJ and 52.1 kJ for the activation energy for VE and styrene respectively were calculated from the slope of the trend line.

5.0 Personnel Supported

Giuseppe R. Palmese (Drexel University)

Xing Geng (postdoctoral researcher, Drexel University)

Justin J. Robertson (M.S., Drexel - graduated March 2009)

6.0 Publications (Attached)

Journal articles:

1. Xing Geng, John J. LaScala, James M. Sands, Giuseppe R. Palmese, Functionalized Fatty Acid as an Environmentally Benign Reactive Diluent Aiding in Processing of Novolac Vinyl Ester Resin for High Temperature Applications, *Composites Research Journal* Volume 2, Issue 4, 2009.
2. John J. La Scala, Xing Geng, et al. "Demonstration of military composites with low hazardous air pollutant content," *2006 American Science Conference preprint*.

Proceedings and Presentations:

1. Xing Geng, John J. La Scala, James M. Sands and Giuseppe R. Palmese, "High Performance Fatty Acid-Based Vinyl Ester Resin for Liquid Molding," SAMPE 2007, Baltimore, MD, June 3-7, 2007.
2. Xing Geng, John J. La Scala, James M. Sands and Giuseppe R. Palmese, "Toughened and High Temperature Stable Vinyl Esters based on Fatty Acid Modifications for Liquid Molding Applications." COMPOSITES & POLYCON 2007 American Composites Manufacturers Association, October 17-19, 2007, Tampa, FL USA

**Hetron 980-35 with Drexel's Bio Rubber
Toughening Additive Comparison
PROGRESS REPORT
October 24, 2009**

David T. Fudge
Matt Grusenmeyer
Stephen M Andersen

Hetron 980-35 with Drexel's Bio Rubber Toughening Additive Comparison PROGRESS REPORT

TABLE OF CONTENTS

	<u>Page</u>
Introduction	3
3 Tex 96 oz/yd ² Glass / Standard and 10% Drexel's Bio Rubber Modified	4
Hetron 980-35 Panel processing summary	
Resin viscosity comparison profile	5
Short Beam Shear Tests	8
DMA summary	13
4 point bending test summary	16
Conclusion	22

Introduction:

Objective

The objective of this part of the program was to evaluate the performance of the introduction of Drexel's Bio Rubber additive in an already existing commercial resin, Hetron 980-35.

Method:

To perform these evaluation tests on the Bio Rubber modified Hetron 980-35 the comparison was made to the base resin to see what qualities, if any had improved. Baseline and testing panels were fabricated consisting of 2 ply's of 3Tex 96oz/yd² 3D woven E-Glass that was infused with each of the two resins. The fabric is oriented in 0-0 arrangement and infused along the 0 degree direction. The panel was post cured at the required temperature and time as set forth by the manufacturer, 280° F for 2 hours. DMA testing, along with short beam shear and 4 point bending tests were performed on the composite at both room (72° F) and elevated temperature (250° F). Two sets of comparative samples were produced and tested during the course of this program. The initial set had a 9% styrene monomer addition to both the normal and modified Hetron 980-35 to simulate the resin in manufacturing conditions in which a higher viscosity of the resin would be favorable. An additional set of test panels was produced leaving the extra styrene out of the mix ratio, to eliminate the possibility that the extra styrene may have been working against the bio rubber additive.

3 Tex 96 oz/yd² Glass / Standard and 10% Drexel's Bio Rubber Modified Hetron 980-35 Panel processing summary:

All four test panels tested were fabricated using two layers of 3Tex 96 oz/yd² 3D woven E-glass fabric. The fabric orientation in one of these composites was 0-0, and infused along the 0 degree direction.

The Vacuum Assisted Resin Transfer Molding (VARTM) process was used to infuse the fabric re-enforcement with both the baseline Hetron 980-35 resin and the Drexel's 10% Bio Rubber modified version. Standard room temperature cure for 24 hours prior to the elevated temperature post-cure of 280° F for 2 hours was done to ensure no damage to the panels occurred during the demolding process.

Lay-up Sequence and Infusion Scheme:

The lay-up sequence is as follows (from bottom to top):

- Tool plate
- Peel ply
- 2 layers 3D 96oz E-Glass
- Peel ply
- Breather Cloth
- Distribution media.
- Vacuum bag

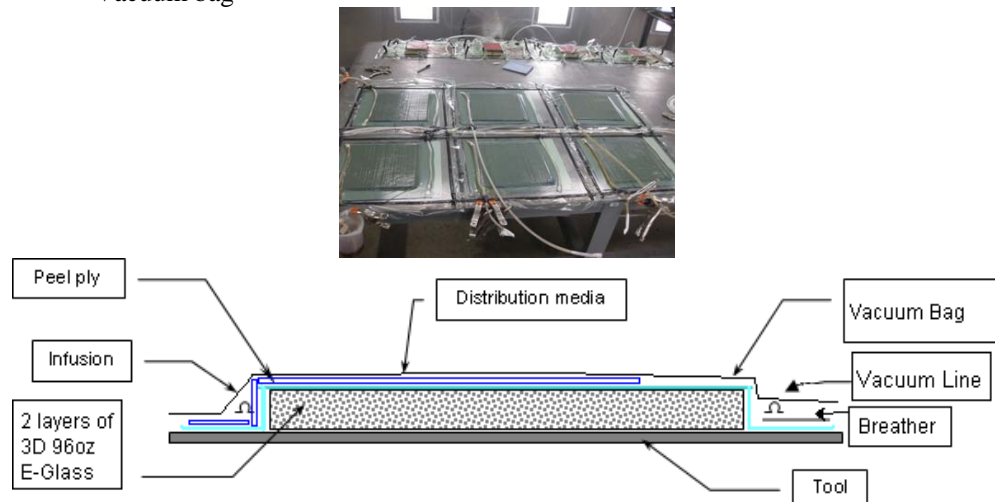


Figure 1: Schematic of VARTM Processing with side Infusion Scheme.

Resin viscosity comparison profile:

All viscosity tests performed were done using a Brookfield Viscometer with a s62 spindle set at 30 RPM.

Initial Viscosity tests of both the pure and 10% modified Hetron 980-35 before the addition of any promoters or catalysts was performed to see the difference the bio rubber toughening agent made in resin viscosity.

Table 1: Viscosity Comparison of both Hetron versions

		Hetron 980-35		10% Modified Hetron 980-35	
		Weight (g)	Viscosity (cP)	Weight (g)	Viscosity (cP)
Viscosity	Sample # 1	65	503	65	842
Trial using	Sample # 2	65	512	65	865
Spindle s62	Sample # 3	65	520	65	868
@ 30 RPM	Average cP		512		858

A mix ratio for both versions of the Hetron 980-35 was selected that had the most favorable results in previous projects and compared with two other manufacturer recommended mix ratios. The mix ratio most favorable for panel processing would be selected for use in panel fabrication.

Table 2: Initial Mix ratios used for Hetron Comparisons

	Hetron 980-35	Styrene	Conap / Cobalt 6%	DMA	Hi - Point 90
Mix Ratio #1	91%	9%	0.25%	0%	1.25
Mix Ratio #2	91%	9%	0.40%	0.05%	1.25%
Mix Ratio #3	91%	9%	0.30%	0.03%	1.25%

The gel times for each of these mix ratios for the normal and Drexel's 10% Bio Rubber Modified resin are shown in the following chart.

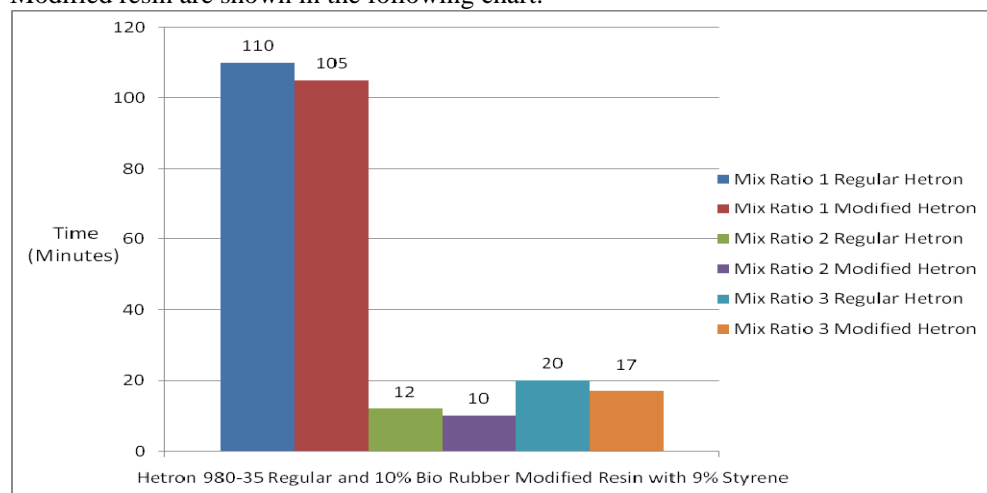


Figure 2: Gel Time Comparison of regular and Modified Hetron per Mix Ratio

The Viscosity Curves of the two Hetron resins with the 9% styrene monomer per each mix ratio are displayed in the following three graphs.

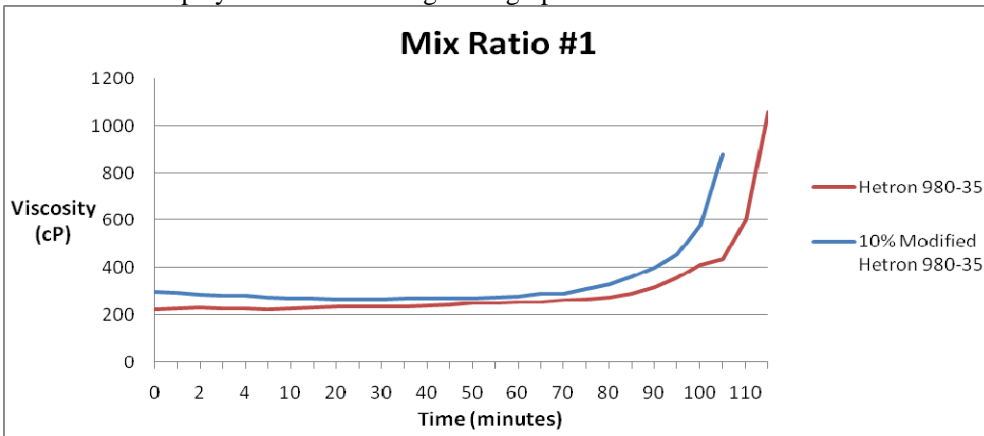


Figure 3: Viscosity over Time Comparison Curves of both Hetron Versions, Mix Ratio 1

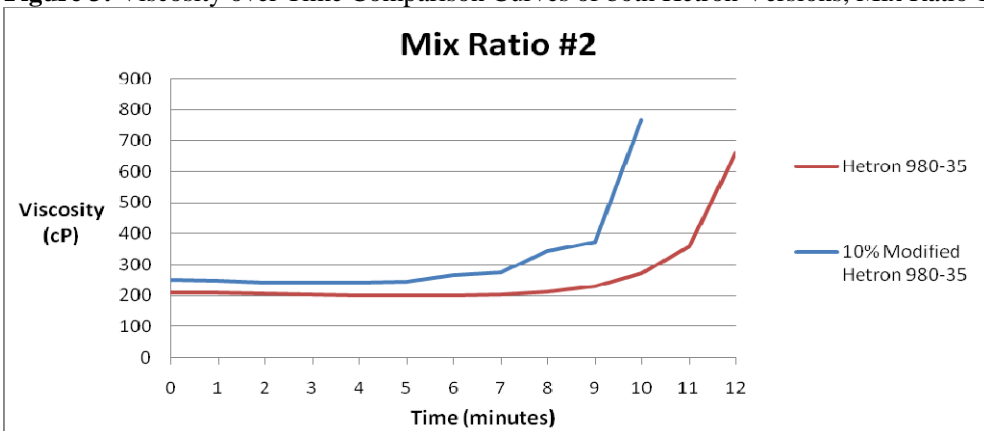


Figure 4: Viscosity over Time Comparison Curves of both Hetron Versions, Mix Ratio 2

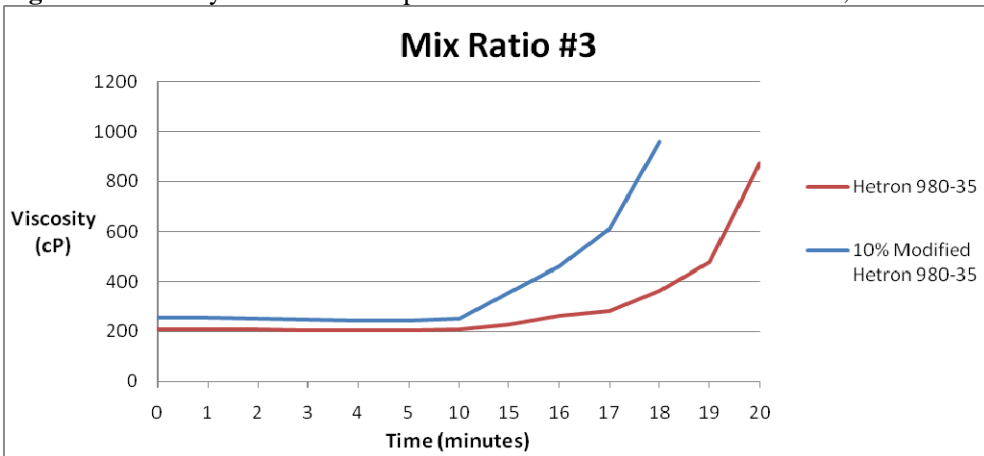


Figure 5: Viscosity over Time Comparison Curves of both Hetron Versions, Mix Ratio 3

Later on in the program when trials began with comparing the standard Hetron 980-35 with the Drexel's 10% Bio Rubber modified version, only Mix Ratio #1 was used. The reasoning behind this choice was because it had the most favorable infusion results, gel time, and mechanical test results. The only change was the exclusion of the 9% styrene in the mix.

Table 3: Mix ratios used for Hetron Comparisons

	Hetron 980-35	Conap / Cobalt 6%	DMA	Hi - Point 90
Mix Ratio #4	100%	0.25%	0%	1.25

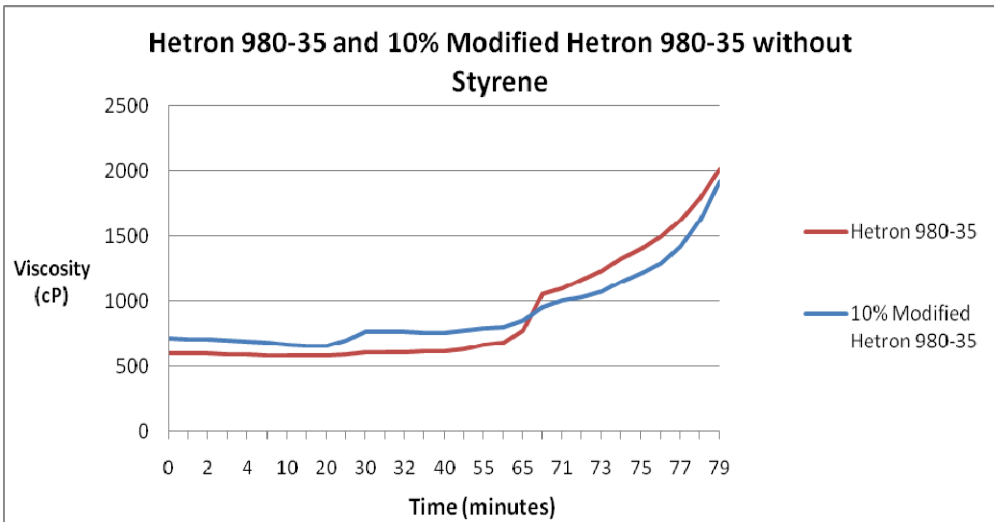


Figure 6: Viscosity over Time Comparison Curves of both Hetron Versions, Mix Ratio 4 which has no additional Styrene

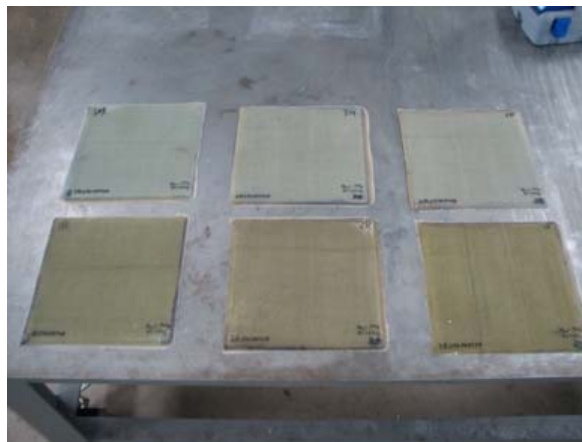


Figure 7: Example of the Panels Fabricated for testing

Short Beam Shear Test Summary:

Inter-laminar shear strength of 2 Layers of 3Tex 96oz/ yd² infused with the Hetron 980-35 and Drexel's 10% Bio Rubber Modified Hetron 980-35 were tested following Short Beam Shear ASTM D2344. Both normal temperature (72°F) and elevated temperature (250°F) testing was preformed. The Short beam test specimens were loaded in a three point bending arrangement, where the specimen ends rested on two supports that permitted lateral movement. The load is then applied by a loading nose centered on the midpoint of the sample. The tool side of each specimen was placed on the supports. The experiment atmosphere was 72°F with a relative humidity of 50%.

Table 4: Specimen dimensions and Testing results of Hetron and Bio Rubber Modified Hetron 980-35 Panels with 9% Styrene

Specimens are designated by the mix ratio number, normal of modified Hetron, and the test sample cut from the panel.

Normal Temp (72° F)							
Specimen	Width (in)	Thickness (in)	Length (in)	Max Load (lbf)	Fsbs (psi)	Avg Fsbs	Standard Deviation
1R-1	0.451	0.221	1.326	665.2	5006	4794	183.5
1R-2	0.452	0.232	1.395	640.3	4565		
1R-3	0.455	0.224	1.344	667.6	4913		
1R-4	0.454	0.219	1.314	616.9	4648		
1R-5	0.449	0.238	1.428	690.2	4839		
1M-1	0.467	0.227	1.362	740.1	5236	5287	162.8
1M-2	0.466	0.232	1.389	739.3	5140		
1M-3	0.465	0.233	1.395	750.6	5207		
1M-4	0.467	0.229	1.371	753	5292		
1M-5	0.463	0.228	1.368	782.8	5562		
2R-1	0.486	0.219	1.314	703.9	4960	4693	214.6
2R-2	0.491	0.235	1.410	690.2	4486		
2R-3	0.485	0.226	1.356	690.2	4723		
2R-4	0.486	0.227	1.362	711.1	4830		
2R-5	0.488	0.228	1.368	662.8	4468		
2M-1	0.485	0.232	1.392	834.4	5556	5018	311.8
2M-2	0.488	0.231	1.389	747.4	4957		
2M-3	0.492	0.243	1.461	778	4870		
2M-4	0.488	0.231	1.386	744.2	4951		
2M-5	0.487	0.240	1.440	740.9	4754		
3R-1	0.474	0.235	1.407	652.3	4406	4642	218.2
3R-2	0.473	0.229	1.374	678.9	4706		
3R-3	0.475	0.239	1.434	669.3	4422		
3R-4	0.473	0.238	1.428	732.9	4888		
3R-5	0.477	0.234	1.404	712.7	4789		
3M-1	0.475	0.240	1.440	788.4	5192	5370	223.2
3M-2	0.475	0.236	1.413	759.5	5092		
3M-3	0.476	0.232	1.392	817.4	5557		
3M-4	0.474	0.243	1.458	830.3	5406		
3M-5	0.473	0.230	1.380	811.8	5603		

High Temp (250° F)

Specimen	Width (in)	Thickness (in)	Length (in)	Max Load (lbf)	Fsbs (psi)	Avg Fsbs	Standard Deviation
1R-6	0.454	0.225	1.350	512.2	3756	3772	100.1
1R-7	0.451	0.234	1.404	549.3	3903		
1R-8	0.455	0.219	1.314	510.6	3843		
1R-9	0.452	0.223	1.338	493.4	3671		
1R-10	0.459	0.222	1.335	502	3686		
1M-6	0.464	0.236	1.419	319.7	2182	2341	132.9
1M-7	0.465	0.232	1.395	358.7	2488		
1M-8	0.464	0.225	1.350	344.3	2470		
1M-9	0.465	0.242	1.452	343.8	2291		
1M-10	0.464	0.237	1.422	333.6	2272		
2R-6	0.484	0.224	1.344	539.9	3731	3513	125.2
2R-7	0.486	0.236	1.416	531.5	3475		
2R-8	0.484	0.236	1.416	523.8	3439		
2R-9	0.480	0.235	1.413	516.5	3423		
2R-10	0.478	0.234	1.404	521.9	3495		
2M-6	0.493	0.233	1.398	360.8	2355	2215	85.3
2M-7	0.489	0.230	1.383	327	2173		
2M-8	0.489	0.233	1.401	340	2233		
2M-9	0.488	0.239	1.434	333.4	2141		
2M-10	0.488	0.235	1.413	332.8	2171		
3R-7	0.473	0.233	1.398	540.7	3675	3552	156.6
3R-8	0.472	0.239	1.434	529.1	3517		
3R-9	0.475	0.228	1.371	543.1	3752		
3R-10	0.475	0.239	1.434	518.4	3421		
3R-11	0.472	0.237	1.425	508.2	3396		
3M-6	0.474	0.240	1.440	322.3	2125	2144	74.1
3M-7	0.474	0.246	1.479	342.4	2197		
3M-8	0.475	0.235	1.410	313.7	2107		
3M-9	0.473	0.233	1.401	329.8	2239		
3M-10	0.475	0.251	1.506	326.4	2053		

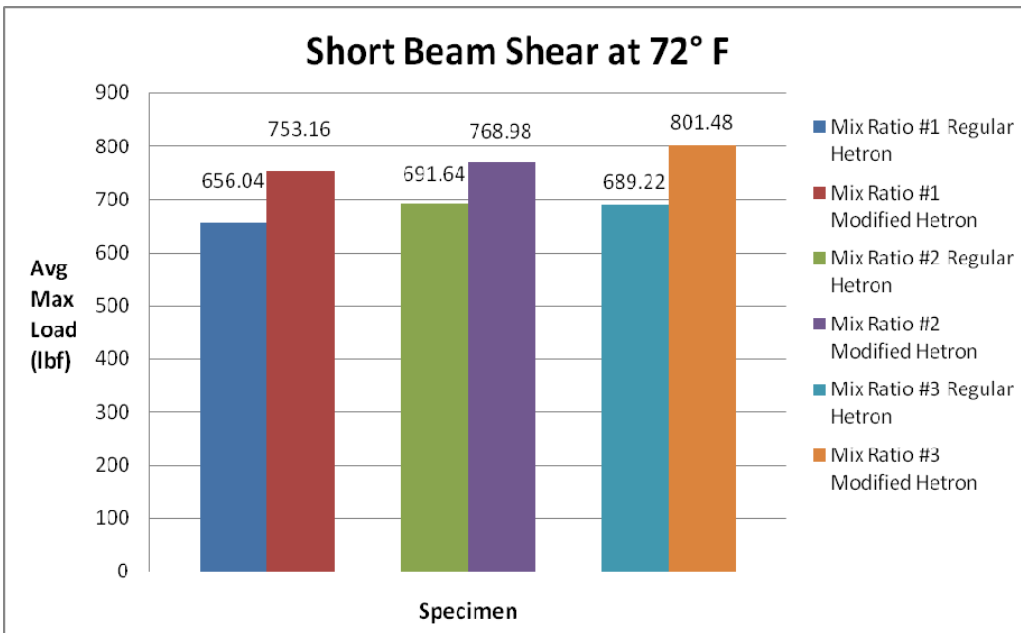


Figure 8 : Short Beam Shear Average Max Load at Room Temperature

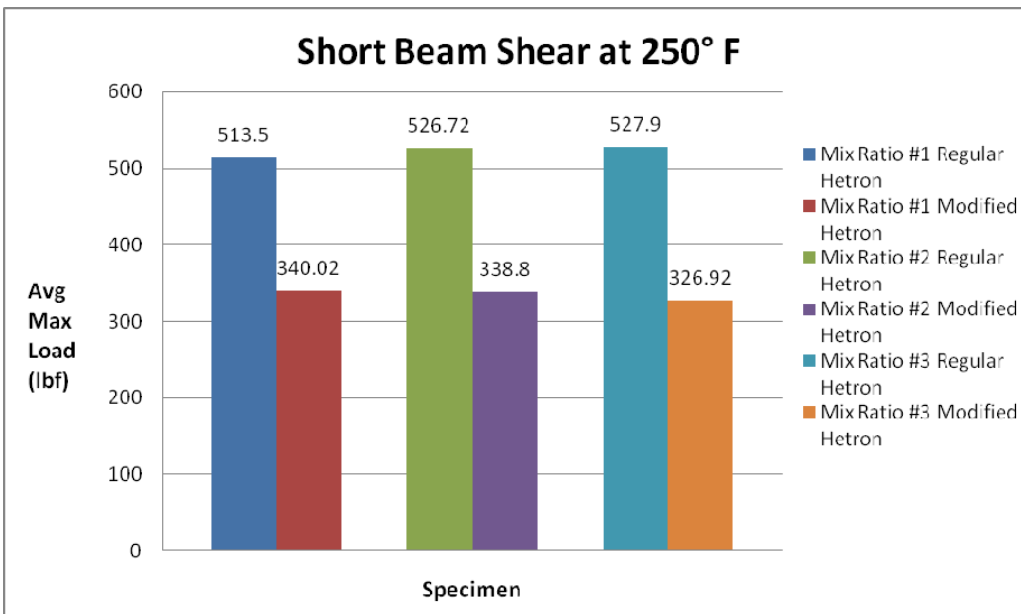


Figure 9 : Short Beam Shear Average Max Load at Elevated Temperature

Table 5: Specimen dimensions and Testing results of Hetron and Bio Rubber Modified
Hetron 980-35 Panels

Room Temp (72° F)

Specimen	Width (in)	Thickness (in)	Length (in)	Max Load (lb)	Short-Beam Strength (psi)	AVG SBS (psi)	Standard Deviation
4R-1	0.432	0.215	1.29	591.1	4773	4968	198.3
4R-2	0.433	0.218	1.305	644.3	5136		
4R-3	0.431	0.217	1.302	623.4	5004		
4R-4	0.431	0.224	1.344	664.4	5173		
4R-5	0.431	0.223	1.338	608.1	4750		
4M-1	0.466	0.234	1.401	693.4	4785	4732	132.3
4M-2	0.474	0.246	1.476	753.8	4849		
4M-3	0.468	0.245	1.47	688.6	4504		
4M-4	0.466	0.252	1.512	746.6	4768		
4M-5	0.471	0.242	1.449	720.8	4753		

High Temp (250° F)

Specimen	Width (in)	Thickness (in)	Length (in)	Max Load (lb)	Short-Beam Strength (psi)	AVG SBS (psi)	Standard Deviation
4R-6	0.433	0.225	1.35	455.8	3509	3783.6	179.4
4R-7	0.43	0.219	1.317	476.8	3789		
4R-8	0.429	0.216	1.296	483.2	3911		
4R-9	0.427	0.223	1.335	473.6	3739		
4R-10	0.429	0.215	1.29	488.9	3971		
4M-6	0.475	0.231	1.383	348.7	2389	2170.5	215.4
4M-7	0.472	0.239	1.437	331	2196		
4M-8	0.468	0.237	1.419	275.4	1868		
4M-9	0.471	0.252	1.512	324.6	2051		
4M-10	0.4695	0.235	1.41	345.5	2349		

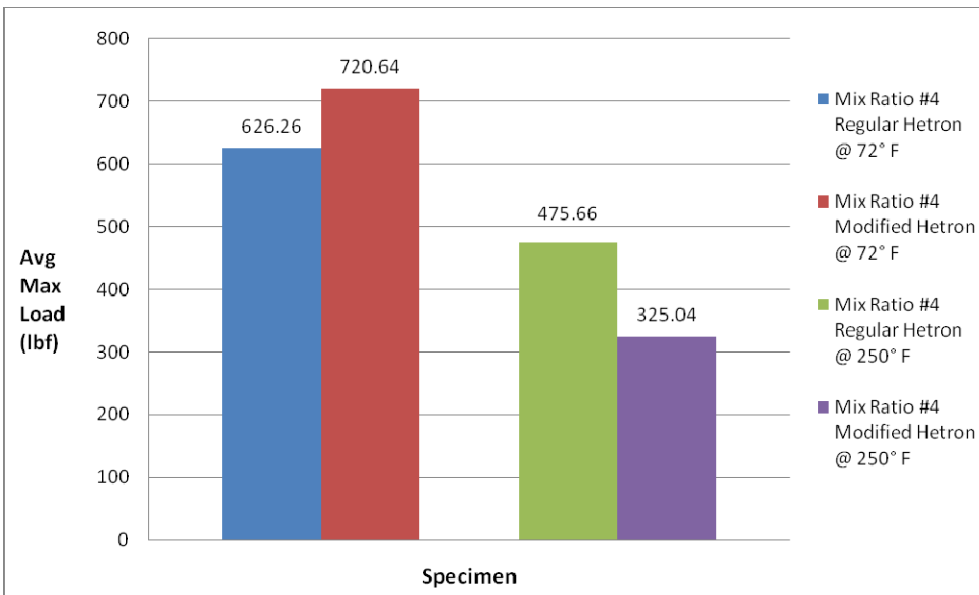


Figure 10: Short Beam Shear Average Max Load at failure at elevated temperature of panels without additional Styrene

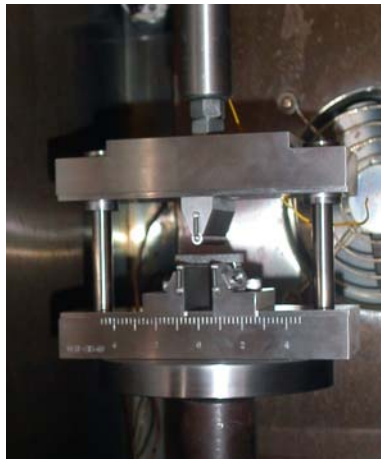


Figure 11 : A typical SBS test set up for elevated temperature.

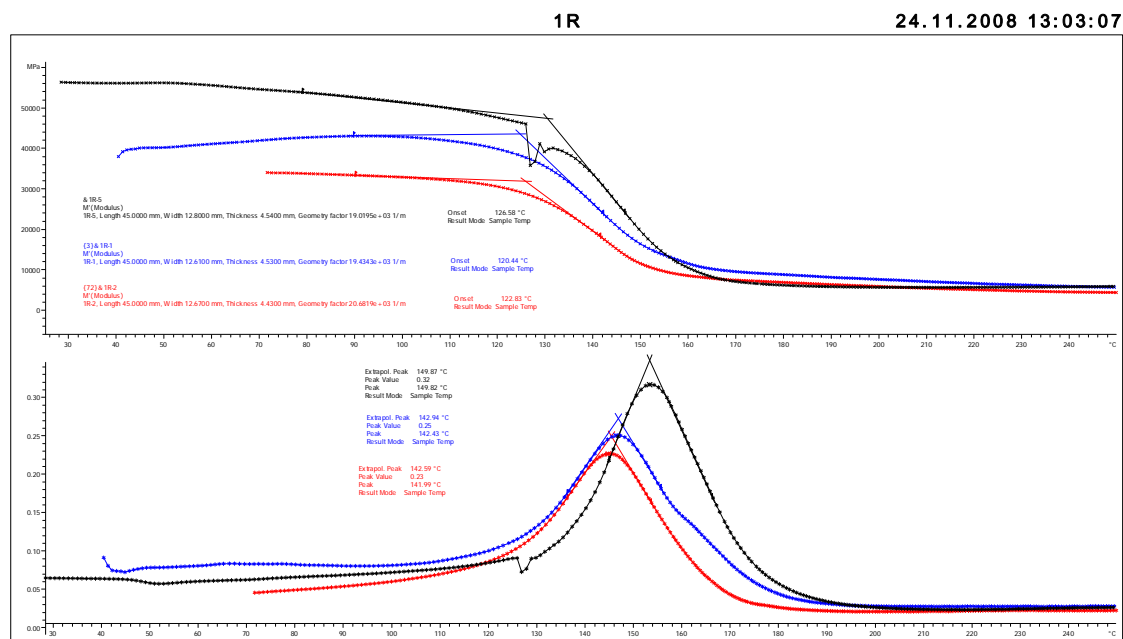
DMA Testing Summary

A course of DMA testing was performed following ASTM E1640-04 to obtain the comparative glass transition temperature between the 3Tex 96oz/yd² infused with the standard Hetron 980-35 and Drexel's 10% Bio Rubber Modified version of Hetron 980-35. The specimens were placed in mechanical oscillation at a fixed frequency of 1 Hz. Samples were clamped in a 3 point bending clamping arrangement and calibrated before testing. In order to reduce thermal noise, the temperature of the experimenting environment was stabilized at 35C for five minutes. Then, the temperature was ramped up to 180C at a rate of 5 deg C/ min. The changes in the visco elastic response of the material were monitored as a function of temperature.

Comparison DMA testing was performed on the set Hetron 980-35 and 10% Bio Rubber Modified Hetron 980-35 panels for each of the 3 mix ratios. The six panels yielded the following results.

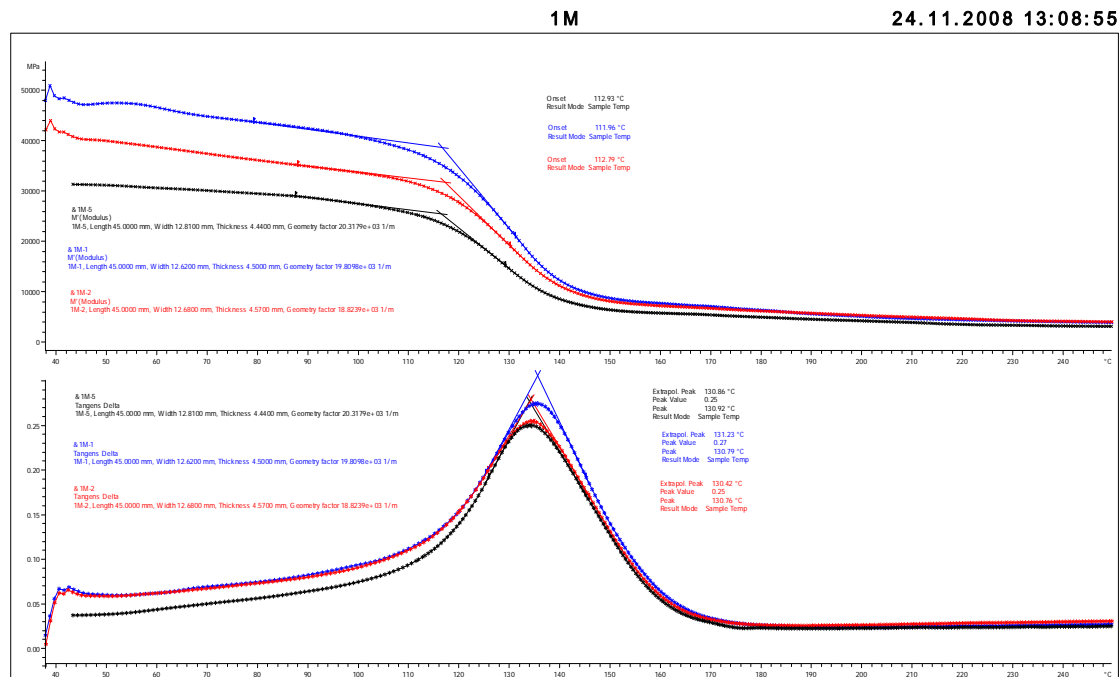
Table 6: DMA comparative results of Hetron 980-35 vs. Bio Rubber Modified Version
all mixes included 9% styrene in the mix ratios

	Test Sample	Onset Temp (C)	Modulus (mPa) @ 250F (107C)	Peak Temp (C)	Peak value	Extrapol. Peak (C)
Mix Ratio 1 Regular Hetron 980-35	a	126	51000	149	0.32	149
	b	120	41000	142	0.25	142
	c	122	32500	141	0.23	142
	Average	123	41500	145	0.27	145
Mix Ratio 1 Modified Hetron 980-35	a	112	26500	130	0.25	130
	b	112	38750	130	0.27	131
	c	112	31500	130	0.25	130
	Average	112	32250	130	0.26	130
Mix Ratio 2 Regular Hetron 980-35	a	119	38000	140	0.3	140
	b	121	39750	139	0.3	140
	c	121	32500	140	0.27	140
	Average	120	36750	140	0.29	140
Mix Ratio 2 Modified Hetron 980-35	a	109	26000	127	0.27	127
	b	108	25500	127	0.26	128
	c	111	26000	128	0.23	128
	Average	110	25833	127	0.25	128
Mix Ratio 3 Regular Hetron 980-35	a	123	31500	141	0.29	141
	b	123	31000	142	0.27	142
	c	123	28000	141	0.24	142
	Average	123	30166	141	0.27	142
Mix Ratio 3 Modified Hetron 980-35	a	108	27500	129	0.26	129
	b	110	25750	129	0.26	129
	c	110	25000	129	0.26	129
	Average	109	26083	129	0.26	129



CCM Lab: METTLER

STAR® SW 9.20



CCM Lab: METTLER

STAR® SW 9.20

Figure 12: Example DMA plots for comparison between the normal and modified Hetron

DMA Testing was repeated on the new set of mix ratio panels that did not contain addition styrene.

Table 7 : DMA comparative results of Hetron 980-35 vs. Bio Rubber Modified Version without the additional styrene

	Test Sample	Onset Temp (C)	Modulus (mPa) @ 250F (107C)	Peak Temp (C)	Peak value	Extrapol. Peak (C)
Mix Ratio 4 Regular Hetron 980-35	1	112	31097	139	0.17	141
	2	105	43551	137	0.23	139
	3	108	50357	137	0.23	139
	4	116	45290	137	0.24	139
	Average	110	42574	138	0.2175	139
Mix Ratio 4 Modified Hetron 980-35	1	98	36302	126	0.28	128
	2	98	40341	127	0.28	128
	3	99	40875	126	0.28	128
	4	97	35485	127	0.25	128
	Average	98	38250	127	0.2725	128

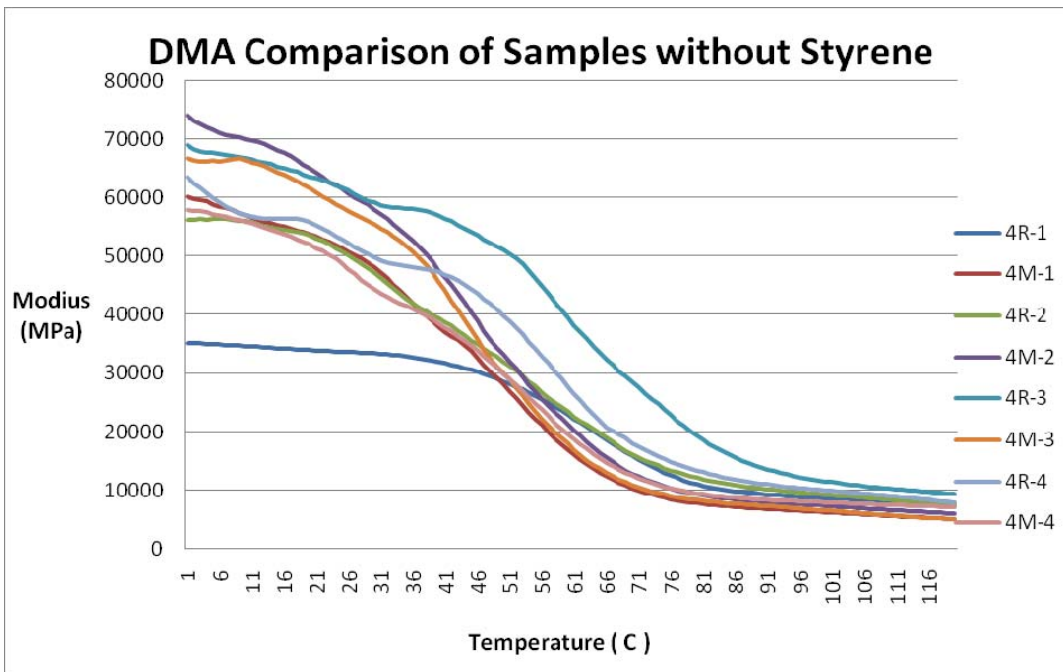


Figure 13 : Example DMA plots for comparison between the normal and modified Hetron without additional Styrene

4 Point Bending Test Summary:

The remaining sections of the panels were prepared for use in the 4 Point Bending Tests. These were performed following ASTM D 6272 in order to compare the flexural properties of the 3Tex 96oz/ yd² infused with the Hetron 980-35 with the Drexel's 10% Bio Rubber Modified Hetron 980-35 composite. The specimens for this experiment were cut along the 0 degree direction of the panel which was also the direction of infusion. Each specimen was tested by resting on two supports and loading at two loading noses. The tool side of the specimen was placed on the supports. The distance between the loading noses was one third of the support span. A 24:1 Span to depth ratio was used due to the loading nose structure. For the elevated temperature 4 point bending test method the same procedure described above for the room temperature tests was followed. However, prior to testing each specimen was conditioned at 250 F for at least 20 minutes.

Deleted:

Test Conditions: 72 F @ 50% humidity , 250 F @ 50% humidity

Load Span Length: 1.6 (in)

Support Span Length: 4.8 (in)

Support span-to-depth ratio: 24:1

Rate of crosshead motion: 0.09 (in/min)



Figure 14: A typical test frame and set up for 4 point bending test

Table 8 : 4 Point Bending Comparison at Room Temperature

Normal Temp(72° F)

Specimen	Max Load (lbf)	Width (in)	Thickness (in)	Load Span (in)	Bending Strength (psi)	Average (psi)	Standard Deviation
1R-1	429.3	0.43	0.224	3.6	71951.5	68919	7417.9
1R-2	380.1	0.427	0.236	3.6	57469.8		
1R-3	476	0.429	0.223	3.6	80323.4		
1R-4	422	0.429	0.229	3.6	67824.2		
1R-5	430.9	0.43	0.232	3.6	67024.6		
1M-1	492.1	0.428	0.225	3.6	81761.1	78485	1826.1
1M-2	517	0.425	0.237	3.6	77966.3		
1M-3	453.4	0.427	0.222	3.6	77562.2		
1M-4	503.4	0.43	0.235	3.6	76315.2		
1M-5	493.7	0.43	0.229	3.6	78818.1		
2R-1	486.4	0.428	0.223	3.6	82270.2	76469	10368.7
2R-2	545.2	0.426	0.227	3.6	89412.2		
2R-3	419.6	0.431	0.233	3.6	64557.8		
2R-4	478.4	0.428	0.221	3.6	82292.1		
2R-5	412.4	0.425	0.234	3.6	63797.0		
2M-1	509	0.429	0.23	3.6	80743.4	88285	6514.3
2M-2	523.5	0.427	0.231	3.6	82711.7		
2M-3	598.4	0.425	0.229	3.6	96657.1		
2M-4	540.4	0.427	0.23	3.6	86025.2		
2M-5	592.7	0.427	0.229	3.6	95288.0		
3R-1	364	0.426	0.227	3.6	59695.6	64030	4303.8
3R-2	379.3	0.428	0.225	3.6	62946.1		
3R-3	410.7	0.43	0.229	3.6	65567.3		
3R-4	372.1	0.425	0.229	3.6	60367.1		
3R-5	441.3	0.427	0.228	3.6	71571.2		
3M-1	492.1	0.434	0.233	3.6	75275.7	78738	2352.5
3M-2	543.6	0.434	0.239	3.6	79030.9		
3M-3	516.2	0.429	0.234	3.6	79110.0		
3M-4	508.2	0.428	0.235	3.6	77733.4		
3M-5	512.2	0.426	0.229	3.6	82539.4		

Table 9 : 4 Point Bending Comparison at Elevated TemperatureElevated Temp
(250° F)

Specimen	Max Load (lbf)	Width (in)	Thickness (in)	Load Span (in)	Bending Strength (psi)	Average (psi)	Standard Deviation
1R-6	319.7	0.431	0.232	3.6	49670.2	49061	4331.8
1R-7	283.5	0.431	0.229	3.6	45155.1		
1R-8	295.6	0.427	0.234	3.6	45514.2		
1R-9	274.6	0.427	0.22	3.6	47889.3		
1R-10	351.1	0.426	0.228	3.6	57076.0		
1M-6	194.9	0.432	0.236	3.6	29161.3	29326	1421.2
1M-7	199.7	0.431	0.228	3.6	32087.3		
1M-8	182.8	0.43	0.232	3.6	28433.7		
1M-9	189.3	0.429	0.238	3.6	28162.3		
1M-10	185.2	0.429	0.238	3.6	28783.7		
2R-6	283.5	0.43	0.228	3.6	45658.1	46527	2153.5
2R-7	282.7	0.427	0.222	3.6	48360.9		
2R-8	301.2	0.442	0.229	3.6	46780.4		
2R-9	261.7	0.43	0.226	3.6	42896.4		
2R-10	290.7	0.43	0.223	3.6	48940.6		
2M-6	168.3	0.429	0.24	3.6	24547.8	25349	2021.9
2M-7	164.3	0.427	0.229	3.6	26530.2		
2M-8	137.7	0.429	0.23	3.6	21869.1		
2M-9	166.7	0.427	0.225	3.6	27761.6		
2M-10	169.1	0.427	0.234	3.6	26036.7		
3R-6	272.2	0.43	0.225	3.6	45014.9	44164	669.8
3R-7	298.8	0.43	0.237	3.6	44536.7		
3R-8	281.9	0.432	0.233	3.6	43271.5		
3R-9	272.2	0.426	0.23	3.6	43483.6		
3R-10	274.6	0.431	0.227	3.6	44511.7		
3M-6	182.8	0.429	0.237	3.6	27342.1	29047	1748.1
3M-7	178.8	0.433	0.234	3.6	27148.8		
3M-8	195.7	0.424	0.239	3.6	29089.2		
3M-9	187.7	0.426	0.231	3.6	29725.8		
3M-10	213.4	0.432	0.236	3.6	31929.3		

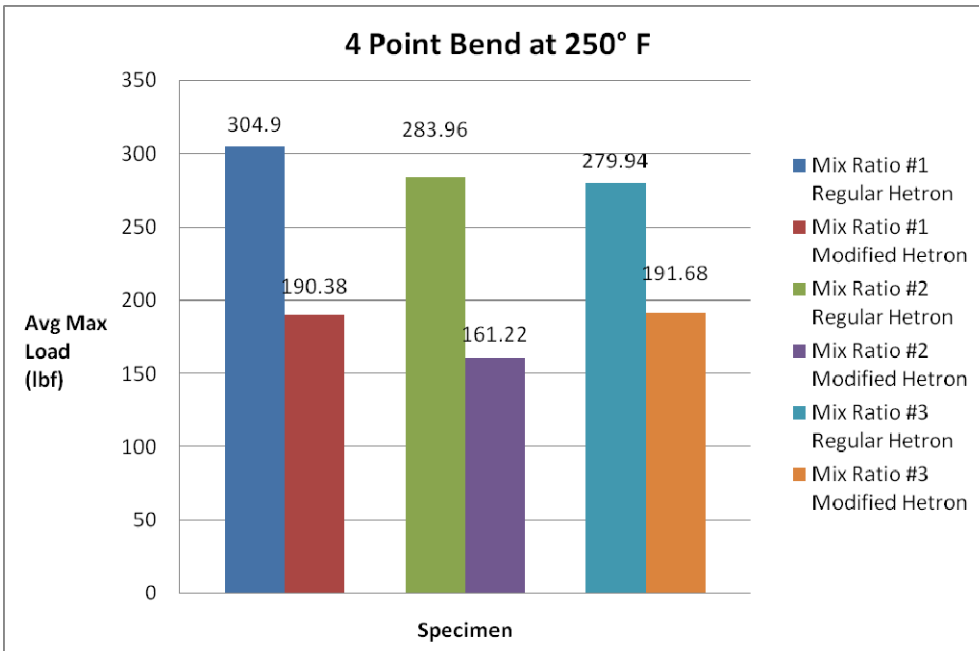
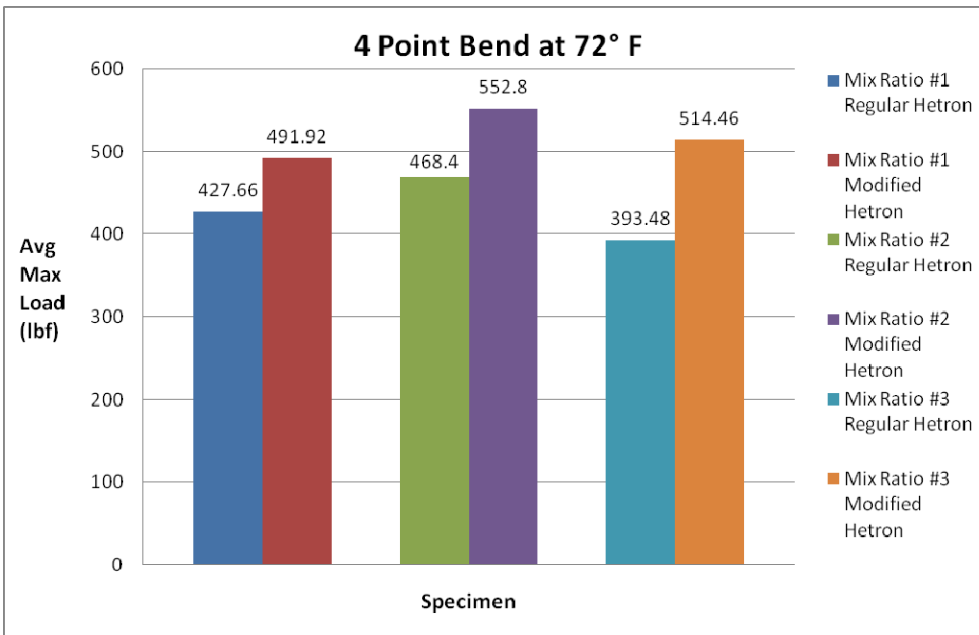


Figure 15 : 4 Point Bending Average Max Load at Room and Elevated Temperatures of the Hetron mixes with additional Styrene

Table 10: 4 point bending test summary

Normal Temp(72° F)

Specimen	Max Load (lb)	Width (in)	Thickness (in)	Load Span (in)	Bending Strength (psi)	AVG Strength (psi)	Standard Deviation
4R-1	560.5	0.555	0.212	3.6	80893.5	70357	10460.2
4R-2	489.7	0.559	0.221	3.6	64570.		
4R-3	460.7	0.556	0.22	3.6	61631.2		
4R-4	578.3	0.561	0.212	3.6	82569.8		
4R-5	471.1	0.559	0.221	3.6	62118.3		
4M-1	697.4	0.605	0.2315	3.6	77433.2	74675	7844.3
4M-2	660.4	0.618	0.243	3.6	65149.1		
4M-3	673.3	0.618	0.24	3.6	68092.6		
4M-4	667.6	0.610	0.224	3.6	78586.7		
4M-5	719.2	0.608	0.225	3.6	84116.9		

Elevated Temp
(250° F)

Specimen	Max Load (lb)	Width (in)	Thickness (in)	Load Span (in)	Bending Strength (psi)	AVG Strength (psi)	Standard Deviation
4R-6	357.6	0.568	0.22	3.6	46828.1	48796	2707.3
4R-7	355.2	0.558	0.217	3.6	48665.6		
4R-8	372.1	0.552	0.22	3.6	50184.7		
4R-9	330.2	0.557	0.216	3.6	45742.2		
4R-10	392.2	0.55	0.221	3.6	52560.9		
4M-6	237.6	0.605	0.2325	3.6	26154.6	27825	1294.8
4M-7	263.4	0.609	0.23	3.6	29433.7		
4M-8	240	0.603	0.23	3.6	27085.7		
4M-9	250.5	0.607	0.2275	3.6	28705.1		
4M-10	242.4	0.605	0.228	3.6	27746.6		

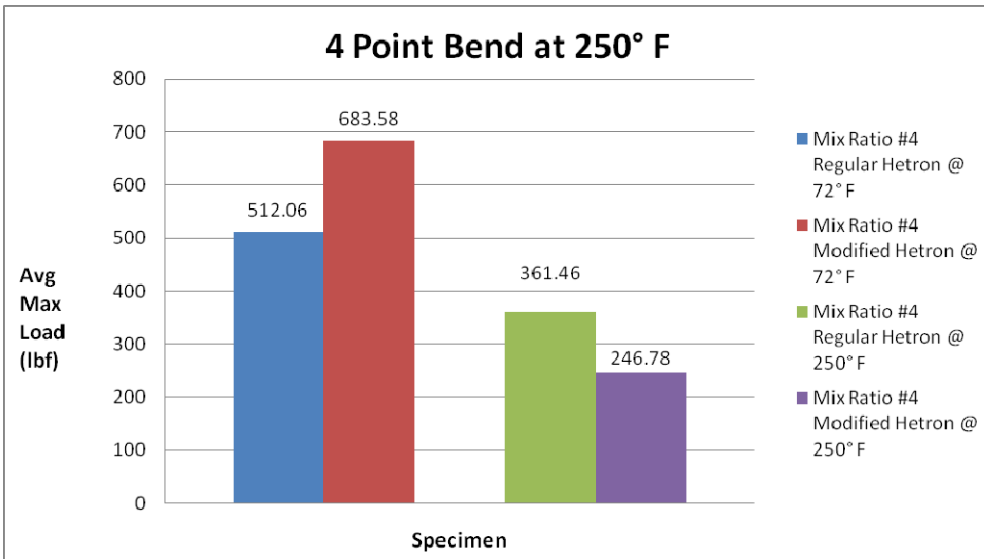
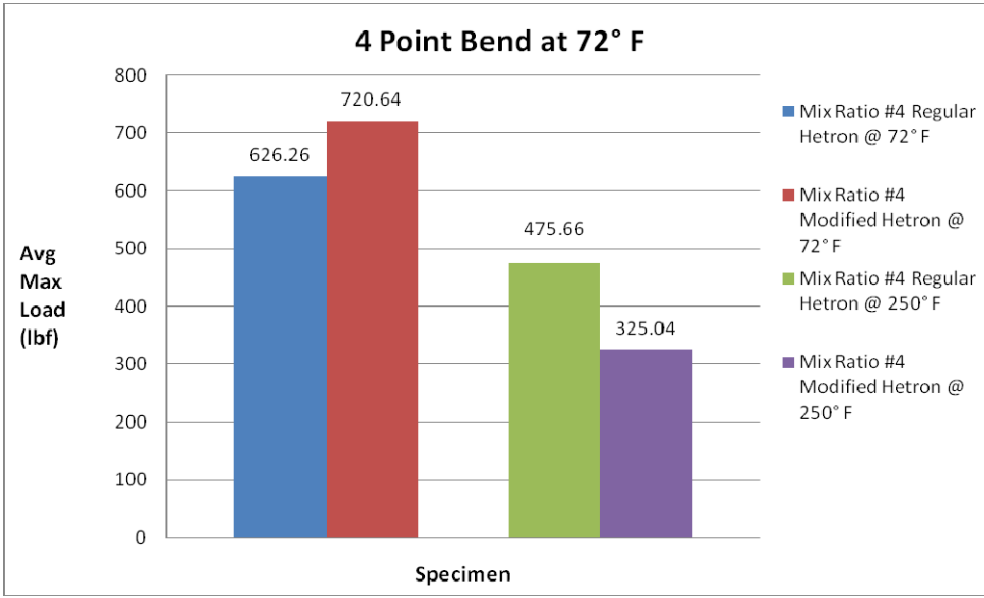


Figure 16 : 4 Point Bending Average Max Load at Room and Elevated Temperatures of the Hetron mixes without Styrene

Conclusion:

Results from the completed testing indicates that the Drexel's Bio Rubber Toughening additive did increase the structural performance of the Hetron 980 & 96 oz/yd² composite in some cases.

The average maximum force applied to the test samples as well as the inter-laminar shear strength of the 10% Bio Rubber Modified Hetron did increase over the regular Hetron 980-35 in the cases where the composite stayed at room temperature. However, as shown, the additive reduced the effective Tg of the resin making the overall composite weaker at higher temperatures in comparison to the regular Hetron resin. This is further proven by the SBS test results performed at 250°F. It is interesting to see that in most cases, the panels with the additional styrene performed better overall than the panels fabricated without the extra styrene. This could be the result of the styrene acting as a solvent on the bio rubber additive further distributing it throughout the composite better than the panels that went without the additional styrene. From the tests shown, the 10% Bio Rubber additive does increase the strength of the composite but with the loss of its effective Tg and an increase of resin viscosity.

Some effective tests for toughened resins, such as impact testing, compression after impact and fracture toughness tests, not performed in this program, would likely better demonstrate the potential performance and durability improvements provided by the increase of the bio-rubber additive. In this case, it would be important that the new resin system still meets the baseline structural objectives and requirements, but the improvements in durability would be quantifiable. Future effort should be focused on this testing and analysis to provide opportunities for insertion of this new technology.

INTENTIONALLY LEFT BLANK.

Appendix D. Gel Time Results

This appendix appears in its original form, without editorial change.

Appendix D

Gel Time Results

Vinyl Ester Gel Time Studies

**Alex Grous
Steve Klankowski**

Table of Contents

List of Figures	3
List of Tables	3
Materials	4
Sample preparation	4
Procedure	5
Results.....	5
Discussion	10
Conclusions.....	11

List of Figures

Figure 1: FAVE-L-25S Gel Times	6
Figure 2: FAVE-O-25S Gel Times	7
Figure 3: 441-400 Gel Times	8
Figure 4: 470HT-400 Gel Times	9

List of Tables

Table 1: In each group one component was varied. Sample 13 was made as an extreme for the 1 weight percent grouping	5
Table 2: Gel Time Results given in minutes	5
Table 3: Actual weight percents of the FAVE-L-25S mixtures and their respective Gel Times	6
Table 4: Actual weight percents of the FAVE-O-25S mixtures and their respective Gel Times	7
Table 5: Actual weight percents of the 441-400 mixtures and their respective Gel Times	8
Table 6: Actual weight percents of the 470HT-400 mixtures and their respective Gel Times	9

Materials

The following materials were used throughout this work:

- Derakane 441-400
- 470HT-400
- FAVE-L-25S batch 1-23-08
- FAVE-O-25S batch 1-23-08
- Trigonox 239 A (Trig) (AkzoNobel Chemicals, Chicago, Illinois) contains 45% cumyl hydroperoxide and acts as the initiator for free radical polymerization.
- Cobalt Naphthenate 6% (CoNap) (Aldrich) is the catalyst for Trigonox in the free radical polymerization.
- N, N-Dimethylaniline (EMD Chemicals Inc). acts as an promoter and speeds the reaction significantly and also aids in fiber wetting
- 2,4-pentanedione (2,4-P) (Alfa Aesar Avocado) is a retarder and slows the reaction allowing for longer working times.

Sample preparation

Approximately 10 grams of resin were poured into a 20ml glass vial, all samples were mixed in Thinky AR-250 planetary centrifugal mixer for 2 minutes at 2000 rpm after each component was added, components were added in the following order when applicable: CoNap, 2,4-P, DMA, Trigonox. Table 1 lists the concentrations of the various components of the initiator package. The first three samples (group 1) held the concentration of Trigonox constant at 1 weight percent and varied the weight percent of CoNap. Samples 4, 5, and 6, (group 2) held Trigonox at 2 weight percent and again varied the weight percent of CoNap. In samples 7, 8 and 9 (group 3) Trigonox was held constant at 2 weight percent and CoNap was held constant at 0.4 weight percent, DMA was varied at weight percents of 0.1, 0.2 and 0.3. Group 4, samples 10, 11 and 12, held the concentration of Trigonox, CoNap and DMA constant at 2 weight percent, 0.4 weight percent and 0.2 weight percent DMA respectively while varying the concentration of 2,4-P at .05, 0.1 and 0.15 weight percent.

Additional mixtures were made to achieve even longer gel times. Sample 13 was formulated to contain the least amount of initiator components, containing 1 weight percent Trigonox and only 0.1 CoNap. Sample 14 contained 1 weight percent Trigonox, 0.1 weight percent CoNap and 0.15 weight percent 2,4-P, sample 14 contained no DMA. Sample 15 also contained 1 weight percent Trigonox but had 0.2 weight percent CoNap, 0.1 weight percent DMA and 0.1 weight percent 2,4-P.

Table 1: In each group one component was varied. Sample 13 was made as an extreme for the 1 weight percent grouping.

Group	Sample ID	Trig wt%	CoNap wt%	DMA wt%	2,4-P wt%
1	1	1	0.2	0	0
	2	1	0.4	0	0
	3	1	0.6	0	0
2	4	2	0.2	0	0
	5	2	0.4	0	0
	6	2	0.6	0	0
3	7	2	0.4	0.1	0
	8	2	0.4	0.2	0
	9	2	0.4	0.3	0
4	10	2	0.4	0.2	0.05
	11	2	0.4	0.2	0.1
	12	2	0.4	0.2	0.15
	13	1	0.1	0	0
	14	1	0.1	0	0.15
	15	1	0.2	0.1	0.1

Procedure

Timing for gel time was started when the Trigonox was added to the sample. To determine the time it took for the resin to gel the vials were flipped about every 30 seconds. When the resin stopped flowing timing was stopped.

Results

Table 2: Gel Time Results given in minutes

ID	FAVE-L-25S	FAVE-O-25S	441-400	470HT-400
1	22	16	6	49
2	10	10	12	16
3	8	7	9	10
4	14	11	12	16
5	7	7	9	8
6	6	6	8	7
7	6	3	6	8
8	5	5	5	6
9	4	4	6	7
10	10	12	16	10±0
11	28	25	26	16.5±.7
12	34	14	31	24±1.4
13	24	14	14	179±84
14	<24hr	<24hr	<24 hr	<24hr
15	99	99	94	105

Table 3: Actual weight percents of the FAVE-L-25S mixtures and their respective Gel Times

ID	Composition FAVE-L-25S	Gel time (mins)
1	1.0057 wt% Trigonox 0.2017 wt% CoNap 0 wt% DMA 0 wt% 2,4-P	22
2	1.0497 wt% Trigonox 0.4016 wt% CoNap 0 wt% DMA 0 wt% 2,4-P	10
3	1.0258 wt% Trigonox 0.6842 wt% CoNap 0 wt% DMA 0 wt% 2,4-P	8
4	1.9453 wt% Trigonox 0.2024 wt% CoNap 0 wt% DMA 0 wt% 2,4-P	14
5	1.9535 wt% Trigonox 0.4301 wt% CoNap 0 wt% DMA 0 wt% 2,4-P	7
6	2.0202 wt% Trigonox 0.6097 wt% CoNap 0 wt% DMA 0 wt% 2,4-P	6
7	2.0888 wt% Trigonox 0.3942 wt% CoNap 0.1366 wt% DMA 0 wt% 2,4-P	6
8	2.0765 wt% Trigonox 0.4029 wt% CoNap 0.1879 wt% DMA 0 wt% 2,4-P	5
9	2.0822 wt% Trigonox 0.4153 wt% CoNap 0.3388 wt% DMA 0 wt% 2,4-P	4
10	1.9446 wt% Trigonox 0.4415 wt% CoNap 0.3213 wt% DMA 0.0625 wt% 2,4-P	10
11	1.9286 wt% Trigonox 0.4541 wt% CoNap 0.2222 wt% DMA 0.1384 wt% 2,4-P	28
12	2.0285 wt% Trigonox 0.3913 wt% CoNap 0.3163 wt% DMA 0.149 wt% 2,4-P	34
13	1.0085 wt% Trigonox 0.104 wt% CoNap 0 wt% DMA 0 wt% 2,4-P	24
14	1.0473 wt% Trigonox 0.1379 wt% CoNap 0 wt% DMA 0.1478 wt% 2,4-P	<24hr
15	0.9664 wt% Trigonox 0.2088 wt% CoNap 0.1224 wt% DMA 0.1056 wt% 2,4-P	99

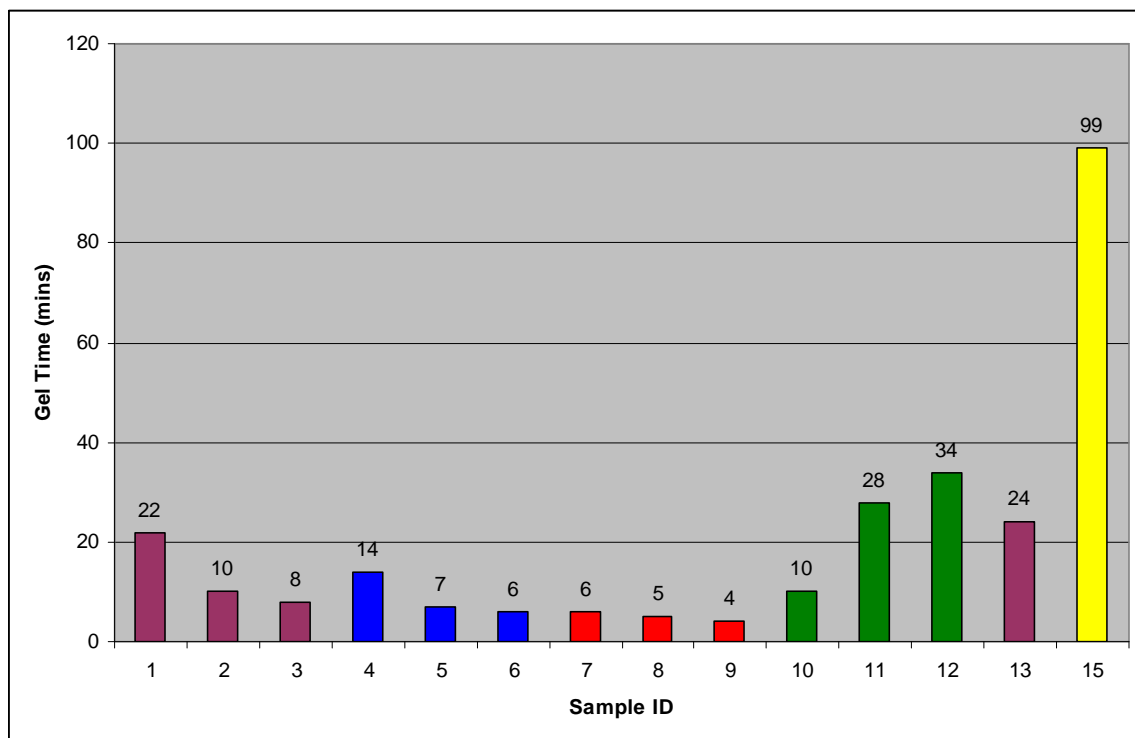


Figure 1: FAVE-L-25S Gel Times

Table 4: Actual weight percents of the FAVE-O-25S mixtures and their respective Gel Times

ID	Composition FAVE-O	Gel time (mins)
1	1.0013 wt% Trigonox 0.2056 wt% CoNap 0 wt% DMA 0 wt% 2,4-P	16
2	0.9441 wt% Trigonox 0.3918 wt% CoNap 0 wt% DMA 0 wt% 2,4-P	10
3	0.9714 wt% Trigonox 0.596 wt% CoNap 0 wt% DMA 0 wt% 2,4-P	7
4	2.0231 wt% Trigonox 0.1954 wt% CoNap 0 wt% DMA 0 wt% 2,4-P	11
5	1.9745 wt% Trigonox 0.3919 wt% CoNap 0 wt% DMA 0 wt% 2,4-P	7
6	2.0419 wt% Trigonox 0.6085 wt% CoNap 0 wt% DMA 0 wt% 2,4-P	6
7	1.943 wt% Trigonox 0.4046 wt% CoNap 0.1406 wt% DMA 0 wt% 2,4-P	3
8	1.9703 wt% Trigonox 0.4066 wt% CoNap 0.2511 wt% DMA 0 wt% 2,4-P	5
9	2.0217 wt% Trigonox 0.4493 wt% CoNap 0.3974 wt% DMA 0 wt% 2,4-P	4
10	2.0114 wt% Trigonox 0.421 wt% CoNap 0.2901 wt% DMA 0.0918 wt% 2,4-P	12
11	1.9707 wt% Trigonox 0.4648 wt% CoNap 0.2296 wt% DMA 0.1393 wt% 2,4-P	25
12	2.0222 wt% Trigonox 0.4007 wt% CoNap 0.2415 wt% DMA 0.0964 wt% 2,4-P	14
13	1.0028 wt% Trigonox 0.099 wt% CoNap 0 wt% DMA 0 wt% 2,4-P	14
14	1.059 wt% Trigonox 0.1022 wt% CoNap 0 wt% DMA 0.1418 wt% 2,4-P	<24 Hr
15	0.9223 wt% Trigonox 0.2276 wt% CoNap 0.1417 wt% DMA 0.1065 wt% 2,4-P	99

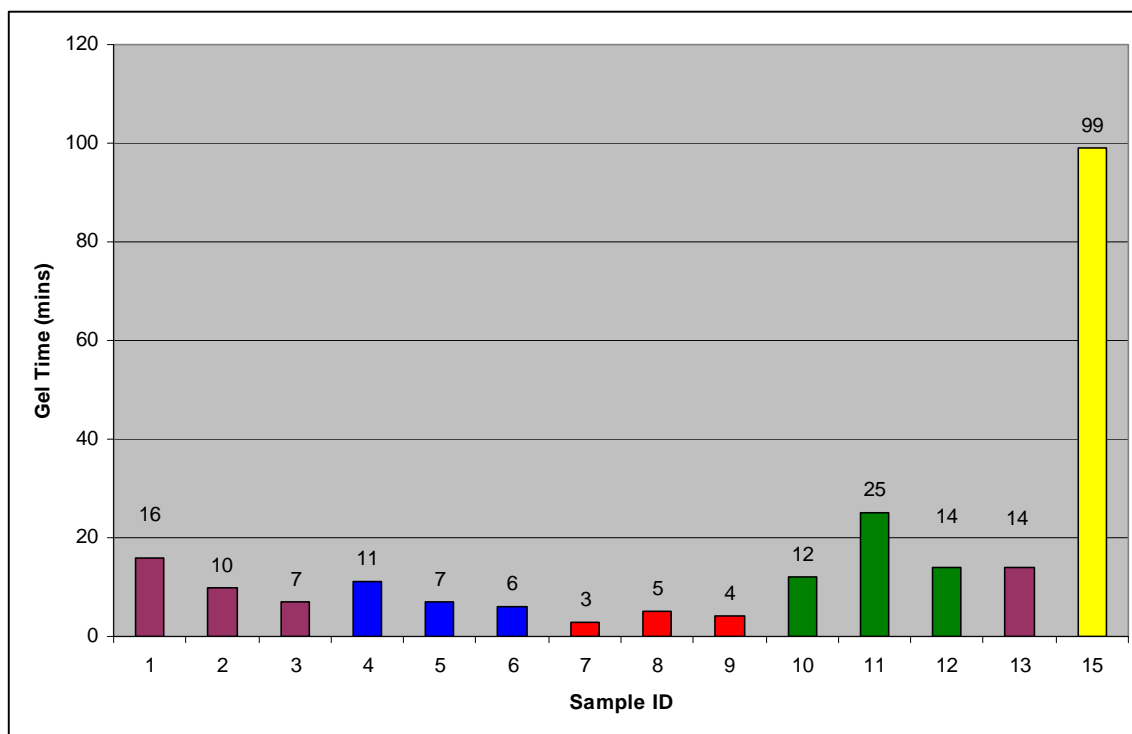


Figure 2: FAVE-O-25S Gel Times

Table 5: Actual weight percents of the 441-400 mixtures and their respective Gel Times

ID	Composition of 441-400	Gel time (mins)
1	1.0734 wt% Trigonox 0.224 wt% CoNap 0 wt% DMA 0 wt% 2,4-P	6
2	1.0161 wt% Trigonox 0.3979 wt% CoNap 0 wt% DMA 0 wt% 2,4-P	12
3	1.0373 wt% Trigonox 0.0612 wt% CoNap 0 wt% DMA 0 wt% 2,4-P	9
4	2.03 wt% Trigonox 0.216 wt% CoNap 0 wt% DMA 0 wt% 2,4-P	12
5	2.0525 wt% Trigonox 0.4239 wt% CoNap 0 wt% DMA 0 wt% 2,4-P	9
6	2.0095 wt% Trigonox 0.6259 wt% CoNap 0 wt% DMA 0 wt% 2,4-P	8
7	2.0065 wt% Trigonox 0.4325 wt% CoNap 0.1218 wt% DMA 0 wt% 2,4-P	6
8	2.0074 wt% Trigonox 0.4081 wt% CoNap 0.2395 wt% DMA 0 wt% 2,4-P	5
9	2.0187 wt% Trigonox 0.4189 wt% CoNap 0.3122 wt% DMA 0 wt% 2,4-P	6
10	2.0015 wt% Trigonox 0.4191 wt% CoNap 0.2295 wt% DMA 0.0628 wt% 2,4-P	16
11	2.0273 wt% Trigonox 0.4086 wt% CoNap 0.2178 wt% DMA 0.1089 wt% 2,4-P	26
12	1.9945 wt% Trigonox 0.4206 wt% CoNap 0.2312 wt% DMA 0.1365 wt% 2,4-P	31
13	1.0724 wt% Trigonox 0.1176 wt% CoNap 0 wt% DMA 0 wt% 2,4-P	14
14	1.0143 wt% Trigonox 0.1056 wt% CoNap 0 wt% DMA 0.1634 wt% 2,4-P	<24hr
15	0.938 wt% Trigonox 0.2001 wt% CoNap 0.2235 wt% DMA 0.1038 wt% 2,4-P	94

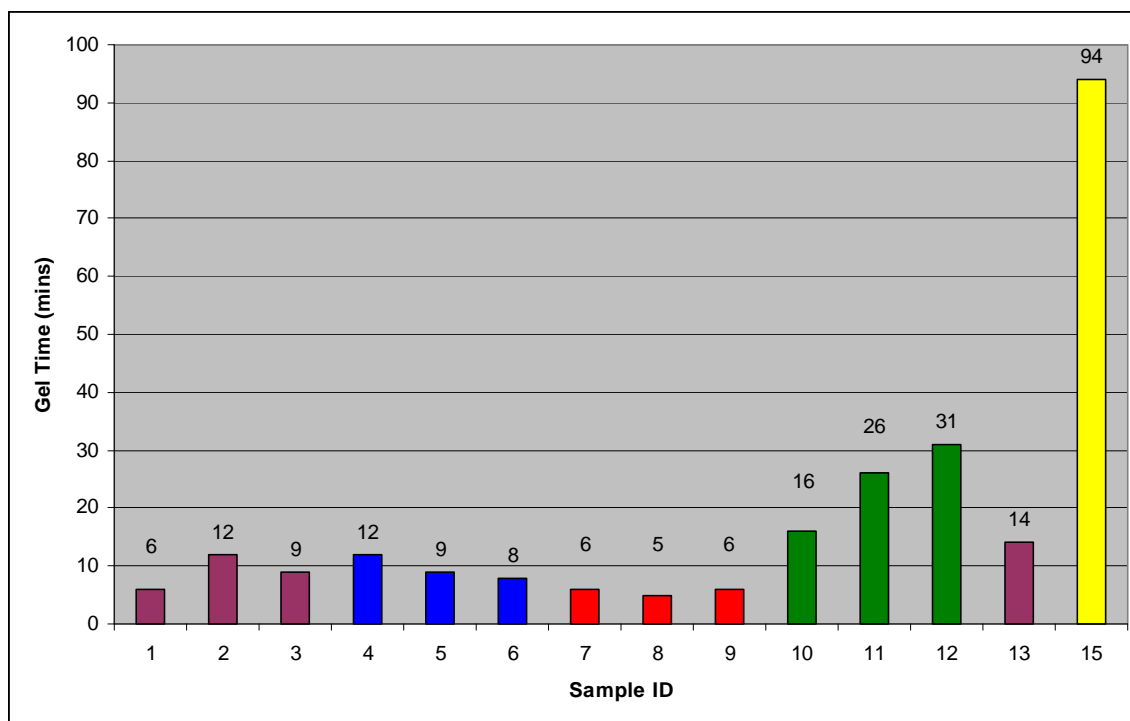


Figure 3: 441-400 Gel Times

Table 6: Actual weight percents of the 470HT-400 mixtures and their respective Gel Times

ID	Composition 470HT-400	Gel time (mins)
1	1.0089 wt% Trigonox 0.2 wt% CoNap 0 wt% DMA 0 wt% 2,4-P	49
2	1.0498 wt% Trigonox 0.4059 wt% CoNap 0 wt% DMA 0 wt% 2,4-P	16
3	1.023 wt% Trigonox 0.618 wt% CoNap 0 wt% DMA 0 wt% 2,4-P	10
4	2.0457 wt% Trigonox 0.214 wt% CoNap 0 wt% DMA 0 wt% 2,4-P	16
5	2.0088 wt% Trigonox 0.4179 wt% CoNap 0 wt% DMA 0 wt% 2,4-P	8
6	2.0176 wt% Trigonox 0.6249 wt% CoNap 0 wt% DMA 0 wt% 2,4-P	7
7	2.033 wt% Trigonox 0.4028 wt% CoNap 0.1049 wt% DMA 0 wt% 2,4-P	8
8	2.0044 wt% Trigonox 0.4167 wt% CoNap 0.1978 wt% DMA 0 wt% 2,4-P	6
9	2.0091 wt% Trigonox 0.4038 wt% CoNap 0.3149 wt% DMA 0 wt% 2,4-P	7
10	2.023 wt% Trigonox 0.41 wt% CoNap 0.203 wt% DMA 0.05 wt% 2,4-P	10
11	2.0244 wt% Trigonox 0.3999 wt% CoNap 0.2119 wt% DMA 0.099 wt% 2,4-P	16
12	2.0046 wt% Trigonox 0.3999 wt% CoNap 0.203 wt% DMA 0.149 wt% 2,4-P	25
10b	2.0219 wt% Trigonox 0.399 wt% CoNap 0.218 wt% DMA 0.057 wt% 2,4-P	10
11b	2.002 wt% Trigonox 0.405 wt% CoNap 0.205 wt% DMA 0.108 wt% 2,4-P	17
12b	2.0376 wt% Trigonox 0.3989 wt% CoNap 0.201 wt% DMA 0.152 wt% 2,4-P	23
13c	1.0068 wt% Trigonox 0.1 wt% CoNap 0 wt% DMA 0 wt% 2,4-P	276
13d	1.0466 wt% Trigonox 0.099 wt% CoNap 0 wt% DMA 0 wt% 2,4-P	122
13e	0.9959 wt% Trigonox 0.099 wt% CoNap 0 wt% DMA 0 wt% 2,4-P	139
14	0.9975 wt% Trigonox 0.1 wt% CoNap 0 wt% DMA 0.1559 wt% 2,4-P	<24 hr
15	1.2276 wt% Trigonox 0.225 wt% CoNap 0.1574 wt% DMA 0.1169 wt% 2,4-P	105

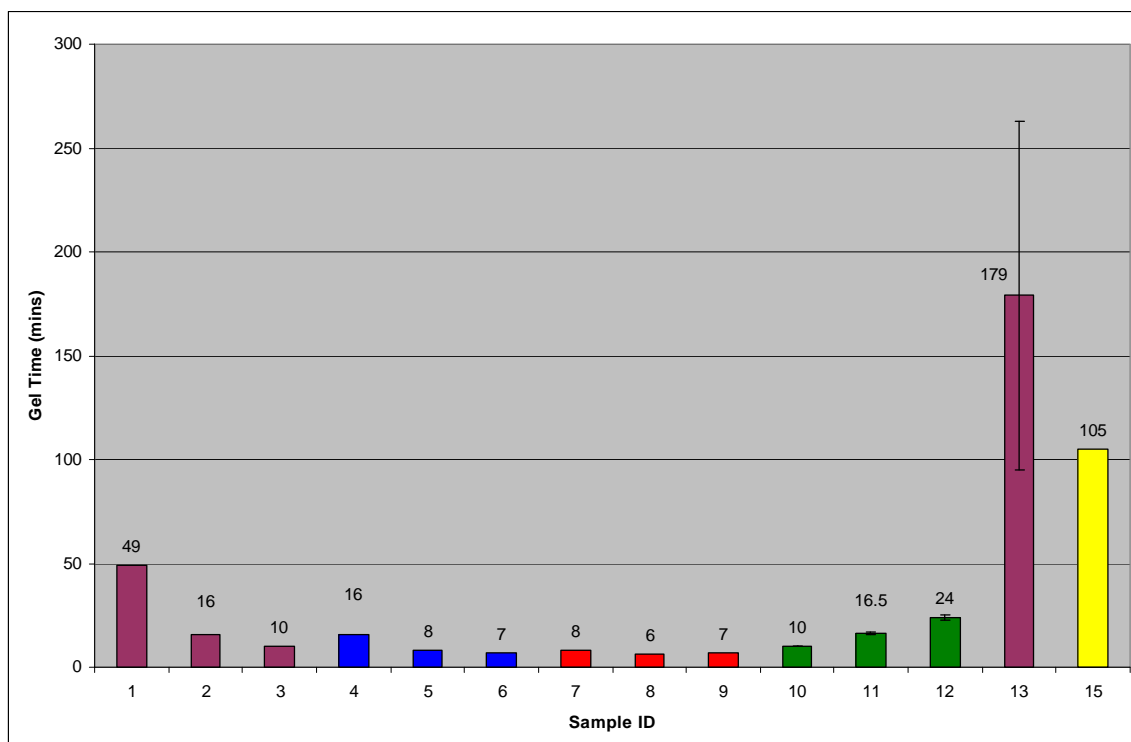


Figure 4: 470HT-400 Gel Times

Discussion

For most resin systems samples, 1-6 and 13, the amount of CoNap directly influenced the gel time exhibiting an inverse correlation between the gel time and concentration of CoNap added. With samples 7-9 the gel time decreased with the addition of DMA. For samples 10-12 the addition of 2,4-P increased the gel time significantly. In all cases sample 14 yielded a gel time that was outside of our range, 2 hours max, and in all cases samples gelled in over 6 hours but less than 24 hours. Sample 15 mixtures yielded a more useable gel time of around 1.5 hours for all resin systems. There were several instances that the expected outcomes did not occur.

FAVE-L-25S exhibited all the expected trends and its gel time can be tailored to range from 4 minutes to 99 minutes.

FAVE-O-25S exhibited most of the expected trends except for sample 13 which should have had a longer gel time than sample 1 because it contained a lower concentration of CoNap, however there is not that significant of a difference. Samples 10-12 are misleading in the graph, but when the compositions of the initiator packages are reviewed it is seen the samples 11 and 12 were reversed, their compositions and corresponding trends are correct, increasing the concentration of 2,4-P slows the gel time. Again FAVE-O-25S can be reacted with different initiator packages to achieve gel times from 3 minutes to 99 minutes.

Derakane 441-400 had a few breaks in the expected trends. sample 1 was much shorter than expected, this should have had a longer gel time than samples sample 2 and 3 because the amount of trigonox remained constant but the concentration of the CoNap was increased. In other reactions this increase decreased the gel times. 441-400 showed that a longer working time could be achieved as well using the sample 15 mixture ratios.

470HT- 400 modeled all the expected trends and showed that CoNap concentration had the most profound effect on the gel times with working times of over 2 hours. 2,4-P concentration had less of an effect on the gel times in this system than the other systems. To make sure this was the case samples 10-12 were retested and results were similar differing only 2 minutes. Sample 13 was retested several times as well, however, the results were not as closely grouped, gel times ranged from 122 minutes to 276 minutes, because of this wide range in gel time alternative mixtures, sample 15, would be better suited for instances where longer gel times are required. 470HT-400 is capable of having a wide range in working times, ranging from 6 minutes to over 105 minutes.

In the neat resin systems there were no visible differences in the uncured resins. Colors were mostly dark purple-dark brown depending on the initiator packages. The darker colors were directly influenced by the concentration of CoNap.

Conclusions

The vinyl ester resin systems tested showed that the gel times could be altered using different initiator packages. Trends reflecting the initiator packages and gel times could be seen in all the resins, however, the direct effect of initiator packages changed from vinyl ester to vinyl ester.

In most of the systems the gel times were limited to less than an hour therefore additional mixtures were need. The initiator packages used in sample 14 yielded gel times to long for our study. Reformulating it with the addition of DMA and more CoNap and lowering the concentration of 2,4-P yielded gel times ranging 93-105 minutes for all the resin systems. When a longer working time is needed the mixture for sample 15 should be used.

E glass 3D (96 oz)/ FAVE-O Panel processing summary:

Two 3D E glass fabric/ FAVE-O resin composites were fabricated using different number of layers. One panel was made using a single layer of 3D E woven fabric with an areal-density of 96 oz/yd². The second one was made using 2 layers of the fabric. In the second laminate, each layer was aligned in the same direction and carefully arranged so that the layers can be interlocked ensuing a bit higher fiber volume fraction. Vacuum Assisted Resin Transfer Molding (VARTM) process was applied with Fatty Acid Vinyl Ester System based on Octanoic acid. Room temperature cure for 24 hours and elevated temperature post-cure, 135 F for 3 hours, were used after the resin infusion.

Lay-up Sequence and Infusion Scheme:

The lay-up sequence is as follows (from bottom to top):

- Tool plate
- Peel ply
- 1 or 2 layers 3D 96oz E glass
- Peel ply
- Breather Cloth
- Distribution media.
- Vacuum bag

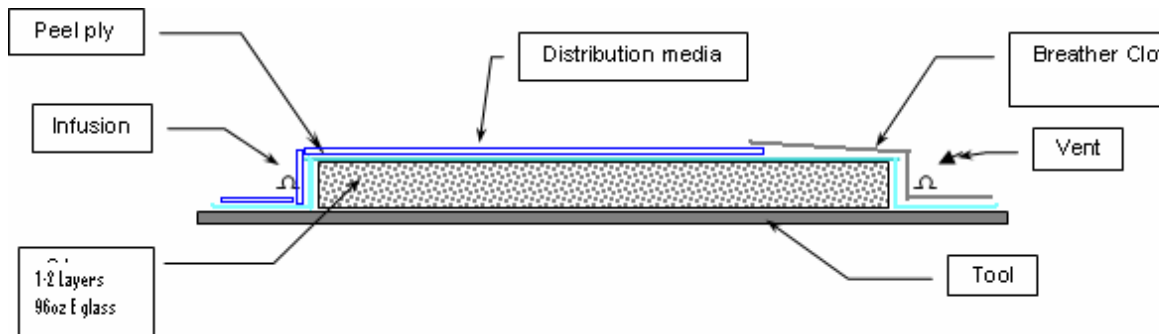


Figure 1. Schematic of VARTM Processing with side Infusion Scheme.

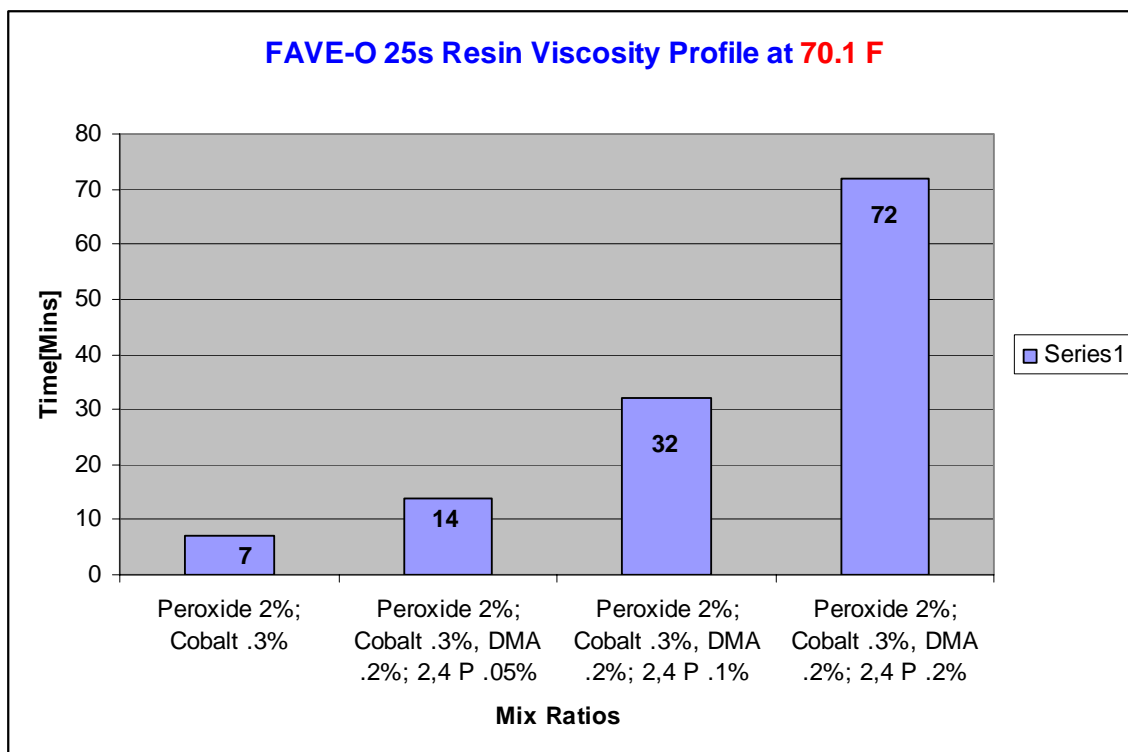


Figure 2. FAVE-O 25s Gel time.

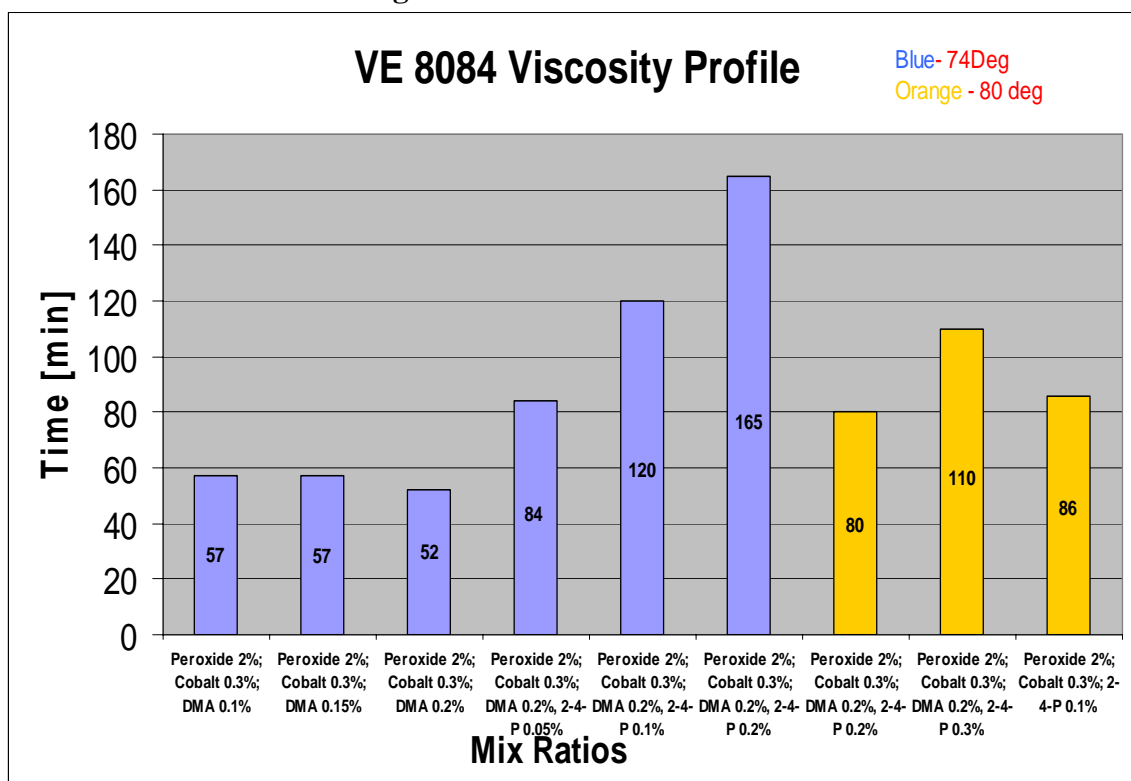


Figure 3. 8084 Gel time.

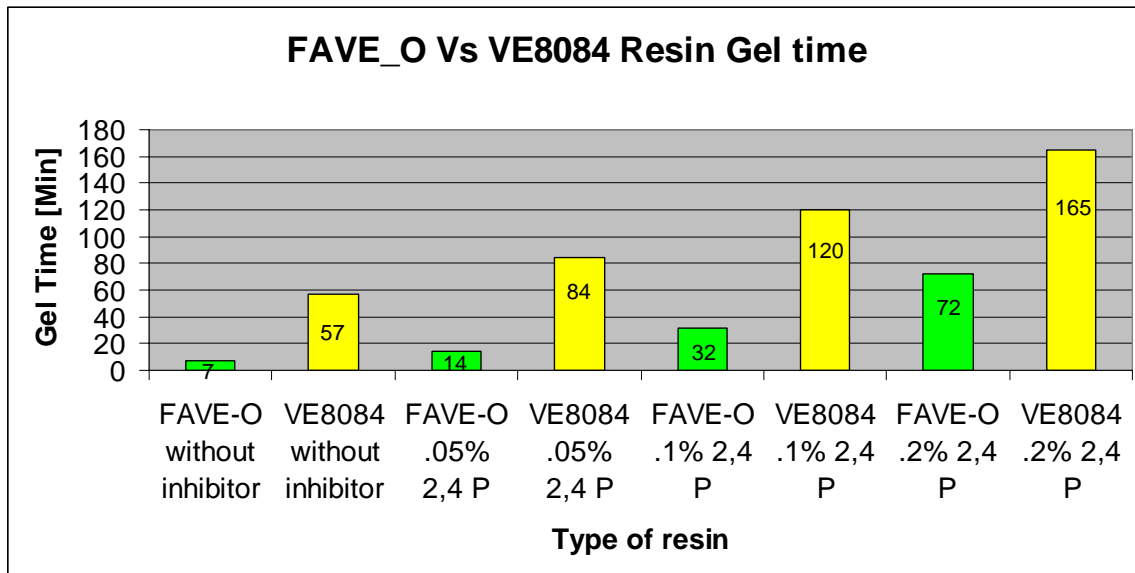
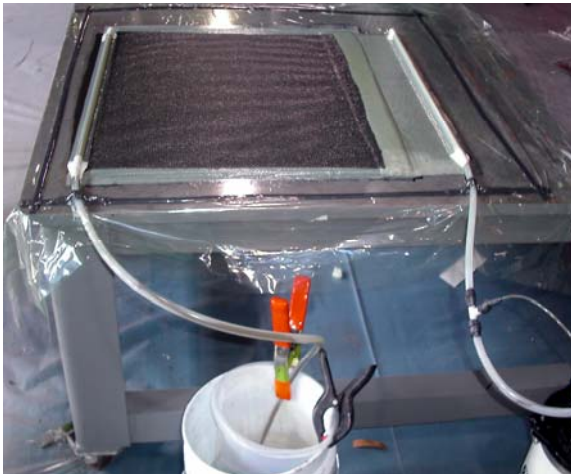


Figure 4. Gel Time Comparison.



Eglass(96oz) / FAVE-O Composite

2 Layers Eglass / FAVE panel processing

VARTM Processing Sheet (1 Layer)

Name(s): Ashiq A Quabili					
Panel ID: Eglass 96oz_1L_FAVE-O					
Fabric	Description				
	Length (L)	24	inches	60.96	cm
	Width (W)	24	inches	60.96	cm

	Aerial Weight (AD)		oz/yd ²	0.00	kg/m ²	
	Number of Layers(n)	1				
	Layup Sequence (against tool)					
	Fabric Weight (W _f , estimated)	0.0	g	0.00	lbs	
	Fabric Weight (W _f , measured)	1260.0	g	2.78	lbs	excluding unravelling: xx.x g
	Single Layer Thickness (estimated)	0.096	inches	2.44	mm	estimation for resin preparation
	AD (dry, psf)	0.00	lbs/ft ²	0.00	kg/m ²	Aerial density of dry preform
Infusion	Date	1/12/2006				
	No. of Distribution Media	1				
	No. of Breather Cloth	1				
	FVF (v _f , initial guess for resin prep.)					fiber volume fraction
	Resin Type	FAVE-O 25s				
	Cure Temperature	70.0	°F	21.1	°C	amb. temp. from a hygrometer
	Resin Density	1.140	g/mL	71.17	lbs/ft ³	liquid resin density
	Minimum Resin Amount		g	0.00	lbs	estimated from the initial FVF
	Resin Prepared	1212.0	g	2.67	lbs	extra about 1000 grams
	Trigonox	24.24	g		oz	
	Conap	3.60	g		oz	
	DMA	2.40				
	2,4 P	1.20	g	0.042	oz	
	Gel time (estimated)	30 mins				from datasheet and amb. temp.
	Time: Resin Gelling	33 Mins				
Panel	Panel Total Weight (W _c)	1743.0	g	3.84	lbs	
	Net Resin (W _r)	483.0	g	1.06	lbs	W _r =W _c -W _f
	Resin Density (ρ _r)	1.14	g/mL	71.17	lbs/ft ³	cured resin density
	Fiber Density (ρ _f)	2.55	g/mL	159.19	lbs/ft ³	S-glass
	Fiber Volume Fraction (v _f)	53.8%				$v_f = (W_f / W_c) (\rho_r / \rho_f) / [1 - (W_f / W_c)(1 - \rho_r / \rho_f)]$
	Resin Volume Fraction (v _r)	46.2%				$v_m = 1 - v_f$ (Approximate)
	Resin vs. Fabric (W _r / W _f)	38.3%				for the same configuration
	Panel Areal Weight (AD)	0.96	lbs/ft ²	4.69	kg/m ²	approximate
	Total Thickness (t)	0.100	inches	2.54	mm	
	Single Layer Thickness (t ₁)	0.096	inches	2.44	mm	
	Single Layer AD	0.961	lbs/ft ²	4.69	kg/m ²	for future reference
Postcure	Date					
	Under Vacuum or Free Standing	Free Standing				
	Ramping Up Time and Temp.	1 Hour				
	Holding Time and Temp.	3Hour @ 135 F				

Ramping Down Time
and Temp.

1 Hour

VARTM Processing Sheet (2 Layers)

Name(s): Ashiq

Panel ID: Eglass_96oz_2L_FAVE-O

Fabric	Description					Plain Weave
	Length (L)	24	inches	60.96	cm	
	Width (W)	24	inches	60.96	cm	
	Aerial Weight (AD)	24	oz/yd ²	13.02	kg/m ²	
	Number of Layers(n)	2				
	Layup Sequence (against tool)					
	Fabric Weight (Wf, measured)	2529.0	g	5.58	lbs	excluding unravelling: xx.x g
	Single Layer Thickness (estimated)	0.096	inches	2.44	mm	estimation for resin preparation
	AD (dry, psf)	0.33	lbs/ft ²	26.04	kg/m ²	Aerial density of dry preform
Infusion	Date	7/31/2006				
	No. of Distribution Media	1				
	No. of Breather Cloth	None				
	FVF (v _f , initial guess for resin prep.)	55%				fiber volume fraction
	Resin Type	FAVE-O 25s				
	Cure Temperature	68.0	°F	20.0	°C	amb. temp. from a hygrometer
	Resin Density	1.140	g/mL	71.17	lbs/ft ³	liquid resin density
	Minimum Resin Amount	2505.0	g	5.52	lbs	estimated from the initial FVF
	Trigonox	50.0	g	0.11	lbs	
	conap	7.50	g	0.26	oz	
	DMA	5.00	g	0.18	oz	
	Inhibitor	2.00	g	0.071	oz	
	Gel time (estimated)	30 Mins				
	Time: Resin Gelling	32 mins				
	Cure Schedule	RT overnight				
Panel	Panel Weight (Wc)	3480.0	g	7.67	lbs	
	Net Resin (W _r)	951.0	g	2.10	lbs	W _r =W _c -W _f
	Resin Density (ρ _r)	1.14	g/mL	71.17	lbs/ft ³	cured resin density
	Fiber Density (ρ _f)	2.55	g/mL	159.19	lbs/ft ³	Sglass
	Fiber Volume Fraction	54.3%				$v_f = (W_f / W_c) (\rho_r / \rho_f) / [1 - (W_f / W_c)(1 - \rho_r / \rho_f)]$
	Resin Volume Fraction (v _r)	45.7%				v _m = 1 - v _f (Approximate)
	Resin vs. Fabric (W _r / W _f)	37.6%				for the same configuration
	Panel Areal Weight (AD)	1.92	lbs/ft ²	9.36	kg/m ²	approximate
	Total Thickness (t)	0.195	inches	4.88	mm	
	Single Layer Thickness (t ₁)	0.096	inches	2.44	mm	
	Single Layer AD	0.959	lbs/ft ²	4.68	kg/m ²	for future reference
Postcure	Date					
	Under Vacuum or Free Standing	Free Standing				
	Ramping Up Time and Temp.	1 hr				
	Holding Time and Temp.	3 hr @135F				

Ramping Down Time and Temp.

1 hr

US Army Research Laboratory

SUMMER RESEARCH TECHNICAL REPORT

Process and Properties of Bio-rubber Modified Vinyl Ester

Resin:

Alexander Grous

Ian McAninch

John La Scala:

DEPARTMENT OF THE ARMY

U.S. ARMY RESEARCH LABORATORY

MATERIALS APPLICATION BRANCH, MATERIALS DIVISION

Attn: AMSRD-ARL-WM-MC

ABERDEEN PROVING GROUND, MD 21005

TABLE OF CONTENTS

	Page Number
List of Figures	2
1. Abstract	3
2. Introduction/Background	4
3. Experiment/Calculations	5
4. Results	7
5. Summary and Conclusions	11
6. References	13

List of Figures

Table 1: In each group one component was varied. Sample 13 was made as an extreme for the 1 weight percent grouping.....	7
Table 2: Gel times, Tg, and G1c corresponding to the different ratios of initiator components also compared against the neat resin system	8
Figure 1: Altering the initiator package concentration the bio rubber toughened 411-350 can yield gel times from 7 minutes to almost 100 minutes. Also with each individual group there were clear trends that correlated the concentration of certain initiator components with the time it took to gel.....	9
Figure 2: Gel time samples once cured exhibited different visible trends which reflect the difference in cure packages and gel times.	10
Figure 3: Dynamic mechanical analysis samples both cured (top) and post cured a 120°C for 2 hours (bottom). Fracture toughness samples exhibited the same trends as the dynamic mechanical analysis samples.....	10
Figure 4: Visible Tg trends followed a loss in Tg caused by addition of Trigonox and a slightly more loss with the addition of dimethylaniline.....	11
Figure 5: GIC values for the selected cure systems and the neat resin system.....	12

1. ABSTRACT

Vinyl Ester (VE) resins are commonly used in polymer matrix composites (PMC) because of their low cost as well as their desired mechanical properties when modified. Some modified resin systems need a higher styrene content to reduce their high viscosity caused by the modifiers. A low HAP modified VE system created at Drexel University may be a viable option for PMCs. During some process' longer working times are needed for the PMCs infuse, this can be achieved by altering the initiator packages. In the case of this bio-rubber toughened vinyl ester system the altering of initiator packages to lengthen and shorten the working time was done and its mechanical properties were evaluated to see if there were any changes. Glass transition temperature was found to vary some but more importantly the fracture toughness of the resin was maintained and was still greater than that of the neat resin.

2. INTRODUCTION/BACKGROUND

Vinyl ester (VE) resins are low cost and are used in polymer matrix composites (PMC) in a variety of applications in marine, ground and aerospace environments. A common method of processing vinyl ester composites is with a vacuum assisted resin transfer molding (VARTM).¹ This is a process in which resin is infused into fiber mats in a mold with vacuum assistance. On larger projects a longer working time is needed for the composite to completely infuse. With vinyl esters different initiator packages can be used to tailor the time of gelation and give it the appropriate amount of time for the resin to infuse the composite.

Vinyl ester resins are a popular choice for producing polymer matrix composites because of their high strength, glass transition temperature, and low cost. However, unmodified vinyl esters generally have poor toughness and contain styrene, a regulated hazardous air pollutant and volatile organic compound². Approaches for toughening vinyl ester resins are blending or reacting vinyl ester resins with different additives and modifiers which generally form a second dispersed phase. The most frequently used modifiers are liquid rubbers which are based on butadiene-acrylonitrile copolymers terminated with various functionalities like vinyl, epoxy and carboxyl.³⁻⁸ It is believed that the rubber cavitation and subsequent shear deformation of the matrix accounts for the enhancement of fracture toughness.⁹⁻¹²

The Clean Air Act (CAA) specifically lists styrene as a hazardous air pollutant (HAP) due to its toxicity and possible carcinogenicity.¹³ Studies have shown that styrene emissions during the manufacture of PMC are a very high percentage of the total styrene emissions because composite manufacturers generally do mixing, infusion, and cure in open molds without any emissions controls. As a result, the Reinforced Plastic Composite National Emissions Standard for Hazardous Air Pollutants (NESHAP) went into effect in 2003 in the U.S.¹⁴ Yet, the cost of NESHAP compliance for current resin systems, processes, and cleaning techniques will be quite expensive and difficult for most businesses to realize.¹⁵ As a result, instead of using emissions controls, PMC fabricators are using low HAP VE alternatives or are switching to non-HAP epoxy resins. These low HAP alternatives include the use of a bimodal molecular weight distribution of VE monomers to decrease the amount of styrene in the system while maintaining low resin viscosities¹⁶ or replacing styrene with non-volatile fatty acid monomers.¹⁷ These efforts will provide an environmentally preferred composite resin system applicable for liquid molding of military and commercial systems.

One such low HAP VE is a bio-rubber toughened system created at Drexel University using a plant oil derived modifier (patent disclosure in progress). This system demonstrated only a slight drop in glass transition temperature (T_g) compared to the neat system, and low viscosity was maintained and it demonstrated a very large increase in toughness.²

By altering the cure temperature, sample size and initiator package the end products were visibly very different in color and clarity. In particular, initiator packages that yielded a fast gel time resulted in a non-phase separated region whereas longer gel times resulted in

more phase separation. We hypothesize that faster cure times prevent segregation of the bio-rubber into separate toughening phases and likely result in a weaker system. The goal of this work is to validate this hypothesis regarding the initiator package. To do so various initiator packages were evaluated and the effects of gel time on thermo-mechanical and fracture properties were investigated.

3. EXPERIMENT/CALCULATIONS

3.1 Materials

The following materials were used throughout this work:

- Bio-rubber Toughened Vinyl Ester Resin (Drexel University) is a rubber toughened vinyl ester resin. The base vinyl ester resin used was Derakane 411-350. This resin was modified with 10 wt% renewable plant oil (rubber) modifier.
- Trigonox 239 A (Trig) (AkzoNobel Chemicals, Chicago, Illinois) contains 45% cumyl hydroperoxide and acts as the initiator for free radical polymerization.
- Cobalt Naphthenate 6% (CoNap) (Aldrich) is the catalyst for Trigonox in the free radical polymerization.
- N, N-Dimethylaniline (EMD Chemicals Inc). acts as an promoter and speeds the reaction significantly and also aids in fiber wetting
- 2,4-pentanedione (2,4-P) (Alfa Aesar Avocado) is a retarder and slows the reaction allowing for longer working times.

3.2 Sample Preparation

Approximately 100 grams of bio-rubber toughened vinyl ester (BR) was poured and mixed in a 200mL container. All samples were mixed in Thinky AR-250 planetary centrifugal mixer for 2 minutes at 2000 rpm after each component was added, components were added in the following order when applicable: CoNap, 2,4-P, DMA, Trigonox. Eight fracture toughness samples, four DMA samples and a gel time vial were poured from the 100g batch. Table 1 lists the concentrations of the various components of the initiator package. The first three samples (group 1) held the concentration of Trigonox constant at 1 weight percent and varied the weight percent of CoNap. Samples 4, 5, and 6, (group 2) held Trigonox at 2 weight percent and again varied the weight percent of CoNap. In samples 7, 8 and 9 (group 3) Trigonox was held constant at 2 weight percent and CoNap was held constant at 0.4 weight percent, DMA was varied at weight percents of 0.1, 0.2 and 0.3. Group 4, samples 10, 11 and 12, held the concentration of Trigonox, CoNap, DMA constant at 2 weight percent, 0.4 weight percent and 0.2 weight percent DMA respectively, and varied the concentration of 2,4-P at .05, 0.1 and 0.15 weight percent. Sample 13 was used as an extreme with 1 weight percent Trigonox and 0.1 weight percent CoNap.

Table 1: In each group one component was varied. Sample 13 was made as an extreme for the 1 weight percent grouping.

Group	Sample ID	Trig wt%	CoNap wt%	DMA wt%	2,4-P wt%
1	1	1	0.2	0	0
	2	1	0.4	0	0
	3	1	0.6	0	0
2	4	2	0.2	0	0
	5	2	0.4	0	0
	6	2	0.6	0	0
3	7	2	0.4	0.1	0
	8	2	0.4	0.2	0
	9	2	0.4	0.3	0
4	10	2	0.4	0.2	0.05
	11	2	0.4	0.2	0.1
	12	2	0.4	0.2	0.15
	13	1	0.1	0	0

3.4 Gel Time Studies

Timing for gel time was started when the Trigonox was added to the sample. To determine the time it took for the resin to gel the vials were flipped about every 30 seconds. When the resin stopped flowing timing was stopped.

3.5 Dynamic Mechanical Analysis

Samples were individually poured into a mold to give each sample the rough dimensions of 60x10x3 mm³. Samples were allowed to cure at room temperature for 16-20 hours and then were post cured at 120°C for 2 hours. Once samples were fully post cured they were polished to remove any imperfections and met even thickness and width. Testing was done on a TA Instruments DMA 2980 using 7.5 µm deflection at 1 Hz with a ramp of 2°C/min from room temperature to 180°C.

3.6 Fracture Toughness

Bars molded to size of 0.25x0.5x2.5in were poured from the master batch of resin and allowed to cure at ambient conditions for 16-20 hours; samples were then post cured for 2 hours at 120°C for 2 hours. Samples were then tested on an Instron 5500R in accordance to ASTM D 5045-93 at ambient temperatures. Due to time restrictions, fracture toughness testing was performed on only samples 2, 5, 8, 9, 11, 12, and 13. These samples were chosen because 2, 5, 8, and 11 represent the middle of each group created and samples 9, 12 and 13 represented the extremes of the test group.

4. RESULTS AND DISCUSSION

4.1 Gel Time Results

Table 2: Gel times, T_g, and G_{1c} corresponding to the different ratios of initiator components also compared against the neat resin system

ID	Composition	Gel time (mins)	T _g °C	G _{1c} (kJ/m ²)
1	1 wt% Trig 0.2 wt% CoNap 0 wt% DMA 0 wt% 2,4-P	27	104.8	
2	1 wt% Trig 0.4 wt% CoNap 0 wt% DMA 0 wt% 2,4-P	14	103	2.0±0.4
3	1 wt% Trig 0.6 wt% CoNap 0 wt% DMA 0 wt% 2,4-P	12	102.3	
4	2 wt% Trig 0.2 wt% CoNap 0 wt% DMA 0 wt% 2,4-P	20	98.1	
5	2 wt% Trig 0.4 wt% CoNap 0 wt% DMA 0 wt% 2,4-P	14	97.7	1.9±0.5
6	2 wt% Trig 0.6 wt% CoNap 0 wt% DMA 0 wt% 2,4-P	12	97.1	
7	2 wt% Trig 0.4 wt% CoNap 0.1 wt% DMA 0 wt% 2,4-P	11	97.1	
8	2 wt% Trig 0.4 wt% CoNap 0.2 wt% DMA 0 wt% 2,4-P	9	96.5	2.0±1.0
9	2 wt% Trig 0.4 wt% CoNap 0.3 wt% DMA 0 wt% 2,4-P	7	94.7	1.8±0.6
10	2 wt% Trig 0.4 wt% CoNap 0.2 wt% DMA 0.05 wt% 2,4-P	31	98.2	
11	2 wt% Trig 0.4 wt% CoNap 0.2 wt% DMA 0.1 wt% 2,4-P	35	96.3	2.5±0.8
12	2 wt% Trig 0.4 wt% CoNap 0.2 wt% DMA 0.15 wt% 2,4-P	98	97.1	2.2±0.6
13	1 wt% Trig 0.1 wt% CoNap 0 wt% DMA 0 wt% 2,4-P	75	104.3	1.8±0.2
	Unmodified 411-350 Vinyl Ester System	NA	123 ²	0.26 ± 0.06 ²

For samples 1-6 and 13 the amount of CoNap directly influenced the gel time exhibiting an inverse correlation between the gel time and concentration of CoNap added. With samples 7-9 the gel time decreased with the addition of DMA. For samples 10-12 the addition of 2,4-P increased the gel time significantly.

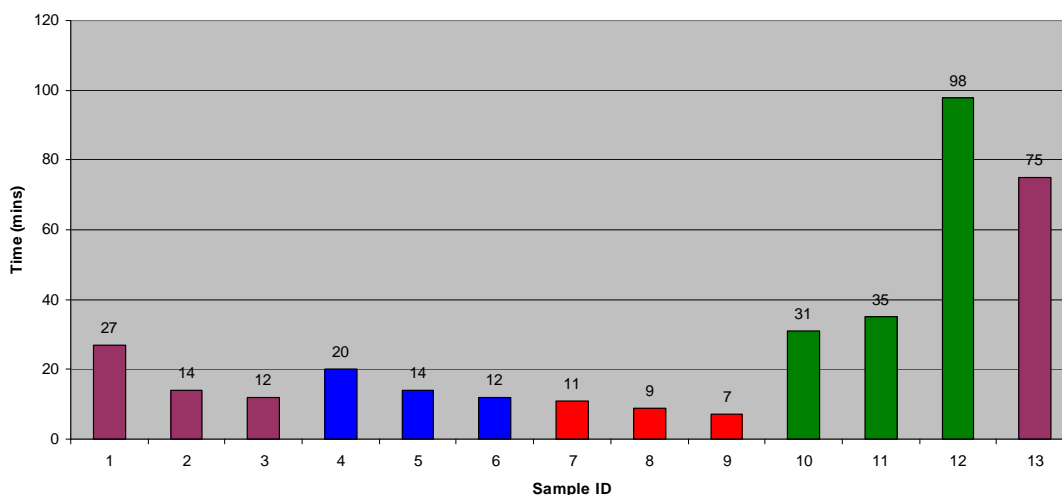


Figure 1: Altering the initiator package concentration the bio rubber toughened 411-350 can yield gel times from 7 minutes to almost 100 minutes. Also with each individual group there were clear trends that correlated the concentration of certain initiator components with the time it took to gel.

There was also a trend in gel time and the visible outcome of the resin samples (Figure 2). Group 1 gel time samples were mostly gray at low concentration of CoNap and got less opaque as the CoNap concentrations increased. This was also the case for the second group of gel time samples. When dimethylaniline was added and the gel time was greatly reduced samples became translucent and very little phase dispersion occurring with sample 9 being almost completely clear. To increase gel time 2,4-P is added, and the addition also causes the most dramatic color changes. Cured samples were green as seen in Figure 2, and this may have to do with the reaction of 2,4-P with CoNap. This is further supported because shortly after mixing the resin systems turned green and the color transformation also happened well before the samples gelled.

For fracture toughness and dynamic mechanical analysis samples (Figure 3), color trends could also be witnessed within and across the different groups with only one difference. Group 3 did not appear translucent (Figure 3) as in did in the gel time samples (Figure 2). Also, sample 13 appeared similar to sample 1 for the mechanical samples (Figure 3), which was not the case for the gel time samples (Figure 2).

Post curing is a processing step in which cured samples are heated at an elevated temperature near or above the glass transition temperature of the polymeric resin for a fixed duration, usually a few hours. It is a common practice to post cure vinyl esters to completely react all of the monomers into the polymeric matrix to maximize glass transition temperature and modulus. When samples were post cured, they turned brown in color likely due to the oxidation of the cobalt in the CoNap. Although the color changed, trends in translucency and clarity were still able to be seen in the post cured samples, i.e. darker cured samples were still darker post cured.

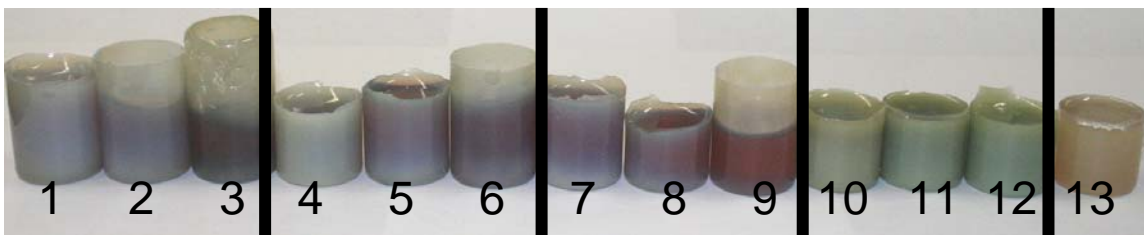


Figure 2: Gel time samples once cured exhibited different visible trends which reflect the difference in cure packages and gel times.

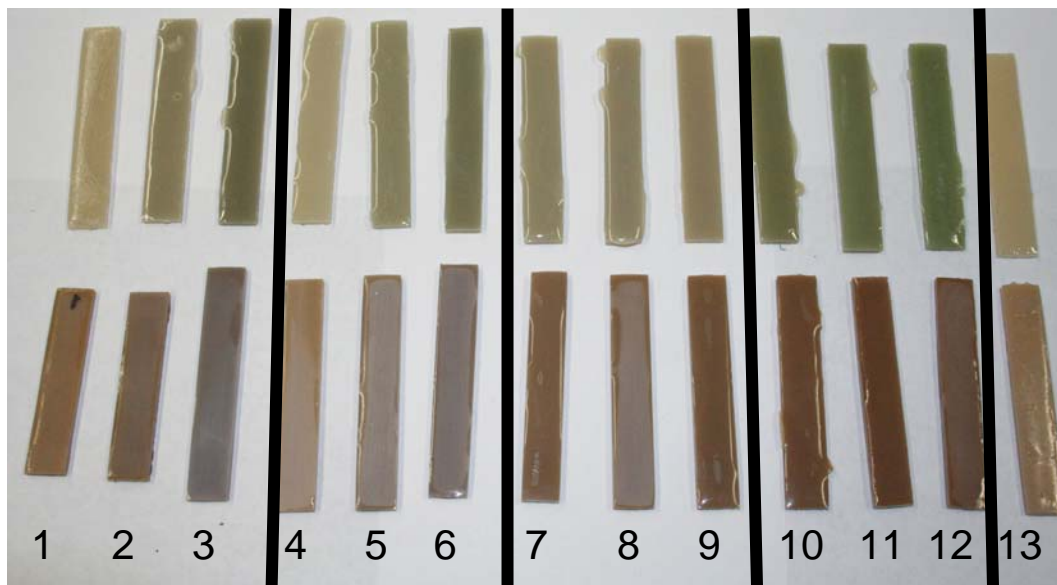


Figure 3: Dynamic mechanical analysis samples both cured (top) and post cured a 120°C for 2 hours (bottom). Fracture toughness samples exhibited the same trends as the dynamic mechanical analysis samples.

4.2 Dynamic Mechanical Analysis Results

Dynamic mechanical analysis was also performed to see if T_g was affected by the different initiator packages. Well defined trends within each group could be seen with the exception of group 4. T_g is a direct function with gel time, shorter gel times lead to a lower T_g which can be seen in Figure 4. The average T_g for groups 1, 2, 3 and 4 were $103.4 \pm 1.3^\circ\text{C}$, $97.6 \pm 0.5^\circ\text{C}$, $96.1 \pm 1.3^\circ\text{C}$, and $97.2 \pm 1.0^\circ\text{C}$, respectively. Compared to the neat resin system (123°C), a lower T_g is expected because the modifiers have a lower T_g than the styrene which it replaces¹⁷.

In groups 1 and 2, gel times were fairly similar for samples 2 and 5 (14 min) and samples 3 and 6 (12 min) yet did not exhibit similar T_g . There was a 6°C drop in T_g between the samples from group 1 and group 2. The concentration of Trigonox was the only variable between the two groups. In fact, the average T_g for 1 weight percent Trigonox was 103.6°C , while for 2 weight percent Trigonox, T_g was 97°C . To validate that there is an inverse relationship with Trigonox concentration and T_g further investigation needs to be done with the effect of the concentration of Trigonox with a neat resin system.

Addition of dimethylaniline possibly caused the T_g to drop further for the third grouping, which had the same concentration of Trigonox as group 2. It is also possible that the $\sim 3^\circ\text{C}$ loss in T_g could also be attributed to the ~ 3 min shorter gel times for group 3 relative to group 2. While the samples with 2,4-P had much longer gel times than the other samples, there was no direct correlation with T_g . Its T_g was similar to those that had shorter gel times which had the same 2 weight percent of Trigonox.

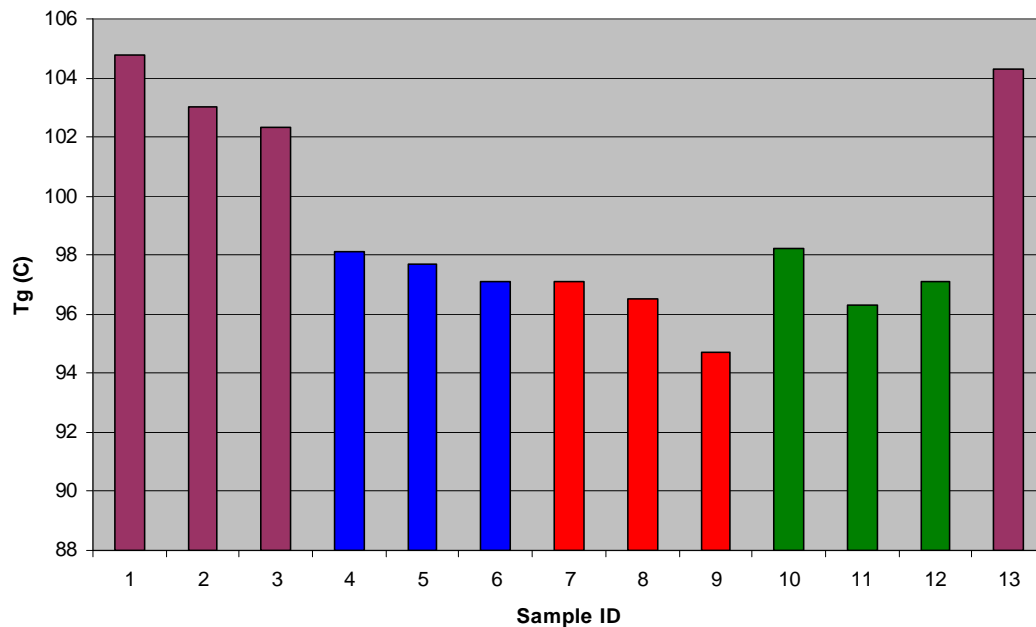


Figure 4: Visible T_g trends followed a loss in T_g caused by addition of Trigonox and a slightly more loss with the addition of dimethylaniline

4.3 Fracture Toughness Results

Figure 5 shows that the fracture toughness is insensitive to the initiator package. The results contained a large amount of experimental error. Although fairly large error bars are typical for standard vinyl ester resins,¹⁷ in this experiment because of the nature of the test these error bars are even larger than usual likely as a result of the toughened 2-phase system. In future work, samples 1, 3, 4, 6, 7, and 10 will be tested to determine whether this trend still holds true. What can be seen in table 2 is that even the sample with the lowest G_{IC} , sample 8, had a much higher fracture toughness ($2.04 \pm 1.0 \text{ kJ/m}^2$) than that of the neat resin system ($0.3 \pm 0.06 \text{ kJ/m}^2$).² This is still almost 4 times tougher than the neat resin system and validates the bio-rubber toughened vinyl ester as an alternative as a

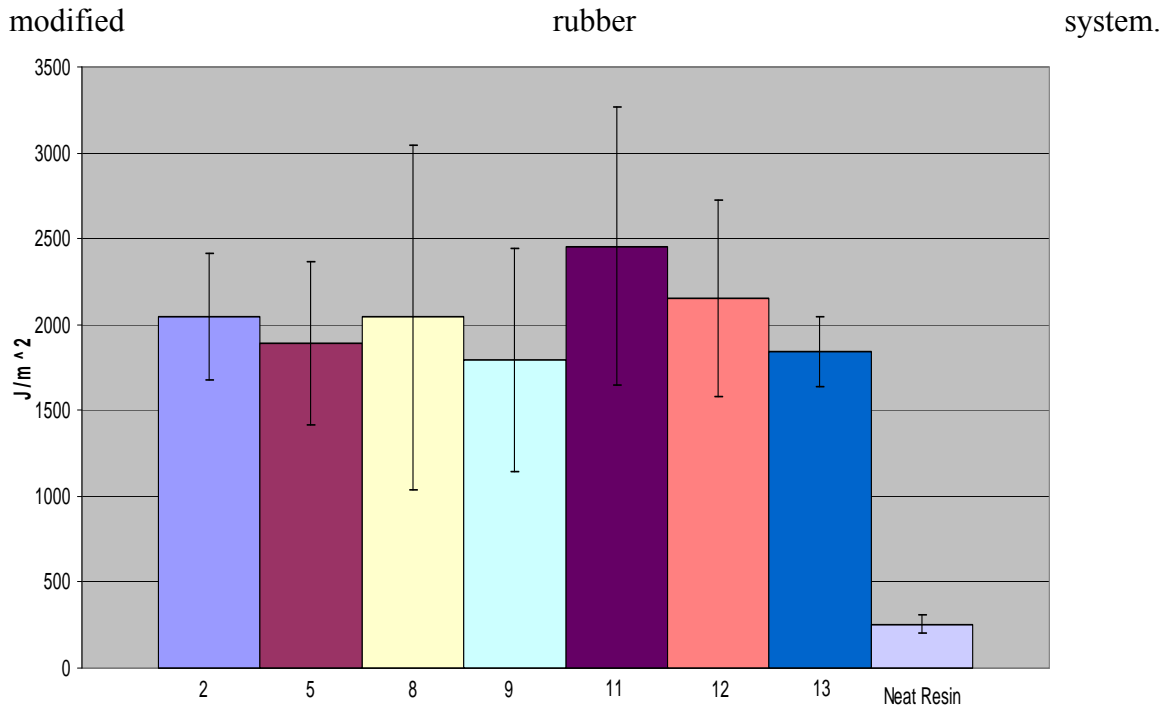


Figure 5: GIC values for the selected cure systems and the neat resin system.

More work needs to be done for the completion of the fracture toughness component of this study; the remaining samples will be done as well as possibly an investigation into the non-post cured samples. After post curing, which is a common practice with vinyl ester resin processing, the samples internal structures are normalized since they will be fully cured. There is a possibility that larger differences in G_{IC} will be observed before post curing, when samples are the most different visibly.

5. SUMMARY AND CONCLUSIONS

Cured bio-rubber toughened 411-350 exhibited a wide range of visible difference, samples that contained dimethylaniline cured very fast, within 10 minutes, and this causes a translucent center with only partial second phase separation. However that translucency did not carry over to the mechanical samples due to a change in geometry. The longer curing ones, particularly group 4 and sample 13 were the most visibly different from the rest. Group 4 had a green color and sample 13 was almost white when it finally cured, these samples exhibited full second phase separation and were uniform in color. When post cured, all samples were normalized to a brown color. Still slight variations in the darkness of brown could be seen, generally when samples were darker during non post cure they were darker after post cure. Despite these variations the overall mechanical properties were only slightly affected.

Glass transition did generally decrease with shorter gel times as it did in Group 3. Group 3 contained dimethylaniline which sped the cure and subsequently caused the translucency which was an indicator that the second phase dispersion did not take place and this could have contributed to the 10°C loss in T_g . That trend did not follow with the

longer curing resins as in group 4 which had a T_g closer to the other systems, rather the loss may be explained by the concentration of Trigonox. When tested, the post cured fracture toughness samples exhibited no overall trends reflecting gel time or initiator package but still maintained a G_{Ic} higher than the neat resin system.

The processability of bio-rubber toughened 411-350 requires no special needs to maintain its mechanical integrity when longer working times are required. Large parts that require a longer working period can be made with just altering the initiator packages without great loss of performance, and despite the wide range of visible differences, the overall mechanical properties remain the same.

REFERENCES

1. A. Cripps et al., *Fibre-reinforced Polymer Composites in Construction*. CIRIA, 2002 pg 41
2. Geng, X., Grous, Alexander T., La Scala, John J., Sands, James M., Palmese, Giuseppe R., Toughening Vinyl Ester Resin Using Novel Bio-based Rubber. SAMPE 2008
3. M.L. Auad, et al., *Polymer*, 42, 3723 (2001)
4. E.J. Robinette, et al., *Polymer*, 45, 6143 (2004)
5. E. Dreerman, et al., *J Appl Polym Sci*, 72, 647 (1999)
6. J.S. Ullet, et al., *Polym Engng Sci*, 35, 1086(1995)
7. D. Stevanovic et al., *Polymer*, 43, 4503(2002)
8. S. Pham, et al., *Polymer*, 36, 3279 (1995)
9. W. Bascom, et al., *J Mater Sci*, 16, 2675(1981)\
10. W. Bascom, et al., *J Appl Polym Sci*, 19, 2545(1975)
11. R. Pearson, et al., *J Mater Sci*, 21, 2475(1986)
12. A. Yee, et al., *J Mater Sci*, 21, 2462(1986)
13. Bassett, S., ed. *Emission Control Strategies: A Guide for Composites Manufacturers*; Ray Publishing, Inc.: Wheat Ridge, CO, 2003.
14. Environmental Protection Agency. Fed. Reg. 2003, 68, 19375.
15. Vallone, J. "NESHAP Requirements Assessment for Miscellaneous Coatings, Adhesives, Sealers, Etc.," Final Report to ARL, Sustainable Painting Operations for the Total Army, 2004
16. La Scala, J. J.; Orlicki, J. A.; Winston, C.; Robinette, E. J.; Sands, J. M.; Palmese, G. R. *Polymer* 2005, 46, 2908.
17. La Scala, J. J.; Sands, J. M.; Orlicki, J. A.; Robinette, E. J.; Palmese, G. R. *Polymer* 2004, 45, 7729.
18. ASTM D 5045-93. Standard Test Methods for Plane-Strain Fracture Toughness and Strain Energy Release Rate of Plastic Materials, Designation D 5045-93; American Society for Testing Materials 1993.

INTENTIONALLY LEFT BLANK.

Appendix E. Publications

This appendix appears in its original form, without editorial change.

Appendix E

Publications

Molecular Relaxation Behavior of Fatty Acid-Based Vinyl Ester Resins

Steven E. Boyd,¹ John J. La Scala,¹ Guiseppe R. Palmese²

¹Army Research Laboratory, AMSRD-WMRD-WM-MC, APG, Maryland 21005

²Department of Chemical Engineering, Drexel University, Philadelphia, Pennsylvania 19104

Received 4 September 2007; accepted 20 December 2007

DOI 10.1002/app.27957

Published online 6 March 2008 in Wiley InterScience (www.interscience.wiley.com).

ABSTRACT: The experimental characterization of the time-dependent properties of fatty acid-based vinyl ester resins with reduced styrene content and emissions was conducted and compared with that of various commercial vinyl ester (VE) resins. Constant heating rate and isothermal, multifrequency sweep experiments were conducted over a wide temperature range using dynamic mechanical analysis. Storage and loss modulus master-curves were formed using time-temperature superposition (TTSP) and analyzed to quantify the molecular relaxation behavior using accepted techniques and theories. Special attention was focused on determining the effect of reducing styrene weight percent on the derived viscoelastic properties. The

fatty acid-based VE resins were found to have similar or slightly inferior thermomechanical properties and a more pronounced viscoelastic response compared with the commercial resins. However, the research definitively demonstrates that the evaluated fatty acid VE resins are a viable replacement to commercial resins in certain applications with concomitant attractive environmental benefits. © 2008 Wiley Periodicals, Inc. *J Appl Polym Sci* 108: 3495–3506, 2008

Key words: viscoelastic properties; thermal properties; relaxation; fatty acid vinyl esters; styrene replacements/alternatives

INTRODUCTION

Vinyl ester (VE) resins are used to make polymer matrix composites for military and commercial civil and infrastructure applications because of their overall good thermal, mechanical, electrical properties, low weight, and low cost compared with conventional materials. These commercial resins typically contain high concentrations (>40 wt %) of reactive diluents, such as styrene (Fig. 1), to decrease viscosity that facilitates the use of conventional room temperature liquid transfer molding techniques to fabricate large scale composites parts and structures. Because styrene is a hazardous air pollutant (HAP) and a volatile organic compound (VOC), the Federal Environmental Protection Agency of the United States of America has introduced legislation that will limit styrene emissions from composite manufacturing.¹ Therefore, replacing all or part of the current

reactive diluents in VE resins with nonvolatile reactive diluents, such as fatty acid (FA) monomers, offers a large environmentally green advantage.

Previous work has shown that specially prepared FA monomers can be blended and cured with VE and unsaturated polyester monomers or resins.^{2–5} This research presented studies of the glass transition temperature, cure kinetics and viscosity for ternary blends of VE, methacrylated fatty acids (MFA), and styrene (Fig. 2) and compared them with Derakane 411-C50 (now replaced by Derakane 411-350).^{2,3} Of particular interest here was the effect of reducing styrene content on monomer and polymer properties and performance. The study found that polymer properties typically decreased with decreasing styrene content with respect to those of the commercial resins. Even so, the observed reduction in properties was minor and reasonably comparable results for room temperature polymer properties such as fracture toughness, flexural strength, and molecular weights of commercial and fatty acid-based VE resins were obtained.³ The comparable cure and ternary polymer properties are quite encouraging because FA monomers are excellent alternatives to styrene because of their low cost and lower volatility. In addition, fatty acids are renewable resources because they are derived from plant oils. Therefore, not only would the use of fatty acids in liquid molding resins reduce VOC emissions, thereby reducing health and environmental risks, but it also would promote global sustainability.

Correspondence to: S. Boyd (boyd@vt.edu).

Contract grant sponsor: SERDP; contract grant number: PP-1271.

Contract grant sponsor: ESTCP; contract grant number: WP-0617.

Contract grant sponsor: ARL; contract grant number: DAAD 19-02-2-0010.

Journal of Applied Polymer Science, Vol. 108, 3495–3506 (2008)
© 2008 Wiley Periodicals, Inc. *This article is a US Government work and, as such, is in the public domain in the United States of America.

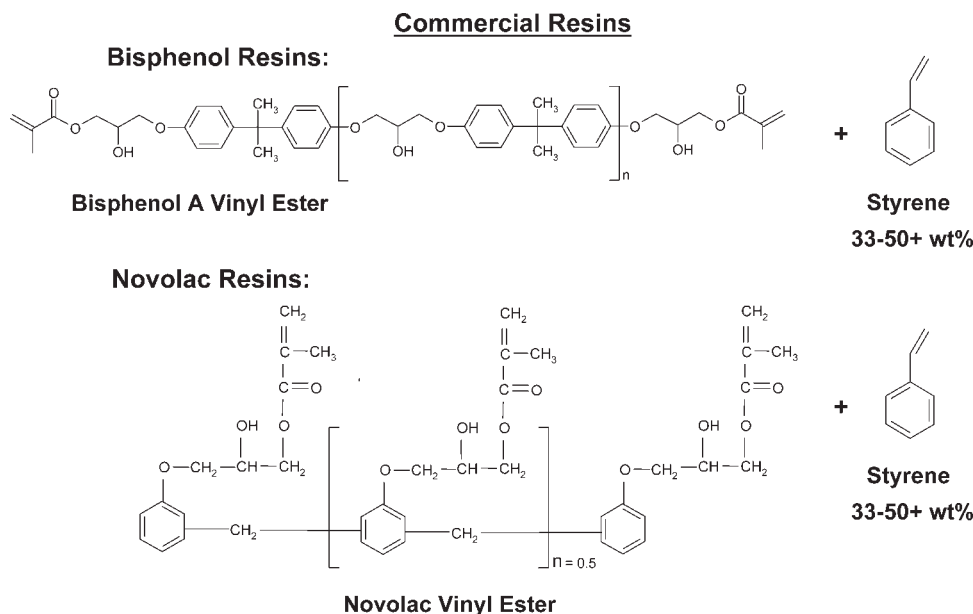


Figure 1 The chemical composition of bisphenol A and novolac based vinyl ester resins.

The current research effort will extend the characterization of fatty acid vinyl ester (FAVE) resins and their commercial counterparts to time-dependent polymer properties. This effort will also present a more detailed determination of properties and one-

to-one comparison of the commercial and FAVE resins. The commercial and FAVE resins selected here are based on current proposed uses in Department of Defense (DoD) applications for glass reinforced composites such as the Marines HMMWV (i.e.,

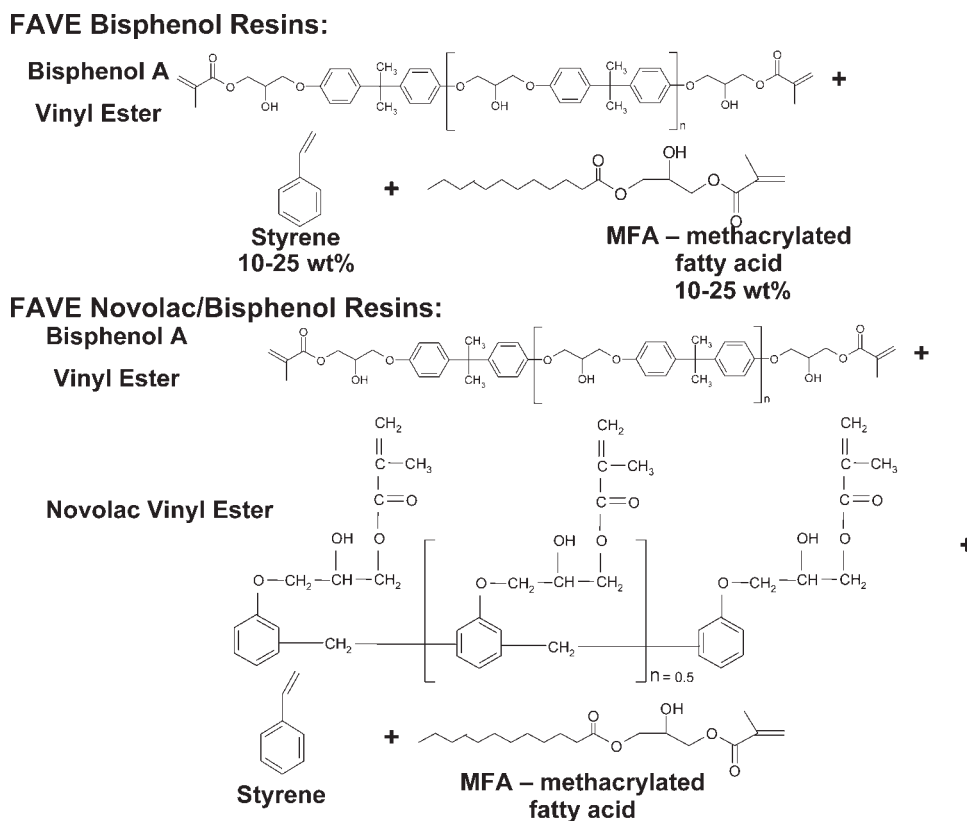


Figure 2 The chemical composition of FAVE resins.

TABLE I
Chemical Formulation of Commercial Resins

Resin	Type	Formulation			
		Bisphenol A VE (wt%)	Novolac VE (wt%)	MFA (wt%)	Styrene (wt%)
Derakane 8084	Toughened Bisphenol A	~ 60 ^a	0	0	40
Hexion 781-2140	Bisphenol A	54	0	0	46
Corve 8100	Bisphenol A	50.5	0	0	49.5
Derakane 441-400	Bisphenol A	67	0	0	33
Derakane 470-300	Novolac	~ 33.5 ^b	~ 33.5 ^b	0	33
Derakane 470HT-400	Novolac	0	67	0	33

^a An unknown percentage of the non-styrene portion of the resin is an elastomer for toughening.

^b Approximately half of the Derakane 470-300 vinyl ester is novolac and half is bisphenol A type.

Humvee) helmet hardtops, Air Force T-38 dorsal covers, mine counter measure (MCM) composite rudders for the Navy, and Army tactical vehicles, including HMMWV hoods, HMMWV transmission containers, and M35A3 truck hoods. Although this work focuses on the neat resin viscoelastic characterization, similar testing/validation is currently underway or planned for FAVE glass reinforced composites.

The viscoelastic characterization is performed using data from constant heating rate and isothermal step, multifrequency sweep experiments, and standard techniques. The accelerated characterizations scheme provided by the time-temperature superposition principle (TTSP)⁶ is used here to reduce the storage and loss modulus data into time-temperature master-curves. The interdependence of the relaxation times and temperature is determined through a temperature shift factor analysis of the Williams-Landel-Ferry (WLF)⁷ type from which the corresponding apparent activation energies can be calculated. The breadth of the relaxation is quantified using the empirical Kohlrausch-Williams-Watts (KWW)^{8,9} function. Comparisons of the glass transition temperature, the molecular weight due to cross-linking, and resistance to thermal softening are also presented. The main emphasis of this work is to not only present a comparison of these resin systems but also to determine whether FAVE resins are a viable alternative to commercial resins, thereby defining the effects of reduced styrene content on various viscoelastic properties of these ternary blends.

EXPERIMENTAL AND MATERIALS

Viscoelastic characterization of both commercial and FAVE resins was primarily conducted through dynamic mechanical analysis (DMA) testing. First, DMA samples were prepared for each resin, and

then a temperature ramp was conducted to assess the degree of cure, determine the breadth of the glass transition range and the glass transition temperature, T_g . Second, isothermal, multifrequency sweep testing was performed over a broad temperature range carefully focusing on the leathery region of the resin identified by the breadth of the glass transition. Finally, TTSP was used to construct master-curves from the storage and loss modulus data and other analyses were employed to determine relevant viscoelastic properties for characterization and comparison purposes.

Materials

Various commercial VE resins (Table I) were used in this work. The commercial resins Coryzn Corve 8100¹⁰ and Hexion 781-2140,¹¹ are bisphenol A-based VEs with high styrene contents. Ashland Derakane 441-400 is a bisphenol A-based VE resin with a low styrene content for a commercial resin (33 wt %).¹² Derakane 470HT-400 is a high temperature VE with a high functionality and low styrene content.¹³ Derakane 470-300 is a blend of low functionality novolac and bisphenol A VE also with a low styrene content.¹⁴ Derakane 8084 is an elastomer toughened bisphenol A VE resin with 40 wt % styrene.¹⁵

FAVE resins were formulated to match the properties of commercial VE resins. Table II lists the FAVE formulations and their compositions. The FAVE formulations were prepared using commercial Derakane resins as their basis and through the addition of MFA and pure VE monomers. MFA monomers were prepared by reacting fatty acids with glycidyl methacrylate at moderate temperature.²⁻⁵ Methacrylated lauric acid (MLau) and methacrylated octanoic acid (MOct) were used in this work. MOct produces resins with slightly higher T_g and lower viscosities, but costs more than MLau. Sartomer CN-151 is a

TABLE II
Chemical Formulation of FAVE Resins

Resin	Type	MFA used	Derakane type	Formulation					
				Derakane (wt %)	CN-151 (wt %)	Total Bisphenol A VE (wt %)	Novolac VE (wt %)	MFA (wt %)	Styrene (wt %)
FAVE-L-10S	FAVE, Bisphenol A	Lauric acid	441-400	20.3	44.7	65	0	25	10
FAVE-L-20S	FAVE, Bisphenol A	Lauric acid	441-400	40.6	24.4	65	0	15	20
FAVE-O-20S	FAVE, Bisphenol A	Octanoic acid	441-400	40.6	24.4	65	0	15	20
FAVE-L-25S	FAVE, Bisphenol A	Lauric acid	441-400	50.8	14.2	65	0	10	25
FAVE-O-25S	FAVE, Bisphenol A	Octanoic acid	441-400	50.8	14.2	65	0	10	25
FAVE-O-470-300-25S	FAVE, Novolac/Bisphenol A	Octanoic acid	470-300	50.8	14.2	~ 39.6 ^a	~ 25.4 ^a	10	25
FAVE-O-HT-25S	FAVE, Novolac/Bisphenol A	Octanoic acid	470HT-400	50.8	14.2	14.2	50.8	10	25

^a Approximately half of the Derakane 470-300 vinyl ester used to partially formulate the FAVE-O-470-300-25S is novolac and half is bisphenol A type, resulting in a slight uncertainty in the novolac and bisphenol A type vinyl ester fraction of this resin.

low molecular weight bisphenol A VE monomer containing no reactive diluent.¹⁶ The total VE content was targeted at 65 wt % for all FAVE formulations. As an example, FAVE-L-25S was formulated by blending 75.8 wt % Derakane 441-400 (of which 50.8 wt % of the total FAVE resin is VE monomers and 25 wt % is styrene) with 14.2 wt % CN-151 and 10 wt % methacrylated lauric acid (MLau). Because of the high viscosity of CN-151, this monomer was heated to 70°C for 10 min prior to adding to the Derakane/MFA solution and then mixed thoroughly. The “L” in “FAVE-L-25S” indicates that the MFA used is MLau, and the “25S” suffix indicates that the resin contains 25 wt % styrene. FAVE-O-20S indicates uses MOct as the MFA and contains 20 wt % styrene.

Neat resins were cured at room temperature using a mixture of Trigonox 239A (Akzo Nobel Chemicals, Chicago, IL), containing 46% cumene hydroperoxide, and cobalt naphthenate (CoNap) (Aldrich). The Trigonox and CoNap weight percents used were 1.5 and 0.375 wt %, respectively, of the total resin weight; however, for more viscous resins such as FAVE-L/O-20S and FAVE-L/O-25S with lower styrene content, the weight percents were reduced to 1 and 0.2%, respectively, to increase gel time and allow for evacuation of air from the mixture. Neat resins were cured overnight in RTV molds with nominal dimensions of 60 mm × 12 mm × 3 mm and then post-cured at 150°C for 2 h. The higher temperature resins such as the Derakane Momentum 470-300 and Derakane 470HT-400 were both cured at 200°C for 2 h. The samples were then wet sanded to ensure uniform cross-sectional area and cut to a length of 50 mm and dried for an additional hour at 40–50°C.

Experimental

All samples were tested on a TA Instruments Q800 DMA using dual cantilever geometry. At least two constant heating rate experiments for each resin were carried out from 30 to 200°C (225°C for the higher temperature novolac-based resins) with a heating rate of 2°C/min and constant oscillatory displacement amplitude of 7.5 μm at 1 Hz. Also, at least two isothermal, multiple frequency sweep tests were conducted over three decades of frequency (0.1 to 30 Hz) at discrete temperatures ranging from 30°C to ~ 170 °C for the bisphenol A type VEs resins and to 200°C for the novolac type VE resins in 5°C steps. The steps were refined to 2 or 3°C in the temperature ranges of the glass transition as identified by the constant heating rate experiments. The oscillatory amplitude was maintained at 7.5 μm to ensure a linearly viscoelastic response over the wide temperature range.

TABLE III
Summary of Thermo-Mechanical and Viscoelastic Properties for Commercial and FAVE Resins

Resin system	<i>n</i>	<i>T_g</i> (°C)	<i>M_c</i> (g/mol)	ΔH_a (kJ/mol)	<i>C₁⁰</i> (°C)	<i>C₂⁰</i> (°C)	<i>f₀</i> (10 ⁻²)
Derakane 8084	0.87	101.8 ± 1.4	828 ± 84	633 ± 13	22.8	104.1	1.9
Hexion 781-2140	0.76 ± 0.01	121.8 ± 0.3	895 ± 86	647 ± 14	17.5	55.0	2.5
Corve 8100	0.75	116.4 ± 0.5	1323 ± 103	608 ± 4	18.6	51.7	2.3
Derakane 441-400	0.76	129.1 ± 1.0	632 ± 18	613 ± 32	21.4	71.4	2.0
Derakane 470-300	0.86	151.8 ± 1.0	280 ± 28	809 ± 35	15.6	57.1	2.8
Derakane 470HT-400	0.86	155.9	171	824 ± 31	18.5	74.1	2.3
FAVE-L-10S	0.88	86.7 ± 0.3	346 ± 22	489 ± 4	26.2	132.5	1.7
FAVE-L-20S	0.83	95.9 ± 2.4	409 ± 62	538 ± 21	20.1	84.7	2.2
FAVE-O-20S	0.82 ± 0.01	99.7 ± 2.1	492 ± 62	540 ± 12	20.5	82.7	2.1
FAVE-L-25S	0.8	108.0 ± 1.9	550 ± 4	16.4	16.4	64.1	2.6
FAVE-O-25S	0.8	106.6 ± 0.8	584 ± 2	17.4	17.4	62.9	2.5
FAVE-O-470-300-25S	0.87	110.2 ± 3.4	605 ± 4	23.0	23.0	105.0	1.9
FAVE-O-HT-25S	0.87	124.2 ± 3.8	595 ± 68	25.4	25.4	108.7	1.7

VISCOELASTIC CHARACTERIZATION

Analysis of the constant heating rate experiments

The constant heating rate experiments yielded storage and loss modulus data versus temperature for each resin. The molecular weight between crosslinks, *M_c*, and the glass transition temperature *T_g* is calculated from this data and gives a means of assessing the crosslink density and its effect on *T_g* and the viscoelastic response (both the *T_g* and *M_c* are listed in Table III). The theory of rubber elasticity is used to calculate *M_c*,

$$M_c = \frac{3RT\rho}{E} \quad (1)$$

Here *E* is the rubbery modulus, *R* is the universal gas constant, *T* is the absolute temperature, and ρ is the sample density.^{17,18} The temperature *T* and rubbery modulus *E* are determined for the calculation of eq. (1) at *T_g* + 40°C (well into the rubbery region) and the sample density ρ that was taken as 1.07 g/cm³ (a common value for the VE resins). Typically, rubber elasticity applies only to polymers with low crosslink densities and would not be expected to give completely accurate crosslink density measurements for highly crosslinked VE systems. However, the results tabulated in Table III are the correct order of magnitude based on more accurate crosslink density calculations¹⁷ and certainly provide a relative means of comparison between commercial and FAVE resin systems.

Another important mechanical property of polymers is the ability to resist thermal softening. To assess the residual stiffness versus temperature, the temperature at which the resin lost 20 and 50% of its

room temperature storage modulus value was identified. The goal of this calculation was to provide an estimated useful operating temperature range for the resins as well as identify which resins were more vulnerable to thermal softening. The thermal softening performance, of course, figures highly into which applications the FAVE resins are best suited as replacements for their commercial counterparts.

Analysis of isothermal step, multiple frequency sweep experiments

The viscoelastic characterization for the commercial and FAVE resins was primarily derived from an analysis of master-curves of storage and loss modulus data. Storage and loss modulus data from multiple frequency sweeps at discrete temperatures were used to form master-curves using TTSP for the resins over a wide temperature range from the glassy to the rubbery regions. The temperature shift factors were fitted to the empirical and free volume derived Williams–Landell–Ferry (WLF) equation in the leathery to rubbery regions about the distortion temperature. The breadth of the distribution of molecular relaxation times was described using a fit to the empirical Kohlrausch–Williams/Watts (KWW) equation.

TTSP is an accelerated characterization scheme that allows for the modeling of long term polymer response to prescribed temperatures and loads using short term data collected over a wide range of temperatures. Multiple frequency sweep storage and loss modulus data was collected over three decades of frequency and shifted into master-curves using time–temperature equivalence. The shifting was performed similar to the reduced variables method described by Ferry⁶ in which a vertical shift or

correction due to the flexible chain theory is applied to both storage modulus E'_{Data} and loss modulus E''_{Data} data before horizontal shifting,

$$\begin{aligned} E'_{\text{MC}} &= E'_{\text{Data}} \frac{T_R \rho_R}{T \rho} \\ E''_{\text{MC}} &= E''_{\text{Data}} \frac{T_R \rho_R}{T \rho} \end{aligned} \quad (2)$$

where T_R and ρ_R are the reference temperature and density at that reference temperature, respectively, and T and ρ are the temperature and density at the new temperature and is plotted against the reduced frequency. This vertical correction further reduces considering that the densities of most polymers do not change significantly in the temperature range where the time-temperature equivalence is valid and the density ratio is approximately one. The vertical shifting procedure does quite well in the leathery and rubbery regions of the polymer to aid in the formation of smooth master-curves, but may cause too much vertical shifting in the glassy region and thus yield incorrect horizontal shift factors.⁶ As a result, shifting of both storage and loss modulus data simultaneously may be required to yield accurate temperature shift factors; an approach that is used for this study.

The temperature shift factor a_T for each resin was analyzed using a WLF type fit to characterize the temperature shift factor versus temperature and calculate the activation energy.¹⁹ The WLF equation is used to characterize the temperature dependence of the distribution of relaxation times in viscoelastic materials.^{6,7} All temperature shifts above the glass transition temperature were fit using a rewrite of the WLF equation,

$$\frac{-1}{\log_{10} a_T} = \frac{C_2^0}{C_1^0} \left(\frac{1}{T - T_R} \right) + \frac{1}{C_1^0} \quad (3)$$

where T_R is the reference temperature, C_1^0 is a dimensionless constant, C_2^0 has dimensions of temperature (usually °C), and the superscript "0" indicates that the reference temperature is not T_g . The fractional free volume f_0 is also calculated once C_1^0 is found,

$$f_0 = \frac{B}{2.303 C_1^0} \quad (4)$$

where B is the Doolittle constant and is usually taken to be one.^{20,21} The apparent activation energy ΔH_a necessary to initiate the viscoelastic relaxation process was calculated using a direct graphical method from a plot of the natural log of the temperature shift factor at temperatures above the glass transition temperature versus the inverse of the temperature in Kelvin,

$$\Delta H_a = R \frac{d(\ln a_T)}{d(1/T)} \quad (5)$$

The resulting calculated slope multiplied by the universal gas constant gives the activation energy values listed in Table III.

The distribution of relaxation times about the glass transition may be described by calculating the coupling parameter n of the empirical Kohlrausch-Williams/Watts (KWW) function.^{8,9} Physically, the coupling parameter reveals the strength of the intermolecular interaction between segmental chains in the polymer and provides a measure of the cooperativity associated with the relaxation process.²² The coupling parameter was determined using the KWW function $\phi_{\text{KWW}}(t)$ proposed by Williams and Watts,

$$\phi_{\text{KWW}}(t) = e^{-\left(\frac{t}{\tau}\right)^{1-n}} \quad 0 < n < 1 \quad (6)$$

where τ is the temperature dependent apparent relaxation time, t is time, and n is the coupling parameter. The KWW function is then substituted into an expression for the complex modulus E^* ,^{23,24}

$$E^* = E'(\omega) - iE''(\omega) = - \int_0^\infty e^{-i\omega t} \left[\frac{d\phi(t)}{dt} \right] dt \quad (7)$$

According to the approach of Weiss et al.,^{24,25} the loss modulus E'' is then given by,

$$E''(\omega) = A z Q_\beta(z) \quad (8)$$

where Q_β is given as,

$$\begin{aligned} Q_\beta(z) &= \frac{1}{\pi} \int_0^\infty e^{-u^\beta} \cos(zu) du \\ \beta &= 1 - n \\ z &= \omega\tau = 2\pi f\tau \end{aligned} \quad (9)$$

Here A is an adjustable constant, τ is the same characteristic relaxation time from eq. (6), f is the frequency, z is a dimensionless spatial variable, and Q_β a probability density function. Numerical methods are required to evaluate Q_β ^{24,25} whose solution may be represented as,

$$\begin{aligned} Q_\beta(z) &= \frac{1}{\pi} \sum_{m=1}^\infty (-1)^{m+1} \frac{\Gamma(1 + \beta m)}{m! z^{1+\beta m}} \sin\left(\frac{\pi m \beta}{2}\right) \\ 0 &\leq \beta \leq 1 \end{aligned} \quad (10)$$

The values A , β , and τ of eq. (8) are curve fitted to loss modulus master-curve data until the polymer loss modulus master-curve in the glass transition

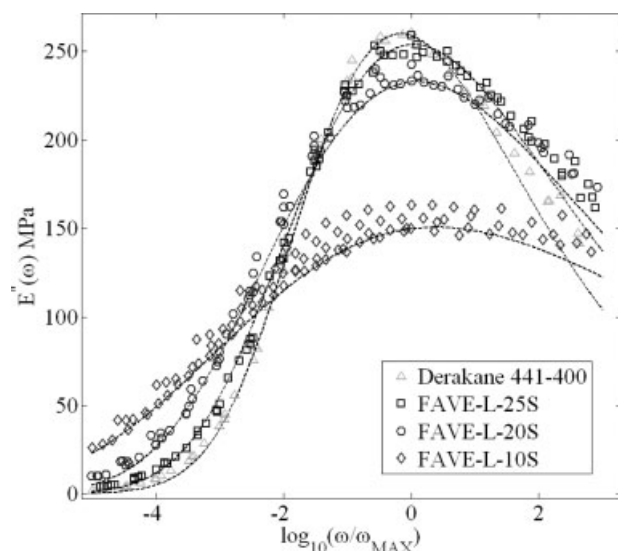


Figure 3 Loss moduli master-curves as a function of frequency normalized at the loss moduli maxima for Derakane 441-400 and FAVE resins based on it in the vicinity of the glass transition temperature along with KWW fit (dashed line).

region is well represented (Fig. 3). The values of the coupling parameter n are listed in Table III.

RESULTS AND DISCUSSION

Thermomechanical polymer properties

Crosslink density is strongly affected by reactive diluent content in the starting resin. From Figure 4, it is clear that the molecular weight due to crosslinking decreased with decreasing styrene content. Although all of the FAVE resins have the same reactive diluent content (35 wt % diluent consisting of styrene and MFA), the molar reactive diluent content increased as the styrene content in the resin increased because MFA monomers have molecular weights 2.75 times (MOct) and 3.3 times (MLau) higher than that of styrene. Therefore, within the FAVE resin, increased styrene content resulted in lower crosslink densities and higher M_c values. The experimental M_c values are listed in Table III and are of the correct order of magnitude for the commercial and FAVE resins.³ Similarly, M_c of the commercial bisphenol A VE resins (i.e., Derakane 441-400, 8084, Hexion 781-2140, and Corve 8100) increased as the styrene content in the resin increased. Furthermore, the FAVE resins had lower M_c values than the commercial bisphenol A type resins because of the lower styrene content in the bisphenol A resins. Even though Derakane 470-300 and Derakane 470HT-400 have the same styrene weight percent as Derakane 441-400, their M_c values were considerably different. Derakane 470HT-400

had the lowest M_c , followed by Derakane 470-300, whereas Derakane 441-400 had the highest value of M_c . This occurred because Derakane 470HT-400 had the highest novolac content. Novolac resins have higher functionality than bisphenol A type resins (Figs. 1 and 2) and produce resins with high crosslink densities.

As with crosslink density, the glass transition temperature is also affected by the amount of reactive diluent in the polymer resin. In this study, the glass transition temperature T_g was determined as the peak of the loss modulus curve versus temperature at an oscillation of 1 Hz.²⁶ Overall, the glass transition temperatures for the FAVE resins are slightly lower than those of the commercial resins. Most notable is the significant drop in T_g for Derakane 8084 compared with the other commercial resins caused by the addition of a plasticizing rubber toughening agent. The two high styrene content resins, Hexion 781-2140 and Corve 8100, both have lower $T_{g,s}$ than Derakane 441-400 because of the presence of more lower T_g styrene ($\sim 100^\circ\text{C}$) to higher T_g VE ($\sim 170^\circ\text{C}$) in the resin's chemical composition. The two novolac type VE resins, Derakane 470-300 and Derakane 470HT-400, have a higher functionality which leads to more crosslinking and thus a higher T_g value. From Figure 5, a decrease in styrene wt % results in a decrease in T_g for the FAVE resins. Though this seems contradictory, it is important to note from Table II that the wt % of reactive diluent (MFA + Styrene) is constant for the FAVE resins at about 35 wt %. The effect here is due to the MFA having a lower intrinsic T_g than the styrene and the VE. As the wt % of MFA increases in the resin chemical composition, the overall T_g of the resin decreases. The difference in T_g between the two novolac type VE resin is more significant for FAVE-O-470-300-25S and FAVE-O-HT-25S than for the commercial resins. Though the "HT" resin is more highly crosslinked

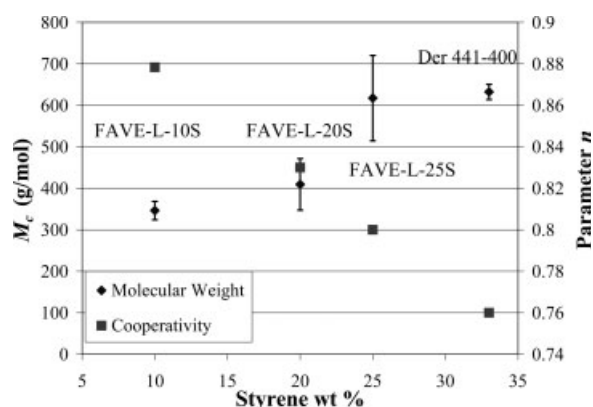


Figure 4 The molecular weight and coupling parameter versus styrene content for Derakane 441-400 and its FAVE resins.

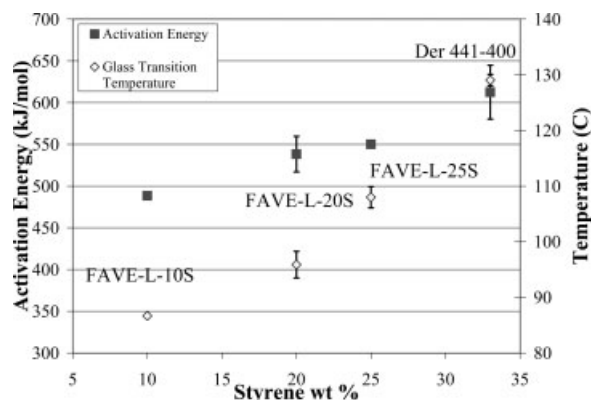


Figure 5 Activation energy and glass transition temperature versus styrene content for Derakane 441-400 and its FAVE resins.

due to a greater novolac wt % (see Table 1 and Table II) and a higher T_g expected, the difference observed here may be due to some experimental error or the unique interaction between the ternary constituents of the FAVE-O-470-300-25S.

The resistance to thermal softening is detailed for the commercial and FAVE resin systems in Figure 6. The temperature at which there is 20% drop in room temperature modulus is reasonably consistent among all the commercial resin systems with the exception of the Derakane 8084 which shows a substantially decreased resistance to thermal softening for both the 20 and 50% drops. Derakane 8084 is toughened with the addition of a proprietary rubber toughening agent which appears to be acting as a plasticizer reducing polymer T_g and thus overall thermal resistance to softening. The Hexion 781-2140 (46 wt % styrene), Corve 8100 (49.5 wt % styrene), and Derakane 441-400 (33 wt % styrene) perform almost identically even though the styrene contents are significantly greater for the Hexion 781-2140 and Corve 8100. This can be explained by noting that increased styrene content leads to a sharper glass transition and thus loss modulus peak versus temperature and a sharper modulus drop in the vicinity of T_g can be expected. Because Derakane 441-400 has less styrene content, its glass transition and peak loss modulus are broader versus temperature and a more gradual modulus drop off is expected; thus, the higher temperature value at 50%. Derakane 470HT-400 and Derakane 470-300 out perform Derakane 441-400 in thermal resistance by about 10°C at the 20% drop-off temperature (glassy region) and a significant 15–25°C at the 50% drop-off temperature (alpha transition region) even though all three resins have the same styrene content. The increase in thermal properties here is given by the higher novolac percent in the Derakane 470 series resins which causes them to be more significantly crosslinked.

The FAVE resins overall had a lower resistance to thermal softening compared with the commercial resins because of the lower styrene content and the presence of long fatty acid groups in the resin. The long aliphatic fatty acid chains pendant to the polymer network increase free volume³ and reduce the T_g and increase the number of relaxation modes. The Derakane 441-400 based FAVE resins (FAVE-L/O-25S, FAVE-L/O-20S and FAVE-L-10S) with decreasing styrene content showed a noticeable downward trend in resistance to thermal softening, as seen in Figure 6. The best FAVE performers are the FAVE-O-470-300-25S and FAVE-O-HT-25S both based on the two commercial novolac VE resins, respectively. Both of these resins compare well to the non-novolac commercial resins with only a 10–20°C difference in softening temperatures and may be selected as viable replacements in certain applications. Also, it is important to note that most of the FAVE resins with at least 20 wt % styrene content had improved resistance to thermal softening than Derakane 8084.

Extent of cure differences among resins could also result in significantly different thermomechanical properties. However, all resins are postcured at high temperatures to ensure complete cure before testing. In addition, previous results indicate that the overall extent of cure for FAVE resins is similar to that of commercial resins.³ However, the results also showed that the extent of styrene conversion is higher, indicating that the extent of cure of VE and MFA components are lower in FAVE resins relative to that of commercial resins.³ However, predicted molecular weight between crosslinks based on the molecular structure of the monomers³ is similar to what was measured and not systematically different for commercial and FAVE resins. Nonetheless, it is possible that these differences in extent of cure could affect thermal softening behavior.²⁷ Yet, the reasons previously described are likely the dominating

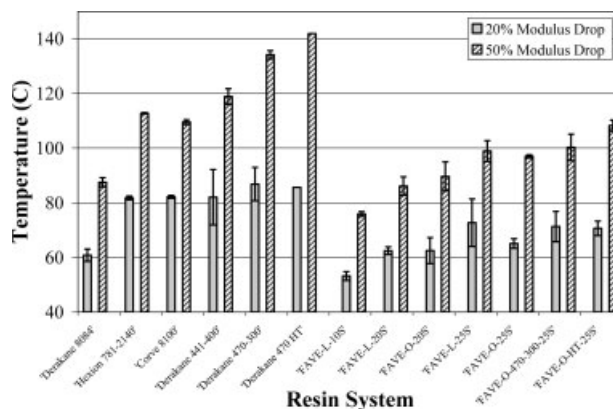


Figure 6 Resin resistance to thermal softening for commercial and FAVE resins.

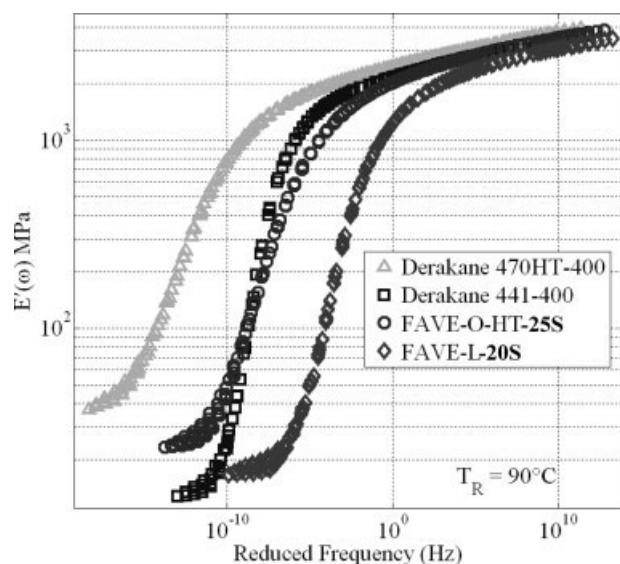


Figure 7 Storage moduli master-curves for selected commercial and FAVE resins.

reasons for differences in T_g , M_c , and thermal softening behavior for FAVE and commercial resins.

Viscoelastic polymer properties

A sampling of storage and loss modulus master-curves constructed for all resins is given in Figures 7 and 8. As described in the Experimental Section, these master-curves were formed using TTSP and temperature shift factors analyzed using the WLF equation eq. (3). The storage modulus master-curves of Figure 7 illustrate a comparison of the commercial and FAVE novolac based VE resins, Derakane 470HT-400 and FAVE-O-HT-25S, along with Derakane 441-400 and FAVE-L-20S. Figure 7 clearly demonstrates that each of the FAVE resins did not perform as well as their commercial counterparts at higher temperatures and to longer periods of time mainly because of the reduced styrene content. The high temperature novolac VE-based Derakane 470HT-400 maintained its modulus to a higher temperature and longer time falling off more gradually because of its high crosslink density. The FAVE-O-HT-25S did not perform as well as Derakane 470HT-400 because of the addition of ~ 14 wt % bisphenol A VE (refer to Table II) and lower styrene content, that reduced overall crosslink density, but performed comparable to the Derakane 441-400 even though it has 8 wt % less styrene. The Derakane 441-400 and FAVE-L are both bisphenol A based VE systems and are more viscoelastic with lower temperature resistance. The modulus of Derakane 441-400 fell off most sharply in the region of the glass transition and obtained the lowest rubbery region modulus. The steep modulus drop can be explained due to the

increased styrene content of the Derakane 441-400 over the FAVE-L-20S which had a more gradual fall off. Overall, the commercial and FAVE resins all had very similar glass region behavior.

The loss modulus master-curves of Figure 8 were formed in the same way using the same temperature shift factors as the storage modulus master-curves. Figure 8 is meant to clearly illustrate the effect of reduced styrene content on loss behavior and response of Derakane 441-400 and the FAVE resins directly based on it. Derakane 441-400 had the highest peak loss followed by FAVE-L-25S (with 25 wt % styrene), FAVE-L-20S (20 wt % styrene), and FAVE-L-10S (10 wt % styrene). It is generally accepted that as the reactive diluent content decreases, the loss modulus peak decreases and the spectra broadens,²⁸ which is supported by Figure 8. The breadth of the loss modulus master-curve also significantly increased with reduced styrene content which is quantified by the coupling parameter n of the KWW equation and also represented in Figure 3 and Table III. Most notable was the peak shift to shorter times on the loss modulus master-curves. Viscoelastically, the shift of the distribution of characteristic relaxation times to shorter time intervals implies that the viscoelastic relaxation process will occur more quickly in materials with lower styrene contents, a result that is supported by this data.

The temperature shift factors found from the master-curve shifting were analyzed using a WLF type analysis. The WLF parameters along with the fractional free volume and the coefficient of thermal expansion due to the change in free volume at a specified temperature are listed for each resin in Table III and are consistent with the theoretical values

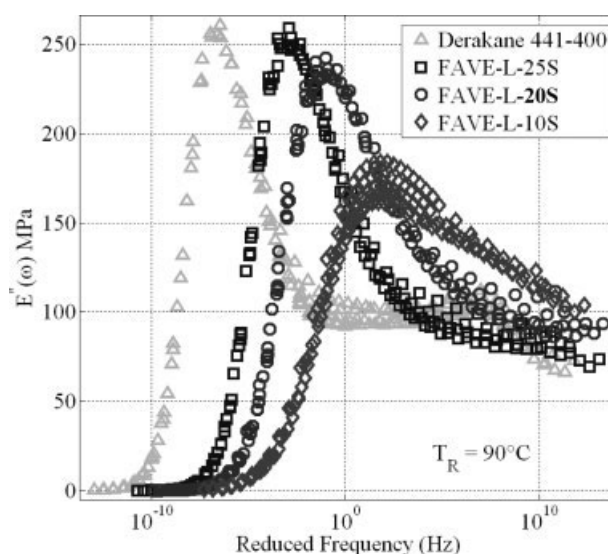


Figure 8 Loss moduli master-curves for Derakane 441-400 and its FAVE resins.

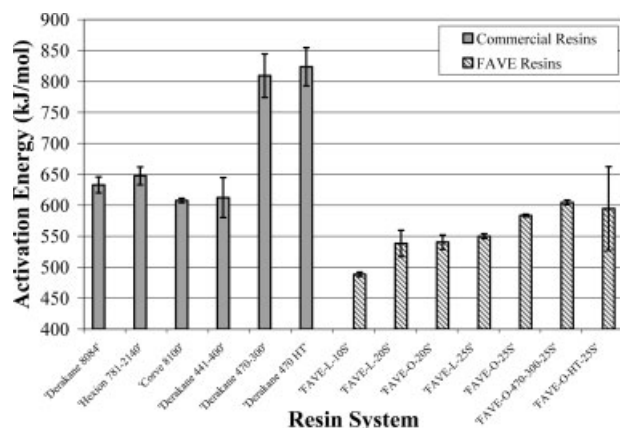


Figure 9 Activation energy comparison for commercial and FAVE resins.

given by Williams et al.⁷ The values also indicate that the assumption of a single accelerating mechanism for the viscoelastic process inherent in TTSP is correct or at least adequate for the current analysis.

Apparent activation energies using the WLF temperature shift factor data were calculated graphically using eq. (5) and are listed in Table III and graphed for comparison in Figure 9. The activation energy values are consistent with the results of previous discussions of the influence of crosslink density, styrene content, and resistance to high temperature softening on the viscoelastic response of these resins and compare well to other calculations listed in the literature.¹⁹ The novolac resins, Derakane 470HT-400 and 470-300, had the highest activation energies due to their high crosslink density compared with the other resin systems considered. The other bisphenol A based commercial resin had approximately the same activation energies, which is not surprising since their storage modulus master-curves and T_g values were all very similar. An interesting result here is that the Derakane 8084 had an activation energy which was similar to the other commercial resins yet had the lowest T_g . The proprietary rubber toughening agent added to Derakane 8084 had a demonstrated plasticizing effect lowering T_g (refer to Table III), but also appears to be inhibiting the onset of the viscoelastic relaxation as indicated by the activation energy value of Figure 9 and the larger coupling parameter n of Table III. This indicates that the rubber toughening agent is likely reacting into the polymer network and providing additional crosslinking,²⁹ but the chemical composition of the rubber toughening agent is nonrigid on the molecular level and thus reduces T_g . The FAVE resins had lower activation energies on average although the two novolac VE-based resins, FAVE-O-470-300-25S and FAVE-O-HT-25S, were comparable to the bisphenol A VE-based commercial resins. The data show that

the activation energy decreased with decreasing styrene content as illustrated in Figure 5 (along with T_g). This occurred because of the resulting broadening of the glass transition.²⁸ In addition, as the styrene content decreased, the MFA content increased resulting in a higher content of pendant aliphatic chains that increase free volume and allow for additional relaxation modes.

The WLF fit constants, C_1^0 and C_2^0 (Table III), are very highly dependent on the WLF fits to the experimental data. Using or omitting a given data point had a significant effect on particular values of these constants. Nonetheless, the trends in values of these constants were simple functions of the polymer molecular structure. Both C_1^0 and C_2^0 increased as the styrene content decreased, as can be seen the FAVE-L series with varying styrene content, or in general, as the crosslink density increased. Derakane 8084 had WLF fit values that were different than expected based on the other resins. This is likely a result of the rubber toughening agent used in this resin that essentially makes this resin's viscoelastic behavior fundamentally different from the other resins. The fractional free volume also behaved regularly with polymer molecular structure for the most part. The values of f_0 (Table III) especially for the FAVE resins, increased with increasing styrene content and with decreasing crosslink density in general. The results for the commercial resins were more scattered. In particular, Derakane 470-300 had a considerably higher f_0 than expected, whereas Derakane 8084 had a lower f_0 than expected. We attribute this to the toughening additive in Derakane 8084 and the fact that f_0 is calculated directly from C_1^0 , which is highly dependent on the WLF fits.

The breadth of the distribution of relaxation times in the viscoelastic process is given by a KWW type analysis. The key parameter is the coupling parameter of eq. (6) which is calculated from a fit of eq. (8) to loss modulus master-curve data as illustrated in Figure 3 (identical to Fig. 8 except with KWW fits and a focus on the glass transition region). This parameter has been used by a number of researchers^{19,22,30,31} to characterize the observed broadening of the loss modulus and $\tan \delta$ curves in neat resins that related to the cooperative motion of the main polymer chains during the glass transition.^{22,32} The values of the coupling parameter n calculated for the commercial and FAVE resins are listed in Table III and are in agreement with values provided by other researchers (see Table I in Ref. 32). From Table III, the highest values of n and thus the broadest distribution of relaxation times are given by the novolac VE-based resins, Derakane 470HT-400 and 470-300, their FAVE counterparts and Derakane 8084. The novolac VE resins are more highly crosslinked requiring a greater degree of cooperative movement

among main chains to fully relax. The large coupling parameter value for Derakane 8084 is probable due to the dispersion of the rubber toughening agent within the chain microstructure inhibiting main chain cooperative motion and the onset of the relaxation. The smaller values of n are given by the commercial resins with the higher styrene contents whose glass transition has been demonstrated to be sharper with a steeper fall-off in the modulus. Most of the FAVE resins have a slightly greater value of the coupling parameter compared with the higher styrene content commercial resins probably because the addition of the methacrylated fatty acids slightly increases the crosslink density. Figure 4 clearly shows that the cooperativity measured by n increases with decreasing styrene content for Derakane 441-400 and the FAVE resins which are based on it. Decreasing the reactive diluent content will decrease the length of the polymer chains generating more crosslinks and higher crosslink density, which will slightly increase the degree of cooperativity between neighboring chains.

SUMMARY AND CONCLUSIONS

Research was conducted to characterize and compare the thermomechanical and time dependent properties of commercially available VE resins and lower styrene content FAVE resins which are based upon them. The FAVE resins were found to have similar or slightly inferior properties compared with the commercial resins. The FAVE resins typically had lower glass transition temperatures and lower resistance to thermal softening. The viscoelastic properties were very dependent upon the degree of crosslinking, and the styrene content, methacrylated fatty acid content and type and functionality of the VE monomer played important roles. From the data presented the viscoelastic relaxation process is accelerated not only by temperature but also by reduced styrene content. Although the glassy region response of the commercial versus FAVE resins was very similar, the novolac VE-based resins would be the best choice for higher temperature applications with a low tolerance for viscoelastic behavior. On the opposite end would be low styrene content resins such as FAVE-L-10S and FAVE-L/O-20S which had the least temperature resistance and most pronounced viscoelastic behavior.

The choice of resin depends greatly upon the anticipated use and desired operating temperature; however, the novolac VE-based FAVE-O-HT-25S was a solid performer for both the thermomechanical and viscoelastic criteria considered, and thus a viable alternative to a number of the commercial resins. The FAVE-O-HT-25S resin also has the added

environmental benefit of lower styrene content and a corresponding reduced styrene gas emission during processing and postcuring. The methacrylated fatty acids which replace some of the styrene content are also a renewable resource. Future work will consist of manufacturing and testing of several types of glass reinforced FAVE composites panels and structures. These composites will be assessed for applications in numerous DoD proposed projects and are expected to have improved thermomechanical and viscoelastic properties over the neat resins.

This research was supported in part by an appointment of one of the authors to the Postgraduate Research Participation Program at the U.S. Army Research Laboratory administered by the Oak Ridge Institute for Science and Education through an interagency agreement between the U.S. Department of Energy and USARL. The authors thank the Ashland Company, Hexion Specialty Chemicals, and CoRezyn for providing the commercial vinyl ester resins and Applied Polymeric Incorporated for preparing many of the FAVE resins. We thank the SERDP PP-1271 and the ESTCP WP-0617 programs for funding this research, and ARL cooperative agreement DAAD 19-02-2-0010.

References

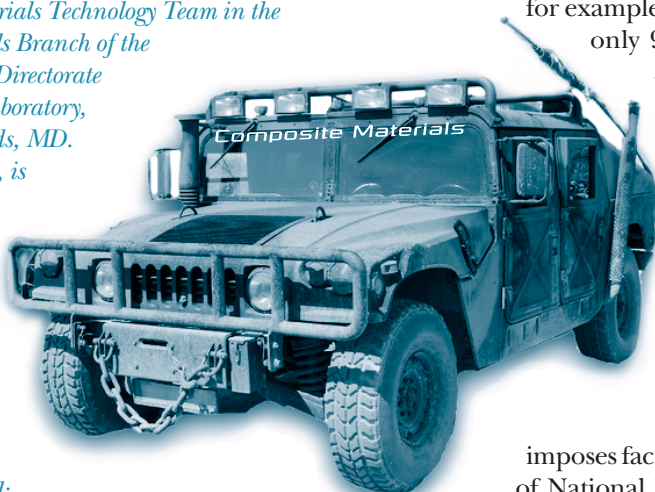
1. National Emissions Standards for Hazardous Air Pollutants: Reinforced Plastic Composites Production, 2003.
2. La Scala, J. J.; Jeyerasingam, A.; Logan, M. S.; Winston, C.; Meyers, P.; Sands, J. M.; Palmese, G. R. *J of Biobased Mater Bioenergy* 2007, 1, 409.
3. La Scala, J. J.; Sands, J. M.; Orlicki, J. A.; Robinette, E. J.; Palmese, G. R. *Polymer* 2004, 45, 7729.
4. Palmese, G. R.; La Scala, J. J.; Sands, J. M. *U.S. Pat. Appl.* 60, 569, 379 (2005).
5. La Scala, J. J.; Sands, J. M.; Palmese, G. R. *AMPTIAC Q* 2005, 8, 118.
6. Ferry, J. D. *Viscoelastic Properties of Polymers*; Wiley: New York, 1980.
7. Williams, M. L.; Landel, R. F.; Ferry, J. D. *J Am Chem Soc* 1955, 77, 3701.
8. Williams, G.; Watts, D. C. *Trans Faraday Soc* 1970, 66, 80.
9. Williams, G.; Watts, D. C.; Dev, S. B.; North, A. M. *Trans Faraday Soc* 1971, 67, 1323.
10. Technical Data Sheet for Corve 8100. Interplastic Corporation, St. Paul, MN, 2007.
11. Technical Data Sheet for Hexion 781-2140. Hexion Specialty Chemicals, Columbus, OH, 2005.
12. Technical Data Sheet for Derakane 441-400 Epoxy Vinyl Ester Resin. Ashland, Columbus, OH, 2004.
13. Technical Data Sheet for Derakane 470HT-400. Ashland, Columbus, OH, 2004.
14. Technical Data Sheet for Derakane 470-300 Epoxy Vinyl Ester Resin. Ashland, Columbus, OH 2004.
15. Technical Data Sheet for Derakane 8084 Epoxy Vinyl Ester Resin. Ashland, Columbus, OH 2004.
16. Technical Data Sheet for Sartomer CN-151. Sartomer, Exton, PA, 2006.
17. Flory, P. J. *Principles of Polymer Chemistry*; Cornell University Press: Ithaca, NY, 1953.
18. Palmese, G. R.; McCullough, R. L. *J Appl Polym Sci* 1992, 46, 1863.

19. Jensen, R. E.; Palmese, G. R.; McKnight, S. H. Dynamic Mechanical Analysis of E-Beam and Thermally Curable IPN Thermosets; Army Research Laboratory, APG, 2002.
20. Berry, G. C.; Fox, T. G. *Adv Polymer Sci* 1967, 5, 261.
21. Doolittle, A. K.; Doolittle, D. B. *J Appl Phys* 1957, 28, 901.
22. Roland, C. M.; Ngai, K. L. *Macromolecules* 1991, 24, 5315.
23. Lindsey, C. P.; Patterson, G. D. *J Chem Phys* 1980, 73, 3348.
24. Weiss, G. H.; Bendler, J. T.; Dishon, M. *J Chem Phys* 1985, 83, 1424.
25. Weiss, G. H.; Dishon, M.; Long, A. M.; Bendler, J. T.; Jones, A. A.; Inglefield, P. T.; Bandis, A. *Polymer* 1994, 35, 1880.
26. Nielsen, L. E.; Landel, R. F. *Mechanical Properties of Polymers and Composites*; Marcel Dekker: New York, 1994.
27. La Scala, J.; Wool, R. P. *Polymer* 2005, 46, 61.
28. Nielsen, L. E. *J of Macromol Sci Rev Macromol Chem* 1969, 3, 69.
29. Robinette, E. J.; Ziaee, S.; Palmese, G. R. *Polymer* 2004, 45, 6143.
30. Verghese, K. N. E.; Jensen, R. E.; Lesko, J. J.; Ward, T. C. *Polymer* 2001, 42, 1633.
31. Sands, J. M.; Jensen, R. E.; Fink, B. K.; McKnight, S. H. *J Appl Polym Sci* 2001, 81, 530.
32. Ngai, K. L.; Plazek, D. J. *Macromolecules* 1991, 24, 1222.

U.S. Military Looks to ENVIRONMENTALLY FRIENDLY COMPOSITE MATERIALS BASED ON FATTY ACID MONOMERS

by John La Scala, James Sands, and Giuseppe Palmese

John J. La Scala, Ph.D., is an engineer in the Materials Application Branch and James M. Sands, Ph.D., is the leader of the Transparent Materials Technology Team in the Survivability Materials Branch of the Weapons Materials Research Directorate of the U.S. Army Research Laboratory, Aberdeen Proving Grounds, MD. Giuseppe R. Palmese, Ph.D., is head of the Department of Chemical and Biological Engineering at Drexel University, Philadelphia, PA, where he runs a research program in nanocomposites, standard composites, and materials from renewable resources. E-mail: jlascale@arl.army.mil; palmese@coe.drexel.edu.



Polymer composites are materials

made by combining a polymer with another class of reinforcing material, such as glass, carbon, and aramid. Composite materials are routinely used by both commercial industry and the U.S. Department of Defense (DOD) because of their high strength-to-weight characteristics that enable lighter and stronger ground, sea, and air structures. Composites are often made by infusing low-viscosity liquid molding resins, such as unsaturated polyester (UPE), vinyl ester (VE), or epoxy resins, into a mold containing reinforcing fibers. UPE and VE resins are preferred resin materials because they offer ease of processing and lower cost in trade for lower performance.

Polymer composites are also used to repair DOD weapons platforms and support equipment that are subject to extremely taxing conditions, and are often damaged during weapons fire and rugged off-road operations. For many damage types, small repairs can increase the field life of the platform significantly. Repair resins, such as Bondo, are used in the field by deployed units and in depots. Many of these repair resins are based on UPE or VE resins.

Unfortunately, aspects of UPE and VE resins have an adverse effect on the environment. UPE and VE resins contain styrene, which is classified as a hazardous air pollutant (HAP) and volatile organic compound (VOC). Fabrication and use of UPE and VE composites produces significant

amounts of volatile emissions during mixing, molding, repair resin application, and even during fielding.¹ In the late 1990s, for example, the composites industry consumed only 9% of the styrene production, but accounted for 79% of the styrene emissions to the atmosphere.² In addition, a recent report made to the U.S. Army states that there are no environmentally friendly repair resins.³ As a result, in 2003 the U.S. Environmental Protection Agency (EPA) established regulations limiting the amount of HAPs that can be used in composite materials, including repair resins.⁴ This regulation

imposes facility-wide emissions limits in the form of National Emissions Standards for Hazardous Air Pollutants (NESHAP), which made compliance through low-emission resins or add-on emissions controls mandatory by April 21, 2006.⁴ It is likely that this regulation will have a significant negative impact on the use of composite materials in the military, as well as commercial applications, unless alternative materials or systems for mitigating HAP emissions during processing of composite parts are developed.

Considering the number of current and future DOD sites using composite resins, the cost of implementing add-on emissions controls would be prohibitive.⁵ Reducing the styrene content in these resins imposes prohibitive viscosity increases, cost increases, and performance reduction.⁶ Various petroleum-based monomers with lower volatilities, such as vinyl toluene, have been used as styrene replacements.⁷ However, even these substitutes still produce significant emissions, and would likely be regulated by EPA if used prevalently.⁴ Additionally, vapor suppressants have been used to reduce emissions, but are often ineffective and have a detrimental effect on composite performance.²

The Army Research Laboratory (ARL) and Drexel University have developed fatty acid monomers that can partially or completely replace styrene in UPE and VE resin systems. The availability and implementation of low-HAP-containing resins would allow DOD facilities to continue manufacturing composites and performing repairs with UPE and VE resins using current practices and facilities, while reducing pollution and health risks.

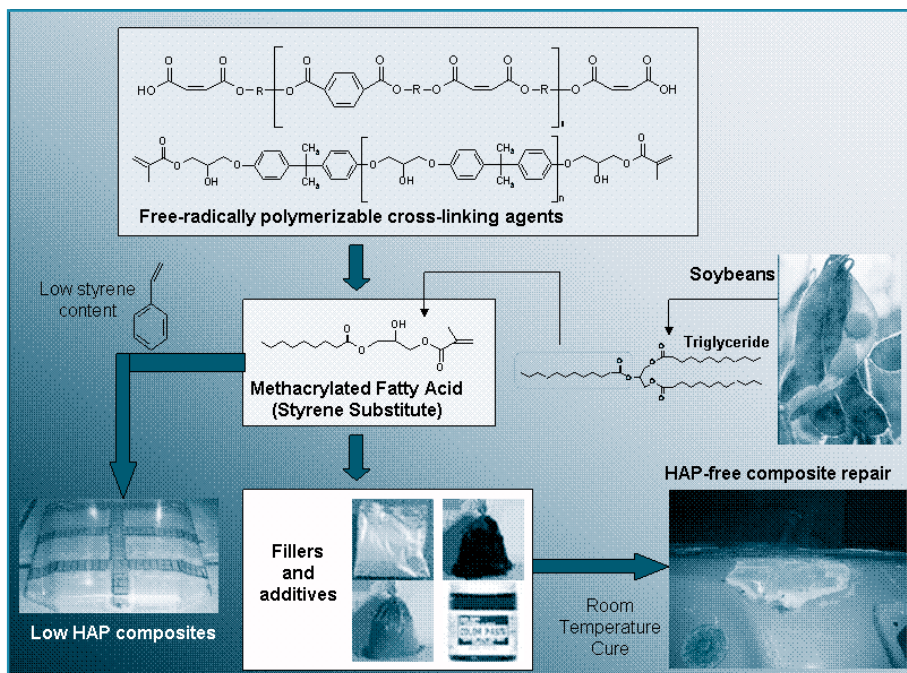


Figure 1. Environmentally friendly VE and UPE resins are made using fatty acid monomers derived from plant oils to replace styrene in commercial repair resins.

FATTY ACID MONOMERS

Typical commercial UPE and VE liquid resins contain 40–60 wt% styrene, while repair resins typically contain 10–30 wt% styrene. These resins are not compliant under EPA regulations. Although some NESHAP-compliant resins have been developed, these generally have shown poor performance. ARL/Drexel has developed a solution for making NESHAP-compliant resins with excellent resin and polymer performance.^{8,9} These resins use fatty acid monomers as a reactive diluent to replace all but 10–25 wt% of the styrene HAP in the VE or UPE resin for liquid molding applications^{6,8} and they can replace all of the styrene in composite repair resins⁹ (see Figure 1).

Triglycerides are the main component of oils derived from plant and animal sources and are composed of three fatty acids connected by a glycerol center.¹⁰ Triglycerides are simply broken down into fatty acids using industrial processes such as acidolysis.¹¹ A number of synthetic routes have been established by ARL/Drexel for making fatty acid-based monomers;⁸ however, the methacrylated fatty

to produce fatty acid monomers, these monomers are inexpensive, with an estimated cost only slightly above that of styrene. Although plant oils have been used to make polymers for years, the use of fatty acid monomers as reactive diluents is a novel concept.⁸

LOW-HAP COMPOSITE RESINS

Ideally, all of the styrene in UPE and VE liquid molding resins could be replaced with fatty acid-based monomers; however, the resulting resin and polymer properties are inferior relative to commercial resins. Therefore, fatty acid

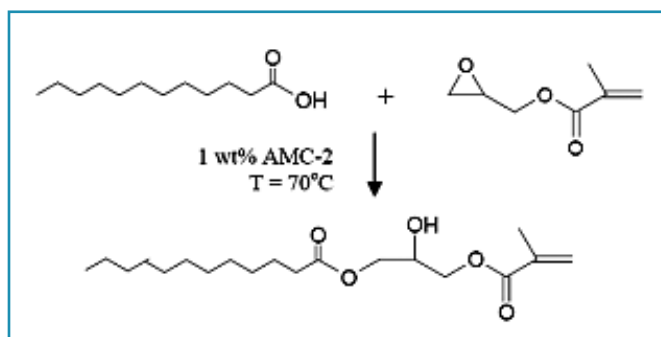


Figure 2. Reaction scheme to produce MFA monomers.

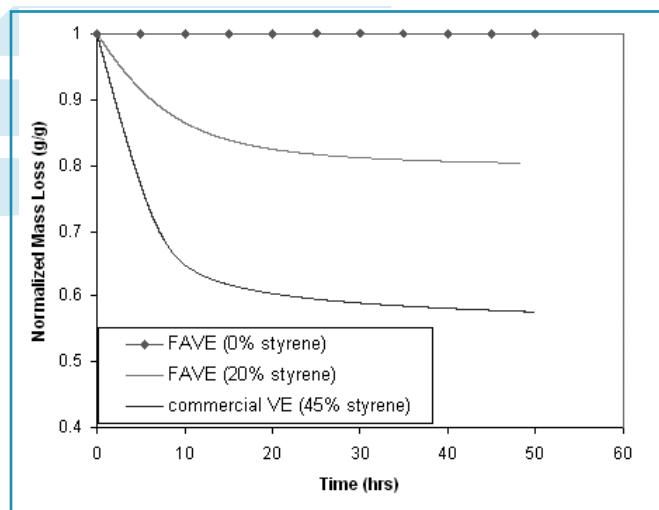


Figure 3. The normalized mass loss (instantaneous mass divided by initial sample mass) as measured in a macro thermo gravimetric analyzer at a constant temperature of 40 °C as a function of time from FAVE and commercial VE resins all containing 55 wt% VE monomers and 45 wt% reactive diluent.



Figure 4. M35-A3 hood prepared using the low-HAP resin.

monomers are used to partially replace styrene. Styrene contents ranging from 10 wt% to 25 wt% (i.e., 25–80% reduction in VOC/HAP content relative to commercial resins) still result in good resin and polymer properties (see Table 1). Overall, the viscosities and mechanical properties of the fatty acid vinyl ester (FAVE) resins are similar to those of commercial resins,^{6,12} while having improved toughness relative to low-HAP commercial products. Thermo gravimetric analysis was used to measure the weight loss at a constant 40 °C as a function of time. The measurements showed that the fatty acid monomers are nonvolatile and that the resins formulated with these monomers produce far fewer emissions (see Figure 3).

In tests, the performance of composites impregnated with low-HAP FAVE resins was very similar to that of commercial resins.^{12,13} To prove that these resins can be used to produce large-scale structures, a composite hood for an M35-A3 truck, measuring 7 feet by 7 feet (see Figure 4) was fabricated using a low-HAP resin containing 15% fatty acid monomers and only 20% styrene. The resin infused very quickly and successfully cured to produce a structural composite part.

Such fabrication successes indicate that low-HAP FAVE resins can be used to replace high-HAP commercial resins used in composite parts on various military structures or platforms. Figure 5 shows various military applications

that use vinyl ester resins, including (a) HMMWV (“Hum-Vee”) hardtop, (b-d) parts for Army tactical vehicles, (e) T-38 aircraft dorsal cover, and (f) composite naval rudders. Currently, DOD is evaluating whether fatty acid-based low-HAP resins can be substituted for commercial VEs for these applications. Current tests have shown certain fatty acid formulations have the necessary properties to compete against commercial VEs. Large-scale composite parts will be fabricated using these low-HAP resins and validated for their use on military platforms.

The composite industry uses approximately 900,000 tons UPE resin annually. Using FAVE resins would approximately halve the styrene emissions in composite manufacture. Assuming sufficient production and acceptance of MFA monomers/resins, approximately 230,000 tons of styrene emissions could be mitigated with this technology. The applications shown in Figure 5 amount to an estimated reduction of 125 tons of resin and 52.5 tons of styrene annually. Simply by substituting commercial resins with FAVE resins, these applications would use only 32.5 tons of styrene annually, reducing emissions by approximately 37%. As a result, the use of these low-HAP resins will reduce the cost associated with styrene emissions and will also benefit worker health and safety by lowering their exposure to HAPs.

HAP-FREE REPAIR RESINS

Repair resins are typically two-part formulations made up of a number of different components. Part A contains the polymeric binder, including a cross-linking agent (e.g., VE or UPE monomers) and a reactive diluent (e.g., styrene), free-radical decomposition promoter, free-radical inhibitors, and various inorganic additives (e.g., talc, magnesium carbonate, chopped glass fiber, cabosil).¹⁴ Part B contains the free-radical initiator and surfactants to enable successful mixing of this hardener into a viscous Part A.¹⁵

Table 1. Properties of low-HAP FAVE resins developed by ARL/Drexel compared to commercial resins.

Property	FAVE Resin	Low-HAP Commercial Resins	Standard Commercial Resins
Styrene Content (wt. %)	10–25	33	45
T _g (°C)	120–130	140	125
Flexural Strength (MPa)	120	130	130
Flexural Modulus (GPa)	3.0	3.5	3.4
Toughness (J/m ²)	200	110	240
Viscosity at 30 °C (cP)	100–1500	312	270
Gel Times	5 min–7 hr	Various	Various
Shrinkage	Low	Moderate	High
Renewable	Partly	No	No
Biodegradable	No	No	No

HAP-free, environmentally-friendly repair resin binders were formulated by blending fatty acid monomers with VE and UPE monomers.⁹ Various compositions of VE/UPE and MFA monomers were used to make a variety of repair resin formulations. Increasing the MFA content reduced resin viscosity and also reduced resin glass transition temperature (T_g) and increased flexibility, allowing for tunability of properties. The T_g of commercial repair resins was easily matched. For example, resins containing 65 wt% MFA and 35 wt% VE monomer had a T_g of approximately 30 °C, similar to that of commercial Bondo resins (25 °C), as measured using dynamic mechanical analysis with a temperature ramp from -50 °C to 120 °C at 1 Hz with 7.5 μ m deflection.

Dimethylaniline was added to the Part A formulation because this chemical promotes free radical cure of benzoyl peroxide initiators, which are typically used in the hardener component. Dimethylaniline content in the amount of 0.1–0.5 wt% was found to be best for adequately curing the repair resin and with sufficient working time.

Inorganic reinforcing fillers were mixed into the resin formulations using high shear mixers. Various inorganic components and contents with various particle sizes were used, including talc, milled glass fibers, magnesium carbonate, sodium metaborate, aluminum oxide, silica thickener, glass microspheres, phenolic, and carbon black. Similar to commercial repair resins, filler contents of 35–50 wt%

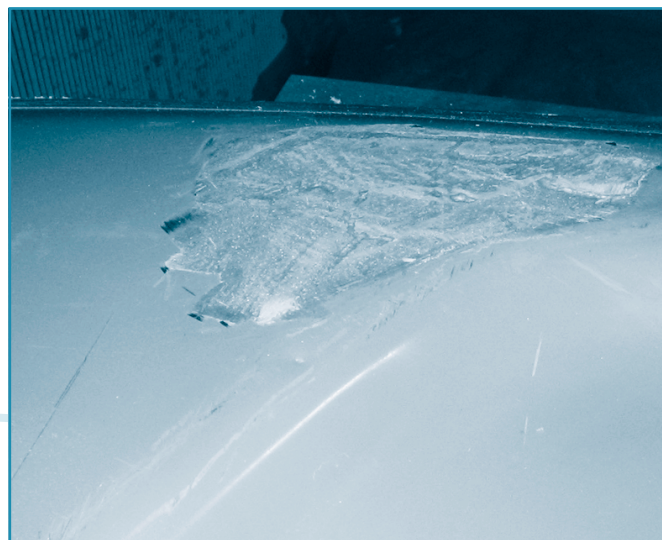


Figure 6. HAP-free fatty acid-based repair resin applied (light area in center of photo) to repair a dent in a truck tailgate.

worked best for producing viscous putty with subsequent good reinforcement of the cured solid.¹⁴ Overall, all of these fillers acted similarly in increasing the viscosity of the uncured resin to that of a putty, while increasing the stiffness of the cured polymer to 3–5 GPa at 0 °C. In particular, filler contents of approximately 25 wt% talc, 15 wt% magnesium carbonate, and 5 wt% glass microspheres or glass fibers were very good at optimizing viscosity and reinforcement. As an added benefit, because these resins contain no styrene, the MFA-based repair resins produce no pungent odor typical of repair resins. Furthermore, this HAP-free repair resin could be simply cured using commercial hardening agents, such as Bondo red cream hardener or other solutions of benzoyl peroxide.^{9,15}

A tailgate of a truck with dents was repaired using a zero-HAP repair resin formulation containing 55 wt% resin (35/65 VE/MFA) and 45 wt% filler (25/15/5 talc/magnesium carbonate/glass microspheres). The application of the resin and curing process was similar to that of commercial repair resins. The resulting repair produced excellent results as shown in Figure 6. The product was able to be sanded down to produce a smooth repaired surface, similar to that of commercial repair resins. Scraping the edges of the repaired area with a razor blade did not result in delamination of the resin thus showing that the repair resin had good adhesive properties with the substrate.

The commercial repair putty industry has sales of approximately 25,000 tons annually and is a US\$100-million industry.

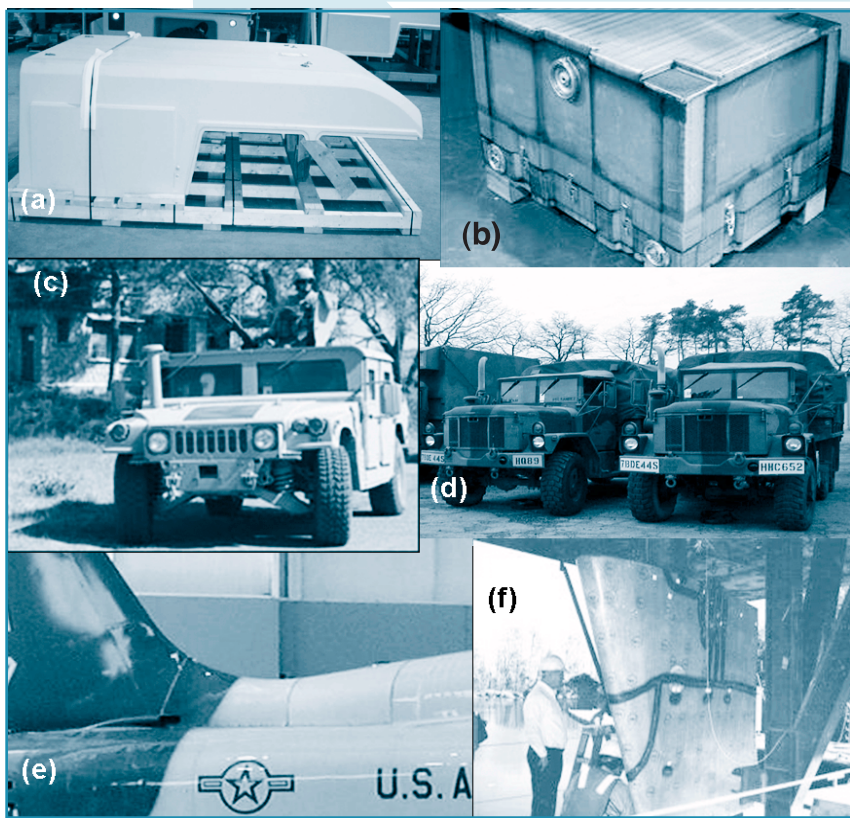


Figure 5. ARL/Drexel low-HAP resins are being demonstrated/validated for use with [a] HMMWV ballistic hardtop, [b] a HMMWV transmission container, composite replacement hoods for [c] HMMWV or [d] M35-A3, [e] T-38 aircraft dorsal cover, and [f] MCM composite naval rudder.

Because commercial repair resins contain 10–30 wt% styrene, substitution with fatty acid-based formulations could result in a 2500–7500 ton reduction in the use of styrene HAPs annually. Using these HAP-free resins also would eliminate costs associated with monitoring or sequestering emissions while eliminating workers' exposure to HAPs, thereby improving worker health and safety. Furthermore, because these resins are nonvolatile, restrictions and costs associated with shipping these resins would be significantly reduced.

SUMMARY

Environmental legislation enacted by EPA has established emissions limits during composite repair and fabrication. Fatty acid monomers can be used to reduce or eliminate styrene in VE and UPE resins for liquid molding and repair applications. The properties of the resulting low-HAP or HAP-free resins are similar to that of commercial resins and are useable to make large-scale composite structures. Currently, DOD is validating these resins for use on a number of weapons platforms, including parts for tactical vehicles, planes, and composite rudders. Overall, the potential for HAP reduction through the use of these monomers is on the order of 50 tons annually for DOD and significantly more in commercial industry. In addition, these resins help reduce worker exposure to HAP chemicals, helping to improve worker health and safety. **em**

REFERENCES

1. Ziaee, S.; Palmese, G.R. Effects of Temperature on Cure Kinetics and Mechanical Properties of Vinyl-Ester Resins. *J. Polym. Sci. B Polym. Phys.* **1999**, *37*, 725-744.
2. Lacovara, B. Reducing Emissions with Styrene Suppressants. CFA [what is CFA?] 1999, 1-5.
3. Task No. 0420, Misc. Adhesives and Sealants Technology Thrust Area; Gap Analysis Report (CDRL A007); Concurrent Technologies Corp., Feb. 2006.
4. National Emissions Standards for Hazardous Air Pollutants: Reinforced Plastic Composites Production, U.S. Environmental Protection Agency, 40 CFR Part 63 *Fed. Regist.* **2003**, *68*, 19375-19443.
5. Vallone, J. NESHAP Requirements Assessment for Miscellaneous Coatings, Adhesives, Sealers, Etc. Final Report to ARL, Sustainable Painting Operations for the Total Army, 2004.
6. La Scala, J.J.; Sands, J.M.; Orlicki, J.A.; Robinette, E.J.; Palmese, G.R. Fatty Acid-Based Monomers as Styrene Replacements for Liquid Molding Resins. *Polymer* **2004**, *45*, 7729-7737.
7. Smeal, T.W.; Brownell, G.L. Laminating Resins Having Low Organic Emissions. U.S. Patent 5,292,841, March 8, 1994.
8. Palmese, G.R.; La Scala, J.J.; Sands, J.M. Fatty Acid Monomers to Reduce Emissions and Toughen Polymers. U.S. Patent Application 11/124,551, May 2005.
9. La Scala, J.J.; Sands, J.M.; Palmese, G.R. Composite Repair Resins Containing Minimal Hazardous Air Pollutants and Volatile Organic Compounds. U.S. Patent Application 11/689,191, 2007.
10. Litchfield, C. *Analysis of Triglycerides*; Academic Press: New York, NY, 1972; p. 3.
11. Gunstone, F.D. *Fatty Acid and Lipid Chemistry*; Blackie Academic and Professional: New York, NY, 1996; pp. 72.
12. Derakane 441-400 Epoxy Vinyl Ester Resin; Technical Data Sheet, Ashland: Columbus, OH, Nov. 2004; available at www.derakane.com.
13. La Scala, J.J.; Jeyerasingam, A.; Logan, M.S.; Winston, C.; Myers, P.; Sands, J.M.; Palmese, G.R. Fatty Acid-Based Vinyl Ester Composites with Low Hazardous Air Pollutant Contents. Accepted for Publication in the *Journal of Biobased Materials and BioEnergy*.
14. Bondo Autobody Filler Repair Kit; MSDS, Bondo Corp.: Atlanta, GA, Oct. 28, 2005; available at www.bondo-online.com.
15. Bondo Red Cream Hardener; MSDS, Bondo Corp.: Atlanta, GA, June 7, 2006; available at www.bondo.com.



AIR & WASTE MANAGEMENT
ASSOCIATION

REQUEST FOR PERMISSION

Manuscript Title: _____

Author(s) _____

The Air & Waste management Association (A&WMA) requests permission to publish and redistribute your manuscript (specified above) in *EM* magazine and in electronic form on the A&WMA Web site, including sales of electronic and paper reprints, and in other publications through republishing agreements with A&WMA.

By signing this release, the Author confirms that the manuscript is not in the public domain and is original on the Author's part except for such excerpts from copyrighted works as may be included with the written permission of the copyright owners. The Author further warrants that the manuscript contains no libelous, obscene, or unlawful statements, and does not infringe upon or violate any copyright, trademark, or other right or the privacy of others. The Author also warrants that in the case of sole authorship, the Author is the sole owner of the manuscript and all copyrights therein, and has full power and authority to register all copyrights therein and to make this Agreement, and that in the case of multiple authorship, these powers of ownership are shared with all other contributing authors. (For U.S. government employees, grant or contract authors, this provision applies only to the extent to which the copyright is transferable.) The Author acknowledges that A&WMA is relying on this release in publishing this manuscript, and agrees to indemnify A&WMA against liability and expense, including reasonable counsel fees, arising from or out of any breach of these warranties.

Considering that the Author(s) retain the copyright to this manuscript, please indicate your agreement to grant the permissions requested for the uses specified above by signing below:

Name: _____ **Title:** _____

Company: _____ **Phone:** _____

Signature: _____ **Date:** _____

Note: In the case of multiple authors, each author must sign a copy of this permission form. In the case of a "work made for hire" (a work prepared by an employee within the scope of his or her employment or commissioned as a work for hire under written agreement), an authorized representative of the employer should sign.

A&WMA Contact:

Lisa Bucher
Managing Editor, *EM*
Air & Waste Management Association
One Gateway Center, Third Floor
Pittsburgh, PA 15222
<http://www.awma.org>

P: (412) 232-3444 x 3159
F: (412) 232-3450
E-mail: lbucher@awma.org



High Performance Fatty Acid-Based Vinyl Ester Resin for Liquid Molding

by Xing Geng, John J. La Scala, James M. Sands, and Giuseppe R. Palmese

ARL-RP-184

July 2007

A reprint from the Proceedings of the SAMPE 2007 Conference, Baltimore, MD, 3–7 June 2007.

NOTICES

Disclaimers

The findings in this report are not to be construed as an official Department of the Army position unless so designated by other authorized documents.

Citation of manufacturer's or trade names does not constitute an official endorsement or approval of the use thereof.

Destroy this report when it is no longer needed. Do not return it to the originator.

Army Research Laboratory

Aberdeen Proving Ground, MD 21005-5069

ARL-RP-184**July 2007**

High Performance Fatty Acid-Based Vinyl Ester Resin for Liquid Molding

John J. La Scala and James M. Sands
Weapons and Materials Research Directorate, ARL

Xing Geng and Giuseppe R. Palmese
Drexel University

A reprint from the *Proceedings of the SAMPE 2007 Conference*, Baltimore, MD, 3–7 June 2007.

Approved for public release; distribution is unlimited.

REPORT DOCUMENTATION PAGE				Form Approved OMB No. 0704-0188	
Public reporting burden for this collection of information is estimated to average 1 hour per response, including the time for reviewing instructions, searching existing data sources, gathering and maintaining the data needed, and completing and reviewing the collection information. Send comments regarding this burden estimate or any other aspect of this collection of information, including suggestions for reducing the burden, to Department of Defense, Washington Headquarters Services, Directorate for Information Operations and Reports (0704-0188), 1215 Jefferson Davis Highway, Suite 1204, Arlington, VA 22202-4302. Respondents should be aware that notwithstanding any other provision of law, no person shall be subject to any penalty for failing to comply with a collection of information if it does not display a currently valid OMB control number. PLEASE DO NOT RETURN YOUR FORM TO THE ABOVE ADDRESS.					
1. REPORT DATE (DD-MM-YYYY) July 2007		2. REPORT TYPE Reprint		3. DATES COVERED (From - To) January 2006–February 2007	
4. TITLE AND SUBTITLE High Performance Fatty Acid-Based Vinyl Ester Resin for Liquid Molding				5a. CONTRACT NUMBER	
				5b. GRANT NUMBER	
				5c. PROGRAM ELEMENT NUMBER	
6. AUTHOR(S) Xing Geng, * John J. La Scala, James M. Sands, and Giuseppe R. Palmese*				5d. PROJECT NUMBER 789531	
				5e. TASK NUMBER	
				5f. WORK UNIT NUMBER	
7. PERFORMING ORGANIZATION NAME(S) AND ADDRESS(ES) U.S. Army Research Laboratory ATTN: AMSRD-ARL-WM-MC Aberdeen Proving Ground, MD 21005-5066				8. PERFORMING ORGANIZATION REPORT NUMBER ARL-RP-184	
9. SPONSORING/MONITORING AGENCY NAME(S) AND ADDRESS(ES)				10. SPONSOR/MONITOR'S ACRONYM(S)	
				11. SPONSOR/MONITOR'S REPORT NUMBER(S)	
12. DISTRIBUTION/AVAILABILITY STATEMENT Approved for public release; distribution is unlimited.					
13. SUPPLEMENTARY NOTES A reprint from the <i>Proceedings of the SAMPE 2007 Conference</i> , Baltimore, MD, 3–7 June 2007. *Department of Chemical Engineering, Drexel University, Philadelphia, PA 19104					
14. ABSTRACT Liquid resins used for molding composite structures are a significant source of volatile organic compounds (VOC) and hazardous air pollutant (HAP) emissions. One effective method of reducing styrene emissions from vinyl ester (VE) resins is to replace some or all of the styrene with fatty acid-based monomers. In our investigation, the styrene was reduced to 20-25 wt% compared to 40-60 wt% associated with commercial products. In addition, fatty acid-based monomers can bring about other benefits like higher toughness, lower exothermal heat and low volume shrinkage. One disadvantage of fatty acid-based VE resins, however, is the reduction in glass transition temperature (T _g) which limits their use in high temperature environments. Therefore, the specific focus of this work was to design high T _g fatty acid-based VE resins with low viscosities and high fracture properties. These high T _g resins were designed by blending fatty acid monomers with novolac vinyl esters. Various low viscosity formulations were established with T _g s as high as 147°C. Moreover, approaches to further improve the fracture toughness of the resin were investigated. Vinyl terminated poly(butadiene-co-acrylonitrile) (VTBN) and epoxy terminated poly(butadiene-co-acrylonitrile) (ETBN) were used as modifiers to these fatty acid vinyl ester resins. Compared with commercial novolac VE resin, marked improvement in fracture toughness (167 J/m ² versus 56 J/m ²) was achieved.					
15. SUBJECT TERMS fatty acid, low-VOC, styrene emission, vinyl ester, liquid molding					
16. SECURITY CLASSIFICATION OF:			17. LIMITATION OF ABSTRACT UL	18. NUMBER OF PAGES 16	19a. NAME OF RESPONSIBLE PERSON John J. La Scala
a. REPORT UNCLASSIFIED	b. ABSTRACT UNCLASSIFIED	c. THIS PAGE UNCLASSIFIED			19b. TELEPHONE NUMBER (Include area code) 410-306-0687

HIGH PERFORMANCE FATTY ACID-BASED VINYL ESTER RESIN FOR LIQUID MOLDING

Xing Geng¹, John J. LaScala², James M. Sands² and Giuseppe R. Palmese¹

¹ Department of Chemical Engineering, Drexel University, Philadelphia, PA 19104

² Army Research Laboratory Aberdeen Proving Ground, MD 21005

ABSTRACT

Liquid resins used for molding composite structures are a significant source of volatile organic compounds (VOC) and hazardous air pollutant (HAP) emissions. One effective method of reducing styrene emissions from vinyl ester (VE) resins is to replace some or all of the styrene with fatty acid-based monomers. In our investigation, the styrene was reduced to 20-25 wt% compared to 40-60 wt% associated with commercial products. In addition, fatty acid-based monomers can bring about other benefits like higher toughness, lower exothermal heat and low volume shrinkage. One disadvantage of fatty acid-based VE resins, however, is the reduction in glass transition temperature (T_g) which limits their use in high temperature environments. Therefore, the specific focus of this work was to design high T_g fatty acid-based VE resins with low viscosities and high fracture properties. These high T_g resins were designed by blending fatty acid monomers with novolac vinyl esters. Various low viscosity formulations were established with T_g s as high as 147°C. Moreover, approaches to further improve the fracture toughness of the resin were investigated. Vinyl terminated poly(butadiene-*co*-acrylonitrile) (VTBN) and epoxy terminated poly(butadiene-*co*-acrylonitrile) (ETBN) were used as modifiers to these fatty acid vinyl ester resins. Compared with commercial novolac VE resin, marked improvement in fracture toughness (167 J/m² versus 56 J/m²) was achieved.

KEYWORDS: Styrene Emission, Vinyl Ester, Liquid Molding

1. INTRODUCTION

Vinyl esters (VE) are one of the most popular resin systems used in polymer matrix composite fabrication for military and commercial applications due to their good properties, low weight and low cost. However, current commercial VE resins generally contain a high concentration of styrene to provide low viscosities suitable for composite fabrication via inexpensive liquid transfer molding techniques. Styrene is a hazardous air pollutant (HAP) and a volatile organic compound (VOC), and its use in composite manufacturing is being limited by the Federal Environmental Protection Agency of the United States of America [1]. Accordingly, fatty acid monomers have been developed and used to replace styrene in VE resins because of their low cost, low volatility, and the fact that they are derived from renewable resources. These monomers allow for the production of high performance composites while using ~20 wt% styrene, compared to 40-60 wt% styrene associated with commercial products [2,3]. Additionally, the use of fatty acid monomers in VE resins can result in other beneficial properties, such as high toughness, low exothermal heat and low volume shrinkage.

One disadvantage associated with the use of fatty acid monomers as reactive diluents to partially or fully replace styrene however, is the low T_g (below 0°C) of their homopolymers compared with that of styrene (~100°C) which limits their use in producing VE resins for high temperature applications. The use of multifunctional novolac VE resins was explored to partially counteract the loss of T_g resulting from fatty acid monomers and to produce high temperature low VOC VE resins. Aside from their high styrene content (33%) relative to fatty acid-based vinyl esters, commercial multifunctional novolac VE systems, such as Derakane 470-300 and 470HT-400, possess low fracture toughness due to their high crosslink densities. Though the presence of fatty acid can lessen this problem to some extent, other effective modifiers have to be employed to improve the fracture toughness to a higher level.

Alternatively, the addition of liquid rubber can be employed to improve the fracture toughness of VE resins [4-7]. Vinyl terminated poly(butadiene-*co*-acrylonitrile) (VTBN) and epoxy terminated poly(butadiene-*co*-acrylonitrile) (ETBN) exhibit significant improvement in certain VE resins, provided that the liquid rubber can form a miscible system with VE monomers and will precipitate completely from the resins resulting in a second phase after cure [4].

The goal of this study is to make low VOC high performance VE resins by using fatty acid to modify current commercial novolac VE resins. Ideally, the resulting resins will have low viscosities suitable for liquid molding, wet T_gs over 120°C, and fracture properties double that of commercial novolac VE resins.

2. MATERIALS AND EXPERIMENTAL PROCEDURE

2.1 Materials Derakane 470HT-400 vinyl ester resin was obtained from Ashland and was used without modification. Epon Resin 160, a novolac epoxy, and Epon 828, a diglycidyl ether of bisphenol A (DGEBA), were purchased from Hexion Specialty Chemicals and was used to synthesize vinyl ester resins. Methacrylic acid was purchased from Aldrich chemicals and was reacted with the epoxy monomers to produce vinyl ester. Two commercial DGEBA vinyl ester resins with $n \sim 0.1$ and containing no styrene, CN 151 and RDX 26936, were obtained from Sartomer and Cytec Surface Specialties Inc., respectively. Methacrylated octanoic acid (MOct) was produced by Applied Poleramic, Inc. and was used without modification. The liquid rubbers used for the toughening study were vinyl terminated poly(butadiene-*co*-acrylonitrile) (Hycar 1300×33) and epoxy terminated poly(butadiene-*co*-acrylonitrile) (Hycar 1300×40) provided by Noveon Solutions.

2.2 Vinyl Ester Resins Preparation Vinyl ester monomers were prepared by reacting methacrylic acid with Epon 160 ($n=0.5$) and Epon 828 ($n=0.098$) to produce VE 160 and VE 828, respectively (Figure 1). The reaction was catalyzed by 1 wt% AMC-2 (Aerojet Chemicals, Rancho Cordova, CA), which is a mixture of 50% trivalent organic chromium complexes and 50% phthalate esters. In order to maintain stability and prevent gelation, 0.01 wt% or 100 ppm hydroquinone was added as an inhibitor. Acid number below 4 and disappearance of the epoxy peak, as seen through Fourier transform infrared spectroscopy (917cm^{-1}), are two indicators for the end of the reaction. Typically, the reaction was allowed to proceed for 2 hours and a green liquid product was obtained.

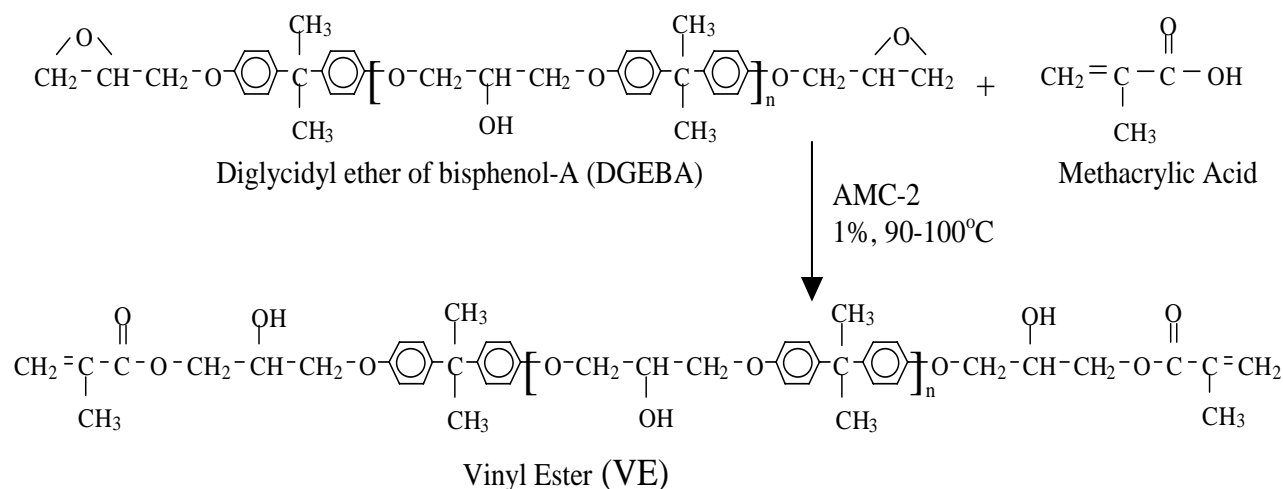


Figure 1: The reaction of DGEBA and methacrylic acid to produce the vinyl ester

2.3 Room Temperature Cure of VE Resins VE resin systems were initiated using Trigonox 239A (Akzo Nobel Chemicals, Chicago, IL), containing 45% cumene hydroperoxide, and cobalt naphthenate (CoNap) (Aldrich) as a catalyst to promote room temperature cure. The Trigonox and CoNap masses used were 1.5% and 0.375%, respectively, of the total resin mass. All resins were allowed to cure at room temperature for 16h. Fracture toughness samples were post-cured at 130°C for 2 h.

2.4 Procedures Dynamic mechanical analysis (DMA) was performed using a TA instruments DMA 2980 at a frequency of 1 Hz and at a heating rate of 2°C/min. Specimens of dimensions 30×12×3 mm³ were tested in single cantilever beam loading configuration.

For the water absorption study, samples with dimensions 30×12×1.5 mm³ were exposed to controlled humidity environments until saturation was reached. Samples were placed 60°C environments with a relative humidity (RH) of 79%. Samples were also immersed in boiling water for 24 hrs. The samples at 60°C and 79% RH were periodically removed from the environments and superficially dried. The samples were weighed to determine the amount of water absorption, and then re-introduced to the humid environment. Saturation was achieved when the sample weight no longer changed with exposure time.

Fourier Transform Infrared Spectroscopy (FTIR) was also used to monitor the water absorption of samples. A Thermo Nicolet Nexus 670 FTIR spectrometer was used. Near IR spectroscopy was conducted in a transmission mode at 16 cm⁻¹ with 32 scans per data point. The water-saturated samples were also tested via DMA to determine the effect of water absorption on Tg.

The viscosities of designed resin systems were evaluated using a Brookfield digital viscometer. The viscosity measurement was taken at 30°C.

3. RESULTS AND DISCUSSION

3.1 Design of High Tg Formulation Fatty acid based resin with dry Tg of 140°C and wet Tg of 120°C is required for certain DoD applications. With this aim, novolac vinyl esters with

multiple functional groups were employed in this study to improve the Tg of fatty acid based resins. Consequently, Derakane 470HT-400 (simplified as Der470HT in this study) was selected because it has the highest Tg among the commercial available VE resins. The goal was to reduce the styrene content in this resin from 33 wt% to 25 wt% or less by replacing styrene with methacrylated octanoic acid, while achieving good performance and processibility. To compensate for the loss of vinyl ester monomer when reducing the amount of styrene, DGEBA based vinyl ester (VE 828) was added to the system. As summarized in Table 1, formulations were designed by adjusting the weight fraction of MOct and Styrene in order to achieve both the performance and processibility at the minimum loading amount of styrene. As can be seen, the formulation of 75.8 wt% Der 470HT, 14.2 wt% VE 828 and 10 wt% MOct gave the highest Tg (147°C) as well as the lowest viscosity (388 cP at 30°C). Because of the excellent properties of this resin, it will be evaluated throughout this paper and abbreviated as FAVE-O-470HT. A representative DMA scan is shown in Fig. 2. The material is in the glassy state at low temperatures, goes through a glass transition at moderate temperatures, and is a rubber at high temperatures. The storage modulus monotonically decreases with temperature, while the loss modulus goes through a maximum. The temperature at which the maximum in the loss modulus occurs was considered the Tg of the material.

Table 1: Representative formulations of VE resins

Formulation No.	Der470HT (wt%)	VE828 (wt%)	MOct (wt%)	Tg (°C) Actual	Styrene (wt%)
1	60.6	29.4	10	147	20
2	60.6	24.4	15	138	20
3	75.8	14.2	10	147	25
4	75.8	9.2	15	136	25

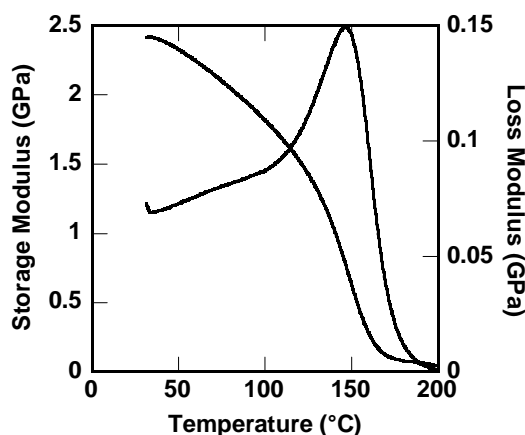


Figure 2: Dynamic mechanical spectrum of the system of 75.8 wt.% Der470HT 14.2 wt.% VE828 and 10 wt.% MOct.

Table 2: Viscosity of designed resins compared with commercial VE resins

Resin	Viscosity (cP) at 30°C
Design 1	780
Design 2	540
Design 3	388
Design 4	296
Der 470HT	290
FAVE-O-470HT *	392

* CN151 was used instead of VE 828

3.3 Water Absorption Study Two different conditions, boiling water for 24 h and 60°C water vapor with humidity as 79% until saturation, were employed in this study to determine the effect of moisture on the thermomechanical properties of fatty acid-based resins. A representative VE resin system of VE 160/MOOct/St (70-5-25) was investigated with respect to water absorption and its influence on Tg. The typical DMA results under 100°C water uptake for 24 h are given in Figure 3. Tgs before and after water uptake are 152°C and 133°C respectively which means water uptake will impart a 19°C decrease in Tg. However, the second and third DMA runs of water absorbed sample (Figure 4), demonstrate that the Tg recovers completely after full removal of water, which indicated no hydrolysis occurred during water absorption of VE resins. DMA spectra of sample exposed to 60°C water vapor for 5 days are shown in Figure 5 and 6, and similar results were obtained.

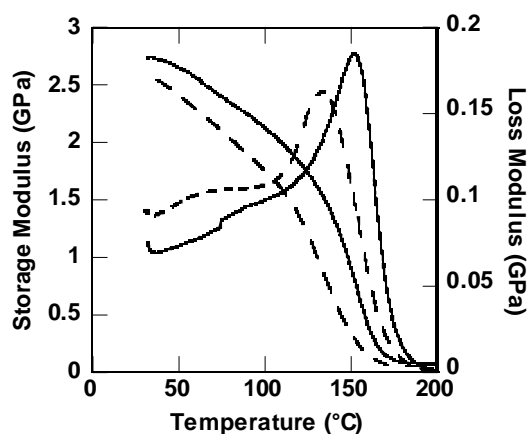


Figure 3: DMA scans of the system of VE scans of water 160/MOOct/St (70-5-25) before (solid) and after (dashed) water uptake in 100°C for 24 hours.

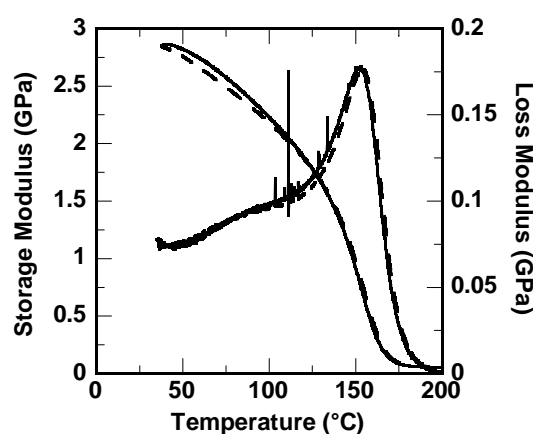


Figure 4: Second (solid) and third (dashed) DMA uptake sample gave Tgs as 152°C and 154°C.

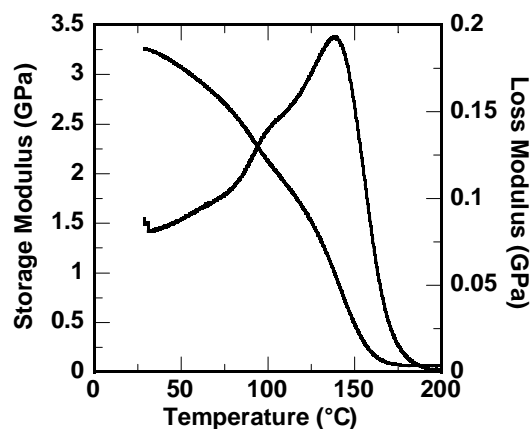


Figure 5: DMA scans of the system of VE 160/MOOct/St (70-5-25) after water uptake at 60°C with RH=79% for 5 days. Resulting sample Tg is 138°C.

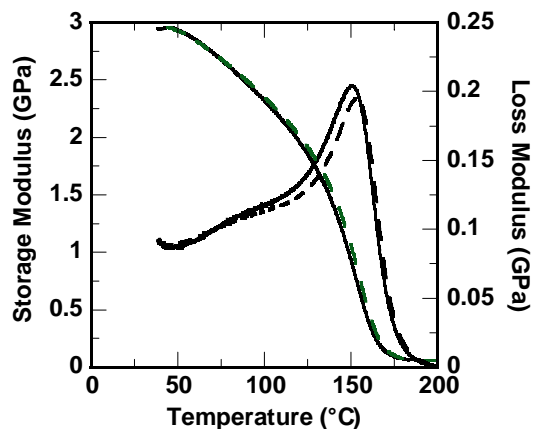


Figure 6: Second (solid) and third (dashed) DMA scans of water uptake sample gave Tgs as 151°C and 153°C.

Near infrared (NIR) spectroscopy was employed to monitor the water uptake of the sample exposed to 60°C during consecutive 7 days with spectra shown in Figure 7. Results show a marked increase in the water peak at $\sim 5100 \text{ cm}^{-1}$. No other changes were observed, and the material is unchanged according to NIR after complete water removal. The NIR results also show that after DMA runs, the water can be fully removed as reflected in the disappearance of water peak in NIR spectra (Figure 8).

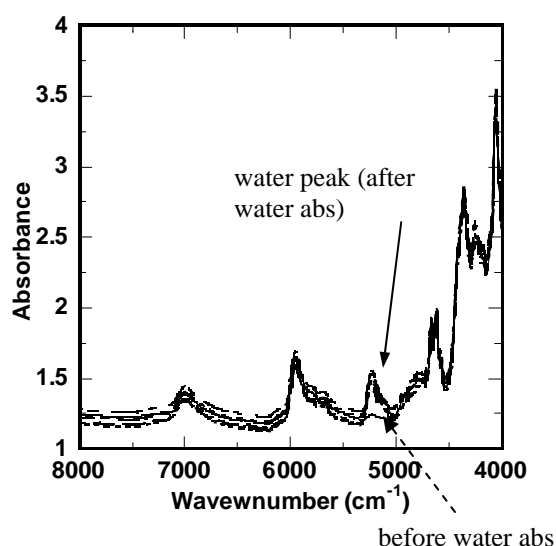


Figure 7: NIR spectra of the system of VE 160/MOOct/St (70-5-25) before and after water uptake in 60°C (RH=79%) for 7 days.

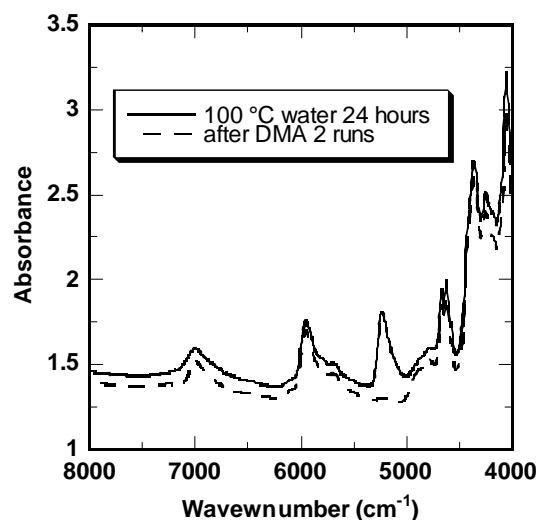


Figure 8: NIR spectra of the sample after water uptake in 100°C for 24 hours and after DMA runs.

The weight gain during the water absorption experiments at 60°C (RH=79%) is shown in Figure 9. It is seen that after 5 days, the water saturation status is reached; the ultimate water absorption percentage is 1.74%. Weight change for a formulation containing 75 wt% VE 160, 5 wt% MOct, and 25 wt% styrene is given in Table 3. Water absorption percentage for 100°C after 24 h and 60°C (RH=79%) after 5 days are 2.25% and 1.62% respectively. These results show that the sample at 100°C will absorb more water and will be correspondingly subject to greater loss in Tg. Accordingly, it can be deduced that water uptake at 100°C for 24 h is a more critical criterion to evaluate the VE resins' resistance to water. The wet Tg of some commercial VE resins were thus measured based on this criterion along with our designed resin system and the results are given in Table 4. The FAVE-O-470HT resin has a moderate wet Tg of 124°C relative to the commercial resins. The Tg is above the goal value of 120°C.

Table 3: The relation between water absorption and Tgs of a formulation containing 75 wt% VE 160, 5 wt% MOct, and 25 wt% styrene.

75VE160-5MOct-25St	Initial	100°C water 24 h	after 1 st run	after 2 nd run	60°C water 5 days	after 1 st run	after 2 nd run
Tg (°C)	152	133	152	154	138	151	153
Sample	0.5812	0.5943	0.578	0.5778			
Weight (g)	0.5930				0.6026	0.5913	0.5911

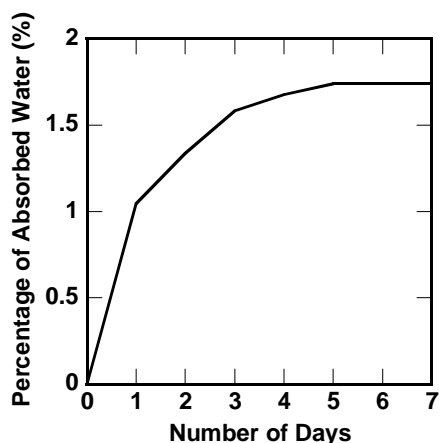


Figure 9: Weight change of sample in 60°C At 79% relative humidity for 7 days

Table 4: Wet Tg of designed resin and commercial VE resins

Resin	Wet Tg after 100°C 24 h (°C)
Derakane 8084	103
Derakane 441-400	125
Derakane 470-300	139
Der 470HT	155
FAVE-O-470HT	124

3.4 Commercial Resin Selection As reported in the previous section, FAVE-O-470HT resin was formulated by blending Derakane 470HT-400 with VE 828, and MOct. This resin has excellent properties, but uses a vinyl ester that is only prepared at the laboratory bench scale. To meet DoD and commercial applications, we must identify the appropriate commercial VE monomer resin as a replacement for VE 828. CN151 and RDX 26929, both of them based on methacrylated diglycidyl ether of bisphenol A epoxy resin, were consequently investigated with regard to their impact on Tg and other properties. Though both of these two resins can produce FAVE-O-470HT resin with slightly different Tg properties (~145°C), when mixed with 33% styrene respectively, the RDX 26939 monomer produced a resin with a significantly higher Tg

(153°C) than the CN151-based resin (132°C), as illustrated in Figure 10 and 11. The difference in T_g properties of these two resins is likely due to lower methacrylate functionality in CN-151.

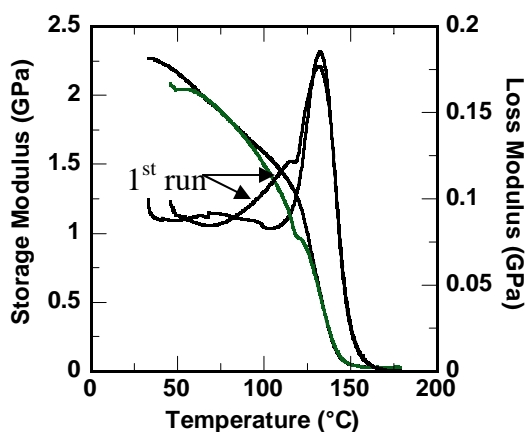


Figure 10 DMA spectra for CN151 with 33% Styrene. T_g of 1st run is 132°C, T_g of 2nd run is 132°C. Fully cure was achieved by heating at 90°C for several days heating.

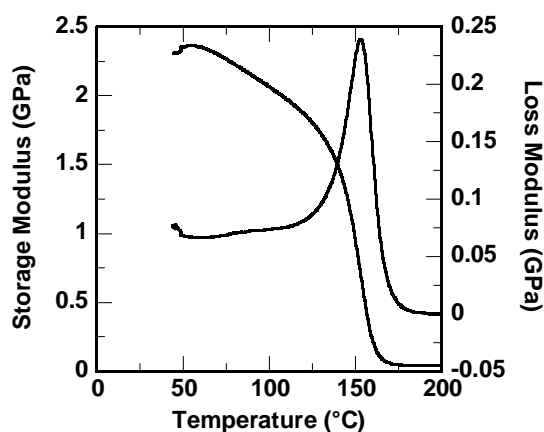


Figure 11 DMA spectrum of sample of RDX 26939 with 33% Styrene. T_g of 153°C shows up in the second run.

3.5 Fracture Toughness Improvement 5% and 10% weight fraction of vinyl terminated poly(butadiene-*co*-acrylonitrile) (VTBN) and epoxy terminated poly(butadiene-*co*-acrylonitrile) (ETBN) were employed to improve the fracture toughness of the designed resin system. The results are summarized in Table 5 along with the fracture toughness of other commercial VE resins for comparison. The rubber modifiers used in this study did not show good miscibility with our high molecular weight, fatty acid-based FAVE-O-470HT resin system. Consequently, the toughening effect was not as good as the commercial toughened vinyl ester resins (Derakane 8084). Nonetheless, marked improvement was achieved with no loss of T_g. Our next work is to develop the appropriate modifiers needed to further improve the fracture toughness of the fatty acid based resin systems.

Table 5 Fracture toughness of liquid rubber modified and commercial VE resins

VE Resins	T _g (°C)	G _{1c} (J/m ²)
Derakane 8084	118	680
Derakane 470HT-400	173	56
FAVE-O-470HT	145	102
5 wt% ETBN FAVE-O-HT	145	135
9 wt% ETBN FAVE-O-HT	151	141
5 wt% VTBN FAVE-O-HT	146	--
9 wt% VTBN FAVE-O-HT	147	167

4. CONCLUSIONS

Novolac vinyl ester resin of Derakane 470-400 was employed in this study to improve the Tg of the fatty acid based low VOC vinyl ester resin. A dry Tg of 147°C and wet Tg of 124°C was achieved along with good processibility. Furthermore, the fracture toughness of the resulting high Tg resin is greatly improved by using liquid rubber as modifiers. However, further investigation needs to be carried out to improve the fracture toughness to a higher level.

5. ACKNOWLEDGEMENTS

The authors are thankful for support from ESTCP under project WP-0167. Moreover, the Drexel University authors acknowledge support for this work via the Army Research Laboratory Cooperative Agreement no. DAAD19-02-2-0010.

6. REFERENCES

1. Environmental Protection Agency. Federal Register, 68, 19375 (2003)
2. J.J. Scala, et al., Polymer, **45** (22), 7729 (2004)
3. J.J. Scala, et al., Polymer, **46** (9), 2908 (2005)
4. E.J. Robinette, et al., Polymer, **45** (18), 6143 (2004)
5. O. Gryshchuk, et al., J. of Appl. Polym. Sci., **84**, 672 (2002)
6. O. Gryshchuk, et al., Polymer, **43** (17), 4763 (2002)
7. M.L. Auad, et al., Polymer, **42** (8), 3723 (2001)

NO. OF
COPIES ORGANIZATION

1 DEFENSE TECHNICAL
(PDF INFORMATION CTR
ONLY) DTIC OCA
8725 JOHN J KINGMAN RD
STE 0944
FORT BELVOIR VA 22060-6218

1 US ARMY RSRCH DEV &
ENGRG CMD
SYSTEMS OF SYSTEMS
INTEGRATION
AMSRD SS T
6000 6TH ST STE 100
FORT BELVOIR VA 22060-5608

1 DIRECTOR
US ARMY RESEARCH LAB
IMNE ALC IMS
2800 POWDER MILL RD
ADELPHI MD 20783-1197

3 DIRECTOR
US ARMY RESEARCH LAB
AMSRD ARL CI OK TL
2800 POWDER MILL RD
ADELPHI MD 20783-1197

ABERDEEN PROVING GROUND

1 DIR USARL
AMSRD ARL CI OK TP (BLDG 4600)

NO. OF
COPIES ORGANIZATION

1 SERDP & ESTCP PROGRAM OFC
 J MARQUSEE
 901 N STUART STREET
 STE 303
 ARLINGTON VA 22203

INTENTIONALLY LEFT BLANK.

Functionalized Fatty Acid as an Environmentally Benign Reactive Diluent Aiding in Processing of Novolac Vinyl Ester Resin for High-Temperature Applications

Xing Geng and Giuseppe R. Palmese
Department of Chemical and Biological Engineering, Drexel University
John J. La Scala and James M. Sands
Army Research Laboratory Aberdeen Proving Grounds

Abstract

Liquid resins used for molding composite structures are a significant source of volatile organic compounds (VOC) and hazardous air pollutant (HAP) emissions. One effective method for reducing styrene emissions from vinyl ester (VE) resins is to replace some or all of the styrene with fatty acid-based monomers. In this investigation, the styrene was reduced to 20 wt% compared to 40-60 wt% associated with commercial products. In addition, fatty acid-based monomers can bring about other benefits like higher toughness, lower exothermal heat and low cure shrinkage. One disadvantage of these fatty acid-based VE resins, however, is the reduction in glass transition temperature (T_g) which limits their use in high-temperature environments. Therefore, the specific focus of this work was to design high T_g fatty acid-based VE resins with low viscosities and high fracture properties. These high T_g resins were designed by blending fatty acid monomers with novolac vinyl esters. Various low viscosity formulations were established with T_g s as high as 147 C. Vinyl terminated poly(butadiene-co-acrylonitrile) (VTBN) and epoxy terminated poly(butadiene-co-acrylonitrile) (ETBN) were used as modifiers to these fatty acid vinyl ester resins. Though marked enhancement in fracture toughness was achieved without sacrificing T_g , further improvement in fracture toughness was limited due to the immiscibility of ETBN and VTBN with VE resins evaluated. The miscibility problem can be mitigated by using high acrylonitrile content carboxyl terminated poly(butadiene-co-acrylonitrile) (CTBN) but in this case a slight loss in T_g was detected. Thus modifiers having appropriate miscibility with VE resins to improve the fracture toughness without sacrificing T_g need to be identified by further work.

Authors

Dr. Geng currently works as a postdoctoral researcher in Department of Chemical and Biological Engineering at Drexel University. He has 15 years working and research experience in water-borne coating, adhesives and high performance polymer composite materials. He earned his PhD in Chemical Engineering from the Drexel University.

Dr. La Scala works at the Army Research Laboratory in Aberdeen, MD in the fields of composites, adhesives, and coatings and has 10 years experience in environmentally friendly polymers and composites. Dr. La Scala holds a PhD in Chemical Engineering from the University of Delaware and a BS in Chemical Engineering from the University of Virginia.

Dr. James M. Sands is the Team Leader of Transparent Materials Technology Team at the U.S. Army Research Laboratory. He has twelve years of experience in adhesive and resin formulation and composite materials fabrication.

Dr. Giuseppe R. Palmese is Professor and Department Head of Chemical and Biological Engineering at Drexel University. He runs a research program in thermosetting polymers and composites with emphasis on elucidating processing-structure-property relationships and multiscale phenomena.

Introduction

Vinyl esters (VE) are one of the most popular resin systems used in polymer matrix composite fabrication for military and commercial applications due to their good properties, low weight and low cost. However, current commercial VE resins generally contain a high concentration of styrene to provide low viscosities suitable for composite fabrication via low-cost liquid transfer molding techniques. Styrene is a hazardous air pollutant (HAP) and a volatile organic compound (VOC), and its use in composite manufacturing is being limited by the Federal Environmental Protection Agency of the United States of America [1]. Accordingly, fatty acid monomers have been developed and used to partially replace styrene in VE resins because of their low cost, low volatility, and because they are derived from renewable resources. These monomers allow for the production of high-performance composites while using ~20 wt% styrene, compared to 40-60 wt% styrene associated with commercial products [2,3]. Additionally, the use of fatty acid monomers in VE resins can result in other beneficial properties, such as high toughness, low exothermal heat and low cure shrinkage.

One disadvantage associated with the use of fatty acid monomers as reactive diluents is the low T_g ($<0^\circ\text{C}$) of their homopolymers compared with that of styrene ($\sim 100^\circ\text{C}$). This limits their use in producing VE resins for high-temperature applications. The use of multifunctional novolac VE resins was explored to partially counteract the loss of T_g resulting from fatty acid monomers and to produce high temperature, low VOC VE resins. Aside from their high styrene content (33%) relative to fatty acid-based vinyl esters, commercial multifunctional novolac VE systems, such as Derakane 470-300 and 470HT-400, possess low fracture toughness due to their high crosslink densities. Though the presence of fatty acid can diminish this problem, other effective modifiers have to be employed to improve fracture toughness further.

Fracture toughness of VE resins can be improved by the addition of liquid rubber modifiers [4-7]. Vinyl terminated poly(butadiene-*co*-acrylonitrile) (VTBN) and epoxy terminated poly(butadiene-*co*-acrylonitrile) (ETBN) provide significant improvement in certain VE resins, provided that the liquid rubber forms a miscible system with VE monomers prior to cure and precipitates completely from the resins resulting in a second phase after cure [4].

The goal of this study is to make low VOC, high-performance VE resins by using fatty acid to modify current commercial novolac VE resins. Ideally, the resulting resins will have low viscosities suitable for liquid molding, T_g s after hydrothermal conditioning (wet T_g) over 120°C , and fracture properties greater than those of commercial novolac VE resins.

Materials and Experimental Procedure

Materials: Commercial novolac vinyl ester resins, named Derakane 470HT-400 and Derakane 470-300 respectively, were obtained from Ashland and were used without modification. Epon Resin 160, a novolac epoxy, and Epon 828, a diglycidyl ether of bisphenol A (DGEBA), were purchased from Hexion Specialty Chemicals and were used to synthesize vinyl ester resins. Methacrylic acid was purchased from Aldrich chemicals and was reacted with the epoxy monomers to produce vinyl ester (Figure 1). Two commercial DGEBA vinyl ester resins with $n \sim 0.1$ and containing no styrene, CN 151 and RDX 26936, were obtained from Sartomer and Cytec Surface Specialties Inc., respectively. Octanoic acid is a fatty acid with eight carbon chain length. Methacrylated octanoic acid (MOct) was produced by Applied Poleramic, Inc. and was used without modification. The liquid rubbers used for the toughening study were vinyl terminated poly(butadiene-*co*-acrylonitrile) (Hycar 1300×33), epoxy terminated poly(butadiene-*co*-acrylonitrile) (Hycar 1300×40) and carboxyl terminated poly(butadiene-*co*-acrylonitrile) (Hycar 1300×13) provided by Noveon Solutions.

Preparation of Vinyl Ester Resin: Vinyl ester monomers were prepared by reacting methacrylic acid with Epon 160 ($n=0.5$) and Epon 828 ($n=0.098$) to produce VE 160 and VE 828, respectively (Figure 1). The

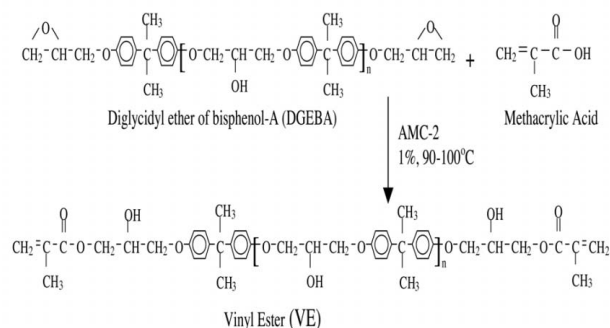


Figure 1: The Reaction of DGEBA and Methacrylic Acid to Produce Vinyl Ester.

reaction was catalyzed by 1 wt% AMC-2 (Aerojet Chemicals, Rancho Cordova, CA), which is a mixture of 50% trivalent organic chromium complexes and 50% phthalate esters. In order to maintain stability and prevent gelation, 0.01 wt% or 100 ppm hydroquinone was added as an inhibitor. Typically, the reaction was allowed to proceed for two hours and a green liquid product was obtained. Acid number below four and disappearance of the epoxy peak (917cm^{-1}) were used as two indicators for the end of the reaction.

Room Temperature Cure of VE Resins: VE resin systems were initiated using Trigonox 239A (Akzo Nobel Chemicals, Chicago, IL), containing 45 percent cumene hydroperoxide, and Cobalt naphthenate (CoNap, OM Group, Inc.), containing 6 percent Cobalt, as a catalyst to promote room temperature cure. The Trigonox and CoNap concentrations were 1.5 percent and 0.375 percent, respectively, of the total resin mass. All resins were allowed to cure at room temperature for 16h. Post-cure was realized by heating at 150 C for 2 hours.

Water Absorption Study: Samples with dimensions $30 \times 12 \times 1.5\text{ mm}^3$ were exposed to a controlled humidity environment (60 C and 79 percent relative humidity) until saturation was reached. The samples were periodically removed and weighed, and then re-introduced to the humid environment. Saturation was achieved when the sample weight no longer changed with exposure time. Immersion in boiling water for 24 hours was also used as a method of sample conditioning.

Fourier Transform Infrared Spectroscopy (FTIR) was used to monitor water absorption of samples. A Thermo Nicolet Nexus 670 FTIR spectrometer was used. Near IR spectroscopy was conducted in transmission mode at 16 cm^{-1} with 32 scans per data point.

Dynamic mechanical analysis (DMA) was performed using a TA instruments DMA 2980 at a frequency of 1 Hz and at a heating rate of 2 C/min. Specimens of dimensions $30 \times 12 \times 3\text{ mm}^3$ were tested in single cantilever beam loading configuration. The temperature at which the maximum in the loss modulus occurs was considered the T_g of the material. The conditioned samples were also tested using DMA and the T_g obtained immediately following conditioning are designated as wet T_g .

Viscosity Measurements: The viscosities of designed

resin systems were evaluated using a Brookfield digital viscometer. Viscosity was measured at 30 C.

Results and Discussion

Design of High T_g Formulation: Fatty acid based resin with dry T_g of 140 C and wet T_g of 120 C is required for certain DoD applications. With this aim, no-volac vinyl esters with multiple functional groups were employed in this study to improve the T_g of fatty acid based resins. Consequently, Derakane 470HT-400 (simplified as Novo-VE in this study) was selected because it has the highest T_g among the commercial available VE resins. The goal was to reduce the styrene content in this resin from 33 wt% to 25 wt% or less by replacing styrene with methacrylated octanoic acid, while achieving good performance and processibility. To compensate for the loss of vinyl ester monomer when reducing the amount of styrene, DGEBA based vinyl ester (VE 828) was added to the system. As summarized in Table 1, formulations were designed by adjusting the weight fraction of MOct and styrene in order to achieve both the performance and processibility at the minimum loading amount of styrene. As can be seen, the formulation of 75.8 wt% Novo-VE, 14.2 wt% VE 828 and 10 wt% MOct gave the best combination of the highest T_g (147°C shown in Figure 2) as well as the lowest viscosity (388 cP at 30°C). At the same time, the styrene content in formulation was reduced to 25 percent compared to the original level of 33 percent. This formulation is marked as FAVE-O-HT for the convenience of further discussion. The material is in the glassy state at low temperatures, goes through a glass transition at moderate temperatures, and is a rubber at high temperatures.

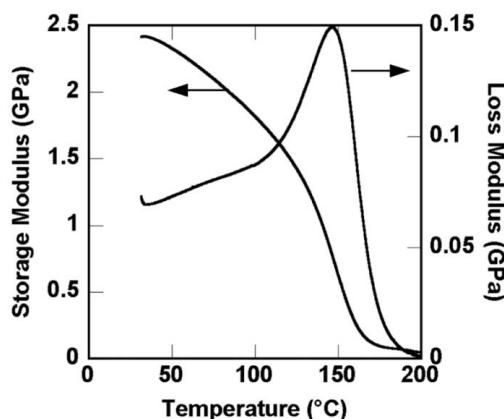


Figure 2: DMA plots for the formulation of 75.8 wt% Novo-VE, 14.2 wt% VE 828 and 10 wt% MOct

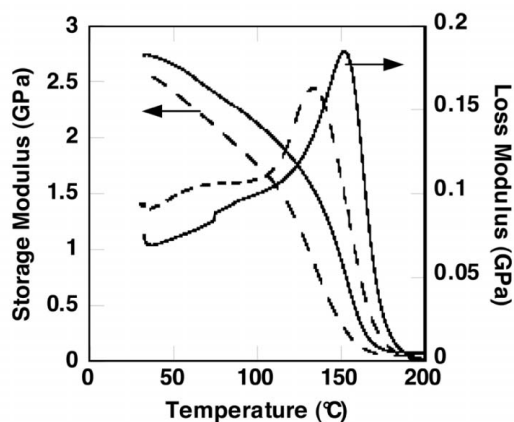


Figure 3: DMA Scans of VE 160/MOOct/St (70-5-25) Before (Solid Line) and After (Dashed Line) 24 h Boiling Water Exposure

Water Absorption Study: Two conditions, boiling water for 24 hours and 60 C humid air with 79 per cent R.H. until saturation, were employed in this study to determine the effect of moisture on the thermomechanical properties of fatty acid-based resins. A representative VE resin system of VE 160/MOOct/St (70-5-25) was investigated with respect to water absorption and its influence on T_g . The typical DMA results for 100 C water uptake are given in Figure 3. T_g s before and after (wet T_g) water uptake are 152 C and 133 C respectively which means water uptake imparts a 19 C decrease in T_g . However, the second and third DMA runs of this sample (Figure 4), demonstrate that the T_g recovers completely after full removal of water. This indicated no hydrolysis occurred during water absorption by VE resins. DMA

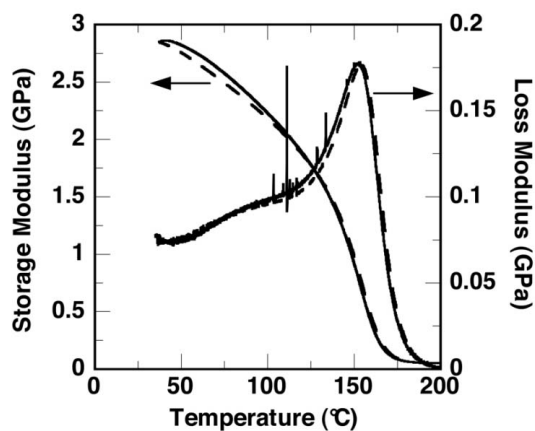


Figure 4: Second (Dashed Line) and Third (Solid Line) DMA Scans of VE 160/MOOct/St (70-5-25) Conditioned for 24 h in Boiling Water.

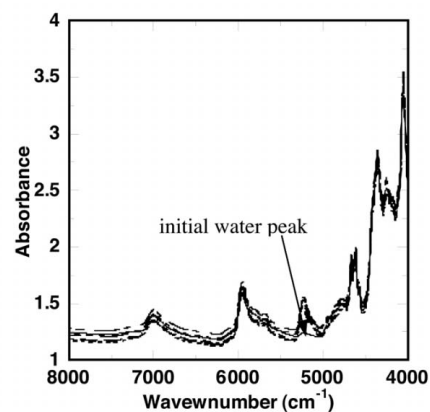


Figure 5: NIR Spectra of VE 160/MOOct/St (70-5-25) Before and After Conditioning in 60°C Humid Air with RH=79% for 7 days

spectra of sample exposed to 60 C water vapor for five days produced similar results.

Near infrared (NIR) spectroscopy was employed to monitor the water uptake of the sample exposed to 60 C (RH=79 percent) on a daily basis for seven consecutive days. The spectra are shown in Figure 5. Results show a marked increase in the water peak at ~5100 cm^{-1} . No other changes were observed, and the material is unchanged according to NIR after complete water removal. The NIR results also show that after DMA runs, the water can be fully removed as reflected in the disappearance of water peak in NIR spectra given in Figure 6.

The weight gain during water absorption experiments

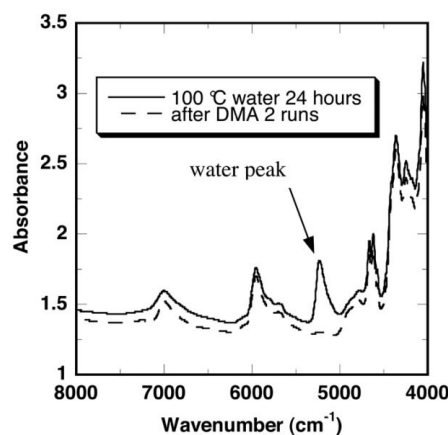


Figure 6: NIR Spectra of VE 160/MOOct/St (70-5-25) After Conditioning in Boiling Water for 24 h (Solid Line) and After DMA Runs (Dashed Line)

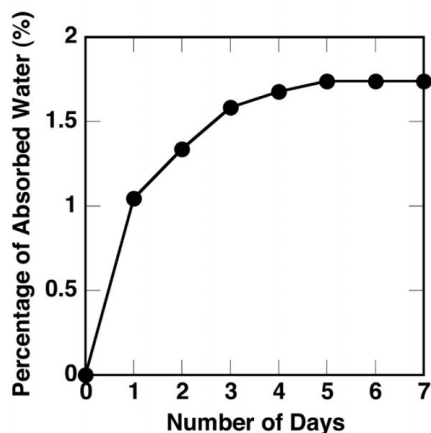


Figure 7: Weight Change of Sample Conditioned in 79% RH, 60°C Humid Air

at 60 C (RH=79 percent) is shown in Figure 7. It can be seen that after five days, saturation is reached; the equilibrium water absorption in this case is 1.74 percent. In another set of experiments, weight change of samples at two stages, after water uptake and after DMA first scan, was measured with results given in Table 3. Water absorptions for 24 hours boiling water and 60 C (RH=79%) after five days are 2.25 percent and 1.62 percent respectively. These results show that the sample at 100 C will absorb more water and will be correspondingly subject to greater loss in T_g . Accordingly, it can be deduced that water uptake at 100 C for 24 hours is a more critical method to evaluate the VE resins' resistance to water absorption. The T_g s following exposure to boiling water for 24 hours were measured for some commercial VE resins as well as our designed resin system and the results are given in Table 4. FAVE-O-HT has a moderate wet T_g of 124 C relative to the commercial resins. The T_g is above our goal value of 120 C.

Commercial Resin Selection: As reported in the previous section, the designed resin has excellent properties, but uses a vinyl ester that has been prepared at the laboratory bench scale. To meet DoD and commercial applications, the appropriate commercial VE monomer resin as a replacement for VE 828 must be identified. CN151 and RDX 26929, both of them based on methacrylated diglycidyl ether of bisphenol A epoxy, were consequently tested in our formulations with regard to their impact on T_g and other properties. Though both of these resins can produce fatty acid based resin with slightly different T_g , when mixed with 33 percent styrene respectively, the RDX 26939 monomer produced a resin with a signif-

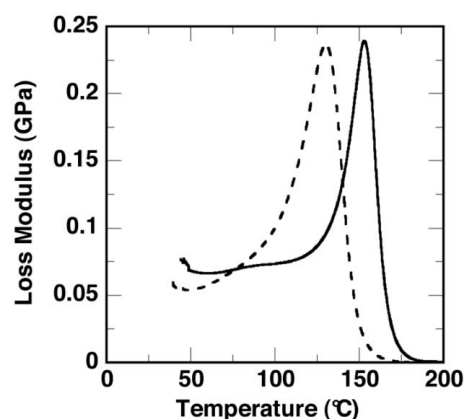


Figure 8: DMA Spectra for CN151 and RDX 26936 with 33% Styrene. RDX 26936 (Solid Line), CN151 (Dashed Line).

icantly higher T_g (153 C) than the CN151-based resin (132 C), as illustrated in Figure 8. Note that post-cure of CN151 was realized by heating at 90 C for several days while the RDX 26926 sample was postcured at 90 C for 10 minutes. The difference in T_g of these two resins is likely due to lower methacrylate functionality in CN-151 and this difference can be eliminated by introducing high functionality novolac VE resin.

Fracture Toughness Improvement: 5 percent and 9 percent weight fraction of vinyl terminated poly(butadiene-co-acrylonitrile) (VTBN) and epoxy terminated poly(butadiene-co-acrylonitrile) (ETBN) were used to improve the fracture toughness (G_{Ic}) of the designed resin system. The results are summarized in Table 5 along with the fracture toughness of other commercial VE resins for comparison. The rubber modifiers used in this study did not show good miscibility with our fatty acid-based resin system. The toughness as measured by G_{Ic} of these systems effect was not as good as the commercial toughened vinyl ester resin (Derakane 8084). Nonetheless, marked improvement was achieved with no loss of T_g . The poor miscibility of VTBN and ETBN is also detrimental to long term storage of the resin. Thus, CTBN with high content of acrylonitrile, 26 percent compared to the 18 percent of VTBN and ETBN, was chosen as a toughener. The results showed the miscibility is highly improved and a transparent solution can be obtained. However, the T_g of the FAVE-O-HT with 10 percent CTBN is 136 C, exhibiting a slight decrease compared to VTBN and ETBN toughened resin systems.

Conclusions

Fatty acid based monomers of methacrylated fatty acids were employed in combination with novolac VE resin to achieve high-temperature resistance, low VOC resin systems. A T_g of 147 C was achieved along with low styrene content and good processability. DMA analysis shows the high temperature resistance of VE resin is reduced by water absorption but the loss is reversible after removal of water. Equilibrium water uptake on exposure to 60 C, 79 percent RH humid air was found to be 1.7 percent. Conditioning for 24 hours in boiling water was found to be a more severe treatment. Under such conditions T_g was reduced to 124 C. This value is greater than our wet T_g goal of 120 C. Additionally, using fatty acid based monomers as a replacement for styrene, fracture toughness improvements were observed. Further improvement is possible with the addition of rubber modifiers.

Acknowledgements

The authors are thankful for support from ESTCP under project WP-0167. Moreover, the Drexel University authors acknowledge support for this work via the Army Research Laboratory Cooperative Agreement no. DAAD19-02-2-0010. Thanks are also due to Ashland Inc. for providing VE resins for this investigation.

References

1. Environmental Protection Agency. Fed Register, 68, 19375 (2003)
2. J.J. Scala, et al., Polymer, 45 (22), 7729 (2004)
3. J.J. Scala, et al., Polymer, 46 (9), 2908 (2005)
4. E.J. Robinette, et al., Polymer, 45 (18), 6143 (2004)
5. O. Gryshchuk, et al., J. of Appl. Polym. Sci., 84, 672 (2002)
6. O. Gryshchuk, et al., Polymer, 43 (17), 4763 (2002)
7. M.L. Auad, et al., Polymer, 42 (8), 3723 (2001)

Table 1: Representative formulations of VE resins

Sample No.	Novo-VE (wt%)	VE828 (wt%)	MOct (wt%)	Styrene (wt%)	T_g (°C)
1	60.6	29.4	10	20	147
2	60.6	24.4	15	20	138
3	75.8	14.2	10	25	147
4	75.8	9.2	15	25	136

Table 2: Viscosity of designed resins compared with commercial VE resins

Resin	Viscosity (cP) at 30°C
Formulation 1	780
Formulation 2	540
Formulation 3	388
Formulation 4	296
Novo-VE	290

Tables continued on next page

Table 3: The relation between water absorption and Tgs of a formulation containing 70 wt% VE 160, 5 wt% MOct, and 25 wt% styrene

75VE160- 5MOct- 25St	Initial	100°C water 24 h	after 2 nd DMA run	60°C (RH=79%) water 5 days	after 2 nd DMA run
<i>T_g</i> (°C)	152	133	154	138	153
Water Absorption (%)	0	2.25	0	--	--
	0	--	--	1.62	0

Table 4: Wet *T_g* of designed resin and commercial VE resins

Resin	Wet <i>T_g</i> after 100°C 24 h (°C)
Derakane 8084	103
Derakane 441-400	125
Derakane 470-300	139
Novo-VE	155
FAVE-O-HT	124

Table 5: Fracture toughness (*G_{1c}*) of liquid rubber modified and commercial VE resins

VE Resins	<i>T_g</i> (°C)	<i>G_{1c}</i> (J/m ²)
Derakane 8084	118	680 ± 160
Novo-VE	173	56 ± 18
FAVE-O-HT	145	102 ± 53
2.5 wt% ETBN FAVE-O-HT	145	135 ± 24
4.5 wt% ETBN FAVE-O-HT	151	141 ± 23
5 wt% VTBN FAVE-O-HT	146	--
9 wt% VTBN FAVE-O-HT	147	167 ± 31
10 wt% CTBN FAVE-O-HT	136	--

RUDDER GETS NEW TWIST WITH COMPOSITES

Engineering Challenge:

A ship rudder with a complex twisted shape that reduces cavitation at ship operating speed and hence reduces both noise levels and maintenance requirements while extending the component's useful life.

Design Solution:

The rudder's complex shape demands a move from existing steel construction to composites, offering the added benefits of weight reduction, reduced acoustic and magnetic signatures and lower warranty costs.

The U.S. Navy's specially contoured ship rudder commands composite construction.

Ship rudder design, historically, has been dictated by the need to minimize hydrodynamic drag, resulting in simple, linear designs, analogous to vertically inclined wings. It is, therefore, far from obvious why the U.S. Navy's latest development is a rudder that is

twisted in such a way that it presents a different angle of attack at different water depths. The reason for this departure from conventional rudder design has to do with the flow of water from the propeller. The primary purpose of a ship's propeller is to drive the hull forward by creating a rapidly moving mass of water in the direction opposite that toward which you wish to move (in accord with Newton's Third Law). However, to perform its task, a propeller must rotate, and this rotation introduces an undesirable secondary effect. As it propels water to the rear (along the 0° axis), it also creates a paddlewheel effect, propelling water to one side at the top of the propeller's arc of travel, and propelling water in the opposite direction at the bottom of its rotation. The combination of forces in the 0° and 90° directions causes water to flow at angles off the rudder's 0° axis. While the direction of the flow that strikes the rudder adjacent to the propeller's hub aligns with the rudder direction, the flow nearer the top and bottom of the propeller's swept area is misaligned with the rudder in one direction at the top of the rudder and misaligned in the opposite direction at the bottom. As a result, the angle of water flow varies along the rudder's span (the distance from top to bottom) and its chord (fore to aft length).

When water flows at high speed and at a slight angle over the rudder surface, the result is an undesirable phenomenon called *cavitation*. Cavitation occurs when water pressure falls to or below vapor pressure and vapor bubbles are formed. Repetitive collapse of these bubbles produces localized stress and vibration. This is bad news for naval ships. First, cavitation will dam-

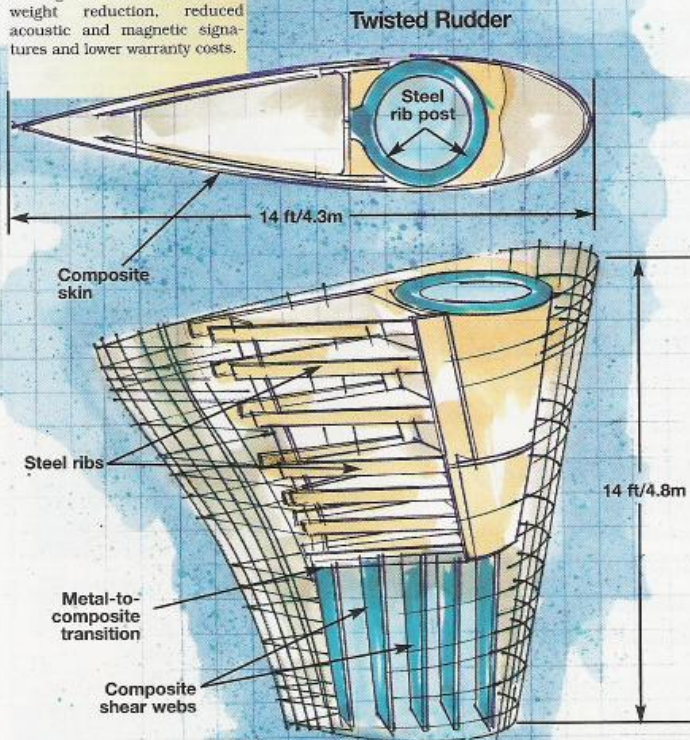


Illustration: Karl Roque

age the surface of the rudder and any protective coatings that have been applied, such as antifouling treatments. On a metal-skinned rudder, coating damage will expose the metal to the corrosive effects of seawater, thus increasing the need for inspection and maintenance. Second, cavitation will create (generate) noise. For a navy destroyer fitted with sonar devices designed to detect very quiet submarines at great distances, noise coming from its own rudder, located less than 500 ft/150m behind the sonar device, handicaps its ability to detect threats.

To alleviate cavitation, Dr. Young T. Shen of the Naval Surface Warfare Center Carderock Div. (NSWCCD, Bethesda, Md.) developed a "twisted rudder" design that incorporates a varying angle of attack from top to bottom (see photo, this page) — one that conforms more closely to the actual water flow pattern. During a development and testing program that was completed in June 2001, trials onboard the USS *Bulkeley*, an DDG 51 Arleigh Burke-class destroyer, using a prototype metal rudder constructed in accord with the new design showed that the proposed solution works well, delaying the onset of cavitation from 23 knots — within the normal operating speed range of Arleigh Burke-class ships — to 29 knots. Tests also demonstrated that the design had no negative impact on speed or steering capability.

COMPOSITE-FOR-METAL MANDATE

Since the original trial, however, the Navy has pursued a composite design for several reasons, not least of which is cost. The complex shape of the rudder's outer surface, for one, calls out for a composite construction, at least for the double curvature skins. "Twisted Rudder rudders are difficult and expensive to build out of steel," says Scott Lewit, president of veteran marine composites manufacturer Structural Composites (Melbourne, Fla.), noting that, unlike many composite-for-metal transformations, a composite solution, in this case, won't increase upfront cost. "The composite rudders are produced from molds that allow us to produce a rudder for about half the steel rudder cost."

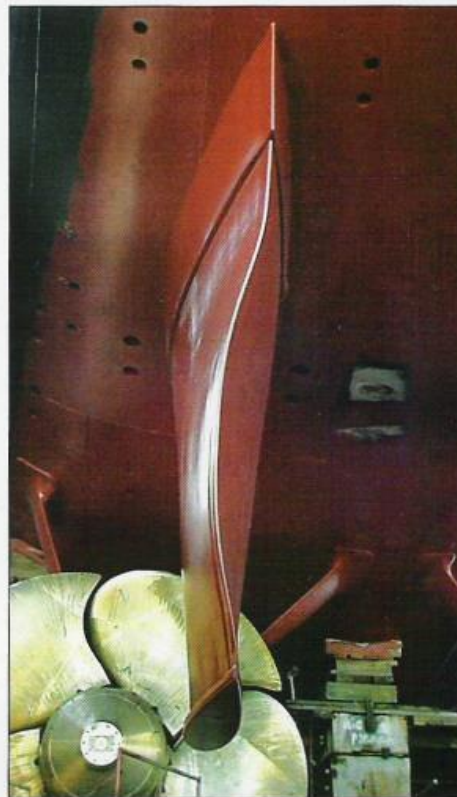
The task of developing the manufacturing method for a composite twisted rudder has been given to Structural Composites. The company was originally awarded a \$904,000 (USD) contract from the Office of Naval Research to build and test composite twisted rudders for DDG-51-class destroyers. This funded development of a demonstration technology, which will be used to test the design's survivability and resistance to environmental degradation. Contract funds above the original amount will come from the

Office of Secretary of Defense's Defense Acquisition Challenge Program. The contract's full value will be \$3.5 million, enough to fund a shipset of rudders for a two-year at-sea evaluation period.

For the demonstrator program, Structural Composites will fabricate a full-size rudder, approximately 14 ft/4.3m across both the span and widest portion of the chord. Fitting the rudder to an existing ship with minimal changes is a requirement, necessitating that trial rudders have the same hub fitting that is used in all-steel designs to facilitate attachment to the rudder rib post on the trial vessel. To avoid an abrupt transition from steel to composite, trial rudders will feature a hybrid steel/composite design developed by Structural Composites and NSWCCD. The design includes a steel inner structure in the top portion of the rudder, provided by Maritime Applied Physics Corp. (Baltimore, Md.), which will transition to a foam-cored composite sandwich structure that features internal shear webs and an external surface of glass/vinyl ester composites, fabricated by Structural Composites (see drawing, p. 60). This steel/composite hybrid is being built with technical assistance from the Navy's NAVSEA 05M3 and NSWCCD personnel.

DESIGN AND MANUFACTURING

For this project, Structural Composites will use its Recirculation Molding process. A variation on light RTM, Recirculation Molding injects resin at relatively low pressure beginning at the lowest point of the mold, counterbalanced by a peristaltic pump that draws only 15 inches of vacuum (about half that drawn in conventional VARTM) through strategically placed vents, says Structural Composites' director of naval projects, Eric Greene. He notes that parts are typically infused vertically to take full advantage of gravity in air evacuation. During infusion, resin is drawn from the mold by vacuum and



Source: NSWCCD

Designed by Dr. Young T. Shen of the Naval Surface Warfare Center, this all-metal "twisted rudder" on the USS *Bulkeley* incorporates a varying angle of attack from top to bottom that conforms more closely to actual water flow patterns. Structural Composites is tasked with development of a hybrid metal/composite solution.

then re-injected to further facilitate removal of any trapped air. The low pressure permits use of a relatively inexpensive clamshell-type composite closed mold. The method permits comolding of the steel "skeleton" and composite sandwich in a single molding cycle.

Recirculation Molding was demonstrated by Structural Composites in a "stepping stone" Navy project called the Mine Countermeasure (MCM) program, in which a smaller untwisted rudder design, with a 7-ft/2.1m span and a chord 6-ft/1.8m wide at top and 5-ft/1.5m wide at bottom, was infused to demonstrate the process and create rudders for the Navy's "minehunter" vessels, on which nonmetallic surfaces help prevent detonation of magnetically triggered mines.

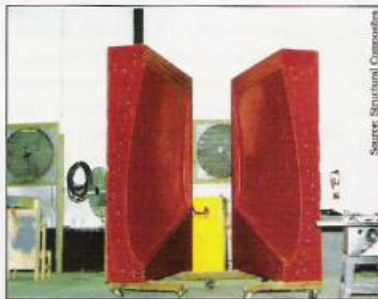
Core material forms made of 7 lb/ft³ (110 kg/m³) polyurethane foam (BASF, Central, S.C.) were used to fill in the general structure around the steel skeleton. On the full-size rudder, sections of formed polyurethane core are bisected by shear webs (vertical blue ribs in the drawing, p. 60) made from biaxial ($\pm 45^\circ$) glass fabric. The composite skins and steel structure are bonded with Plexus MA-310 supplied by ITW Plexus (Danvers, Mass.) though distributor Prairie Technology (Orlando, Fla.). The core, shear webs and steel skeleton are wrapped with (nominally) 25 plies (alternated at near 0° and 90° angles) of E-LM 1810 Uni, a reinforcement fabric consisting of unidirectional E-glass fibers (18 oz/yd²) stitched to 1.0 oz/ft² binder-free chopped strand mat, from Vectorply Corp. (Phenix City, Ala.), with strategically placed EnkaFusion 8004 infusion media, supplied by Colbond (Enka, N.C.). Because the rudder is infused vertically, reinforcements are tacked in place using Infuzene Vacuum Infusion Enabler (Westech Aerosol Corp., Port Orchard, Wash.), a spray-on material designed to solubilize during infusion and disperse in the resin to prevent binder-related interference with fiber/resin adhesion.

The full-scale rudder assembly is then encased in the mold and infused with 8100-50 vinyl ester resin from Interplastic Corp. - Thermoset Resins Div. (St. Paul, Minn.) catalyzed with Luperox DHD-9 from Arkema (Philadelphia, Pa.).

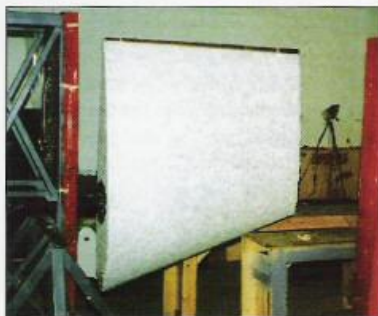
STEERING TOWARD SUCCESS

The infusion process for the Twisted Rudder will build upon lessons learned

from the Navy ManTech-sponsored MCM project. A trial run on a full-scale rudder (sans steel component) is slated for this month, to prove the composite manufacturing method. Assuming all goes well, the process will be repeated in September



The composite clamshell mold for the 7-ft by 5-ft (1.8m by 1.5m) MCM rudder. A similar mold will be built for the larger Twisted Rudder demonstrator.



The complete MCM rudder layout is attached in place on the framework at right (using the encased metal rudder rib post). This arrangement facilitates loading the part into the mold.




Structural Composites infused the MCM rudder in the mold vertically, using its Recirculation Molding technology, a variation on light RTM.

with the steel hub structure in place. Finished rudders must be ready for installation in the March-May 2007 timeframe, when the test vessel is in port.

Greene anticipates multiple benefits for the Navy. On the MCM Rudder pro-

gram, the use of composites enabled a 50 percent reduction in rudder weight from 5,772/lb to 2,820/lb. Use of a lighter rudder also affects the trim of the vessel, permitting removal of counterweighting ballast from the bow. In the full-size Twisted Rudder to come, acquisition cost and survivability are the primary program drivers. The yacht-quality rudder surface will offer less form drag, which will translate to reduced fuel consumption. More importantly, the rudder's cavitation-reducing twist will minimize erosion damage and significantly reduce maintenance costs. "The noncorrosive structure will not deteriorate when subject to the aggressive environment downstream of the propellers," says Greene.

Greene believes that the composite rudders also may offer a much more survivable solution for surface combatant appendages. One of the most difficult challenges in designing a rudder for a naval ship is the ability to withstand underwater explosions, says Greene, noting that "the MCM design has been being optimized and tested for underwater blast resistance."

Although the demonstrator program only covers development of the hybrid steel/composite rudder, Greene says integration of a carbon fiber rudder post into the structure will produce a significantly lighter and stronger rudder/shaft assembly. He believes that an all-composite rudder could be viable for the DDG 1000-class destroyer, with the potential to reduce the magnetic and electrical "signatures" of the Navy's future surface combatant ship, which is currently in the design and demonstration stage. 

— Bob Griffiths, Contributing Writer

use goComp.biz

Arkema, arkema.gocomp.biz/8
 BASF Corp., basf.gocomp.biz/3
 Colbond Inc., colbond-usa.gocomp.biz/7
 Interplastic Corp. - Thermoset Resins Div.,
interplastic.gocomp.biz/11
 ITW Plexus, itwplexus.gocomp.biz/28
 Vectorply Corp., vectorply.gocomp.biz/10
 Westech Aerosol Corp., infuzene.gocomp.biz/8

Biobased Solutions

Spring 2007

FOR GOVERNMENT

New Executive Order Requires Government to Strengthen Environmental Stewardship and Energy Efficiency

On January 24, the White House issued Executive Order 13423, *Strengthening Federal Environmental, Energy, and Transportation Management*. This executive order requires Federal agencies to lead by example in advancing the nation's energy security and environmental performance through effective environmental, energy, and transportation management. It consolidates and strengthens five existing executive orders and two memorandums of understanding and establishes new and updated goals, practices, and reporting requirements for environmental, energy, and transportation performance and accountability. For example, among the highlights that could lead to greater use of soy-based products are the following directives:

- Expand purchases of environmentally-sound goods and services, including biobased products;
- Increase purchase of alternative fuel, hybrid, and plug-in hybrid vehicles when commercially available;
- Reduce petroleum consumption in fleet vehicles by 2% annually through 2015;
- Increase alternative fuel consumption by at least 10% annually;
- Reduce greenhouse gas emissions through reduction of energy intensity by 3% annually or 30% by 2015;
- Purchase at least 50% of current renewable energy from new renewable sources (in service after January 1, 1999).

For more details on this executive order, please visit:
www.whitehouse.gov/news/releases/2007/01/20070124-2.html

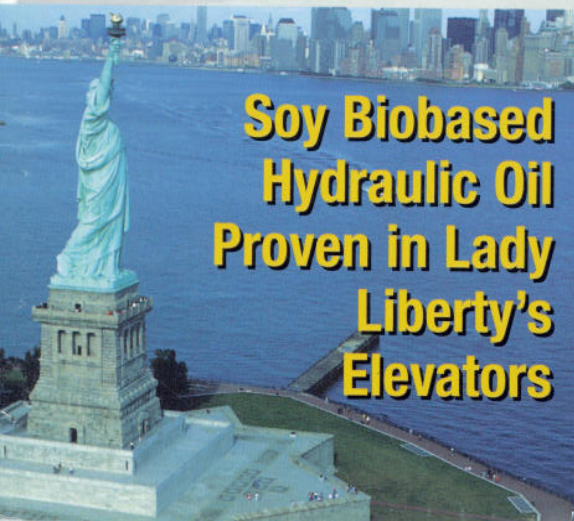


The Naval Weapons Industrial Reserve Plant clean up effort included the digging of trenches for the "biowalls" that were made of soybean oil mixed with compost, wood chips and crushed limestone. Several years later, emulsified soybean oil was injected into the "biowalls" to sustain the biological community that was degrading the perchlorate.

Soy Oil 'Walls' Win Against Perchlorate Texas Military Facility Gets EPA, State OK for Reuse

The successful remediation of more than 50 years of contamination—including perchlorate—earned a 9,700-acre U. S. Navy facility the "Ready for Reuse" (RFR) Determination by the U.S. Environmental Protection Agency (EPA) and the Texas Commission on Environmental Quality (TCEQ). One hero of this accomplishment is the soybean, or to be more precise its derivative, soy oil, which cleaned up the chemicals and saved millions of dollars.

continued on page 4



Soy Biobased Hydraulic Oil Proven in Lady Liberty's Elevators

Five Years of Flawless Performance

Based on almost five years of flawless performance at the Statue of Liberty, a number of events are about to happen that will make the well-proven benefits of soy biobased hydraulic fluid for elevators more available to users throughout the Federal government.

First, the elevator industry's acceptance of soy-based hydraulic fluids

represents a significant step in the use of biobased products. AgriTech Brands, a division of Bunge Oils, commercialized the product in January 2006 after extensive testing both in the laboratory and during application testing at the Statue of Liberty. "Agri-Tech has placed the product in multiple elevator operations across the United States with most of the major equipment

continued on page 3



Administration Outlines Biobased Provisions in 2007 Farm Bill

In January, the U.S. Department of Agriculture (USDA) outlined its 2007 Farm Bill proposal, which includes a number of provisions to encourage greater use of biobased products. According to USDA, "The Federal Procurement of Biobased Products program helps develop the market for biobased products by encouraging the purchase of these products by the Federal government. Through Federal government purchases, the commercial viability of these products could be established and government demand for biobased products increased, thus leading to wider public acceptance, increased demand, and increased production of a greater variety of biobased products."

Among the Farm Bill's biobased provisions are:

- Reauthorization of the Federal Procurement of Biobased Products program to improve its effectiveness and invest \$18 million over 10 years to expand and improve the program. It is currently funded at \$1 million a year.
- The authorization of \$800,000 in annual mandatory funding to enable USDA to provide assistance to other Federal agencies in implementing the procurement program as well as audit manufacturers on their claims.
- The creation of the Agricultural Bioenergy and Biobased Products Research Initiative to enhance the production and conversion of biomass to renewable fuels and related products. \$500 million over 10 years would be dedicated to advance the fundamental scientific knowledge for improved production of renewable fuels and biobased products.

In addition, USDA proposes that the \$1 million in annual mandatory funding currently provided for testing should be continued and expanded to include environmental and performance testing for the purposes of public information as well as for designation of items for procurement.

For more details on the Administration's 2007 Farm Bill proposal, please visit www.usda.gov and follow the links to the Energy & Research Titles.

Army's Soy-based Resin for Composite Shows 'Tremendous' Potential

If it's not metal or rubber and it isn't really plastic that is common in homes, then it's known as a composite—a durable product that is tough enough for bumpers on cars as well as hoods of military Humvees and farm machinery. Composites are used because they are light in weight and more durable than metal or rubber. They can be less expensive too.

To date, composites of this sort are made from petroleum-based thermo set resins which have two problems. First, this kind of composite contains styrene monomer, a suspected carcinogen that may escape during molding and finishing or during repair. The U.S. Environmental Protection Agency (EPA) has recently enacted new emission standards for styrene. Second, as a petroleum-based product, its widespread use increases U.S. dependence on foreign oil.

However, John LaScala, of the U.S. Army Research Laboratory (ARL) at Aberdeen Proving Ground in Maryland, did research work with soy-based vinyl-ester resins while getting his doctorate in engineering at the University of Delaware. He brought that expertise with him when he came to Drexel University as a postdoctoral scientist in 2002 and to ARL in 2003.



photo credit: U.S. Army

John LaScala (left), of the U.S. Army Research Laboratory (ARL) and his colleague, John Brown, display the truck hood of a M35A3 vehicle made from a soy-based composite. Their product performs equal to, or better, than its petroleum-based counterpart and reduces styrene emissions by 20-78 percent.

Working under funds provided by the Strategic Environmental Research and Development Program (SERDP), a joint effort of EPA and the Departments of Defense and Energy, LaScala and his team have developed a soy-based composite. Their product performs equal to, or better, than its petroleum-based counterpart and reduces styrene emissions by 20-78 percent.

"This means that soldiers working to repair vehicles can work more safely. It also means that military repair shops can meet EPA standards without emission control systems, which can easily cost \$1 million per installation," LaScala explains.

continued on page 6

Biobased Purchasing Requirements Proposed to be Added to the Federal Acquisition Regulation

On December 26, 2006, the Department of Defense (DoD), the General Services Administration (GSA), and the National Aeronautics and Space Administration (NASA) proposed a rule to revise the Federal Acquisition Regulation (FAR) to implement procurement preference provisions for biobased products. The FAR contains the uniform policies and procedures for acquisition by all executive agencies and is jointly issued by DoD, GSA, and NASA.

The proposal adds biobased provisions to FAR Part 7 (acquisition planning), Part 11 (describing Agency needs), Part 12 (acquisitions of commercial product), Part 13 (simplified acquisitions) and Part 23 (use of products containing recovered materials and biobased products). The proposed FAR provisions would require executive agencies to consider the maximum practical use of biobased products when considering specifications, describing Government requirements, and developing source-selection factors. The proposal includes definitions of biobased product and USDA-designated items, requirements for agencies to establish affirmative procurement programs for biobased products, procedures for contracting officers when purchasing products or services, requirements for solicitation provisions and contract clauses, and provisions for monitoring contractor compliance.

Meanwhile, Federal agencies in general have been reporting on biobased product purchasing. Specifically they have been reporting on the creation of the infrastructure that will be needed to implement the USDA program: Incorporation of biobased product purchasing into their agency green purchasing plans and policies, training their staff, review of specifications, and testing of products through pilot projects.

A copy of the FAR proposal can be found at <http://a257.gakamaitech.net/7/257/2422/01jan20061800/edocket.access.gpo.gov/2006/pdf/06-9846.pdf>.

Army's Soy-based Resin Shows Potential

continued from page 5

The biobased composite has very wide application, not only in vehicles but also in aircraft and ships, both military and civilian. The various branches of the military are currently laboratory testing the product and are planning to field test it next year. If all goes as expected, mass production of original equipment and parts could begin in 2009. Meanwhile, commercialization of the product has begun with a licensing agreement with Vertachem Corp., which is in the early stages of introducing the product to major resin manufacturers.

Like many entrepreneurial enterprises, Vertachem came into being as a result of a joint MBA project between Tom Watchko and David Epstein, cofounders of the company. "We've also had some very good help from the United Soybean Board (USB), specifically from Tom Doyle, who is with OmniTech International, USB's technical consulting firm," Watchko says. "Tom Doyle, who knows the resins industry inside and out, has helped us in many ways—from finding suppliers of soy-based raw material, to opening the doors of the big resin manufacturers, as well as providing good, sound business advice that only comes from industry experience. We appreciate his efforts and we appreciate USB for providing Tom as a resource to us."

"This product with its twin attributes of being environmentally friendly and being made from a renewable resource has everything going for it. Its potential is tremendous," Doyle says.

And yes, since the U.S. Army owns the patent, it should profit as well. Also, LaScala is working on a similar product, a biobased resin that is used in vehicle body repair. That's another potentially high-volume composite use that's green and made from naturally renewable soybeans.



A truck hood is one of the many potential applications for the new biobased composite. The Army owns the patent for the product that could be used in military or civilian aircraft or ships.

For more information write:
United Soybean Board

16640 Chesterfield Grove Rd., Suite 130 • Chesterfield, MO 63005-1429

To reach Biobased Solutions for Government directly:

Call: 1-800-989-USB1 (1-800-989-8721) • Or E-mail: merker@smithbucklin.com

USB Publication Code 7354/7406-032007-2000



Biobased Solutions for Government is a quarterly newsletter published by the United Soybean Board (USB) for people involved in government purchasing. This newsletter is provided for information only. The USB does not endorse, promote or make any representations regarding any specific suppliers mentioned herein.



Because of the potential for biobased products to create new markets for soybeans, U.S. soybean farmers have invested millions of dollars to research, test and promote biobased products. Much of this work was done through the United Soybean Board (USB), which is composed of 64 U.S. soybean farmers appointed by the U.S. Secretary of Agriculture to invest soybean checkoff funds. As stipulated in the Soybean Promotion, Research and Consumer Information Act, USDA's Agricultural Marketing Service has oversight responsibilities for the soybean checkoff.



INTENTIONALLY LEFT BLANK.

Appendix F. Air Force Composite Testing

This appendix appears in its original form, without editorial change.

Appendix F

Air Force Composite Testing



DEPARTMENT OF THE AIR FORCE
HEADQUARTERS OGDEN AIR LOGISTICS CENTER (AFMC)
HILL AIR FORCE BASE, UTAH

MEMORANDUM FOR: AFRL/RXS-OLH (Frank Bruce 6-3325)

19 Nov 07

FROM: OO-ALC/MADLM

SUBJECT: Metallurgical Report 7406-07; Composite Panel Tests

1. INTRODUCTION:

Six fiberglass panels were submitted to the materials laboratory for testing. Each of the panels was to be subjected to tensile, compressive, and short beam shear testing.

2. IDENTIFICATION:

The table below shows notations which were made on the panels before submittal, and the corresponding number assigned to the panel.

Notes written on panel	Panel Number
Trial 1 1/16/07	1
Trial #1 1/16/07	2
Trial 2 1/16/07 1 ply red distrib. media	3
Trial 2 Entrafusion media 7004 m = 400g	4
Trial 2 1/16/07 Double ply distrib. Media m = 400g	5
FAVE -L-25S 8 ply 7500 2 Oct 07	6

For each sample the results tables list first the panel number, then an abbreviation for the type of testing (C = compression T = tension, SBS = Short Beam Shear), and lastly the sample number.

3. TESTING:

- a. Tensile testing was accomplished by testing samples to failure as per ASTM D3039. The sample size chosen was 5 inches long by ½ inch wide. The coupons were tabbed on the ends using a 1 and ½ inch long, 1/16 of an inch thick tab. This leaves a gage length of 2 inches. Strain gages were bonded to each sample for computation of tensile modulus. Five coupons from each panel were tested. Data from all of the coupons tested are listed in Table One.
- b. Compression testing was accomplished in accordance with ASTM D6641. Five samples from each panel were tested. Strain gages were also bonded to the compression samples for computation of compressive modulus. Results are listed for each sample tested in Table Two.
- c. Short beam shear testing was accomplished in accordance with ASTM D2344. Five samples from each panel were tested; results for each sample are listed in Table Three.

- d. Glass transition temperature (T_g) was determined using a DSC (Differential Scanning Calorimeter) from TA Instruments. Samples were cut from the panels and contained both resin and glass fibers. It is unknown how the presence of glass fibers affects the T_g of the resin. At least two samples from each panel were analyzed. Results are given in Table Four.
- e. Results listed in red in the data tables were considered to be outlying data, and were not used to compute panel averages

4. ADDITIONAL INFORMATION:

For additional information concerning mechanical testing, please contact Scot Frew, MXDEB, DSN 586-4513, commercial 801-586-4513, voice mail 801-586-4513, or e-mail at Scot.Frew@hill.af.mil. For additional information concerning thermal testing, please contact Wes Finneran, MXDEA, DSN 586-4516, commercial 801-586-4516, voice mail 801-586-4516, or e-mail at Wes.Finneran@hill.af.mil.

Table One

Sample	Tensile strength (ksi)	Tensile Modulus (ksi)
1-T1	33.5	2564
1-T2	31.9	2440
1-T3	31.9	2865
1-T4	31.3	2560
1-T5	33.1	2574
Set Ave.	32.4	2601
2-T1	31.7	2270
2-T2	33.6	2903
2-T3	34.1	2673
2-T4	30.7	2659
2-T5	29.7	2010
Set Ave.	32.0	2503
3-T1	40.0	2732
3-T2	39.1	2610
3-T3	38.8	2455
3-T4	38.5	2881
3-T5	37.6	2527
Set Ave.	38.8	2641

Sample	Tensile strength (ksi)	Tensile Modulus (ksi)
4-T1	32.9	3835
4-T2	32.6	2028
4-T3	36.3	2701
4-T4	33.5	2374
4-T5	32.4	2423
Set Ave.	33.5	2382
5-T1	30.9	2514
5-T2	32.3	2366
5-T3	32.5	2856
5-T4	33.5	2316
5-T5	33.4	3939
Set Ave.	32.5	2513
6-T1	32.9	2855
6-T2	33.5	3250
6-T3	35.9	2918
6-T4	33.2	3454
6-T5	34.1	3101
Set Ave.	33.9	3116

Table Two

Sample	Compressive strength (ksi)	Compressive Modulus (ksi)
1-C1	18.1	3121
1-C2	18.8	3581
1-C3	17.3	73.1
1-C4	15.0	3368
1-C5	18.8	3167
Set Ave.	17.6	3309
2-C1	13.4	3584
2-C2	4.2	888
2-C3	15.8	3237
2-C4	11.5	3689
2-C5	14.6	2.0
Set Ave.	13.8	3503
3-C1	19.3	3557
3-C2	17.1	2885
3-C3	18.0	3623
3-C4	17.5	3171
3-C5	20.1	3663
Set Ave.	18.4	3380

Sample	Compressive strength (ksi)	Compressive Modulus (ksi)
4-C1	18.4	2916
4-C2	20.8	2523
4-C3	19.2	3004
4-C4	20.8	2688
4-C5	21.7	3214
Set Ave.	20.2	2869
5-C1	5.0	912
5-C2	19.4	4735
5-C3	19.8	4477
5-C4	18.0	2985
5-C5	17.7	2675
Set Ave.	18.7	3718
6-C1	20.2	3336
6-C2	21.7	3159
6-C3	21.6	4309
6-C4	22.0	3780
6-C5	20.0	3398
Set Ave.	21.13	3596

Table Three

Sample	SBS strength (ksi)
1-SBS1	36.1
1-SBS2	35.9
1-SBS3	33.3
1-SBS4	37.1
1-SBS5	32.1
Set Ave.	34.9
2-SBS1	32.6
2-SBS2	22.4
2-SBS3	24.5
2-SBS4	17.7
2-SBS5	18.9
Set Ave.	20.6
3-SBS1	19.6
3-SBS2	23.7
3-SBS3	22.5
3-SBS4	18.9
3-SBS5	20.1
Set Ave.	21.0

Sample	SBS strength (ksi)
4-SBS1	17.9
4-SBS2	18.6
4-SBS3	20.2
4-SBS4	15.1
4-SBS5	17.4
Set Ave.	17.8
5-SBS1	18.7
5-SBS2	17.3
5-SBS3	21.3
5-SBS4	16.4
5-SBS5	16.9
Set Ave.	18.1
6-SBS1	18.5
6-SBS2	17.0
6-SBS3	19.0
6-SBS4	15.7
6-SBS5	18.4
Set Ave.	17.7

Table Four

Panel number	T_g Run 1 (°F)	T_g Run 2 (°F)	T_g Average (°F)
1	145.9	144.6	145.2
2	145.9	143.1	144.5
3	146.7	143.4	145.1
4	142.6	142.8	142.7
5	142.3	144.3	143.3
6	139.9	137.5	138.7

Prepared By:

Approved By:

KYLE CHAPMAN
Materials Engineer
Material/Chemical Flight
809 Maintenance Support Squadron

GEORGE LAFIGUERA
Director
Material/Chemical Flight
809 Maintenance Support Squadron

Reviewed By:

Approved By:

WELDON W. BETTS
Team Lead
Material/Chemical Flight
809 Maintenance Support Squadron

Dr. DAVID HANSEN
Director
809 Maintenance Support Squadron



This laboratory is accredited by the American Association for Laboratory Accreditation (A2LA) and the results shown in this test report have been determined in accordance with the laboratory's terms of accreditation unless stated otherwise. This report may not be reproduced, except in full, without laboratory approval.

Appendix G. Navy Resin Testing

This appendix appears in its original form, without editorial change.

Appendix G

Navy Resin Testing



DEPARTMENT OF THE NAVY
NAVAL SURFACE WARFARE CENTER, CARDEROCK DIVISION
9500 MACARTHUR BOULEVARD
WEST BETHESDA MD 20817-5700

IN REPLY REFER TO
9078
Ser 65-40
4 June 2009

From: Commander, Naval Surface Warfare Center, Carderock Division
To: Department of the Army, U.S. Army Research Laboratory, AMSRD-ARL-WM-MC,
Aberdeen Proving Ground, MD 21005 (Attn: John LaScala)

Subj: Environmental Security Technology Certification Program (ESTCP) Low HAP/VOC
Program

Ref: (a) Environmental Security Technology Certification Program Funding Documents
W74RDV90301105, W74RDV73615721, W74RDV70657281 and Army Research
Lab Funding Document Number MIPR6FARL80163

Encl: (1) NSWCCD ESTCP Low HAP/VOC Testing Report

1. Reference (a) requested the Naval Surface Warfare Center, Carderock Division (NSWCCD) to participate in this tri-service program to evaluate several low hazardous air pollutants/volatile organics vinyl ester resin systems for possible use in naval applications. The MCM rudder application was chosen as a possible use for this resin system and a variety of testing was performed to evaluate this resin for use in that specific application. Several batches of different types of resins were received at NSWCCD and composite manufacturing and testing were performed in house. Enclosure (1) is the final report of these tests. A follow on report will document the oversight of the fabrication of the MCM rudder demonstration articles as well as the destructive evaluation of one of these articles.

2. Comments or questions may be referred to Dr. Roger M. Crane, Code 655, phone: (301) 227-5126 or e-mail: roger.crane@navy.mil.

E. A. RASMUSSEN
By direction

Copy to:

NAVSURFWARCN CARDEROCKDIV
BETHESDA MD [Codes 65 and 655 (R. Crane and
M. Foley)]

Department of the Army, U.S. Army Research
Laboratory, AMSRD-ARL-WM-MC, Aberdeen Proving
Ground, MD 21005 (Attn: John LaScala)

NSWC CD ESTCP Low HAP/VOC Program		
Subject:	ESTCP Low VOC Material Characterization	
Maureen E Foley, Timothy Dapp, John Kim and Roger Crane		Date: 4/30/2009

1.0 Background

Through an Environmental Security Technology Certification Program (ESCTP), NSWC Carderock Division was tasked with evaluating a low volatile organic compound (VOC) vinyl ester (VE) resin system that could be considered for further use in Navy applications. Whereas most current vinyl ester systems contain 40-60 weight percent of styrene, the low VOC vinyl ester resin systems cuts this styrene content in half and replaces it with a Fatty Acid (FA) monomer as a reactive diluent. In the case of the NSWCDD task, the reactive diluent in the system was methacrylate lauric acid (FAVE-L). Two different concentrations of FAVE-L were evaluated in this program. Initially, a 20wt% styrene product (FAVE-L-20S) was evaluated. It was determined that this system exhibited a slightly lower glass transition temperature than desired therefore an alternate resin system with 25wt% styrene (FAVE-L-25S) was also evaluated. Baseline composite material properties were also determined for Ashland's Derakane 510A-40 vinyl ester system and Interplastic CORESYZN 8100 which are currently used in several Navy applications.

2.0 Test Plan

The test plan was broken down into two main parts. The first being the characterization of the FAVE-L-20S resin system and the second being the characterization of the FAVE-L-25 and Derakane 510A resin systems.

2.1 FAVE-L-20S

The following test plan was developed to characterize the room temperature dry (RTD) and Elevated Temperature Wet (ETW) properties of glass fiber reinforced FAVE-L-20S composite systems for possible future use in naval applications such as the composite twisted rudder program. The test plan consisted of physical attribute characterization such as fiber volume fraction and density and mechanical testing to determine the tensile, compressive, shear and toughness properties. A series of samples are also underwent environmental exposure to 50°C at 80% RH with moisture uptake monitoring occurring. After moisture equilibrium was reached, these samples were tested to determine the effect of environmental properties on the tensile, compressive, shear and toughness properties of the composite material. Similar vinyl ester composite systems have reached moisture equilibrium after 2.5 months under these conditions.

2.1.1 Panel Fabrication

A total of four panels were fabricated at NSWCCD for evaluation of the FAVE-L-20s resin system. These panels were made using standard VARTM techniques and the resin and fabric as shown below. A summary of the fiber orientation of the four different panels is shown in Table 1.

Resin: FAVE-L-20S (Fatty Acid Vinyl Ester, -L (Methacrylate Lauric Acid))
 65 wt% Bisphenol A Vinyl Ester
 20% Styrene
 15 wt% Methacrylate Lauric Acid

Formulation: 97.25 wt% FAVE-L-20S Resin
 2.0 wt% Methyl Ethyl Ketone Peroxide (MEKP) (Cadox L-50a)
 0.3 wt% Cobalt Napthenate 6% (CoNap6%)
 0.25 wt% 2,4-Pentanedione (2,4-P)
 0.2 wt% Dimethylaniline (DMA)

Fabric: SW1810 Uni/Mat Fabric from Fiber Glass Industries - Nominally an 18 oz/yd² unidirectional E-glass fibers stitched to 10 oz/yd² binder-free chopped strand mat (similar architecture to twisted rudder program)

Table 1 Panel Identification and Fiber Orientation

Panel	Layup	Denoted
061001	[0] ₁₀	Uni
061002	[0/+45/90/-45] _s	Quasi
061201	[0/90] _{4s}	Cross-Ply
070201	[0] ₈	Uni

2.1.2 Physical Properties Characterization

2.1.2.1 Density

The density of both the neat resin and composite pieces taken from each panel was tested according to the guidelines of ASTM D792. The results are summarized in Table 2. The results show fairly consistent composite panel densities for the 8 ply composite panel regardless of ply layup. The quasi panel exhibited a slightly higher density than the unidirectional or cross-ply panels.

Table 2 Summary of Density Measurements (ASTM D792)

Panel	Type	Density (g/cm ³)
-	Neat Resin	1.167 ± 0.002
061001	Uni	1.838 ± 0.021
061002	Quasi	1.854 ± 0.003
061201	Cross-Ply	1.847 ± 0.009
070201	Uni	1.849 ± 0.015

The fiber, resin and void fraction were determined using the burnout method as described in ASTM D3171. An E-Glass fiber density was assumed to be 2.59 g/cm³ for these calculations¹. The results of these tests are shown in Table 3. Detailed specimen level results are shown in Appendix A.

Table 3 Summary of Constituent Material Measurements (ASTM D3171)

Panel	Type	% Fiber Volume Fraction	% Resin Volume Fraction	% Void Volume Fraction
061001	Uni	47.74 ± 1.33	51.60 ± 1.19	0.65 ± 0.15
061002	Quasi	48.74 ± 0.09	50.72 ± 0.03	0.54 ± 0.12
061201	Cross-Ply	48.11 ± 0.47	51.53 ± 0.27	0.35 ± 0.20

2.1.2.2 Tension Testing

Samples were prepared using standard machining techniques to ASTM D638 Type III specimen dimensions. Two sets of specimens were prepared. One set had the outer plies of the composite oriented in the 0° direction along the axis of the specimen while the other had set the outer plies oriented in the 90° direction perpendicular or transverse to the axis of the specimen. The average of three measurements was used to determine the width and thickness of the samples in the gage length of the specimen. Vishay strain gages of type CEA-06-125WT-350, gage factor 2.15 were attached to the center of the gage length to allow for the calculation of the elastic modulus and Poisson's ratio. Specimens were tested using a Southwark-Emery 60 kip load frame with a 60 kip load cell. Samples were loaded at a rate of 0.2 inch per minute. Prior to testing, the grips were vertically aligned using a stock metal piece. This was found to be the best method to ensure that the grips remained aligned during testing due to the large amount of play that is present in the load train system of the machine.

The results of test are shown in the following table. Detailed specimen level results are included in Appendix B.

¹ Fiber Glass Industries (www.fiberglassindustries.com)

Table 4 ASTM D638 Tension Test Results

Panel ID	Type	Tensile Strength (ksi)		Elastic Modulus* (Msi)		Poisson's Ratio* (v)	
		0°	90°	0°	90°	0°	90°
061001	Uni	89.93 ± 3.88	11.37 ± 0.73	4.84 ± 0.07	1.18 ± 0.19	0.307 ± 0.014	0.112 ± 0.025
061002	Quasi	39.92 ± 0.48	41.92 ± 2.47	2.69 ± 0.03	2.92 ± 0.24	0.325 ± 0.018	0.319 ± 0.02
061201	Cross- Ply	53.20 ± 3.29	55.41 ± 1.83	3.28 ± 0.14	3.17 ± 0.27	0.176 ± 0.018	0.185 ± 0.021

*Range of 1000 to 3000in/in

2.1.2.3 Compression Testing:

Samples were prepared using standard machining techniques to ASTM D695 specimen dimensions. Two sets of specimens were prepared. One set had the outer plies of the composite oriented in the 0° direction along the axis of the specimen while the other had set the outer plies oriented in the 90° direction perpendicular or transverse to the axis of the specimen. The average of three measurements was used to determine the width and thickness of the samples in the gage length of the specimen. Vishay strain gages of type CEA-06-062UW-350 were attached to the center of the gage length to allow for the calculation of the elastic modulus. Specimens were tested using a Southwark-Emery 60 kip load frame with a 60 kip load cell. Samples were loaded at a rate of 0.05 inch per minute.

The results of test are shown in the following table. Detailed specimen level results are included in Appendix C.

Table 5 ASTM D695 Compression Test Results

Panel ID	Type	Compressive Strength (ksi)		Elastic Modulus* (Msi)	
		0°	90°	0°	90°
061001	Uni	53.64 ± 5.99	21.14 ± 0.76	5.03 ± 0.28	2.55 ± 0.65
061002	Quasi	37.95 ± 1.35	35.34 ± 1.27	3.06 ± 0.08	3.71 ± 0.36
061201	Cross-Ply	37.02 ± 3.67	43.83 ± 0.95	3.71 ± 0.18	3.74 ± 0.81

*Range of 1000 to 3000in/in

2.1.2.4 Shear Testing

Samples were prepared using standard machining techniques to ASTM D5379 V-notch shear specimen dimensions. One set of specimens were prepared with the outer plies of the composite oriented in the 0° direction along the length of the specimen. The average of three dimensions was used to determine the width and thickness of the samples in the gage length of the specimen. Vishay strain gages of type CEA-06-062WT-350 were attached at the center of the specimen as called out in the ASTM D5379 to allow for the calculation of the shear modulus. Specimens were tested using a Southwark-Emery 60 kip load frame with a 60 kip load cell. Samples were loaded at a rate of 0.05 inch per minute.

The results of test are shown in the following table. Detailed specimen level results are included in Appendix D.

Table 6 ASTM D5379 V-Notch Shear Test Results

Panel ID	Type	Shear Modulus* (Msi)	Ultimate Shear Strain (in/in)	Shear Strength (ksi)		
				@ 0.2% offset	@ 5% Strain	Ultimate
		0°	0°	0°	0°	0°
061001	Uni	0.79 ± 0.10	0.059 ± 0.010	8.12 ± 0.44	14.36 ± 1.67	15.15 ± 0.96
061002	Quasi	1.07 ± 0.13	0.026 ± 0.002	15.41 ± 3.96	-	20.21 ± 1.15
061201	Cross-Ply	0.82 ± 0.13	0.082 ± 0.021	8.59 ± 1.43	16.40 ± 0.53	17.30 ± 0.78

*Range of 1000 to 4000in/in

2.1.3 Environmental Conditioning

A total of 21 samples underwent environmental exposure at 50°C and 80%RH. These included samples to perform tension and compression (as outlined in the previous sections) and also short beam shear (ASTM D2344) and interlaminar toughness (ASTM D5528). Samples were weighed at prescribed intervals to monitor the percent moisture uptake over time. After the percent moisture has reached the equilibrium state as defined by ASTM D5229 the samples were tested to determine the effect of temperature and moisture on the composite material. The percent weight gain of the samples over time is included as a reference in Figure 2. The varying volume/surface area of the different samples appears to contribute to a difference in the percent weight gain of each different sample type. The slight drop in the moisture uptake curve at 38.5 hr ½ was due to loss of humidity chamber conditions. After 140 days exposure, the samples appeared to reach an equilibrium saturation level. Samples taken from the same panel (070201) that have been aged at room temperature were also tested at the same time for direct comparison.

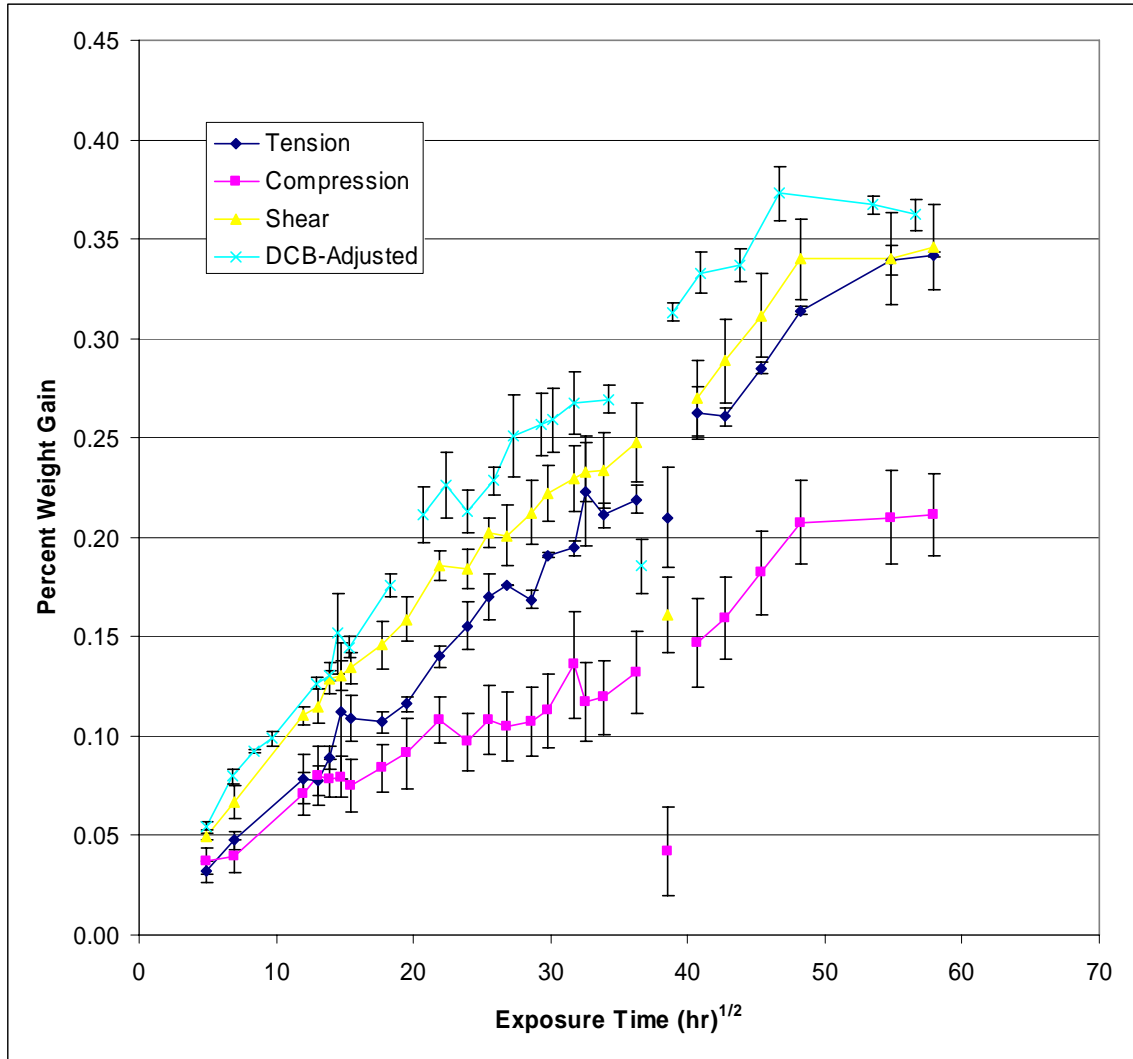


Figure 2 Percent Weight Gain versus Exposure Time for FAVE-L Composite Samples that are Undergoing 50°C and 80%RH.

2.1.3.1 Tension Testing

The tension tests were performed in the same manner as in the previous section. The results of the room temperature dry and elevated temperature wet test specimens that were taken from the same panel are shown in the following table and figures. Detailed specimen level results are included in Appendix B. The results indicate a small decrease in average tensile strength (5%) after the elevated temperature wet exposure. This level of change is just above the coefficient of variation of the sample population of 4%. There was no noticeable change in the tensile modulus after the elevated temperature wet exposure.

Table 7 ASTM D638 Tension Test Results (RTD and ETW)

Panel ID	Type	Conditioning	Tensile Strength (ksi)	Elastic Modulus* (Msi)
061001	Uni	As- Manufactured	89.9±3.9	4.8±0.1
070201	Uni	Room Temperature Dry	89.1±3.8	5.0±0.1
070201	Uni	Elevated Temperature Wet	85.1±3.6	4.8±0.3

*Range of 1000 to 3000in/in

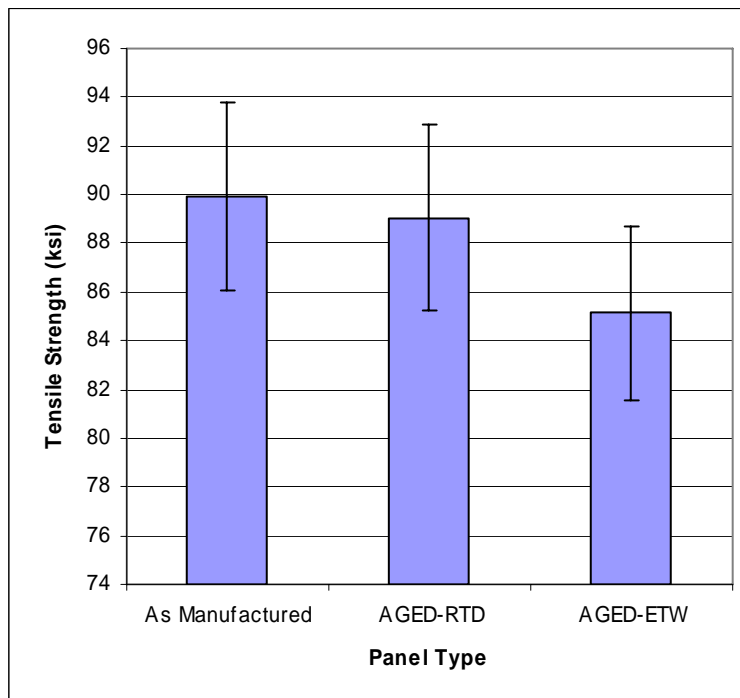


Figure 3 Summary of Tension Tests – Strength Results

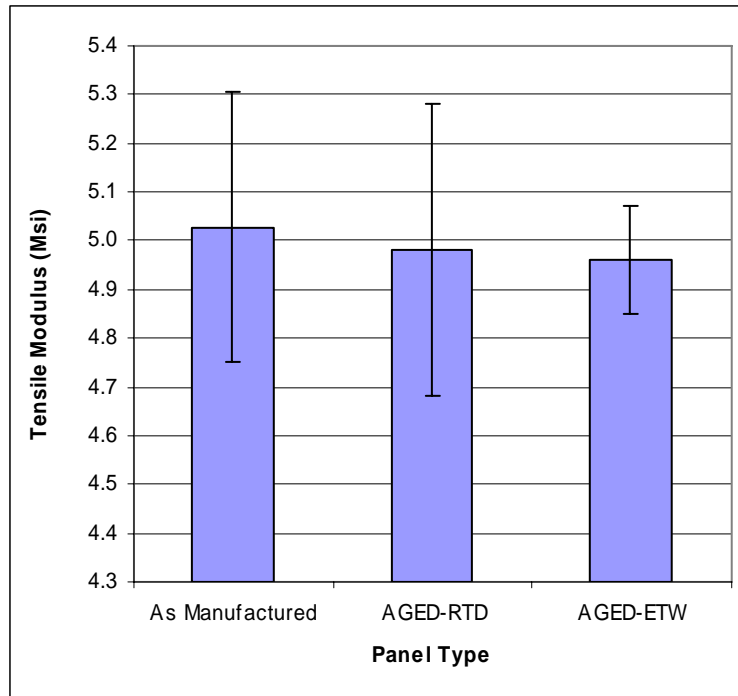


Figure 4 Summary Tension Tests – Modulus Results

2.1.3.2 Compression Testing:

The compression tests were performed in the same manner as in the previous section. The results of the room temperature dry and elevated temperature wet test specimens that were taken from the same panel are shown in the following table and figures. Detailed specimen level results are included in Appendix C. The results indicate that there was no significant change in the compressive strength or modulus after the elevated temperature wet exposure.

Table 8 ASTM D695 Compression Test Results

Panel ID	Type	Conditioning	Compressive Strength (ksi)	Elastic Modulus* (Msi)
061001	Uni	As-Manufactured	53.6±6.0	5.0±0.3
070201	Uni	Room Temperature Dry	47.5±6.1	5.0±0.3
070201	Uni	Elevated Temperature Wet	44.8±7.0	5.0±0.1

*Range of 1000 to 3000in/in

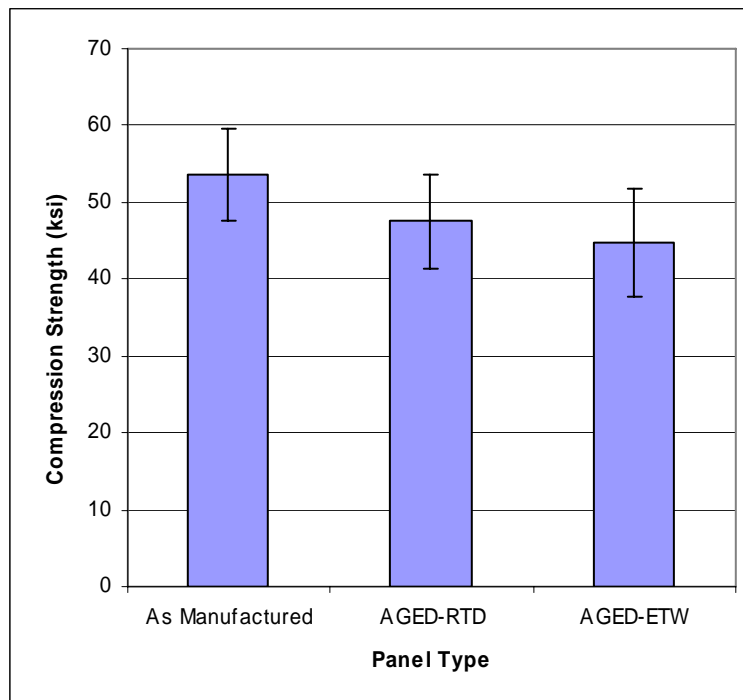


Figure 5 Summary of Compression Tests – Strength Results

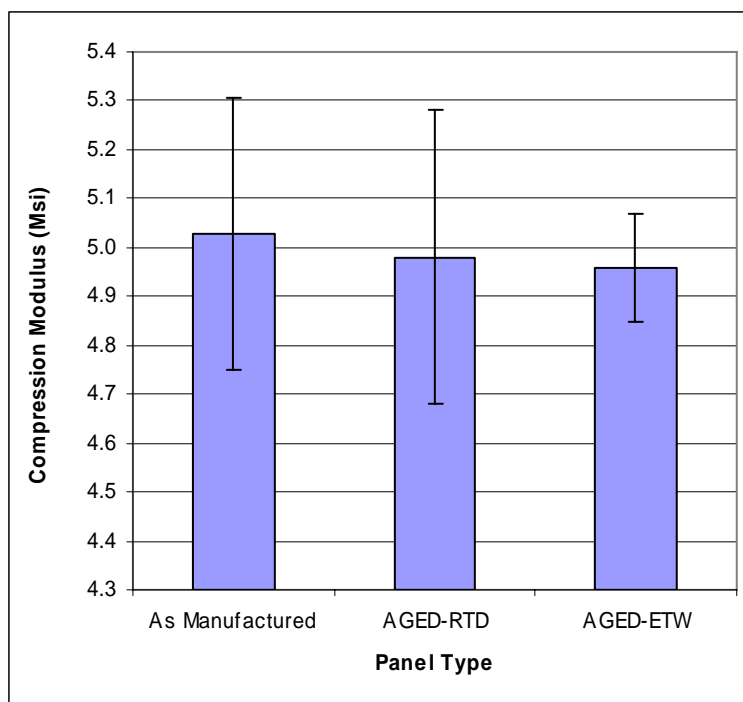


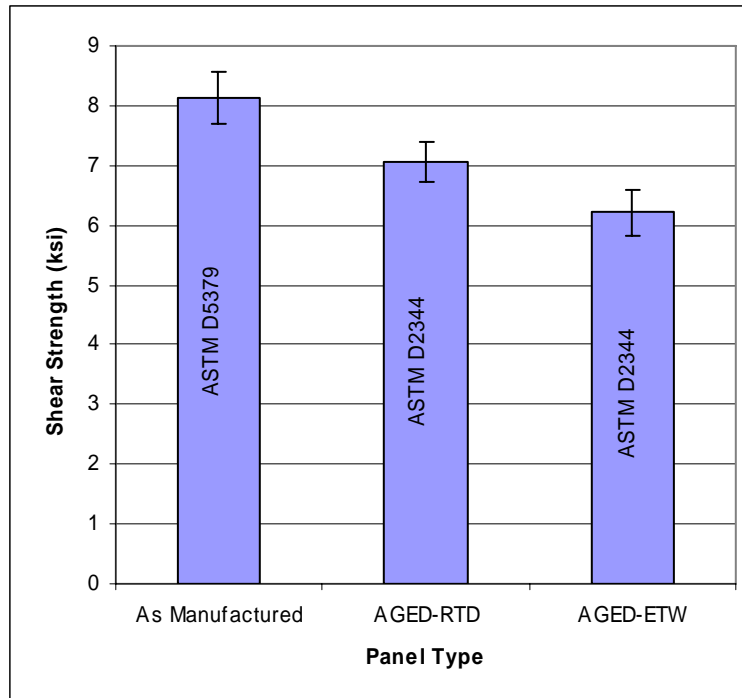
Figure 6 Summary of Compression Tests – Strength Results

2.1.3.3 Shear Testing

Samples were prepared using standard machining techniques to ASTM D2344 short beam shear specimen dimensions. One set of specimens were prepared with the outer plies of the composite oriented in the 0° direction along the length of the specimen. The average of three dimensions was used to determine the width and thickness of the samples in the gage length of the specimen. Specimens were tested using a Southwark-Emery 60 kip load frame with a 60 kip load cell. Samples were loaded at a rate of 0.05 inch per minute using a three point bend type fixture with a span to depth ratio of 4. This type of test was selected for use over the V-notch test due to the ease of machining and the V-notch non-ideal failure of composites with off-axis fibers. The results of the room temperature dry and elevated temperature wet test specimens that were taken from the same panel are shown in the following table and figures. Detailed specimen level results are included in Appendix E. The results indicate that there was a 12% decrease in short beam shear strength after the elevated temperature wet exposure.

Table 10 Shear Test Results

Panel ID	Type	Conditioning	Shear Strength (ksi)
061001	Uni	As-Manufactured	8.1±0.4 (ASTMD5379)
070201	Uni	Room Temperature Dry	7.1±0.3 (ASTM D2344)
070201	Uni	Elevated Temperature Wet	6.2±0.4 (ASTM D2344)

**Figure 7 Summary of Shear Tests – Strength Results**

2.1.3.4 Mode I Interlaminar Fracture Toughness (DCB) Testing

Samples were prepared using standard machining techniques to ASTM D5528 specimen dimensions. One set of specimens was prepared with the outer plies of the composite oriented in the 0° direction along the length of the specimen. Piano hinges were attached to the composite specimens using epoxy adhesive. Crack gauges of type TK-09-CPS05-001 by Vishay Measurements were attached to the side of the specimen to monitor the crack advancement. The average of three dimensions was used to determine the width

and thickness of the samples of the specimen. Specimens were tested using an Instron 4202 load frame with a 2000 pound load cell at a rate of 0.2 in/min. The use of crack gauges has been seen to automate the testing process and to eliminate the ambiguity of the operator visual noting the crack tip displacement. The results of the room temperature dry and elevated temperature wet test specimens that were taken from the same panel are shown in the following table and figures. Three different G_{Ic} values are reported. The onset is defined as when the crack gage shows the onset of crack tip displacement. The non-linear (NL) offset is defined as the G_{Ic} value calculated when the load versus displacement curve is no longer linear. Finally, the propagation value is the G_{Ic} value after 0.25 inches of crack tip displacement. These three values have been defined and used in the past in Navy programs². Detailed specimen level results are included in Appendix F. The results indicate that there was a slight increase in all the G_{Ic} values after the elevated temperature wet exposure as compared to the room temperature dry specimens.

Table 11 Mode I Interlaminar Toughness Results

Panel ID	Type	Conditioning	G_{Ic} (in-lb/in ²)		
			Onset	Propagation	Steady State
070201	Uni	Room Temperature Dry	0.56±0.24	1.63±0.23	3.11 ± 0.10
070201	Uni	Elevated Temperature Wet	0.98±0.21	2.25±0.36	3.76 ± 0.65

²Maureen Foley, Timothy Dapp, John Kim and Roger Crane, The Effect of Peel Ply and Surface Preparation on Secondary Bonding in VARTM Applications, NSWCCD-65-TR-2009/36, 2009.

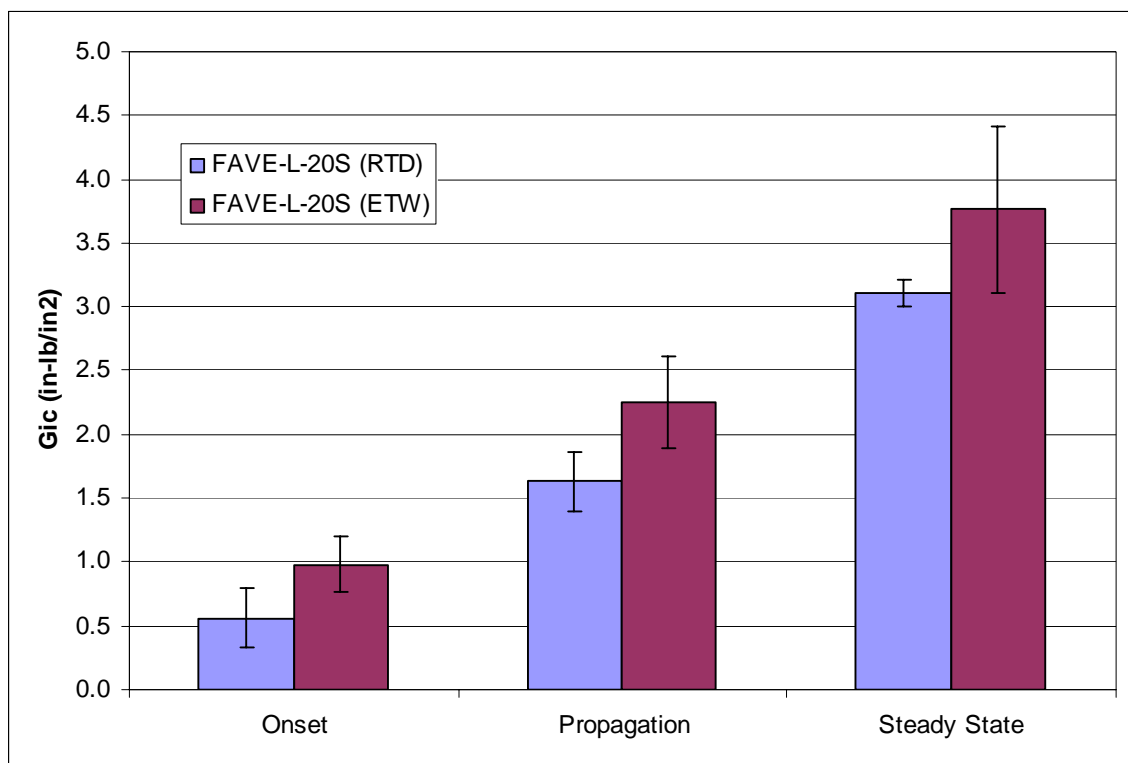


Figure 8 Mode I Interlaminar Toughness Results

2.1.4 Thermal Property Characterization - Dynamic Mechanical Analysis:

A dynamic mechanical analysis was performed on a neat resin sample of the FAVE-L-20S resin using a TA Instruments DMA. The sample was run in the single cantilever bending mode at a frequency of 1 Hz. The temperature ramp rate was set to 2°C/min from 30° to 150°C. The results, shown in Figure1, were analyzed according to ASTM E1640 and the T_g values are shown in Table 12.

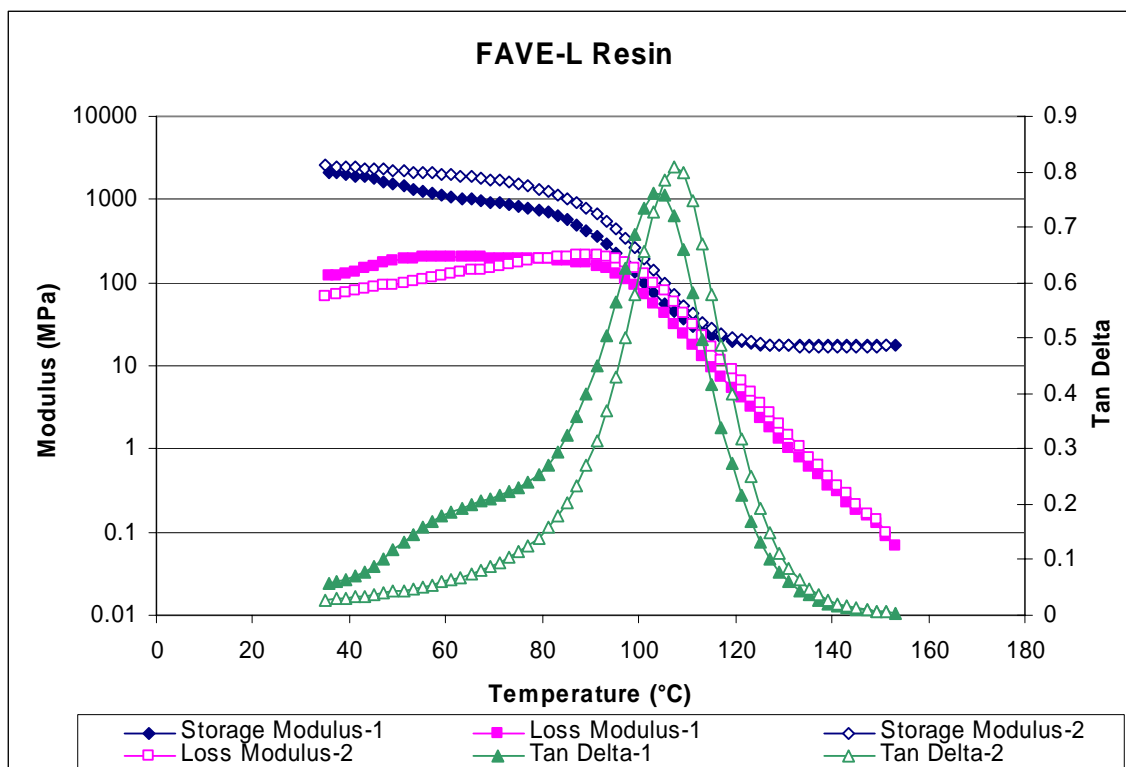


Figure 9 DMA Results for the FAVE-L-20S Resin Material

Table 12 Glass Transition Temperature Results as Determined by the Dynamic Mechanical Thermal Analysis Test for the FAVE-L-20S Resin

FAVE-L-20S	Glass Transition Temperature, T_g , (°C) as determined by		
	Extrapolated Onset of change of the storage modulus*	Peak of Loss Modulus	Peak of Tan Delta Curve
1 st Heating	78.9	-	105
2 nd Heating	73.8	89.2	107

*Typical Navy Design Criteria

The FAVE-L-20S resin system was originally selected for characterization based on the published data on the T_g of the system being greater than 100°C. Since, using DMA and the extrapolated onset of the change of the storage modulus, the T_g is below 80°C it was determined that another formulation of the FAVE product line should be considered. Several additional samples were relieved from the Army Research Lab for consideration. These were the FAVE-L-25S and FAVE-O-25S which contains slightly more styrene at 25wt%. The O designation denotes the change in the fatty acid to methacrylated octanoic acid instead of the methacrylated lauric acid. Similar DMA tests were run on these samples as well as baseline samples of the Ashland Derakane 510A and 8084 as well as the Interplastic CoRezyn CORVE 8100 which are commercially available vinyl esters that are being used in Navy applications. The results of the DMA scans are given in

Appendix G and summarized in Table 13. Also included in the Table for reference purposes are the AOC K018 vinyl ester resin system.

Table 13 Glass Transition Temperature Results as Determined by the Dynamic Mechanical Thermal Analysis Test for a Variety of Resin Systems

		Glass Transition Temperature, T _g , (°C) as determined by		
		Extrapolated Onset of change of the storage modulus*	Peak of Loss Modulus	Peak of Tan Delta Curve
FAVE-L-20S	1 st Heating	78.9	-	105
	2 nd Heating	73.8	89.2	107
FAVE-L-25S	1 st Heating	84.2	98.2	114
	2 nd Heating	96.2	106	122
FAVE-O-25S	1 st Heating	82.4	100	116
	2 nd Heating	94.4	110	124
Derakane 510A	1 st Heating	101	114	128
	2 nd Heating	111	124	136
Derakane 8084	1 st Heating	73.0	80.2	118
	2 nd Heating	85.0	110	130
CORVE 8100	1 st Heating	108	110	122
	2 nd Heating	112	114	126

*Typical Navy Design Criteria

The DMA results indicated that the FAVE-L-25S would be a good low VOC resin system to evaluate further since it would be comparable to a resin system that has temperature properties that fall between the Derakane 8084 and Derakane 510A resin systems. It is a little lower in T_g than the current CORVE 8100 resin system currently used in the MCM rudder application. The FAVE-O-25S also would fit into this category, but it is predicted to more expensive to produce than the FAVE-L-25S.

2.2 FAVE-L-25S, Derakane 510A and CORVE 8100 Resin Characterization

The following test plan was developed to characterize the room temperature dry (RTD) properties of glass fiber reinforced FAVE-L-25S, Derakane 510A and CORVE 8100 composite systems. The Derakane 510A resin was tested so as to provide baseline materials properties for a non-low VOC resin system currently in use in Navy applications. The CORVE 8100 was also tested as it is the current resin system used in the MCM rudder application. The test plan consisted of physical attribute characterization such as fiber volume fraction and density and mechanical testing to determine the tensile, compressive, shear and toughness properties. Initial studies also looked at the gel time for different formulations and also the flow rate through the fabricated panels.

2.2.1 Gel Time Study

A series of tests were performed with the FAVE-L-25S resin system prior to the infusion of panels to determine the appropriate formulation for the desired gel time. A 5 hour gel time would be desired for manufacturing of large scale parts whereas a slightly shorter gel time would be desirable for small scale laboratory parts. An initial test was performed with the same formulation as the FAVE-L-20S resin system but with the Trigonox 239A catalyst and this yielded a gel time of 6 hours with the samples still tacky to the touch. Some variations on this formulation were attempted as shown in Table 14, but this only resulted in longer gel times. The catalyst was then switched back to the Cadox L-50 MEKP material for Trial B as shown in Table 15. In general this yielded approximately the same gel times with the samples a little less tacky to the touch. Finally, the DMAA (N,N-Dimethylacetamide) component was switched to DMA (N,N-Dimethylaniline) which had been used in the past in vinyl ester formulations. This resulted in formulations that fully cured and were not tacky to the touch once cured. Formulations for a short term gel time (~1 hour) and longer one (4-5 hours) were tested. The trial denoted 2C was used for panel fabrication for characterization purposes and the trial 1C is recommended for large part fabrication.

Table 14 Gel Time Study – Trial A

Fave-L-25S	Trial (wt%)					
Component	1A	2A	3A	4A	5A	6A
CoNap	0.3	0.3	0.3	0.3	0.25	0.3
2,4 P	0.25	0.25	0.3	0.3	0.3	-
DMAA	0.2	-	-	-	-	-
Trigonox	2.0	2.0	2.0	1.5	1.0	1.5
Gel Time	6 hrs*	Overnight*	Overnight*	Overnight*	Overnight*	20 min*

*Samples tacky to touch once cured

Table 15 Gel Time Study – Trial B

Fave-L-25S	Trial (wt%)				
Component	1B	2B	3B	4B	5B
CoNap	0.3	0.3	0.3	0.3	0.25
2,4 P	0.25	0.25	0.3	0.3	0.3
DMAA	0.2	-	-	-	-
Cadox L-50a	2.0	2.0	2.0	2.0	1.5
Gel Time	7 hrs*	2.5 hrs*	10+ hrs*	10+ hrs*	10+ hrs*

*Samples less tacky to touch once cured than first set of Trials

Table 16 Gel Time Study – Trial C

Fave-L-25S	Trial (wt%)	
Component	1C	2C
CoNap	0.3	0.3
2,4 P	0.25	0.1
DMA	0.2	0.2
Cadox L-50a	1.5	1.5
Gel Time	4-5 hrs	50 minutes

Samples not tacky to touch once cured

2.2.2 Panel Fabrication

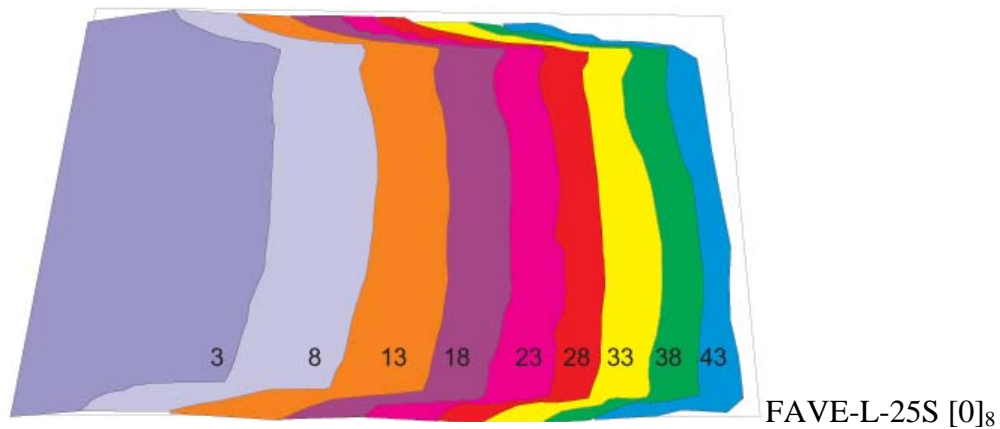
A total of two panels were fabricated at NSWCCD for evaluation of the FAVE-L-25S and Derakane 510A resin systems. These panels were made using standard VARTM techniques with the same fabric as in the previous section and the resin as shown below in Table 17.

Table 17 Panel Identification and Fiber Orientation

Panel	Layup	Resin/Formulation	
070801	[0] ₈	FAVE-L-25S	0.3% CoNap 0.1% 2,4 P 0.2% DMA 1.5% Cadox L-50
070902	[0/90] ₄	FAVE-L-25S	0.3% CoNap 0.1% 2,4 P 0.2% DMA 1.5% Cadox L-50
070903	[0] ₈	Derakane 510A	0.25% CoNap 0.1% 2,4 P 1.25% Trig 239A
080304	[0] ₁₀	CORVE 8100	0.1% CoNap 1.25% Cadox L-50

Flow/Viscosity Study

As the panels shown in Table 17 were being infused, an outline of the infusion flow front was drawn on the bag at specified time intervals. Photographs were taken at the end of the infusion and a flow front with time graph was constructed for each of the panels as shown in the following Figures.



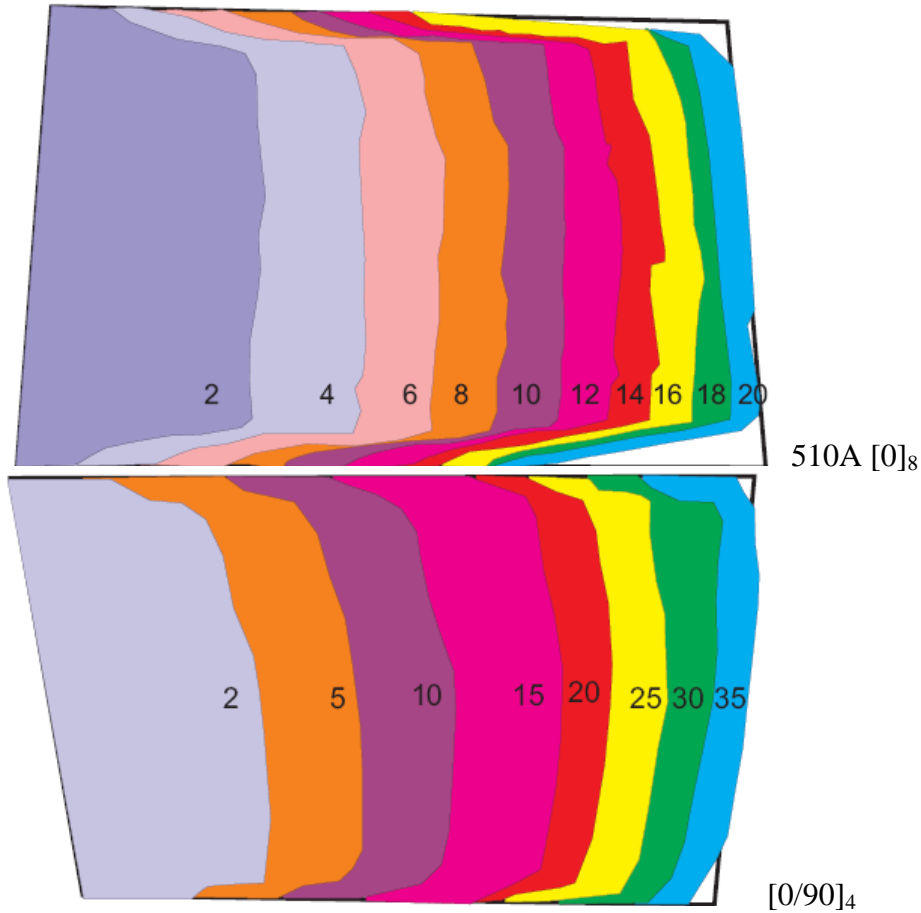


Figure 10 Flow Study Results Indicating Movement of Flow Front with Time Denoted in Minutes for Three Different Panel Types

The flow study results indicated that the FAVE-L-25 S resin appears to infuse at a much slower rate than the Derakane 510A resin in a unidirectional panel (43 minutes versus 20 minutes). The addition of 90° plies appears to aid in speeding up the flow front by decreasing the infusion time from 43 minutes to 35 minutes. A brief check of the resin viscosities with a Model RV Brookfield viscometer yielded higher than expected viscosities for the FAVE-L resin systems as shown in Table 18.

Table 18 Viscosity of Resin Systems

Type	Viscosity (cPoise)
FAVE-L-20S	1992±11
FAVE-L-25S	1171±99
Derakane 510A	520±0
Corve 8100	100*

* Interplastic Data Sheet Value

2.2.3 Physical Properties Characterization

2.2.3.1 Density

The density of both the neat resin and composite pieces taken from each panel was tested according to the guidelines of ASTM D792. The results are summarized in Table 19. The results show fairly consistent composite panel densities for the 8 ply composite panel regardless of ply layup.

Table 19 Summary of Density Measurements (ASTM D792)

Panel	Type	Density (g/cm ³)
-	Neat Resin FAVE-L-25S	1.17±0.002
-	Neat Resin Derakane 510A	1.35±0.008
	Neat Resin CORVE 8100	1.14
070801	Composite FAVE-L-25S	1.84±0.003
070903	Composite Derakane 510A	1.91±0.005
080304	Composite CORVE 8100	1.83±0.002

The fiber, resin and void fraction were determined using the burnout method as described in ASTM D3171. An E-Glass fiber density was assumed to be 2.59 g/cm³ for these calculations³. The results of these tests are shown in Table 20. Detailed specimen level results are shown in Appendix A.

³ Fiber Glass Industries (www.fiberglassindustries.com)

Table 20 Summary of Constituent Material Measurements (ASTM D3171)

Panel	Type	% Fiber Volume Fraction	% Resin Volume Fraction	% Void Volume Fraction
070801	Composite FAVE-L-25S	47.9±0.2	51.5±0.3	0.6±0.2
070903	Composite Derakane 510A	47.0±0.4	51.7±0.4	1.30±0.06
080304	Composite CORVE 8100	49.6 ± 0.2	49.6 ± 0.2	0.82 ± 0.03

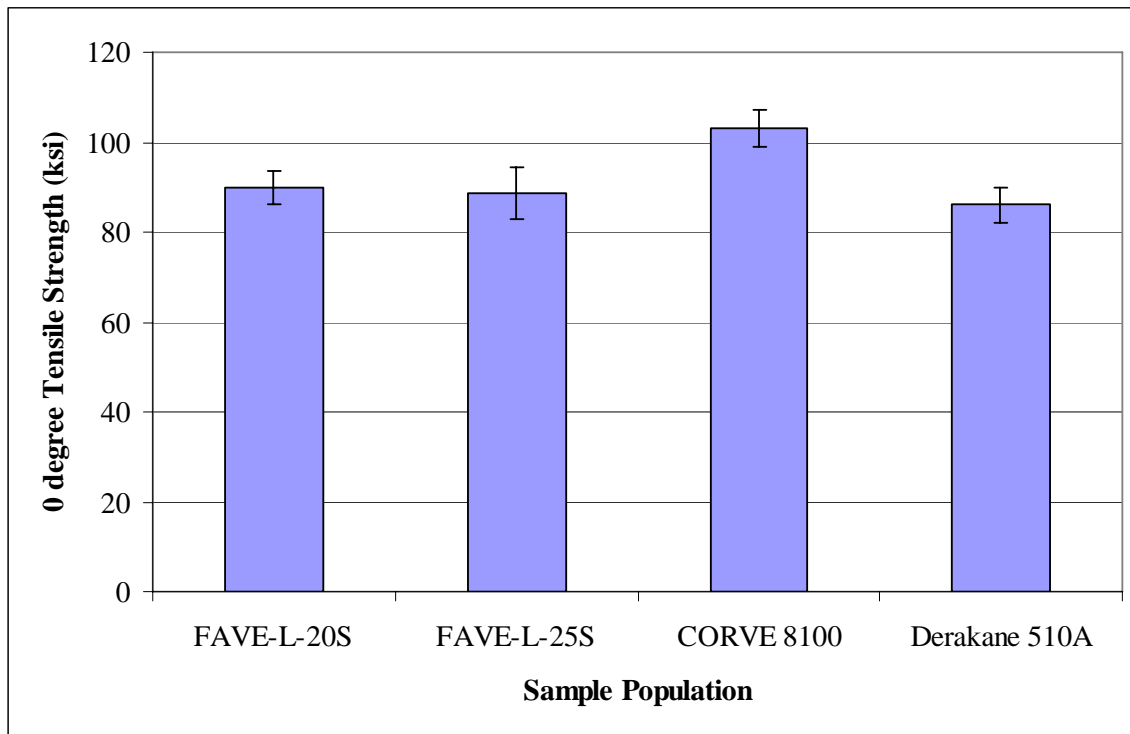
2.2.3.2 Tension Testing

The tension tests were performed in the same manner as in the previous FAVE-L-20S section. The results of test are shown in the following table. Detailed specimen level results are included in Appendix B. The results indicate the FAVE-L-20S, FAVE-L-25S, and Derakane 510A composite systems all appear to exhibit similar tensile strengths and tensile modulus within the uncertainty of the test. The CORVE 8100 composite appears to have a slightly higher tensile strength and modulus.

Table 21 ASTM D638 Tension Test Results

Panel ID	Type	Tensile Strength (ksi)	Elastic Modulus* (Msi)
061001	Composite FAVE-L-20S [0°]	89.9 ± 3.9	4.8 ± 0.07
070801	Composite FAVE-L-25S [0°]	88.6±5.8	4.6±0.3
070903	Composite Derakane 510A [0°]	86.0±3.9	4.6±0.2
08304	Composite CORVE 8100 [0°] [90°]	103.2 ± 4.1 15.6 ±0.6	5.1 ± 0.4 2.1 ±0.1

*Range of 1000 to 3000in/in

**Figure 11 Tensile Strength Results**

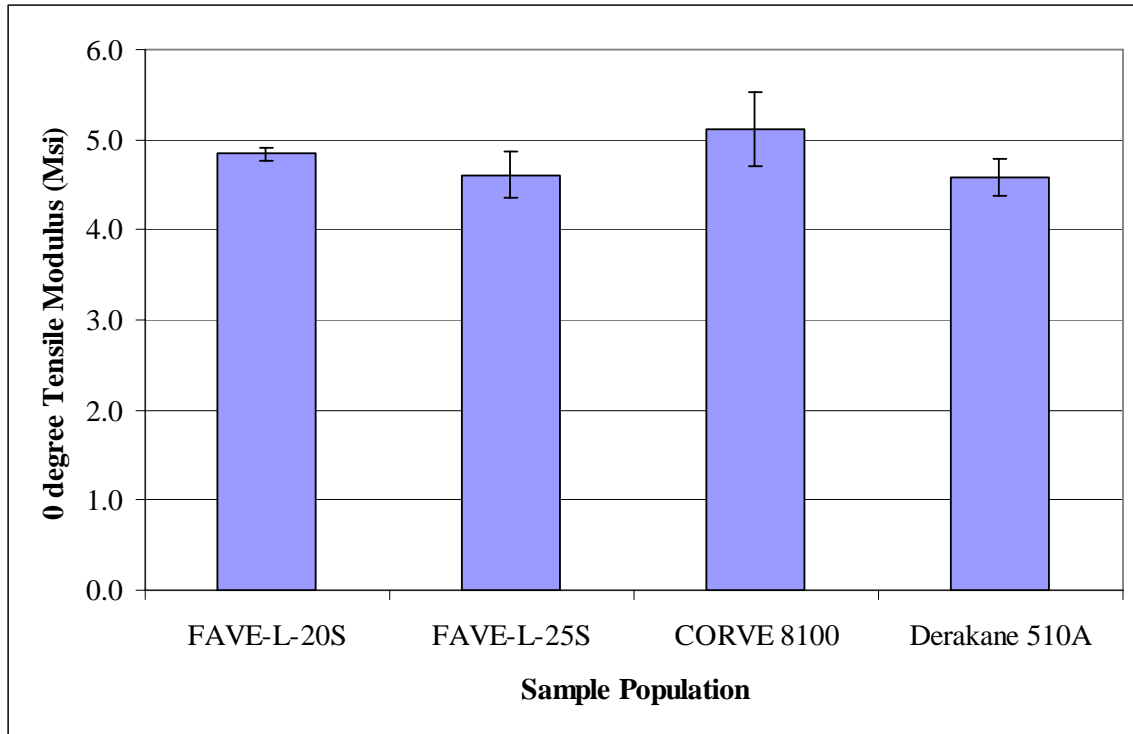


Figure 12 Tensile Modulus Results

2.2.3.3 Compression Testing:

The compression tests were performed in the same manner as in the FVE-L-20S previous section. The results of test are shown in the following table. Detailed specimen level results are included in Appendix C. The results indicate that the FAVE-L-25S, Derakane 510A and CORVE 8100 composite systems exhibit significantly higher compressive strengths than the FAVE-L-20S. All three resin systems exhibit comparable compressive moduli. The FAVE-L-25S exhibits a higher strength but a lower modulus than the current 8100 MCM rudder material.

Table 22 ASTM D695 Compression Test Results

Panel ID	Type	Compressive Strength (ksi)	Elastic Modulus* (Msi)
061001	Composite FAVE-L-20S [0°]	53.6 ± 6.0	5.03 ± 0.3
070801	Composite FAVE-L-25S [0°]	83.0±2.2	4.52±0.2
070903	Composite Derakane 510A [0°]	79.3±4.0	4.5±0.2
08304	Composite CORVE 8100 [0°] [90°]	63.1 ± 4.4	5.1 ± 0.6
		21.8 ± 0.6	1.8 ± 0.1

*Range of 1000 to 3000in/in

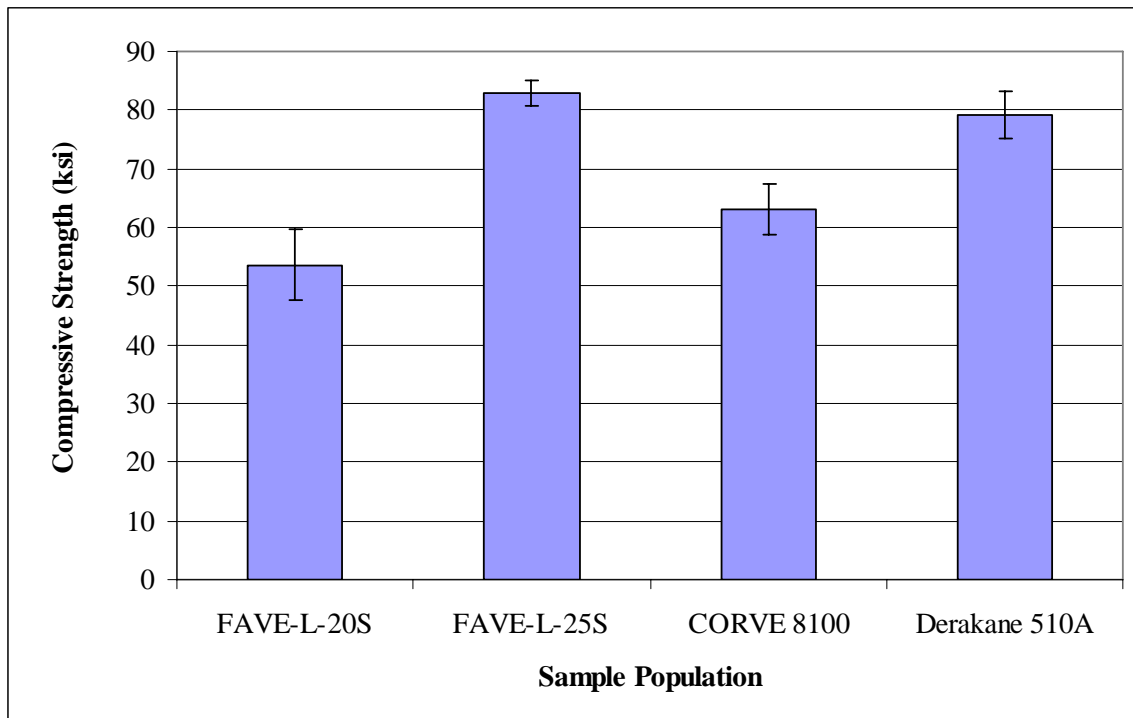


Figure 13 Compressive Strength Results

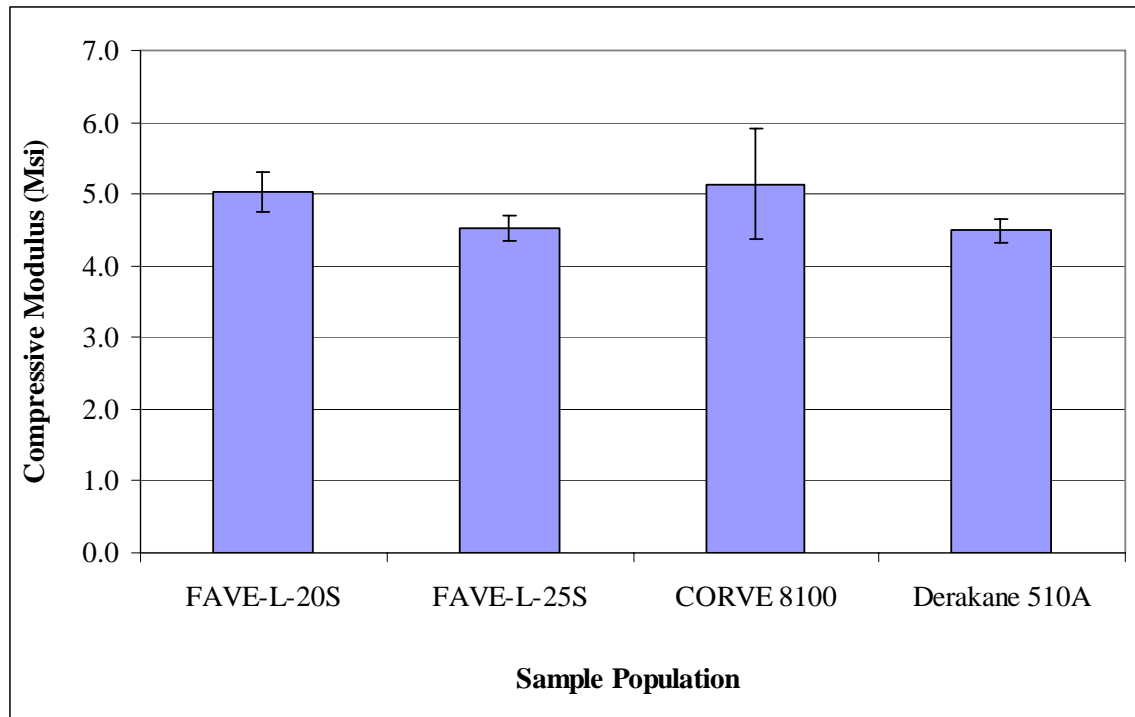


Figure 14 Compressive Modulus Results

2.2.3.4 Shear Testing

The shear tests were performed according to ASTM D2344 (Short Beam Shear). The results of test are shown in the following table. Detailed specimen level results are included in Appendix D. The results indicate the FAVE-L-20S and FAVE-L-25S appear to have slightly higher short beam shear strengths than the CORVE 8100 and Derakane 510A composite systems.

Table 23 Shear Test Results (ASTM D2344)

Panel ID	Type	Shear Strength (ksi)
070201	Composite FAVE-L-20S [0°]	7.1±0.3
070801	Composite FAVE-L-25S [0°]	7.2±0.03
070903	Composite Derakane 510A [0°]	6.2±0.03
08304	Composite CORVE 8100 [0°] [90°]	6.5 ± 0.1 4.0 ± 0.2

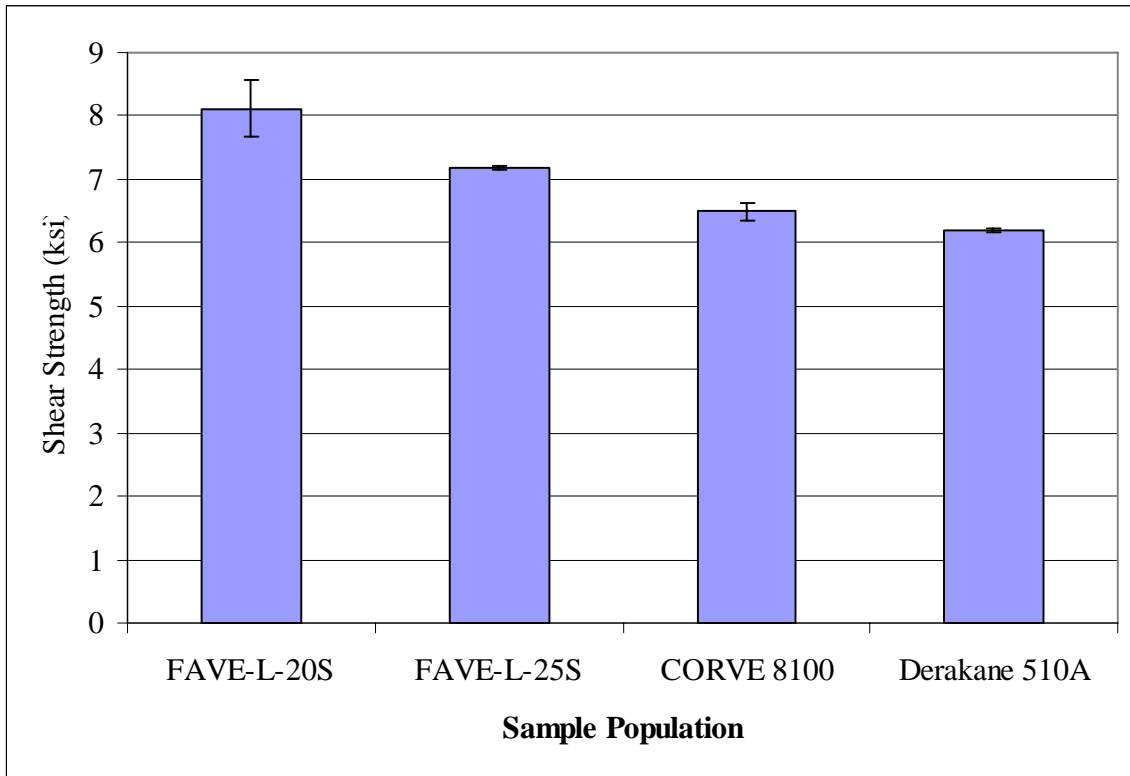


Figure 15 Shear Strength Results

2.2.3.5 Mode I Interlaminar Fracture Toughness (DCB) Testing

Specimens were prepared and tested as in the previous FAVE-L-20S section. The results of the tests are summarized in Table 24 and Figure 16. The onset of the G_{Ic} was defined as when the crack gage indicated that the crack started to open. The propagation value is taken as the G_{Ic} value after 0.25 in of crack growth. Since these specimens appear to exhibit an increasing G_{Ic} as the crack propagates and then flattens out after 1 inch of crack growth as shown in Figure 16, a steady state G_{Ic} value was determined by averaging the G_{Ic} values from 1 to 1.6 inch of crack growth. The results indicate that the FAVE-L-25S composite exhibits similar room temperature dry toughness properties across the board (Onset, Propagation and Steady State) as the FAVE-L-20S. The Derakane 510A and CORVE 8100 composites exhibited close to double the toughness of the FAVE systems across the board. The effect of post cure of 4 hours at 160°F was also investigated to see if this raised the toughness values. The results indicate that there was no change in the toughness within the scatter of the test after the post cure.

**Table 24 Mode I Interlaminar Toughness Results (Room Temperature Dry)
(Glass Fabric SW1810)**

Panel ID	Type	G_{Ic} (in-lb/in ²)		
		Onset	Propagation	Steady State
070201	Composite FAVE-L-20S	0.56±0.24	1.63±0.23	3.11±0.10
070801	Composite FAVE-L-25S	0.62±0.16	1.57±0.24	3.68±0.25
070801	Composite FAVE-L-25S (Post Cured)	0.29±0.05	1.45±0.24	3.47±0.92
070903	Composite 510A	1.15±0.29	3.01±0.59	6.70±0.60
070903	Composite 510A (Post Cured)	1.27±0.16	3.40±0.47	6.88 ±0.39
080304	Composite 8100	0.38 ±0.20	2.76±0.12	6.02±0.37
080304	Composite 8100 (Post Cured)	0.20±0.15	2.99±0.47	6.38 ±0.60

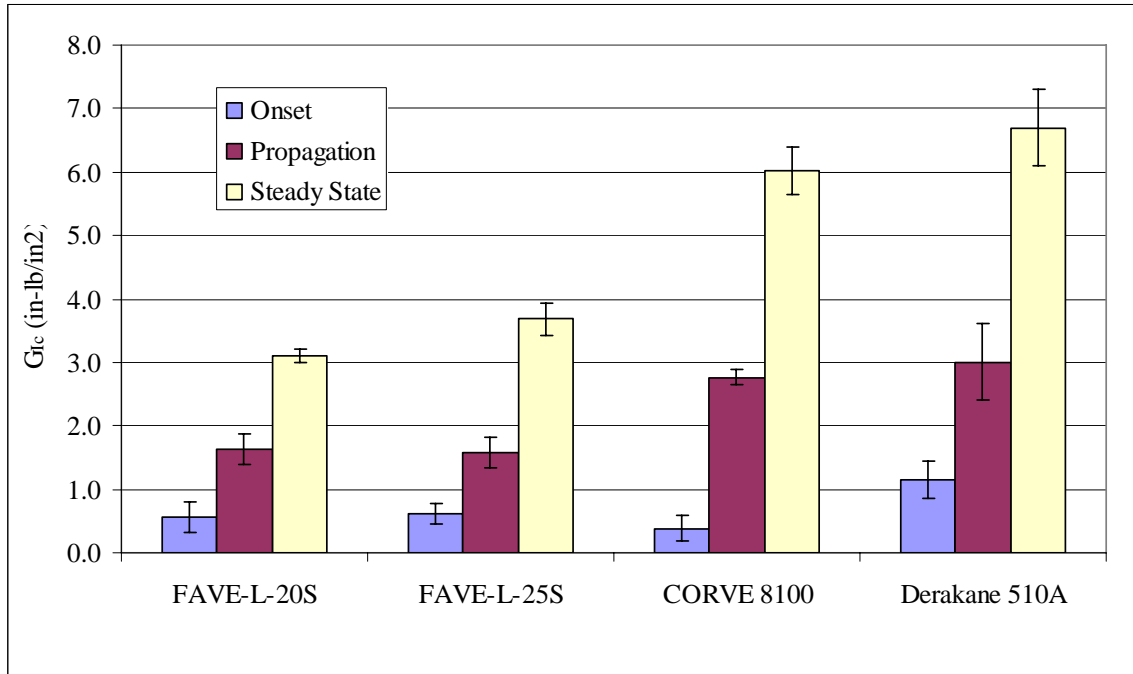


Figure 16 Mode I Interlaminar Toughness Results

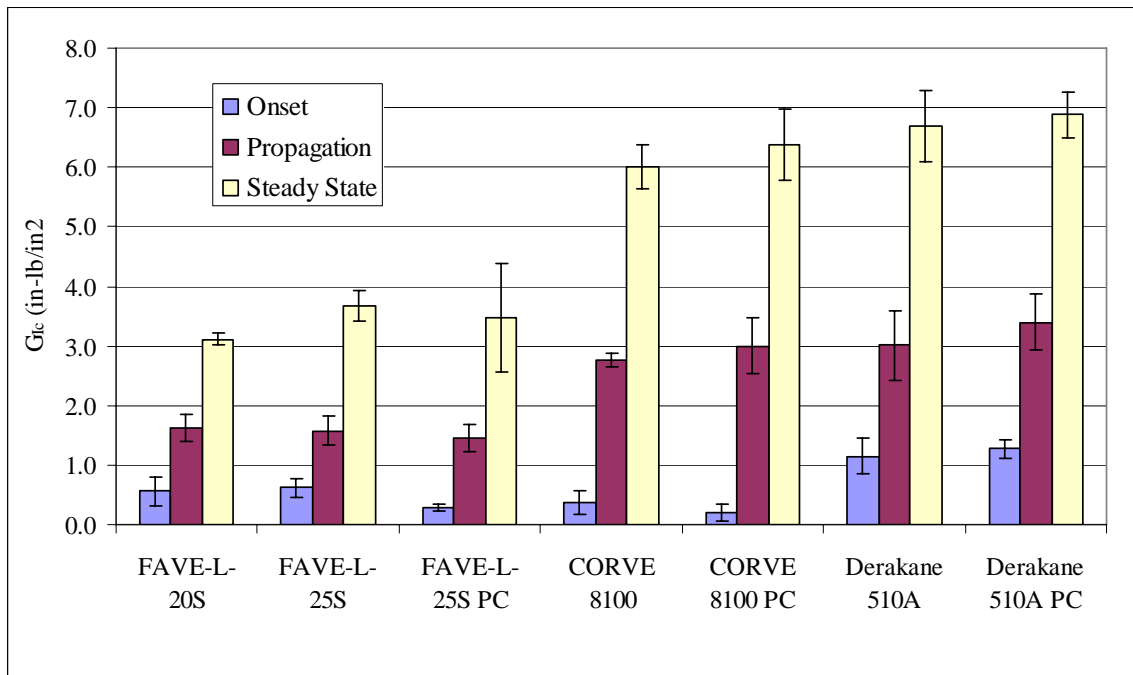


Figure 17 Mode I Interlaminar Toughness Results Effect of Post Cure

2.2.3.6 Carbon Fiber Mode I Interlaminar Fracture Toughness (DCB) Testing

A series of tests were also performed by infusing the FAVE-L-25S, 510A and West Systems Epoxy into a T700 FOE size, 9 oz/sq yd plain weave carbon fiber woven roving to determine if the FAVE-L-25S might exhibit any better bonding to carbon fiber than the baseline 510A used in Navy designs. The results indicated that the FAVE-L-25S exhibited significantly lower G_{Ic} values than the 510A and the West Systems Epoxy as shown in Table 25 and Figure 18.

**Table 25 Mode I Interlaminar Toughness Results (Room Temperature Dry)
(Carbon Fiber Fabric T700 FOE Size, Plain Weave, 9 oz/sq yd)**

Panel ID	Type	G_{Ic} (in-lb/in ²)		
		Onset	Propagation	Steady State
080305	Composite FAVE-L-25S with Carbon Farbic	0.14±0.007	0.91±0.18	1.76±0.20
080401	Composite 510A with Carbon Fiber Fabic	1.16±0.37	2.77±0.67	4.49±0.60
080502	Composite West Systems 117LV with Carbon Fiber Fabric	0.29±0.23	2.4±0.38	4.07±0.34

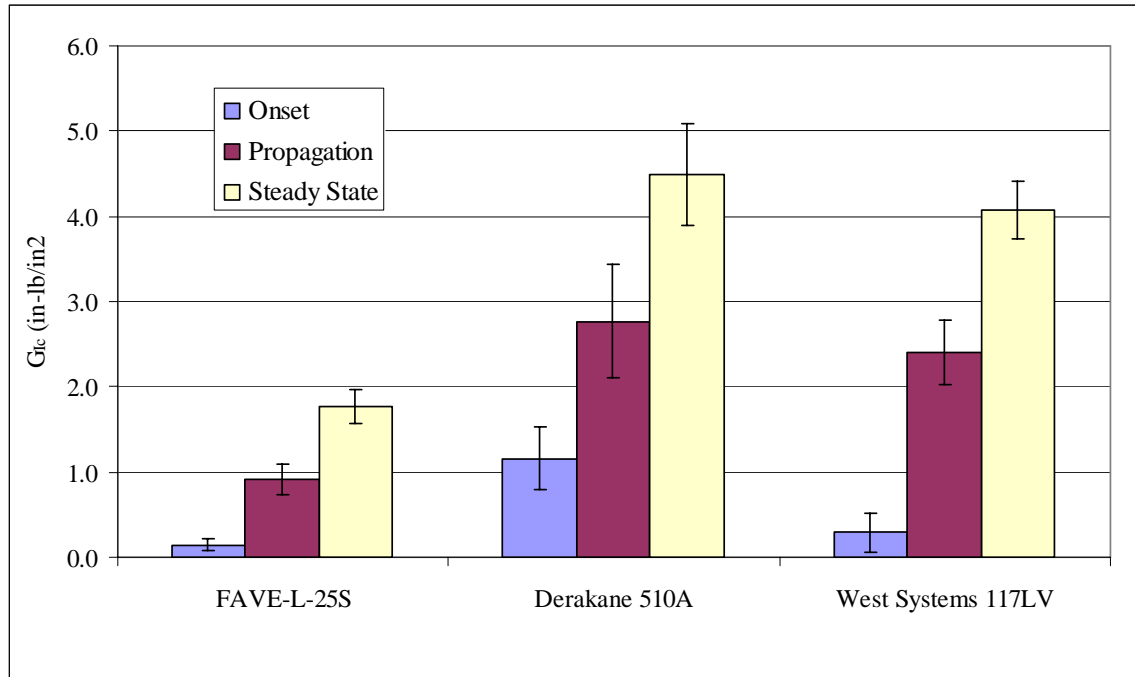


Figure 18 Mode I Interlaminar Toughness Results for Carbon Fiber Reinforced Vinyl Ester Systems

3.0 Conclusions

A variety of tests were performed in support of this several year ESTCP Low HAP/VOC composite resin system. Several different low VOC resins were evaluated and a final down selection of the FAVE-L-25S was made. Extensive materials testing and processing studies were performed and compared to other typical Navy vinyl ester resin systems. In general, the system was able to be processed using standard VARTM practices with formulation variations allowing for short and long infusion times. The quality of the composites parts with the FAVE-L-25S was similar in density, fiber volume fraction, and void content as the Derakane 510A and CORVE 8100 resin systems. The glass transition temperature of the FAVE-L-25S is lower than the Derakane 510A and CORVE 8100 and closer to the Derakane 8084 resin. Composites made with the Derakane 510A, CORVE 8100 and FAVE-L-25S all exhibited similar mechanical properties (tensile, compressive and shear). However, the FAVE-L-25S exhibited significantly lower Mode I interlaminar fracture toughness than the Derakane 510A and CORVE 8100 materials. This appeared to be the case whether or not the part was postcured and occurred with both glass and carbon fiber composites. In general this FAVE-L-25S resin appears promising and might be considered for future composite applications where a low HAP/VOC system is required and the interlaminar fracture toughness is not critical to the design.

Appendix A

Density Measurements

MATERIAL. VE FAVE-L-20S (neat resin)

	WT. SPECIMEN (g)	WT. WIRE in H2O (g)	WT. /WIRE & SPEC. in H2O (g)	WT of Spec in H2O (g)	SPECIFIC GRAVITY	Density (g/cm3)
1	4.0039	4.4670	5.0564	0.5894	1.1726	1.1697
2	3.5978	4.4965	5.0166	0.5201	1.1690	1.1661
3	4.4931	4.5039	5.1563	0.6524	1.1699	1.1669
4	5.7141	4.5108	5.3313	0.8205	1.1677	1.1647
5	5.8058	4.5087	5.3448	0.8361	1.1682	1.1653
				<i>MEAN</i>	1.1695	1.1666
				<i>STD.DEV.</i>	0.0019	0.0019

MATERIAL. VE FAVE-L-25S (neat resin)

	WT. SPECIMEN (g)	WT. /WIRE & SPEC. in H2O (g)	WT of Spec in H2O (g)	SPECIFIC GRAVITY	Density (g/cm3)
	6.0896	0.9194	0.9194	1.1778	1.1749
	6.0878	0.9054	0.7814	1.1747	1.1718
				<i>MEAN</i>	1.1733
				<i>STD.DEV.</i>	0.002

MATERIAL. CORVE 8100

	WT. SPECIMEN (g)	WT. /WIRE & SPEC. in H2O (g)	WT of Spec in H2O (g)	SPECIFIC GRAVITY	Density (g/cm3)
1	4.3054	0.5283	0.5283	1.1399	1.1370

MATERIAL. Derakane 510A

	WT. SPECIMEN (g)	WT of Spec in H2O (g)	WT of Spec in H2O (g)	SPECIFIC GRAVITY	Density (g/cm3)
	2.0949	0.5437	0.5437	1.3505	1.3471
	2.9422	0.7814	0.7814	1.3616	1.3582
				<i>MEAN</i>	1.3527
				<i>STD.DEV.</i>	0.008

MATERIAL. Derakane 8084

	WT. SPECIMEN (g)	WT of Spec in H2O (g)	WT of Spec in H2O (g)	SPECIFIC GRAVITY	Density (g/cm3)
	1.2750	0.1621	0.1621	1.1457	1.1428
	2.4427	0.3159	0.7814	1.1485	1.1457
				<i>MEAN</i>	1.1442
				<i>STD.DEV.</i>	0.002

I.D. NO.: 061001

MATERIAL: GL(Uni Mat)(0)_g/VE(FAVE-L-20S)

	WT. SPECIMEN (g)	WT. WIRE in H2O (g)	WT. /WIRE & SPEC. in H2O (g)	WT of Spec in H2O (g)	SPECIFIC GRAVITY	Density (g/cm3)
1	5.5172	0.5824	3.1338	2.5514	1.8603	1.8556
2	5.4045	0.5824	3.0350	2.4526	1.8309	1.8263
3	5.8075	0.5882	3.2554	2.6672	1.8493	1.8447
4	5.5544	0.5882	3.1201	2.5319	1.8377	1.8331
5	5.1304	0.5827	2.9190	2.3363	1.8362	1.8316
				MEAN	1.8429	1.8383
				STD.DEV.	0.0208	0.0208

	WT. CRUCIBLE (g)	WT. FIBER in CRUCIBLE (g)	WT. FIBER (g)	WT. RESIN (g)
1	15.3680	19.1279	3.7599	1.7573
2	15.9774	19.5750	3.5976	1.8069
3	15.6919	19.6171	3.9252	1.8823
4	16.7207	20.4514	3.7307	1.8237
5	19.8805	23.3102	3.4297	1.7007

	FIBER CONTENT	RESIN CONTENT	FIBER VOL. FRACTION	RESIN VOL. FRACTION
1	68.1487	31.8513	48.8256	50.6895
2	66.5667	33.4333	46.9380	52.3657
3	67.5885	32.4115	48.1397	51.2781
4	67.1666	32.8334	47.5376	51.6180
5	66.8505	33.1495	47.2745	52.0715
MEAN	67.2642	32.7358	47.7431	51.6046
STD.DEV.	1.1186	1.1186	1.3347	1.1852

	VOID CONTENT %	DENSITY OF FIBERS :	2.59
1	0.4849	DENSITY OF MATRIX :	1.166
2	0.6963		
3	0.5821		
4	0.8444		
5	0.6540		
MEAN	0.6523	DATE :	3/8/2007
STD.DEV.	0.1495		

I.D. NO.: 061002

MATERIAL: GL(Uni Mat)(Quasi(0/+45/90/-45)_s)/VE(FAVE-L-:

	WT. SPECIMEN	WT. WIRE in H2O	WT. /WIRE & SPEC. in H2O	WT of Spec in H2O (g)	SPECIFIC GRAVITY	Density (g/cm3)
1	6.7100	0.5840	3.6771	3.0931	1.8552	1.8505
2	6.6132	0.5840	3.6251	3.0411	1.8513	1.8467
3	6.8828	0.5864	3.7596	3.1732	1.8554	1.8508
4	6.5137	0.5864	3.6117	3.0253	1.8672	1.8626
5	6.7869	0.5855	3.7287	3.1432	1.8626	1.8580
				MEAN	1.8584	1.8537
				STD.DEV.	0.0027	0.0027

	WT. CRICUBLE (g)	WT. FIBER in CRUCIBLE (g)	WT. FIBER (g)	WT. RESIN (g)
1	15.7332	20.3124	4.5792	2.1308
2	16.8223	21.3330	4.5107	2.1025
3	17.3394	22.0144	4.6750	2.2078
4	17.5650	22.0050	4.4400	2.0737
5	15.2377	19.8494	4.6117	2.1752

	FIBER CONTENT	RESIN CONTENT	FIBER VOL. FRACTION	RESIN VOL. FRACTION
1	68.2444	31.7556	48.7603	50.3988
2	68.2075	31.7925	48.6333	50.3532
3	67.9229	32.0771	48.5364	50.9151
4	68.1640	31.8360	49.0196	50.8550
5	67.9500	32.0500	48.7452	51.0706
MEAN	68.0978	31.9022	48.7389	50.7186
STD.DEV.	0.0261	0.0261	0.0898	0.0323

	VOID CONTENT %	DENSITY OF FIBERS :	2.59
1	0.8409	DENSITY OF MATRIX :	1.166
2	1.0136		
3	0.5484		
4	0.1254		
5	0.1842		
MEAN	0.5425	DATE :	3/8/2007
STD.DEV.	0.1221		

I.D. NO.: 061201

MATERIAL: GL(Uni Mat)(0/90)_{4s}/VE(FAVE-L-20S)

	WT. SPECIMEN (g)	WT. WIRE in H2O (g)	WT. /WIRE & SPEC. in H2O (g)	WT of Spec in H2O (g)	SPECIFIC GRAVITY	Density (g/cm3)
1	6.2276	0.5956	3.4536	2.8580	1.8482	1.8436
2	6.3848	0.5922	3.5462	2.9540	1.8610	1.8564
3	6.3950	0.5913	3.5377	2.9464	1.8544	1.8497
4	6.4249	0.5934	3.5367	2.9433	1.8454	1.8408
5	6.3414	0.5923	3.5045	2.9122	1.8492	1.8446
				MEAN	1.8516	1.8470
				STD.DEV.	0.0091	0.0091

	WT. CRUCIBLE (g)	WT. FIBER in CRUCIBLE (g)	WT. FIBER (g)	WT. RESIN (g)
1	19.8801	24.0797	4.1996	2.0280
2	15.7332	20.0685	4.3353	2.0495
3	16.8223	21.1287	4.3064	2.0886
4	17.5655	21.8748	4.3093	2.1156
5	16.7199	21.0057	4.2858	2.0556

	FIBER CONTENT WT%	RESIN CONTENT WT%	FIBER VOL. FRACTION %	RESIN VOL. FRACTION %
1	67.4353	32.5647	48.0002	51.4878
2	67.9003	32.0997	48.6673	51.1054
3	67.3401	32.6599	48.0933	51.8116
4	67.0719	32.9281	47.6695	51.9839
5	67.5844	32.4156	48.1340	51.2814
MEAN	67.4664	32.5336	48.1129	51.5340
STD.DEV.	0.3288	0.3288	0.4717	0.2704

	VOID CONTENT %	DENSITY OF FIBERS :	2.59
1	0.5121	DENSITY OF MATRIX :	1.166
2	0.2273		
3	0.0951		
4	0.3465		
5	0.5845		
MEAN	0.3531	DATE :	3/8/2007
STD.DEV.	0.2013		

I.D. NO.: 070201

MATERIAL: VE FAVE-L-20S /UniMat (0)₈

	WT. SPECIMEN (g)	WT. WIRE in H2O (g)	WT. /WIRE & SPEC. in H2O (g)	WT of Spec in H2O (g)	SPECIFIC GRAVITY	Density (g/cm3)
1	4.8320	4.5055	6.7418	2.2363	1.8615	1.8569
2	4.8245	4.5064	6.7178	2.2114	1.8463	1.8417
3	4.7650	4.5076	6.7193	2.2117	1.8662	1.8615
4	4.7932	4.5080	6.7416	2.2336	1.8726	1.8680
5	4.9602	4.5093	6.7784	2.2691	1.8432	1.8386
				<i>MEAN</i>	1.8540	1.8493
				<i>STD.DEV.</i>	0.0150	0.0150

I.D. NO.: 070801

MATERIAL: GL/VE

FAVE-L-25S (Uni/SW1810 Rudder Fabric) 8 plies

	WT. in Air SPECIMEN	WT. in H2O SPECIMEN	SPECIFIC GRAVITY	Density (g/cm3)
1	7.1343	3.2697	1.8461	1.8414
2	7.3982	3.3981	1.8495	1.8449
3	7.3554	3.3823	1.8513	1.8467
4	7.0938	3.2659	1.8532	1.8486
5	7.3033	3.3453	1.8452	1.8406
6	7.3708	3.3887	1.8510	1.8464

MEAN 1.8494 1.8447
STD.DEV. 0.0031 0.0031

	CRUCIBLE #	WT. CRICUBLE (g)	WT. FIBER in CRUCIBLE (g)	WT. FIBER (g)	WT. RESIN (g)
1	3	17.5888	22.3652	4.7764	2.3579
2	2	17.3157	22.2773	4.9616	2.4366
3	41	15.3104	20.2643	4.9539	2.4015
4	K	15.7304	20.5040	4.7736	2.3202
5	H	15.6891	20.6055	4.9164	2.3869
6	52	17.0742	22.0518	4.9776	2.3932

	FIBER CONTENT	RESIN CONTENT	FIBER VOL. FRACTION	RESIN VOL. FRACTION	Theoretical Density (g/cm3)
1	66.95	33.05	47.60	51.88	1.851
2	67.06	32.94	47.77	51.80	1.853
3	67.35	32.65	48.02	51.40	1.857
4	67.29	32.71	48.03	51.54	1.856
5	67.32	32.68	47.84	51.28	1.857
6	67.53	32.47	48.14	51.11	1.860
MEAN	67.25	32.75	47.90	51.50	
STD.DEV.	0.21	0.21	0.20	0.30	

	VOID CONTENT	DENSITY OF FIBERS : 2.59	DENSITY OF MATRIX : 1.1730
1	0.52		
2	0.43		
3	0.58		
4	0.43		
5	0.88		
6	0.75		
MEAN	0.60		
STD.DEV.	0.18	DATE : Sept 18 2007	

I.D. NO.: 070903

MATERIAL: GL/VE

510A - (Uni/SW1810 Rudder Fabric) 8 plies

	WT. in Air SPECIMEN	WT. in H2O SPECIMEN	SPECIFIC GRAVITY	Density (g/cm3)
1	7.8210	3.7494	1.9209	1.9161
2	7.8369	3.7362	1.9111	1.9063
3	7.9398	3.8100	1.9226	1.9178
4	7.4951	3.5835	1.9161	1.9113
5	7.7841	3.7317	1.9209	1.9161
6	8.0349	3.8655	1.9271	1.9223

MEAN 1.9198 1.9150
STD.DEV. 0.0055 0.0055

	CRUCIBLE #	WT. CRICUBLE (g)	WT. FIBER in CRUCIBLE (g)	WT. FIBER (g)	WT. RESIN (g)
1	3	15.9032	20.8788	25.4273	4.9756
2	2	17.3356	22.2732	22.3713	4.9376
3	41	16.8192	21.8798	23.8221	5.0606
4	K	17.5622	22.2987	30.2921	4.7365
5	H	17.9115	22.8701	26.9229	4.9586
6	52	15.2338	20.3759	24.5974	5.1421

	FIBER CONTENT	RESIN CONTENT	FIBER VOL. FRACTION	RESIN VOL. FRACTION	Theoretical Density (g/cm3)
1	63.62	36.38	47.06	51.64	1.941
2	63.00	37.00	46.37	52.24	1.933
3	63.74	36.26	47.19	51.51	1.943
4	63.19	36.81	46.64	52.11	1.936
5	63.70	36.30	47.13	51.52	1.942
6	64.00	36.00	47.50	51.27	1.946
MEAN	63.54	36.46	46.98	51.71	
STD.DEV.	0.37	0.37	0.41	0.38	

	VOID CONTENT	DENSITY OF FIBERS :	2.59
1	1.30	DENSITY OF MATRIX :	1.3500
2	1.39		
3	1.29		
4	1.26		
5	1.36		
6	1.24		
MEAN	1.30	DATE :	Sept 18 2007
STD.DEV.	0.06		

I.D. NO.: 080304

MATERIAL: GL(Uni Mat)(0)/VE(CORVE 8100)

	WT. SPECIMEN (g)	WT. /WIRE & SPEC. in H2O (g)	WT of Spec in H2O (g)	SPECIFIC GRAVITY	Density (g/cm3)
1	8.2039	3.7450	3.7450	1.8399	1.8353
2	7.7688	3.5405	3.5405	1.8373	1.8327
3	7.3643	3.3464	3.3464	1.8329	1.8283
4	7.8045	3.5313	3.5313	1.8264	1.8218
5	7.7809	3.5464	3.5464	1.8375	1.8329
			MEAN	1.8348	1.8302
			STD.DEV.	0.0018	0.0018

	WT. CRUCIBLE (g)	WT. FIBER in CRUCIBLE (g)	WT. FIBER (g)	WT. RESIN (g)
1	15.9752	21.6734	5.6982	2.5057
2	15.7283	21.1083	5.3800	2.3888
3	16.8170	21.8946	5.0776	2.2867
4	15.3987	20.7820	5.3833	2.4212
5	15.6875	21.0546	5.3671	2.4138

	FIBER CONTENT WT%	RESIN CONTENT WT%	FIBER VOL. FRACTION	RESIN VOL. FRACTION
1	69.4572	30.5428	49.9899	49.1710
2	69.2514	30.7486	49.7725	49.4336
3	68.9488	31.0512	49.4347	49.7987
4	68.9769	31.0231	49.2797	49.5776
5	68.9779	31.0221	49.5804	49.8778
MEAN	69.1224	30.8776	49.6115	49.5717
STD.DEV.	0.1456	0.1456	0.1538	0.1856

	VOID CONTENT
1	0.8390
2	0.7940
3	0.7666
4	1.1427
5	0.5418
MEAN	0.8168
STD.DEV.	0.0319

DENSITY OF FIBERS : 2.55

DENSITY OF MATRIX : 1.14

DATE : 4/15/2009

ENGINEER: M.Foley

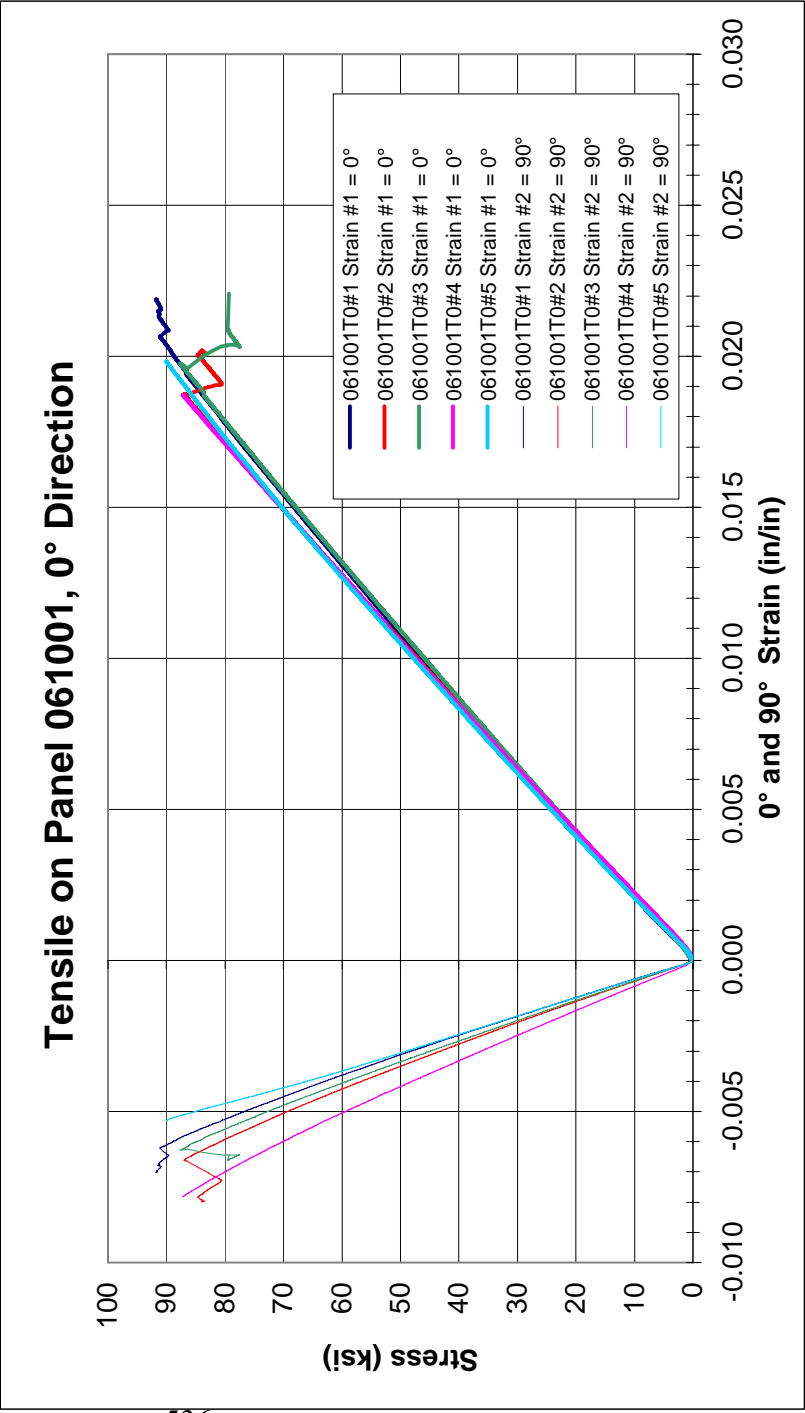
Appendix B

ASTM D638 Tension Test Measurements

Tensile Test ASTM D638, Tested on Panel 061001, 0° Direction

Date	Sample ID	Test #	Width (in.)	Thickness (in.)	Peak Load (lbf)	Tensile Strength (ksi)	Poisson's Ratio (n)	E (MSI) Range of 1000 to 3000in/in	Memo
30-Nov-06	061001T0#1	4338	0.7442	0.2575	17663.2	92.17	0.2922	4.89	Split and delaminated, 4.89 Mpsi
30-Nov-06	061001T0#2	4336	0.7415	0.2580	16639.8	86.98	0.3204	4.86	Split and delaminated, 4.86 Mpsi
30-Nov-06	061001T0#3	4335	0.7442	0.2567	16741.1	87.63	0.3084	4.76	Split and delaminated, 4.76 Mpsi
30-Nov-06	061001T0#4	4344	0.7403	0.2567	16563.8	87.16	0.3897	4.95	Split and delaminated, 5.12 Mpsi / Redo 4.95 Mpsi
30-Nov-06	061001T0#5	4341	0.7465	0.2550	18220.3	95.72	0.2985	5.03	Split and delaminated, 5.03 Mpsi
					AVG	89.93	0.3070	4.84	
					STDEV	3.88	0.014	0.07	
					%COV	4.31	4.62	1.36	

All specimen measured after gaged.

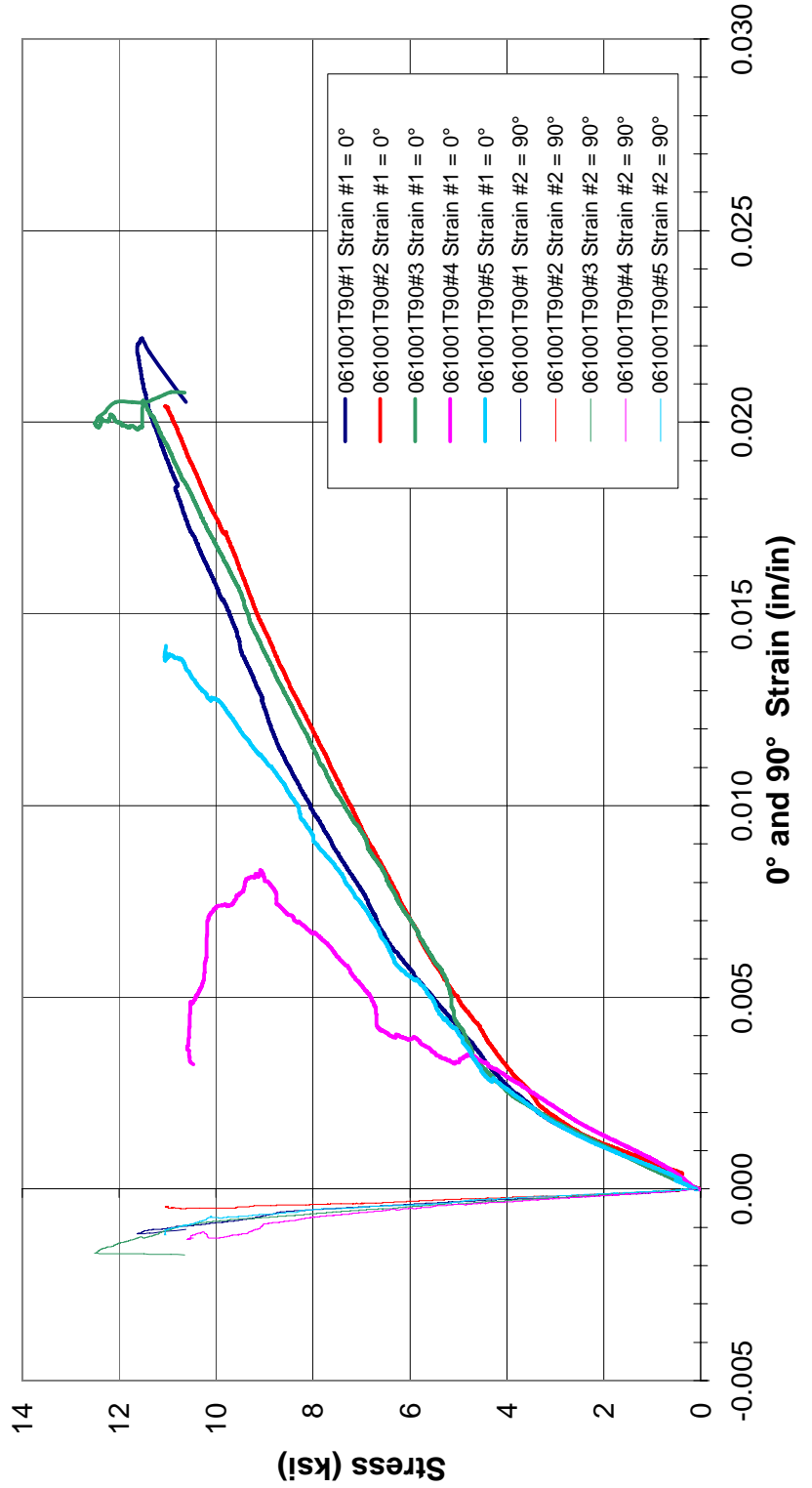


Tensile Test ASTM D638, Tested on Panel 061001, 90° Direction

Date	Sample ID	Test #	Width (in.)	Thickness (in.)	Peak Load (lbf)	Tensile Strength (ksi)	Poisson's Ratio (n)	E(msi) Range of 500 to 1500in/in	Memo
30-Nov-06	061001T90#1	4340	0.7440	0.2570	2224	11.63	0.1289	1.99	Shear in middle, 1.09 mpsi
30-Nov-06	061001T90#2	4339	0.7465	0.2568	2117	11.04	0.0837	1.83	Shear in middle, 0.81 mpsi
30-Nov-06	061001T90#3	4334	0.7487	0.2592	2426	12.50	0.1241	1.61	Shear in middle, 1.09 mpsi
30-Nov-06	061001T90#4	4344	0.7450	0.2560	2021	10.60	0.1252	1.54	Shear in middle, 1.26 mpsi
30-Nov-06	061001T90#5	4337	0.7478	0.2473	2046	11.06	0.1049	1.74	Shear in middle, 1.09 mpsi
					AVG	11.37	0.1122	1.81	
					STDEV	0.73	0.025	0.19	
					%COV	6.45	22.15	10.68	

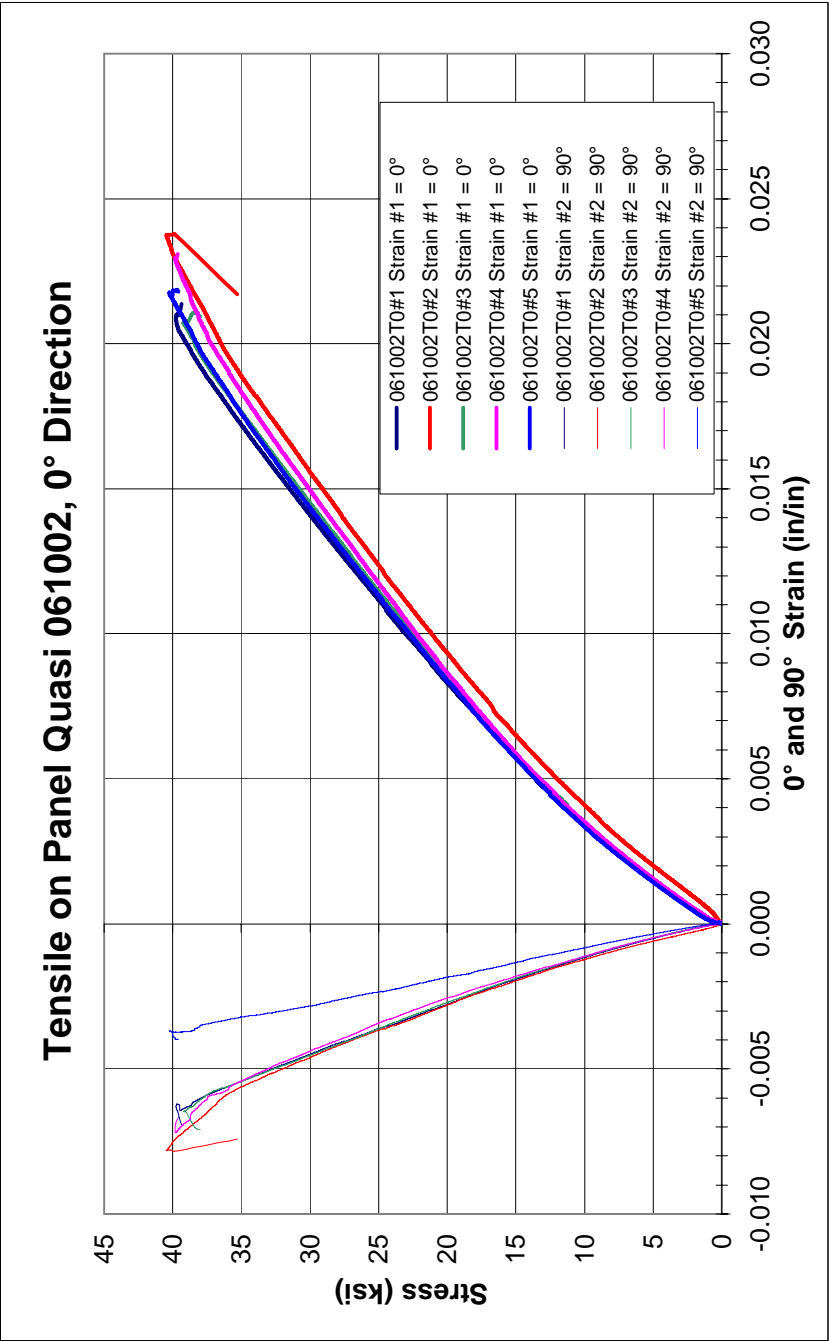
All specimen measured after gaged.

Tensile on Panel 061001, 90° Direction



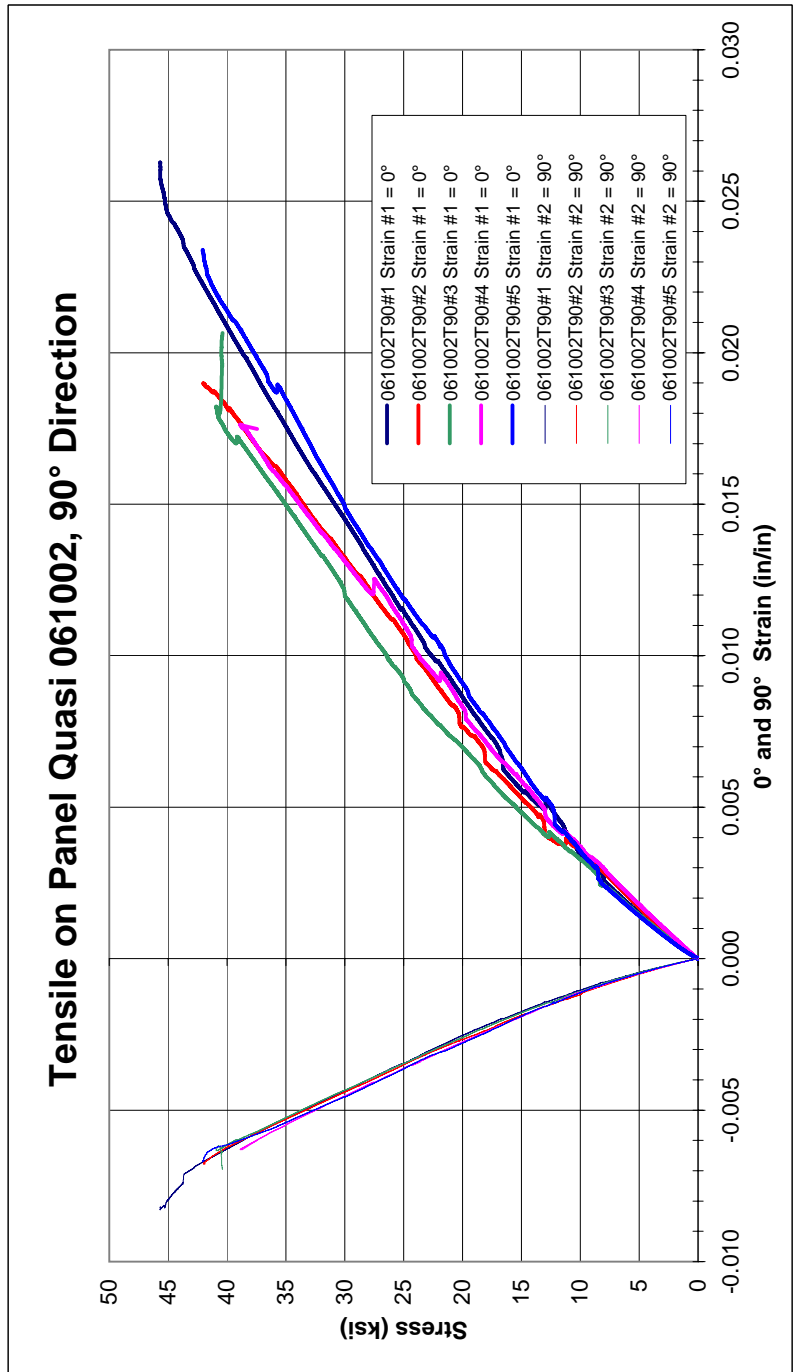
Tensile Test ASTM D638, Tested on Panel Quasi 061002, 0° Direction

Date	Sample ID	Test #	Width (in.)	Thickness (in.)	Peak Load (lbf)	Tensile Strength (ksi)	Poisson's Ratio (n)	E (MSI) Range of 1000 to 3000in/in	Memo
5-Nov-06	061002T0#1	4348	0.7509	0.2162	6456.87	39.77	0.3398	2.72	
5-Nov-06	061002T0#2	4346	0.7509	0.2164	6578.04	40.48	0.3045	2.66	
5-Nov-06	061002T0#3	4350	0.7519	0.2166	6389.98	39.25	0.3307	2.69	
5-Nov-06	061002T0#4	4349	0.7516	0.2131	6381.39	39.84	0.3175	2.73	
5-Nov-06	061002T0#5	4347	0.7509	0.2187	6611.68	40.26	0.2492	2.80	
					AVG	39.92	0.3250	2.69	
					STDEV	0.48	0.018	0.03	
					%COV	1.20	5.63	1.09	



Tensile Test ASTM D638, Tested on Panel Quasi 061002, 90° Direction

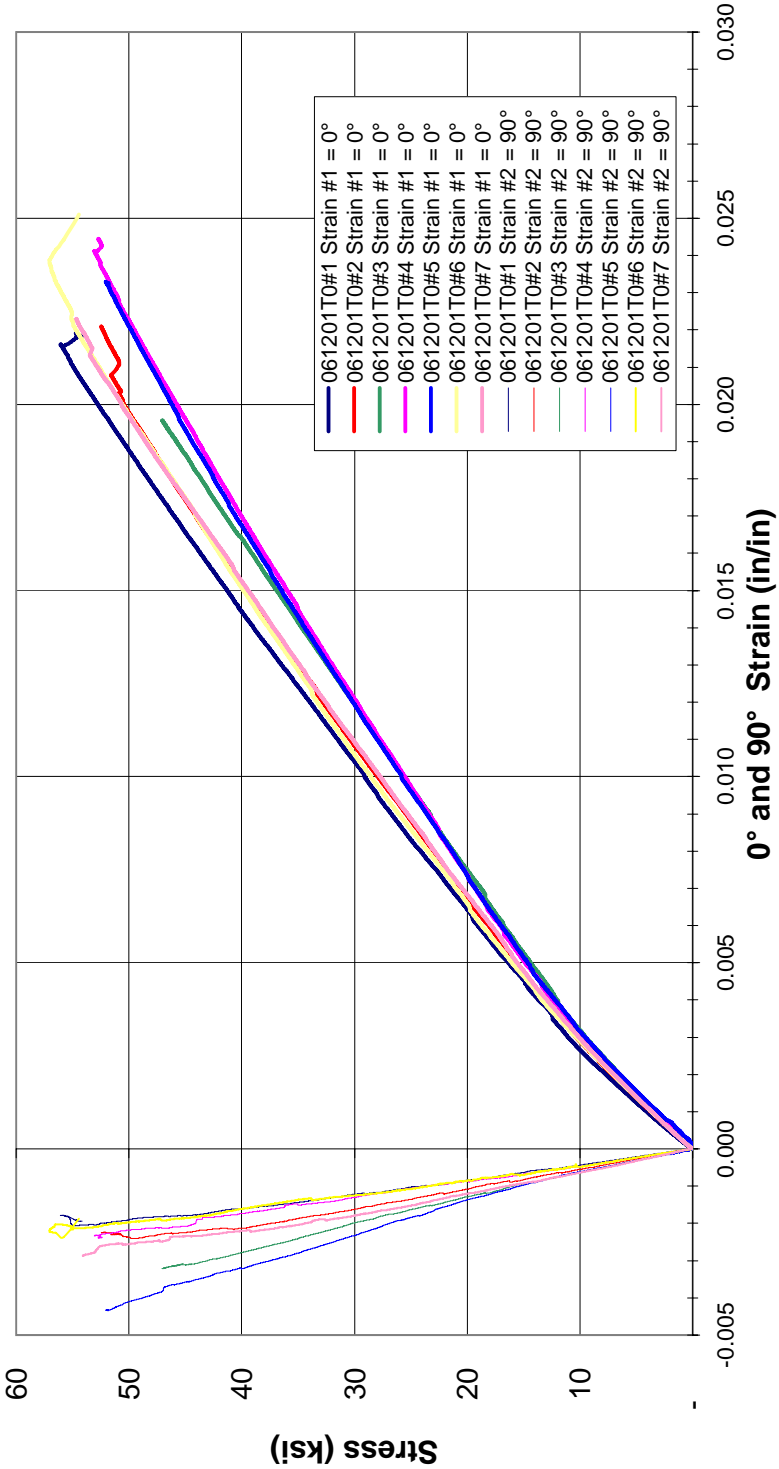
Date	Sample ID	Test #	Width (in.)	Thickness (in.)	Peak Load (lbf)	Tensile Strength (ksi)	Poisson's Ratio (n)	E (MSI) Range of 1000 to 3000in/in	Memo
5-Nov-06	061002T90#1	4355	0.7500	0.2128	7290.36	45.68	0.308	2.98	
5-Nov-06	061002T90#2	4357	0.7500	0.2227	7017.63	42.02	0.307	2.65	
5-Nov-06	061002T90#3	4353	0.7494	0.2159	6620.54	40.92	0.343	3.13	
5-Nov-06	061002T90#4	4356	0.7515	0.2198	6423.37	38.89	0.293	2.68	
5-Nov-06	061002T90#5	4354	0.7530	0.2188	6932.99	42.08	0.347	3.03	
					AVG	41.92	0.319	2.92	
					STDEV	2.47	0.02	0.24	
					%COV	5.89	6.43	8.38	



Tensile Test ASTM D638, Tested on Panel Cross Ply 061201, 0° Direction

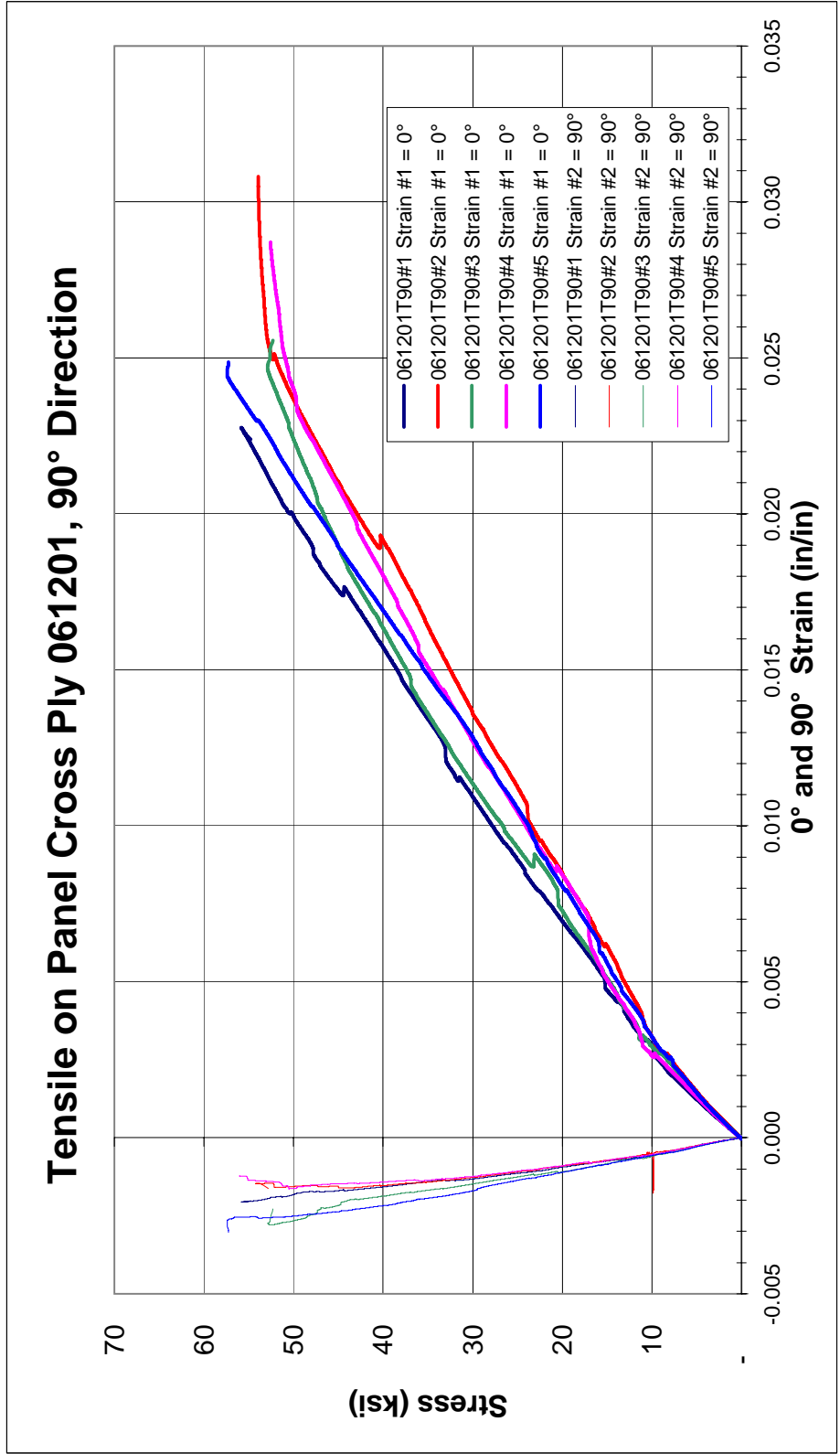
Date	Sample ID	Test #	Width (in.)	Thickness (in.)	Peak Load (lbf)	Tensile Strength (ksi)	Poisson's Ratio (v)	E (MSI) Range of 1000 to 3000in/in	Comments (Failure Location)
27-Feb-07	061201T0#1	4511	0.7553	0.2165	9,165.81	56.05	0.1587	3.53	Top Radius
27-Feb-07	061201T0#2	4512	0.7526	0.2198	8,677.53	52.46	0.1884	3.35	Top Radius
27-Feb-07	061201T0#3	4514	0.7545	0.2216	7,864.48	47.04	0.1956	3.11	Bottom Radius
27-Feb-07	061201T0#4	4515	0.7561	0.2186	8,770.74	53.06	0.1519	3.15	Middle of Gage Length
27-Feb-07	061201T0#5	4516	0.7542	0.2162	8,485.88	52.04	0.1941	3.24	Bottom Radius
1-Mar-07	061201T0#6	4522	0.7452	0.2144	9,116.70	57.06	0.1638	3.33	Middle of Gage Length
1-Mar-07	061201T0#7	4523	0.7439	0.2178	8,859.09	54.68	0.1793	3.26	Bottom Radius
					AVG	53.20	0.1760	3.28	
					STDEV	3.29	0.018	0.14	
					%COV	6.19	10.13	4.26	

Tensile on Panel Cross Ply 061201, 0° Direction



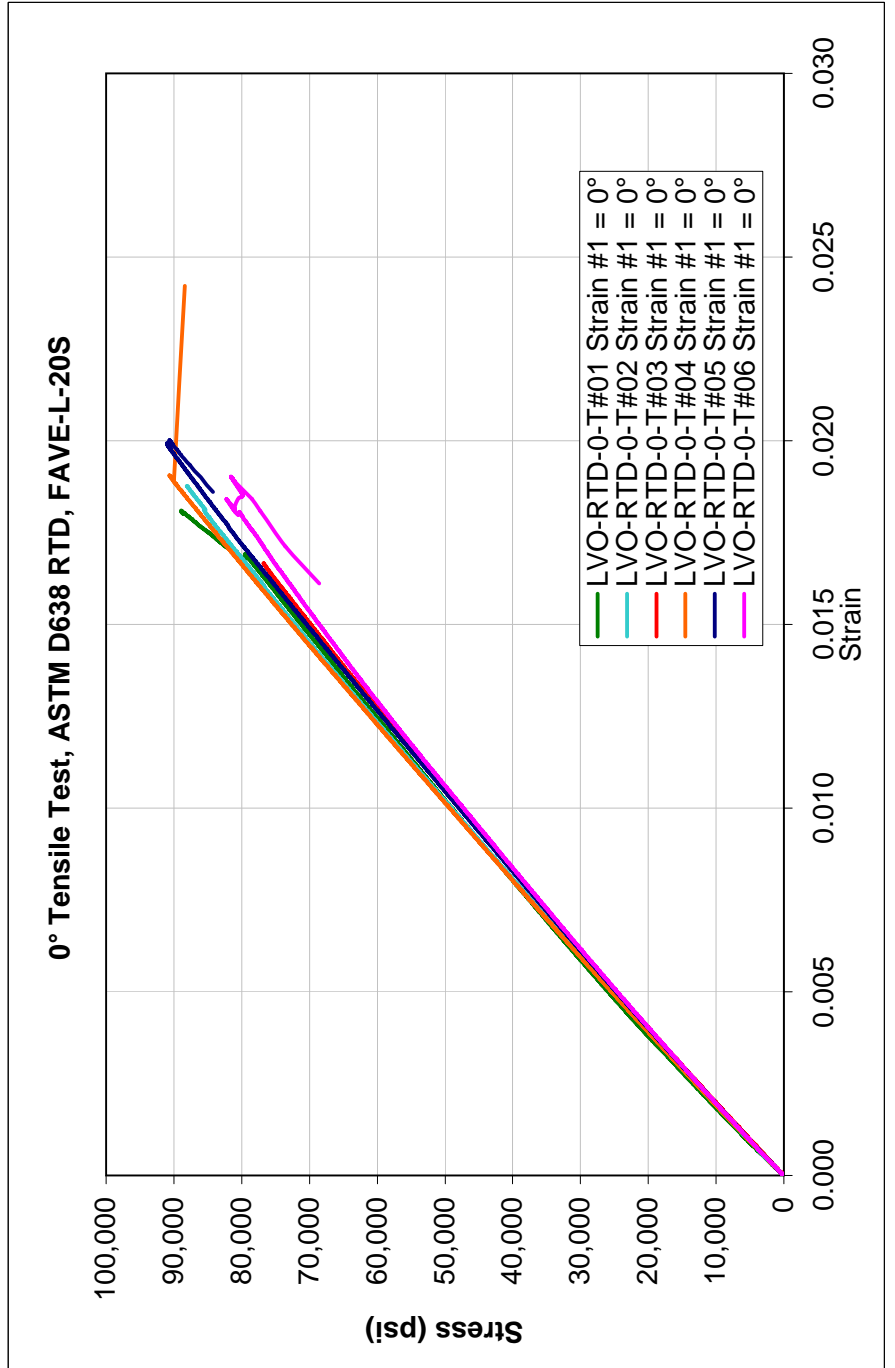
Tensile Test ASTM D638, Tested on Panel Cross Ply 061201, 90° Direction

Date	Sample ID	Test #	Width (in.)	Thickness (in.)	Peak Load (lbf)	Tensile Strength (ksi)	Poisson's Ratio (ν)	E (MSI) Range of 1000 to 3000in/in	Comments (Failure Location)
1-Mar-07	061201T90#1	4517	0.7450	0.2119	8,814.45	55.84	0.1942	3.26	Bottom Radius
1-Mar-07	061201T90#2	4518	0.7453	0.2142	8,656.38	54.22	0.1541	2.99	Middle of Gage Length
1-Mar-07	061201T90#3	4519	0.7417	0.2161	8,480.22	52.91	0.1983	3.18	Middle of Gage Length
1-Mar-07	061201T90#4	4520	0.7472	0.2176	9,210.80	56.65	0.2037	3.57	Bottom Radius
1-Mar-07	061201T90#5	4521	0.7426	0.2171	9,255.60	57.41	0.1738	2.87	Middle of Gage Length
					AVG	55.41	0.1848	3.17	
					STDEV	1.83	0.021	0.27	
					%COV	3.30	11.12	8.51	



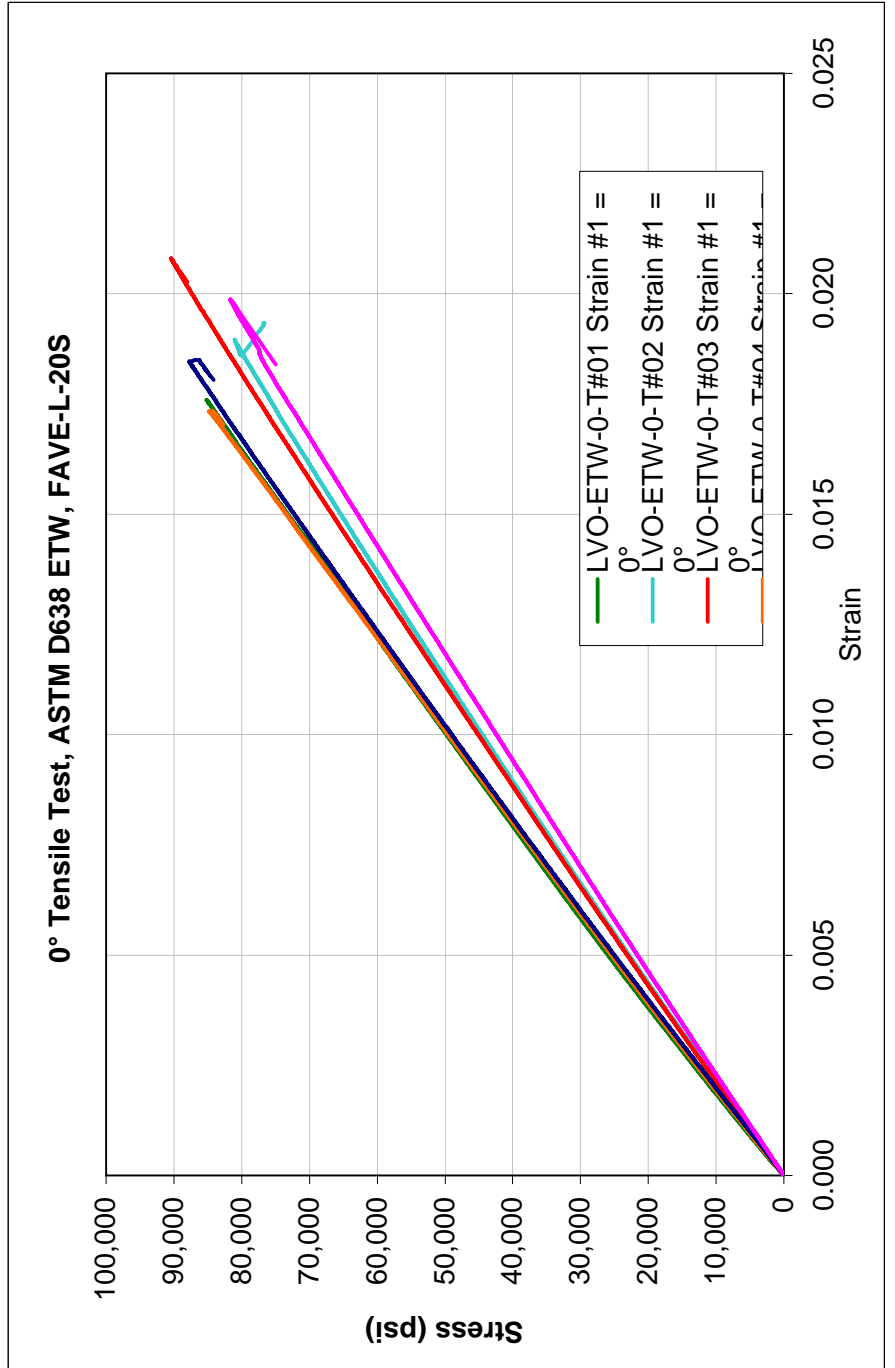
0° Tensile Test, ASTM D638 RTD, FAVE-L-20S

Date	Sample ID	Test #	Width (in.)	Thickness (in.)	Peak Load (lbf)	Tensile Strength (ksi)	E (MSI) Range of 1000 to 3000in/in
26-Jul-07	LVO-RTD-0-T#01	4677	0.7439	0.2117	14,014	88.98	5.17
31-Jul-07	LVO-RTD-0-T#02	4684	0.7493	0.2034	13,422	88.07	5.04
31-Jul-07	LVO-RTD-0-T#03	4685	0.7421	0.2072	14,364	93.39	4.98
31-Jul-07	LVO-RTD-0-T#04	4686	0.7429	0.2135	14,375	90.64	5.08
31-Jul-07	LVO-RTD-0-T#05	4687	0.7445	0.2037	13,815	91.07	4.96
31-Jul-07	LVO-RTD-0-T#06	4688	0.7425	0.2236	13,648	82.21	4.92
					AVG	89.06	5.03
					STDEV	3.82	0.09
					%COV	4.29	1.80



0° Tensile Test, ASTM D638 ETW, FAVE-L-20S

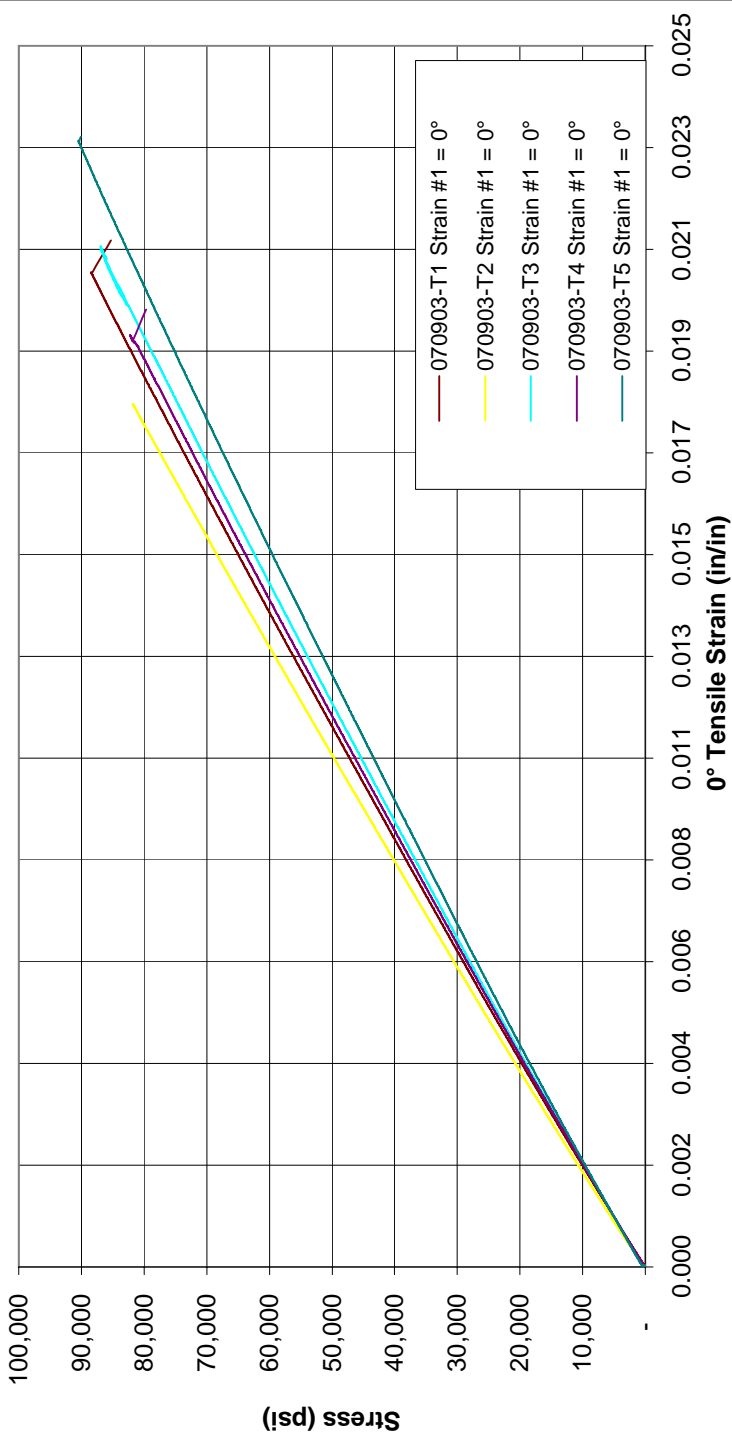
Date	Sample ID	Test #	Width (in.)	Thickness (in.)	Peak Load (lbf)	Tensile Strength (ksi)	E (MSI) Range of 1000 to 3000in/in
26-Jul-07	LVO-ETW-0-T#01	4678	0.7410	0.2005	12,655	85.16	5.19
26-Jul-07	LVO-ETW-0-T#02	4679	0.7491	0.2240	13,602	81.06	4.61
26-Jul-07	LVO-ETW-0-T#03	4680	0.7445	0.2081	14,007	90.43	4.66
26-Jul-07	LVO-ETW-0-T#04	4681	0.7445	0.2069	13,058	84.79	5.12
26-Jul-07	LVO-ETW-0-T#05	4682	0.7476	0.2128	13,953	87.70	5.04
26-Jul-07	LVO-ETW-0-T#06	4683	0.7471	0.2160	13,187	81.70	4.35
					AVG	85.14	4.83
					STDEV	3.55	0.33
					%COV	4.17	6.92



0° Tension Test, ASTM D695, ESTCP, EGlass/510A Resin

Date	Sample ID	Test #	Width (in.)	Thickness (in.)	Peak Load (lbf)	Tensile Strength (ksi)	E (MSI) Range of 1000 to 3000in/in	Memo
3-Oct-07	LV070903-0-T-#01	4769	0.7487	0.2438	16148	88.48	4.70	
3-Oct-07	LV070903-0-T-#02	4770	0.7598	0.2452	15235	81.78	4.87	
3-Oct-07	LV070903-0-T-#03	4771	0.7507	0.2538	16567	86.96	4.49	
3-Oct-07	LV070903-0-T-#04	4772	0.7608	0.2430	15207	82.25	4.56	
3-Oct-07	LV070903-0-T-#05	4773	0.7618	0.2487	17153	90.52	4.31	
					AVG	86.00	4.58	
					STDEV	3.86	0.21	
					%COV	4.48	4.60	

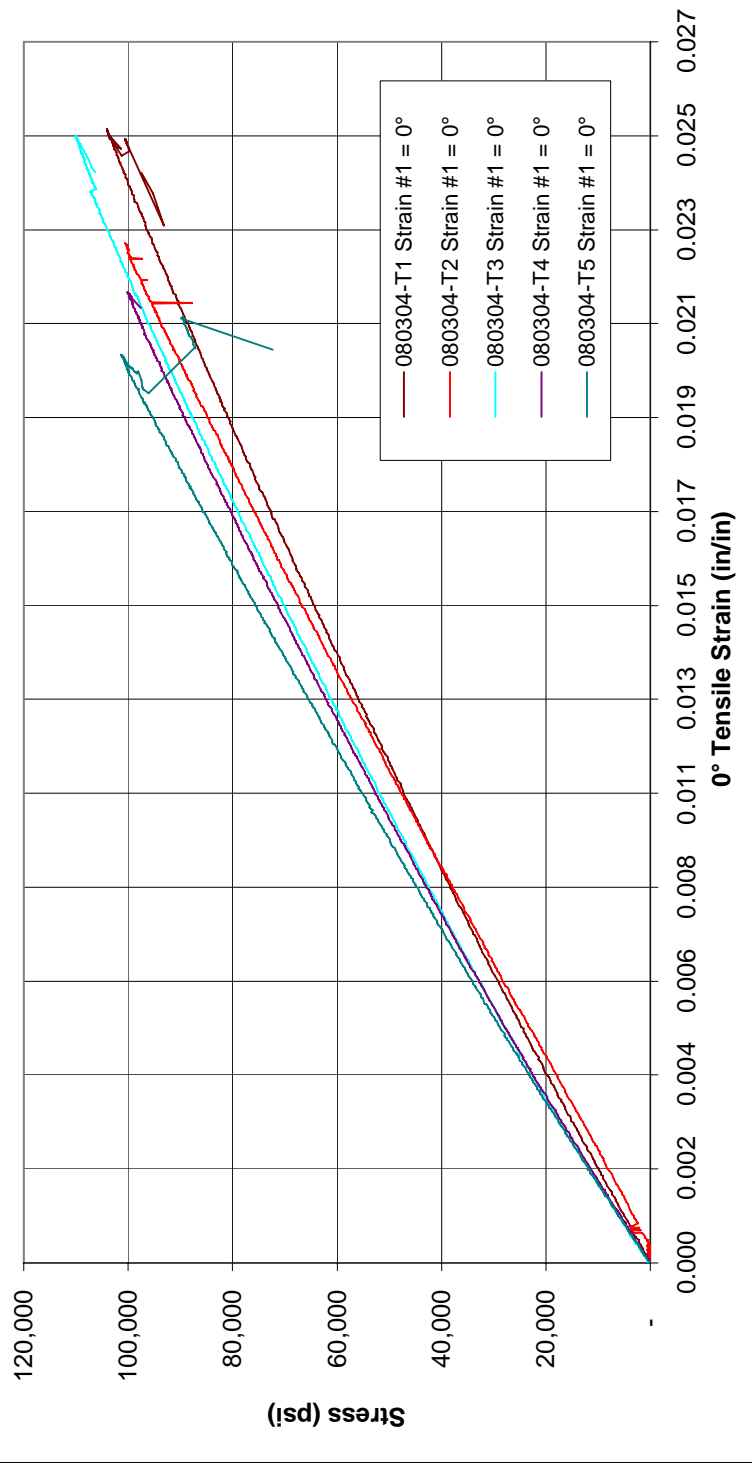
0° Tension Test, ASTM D695, ESTCP, EGlass/510A Resin



0° Tension Test, ASTM D695, ESTCP, EGlass/8100 Resin

Date	Sample ID	Test #	Width (in.)	Thickness (in.)	Peak Load (lbf)	Tensile Strength (ksi)	E (MSI) Range of 1000 to 3000in/in	Memo
27-Mar-09	080304 0° T #1	1	0.7360	0.2567	19,658	104.05	4.71	
27-Mar-09	080304 0° T #2	2	0.7345	0.2575	19,022	100.57	4.62	
27-Mar-09	080304 0° T #3	3	0.7352	0.2552	20,654	110.08	5.39	
27-Mar-09	080304 0° T #4	4	0.7365	0.2680	19,775	100.19	5.36	
27-Mar-09	080304 0° T #5	5	0.7388	0.2468	18,475	101.32	5.46	
					AVG	103.24	5.11	
					STDEV	4.11	0.41	
					%COV	3.98	7.95	

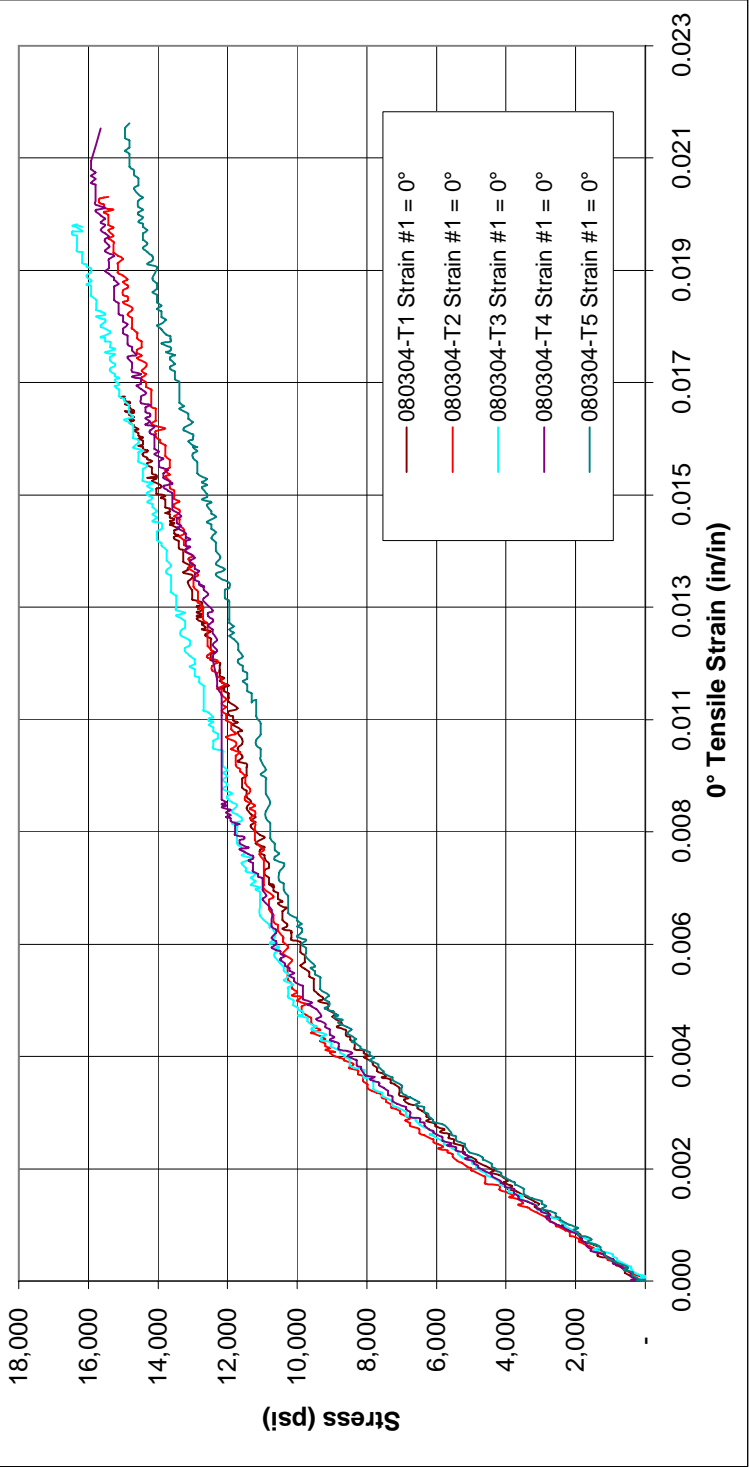
0° Tension Test, ASTM D695, ESTCP, EGlass/8100 Resin



90° Tension Test, ASTM D695, ESTCP, EGlass/8100 Resin

Date	Sample ID	Test #	Width (in.)	Thickness (in.)	Peak Load (lbf)	Tensile Strength (ksi)	E (MSI) Range of 1000 to 3000in/in	Memo
27-Mar-09	080304 90° T #1	6	0.7392	0.2553	2846	15.08	1.98	
27-Mar-09	080304 90° T #2	7	0.7362	0.2452	2832	15.69	2.21	
27-Mar-09	080304 90° T #3	8	0.7337	0.2467	2979	16.46	2.20	
27-Mar-09	080304 90° T #4	9	0.7458	0.2533	3007	15.91	2.07	
27-Mar-09	080304 90° T #5	10	0.7392	0.2538	2804	14.95	1.97	
					AVG	15.62	2.09	
					STDEV	0.62	0.12	
					%COV	3.97	5.52	

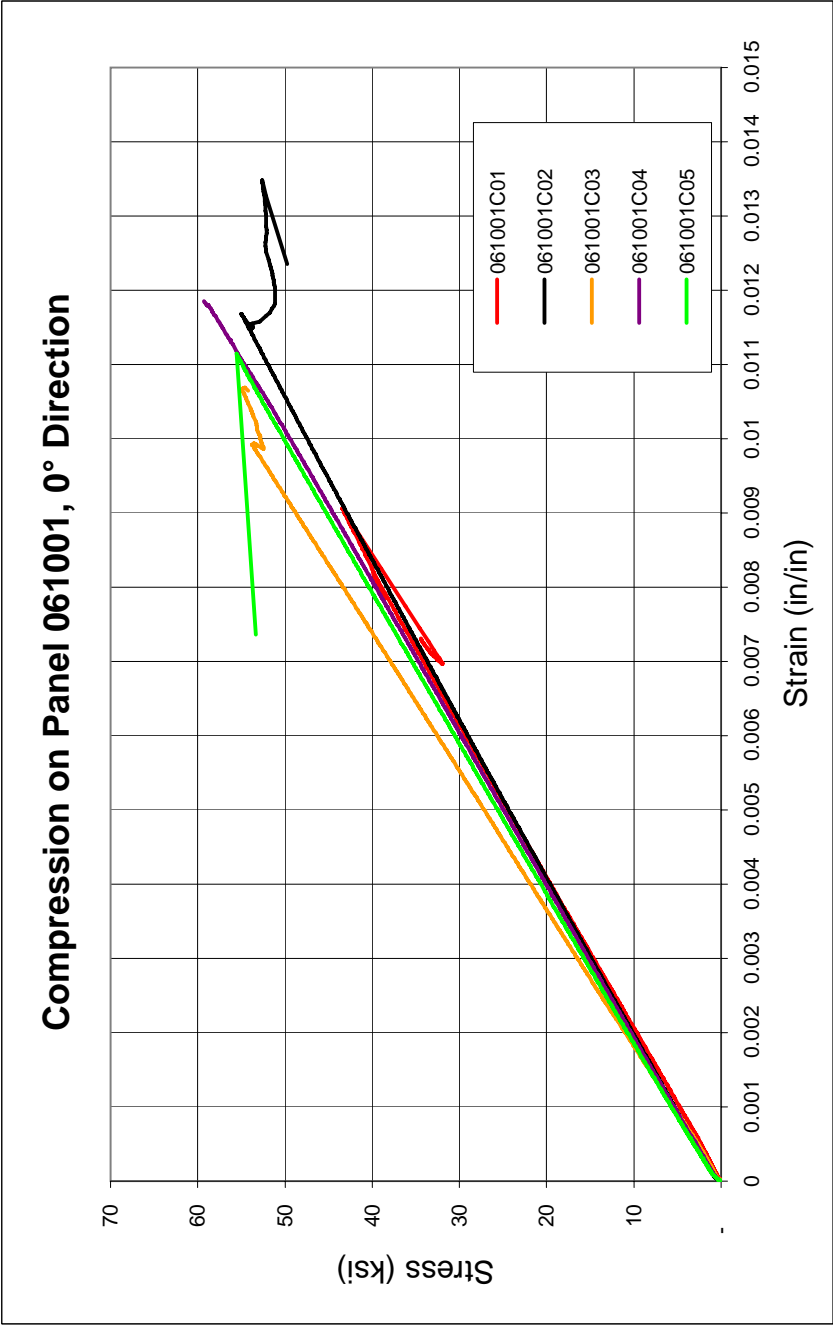
90° Tension Test, ASTM D695, ESTCP, EGlass/8100 Resin



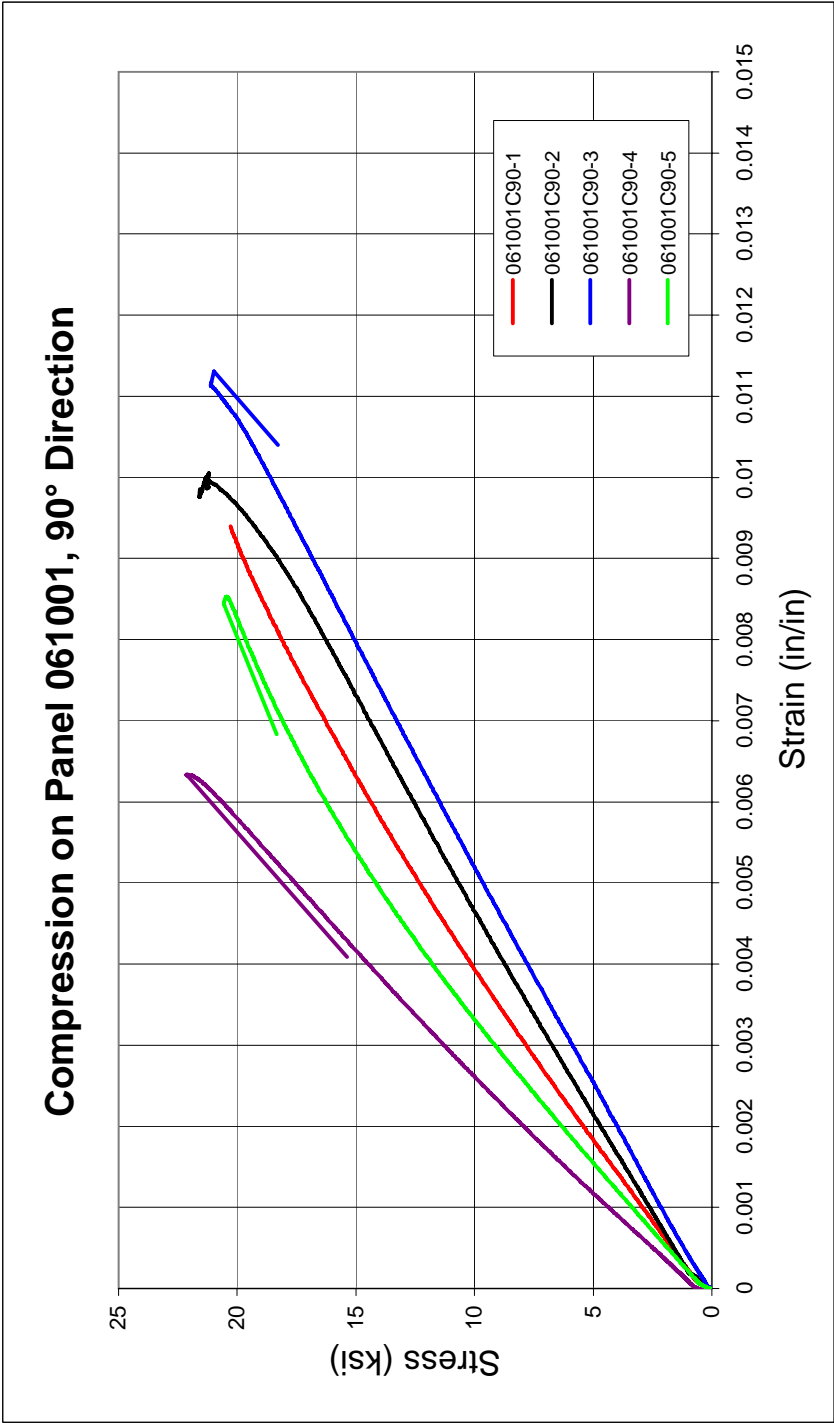
Appendix C

ASTM D695 Compression Test Measurements

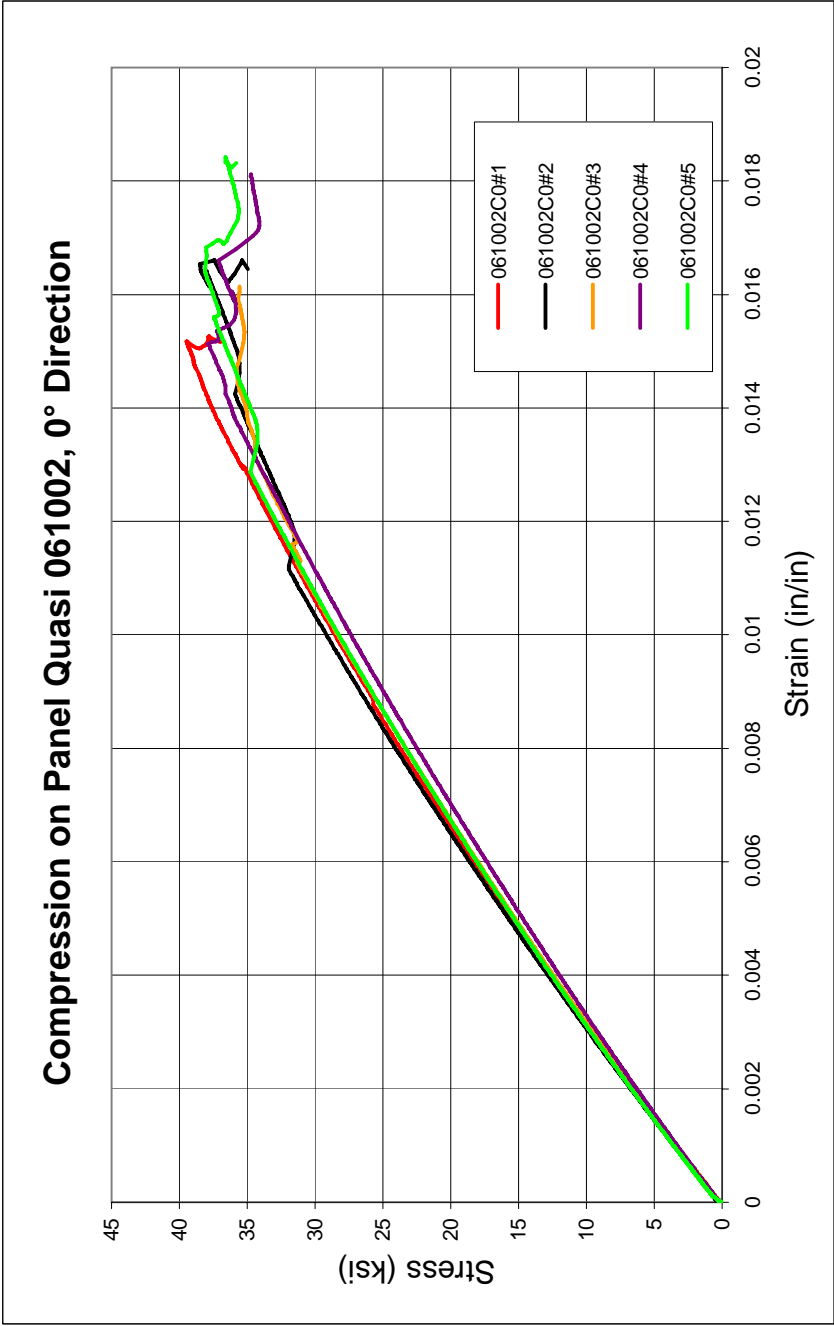
Compression on Panel 061001, 0° Direction									
Date	Sample ID	Data #	Width (in.)	Thickness (in.)	Peak Load (lbf)	Strength (ksi)	E(msi) Range of 1000 to 3000in/in	Memo	
6-Nov-06	061001C01	4323	0.5023	0.2667	5819.86	43.43	4.945	Crushed top & bottom, 4.95 Mpsi	
6-Nov-06	061001C02	4325	0.5007	0.2622	7221.34	55.00	4.782	Crushed top and split middle, 4.75 Mpsi	
6-Nov-06	061001C03	4332	0.5003	0.2575	7074.12	54.92	5.503	Crushed top & bottom, 5.46 Mpsi	
6-Nov-06	061001C04	4329	0.5065	0.2590	7780.64	59.30	4.910	Split in center, 4.91 Mpsi	
6-Nov-06	061001C05	4327	0.5045	0.2653	7433.30	55.56	5.002	Split in center, 4.99 Mpsi	
				AVG	7066	53.64	5.028		
				STDEV	745	5.99	0.277		
				%COV	10.55	11.16	5.51		



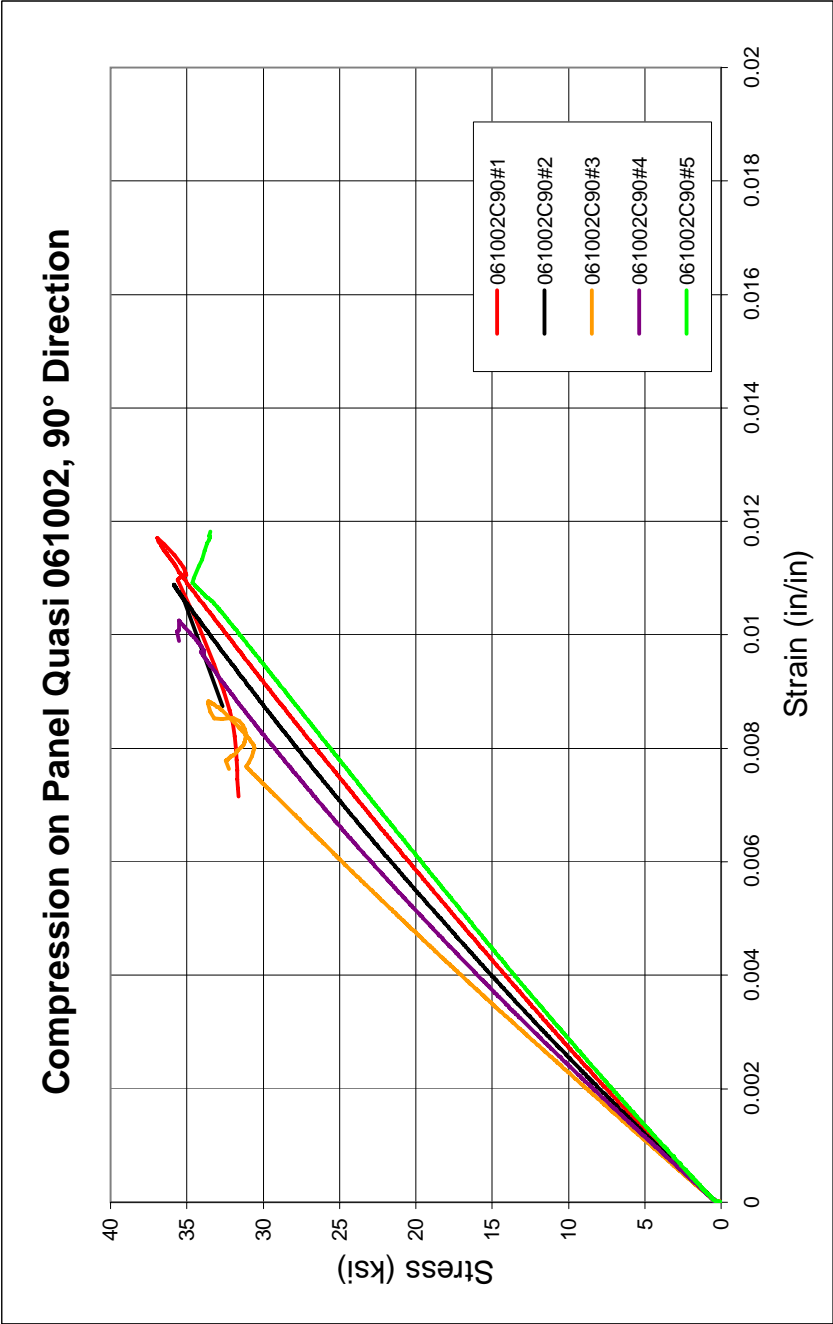
Compression on Panel 061001, 90° Direction									
Date	Sample ID	Data #	Width (in.)	Thickness (in.)	Peak Load (lbf)	Strength (ksi)	E(msi) Range of 1000 to 3000in/in	Memo	
6-Nov-06	061001C90-1	4325	0.4983	0.2535	2561.84	20.28	2.472	Split lower part from middle, 2.47 Mpsi	
6-Nov-06	061001C90-2	4325	0.5053	0.2660	2903.40	21.60	2.062	Split and delaminated middle part, 2.04 Mpsi	
6-Nov-06	061001C90-3	4330	0.5063	0.2538	2713.27	21.11	1.858	Split in center, 1.87 Mpsi	
6-Nov-06	061001C90-4	4328	0.5018	0.2585	2872.00	22.14	3.462	Split in center, 3.30 Mpsi	
6-Nov-06	061001C90-5	4331	0.5032	0.2612	2701.42	20.56	2.899	Split in center, 2.90 Mpsi	
				AVG	2750	21.14	2.551		
				STDEV	139	0.76	0.648		
				%COV	5.06	3.58	25.39		



Compression on Panel Quasi 061002, 0° Direction								
Date	Sample ID	Data #	Width (in.)	Thickness (in.)	Peak Load (lbf)	Strength (psi)	E(msi) Range of 1000 to 3000in/in	Memo
6-Nov-06	061002C0#1	4360	0.5082	0.2147	4306.14	39.47	3.110	
6-Nov-06	061002C0#2	4366	0.5100	0.2114	4149.29	38.49	3.133	
6-Nov-06	061002C0#3	4367	0.5063	0.2183	3955.84	35.80	3.073	
6-Nov-06	061002C0#4	4359	0.5051	0.2180	4168.58	37.86	2.935	
6-Nov-06	061002C0#5	4362	0.5053	0.2144	4128.96	38.13	3.053	
				AVG	4142	37.95	3.061	
				STDEV	125	1.35	0.077	
				%COV	3.02	3.55	2.51	



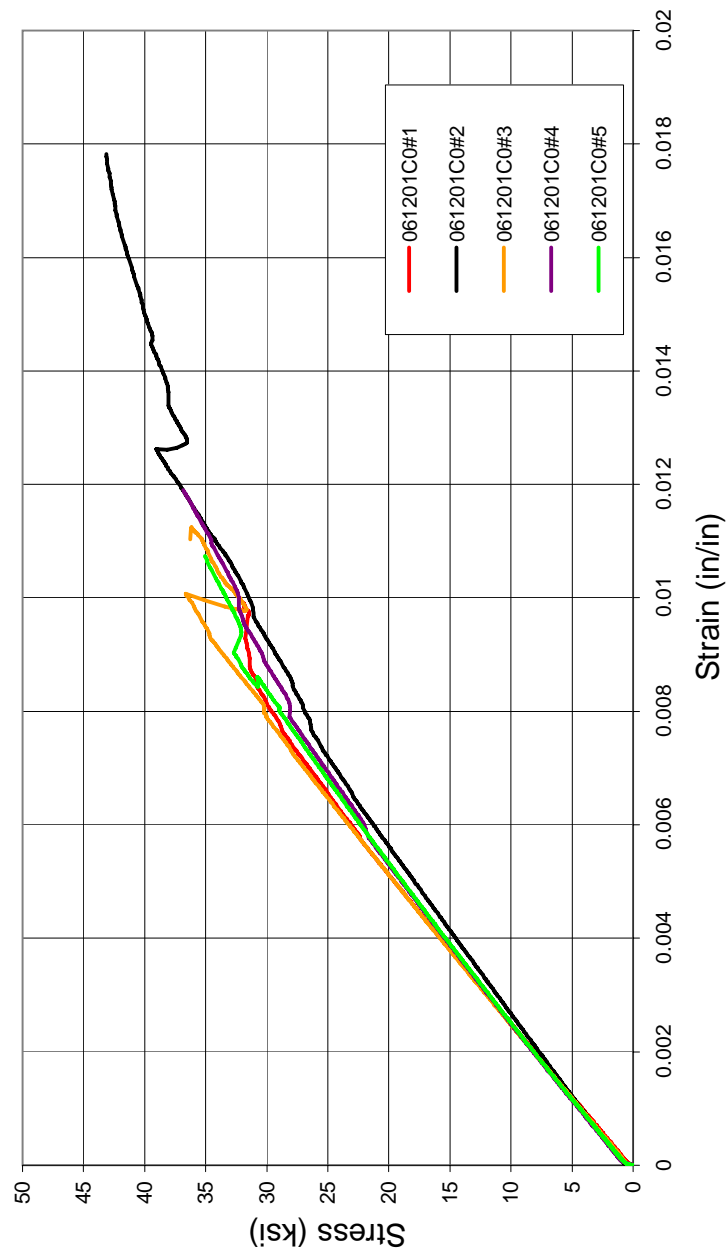
Compression on Panel Quasi 061002, 90° Direction									
Date	Sample ID	Data #	Width (in.)	Thickness (in.)	Peak Load (lbf)	Strength (ksi)	E(msi) Range of 1000 to 3000in/in	Memo	
6-Nov-06	061002C90#1	4363	0.5090	0.2163	4067.80	36.95	3.439		
6-Nov-06	061002C90#2	4365	0.5052	0.2186	3958.62	35.86	3.693		
6-Nov-06	061002C90#3	4364	0.5055	0.2139	3633.35	33.61	4.176		
6-Nov-06	061002C90#4	4359	0.5052	0.2198	3926.12	35.66	3.937		
6-Nov-06	061002C90#5	4362	0.5072	0.2185	3835.35	34.62	3.293		
				AVG	3884	35.34	3.708		
				STDEV	163	1.27	0.359		
				%COV	4.20	3.60	9.69		



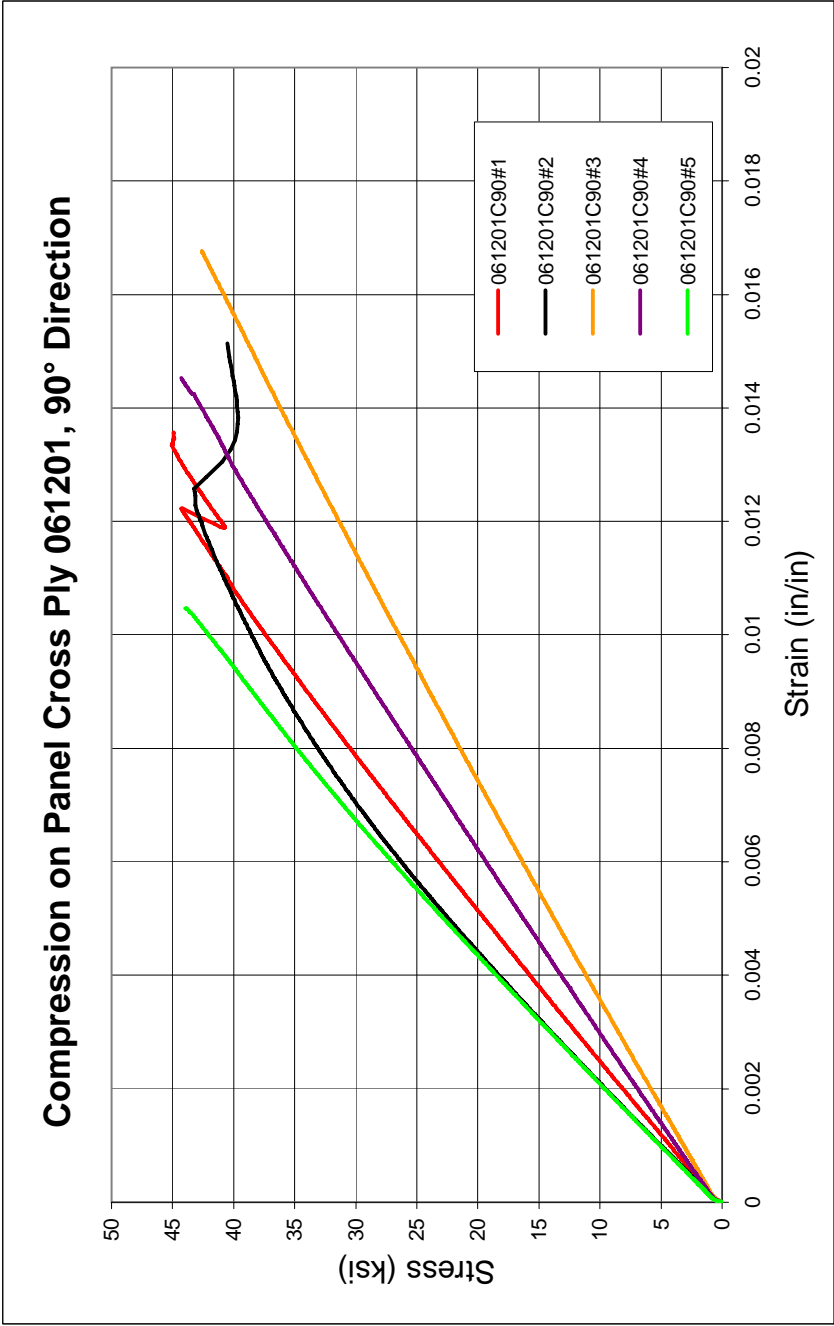
Compression on Panel Cross Ply 061201, 0° Direction

Date	Sample ID	Data #	Width (in.)	Thickness (in.)	Peak Load (lbf)	Strength (ksi)	E(msi) Range of 1000 to 3000in/in	Memo
6-Mar-06	061201C0#1	4531	0.5036	0.2164	3648.01	33.47	3.883	Middle
6-Mar-06	061201C0#2	4532	0.5037	0.2174	4721.00	43.11	3.447	Above Middle
6-Mar-06	061201C0#3	4533	0.5025	0.2147	3952.15	36.63	3.869	Middle
6-Mar-06	061201C0#4	4534	0.5080	0.2196	4112.19	36.85	3.649	Middle
6-Mar-06	061201C0#5	4535	0.5090	0.2176	3885.09	35.06	3.703	Middle
				AVG	4064	37.02	3.710	
				STDEV	404	3.67	0.179	
				%COV	9.93	9.90	4.83	

Compression on Panel Cross Ply 061201, 0° Direction

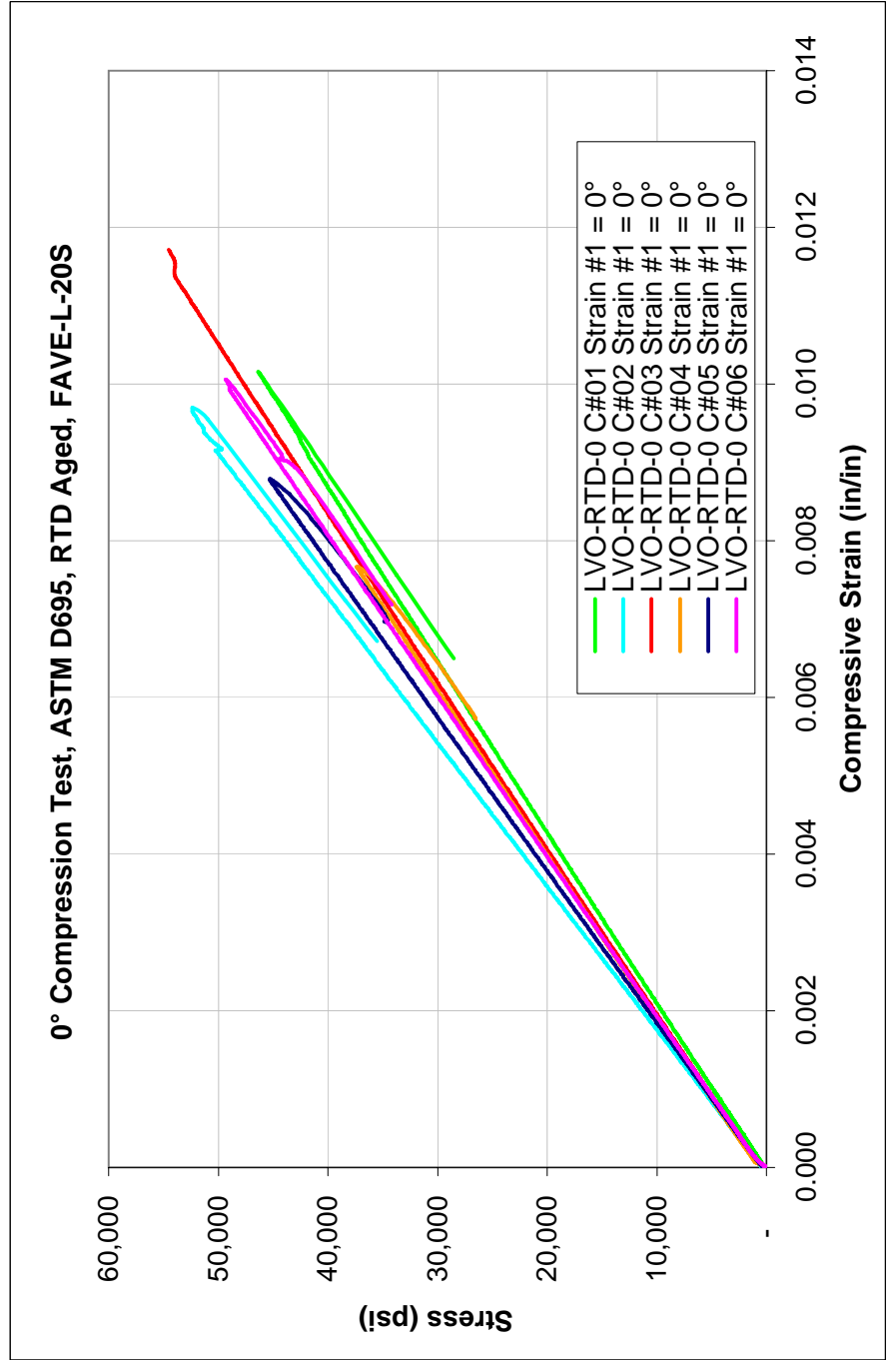


Compression on Panel Cross Ply 061201, 90° Direction									
Date	Sample ID	Data #	Width (in.)	Thickness (in.)	Peak Load (lbf)	Strength (psi)	E(msi) Range of 1000 to 3000in/in	Memo	
6-Mar-06	061201C90#1	4536	0.4977	0.2207	4946.94	45.05	3.863	Middle	
6-Mar-06	061201C90#2	4537	0.5052	0.2143	4682.15	43.23	4.495	Middle	
6-Mar-06	061201C90#3	4538	0.4945	0.2202	4639.34	42.60	2.680	Middle	
6-Mar-06	061201C90#4	4539	0.4957	0.2187	4802.81	44.31	3.172	Middle	
6-Mar-06	061201C90#5	4540	0.4937	0.2143	4649.97	43.95	4.496	Middle	
				AVG	4744	43.83	3.741		
				STDEV	131	0.95	0.806		
				%COV	2.75	2.17	21.56		



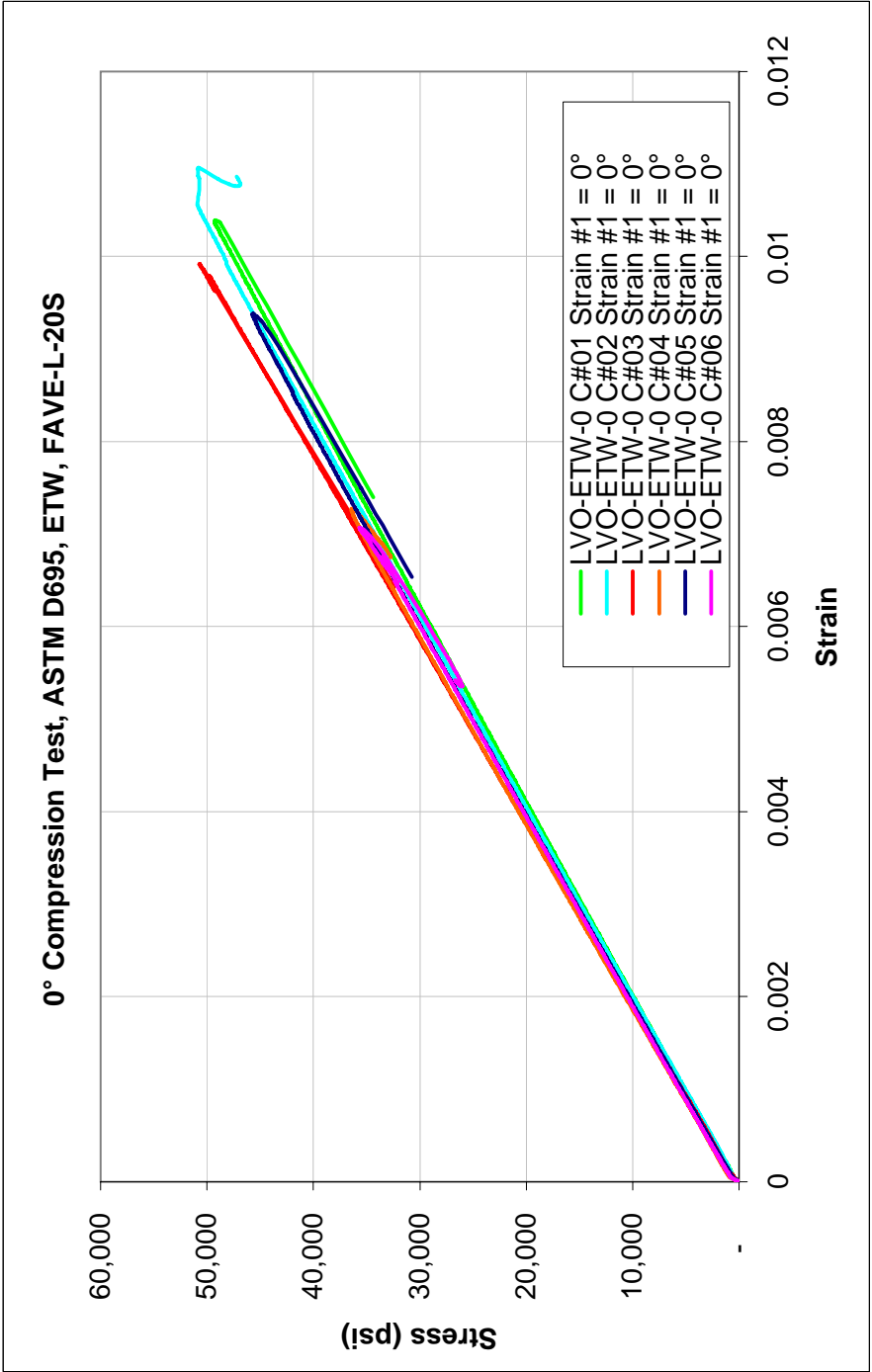
0° Compression Test, ASTM D695, RTD Aged, FAVE-L-20S

Date	Sample ID	Test #	Width (in.)	Thickness (in.)	Peak Load (lbf)	Tensile Strength (ksi)	E (MSI) Range of 1000 to 3000in/in	Memo
25-Jul-07	LVO-RTD-0 C#01	4664	0.5036	0.2148	5,013	46.33	4.65	Crushed Top of Specimen
25-Jul-07	LVO-RTD-0 C#02	4665	0.4958	0.2037	5,290	52.38	5.46	Crushed Top of Specimen
25-Jul-07	LVO-RTD-0 C#03	4666	0.4943	0.2147	6,515	54.53	4.80	Crushed Top of Specimen
25-Jul-07	LVO-RTD-0 C#04	4667	0.4986	0.2214	6,308	37.36	4.83	Crushed Top of Specimen
25-Jul-07	LVO-RTD-0 C#05	4668	0.5011	0.2019	7,024	45.31	5.18	Shear in Middle of Specimen
25-Jul-07	LVO-RTD-0 C#06	4669	0.4871	0.2284	5,492	49.34	4.93	Crushed Top of Specimen
					AVG	47.54	4.98	
					STDEV	6.09	0.30	
					%COV	12.81	5.95	

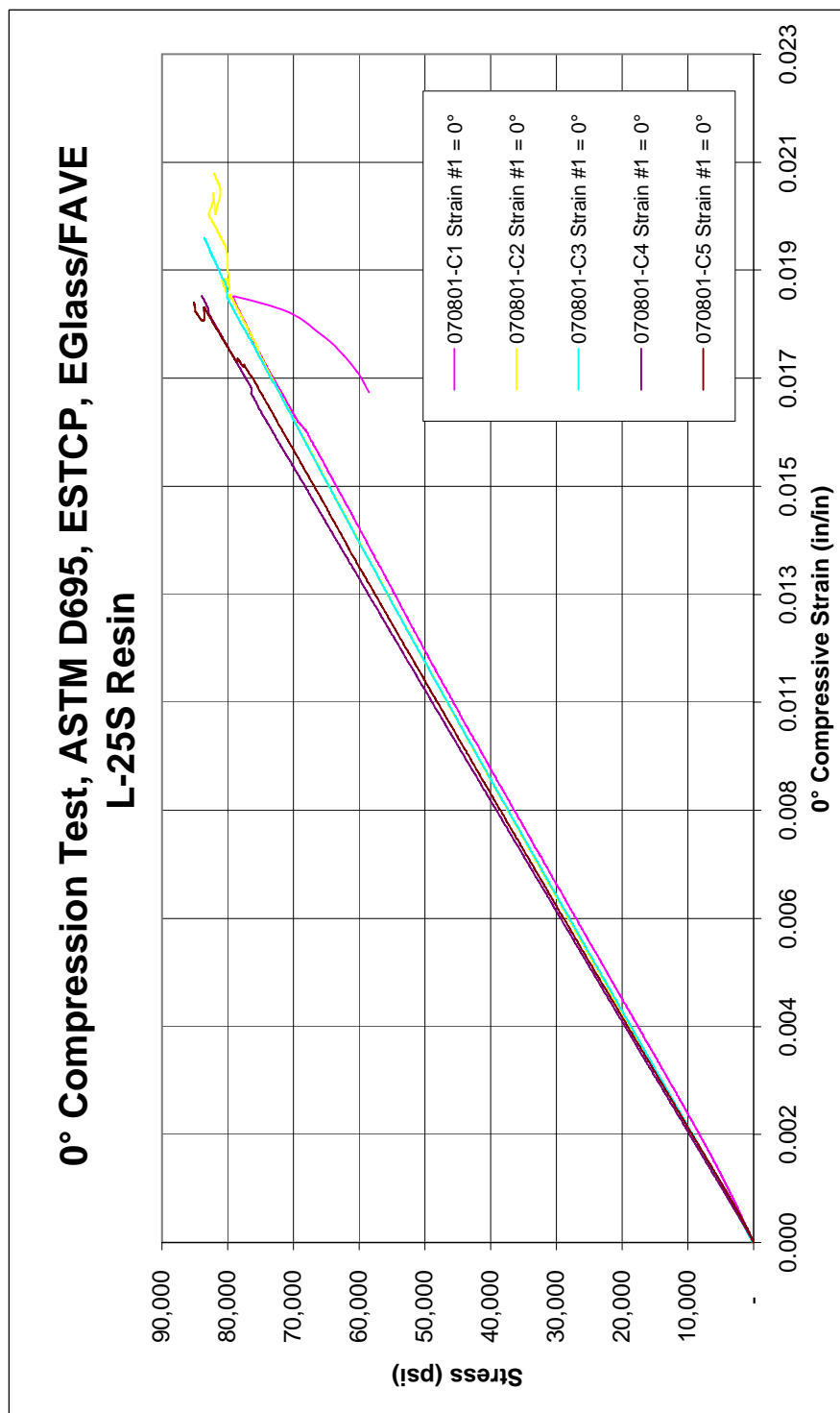


0° Compression Test, ASTM D695, ETW, FAVE-L-20S

Date	Sample ID	Test #	Width (in.)	Thickness (in.)	Peak Load (lbf)	Tensile Strength (ksi)	E (MSI) Range of 1000 to 3000in/in	Memo
26-Jul-07	LVO-ETW-0 C#01	4670	0.5067	0.2146	5,357	49.28	4.83	Crushed Bottom/Interlaminar Shear
26-Jul-07	LVO-ETW-0 C#02	4671	0.4964	0.2157	5,447	50.87	4.92	Interlaminar Shear/ Crush Bottom
26-Jul-07	LVO-ETW-0 C#03	4672	0.4974	0.2113	5,329	50.70	5.14	Interlaminar Shear/ Crush Bottom
26-Jul-07	LVO-ETW-0 C#04	4673	0.4944	0.2049	6,249	36.46	5.05	Crushed Top of Specimen
26-Jul-07	LVO-ETW-0 C#05	4674	0.4980	0.2120	4,827	45.71	4.96	Crushed Top Radius of Specimen
26-Jul-07	LVO-ETW-0 C#06	4675	0.4945	0.2057	4,704	35.68	4.89	Crushed Top of Specimen
					AVG	44.79	4.96	
					STDEV	7.00	0.11	
					%COV	15.64	2.28	



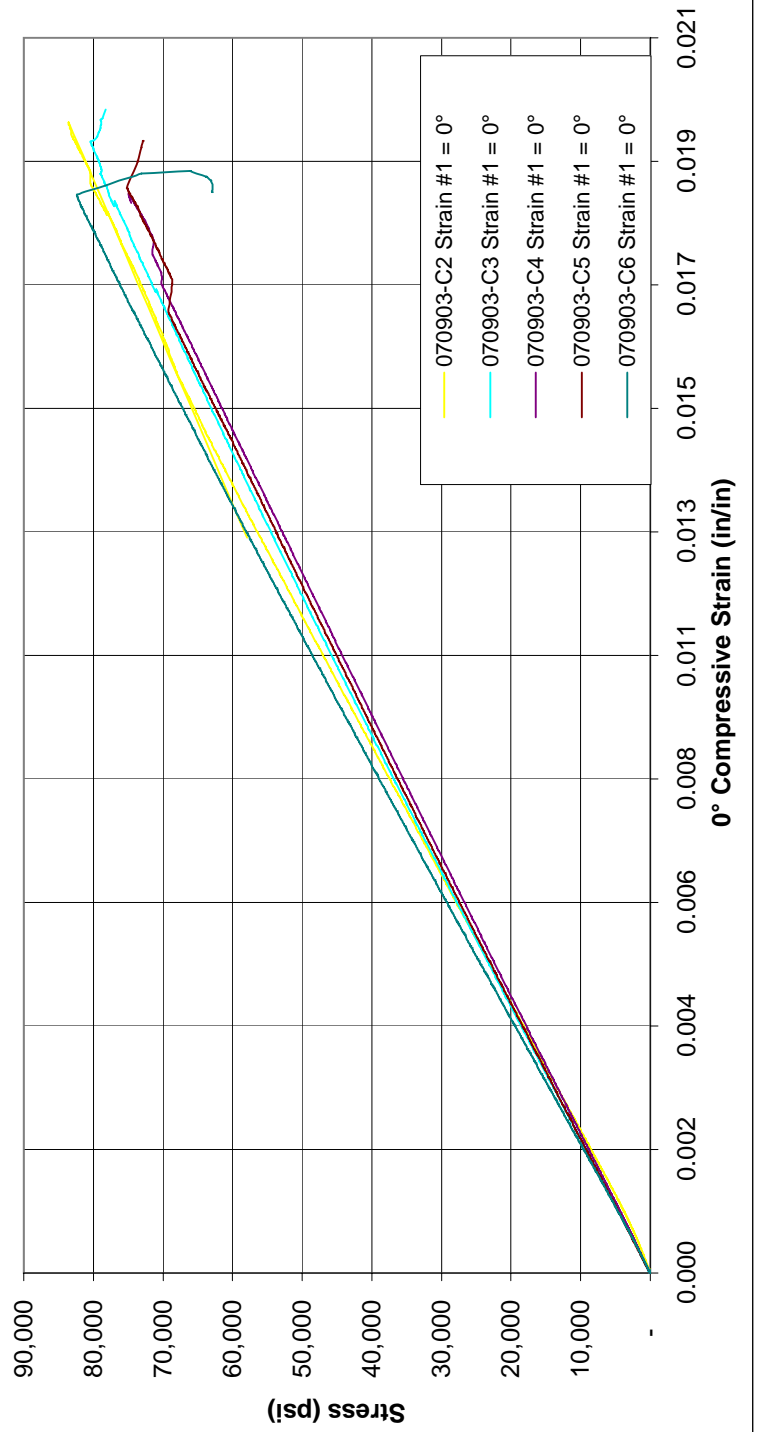
0° Compression Test, ASTM D695, ESTCP, EGlass/FAVE-L-25S Resin

[illegible]

0° Compression Test, ASTM D695, ESTCP, EGlass/510A Resin

Date	Sample ID	Test #	Width (in.)	Thickness (in.)	Peak Load (lbf)	Compressive Strength (ksi)	E (MSI) Range of 1000 to 3000in/in	Memo
10-Oct-07	LV070903-0-C-#02	4780	0.5013	0.2552	10686	83.55	4.57	Crush at top of specimen
10-Oct-07	LV070903-0-C-#03	4781	0.5043	0.2528	10256	80.44	4.47	Shear at middle
10-Oct-07	LV070903-0-C-#04	4782	0.5032	0.2492	9399	74.95	4.29	Crush at top of specimen
10-Oct-07	LV070903-0-C-#05	4783	0.5042	0.2518	9545	75.16	4.39	Shear bottom radius
10-Oct-07	LV070903-0-C-#06	4784	0.5013	0.2448	10102	82.33	4.72	Shear at middle
					AVG	79.29	4.49	
					STDEV	4.02	0.16	
					%COV	5.07	3.65	

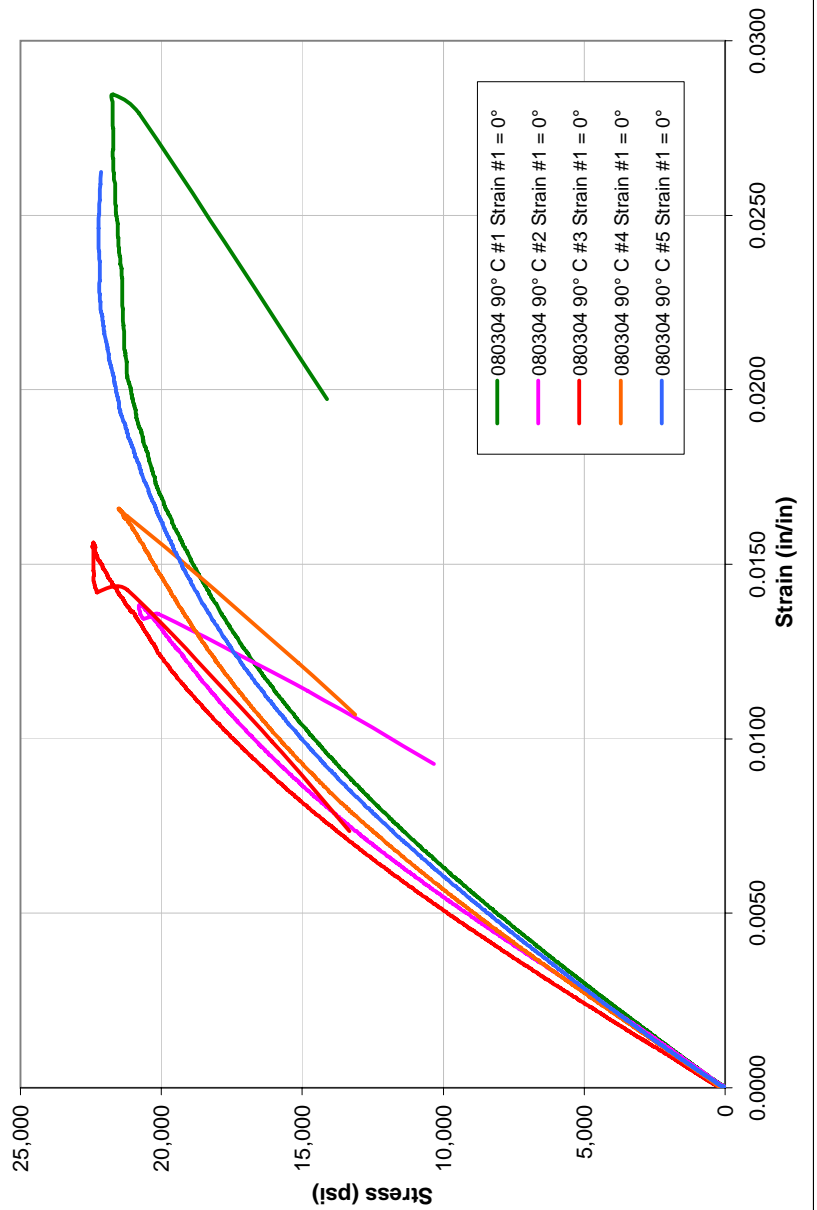
0° Compression Test, ASTM D695, ESTCP, EGlass/510A Resin



Compression Test, ASTM D695, RTD, Low VOC, 90°, Corve 8100/SW180 Glass Fabric

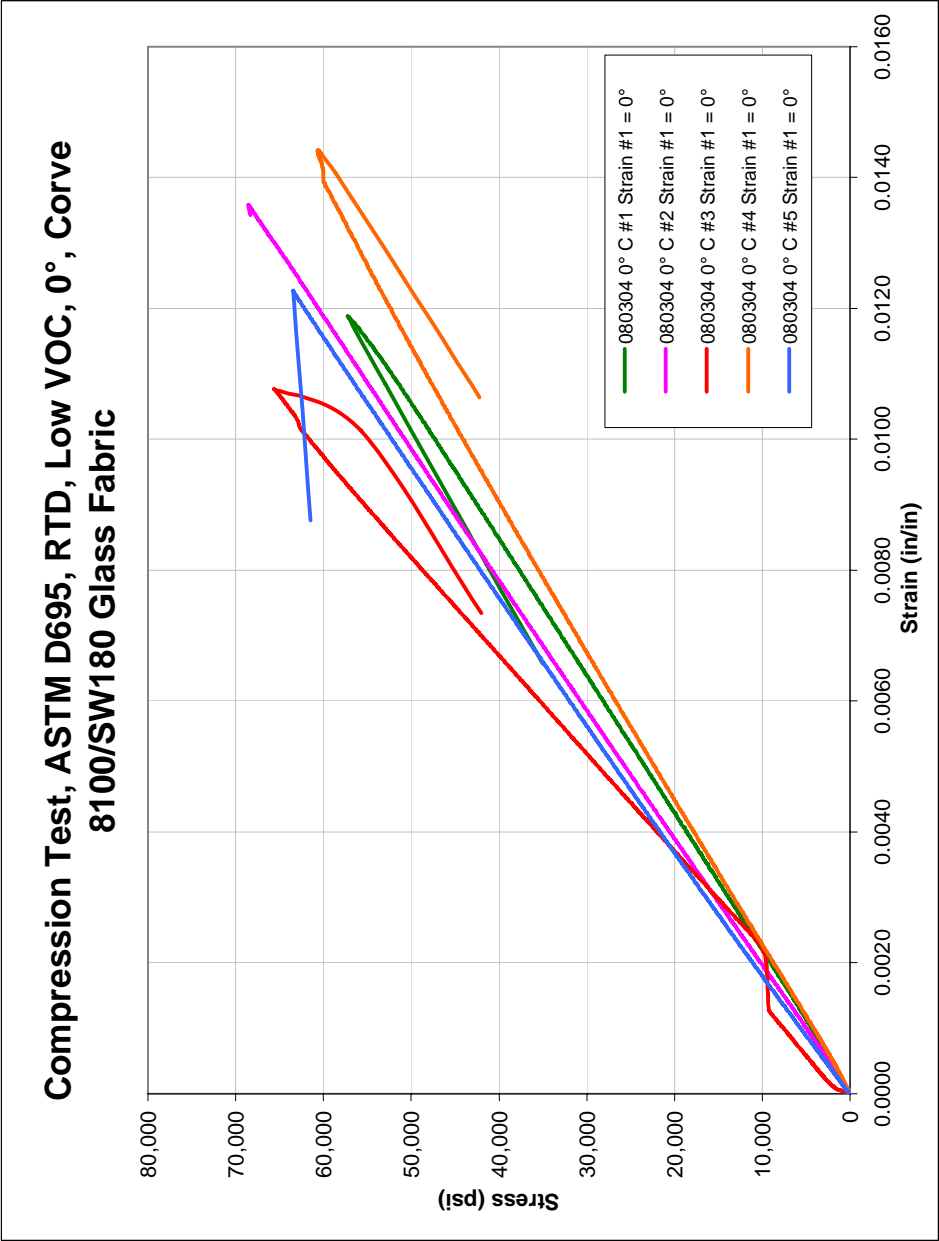
Date	Sample ID	Test #	Width (in.)	Thickness (in.)	Peak Load (lbf)	Compression Strength (ksi)	E (MSI) Range of 1000 to 3000in/in	Memo
10-Jun-08	080304 90° C #1	4895	0.4943	0.2455	2638	21.73	1.64	Middle Gage Length Failure
10-Jun-08	080304 90° C #2	4896	0.4978	0.2627	2720	20.80	1.85	Middle Gage Length Failure
10-Jun-08	080304 90° C #3	4897	0.4953	0.2483	2762	22.46	1.98	Middle Gage Length Failure
10-Jun-08	080304 90° C #4	4898	0.4943	0.2560	2722	21.52	1.80	Bottom Radius Failure
10-Jun-08	080304 90° C #5	4899	0.4953	0.2457	2706	22.24	1.69	Middle Gage Length Failure
					AVG	21.75	1.79	
					STDEV	0.65	0.14	
					%COV	3.00	7.54	

Compression Test, ASTM D695, RTD, Low VOC, 90°,
Corve 8100/SW180 Glass Fabric



Compression Test, ASTM D695, RTD, Low VOC, 0°, Corve 8100/SW180 Glass Fabric

Date	Sample ID	Test #	Width (in.)	Thickness (in.)	Peak Load (lbf)	Compression Strength (ksi)	E (MSI) Range of 1000 to 3000in/in	Memo
10-Jun-08	080304 0° C #1	4894	0.4917	0.2587	7283	57.26	4.35	Crush Top
10-Jun-08	080304 0° C #2	4900	0.4908	0.2458	8270	68.57	5.05	Top Radius Section Fracture
10-Jun-08	080304 0° C #3	4901	0.1941	0.2467	7947	65.62	6.24	Bottom Radius Section Fracture
10-Jun-08	080304 0° C #4	4902	0.4925	0.2525	7548	60.68	4.53	Crush Top
10-Jun-08	080304 0° C #5	4903	0.4910	0.2538	7906	63.45	5.54	Crush Bottom
					AVG	63.12	5.14	
					STDEV	4.37	0.77	
					%COV	6.93	14.96	

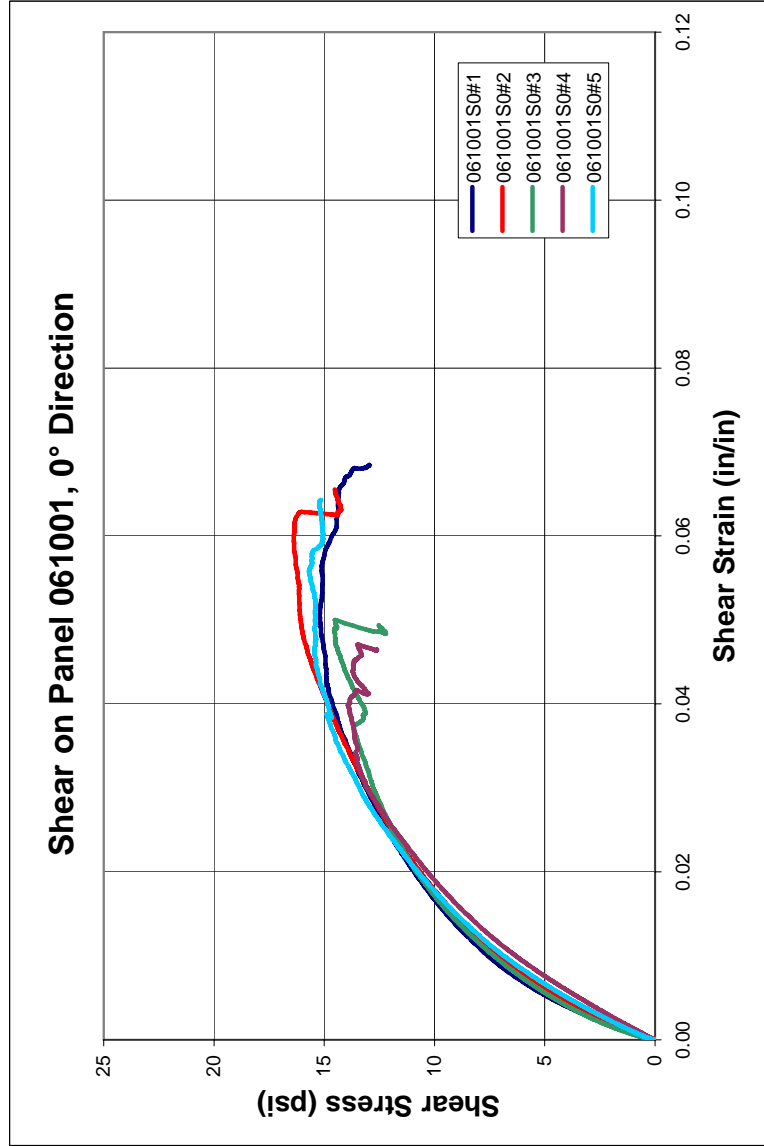


Appendix D

ASTM D5379 V-Notch Shear Test Measurements

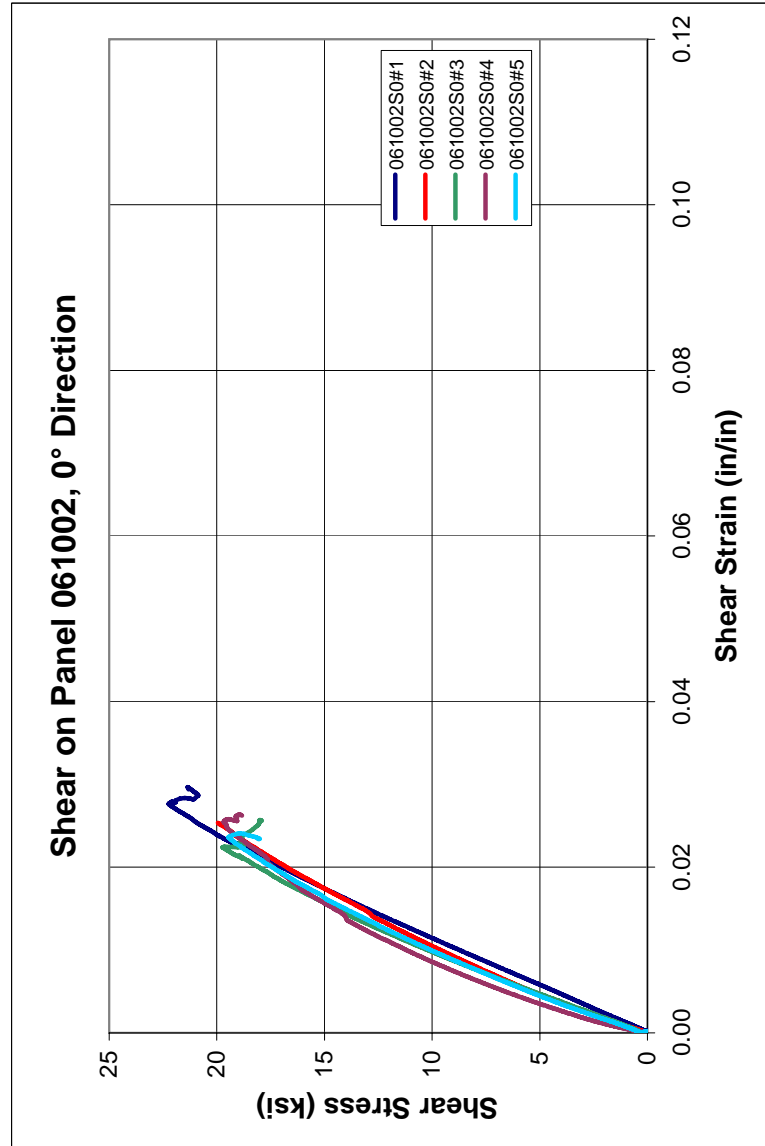
Shear Test ASTM D5379, Tested on Panel 061001 0° Direction

Date	Sample ID	Test #	Width (in)	Thickness (in)	G (Msi) (range of 1,000 to 4,000 μ ε)	Shear Stress @ 0.2% Offset (ksi)	Shear Stress @ 5% strain (ksi)	Maximum Shear Stress (ksi)	Maximum Shear Strain
8-Mar-07	061001S0#1	4541	0.4490	0.2488	0.915	7.83	15.19	15.20	0.068
8-Mar-07	061001S0#2	4542	0.4498	0.2475	0.789	7.98	16.07	16.39	0.066
8-Mar-07	061001S0#3	4543	0.4517	0.2580	0.856	7.80	12.52	14.55	0.050
8-Mar-07	061001S0#4	4544	0.4493	0.2475	0.642	8.88	12.61	13.93	0.047
8-Mar-07	061001S0#5	4545	0.4500	0.2543	0.757	8.08	15.42	15.69	0.064
Average:					0.792	8.12	14.36	15.15	0.059
stdev					0.10	0.44	1.67	0.96	0.010
COV (%):					13.08%	5.44%	11.64%	6.33%	16.60%



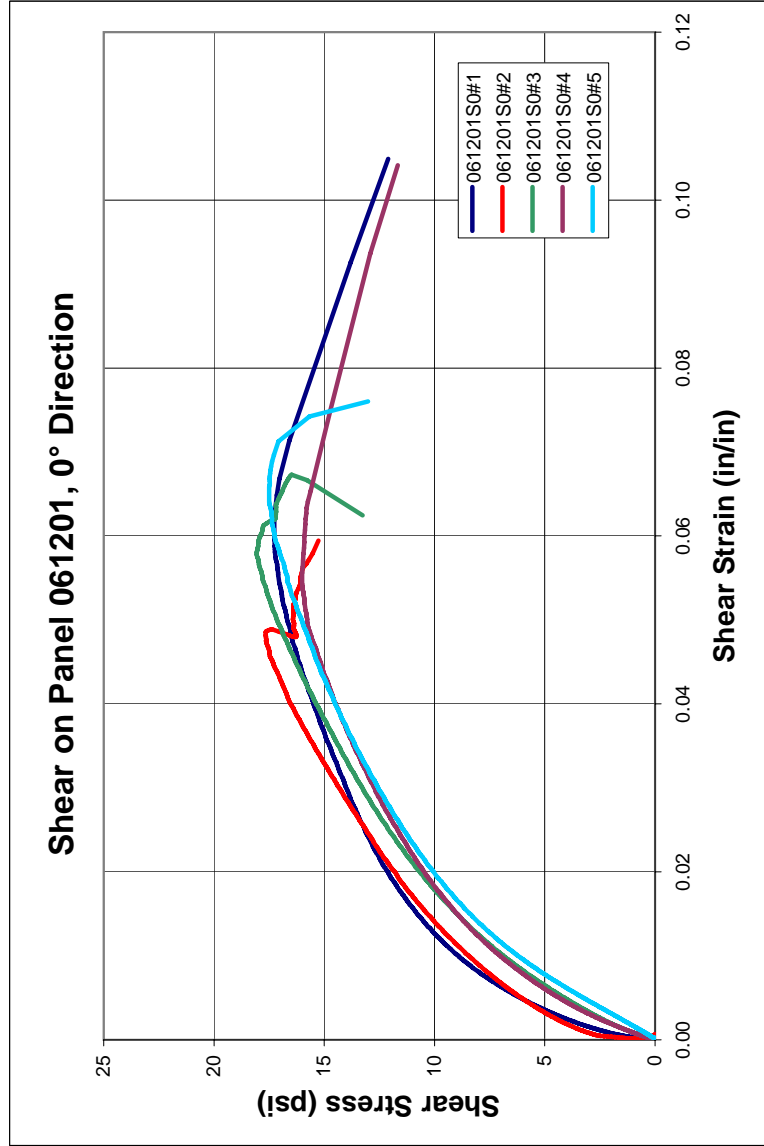
Shear Test ASTM D5379, Tested on Panel 061002 0° Direction

Date	Sample ID	Test #	Width (in)	Thickness (in)	G (Msi) (range of 1,000 to 4,000 $\mu\epsilon$)	Shear Stress @ 0.2% Offset (ksi)	Shear Stress @ 5% strain (ksi)	Maximum Shear Stress (ksi)	Maximum Shear Strain
8-Mar-07	061002S0#1	4546	0.4543	0.2033	0.880	21.60	-	22.24	0.030
8-Mar-07	061002S0#2	4547	0.4550	0.2058	1.102	11.61	-	19.95	0.025
8-Mar-07	061002S0#3	4548	0.4555	0.2008	1.042	16.92	-	19.73	0.026
8-Mar-07	061002S0#4	4549	0.4580	0.2033	1.225	13.60	-	19.68	0.026
8-Mar-07	061002S0#5	4550	0.4538	0.1948	1.103	13.33	-	19.45	0.025
Average:					1.070	15.41	-	20.21	0.026
stdev					0.13	3.96	-	1.15	0.002
COV (%):					11.73%	25.68%	-	5.67%	7.41%



Shear Test ASTM D5379, Tested on Panel 061201 0° Direction

Date	Sample ID	Test #	Width (in)	Thickness (in)	G (Msi) (range of 1,000 to 4,000 $\mu\epsilon$)	Shear Stress @ 0.2% Offset (ksi)	Shear Stress @ 5% strain (ksi)	Maximum Shear Stress (ksi)	Maximum Shear Strain
8-Mar-07	061201S0#1	4551	0.4585	0.1982	1.016	9.50	16.67	17.27	0.105
8-Mar-07	061201S0#2	4552	0.4587	0.2008	0.764	10.62	16.41	17.66	0.059
8-Mar-07	061201S0#3	4553	0.4515	0.2007	0.777	7.83	17.13	18.07	0.067
8-Mar-07	061201S0#4	4554	0.4570	0.1993	0.864	7.14	15.77	16.01	0.104
8-Mar-07	061201S0#5	4555	0.4537	0.1983	0.674	7.86	16.03	17.51	0.076
Average:					0.819	8.59	16.40	17.30	0.082
stdev					0.13	1.43	0.53	0.78	0.021
COV (%):					15.78%	16.63%	3.25%	4.50%	25.57%



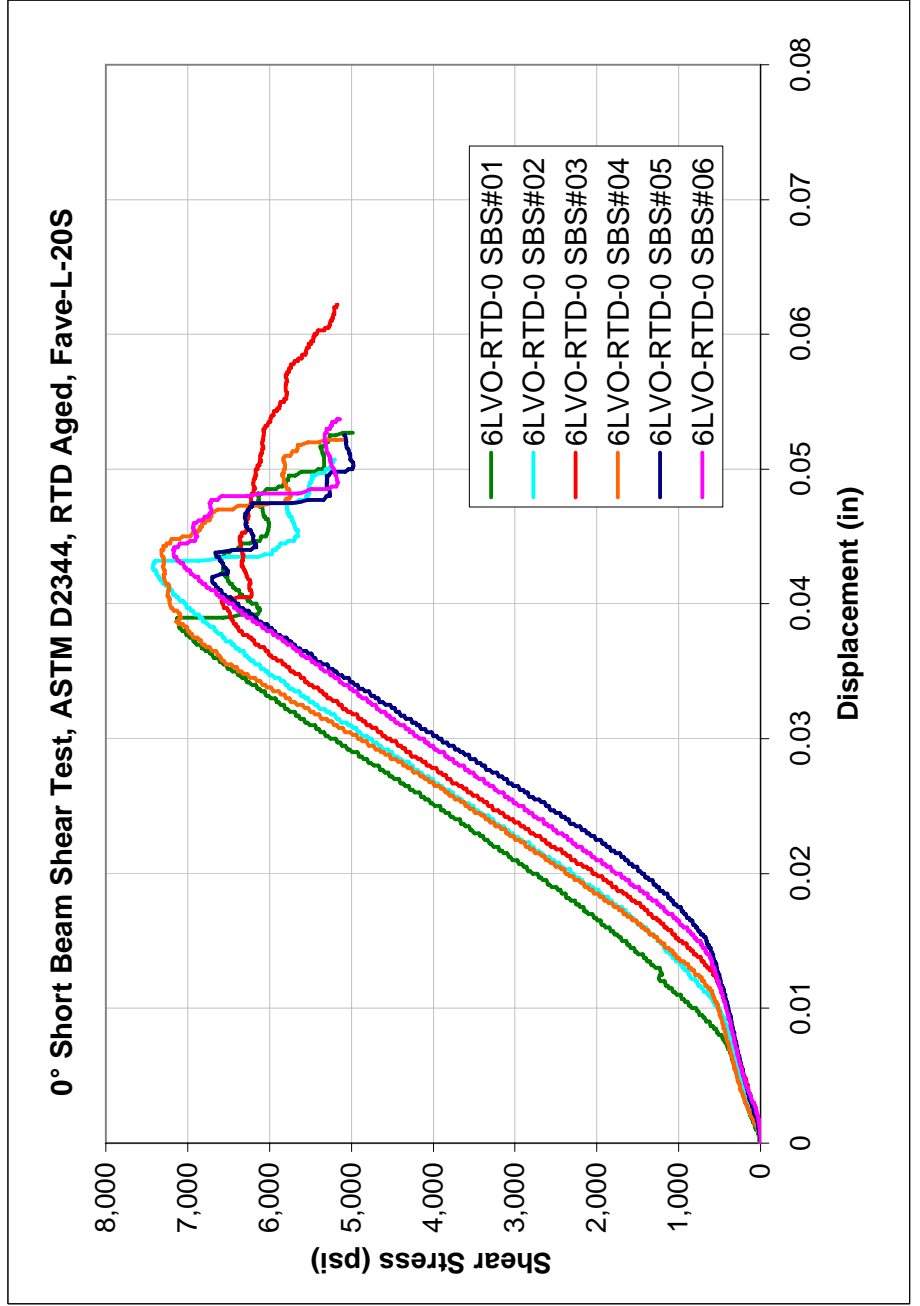
Appendix E

ASTM D2344 Short Beam Shear Test Measurements

0° Short Beam Shear Test, ASTM D2344, RTD Aged, Fave-L-20S

Date	Sample ID	Test #	Width (in.)	Thickness (in.)	Peak Load (lbf)	Shear Strength (ksi)
25-Jul-07	6LVO-RTD-0 SBS#01	4652	0.4879	0.2136	990.4	7,127.5
25-Jul-07	6LVO-RTD-0 SBS#02	4653	0.4962	0.2198	1032.0	7,427.1
25-Jul-07	6LVO-RTD-0 SBS#03	4653	0.5093	0.2334	914.9	6,584.3
25-Jul-07	6LVO-RTD-0 SBS#04	4655	0.4958	0.2310	1017.4	7,321.9
25-Jul-07	6LVO-RTD-0 SBS#05	4656	0.4844	0.2074	931.4	6,702.6
25-Jul-07	6LVO-RTD-0 SBS#06	4657	0.4965	0.2182	997.2	7,176.3
					AVG	7056.6
					STDEV	339.2
					%COV	4.81

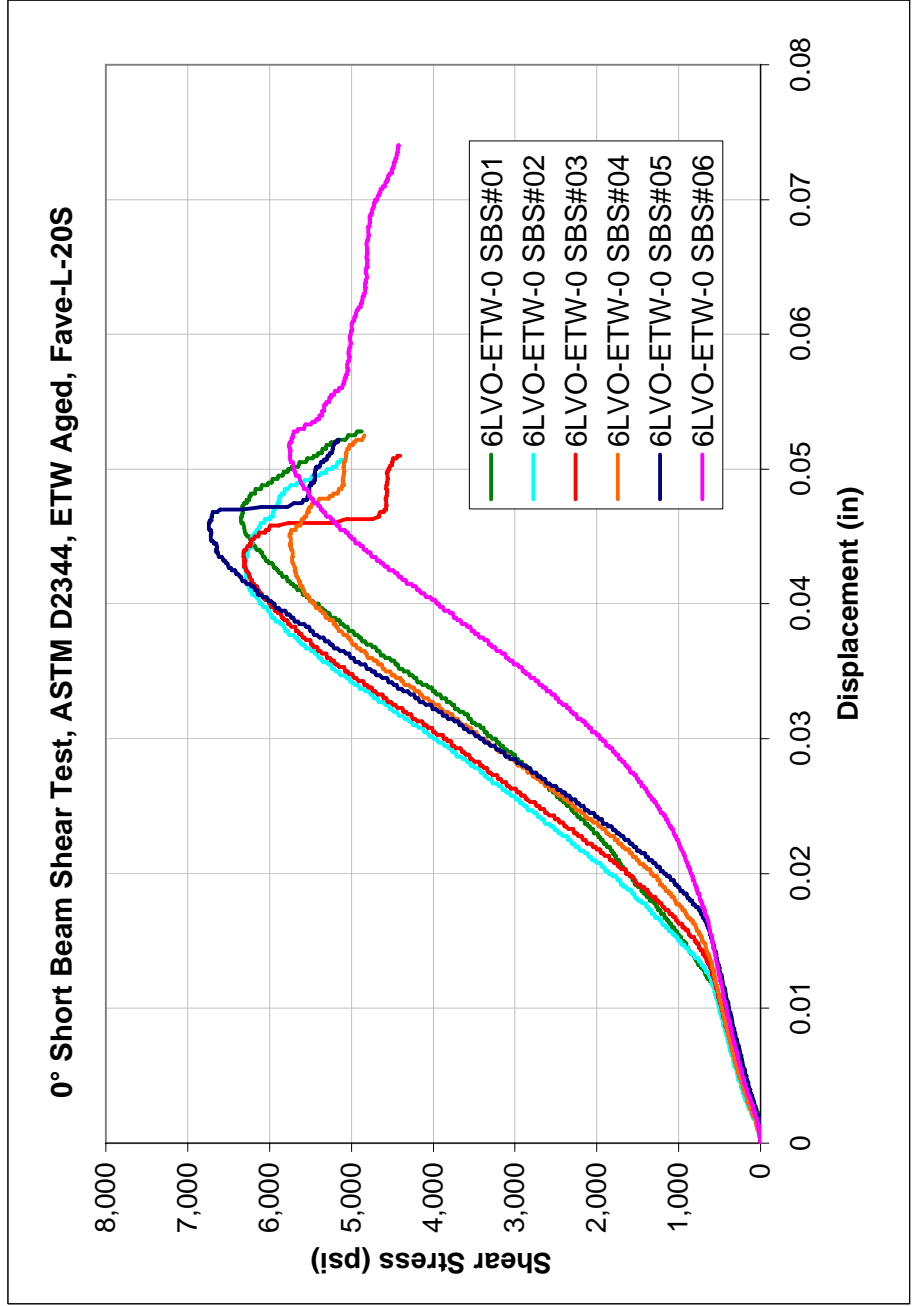
Support Span 0.8823



0° Short Beam Shear Test, ASTM D2344, ETW Aged, Fave-L-20S

Date	Sample ID	Test #	Width (in.)	Thickness (in.)	Peak Load (lbf)	Shear Strength (ksi)
25-Jul-07	6LVO-ETW-0 SBS#01	4652	0.4879	0.2136	882.7	6,352.7
25-Jul-07	6LVO-ETW-0 SBS#02	4653	0.4962	0.2198	877.9	6,318.2
25-Jul-07	6LVO-ETW-0 SBS#03	4653	0.5093	0.2334	878.4	6,321.7
25-Jul-07	6LVO-ETW-0 SBS#04	4655	0.4958	0.2310	799.8	5,755.6
25-Jul-07	6LVO-ETW-0 SBS#05	4656	0.4844	0.2074	937.1	6,744.1
25-Jul-07	6LVO-ETW-0 SBS#06	4657	0.4965	0.2182	800.9	5,764.1
					AVG	6209.4
					STDEV	383.4
					%COV	6.18

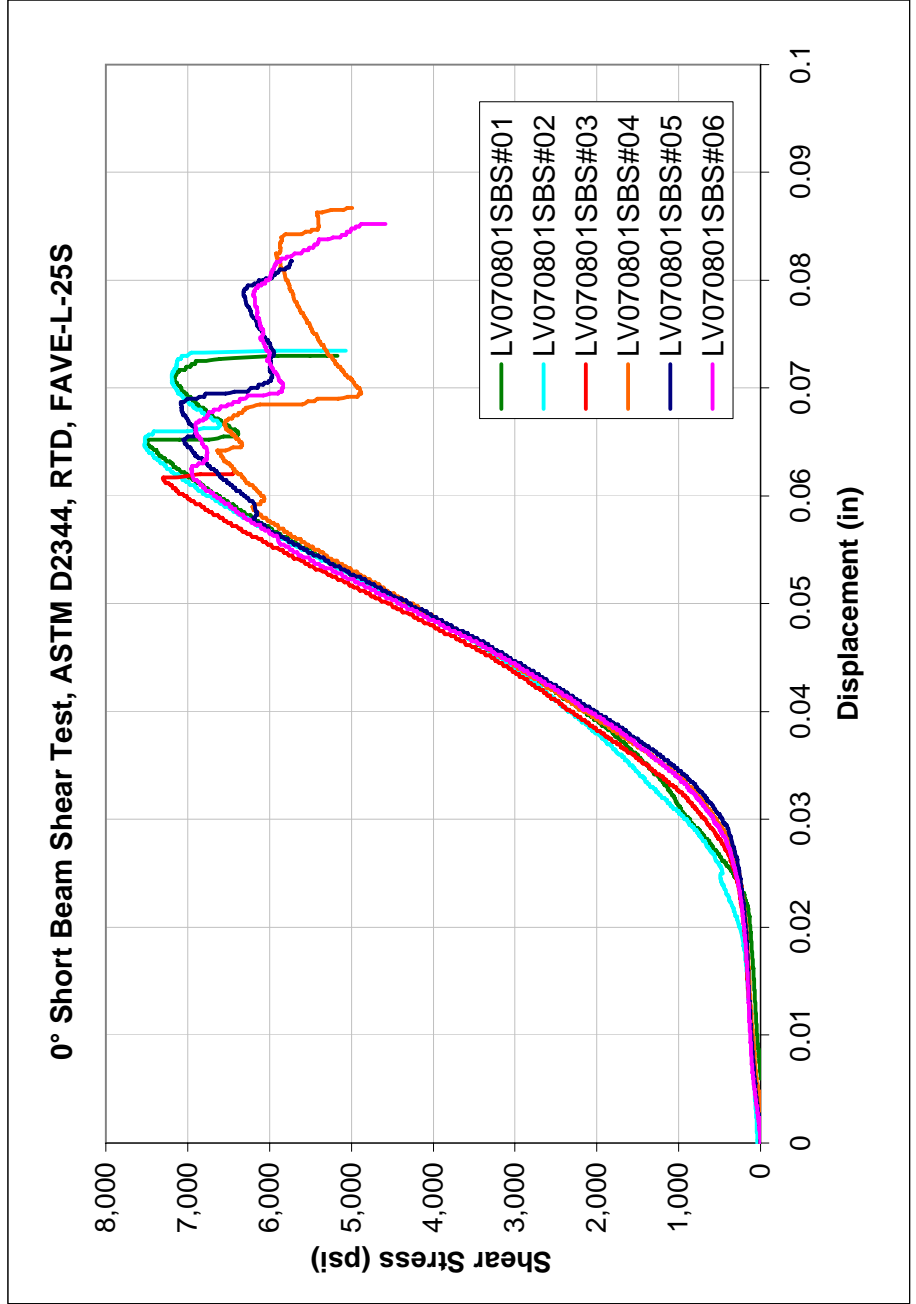
Support Span 0.8765



0° Short Beam Shear Test, ASTM D2344, RTD, FAVE-L-25S

Date	Sample ID	Test #	Width (in.)	Thickness (in.)	Peak Load (lbf)	Shear Strength (ksi)	Memo
25-Sep-07	LV070801-SBS#01	4752	0.4878	0.2442	1191.1	7.50	Interlaminar
25-Sep-07	LV070801-SBS#02	4753	0.4967	0.2453	1195.7	7.53	Interlaminar
25-Sep-07	LV070801-SBS#03	4754	0.4965	0.2500	1159.1	7.30	Interlaminar
25-Sep-07	LV070801-SBS#04	4755	0.4960	0.2347	1054.1	6.64	Interlaminar
25-Sep-07	LV070801-SBS#05	4756	0.4937	0.2470	1125.6	7.09	Molding Side/Interlaminar
25-Sep-07	LV070801-SBS#06	4757	0.5010	0.2488	1105.2	6.96	Molding Side/Interlaminar
					AVG	7.17	
					STDEV	0.34	
					%COV	4.79	

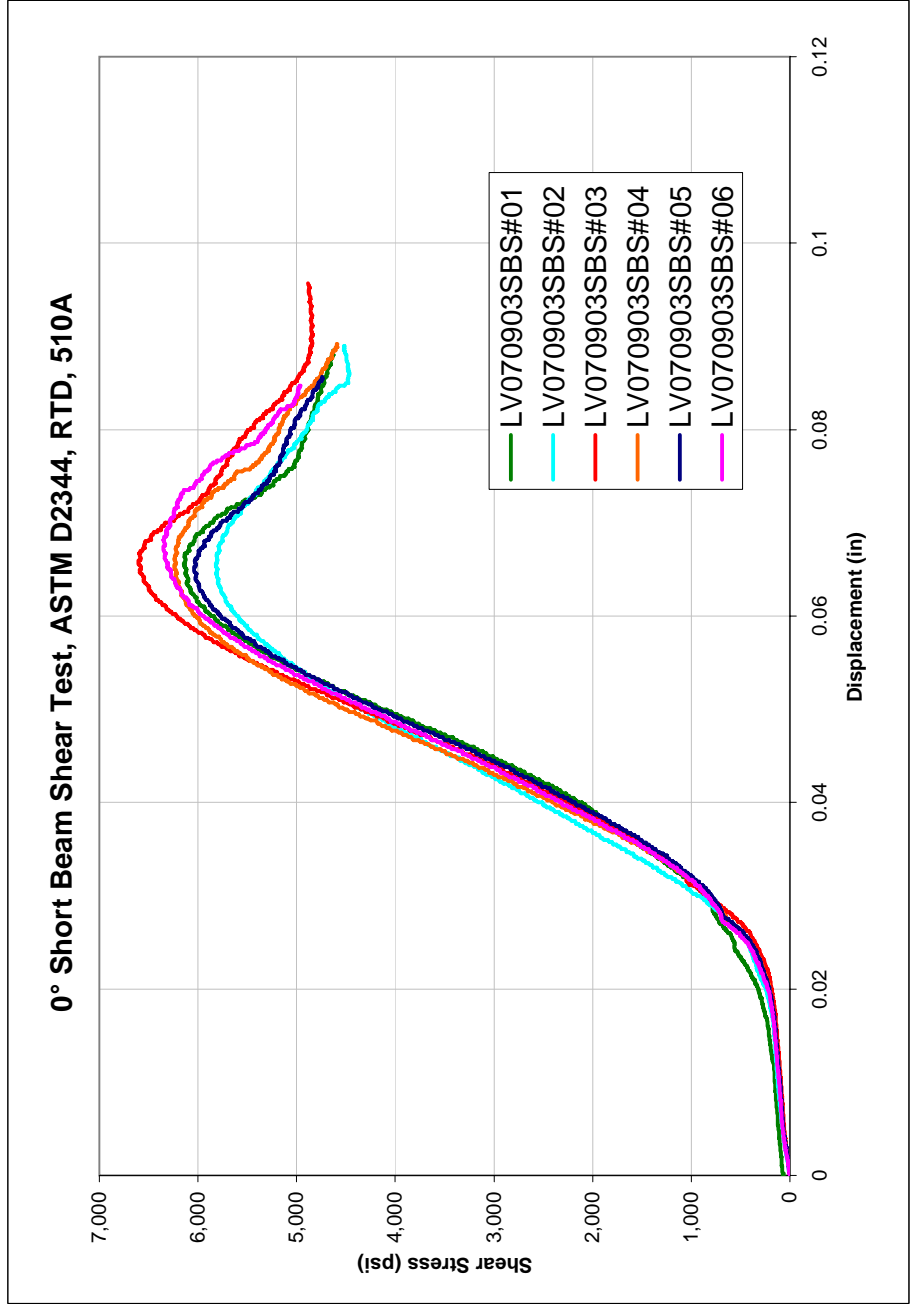
Support Span 0.98



0° Short Beam Shear Test, ASTM D2344, RTD, 510A

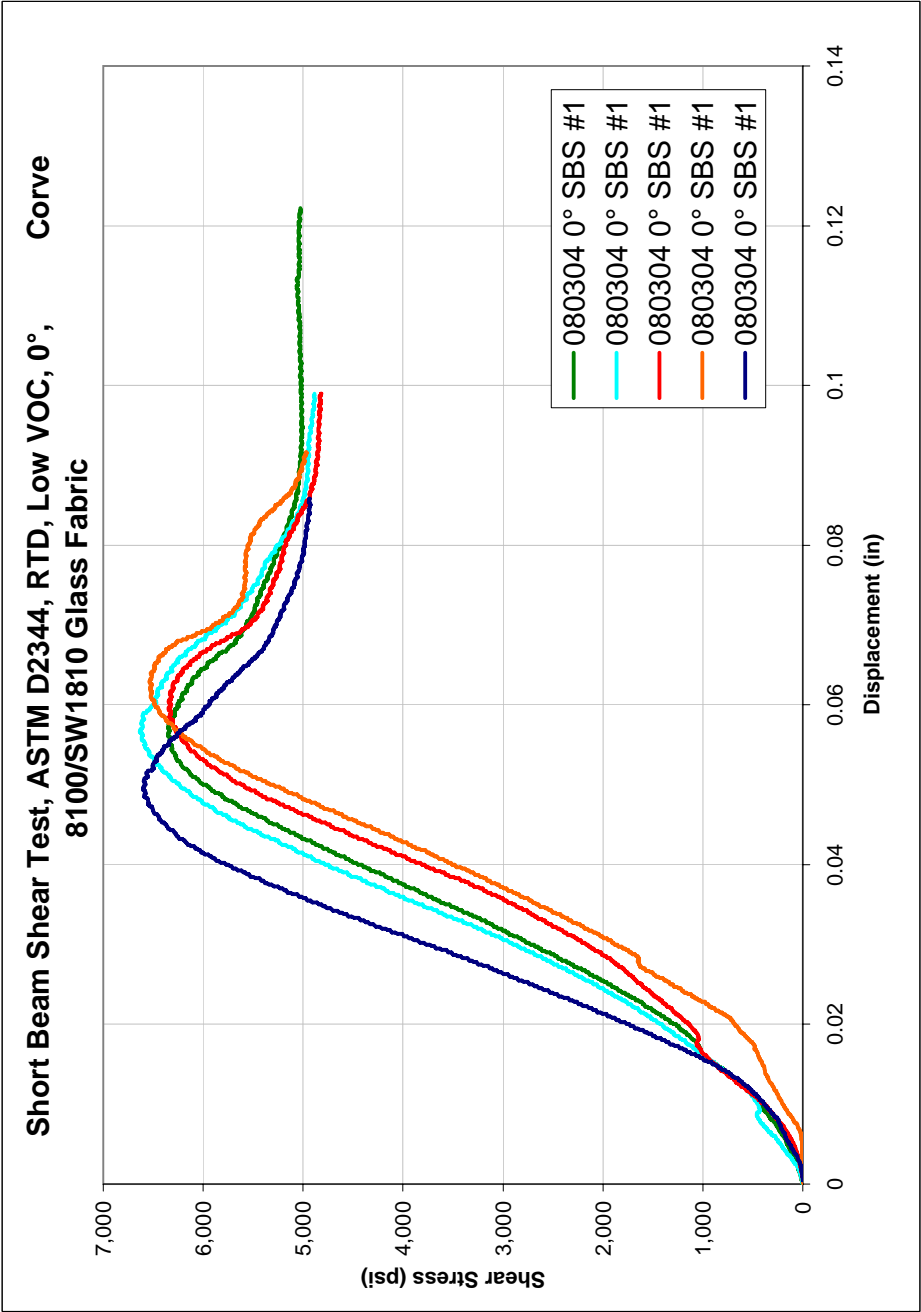
Date	Sample ID	Test #	Width (in.)	Thickness (in.)	Peak Load (lbf)	Shear Strength (ksi)	Memo
25-Sep-07	LV070903-SBS#01	4761	0.4987	0.2490	1017.4	6.14	Molding Side/Interlaminar
25-Sep-07	LV070903-SBS#02	4759	0.4967	0.2365	964.0	5.82	Molding Side/Interlaminar
25-Sep-07	LV070903-SBS#03	4760	0.5020	0.2433	1093.9	6.61	Bagging Side/Interlaminar
25-Sep-07	LV070903-SBS#04	4758	0.4988	0.2375	1033.5	6.24	Bagging Side/Interlaminar
25-Sep-07	LV070903-SBS#05	4762	0.4872	0.2410	1000.4	6.04	Bagging Side/Interlaminar
25-Sep-07	LV070903-SBS#06	4763	0.4958	0.2382	1051.8	6.35	Molding Side/Interlaminar
					AVG	6.20	
					STDEV	0.27	
					%COV	4.34	

Support Span 0.9637



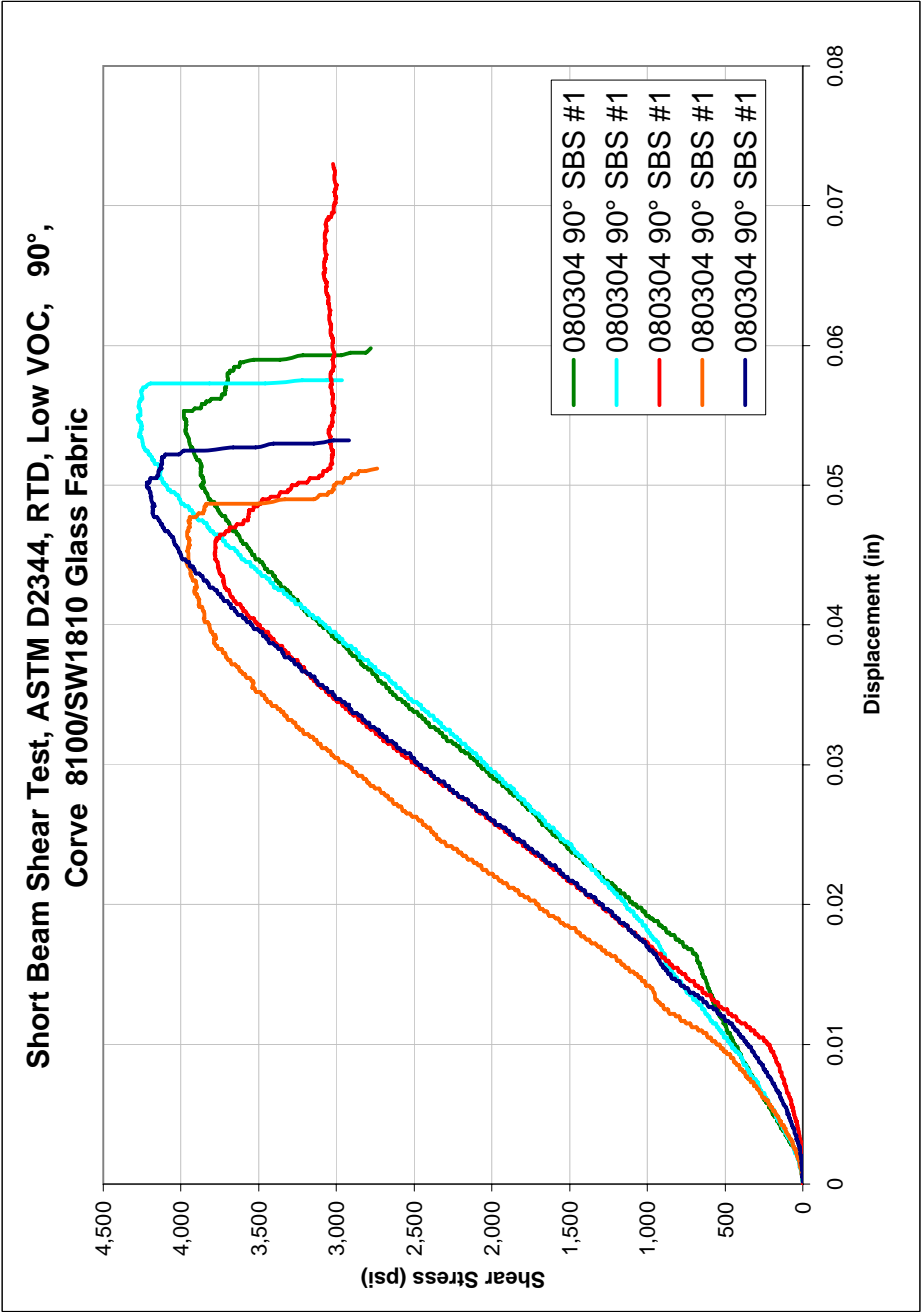
Short Beam Shear Test, ASTM D2344, RTD, Low VOC, 0°,
Corve 8100/SW1810 Glass Fabric

Date	Sample ID	Test #	Width (in.)	Thickness (in.)	Peak Load (lbf)	Shear Strength (psi)	Memo
27-May-08	080304 0° SBS #1	4884	0.4970	0.2442	1,028.5	6,355.8	
27-May-08	080304 0° SBS #1	4885	0.4945	0.2477	1,083.4	6,633.5	
27-May-08	080304 0° SBS #1	4886	0.4958	0.2545	1,067.9	6,347.2	
28-May-08	080304 0° SBS #1	4887	0.4953	0.2495	1,077.0	6,536.5	
28-May-08	080304 0° SBS #1	4888	0.4960	0.2383	1,040.6	6,603.2	
					AVG	6,495.2	
					STDEV	135.85	
					%COV	2.09	
Support Span		0.9873		inch			



Short Beam Shear Test, ASTM D2344, RTD, Low VOC, 90°,
 Corve 8100/SW1810 Glass Fabric

Date	Sample ID	Test #	Width (in.)	Thickness (in.)	Peak Load (lbf)	Shear Strength (psi)	Memo
28-May-08	080304 90° SBS #1	4889	0.4958	0.2480	653.0	3,982.8	
28-May-08	080304 90° SBS #1	4890	0.4955	0.2498	705.8	4,276.7	
27-May-08	080304 90° SBS #1	4891	0.4950	0.2457	613.7	3,784.4	
28-May-08	080304 90° SBS #1	4892	0.4960	0.2498	654.8	3,963.4	
28-May-08	080304 90° SBS #1	4893	0.4948	0.2442	680.0	4,221.0	
					AVG	4,045.7	
					STDEV	201.91	
					%COV	4.99	
Support Span			0.9873	inch			



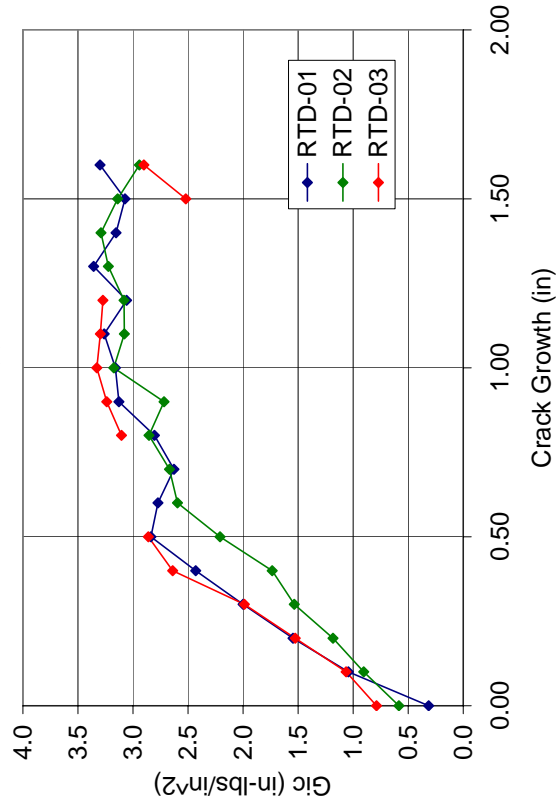
Appendix F

ASTM D5528 Mode I Interlaminar Fracture Toughness (DCB) Test Measurements

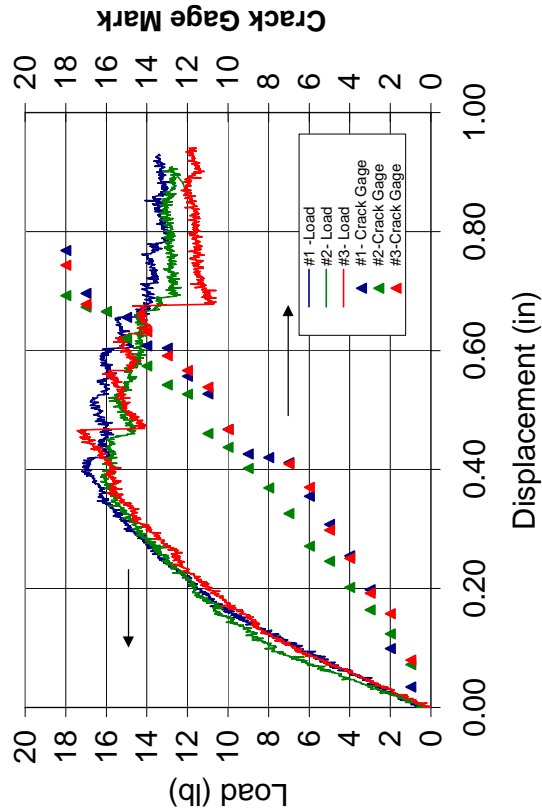
DCB Results Summary - FAVE-L-20S-RTD

Sample ID	Width	Thickness	ao	Gic (in-lb/in ²)		
				Onset	Propagation	Steady State
FAVE-L-20S-1	0.9965	0.2220	2.0650	0.31	1.77	3.19
FAVE-L-20S-1	1.0005	0.2235	1.9745	0.59	1.36	3.13
FAVE-L-20S-3	0.9950	0.2220	1.9780	0.79	1.76	3.00
average				0.56	1.63	3.11
stdev				0.24	0.23	0.10
Cov (%)				42.49	14.39	3.22

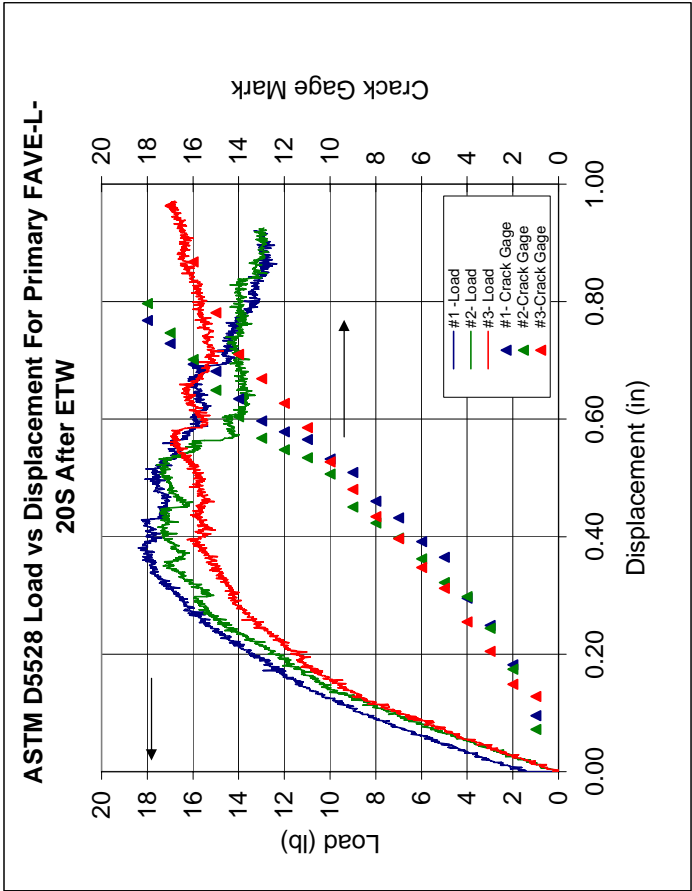
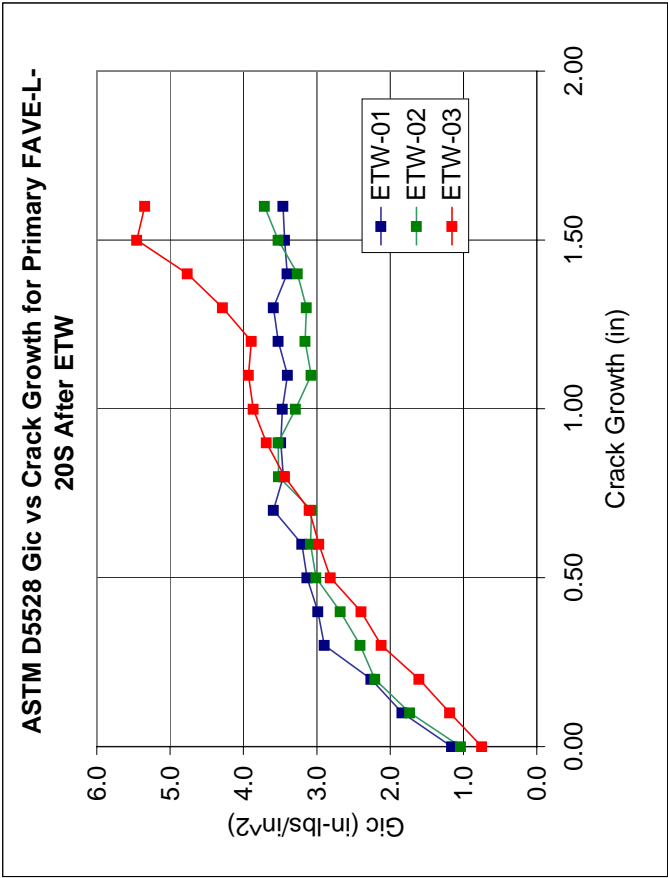
ASTM D5528 Gic vs Crack Growth for Primary FAVE-L-20S



ASTM D5528 Load vs Displacement For Primary FAVE-L-20S

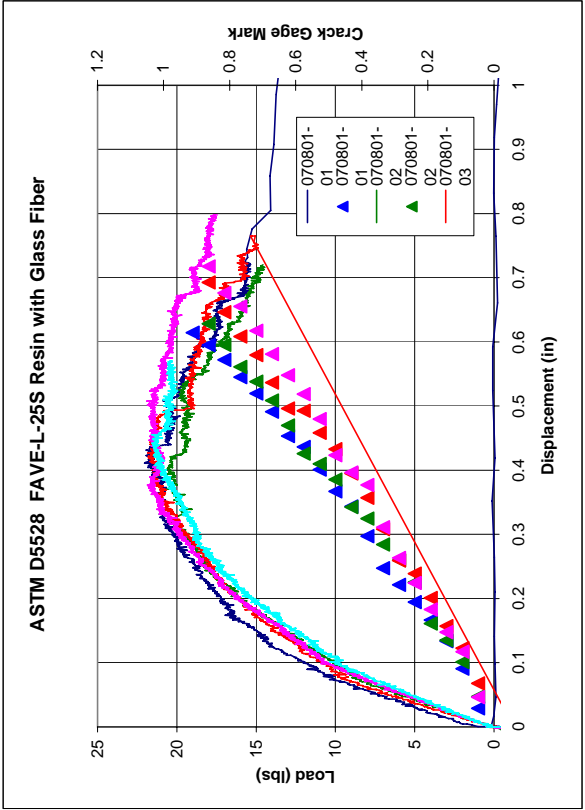
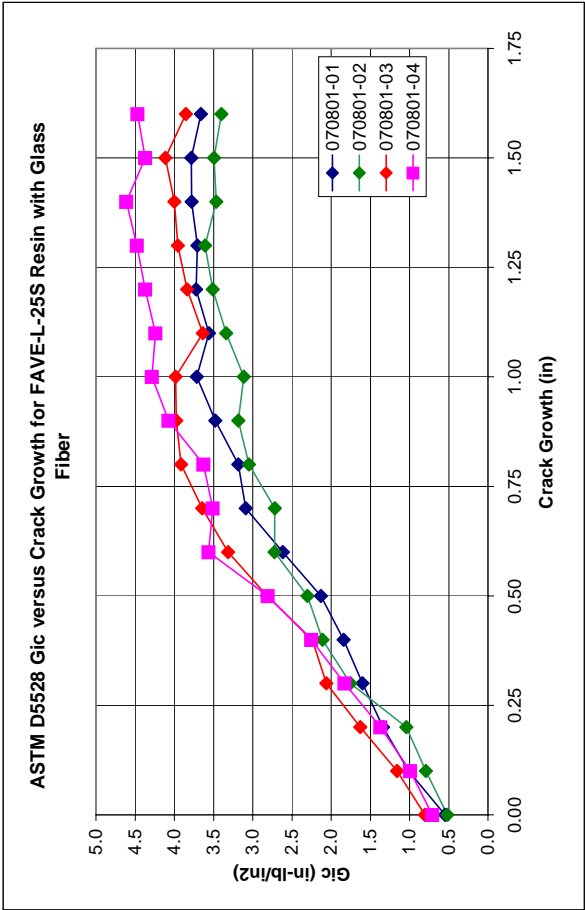


Sample ID	Width	Thickness	ao	Gic (in-lb/in ²)		
				Onset	Propagation	Steady State
FAVE-L-20S-1ETW	0.9955	0.2220	1.9925	1.16	2.58	3.47
FAVE-L-20S-1ETW	0.9975	0.2140	2.0120	1.04	2.31	3.31
FAVE-L-20S-3ETW	0.9965	0.2145	1.9740	0.75	1.86	4.51
average				0.98	2.25	3.76
stdev				0.21	0.36	0.65
Cov (%)				21.48	16.05	17.28



DCB Results Summary - FAVE-L-25S

Sample ID	Width	Thickness	ao	Gic (in-lb/in2)		
				Onset	Propagation 1	Steady State
070801-01	0.9890	0.2505	1.8995	0.55	1.47	3.70
070801-02	0.9930	0.2460	1.8570	0.52	1.40	3.42
070801-03	0.9895	0.2465	1.9020	0.80	1.84	3.91
070801-04	0.9935	0.2445	1.9310	0.71	1.60	4.40
070801-05	0.9910	0.2415	1.9750		Gage Malfunction	
		average		0.62	1.57	3.68
		stdev		0.16	0.24	0.25
		Cov (%)		25.33	15.25	6.72

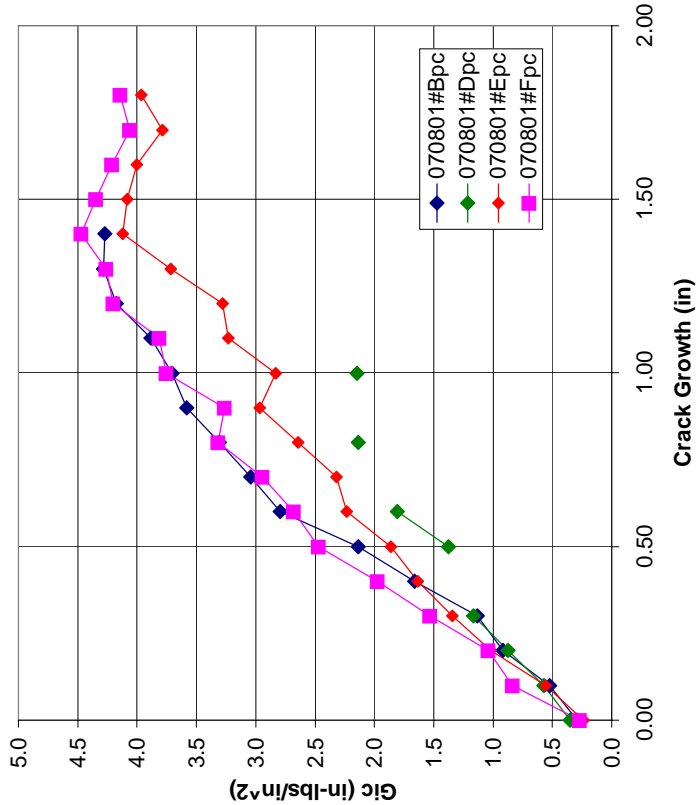


FAVE-L- 25S Post Cured, Double Cantilever Beam, ASTM 5528

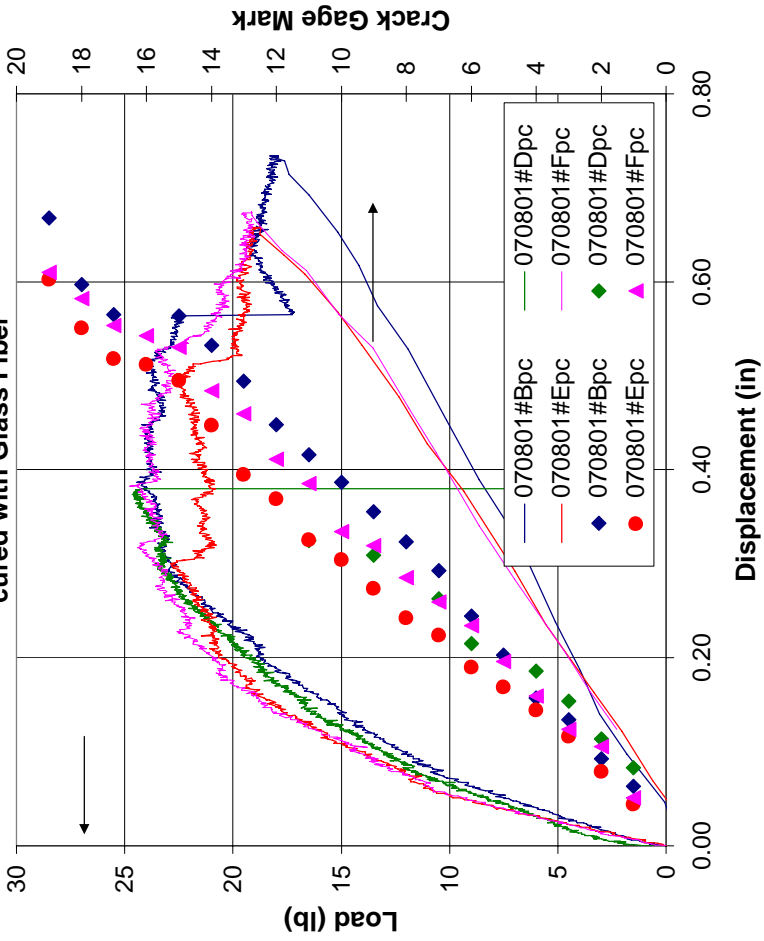
Date	Sample ID	Resistance (Ohms)	Initial Crack Length, a ₀ (in)	hinge (in)	Width 1 (in.)	Width 2 (in.)	Width 3 (in.)	Average Width (in.)	Thickness 1 (in.)	Thickness 2 (in.)	Thickness 3 (in.)	Average Width (in.)	Max Load (lbs at in)	GI Onset (in-lbs/in ²)	GI Propagation (in-lbs/in ²)	GI Steady State (in-lbs/in ²)
15-Apr-08	070801#Bpc	1.0000	1.8015	0.09	0.9855	0.9900	0.9895	0.9883	0.2450	0.2415	0.2325	0.2397	24.44	0.29	1.40	4.06
15-Apr-08	070801#Epc	1.0000	1.66	0.09	0.9915	0.9900	0.9885	0.9900	0.2435	0.2385	0.2365	0.2395	22.87	0.24	1.49	3.54
15-Apr-08	070801#Fpc	1.0000	1.656	0.09	0.9845	0.9875	0.9895	0.9872	0.2400	0.2345	0.2385	0.2377	24.77	0.27	1.75	4.14
29-Jan-08	070801#Dpc	1.0000	1.7375	0.09	0.9935	0.9935	0.9935	0.9935	0.2340	0.2340	0.2340	0.2340	24.65	0.35	1.17	2.15
												AVG	24.18	0.29	1.45	3.47
												STDEV	0.89	0.05	0.24	0.92
												%COV	3.67	16.55	16.78	26.61

Loading Rate 0.2 in/min
Load Scale 100 lbs

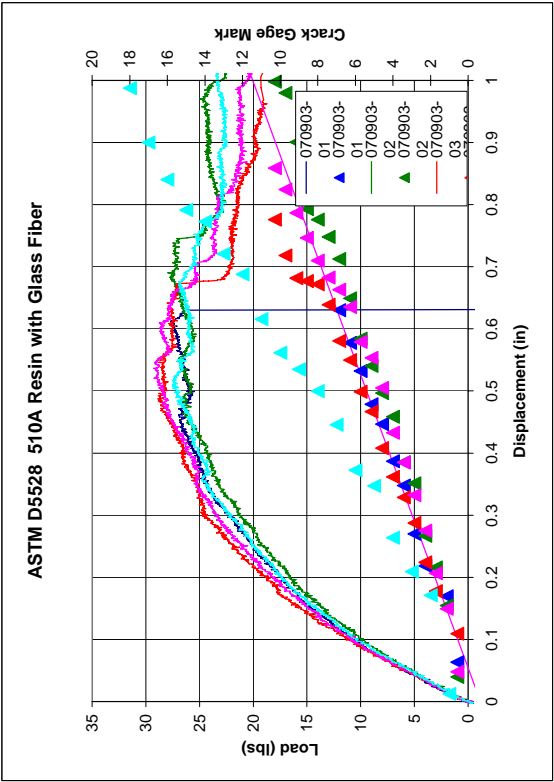
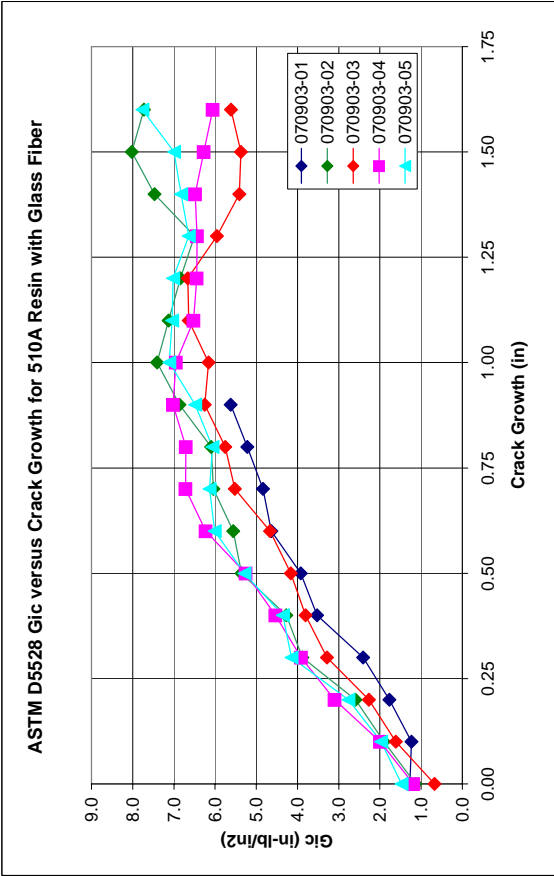
ASTM D5528 Gic vs Crack Growth for FAVE-L-25S Post cured with Glass Fiber



ASTM D5528 Gic vs Crack Growth for FAVE-L-25S Post cured with Glass Fiber

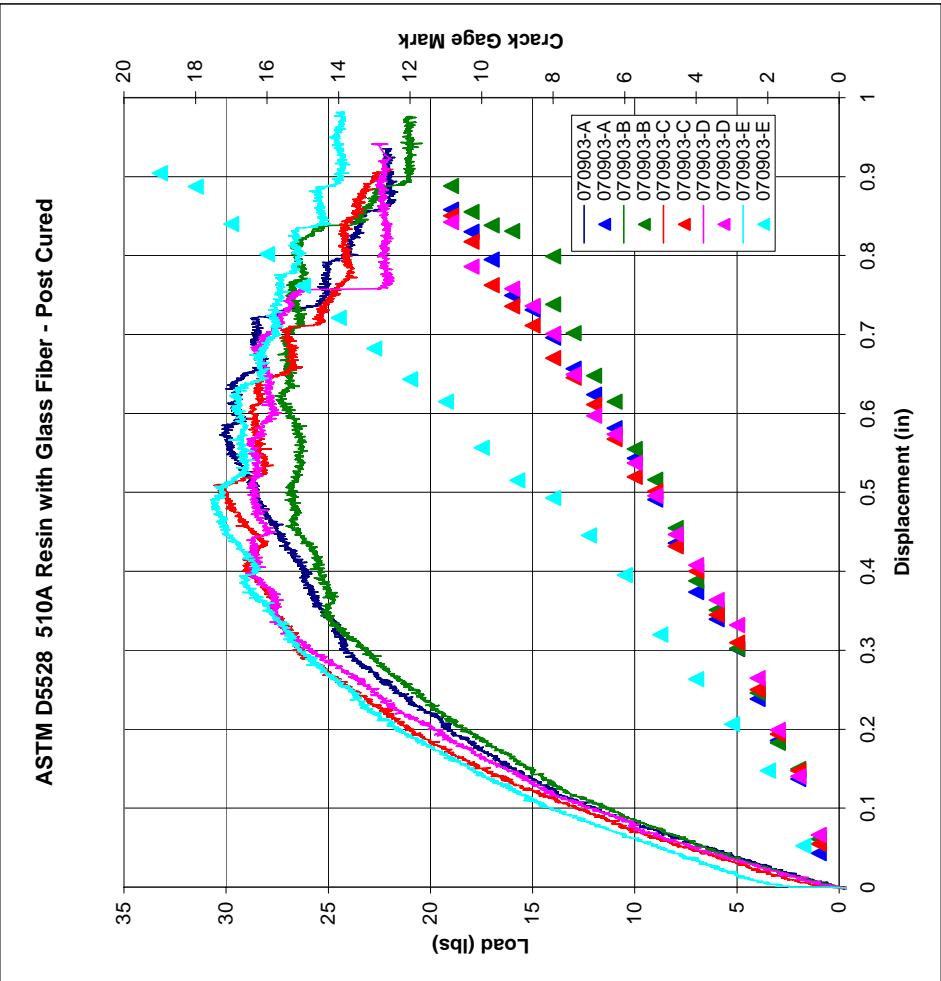
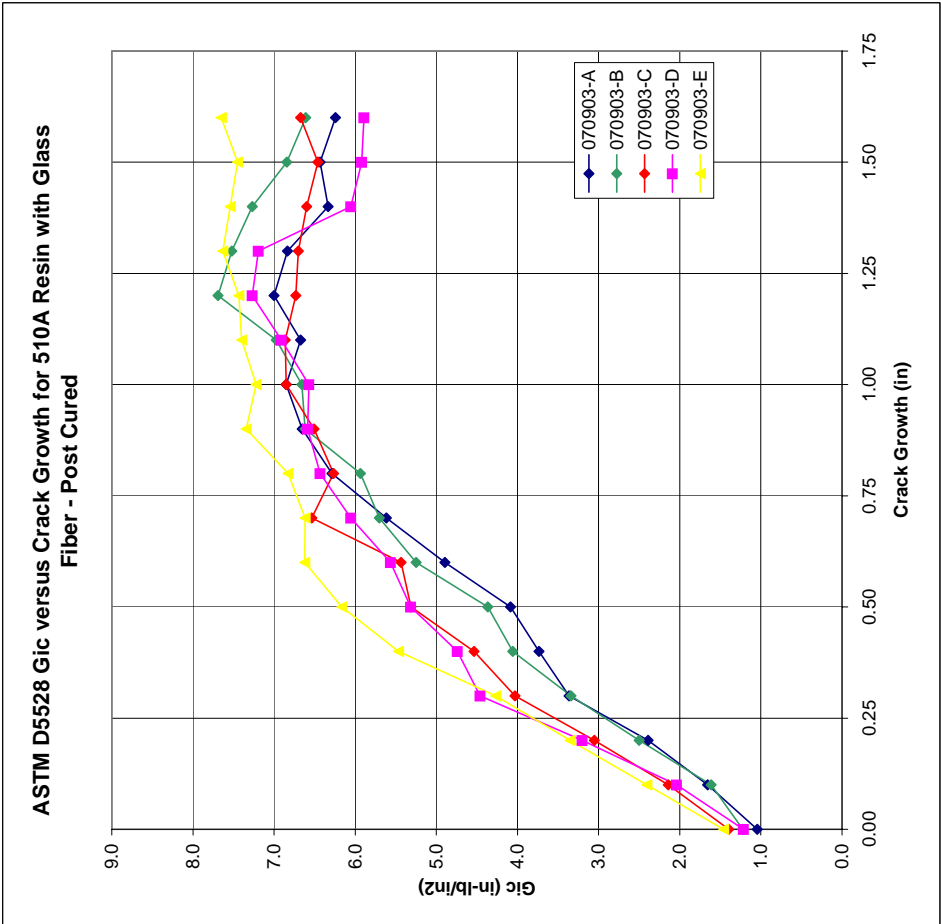


Sample ID	Width	Thickness	ao	Load	Gic (in-lb/in2)	
					Onset	Propagation
070903-01	0.990	0.242	1.906	27.69	1.28	2.09
070903-02	0.990	0.236	1.908	27.94	1.14	3.24
070903-03	0.993	0.242	1.886	28.88	0.68	2.78
070903-04	0.995	0.245	1.880	29.27	1.19	3.51
070903-05	0.994	0.246	1.886	27.53	1.48	3.46
			average	28.26	1.15	3.01
			stddev	0.77	0.29	0.59
			Cov (%)	2.72	25.56	19.64
						8.94



DCB Results Summary-510A Post Cured Material

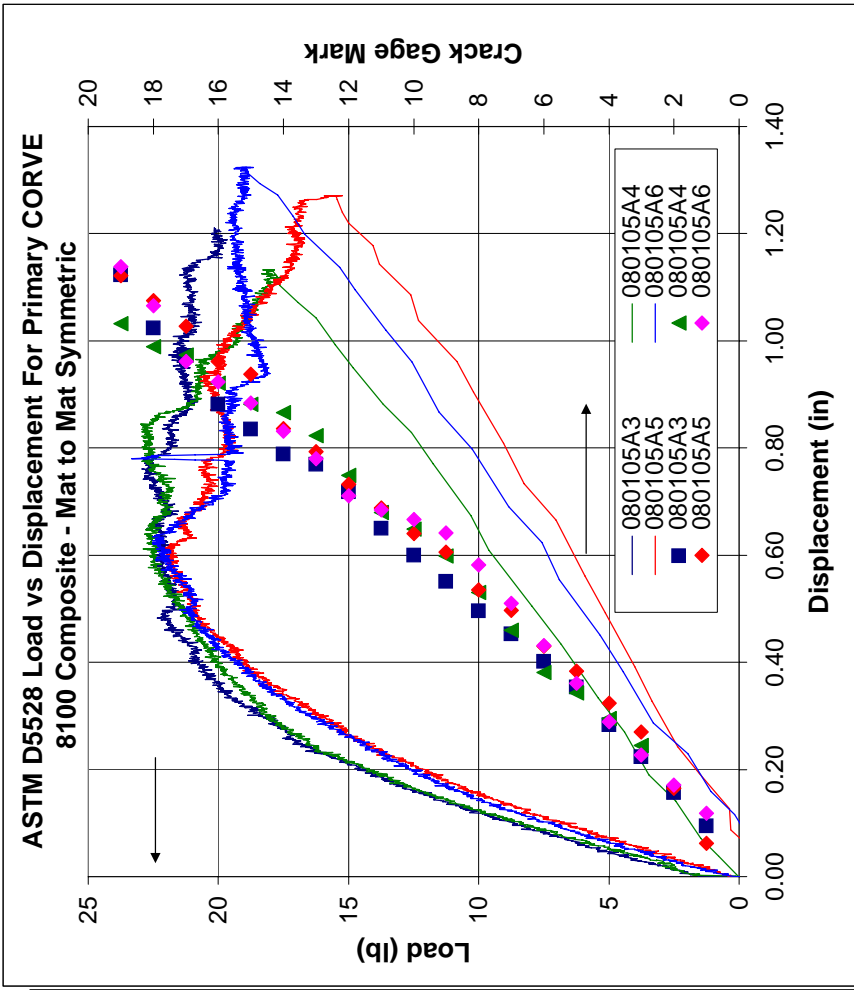
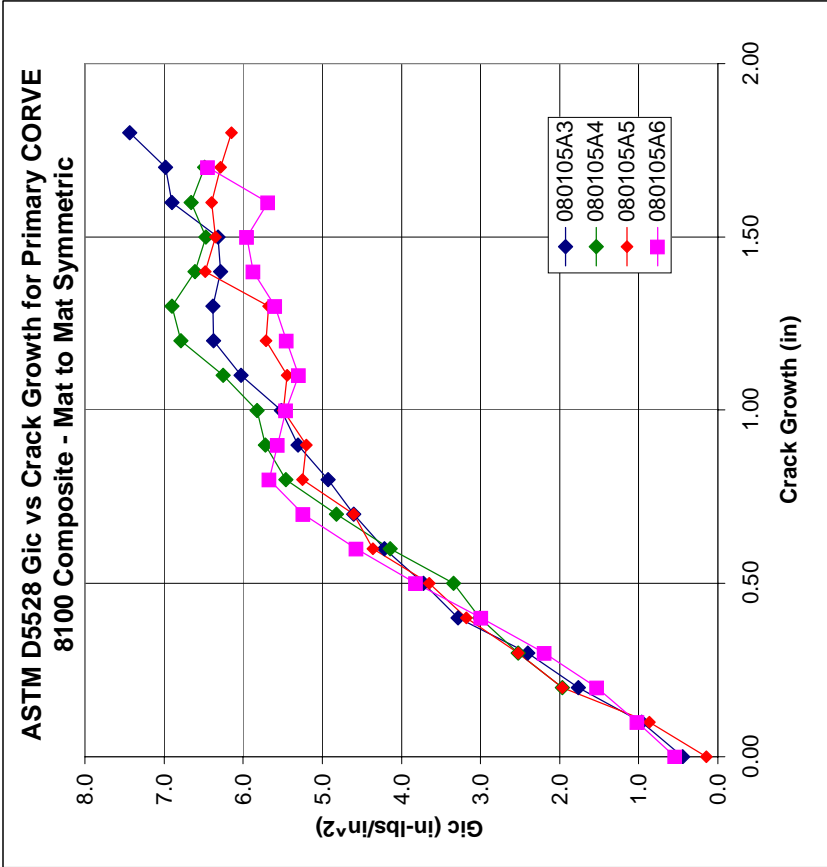
Sample ID	Width	Thickness	ao	Gic (in-lb/in2)		
				Onset	Propagation	Steady State
070903-A	1.0000	0.2515	1.9085	1.04	2.88	6.62
070903-B	1.0010	0.2525	1.9335	1.22	2.92	7.08
070903-C	0.9930	0.2565	1.8625	1.40	3.54	6.70
070903-D	0.9925	0.2525	1.9030	1.22	3.83	6.54
070903-E	0.9965	0.2525	1.9045	1.46	3.81	7.48
average				1.27	3.40	6.88
stdev				0.16	0.47	0.39
Cov (%)				12.97	13.79	5.66



Double Cantilever Beam, ASTM 5528 Primary CORVE 8100 SW1810 Glass Fabric (Mat to Mat)

Date	Sample ID	Resistance (Ohms)	Initial Crack Length, a ₀ (in)	hinge (in)	Width 1 (in.)	Width 2 (in.)	Width 3 (in.)	Average Width (in.)	Thickness 1 (in.)	Thickness 2 (in.)	Thickness 3 (in.)	Average Width (in.)	Max Load (lbs at in)	GI Onset (in-lbs/in ²)	GI Propagation (in-lbs/in ²)	GI Steady State (in-lbs/in ²)
27-Mar-08	080105A3	0.8000	1.979	0.09	0.9680	0.9680	0.9680	0.9680	0.2105	0.2105	0.2105	0.2105	22.94	0.45	2.8443	6.15
27-Mar-08	080105A4	0.9000	1.9705	0.09	0.9645	0.9645	0.9645	0.9645	0.2205	0.2205	0.2205	0.2205	22.98	-	2.7640	6.47
27-Mar-08	080105A5	0.9000	1.986	0.09	0.9755	0.9755	0.9755	0.9755	0.2155	0.2155	0.2155	0.2155	22.12	0.15	2.8521	5.86
27-Mar-08	080105A6	0.8000	1.997	0.09	0.9890	0.9930	0.9910	0.9910	0.2070	0.2420	0.2035	0.2175	23.34	0.54	2.5921	5.61
												AVG	22.84	0.38	2.76	6.02
												STDEV	0.52	0.20	0.12	0.37
												%COV	2.26	54.10	4.37	6.22

Loading Rate 0.2 in/min
Load Scale 100 lbs

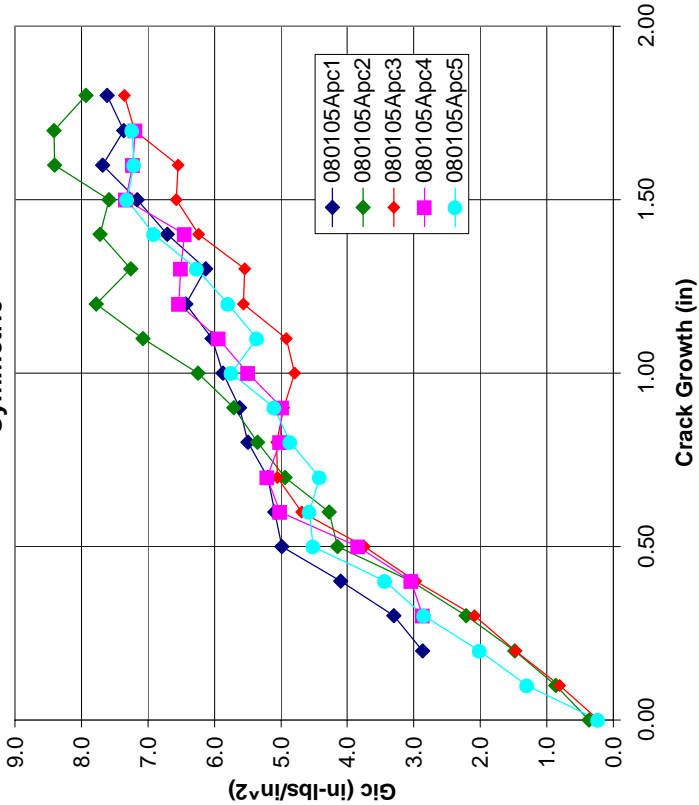


Double Cantilever Beam, ASTM 5528 Post Cured Primary CORVE 8100 SW1810 Glass Fabric (Mat to Mat)

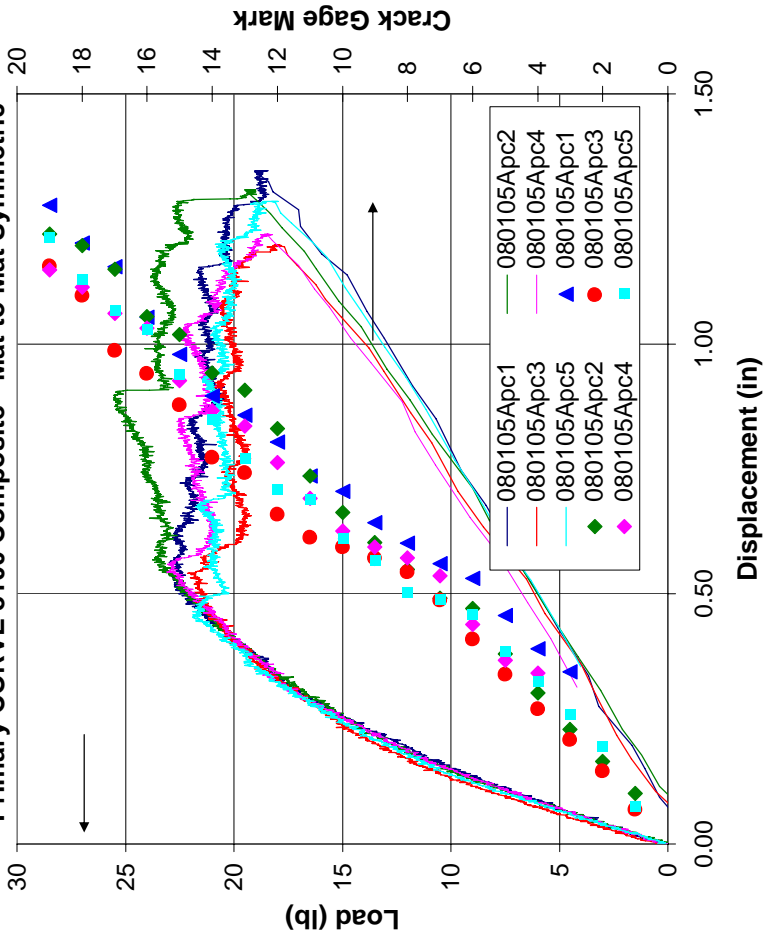
Date	Sample ID	Resistance (Ohms)	Initial Crack Length, a_0 (in)	hinge (in)	Width 1 (in.)	Width 2 (in.)	Width 3 (in.)	Average Width (in.)	Thickness 1 (in.)	Thickness 2 (in.)	Thickness 3 (in.)	Average Width (in.)	Max Load (lbs at in)	GI Onset (in-lbs/in ²)	GI Propagation (in-lbs/in ²)	GI Steady State (in-lbs/in ²)
9-Apr-08	080105Apc1	0.80	2.04	0.09	0.9785	0.9910	0.9920	0.9872	0.2055	0.2085	0.2115	0.2085	22.98	-	3.70	6.39
9-Apr-08	080105Apc2	1.00	1.9915	0.09	0.9855	0.9845	0.9895	0.9865	0.2020	0.1945	0.2065	0.2010	25.55	0.36	2.63	7.28
9-Apr-08	080105Apc3	0.90	1.983	0.09	0.9850	0.9880	0.9875	0.9868	0.2035	0.2040	0.1990	0.2022	22.12	0.22	2.53	5.60
9-Apr-08	080105Apc4	1.00	1.992	0.09	0.9815	0.9785	0.9800	0.9800	0.2050	0.1995	0.2050	0.2032	23.11	0.00	2.95	6.38
9-Apr-08	080105Apc5	0.80	2.0005	0.09	0.9825	0.9790	0.9805	0.9807	0.1990	0.2045	0.2035	0.2023	21.88	0.23	3.14	6.23
												AVG	23.13	0.20	2.99	6.38
												STDEV	1.45	0.15	0.47	0.60
												%COV	6.29	73.91	15.56	9.37

Loading Rate 0.2 in/min
Load Scale 100 lbs

ASTM D5528 Gic vs Crack Growth for Post Cured Primary CORVE 8100 Composite - Mat to Mat Symmetric



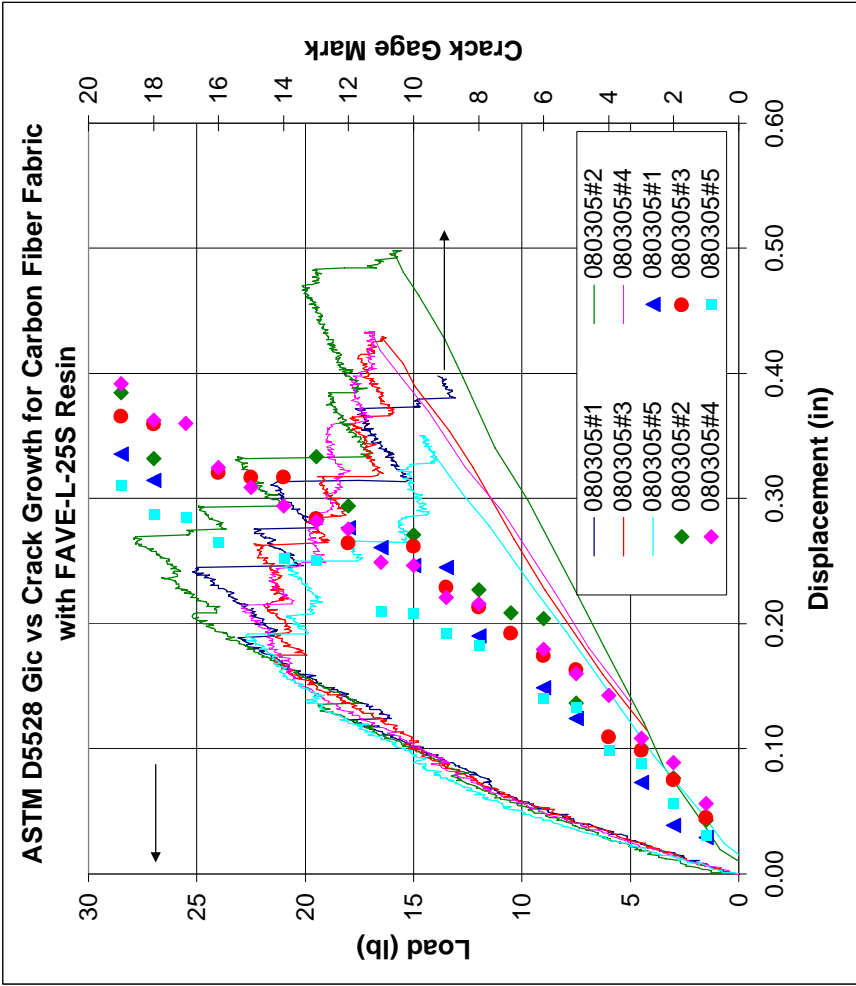
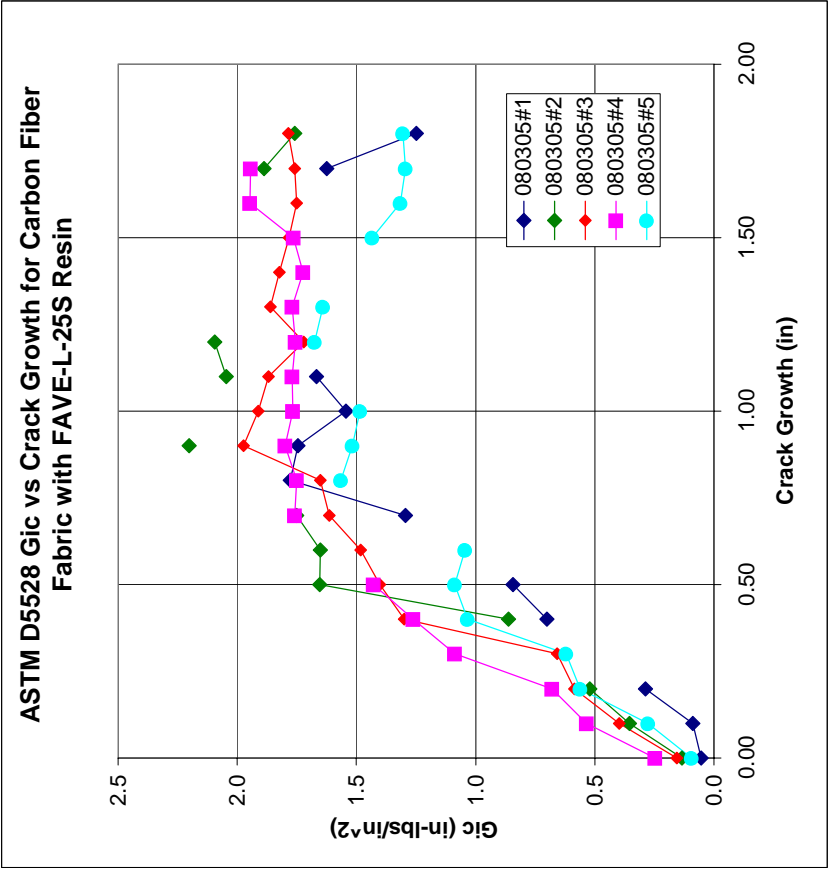
ASTM D5528 Load vs Displacement For Post Cured Primary CORVE 8100 Composite - Mat to Mat Symmetric



Double Cantilever Beam, ASTM 5528 for Carbon Fiber Fabric with FAVE-L-25S Resin

Date	Sample ID	Resistance (Ohms)	Initial Crack Length, a0 (in)	hinge (in)	Width 1 (in.)	Width 2 (in.)	Width 3 (in.)	Average Width (in.)	Thickness 1 (in.)	Thickness 2 (in.)	Thickness 3 (in.)	Average Width (in.)	Max Load (lbs at in)	GI Onset (in-lbs/in^2)	GI Propagation (in-lbs/in^2)	GI Steady State (in-lbs/in^2)
9-Apr-08	080305#1	0.9000	1.944	0.09	0.9935	0.9955	0.9970	0.9953	0.2560	0.2530	0.2595	0.2562	25.19	0.05	0.7009	1.61
9-Apr-08	080305#2	1.0000	1.983	0.09	0.9980	0.9985	0.9955	0.9973	0.2500	0.2500	0.2450	0.2483	27.90	0.13	0.8615	2.07
9-Apr-08	080305#3	1.0000	2.0165	0.09	0.9960	0.9945	0.9945	0.9950	0.2535	0.2500	0.2510	0.2515	22.36	0.16	0.9795	1.83
9-Apr-08	080305#4	0.9000	2.029	0.09	0.9920	0.9910	0.9915	0.9915	0.2515	0.2570	0.2495	0.2527	22.95	0.25	1.1751	1.76
9-Apr-08	080305#5	1.0000	1.9655	0.09	0.9965	0.9990	1.0000	0.9985	0.2495	0.2545	0.2580	0.2540	22.74	0.09	0.8262	1.56
												AVG	24.23	0.14	0.91	1.76
												STDEV	2.33	0.07	0.18	0.20
												%COV	9.62	52.76	19.70	11.53

Loading Rate 0.2 in/min
Load Scale 100 lbs

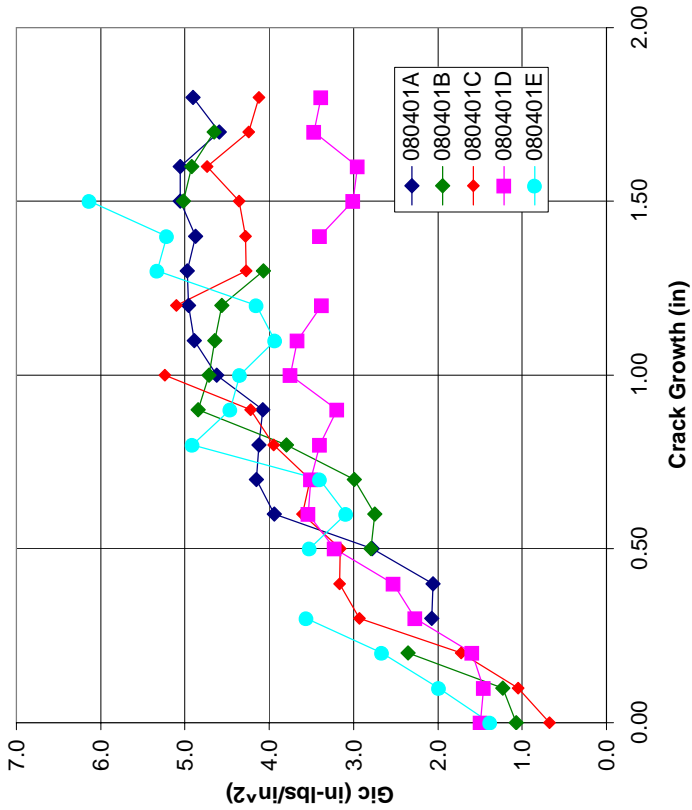


510A Resin with Carbon Fiber Fabric, Double Cantilever Beam, ASTM 5528

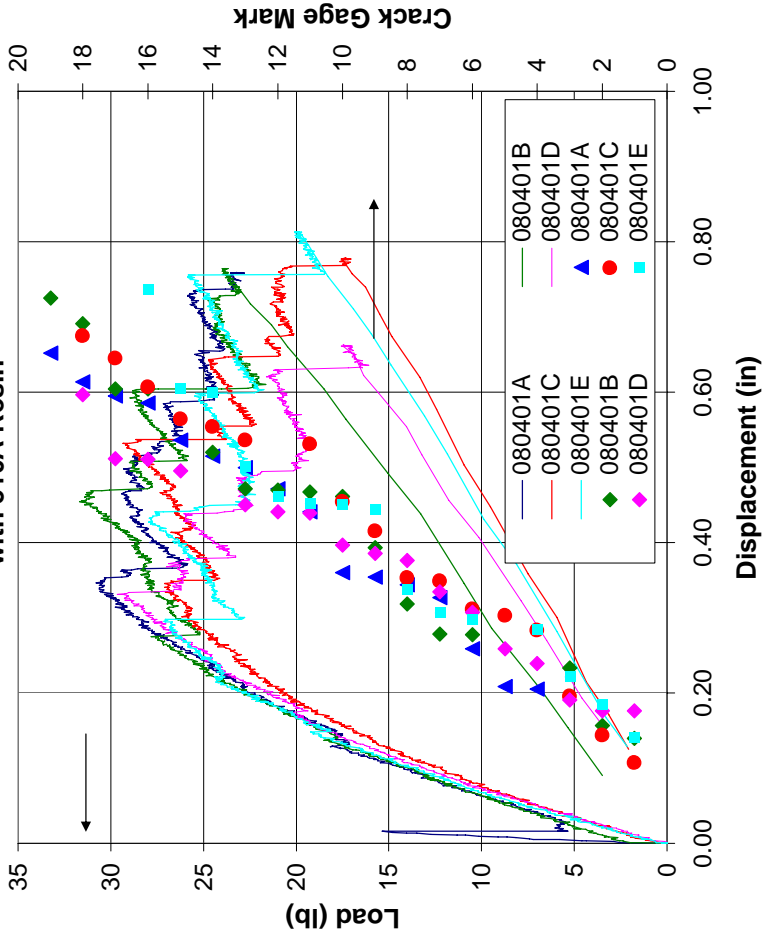
Date	Sample ID	Resistance (Ohms)	Initial Crack Length, a ₀ (in)	hinge (in)	Width 1 (in.)	Width 2 (in.)	Width 3 (in.)	Average Width (in.)	Thickness 1 (in.)	Thickness 2 (in.)	Thickness 3 (in.)	Average Width (in.)	Max Load (lbs at in)	GI Onset (in-lbs/in ²)	GI Propagation (in-lbs/in ²)	GI Steady State (in-lbs/in ²)
24-Apr-08	080401A	1.0000	1.9815	0.09	0.9935	0.9945	0.9930	0.9937	0.2990	0.3040	0.2975	0.3002	30.78	-	2.0676	4.90
28-Apr-08	080401B	1.0000	2.0065	0.09	0.9955	0.9955	0.9945	0.9952	0.2985	0.2965	0.2980	0.2977	31.69	1.07	-	4.60
28-Apr-08	080401C	1.0000	2.074	0.09	0.9940	0.9940	0.9950	0.9943	0.2910	0.2960	0.2985	0.2952	29.34	0.67	3.0500	4.65
28-Apr-08	080401D	1.0000	2.053	0.09	0.9950	1.0040	1.0110	1.0033	0.2965	0.2925	0.2945	0.2945	29.66	1.50	2.4006	3.44
28-Apr-08	080401E	1.0000	2.0525	0.09	0.9925	0.9945	0.9975	0.9948	0.2975	0.2935	0.2950	0.2953	27.96	1.38	3.5581	4.85
													AVG 29.89	1.16	2.77	4.49
													STDEV 1.42	0.37	0.67	0.60
													%COV 4.77	31.90	24.04	13.35

Loading Rate 0.2 in/min
Load Scale 100 lbs

ASTM D5528 Gic vs Crack Growth for Carbon Fiber Fabric with 510A Resin

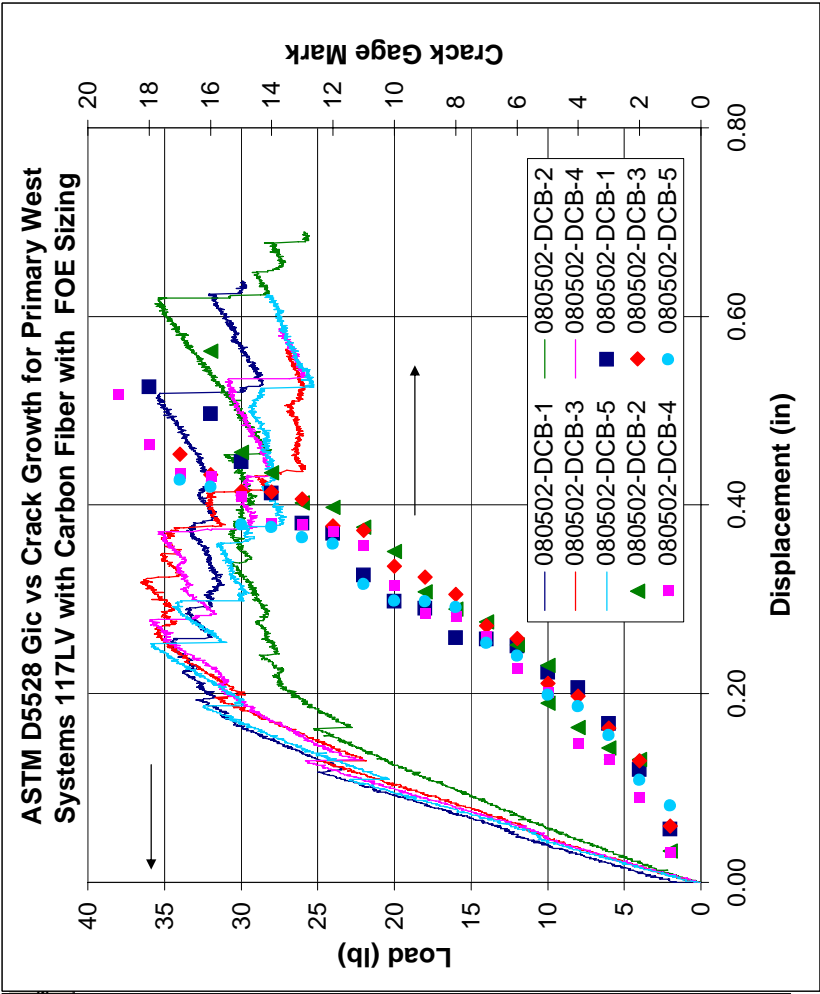
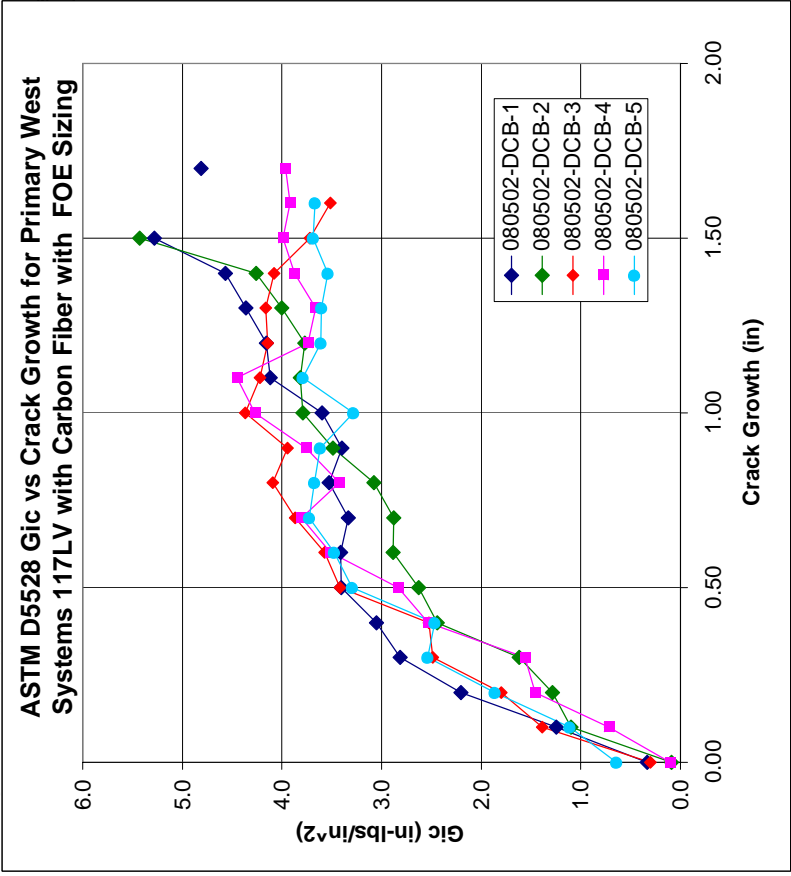


ASTM D5528 Gic vs Crack Growth for Carbon Fiber Fabric with 510A Resin



West Systems 117LV with Carbon Fiber with FOE Sizing, Double Cantilever Beam, ASTM 5528

Date	Sample ID	Resistance (Ohms)	Initial Crack Length, a ₀ (in)	hinge (in)	Width 1 (in.)	Width 2 (in.)	Width 3 (in.)	Average Width (in.)	Thickness 1 (in.)	Thickness 2 (in.)	Thickness 3 (in.)	Average Width (in.)	Max Load (lbs at in)	GI Onset (in-lbs/in ²)	GI Propagation (in-lbs/in ²)	GI Steady State (in-lbs/in ²)
9-Jul-08	080502-DCB-1	1.0000	1.936	0.09	0.9950	0.9965	0.9960	0.9958	0.2705	0.2700	0.2735	0.2713	35.52	0.33	2.9328	4.55
9-Jul-08	080502-DCB-2	1.0000	2.050	0.09	0.9950	0.9945	0.9950	0.9948	0.2745	0.2720	0.2680	0.2715	35.60	0.09	2.0298	4.25
9-Jul-08	080502-DCB-3	1.0000	2.001	0.09	0.9935	0.9965	0.9985	0.9962	0.2630	0.2720	0.2705	0.2685	36.52	0.30	2.5056	3.97
9-Jul-08	080502-DCB-4	1.0000	1.972	0.09	1.0015	1.0020	1.0080	1.0038	0.2625	0.2695	0.2675	0.2665	35.94	0.10	2.0447	3.94
9-Jul-08	080502-DCB-5	1.0000	1.925	0.09	0.9960	0.9950	0.9965	0.9958	0.2695	0.2705	0.2725	0.2708	35.91	0.65	2.5034	3.65
												AVG	35.90	0.29	2.40	4.07
												STDEV	0.40	0.23	0.38	0.34
												%COV	1.10	76.38	15.69	8.36



Appendix G

ASTM E 1640 Dynamic Mechanical Analysis – Glass Transition Temperature

Naval Surface Warfare Center
Carderock Division Code 616
9500 MacArthur Blvd
West Bethesda, MD 20817-5700

Thermal Behavior of FAVE Composite Materials

Prepared by:

Dr. Steven Dallek
G/J Associates
Annapolis, MD

Submitted to:

Dr. Maureen E. Foley
Code 6550

17 July 2007

Glass Transition Temperatures (°C)

<u>File</u>	<u>Sample</u>	<u>Tg (E')</u>	<u>Tg (E'')</u>	<u>Tg (tan δ)</u>
Fave-I.001	FAVE-L-20S	78.9	-	105
Fave-I.002	FAVE-L-20S	73.8	89.2	107
Foley-2.001	FAVE-L-25S	84.2	98.2	114
Foley-2.002	FAVE-L-25S	96.2	106	122
Foley-1.001	FAVE-O-25S	82.4	100	116
Foley-1.002	FAVE-O-25S	94.4	110	124
Foley-3.001	510A	101	114	128
Foley-3.002	510A	111	124	136
Foley-5.001	DERAKANE 8084	73.0	80.2	118
Foley-5.002	DERAKANE 8084	85.0	110	130
Foley-9.001	CORVE 8100	108	110	122
Foley-9.002	CORVE 8100 **	112	114	126
Foley-10.001	CORVE 8100PC	90.4	110	122
Foley-10.002	CORVE 8100PC***	---	---	---
Foley-4.001	RS	82.2	92.2	106
Foley-4.002	RS	101	114	122
Foley-7.001	AOC K018	90.7	108	128
Foley-7.002	AOC K018	123	112	144
Foley-8.001	AOC K018PC	102	102	128
Foley-8.002	AOC K018PC*	---	---	---

*sample yielded – data not stored

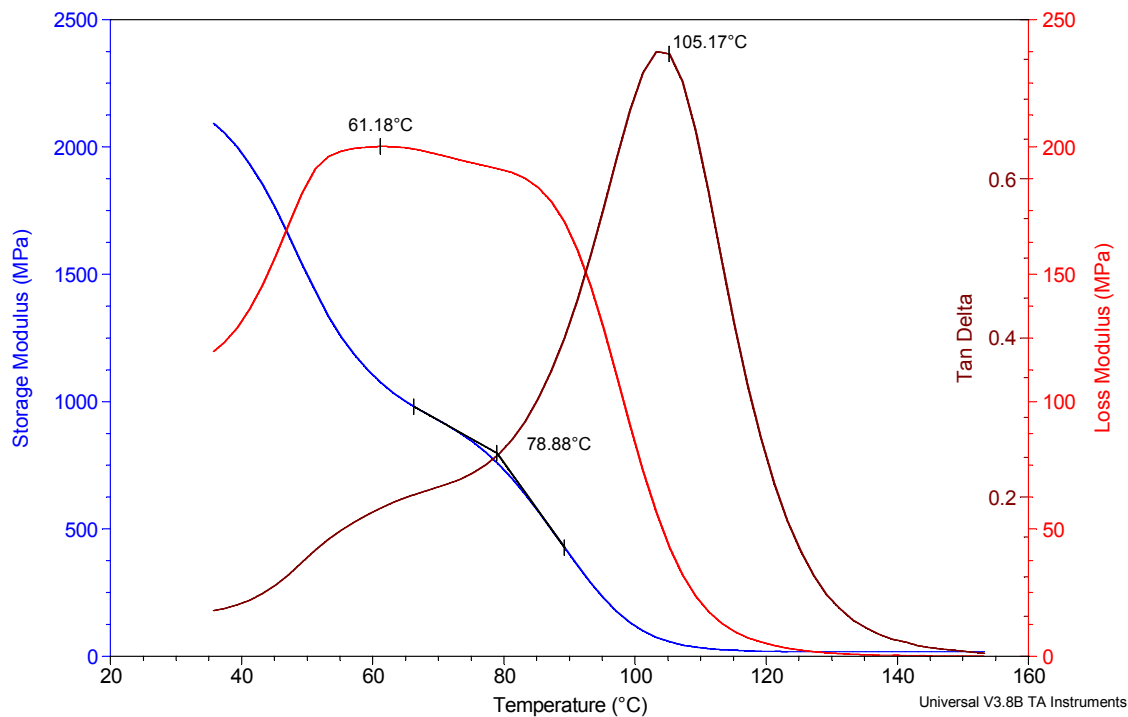
**sample yielded – data stored

*** computer problems – data corrupted

Sample: FAVE-L
 Size: 9.8400 x 9.9700 x 1.7200 mm
 Method: Temp Step / Freq Sweep
 Comment: torque: 6 in-lb

DMA

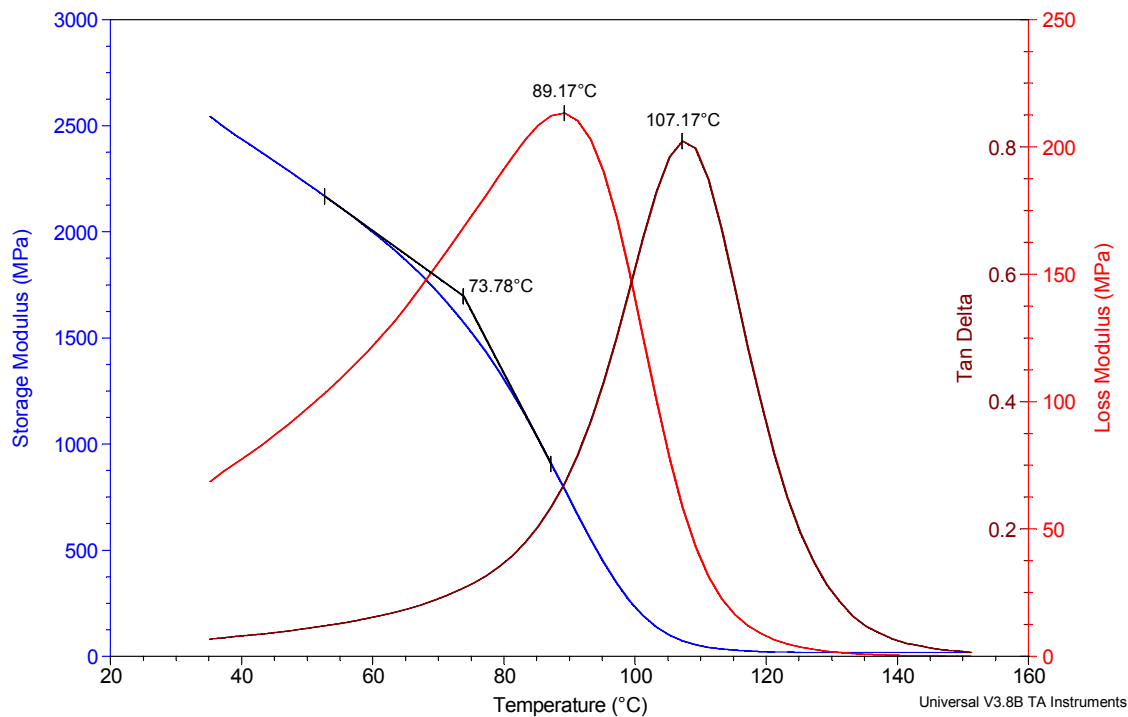
File: C:\TA\Data\DMA\fave-l.001
 Run Date: 26-Mar-07 08:25
 Instrument: DMA Q800 V3.13 Build 74



Sample: FAVE-L
 Size: 9.8400 x 9.9700 x 1.7200 mm
 Method: Temp Step / Freq Sweep
 Comment: torque: 6 in-lb

DMA

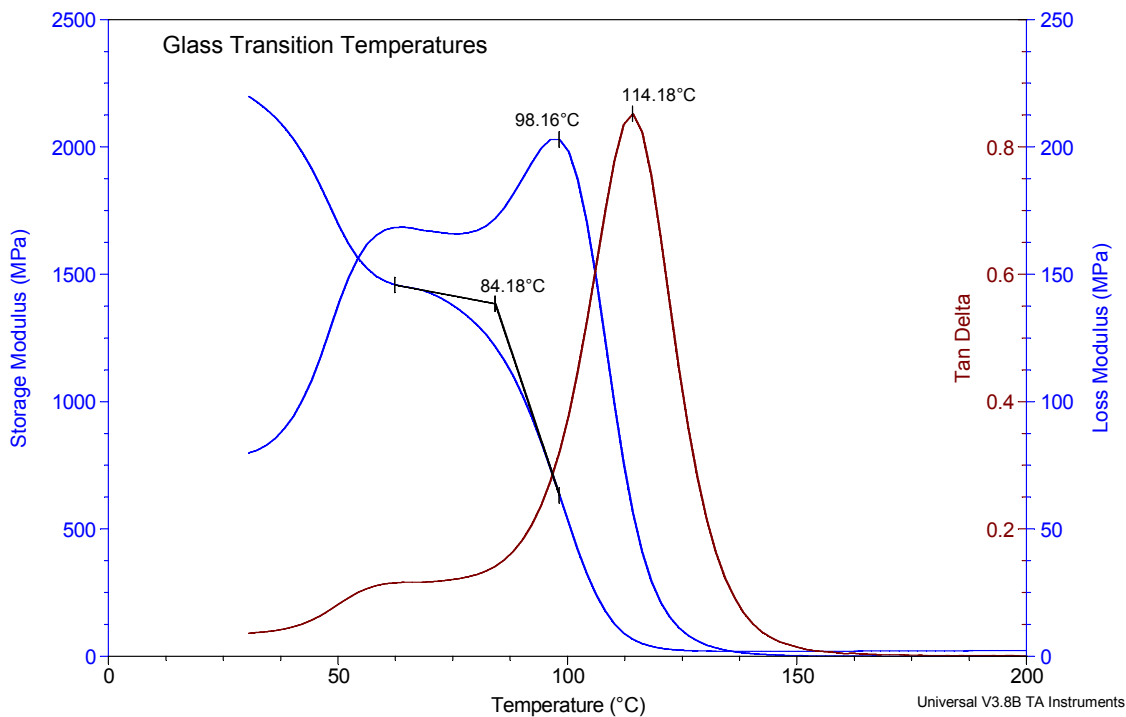
File: C:\TA\Data\DMA\fave-l.002
 Run Date: 27-Mar-07 05:58
 Instrument: DMA Q800 V3.13 Build 74



Sample: FAVE-L-25S
 Size: 9.9000 x 10.0300 x 2.4400 mm
 Method: Temperature Ramp
 Comment: torque: 10 in-lb

DMA

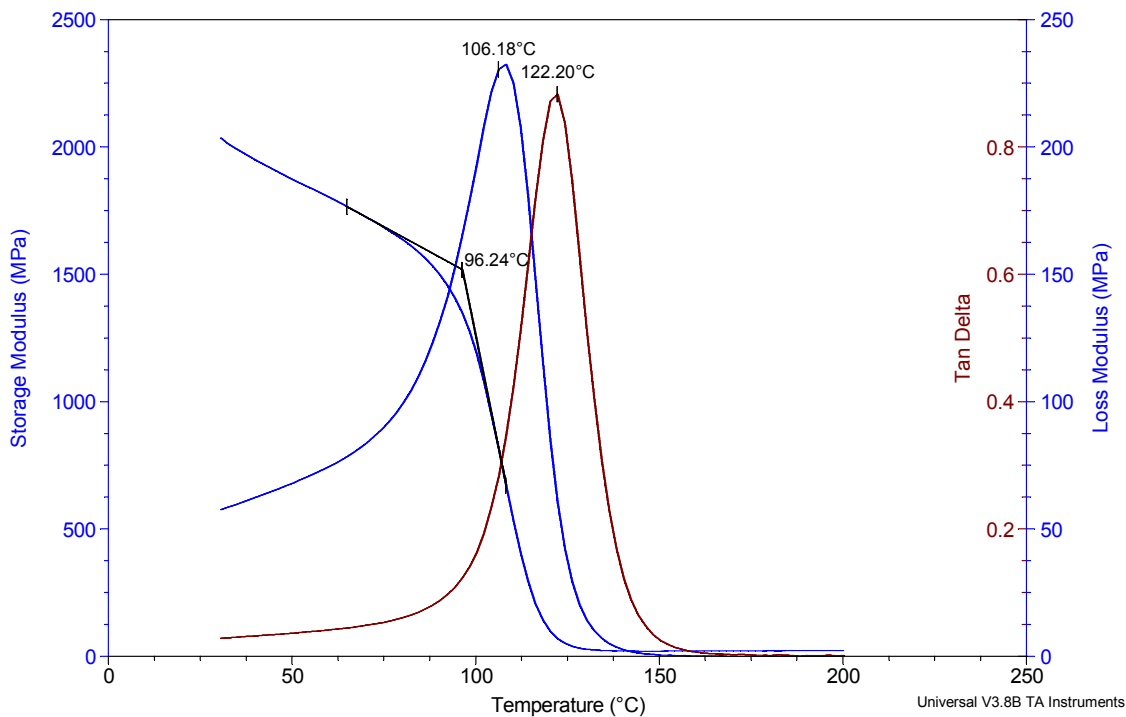
File: C:\TA\Data\DMA\foley-2.001
 Run Date: 02-Jul-07 08:25
 Instrument: DMA Q800 V3.13 Build 74



Sample: FAVE-L-25S
 Size: 9.9000 x 10.0300 x 2.4400 mm
 Method: Temperature Ramp
 Comment: torque: 10 in-lb

DMA

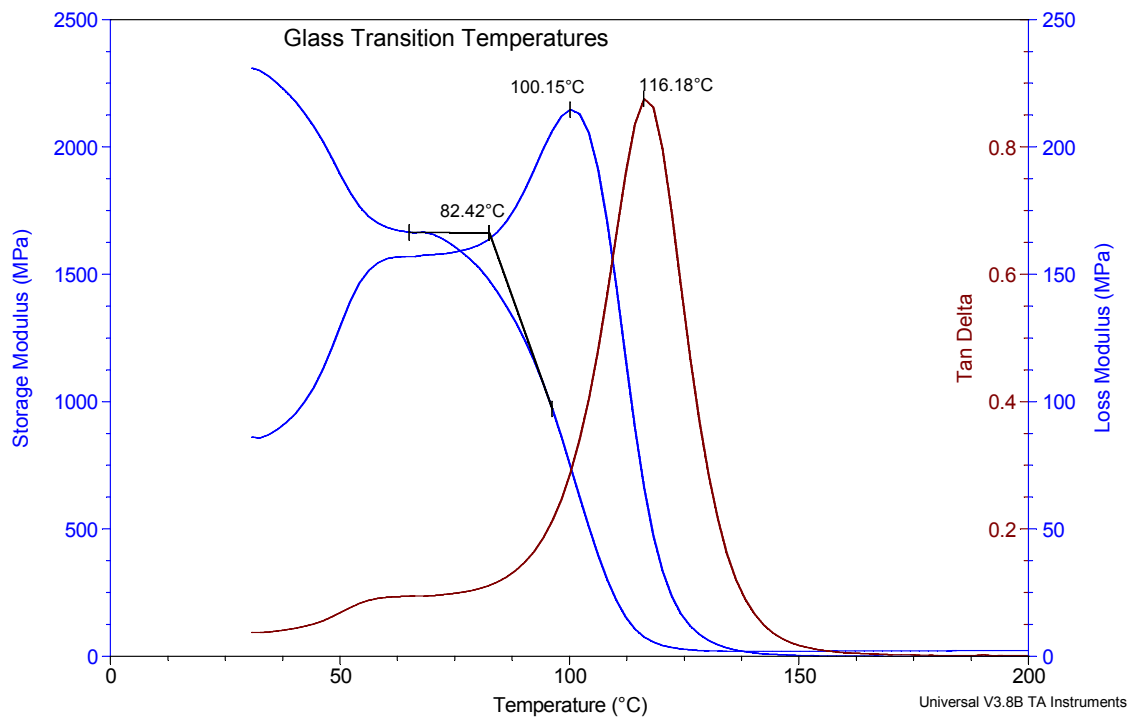
File: C:\TA\Data\DMA\foley-2.002
 Run Date: 03-Jul-07 06:09
 Instrument: DMA Q800 V3.13 Build 74



Sample: FAVE-O-25S
 Size: 9.8000 x 11.0600 x 2.5700 mm
 Method: Temperature Ramp
 Comment: torque: 6 in-lb

DMA

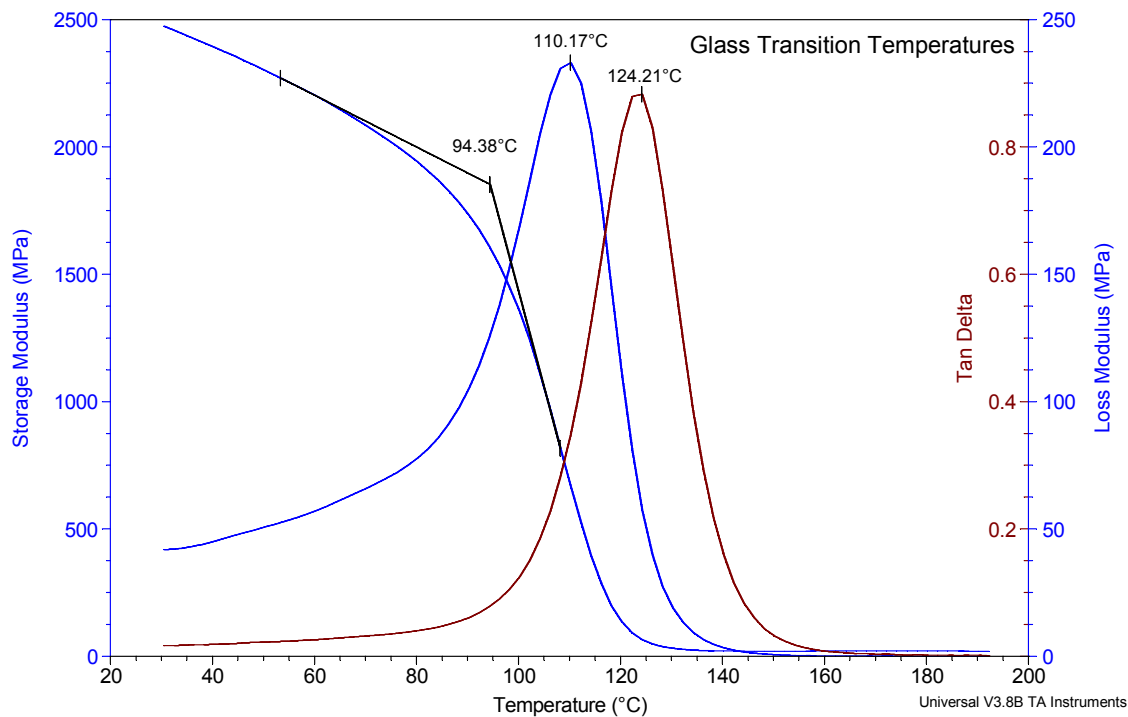
File: C:\TA\Data\DMA\foley-1.001
 Run Date: 26-Jun-07 14:05
 Instrument: DMA Q800 V3.13 Build 74



Sample: FAVE-O-25S
 Size: 9.8000 x 11.0600 x 2.5700 mm
 Method: Temperature Ramp
 Comment: torque: 6 in-lb

DMA

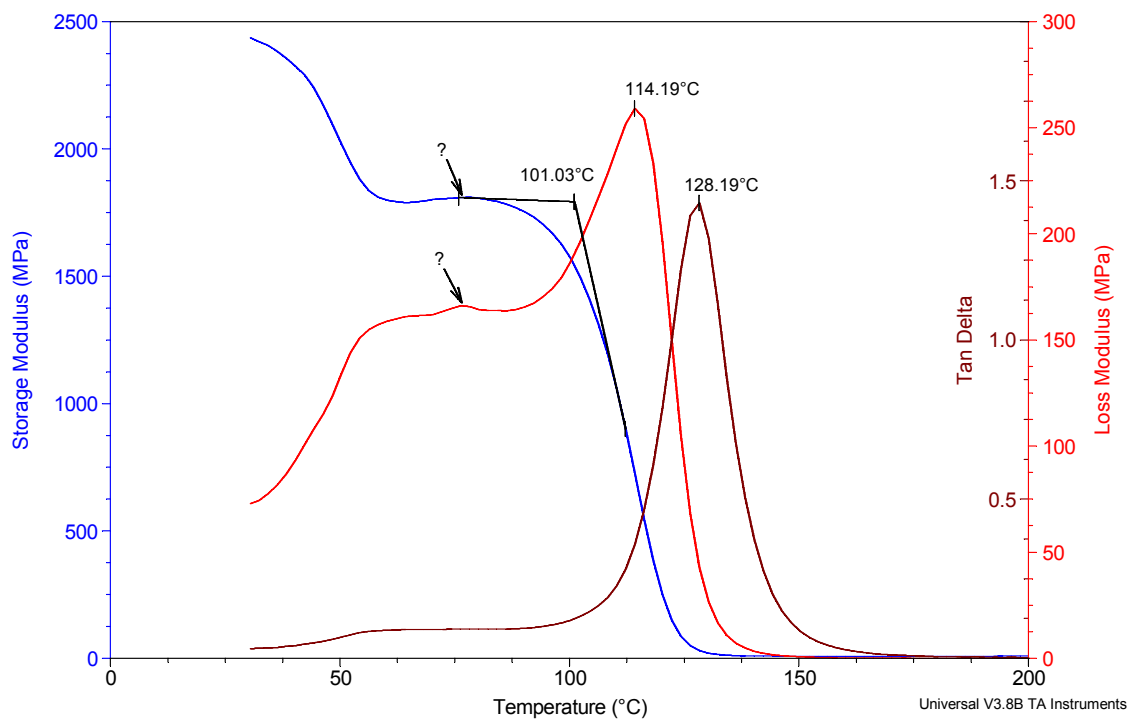
File: C:\TA\Data\DMA\foley-1.002
 Run Date: 27-Jun-07 06:29
 Instrument: DMA Q800 V3.13 Build 74



Sample: 510A
 Size: 9.9000 x 9.4500 x 2.1100 mm
 Method: Temperature Ramp
 Comment: torque: 10 in-lb

DMA

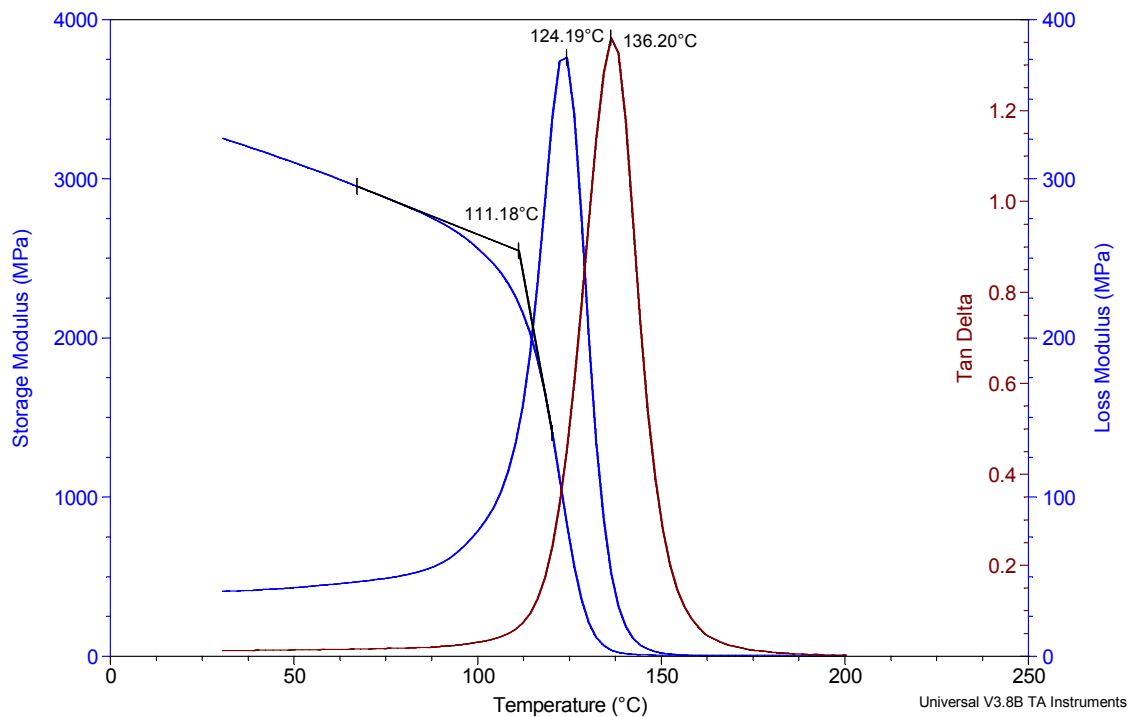
File: C:\TA\Data\DMA\foley-3.001
 Run Date: 05-Jul-07 06:14
 Instrument: DMA Q800 V3.13 Build 74



Sample: 510A
 Size: 9.9000 x 9.4500 x 2.1100 mm
 Method: Temperature Ramp
 Comment: torque: 10 in-lb

DMA

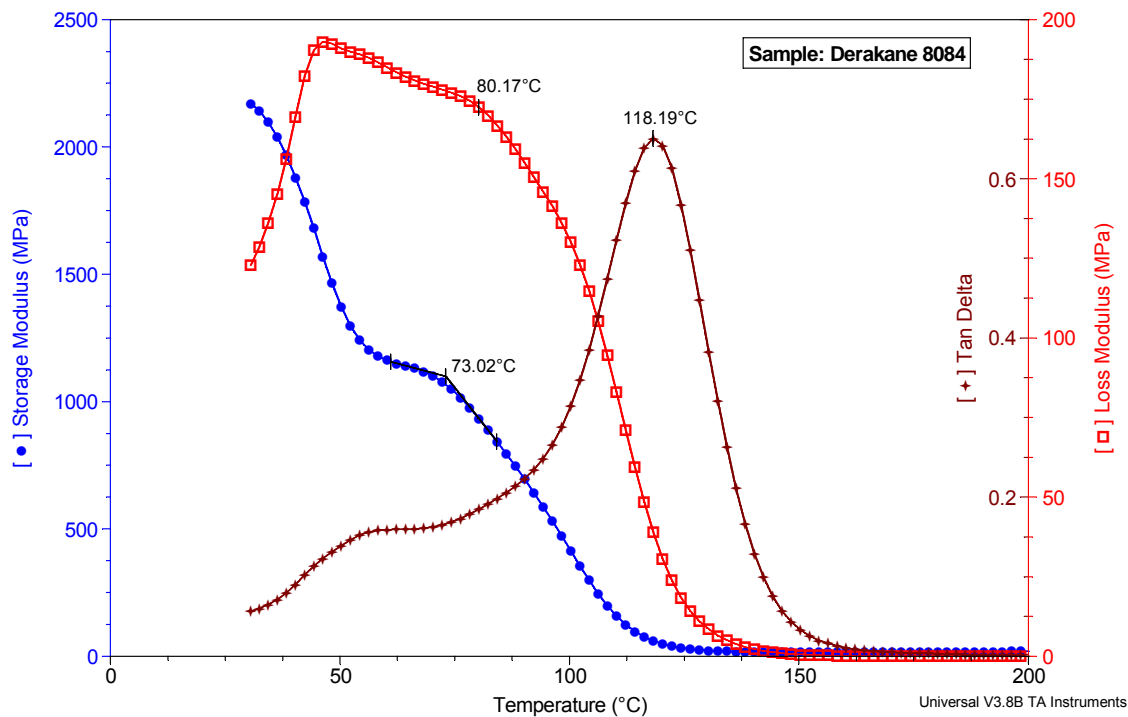
File: C:\TA\Data\DMA\foley-3.002
 Run Date: 09-Jul-07 06:42
 Instrument: DMA Q800 V3.13 Build 74



Sample: Derakane 8084
 Size: 9.9000 x 11.7300 x 2.1400 mm
 Method: Temperature Ramp
 Comment: torque: 10 in-lb

DMA

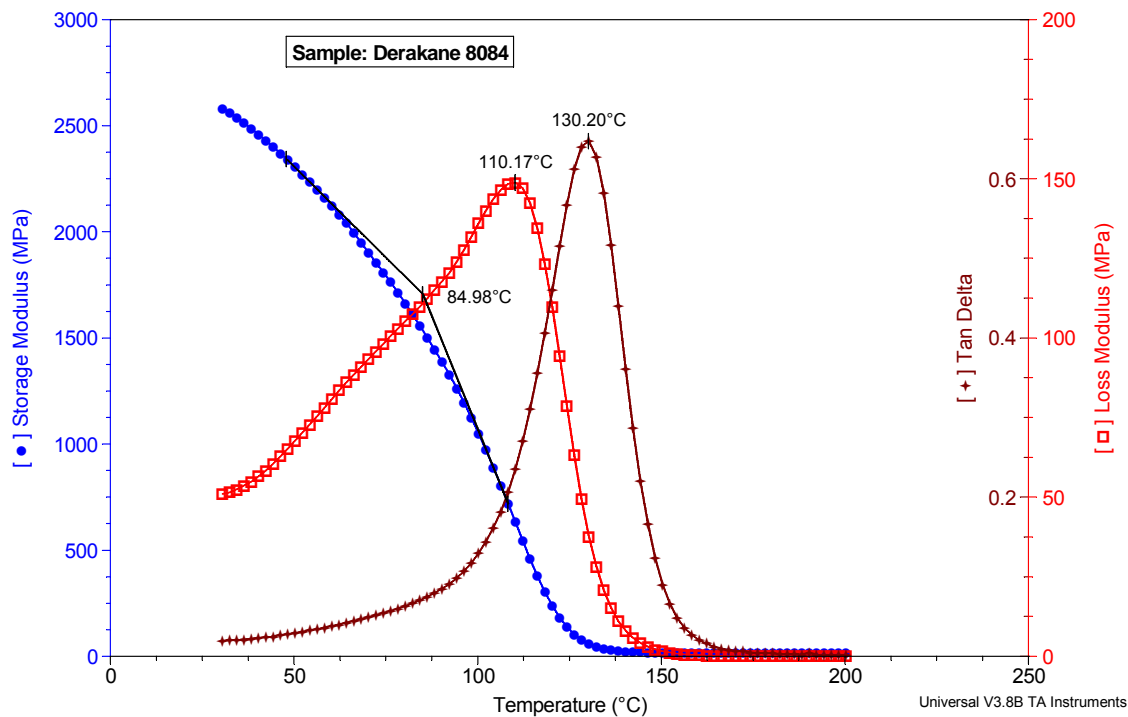
File: C:\TA\Data\DMA\foley-5.001
 Run Date: 16-Jul-07 06:45
 Instrument: DMA Q800 V3.13 Build 74



Sample: Derakane 8084
 Size: 9.9000 x 11.7300 x 2.1400 mm
 Method: Temperature Ramp
 Comment: torque: 10 in-lb

DMA

File: C:\TA\Data\DMA\foley-5.002
 Run Date: 17-Jul-07 06:10
 Instrument: DMA Q800 V3.13 Build 74



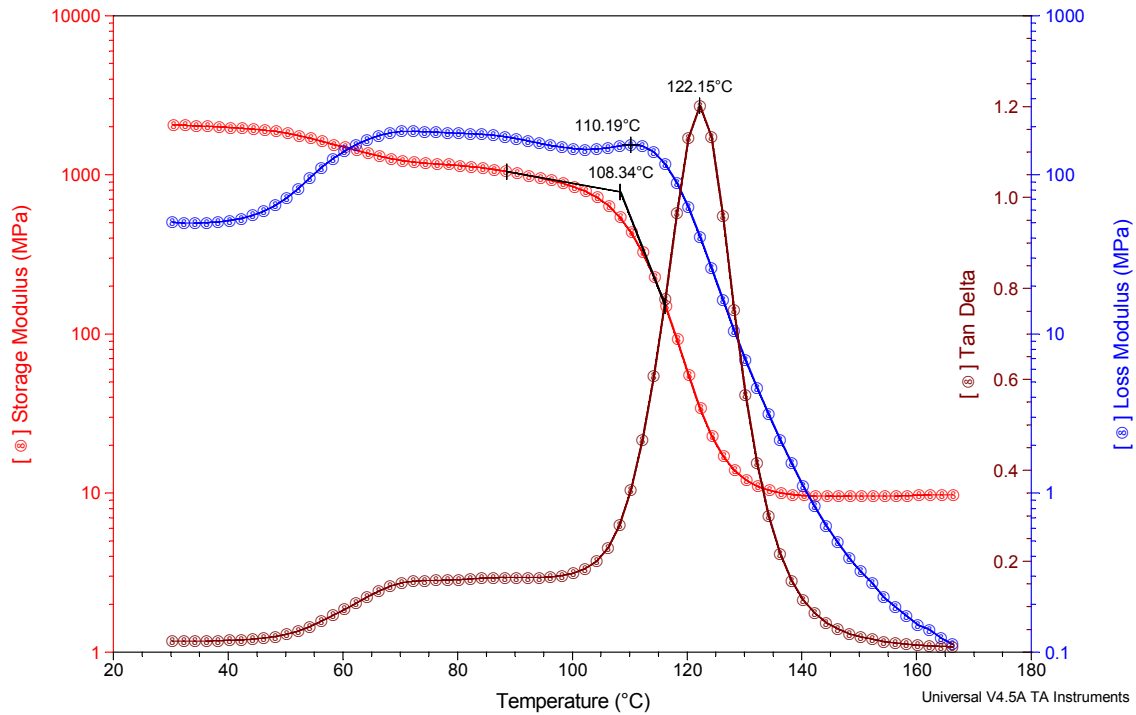
CORVE 8100

Sample: 080101A
Size: 9.5500 x 11.9800 x 1.7900 mm
Method: Temp Step / Freq Sweep

DMA

File: C:\TA\Data\DMA\Foley\foley-9.001

Run Date: 21-Feb-2008 06:41
Instrument: DMA Q800 V7.5 Build 127

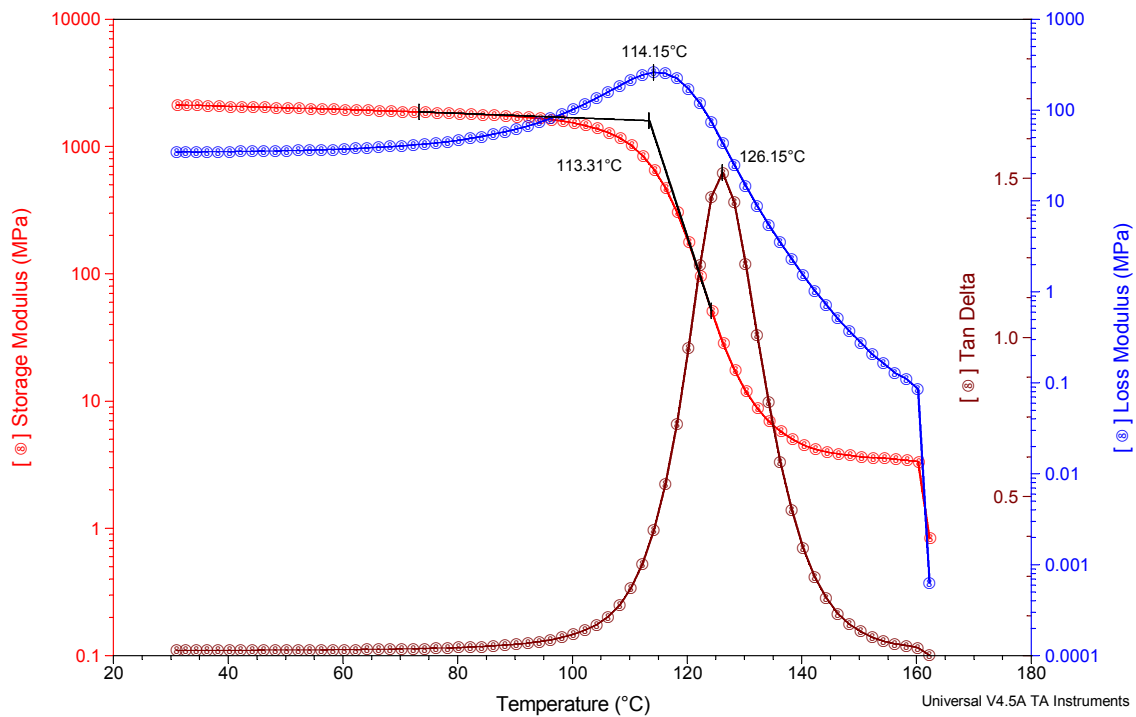


Sample: 080101A CORVE 8100
Size: 9.5500 x 11.9800 x 1.7900 mm
Method: Temp Step / Freq Sweep

DMA

File: C:\TA\Data\DMA\Foley\foley-9.002

Run Date: 21-Feb-2008 12:43
Instrument: DMA Q800 V7.5 Build 127



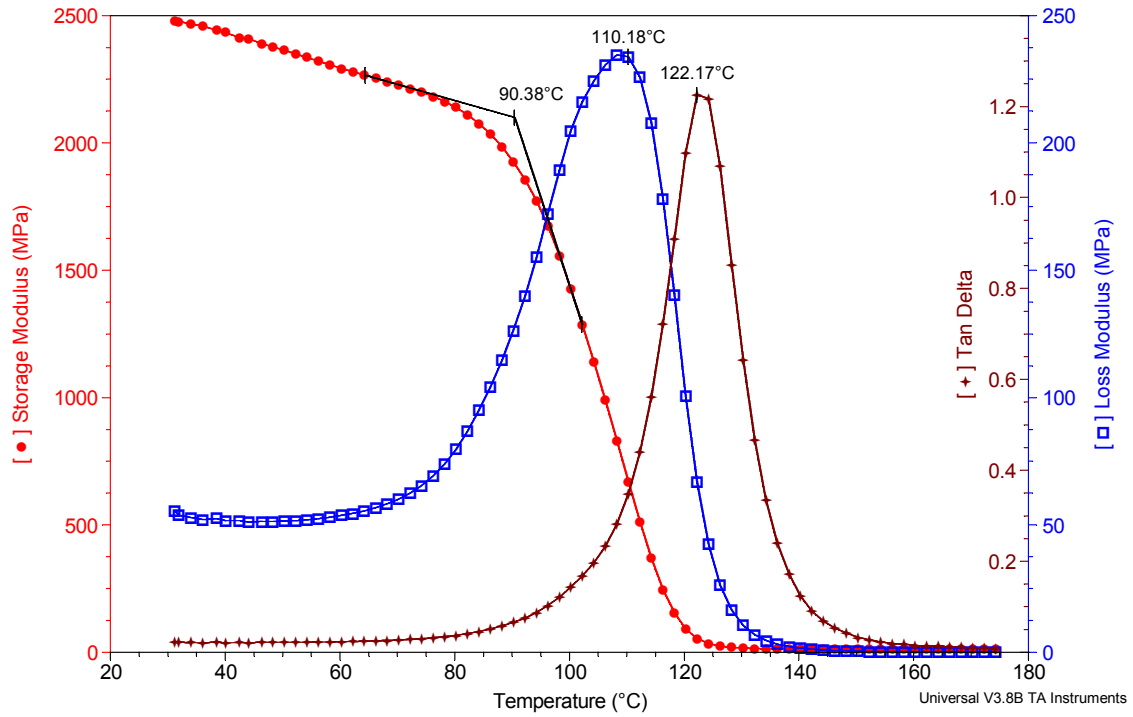
CORVE 8100 PC

Sample: 08101APC
Size: 9.6200 x 12.6800 x 1.9500 mm
Method: Temperature Ramp

DMA

File: C:\TA\Data\DMA\Foley\foley-10.001

Run Date: 26-Feb-08 07:32
Instrument: DMA Q800 V7.5 Build 127

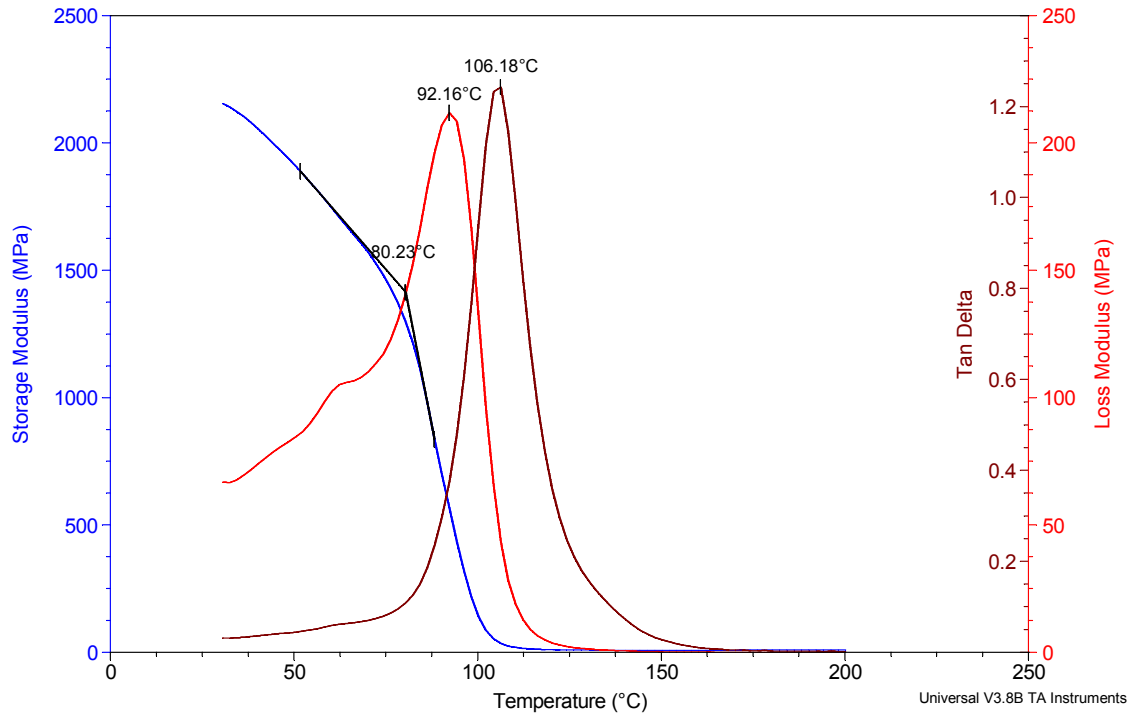


Rick Strand Formulation

Sample: RS
Size: 10.1100 x 10.9500 x 2.8300 mm
Method: Temperature Ramp
Comment: torque: 10 in-lb

DMA

File: C:\TA\Data\DMA\foley-4.001
Run Date: 10-Jul-07 06:20
Instrument: DMA Q800 V3.13 Build 74

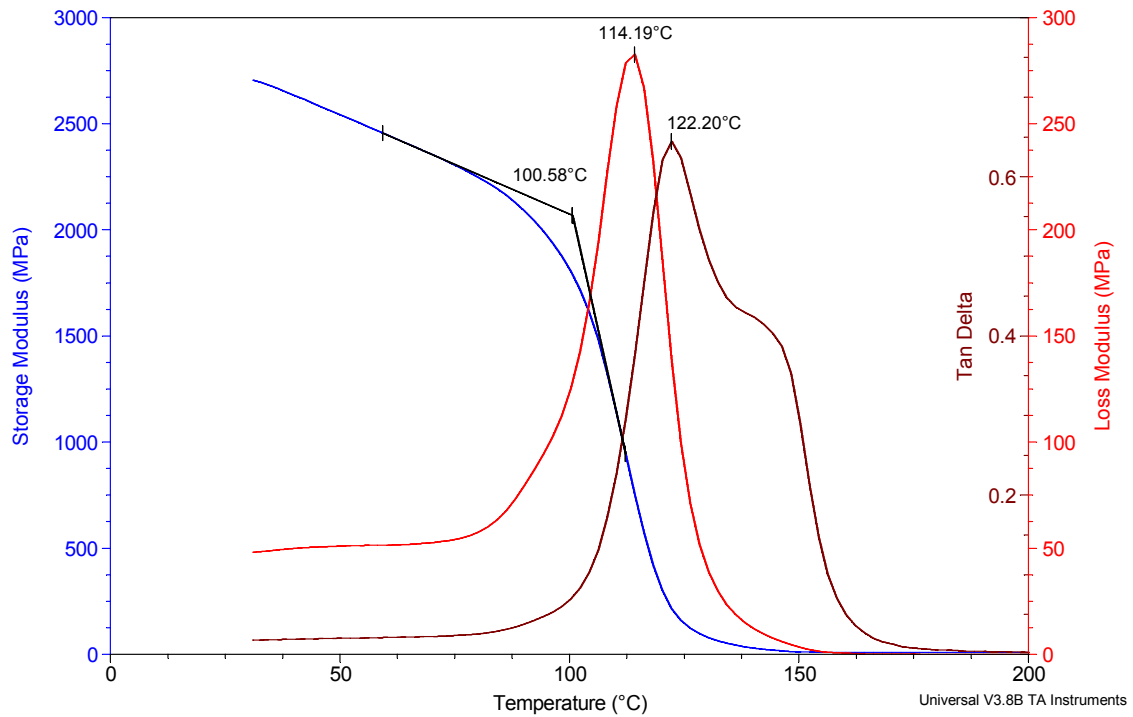


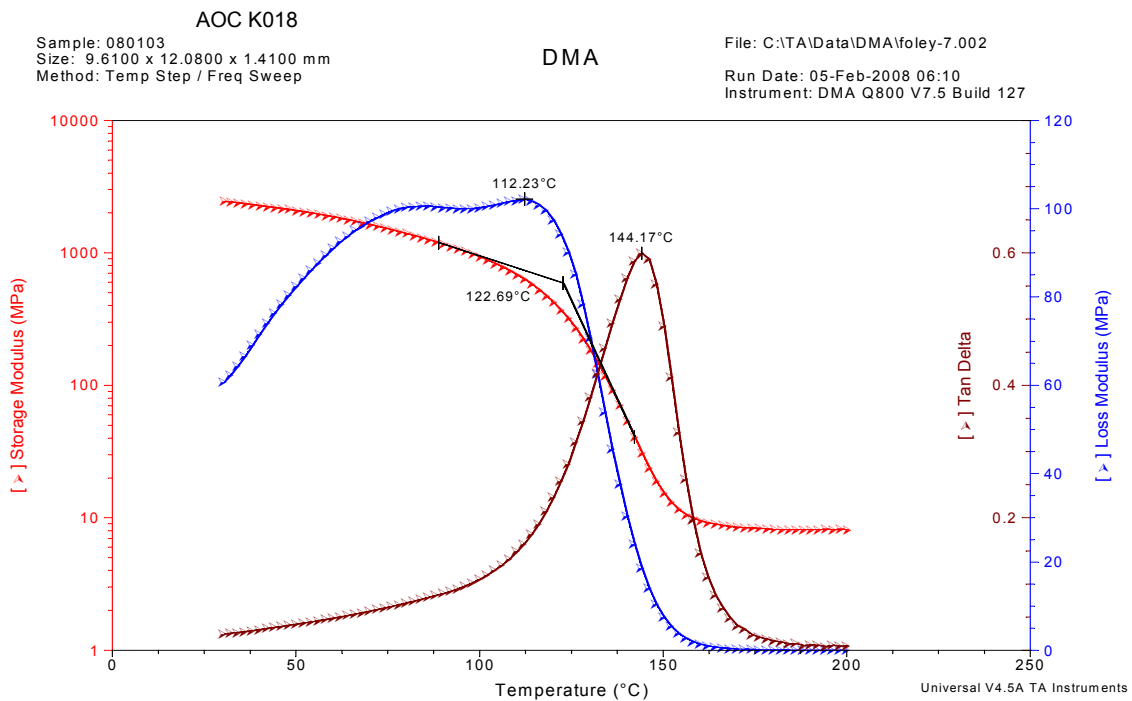
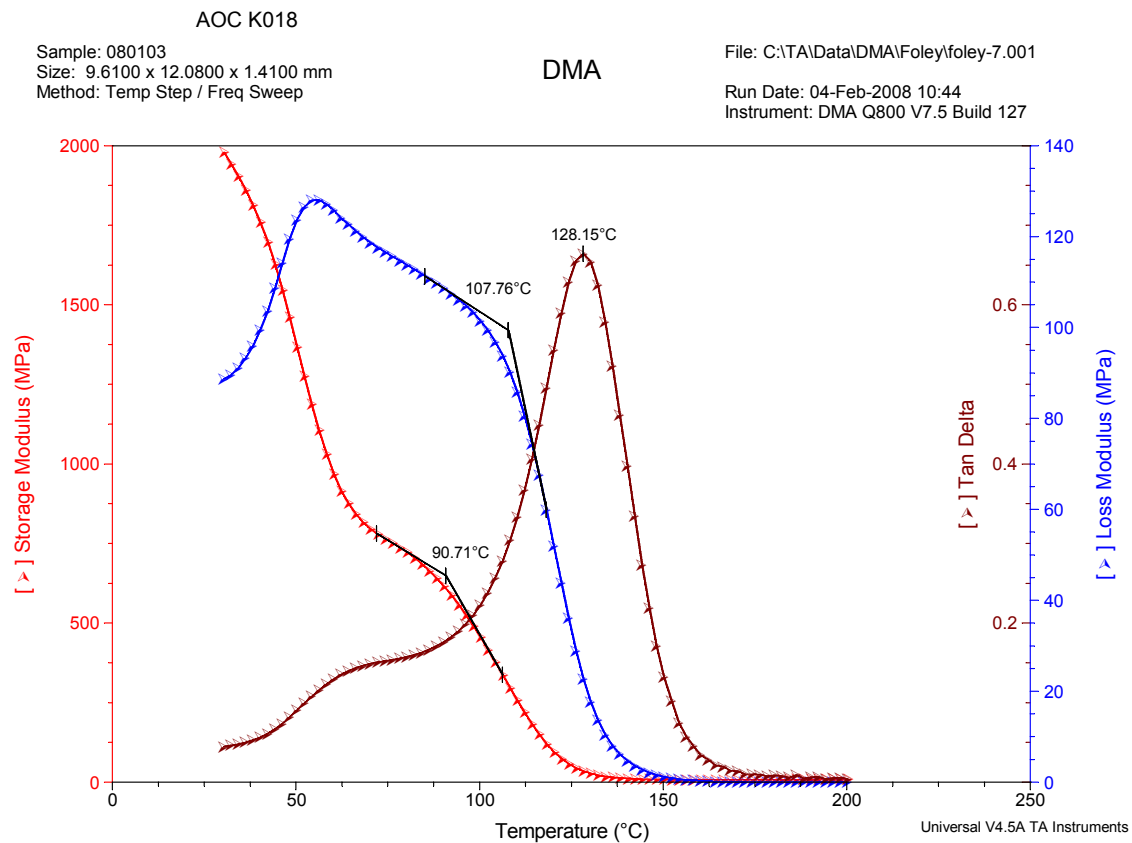
Rick Strand Formulation

Sample: RS
Size: 10.1100 x 10.9500 x 2.8300 mm
Method: Temperature Ramp
Comment: torque: 10 in-lb

DMA

File: C:\TA\Data\DMA\foley-4.002
Run Date: 11-Jul-07 06:05
Instrument: DMA Q800 V3.13 Build 74





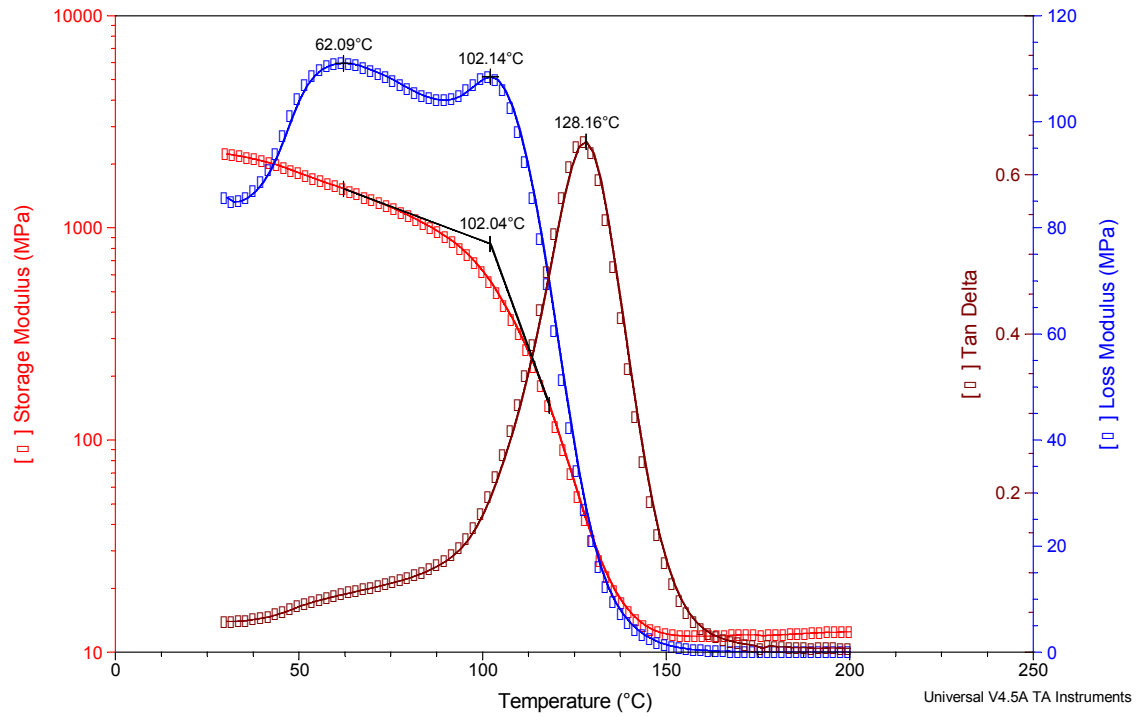
AOC K018 PC

Sample: 080103PC
Size: 9.5900 x 12.2500 x 1.8500 mm
Method: Temp Step / Freq Sweep

DMA

File: C:\TA\Data\DMA\foley-8.001

Run Date: 19-Feb-2008 06:17
Instrument: DMA Q800 V7.5 Build 127



Appendix H. Army and Marines Composite Panel Testing Results

This appendix appears in its original form, without editorial change.

Appendix H

Army and Marines Composite Panel Testing Results

**Low HAP/VOC Compliant Resins validation for
Military Applications
PROGRESS REPORT
December 19, 2006**

Ashiq A. Quabili
Stephen M Andersen

LOW HAP/VOC COMPLIANT RESINS VALIDATION FOR MILITARY APPLICATIONS PROGRESS REPORT

TABLE OF CONTENTS

	<u>Page</u>
Objective	3
E glass 3D (96 oz)/ FAVE-O 25s Panel processing summary	4
Resin viscosity profile	5
VARTM processing sheet	7
Short beam shear test outline	10
Short beam shear at elevated temperature	13
DMA summary	14
4 point bending test summary	18
4 point bending test at elevated temperature	20
Performance objectives for Army Tactical vehicles with appropriate fabric reinforcement for application	23

Objective:

The objective of this program is to validate the performance of low HAP/ VOC compliant resins so that they can be used as an alternative to the existing Vinyl Ester resin system which is headed toward greater use in DoD applications. In order to perform some screening tests on the Fatty acid Vinyl Ester resin, initially, a single panel of Eglass/FAVE-O 25s resin has been fabricated using 2 layers of 3D woven fabric with areal density of 96 oz/yd². The fabric is oriented in 0-90 arrangement. The panel is post cured at a low temperature, 135 F for 3 hours. DMA, Room temperature short beam shear and 4 point bending tests are performed on this composite. The results, however, show that the performance is not optimized due to the 0-90 orientation and low temperature post cure cycle. All the tests have been redone with another 2 layer-Eglass96oz /FAVE-O 25s composite. This time, the fabric orientation is 0-0, and the post cure cycle is 135C for 3 hours. For comparison with vinyl Ester 8084 system, a panel with 2 layer- Eglass 96oz/ VE 8084 with 0-0 fabric orientation is made under the same conditions. Room temperature DMA, short beam shear, 4 point bending tests are performed on both FAVE-O 25s and VE8084 based composites.

E glass 3D (96 oz)/ FAVE-O 25s Panel processing summary:

Two E glass / FAVE-O 25s resin composites were fabricated using 2 layers of 3D E-glass woven fabric with an areal-density of 96 oz/yd². The fabric orientation in one of these composites was 0-90. In the other laminate, each layer was aligned in the same direction and carefully arranged so that the layers can be interlocked ensuring a higher fiber volume fraction. Another panel with 2 layers of Eglass 96oz and VE8084 was made under the same conditions, following the 0-0 fabric orientation.

Vacuum Assisted Resin Transfer Molding (VARTM) process was applied with Fatty Acid Vinyl Ester System based on Octanoic acid. Room temperature cure for 24 hours and elevated temperature post-cure, 135 C for 3 hours, were used after the resin infusion.

Lay-up Sequence and Infusion Scheme:

The lay-up sequence is as follows (from bottom to top):

- Tool plate
- Peel ply
- 2 layers 3D 96oz E-Glass
- Peel ply
- Breather Cloth
- Distribution media.
- Vacuum bag

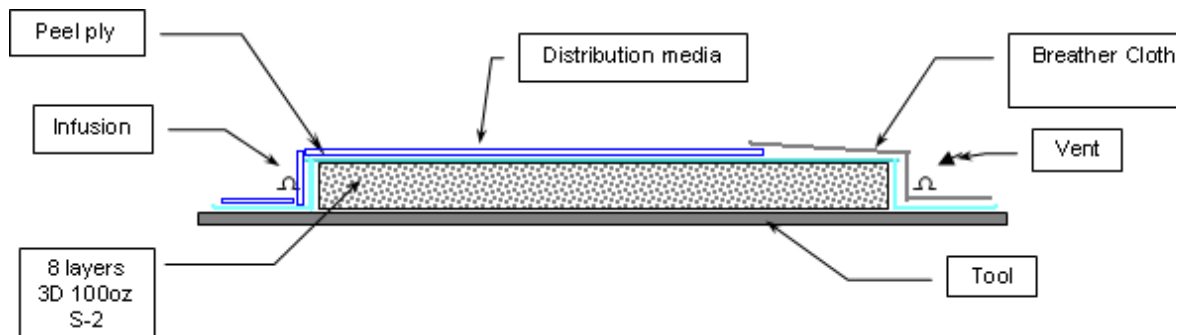
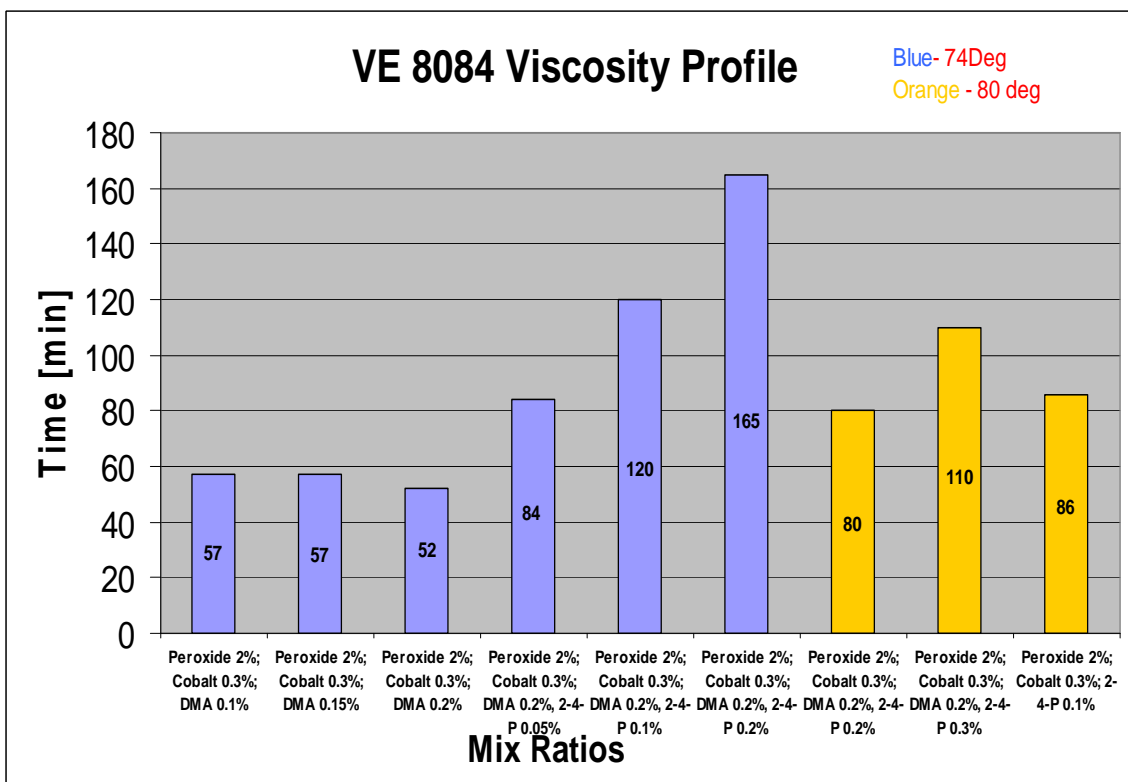
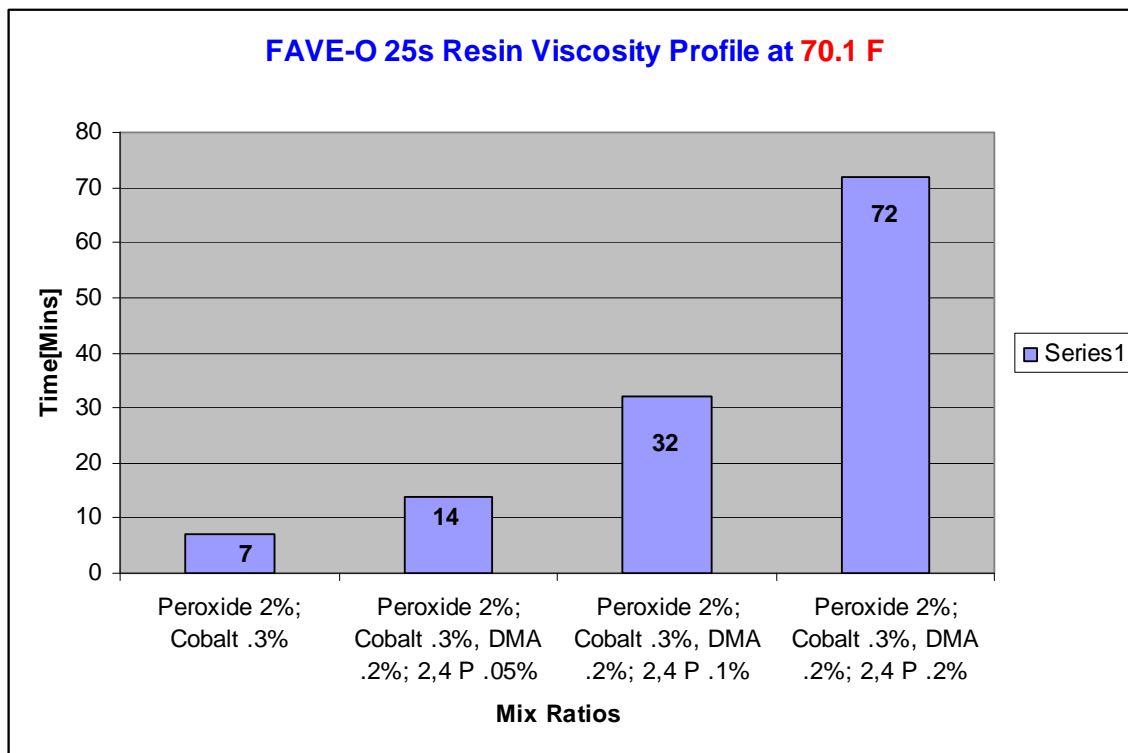


Figure 1: Schematic of VARTM Processing with side Infusion Scheme.



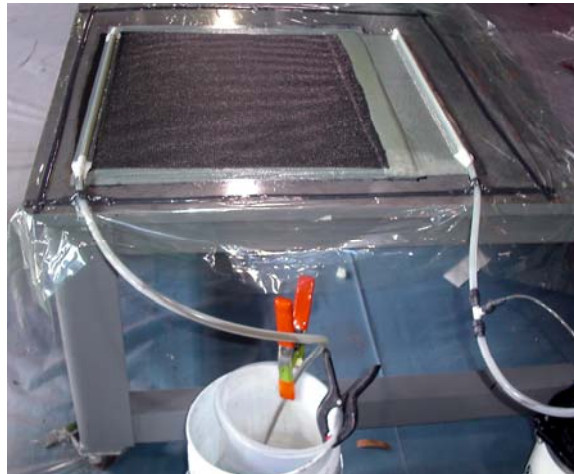
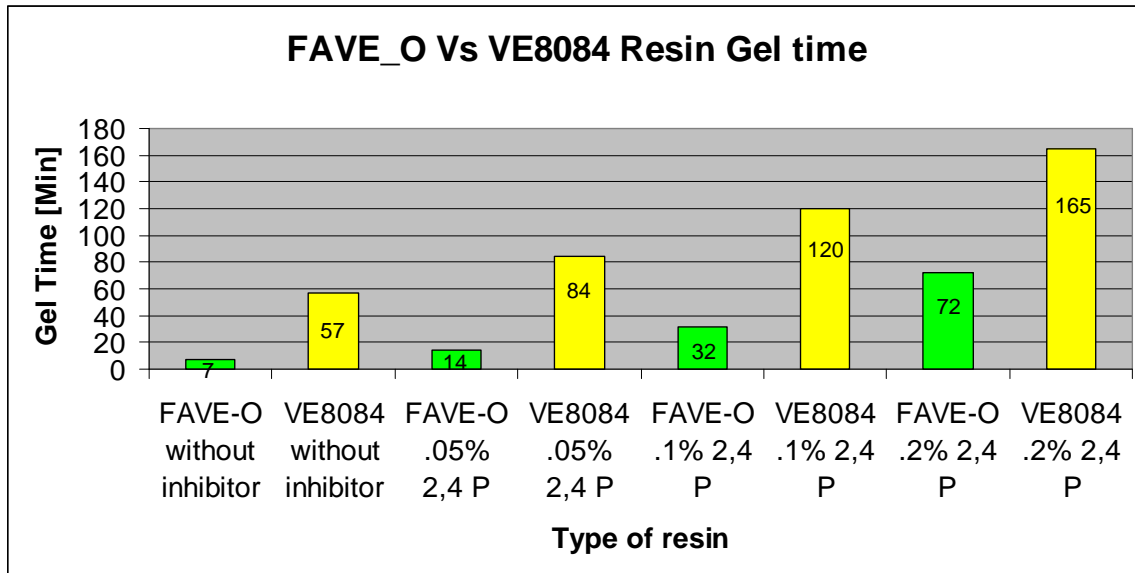


Figure 2: Eglass / FAVE panel processing

VARTM Processing Sheet (2 Layers) 0-90 Orientation

Name(s): Ashiq				
Panel ID: Eglass_96oz_2L_FAVE-O				
Fabric	Description			Plain Weave
	Length (L)	24 inches	60.96 cm	
	Width (W)	24 inches	60.96 cm	
	Aerial Weight (AD)	24 oz/yd ²	13.02 kg/m ²	
	Number of Layers(n)	2		
	Layup Sequence (against tool)			
	Fabric Weight (Wf, measured)	2529.0 g	5.58 lbs	excluding unravelling: xx.x g
	Single Layer Thickness (estimated)	0.096 inches	2.44 mm	estimation for resin preparation
	AD (dry, psf)	0.33 lbs/ft ²	26.04 kg/m ²	Aerial density of dry preform
Infusion	Date	7/31/2006		
	No. of Distribution Media	1		
	No. of Breather Cloth	None		
	FVF (v _f , initial guess for resin prep.)	55%		
	Resin Type	FAVE-O 25s		
	Cure Temperature	68.0 °F	20.0 °C	amb. temp. from a hygrometer
	Resin Density	1.140 g/mL	71.17 lbs/ft ³	liquid resin density
	Minimum Resin Amount	2505.0 g	5.52 lbs	estimated from the initial FVF
	Trigonox	50.0 g	0.11 lbs	
	conap	7.50 g	0.26 oz	
	DMA	5.00 g	0.18 oz	
	Inhibitor	2.00 g	0.071 oz	
	Gel time (estimated)	30 Mins		
	Time: Resin Gelling	32 mins		
	Cure Schedule	RT overnight		
Panel	Panel Weight (Wc)	3480.0 g	7.67 lbs	
	Net Resin (W _r)	951.0 g	2.10 lbs	W _r =W _c -W _f
	Resin Density (ρ _r)	1.14 g/mL	71.17 lbs/ft ³	cured resin density
	Fiber Density (ρ _f)	2.55 g/mL	159.19 lbs/ft ³	Sglass
	Fiber Volume Fraction	54.3%		
	Resin Volume Fraction (v _r)	45.7%		
	Resin vs. Fabric (W _r / W _f)	37.6%		
	Panel Areal Weight (AD)	1.92 lbs/ft ²	9.36 kg/m ²	approximate
	Total Thickness (t)	0.195 inches	4.88 mm	
	Single Layer Thickness (t ₁)	0.096 inches	2.44 mm	
	Single Layer AD	0.959 lbs/ft ²	4.68 kg/m ²	for future reference
Postcure	Date			
	Under Vacuum or Free Standing	Free Standing		
	Ramping Up Time and Temp.	1 hr		
	Holding Time and Temp.	3 hr @135F		
	Ramping Down Time and Temp.	1 hr		

Name(s): Ashiq A Quabili		0-0 Orientation				
Panel ID: Eglass 96oz_2L_VE8084						
Fabric	Description	0-0 Deg Fabric Orientation				
	Length (L)	12.5	inches	31.75	cm	
	Width (W)	13	inches	33.02	cm	
	Aerial Weight (AD)		oz/yd ²	0.00	kg/m ²	
	Number of Layers(n)	2				
	Layup Sequence (against tool)					
	Fabric Weight (Wf, estimated)	0.0	g	0.00	lbs	
	Fabric Weight (Wf, measured)	780.0	g	1.72	lbs	excluding unravelling: xx.x g
	Single Layer Thickness (estimated)	0.096	inches	2.44	mm	estimation for resin preparation
	AD (dry, psf)	0.00	lbs/ft ²	0.00	kg/m ²	Aerial density of dry preform
Infusion	Date	8/5/2006				
	No. of Distribution Media	1				
	No. of Breather Cloth	1				
	FVF (v _f , initial guess for resin prep.)					fiber volume fraction
	Resin Type	VE 8084				
	Cure Temperature	70.0	°F	21.1	°C	amb. temp. from a hygrometer
	Resin Density	1.140	g/mL	71.17	lbs/ft ³	liquid resin density
	Minimum Resin Amount		g	0.00	lbs	estimated from the initial FVF
	Resin Prepared	1000.0	g	2.20	lbs	extra about 1000 grams
	Trigonox	20.00	g		oz	
	Conap	3.00	g		oz	
	DMA	2.00	g			
	2,4 P			0.000	oz	
	Gel time (estimated)	30 mins				from datasheet and amb. temp.
	Time: Resin Gelling	33 Mins				
Panel	Panel Total Weight (Wc)	1031.0	g	2.27	lbs	
	Net Resin (W _r)	251.0	g	0.55	lbs	W _r =W _c -W _f
	Resin Density (ρ _r)	1.14	g/mL	71.17	lbs/ft ³	cured resin density
	Fiber Density (ρ _f)	2.55	g/mL	159.19	lbs/ft ³	S-glass
	Fiber Volume Fraction (v _f)	58.1%				v _f = (W _f / W _c) (ρ _r / ρ _f) / [1- (W _f / W _c)(1-ρ _r / ρ _f)]
	Resin Volume Fraction (v _r)	41.9%				v _m = 1 - v _f (Approximate)
	Resin vs. Fabric (W _r / W _i)	32.2%				for the same configuration
	Panel Areal Weight (AD)	2.01	lbs/ft ²	9.83	kg/m ²	approximate
	Total Thickness (t)	0.196	inches	4.98	mm	
	Single Layer Thickness (t ₁)	0.096	inches	2.44	mm	
Single Layer AD	1.007	lbs/ft ²	4.92	kg/m ²		
Postcure	Date					
	Under Vacuum or Free Standing	Free Standing				
	Ramping Up Time and Temp.	1 Hour				
	Holding Time and Temp.	3Hour @ 135 C				

VARTM Processing Sheet

Name(s): Ashiq					
Panel ID: Eglass_96oz_2L_FAVE-O					
Fabric	Description				Plain Weave
	Length (L)	12.5	inches	31.75	cm
	Width (W)	14	inches	35.56	cm
	Aerial Weight (AD)		oz/yd ²	0.00	kg/m ²
	Number of Layers(n)	2			
	Layup Sequence (against tool)				
	Fabric Weight (Wf, measured)	856.0	g	1.89	lbs
	Single Layer Thickness (estimated)	0.096	inches	2.44	mm
	AD (dry, psf)	0.00	lbs/ft ²	0.00	kg/m ²
Infusion	Date	8/5/2006			
	No. of Distribution Media	1			
	No. of Breather Cloth	None			
	FVF (v _f , initial guess for resin prep.)	55%			
	Resin Type	FAVE-O 25s			
	Cure Temperature	68.0	°F	20.0	°C
	Resin Density	1.140	g/mL	71.17	lbs/ft ³
	Minimum Resin Amount	1000.0	g	2.20	lbs
	Trigonox	20.0	g	0.04	lbs
	conap	3.00	g	0.11	oz
	DMA	2.00	g	0.07	oz
	Inhibitor	0.50	g	0.018	oz
	Gel time (estimated)	30 Mins			
	Time: Resin Gelling	32 mins			
	Cure Schedule	RT overnight			
Panel	Panel Weight (Wc)	1177.0	g	2.59	lbs
	Net Resin (W _r)	321.0	g	0.71	lbs
	Resin Density (ρ _r)	1.14	g/mL	71.17	lbs/ft ³
	Fiber Density (ρ _f)	2.55	g/mL	159.19	lbs/ft ³
	Fiber Volume Fraction	54.4%			
	Resin Volume Fraction (v _r)	45.6%			
	Resin vs. Fabric (W _r / W _f)	37.5%			
	Panel Areal Weight (AD)	2.14	lbs/ft ²	10.42	kg/m ²
	Total Thickness (t)	0.200	inches	5.08	mm
	Single Layer Thickness (t _l)	0.096	inches	2.44	mm
	Single Layer AD	1.068	lbs/ft ²	5.21	kg/m ²
Postcure	Date				
	Under Vacuum or Free Standing	Free Standing			
	Ramping Up Time and Temp.	1 hr			
	Holding Time and Temp.	3 hr @135C			
	Ramping Down Time and Temp.	1 hr			

Short beam shear test Outline

Inter-laminar shear strength of 2 Layers of 3Tex Eglass 96oz/ VE8084 and FAVE-O 25s composites were tested following Short Beam Shear ASTM D2344. The Short beam test specimens were loaded in three point bending arrangement, where the specimen ends rested on two supports that permitted lateral movement, the load being applied by a loading nose centered on the midpoint of the sample. The tool side of each specimen was placed on the supports. The experiment atmosphere was 72 F with a relative humidity of 55%.

Table 1: Specimen dimensions

SBS	b (in)	H (in)	L (in)
8084			
1	0.399	0.180	1.160
2	0.398	0.180	1.161
3	0.395	0.180	1.161
4	0.400	0.182	1.600
5	0.370	0.181	1.640
FAVE-O 25s			
1	0.397	0.187	1.156
2	0.396	0.189	1.155
3	0.410	0.195	1.156
4	0.393	0.193	1.156
5	0.388	0.183	1.155

Specimen 1 to 5

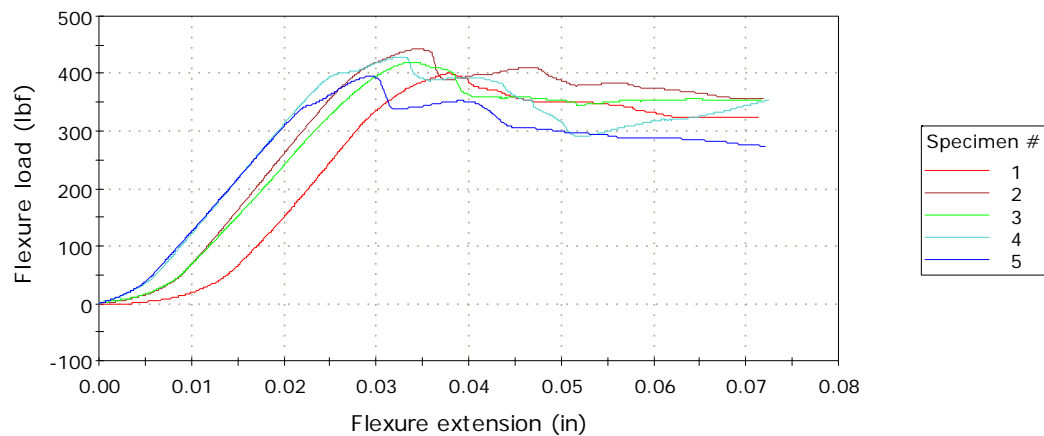


Figure 3: Eglass96oz/ VE8084 samples.

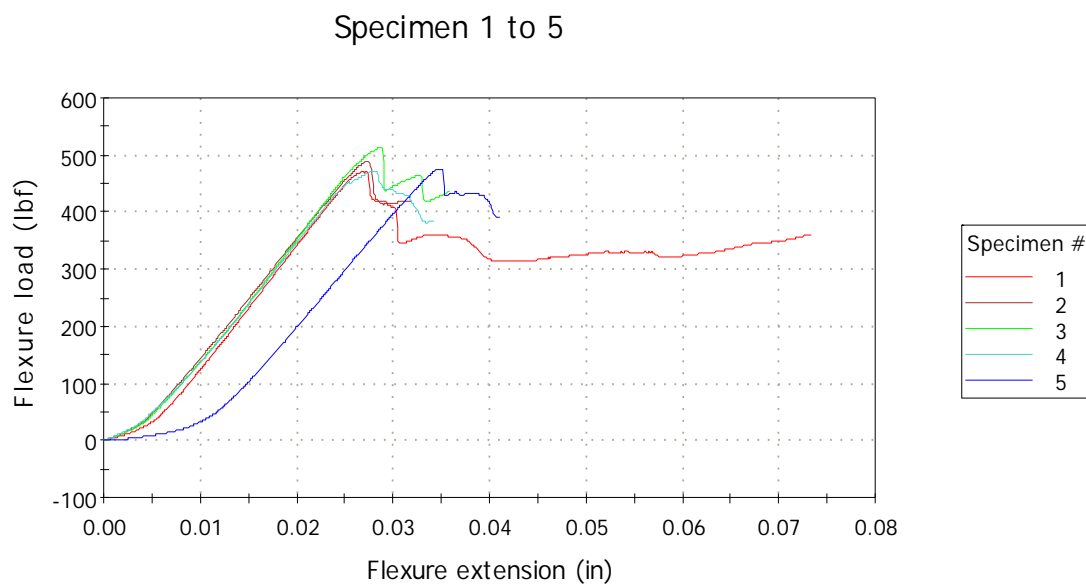


Figure 4: Eglass96oz/ FAVE O 25s samples.

Table 2: SBS at RT test results

Sample ID	Extension at Maximum Flexure load (in)	Maximum Flexure load (lbf)
Eglass96/VE8084		
1	-0.03775	400
2	-0.03442	443
3	-0.03425	420
4	-0.03275	429
5	-0.02959	395
Eglass96oz/FAVE-O 25s		
1	-0.02684	471
2	-0.02725	489
3	-0.02884	513
4	-0.02800	472
5	-0.03509	474

Table 3: Test result summary

Sample ID	Pmax(lbf)	Fsbs(psi)	Avg Fsbs(psi)	STD Dev
Eglass96/VE8084				
1	400	4182		
2	443	4640	4422	162
3	420	4437		
4	429	4420		
5	395	4429		
Eglass96/FAVE-O 25s				
1	471	4760		
2	489	4900		
3	512	4810	4830	131
4	472	4667		
5	474	5012		

Short Beam Shear at Elevated Temperature:

Elevated temperature short beam shear tests were followed by the same procedure described above for the room temperature tests. Each specimen was conditioned at 250 F for at least 20 minutes prior to test. Specimen size, support span lengths are given bellow:

Table 4: Specimen dimensions

SBS	b(in)	H(in)	L(in)
FAVE-O 25s			
1	0.400	0.192	1.156
2	0.400	0.193	1.155
3	0.400	0.194	1.156
4	0.400	0.193	1.156
5	0.400	0.193	1.155

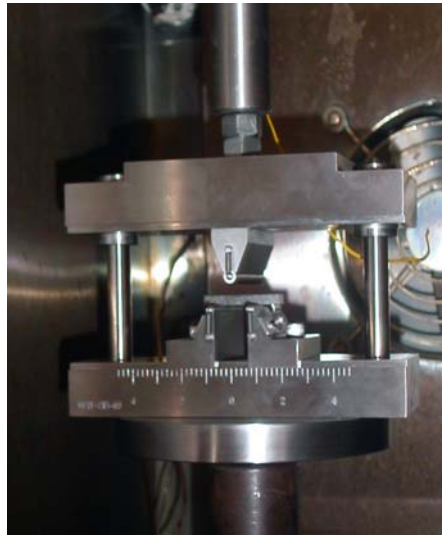


Figure 5: A typical SBS test set up for elevated temperature.

Table 5: Test result

ID	Pmax (lbs)	Fsbs (psi)	Average Fsbs (psi)	Std Dev
FAVE-O 25s				
1	119	1168	872	188
2	97	947		
3	81	786		
4	77	751		
5	73	709		

DMA Summary

DMA test was performed following ASTM E1640-04 to obtain the glass transition temperature of the FAVE resin/ Eglass composite. The first sample was taken from the 0-90 oriented FAVE/2layers Eglass 96oz composite which was post cured at a low temperature (3 hours at 135F). The specimen was placed in mechanical oscillation at a fixed frequency of 1 Hz. Samples were clamped in a 3 point bending clamping arrangement and calibrated before testing. In order to reduce thermal noise, the temperature of the experimenting environment was stabilized at 35C for five minutes. Then, the temperature was ramped up to 180C at a rate of 5 deg C/ min. The changes in the viscoelastic response of the material were monitored as a function of temperature.

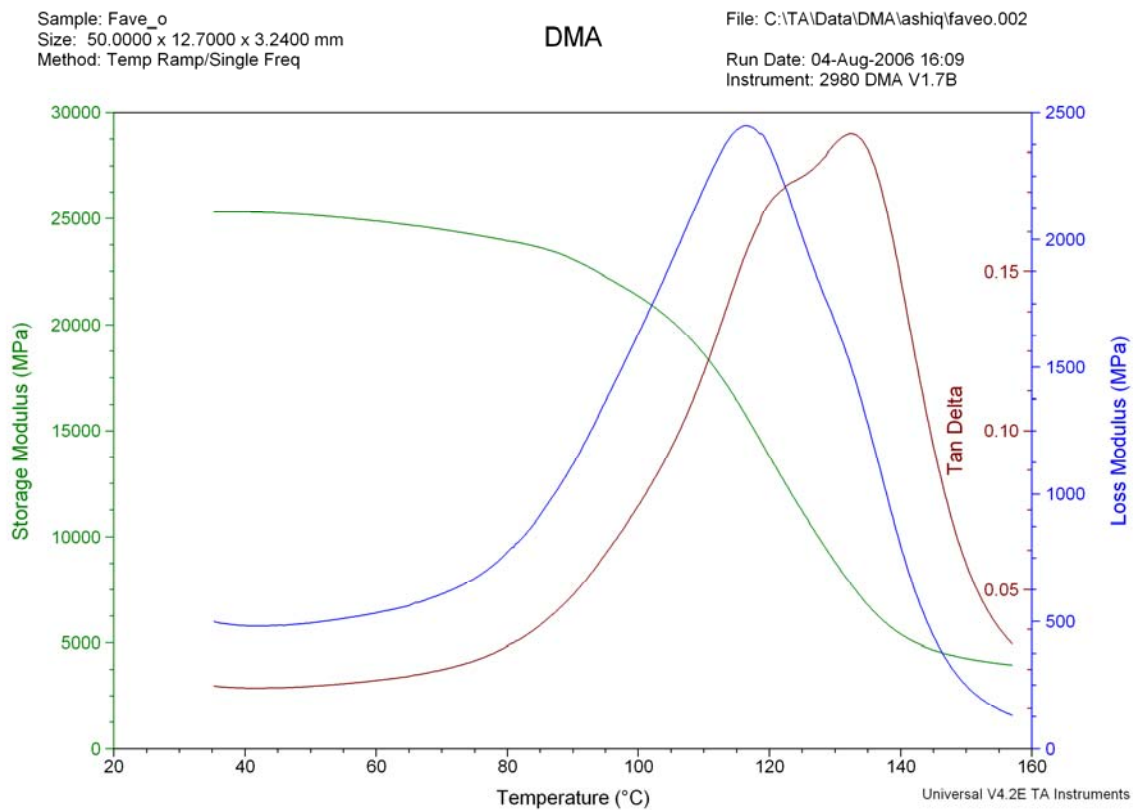


Figure 6: DMA plot for FAVE/ E96oz Sample, cured at 135 F

Three more specimens from the same composite panel were used to perform DMA tests. The conditions were identical to the first test. However, this time, each specimen was post cured relatively at high temperature (3 hours at 135C). There was no significant change in Glass Transition Temperature in the following experiments.

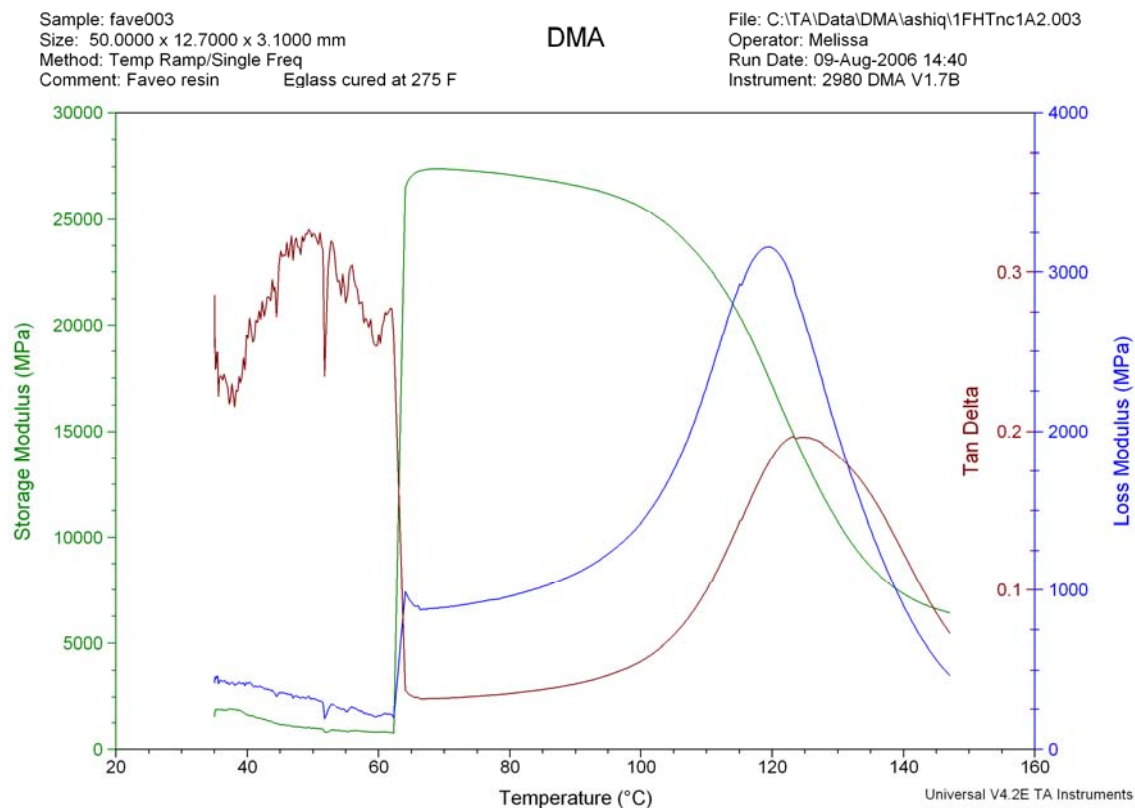


Figure 7: DMA plot for FAVE/ E96oz Sample, cured at 135 C

All the samples were post cured at a higher temperature, 275F for 3 hours and resulted repeating the plot above. Therefore, the Tg of this FAVE/Eglass composite was taken by observing the extrapolated onset to the change in the storage modulus in going from firm, breakable region to the ductile, rubbery region of the material under test. By constructing a tangent to the storage modulus curve below, the Tg was identified as 106C.

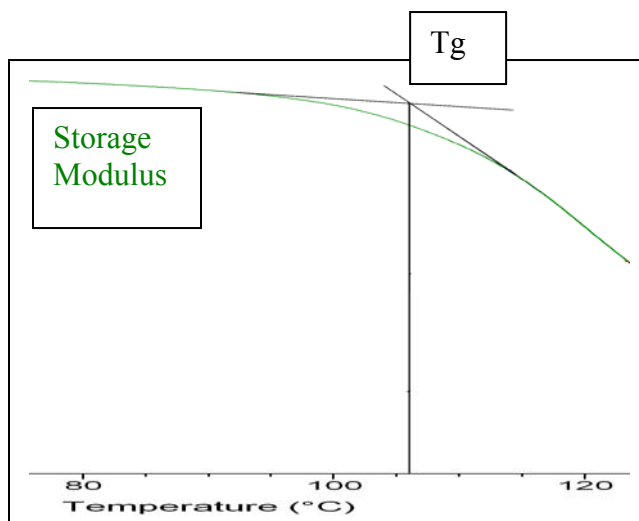


Figure 8: Tangent to the Storage Modulus

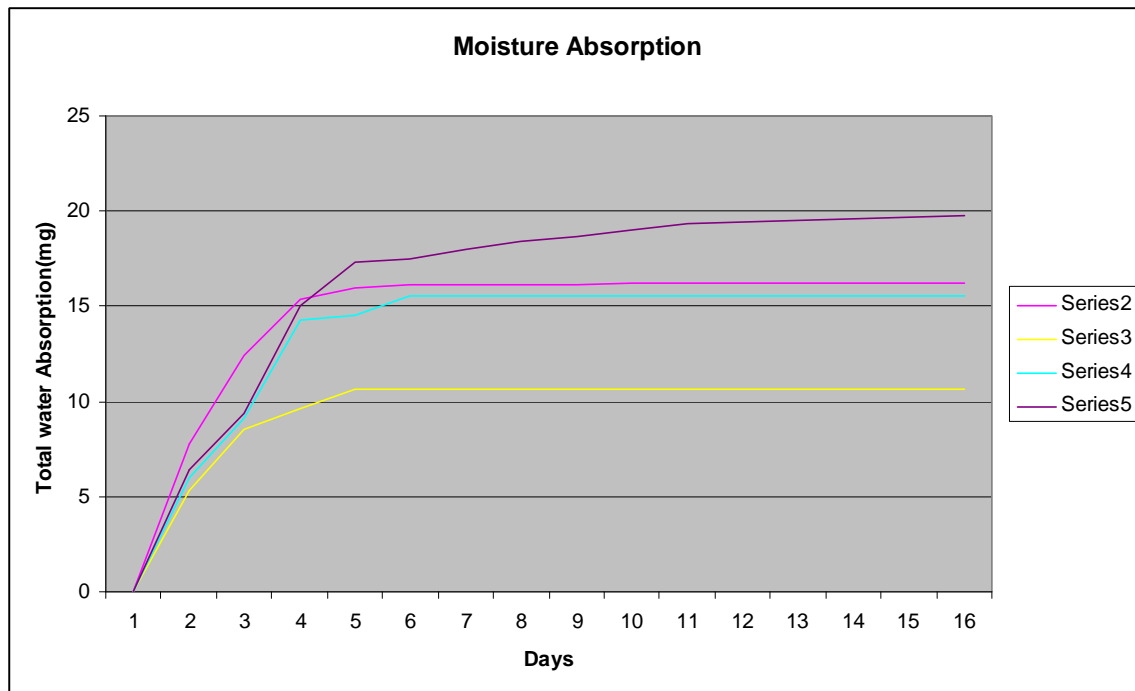
DMA (Wet TG):

In order to obtain the wet T_g of the FAVE/Eglass composite, the specimens are submerged in water at 60 C, with 100% relative humidity. The following table shows the total water absorption of each specimen during the three week conditioning period.

Table 6: Moisture Absorption

Day	Specimen4 (mg)	Specimen5 (mg)	Specimen6 (mg)	Specimen7 (mg)
1	0	0	0	0
2	7.80	5.30	6.0	6.4
3	12.40	8.50	9.1	9.4
4	15.40	9.60	14.3	15.0
5	16.00	10.60	14.5	17.3
6	16.10	10.60	15.5	17.5
7	16.14	10.62	15.5	18.0
8	16.15	10.62	15.5	18.4
9	16.17	10.60	15.5	18.7
10	16.18	10.62	15.5	19.0
11	16.19	10.62	15.5	19.3
12	16.20	10.62	15.5	19.4
13	16.20	10.63	15.5	19.5
14	16.20	10.62	15.5	19.6
15	16.20	10.62	15.5	19.7
16	16.20	10.62	15.5	19.8

The following plot shows the water absorption rate and the saturation point as well.

**Figure 9: Plot-moisture absorption vs time**

DMA test is performed following ASTM E1640-04 to obtain the wet Tg of the FAVE-O 25s resin/ Eglass composite.

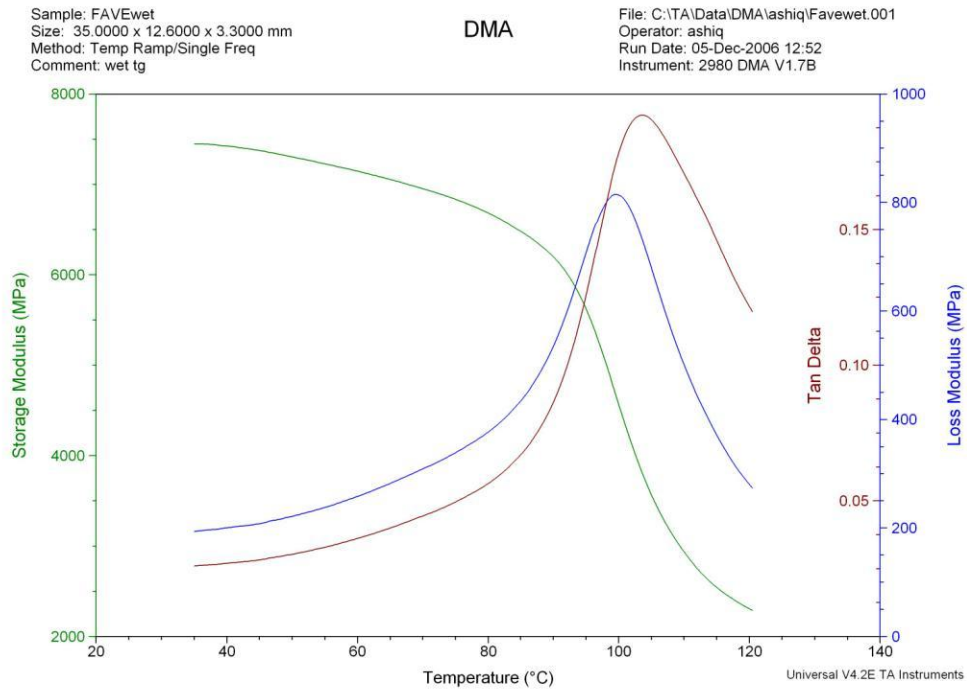


Figure 10: DMA plot for FAVE/E96oz sample, cured at 135C, conditioned at 60C

From the plot above, the wet Tg of FAVE-O 25s is identified as 90C.

4 Point Bending Test Summary:

4 point test were performed following ASTM D 6272 in order to determine the flexural properties of Eglass96 oz / VE 8084 and Eglass96/ FAVE composites. The specimens for this experiment were cut in the lengthwise (fabric wrap) direction of the panel. Each specimen was tested by resting on two supports and loading at two loading noses. The tool side of the specimen was placed on the supports. The distance between the loading noses was one third of the support span. 24:1 Span to depth ratio was used due the loading nose structure. The specimen size, load span length, support span length etc are given bellow:

Test Condition: 72 F, 55% humidity

Load Span Length: 1.6 (in)

Support Span Length: 4.8 (in)

Support span-to-depth ratio: 24:1

Rate of crosshead motion: 0.09 (in/min)



Figure 9: A typical test frame and set up for 4 point bending test

Table 7: Specimen dimensions

4 pt bend	b (in)	h (in)	L (in)	support span (in)
8084				
1	0.470	0.183	5.960	4.800
2	0.470	0.180	5.960	4.800
3	0.470	0.184	5.960	4.800
4	0.470	0.186	5.960	4.800
5	0.455	0.183	5.960	4.800
6	0.470	0.183	5.960	4.800
FAVE-O25s				
1	0.497	0.197	5.957	4.800
2	0.500	0.199	5.959	4.800
3	0.500	0.196	5.960	4.800
4	0.495	0.197	5.960	4.800
5	0.500	0.197	5.964	4.800

Table 8: 4 point bending test results

ID	Pmax (lbs)	m (lbs/in)
8084		
1	214	475
2	177	415
3	224.	498
4	227	488
5	218	489
6	214	493
FAVE-O25s		
1	258	630
2	259	631
3	231	569
4	249	586
5	263	629

Table 9: 4 point bending test summary

ID	Bending Modulus (psi)	Average Modulus (psi)	Std Dev	Bending strength (psi)	Avg Strength (psi)	Std Dev
8084						
1	3832182	3851956	197589	65248	64963	4701
2	3521535			55747		
3	3954219			67657		
4	3751357			67043		

5	4072724			68669		
6	3979719			65413		
FAVE-O 25s						
1	3853760	3702431	143733	64135	62425	2837
2	3720990			62832		
3	3515018			57728		
4	3601385			62348		
5	3821001			65079		

4 point bending test at elevated temperature:

Elevated temperature 4 point bending test method was followed by the same procedure described above for the room temperature tests. Each specimen was conditioned at 250 F for at least 20 minutes prior to test. Specimen size, support span lengths are given bellow:

Table 10: Specimen dimensions

4 pt bend	b (in)	h (in)	L (in)	support span (in)
8084				
1	0.500	0.183	5.960	4.800
2	0.500	0.183	5.960	4.800
3	0.496	0.182	5.960	4.800
4	0.500	0.182	5.960	4.800
5	0.472	0.182	5.960	4.800
6	0.500	0.182	5.960	4.800
FAVE-O 25s				
1	0.514	0.195	5.957	4.800
2	0.496	0.190	5.959	4.800
3	0.500	0.190	5.960	4.800
4	0.500	0.196	5.960	4.800
5	0.440	0.190	5.964	4.800
6	0.440	0.195	5.964	4.800
7	0.450	0.190	5.964	4.800



Fig10: Conditioning specimens inside a chamber



Fig 11: A typical 4 point bending test setup at elevated temperature.

Table 11: 4 point bending test results:

ID	Pmax (lbs)	m (lbs/in)
8084		
1	45	287
2	42	284
3	45	205
4	61	370
5	43	296
6	48	354
FAVE-O 25s		
1	39	308
2	52	352
3	36	308
4	34	303
5	24	298
6	26	383
7	21	308

Table 12: 4 point bending test Summary

ID	Bending Modulus (psi)	Average Modulus (psi)	Std Dev	Bending strength (psi)	Avg Strength (psi)	Std Dev
8084						
1	2177379	2320161	454609	12974	13841	2032
2	2149276			11958		
3	1596777			13270		
4	2853706			17785		
5	2415320			13153		
6	2728512			13908		
FAVE						
O 25s						
1	1879418	2106358	240973	9642	9474	2484
2	2402532			14119		
3	2083830			9594		
4	1869166			8696		
5	2296842			7398		
6	2731463			7393		
7	2319894			6425		

The following table summarizes the expected performance and actual performance on room temperature screening tests of Eglass/FAVE composite.

Table 13: Performance objectives and actual performance for Army Tactical vehicles with appropriate fabric reinforcement for application

Type of Performance Objective	Primary Performance Criteria	Expected Performance (Metric)	Actual Performance
Quantitative	Dry T _g through DMA test - HMMWV Hood - M35A3 Hood - HMMWV Container	> 250°F > 250°F > 200°F	222°F *The T _g only meets requirement for HMMWV Container.
Quantitative	Flexural Strength at RT (ASTM D790) - HMMWV Hood - M35A3 Hood	≥ 55 ksi ≥ 55 ksi	62.4 ksi
Quantitative	Flexural Modulus at RT (ASTM D790) - HMMWV Hood - M35A3 Hood	≥ 3.7 Msi ≥ 3.7 Msi	3.7 Msi
Quantitative	SBS Strength at RT (ASTM D2344) - HMMWV Hood - M35A3 Hood	≥ 4.5 ksi ≥ 4.5 ksi	4.8 ksi
Quantitative	Wet T _g through DMA test - HMMWV Hood - M35A3 Hood - HMMWV Container	> 225°F > 225°F > 180°F	195F
Quantitative	Flexural Strength at 250°F (ASTM D790) - HMMWV Hood - M35A3 Hood	≥ 30 ksi ≥ 30 ksi	9.5 ksi
Quantitative	Flexural Modulus at 250°F (ASTM D790) - HMMWV Hood - M35A3 Hood	≥ 3.0 Msi ≥ 3.0 Msi	2.1 Msi
Quantitative	SBS Strength at 250°F (ASTM D2344) - HMMWV Hood - M35A3 Hood	≥ 3.0 ksi ≥ 3.0 ksi	0.87 ksi

Quantitative	Resin fills part in allotted time	Fabricator comments and approval	Yes
Quantitative	Resin gels in correct amount of time	Fabricator comments and approval	Yes. The resin gels more rapidly than the VE 8084 gel time.
Quantitative	Resin fully wets fibers	Fabricator comments and approval	Yes

Conclusion:

The test results show that at room temperature, the FAVE-O 25s resin meets the expected performance in short beam shear strength, flexural modulus and strength. However, the resin system fails drastically when the test is performed at elevated temperature (250 F). A part of the reason of this failure is because of the low T_g of the resin system. ARL is currently developing a modified version of FAVE with higher T_g. In near future, some screening tests should be performed on the new resin system in order to validate its performance.

ESTCP- FAVE-O-25 S , FAVE- L25S and FAVE-O-HT Resin Characterization Four Point Bend and Short Beam Shear

4 pt bend flexure and short beam shear test

- For 4 pt bend test (ASTM D6272)
 - span used 4.8", loading span – 1.6"
 - Specimen cross section 0.5" x 0.19"
 - 5 specimens tested for room temp and elevated temp each
- For short beam shear (ASTM D2344)
 - span used 0.8"
 - specimen cross section 0.38" x 0.19"
 - 5 specimens tested for room temp and elevated temp each

VARTM Processing parameters

resin	Fiber wt %	Post cure
FAVE-O-HT 1 st set tests	73	266°F for 2 hrs
FAVE-O-HT 2 nd set tests	74	266°F for 2 hrs
FAVE-O-HT 3 rd -latest tests	72	266°F for 2 hrs
FAVE-O-25S	73	135°F for 3 hrs
FAVE-L25S	72	257°F for 2 hrs

VARTM- 2 layers of 3D woven 96oz E-Glass fabric

ESTCP tests

		4 pt bend RT	4 pt bend 250F	SBS RT	SBS 250 F
Army Requirement	Strength ksi	55.0	30.0	4.50	3.00
	Modulus msi	3.70	3.00	-	-
FAVE-O-HT-1 st set tests	Strength ksi	56.60	29.20	3.70	2.90
	Modulus msi	3.67	2.69	-	-
FAVE-O-HT-2 nd set tests	Strength ksi	62.00	38.80	4.08	3.20
	Modulus msi	3.76	2.90	-	-
FAVE-O-HT-3 rd - latest set tests	Strength ksi	71.00 ± 1.00	42.00 ± 2.00	4.30 ± 0.20	3.80 ± 0.08
	Modulus msi	3.65 ± 0.13	3.36 ± 0.04	-	-
FAVE-O-25S	Strength ksi	62.00	9.40	4.80	0.90
	Modulus msi	3.70	2.10	-	-
FAVE--L25S	Strength ksi	70.00	15.90	5.10	1.20
	Modulus msi	3.85	2.23	-	-

Summary

- Latest test results are highlighted in red
- FAVE-O-HT High temp resin meets (considering the scatter) the requirement for room temp and elevated temp flexural modulus/strength and SBS strength
- FAVE-O-25S and FAVE-L25S meets the requirement for RT but not for elevated temp flexural strength/modulus and SBS strength

Low VOC M35 Hood

Deflection and Durability Tests



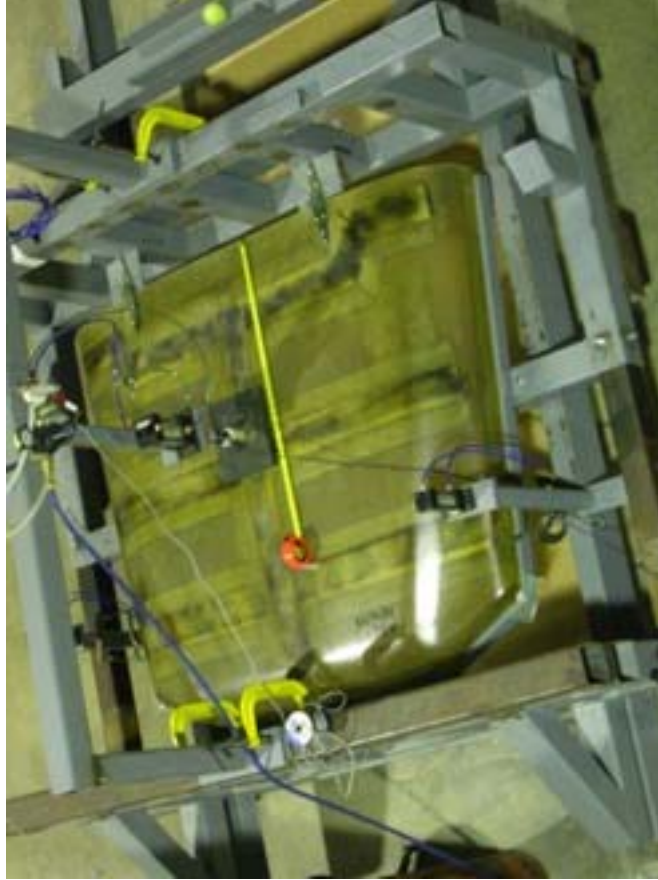
- Hood in test fixture with center and corner handle load actuators.



- Test will be conducted at room temperature.
- 250 lb load applied to the outside surface over a maximum 10"x10" area.
- The load will be applied at the center and front areas of the hood.
- The deflection will be measured at the point of application of the load but on the opposite surface.
- Plot of load vs deflection will be obtained.
- **Test pass criteria:**
 - Elastic deflection must not exceed 0.50".
 - No permanent deformation.
 - No separation of reinforcements from the hood.
 - No cracks allowed.

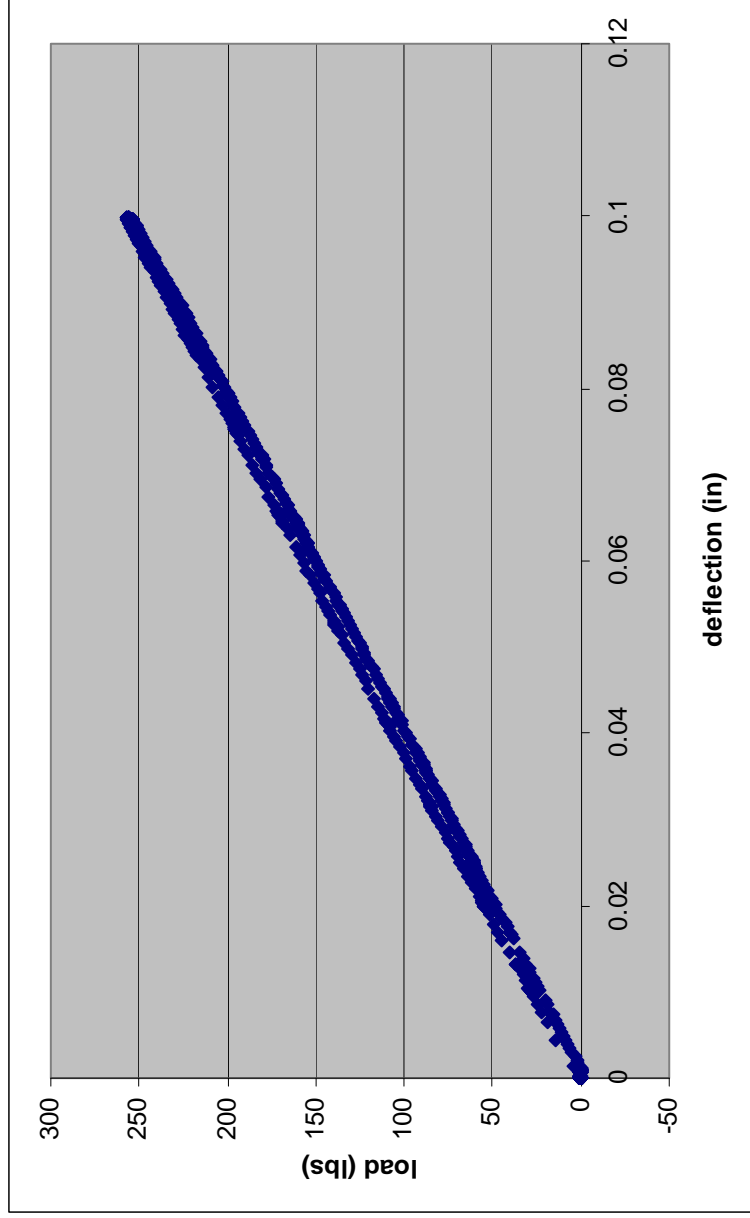


Top Center Load



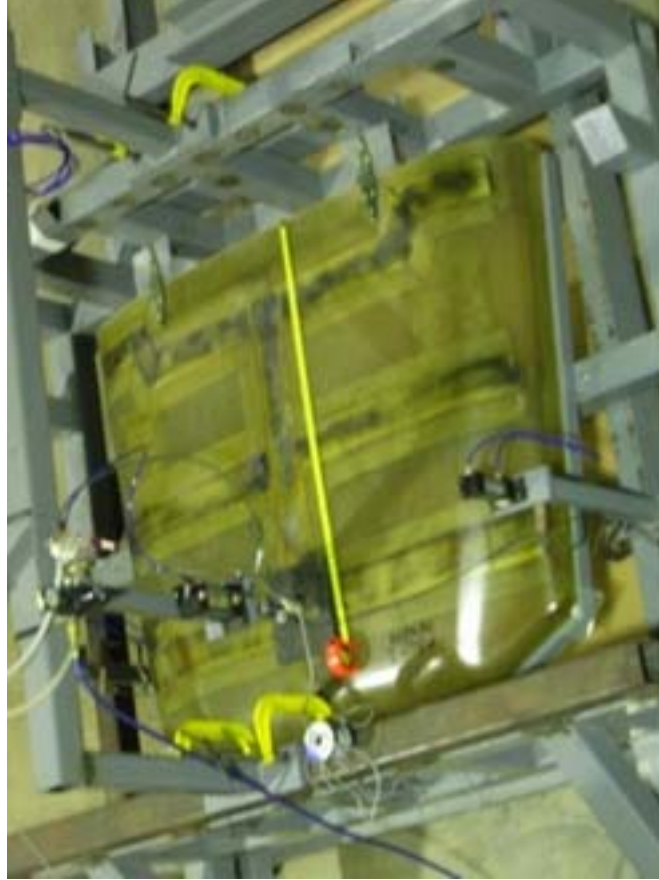
- No permanent deformation.
- No separation of reinforcements from the hood.
- No cracks.
- **Test passed.**

Initial Top Center load



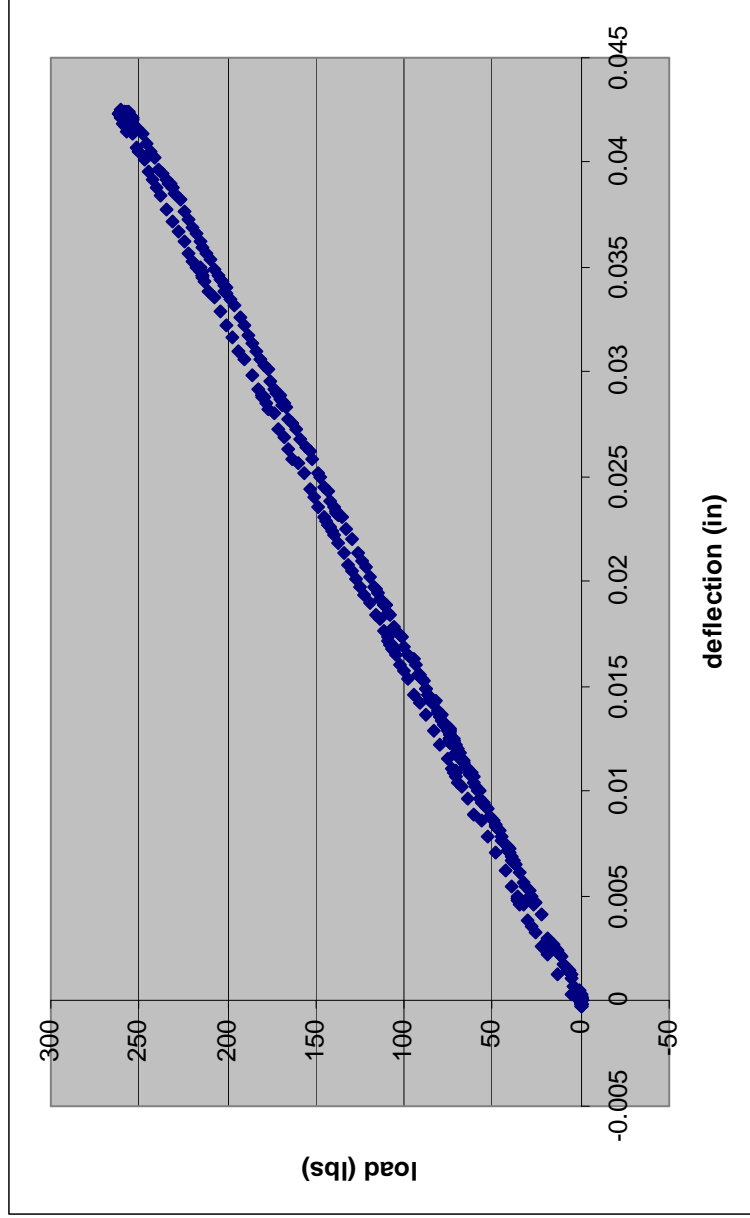
- Elastic deflection 0.10" at 250 lbs.
- Much less than 0.50" allowed
- **Test passed.**

Top Front Load



- No permanent deformation.
- No separation of reinforcements from the hood.
- No cracks.
- **Test passed.**

Initial Top Front Load



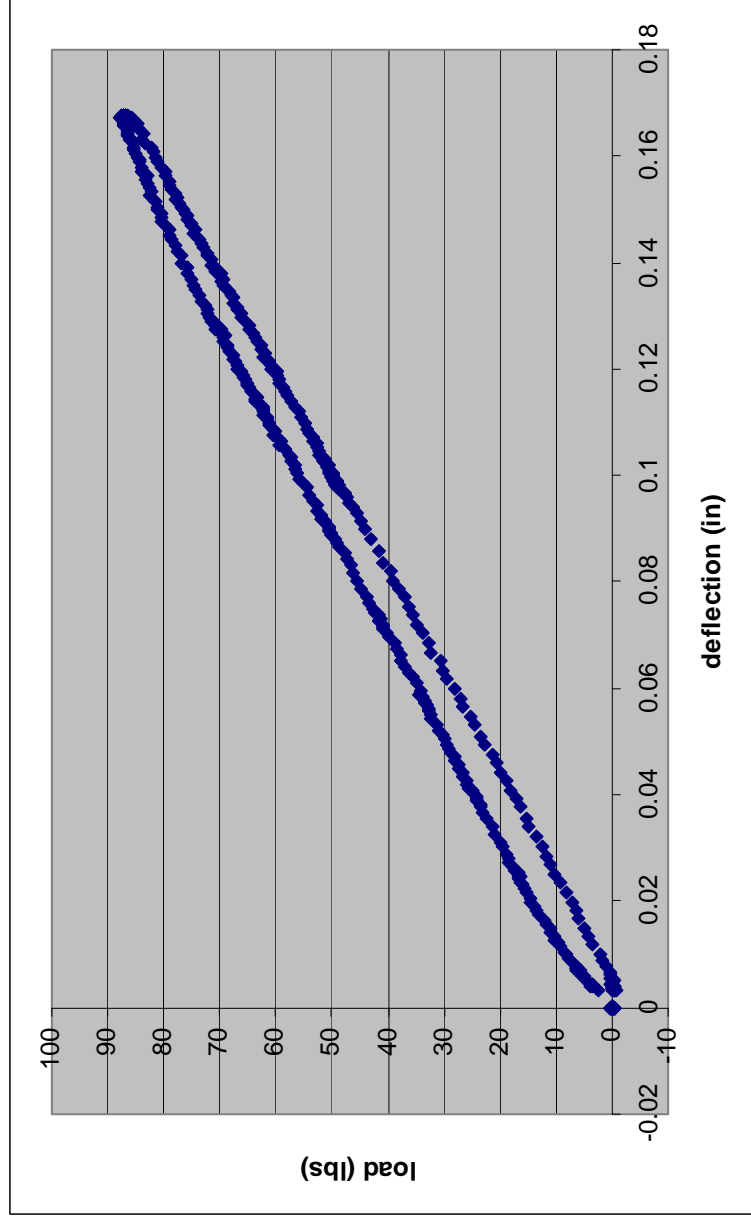
- Elastic deflection 0.04" at 250 lbs.
- Much less than 0.50" allowed
- **Test passed.**

- Test will be conducted at room temperature.
- An upward load will be applied at the corner lift handles
- The center latch will be engaged and both right and left sides will be tested (separately).
- Displacement of the hood corner above the fixture will be measured.
- Plots of load vs deflection will be obtained.
- The lifting load will not exceed 100 lbs.
- **Test pass criteria:**
 - Load to lift the corner 0.375" shall be greater than 50 lbs.
 - No permanent deformation.
 - No separation of reinforcements from the hood.
 - No cracks allowed.





- No permanent deformation.
- No separation of reinforcements from the hood.
- No cracks.
- **Test passed.**



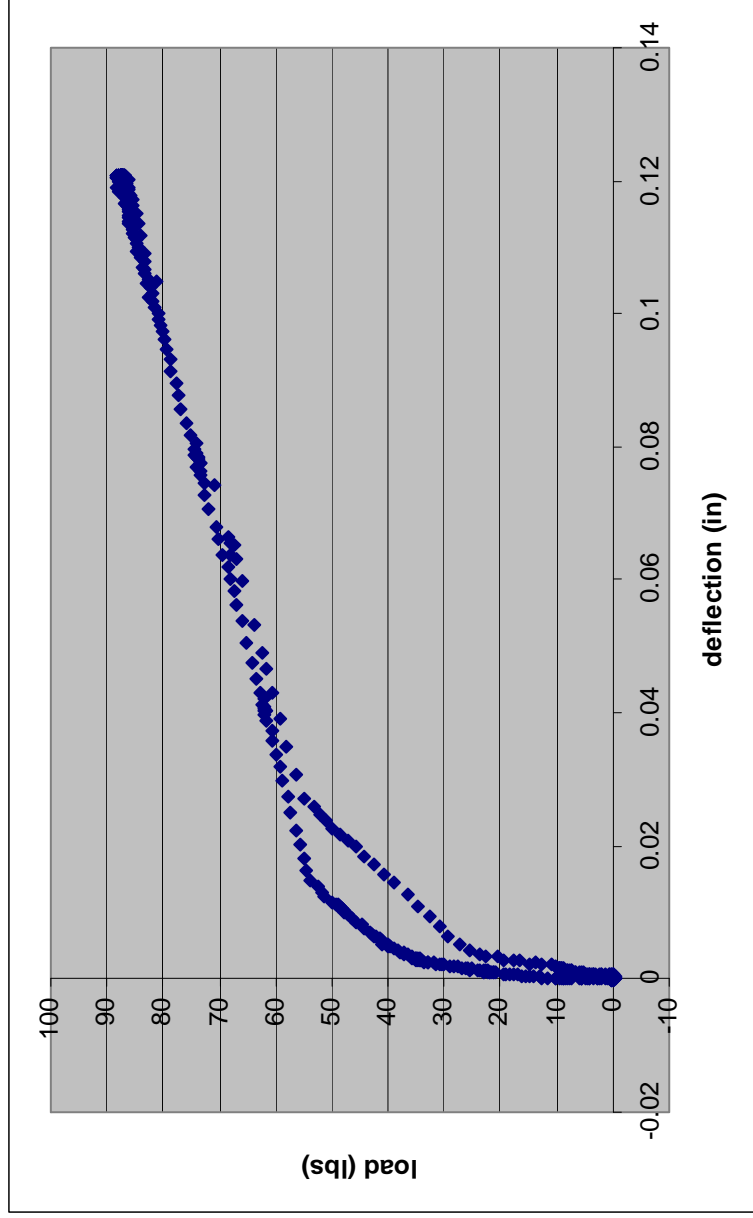
- Elastic deflection 0.16" at 85 lbs.
- More than 50 lbs required to lift corner 0.375"
- **Test passed.**

Passenger Corner Lift



- No permanent deformation.
- No separation of reinforcements from the hood.
- No cracks.
- **Test passed.**

Initial Passenger Corner Lift



- Elastic deflection 0.12" at 85 lbs.
- More than 50 lbs required to lift corner 0.375"
- **Test passed.**



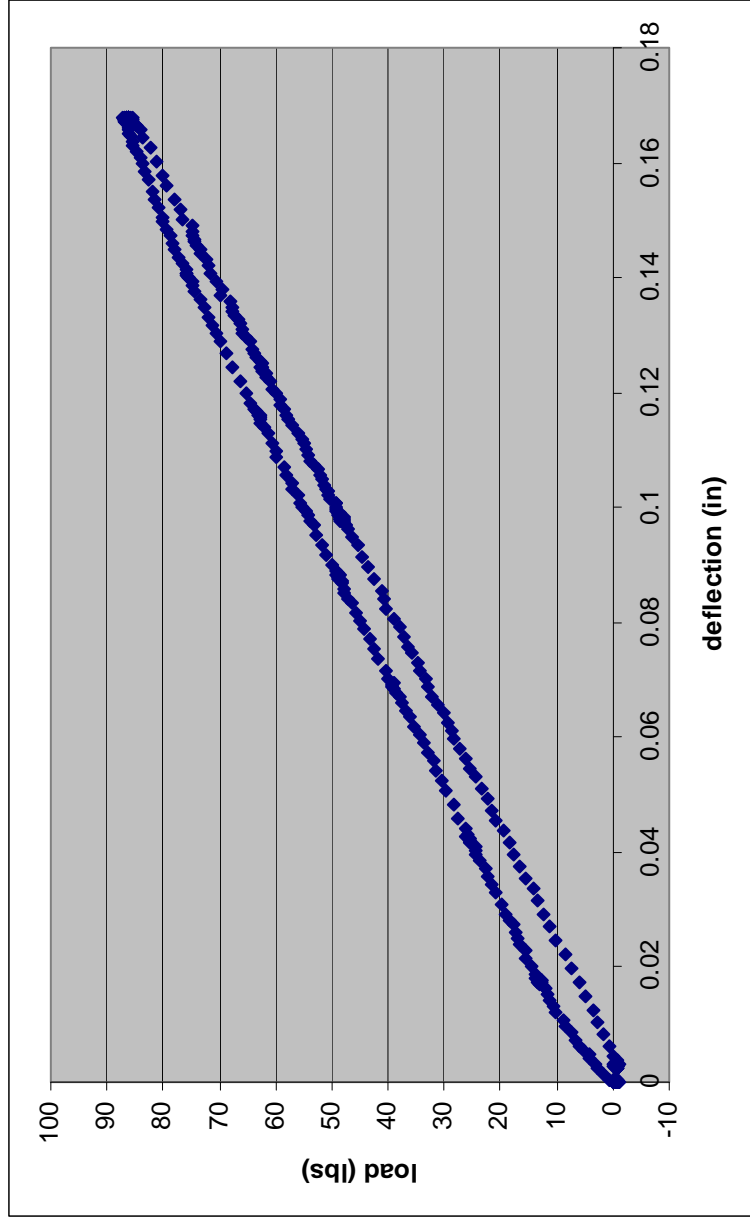
- Test will be conducted at room temperature.
- 50 lb upward loads will be applied at the corner lift handles with the center latch engaged.
- The loads will be applied in alternating fashion (right then left) over a 8 hour period at 10 cycles per minute.
- Upon completion plots of load vs deflection will be obtained.
- **Test pass criteria:**
 - No permanent deformation.
 - No separation of reinforcements from the hood.
 - No cracks allowed.
 - No broken fibers shall be visible on areas where the hood contacts the fixture.



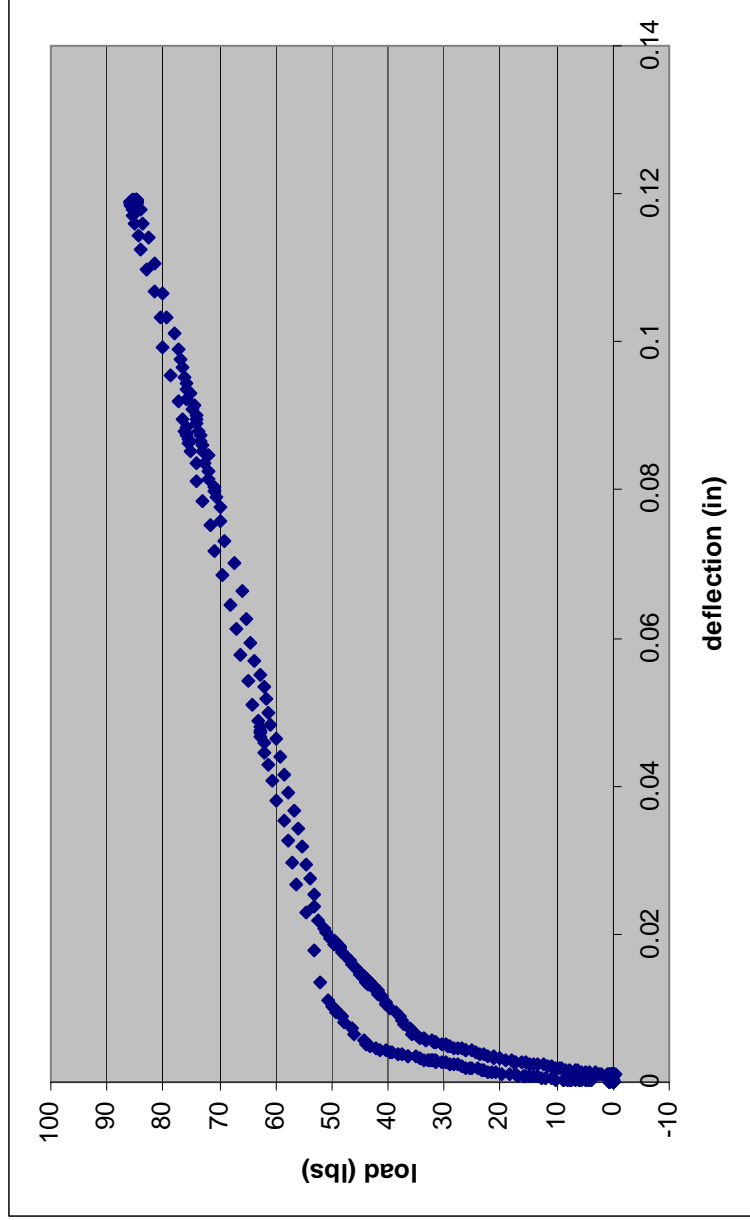
Cyclic Handle Load



- No permanent deformation.
- No separation of reinforcements from the hood.
- No cracks.
- No broken fibers visible on areas where the hood contacts the fixture
- **Test passed.**



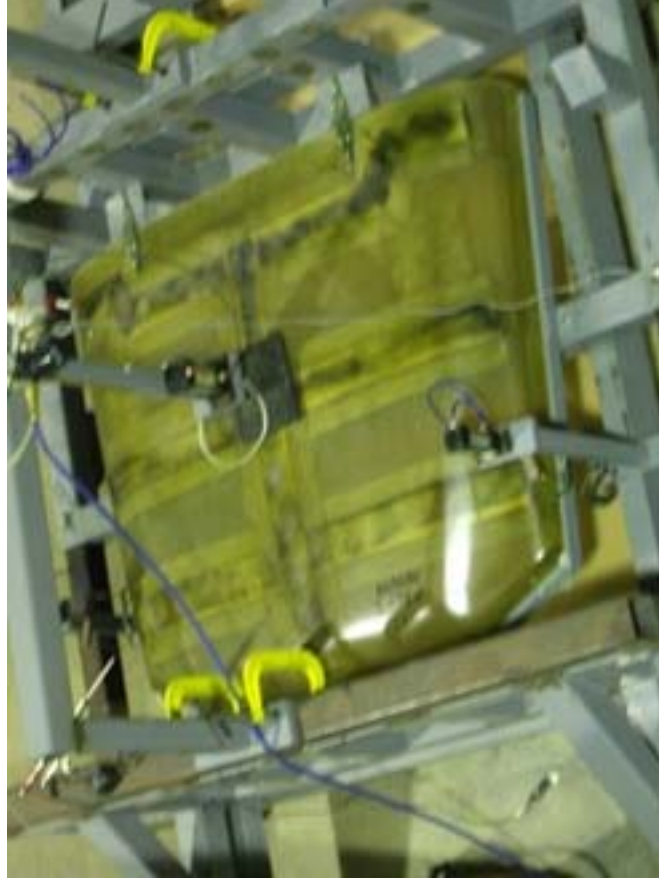
- Elastic deflection 0.16" at 85 lbs.
- More than 50 lbs required to lift corner 0.375".
- No significant change in stiffness after cyclic loading.
- **Test passed.**



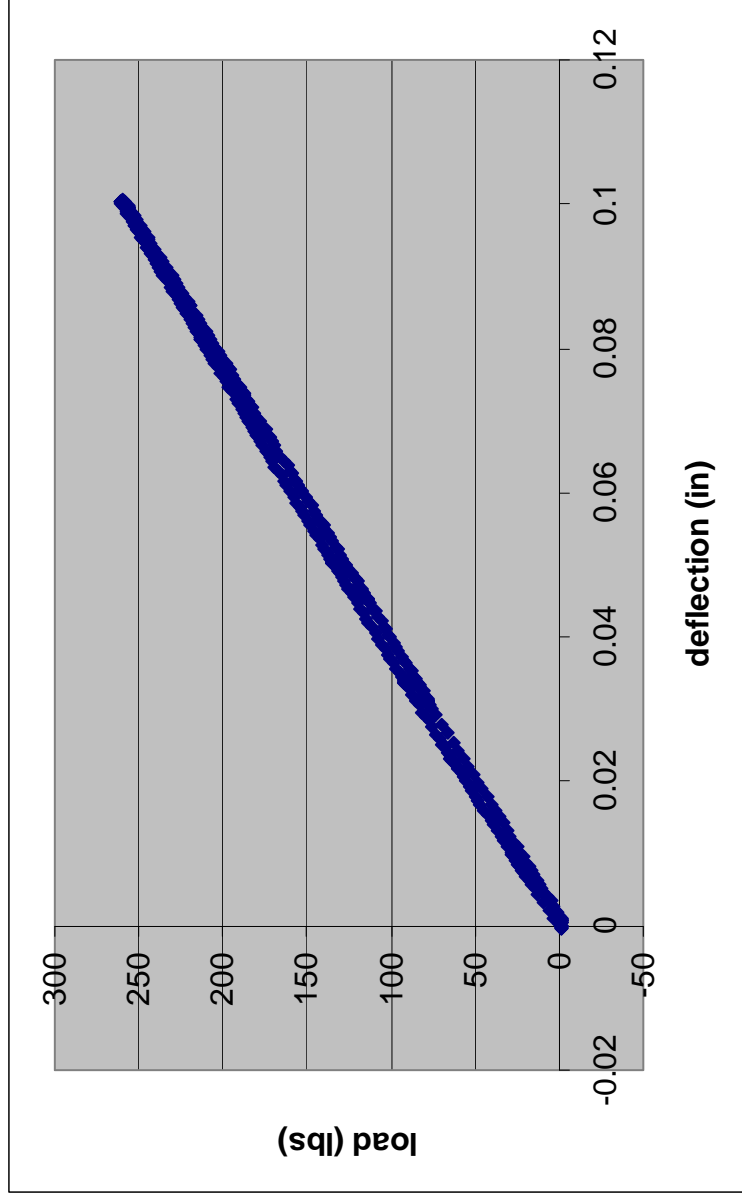
- Elastic deflection 0.12" at 85 lbs.
- More than 50 lbs required to lift corner 0.375".
- No significant change in stiffness after cyclic loading.
- **Test passed.**

- Test will be conducted at room temperature.
- A 250 lb load will be applied to the outside surface of the hood at a central location.
- The load will be cycled on and off for 100,000 cycles at 1 cycle per second.
- Upon completion a plot of load vs deflection will be obtained.
- **Test pass criteria:**
 - No permanent deformation.
 - No separation of reinforcements from the hood.
 - No cracks allowed.
 - No broken fibers shall be visible on areas where the hood contacts the fixture.



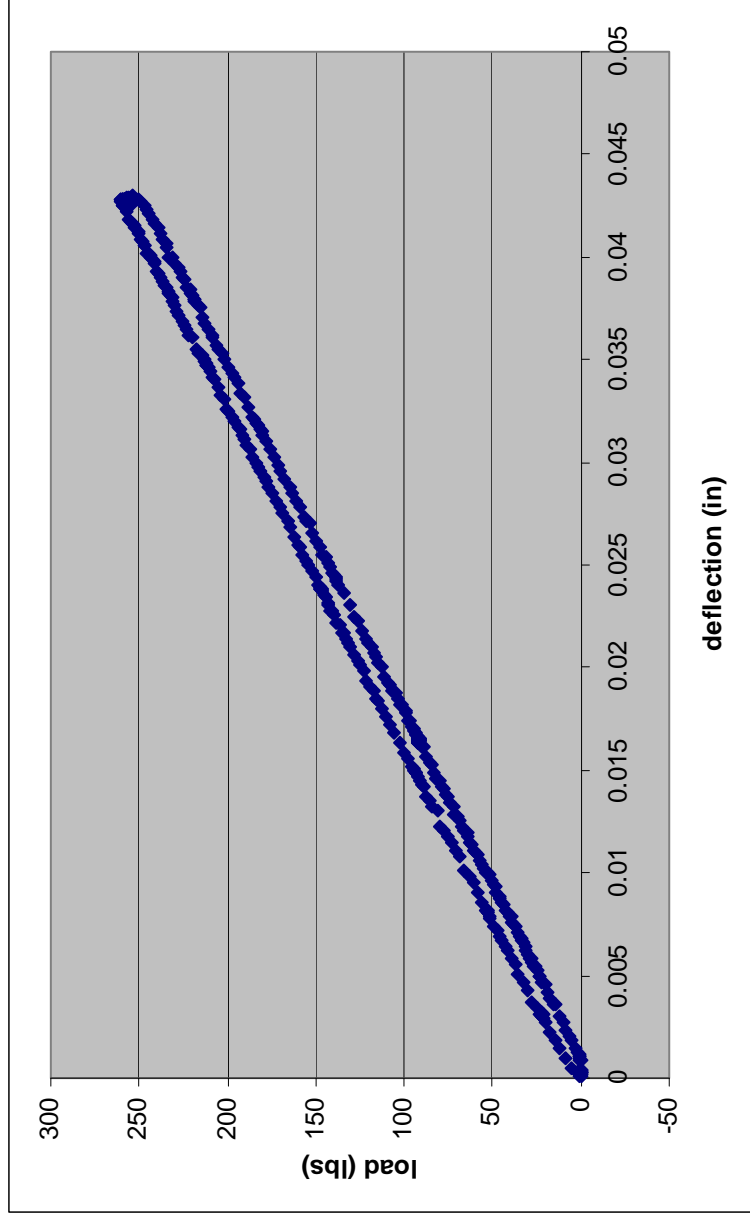


- No permanent deformation.
- No separation of reinforcements from the hood.
- No cracks.
- No broken fibers visible on areas where the hood contacts the fixture
- **Test passed.**



- Elastic deflection 0.10" at 250 lbs.
- Much less than 0.50" allowed
- No significant change in stiffness after cyclic loading.
- **Test passed.**

Final Top Front Load

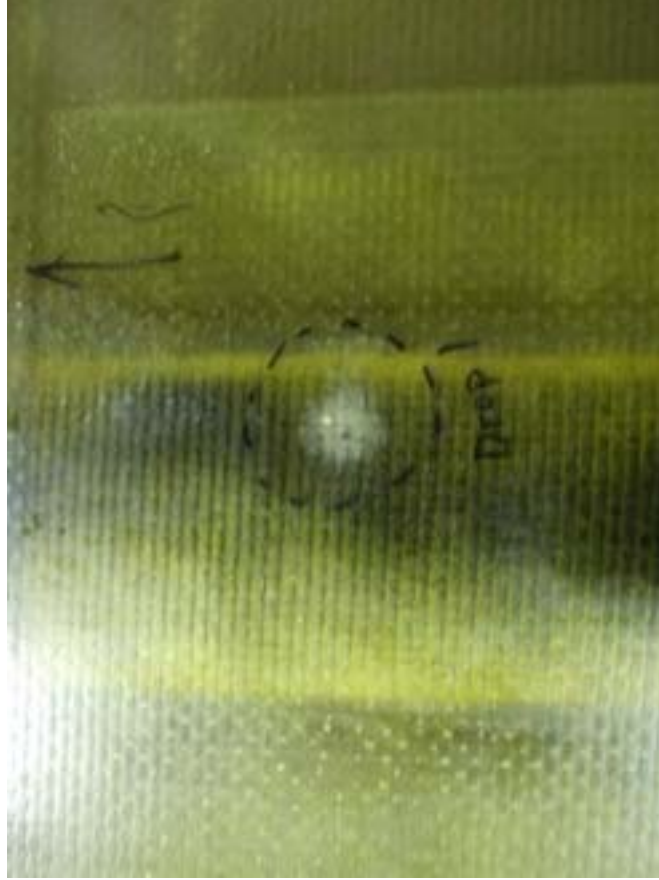


- Elastic deflection 0.04" at 250 lbs.
- Much less than 0.50" allowed
- No significant change in stiffness after cyclic loading.
- **Test passed.**

- Test will be conducted at room temperature.
- 2 lb steel ball will be dropped on the hood.
- The ball will undergo a 6' drop.
- Impact will occur at the following locations:
 - On stiffener
 - Next to stiffener
 - Between stiffeners
 - On small radius surface
 - On large radius surface
- Test pass criteria:
 - No permanent deformation.
 - No separation of reinforcements from the hood.
 - No cracks allowed.

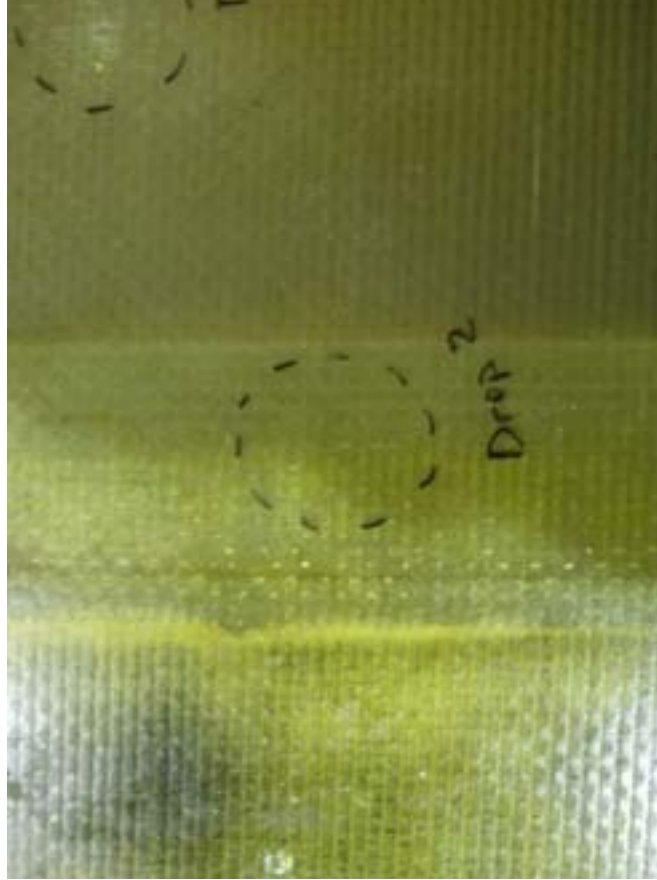


Impact 1 - on stiffener



- No permanent deformation.
- No separation of reinforcements from the hood.
- No cracks.
- **Test passed.**

Impact 2 - next to stiffener



- No permanent deformation.
- No separation of reinforcements from the hood.
- No cracks.
- **Test passed.**

Impact 3 – between stiffeners



- No permanent deformation.
- No separation of reinforcements from the hood.
- No cracks.
- **Test passed.**



Impact 4 – large radius corner



- No permanent deformation.
- No separation of reinforcements from the hood.
- No cracks.
- **Test passed.**

Impact 5, 6 – small radius corner



- No permanent deformation.
- No separation of reinforcements from the hood.
- No cracks.
- **Test passed.**

INTENTIONALLY LEFT BLANK.

Appendix I. Navy Composite Rudder Demonstration and Validation Report

This appendix appears in its original form, without editorial change.

Appendix I

Navy Composite Rudder Demonstration and Validation Report



DEPARTMENT OF THE NAVY
NAVAL SURFACE WARFARE CENTER, CARDEROCK DIVISION
9500 MACARTHUR BOULEVARD
WEST BETHESDA MD 20817-5700

IN REPLY REFER TO

9078
Ser 65-08
30 Oct 09

From: Commander, Naval Surface Warfare Center, Carderock Division
To: Department of the Army, U.S. Army Research Laboratory, AMSRD-ARL-WM-MC,
Aberdeen Proving Ground, MD 21005 (Attn: John LaScala)
Subj: Environmental Security Technology Certification Program (ESTCP) Low HAP/VOC
Ref: (a) Environmental Security Technology Certification Program Funding Documents
W74RDV90301105, W74RDV73615721, W74RDV70657281 and Army Research
Lab Funding Document Number MIPR6FARL80163

Encl: (1) *NSWCCD ESTCP MCM Rudder Demonstration Report*

1. Reference (a) requested the Naval Surface Warfare Center, Carderock Division (NSWCCD) to participate in this tri-service program to evaluate several low hazardous air pollutants/volatile organics vinyl ester resin systems for possible use in naval applications. The Mine Countermeasure (MCM) ship rudder application was chosen as a possible use for this resin system and two full-scale MCM rudders were fabricated under this program by Structural Composites Inc., Melbourne, FL. Enclosure (1) is a draft final report documenting the fabrication of these MCM rudders as well as the destructive evaluation performed on one of the rudders to evaluate the manufacturing quality. A final report will be issued when the results of the full-scale non-destructive evaluation using the SIDER technique have been completed.
2. Comments or questions may be referred to Dr. Roger M. Crane, Code 655, phone (301) 227-5126, e-mail, Roger.Crane@navy.mil.

E. A. RASMUSSEN
By direction

Copy to:

NAVSURFWARCEN CARDEROCKDIV
BETHESDA MD [Codes 65, 655,
655(Crane, Foley,)]

Department of the Army, U.S. Army Research
Laboratory, AMSRD-ARL-WM-MC, Aberdeen Proving
Ground, MD 21005 (Attn: John LaScala)

NSWC CD ESTCP Low HAP/VOC Program	
Subject:	ESTCP Mine Counter Measure Class Rudder Demonstration
Maureen E Foley, Timothy Dapp, John Kim and Roger Crane	Date: 10/20/2009

Introduction

Through an Environmental Security Technology Certification Program (ESCTP), NSWC Carderock Division was tasked with evaluating a low volatile organic compound (VOC) vinyl ester (VE) resin system that could be considered for further use in Navy applications. Whereas most current vinyl ester systems contain 40-60 weight percent of styrene, the low VOC vinyl ester resin systems cuts this styrene content in half and replaces it with a Fatty Acid (FA) monomer as a reactive diluent. In the case of the NSWCCD task, the reactive diluent in the system was methacrylate lauric acid (FAVE-L). A detailed characterization of several FAVE resins was performed and results compared to several resins currently used in Navy applications¹. The FAVE-L-25S (25 wt% styrene) was selected to demonstrate the viability of this fatty acid vinyl ester resin technology in fabrication of medium/large scale infusion process required for the approximately 6 foot tall MCM rudder. Structural Composites, INC. of Melbourne, FL was selected as the manufacturer since they had been extensively involved in the development of the manufacturing process for the DDG51 Composite Twisted Rudder and also owned the molds and equipment that was used to make the one pair of composite Mine Counter Measure Class (MCM) rudders that are currently fielded in the fleet².

Background

A total of 2 MCM rudder demonstration articles were fabricated by Structural Composites INC. of Melbourne, FL. The main difference between the two rudders was that the first rudder has a fabricated representative composite hub whereas the second rudder was only foam filled and did not contain a hub. The second rudder would be used for evaluation of the process by performing destructive evaluation whereas the first rudder would be held intact for potential further testing. In addition, a SIDER non destructive test will be performed to confirm the quality of the part.

Fabrication Process

The MCM rudder for this demonstration process was made using the same glass fiber reinforcement and fiber layup as with the DDG51 Composite Twisted Rudder (CTR). The SW1810 Uni/Mat fabric from Fiber Glass Industries – Nominally an 18oz/yd²

¹ Maureen Foley, Timothy L. Dapp, John Kim, and Roger Crane, ESTCP Low VOC Material Characterization, NSWCCD-65-2009/45, (in preparation).

² Composite Marine Control Surface (Rudder) Program (TDL 95-11) Final Report, Lockheed Martin Aeronautical Systems Company, December 1997.

unidirectional E-glass fibers stitched to a 10 oz/yd² binder-free chopped strand mat. The main fabrication process difference was that these rudders were fabricated using a 2-step infusion process rather than the single stage resin recirculation process that was used to fabricate the in-service MCM rudders. It was found as a result of the DDG51 CTR program³ that the risk to a program is substantially reduced by the use of a multi-step infusion process for thick section composite parts by allowing the possibility of repair after each infusion step. 5 layers of fabric were laid up on the part for each infusion step using an alternating 0/90° layup with the mat side placed against the part.

Rudder One Fabrication

Structural Composites decided to fabricate a composite hub for this rudder. Initial inquiries into the cost of a metallic bronze hub was in excess of \$50K which was well outside the boundaries of this demonstration. The hub was constructed using the metallic version as a guideline and also taking into account the hub and flange design of the DDG51 CTR. The hub was made in several stages with the circular hub formed around a steel cylinder. The flanges were fabricated separately and then secondarily bonded to the main hub. Figure 1 shows a series of photos that were taken of the composite hub fabrication process.

After the hub was manufactured, the part was placed into the foaming mold and a 2 part polyurethane foam was blown into place. As part of this process demonstration, risk reduction trials for the DDG51 class rudder composite manufacturing process were evaluated where possible. One of these trials involved the fabrication of vertical shear ties located near the tip of the rudder. In the case of the CTR, there were issues ensuring that the full thickness of the shear ties was fully and uniformly infused. Therefore for this demonstration, a new process was evaluated to make the cut outs in the foam required for the placement of the shear ties. In this case, a wooden preform was molded into the foam at the desired shear tie location. Once the foaming was complete, the wooden performs were removed leaving a uniform cut out in the foam for the insertion of the fabric that was used to make the shear tie. As will be shown in the destructive evaluation portion of the second rudder, this method yielded very uniform shear ties with minimal (if any) voids.

After the foaming was complete, the glass preform shear ties were installed into the foam in the desired locations and then infused. Figure 2 shows pictures of the foaming and shear tie fabrication process. It should be noted that the orange/pinkish color on the foam is fairing compound that was used to fill in the surface holes. The rudder was then placed on the assembly stand and the glass fiber was wrapped to the required layup. To reduce the risk to the program, half of the required layers were infused at a time.

³ Composite Twisted Rudder Manufacturing Guide prepared by Structural Composites for the Office of Naval Research under contract No. N00014-06-D-0045, June 2008.

Figure 1 Fabrication of MCM Composite Hub



MCM Rudder Tooling



Infused Hub Stiffener



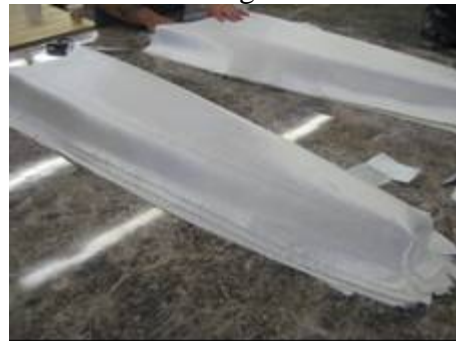
E-Glass Wrapped Cylinder



Infused E-glass Hub



Foam cut outs for Flange Fabrication



Foam Overwrapped with E-Glass



Flange Infusion



Composite Hub Assembly

Figure 2 Foaming and Shear Ties Fabrication of MCM Rudder



Foam Form with Embedded Flanges from the Composite Hub Present



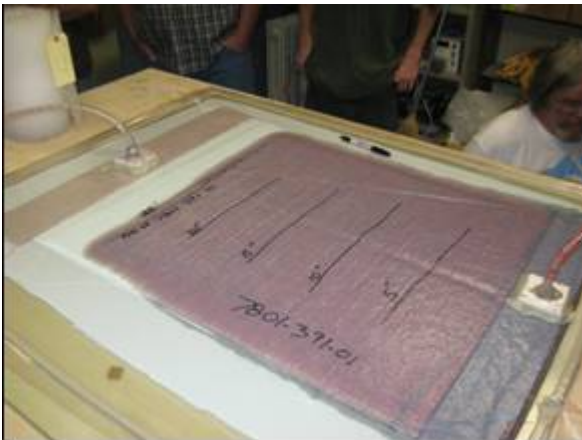
Foam Form with Embedded Flanges from the Composite Hub Present



Vertical Shear Ties Inserted into Slots



Shear Ties in Place with Flange Overwraps



Infusion of Vertical Shear Ties



Infusion of Horizontal Flanges

Figure 2 Foaming and Shear Ties Fabrication of MCM Rudder (continued)



Foam Form with Vertical Shear Ties and Horizontal Flanges Infused

The first infusion for Rudder One was witnessed by Roger Crane (Code 655). One of the key issues in the Vacuum-Assisted-Resin-Transfer-Molding process is the control of the vacuum bag seal. It is extremely important that there are very minimal (if any) leaks in the bag seal to ensure that no air is pulled into the part during the manufacturing stage. As parts get larger, it becomes more and more difficult to find leaks in the seams. Generally a leak down test was performed prior to infusion. The requirement being that, the vacuum pressure in the bag cannot drop more than 1" of mercury over 15 minutes. If this requirement is not met, then the bag seal is inspected again to determine where the leak is originating and is repaired.

Structural Composites Inc. uses a unique combination of vacuum bagging materials in the infusions. The resin distribution media is fairly open allowing very fast movement of the resin along the surface of the part. The distribution media used in this application is also very stiff and has sharp edges where it has been trimmed. It is believed that these sharp edges might have contributed to issues with vacuum leaks developing during the infusion process. It was determined in the DDG51 CTR Program through a peel ply study⁴, that a heat scoured peel ply provides the best surface for secondary bonding. Several infusion lines are used in this vertical infusion. The initial 2 ports are located at the base of the rudder as it sits on the infusion platform. Once flow is past the next line of infusion the next set of inlet ports are opened. All lines are kept open until the resin gels in the buckets. In some instances, if a leak appears in the part, an additional inlet/outlet port may be quickly added to minimize the affect of the leak. In this infusion, the trailing edge tip of the rudder was the last to infuse.

⁴ Maureen E Foley, Timothy L. Dapp, John S. Kim and Roger Crane, The Effect of Peel Ply and Surface Preparations on Secondary Bonding in VARTM Applications, NSWCCD-65-TR-2009/36, March 2009.

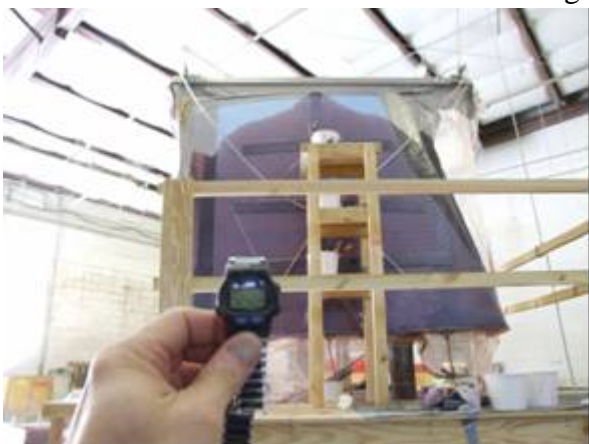
Figure 3 MCM Rudder One- Infusion 1



MCM Rudder Before Infusion One



MCM During Infusion One



MCM Rudder Towards End of Infusion

Figure 3 MCM Rudder One- Infusion 1 (continued)



MCM Rudder After Infusion One

The first infusion yielded a good outer face sheet laminate. The whiteness of the part are surface scrapes from removing the white heat scoured peel ply. It was found that this peel ply would tear as it was being removed from the part which necessitated removing the peel ply in smaller pieces using mechanical assistance. A significant effort in both time and labor was required to remove the vacuum bag and distribution media for the first layer infusion. In subsequent infusion, an additional layer of Super Release Blue peel ply was used over the heat scoured peel ply to aid in the removal of the bag and distribution media.

A similar process was performed with the second infusion of rudder one. Figure 4 shows the progression of the infusion up the MCM rudder from the base to the tip. This infusion (and all subsequent face sheet) infusions were witnessed by Maureen Foley (Code 655). Structural Composites, INC., decided to wrap the rudder with pallet wrap prior to placing the vacuum bag over the part. It was hoped that by holding the glass fabric more tightly in place prior to application of the vacuum it would minimize the wrinkling on the leading edge. After infusion, (Figure 5) it was seen that wrinkling still occurred on the leading edge. In this case, the overlaps in the pallet wrap layers caused areas of excess resin pockets to form along the faces of the rudder as well as the root of the rudder. After the infusion, the rudder was carefully removed from the assembly stand that was also used as an infusion station (Figure 6).

In general, the face sheet infusions took approximately 1 hour to infuse through the vertical height of the rudder. Initially there was concern that the nominally higher viscosity of the FAVE-L-25S resin (400 cps) compared to the CORVE 8100 resin (100 cps) would cause problems with the infusion, but the infusions were fairly well behaved. The only manufacturing concern with the FAVE-L-25S was that it did not appear to have a very stable gel time with a given mix ratio. Before each infusion, a gel time test was performed and the mix ratio varied accordingly to meet the desired 1- 1.5 hour gel time. During the infusion, the mix ratio of the buckets mixed later in the infusion contains higher amounts of catalyst so that they would gel at approximately the same time as the first buckets that were mixed.

Figure 4 **MCM Rudder One- Infusion 2**



Start 1315



1402



1412



1412



1414



1415



1417 Infusion Complete



1418 Infusion Complete

Figure 5 **Completed MCM Rudder One**



Trailing Edge



Wrinkling(or Excess Resin) Evident near Root of the Rudder

Figure 5 **Completed MCM Rudder One (continued)**



Some Wrinkling on Leading Edge



Some excess resin pockets

Figure 6 Unloading MCM Rudder One From Fabrication Fixturing



Rudder Two Fabrication

The second rudder that was fabricated under this demonstration project did not have a composite hub. Instead it simply had a steel cylinder to which several pieces of steel were welded on to provide a flange type support. The purpose of the flange was simply to ensure that the steel cylinder would not rotate within the foam ensuring that the glass wrapping process could take place.

Figure 7 shows some additional steps of the fabrication process. Initially the full foam preform was molded and faired as needed. The vertical shear tie foam area was removed and wooden preform installed for the second foaming step which yielded very uniform shear tie slots. The vertical shear ties were installed and infused as with Rudder One.

Figure 7 MCM Rudder Two- Foaming and Shear Tie Fabrication



Foam Preform



Mold for Shear Tie Slot Fabrication



Shear Tie Slots



Shear Tie Infusion



Shear Ties Infused

Figure 8 shows part of the glass wrapping process. The SW1810 is wrapped around the rudder using a fixture that was developed under a previous program. The mat side of the glass fabric was placed against the foam in alternating 0/90 layers for a total lay up of (0/90/0/90/0) for each infusion.

Figure 8 MCM Rudder Two- Glass Wrapping



0° Plies



90° Plies

During the infusions of Rudder Two, two caul plates were evaluated to investigate if their use would minimize the wrinkling of the glass fabric around the edges of the rudder. Glass fiber reinforced caul plates were fabricated using the MCM molds and placed on the middle of the tip of the rudder and about one fourth of the way down from the root on the leading edge. Figure 9 shows the caul plates installed with the distribution media prior to the installation of the vacuum bag.

Figure 9 **MCM Rudder Two- Caul Plate Locations**



Caul Plate on Tip of Rudder



Caul Plate on Leading Edge of Rudder

A progression of the MCM Rudder Two infusion one can be seen in Figure 10. As with the previous infusions, the infusion time was approximately 1 hour. Figure 11 shows different views of the MCM Rudder Two after the first infusion. The results are similar to the previous infusions. In the areas where the caul plate was used, it appeared that wrinkling was prevented in the glass fabric in the immediate area. However the use of the caul plate caused the wrinkle to move to an area not covered by the caul plate. On one side of the rudder there was a large black inclusion as circled in red in Figure 11. Upon further inspection, this was found to be a piece of vacuum tape that was removed before the next infusion. This incidence was somewhat indicative of the kinds of manufacturing defects can occur when quality checks are not adhered to on the production floor.

Figure 10 MCM Rudder Two- Infusion One



1307



1315



1323



1329



1330



1333



1338



1358

Figure 11 MCM Rudder Two- After Infusion One



Side 1



Side 2



Area on Tip where Caul Plate was Used



Near Root



Leading Edge (Large Inclusion circled in Red)



A progression of the MCM Rudder Two infusion two can be seen in Figure 12. As with the previous infusions, the infusion time was approximately 1 hour. Figure 13 shows different views of the MCM Rudder Two after the second infusion. The results are similar to the previous infusions. In the areas where the caul plate was used, it appeared that it did prevent wrinkling in the glass fabric in the immediate area, but the wrinkle moved to an area not covered by the caul plate. A destructive analysis will be performed in these areas to confirm these findings.

Figure 12 MCM Rudder Two- Infusion Two



1246



1259



1312



1314



1317



1320

Figure 12 MCM Rudder Two- Infusion Two (continued)



1327



1329



1332



1336



1340



1350



1409



1429

Figure 13 MCM Rudder Two- After Infusion Two



Face 1



Face 2



Base of Rudder



Leading Edge of Rudder, Wrinkle is displaced where caul plate was located

Destructive Evaluation of Rudder Two

A. Face Sheet Core Samples

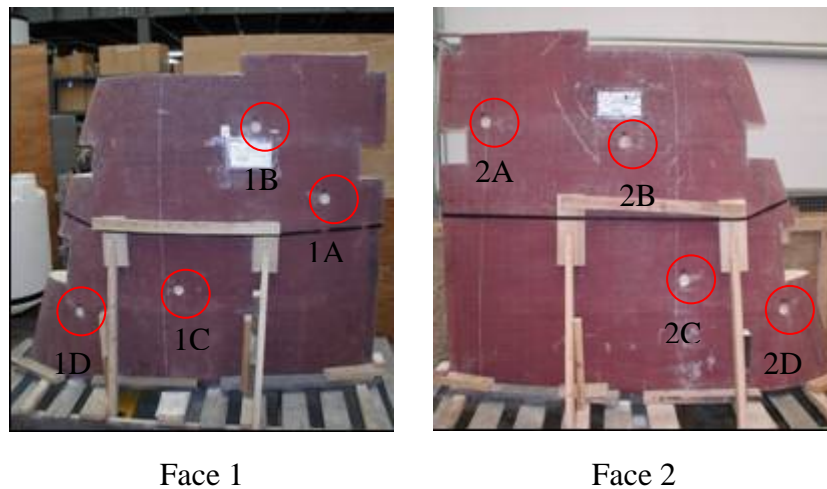
Four samples were extracted using a core drill from each face of the rudder to determine an average face sheet thickness. Figure 14 shows photos of the two faces with the locations marked where the samples were removed. The results are shown in Table 1. The results show fairly good agreement from one face to another on thickness of the face sheet material. The average of samples does not include the B samples, which were taken in the area of the vertical shear ties and therefore have an additional thickness due to the shear tie overwraps.

Table 1 Core Drill Samples Thicknesses from Rudder Faces

Sample	Face 1 (inch)	Face 2 (inch)
A	0.3755	0.3790
B*	0.5010	0.5205
C	0.3600	0.3495
D	0.4105	0.4115
Average \pm StDev	0.382 ± 0.026	0.380 ± 0.031

*Average does not include B Samples

Figure 14 MCM Rudder Two – Locations of Face Sheet Samples

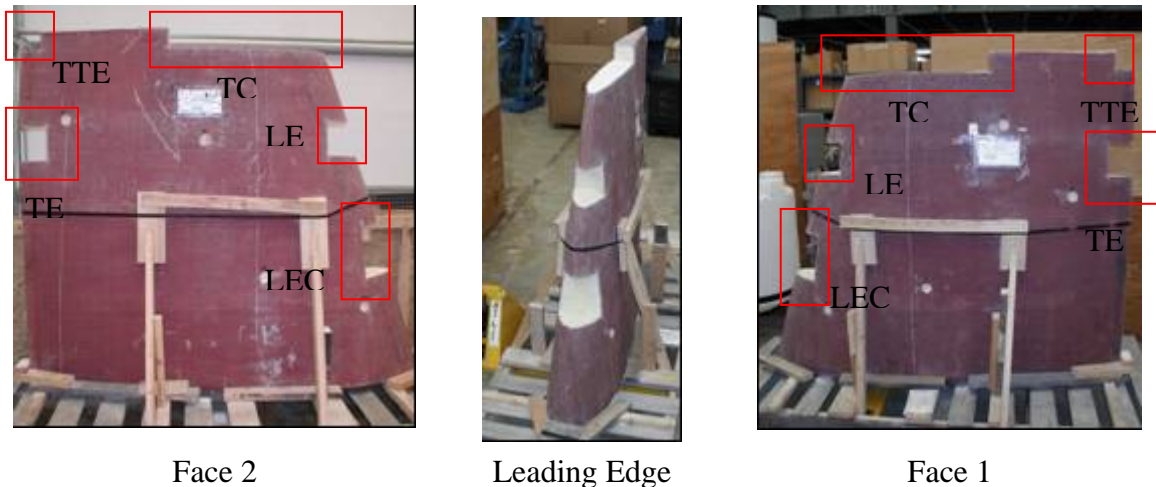


B. Rudder Cross Sections

Around the edges of Rudder Two, large pieces of composite were removed so that a detailed analysis could be performed on the cross section of the composite. Two locations were removed on the leading edge: One in the area of caul plate use (LEC) and the other away from the caul plate location (LE). Similarly, two pieces from the tip of the rudder were removed for inspection: One through the 2 shear ties and caul plate area

(TC) and other at the corner of the tip and trailing edge (TTE). The remaining piece was removed from middle of the trailing edge (TE). All sides of the composites pieces that were removed were polished using standard polishing techniques so that an overall snapshot of the quality of the composite part such as fiber ply alignment and void/resin/fiber ratio could be obtained.

Figure 15 MCM Rudder Two – Locations of Rudder Cross Sections



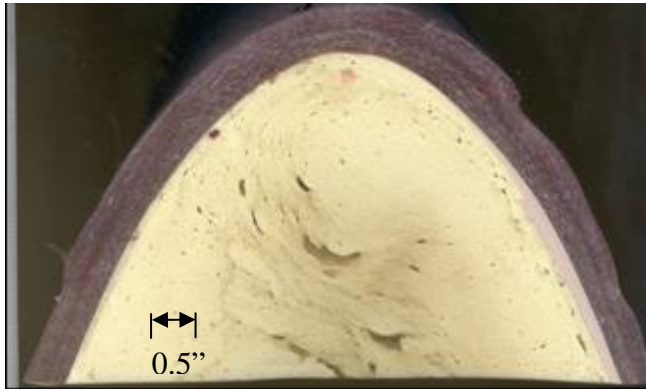
1. Leading Edge - Caul Plate Area (LEC)

A large piece of composite was removed on the leading edge in the area where the caul plate was in place during the two infusions. All edges of the part were polished and results are shown in Figures 16 and 17. Results indicate that the caul plate appeared to shift the wrinkling from the leading edge to the edge of the caul plate.

2. Leading Edge - Away from Caul Plate Area (LE)

A large piece of composite was removed on the leading edge in an area away from the caul plate. All edges of the part were polished and results are shown in Figure 18. Results indicate that there was a substantial amount of wrinkling along the leading edge due to non-uniform compression of the glass fabric plies during the application of vacuum. These types of wrinkles are expected with this manufacturing process and were also evident in the CTR. As compared to the results in the previous section, the wrinkles in this part were much more pronounced than the ones in the caul plate area.

Figure 16 MCM Rudder Two – Leading Edge Near Caul Plate

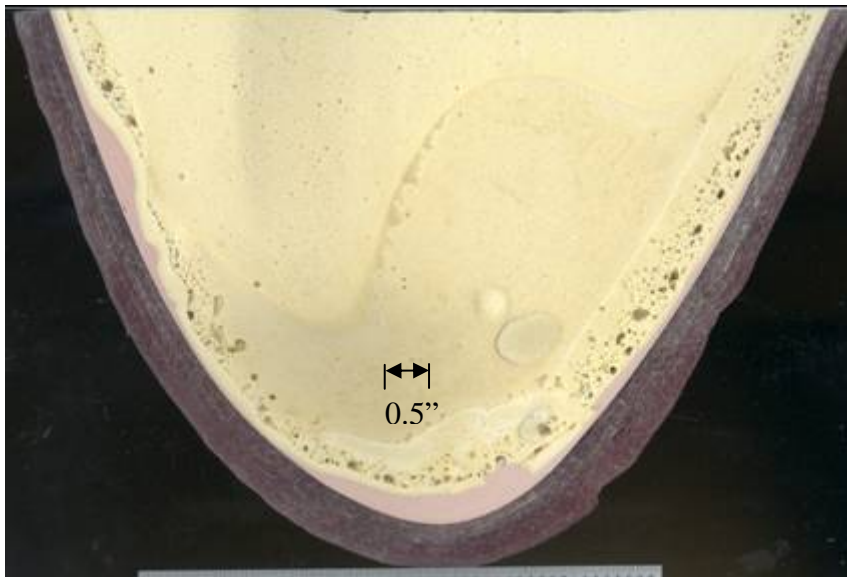


- Nearly uniform composite part along the leading edge.
- Wrinkled moved to location at edge of caul plate away from leading edge



- Nearly uniform composite part with minimal voids

Figure 17 MCM Rudder Two – Leading Edge Near Caul Plate (continued)



- Nearly uniform composite part along the leading edge.
- Wrinkled moved to location away from leading edge

Figure 18 MCM Rudder Two – Leading Edge Away from Caul Plate



- Large wrinkle present in both infusions at the leading edge.
- Nearly uniform composite part away from the leading edge.
- Resin rich areas present within the wrinkle

- Nearly uniform composite part with minimal voids

- Large wrinkle present in both infusions at the leading edge.
- Nearly uniform composite part away from the leading edge.
- Resin rich areas present within the wrinkle.

3. Tip – Shear Ties and Caul Plate Area (TC)

A large piece of composite was removed on the tip of the rudder that included an area through the two shear ties. All edges of the part were polished and results are shown in Figure 19. Results indicate a fairly uniform cross-section within the shear ties, with minimal (if any) voids. The layer of distribution media (blue) that was left in the part can be seen in the resin rich layer in the center of the shear tie. While the composite areas look very uniform, the foam regions are less than homogeneous. In general, the foam is used to fill up the space and not required to take any load. It is uncertain whether the voids in the foam region are critical. While the new technique to fabricate consistent shear ties appears to have worked, there has been some degradation in the quality of the foam in the areas around the shear ties.

The cross section of the part where the caul plate was located shows a uniform composite sample with continuous plies going around one of the sides of the tip. The other side which did not have the caul plate, showed some minimal wrinkling with some resin rich areas.

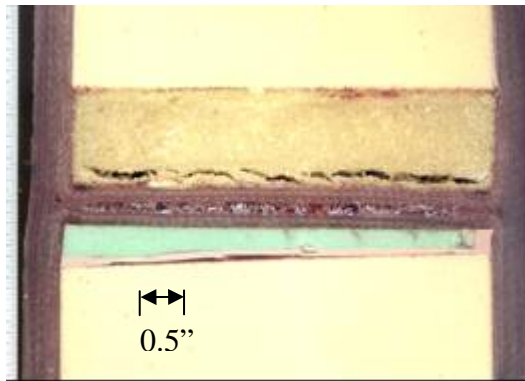
4. Corner of Tip and Trailing Edge (TTE)

A large piece of composite was removed from the corner of the rudder at the tip and leading edge. All edges of the part were polished and results are shown in Figure 20. The trailing edge side of the part showed fairly uniform glass layers going around the trailing edge. In contrast, the tip side of the part exhibited significant wrinkling of the layers especially in the second infusion.

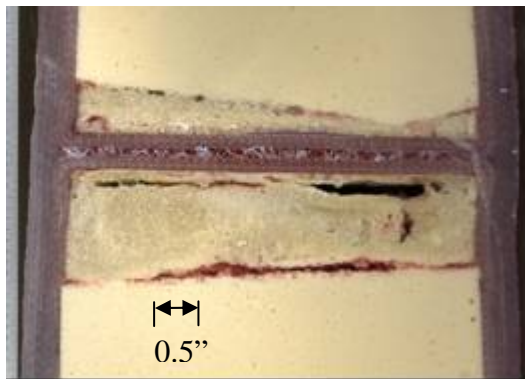
5. Middle of the Trailing Edge (TE)

A large piece of composite was removed from the middle of the trailing edge of the rudder. All edges of the part were polished and results are shown in Figure 21. The results indicate that the glass layers appear to be continuous and uniform around the trailing edge with minimal (in any) wrinkling.

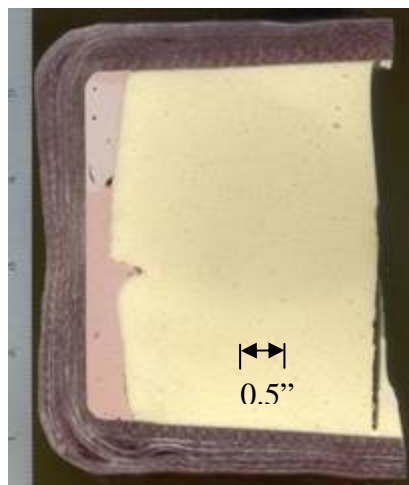
Figure 19 MCM Rudder Two – Shear Ties and Caul Plate Area



- Nearly uniform composite part along the faces of the rudder and along the shear tie.
- Several layers of foam present within the part.
- Green Foam may be HP80 Diab foam.
- Cracks in foam may provide locations to trap water

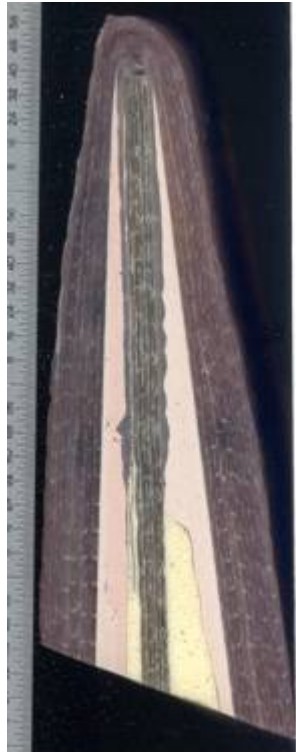


- Nearly uniform composite part along the faces of the rudder and along the shear tie.
- Several layers of foam present within the part.
- Cracks in foam may provide locations to trap water



- Nearly uniform composite part along the faces of the rudder and along the tip of the rudder
- Thick layer of fairing (pink) compound at tip of part
- Top corner where caul plate was appears to have minimal wrinkling
- Bottom corner appears to have minimal wrinkling with some resin rich areas.

Figure 20 MCM Rudder Two – Corner of Tip and Trailing Edge



- Nearly uniform composite part along the faces of the rudder and around the trailing edge of the rudder.
- Thick layer of fairing (pink) compound in trailing edge region.
- Uniform composite material in trailing edge stiffener piece.

0.25"



- Nearly uniform composite part along the faces of the rudder.
- Some wrinkling of the composite at the tip of the rudder which appears to be more significant in the infusion two plies.
- Thick layer of fairing (pink) compound at tip of part

0.25"

Figure 21 MCM Rudder Two – Middle of Trailing Edge



0.5"

- Nearly uniform composite part along the faces of the rudder and around the trailing edge of the rudder.
- Thick layer of fairing (pink) compound in trailing edge region.
- Uniform composite material in trailing edge stiffener piece.



0.5"

- Nearly uniform composite part along the faces of the rudder.
- Thick layer of fairing (pink) compound in trailing edge region.
- Uniform composite material in trailing edge stiffener piece.



0.5"

- Nearly uniform composite part along the faces of the rudder and around the trailing edge of the rudder.
- Thick layer of fairing (pink) compound in trailing edge region.
- Uniform composite material in trailing edge stiffener piece.

Conclusions

The FAVE-L-25S low HAP/VOC resin system was used to fabricate 2 full-scale MCM Rudder demonstration articles. The resin system was able to be processed using the standard marine grade VARTM materials and techniques to fabricate good quality composite parts. The higher viscosity of the FAVE-L-25S as compared to the baseline resin system (CORVE 8100) did not appear to adversely affect the manufacturability of the part. The FAVE-L-25S did appear to be slightly more affected by changes over time and of processing conditions than other commercially available resin systems which required closer monitoring using gel time tests prior to infusion and adjustments to the mixing ratios as the part was being infused. Several manufacturing processes were evaluated under this program for risk reduction of the DDG51 CTR manufacturing. The new method for the manufacturing and placement of the shear tie structure appears to be very successful. In addition, there was a moderate improvement in the wrinkling on the leading edge and tip with the use of caul plates.

Acknowledgements

NSWCCD would like to thank John LaScala at the Army Research Lab, Aberdeen, MD., for the funding of this 3 year tri-service ESTCP project which culminated in the fabrication of these demonstration articles. NSWCCD would also like to thank the contractor on this project, Structural Composites INC., for all the work they performed in the fabrication of the MCM rudders and for the photographs taken of the MCM fabrication process while NSWCCD personnel were not on-site.

Appendix J. Sioux Manufacturing Corp. Report

This appendix appears in its original form, without editorial change.

Appendix J

Sioux Manufacturing Corp. Report

FINAL REPORT

Name and Address:

Sioux Manufacturing Corporation
PO Box 400
1115 Dakotah Drive
Fort Totten, ND 58335

Contract Number: W911QX-07-P-0813

Program: Low HAP Composites for Army Tactical Vehicles

Date of Report: March 15, 2008

Period Covered: October 1, 2007 – February 28, 2009

Name and telephone number of preparer of report:

Dr. Dana T. Grow
(701) 766-4211 ext 313

I. Introduction

Under this contract, Sioux Manufacturing Corporation has fabricated:

- 1) two M35A3 hoods from FAVEL resin
- 2) two M35A3 hoods from Vantico 8605 epoxy resin
- 3) two HMMWV transmission container from FAVEL resin
- 4) two HMMWV transmission container from Ashland 8084 Vinyl Ester resin

These parts were previously fabricated under another program conducted by Sioux Manufacturing Corporation and the University of Delaware Center for Composite Materials which investigated the feasibility of converting metal parts to composite parts in the wheeled vehical fleet. Under this contract the University of Delaware designed and Sioux Manufacturing built, over one hundred M35A3 hoods, ten sets of composite armored doors for the HMMWV, five HMMWV transmission containers and a mine blast test specimen. The program investigated using vinyl ester resins for parts requiring a use temperature at ambient and using epoxy resin for parts requiring higher temperature performance, such as the M35A3 hood. One of the problems with vinyl ester resins in general is the use styrene as a solvent and in the curing reaction.

ARL has sythsize low-HAP vinyl ester resins to reduce the amount of styrene in the production workplace, to reduce the possiblility of diffusion of styrene from cured in a confined enclosure, and to enable recycling of these materials. Sioux manufacturing has fabricated one M35A3 hood and one HMMWV transmission container from FAVL resin, a low HAP resin orignally sythesized at Army Research Laboratories and now available from Applied Polymeric, Inc. of Benicia, CA.

Shown below in Table(1) is a comparison of the three resins employed in this study.

Table(1). Some Neat resin properties

resin	Density (g/ml) Neat resin	Dynamic Viscosity (cP)	Flexural strength (MPa)	Flexural Modulus (GPa)	Glass transition temperat ure (oC)
FAVE-L25	1.07	550	110	3.2	120
Vantico 8605	1.06	500-700			153 (E' onset, dry)
Derakane 8084	1.14	360	130	3.3	115

II. Procedure

SMC utilized the procedures developed for the UN/CCM effort in the fabrication of the ARL hood and container. No difficulties were encountered during the infusion process of either the box or the hood.

IIA. M35A3 hood

The major steps in hood production are:

- 1) cut 3Tex 96 oz main ply
- 2) stiffeners consisting of a foam core and wrapping ply are purchased pre-cut
- 3) lay-up plies and stiffeners. Place additional reinforcement plies over the stiffeners and along the perimeter of the hood
- 4) bag part
- 5) mix resin, CoNap, and MEKP and infuse with FAVEL vinyl ester resin or vantico 8605 epoxy resin
- 6) post-cure part
- 7) trim hood in router
- 8) drill holes for hardware
- 9) bond safety latch and handles

Below are some pictures of the infusion process

1. Bagged hood



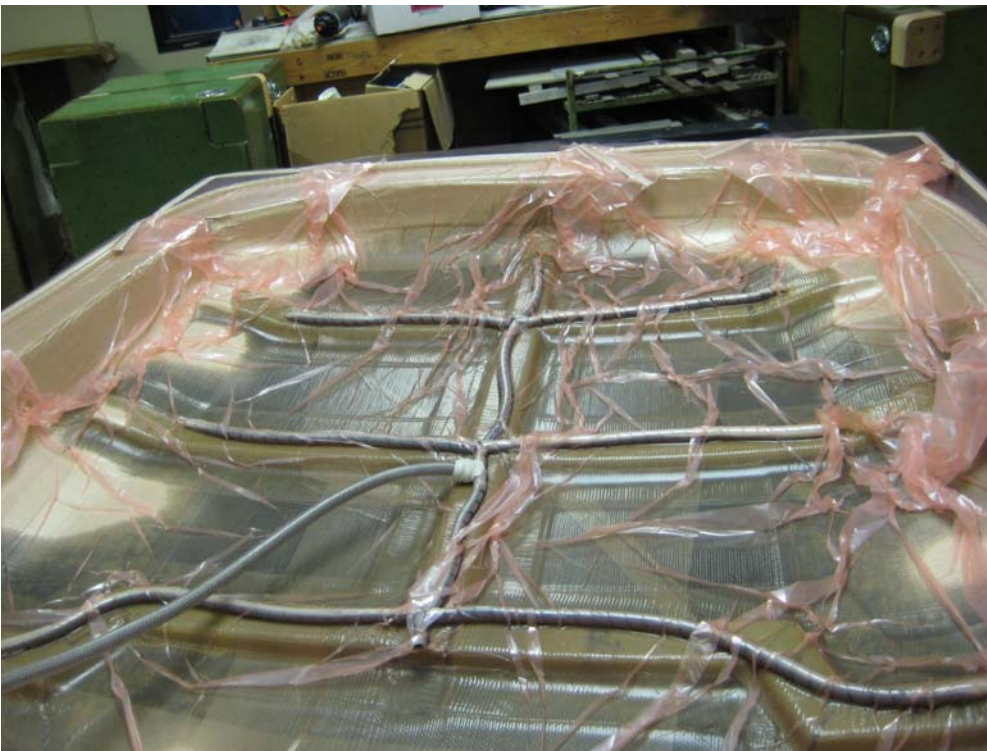
2) At start of infusion



3) After 10 minutes of resin infusion



4) After 19 minutes of resin infusion



5) After 51 minutes



6) Completed hood



IIB. HMMWV Transmission Container

The major steps in box production are:

- a. cut 3Tex plies
- b. cut and drill foam
- c. lay-up plies and foam
- d. bag part
- e. mix resin, CoNap, and MEKP and infuse with FAVEL or 8084 vinyl ester resin
- f. post-cure part
- g. cut holes for hardware
- h. add hardware
- i. trim top of box
- j. cut aluminum rails
- k. attach rails to box
- l. cut metal for internal cradle
- m. assemble cradle

Shown below are some pictures of the box fabrication process:

1) Bagged box



2) Infusion



3) Top and Bottom



4) Bottom with hardware



5) Top with hardware



6) Bottom with hardware



7) Assembled box



III.Conclusions

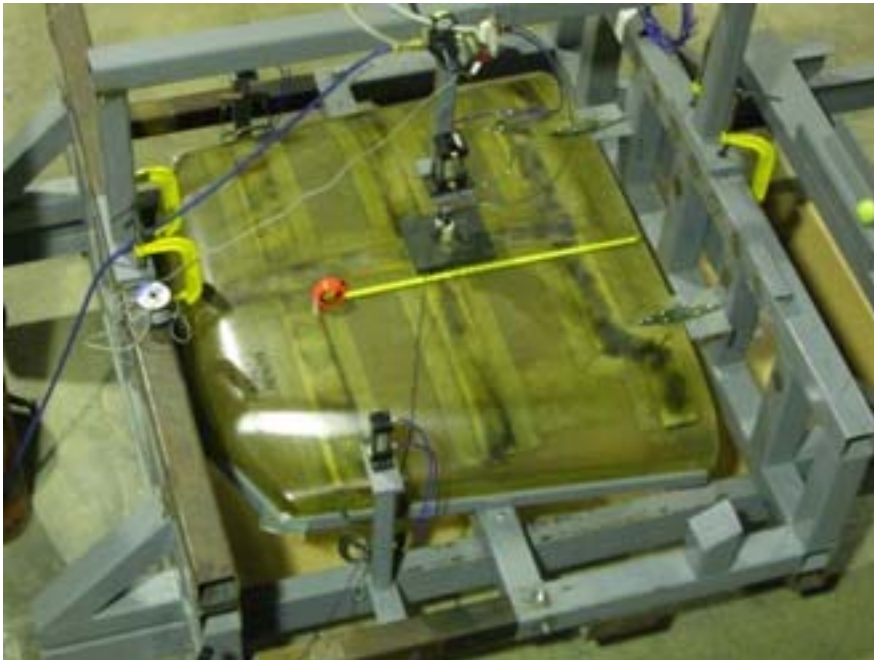
1. The FAVEL resin infused as well as, or better than, the competing vinyl ester or epoxy resins.
2. The M35 hood has been tested at the University of Delaware, Center for Composite Materials and has passed a series of performance tests including deflection and durability, flexural, and impact.
3. The HMMWV transmission transport container is scheduled to undergo a series of performance test at UD/CCM.
4. The FAVEL resin should be considered for a more extensive series of trials comprising production of 100 or more M35A3 hoods split between the epoxy and FAVE resins. These hoods could then be placed on trucks for long-term performance evaluation

APPENDIX I

Testing of Low-VOC M35 Hood

Testing was conducted by Dr. Nick Schevchenko of the University of Delaware Center for Composite Materials. Some of the key results are listed below.

A) Deflection and Durability Tests – hood was placed in a test rig and actuators were attached. A static load was placed on the surface.



Test Procedure:

- Test conducted at room temperature
- 250 lb load applied to the outside surface over a maximum 10"x10" area
- The load applied at the center and front areas of the hood
- The deflection measured at the point of application of the load but on the opposite surface
- Plot of load vs deflection obtained
- Test pass criteria:
 - Elastic deflection must not exceed 0.50"
 - No permanent deformation
 - No separation of reinforcements from the hood
 - No cracks allowed

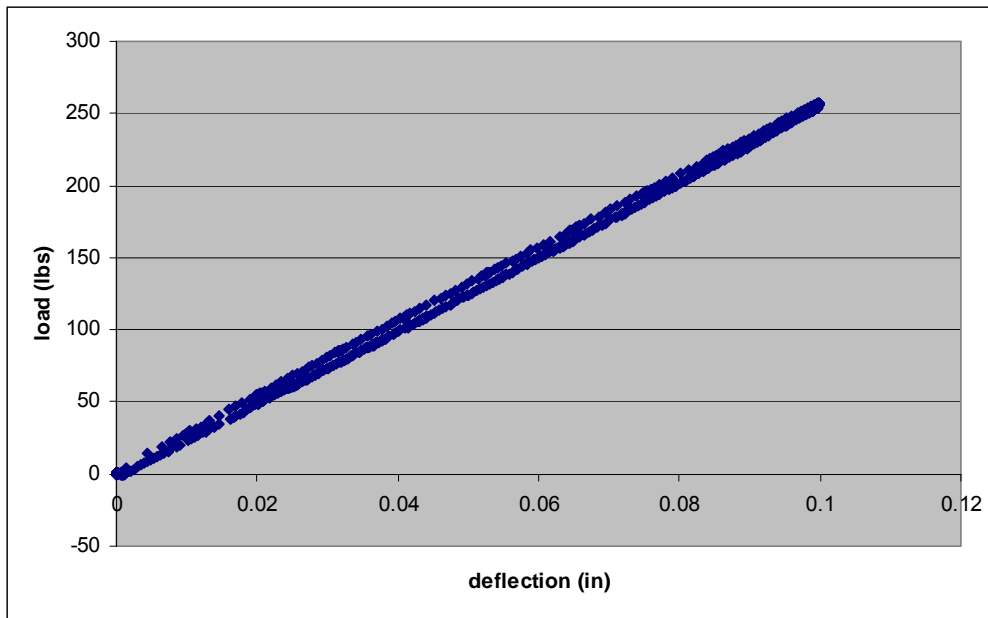
Results:

- No permanent deformation

- No separation of reinforcements from the hood
- No cracks
- Test passed

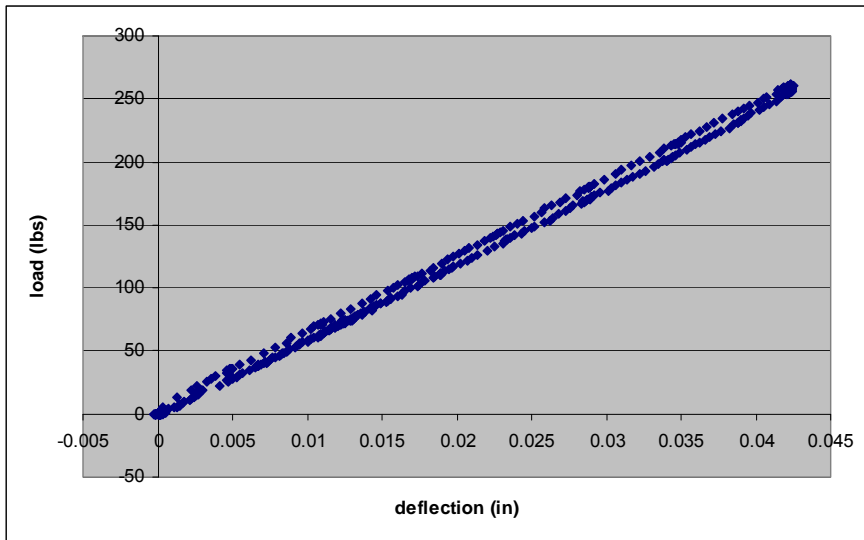
1. Initial Top Center Load

- Elastic deflection 0.10" at 250 lbs.
- Much less than 0.50" allowed
- Test passed.



2. Initial Top-Front Load

- Elastic deflection 0.04" at 250 lbs.
- Much less than 0.50" allowed
- Test passed.



B) Flexural Strength

- Test conducted at room temperature
- An upward load is applied at the corner lift handles
- The center latch engaged and both right and left sides will be tested (separately)
- Displacement of the hood corner above the fixture measured
- Plots of load vs deflection obtained
- The lifting load will not exceed 100 lbs
- Initial Driver corner lift – 0.16" deflection at 85 lb_f
- Initial passenger corner lift – 0.12" deflection at 85 lb_f
- Test pass criteria:
 - Load to lift the corner 0.375" shall be greater than 50 lbs.
 - No permanent deformation.
 - No separation of reinforcements from the hood.
 - No cracks allowed.

Cyclic Handle Load:

- Test conducted at room temperature
- 50 lb upward loads will be applied at the corner lift handles with the center latch engaged
- The loads will be applied in alternating fashion (right then left) over a 8 hour period at 10 cycles per minute
- Upon completion plots of load vs deflection will be obtained
- Test pass criteria:
 - No permanent deformation.
 - No separation of reinforcements from the hood.
 - No cracks allowed.
 - No broken fibers shall be visible on areas where the hood contacts the fixture

Results

Test Passed

The driver and passenger corner lift tests were repeated with only 0.12" deflection for 85 lb_f.

C) Durability Tests

- Test conducted at room temperature
- A 250 lb load applied to the outside surface of the hood at a central location
- The load cycled on and off for 100,000 cycles at 1 cycle per second
- Upon completion a plot of load vs deflection was obtained.
- Test pass criteria:
 - No permanent deformation
 - No separation of reinforcements from the hood
 - No cracks allowed
 - No broken fibers shall be visible on areas where the hood contacts the fixture

Results

- No permanent deformation
- No separation of reinforcements from the hood
- No cracks
- No broken fibers visible on areas where the hood contacts the fixture
- Test passed
- Top-center load and top-front load tests were repeated with passing results

D) Impact Resistance

- Test will be conducted at room temperature.
- 2 lb steel ball will be dropped on the hood.
- The ball will undergo a 6' drop.
- Impact will occur at the following locations:
 - On stiffener
 - Next to stiffener
 - Between stiffeners
 - On small radius surface
 - On large radius surface
- Test pass criteria:
 - No permanent deformation
 - No separation of reinforcements from the hood
 - No cracks allowed

Results

All tests passed

APPENDIX II.

HMMWV TRANSMISSION CONTAINER TEST PLAN

I. A-A-52462

The tests to be conducted are listed in the specification A-A-52462, Commercial Item Description, Containers, Shipping and Storage: Metal, Reusable; for engines, transmissions, differentials, transfers, and Similar Assemblies (metric)

1. Air leakage

Container is pressured to:

69 kPa for Type I Container and
34 kPa for Type II containers.

and is to show no evidence of air leakage.

2. Handling Tests

Container is loaded with a dummy load and subjected to the following drops onto a concrete surface:

- a) edgewise drop test – one end is raised 15 cm and the other end is allowed to drop from heights of 30, 60, and 90 cm
- b) cornerwise drop test - one corner is supported at a height of 15 cm and a block 30 cm in height is placed under the other corner. The lowest point of the opposite end is allowed to fall from heights of 30, 60, and 90 cm. Test is applied to two diagonal corners.
- c) tip over test – packed container is tipped over to one side and then the other
- d) impact test – the container is suspended as a pendulum from cables and allowed to swing into a barrier. The test is applied to each end.
- e) Flatwise drop test – box is dropped once from a height of 15 cm and 30 cm.

Contents are examined for damage after the handling tests are conducted.

II. SAE ARP1967

An alternative specification with more rigorous requirements is SAE-ARP1967 “CONTAINERS, SHIPPING AND STORAGE, AIRCRAFT ENGINES AND MODULES – METAL, REUSABLE

Tests include

1. Leak test – prototype test – pressurize to 10 kPa or pull a vacuum of 7 kPa. Stabilize for 30 minutes.
The pressure should change less than 0.2 kPa in 30 minutes.
2. Leak test - acceptance test – pressurize to 10 kPa. Stabilize for 30 minutes. Pressure should change less than 0.086 kPa in 15 minutes.
3. Drop tests
 - a. rotational edge drop test – per ASTM D6179, Method A
 - b. rotational corner drop test – per ASTM D4169, Method B
 - c. free fall drop test – ASTM D5276
 - d. tipover test - ASTM D6179, method G
 - e. vibration test – ASTM D999, Method B
 - f. lateral impact test – per ASTM D880, Procedure B, 179, Test Method B – Incline Impact Test
4. Static Loading – per ASTM D4577. Container shall be subjected to the load for 168 h at 60 °C and 96% relative humidity.
5. Handling Characteristics
 - a. hoisting & tiedown - per ASTM D4169 & ASTM D1083
 - b. form & fit test
6. Mechanical Handling Tests
 - a. fork lift truck transport
 - b. sling hoisting
 - c. push test
 - d. towing test
 - e. stack test
 - f. pallet jack compatibility
 - g. weight test – production containers must weigh less than 4% more or more than 2% less than prototype container.

II. SAE ARP1967 “Containers, shipping and Storage, Aircraft Engines and Modules – metal, Reusable”

This is a second specification that can be consulted for testing parameters.

1. Requirements

Container must have

- a. desiccant port
 - b. lifting handles
 - c. latches – no accidental opening
 - d. humidity indicator
 - e. pressure relief valve
 - f. drainage plug
 - g. forklift and pallet jack tie pockets
2. Leakage test
- a. Pressurize to 10 kPa, $\Delta P < 0.2$ Pa in 30 minutes
 - b. Pull a vacuum of 7 Pa, $\Delta P < 0.2$ Pa in 30 minutes
3. Drop tests
- a. Rotational Edge Drop Test per ASTM D6179 Method A
 - b. Rotational Corner Drop Test per ASTM D6179, Test Method B
 - c. Unsupported free fall drop test per ASTM D6179 Method D
 - d. Tipover Test per ASTM D6179, Method G
 - e. Vibration Test per ASTM D999 Test Method B
 - f. Later Impact Test per ASTM D880, Procedure B, 179, Test Method B

INTENTIONALLY LEFT BLANK.

Appendix K. Concurrent Technology Corporation Life Cycle Analysis

This appendix appears in its original form, without editorial change.

Appendix K

CTC Life Cycle Analysis

May 22, 2009

CTC/TMG-CL2123-09

U.S. Army SAIE-ESOH
Environmental Technology Office (ATTN: Mr. Thomas Moran)
1235 South Clark Street, Suite 307
Arlington, VA 22202-3263

SUBJECT: Final Cost and Performance Summary (CDRL A007), dated May 22, 2009

REFERENCE:

- (1) Electronic Mail to Tamara Goller (*CTC*) from Darlene Bader-Lohn (USAEC), dated May 14, 2009, Subject: NDCEE Task 535, Draft Cost and Performance Summary, dated May 4, 2009
- (2) Task No. 0535, "Life-Cycle Cost Analysis of Low HAP/VOC Compliant Resins for Military Applications" approved September 23, 2008
- (3) Contract Number W74V8H-04-D-0005

Dear Mr. Moran:

Concurrent Technologies Corporation (*CTC*) is pleased to submit one (1) copy of the Subject Deliverable in response to Reference (1) Government comments and in accordance with the Reference (2) Task under the Reference (3) Contract. The Contractor, *CTC*, hereby declares that, to the best of its knowledge and belief, the technical data delivered herewith under the Reference (3) Contract is complete, accurate, and complies with all requirements of the contract. If you should require technical clarification, please call Mr. Jerry Baughn at (904) 486-4006. For contractual issues, please call the undersigned at the above direct-dial number.

Very truly yours,

Tamarca N. Goller

Tamara Goller
Contracts Administrator

/bem

Enclosures: as stated

cc: Dr. John La Scala, AMSRD-ARL-WM-MC
 Ms. Darlene Bader-Lohn, IMAE-ATT

Attachment A
NDCEE Response to Government Comments

In Reference to the letter dated May 14, 2009 with Subject:
“NDCEE Task 535, Draft Cost and Performance Summary, dated May 4, 2009”

Government Comment 1: Executive Summary Paragraph 2: Change: “Pending” to “Pended” and add U.S patent # 7,524,909.

- **NDCEE Response:** Changed “Pending” to “Pended” and added the patent number.

Government Comment 2: Section 3.3 Paragraph 5: Add the sentence “Based on this analysis, the price of MLau was estimated to be \$2.82/lb and the price of MOct was estimated to be \$4.18/lb.”

- **NDCEE Response:** The sentence was added with a modification. The sentence was changed to read, “Based on this analysis, the price of MLau was estimated to be \$2.91/lb and the price of MOct was estimated to be \$4.38/lb.” After further analysis, the price mark-up discussed in this section changed. The markup is discussed and analyzed in Section 3 and throughout Section 4. Please note that the referenced section is now Section 4.3 due to the addition of Section 3.

Government Comment 3: Section 3.4 Paragraph 4: Add the following: “If manufactured by a small company, the price of FAVE-L-25S, FAVE-O-25S, FAVE-L-HT, and FAVE-O-HT would be \$4.29/lb, \$4.42/lb, \$5.16/lb, and \$5.27/lb, respectively. If a large resin manufacturer like Ashland were to manufacture this resin, the 35% markup can be assumed to be already taken into account in the cost of the VE components and the 35% markup already added to the fatty acid monomer cost. Materials handling, etc costs will also be taken into account in the quoted prices for the baseline resins. Stirring and heating costs are negligible. Therefore, the price of these resins if produced by a large resin manufacturer for FAVE-L-25S, FAVE-O-25S, FAVE-L-HT, and FAVE-O-HT would be \$3.17/lb, \$3.27/lb, \$3.77/lb, and \$3.87/lb, respectively.”

- **NDCEE Response:** These sentences were added with modifications. Since the first submission of this report, further research has been conducted and additional calculations were performed. This information appears in Section 4.4 on page 17.
- Government Comment 4:** Table 7 under Total for Materials, Labor, and Energy add: “(Large Manufacturer Price)”
- **NDCEE Response:** This was added with modifications. Since the first submission of this report, further research has been conducted and additional calculations were performed. This information appears in Section 4.4 on page 17.

Government Comment 5: Table 7 under Cost with 35% markup add “(Small manufacturer Price)”

- NDCEE Response: This was added with modifications. Since the first submission of this report, further research has been conducted and additional calculations were performed. This information appears in Section 4.4 on page 17

Government Comment 6: Table 9. Total Material Cost for Incumbent and Replacement Resins add “if resin is manufactured by a small manufacturer.”

- NDCEE Response: Table 9, now Table 12, is entitled “Total Material Cost for Incumbent and Replacement Resins with No Engineering Controls.” This includes prices for both small and large manufacturers.

Government Comment 7: Update Table 9.

- NDCEE Response: Table 9 is now Table 12, and was updated to reflect the costs for both small and large resin manufacturers.

Government Comment 8: Section 4.1 paragraph 1, questioned whether the following is true? “Furthermore, it is assumed that the replacement FAVE resins with a styrene content reduced by 15 wt% are exempt from the control device requirement.”

- NDCEE Response: From the research conducted by the NDCEE, every indication points to the FAVE resins being exempt from requiring a pollution control device. This is due to the 15 wt% styrene as well as the Vacuum Assisted Resin Transfer Molding (VARTM) manufacturing process. Please note that the referenced section is now Section 5.1 due to the addition of Section 3.

Government Comment 9: Section 4.1 paragraph 3, explain why “The higher priced unit was used in subsequent calculations.”

- NDCEE Response: The higher price was used because it was more representative of an average price for the RTO units. Please note that the referenced section is now Section 5.1 due to the addition of Section 3.

Government Comment 10: Section 4.1 paragraph 4, Change sentence number 4 to read “This assumption will likely over estimate the cost of the RTO is a conservative assumption, as because a facility with an RTO would probably manufacture several different composite products.”

- NDCEE Response: The section (now Section 5.1) was rewritten and reflects this comment.

Government Comment 11: Section 4.1 paragraph 4, Add the following sentence #5: “Therefore, we will also calculate the cost for the RTO for a facility using 75% of the capacity of the RTO.”

- NDCEE Response: The direction taken by the NDCEE was not using the RTO at a 75% capacity. A worst case scenario and realistic scenario were assumed for RTO usage, and costs were calculated accordingly. These details can be found in Sections 5 and 6.

Government Comment 12: Section 4.1 paragraph 4, Questioned whether the following is truly the case: “There is no RTO cost per part for the FAVE resins because it assumed that an RTO is unnecessary for these resins.”

- NDCEE Response: The RTO costs for FAVE resins has been added and this is explained in Table 19 on page 30.

Government Comment 13: Section 5.2: Add a table 12 for the cost of the resin assuming the manufacturer uses 75% or so of the capacity of the RTO.

- NDCEE Response: A different approach was taken by the NDCEE. Tables 15 and 17 were added to reflect a “worst case scenario” cost for the RTO and a “realistic scenario” cost for the RTO is shown in Tables 16 and 18. This is described in the text in Section 6.2.

Government Comment 14: Table 10. “Not really as it doesn’t account for the cost of the fibers or manufacture or does it? Also, I would recommend breaking out the costs on this table to make them clearer (resin contribution, RTO capital costs, RTO operating costs, etc.”

- NDCEE Response: This information is now reflected in Tables 115 through 18. The costs are broken out to make it more transparent and are also included in Appendix B.

NDCEE TASK 535: LIFE-CYCLE COST ANALYSIS OF LOW HAP/VOC COMPLIANT RESINS FOR MILITARY APPLICATIONS

Final Cost and Performance Summary

May 22, 2009

Distribution Statement "D" applies
Distribution is authorized to the DoD and DoD contractors only.

Requests for this document shall be referred to:
Office of the Assistant Secretary of the Army Installation and Environment
SERDP and ESTCP Program Office
901 North Stuart Street, Suite 303
Arlington, VA 22203

Contract No. W74V8H-04-D-0005
Task No. 0535
CDRL A007

Prepared by
National Defense Center for Energy and Environment (NDCEE)

Submitted by
Concurrent Technologies Corporation
100 CTC Drive
Johnstown, PA 15904

REPORT DOCUMENTATION PAGE			Form Approved	
Public reporting burden for this collection of information is estimated to average 1 hour per response, including the time for reviewing instructions, searching existing data sources, gathering and maintaining the data needed, and completing and reviewing the collection of information. Send comments regarding this burden estimate or any other aspect of this collection of information, including suggestions for reducing this burden to Washington Headquarters Services, Directorate for information operations and Reports, 1215 Jefferson Davis Highway, Suite 1204, Arlington, VA 22202-4302, and to the Office of Management and Budget, Paperwork Reduction Project (0704-0188), Washington, DC 20503.				
1. AGENCY USE ONLY (Leave blank)		2. REPORT DATE May 22, 2009		3. REPORT TYPE AND DATES COVERED Final (September 23, 2008 – May 22, 2009)
TITLE AND SUBTITLE Cost and Performance Summary			4. FUNDING NUMBERS Contract: W74V8H-04-D-0005 Task: 0535	
5. AUTHOR(S) Heather Brent, Jane Pitchford, Shannon Lloyd, and Jerry Baughn				
6. PERFORMING ORGANIZATION NAME(S) AND ADDRESS(ES) National Defense Center for Energy and Environment Operated by Concurrent Technologies Corporation 100 CTC Drive Johnstown, PA 15904			7. PERFORMING ORGANIZATION REPORT NUMBER	
8. SPONSORING/MONITORING AGENCY NAME(S) AND ADDRESS(ES) NDCEE Program Office (Office of the Assistant Secretary of the Army for Installations and Environment) 1235 South Clark Street, Suite 307 Arlington, VA 22202-3263 Program Manager: Mr. Tom Moran, NDCEE Program Manager, 410-436-5910			9. SPONSORING/MONITORING AGENCY REPORT NUMBER NDCEE-CR-2009-089	
10. SUPPLEMENTARY NOTES				
12a. DISTRIBUTION/AVAILABILITY STATEMENT Distribution authorized to the DoD and DoD contractors only.			12b. DISTRIBUTION CODE	
13. ABSTRACT (Maximum 200 words) The National Defense Center for Energy and Environment (NDCEE), operated by Concurrent Technologies Corporation (CTC), was tasked to perform a life-cycle cost analysis (LCCA) for liquid resins that are being developed to replace standard commercial resins. Liquid resins used for molding composite structures are a significant source of volatile organic compounds (VOC) and hazardous air pollutant (HAP) emissions from chemicals such as styrene. The Reinforced Plastic Composites National Emission Standards for Hazardous Air Pollutants (NESHAP) rule requires many facilities that use thermoset resins to implement add-on control devices to capture volatile emissions from composite processing in order to use the high performance commercial resins. This NDCEE task will support the Environmental Security Technology Certification Program (ESTCP) project effort by evaluating and comparing the costs of Fatty Acid Vinyl Ester (FAVE) resins to those of standard Vinyl Ester (VE) resins currently in use. The goal is to quantify the life cycle costs of implementing FAVE resins versus using standard VE resins combined with facility modifications to meet NESHAP requirements. This report details the life cycle cost analysis.				
14. SUBJECT TERMS LCCA, styrene, resins			15. NUMBER OF PAGES 34	
			16. PRICE CODE	
17. SECURITY CLASSIFICATION OF REPORT Unclassified	18. SECURITY CLASSIFICATION OF THIS PAGE Unclassified	19. SECURITY CLASSIFICATION OF ABSTRACT Unclassified	20. LIMITATION OF ABSTRACT None	

TABLE OF CONTENTS

	Page
LIST OF ACRONYMS	iii
EXECUTIVE SUMMARY	iv
1.0 INTRODUCTION.....	1
2.0 PROCESS DESCRIPTION	2
2.1 Standard VE Resin.....	2
2.2 Fatty Acid Vinyl Ester Resin	3
2.3 Vacuum Assisted Resin Transfer Molding	6
3.0 APPLICATION MANUFACTURING.....	7
4.0 RESIN COST ESTIMATION	8
4.1 Incumbent VE Resins	10
4.2 Replacement FAVE Resin Components.....	10
4.3 Methacrylated Fatty Acid Monomers	11
4.4 Fatty Acid Vinyl Ester Resins.....	14
4.5 Material Costs by Application	17
5.0 ENGINEERING CONTROLS	19
5.1 Pollution Control Equipment	19
6.0 ECONOMIC ANALYSIS	23
6.1 Cost Model / Assumptions.....	23
6.2 Cost Analysis and Comparison.....	24
7.0 ENVIRONMENTAL IMPACT	30
7.1 Preparation of Incumbent Resin (Derakane 8084).....	31
7.2 Preparation of Replacement Resin (FAVE-L-25S)	32
8.0 CONCLUSIONS	34

LIST OF FIGURES

Figure 1. Potential DoD Applications for FAVE Resins	2
Figure 2. Chemical Composition of Bisphenol A-based VE Resins	3
Figure 3. Reaction Scheme to Produce MFA Monomers	3
Figure 4. Chemical Composition of FAVE Resins.....	4
Figure 5. Schematic Illustration of Composite Manufacturing Process	6
Figure 6. Illustration of VARTM	7
Figure 7. Monomer Synthesis Steps	12
Figure 8. Adwest's RETOX Dual Chamber RTO Oxidizer System Requirements.....	20
Figure 9. Aspects of the Product Life Cycle Compared for the Two Resin Systems.....	31
Figure 10. Derakane 8084 Process Flow Diagram	32
Figure 11. FAVE-L-25S Process Flow Diagram.....	33

Figure 12. Methacrylated Lauric Acid Process Flow Diagram	33
Figure 13. Derakane 441-400 Process Flow Diagram	34

LIST OF TABLES

Table 1. Incumbent and Replacement Resin for Selected Composite Military Applications	5
Table 2. Projected Scale of Operations for Various Demonstrations, as provided by ARL	7
Table 3. Styrene Emissions from Manufacturing Composite Applications	8
Table 4. Cost of Incumbent VE Resins	10
Table 5. Cost of Replacement FAVE Resin Components.....	11
Table 6. Prices Quoted by API for MLau and MOct	12
Table 7. Estimated Breakdown of Current Costs for Small Resin Manufacturer to Produce 55-Gallon Batch of Monomers.....	13
Table 8. Prices Quoted by API for FAVE Resins	14
Table 9. Estimated Breakdown of Costs to Produce 55-Gallons of Resins for Small Resin Manufacturer	16
Table 10. FAVE Resin Costs for Large Resin Manufacturer	17
Table 11. Material Requirements for VARTM Production of VE Resins.....	18
Table 12. Total Material Cost for Incumbent and Replacement Resins with No Engineering Controls	18
Table 13. Price quotes obtained for Regenerative Thermal Oxidizers	21
Table 14. RTO Capital and Operating Costs Spread Over a 15-Year Economic Lifetime	22
Table 15. Worst Case Total Estimated Cost / Part with Resin Prices from Small Mfr	25
Table 16. Realistic Scenario Total Estimated Cost / Part with Resin Prices from Small Mfr.....	26
Table 17. Worst Case Total Estimated Cost / Part with Resin Prices from Large Mfr	27
Table 18. Realistic Scenario Total Estimated Cost / Part with Resin Prices from Large Mfr.....	28
Table 19. RTO Usage Price Increase for FAVE Resins	30

LIST OF APPENDICES

Appendix A Resin and Monomer Price List, Monomer and Resin Price Calculations
Appendix B Cost Analysis Calculations

LIST OF ACRONYMS

API	Applied Polymerics, Inc.
ARL	Army Research Laboratory
CEA	Cost effectiveness analysis
cfm	Cubic feet per minute
CTC	Concurrent Technologies Corporation
DoD	Department of Defense
EIA	Economic Impact Analysis
EPA	Environmental Protection Agency
ESTCP	Environmental Security Technology Certification Program
FAVE	Fatty acid vinyl ester
HAP	Hazardous air pollutant
HMMWV	High Mobility Multipurpose Wheeled Vehicle
hp	Horsepower
lb	Pound
LCA	Life cycle assessment
LCCA	Life cycle cost analysis
MCM	Mine countermeasure
MFA	Methacrylated fatty acid
MLau	Methacrylated lauric acid
MOct	Methacrylated octanoic acid
NAICS	North American Industry Classification System
NDCEE	National Defense Center for Energy and Environment
NESHAP	National Emission Standards for Hazardous Air Pollutants
PM	Preventative maintenance
RDT&E	Research, development, test and evaluation
RTO	Regenerative thermal oxidizer
TRI	Toxics Release Inventory
VARTM	Vacuum Assisted Resin Transfer Molding
VE	Vinyl ester
VOC	Volatile organic compounds

EXECUTIVE SUMMARY

The National Defense Center for Energy and Environment (NDCEE), operated by Concurrent Technologies Corporation (CTC), was tasked to perform a life cycle cost analysis (LCCA) for liquid resins that are being developed to replace standard commercial resins. Liquid resins used for molding composite structures are a significant source of volatile organic compounds (VOC) and hazardous air pollutant (HAP) emissions from chemicals, such as styrene. The Reinforced Plastic Composites National Emission Standards for Hazardous Air Pollutants (NESHAP) rule requires many facilities that use thermoset resins to implement add-on control devices to capture volatile emissions from composite processing in order to use the high performance commercial resins.

One method of reducing styrene emissions from vinyl ester (VE) resins is to replace some or all of the styrene with fatty acid-based monomers. Fatty acid monomers are ideal candidates because they are inexpensive, have low volatilities, and are derived from renewable resources. The US Army Research Laboratory (ARL) has developed a patented technology (U.S patent # 7,524,909) that allows for the formulation of high performance composite resins with no more than 25 weight percent (wt %) styrene. High performance fatty acid vinyl ester (FAVE) resins are currently being demonstrated/validated for Department of Defense (DoD) use for Army tactical vehicles, including High Mobility Multipurpose Wheeled Vehicle (HMMWV) hoods, Marines HMMWV helmet hardtops, Air Force T-38 aircraft dorsal covers, and mine countermeasure (MCM) composite rudders for Navy ships through Environmental Security Technology Certification Program (ESTCP) Project WP-0617.

This NDCEE task is supporting the ESTCP project effort by evaluating and comparing the life cycle costs of FAVE resins to those of standard VE resins currently in use. The goal is to quantify the life cycle costs of implementing FAVE resins versus using standard VE resins combined with facility modifications to meet NESHAP requirements. This report details the life cycle cost analysis.

The costs per pound and costs per part were calculated for each different resin formulation, for resins produced by a small manufacturer (higher prices) and resins produced by a large manufacturer (lower prices). The FAVE resin estimated prices were compared to the market prices of the incumbent resins with incremental costs for engineering controls. Upon reviewing the final costs among the different resin formulations, it is obvious that the epoxy resins remain the most expensive option. Even with the reduced burden of environmental reporting, the epoxy resin costs are two to four times higher than any other resin.

For every application in which the FAVE resins were produced by a small manufacturer, the cost per pound and cost per part are less for the incumbent resin using pollution control equipment than for the replacement FAVE resin. The incrementals cost with engineering controls amounts to pennies per pound. For the Hetron, Hexion, and CoRezyn incumbent resins, the costs with engineering control costs included is still significantly less than the cost of materials for the replacement FAVE resins for a small resin manufacturer.

If the FAVE resins were manufactured on a large scale, the costs and subsequently the price could be reduced even further. If the FAVE resins were manufactured on a large scale by a company such as Ashland Chemical, the FAVE prices would be competitive with some incumbent resin prices. The FAVE-L-25S and the FAVE-O-25S are less expensive than the Derakane 8084 by 17% and 13%, respectively. The FAVE-L-HT and the FAVE-O-HT are both about 35% more than the Hetron 980 and nearly identical in price to the Derakane 8084. Even the least expensive FAVE resin, the FAVE-L-25S, is more expensive than the Hexion and CoRezyn incumbent resins, probably due to the higher styrene content in these resins. A less expensive resin may be more economical in the FAVE resin formula than Derakane 441-400 or Derakane 470HT-400. If determined to be comparable in quality and performance to the Derakane products, the Hetron 980/35 should be considered for use in the FAVE resin formulas since all of these products contain approximately 35% styrene.

Not included in this cost analysis is the environmental life cycle assessment of the different resin formulations. An LCA would quantify the inputs and outputs for each life cycle stage and assess the total environmental impact of a product. A Consequential LCA is recommended to identify significant differences in the environmental burdens of using one product instead of another.

1.0 INTRODUCTION

The National Defense Center for Energy and Environment (NDCEE), operated by Concurrent Technologies Corporation (CTC), was tasked to perform a life-cycle cost analysis (LCCA) for liquid resins that are being developed to replace standard commercial resins. Liquid resins used for molding composite structures are a significant source of volatile organic compounds (VOC) and hazardous air pollutant (HAP) emissions. Reactive diluents in vinyl ester (VE) and unsaturated polyester resins, such as styrene and methyl methacrylate, are used to reduce the resin viscosity to enable liquid molding. However, these diluents are VOCs and HAPs. Typical commercial resins contain 40-60 weight percent (wt %) styrene.

Under the Reinforced Plastic Composites National Emission Standards for Hazardous Air Pollutants (NESHAP) rule, the Environmental Protection Agency has established regulations limiting the amount of VOCs, HAPs, and heavy metals that can be emitted from certain industrial sources. The Reinforced Plastic Composites NESHAP, promulgated April 21, 2003 with a compliance date of April 21, 2006, required many facilities that use thermoset resins to implement add-on control devices to capture volatile emissions from composite processing in order to use the high performance commercial resins.¹ As a result, some manufacturers have attempted to formulate NESHAP-compliant VE resins to eliminate the need for pollution control equipment. Studies have shown that current NESHAP-compliant VE resins have poor fracture properties, poor processability, and higher cost.² The alternative is to use more expensive epoxy resins, which could cost approximately three times more than standard VE resins, or to reduce the usage of composites in the Department of Defense (DoD), which would make it difficult to realize the initiative to make a lighter, faster, and more maneuverable military.

One method of reducing styrene emissions from VE resins is to replace some or all of the styrene with fatty acid-based monomers. Fatty acid monomers are ideal candidates because they are inexpensive, have low volatilities, and are derived from renewable resources. The US Army Research Laboratory (ARL) has developed a patent pending technology that allows for the formulation of high performance composite resins with no more than 25 wt % styrene. These resins have low viscosities suitable for vacuum infusion methods, and have excellent polymer and composite properties.³

The high performance fatty acid vinyl ester (FAVE) resins developed by ARL are currently being demonstrated/validated for DoD use for Army tactical vehicles, including High Mobility Multipurpose Wheeled Vehicle (HMMWV) ballistic hardtops (Figure 1, photo a), HMMWV transmission containers (Figure 1, photo b), HMMWV composite

¹ Environmental Protection Agency. 40 CFR 63, subpart WWWW, National Emission Standards for Hazardous Air Pollutants: Reinforced Plastics Composites, Final Rule Amendments August 25, 2005.

² J.J. La Scala, T. Glodek, C. Lochner, X. Geng, A. Quabili, K. Patterson, F. Bruce, E. Bartling, C. Johnson, P. Myers, S. Boyd, S. Andersen, L. Coulter, R. Crane, J. Gillespie, J.M. Sands, M. Starks, J. Gomez, and G.R. Palmese, Demonstration of Military Composites with Low Hazardous Air Pollutant Content, ARL Technical Report ARL-RP-185, July 2007.

³ *Ibid.*

replacement hoods (seen for M939 in Figure 1, photo c and for M35A3 in photo d), Air Force T-38 aircraft dorsal covers (Figure 1, photo e), and Mine Countermeasure (MCM) composite rudders for Navy ships (Figure 1, photo f) through Environmental Security Technology Certification Program (ESTCP) Project WP-0617.



Figure 1. Potential DoD Applications for FAVE Resins

This NDCEE task is supporting the ESTCP project effort by evaluating and comparing the life cycle costs of FAVE resins to those of the standard VE resins currently used in these applications. The goal is to quantify the life cycle costs of implementing FAVE resins versus using standard VE resins combined with facility modifications to meet NESHAP requirements. This report details the life cycle cost analysis.

2.0 PROCESS DESCRIPTION

2.1 Standard VE Resin

VE resins are used to make polymer matrix composites for military and commercial civil and infrastructure applications because of their good thermal, mechanical, and electrical properties, low weight, and low cost compared with conventional materials. All of the commercial VE resins used for a baseline in

this project are bisphenol A-based VEs with high styrene contents.⁴ The chemical composition of these resins is shown in Figure 2.

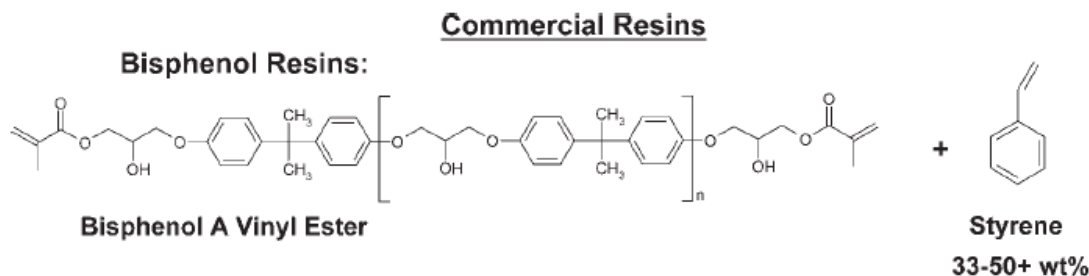


Figure 2. Chemical Composition of Bisphenol A-based VE Resins⁵

2.2 Fatty Acid Vinyl Ester Resin

FAVE resins are low HAP/VOC alternatives to commercial VE resins. These resins use methacrylated fatty acid (MFA) monomers as a reactive diluent to replace all but 10-25 wt % of the styrene.

Synthesizing the Methacrylated Fatty Acid Monomer

The first step for making FAVE resins is MFA monomer synthesis. The MFA monomer is produced in a simple addition reaction. Glycidyl methacrylate is reacted with a stoichiometric equivalent of fatty acid. The reaction is catalyzed using an accelerator called AMC-2[®] from AMPAC Fine Chemicals. Two different fatty acid monomers are being used to produce MFAs: lauric acid and octanoic acid. Lauric acid and octanoic acid react with glycidyl methacrylate to become methacrylated lauric acid (MLau) and methacrylated octanoic acid (MOct), respectively. The reaction is depicted in Figure 3. More detail about the specific formulations used by ARL is provided in Section 3.

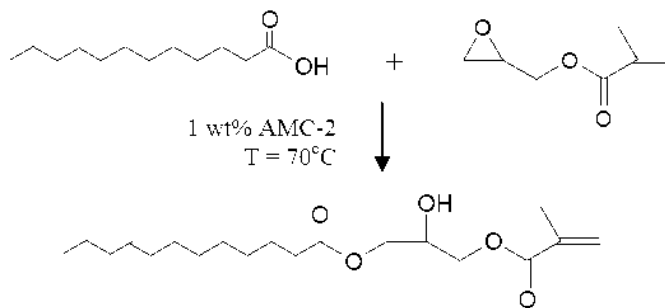


Figure 3. Reaction Scheme to Produce MFA Monomers⁶

⁴ S.E. Boyd, J.J. La Scala, G.R. Palmese, Molecular Relaxation Behavior of Fatty Acid-Based Vinyl Ester Resins, *Journal of Applied Polymer Science*, 108(6) 3495 - 3506, 2008.

⁵ *Ibid.*

Blending the Fatty Acid Vinyl Ester Resins

Four resin systems are being explored as replacements for the current commercial VE resins: FAVE-L-25S, FAVE-O-25S, FAVE-L-HT, and FAVE-O-HT. Earlier formulas, known as FAVE-L and FAVE-O, were included in the Subtask 2 report for pricing purposes but are no longer being considered for production. Each resin system is prepared by mixing two different commercial low-HAP VE resins with one of the fatty acid monomers (MLau or MOct). An example of the FAVE Resins synthesis can be seen in Figure 4.

FAVE Bisphenol Resins:

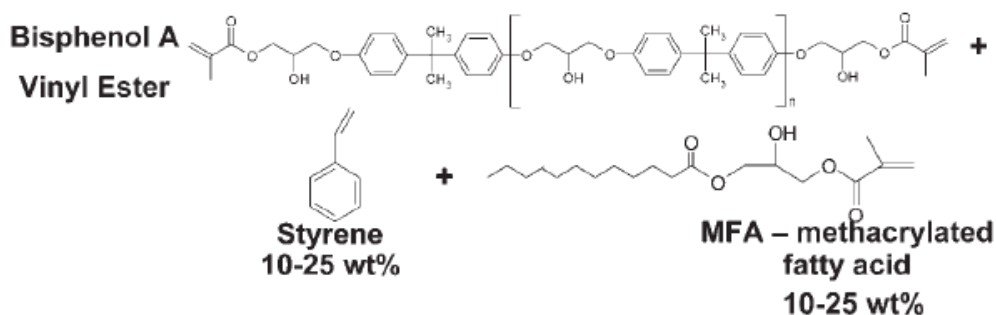


Figure 4. Chemical Composition of FAVE Resins⁷

Selecting the Resin System

The low HAP/VOC FAVE resin systems are being considered for six military applications. Table 1 lists the composite systems currently used for each application as well as the proposed replacement resins. Four commercial VE resin systems are currently used for these applications. Ashland Inc.'s Derakane[®] 8084 is used to produce the HMMWV transmission container and Amtech HMMWV hardtop. Ashland Inc.'s Hetron[®] 980/35 is used to produce the M939 hood and M35A3 hood. Hexion Specialty Chemical's Hexion 781-2140 is used to produce the T-38 dorsal cover. Interplastic Corporation's Corezyn[®] Corve 8100 is used to produce Navy rudders, such as the MCM rudder. FAVE-L-25S or FAVE-O-25S is the targeted replacement resin for the HMMWV transmission container. FAVE-L-25S is the targeted replacement for the T-38 dorsal cover and MCM rudder applications. To obtain the necessary heat distortion temperatures, FAVE-O-HT or FAVE-L-HT must be used for the M939 hood, M35A3 hood, and Amtech HMMWV hardtop. FAVE-L-25S is also being considered for the Amtech HMMWV hardtop. An epoxy resin, Huntsman Advanced Materials' RenInfusion[®] 8605/Ren 8605 is also being considered for use in the M35A3 and M939 applications.

⁶ J.J. La Scala, T. Glodek, C. Lochner, X. Geng, A. Quabili, K. Patterson, F. Bruce, E. Bartling, C. Johnson, P. Myers, S. Boyd, S. Andersen, L. Coulter, R. Crane, J. Gillespie, J.M. Sands, M. Starks, J. Gomez, and G.R. Palmese, Demonstration of Military Composites with Low Hazardous Air Pollutant Content, ARL Technical Report ARL-RP-185, July 2007.

⁷ S.E. Boyd, J.J. La Scala, G.R. Palmese, Molecular Relaxation Behavior of Fatty Acid-Based Vinyl Ester Resins, Journal of Applied Polymer Science, 108(6) 3495 - 3506, 2008.

Table 1. Incumbent and Replacement Resin for Selected Composite Military Applications

Application	Service	Incumbent Resin	Replacement Resin
HMMWV Transmission Container	Army	Derakane 8084	FAVE-L-25S or FAVE-O-25S
M939 hood	Army	Hetron 980/35 or Huntsman RenInfusion 8605/Ren 8605	FAVE-L-HT or FAVE-O-HT
M35A3 hood	Army	Hetron 980/35 or Huntsman RenInfusion 8605/Ren 8605	FAVE-L-HT or FAVE-O-HT
Amtech HMMWV hardtop	Marines	Derakane 8084	FAVE-L-HT, FAVE-O-HT, or FAVE-L-25S
T-38 Dorsal Cover	Air Force	Hexion 781-2140	FAVE-L-25S
MCM Rudder	Navy	Corve 8100	FAVE-L-25S

Manufacturing the Composites

The process for manufacturing composites is illustrated in Figure 5. If a FAVE replacement resin is to be used, then the process begins with MFA monomer synthesis. This mixture is stirred and gently heated at a controlled temperature for about four hours. The MFA monomer is then blended with the other materials to make the resin (see formulations in Tables 5 and 7). The synthesis and blending steps (blue box) are not required for the current VE resins.

While the rest of the steps vary for different applications, they are the same regardless of whether the current VE or a replacement FAVE is used. The resin is blended with a catalyst (cobalt naphthenate) and initiator (Trigonox 239[®] or methyl ethyl ketone peroxide), regardless of whether an incumbent or replacement resin are used. Following the catalyst and initiator blending step, the prepared resin is injected into the mold, cured, de-molded, sanded, and painted. Except for the MCM rudder, it is unlikely that the resin parts will be postcured.

Overall, the FAVE resins will be drop-in replacements for commercial VE resins. Consequently, composite manufactures will not require any process changes when switching to the FAVE resins.

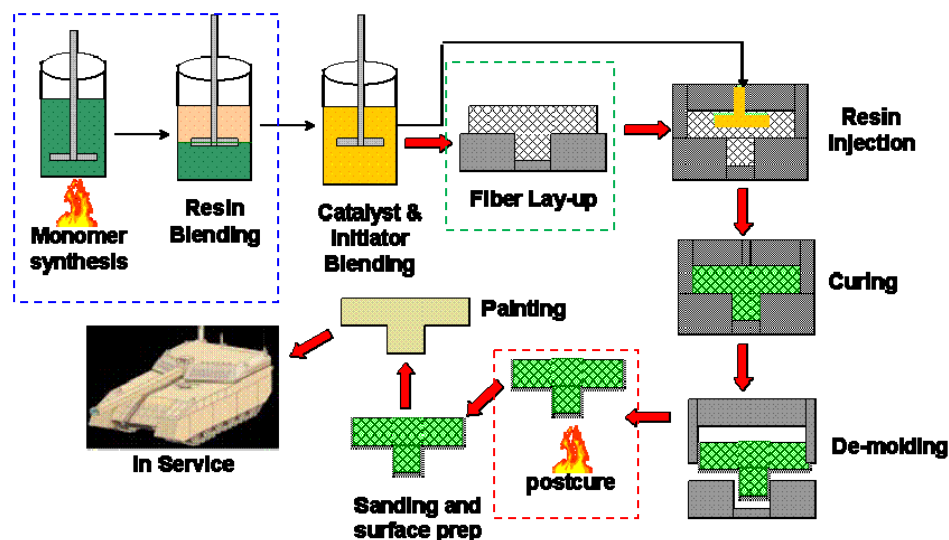


Figure 5. Schematic Illustration of Composite Manufacturing Process

2.3 Vacuum Assisted Resin Transfer Molding

There are various composite molding processes that are used to manufacture composite structures. The molding process evaluated in this analysis is Vacuum Assisted Resin Transfer Molding (VARTM). VARTM is an infusion process where a vacuum draws a resin into a one-sided mold.⁸ First, dry fabric or a preform is laid up on one-sided tooling and covered with a vacuum bag. The air is evacuated by a vacuum pump and then liquid resin from an external reservoir is drawn into the mold by the vacuum. A vacuum is created between the preform and the vacuum bag, which allows for an even thickness mold. After the molded part is cured, which can be several hours for a large part, the structure is opened and the molded part is released. VARTM is considered by the Environmental Protection Agency (EPA) to be a closed molding process.⁹ This process is illustrated in Figure 6.

⁸ http://www.engr.ku.edu/~rhale/ae510/websites_f02/vartmwebsite/

⁹ US EPA Technology Transfer Network, Clearinghouse for Inventories and Emission Factors, AP-42 Section 4.4 Polyester Resin Plastics Products Fabrication, February 2007.

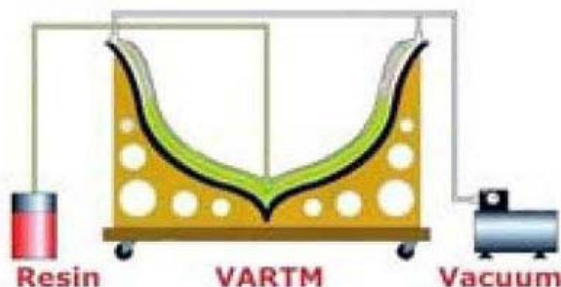


Figure 6. Illustration of VARTM ¹⁰

3.0 APPLICATION MANUFACTURING

The various applications listed in Table 1 are made by small to medium sized composites manufacturers scattered through the US, often near DoD installations. The size of the parts and the production volume vary widely, as seen from information provided by ARL in Table 2.

Table 2. Projected Scale of Operations for Various Demonstrations, as provided by ARL ¹¹

Application	Total Mass per Part	Resin Mass per Part	Estimated Production	Total Resin Weight	Styrene Reduction through low HAP Resins	Location
M35A3 hood	52 lbs	18 lbs	100/yr	1800 lbs/yr	~450 lbs/yr	Fort Totten, ND
M939 hood	60 lbs	20 lbs	5000/yr	100,000 lbs/yr	~25,000lbs/yr	Fort Totten, ND
HMMWV transmission container	110 lbs	35 lbs	500/yr	17,500 lbs/yr	~4000 lbs/yr	Fort Totten, ND
HMMWV hardtop	1400 lbs	220 lbs	480/yr	100,000 lbs/yr	~25,000 lbs/month	Wapato, WA
T-38 Dorsal cover	10 lbs	4 lbs	40/yr	160 lbs/yr	~80 lbs/yr	Hill AFB, Utah
Composite rudder for MCM	1400 lbs	190 lbs	5/yr	960 lbs/yr	240 lbs/yr	Annapolis, MD

Styrene Emissions

The styrene emissions from the manufacturing of these parts can be estimated based on the amount of styrene in the part and the accepted styrene emission factor. The styrene

¹⁰ VARTM, http://www.an-cor.com/images/laminating_methods/vartm.jpg

¹¹ J.J. La Scala, Information for CTC for Life Cycle Analysis Modeling, October 21, 2008.

content varies from 35-50%, depending on the resin, but an average value of 40% styrene was used throughout the calculations. According to EPA's AP-42 emission factor for resin for a closed molding process, 1-3 % of the starting monomer is emitted.¹² The highest value in the range was used in the calculations as a conservative estimate. Table 3 shows the anticipated styrene emission rate for a hypothetical composites manufacturer near Ft. Totten, ND that only manufactures the M35A3 Hood, the M939 Hood, and the HMMWV Transmission Container using the VARTM method. It is assumed no other parts are made in the facility and the total annual production is 5,600 pieces per year (based on estimated production in Table 2). It is assumed the facility operates two eight-hour shifts per day, five days per week, 51 weeks per year, for a total of 4,080 hours per year. An average styrene emission rate was calculated to be 0.35 lbs styrene per hour by dividing the annual styrene emissions by the operating hours.

Table 3. Styrene Emissions from Manufacturing Composite Applications

Part	Lbs Resin/ Part	Lbs Styrene/ Part	Styrene Emissions/ Part (lbs)	Annual Production (pieces)	Annual Styrene Emissions (lbs)
M35A3 hood	18	7.2	0.22	100	22
M939 hood	20	8	0.24	5,000	1,200
HMMWV transmission container	35	14	0.42	500	210
TOTAL			0.88	5,600	1,432
Total Annual Operating Hours					4,080
Average Styrene Emission Rate					0.35

4.0 RESIN COST ESTIMATION

Many factors contribute to the total cost of using a new material. These include the costs of developing and producing the alternative material, forming components, maintaining equipment, assembling components on tactical vehicles, complying with environmental and safety regulations, and disposing of waste. The actual cost incurred depends on raw material and energy prices, production methods, labor rates, and regulatory requirements, which depend on market conditions, production volumes, as well as other factors. Cost estimates for the incumbent and replacement resins are developed based on data collected from manufacturers, distributors, and the ARL, as well as many underlying assumptions. The cost estimation procedure, input data, underlying assumptions and results for each of the resin systems are described and presented in subsequent sections.

¹² US EPA Technology Transfer Network, Clearinghouse for Inventories and Emission Factors, AP-42 Section 4.4 Polyester Resin Plastics Products Fabrication, February 2007.

It is relatively straightforward to calculate costs for raw materials, energy, and labor, as detailed in this section of this report. But without realistic figures for facility rent and maintenance, overhead labor, equipment costs, etc., it is difficult to estimate hidden costs often grouped together as “other”. Profit estimates, often treated like another fixed cost, are also factored into a product’s price. There are many different methods for pricing a product to cover both costs and profit, ranging from cost-plus pricing to competitive pricing to markup pricing.¹³ For small businesses selling resin to low-volume users (such as hobbyists or small research groups), the markup on the materials can be as high as 100% or more.¹⁴ Even industry experts cannot predict or explain the pricing strategy for resins. A conversation with Mr. Keith Johnson¹⁵, a subject matter expert with over 30 years in the resin industry, revealed that resin pricing depends on current market prices, and (profit) margins vary by manufacturer. In an earlier conversation between ARL and Mr. Johnson, a 35% markup for resin was discussed as a typical resin pricing strategy, but Mr. Johnson refuted this value in a more recent conversation with the project team.

It is generally accepted that prices will decrease with increasing production volume, as costs are spread out over a larger quantity of products. Based on resin price inquiries during the Subtask 2 portion of this project as well as conversations with ARL, it appears as though the markup on resin costs does not drop off sharply with increasing volume. Instead, the prices change only slightly with increasing volume, if at all, implying a minimal markup of resin costs. By this logic, resin markup is probably not very high for the market and it is unlikely that a medium to large size resin manufacturer would have a very high markup in their resin prices.

More concrete evidence of resin markup can be found in the US Census Bureau’s Annual Survey of Manufactures for Plastics Material and Resin Manufacturing (North American Industry Classification System (NAICS) code 325211).¹⁶ For the year 2006 (the most recent year available), if you divide the “Value of Product Shipments” by the “Total Cost of Materials”, you get the ratio 1.45.¹⁷ According to the definition of the term “Value of Product Shipments”, this item covers the received or receivable net selling values (in other words, sales). The term “Total Cost of Materials” refers to direct charges actually paid or payable for items consumed or put into production during the year, including freight charges, the cost of materials, and fuel consumed. Therefore, 1.45 represents the sales to cost of materials ratio and can be used to calculate the sale price of a resin or determine the markup that is factored into a price of a resin. The EPA used this approach to compute the market prices of Reinforced Plastics Composites (RPCs) in the Economic

¹³ Entrepreneur Magazine, “Pricing a Product”, 2009, <http://www.entrepreneur.com/encyclopedia/term/82380.html>

¹⁴ J.R. Boyer, Compilation of a Materials Cost Database for a WEB-based Composites Cost Estimator, Massachusetts Institute of Technology, June 2001.

¹⁵ Telephone conversation with Mr. Keith Johnson on May 4, 2009.

¹⁶ US Census Bureau, 2006 Annual Survey of Manufactures, NAICS code 325211, release date 11/18/08, <http://www.census.gov/mcd/asm-as1.html>

¹⁷ 2006 Value of Product Shipments = \$78,410,325,000 and the 2006 Total Cost of Materials = \$54,017,672,000.

Impact Analysis of the Final Reinforced Plastics NESHAP.¹⁸ To find the markup percentage, divide the markup value (the difference between the sales and the cost) by the total cost. According to the 2006 US Census data for the resin industry, the markup is 45%. This figure will be used as the final markup estimate in all of the resin pricing estimations.

4.1 Incumbent VE Resins

The incumbent VE resins can be readily purchased in a blended form ready for molding. The purchase price for each incumbent resin currently used in the tactical vehicle applications was obtained from the manufacturer or one of their distributors. Because this is a comparison study and both incumbent and replacement resins would be shipped to the same composite manufacturing location, shipping costs were not considered. The resin prices were quoted in price per pound for a drum (55 gal) of each product. These prices, as well as the data sources and dates, are listed in Table 4.

For certain chemicals, the price quoted depended upon the quantity that would be ordered, with larger volumes fetching cheaper prices. For these situations, the least expensive prices were assumed in anticipation of large-scale production. For the Hetron 980, the higher price was used because it was assumed that the quantity ordered for resin production would be less than 40,000 pounds. The prices for all chemicals, including the incumbent resins, are located in Appendix A.

Table 4. Cost of Incumbent VE Resins

Resin	Price/lb	Source
Derakane 8084	\$3.43	Ashland (October 2008, verified Feb. 2009)
Hetron 980/35	\$2.36	Ashland Specialty Chemicals (February 2009)
Huntsman RenInfusion 8605 / Ren 8605	\$13.27	Freeman Composites (February 2009)
Hexion 781-2140	\$2.49	Hexion Specialty Chemicals (October 2008, verified Feb. 2009)
CoRezyn Corve 8100	\$2.00	Interplastic (February 2009)

4.2 Replacement FAVE Resin Components

The replacement FAVE resins currently serve a niche market and are not as readily available as the incumbent VE resins. The ARL has purchased both the blended replacement resins, which were ready for molding, as well as the

¹⁸ US EPA, Economic Impact Analysis of the Final Reinforced Plastics NESHAP, Final Report, August 2002, pg 4-4.

components of replacement resins, which the ARL blended into resin prior to molding. The blended FAVE resins have been acquired from one supplier at a low volume. If the replacement resins are adopted for use in tactical vehicles, it is expected that composites manufacturers will purchase higher volumes ready for molding. Since material prices are volume-dependent, this would likely reduce the purchase price of the blended replacement resins.

The ARL obtained costs for the replacement FAVE resin components in 2006. As part of this task, the NDCEE acquired current prices from manufacturers or one of their distributors. As with the incumbent resins, the prices were quoted in price per pound for a drum (55 gal) of each product with no shipping costs. The 2006 and updated prices, as well as the data sources and dates, are listed in Table 5. Ashland Specialty Chemicals would not provide a price for Aropol 914 since the product is not currently sold commercially. For this analysis, ARL's price for Aropol was used. All other updated prices were between 0 and 83 percent higher than the prices obtained by the ARL in 2006. These differences demonstrate how prices can change with time, as well as the difficulty in estimating the future material cost. The updated prices are used in the remainder of the analysis.

Table 5. Cost of Replacement FAVE Resin Components

Resin	2006 Price/lb	Updated Price/lb	Source	Change
Lauric Acid	\$0.65	\$0.65	Twin Rivers (April 2009)	0%
Octanoic Acid	\$1.20	\$2.19	Acme-Hardesty Co. (April 2009)	83%
Glycidyl methacrylate	\$2.75	\$3.50	NOF America Corporation (January 2009)	27%
AMC-2 catalyst	\$32.20	\$36.62	AMPAC Fine Chemicals (October 2008)	14%
Derakane 441-400	\$2.50	\$3.07	Ashland (October 2008, verified Feb. 2009)	23%
Aropol 914	N/A	\$3.29	Price quoted to ARL	N/A
Derakane 470HT-400	\$3.00	\$3.95	Ashland (October 2008, verified Feb. 2009)	32%

4.3 Methacrylated Fatty Acid Monomers

The methacrylated fatty acid monomer production process was discussed with Applied Polyramics, Inc. (API), the small resin blender in Benicia, California used by ARL.¹⁹ In addition, API quoted the prices provided in Table 6 for volumes of 5- and 55-gallons. The information gleaned from API is used here to estimate the current price breakdown for MLau and MOct. Future prices are then estimated based on increased production volumes. API uses the same process, shown in Figure 7, to synthesize both MLau and MOct. A variety of costs are

¹⁹ Telephone conversation with Mr. Rich Moulton of Applied Polyramics in March 2009.

incurred during this process. Here, they are categorized as material, labor, and energy costs. Other costs not itemized in the tables are costs for equipment, tooling, maintenance, overhead labor, building and capital, and profit.

Table 6. Prices Quoted by API for MLau and MOct

Monomer	5-Gallon Price/lb	55-Gallon Price/lb
MLau	\$8.40	\$7.00
MOct	\$8.40	\$7.00

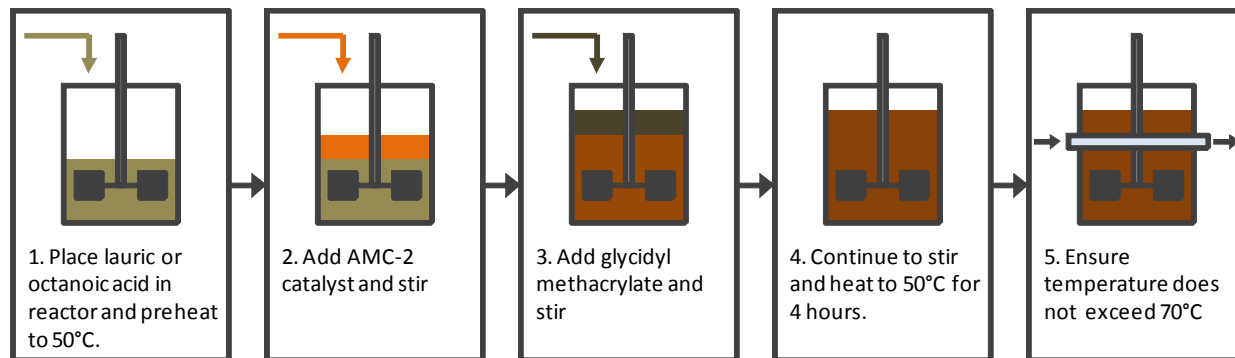


Figure 7. Monomer Synthesis Steps

The costs to produce 55 gallons of MLau and MOct by a small resin blender are estimated in Table 7. The material costs are derived using monomer formulas provided by the ARL and the component costs from Table 5. The labor costs were derived from production information provided by API. According to API, for a small resin blending operation, very little labor is required to blend the raw materials into an MFA monomer. To make a 55-gallon drum batch, about one-half hour is required to pour the ingredients into a drum, seal it, and place it on a drum roller for mixing. A generic fully burdened rate of \$65 per hour was assumed for a technician.

The energy requirements for producing a 55-gallon batch were also obtained from a discussion with API. According to API, it is not necessary to preheat the lauric or octanoic acid prior to blending, as long as the mixing tank is placed in a warm room. Even octanoic acid, which is a solid at temperatures below 63 degrees Fahrenheit, melts readily in a warm temperature and melts completely during the exothermic reaction that occurs when other materials are added. Therefore, there are no energy inputs required for heating the mixture. Temperature control, to prevent overheating during the exothermic reaction, could be achieved by placing the mixing tank in a cool water bath. No costs were assumed for the water.

After the raw materials are poured into a drum, the drum is sealed and placed on a drum roller for six to eight hours. An average size drum roller has a one horsepower (HP) engine. Using an average electricity rate for Benicia, California (the location of the current resin blender), the electricity cost for blending a batch

of monomer on a drum roller for seven hours totals \$0.73. In Table 7, the sum of the raw materials, labor, and energy costs was multiplied by various markup percentages to estimate the other costs. These costs would include equipment, tooling, maintenance, overhead labor, and building and capital costs, as well as the manufacturer's profit. To prevent double-counting some costs, the 45% markup is applied to the sum of materials cost only, not the cost with energy and labor factored into the calculations. This is based on data descriptions from the US Census Bureau data. The prices charged by API for MLau and MOct appear to be greater than the 100% markup of all costs. When questioned, API would not reveal their pricing strategy, citing only market prices and competition as determining factors. The markup in this report was assumed to be 45%. Based on this analysis, the price of MLau was estimated to be \$2.91/lb and the price of MOct was estimated to be \$4.38/lb.

Table 7. Estimated Breakdown of Current Costs for Small Resin Manufacturer to Produce 55-Gallon Batch of Monomers

Cost Category			MLau (Batch = 438 lbs)		MOct (Batch = 452 lbs)	
Materials	Component	Cost/lb	Wt%	Cost/lb	Wt%	Cost/lb
	Lauric Acid	\$0.65	58.5%	\$0.38		
	Octanoic Acid	\$2.19			50.4%	\$1.10
	Glycidyl methacrylate	\$3.50	41.5%	\$1.45	49.6%	\$1.74
	AMC-2 catalyst	\$36.62	0.5%	\$0.18	0.5%	\$0.18
	Total			\$2.01		\$3.02
Labor	Process	Labor	Time	Cost/lb	Time	Cost/lb
	Material Handling	\$65/hr	0.5 hr	\$0.07	0.5 hr	\$0.07
	Total			\$0.07		\$0.07
Energy	Process	Cost/ kWh	kWh	Cost/lb	kWh	Cost/lb
	Stirring	\$0.14	5.22	\$0.002	5.22	\$0.002
	Heating	\$0.14	n/a	--	n/a	--
	Total			\$0.002		\$0.002
Total for Materials, Labor, and Energy				\$2.09		\$3.10
Cost with 35% markup				\$2.82		\$4.19
Materials with 45% markup				\$2.91		\$4.38
Cost with 100% markup				\$4.18		\$6.20
Price Quoted by API				\$7.00		\$7.00

4.4 Fatty Acid Vinyl Ester Resins

The FAVE resin production process was discussed with API. In addition, API quoted the prices provided in Table 8 for five-gallon volumes. No prices were quoted for larger volumes because API had not yet made larger volumes of the resins. The information gathered from API is used to estimate the current price breakdown for FAVE resins. Future prices are then estimated based on increased production volumes. A variety of costs are incurred during this process. Here, they are categorized as material, labor, and energy costs. Other costs not itemized in the tables are costs for equipment, tooling, maintenance, overhead labor, building and capital, and profit.

Table 8. Prices Quoted by API for FAVE Resins

Resin	5-Gallon Price/lb
FAVE-L-25S	\$6.25
FAVE-O-25S	\$6.25
FAVE-L-HT	Not available
FAVE-O-HT	Not available

The costs to produce 55 gallons of the FAVE resins are estimated in Tables 9 and 10. Table 9 shows the estimated costs for a small resin manufacturer to produce the various resins. The material costs are derived using resin formulas provided by the ARL and the material costs from Table 5. It was assumed that the small resin manufacturer must purchase the Derakane resins at market price. The labor costs were derived from production information provided by API. According to API, for a small resin blending operation, very little labor is required to blend the monomer and other raw materials into a resin. To make a 55-gallon drum batch, about one-half hour is assumed to pour the ingredients into a drum and mix it gently by hand, although API indicated that even less time is required for this step. A generic fully burdened rate of \$65 per hour was assumed for a technician. According to API, no additional energy costs were necessary for heating or mixing the resin.

To estimate the costs to produce the FAVE resins, it was assumed that the resins were blended by the same company and in the same location as the MLau and MOct monomers. Consequently, shipping costs were not considered. Furthermore, by assuming the monomer manufacturer also blends the resins, then raw material costs are assumed for all components, rather than a marked-up price for the monomers. This assumption was supported by Keith Johnson, who said that one markup is often applied to all raw materials, regardless of their source. Likewise, labor and energy costs for making the monomers are listed again for the resin blending costs, so that Table 9 provides a complete cost for making the resin that includes all costs for making the monomers. The sum of the raw materials, labor, and energy costs was multiplied by various markup percentages to estimate the other costs. These costs would include equipment, tooling, maintenance,

overhead labor, and building and capital costs, as well as the manufacturer's profit. In accordance with the sales to cost of materials ratio using the US Census Bureau data, the 45% markup is applied to the sum of materials cost only, to prevent double-counting some costs. The markup for our purposes was assumed to be 45%.

Table 9. Estimated Breakdown of Costs to Produce 55-Gallons of Resins for Small Resin Manufacturer

Cost Category		FAVE-L-25S (Batch = 491 lbs)		FAVE-O-25S (Batch = 493 lbs)		FAVE-L-HT (Batch = 488 lbs)		FAVE-O-HT (Batch = 490 lbs)	
		Component	Cost/lb	Wt%	Cost/lb	Wt%	Cost/lb	Wt%	Cost/lb
Materials		Derakane 441-400	\$3.07	54%	\$1.66	54%			
		Derakane 470HT-400	\$3.95			73%	\$2.88	73%	\$2.88
		Aropol 914	\$3.29	36%	\$1.18	36%	\$0.56	17%	\$0.56
		MLau	\$2.01	10%	\$0.20	10%	\$0.20		
		MOct	\$3.02			10%		10%	\$0.30
		Total			\$3.04		\$3.14		\$3.74
Labor		Process	Labor	Time	Cost/lb	Time	Cost/lb	Time	Cost/lb
		Material Handling	\$65/hr	1 hr	\$0.13	1 hr	\$0.13	1 hr	\$0.13
		Total			\$0.13		\$0.13		\$0.13
Energy		Process	Cost/ kWh	kWh	Cost/lb	kWh	Cost/lb	kWh	Cost/lb
		Stirring	\$0.14	5.22	\$0.002	5.22	\$0.002	5.22	\$0.002
		Heating	\$0.14	n/a	--	n/a	--	n/a	--
		Total			\$0.002		\$0.002		\$0.002
Total for Materials, Labor, and Energy									
Cost with 35% markup					\$3.17		\$3.27		\$3.87
					\$4.29		\$4.42		\$5.23
Materials with 45% markup					\$4.41		\$4.55		\$5.43
Price Quoted by API					\$6.25		\$6.25		

Table 10 shows the estimated costs for a large resin manufacturer, such as Ashland Chemical, to produce the various resins. Because the Derakane resin and Aropol production costs are not available, the market or sales price is used for these materials. It is assumed that a 45% markup is already factored into the sales price. Likewise, the MFA monomer prices are listed with the 45% markup included. It is assumed that all labor, energy, profit, and other costs are already factored into sales price, including the costs associated with blending of the FAVE resins. The total costs, including profit, to produce FAVE resins for a large manufacturer are presented as the total in Table 10.

Table 10. FAVE Resin Costs for Large Resin Manufacturer

Materials		FAVE-L-25S		FAVE-O-25S		FAVE-L-HT		FAVE-O-HT	
Component	Cost/lb	Wt%	Cost/lb	Wt%	Cost/lb	Wt%	Cost/lb	Wt%	Cost/lb
Derakane 441-400	\$3.07	54%	\$1.66	54%	\$1.66				
Derakane 470HT-400	\$3.95					73%	\$2.88	73%	\$2.88
Aropol 914	\$3.29	36%	\$1.18	36%	\$1.18	17%	\$0.56	17%	\$0.56
MLau, with 45% markup	\$2.91	10%	\$0.29			10%	\$0.29		
Moct, with 45% markup	\$4.38			10%	\$0.44			10%	\$0.44
Total			\$3.13		\$3.28		\$3.73		\$3.88

As the fatty acid monomers and FAVE resins move from research, development, test and evaluation (RDT&E) to production, the production processes will likely be more automated and alternative methods for producing the materials may be explored. If they are adopted in large-scale commercial applications, additional economies of scale as well as competition in the marketplace may be realized. It is difficult to estimate how this progression would impact the cost of FAVE resins. Material prices can be expected to decrease until they reach a value equal to the cost of production plus some profit at high volumes.²⁰ The FAVE resin prices calculated for this report range from: \$3.13 - \$4.41 per lb for FAVE-L-25S; \$3.28 - \$4.55 per lb for FAVE-O-25S; \$3.73 - \$5.28 per lb for FAVE-L-HT; and \$3.88 - \$5.43 per lb for FAVE-O-HT.

4.5 Material Costs by Application

A variety of material losses can occur during part production. The losses currently occurring during VARTM production using the incumbent VE resins and the resulting material requirements are provided in Table 11. This

²⁰ Boyer, J.M., "Compilation of a Materials Cost Database for a WEB-Based Composites Cost Estimator, B.S. Thesis, Massachusetts Institute of Technology, June 2001, Thesis Supervisor: Timothy G. Gutowski.

information was provided by the ARL. Similar losses can be expected for the FAVE resins.

Table 11. Material Requirements for VARTM Production of VE Resins

Part	Mass (lbs)	Trim Loss (%)	Waste (%)	Total Material Requirement (lbs)
HMMWV Transmission Container	35	0	5	36.75
M939 Hood	20	5	5	22
M35A3 Hood	18	5	5	19.8
HMMWV Hardtop	220	5	5	242
T-38 Dorsal Cover	4	7	5	4.48
MCM Rudder	190	0	5	199.5

Using the monomer and resin price calculations detailed in Tables 7, 9 and 10 and the resin mass per part information obtained from ARL, the resin cost per part was calculated using resin prices from both small scale and large scale manufacturers (Table 12). The resin price per pound and the corresponding price per part (for each application) are provided for the incumbent VE resin (shaded in gray) and the proposed replacement resin (no shading). For the small resin manufacturer, the FAVE resin costs with 45% markup were used in this table.

Table12. Total Material Cost for Incumbent and Replacement Resins with No Engineering Controls

Application	Resin used per Part (lbs)	Resin	Cost/lb Small Mfr	Cost/part Small Mfr	Cost/lb Large Mfr	Resin Cost/part Large Mfr
HMMWV Transmission Container	36.75 lbs	Derakane 8084	\$3.43	\$126.05	\$3.43	\$126.05
		FAVE-L-25S	\$4.41	\$162.07	\$3.13	\$115.03
		FAVE-O-25S	\$4.55	\$167.21	\$3.28	\$120.54
M939 Hood	22 lbs	Hetron 980/35	\$2.46	\$54.12	\$2.46	\$54.12
		Huntsman RenInfusion 8605 / Ren 8605	\$13.27	\$291.94	\$13.27	\$291.94
		FAVE-L-HT	\$5.28	\$116.16	\$3.73	\$82.06
		FAVE-O-HT	\$5.43	\$119.46	\$3.88	\$85.36
M35A3 Hood	19.8 lbs	Hetron 980/35	\$2.46	\$48.71	\$2.46	\$48.71
		Huntsman RenInfusion 8605 / Ren 8605	\$13.27	\$262.75	\$13.27	\$262.75
		FAVE-L-HT	\$5.28	\$104.54	\$3.73	\$73.85
		FAVE-O-HT	\$5.43	\$107.51	\$3.88	\$76.82

Table12. Total Material Cost for Incumbent and Replacement Resins with No Engineering Controls (Continued)

Application	Resin used per Part (lbs)	Resin	Cost/lb Small Mfr	Cost/part Small Mfr	Cost/lb Large Mfr	Resin Cost/part Large Mfr
Amtech HMMWV Hardtop	242 lbs	Derakane 8084	\$3.43	\$830.06	\$3.43	\$830.06
		FAVE-L-25S	\$4.41	\$1,067.22	\$3.13	\$757.46
		FAVE-L-HT	\$5.28	\$1,277.76	\$5.28	\$1,277.76
		FAVE-O-HT	\$5.43	\$1,314.06	\$5.43	\$1,314.06
T-38 Dorsal Cover	4.48lbs	Hexion 781-2140	\$2.49	\$11.16	\$2.49	\$11.16
		FAVE-L-25S	\$4.41	\$19.76	\$3.13	\$14.02
MCM Rudder	199.5 lbs	CoRezyn Corve 8100	\$2.00	\$399.00	\$2.00	\$399.00
		FAVE-L-25S	\$4.41	\$879.80	\$3.13	\$624.44

Note: The shaded areas indicate the incumbent VE resin information.

5.0 ENGINEERING CONTROLS

5.1 Pollution Control Equipment

In light of the Reinforced Plastic Composites NESHAP that took effect in April 2006, it is assumed, based on information from ARL, that composite manufacturers employing VARTM technology are required to implement add-on control devices to capture volatile emissions from conventional styrene-based commercial resins. Furthermore, it is assumed that the replacement FAVE resins with a styrene content reduced by 15 wt% are exempt from the control device requirement.

Various air pollution control devices were studied and it was determined that a regenerative thermal oxidizer (RTO) would be the most beneficial technology for composites manufacturing. The RTO eliminates the VOC emissions through high temperature catalytic oxidization and subsequently releases carbon dioxide and water vapor as a result. The high temperatures necessary for RTO operation are achieved initially by burning natural gas, but energy from the hot exhaust air is recuperated to heat the process air coming into the RTO. This allows for added efficiency and inherent energy savings.²¹ Most RTOs are rated for 95% energy recovery. The following schematic details the air flow within an RTO.

²¹ Anguil Environmental, "Regenerative Thermal Oxidizer", <http://www.anguil.com/prregthe.php>

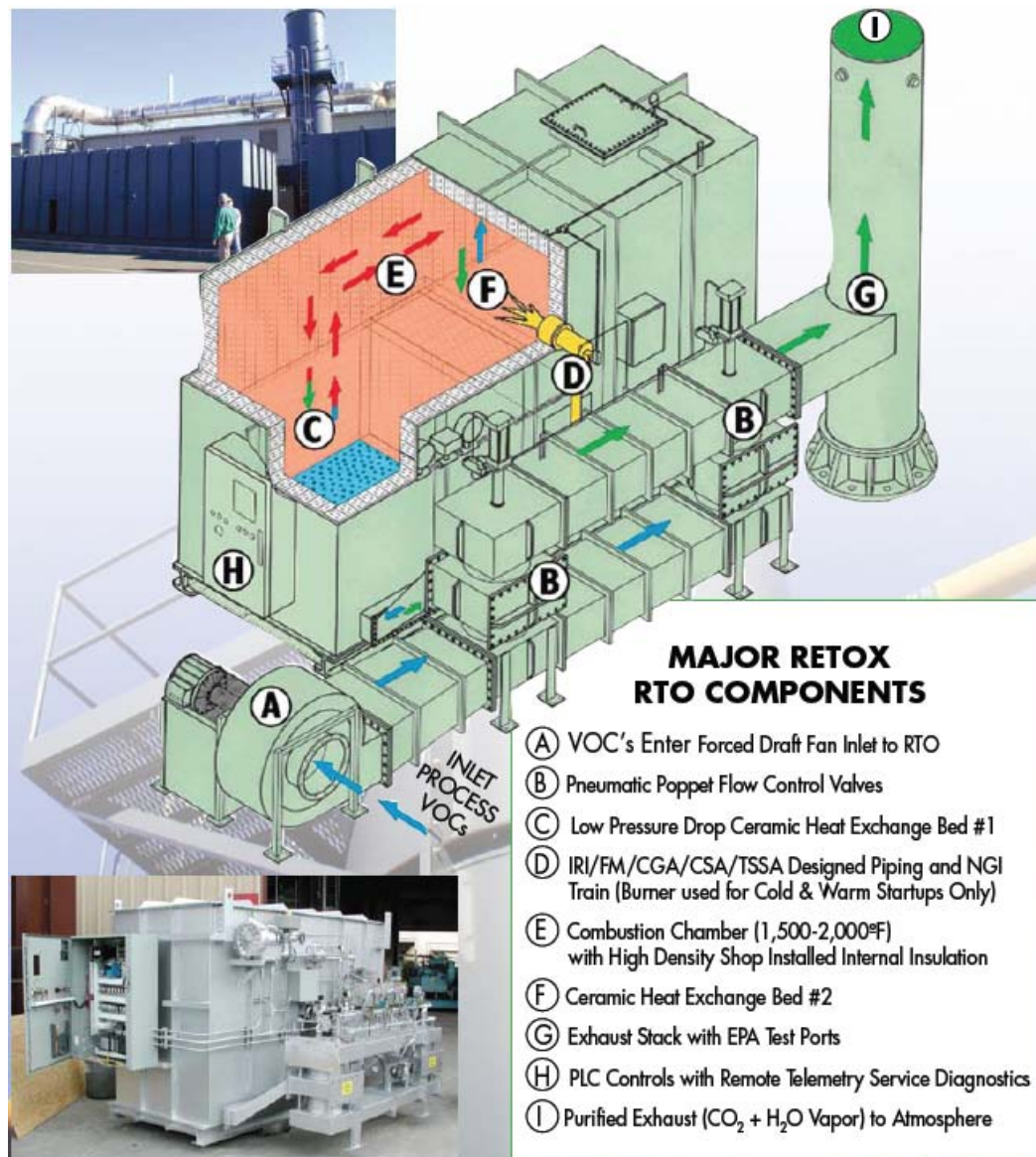


Figure 8. Adwest's RETOX Dual Chamber RTO Oxidizer System Requirements²²

Price quotes for RTOs were obtained from multiple vendors for sizes ranging from 25,000 cubic feet per minute (cfm) – 35,000 cfm because this seemed to be the appropriate size RTO for a small to medium-sized composites manufacturer. As additional research was conducted and process calculations were performed, these sizes proved to be much too large for small to medium sized composites manufacturers using the VARTM process. Based on the styrene emissions calculations using an EPA emission factor (see Section 3.0 of this report), the RTO size was reduced to a 2,000 cfm unit. See Table 13 for a listing of RTO sizes and prices researched during this process.

²² Adwest Technologies, Inc. 2009 RETOX RTO Portfolio Brochure, Anaheim, California. www.adwestusa.com

Table 13. Price quotes obtained for Regenerative Thermal Oxidizers

RTO Manufacturer	RTO Size	Price (Including all equipment, freight, and installation)
Adwest Technologies, Inc.	25,000 cfm	\$439,800 (does not include freight)
Adwest Technologies, Inc	6,5000 cfm	\$211,800 (does not include freight)
Tellkamp Systems, Inc.	35,000 cfm	\$585,000
Tellkamp Systems, Inc.	2,000 cfm	\$265,000
Ship & Shore*	25,000 cfm	\$361,676 (does not include freight)

* Price estimate obtained from Bedford Materials. Bedford Materials purchased a 25,000 cfm from Ship & Shore for a similar price. Bedford Materials noticed that Ship & Shore's quote was about 20% less than the quote for the comparable Adwest RTO.

From the calculations in Table 3, an average styrene emission rate was calculated to be 0.35 lbs styrene per hour going to an RTO. As a conservative estimate, this figure was rounded up to 2.0 lbs /hour to size an RTO for this hypothetical facility. For a small- to medium-sized composite manufacturer that emits an average of 2 lbs of styrene per hour, a 2,000 cfm RTO would provide ample destruction efficiency for this process. A price quote of \$265,000 for the 2,000 cfm unit was received from Tellkamp Systems, Inc. in April 2009. This price includes the installation and shipping to a facility in Northern California. An additional price quote was received from Adwest Technologies, Inc. for a comparable 6,500 cfm unit for \$211,800, including all equipment, and installation, but not shipping. The higher priced unit was used in subsequent calculations because it appeared to be a more complete price quote for a more appropriately sized RTO.

The annualized RTO costs are summarized in Table 14. The total capital investment for the RTO is a sum of the direct and indirect costs. The direct costs were obtained from vendor quotes and include any auxiliary equipment, instrumentation, installation, and freight. The indirect costs can be estimated from the EPA's Air Pollution Control Cost Manual.²³ According to the formula, the indirect costs, which include engineering, construction and field expenses, contractor fees, start-up costs, performance tests, and contingencies, can be estimated by multiplying the direct costs by 0.31. The total capital investment for the RTO was divided over 15 years, the assumed lifetime of the RTO.

²³ EPA Air Pollution Control Cost Manual, 6th Edition, January 2002.

Table 14. RTO Capital and Operating Costs Spread Over a 15-Year Economic Lifetime

Annualized RTO Costs			
RTO Capital Costs	Cost Category	Total Cost	Annualized Cost
	RTO Direct Cost (incl. freight and installation)	\$265,000	\$17,666.67
	RTO Indirect Cost (Engineering, contractor fees, start-up, etc.)	\$82,150	\$5,476.67
	Total	\$347,150	\$23,143.33
RTO Maintenance (Labor and Parts)	Cost Category	Unit	Annualized Cost
	Perform visual inspection 2-3 hours per month	30 hrs/year	\$1,950.00
	Lubrications/replace gaskets, bearings, belts, etc. 10-12 hours/year	11 hrs/year	\$715.00
	Maintenance Materials	\$1,000	\$1,000.00
	Total		\$3,665.00
RTO Energy Usage	Cost Category	Unit	Annualized Cost
	Electricity to run 10 HP fan on RTO for 24/7	\$0.77/hour	\$6,745.20
	Natural gas for RTO for 24/7	\$1.22/hour	\$10,687.20
	Total		\$17,432.40
Total Annual Costs to use RTO			\$44,240.73

Other costs associated with RTO operation, such as operating energy costs and annual preventative maintenance (PM) costs, were also factored into the total cost to use the RTO. According to the Tellkamp Systems sales engineer, most RTOs would require a few minutes of daily visual inspections (totaling 2-3 hours per month) and an annual shutdown period (10-12 hours per year) to perform lubrications and replace bearings, belts, gaskets, or other parts in need of repair. Maintenance costs for consumable parts would be approximately \$1,000 per year.

The energy costs for the 2,000 cfm RTO were calculated to be \$1.99 per hour, assuming 24 hour operation of the RTO to maintain the proper temperature required for the permitted VOC destruction efficiency. Assuming an average electricity rate of \$0.11/kWh for a 10 HP fan, the electricity costs for the RTO total \$0.77 per hour. Assuming a 2 lb/hr styrene input to the RTO (which could be hard to maintain at a constant rate and would therefore require additional natural gas to supplement the VOC input and maintain the RTO temperature), the natural gas cost would be \$1.22 per hour for a rate of \$6.50 per dekatherm. These operating costs were also factored into the total RTO cost in Table 14.

6.0 ECONOMIC ANALYSIS

In this LCCA, two courses of action have been explored for vinyl ester resins: (1) continue using incumbent VE resins, which are assumed will require composite manufacturers to install and use pollution control equipment; or (2) adopt replacement FAVE resins, which are assumed will not require pollution controls. Both options are expected to increase the costs for a composites manufacturer and consequently, the DoD's costs to purchase the composite products. Since vacuum infusion molding, or VARTM, is considered by the EPA to be a closed molding process, it is unknown what, if any, requirements must be met to ensure compliance under the NESHAP rule. As a compliance evaluation is out of the scope of this project, it is assumed that these two scenarios are required to ensure compliance with the Reinforced Plastic Composites NESHAP rule.

A cost effectiveness analysis (CEA) was performed to evaluate which of these options is more cost effective at meeting the goal of maintaining tactical vehicle performance while also meeting NESHAP requirements. CEA was used to compare the relative costs and outcomes of the two courses of action. It can be assumed that the outcomes of the two approaches are similar; that is, tactical vehicle performance is maintained and NESHAP requirements are met. Only the costs that differ between the two courses of actions are included in the analysis. A 15-year study period was used. Annual production volumes are assumed to stay constant over the fifteen years.

6.1 Cost Model / Assumptions

When determining which cost model would give the appropriate results for this analysis, it was determined a custom analysis was necessary. The models traditionally used by CTC, Environmental Cost Analysis Methodology (ECAM) and Pollution Prevention (P2) Finance, are not relevant because ARL/DoD is not making an investment, but rather purchasing products from companies that may have to make this investment. Therefore, a project specific cost model was created in Excel by the project team.

The annualized costs for RTO equipment, labor, and utilities (see Table 14) were divided by the annual RTO throughput to calculate a cost per pound for operating the RTO. To perform these calculations, several assumptions were made. These are summarized below:

- RTO capital cost:
 - Assume an RTO is the best solution for ensuring compliance with NESHAP rule
 - Assume a 2,000 cfm unit is the correct size for this scenario
 - Assume the EPA's indirect cost formula correctly captures these costs
 - Assume an economic life of 15 years for the RTO
- RTO Maintenance:
 - Assume a burdened labor rate of \$65/hour for a technician
 - Assume RTO consumable materials total \$1,000 annually

- Assume RTO maintenance requirements total 41 hours of labor annually
- Utilities for the RTO:
 - Assume an average electricity rate of \$0.11/kWh, based on inquiries near Fort Totten, ND; Wapato, WA; Hill AFB, UT; and Annapolis, MD
 - Assume an average natural gas rate of \$6.50/dekatherm, based on inquiries near Fort Totten, ND; Wapato, WA; Hill AFB, UT; and Annapolis, MD
 - Assume the RTO must keep running 24 hours a day, every day, regardless of the production schedule. Many air permits require RTOs to stay at a certain temperature to meet the required VOC destruction efficiency, and they don't respond quickly to temperature fluctuations.
- Production:
 - Assume the production estimates in Table 2 are reliable estimates
 - For the worst case scenario, assume only one line of production is routed to the RTO.
 - For the more realistic scenario, assume all Ft. Totten, ND parts (for Army vehicles) are made in one facility. Assume that all three product lines go to the same RTO and no other products go to the RTO.
 - Assume the Ft. Totten facility example is representative for all applications, even those with very small annual production estimates. Assume the cost per pound increase from RTO usage can be applied to all applications.
- Environmental, Health, and Safety Compliance:
 - Assume that the annual costs for preparing Toxics Release Inventory (TRI) reports are the same for both VE and replacement resins. For the Ft. Totten facility example, the reporting threshold for processing styrene (10,000 lbs per year) is exceeded for both the incumbent and replacement FAVE resins.
 - Assume that no TRI reporting is required for an epoxy resin. According to the EPA, the annual burden for completing a TRI report for one chemical is \$630. If this cost were divided by an average annual production rate (assume 5,000 parts per year), the cost savings for an epoxy resin for not completing a TRI report is approximately \$0.13 per part.
 - Assume that a baseline Industrial Hygiene survey and personal air sampling must be performed for facilities using incumbent resins and for facilities using replacement FAVE resins.

6.2 Cost Analysis and Comparison

In order to complete a cost analysis and comparison, it was necessary to determine the incremental variable costs associated with using a pollution control device. The annualized costs for RTO equipment, labor, and utilities (see Table 14) were divided by the annual RTO throughput to calculate a cost per pound for operating the RTO. Once calculated, these costs were compared to the prices of the replacement FAVE resins.

A cost comparison was performed on both the cost per pound and cost per part for each of the products listed in Tables 15 through 18. The incremental costs for RTO usage were calculated using a worst case scenario (with only one line of production routed to the RTO) and a more realistic scenario (with three production lines routed to the RTO). Tables 15 and 16 show the costs using resin prices from a small resin manufacturer and Tables 17 and 18 show the costs using resin prices from a large resin manufacturer.

For the worst case scenario, it was assumed that only one line of production is routed to the RTO. Obviously, it would be cost prohibitive to operate in this manner, and the costs reflect this unrealistic scenario. It is highly unlikely a composite manufacturer would operate a pollution control device so far under its capacity. Only the applications that are heavy and/or are produced in high volume show a reasonable cost. The detailed calculations for these prices can be found in the spreadsheets in Appendix B.

For the more realistic scenario, it was assumed all Ft. Totten, ND parts (for Army vehicles) are made in one facility and all three product lines go to the same RTO. It was further assumed that no other products go to the RTO. The calculations were completed for the HMMWV transmission container, the M939 Hood, and the M35A3 Hood and these incremental variable costs per pound were then applied to the other applications. It was assumed that the Ft. Totten facility example is representative for all applications, even those with very small annual production estimates. The cost per pound increase from RTO usage, \$0.34 per pound regardless of the resin, was then applied to all applications.

Table 15. Worst Case Total Estimated Cost / Part with Resin Prices from Small Mfr

Application	Resin	RTO Maintenance Labor and Parts (\$/lb)	RTO Purchase (\$/lb)	RTO Utilities (\$/lb)	Material (\$/lb)	Total (\$/lb)	Total Cost/part
HMMWV Transmission Container	Derakane 8084	\$0.20	\$1.26	\$0.95	\$3.43	\$5.84	\$214.53
	FAVE-L-25S					\$4.41	\$162.07
	FAVE-O-25S					\$4.55	\$167.21
M939 Hood	Hetron 980/35	\$0.03	\$0.21	\$0.16	\$2.46	\$2.86	\$62.97
	Huntsman RenInfusion 8605 / Ren 8605					\$13.27	\$291.94
	FAVE-L-HT					\$5.28	\$116.16
	FAVE-O-HT					\$5.43	\$119.46

Table 15. Worst Case Total Estimated Cost / Part with Resin Prices from Small Mfr (Continued)

Application	Resin	RTO Maintenance Labor and Parts (\$/lb)	RTO Purchase (\$/lb)	RTO Utilities (\$/lb)	Material (\$/lb)	Total (\$/lb)	Total Cost/part
M35A3 Hood	Hetron 980/35	\$1.85	\$11.69	\$8.80	\$2.46	\$24.80	\$491.12
	Huntsman RenInfusion 8605 / Ren 8605					\$13.27	\$262.75
	FAVE-L-HT					\$5.28	\$104.54
	FAVE-O-HT					\$5.43	\$107.51
Amtech HMMWV Hardtop	Derakane 8084	\$0.03	\$0.20	\$0.15	\$3.43	\$3.81	\$922.23
	FAVE-L-25S					\$4.41	\$1,067.22
	FAVE-L-HT					\$5.28	\$1,277.76
	FAVE-O-HT					\$5.43	\$1,314.06
T-38 Dorsal Cover	Hexion 781-2140	\$20.45	\$129.15	\$97.28	\$2.49	\$249.37	\$1,117.17
	FAVE-L-25S					\$4.41	\$19.76
MCM Rudder	CoRezyn Corve 8100	\$2.67	\$23.20	\$17.48	\$2.00	\$45.35	\$9,047.15
	FAVE-L-25S					\$4.41	\$879.80

Note: The shaded areas indicate the incumbent VE resin information.

Table 16. Realistic Scenario Total Estimated Cost / Part with Resin Prices from Small Mfr

Application	Resin	RTO Maintenance Labor and Parts (\$/lb)	RTO Purchase (\$/lb)	Utilities (\$/lb)	Material (\$/lb)	Total \$/lb	Total Cost/part
HMMWV Transmission Container	Derakane 8084	\$0.03	\$0.18	\$0.13	\$3.43	\$3.77	\$138.52
	FAVE-L-25S					\$4.41	\$162.07
	FAVE-O-25S					\$4.55	\$167.21
M939 Hood	Hetron 980/35	\$0.03	\$0.18	\$0.13	\$2.46	\$2.80	\$61.59
	Huntsman RenInfusion 8605 / Ren 8605					\$13.27	\$291.94
	FAVE-L-HT					\$5.28	\$116.16
	FAVE-O-HT					\$5.43	\$119.46

Table 16. Realistic Scenario Total Estimated Cost / Part with Resin Prices from Small Mfr (Continued)

Application	Resin	RTO Maintenance Labor and Parts (\$/lb)	RTO Purchase (\$/lb)	Utilities (\$/lb)	Material (\$/lb)	Total \$/lb	Total Cost/part
M35A3 Hood	Hetron 980/35	\$0.03	\$0.18	\$0.13	\$2.46	\$2.80	\$55.43
	Huntsman RenInfusion 8605 / Ren 8605					\$13.27	\$262.75
	FAVE-L-HT					\$5.28	\$104.54
	FAVE-O-HT					\$5.43	\$107.51
Amtech HMMWV Hardtop	Derakane 8084	\$0.03	\$0.18	\$0.13	\$3.43	\$3.77	\$912.34
	FAVE-L-25S					\$4.41	\$1,067.22
	FAVE-L-HT					\$5.28	\$1,277.76
	FAVE-O-HT					\$5.43	\$1,314.06
T-38 Dorsal Cover	Hexion 781-2140	\$0.03	\$0.18	\$0.13	\$2.49	\$2.83	\$12.68
	FAVE-L-25S					\$4.41	\$19.76
MCM Rudder	CoRezyn Corve 8100	\$0.03	\$0.18	\$0.13	\$2.00	\$2.34	\$466.83
	FAVE-L-25S					\$4.41	\$879.80

Note: The shaded areas indicate the incumbent VE resin information.

Table 17. Worst Case Total Estimated Cost / Part with Resin Prices from Large Mfr

Application	Resin	RTO Maintenance Labor and Parts (\$/lb)	RTO Purchase (\$/lb)	Utilities (\$/lb)	Material (\$/lb)	Total \$/lb	Total Cost/part
HMMWV Transmission Container	Derakane 8084	\$0.20	\$1.26	\$0.95	\$3.43	\$5.84	\$214.53
	FAVE-L-25S					\$3.13	\$115.03
	FAVE-O-25S					\$3.28	\$120.54
M939 Hood	Hetron 980/35	\$0.03	\$0.21	\$0.16	\$2.46	\$2.86	\$62.97
	Huntsman RenInfusion 8605 / Ren 8605					\$13.27	\$291.94
	FAVE-L-HT					\$3.73	\$82.06
	FAVE-O-HT					\$3.88	\$85.36

Table 17. Worst Case Total Estimated Cost / Part with Resin Prices from Large Mfr (Continued)

Application	Resin	RTO Maintenance Labor and Parts (\$/lb)	RTO Purchase (\$/lb)	Utilities (\$/lb)	Material (\$/lb)	Total \$/lb	Total Cost/part
M35A3 Hood	Hetron 980/35	\$1.85	\$11.69	\$8.80	\$2.46	\$24.80	\$491.12
	Huntsman RenInfusion 8605 / Ren 8605					\$13.27	\$262.75
	FAVE-L-HT					\$3.73	\$73.85
	FAVE-O-HT					\$3.88	\$76.82
Amtech HMMWV Hardtop	Derakane 8084	\$0.03	\$0.20	\$0.15	\$3.43	\$3.81	\$922.23
	FAVE-L-25S					\$3.13	\$757.46
	FAVE-L-HT					\$3.73	\$902.66
	FAVE-O-HT					\$3.88	\$938.96
T-38 Dorsal Cover	Hexion 781-2140	\$20.45	\$129.15	\$97.28	\$2.49	\$249.37	\$1,117.17
	FAVE-L-25S					\$3.13	\$14.02
MCM Rudder	CoRezyn Corve 8100	\$2.67	\$23.20	\$17.48	\$2.00	\$45.35	\$9,047.15
	FAVE-L-25S					\$3.13	\$624.44

Note: The shaded areas indicate the incumbent VE resin information.

Table 18. Realistic Scenario Total Estimated Cost / Part with Resin Prices from Large Mfr

Application	Resin	RTO Maintenance Labor and Parts (\$/lb)	RTO Purchase (\$/lb)	Utilities (\$/lb)	Material (\$/lb)	Total \$/lb	Total Cost/part
HMMWV Transmission Container	Derakane 8084	\$0.03	\$0.18	\$0.13	\$3.43	\$3.77	\$138.52
	FAVE-L-25S					\$3.13	\$115.03
	FAVE-O-25S					\$3.28	\$120.54
M939 Hood	Hetron 980/35	\$0.03	\$0.18	\$0.13	\$2.46	\$2.80	\$61.59
	Huntsman RenInfusion 8605 / Ren 8605					\$13.27	\$291.94
	FAVE-L-HT					\$3.73	\$82.06
	FAVE-O-HT					\$3.88	\$85.36

Table 18. Realistic Scenario Total Estimated Cost / Part with Resin Prices from Large Mfr (Continued)

Application	Resin	RTO Maintenance Labor and Parts (\$/lb)	RTO Purchase (\$/lb)	Utilities (\$/lb)	Material (\$/lb)	Total \$/lb	Total Cost/part
M35A3 Hood	Hetron 980/35	\$0.03	\$0.18	\$0.13	\$2.46	\$2.80	\$55.43
	Huntsman RenInfusion 8605 / Ren 8605					\$13.27	\$262.75
	FAVE-L-HT					\$3.73	\$73.85
	FAVE-O-HT					\$3.88	\$76.82
Amtech HMMWV Hardtop	Derakane 8084	\$0.03	\$0.18	\$0.13	\$3.43	\$3.77	\$912.34
	FAVE-L-25S					\$3.13	\$757.46
	FAVE-L-HT					\$3.73	\$902.66
	FAVE-O-HT					\$3.88	\$938.96
T-38 Dorsal Cover	Hexion 781-2140	\$0.03	\$0.18	\$0.13	\$2.49	\$2.83	\$12.68
	FAVE-L-25S					\$3.13	\$14.02
MCM Rudder	CoRezyn Corve 8100	\$0.03	\$0.18	\$0.13	\$2.00	\$2.34	\$466.83
	FAVE-L-25S					\$3.13	\$624.44

Note: The shaded areas indicate the incumbent VE resin information.

This incremental cost increase for RTO usage was compared to the information found in the EPA's "Economic Impact Analysis of Final Reinforced Plastics NESHAP." In this document in Table 4-4, the compliance costs and market price changes resulting from the NESHAP regulation are summarized for the year 1997. For the recommended alternative, the mean incremental variable compliance cost across all industries is \$0.06 per pound, with a maximum value increase of \$1.08 per pound.²⁴ For the Land Transportation industry, the incremental cost was expected to increase to \$0.05 per pound as a mean, and \$0.20 per pound maximum.

The cost analysis provided in this report assumes that all cost increases would be directly translated to the composites manufacturer, and thus, the DoD. According to the EPA's Economic Impact Analysis (EIA), the increased cost of production due to the regulation is expected to slightly increase the price of composites and marginally reduce their production/consumption from baseline levels.²⁵ However, according to the EIA, the price impacts are attenuated by the existence of a

²⁴ US EPA, Economic Impact Analysis of the Final Reinforced Plastics NESHAP, Final Report, August 2002, pg 4-15.

²⁵ Ibid.

perfect substitute for the regulated reinforced plastic composites (RPC) products, such as a part made out of a different material. Therefore, the incremental cost associated with RTO usage could indeed be closer to the EPA's \$0.20 per pound value for land transportation RPC products.

Finally, an RTO usage incremental cost can be calculated in the event that FAVE resin composite parts also use an RTO for air pollution control. For this scenario, one can assume a facility in which many different composites parts are being manufactured using a variety of processes, such as open molding, VARTM, etc., and all of the emissions from these processes are being routed to the RTO. If one of these production lines replaced their incumbent resin with a FAVE resin, it is unlikely they would discontinue the RTO treatment of those emissions. In other words, the emissions from this process would still be routed to the RTO and, as a result, some the FAVE resins would incur some of the RTO costs. One way to estimate the costs for this scenario would be to create a ratio of the FAVE resin styrene content to the incumbent resin styrene content and multiply this by the \$0.34 per pound increase for the RTO usage. This is estimated below in Table 19. The styrene content of all FAVE resins is 25%.

Table 19. RTO Usage Price Increase for FAVE Resins

Resin	Styrene Content	Ratio of FAVE resin styrene content to incumbent resin styrene content	Cost per pound
Derakane 8084	40%	0.625	\$0.21
Hetron 980/35	35%	0.714	\$0.24
Hexion 781-2140	46%	0.543	\$0.18
CoRezyn Corve 8100	49.5%	0.505	\$0.17

The cost per pound for a particular resin in this table would then be added to the FAVE resin cost per pound that is replacing this resin.

7.0 ENVIRONMENTAL IMPACT

Materials, energy, water and other inputs are required to extract, process, and transport raw materials and to manufacture, transport, use, and retire composite structures used in military applications. In addition to consuming resources, these activities result in environmental discharges and generate waste. These aspects of the incumbent and replacement resins are not captured in the CEA provided above. Life cycle assessment (LCA) is an analytical process for quantifying the inputs and outputs for each life cycle stage and assessing the total environmental impact of a product. Consequential LCA is used to identify significant differences in the environmental burdens of using one product instead of another. In the following diagrams, consequential LCA is used to evaluate the environmental implications of substituting one of the replacement FAVE resin systems (i.e., FAVE-L-25S) for one of the incumbent VE resin systems (i.e., Derakane 8084). Figure 9 shows the product life cycle associated with using these resin systems in

structural composites. The FAVE resins will be drop-in replacements for commercial VE resins. The resource extraction and resin blending stages will be different for both resin systems. During an LCA, all of the inputs and outputs associated with these stages are evaluated. No process changes are expected in the composite molding, use, or retirement stages. Since the styrene emissions during these stages depend on the composition of the composite, they would be evaluated.

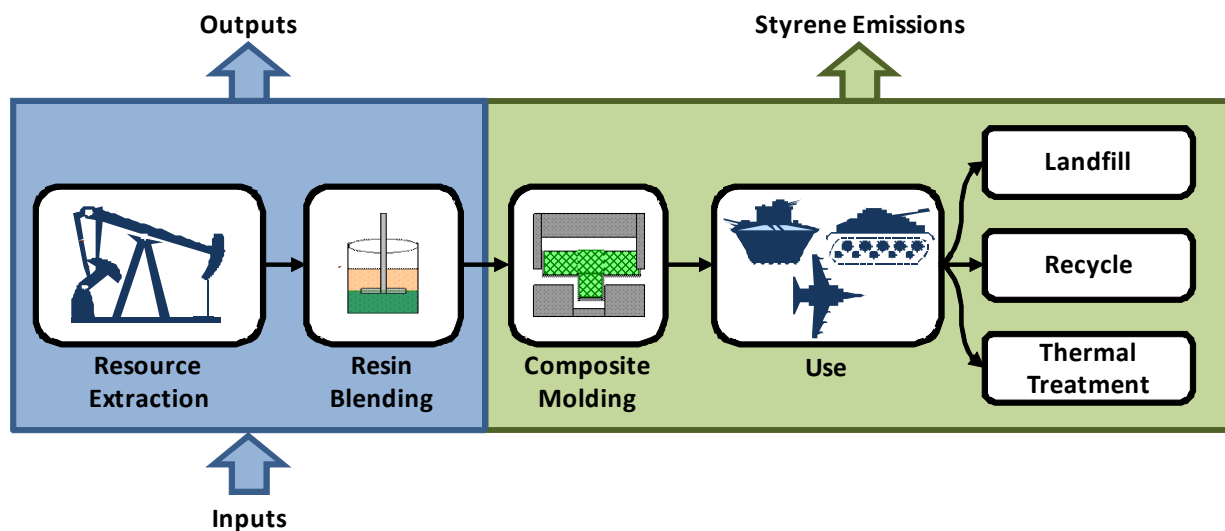


Figure 9. Aspects of the Product Life Cycle Compared for the Two Resin Systems

To identify the cradle-to-gate flows from preparing the incumbent and replacement resin, process flow diagrams were developed based on technical literature and reference books.²⁶ Since little detailed information is available from the resin producers, processes that have the greatest industrial performance were assumed. Several of the operations included in the process flow diagrams produce co-products. However, only the chemicals used in producing the incumbent and replacement resins are shown. If an LCA were to be performed, the next step would be to quantify the inputs and outputs associated with preparing each material or chemical shown in the process flow diagrams.

7.1 Preparation of Incumbent Resin (Derakane 8084)

Derakane 8084 is an elastomer-modified Bisphenol-A epoxy vinyl ester. It is 60 wt% Bisphenol A and 40 wt% styrene, with an unknown percentage of the non-styrene portion being an elastomer for toughening.²⁷ The assumed process flow diagram for producing Derakane 8084 is shown in Figure 10.

²⁶ In particular, the Kirk-Othmer Encyclopedia of Chemical Technology and Speight's 2002 Chemical and Process Design Handbook were consulted.

²⁷ S.E. Boyd, J.J. La Scala, G.R. Palmese, Molecular Relaxation Behavior of Fatty Acid-Based Vinyl Ester Resins, *Journal of Applied Polymer Science*, 108(6) 3495 - 3506, 2008.

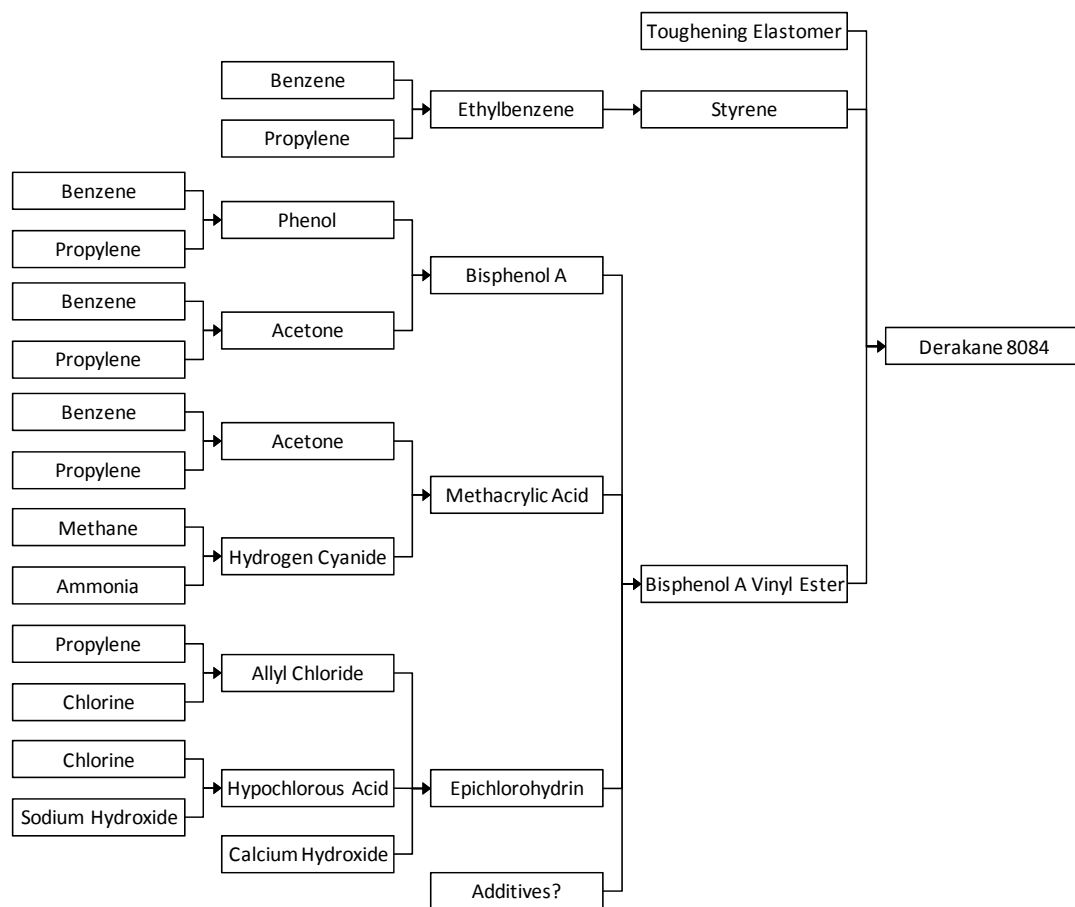


Figure 10. Derakane 8084 Process Flow Diagram

7.2 Preparation of Replacement Resin (FAVE-L-25S)

The replacement resin FAVE-L-25S has many of the same ingredients as the Derakane 8084, but a portion of the styrene is replaced with a methacrylated fatty acid monomer that contains plant-derived ingredients. The assumed process flow diagram for the FAVE-L-25S replacement resin is shown in Figure 11.

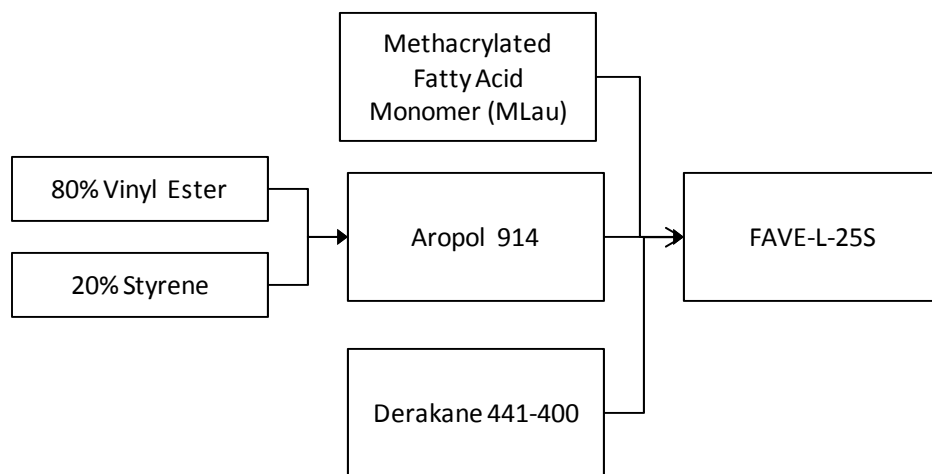


Figure 11. FAVE-L-25S Process Flow Diagram

The MLau monomer and Derakane 441-400 can be dissected further into their own process flow diagrams. The assumed process flow diagram for the MLau monomer is shown in Figure 12.

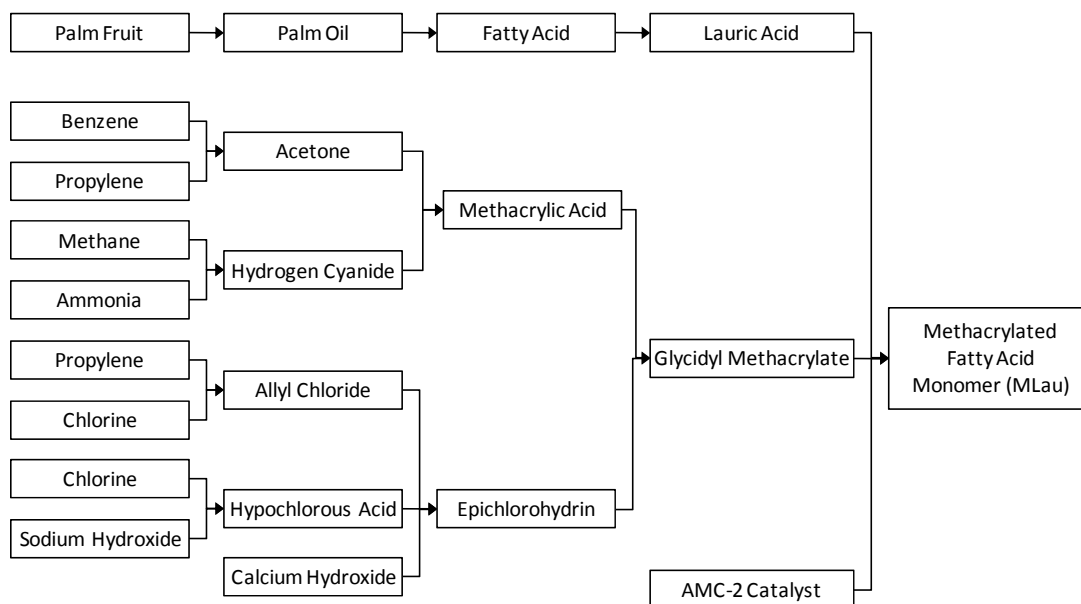


Figure 12. Methacrylated Lauric Acid Process Flow Diagram

Derakane 441-400, the vinyl ester portion of the FAVE-L-25S replacement resin, is also a Bisphenol-A epoxy vinyl ester, but without the elastomer-modified component. It is 67 wt% Bisphenol A and 33 wt% styrene. The assumed process flow diagram for producing Derakane 8084 is shown in Figure 1013.

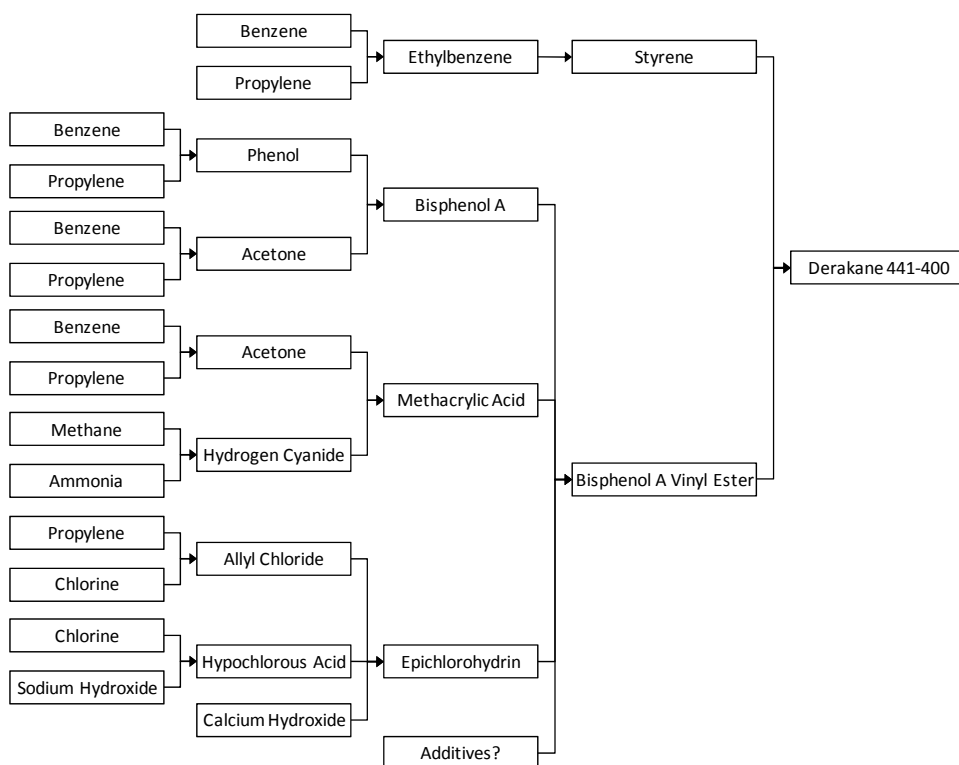


Figure 13. Derakane 441-400 Process Flow Diagram

8.0 CONCLUSIONS

This Life Cycle Cost Analysis details the costs of implementing FAVE resins versus using standard VE resins combined with facility modifications to meet NESHAP requirements. Tables 15 through 18 summarize the anticipated life cycle costs on a per pound and per part basis. The worst case scenarios (Tables 15 and 17) shows costs that are so unrealistic that this scenario should not be considered further. Only the applications that are heavy (such as the HMMWV hardtop) and/or are produced in high volume (such as the M939 hood) show a reasonable cost. It is highly unlikely a composite manufacturer would operate a pollution control device so far under its capacity. As detailed in Table 16 (for resin prices from a small manufacturer), for every application, the cost per pound and cost per part are less for the incumbent resin using pollution control equipment than for the replacement FAVE resin. The incremental cost with RTO usage amounts to pennies per pound. It should be noted that this cost analysis assumes all costs are translated directly to the consumer. As discussed in the EPA's EIA, however, some of these costs are likely to be absorbed by the composites manufacturers. A close look at the calculations in Appendix B shows a sensitivity to RTO throughput, but it is likely that composites manufacturers would maximize the number of parts going to the RTO.

Upon reviewing the final costs among the different resin formulations, it is obvious that the epoxy resins remain the most expensive option. Even with the reduced burden of

environmental reporting, the epoxy resin costs are two to four times higher than any other resin. For the Hetron, Hexion, and CoRezyn incumbent resins, the costs with the RTO usage included are still significantly less than the replacement FAVE resins costs, if the resins were produced by a small manufacturer.. For the Derakane 8084, it is possible that the FAVE resin prices could be competitive. As shown in Table 16, if the markup on the FAVE resin prices were reduced to a 19% margin (instead of 45%), the FAVE resin prices would be similar to the costs of Derakane 8084 with incremental costs of RTO usage included.

If the FAVE resins were manufactured on a large scale by a company such as Ashland Chemical (Table 18), the FAVE prices would be competitive with some incumbent resin prices. The FAVE-L-25S and the FAVE-O-25S are less expensive than the Derakane 8084 by 17% and 13%, respectively. The FAVE-L-HT and the FAVE-O-HT are both about 35% more than the Hetron 980 and nearly identical in price to the Derakane 8084. Even the least expensive FAVE resin, the FAVE-L-25S, is more expensive than the Hexion and CoRezyn incumbent resins, probably due to the higher styrene content in these resins. A less expensive resin may be more economical in the FAVE resin formula than Derakane 441-400 or Derakane 470HT-400. If determined to be comparable in quality and performance to the Derakane products, the Hetron 980/35 should be considered for use in the FAVE resin formulas since all of these products contain approximately 35% styrene.

Not included in this cost analysis is the environmental life cycle assessment of the different resin formulations. An LCA would quantify the inputs and outputs for each life cycle stage and assess the total environmental impact of a product. A Consequential LCA is recommended to identify significant differences in the environmental burdens of using one product instead of another.

Appendix A

Resin and Monomer Price List, Monomer and Resin Price Calculations



replacement resin
info-new formula rev'

Appendix B

Cost Analysis Calculations



All Cost
Info_modified FAVE p

INTENTIONALLY LEFT BLANK.

Appendix L. Drexel MFA Production and Cost Report

This appendix appears in its original form, without editorial change.

Appendix L

Drexel MFA Production and Cost Report

Polymers from Renewable Fatty Acid Monomers

Synthesis of MFA Monomers

Design Team 9
Nicole Galante
Colleen Mackey
Michael Matt
Thomas Salerno

April 30, 2007

Academic Advisor: Dr. Giuseppe Palmese

Industrial Advisor: Mr. Steven Schon

Department of Chemical and Biological Engineering Drexel University, Philadelphia, PA
19104

Drexel University
3141 Chestnut Street
Philadelphia, PA 19104

April 30, 2007

Giuseppe R. Palmese, Ph.D.
Professor and Department Head
Chemical and Biological Engineering
3141 Chestnut Street
Philadelphia, PA 19104

Dear Dr. Palmese:

In this report you will find the completed feasibility study for plant that will produce Methacrylated Fatty Acids (MFA). MFA is a new chemical that will be used to replace some of the styrene in vinyl ester resins to effectively reduce harmful emissions created by the styrene diluent. The purpose of this design simulation was to create a process and plant to produce MFA, and then assess if such a plant was economically advantageous. This study includes scope, background, process design, process flow diagrams, plot plan, sample calculations, economic analysis, safety and environmental concerns, results, and conclusions.

We appreciate all of the guidance and consultation you have provided throughout this process. We encourage you to contact any of the team members with any questions or concerns you may have.

Sincerely,



Nicole Galante



Michael Matt



Colleen Mackey

Thomas Salerno



Executive Summary

The feasibility of this study was determined by performing an economic analysis on two different levels of production: 5 million and 55 million pounds of MFA produced per year. While the design discussed throughout the paper is for 5 million pounds, the extra analysis was performed to see if a higher production rate would create a more profitable plant.

The proposed site for the plant is in Freeport, Texas. This location allows for easy transportation of the reactants and product. It is also located near a glycidyl methacrylate (GM) plant to cut down on transportation costs of the most expensive raw material.

The current selling price of styrene is 88 cents per pound. The price of MFA will be set at \$1.17 per pound. Due to high raw material costs, particularly those from GM, MFA must be set at a higher price than styrene. The biggest risk in the project stems from the dependence the team has on negotiating a low cost-high volume contract with Dow for GM.

After performing an economic assessment on the plant designed, which will produce 5 million pounds of MFA per year, the IRR was determined to be -15%. From this, it is recommended that the project not go forward. However, if production is increased by a factor of 4 to 20 MM pounds per year, the breakeven point is reached. For the process to actually be profitable, an economic assessment was also done on a plant that would produce 55 million pounds of MFA per year. The IRR for a plant producing 55 million pounds is 21%, a much more favorable number. If the market will respond to that large of a production rate for MFA, building a plant with a higher capacity that is profitable is something for the venture company to consider.

Marketing the MFA will be a difficult task. Current methods for treating styrene emissions offer a way for companies to put into place equipment that will treat the toxic emissions, without having to add another raw material into their vinyl ester resin. The challenge on this front will be convincing the companies that MFA is a better choice, or, that paired with emissions equipment it will be an efficient alternative to reducing emissions. However, if no legislation is passed that requires styrene emissions to be lowered, there is no place for MFA in the market.

While many economic challenges have surfaced in the design of the MFA plant, future effects – such as legislation or brokering a deal with Dow on the price of GM – will ultimately decide the fate of this project.

Abstract

Styrene emissions in vinyl ester resins can release harmful volatile organic compounds (VOCs) into the environment. Styrene has also recently been identified as a carcinogen, resulting in new emissions standards set by the EPA in recent legislation. Emission reduction of these VOCs can be achieved by partially replacing the styrene with methacrylated fatty acid monomers (MFA) in vinyl ester resins.

MFAs are produced from a reaction between glycidyl methacrylate (GM) and lauric acid in the presence of the AMC-2 catalyst. These reactants will be mixed and heated in a static mixer before entering the reactor. This reaction will take place in a coiled tubular flow reactor, determined to be the most feasible choice after taking into account factors such as heat of reaction and production rate per year.

As MFA is not made commercially, the team will assess the feasibility of large-scale production of this monomer. Feasibility analysis of the lab scale process showed this product cannot be made for a profit, thus the team has performed two optimization studies. The first examined multiple arrangements of the reaction system to reduce capital and utility costs. The second involved sketching the process to produce GM, a specialty chemical from DOW, to act as a support when setting up a lower cost – high volume contract, which would reduce the raw material costs. The economics were then compared to alternative methods of reducing styrene emissions to determine the success of converting this process to industrial scale.

Table of Contents

1.	Introduction	1
1.1.	Background.....	1
1.2.	Production of MFA	2
1.3.	Future MFA Plant.....	3
2.	Design Bases.....	4
2.1	Project Scope	4
2.1.1	Products.....	4
2.1.2	Production Rate.....	4
2.1.3	Continuous Tubular Flow Reactor	4
2.1.4	Raw Materials.....	4
2.1.5	Utilities.....	4
2.1.6	Plant Location.....	4
2.2	Location of Plant	5
2.3	Size of Plant	5
2.4	Storage and Shipment of Products	6
2.5	Raw Materials	6
2.6	Major Design Assumptions	6
2.7	Ancillaries Design	7
3.	Process Description	8
3.1	MFA Monomer Process Description	8
3.1.1	Section 110 – Lauric Acid Feed Preparation	10
3.1.2	Section 120 – GM Feed Preparation.....	11
3.1.3	Section 130 – AMC-2 Catalyst Feed Preparation.....	12
3.1.4	Section 200 – Reactor	12
3.1.5	Section 300 – Packaging.....	14
3.2	MFA Monomer Stream Tables	15
3.2.1	MFA Process Stream Tables	15
3.3	Reactor Process Description	16
3.3.1	Reaction Kinetics	16
3.3.2	Continuous Tubular Flow Reactor	17
3.3.3	Finishing Tanks – Complete Conversion	20
3.3.4	Alternative Reactors Considered	24
	Straight Batch.....	24
	Semi-batch.....	29
	In summary:.....	30
	CTFR – tubular reactor submersed in vessel	30
	CTFR – jacketed tubular reactor	31
	Straight Batch	32
	Semi – Batch.....	32
4.	Process Flow Diagrams	33
4.1	MFA Process Stream Tables.....	33
5.	Equipment List	35
5.1	MFA Plant Tank, Vessel, and Reactor List.....	35

5.2	<i>MFA Plant Pump List</i>	35
5.3	<i>MFA Plant Heat Exchanger List</i>	35
6.	Operating Requirements	35
	Utilities	36
	Catalyst	36
	Labor Requirements: Operating + Maintenance	36
7.	Process Safety Considerations	38
7.1	<i>Reactor Safety</i>	38
7.2	<i>Catalyst Safety</i>	38
7.3	<i>Lauric Acid Safety</i>	38
7.4	<i>Glycidyl Methacrylate Safety</i>	39
7.5	<i>Utility Loss Concerns</i>	40
8.	Environmental and Waste Considerations	41
8.1	<i>Environmental Concerns</i>	41
8.2	<i>Waste Concerns</i>	42
8.1.1	<i>Material Intensity</i>	42
8.1.2	<i>Energy Intensity</i>	42
8.1.3	<i>Water Intensity</i>	43
8.1.4	<i>Toxic Release</i>	44
8.1.5	<i>Greenhouse Gases</i>	44
9.	Economics	46
9.1	<i>Introduction</i>	46
9.2	<i>Overview of the Market for MFA Monomer</i>	47
	Market Size:	47
	Market Competition:	47
	Alternative 1: Reducing Styrene Emissions with Specialized Equipment:	49
	Alternative #2: Replacing Styrene with MFA - Setting the price for MFA	50
	Alternative #3: Replacing Styrene with Current Monomer	52
9.3	<i>Economic Analysis for 5 Million Pound Per Year Plant</i>	53
	Capital Costs	53
	Manufacturing Costs	54
	15-Year Cash Flow Analysis	58
	MFA Production Scale-up	60
9.4	<i>Economic Analysis for 5 Million Pound Per Year Plant</i>	61
	Capital Costs	61
	Manufacturing Costs	62
	15-Year Cash Flow Analysis	64
	Sensitivity Analysis	66
	Monte Carlo Analysis	68
	Summary of Acceptable GM and MFA price combinations	71
	Effect of Percent Emission Reduction on IRR	74
9.5	<i>Conclusions and Recommendations</i>	75
10.	Calculations	77
10.1.	<i>Centrifugal Pumps</i>	77
10.2.	<i>Positive Displacement Pumps</i>	81
10.3	<i>Shell and Tube Heat Exchangers</i>	82

10.4	<i>Storage Tanks</i>	84
10.5	<i>Continuous Tubular Reactor with Heat Exchange</i>	86
10.6	<i>Coiled CTFR</i>	91
10.7	<i>Batch Reactor</i>	92
10.8	<i>Utilities for Storage Tanks</i>	95
10.9	<i>Cash Flow Analysis (Year 1)</i>	97
10.10	<i>Cost of Manufacturing</i>	100
10.11	<i>Capital Costs</i>	101
10.12	<i>MFA Price</i>	102
10.13	<i>Sensitivity</i>	103
10.14	<i>Hess's Law</i>	104
10.15	<i>Decanter Size</i>	106
10.16	<i>Probability Distributions for Monte Carlo</i>	108
11.	<i>Process Optimization</i>	110
12.	<i>Conclusions and Recommendations</i>	116
13.	<i>Important Data and Properties Used</i>	119

Figure list for Design Report

Figure or Table Number	Description
Figure 3.1	Preliminary flow diagram
Table 3.1	List of streams on the PFD
Table 3.2	Detailed list of streams on the PFD
Table 3.3	PFR Temperature and catalyst wt% versus reactor length and residence time
Figure 3.2	Temperature profiles of reactor system for first 10 minutes
Table 3.4	Temperature and exit conversion versus reaction time
Table 3.5	Sensitivity of Heat Transfer Coefficient versus Heat of Reaction at 80 C, 0.1 wt% catalyst, 16 operating hours per day
Table 3.6	Number of reactors needed to meet yearly production for worst-case heat transfer/heat of reaction
Table 4.1	List of streams on the PFD.
Table 4.2	Detailed list of streams on the PFD.
Table 4.3	Detailed list of stream on the PFD.
Table 5.1	MFA tank vessel and reactor list
Table 5.2	MFA pump list
Table 5.3	MFA heat exchanger list
Table 6.1	Cooling water utilities
Table 6.2	Chilled water utilities
Table 6.3	Steam utilities
Table 6.4	Power utilities
Table 6.5	Catalyst utilities
Figure 9.1	Total expenditures for first 15 years of operation.
Figure 9.2	Breakdown of fixed capital investment (Gross root cost of each piece of equipment)
Figure 9.3	Breakdown of direct manufacturing costs
Figure 9.4	Breakdown of fixed manufacturing costs
Figure 9.5	Breakdown of general manufacturing expense
Figure 9.6	IRR as a function of production
Figure 9.7	Total expenditures for first 15 years of operation
Figure 9.8	Breakdown of direct manufacturing costs
Figure 9.9	Cumulative present worth discount rate at 12%
Figure 9.10	After tax cash flow (Present value) discount rate at 12%
Figure 9.11	IRR sensitivity study.
Figure 9.12	Contributors to IRR
Figure 9.13	IRR cumulative frequency
Figure 9.14	Correlation of IRR with MFA and GM prices
Figure 9.15	IRR as a function of percent reduction in styrene emissions
Figure 9.16	Conclusive economic analysis numbers
Figure 10.1	Arkema cost estimating spreadsheet

Figure 10.2	Average utilities cost
Figure 11.1	Temperature profiles of reactor system for adiabatic operation versus tempered water @ 110°C, 90 L/min
Figure 11.2	Temperature profiles of reactor system and tempered water streams for entire length of reactor.

Figure list for GM Appendix

Figure or Table Number	Description
Table 2.1	Heuristics used for GM plant
Figure 3.1	GM Flowsheet, Diagram Part 1
Figure 3.2	GM Flowsheet, Diagram Part 2
Table 4.1	GM Process Stream Table
Table 4.2	GM Process Stream Table
Table 5.1	GM tank vessel and reactor list
Table 5.2	GM pump list
Table 5.3	GM heat exchanger list
Figure 6.1	Utility usage summary for GM plant
Figure 6.2	Utility cost summary for GM plant
Figure 6.3	Waste treatment cost summary for GM plant
Figure 6.4	Catalyst cost summary for GM plant
Figure 7.1	Wastewater minimization in GM plant
Figure 7.2	Epichlorohydrin minimization in GM plant
Figure 8.1	Equipment summary for GM plant
Figure 8.2	Manufacturing cost summary for GM plant
Figure 8.3	Distribution of unit costs to produce GM
Figure 9.1	Diethyl ether data (Felder)
Figure 9.2	Stream 20 data

1. Introduction

1.1. *Background*

Vinyl ester resins are used to coat and protect many products, from surfboards and boats to military tanks and helmets. Due to the high viscosity of monomers a diluent must be added to the formulation to allow these resins to adapt to various liquid molds. Recently, the Federal Environmental Protection Agency (EPA) passed legislation to tackle the issue of hazardous emissions from composite manufacturing. Throughout the process of composite manufacturing and through the lifetime of the product, volatile organic compounds (VOC) are emitted to the environment. By passing the “National Emissions Standards for Hazardous Air Pollutants: Reinforced Plastic Composites Production”, new emissions standards to combat this pollution have been enacted. Styrene, a diluent often used in vinyl ester resins, is classified as a possible human carcinogen (EPA website) and was specifically targeted in this bill as a hazardous air pollutant (HAP). This has created a need in the market for a product that can act as a diluent, but will not release VOCs or be classified as a HAP.

This focus of this project is the production of a methacrylated fatty acid (MFA) monomer, which is one prospective product that could replace styrene in VE resins. It has been shown that when MFA replaces up to 55% of the styrene in the vinyl ester resin, the resulting product displays equal thermo-mechanical behavior at acceptable viscosities. Using MFA in place of styrene has many benefits, besides trying to comply with the new EPA-set standards. The monomers have low

Written By: CM
Checked: TS

1

volatilities and are globally sustainable since one of the reactants to produce MFA comes from a natural source. By using a mix of MFA and styrene in the vinyl ester resin, VOC emissions can be reduced by 50 to 85 percent, depending on the amount of styrene replaced.

The target market for MFA is the surfboard and military industries. Potential uses are to coat surfboards, Army tactical vehicles, dorsal covers and Navy rudders, to name a few. In order for the target industries to accept this product, MFA must have a comparable price to what is currently on the market.

1.2. *Production of MFA*

The monomer is made in a continuous process that uses a coiled tubular flow reactor (CTFR). The feed into the reactor will be a one to one stoichiometric ratio of lauric acid to glycidyl methacrylate (GM). In addition to these chemicals, a catalyst, AMC-2, will be used to increase the reaction rate. While at higher temperatures the reaction can complete faster, it also poses a risk for a runaway polymerization, which would cause the reactants to gel, in turn shutting down the operation to allow the coils to be replaced. The reactor will be submerged in a baffled vessel containing cooling water in order to remove the exothermic heat generated and to maintain safe operating temperature for the reactor. Once the reaction has completed, the product will be emptied from the reactor and sent to intermediate tankage. No purification step is needed as the reaction is allowed to fully complete, but the MFA will contain trace amounts of catalyst and impurities from GM. However, since these impurities

Written By: CM
Checked: *IB*

2

are below 2wt%, it will not affect its performance, safety or positive effect on the environment.

1.3. *Future MFA Plant*

The plant is sized for 5,000,000 pounds of production of the MFA monomer per year. While this is a small production rate, it is noted that MFA is new to the market and is not yet accepted in the industry. Since there can be no data collected or market studies performed to see how consumers will react to this change in product, it was decided that the plant should start small in order to not lose any profit by creating a large supply that has no demand. However, it is expected that the production rate and the plant's capacity will quickly increase as MFA takes the place of styrene.

Vinyl ester resin sales reach \$2 billion annually and are sold at a price of \$2.50 per pound (SRI). If MFA monomer takes the place of 25 percent of the styrene used in these resins, there is a potential market for a production of 200 million pounds of MFA monomer per year. Although consumers will be unfamiliar with the product, once on the market, the reliability of the MFA monomer can be demonstrated.

Written By: CM
Checked: TS

2. Design Bases

2.1 Project Scope

2.1.1 Products

- Methachrylated Fatty Acid (MFA)
- 98% Purity

2.1.2 Production Rate

- 5 MM lb/yr of MFA
- Operating Hours:
 - 5 days/week
 - 2 – 12 hour shifts/day
 - 50 weeks/year
- 100% conversion of reactants

2.1.3 Continuous Tubular Flow Reactor

- MFA is produced in a Continuous Tubular Flow Reactor that is approximately 1000 meters long with 25.4 mm (1-inch nominal) diameter tubing.
- Tubing is coiled and submersed in a two stage cooling water vessel
- 77 minute residence time
- CFTR will operate at 110°C, and with 0.25 wt% AMC-2 catalyst

2.1.4 Raw Materials

- Lauric Acid – 99.9% pure
- Glycidyl Methacrylate (GM) – 98% pure
- AMC-2 catalyst – homogeneous

2.1.5 Utilities

- Assumed available outside batter limits
- Cooling Water available at 33 C, max return at 40.6 C
- Low Pressure Steam available at 2 bar
- Chilled Water available at 10 C, max return at 16 C
- Power received from local grid

2.1.6 Plant Location

- Freeport, TX
- Close proximity to Dow's GM plant.

Written By: CM
Checked: TS

2.2 Location of Plant

The plant will be located in Freeport, TX with access to railroads, highways and boat transportation. This location also provides tax incentives such as full, partial, or deferred tax abatements; infrastructure grants; Tax Increment Financing; Enterprise Zones; energy cost abatement and tax credits (Sears). There are also benefits for being located in a Foreign Trade Zone, such as custom duty deferral (Sears). This location is near one of the largest manufacturing sites for GM in the United States and therefore will reduce the cost of transportation for that material. Also, because shipments can be received more frequently, the storage capacity can be reduced to save on capital costs. Lastly, as an added benefit to this location, Freeport has over 7,500 acres open for development (Sears), so future growth of the plant is possible.

2.3 Size of Plant

The production rate will be 5 million pounds of MFA per year, made in one CTFR. However, the final goal of MFA is to capture 40% of the VE resin market by replacing 25% of the styrene in the resins. The start-up plant will only need two acres of land for its production, storage and auxiliary facilities. While this may seem like a small plant for start-up, MFA will be new to the market and there is a big risk in selling this product. Therefore, the plant will run small.

Written By: CM
Checked: *TS*

5

2.4 Storage and Shipment of Products

The effluent of the CTFR will be sent to one of two intermediate storage tanks for a minimum of three hours. This will allow the reaction to go to completion and cool before being transferred to a final storage tank, which will be maintained at room temperature. The MFA can then be loaded into drums or totes.

2.5 Raw Materials

- Lauric Acid
 - Delivered in heated tanker trucks every Saturday
 - 99.9% purity
- Glycidyl Methacrylate
 - Transported from Dow's local plant twice per week
 - Received in totes
 - Stored in separate building
- AMC-2 Catalyst
 - Shipped from Aerojet Chemicals
 - Received in 55 gal drums
 - Chromium (III) based

2.6 Major Design Assumptions

- Legislation will pass reducing the maximum amount of styrene emissions in composite manufacturing before construction of an MFA plant is complete.
- A study estimate has been done to determine the cost of manufacturing for GM. This was done in order to use as a bargaining chip with DOW to enter into a low cost-high volume contract.
- The plant is in Texas to be near the site from which the GM will be bought.

Written By: CM
Checked: JS

- 98% purity of MFA is sufficient to achieve desired performance.
- The heat of reaction is -230 J/g.
- The plant will not be self-sufficient.

2.7 *Ancillaries Design*

- The first building will consist of the production and packaging space as well as the control center.
- Loading docks will be located at the building that houses the production and packaging spaces. There will be two loading docks, one for deliveries and one for shipments.
- A raw materials storage section will also be connected to the production and packaging building. This storage building will hold both the catalyst and lauric acid.
- GM will be stored separately from the production building. This is because of the risk GM has to auto-polymerize if stored incorrectly. This building will consist of three walls made of blowout panels and one open wall. This open wall will be facing away from the rest of the plant in case of any accident.
- The third and final building will consist of office units for administration employees, a reception area and a small cafeteria for employees to take their breaks in.

Written By: CM
 Checked: *ts*

7

3. Process Description

3.1 MFA Monomer Process Description

The MFA monomer plant has five sections associated with the process:

- Section 110 - Lauric Acid Feed Preparation
- Section 120 - GM Feed Preparation
- Section 130 - AMC-2 Catalyst Feed Preparation
- Section 200 - Reactor
- Section 300 - Product Packaging

The following is a general preliminary flow diagram for the process. The main equipment needed and the overall flow of the process is shown. More detailed flow diagrams for each section can be found in the PFD section of this report.

Written By: NHG
Checked: MPM

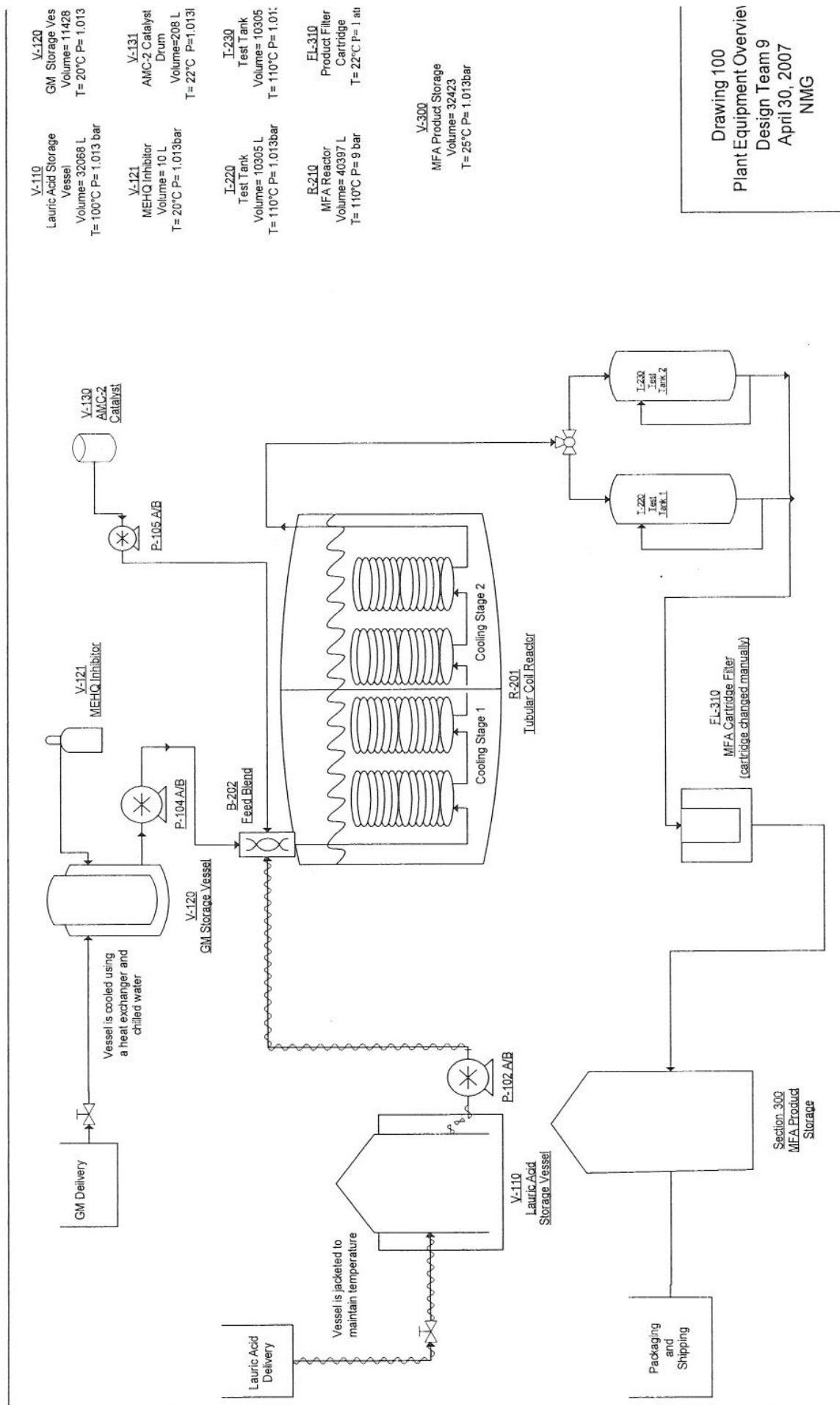


Figure 3.1 – Preliminary flow diagram

Written By: NMG
Checked: MFM

Drawing 100
Plant Equipment Overview
Design Team 9
April 30, 2007
NMG

MFA monomer is a product of the reaction between lauric acid and glycidyl methacrylate using a homogeneous chromium based catalyst. A tubular reactor in a 110°C temperature bath will be used to produce the MFA monomer. The lauric acid, glycidyl methacrylate, and AMC-2 catalyst will be fed into an in-line static mixer by metering pumps. The static mixer will then blend the reactants and charge the reactor. The mixture will react along the length of the reactor and the exotherm will be controlled by the temperature bath. The exiting product from the reactor goes to finishing tanks, so the reaction can fully complete and quality control can be enacted to ensure the product is within specification. After ensuring quality of the MFA monomer, the product will be pumped through a filter and held in a storage tank. The product will be packaged directly from the storage tank into drums and totes. This plant will require low-pressure steam, nitrogen, chilled water, and poor air. To examine this process in more detail each section is described thoroughly below.

3.1.1 Section 110 – Lauric Acid Feed Preparation

Lauric acid is a solid at room temperature, but for this process it is needed in its liquid form. Therefore, the acid will be delivered by a heated tanker truck and kept above its melting point of 45°C. To ensure that the reactor feed system is not affected, it needs to come in on a weekend when the reactor is not operating.

A centrifugal pump, P-101, will be used to transport the lauric acid from the truck to the storage vessel (V-110). The piping that connects the delivery truck to the tank will be heat traced to keep the acid liquefied. The storage tank for the

Written By: NMG
Checked: MFM

10

lauric acid will be heated to 100°C by an external heating jacket. Low-pressure steam is the heating medium for the jacket. The steam flow-rate for the heat up to 100°C will be approximately 700 std L/min for 24 hours. A temperature controller will be used to measure the temperature inside the vessel and correct for the amount of steam needed by regulating the steam control valve. After 24 hours, the flow-rate will be reduced to an average rate of 300 std L/min to keep the tank at 100 C.

When charging the reactor, a flow controller will be used to meter the correct flow-rate of lauric acid. This flow controller will be connected to a volume ratio controller that will be at a 1.65:1 set point of lauric acid to GM. While in storage, nitrogen will be used to maintain an inert atmosphere in V-110 because of lauric acid's low flash point. The lauric acid will be discharged from the storage tank by a metering pump and excess will be sent back into the tank through a pump around loop. The lauric acid will mix with the GM and catalyst before entering the reactor. Lauric acid will be stored at 100°C, so when it is mixed with the other reactants the reactor feed will be approximately 60°C.

3.1.2 Section 120 – GM Feed Preparation

Glycidyl Methacrylate (GM) will be delivered in totes and a centrifugal pump, P-103 will be used for unloading the GM into the jacketed storage tank (V-120). To maintain stability and prevent homo-polymerization, GM requires an inhibitor. A replenishing tank of hydroquinone mono methyl ether (MEHQ) inhibitor (V-121) will thus be present on site. If homo-polymerization occurs, the temperature within the storage tank will increase and set off an alarm, which will

Written By: NMG
Checked: MFM

11

alert the operator to add MEHQ inhibitor. The concentration of MEHQ in the storage tank should never exceed 100ppm.

In addition, V-120 will be padded with poor air and kept at 20°C by circulating chilled water through an external double pipe heat exchanger, E-120. Flow and ratio controllers will meter the correct amount of GM to be charged to the reactor by adjusting a regulating valve. A metering pump will feed the regulating valve as well as re-circulate the GM in the storage tank. Before entering the reactor, GM will be mixed with catalyst and the heated lauric acid and will enter the reactor at 60°C.

3.1.3 Section 130 – AMC-2 Catalyst Feed Preparation

AMC-2 catalyst exists as a liquid at room temperature and will be delivered in 55-gallon drums. Two 55-gallon drums will be connected to a metering pump, P-105, by a three-way valve. The drums will be on weighing scales and a weight controller will operate the pump to send the correct amount of catalyst to the reactor. The weight controller will also serve to alert operators when a new drum is needed. The AMC-2 catalyst will mix with the 100°C lauric acid and GM in the static mixer before entering the reactor.

3.1.4 Section 200 – Reactor

The reactor consists of four units of coiled tubing, which are submerged in two, individually controlled temperature baths, contained within one cylindrical vessel. The feed to the reactor unit comes from an inline static mixer at 60°C.

The feed stream will leave the mixer and enter the first reactor stage, and come

Written By: NMG
Checked: MFM

12

into contact with 110°C tempered water. This water, in addition to the reaction exotherm, will allow the reactants to reach the reacting temperature, 110°C. As the reactants progress down the reactor, each feed will enter and exit each coil at the bottom. After the reactor flow exits the second coil pack, it will enter the second bath, at which the tempered water temperature will be fresh at 110.5°C. The reaction will continue through the remaining two coil packs and then exit the vessel.

The tempered water will be circulated through the loop by two centrifugal pumps, P-201, and P-203, and will flow co-currently with the reactor coils with the aide of baffles. The water will act as a heat sink for the heat of the reaction, and the temperature of the water will follow the reactor temperature closely. The temperature of the tempered water entering each of the two stages will be controlled continuously through the external loop with cooling water from E-202/E-203, and intermittently with direct low-pressure steam injection. The heat exchangers have been oversized to accommodate more than 100% additional cooling if needed. Direct steam injection is only necessary during start-up, which will be once per week.

If the reaction reaches temperatures at which it cannot be controlled by cooling water, polymerization will occur and damage the product. Polymerization will cause the product to “gel” and the temperature rise will be significant. The plant will have extra coil packs in stock as a replacement if the product gels.

Written By: *NMG*
Checked: *MFm*

13

The reactor product will exit the coils and flow into one of two completion tanks, T-220 or T-230. A three-way valve will be employed to regulate the filling of each tank. Each tank is sized to contain the daily production rate of MFA. The tank temperature will be controlled continuously at 110°C, with an external pump-around, by pumping MFA with P-203/P-204 through a double pipe heat exchanger, E-220/E-230. After the first tank is full, production will be routed to the second tank. The product in the first tank will continue reacting until completion, which will take approximately 30 minutes, at 110°C. After the reaction goes to completion, the tank will be cooled down to 40°C. This will take about 1.5 hours. During this cool down period, quality control measures will take place to ensure that the product is within specification. Once the product quality is assured, the product will be loaded to the final product tank, V-300. When the second tank is full, production will be routed to the first tank and the procedure will be repeated.

3.1.5 Section 300 – Packaging

The product in the completion tanks will be pumped by P-203/P-204 into the final storage tank, V-300, which is capable of holding three days capacity. After exiting the completion tanks, the product will pass through a cartridge filter to remove any impurities that could build up in the system.

Totes and 55-gallon drums have been selected for the packaging medium and will be connected to the same packing pump by a three-way valve. The packaging pump, P-301 will be connected to the storage tank and will deliver

product to the drums or totes. A shipping dock will be located near the packaging area for ease of product loading.

3.2 MFA Monomer Stream Tables

3.2.1 MFA Process Stream Tables

Table 3.1 – List of streams on the PFD.

Stream No.	Description
101a	LA offsite receiving to inlet of LA offsite pump
101	LA offsite pump to LA tank
102	LA pump to pump-around loop
103/201	LA to reactor
104	From offsite receiving to inlet of GM offsite pump (outside)
105	GM offsite pump to GM tank (outside)
106	GM tank to GM metering pump (outside)
107	GM pump to pump-around loop
108/202	GM to reactor
109	AMC-2 to metering pump
110/203	AMC-2 reactor feed pump to reactor
204	Combined Stream to reactor
205	Reactor Outlet to Completion Tanks
206	Completion Tank 1 pump-around
207	Completion Tank 2 pump-around
208	MFA to Product Storage
301	MFA to Product Storage
302	MFA to Packaging (drum/ tote)

Table 3.2 – Detailed list of streams on the PFD.

Stream No.	101a	101	102	103/201	104	105
Temperature (°C)	50.00	50.00	100.00	100.00	20.00	20.00
Pressure (barg)	0.10	1.43	0.10	23.21	0.10	1.97
Vapor Fraction	0.00	0.00	0.00	0.00	0.00	0.00
Mass flow (kg/min)	912.00	912.00	3.52	3.52	912.00	912.00
Mole Flow (mol/min)	4560.00	4560.00	17.61	17.61	6415.76	6415.76
Volumetric Flow (L/min)	1048.28	1048.28	4.05	4.05	876.92	876.92
Component mole flow (mol/min)						
Lauric Acid	4560.00	4560.00	17.61	17.61		
Glycidyl Methacrylate					6287.44	6287.44
MEHQ Inhibitor					0.64	0.64
GM Impurities					127.67	127.67
AMC-2 Catalyst						
Methacrylated Fatty Acid						

Written By: MPM
Checked: NMG

Stream No.	106	107	108/202	109	110/203	204
Temperature (°C)	20.00	20.00	20.00	25.00	25.00	100.00
Pressure (barg)	0.10	23.48	23.48	0.10	23.46	20.00
Vapor Fraction	0.00	0.00	0.00	0.00	0.00	0.00
Mass flow (kg/min)	2.55	2.55	2.55	0.01	0.01	6.08
Mole Flow (mol/min)	17.97	17.97	17.97	0.04	0.04	35.63
Volumetric Flow (L/min)	2.45	2.45	2.45	0.01	0.01	6.51
Component mole flow (mol/min)						
Lauric Acid						17.61
Glycidyl Methacrylate	17.61	17.61	17.61			17.61
MEHQ Inhibitor	0.00	0.00	0.00			0.00
GM Impurities	0.36	0.36	0.36			0.36
AMC-2 Catalyst				0.04	0.04	0.04
Methacrylated Fatty Acid						

Stream No.	205	206	207	208	301	302
Temperature (°C)	100.00	25.00	25.00	25.00	25.00	25.00
Pressure (barg)	2.00	0.10	1.98	1.98	1.98	1.98
Vapor Fraction	0.00	0.00	0.00	0.00	0.00	0.00
Mass flow (kg/min)	6.08	6.08	6.08	6.08	6.08	6.08
Mole Flow (mol/min)	18.90	18.02	18.02	18.02	18.02	18.02
Volumetric Flow (L/min)	6.51	6.51	6.51	6.51	6.51	6.51
Component mole flow (mol/min)						
Lauric Acid	0.88					
Glycidyl Methacrylate	0.88					
MEHQ Inhibitor	0.00	0.00	0.00	0.00	0.00	0.00
GM Impurities	0.36	0.36	0.36	0.36	0.36	0.36
AMC-2 Catalyst	0.04	0.04	0.04	0.04	0.04	0.04
Methacrylated Fatty Acid	16.73	17.61	17.61	17.61	17.61	17.61

3.3 Reactor Process Description

3.3.1 Reaction Kinetics

The production of MFA involves the liquid phase reaction between lauric acid (LA) and glycidyl methacrylate (GM). The overall reaction rate is aided by the presence of AMC-2, a Chromium III based homogeneous catalyst. Due to the high cost of the catalyst the environmental concerns, being that it is

Written By: MFM
 Checked: NMG

Chromium based, 0.25 wt% is the maximum amount used. In addition, if more than 0.25 wt% were to be used, MFA would not be able to make the 98% purity target. The reaction follows the rate equation shown below:

$$(3.1) \quad -r_E = \frac{d[E]}{dt} = 1.16 \times 10^8 e^{\left(\frac{-7657}{T}\right)} [E]^{0.79} [C]^{0.88}$$

Here, [E] is the dimensionless concentration (iE_t/E_0) of GM and [C] is the amount of AMC-2 catalyst present in wt%. Also, T is the operating temperature, in Kelvin, for the reactor. The time reference for this rate law is minutes.

For MFA production, the heat of reaction has been estimated to be -230 J/g. This highly exothermic value is a result of the opening of an epoxide ring during reaction. The value was derived from several laboratory experiments.

3.3.2 Continuous Tubular Flow Reactor

The selection of the continuous tubular flow reactor stems from the advantages of continuous operation. This enables the plant to be easily scaled up to higher production levels and saves costs for operating labor. The reaction takes place continuously over 77 minutes of residence time in approximately one thousand meters of coiled tubing contained within two separate water- filled compartments. Each coil consists of 25.4 mm (1 in.) tubing coiled to a diameter of 1 m with 25.4 mm (1 in.) of spacing between successive loops. Since the reaction requires 1000 meters of tubing, the vessel contains four coil “packs” to

ensure the vessel's height is reasonable for providing easy removal. Furthermore, each pack can be individually disconnected and removed from the vessel for replacement.

The reactor coils will be constructed of 25.4 mm (1 in.) 316 SS nominal pipe providing additional heat transfer area compared to a typical batch vessel. While shell and tube heat exchangers have heat transfer coefficient benefits over jacketed vessels, the coiled reactor design does not have the same flow characteristics due to the relatively low flow-rate of water through the tanks. Therefore, the overall heat transfer coefficient for the water/reactor coil is estimated at 60 Btu/hrft²F (TBWS, 343). While this value is comparable to the heat transfer coefficient for a jacketed vessel, there is, due to a significant improvement in total surface area, better heat transfer.

Table 3.3 – PFR Temperature and catalyst wt% versus reactor length and residence time

Temperature	Exit	Volume	Catalyst	Length of 1" tube	Residence Time
Degrees C	Conversion	L	wt%	ft	Min
100	0.95	1409	0.25	8296	232
100	0.95	8307	0.09	48895	1369
110	0.95	825	0.25	4854	136
110	0.95	2026	0.09	11927	334

****Note:** Values in table 3.3 are pre-optimization numbers.**

As can be seen in Table 3.3 above, in order for the PFR to have a reasonable volume and residence time, it needs to be operated at temperatures above 110°C with a catalyst concentration greater than or equal to 0.25 wt%.

Written By: MFM
Checked: NAG

18

Lauric acid can undergo an oxidation reaction above 130°C, so the PFR will operate at the least 15°C, greater than 10% of 130°C, below that limit as a safety factor. For the MFA product to remain at its intended purity of 98%, the process will operate at a maximum of 0.25 wt% catalyst to maximize the rate of reaction.

The reactor is designed to operate at 110°C, and because the reactants will not be stored at that temperature, they must be heated to the reaction temperature. Due to stability concerns, GM will be stored at 20°C to prevent homo-polymerization. Lauric acid will be stored above 50°C because its melting point is 45°C. There have been three identified options for this problem: mix all reactants at their minimum storage temperatures and heat the reacting mixture using the MFA product; heat up the GM/LA each in one exchanger using the MFA product; or utilize the tempered water and additional reactor length.

This heat integration is not necessary for such a small plant and this system would require additional controls for startup. Through cost comparisons, adding length to the reactor is the cheapest alternative rather than a pre-heat exchanger. Thus, the reactor is designed to allow the heat of reaction as well as the tempered water system to quickly heat the reactants to the proper operating temperature of 110°C.

Figure 3.2 below, is a comparison of using tempered water to heat the reactor feed and keeping the coil exposed to air. The total flow-rate for the reactants is 6.51 L/min @ 60°C, while the flow-rate of the tempered water is 90 L/min @ 110°C. Due to the contact with the comparatively higher flow, and

Written By: MFM
Checked: NMJ

19

warmer tempered water, the reacting fluid is able to heat up to 110°C within 3 minutes of residence time.

The optimization of the design of this reactor system, such as temperatures, flow-rates, sizing will be discussed further in the optimization section of this report.

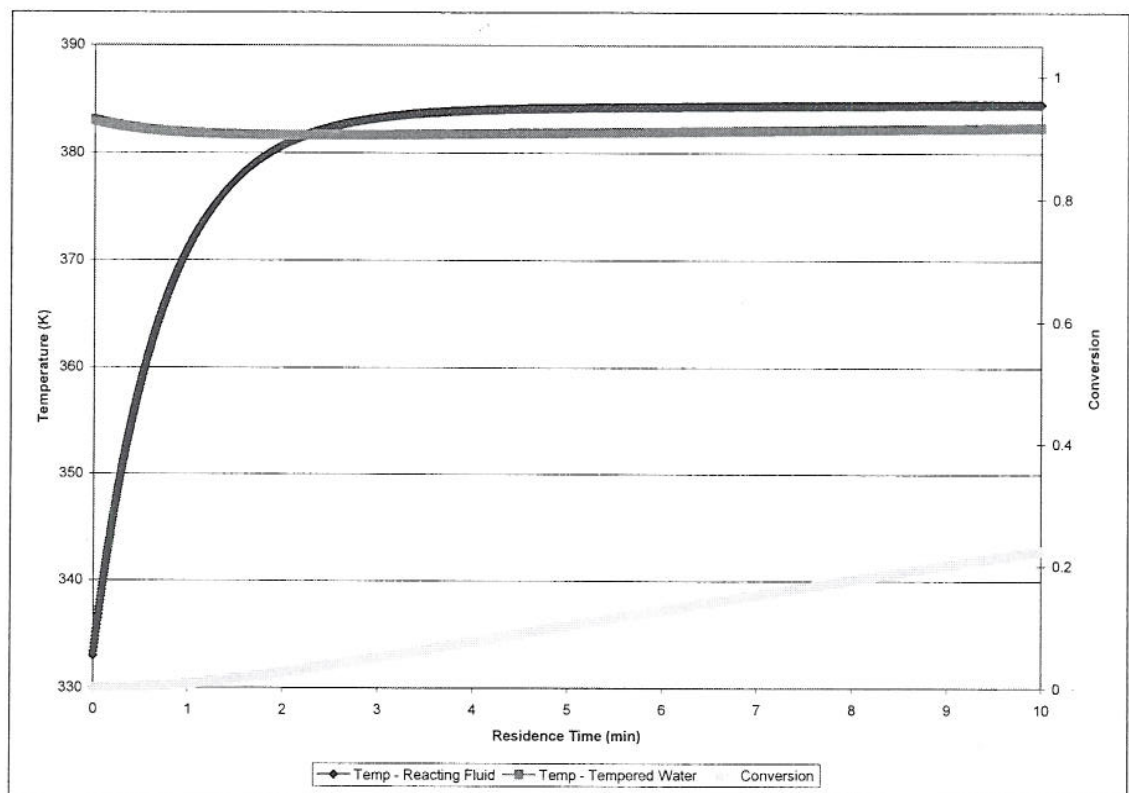


Figure 3.2 – Temperature profiles of reactor system for first 10 minutes

3.3.3 Finishing Tanks – Complete Conversion

One method to reduce the amount of residence time is to decrease the required exit conversion from the reactor. The material exiting the reactor can be transferred to a holding tank, either T-220 or T-230, where the reaction can

Written By: MFM
Checked: NMG

continue until completion. There is less control needed for these tanks as the rate of heat released is significantly reduced at this level of conversion.

This was intended for batch operation, since the designed batch reactors had to be run at lower temperatures compared to a tubular reactor. However, this optimization still applies to the continuous setup, because the concentrations of the reactants are so low, the remaining 5% will take an additional 575 meters and 47 minutes of residence time. In Table 3.4 below, values for the time required for a batch to complete are compared to exit conversion.

Table 3.4 – Temperature and exit conversion versus reaction time.

Temperature	Catalyst Present	Exit Conversion	Time Required to Reach Target Conversion
°C	wt%		min
70	0.15	0.8	310
70	0.15	0.9	414
70	0.15	0.95	504
80	0.15	0.8	164
80	0.15	0.9	220
80	0.15	0.95	268
90	0.15	0.8	90
90	0.15	0.9	121
90	0.15	0.95	147

Written By: MPM
Checked: NMG

The operation chosen is to have the reaction go to 95% completion, where the heat generated will be less than at 80%, and the reaction will need less time to finish. The two intermediate tanks, T-220, T-230 are a necessity in the base case because the plant needs intermediate tanks for proper testing of the final MFA product before it is loaded to the final tank.

For 95% conversion to 100%, at 110°C, it takes 30 minutes for a full tank to go to complete conversion. After this, the external pump-around/heat exchanger will cool the MFA down to 40°C. This will take an additional 1.5 hours. Due to the two extra hours needed once the tank is full and the required testing, two tanks will be needed, each capable of holding 24 hours of production. MFA will then be transferred to the final tank, which can offload to totes or drums and go out for delivery.

Another option, which can be used in addition to the previous operation, is to load the final product from the CTFR directly to 55-gallon drums, at 95% conversion. If the drums are loaded at 25°C, it will take about 12 days to complete the reaction. For those 12 days material can be staged in a temperature controlled warehouse and then be shipped out to customers. MFA has not been produced on this scale before and this will be a target area to improve operation down the road after production has stabilized. At this time, loading product directly into drums is too risky, because there is no easy way to correct the drums which do not meet specifications due to small errors in stoichiometric ratios.

The assumption cannot be made that the product coming out of the PFR will be in the correct stoichiometric proportions for the reaction to complete in

Written By: MFM
Checked: NMJ

22

the drums. Until this is known, all products for one day of production will feed into one storage tank. This is to ensure that if everything is fed into the reactor at the correct proportions, they will still be maintained in the final tankage. This is all done to ensure product quality.

Continuous Tubular Flow Reactor Concerns

The flow reactor operates continuously 24 hours a day for 5 days a week at a relatively low flow-rate, 6.51 L/min, to meet total yearly demand of 5,000,000 pounds. It was previously thought that the viscosity would be increasing from 1 cP to 10 cP as the reactants flow through the reactor and react to form MFA. Since the reaction is occurring within a 1 in. pipe, the resulting Reynolds number, based on that viscosity, flow-rate, and pipe diameter comes to 800, and laminar flow. If the reactant flow within the reactor is laminar, then that would mean that there could be dispersion effects and unequal conversion along the tube diameter resulting in significantly less overall conversion. This could be remedied with inline static mixers, but making sure that the flow is turbulent would save a significant investment.

The breaking point between turbulent flow and the transitional flow between laminar and turbulent is when the MFA viscosity at 110°C is 1.7 cP. So, if the viscosity of MFA at 110°C is less than 1.7 cP, the flow will be turbulent. Based on recent experimental data from Dr. Palmese, MFA viscosity at 110°C is below 1 cP.

Written By: MFM
Checked: NMS

23

A similar concern has been expressed over the flow regime of the tempered water in the reactor. The reactor design, as well as the tempered water flow-rates, has been optimized to ensure that the tempered water flow will be turbulent. Because of the uncertainty of the tempered water streams, and to be conservative with heat transfer, a heat transfer coefficient of $280 \text{ W/m}^2\text{K}$ has been selected.

3.3.4 Alternative Reactors Considered

A plant of this type has never been designed before, so the process to research the reactor went through many stages. Different alternatives considered were a batch operation, semi-batch, varying continuous designs, and finally, the coiled reactor. The information contained within this section is here for reference purposes and show the progress throughout the project in order to identify the pros and cons of each design along the way.

Straight Batch

The first reactor design considered was the “straight” batch reactor in which the total quantity of reactants and catalyst are fed into a vessel, which react until completion. After the reaction continues to the desired conversion, the contents of the reactor are transferred out of the reactor to the next stage and fresh reactants are fed. This operation was considered first because it mimicked the method used in the lab scale experiments of this product.

Written By: MFM
Checked: NMG

24

The first hurdle of designing the batch reactor was the fact that the reaction to form MFA is highly exothermic, and it is very important to maximize heat transfer. Unfortunately, batch reactors have difficulty adding or removing heat. Typically, batch reactors can utilize a cooling jacket with a variable flow of cooling water, or a pump-around can be used to circulate the reactor contents through an external heat exchanger to remove heat. Because of the risk of forming hot spots in an external circuit, external heat exchange would not be an option. Another method to aide in heat removal is to use a heat carrier, which acts as a heat sink and slows the temperature increases. The final product can only have limited impurities and inert compounds, so this option is not feasible. The remaining practical method is to utilize a cooling water jacket.

The reactor radius determines the available heat transfer area of the cooling jacket. The area, $A \propto r^2$, so in effect the volume, $V \propto r^3$. As a result the area to volume ratio, $A/V \propto 1/r$, and as r increases, A/V decreases. From the processing viewpoint, as the radius is increasing the ability to remove heat is decreasing relative to the increasing reacting volume. As a safety factor to mitigate risk, batch reactors should be sized below the maximum volume based on the A/V ratio for the reaction and reaction conditions so that the heat generated will never exceed the ability to remove heat. If the maximum size is not big enough to support the required production rate, several batch reactors will need to be used to meet yearly production requirements because of this minimum reactor size. The analysis on this concept of a maximum reactor size for production of MFA is explained below.

Written By: MFM
Checked: NMG

25

In table 3.5, a comparison between the effect of the uncertainty of the overall heat transfer coefficient and the heat of reaction versus the maximum size of the reactor from those conditions is shown. For operation at 80 C and 0.1 wt% catalyst present, the time for 95% conversion of the reactants is 436 minutes. The maximum diameter and volume is determined from a given U and heat of reaction. In the fourth row, both values are the normal estimated values, 60 Btu/hrft²F and -900kJ/mol respectively. These conditions allow a maximum diameter of 0.77 meters or a volume of 717 liters. From the reaction time required of 436 minutes and for a 16-hour operating day for 5 days/week, 50 weeks per year, the size of the batch must be 2343 liters. To meet this production requirement, there must be more than 3.3 reactors.

If the accuracy of the heat transfer coefficient or the heat of reaction is off by 20%, the amount of reactors needed becomes more infeasible from the normal case of 3.3 reactors to 11.2 reactors needed.

Table 3.5 – Sensitivity of Heat Transfer Coefficient versus Heat of Reaction at 80 C, 0.1 wt% catalyst, 16 operating hours per day

	Delta from Estimated Value		Reaction Time Required		Max Diameter	Max Size Reactor	Production needed	# of Maximum Sized Reactors
	Overall Heat Transfer Coefficient	Heat of reaction	minutes	hours	m	L	–L/batch	to meet production
Worst Case	-20%	+20%	382.63	6.38	0.51	208	2343	11.2
↓	Normal	+20%			0.63	393	2343	6.0
	-20%	Normal			0.65	431	2343	5.4
	Normal	Normal			0.77	717	2343	3.3
Best Case	+20%	-20%			0.815	850	2343	2.8

To be conservative, the reactor sizing must be considered under the worst conditions, which is when the heat of reaction is 20% greater than estimated, and the overall heat transfer coefficient is 20% lower than estimated. This is reasonable because the heat of reaction has not been verified in the laboratory and the overall heat transfer coefficient can be affected if there is a build up of film on the walls of the reactor. As can be seen in table 3.7, the maximum reactor diameter is 0.51 m giving a max volume of 208 L. To meet yearly production, 11.2 reactors would be needed. As temperature is lowered, and catalyst concentration is reduced, reactor sizes can be larger. The operating

Written By: MFM
Checked: NMG

temperature decrease outweighs the time increase by having a slower reaction.

As can be seen below in table 3.6, if temperatures are reduced to 60°C and the catalyst is present at 0.1 wt%, three 1692 L reactors must be used to meet yearly production.

Table 3.6 – Number of reactors needed to meet yearly production for worst-case heat transfer/heat of reaction

Temperature	Catalyst	Reaction Time Required		Max Diameter	Max Size Reactor	Production needed	# of Maximum Sized Reactors
C	wt%	minutes	hours	m	L	L / batch	to meet production
						One Reactor	
80	0.15	267.80	4.46	0.36	73	1562	21.3
80	0.1	382.63	6.38	0.51	208	2343	11.2
60	0.15	985.38	16.42	0.71	562	4686	8.3
60	0.1	1407.88	23.46	1.025	1692	4686	2.8

This exercise with batch reactors shows that to meet yearly demand the MFA plant would need several larger reactors that operate at medium to low temperatures. The cost of building several large reactors greatly outweighs the benefit of having versatile production.

In addition, while batch reactors utilize agitators to keep the solution well mixed, it is possible for hot spots to occur in the reactor, and lead to overheating at those areas of the reactor. This overheating could lead to a runaway polymerization that, at the very least, could destroy the entire batch of MFA, and at most start a violent reaction that could lead to an overpressure of the reactor.

Written By: MPM
Checked: NMG

28

Higher capital funds are needed to buy several larger reactors and because of the possibility for hot spots to occur due to non-uniform mixing, the CTFR was selected over batch operation.

However, because the previously assumed heat of reaction, -900 kJ/mol is approximately 10 times higher than has been identified recently in the lab, the previous arguments hold only in theory. However, if the heat of reaction is larger than the new estimate, the thinking provided above points to continuous operation.

Furthermore, as will be explained in the economics section, for the plant to be profitable it will need to be sized to 55 MM lb.yr. Batch operation is tougher to scale up, requiring purchasing of additional reactors and hiring of more operators. Due to the advantages of continuous operation, and the ease of scalability, the final decision was to stay with the tubular coiled reactor.

Semi-batch

After it was determined that the straight batch configuration would not work, an alternative was identified, the semi-batch reactor, also known as fed-batch. In this operation, all of the lauric acid and AMC-2 catalyst are batch fed into the reactor. When the reaction is scheduled to start, GM will be dripped in at a constant flow-rate until the intended conversion is completed. The benefit of this operation is that less GM will be present at all times, so the propensity for the reaction to auto-polymerize or runaway is significantly less than straight batch. However, this comes at a cost of time. Semi-batch operation on average

Written By: MFM
Checked: NMG

29

takes 30% longer to reach the same conversion as straight batch. This is because the concentration of GM will be so low in the reactor, and thus the reaction rate will be lower. Because the reaction rate is lower, the reactor will need to be operated at a higher temperature to meet the same batch times as the straight batch configuration. But because the semi-batch reactor utilizes the same cooling water jacket, it has the same disadvantages for scaling up production from a heat transfer standpoint.

This led to the consideration of a continuous flow reactor, due to the great heat transfer characteristics and higher heat transfer area. However because the heat of reaction was over-estimated, like the straight batch, the semi-batch reactor would also work.

In conclusion, the continuous tubular flow reactor was selected over the batch reactors mainly because of the simplicity of the everyday production. There are no schedules for loading and unloading like in batch, so the operators must make sure everything is running at the right flow-rates/temperatures. Because of this, the requirements for operators are significantly less.

In summary:

CTFR – tubular reactor submersed in vessel

- Advantages
 - Cheapest of compared reactor designs – no jacketed piping
 - Continuous operation – great for medium to large scale production
 - Great heat transfer

Written By: MFM
Checked: NAL

30

- Can operate at higher temperatures, lower residence time
- Upgraded temperature control over jacketed PFR
- 1" tubing gives higher Re number – turbulent flow
- Disadvantages
 - 1000 feet of 1" tubing
 - Relatively more complex temperature control configuration
 - Not as versatile as batch for small scale production
 - Higher catalyst wt% is needed
 - Maintaining correct stoichiometric flows to the reactor

CTFR – jacketed tubular reactor

- Advantages
 - Lower price in comparison to batch
 - Continuous operation – ideal for medium to large scale production
 - Ideal heat transfer
 - Can operate at higher temperatures
 - For 3" pipe, 200 meters of length
- Disadvantages
 - Non-ideal at low flow-rates
 - Parabolic velocity profile
 - Dispersion effects
 - Poor temperature control
 - Large lengths of jacketed pipe - expensive

Straight Batch

- Advantages
 - Versatile for small scale production
 - Good temperature control
- Disadvantages
 - Agitation will never provide perfect mixing and hot spots may develop
 - Expensive compared to continuous tubular reactors
 - All reactants at once could create a safety concern for GM

Semi – Batch

- Advantages
 - GM dripped in reduces auto polymerization and runaway reaction safety concern
 - Versatile for small scale production
 - Good temperature control
- Disadvantages
 - Need to operate at higher reactor temperatures to match straight batch reaction times
 - Agitation will never provide perfect mixing and hot spots may develop
 - Poor heat transfer limits size of reactor
 - Expensive compared to continuous tubular reactors

4. Process Flow Diagrams

4.1 MFA Process Stream Tables

Table 4.1 – List of streams on the PFD.

Stream No.	Description
101a	LA offsite receiving to inlet of LA offsite pump
101	LA offsite pump to LA tank
102	LA pump to pump-around loop
103/201	LA to reactor
104	From offsite receiving to inlet of GM offsite pump (outside)
105	GM offsite pump to GM tank (outside)
106	GM tank to GM metering pump (outside)
107	GM pump to pump-around loop
108/202	GM to reactor
109	AMC-2 to metering pump
110/203	AMC-2 reactor feed pump to reactor
204	Combined Stream to reactor
205	Reactor Outlet to Completion Tanks
206	Completion Tank 1 pump-around
207	Completion Tank 2 pump-around
208	MFA to Product Storage
301	MFA to Product Storage
302	MFA to Packaging (drum/ tote)

Table 4.2 – Detailed list of streams on the PFD.

Stream No.	101a	101	102	103/201	104	105
Temperature (°C)	50.00	50.00	100.00	100.00	20.00	20.00
Pressure (barg)	0.10	1.43	0.10	23.21	0.10	1.97
Vapor Fraction	0.00	0.00	0.00	0.00	0.00	0.00
Mass flow (kg/min)	912.00	912.00	3.52	3.52	912.00	912.00
Mole Flow (mol/min)	4560.00	4560.00	17.61	17.61	6415.76	6415.76
Volumetric Flow (L/min)	1048.28	1048.28	4.05	4.05	876.92	876.92
Component mole flow (mol/min)						
Lauric Acid	4560.00	4560.00	17.61	17.61		
Glycidyl Methacrylate					6287.44	6287.44
MEHQ Inhibitor					0.64	0.64
GM Impurities					127.67	127.67
AMC-2 Catalyst						
Methacrylated Fatty Acid						

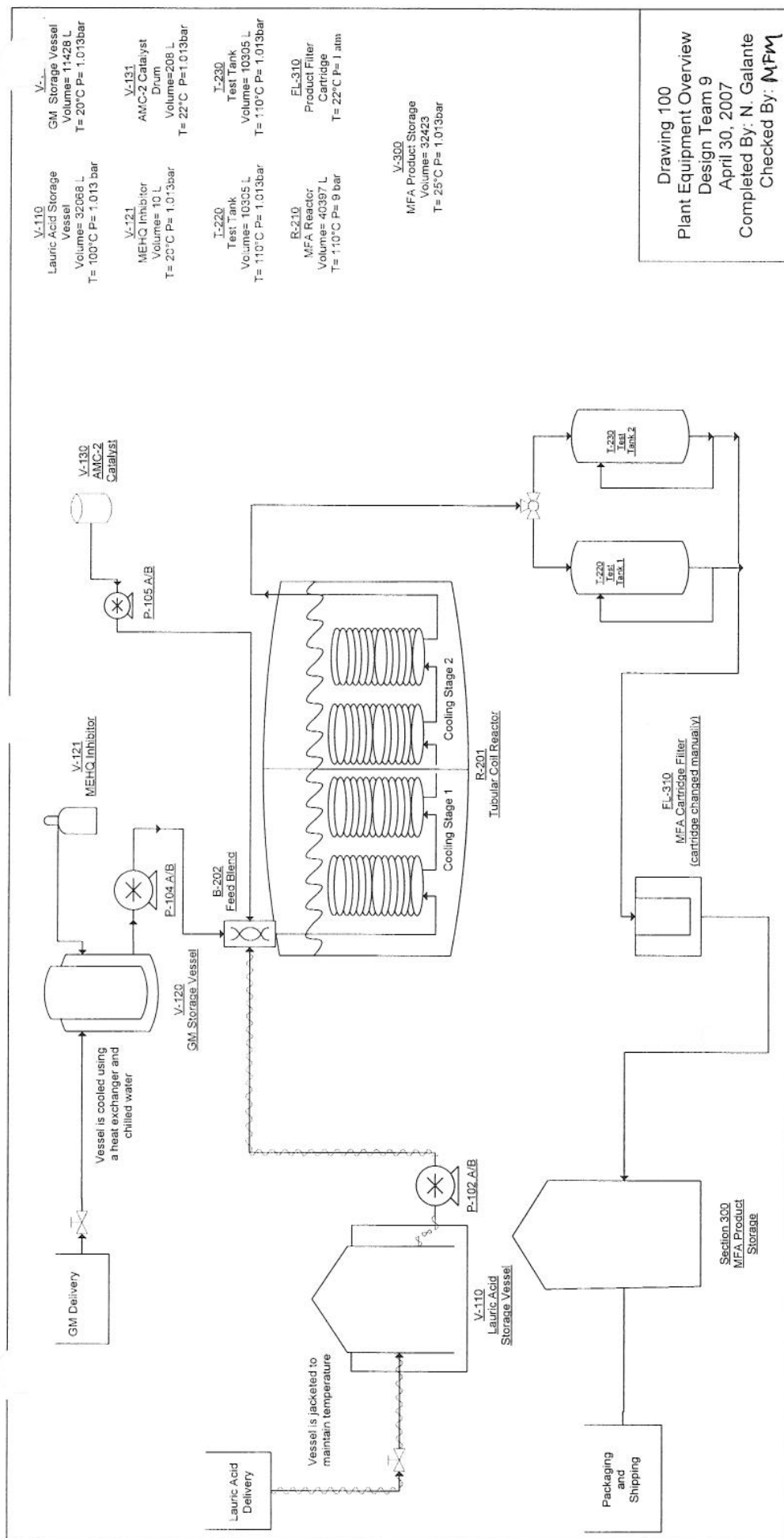
Written By: MFM
Checked: NMG

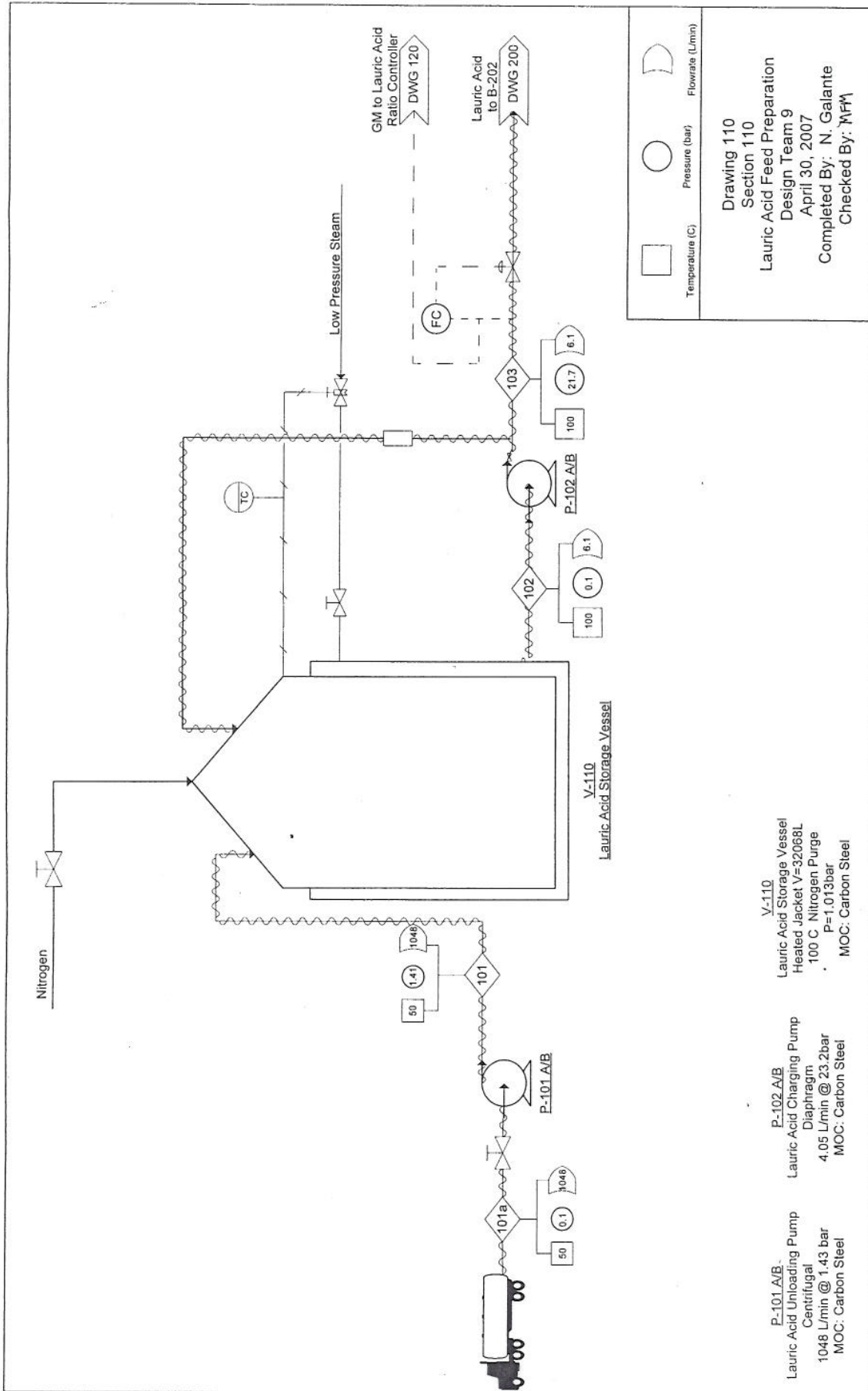
Stream No.	106	107	108/202	109	110/203	204
Temperature (°C)	20.00	20.00	20.00	25.00	25.00	100.00
Pressure (barg)	0.10	23.48	23.48	0.10	23.46	20.00
Vapor Fraction	0.00	0.00	0.00	0.00	0.00	0.00
Mass flow (kg/min)	2.55	2.55	2.55	0.01	0.01	6.08
Mole Flow (mol/min)	17.97	17.97	17.97	0.04	0.04	35.63
Volumetric Flow (L/min)	2.45	2.45	2.45	0.01	0.01	6.51
Component mole flow (mol/min)						
Lauric Acid						17.61
Glycidyl Methacrylate	17.61	17.61	17.61			17.61
MEHQ Inhibitor	0.00	0.00	0.00			0.00
GM Impurities	0.36	0.36	0.36			0.36
AMC-2 Catalyst				0.04	0.04	0.04
Methacrylated Fatty Acid						

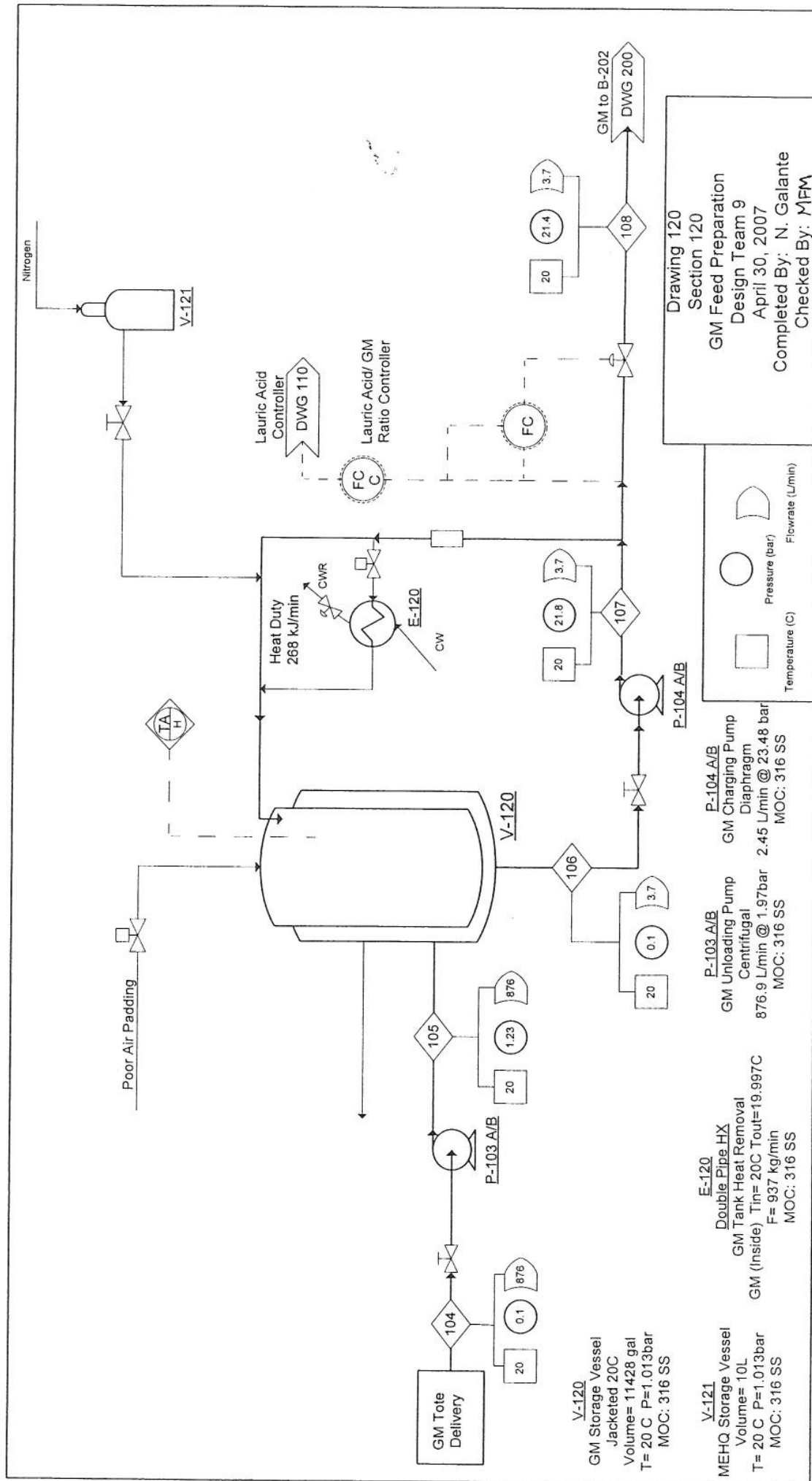
Table 4.3 – Detailed list of streams on the PFD.

Stream No.	205	206	207	208	301	302
Temperature (°C)	100.00	25.00	25.00	25.00	25.00	25.00
Pressure (barg)	2.00	0.10	1.98	1.98	1.98	1.98
Vapor Fraction	0.00	0.00	0.00	0.00	0.00	0.00
Mass flow (kg/min)	6.08	6.08	6.08	6.08	6.08	6.08
Mole Flow (mol/min)	18.90	18.02	18.02	18.02	18.02	18.02
Volumetric Flow (L/min)	6.51	6.51	6.51	6.51	6.51	6.51
Component mole flow (mol/min)						
Lauric Acid	0.88					
Glycidyl Methacrylate	0.88					
MEHQ Inhibitor	0.00	0.00	0.00	0.00	0.00	0.00
GM Impurities	0.36	0.36	0.36	0.36	0.36	0.36
AMC-2 Catalyst	0.04	0.04	0.04	0.04	0.04	0.04
Methacrylated Fatty Acid	16.73	17.61	17.61	17.61	17.61	17.61

Written By: MFM
Checked: NAL







Drawing 120

Section 120

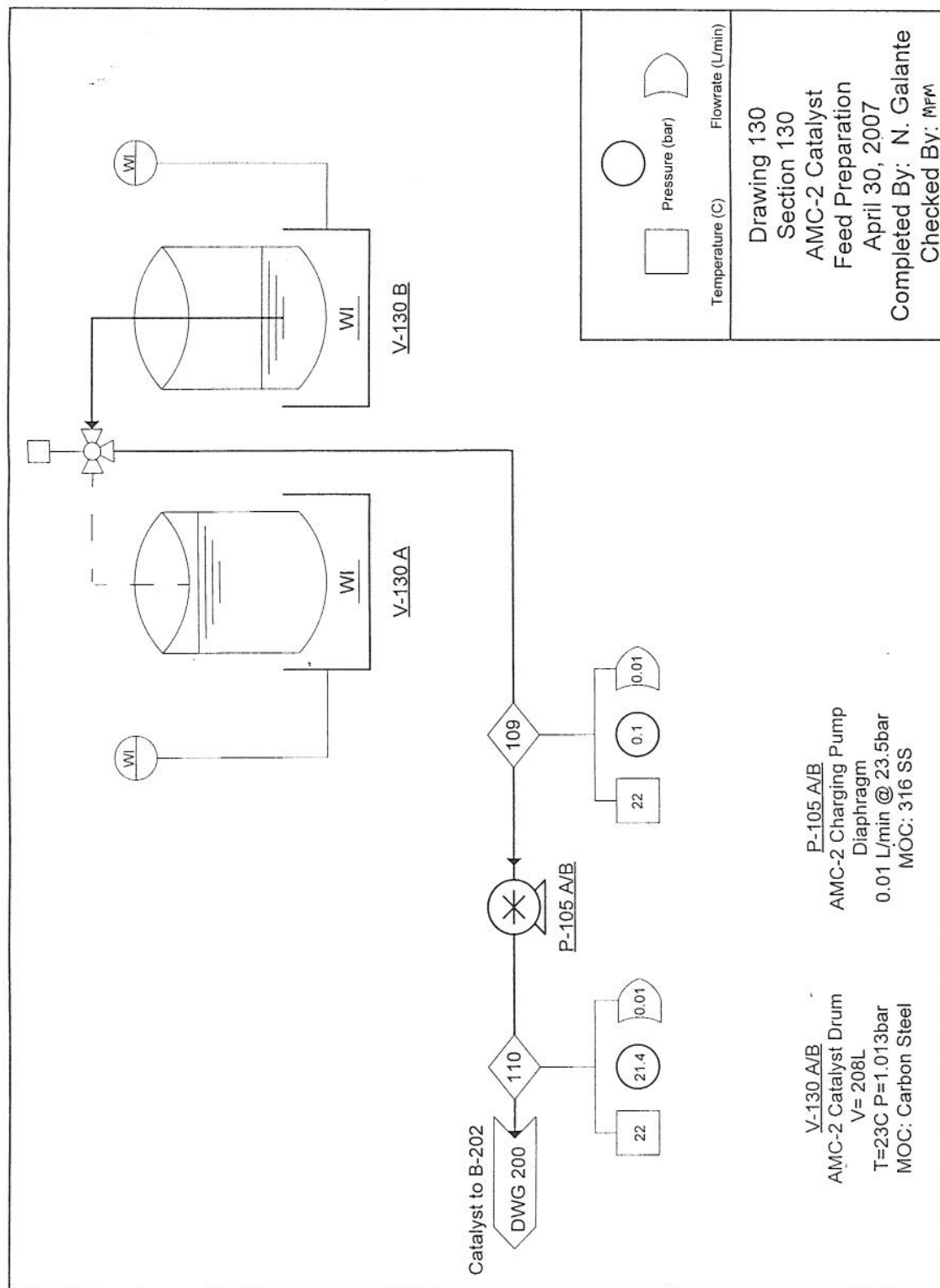
GM Feed Preparation

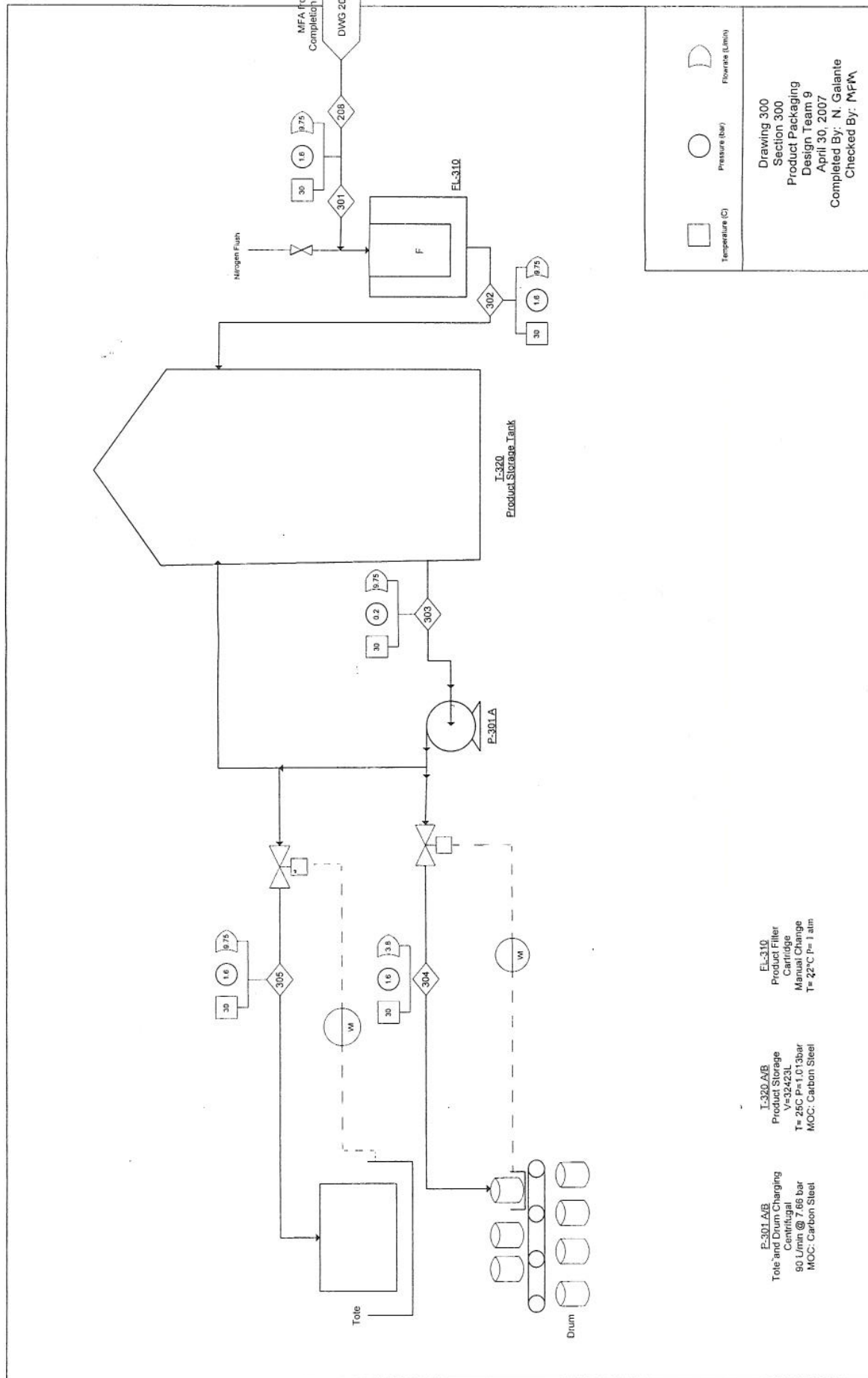
Design Team 9

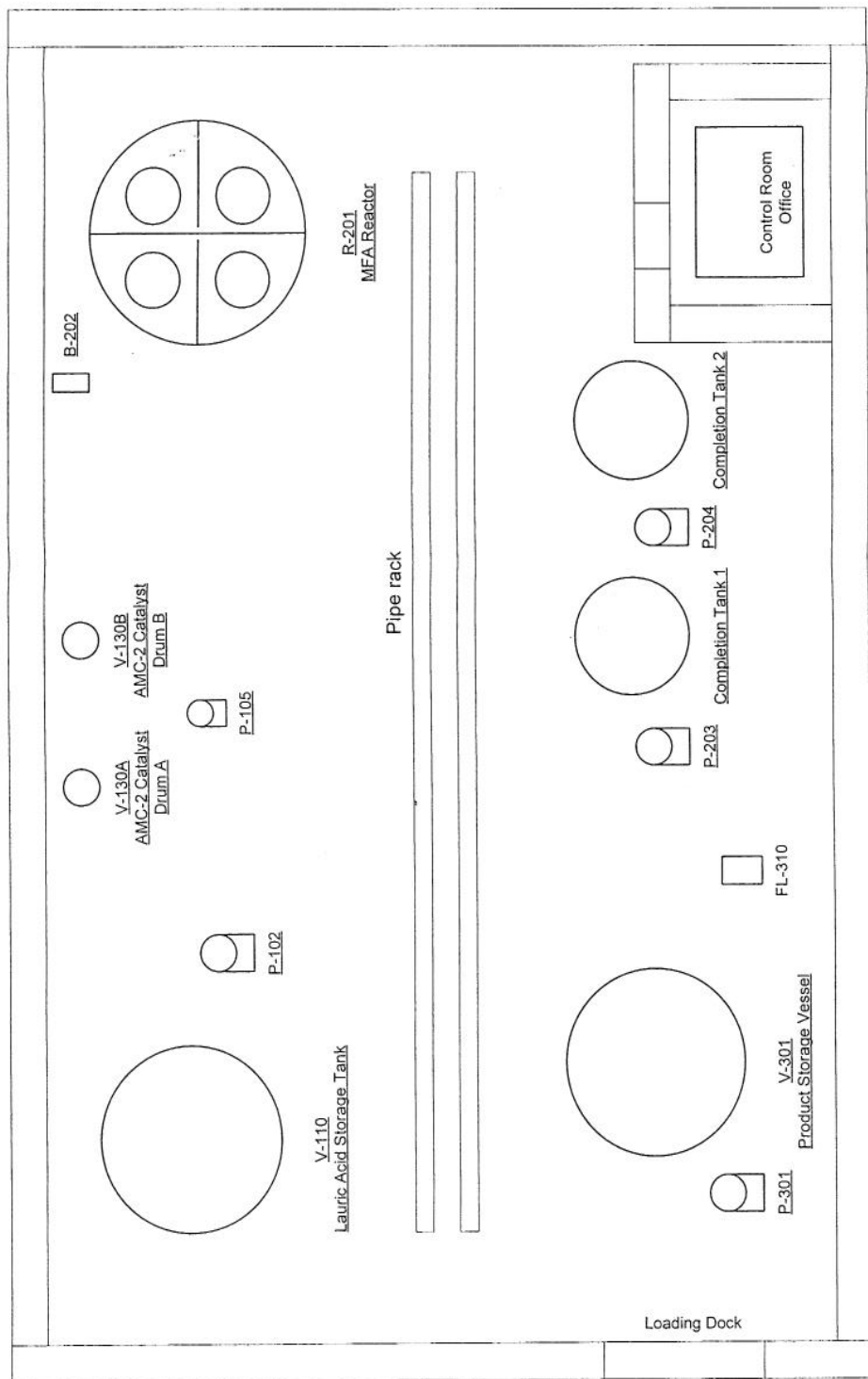
April 30, 2007

Completed By: N. Galante

Checked By: MFM



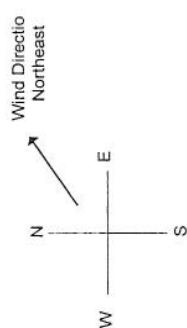
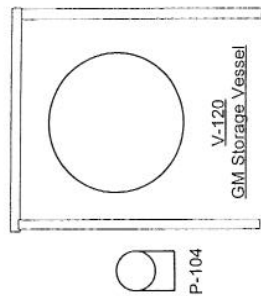




Office Building

Top (Aerial) View

Scale: 1 inch= 1 foot



Site Plan
MFA Plant
Design Team 9
April 30, 2007
Completed By: N. Galante
Checked By: MFM

5. Equipment List

5.1 MFA Plant Tank, Vessel, and Reactor List

Table 5.1 – MFA tank vessel and reactor list

Equipment ID	Description	MOC	Size (liters)	Temperature, C	Pressure, bara
V-110	Lauric Acid Storage Vessel	Carbon Steel	32068	100	1.013
V-120	GM Storage Vessel	316L SS	11428	20	1.013
V-121	MEHQ Storage Vessel	316L SS	10	20	1.013
V-130	AMC-2 Drum	316L SS	208	23	1.013
R-201	Tubular Reactor	316L SS	40397	110	9.0
T-220	Completion Tank 1	316L SS	10305	110	1.013
T-230	Completion Tank 2	316L SS	10305	110	1.013
V-300	Product Storage	Carbon Steel	32423	25	1.013

5.2 MFA Plant Pump List

Table 5.2 – MFA plant pump list

Pump ID	Description	Type	MOC	Duty (kW)	Flow (L/min)	Pout (barg)
P-101	Lauric Acid Unloading	Centrifugal	Carbon Steel	4.44	1048.3	1.43
P-102	Lauric Acid Reactor Charge	Diaphragm	Carbon Steel	0.86	4.05	23.21
P-103	GM Unloading	Centrifugal	316L SS	5.17	876.9	1.97
P-104	GM Reactor Charge	Diaphragm	316L SS	0.53	2.45	23.48
P-105	AMC-2 Reactor Charge	Diaphragm	316L SS	0.002	0.01	23.46
P-201	Tempered Water Loop	Centrifugal	316L SS	1.37	90.0	7.66
P-202	Tempered Water Loop	Centrifugal	316L SS	1.37	90.0	7.66
P-203	Test Tank 1 Pump Around	Centrifugal	316L SS	5.68	936.7	1.98
P-204	Test Tank 2 Pump Around	Centrifugal	316L SS	5.68	936.7	1.98
P-301	Product Packaging	Centrifugal	Carbon Steel	0.54	90.0	2.06

5.3 MFA Plant Heat Exchanger List

Table 5.3 – MFA Heat exchanger list.

Exchanger ID	Inside	Outside	Inside Inlet Temp	Tube Flowrate	Inside Outlet Temp	Outside Inlet Temp	Outside Flowrate	Outside Outlet Temp
E-120	GM	Chilled Water	20 C	877 L/min	19.997 C	10 C	3.72 L/min	15.6 C
E-202	Tempered Water	Cooling Water	110 C	90 L/min	111 C	33.3 C	150 L/min	40.6 C
E-203	Tempered Water	Cooling Water	117 C	108 L/min	107 C	33.3 C	150 L/min	40.6 C
E-220	MFA	Cooling Water	110 C	937 L/min	97.3 C	33.3 C	459 L/min	40.6 C
E-230	MFA	Cooling Water	110 C	937 L/min	97.3 C	33.3 C	459 L/min	40.6 C

Written By: MFM
Checked: NMW

6. Operating Requirements

Utilities

Table 6.1 – Cooling water utilities

Cooling Water					
		To MFA T-220/T-230	To E-202	To E-203	Total
Normal Flow	L/min	459.4	24.9	15.0	499.3
Max Flow	L/min	489.5	108	108	705.5
Total Weekly Flow	L	4934608	251225	150735	5336568

Table 6.2 – Chilled water utilities

Chilled Water		
		To GM V-120
Normal Flow	L/min	3.7
Max Flow	L/min	9.3
Total Weekly Flow	L	65701

Table 6.3 – Steam utilities

Steam					
		To LA V-110	To Reactor S1	To Reactor S2	Total
Normal Flow	std L/min	321.4	0	0	321.4
Max Flow	std L/min	728.6	12.43	12.43	753.4
Total Weekly Flow	L	3826015	2327	2327	3830668

Table 6.4 – Power utilities

Power		
Pumps	kW	25.5

Catalyst

Table 6.5 – Catalyst utilities

AMC-2 Catalyst		
		To Reactor
Normal Flow	L/min	0.008
Total Weekly Flow	L	56

Labor Requirements: Operating + Maintenance

Due to the small capacity of the continuous, automated process designed for production of MFA, the demand for workers is low. It is estimated that two operators

Written By: MFA
Checked: NMA

will be sufficient to handle daily responsibilities such as loading catalyst, checking temperature gauges, and guiding product packing.

The low number of capital equipment allows our plant to operate without a full time maintenance person. Contractors will perform all repairs that are needed in the plant. To allow for two to three days for shutdown, to wait for contractors, an inventory of two weeks will be kept on site.

Since this plant produces a new chemistry, it is recommended to have both a chemist and an engineer to handle trouble-shooting issues, which have not been revealed in laboratory experiments. For costing purposes, a chemist has been priced at 30% above an operator, whereas an engineer is priced at 70% above an operator.

Written By: NMS
Checked: MPM

37

8. Environmental and Waste Considerations

8.1 Environmental Concerns

The largest environmental concern for this process comes from the risk of a chemical spill or fire. While the process will take place inside a building, any spill can run the risk of contaminating the environment depending on its severity. In order to prepare for such an event, the facility will be supplied with various barriers and dikes that can be placed on the ground to halt the spill. These spill barriers can affix to different surfaces, from smooth concrete to asphalt, and can stop the spill from spreading inside or outside the building. Should the spill go outside, any barrier that can be fixed to asphalt is placed around gutters or drains so as to stop the chemical from getting into the environment and water systems. These barriers will also help contain the spill until a team can reach the site and properly handle the situation.

There is also a danger of triggering GM into a runaway polymerization reaction. While the storage facility for GM is being built to safely handle a fire and protect the employees, the environment must also be taken into consideration. Should this reaction occur, an employee would immediately call the local fire department to put out the fire. The building will also be equipped with smoke sensitive sprinklers that will be set off to control the fire before the fire department comes.

The catalyst that is to be used in this reaction, AMC-2, is a chromium (III) based catalyst. Due to chromium's toxicity, the amount of catalyst used is to be kept at a low level since it will remain in the final product. The way to lower

Written By: CM
Checked: NMG

41

the level of catalyst is to have the reaction run at the highest temperature possible, yet in a safe manner. The amount of catalyst used per batch is .25 weight percent, leaving only trace amounts of catalyst in the product.

8.2 Waste Concerns

To focus on minimizing waste, five environmental metrics were. These metrics measured were material, energy, and water intensity, toxic release and greenhouse gases. Using these measurements, the process was then refined to minimize the waste and environmental harm the process causes.

8.1.1 Material Intensity

Material intensity is measured by the following equation

$$(8.1) \frac{\text{Mass of Raw Materials} - \text{Mass of Products}}{\text{Output}}$$

where output is the mass of primary products, sales revenue of primary products or revenues less expenses. For the process, the reaction goes to completion, meaning that there are no reactants left at the end of a batch, just products. This makes the numerator zero, thus the material intensity for this process is zero. While MFA is being made to alleviate toxic emissions on the environment, the process to make it is environmentally friendly, too, in not wasting any of the raw materials needed.

8.1.2 Energy Intensity

To calculate the energy intensity, the following equation was used

Written By: CM
Checked: NMK

42

$$(8.2) \frac{\text{Total Energy per year}}{\text{Output}}$$

where again, the output is the mass of primary products, sales revenue of primary products or revenues less expenses. The total energy used by the plant is found in the utility tables, and this number is used to calculate the energy intensity. The energy used in this plant comes from the pumps, which use 25.5 kW of energy per week. The plant runs fifty weeks a year, so the total amount of energy is 1275 kW per year. This number converted into Btu/h is 4350300 Btu/h. This number is then put into equation 8.2 and the numbers for energy intensity are .87 Btu/h/MM lb of MFA, .75 Btu/h/\$ of revenue and -.096 Btu/h/\$ of cash flow. These numbers are very low, showing a good correlation between energy consumed and the amount of product produced. Since the plant requires so little equipment, it helps contribute to its environmentally friendly benefits.

8.1.3 Water Intensity

To calculate the water intensity, the following equation was used,

$$(8.3) \frac{\text{Mass of Fresh Water Consumed}}{\text{Output}}$$

where the mass of fresh water consumed is taken from the utility tables. This number is the sum of cooling water and chilled water, which is 270113450 L/year. This is plugged into equation 8.3 and the results are 54.02 L/MM lb of MFA, 46.57 L/\$ revenue and -5.94 L/\$ revenue less expenses. These numbers show that the process does use water in a larger

proportion than what is produced. However, some choices that affected the amount of water used, such as placing the GM tank in a separate building, were done to keep the process safe. Therefore, the amount of water used can be justified.

8.1.4 Toxic Release

To calculate the toxic release, the following equation is followed

$$(8.4) \frac{\text{Mass of Toxic Pollutant in Emissions and Waste}}{\text{Output}}$$

Since none of the raw materials are wasted in this process, and the reactants used are not listed on the EPA Toxic Chemical Release Inventory (EPA Website), the numerator for this equation is zero. Therefore, the toxic release factor is also zero for this process, again displaying how environmentally friendly the process to produce MFA is.

8.1.5 Greenhouse Gases

The last factor to be calculated is the release of greenhouse gases, which is done with the following equation.

$$(8.5) \frac{\text{CO}_2 \text{ Equivalents from Fuel, Emissions, Waste}}{\text{Output}}$$

The CO₂ equivalent for the fuel, emissions and waste was calculated through correlations presented in senior design. These correlations helped correlate the energy, water, steam and other utilities to the amount of carbon dioxide release. Only correlations relevant to the process were considered. After these numbers were calculated, they were plugged into equation 8.5 and were found to be .000331 tons CO₂/MM of MFA,

.00285 tons of CO₂/\$ revenue and -.000036 tons of CO₂/\$ revenue less expenses. These numbers show just how little greenhouse gases are released in this process. The correlation between the amount of product, revenue and cash flow produced is very low, showing again how this process doesn't harm the environment, one of the great benefits in trying to get MFA onto the market.

Written By: CM
Checked: NMG

45

9. Economics

9.1 Introduction


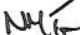
This section of the report will describe the economic analysis for the production of MFA as outlined earlier, and the techniques used to arrive at these predictions.

The section opens with a brief overview of the market for the MFA monomer, including the total size of the market, the potential competition, and the reasoning behind the chosen production level.

Next, a preliminary economic analysis is performed for an MFA plant producing 5 million pounds of monomer per year as was the designed in detail in this report. This analysis will include the approach used to calculate the capital costs as well as the manufacturing costs for the plant designed. Furthermore, a 15-year economic forecast will be presented for this plant, which reveals its negative financial position in the base case. From this data, the team has suggested an increase in production to 55 million pounds per year to achieve profitability.

The 55 million pound per year plant will then be presented in detail along with the assumptions made in its calculation. Along with the 15-year economic analysis, a sensitivity study will be performed to quantify the risk involved for VertaChem, the MFA business proprietor, to invest in this venture.

Finally, preliminary conclusions will be made to summarize the data presented.

Written By: 
Checked: 

46

9.2 Overview of the Market for MFA Monomer

Market Size:

Currently MFA monomer is not produced or sold commercially. Its function is to act as a partial replacement for styrene in the VE resins system in order to reduce the volatile emissions by 50-85%, depending on the amount of styrene replaced. The current plan is to replace 50% of the styrene used, or 22.5wt% of the total VE resin, with an equal weight of MFA monomer. Thus, in order to determine the total market size for MFA monomer, the market for VE resins must first be considered.

Currently, SRI Consulting has reported that the market for VE resins has been steady at 2 billion pounds per year (SRI REPORT). The maximum market for MFA is then determined by assuming that all production companies of this product decide to switch to the new formulation, incorporating 22.5wt% of MFA into the resin. This sets the total market size to 500 million pounds. However, this maximum is not possible to achieve as many companies may decide to not change the formulation or use alternatives to MFA.

Market Competition:

The market for MFA monomer will only exist if legislation is passed restricting the emission of hazardous air pollutants (HAPs) and volatile organic compounds (VOCs) that are produced in the production of vinyl ester resins (VE). The HAPs and VOCs are produced from the styrene used to produce the VE resin. The amount of HAPs and VOCs produced is a direct function of the amount of styrene used in the manufacturing of the resin. If the amount of styrene can be reduced, the amount

Written By: *TS*
Checked: *NMG*

47

of emissions can in turn be reduced. The economics section of the MFA monomer plant has been determined assuming that the legislation reducing HAP and VOC emissions is passed.

With new legislature being passed mandating the reduction of styrene emissions made in the production of VE resins, companies producing the product are left with two choices. The first would be to adjust their current process and the second is to shut their plants down. Since most of the corporations involved in the manufacture of VE resin products are run by small companies, it is unlikely that they will be willing to end their business ventures. This would leave them with no income and remaining fixed costs from their plants to be paid. Thus, it can be assumed that the multitude of vendors will make one of the following three alternatives.

First, companies can install and fuel equipment that can increase the airflow through the plant to effectively dilute the styrene concentration. Reports have been published by the Environmental Compliance and Risk Management (ECRM) on the effectiveness and cost of this alternative and will be explored in the next section. The second alternative involves incorporating the new product, MFA, into their production. The third alternative is that companies may choose to replace a portion of the styrene used by increasing the amount of VE resin. Essentially they would be reducing the weight percent of styrene used in the resin. The costs and benefits associated with the latter two alternatives will be explored later in this report.

Competition was not a concern when determining the percent of the market that could be captured. This is due to the fact that no other product currently being produced or patented has the effect of reducing the VOC emissions while still

Written By: TS
Checked: NMG

48

maintaining the properties required for ease of production and the properties required in the resulting polymer [SERDP report]. Instead, the percentage of companies that will choose the MFA alternative over the aforementioned competing alternatives was analyzed.

Alternative 1: Reducing Styrene Emissions with Specialized Equipment:

An engineering survey has been completed concerning the amount of styrene emissions from composites manufacturing in California. The study centered on determining the price of reducing styrene emissions by 50%. In this document, the company has outlined a hierarchy required by the government to handle these dangerous emissions. This hierarchy has been outlined below:

- 1. Reduction of ambient styrene levels at the source of emission through modification of raw materials or their methods of application. For composites, this might be accomplished by reducing styrene content in resins, employing vapor suppressants, or reducing atomization (fine droplet formation) during application of gelcoat and resin.*
- 2. Engineering controls such as production line reconfiguration and ventilation improvements to reduce styrene concentrations in the breathing zone of workers. For composites, this might involve modification of work enclosures (booths or rooms), repositioning of work or operators within enclosures, redirection of supply and exhaust flow, and increasing ventilation airflows.*
- 3. Education or administrative controls such as worker rotation.*

Written By: *TS*
Checked: *NHG*

49

4. Use of supplied air or air purifying respirators to reduce inhalation exposures.

As is explained in this report, each company must follow this hierarchy from the top down, accepting the first 'feasible' solution to ensure the best alternative measures have been taken to protect the workers and the environment. Solution #1, unfortunately, was not cost feasible at the time as no product was able to successfully reduce the emissions in a cost effective fashion.

A complete engineering study was performed on six plants to assess the cost of installing styrene emission reducing equipment.

The company found that in four of the six plants installing increased ventilation equipment could not reduce emissions to the required minimum level. This failure results in requiring complete construction of new buildings to house the existing machine area. Thus, in 66% of the plants, the ventilation improvements still had to be accompanied by increase in personal protection equipment and training to their workers. This leaves them at a higher risk than if the emissions could have been reduced to the correct value from the source.

The details from the two plants in which cost estimates were made show that constructing equipment to reduce emissions can be effective but costly.

Alternative #2: Replacing Styrene with MFA - Setting the price for MFA

As was previously mentioned, MFA is not currently sold on the market, so no price is available to base the economic analysis on. Instead, the team has set the price of MFA to compete with the alternative just presented.

Written By: *TJ*
Checked: *NMG*

50

It is recommended that the price of MFA be set to such a value as to have the increased raw material cost for the plants purchasing MFA to equal the increased utility and equipment costs discovered from Alternative #1.

The price should not be set any higher than the comparative price of ventilation equipment because MFA offers no performance enhancement to the product.

Although it does increase some mechanical properties of the resultant resin, it also decreases other sought after properties. However, a slight price increase may be acceptable considering the solution offers reducing the emissions from their source and not relying on second hand alternatives which may fail to work if the equipment breaks.

However, the price for MFA does not have to be reduced lower than the cost of Alternative #1. At equal cost levels, it initially appears there exists no preference for choosing either option. However there are two strong reasons that suggest most companies will turn to the MFA solutions over the other two. First, if legislation does get passed, it will probably recommend a similar hierarchy to what has been previously presented. Following this hierarchy, most companies will show preference to the first option, which involves purchasing MFA monomer. Second, as was noted in the ECRM study, an estimated 50% of current plants would have to redesign new production facilities in order to provide enough area for Alternative #1 to work. For at least half of the plants, installing styrene emission equipment by itself will not solve the problem.

Written By: *TS*
Checked: *NMG*

51

The conducted study predicted the effective annual cost of Alternative #1, for a 50% reduction in emissions is \$.093/lb of product. Therefore, the selling price of MFA, which would increase the costs of production by an equal amount, is \$1.17/lb.

It should be noted, however that the choice of comparing a 50% reduction in styrene emissions was chosen by ECRM researching the cost estimate. It is not possible, at this stage, to determine the actual value of styrene emissions that the legislation that will reduce. For simplicity, the team has performed a complete cost estimate assuming a 50% reduction, following the recommendation of ECRM. Later in the report the effect the percent emissions has on the IRR will be compared.

Alternative #3: Replacing Styrene with Current Monomer

Research by Dr. Palmese and his team reveals that replacing the same amount of styrene with MFA or more of another monomer produces significantly different effects in the resultant resin. The latter will produce a polymer with less desirable properties than both the existing resin and the resin made with MFA. From a performance standpoint, replacing styrene with vinyl ester resin is at a disadvantage.

Furthermore, current prices for monomers used in the resins are at \$2.50/ lb. Thus, as can be seen from the previous table showing the price of MFA and effective price rise of styrene emission equipment per pound of product, this alternative is less attractive from a cost standpoint.

These two factors combine to ensure the percent of companies choosing this alternative will be set below 5%.



Written By: *TS*
Checked: *NM*

9.3 Economic Analysis for 5 Million Pound Per Year Plant

Capital Costs

Design Assumptions

- Each piece of equipment was designed based off of heuristic calculations used in the material and energy balance of the MFA flowsheet.
- Costs were determined by using past cost figures
 - Pumps and Heat Exchangers were designed in Capcost
 - Tanks and Reactors were designed using tools provided by Mr. Schon from Arkema.
- Any equipment below the minimum size in which data was available was priced at that lowest value. This should result in a conservative estimate for these pieces of equipment.
- Installation, shipping, and other overhead costs for each piece of equipment was calculated from either the Grass Roots calculation presented in TBWS, or from empirical cost multipliers provided by Arkema's research.
- Land Costs were assumed to be close to the average used by default in Capcost of \$1.2 million.

Written By: 
Checked: 

53

Table 9.1: Capital cost summary for MFA plant.

Capital Cost Summary for MFA Plant							
Exchangers	Type of Exchanger	Shell Pressure (bar)	Tube Pressure (bar)	MOC	Area (square meters)	Purchased Equipment Cost	
E-101	Double Pipe		4.4	Stainless Steel / Carbon Steel	1	\$	2,210
E-102	Double Pipe		8.4	Carbon Steel / Carbon Steel	1.3	\$	2,370
E-103	Double Pipe		8.4	Carbon Steel / Carbon Steel	1.3	\$	2,370
E-104	Double Pipe		4.4	Stainless Steel / Carbon Steel	3.2	\$	2,960
E-105	Double Pipe		4.4	Stainless Steel / Carbon Steel	3.2	\$	2,960

Pumps (with drives)	Pump Type	Power (kilowatts)	# Spares	MOC	Discharge Pressure (bar)	Purchased Equipment Cost	
P-101	Centrifugal	4.54	1	Stainless Steel	1.3	\$	6,190
P-102	Positive Displacement	1	1	Stainless Steel	21.3	\$	6,000
P-103	Centrifugal	3.77	1	Stainless Steel	1.3	\$	5,920
P-104	Positive Displacement	1	1	Stainless Steel	21.3	\$	6,000
P-105	Positive Displacement	1	1	Stainless Steel	21.3	\$	6,000
P-106	Centrifugal	4.2	1	Stainless Steel	1.3	\$	6,070
P-107	Centrifugal	4.2	1	Stainless Steel	1.3	\$	6,070

User Added Equipment	Description	Installation Factor	Purchased Equipment Cost	
Z-101	Storage Tank T-110	3.09	\$	49,400
Z-102	Storage Tank T-120	3.09	\$	49,400
Z-103	Catalyst Hopper T-130	3.09	\$	26,000
Z-104	Storage Tank T-140	3.09	\$	49,400
Z-105	Storage Tank T-150	3.09	\$	49,400
Z-106	Storage Tank T-310	3.09	\$	41,400
Z-107	MFA Reactor R-110	5.4	\$	486,225

Element of Cost	Pricing basis:	Unit of Measure	Furnish Price	Install Price	Furnish & Install Price
Loading/Unloading Spots:					
Tank Truck	Closed Dome, scale, process sewer, rack, utilities & FP, loading equipment, & shelter. Based on 100 million lbs / year capacity.	EACH			\$200,000
Conveying & Packing Systems					
25 kg (50 lbs.) bag packer - Automatic bag placing	Includes 2 each single spout bag filling machines with common off take conveyor, check weigher, reject conveyor, all incoming ducting from screw outlet, buffer tank, compressor, instrumentation, power supplies etc.	EACH			\$585,000

Manufacturing Costs

Design Assumptions

- The breakdown of variable costs was chosen based off of recommendations from TBWS with a few exceptions.
 - Maintenance and repairs were doubled from the suggested value.
- Since the plant has few pieces of equipment, it will not require a permanent maintenance team.

Written By: *AS*
 Checked: *NMG*

- Direct supervisory and clerical labor can be reduced by 50% as the size of this plant will require less on site need for these employees.
- From recommendations from Drexel Professors, SG&A is assumed to be as 1% of the cost of sales, which allows this number to scale with production as should be expected. The assumed breakdown of this value is taken from suggestions of TBWS.

The total expenditure over 15 years of operation of the plant is dominated by direct manufacturing expenses, which includes raw material costs, utility costs, labor costs, and other similar costs. However a significant percentage is needed for fixed capital investment, such as purchase of buildings, equipment, and land. This is the same for fixed manufacturing expenses such as plant overhead, employee benefits, and local taxes.

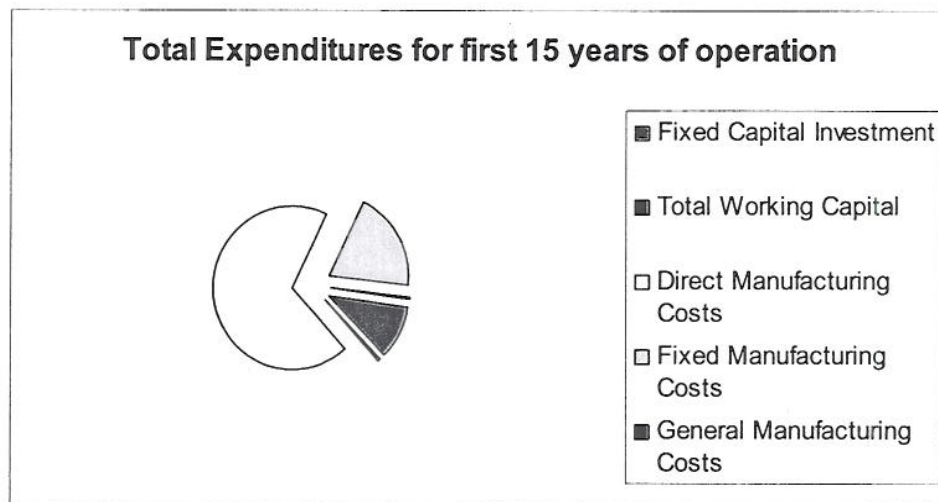


Figure 9.1 – Total expenditures for first 15 years of operation.

Looking more closely at the fixed capital investment, the bulk of the cost is incurred in purchasing the reactor coils.

Written By: *AS*
 Checked: *NMG*

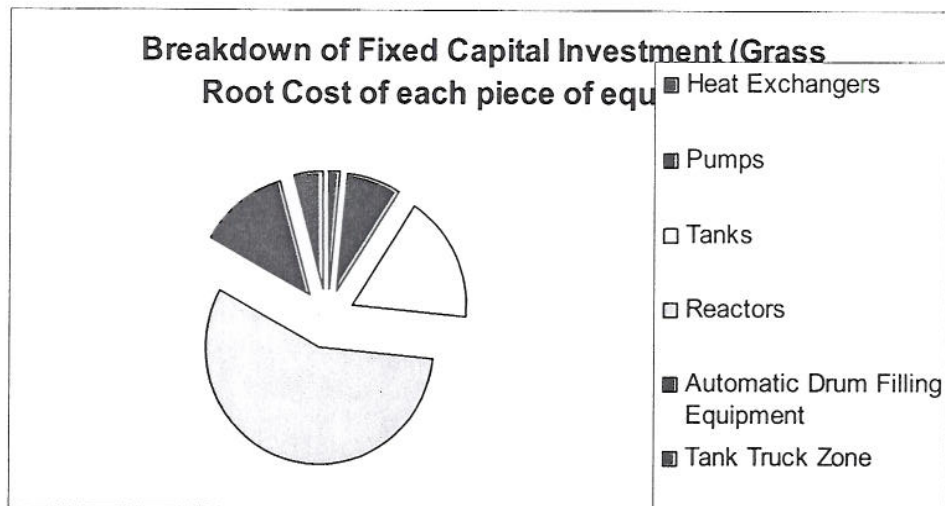


Figure 9.2 – Breakdown of fixed capital investment (Grass root cost of each piece of equipment)

The direct manufacturing costs are controlled by the cost of the raw materials. However, the cost of operating labor also plays a significant role in this figure. It is important for later analysis of this plant to note that the cost of raw materials will scale directly with the plant, whereas the number of operators needed only increases roughly with the root of production.

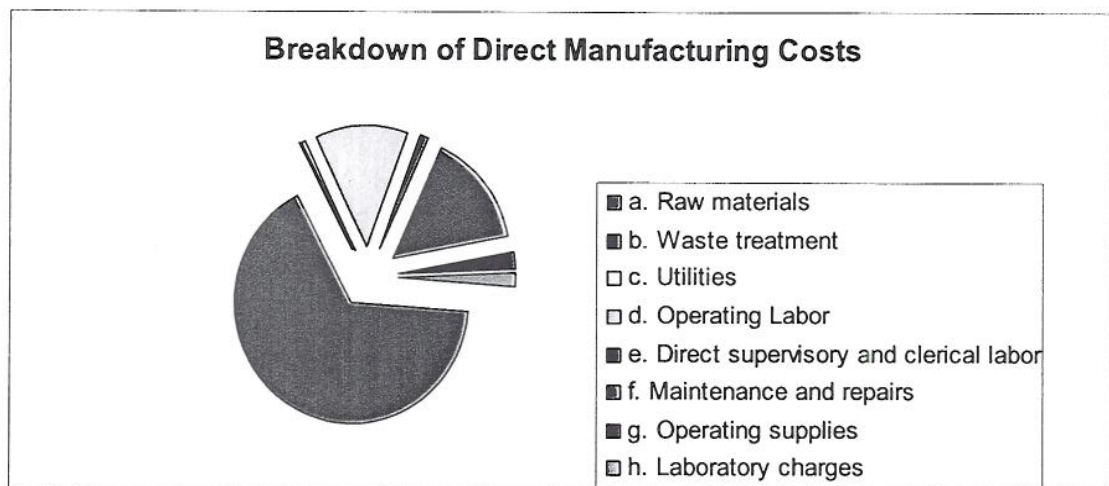


Figure 9.3 – Breakdown of direct manufacturing costs

Written By: *AS*
 Checked: *NMG*

Fixed manufacturing expenses are controlled by the plant overhead costs, which receives its greatest charge from employee benefits.

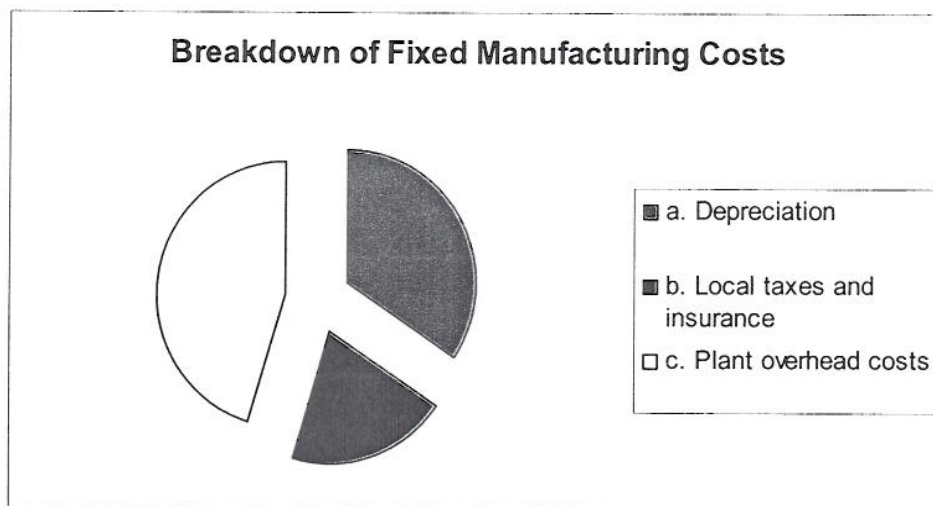
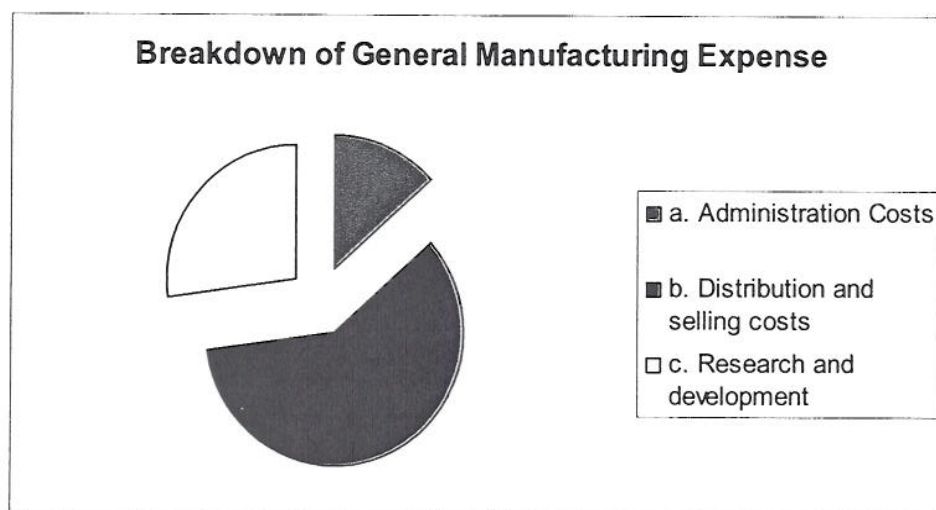


Figure 9.4 – Breakdown of fixed manufacturing costs

Finally, the costs of marketing, advertising, and distribution of the MFA monomer control general manufacturing expenses. Since this is a new product, a good marketing campaign is important. Research and development was also priced at a large value to examine the effects that industrial scale manufacturing of this product will have on its properties in the VE resin.


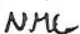


Written By: *B*
 Checked: *mm*
 Figure 9.5 – Breakdown of general manufacturing expense

15-Year Cash Flow Analysis

Design Assumptions

- Working Capital
 - The working capital was assigned to be 12% of expected revenues.
This value turns out to be \$.19MM in the first year
 - Typical capital required is based off having a half-month supply of operation. The time scale was chosen to be the turnover of the raw materials brought in and converted to revenue from the sale of MFA. Assuming the majority of this value will come from raw materials, the plant should have on hand \$.169MM. The previous estimate shows the plant to be in a sufficient financial position.
- Income Tax Rate
 - Federal tax rates average 35% with small variations
- Inflation Rate
 - A 3% inflation is assumed for all manufacturing costs. This value will also be used to inflate the price of MFA.
- Capital Expenditures
 - The following table was used to purchase capital for the MFA plant.
- Start-up Costs
 - The following table was used to predict additional capital expenses incurred during construction of the MFA plant.


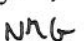
Written By: 
Checked: 

58

- Land Costs
 - An average cost of land, obtained by the default setting in CAPCOST, is \$1.25MM

Conclusions

- The cash flow analysis reveals that the company investing in the MFA plant will end up losing money. An estimated IRR of -7% was obtained at the end of 15 years
- Variable cost Analysis
 - Analysis of the cumulative present worth of the plant reveals that each year of operation the plant loses more money. The costs of manufacturing MFA at this level outweigh the revenues that can be obtained.
 - The price of MFA, however, is above the cost of the sum of raw materials, utilities, and SG&A, which directly scale with production.
 - As production is increased, Fixed Capital Investment will increase according to the 0.6 rule.
 - Operating labor will scale roughly to the root of production for a continuous process as the pieces of equipment will not grow in number only in size. Similarly fixed costs, which are controlled by employee benefits, should be scaled in the same way.
- Scaling the plant in production will enable this process to be profitable.

Written By: 
 Checked: 

59

MFA Production Scale-up

Scaling Assumptions

- All raw materials and catalyst scale directly with increased production.
- Utilities scale directly with increased production
- Fixed Capital Investment scales with production following the 0.6 rule
- Operating Labor will scale with production to the 0.3 power
 - It is assumed that labor increases only slightly with increased production because the process is continuous and, in the limit of moderate increases in capacity, most of the equipment will only grow in size and not number. Thus the number of operators needed remains close to the initial value.

Results

- At the current design capacity of 5 MM pounds per year the IRR is -7%
- Production must be increased by a factor of 4 to 20 MM pounds per year to reach the breakeven point.
 - IRR at 20 MM pounds per year is 0%
- Production must be increased by a factor of 8 to 40 MM pounds per year to reach above the hurdle rate of 12%
 - IRR at 40 MM pounds per year is 13%
- The team recommends that production be increased to 1100% of its original value.
 - Production of 55 MM pounds per year

Written By: TS
Checked: NMG

60

- IRR at base case is 22%

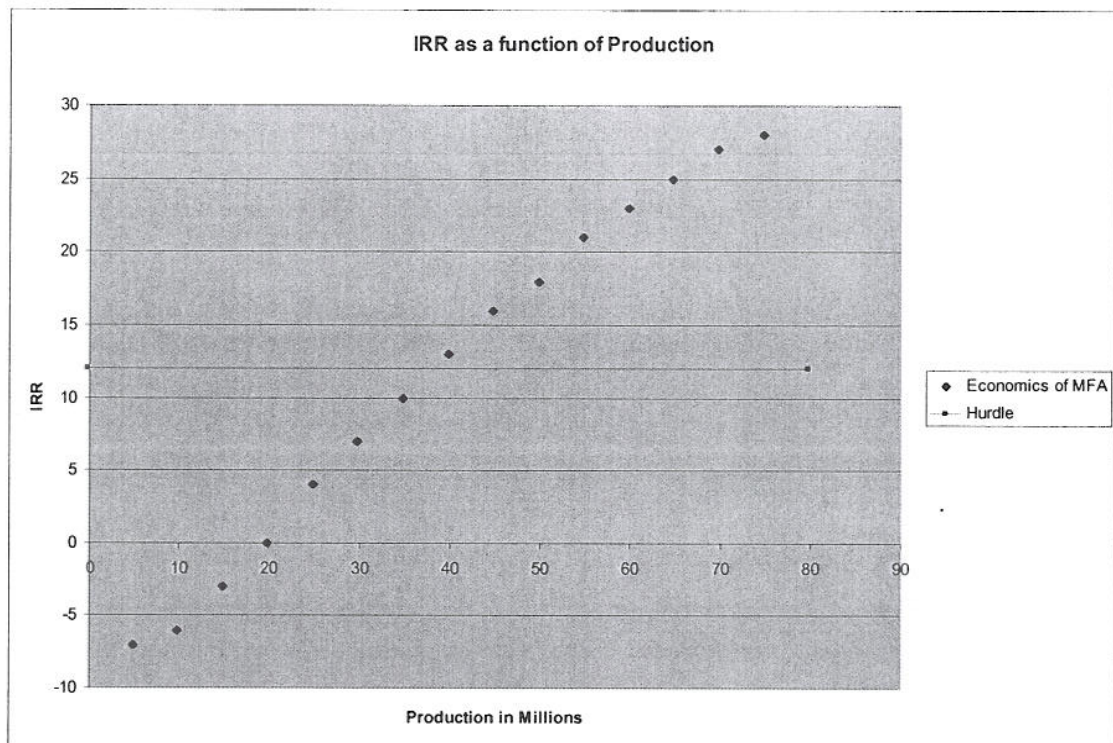


Figure 9.6 – IRR as a function of production

9.4 Economic Analysis for 5 Million Pound Per Year Plant

Capital Costs

Capital Costs were assumed to scale via the six-tenths rule. This is a good assumption for a continuous process where the residence time of the process equipment can increase in size as well as in number.

The breakdown of capital costs and assumptions made stays the same as the 5 MM pound capacity plant.

Written By: *ES*
 Checked: *NMG*

Manufacturing Costs

Due to the different levels of scaling for the important parameters used to determine the total manufacturing costs, two of the breakdown charts show significant changes.

First, the total expenditures of the MFA plant in the first 15 years of operation became more dominated by the direct manufacturing costs.

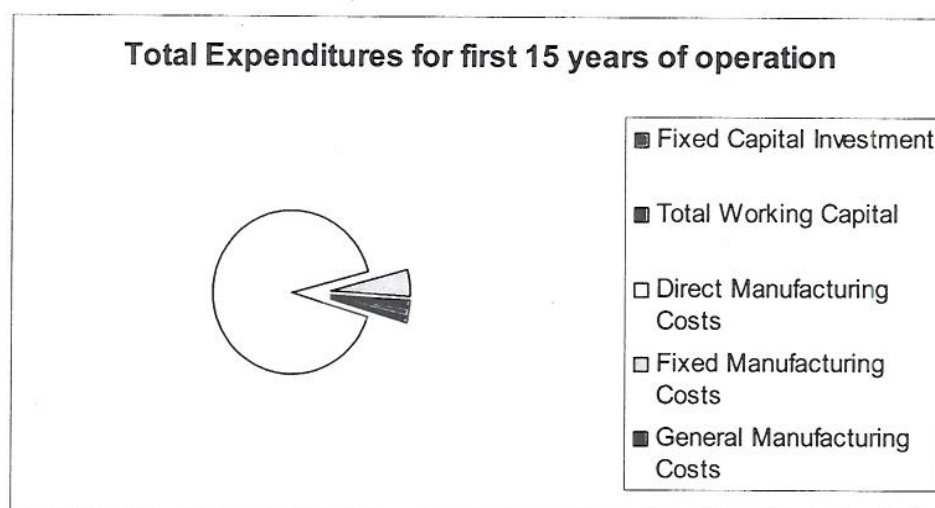


Figure 9.7 – Total expenditures for first 15 years of operation.

Secondly, the break down of the direct manufacturing costs also changes. This is due to the percent required by raw materials is significantly higher than all other costs, and even grew larger than the cost of operating labor.

Written By: *B*
Checked: *NML*

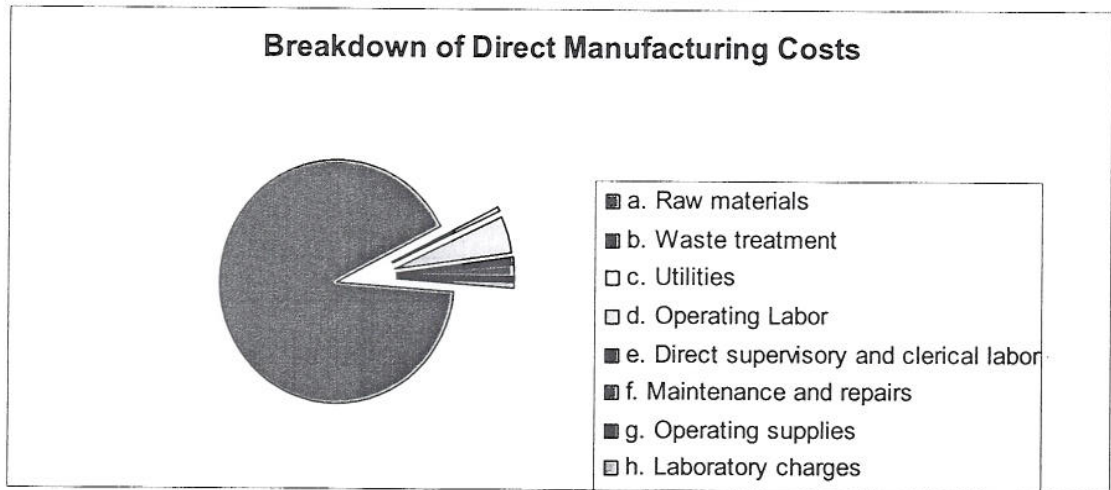


Figure 9.8 – Breakdown of direct manufacturing costs

As was noted earlier, the price of MFA is maintained above the variable costs of raw materials and utilities. However, upon including the semi-fixed costs, such as operating labor and plant overhead for the 5 MM capacity plant, the result is a loss of money per pound of product. As can be seen from the charts above, the raw materials now become a larger percentage of the costs over utilities. And the direct manufacturing costs become larger over the fixed costs. This allows for the plant to produce MFA at a profit.

A summary of the plants raw material requirements, utility requirements, operating labor requirements and fixed capital investment (FCI) is shown below.

Written By: *BF*
 Checked: *MFM*

Capital Cost Investment	\$	19.61
-------------------------	----	-------

Cost of Utilities	Type	Amount per year	Cost (\$/Month)	Yearly Cost (\$M)
Electricity (kWh)	110V-440V	1651653	0.060	0.09
Low Pressure Steam (kg)	lps	2380131	0.016	0.03
Cooling Water (cubic m)	cw	54328	0.015	8.041E-0
Chilled Water (kg)	cw	723435	0.000185	1.338E-0
Total Cost of Utilities				0.13

Cost of Operating Labor	
Number of Shifts	5
Number of Operators per Shift	4.5
Base Salary per Operator (\$/yr)	54000
Total Cost of Operating Labor (\$MM)	1.215

Following the same method as outlined for the 5 MM pound capacity plant, a complete economic analysis was completed on the MFA plant at 55 MM pounds per year with the following conclusions drawn for the base case.

- The net present value (NPV) after 15 years of the MFA plant is \$14.50 MM
- The discounted cash flow rate of return (DCFROR) or the IRR after 5 years is 22%.
 - This value is nearly double the hurdle rate of 12%.
- The discounted payback period (DPBP) is 9 years.

64

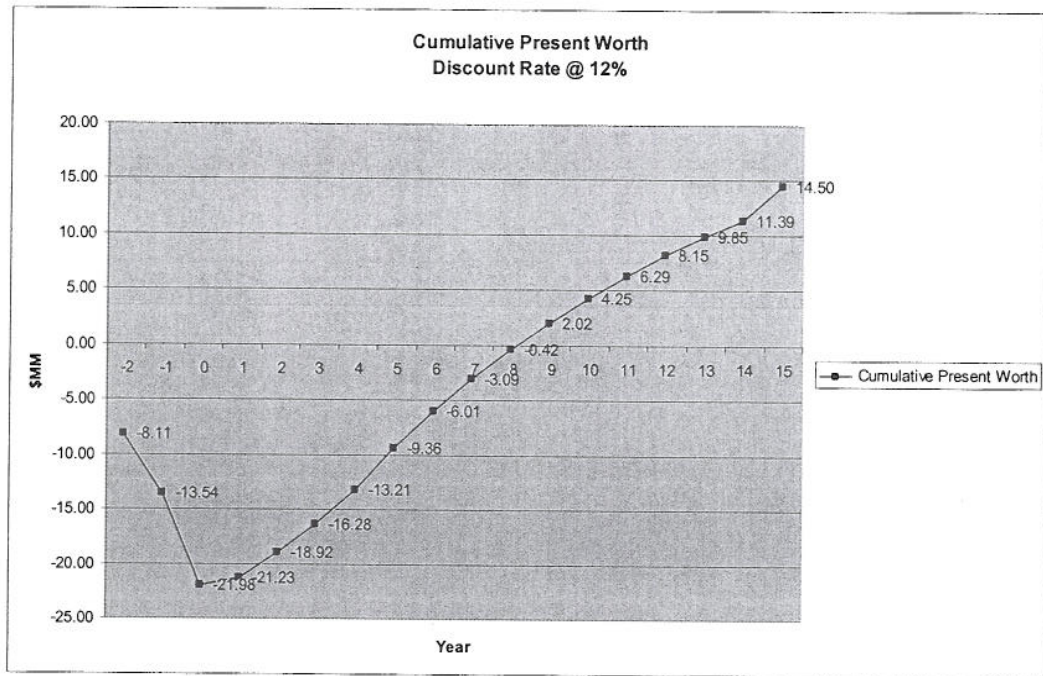


Figure 9.9 – Cumulative present worth discount rate at 12%

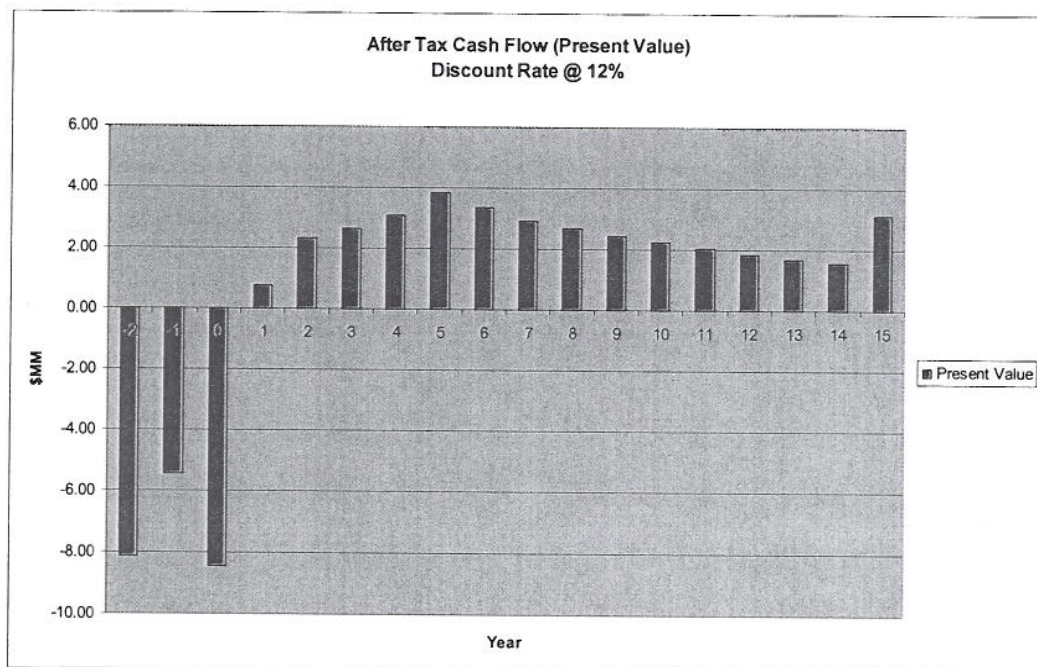


Figure 9.10 – After tax cash flow (Present value) discount rate at 12%

Written By: *TS*
 Checked: *MPM*

Sensitivity Analysis

In order to identify the primary variables responsible for the reported IRR at 55 MM pounds, the team has performed a sensitivity study on a number of variables in the process. The list includes


- Price of Raw Materials (GM and Lauric Acid)
- Price of Product (MFA)
- Capacity of Plant (MM of pounds per year the market allows)
- Fixed Capital Investment
- Operating Costs

Each input was varied from 50% to 150% of its value in the base case, with the IRR being measured at certain intervals.

The measurement calculated for each variable was the sensitivity factor. This is defined as the change in IRR produced by a 10% increase in the independent variable. Thus this measure predicts how much the IRR will change when each of the six parameters increases by 10% of its original value.

Results

- The most sensitive values are the GM price and the MFA price.
 - GM has a sensitivity value of -6.13
 - MFA has a sensitivity value of 10.5
- The moderately sensitive variables include Lauric Acid price and capacity.
 - Lauric Acid has a sensitivity of -1.72

Written By: 
Checked: MFM

66

- Capacity has a sensitivity of 2.19
- Both FCI and Operating Costs had minor effects on the IRR value
 - FCI has a sensitivity of -.42
 - Operating Cost has a sensitivity of -.22
- The results of the test are summarized in the graph below.

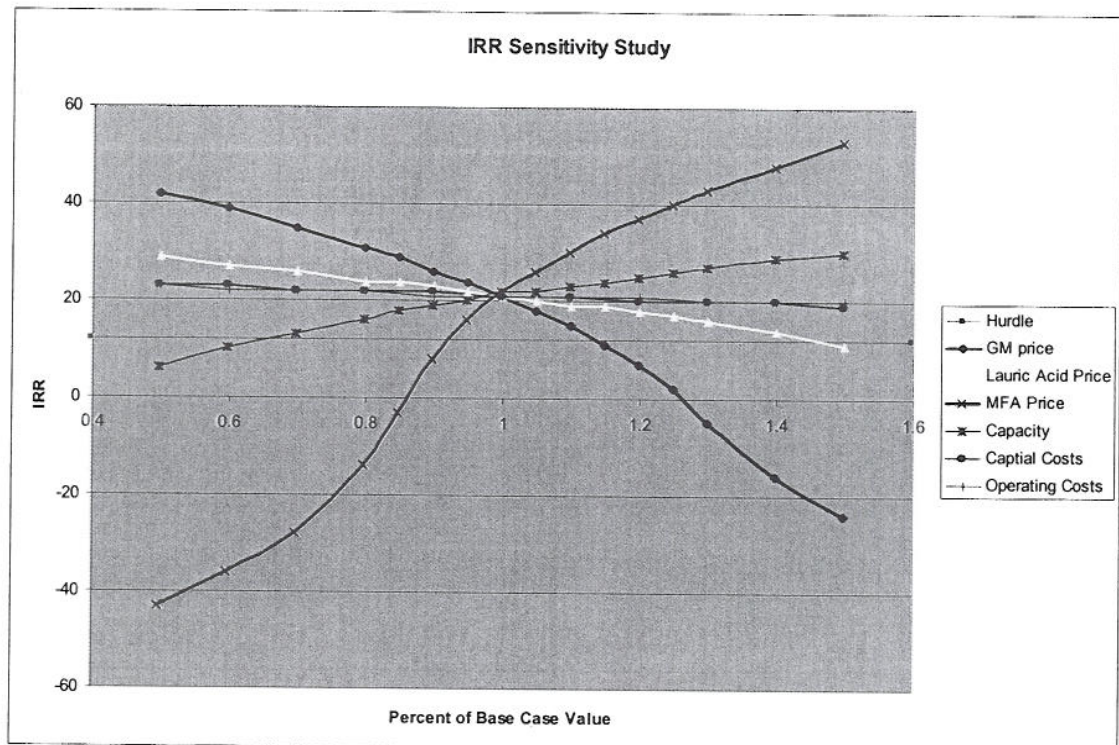


Figure 9.11 – IRR sensitivity study.

Conclusions

- The primary variables to be concerned with are the price of GM and the selling price of MFA. With the base case IRR at 22%, it is seen that a change of over 10% in the wrong direction of either variable - increase for GM, decrease for MFA - could decrease the IRR to below hurdle. Furthermore, a 25% change in the wrong direction could make the plant unprofitable.

Written By: *AS*
 Checked: *MMW*


- This higher than average sensitivity in two of the parameters affecting the production of MFA is a concern for the company contemplating investing in this venture.

Monte Carlo Analysis

Due to the high sensitivity of an MFA plant to the raw material and product prices, it is necessary to quantify the risk involved in investing in such a venture. To determine the risk associated with creating an MFA plant, the team has determined probable variations in each of the major parameters from the base case prediction. Each parameter was given a triangular probability distribution, assigning its most likely value to be that in the base case, and the lowest and highest values taken from the probable distributions assigned. Samples of the probability distributions are shown in the appendix. One hundred random combinations of the variables were then tested with the IRR reported.

The following is a list of the variation in each parameter measured

- GM Price (-25% to 40%)
 - The current price of GM for lab scale quantities is \$4.25/lb. The team performed a cost analysis on a patented procedure to manufacture GM and discovered the actual price may be closer to \$1.38/lb. However, this does not guarantee the MFA plant will be able to convince Dow to sell GM at this price. Thus, it was varied as much as 40%.

Written By: 
 Checked: MFM

68

- MFA Price (-25% to 25%)
 - The price of MFA was determined by the utility and capital costs of installing equipment capable of reducing the concentration of styrene in the air. These prices tend not to vary too significantly from reported values.
- Lauric Acid Price (-20% to 20%)
 - This price was taken from the literature. Prices for common commodities tend to be stable around the common selling price.
- Capacity of Plant (-25% to 50%)
 - The current level of 55 MM pounds per year is roughly 25% of the market. This implies that one forth of the producers of VE resins will chose to use MFA to solve the styrene emissions problem over the other two alternatives. Based on previous arguments, it is probable that half of the market could be captured, and a smaller chance that less will be captured in the base case.
- Capital Costs (-10% to 25%)
 - Through the use of old data on equipment, the estimates for the plant should be fairly accurate
- Operating Costs (-20% to 20%)
 - Due to the small size of the plant, the team is confident that the number of operators needed is correct

Written By: *TS*
 Checked: *MFM*

The data provided by this simulation shows the sensitivity of the plant to the variables measured. Those variables with high slopes and moderate correlations have the largest effect on the IRR. It also reveals the confidence level in the IRR an MFA plant is capable of earning.

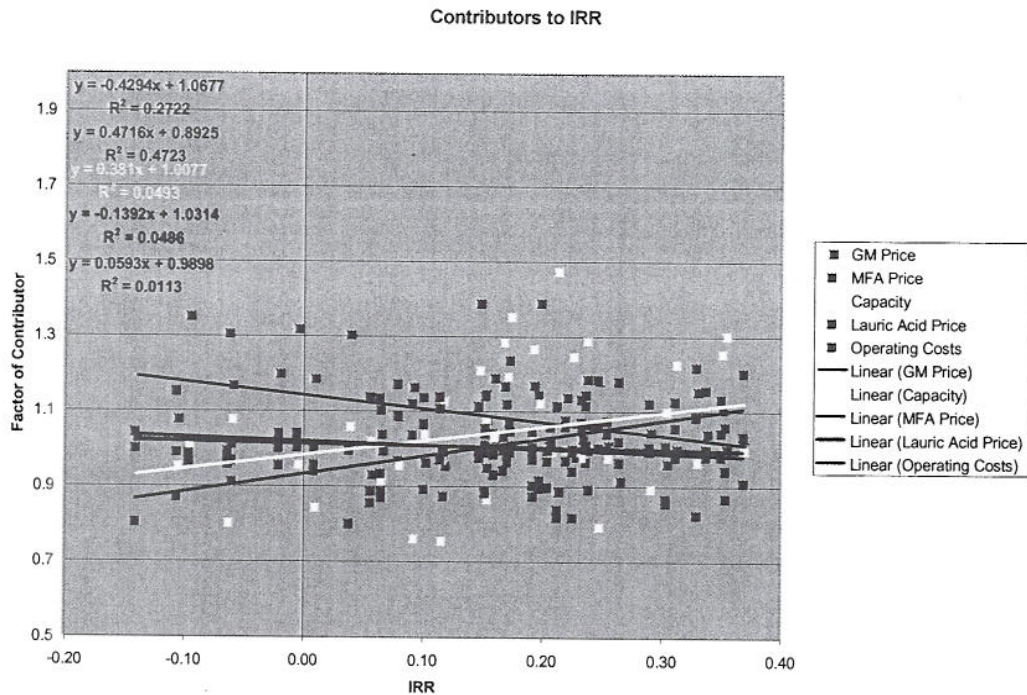


Figure 9.12 – Contributors to IRR

Written By: *15*
 Checked: MFM

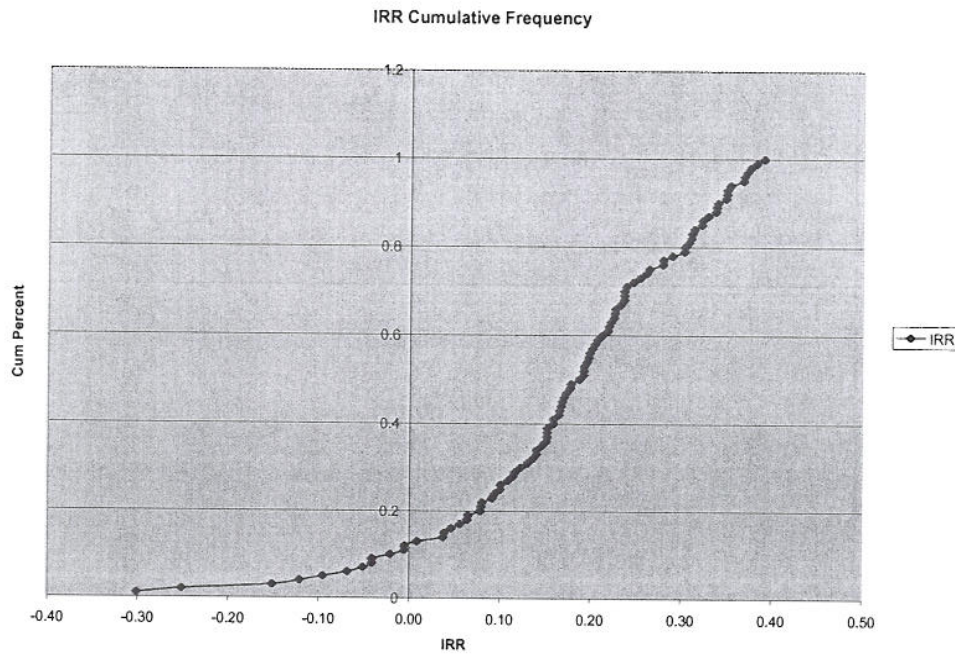



Figure 9.13 – IRR cumulative frequency

Results

- MFA and GM are the biggest contributors to the IRR
 - Both have large slopes and moderate correlations
- IRR in Base Case is 22%
- IRR average for 100 cases is 18%
- Probability that IRR is above .00 is 89%
- Probability that IRR is above hurdle of .12 is 71%

Summary of Acceptable GM and MFA price combinations

In both the sensitivity studies and the Monte Carlo analysis, it was found that the biggest contributors to the profitability of an MFA plant is the cost of GM, and the selling price of MFA. It is highly recommended that further research be done in

Written By: 
 Checked: MFM

these two areas to determine a high confidence number for each of these variables. Once a definite value has been set it will be possible to obtain a better prediction on the expected IRR.

To summarize the effects each variable has on the IRR, the team has prepared a graph that lays out the predicted IRR for all possible combinations of these variables. Once the proper quadrant of the graph is identified, we can quickly determine the profitability of an MFA plant. Note that MFA price has been varied from +25% to -25% of its expected value, the price of GM has been varied from -15% to +40% of its predicted value. Therefore, the probability of each section of the graph is not equal. There is a higher probability of being around the vertical brown line, less chance of being around the vertical red line, and the least chance of being around the orange line.

Written By: *TS*
Checked: MFM

72

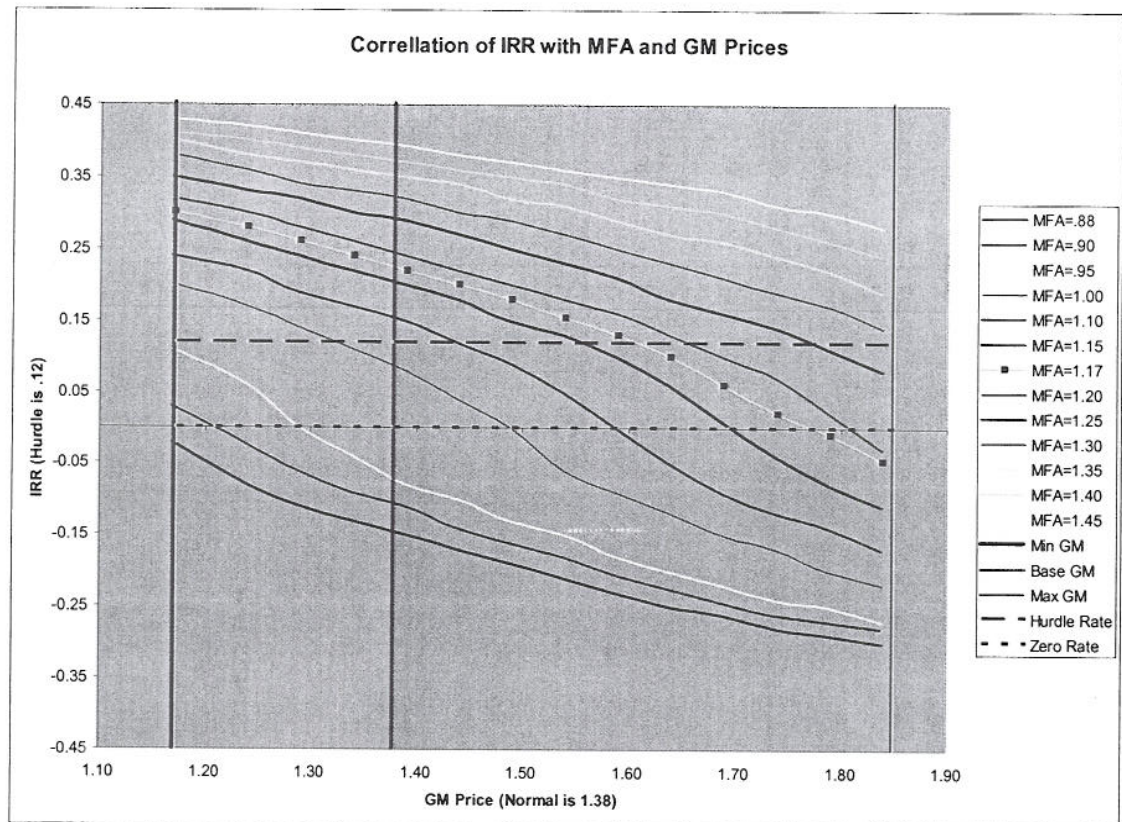


Figure 9.14 – Correlation of IRR with MFA and GM prices

Results

- The base case MFA, shown as the beige line with black dots, has a 70% chance of being above hurdle and a 90% chance of being profitable.
- As the price of MFA increases the expected IRR slowly increase.
 - An MFA price of \$1.30/lb (11% increase) is always above hurdle
- As the price of MFA falls, the expected IRR falls significantly
 - An MFA price of \$.95/lb (19% decrease) is always below hurdle
 - An MFA price of \$.88/lb (25% decrease) is always unprofitable


Written By: TS
Checked: MFM

Effect of Percent Emission Reduction on IRR

As mentioned before, the price of MFA is determined by the cost of installing and fueling styrene emission reducing equipment. However, different levels of styrene reduction will bring different costs. It is the purpose of this section to summarize the expected IRR's as a function of percent reduction of styrene emissions required by legislation

Assumptions

- Capital costs scale with percent styrene reduction capacity via the six tenths rule
- Operating costs scale with percent styrene reduction capacity directly.
- The minimum styrene content of fatty acid resins, based on acceptable viscosity and polymer performance characteristics, is 10-12%. This implies the maximum reduction of styrene emissions Alternative #2 can produce is 80%.
 - To reduce emissions above this level, say 90%, companies must use 10% styrene and 35% MFA in their resin, as well as purchase and fuel equipment capable of reducing emissions the additional 10%.

Written By: 
Checked: MFM

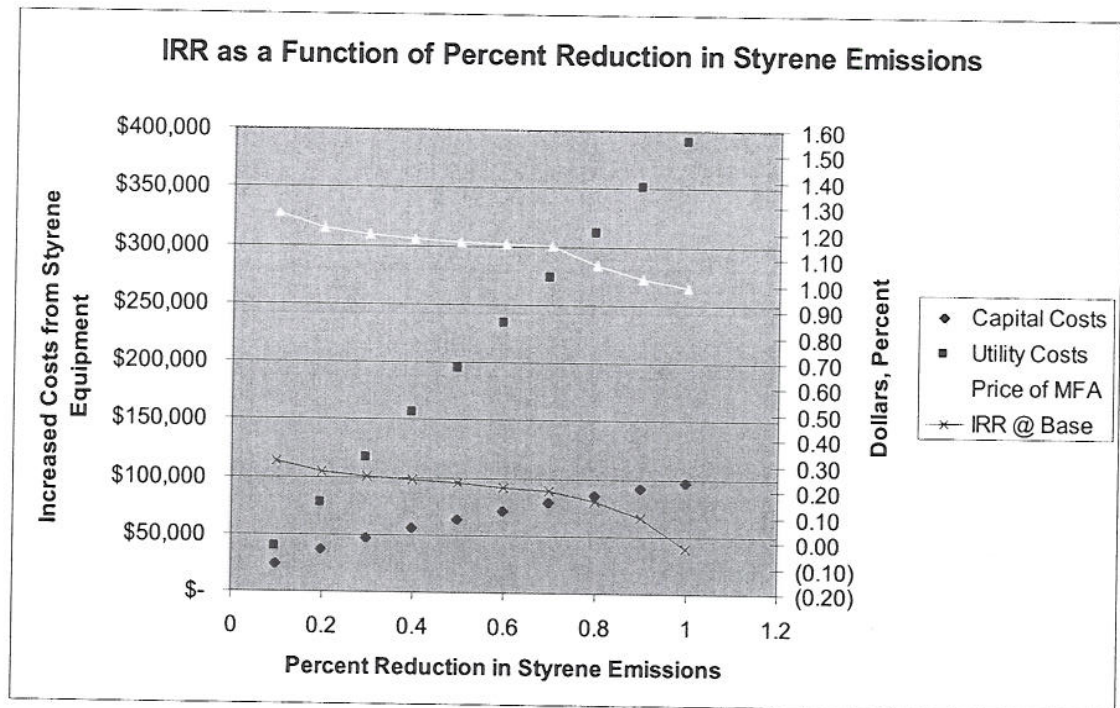


Figure 9.15 – IRR as a function of percent reduction in styrene emissions

Results

- If the required reduction of styrene emissions is 86.3% or below, an MFA plant will be above hurdle.
- If the required reduction of styrene emissions is 96.6% or below an MFA plant will be profitable.

9.5 Conclusions and Recommendations

In order for the economic of an MFA plant to be attractive, production levels must be set to 55MM pounds per year. However, this level poses great risk for the potential investors in MFA production.

First, this is roughly 25% of the market. Although we have proven that MFA will be chosen more often than its competitors (66% of current plants would require

Written By: TS
Checked: MFM

complete building reconstruction in order for Alternative #1 to be successful), we must also take into account entry of alternative products similar to MFA. Thus we have assumed a 60% chance an MFA plant can hold on to 25% of the market for the projected 15 year. Secondly, as of 2007, there has been no legislation passed restricting the level of styrene emissions. Until this passes, there is no real market for MFA. Also, if the legislation calls for a reduction of 86% styrene emissions, the plant is on the cusp of the hurdle rate. For reduction of emissions greater than 96%, an MFA plant is no longer profitable. Thus we will assume a 50% chance that legislation will pass with a favorable criterion set for styrene.

Figure 9.6 below summarizes the total risk involved in construction of this plant. Overall, an MFA plant has a 21.3% chance of being above hurdle.

Obstacle	Probability
MFA Plant operating above hurdle rate	0.71
Capturing 22% of Market	0.60
Styrene Legislation being passed	0.50
Cumulative Probability of Success	21.3%

Figure 9.16 – Conclusive economic analysis numbers

At this time, the risk is too high for the required investment. We suggest a no/go on this project until the primary variables obtain a conclusive and confident value.

Written By: *TS*
 Checked: *MTM*

10. Calculations

The calculation section for the GM plant has been merged with the MFA plant calculations to prevent any discrepancies. Assumptions for both designs will be discussed in each section, however, only one example (either MFA or GM) will be used for each calculation.

10.1. *Centrifugal Pumps*

All pumps can be centrifugal since the GM process contains only liquid feeds and liquid products, as well as highly soluble salts and catalysts, which can be assumed completely dissociated in the liquid phase. For the MFA plant however, centrifugal pumps can only be used for the circulation of the tempered water or loading/unloading tankage. The shaft power required of each pump is directly obtained from the following heuristic given by TBWS

$$(10.1) \text{ Power (kW)} = \frac{1.67 * \text{Flowrate} \left(\frac{\text{m}^3}{\text{hr}} \right) * \Delta P (\text{bar})}{\text{Efficiency}}$$

This equation requires three pieces of information: the volumetric flow rate through the pump, the pressure rise given to the material, and the efficiency. For the latter, the efficiency will vary with flow rate; however, an average of 70% can be used as a conservative estimate. For the MFA plant, 60% was used because of the lower flow rates. The volumetric flow rate is obtained from the

Written By: *TS*
Checked: MFM

77

material balance of the system. Finally, the pressure rise given to the material must be sufficient to flow the material through a piping network and into its destination vessel operating at some pressure.

To calculate this last number, heuristics from TBWS will be used. On average, pressure drop of a liquid flowing through a pipe is 2 psi / 100 feet. Also, preliminary estimates of line pressure drops in plants reveal an average equivalent length of 100 ft. If the pipe contains control valves, an additional 10 psi must be added to obtain this control. In the plant, each pump must be able to overcome 12 psi of pressure drop before reaching its desired reactor.

In calculating the ultimate pressure rise, two more factors were considered. First, if the material must flow through a heat exchanger, an additional 2 psi must be overcome. Second, the pressure of the material must always be greater than the pressure of the discharge tank by at least 2 psi. Combining, the design pressure rise is equal to

$$(10.2) \quad \Delta P(\text{psi}) = 12 + 2 * (\# \text{ of heat exchangers}) + (2 + P_{\text{discharge unit}})$$

As an example, consider stream 4 in the GM plant. From the flow diagram, it can be seen that the material must flow through one heat exchanger and discharge into R-201 operating at 1 bar pressure. The pressure rise is calculated as

Written By: *TS*
Checked: *MFM*

78

$$\Delta P(\text{bar}) = \left(\frac{12 + 2 * (1) + (2 + 1)}{1.01} \right) = 16.8$$

From the stream table, it can be seen that the volumetric flow rate is 816587.8 L/hr. Assuming the efficiency is 70%, the power requirement is

$$\text{Power (kW)} = \frac{1.67 * 816.6 \left(\frac{\text{m}^3}{\text{hr}} \right) * 16.8(\text{bar})}{\text{Efficiency}} = 37.9$$

The last pump related calculation is the NPSH_A. This value must be greater than the NPSH_R dictated by the pump manufacturer. The available NPSH is the total suction head, in meters of liquid absolute, determined at a datum elevation, minus the vapor pressure of the liquid in meters absolute.

$$(10.3) \quad NPSH_A = (h_p - h_{vpa} + h_{st} - h_{fs} - h_a) \left(\frac{1}{1.1} \right)$$

h_p = absolute pressure head in meters on the surface of the liquid supply level

h_{vpa} = Vapor pressure of the liquid converted to meters

h_{st} = Static height in meters difference between liquid level and pump datum.

The pump datum level is assumed to be 0.2 meters

h_{fs} = All suction line losses converted from pressure to meters

h_a = Acceleration head losses (applicable for PD pumps)

The 1.1 is a 10% safety factor.


Written By: *ts*
Checked: *MFW*

79

For the MFA plant it was easier to evaluate the NPSH as a pressure and then convert that value to the equivalent head in meters. MFA P-203/P-204 will be used as an example to walk through the typical assumptions. Because the tank operates at atmospheric pressure $h_p = 1.013$ bar. The vapor pressure for MFA was assumed to be the worst case, which is the vapor pressure of GM: $h_{vpa} = 0.0133$ bar. h_{st} = minimum liquid level of the tank - pump datum level. In this case the liquid level was assumed to provide a pressure of 0.1 bar and the pump datum level was 0.2 meters. The suction line losses were determined to be 0.06 bar through 12 meters of equivalent length.

$$NPSH_A = \left[\frac{(1.013 + 0.1 - 0.6 - 0.0133)}{0.0981 * 0.935} - 0.2 \right] \left(\frac{1}{1.1} \right) = 9.75m$$

For the MFA pump design spec sheets the 7.6 meter convention is maintained. That is, NPSH available seldom exceeds 25 ft in practical design. Even when it does, the actual value seldom influences pump selection. As a convention, when the NPSH available is calculated to be higher than 7.5 meters, a value of 7.6 meters “minimum” is specified, rather than the actual value.

Written By: 
 Checked: MFM

80

CAPCOST was used to estimate the capital costs of each pump. The required inputs are the type, material of construction, discharge pressure, and power requirement. This calculation is based off of recorded data for pumps and uses correlations to adjust the cost for size of the unit and inflation. A complete procedure of this can be found in TBWS.

Performed By: Tom Salerno

Checked By: M. Matt

10.2. *Positive Displacement Pumps*

Because the MFA reactor, R-201 needs to operate at very precise and relatively low flow rates, metering pumps are used to charge the reactor. The Power and ΔP equations still hold true except for two small changes. Because the positive displacement pump is a metering pump, the mechanical efficiency is assumed to be 20% (proprietary source). In addition, an acceleration head loss must be included for pump sizing as well as for NPSH concerns. Acceleration head loss occurs because at the instant that the suction valve opens on a positive displacement pump or other controlled volume pump, the liquid must be accelerated into the cylinder.

Estimated Acceleration Head Loss (ft or m),

$$(10.4) \quad ha = \frac{LVnC}{Kg}$$

Written By: MFM

Checked: MJ

81

Where L = length of the suction line from the nearest upstream vessel to the pump

V = Average velocity in the suction line

n = Pump speed, rpm

C = A constant to account for pump geometry, units, and other factors

K = A factor representing the relative compressibility of the liquid

G = Gravitational constant

To take MFA P-105 as an example, $L = 6.096$ m (should be as small as possible),

$V = 0.44704$ m/s, $n = 60$ rpm, $C = 0.2$, $K = 2$, $G = 9.82$ m/s².

$$ha = \frac{(6.096) * (0.44704) * (60) * (0.2)}{(2) * (9.82)} = 1.67m$$

Performed By: M. Matt

Checked By: Tom / a / com

10.3 *Shell and Tube Heat Exchangers*

Similar to centrifugal pumps, the design of the shell and tube heat exchangers for the GM and MFA plants was based off of heuristics. As mentioned previously, two equations for calculation of the heat required for the process streams are used - the area required for the heat exchanger and the flow rate required of the chosen utility.

Written By: MFM

Checked: AS

82


$$(10.5) \quad Q = \dot{m} C_p \Delta T$$

$$(10.6) \quad Q = U A F \Delta T_{lm}$$

From this equation, the value for U has been estimated to be $850 \frac{W}{m^2 K}$ by

TBWS for shell and tube heat exchangers utilizing steam or cooling water. The value of F can be at a minimum .9 before replacement of the heat exchanger because of fouling is necessary. Using this as a conservative estimate for the 1-1 shell and tube heat exchanger is satisfactory. Finally, estimation of the utility temperature for heating is done using the common temperatures of low-pressure steam of 250-275 F, or medium pressure steam of 285-300 F. For the GM cooling requirements it uses the common temperature of cooling water at 80-90 F. For the MFA plant it was assumed that the cooling water is available at 92F (33.3 C) and is returned at 105 F (40.6 C).

For an example of this, please consider Stream 5 in the GM section. The material balance of the plant shows that 408.3 kmole/hr of methacrylic acid must be heated from its storage temperature of 40°C to the reactor temperature of 70°C . The heat capacity of methacrylic acid is recorded as 123.1 kJ/kmole K . The heat required for this stream is

Written By: 
 Checked: MFM

83

$$Q = \dot{m} C_p \Delta T = 408.3 \left(\frac{\text{kmole}}{\text{hr}} \right) * \left(\frac{\text{hr}}{3600 \text{ sec}} \right) * 123.1 \left(\frac{\text{kJ}}{\text{kmole K}} \right) * (343\text{K} - 303\text{K})$$

$$Q = 558.5 \text{ kJ/sec}$$

The heat exchanger area required is then,

$$\Delta T_{lm} = \frac{(T_{util,in} - T_{s,out}) - (T_{util,out} - T_{s,in})}{\ln \left(\frac{(T_{util,in} - T_{s,out})}{(T_{util,out} - T_{s,in})} \right)} = \frac{(408 - 343) - (398 - 303)}{\ln \left(\frac{(408 - 343)}{(398 - 303)} \right)} = 74.55 \text{ K}$$

$$A = \frac{Q}{U F \Delta T_{lm}} = \frac{558.5 \text{ kJ/sec}}{0.85 \frac{\text{kJ}}{\text{m}^2 \text{ sec}} * 9 * 74.55 \text{ K}} = 9.8 \text{ m}^2$$

Finally, the required utility flow rate is

$$\dot{m} = \frac{Q}{C_p \Delta T} = \frac{558.5 \text{ kJ/sec} * \frac{3600 \text{ sec}}{\text{hr}}}{37.37 \frac{\text{kJ}}{\text{kmole K}} (408\text{K} - 398\text{K})} = 5433 \frac{\text{kmole}}{\text{hr}} \text{ lps}$$

Performed By: Tom Salerno

Checked By: M.M.H

10.4 Storage Tanks

For the GM plant, it was assumed that deliveries will be made to the plant every two days. For the MFA plant, it was assumed that GM would be received every

Written By: TS
Checked: MFM

three days and the lauric acid would be received weekly. So the size of the storage tanks must be large enough to hold these capacities. For the GM plant a safety factor of 10% will be added to the design of the tank to allow for vapor space. However, for the MFA plant tanks, a 20% factor will be used. The volume of each tank is calculated from

$$(10.7) \quad V(m^3) = 2.2 * (Daily Capacity (m^3 / day))$$

It is assumed for each of these tanks that the L/D ratio is 1.5, a common value for process tanks. The diameter of the column can be calculated as

$$(10.8) \quad V = \frac{\pi}{4} D^2 * L = \frac{\pi}{4} D^2 * 1.5 * D = 1.5 \frac{\pi}{4} D^3$$

$$D(m) = \left(\frac{4 * V(m^3)}{1.5 * \pi} \right)^{1/3}$$

As an example, consider the storage tank for methacrylic acid TK-202. From Stream 5, the daily requirement of methacrylic acid is 34594 L/hr. Therefore, the volume of the tank must be

$$V(m^3) = 2.2 * \left(34594 (L/hr) * \frac{m^3}{1000L} * \frac{8hr}{day} \right)$$

$$V(m^3) = 608.86$$

Written By: MFM
Checked: B

85

And the diameter of the tank is

$$D(m) = \left(\frac{4 * 608.86(m^3)}{1.5 * \pi} \right)^{1/3} = 8.03$$
$$L(m) = 1.5 * D(m) = 1.5 * 8.03(m) = 12.04$$

Performed By: M. Mott

Checked By: [Signature]

10.5 Continuous Tubular Reactor with Heat Exchange

The designs of all plug flow reactors in the GM and MFA plants follow a numerical approach in solving the differential equations developed by Fogler.

Since every reaction considered is exothermic, the models will be produced based from derivations made in the book where the heat is carried away via heat exchange with cooling water jackets around the pipe.

Written By: M. Mott
Checked: 15

To illustrate the technique, consider the GM reactor, R-201, where sodium hydroxide and methacrylic acid combine to form sodium methacrylate and water. The mole balances of each species, where F_i is the molar flow rate of species i,

$$\begin{aligned}
 (10.9) \quad & \frac{dF_{SH}}{dV} = -r_{SH} \quad SH = \text{sodium hydroxide} \\
 & \frac{dF_{MA}}{dV} = -r_{MA} \quad MA = \text{methacrylic acid} \\
 & \frac{dF_{SM}}{dV} = -r_{SM} \quad SM = \text{sodium methacrylate} \\
 & \frac{dF_W}{dV} = -r_W \quad W = \text{water}
 \end{aligned}$$


The rate of reaction was derived earlier and is

$$\begin{aligned}
 (10.10) \quad & \text{rate} = .3487 \exp \left[(5084.9) \left(\frac{1}{273 + 36.6} - \frac{1}{T} \right) \right] [SH][MA] \\
 & [SH] = \text{molar concentration of sodium hydroxide} \\
 & [MA] = \text{molar concentration of methacrylic acid}
 \end{aligned}$$

The molar concentration is related to the molar flow rate as

$$(10.11) \quad F_i = Q^*[i] \quad \text{where } Q = \text{volumetric flow rate}$$

Combine equations 9.8 and 9.9 gives

Written By: 
 Checked: MPM

$$(10.12) \quad r = .3487 \exp \left[(5084.9) \left(\frac{1}{273 + 36.6} - \frac{1}{T} \right) \right] \frac{F_{SH}}{Q} * \frac{F_{MA}}{Q}$$

$$\text{where } r = -\frac{dF_{SH}}{dV} = -\frac{dF_{MA}}{dV} = \frac{dF_{SM}}{dV} = \frac{dF_W}{dV}$$

Equation 9.10 is then rewritten in terms of residence time by applying

$$\theta = V / Q = \text{residence time}$$

$$(10.13) \quad \frac{dF_i}{dV} = \frac{dF_i}{dV} \frac{Q}{Q} = \frac{dF_i}{d\theta Q} = \frac{1}{Q} \frac{dF_i}{d\theta}$$

Thus, the mole balances on each species is

$$(10.14) \quad \frac{dF_i}{d\theta} = \frac{.3487}{Q} \exp \left[(5084.9) \left(\frac{1}{273 + 36.6} - \frac{1}{T} \right) \right] F_{SH} * F_{MA}$$


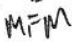
$$\frac{dF_i}{d\theta} = Q * r$$

Next, an energy balance is performed on this system to account for heat exchange with cooling water outside of the PFR and the heat produced by the reaction in the PFR. Fogler gives the result of this balance as

$$(10.15) \quad \frac{dT}{dV} = \frac{Ua(T_w - T) + r * \Delta H_{rxn}}{\sum F_i C_{p,i}}$$

$$\frac{dT_w}{dV} = \frac{Ua(T - T_w)}{F_w C_{p,w}}$$

$$\text{where } a = \text{Unit Heat Transfer Area} = \frac{4}{D}$$

Written By: 
 Checked: 

Once again, this equation is rewritten in terms of residence time as

$$\frac{dT}{d\theta} = Q \frac{Ua(T_w - T) + r^* \Delta H_{rxn}}{\Sigma F_i C_{p,i}}$$

$$(10.16) \quad \frac{dT_w}{d\theta} = Q \frac{Ua(T - T_w)}{F_{CW} C_{p,w}}$$

where F_{CW} = molar flow of cooling water

Utilizing Euler's method to solve these coupled differential equations, inlet conditions of the reactor are assessed first. The streams entering R-201 are streams 6 and 7. From these streams the inlet conditions are

$$F_{MA} = 6804 \text{ mol / min}$$

$$F_{SH} = 6804 \text{ mol / min}$$

$$F_{SM} = 0 \text{ mol / min}$$

$$F_W = 744806 \text{ mol / min}$$

$$T_{in} = 343 \text{ K}$$

$$T_w = 323 \text{ K}$$

Choosing a residence time of .001 minutes, the conditions of the reactor are calculated as

$$V = \theta * Q = .001 \text{ min} * 14186 \text{ L / min} = 14.186 \text{ L}$$

$$Length = V / A = \frac{14.186 \text{ L}}{\frac{\pi}{4} D^2} = \frac{.014186 \text{ m}^3}{\frac{\pi}{4} (.508 \text{ m})^2}$$

$$Length = .07 \text{ meters down the PFR}$$

Written By: *TS*
 Checked: *MFM*

From equation 9.12

$$F_{i,t+1} = F_{i,t} + \Delta\theta * \left(\frac{.3487}{Q} \exp \left[(5084.9) \left(\frac{1}{273 + 36.6} - \frac{1}{T} \right) \right] F_{SH} * F_{MA} \right)$$

$$F_{i,t+1} = F_{i,t} + .001 * \left(\frac{.3487}{14186} \exp \left[(5084.9) \left(\frac{1}{273 + 36.6} - \frac{1}{343} \right) \right] 6804 * 6804 \right)$$

$$F_{i,t+1} = F_{i,t} + (4.812)$$

The flow rate of sodium hydroxide at this time step will be

$$F_{NaOH,1} = F_{NaOH,0} - (4.812)$$

$$F_{NaOH,1} = 6804.898 - (4.812) = 6800.086 \text{ mole / min}$$

Similarly, the temperature of the process stream and the cooling water stream are calculated using Euler's method,

Written By: *DS*
 Checked: *MFV*

$$T_{i+1} = T_i + \Delta\theta * Q \frac{Ua(T_{w,i} - T_i) + r_i * (\Delta H_{rxn})}{\Sigma F_i C_{p,i}}$$

$$T_1 = T_0 + .001 * 14186 \frac{(51) \frac{4}{.508} (298 - 343) + (.339) * (50.2)}{(6804 * .1706 + 6804 * .1231 + 744806 * .075312)}$$

$$T_1 = 343 - .0002534 = 342.99975 \text{ K}$$

$$T_{w,i+1} = T_{w,i} + \Delta\theta * Q \frac{Ua(T - T_w)}{F_{CW} C_{p,w}}$$

$$T_{w,1} = T_{w,0} + (.001) * 14186 \frac{(51) \frac{4}{.508} (343 - 298)}{5000 * .075312}$$

$$T_{w,1} = 298 + .009655 = 298.009655 \text{ K}$$

This procedure is continued down the length of the PFR until the desired conversion is met.

Performed By: Tom Salerno
 Checked By: [Signature]

10.6 Coiled CTFR

The length of pipe is determined from the procedure outlined in section 10.5. The length of pipe is assumed to be 24.5 mm (1 in.) nominal diameter (1.315 OD), coiled to a diameter of 1 m with 24.5 mm (1 in.) of spacing between successive coils.

Written By: MM
 Checked: [Signature]

The amount of coils per pack is equal to:

$$\# \text{ Coils per coil pack} = \text{Height of Vessel (in)} / (\text{Piping OD} + \text{Spacing Between Coils})$$

$$\text{Length of coil pack} = \# \text{ of Coils} * \text{Circumference of Coil} = \# \text{ of Coils} * \pi d$$

Where d is the diameter of a coil in feet.

$$\# \text{ of coil packs needed} = \text{Length needed for reactor} / \text{Length of coil pack}$$

10.7 Batch Reactor


The sample calculations for the batch reactors are included for reference purposes.

Reaction time

$$(10.16) \quad t = - \int_{C_{A0}}^{C_{Af}} \frac{dC_A}{-r_A} = - \int_{[E]_0}^{[E]_f} \frac{d[E]}{-r_E}$$

Where t is in minutes, $[E]_f$ and $[E]_0$ are the final and initial concentrations of GM respectively, and $-r_E$ is the rate of reaction for GM.

Inserting the rate equation into the denominator, and integrating between bounds:

Written By: MFM
Checked: 


92

$$(10.17) \quad t = - \left(\frac{1}{1.16 \times 10^8 e^{\left(\frac{-7657}{T}\right)} [C]^{0.88}} \right) \int_{[E]_0}^{[E]_f} \frac{d[E]}{[E]^{0.79}} = - \left(\frac{4.7619 ([E]_f^{0.21} - [E]_0^{0.21})}{1.16 \times 10^8 e^{\left(\frac{-7657}{T}\right)} [C]^{0.88}} \right)$$

Cooling ability of the reactor vs. the heat of reaction generated

The same equations for heat transfer used for the PFR were used for Batch, with one exception: the SA available for heat transfer as well as the volumes for the reactor were varied to compare the effect that increasing reactor size had on the ability to remove heat.

The overall heat transfer coefficient for a jacketed stainless steel vessel was estimated from several sources, including Chemical Process Equipment, TBWS, and from meeting with Mr. S. Schon. Chemical Process Equipment lists a value between 30-120 Btu/(hr*ft²*F), when brine is the jacket fluid and when an organic is the fluid inside the vessel. It also lists values of 24.4 and 72.3 for a water/paraffin wax system when the vessel is copper or cast iron respectively. Mr. Schon has suggested 60 Btu/(hr*ft²*F) and since this value seems to fall within the literature ranges, that value has been used with sensitivities of 48 and 72, which are +-20% from 60.

Written By: MPM
 Checked: 

93

Surface Area for Cooling Jacket

$$(10.18) \quad SA = \pi \left(\frac{d}{2} \right)^2 + 4 \frac{H}{D} 0.8 \pi \left(\frac{d}{2} \right)^2$$

Where d is the diameter of the reactor in meters, H/D is the ratio of the height of the reactor vs. the reactor diameter, and 0.8 is a multiplier assuming that 80% of the wall surface area is available for heat exchange. The H/D ratio used was 2:1.

Volume of the Reactor as a function of diameter

$$(10.19) \quad V = 1000 * 0.25 * \frac{H}{D} \pi d^3$$

1000 is the conversion factor for converting m³ to L.

As d increases, so does the volume of the reactor, thus increasing the heat generated by the reaction. In addition the surface area for heat exchange increases, thus increasing the ability to remove heat. As has been discussed in the body of the report, there is a maximum diameter where $Q_{cool} = Q_{tot}$ and if the size of the reactor increases any more the total heat generated will exceed the ability to cool.

Performed By: MMA

Checked By: For Fakruo

Written By: MPM
Checked: TJ


10.8 Utilities for Storage Tanks

This section is a combination of both sections 9.2 and 9.3 because it takes into account equations from each. Several of the MFA plant tanks require utilities such as steam, cooling water, or chilled water. The assumptions for these utilities are shown in our scope assumptions in section 2.1.

The requirements for tank utilities are due to heat transfer with the environment due to temperature gradients. To use V-110 as an example, it is required that the lauric acid in storage tank V-110 be maintained at 100C. This is partly to keep the lauric acid liquefied and also as a requirement for the reactor operation. V-110 is assumed to be indoors with a constant ambient temperature of 25C.

Using equation 10.6, the Q released to the environment is equal to the surface area of the tank in this case equal to 35 m² multiplied by the heat transfer coefficient, which to be conservative is assumed to be $10 \frac{W}{m^2 K}$, multiplied by the temperature difference which is equal to 75 degrees Celsius.

$$Q = 35 * 10 * 75 = 26.250 \text{ kJ/s}$$

Written By: MPM
Checked: 

95

To find the steam needed to compensate for this loss to the environment, the Q released is divided by the heating value of the steam. The steam for the MFA plant is assumed to be 2 bar steam, which has an evaporative heating value of 2201.6 kJ/kg.

$$(10.20) \quad F_{steam} (L/min) = \frac{Q}{\Delta H} \hat{V} * 60 \frac{s}{min} * 1000 \frac{L}{m^3}$$

V-hat is the specific volume of steam, which at 2.0 bar is 0.885 m³/kg. Inserting the pertinent values:

$$F_{steam} (std L/min) = \frac{26.25 \frac{kJ}{s}}{2201.6 \frac{kJ}{kg}} 0.885 \frac{m^3}{L} * 60 \frac{s}{min} * 1000 \frac{L}{m^3} = 642.8 std L/min$$

Since the surface area of fluid in contact with the tank is changing continuously, and because the 642.8 L/min flowrate was calculated using a full tank of lauric acid, an average value (i.e. tank is half full) would simply be half or 321.4 L/min as can be seen in Table 6.3 in the utilities section under steam usage.

Performed By: M. Mutt

Checked By: Tom Sg/emu

Written By: M. Mutt
Checked: B

10.9 Cash Flow Analysis (Year 1)

Plant Capital

- All capital expenditures including equipment, reactors, and land costs were paid in years -2, -1, 0.
- Capital Equipment Costs=\$0
- Land Costs=\$0

Plant Capacity

- It is assumed that the MFA plant will be operating at 25% of capacity within the first year of operation

$$\text{Capacity} = .25 * \text{Design Capacity}$$

- $$\text{Capacity} = .25 * 55 \left(\frac{\text{MM lb}}{\text{yr}} \right)$$

$$\text{Capacity} = 13.75 \left(\frac{\text{MM lb}}{\text{yr}} \right)$$

Revenues

- Price

$$\text{Price} = (\text{MFA Selling Price})_{2007} * (1 + \text{Inflation})^{2010-2007}$$

- $$\text{Price} = (1.17)_{2007} * (1 + .03)^{2010-2007}$$


$$\text{Price} = \$1.28 / \text{lb}$$

- Sales

$$\text{Sales} = \text{Capacity} * \text{Price}$$

- $$\text{Sales} = 13.75 * 10^6 \frac{\text{lb}}{\text{yr}} * \$1.28 / \text{lb}$$

$$\text{Sales} = \$17.56 \text{MM}$$

Written By: 
Checked: MPM

- Total Revenue

- $Total\ Revenue = Sales = \$17.56MM$

Expenses

- Cost of Manufacturing (without depreciation or SG&A)

- $COM_d = (Direct\ Manufacturing\ Cost + Fixed\ Manufacturing\ Cost)_{2007} * (1 + Interest\ Rate)^{2010-2007}$
 $COM_d = ($.934/lb + $.034/lb) * (1 + .03)^{2010-2007}$
 $COM_d = \$1.056/lb$

- SG&A

- It is assumed SG&A is 1% of sales

$$SG\ \&\ A = .01 * Total\ Revenue$$

- $SG\ \&\ A = .01 * \$17.56MM$

$$SG\ \&\ A = \$1.75MM$$

- Total Expenses

$$Total\ Expenses = COM_d * Capacity + SG\ \&\ A$$

- $Total\ Expenses = \$1.056/lb * 13.75MMlb + \$1.76MM$

$$Total\ Expenses = \$14.69MM$$

Depreciation

- Using the MACRS method of depreciation, the first years allowable depreciation is 20% of FCI

$$Depreciation = .20 * FCI$$

- $Depreciation = .20 * \$15.05MM$

$$Depreciation = \$3.01MM$$

Written By: *TS*
 Checked: *MFM*

Taxes

- Taxable Income

$$\text{Taxable Income} = \text{Revenues} - \text{Expenses} - \text{Depreciation}$$

- $\text{Taxable Income} = \$17.56\text{MM} - \$14.69\text{MM} - \3.01MM

$$\text{Taxable Income} = -\$1.14\text{MM}$$

- Tax or Tax Credits

$$\text{Tax} = \text{Income Tax Rate} * \text{Taxable Income}$$

- $\text{Tax} = .35 * (-\$1.14\text{MM})$

$$\text{Tax} = -\$0.39\text{MM}$$

- After Tax Net Profit

$$\text{After Tax Net Profit} = \text{Taxable Income} - \text{Tax}$$

- $\text{After Tax Net Profit} = -\$1.14\text{MM} + \$0.39\text{MM}$

$$\text{After Tax Net Profit} = -\$0.75\text{MM}$$

Working Capital

- Total Working Capital is assumed to be 12% of Revenues

$$\text{Total Working Capital} = .12 * \text{Revenues}$$


- $\text{Total Working Capital} = .12 * \17.56MM

$$\text{Total Working Capital} = \$2.11\text{MM}$$

- Net Working Capital is how much needs to be added to the current account to meet the Total Working Capital requirement.

- $\text{Net Working Capital} = (\text{Total Working Capital})_{2010} - (\text{Total Working Capital})_{2009}$

$$\text{Net Working Capital} = \$2.11\text{MM} - 0 = \$2.11\text{MM}$$

Written By: 
Checked: MFM

After Tax Cash Flow

$$ATCF = \text{After Tax Net Profit} - \text{Capital Expenditure} - \text{Land Cost} - \text{Startup Cost} \\ + \text{Depreciation} - \text{Net Working Capital} + \text{Working Capital Recovery}$$

$$ATCF = -\$0.09\text{MM} - 0 - 0 - 0 + \$3.01\text{MM} - \$2.11\text{MM} + 0$$

$$ATCF = \$0.81\text{MM}$$

Present Value of After Tax Cash Flow

$$(ATCF)_{PV} = ATCF * (1 + \text{Discount Rate})^{2010-2007}$$

$$(ATCF)_{PV} = \$0.81\text{MM} * (1 + .12)^{2010-2007}$$

$$(ATCF)_{PV} = \$0.58\text{MM}$$

Performed By: Tom Salerno

Checked By: M. Mull

10.10 Cost of Manufacturing

The costs of manufacturing were calculated using formulas in TBWS. However, the costs of SG&A were taken from recommendations of Drexel Professors in CHE483 lectures to be 1% of Sales. Thus SG&A will vary with the amount sold.

Written By: TS
Checked: MF

100

Fixed Capital Investment	Capcost	15.05
--------------------------	---------	-------

1. Direct manufacturing costs		
a. Raw materials	Crm	48.508
b. Waste treatment	Cwt	0.000
c. Utilities	Cut	0.326
d. Operating Labor	Col	1.215
e. Direct supervisory and clerical labor	0.18*Col	0.219
f. Maintenance and repairs	.06*FCI	0.903
g. Operating supplies	.009*FCI	0.135
h. Laboratory charges	.15*Col	0.182
i. Patents and royalties	.03*COM	2.028
Total Direct Manufacturing Costs		51.379

-0.10935 Less necessary because we have a small plant

-2.027887 Our process requires no patents

2. Fixed manufacturing costs		
a. Depreciation	---	---
b. Local taxes and insurance	.032*FCI	0.481
c. Plant overhead costs	.708*Col+.036*FCI	1.402
Total Fixed Manufacturing Costs		1.883

3. General Manufacturing Expenses (SG&A)		
a. Administration Costs	3.1% of SG&A	0.004
b. Distribution and selling costs	66.6% of SG&A	0.093
c. Research and development	30.2% of SG&A	0.042
Total General Manufacturing Expenses		0.140

Performed By: Tom Salerno

Checked By: M. Mott

10.11 Capital Costs

All pumps and heat exchangers were priced using CAPCOST. All tanks and reactors were priced using tools provided by Mr. Schon and Arkema. The following is the procedure used to calculate the installation cost of R-210.

The bare cost was found using Arkema's cost estimating spreadsheet. Then an installation factor was found using another Arkema spreadsheet to find the total cost of installing and purchasing this reactor.

Written By: MS
Checked: MM

Table 10.1 – Arkema cost estimating spreadsheet.

Estimating Investment Manual, Version 4				
Item No. ->				
Description ->				
Equip. Title	Continuous-Tube-In-Shell Reactor; Tubes=2000-6000psig, Shell=Vacuum-450psig			
Equip. Code		C_CTISR_A	MAX	MIN
Shell & Tube Reactor (Converters)	No			
Total External Surface Area of Tubes, s.f. ->		-----		
Total Adjustment Factor (additive)		-----	Guess over	Guess less
*Full Radiography (Y/N)->	y	-----	Max (Y/N) ?	Min (Y/N) ?
*Stress Relief (Y/N)->	y	-----	y	y
*Tubes attached to tubesheets by both welding and rolling (Y/N) ->	y	-----	1,636	
*Hub Ring for attaching the shell to tubesheet machined from forging as an integral part of the tubesheet(Y/N)	y	-----		
Subtotal ->		-----		
Continuous-Tube-In-Shell Reactor	Yes			
Tubes-316L 2000-6000psig; Shell-c.s./s.s. vacuum-450psig				
Tube Surface Area, sq.ft. ->	1,720	\$ 247,740	3,000	500
Tank-Type, Agitated Reactor	No			
Capacity, Gal. ->	5,000	-----		
Total Adjustment Factor (additive)		-----		
*Full Radiography (Y/N) ->	y	-----		
*Stress Relief (Y/N) ->	y	-----		
Subtotal ->		-----		
Total 1975 Cost->		\$ 247,740		
Current Date	2007	196%	Exchanger Index	
Current Cost		\$ 486,225		
Year Delivered ->	2007	196%	Exchanger Index	
Delivered Cost ->		\$ 486,225		
Purchased Equipment Cost	\$ 486,225.11			
Installation Factor	5.39			
Total Cost	\$ 2,620,753.36			

Performed By: Tom Salerno

Checked By: M. Matt

10.12 MFA Price

The selling price of MFA was calculated to have the increased cost of purchasing MFA for inclusion in production of VE resins to equal to the cost to install and fuel styrene reducing emission equipment.

From reported data

Table 10.2 - Average utilities cost

Written By: MF
 Checked: MF

Estimating Styrene Impact (Year =>)	2001
Electricity Cost Plant 1	\$ 197,019
Electricity Cost Plant 5	\$ 106,868
Average Electricity Cost	\$ 151,943
Feul Gas Cost Plant 1	\$ 32,598
Feul Gas Cost Plant 2	\$ 54,210
Average Feul Gas Cost	\$ 43,404
Equiv Cap Cost Plant 1	\$ 39,165
Equiv Cap Cost Plant 5	\$ 89,315
Average Equiv Cap Cost	\$ 64,240
Average Total Cost	\$ 259,587

The average production of Plant 5 is 2.78MM lb/year. Thus the effective cost of installing styrene emission reducing equipment is \$.0934 per pound of product.

The cost increase due to MFA inclusion in VE resins is calculated as

- $Cost_{MFA} = (\$_{MFA} - \$_{Styrene}) * \%_{reduction} * Initial \%_{Styrene} \text{ in resin}$
- The reduction of styrene emissions studied in the paper averaged 50%
- The average styrene concentration present in the VE resins was 40%

$$Cost_{MFA} = (\$_{MFA} - \$_{.70}) * .5 * .40$$

$$\$_{.0934} = (\$_{MFA} - \$_{.70}) * .5 * .40$$

$$\$_{MFA} = 1.17$$

Performed By: Tom Salemi

Checked By: M. Malt

10.13 Sensitivity

The measurement calculated for each variable was the sensitivity factor. This is defined as the change in IRR produced by a 10% increase in the independent

Written By: BS
 Checked: MFM

variable. Thus this measure predicts how much the IRR will change when each of the six parameters increases by 10% of its original value.

$$S = \left(\frac{IRR_{new} - IRR_{base}}{\frac{\$GM_{new} - \$GM_{base}}{\$GM_{base}} * .10} \right)$$

$$S = \left(\frac{18 - 21}{\frac{\$1.449 - \$1.38}{\$1.38} * .10} \right) = -6$$

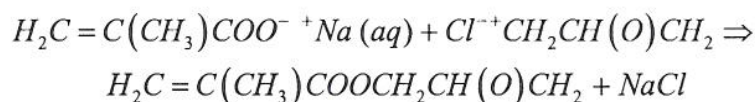
Performed By: Tom Salerno

Checked By: M. Mat

10.14 Hess's Law

The heat release for the reaction producing GM was calculated using Hess's Law. For this calculation the heat of formation of each species was required. The following is the values used and their sources.

Reaction Chemistry



Heats of Formation

Written By: B
 Checked: MFM

- Sodium Methacrylate(aq)
 - $\Delta H_f = -164.2 \text{ kJ / mole}$
 - Hess's Law from Reaction #1
- Epichlorohydrin (liq)
 - $\Delta H_f = -149 \text{ kJ / mole}$
 - Knovel Critical Tables
- Glycidyl Methacrylate (liq)
 - $\Delta H_f = -455.4 \text{ kJ / mole}$
 - Knovel Critical Tables
- Sodium Chloride (aq)
 - $\Delta H_f = -407.2 \text{ kJ / mole}$
 - Knovel Critical Tables

$$\Delta H = \left(\sum \Delta H_f \right)_{\text{products}} - \left(\sum \Delta H_f \right)_{\text{reactants}}$$

$$\Delta H = -(455.4 + 407.2) + (164.2 + 149)$$

$$\Delta H = -549.4 \text{ kJ / mole}$$

Performed By: Tom Iwano

Checked By: M. Malt

Written By: B
 Checked: MPM

10.15 Decanter Size

Both decanters present in the GM subsection of the report are continuous with 30 minute residence times. A safety factor of 50% was used for both decanters. The following is a sample calculation for R-203.

$$\text{Volume} = \text{Safety Factor} * \text{Flowrate} * \text{Residence Time}$$

$$\text{Volume} = 1.5 * 146419 \left(\frac{\text{L}}{\text{hr}} \right) * .5 \text{hr}$$

$$\text{Volume} = 109800 \text{ L}$$


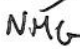
The phase separation section of the GM plant was designed using Aspen. The following is the input summary and results obtained.

Performed By: Tom Falcow

Checked By: M. Matt

Written By: TS
Checked: MPM

Aspen Printout Following Page

Written By: 
Checked: 

107

r203.tmp

```
;
;Input Summary created by Aspen Plus Rel. 13.2 at 13:41:20 Thu Mar 8, 2007
;Directory J:\GM ASPEN  Filename C:\DOCUME~1\DESIGN~1\LOCALS~1\Temp\~apd1.tmp
;
```

DYNAMICS

DYNAMICS RESULTS=ON

TITLE 'GM Flash'

IN-UNITS ENG

DEF-STREAMS CONVEN ALL

DATABANKS PURE13 / AQUEOUS / SOLIDS / INORGANIC / &
NOASPENPCD

PROP-SOURCES PURE13 / AQUEOUS / SOLIDS / INORGANIC

COMPONENTS

ALPHA-01 C3H5ClO /
WATER H2O /
SODIU-01 NaOH /
METHA-01 C4H6O2-D5 /
SODIU-02 NaCl /
GM C7H10O3

FORMULA GM C7H10O3

FLOWSHEET

BLOCK B4 IN=1 OUT=2 3

PROPERTIES RK-SOAVE

STRUCTURES

STRUCTURES GM C1 C2 D / C1 C3 S / C1 C4 S / C4 O5 &
D / C4 O6 S / O6 C7 S / C7 C8 S / C8 O9 S / &
C8 C10 S / C10 O9 S

ESTIMATE ALL

PROP-DATA PCES-1

IN-UNITS ENG

PROP-LIST TC / PC / VC / ZC / DGFORM / OMEGA / DHVLB / &
VB / VLSTD / RKTZRA

PVAL GM 751.8453528 / 491.9720452 / 6.623634635 / &
.2506405000 / -1.0678848E+5 / .4643656020 / 19659.10211 / &
2.425480991 / 1.992164495 / .2476308700

PROP-LIST VLSTD

PVAL SODIU-01 .3594623290

PROP-DATA USRDEF

IN-UNITS ENG TEMPERATURE=K MOLE-ENTHALP='J/kmol'

PROP-LIST TB / MW / SG / DHFORM

PVAL GM 469 / 142 / 1.071 / -455400

PROP-DATA CPIG-1

IN-UNITS ENG

PROP-LIST CPIG

PVAL GM 36.36301315 .0588804593 -1.8194955E-5 5.5636601E-10 &
0.0 0.0 44.33000365 1520.329992 8.605426579 &

Page 1

2.68074785E-3 1.500000000

PROP-DATA DHVLWT-1

IN-UNITS ENG

PROP-LIST DHVLWT

PVAL SODIU-01 48929.12511 613.1299991 2.100213590 &
-5.162744530 613.1299991PVAL GM 25121.30232 127.0400030 .5805131300 -.3924290720 &
127.0400030

PROP-DATA KLDIP-1

IN-UNITS ENG

PROP-LIST KLDIP

PVAL GM -.0294587278 8.07947468E-4 -2.5958872E-6 &
3.39385593E-9 -1.682998E-12 384.5300009 739.7301991

PROP-DATA MULAND-1

IN-UNITS ENG

PROP-LIST MULAND

PVAL GM -4.265524133 2410.200143 1.90374827E-7 384.5300009 &
448.9665156

PROP-DATA PLXANT-1

IN-UNITS ENG

PROP-LIST PLXANT

PVAL GM 2336.549891 -1.1640377E+5 0.0 .3328960838 &
-366.4510330 -2.284514E-17 6.000000000 127.0400030 &
252.5900020

PROP-DATA SIGDIP-1

IN-UNITS ENG

PROP-LIST SIGDIP

PVAL SODIU-01 588.2138740 1.222222220 1.7883133E-10 &
-1.989210E-10 7.9947794E-11 2834.329981 4514.809968
PVAL GM 73.33764710 1.222222220 -3.500641E-10 3.9270352E-10 &
-1.563979E-10 384.5300009 727.6150454

PCES-PROP-DATA

IN-UNITS ENG PRESSURE=atm TEMPERATURE=C PDROP=psi

PL GM 52.8 .00222 / 62.66 .00417 / 97.5 .028 / 114.56 &
.0614 / 122.55 .086

STREAM 1

SUBSTREAM MIXED TEMP=25. <C> PRES=1.82 <bar>

MOLE-FLOW ALPHA-01 2062.15 <kmol/hr> / WATER &
45085. <kmol/hr> / SODIU-01 11.32 <kmol/hr> / METHA-01 &
11.32 <kmol/hr> / SODIU-02 377.3 <kmol/hr> / GM &
377.3 <kmol/hr>

BLOCK B4 DECANter

PARAM TEMP=25. <C> PRES=1. <bar> LL-METH=EQ-SOLVE &

L2-COMPS=ALPHA-01 GM

EO-CONV-OPTI

STREAM-REPOR MOLEFLOW

PROPERTY-REP PCES

;
;
;
;
;
;
;

BLOCK: B4 MODEL: DECANTER

```

-----
INLET STREAM:          1
FIRST LIQUID OUTLET:   2
SECOND LIQUID OUTLET:  3
PROPERTY OPTION SET:    RK-SOAVE  STANDARD RKS EQUATION OF STATE

```

```

*****
*
*      VAPOR PRESENT IN FEED TO BLOCK
*
*****

```

```

***  MASS AND ENERGY BALANCE  ***
                                IN      OUT      RELATIVE DIFF.
TOTAL BALANCE
MOLE(LBMOL/HR)                 105655.    105655.    0.000000E+00
MASS(LB/HR )                   0.238115E+07  0.238115E+07  -0.542534E-07
ENTHALPY(BTU/HR )              -0.127289E+11 -0.128229E+11  0.733229E-02

```

*** INPUT DATA ***

```

LIQUID-LIQUID SPLIT, TP SPECIFICATION
SPECIFIED TEMPERATURE          F              77.0000
SPECIFIED PRESSURE              PSI            14.5038
CONVERGENCE TOLERANCE ON EQUILIBRIUM              0.10000E-03
MAXIMUM NO ITERATIONS ON EQUILIBRIUM              30
EQUILIBRIUM METHOD              EQUATION-SOLVING
KLL COEFFICIENTS FROM          OPTION SET OR EOS
KLL BASIS                      MOLE
KEY COMPONENT(S):              ALPHA-01  GM

```

*** RESULTS ***

```

OUTLET TEMPERATURE          F              77.000
OUTLET PRESSURE              PSI            14.504
CALCULATED HEAT DUTY        BTU/HR        -0.94021E+08
MOLAR RATIO 1ST LIQUID / TOTAL LIQUID          0.94540

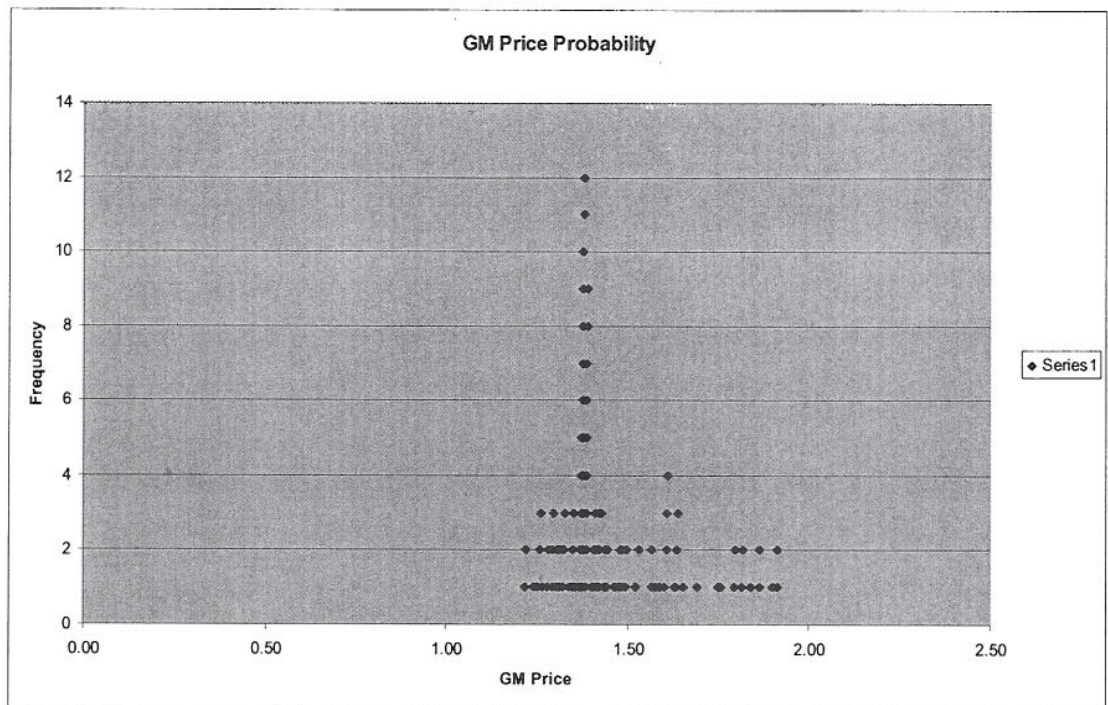
```


L1-L2 PHASE EQUILIBRIUM :

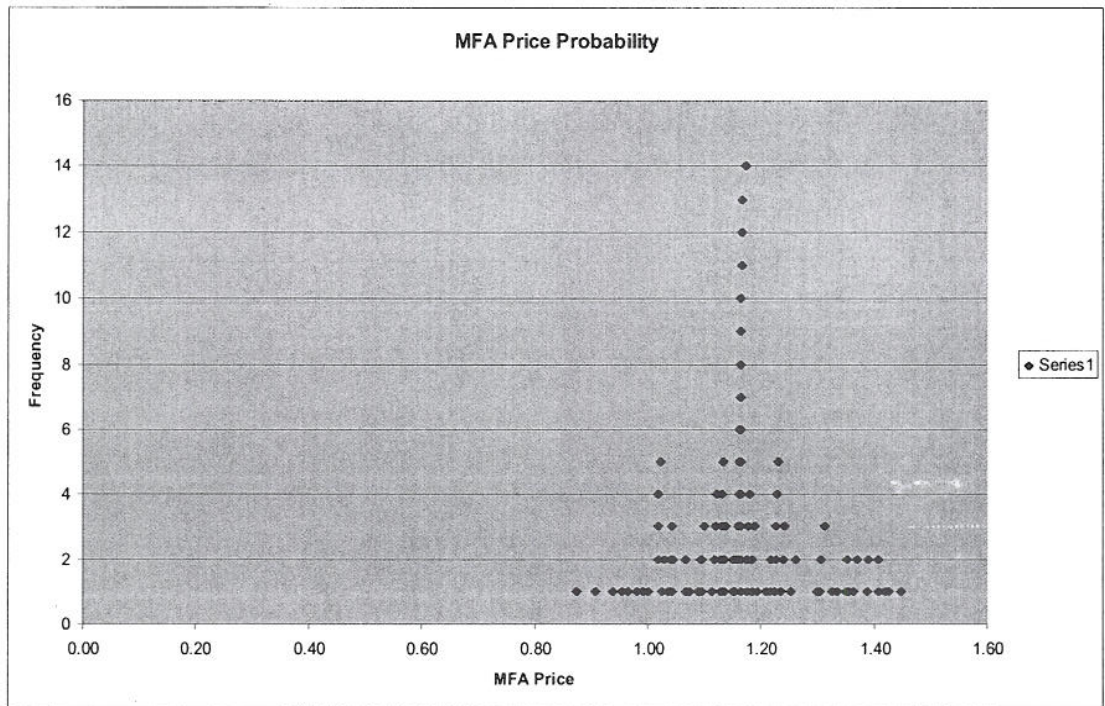
COMP	F	X1	X2	K
ALPHA-01	0.043029	0.392025-06	0.78810	2,010,330.
WATER	0.94075	0.99169	0.058773	0.059266
SODIU-01	0.00023621	0.00024858	0.219402-04	0.088262
METHA-01	0.00023621	0.163452-08	0.0043262	2,646,780.
SODIU-02	0.0078728	0.0080627	0.0045850	0.56867
GM	0.0078728	0.130414-11	0.14420	0.110567+12

10.16 Probability Distributions for Monte Carlo

The values of each variable were assigned a probability such that the most frequent value will be the base case, and the total fluctuation will vary from the worst to the best case with a descending probability.



Written By: 
Checked: MFM



Performed By: Tom Salcrao

Checked By: M. Hall

Written By: B
 Checked: MPM

11. Process Optimization

The main area of optimization for this design was in the reactor design. Initially, when the reactor was a batch vessel, it had to be sized based on the maximum heat load that could be transferred out of the reactor, as was discussed in the alternative reactors section. There was an optimization of the maximum size of the reactor, which was determined by the conditions in the reactor such as catalyst present and temperature. At higher temperatures the maximum reactor size was smaller, so many reactors were needed to meet the total yearly production. At lower temperatures the maximum reactor size could be larger, but because the temperatures were low the reaction took longer to go to completion. Therefore, it was a trade-off between total reaction time and the number of reactors needed.

Because this design embraces continuous operation, the optimization for batch operation is not valid. There were two main optimizations within the design of the coiled tubular flow reactor. The first was to optimize the temperature profiles of the reactor contents to reduce the total residence time needed in addition to providing a simple way to heat up the reactants to the proper reaction temperature of 110°C. Another area of optimization was the design of the tempered water loop and the design of the reactor vessel to improve the flow characteristics of the tempered water.

Optimization of Tempered Water Flow-rate

As was discussed in section 3.3.2, there was a need to heat up the reactants from the feed temperature, 60°C, to the reactor operating temperature 110°C. The first design was to use a length of extra coil that would not be submersed in any cooling water and utilize the heat of reaction. However, at low temperatures the reaction rate is so low, starting at 60°C, and the reaction took as much as 70 minutes to get up to 110°C. As a result, the total residence time increased by as much as 100%.

The solution to this was that instead of running one coil pack adiabatically, the coils could be submerged in the reactor vessel and come into contact with the warm tempered water stream. Because the tempered water stream needs to enter the reactor close to the reactor operating temperature, there would be a gradient of almost 50°C. At a tempered water inlet flow-rate of 90 L/min @ 110°C the reactor flow of 6.51 L/min is able to heat up to 110°C within 3 minutes of residence time. This comparison can be seen below in Figure 11.1.

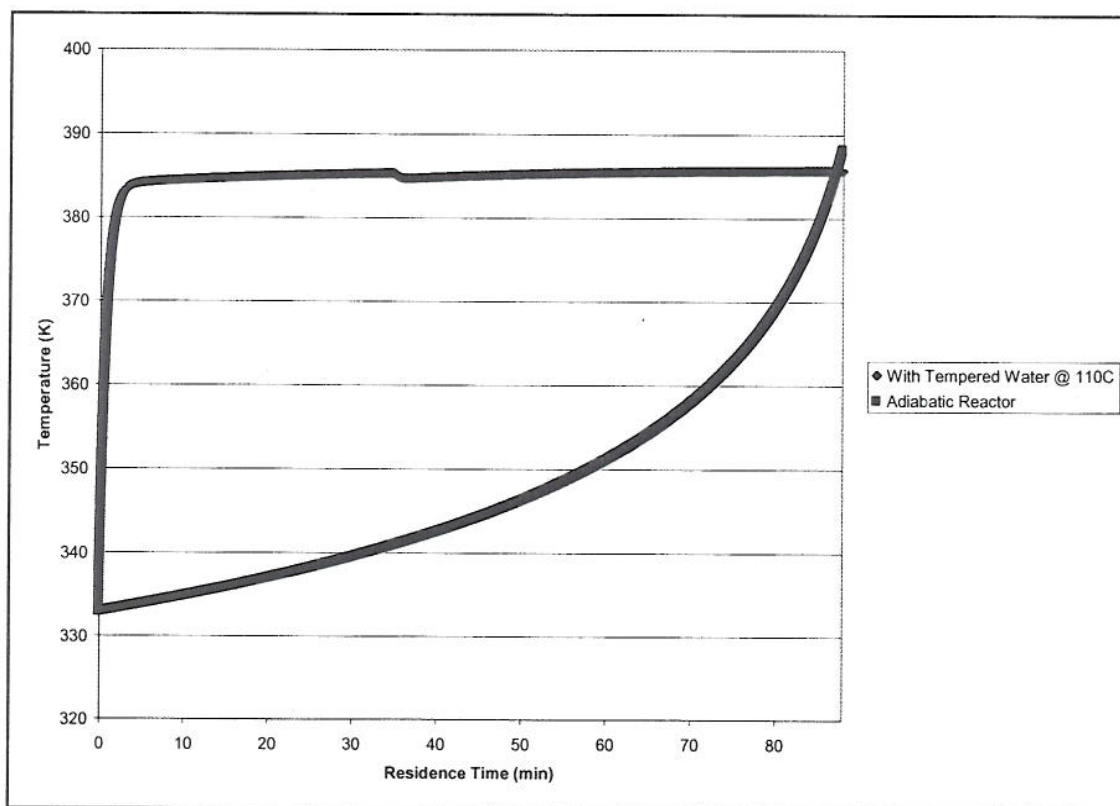


Figure 11.1 – Temperature profiles of reactor system for adiabatic operation versus Tempered Water @ 110°C, 90 L/min

The 90 L/min flow-rate for the tempered water going to the first stage of the reactor was selected because first, it needs to be able to heat up the reactants to 110°C quickly. Secondly, the high flow-rate enables water to act as an excellent heat sink for the heat of reaction. As can be seen below in figure 11.2, the water temperature follows the reactor temperature closely and prevents the temperature of the reactor from getting too high. If a lower flow-rate was chosen, the reactor temperature would increase over the limit of 110 to 115°C. Increasing the flow-rate over 90 L/min is not necessary because the temperature profile of both the reactor as well as the bath would just become more flat. Since it is desired that the temperature still increase to some degree, 90 L/min is the optimization point.

Written By: MFM
Checked: CM

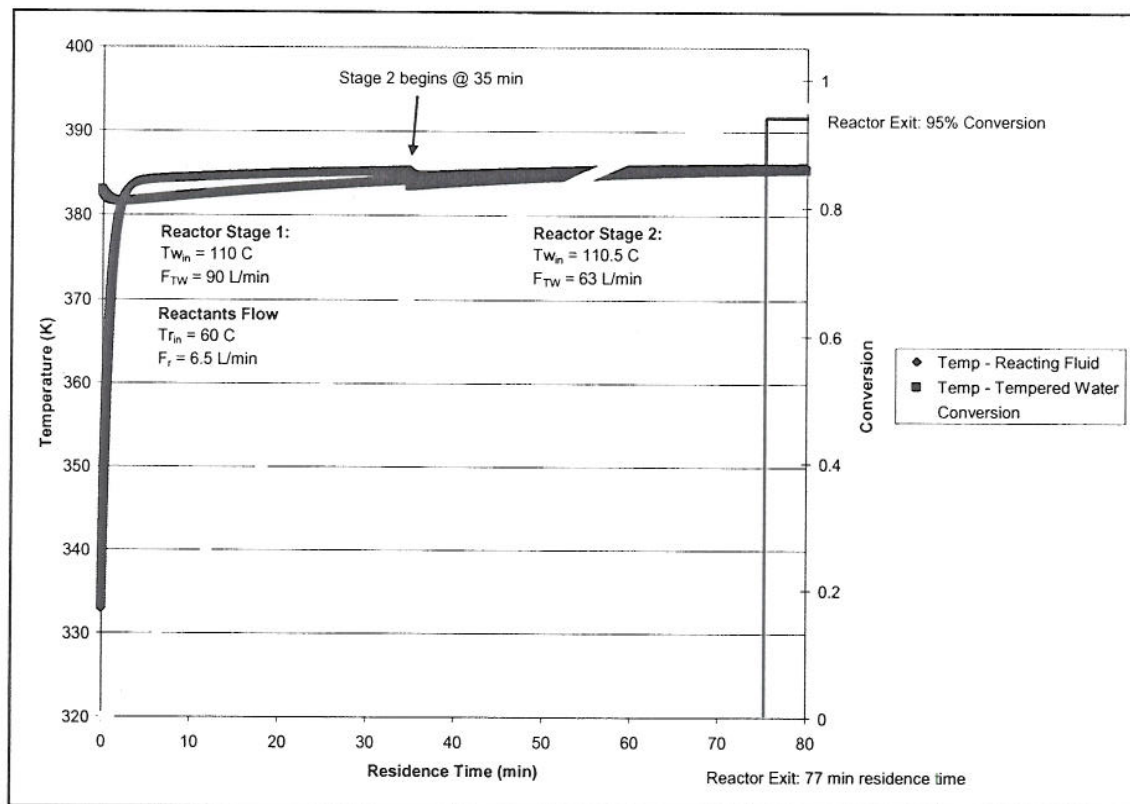


Figure 11.2 – Temperature profiles of reactor system and tempered water streams for entire length of reactor

The reactor vessel is divided in half, with each having two compartments, one for each coil pack. Each half has its own tempered water loop. Having two tempered water loops is important for operation of the last two reactor coils and for additional controllability of the reactor. The second half of the reaction, because the concentrations of the reactants will be lower, the reaction rate will be lower, and thus the heat of reaction will be less. If the tempered water bath is controlled by one loop, the temperature at the end of the reactor would slowly decrease. But, by decreasing the flow from 90 L/min to 63 L/min, the temperature profile of the reactor can remain much steadier and even increase slightly to maximize the reaction

rate at the lower concentrations. By optimizing this flow-rate the total residence time can be reduced by several minutes.

To even optimize the reactor more, four separate tempered water loops could have been used. However, it was decided to save costs on buying two additional centrifugal pumps, two heat exchangers, valves, piping and controls. The incremental cost of using more than two separate loops outweighs the incremental benefits of having additional independent controllability. Therefore, it was decided to use just two tempered water loops instead.

Dimensions/Sizing of the Reactor Vessel

Also in regards to the optimization reactor design, the sizing of the reactor vessel, which the tempered water flows through, was optimized to promote turbulent flow through the reactor. The variables for the Reynolds number are the diameter of the tube, in this case the equivalent diameter of the compartment, the velocity of the water, the density of the water, and the viscosity at the operating temperature.

Initially, the sizing of the vessel was done through a “back of the envelope” calculation, which was based on a diameter of the reactor coils equal to 1.5 meters and then adding a few extra meters of diameter for extra spacing. The result was a vessel diameter of 6.1 meters and a vessel height of 3.81 meters. The height was determined by the reactor length needed (1000 m) and coiling the piping in four

Written By: MFM
Checked: CM

114


separate coil packs. Because the diameter was so oversized, the individual compartments of the vessel were too large and so the velocity of the water flowing was very low. Using a vessel diameter of 6.1 meters, and a flow-rate of 90 L/min the resultant Reynolds number was ~ 1000 , so laminar flow.

To achieve turbulent flow, the reactor dimensions could be optimized. By decreasing the required coil diameter to 1 meter instead of 1.5 meters, and by being less generous on the required spacing, the diameter of the vessel was reduced to 3 meters from 6.1 meters. So by reducing to a 3 meter diameter vessel the characteristic length of the equivalent diameter is reduced, but the velocity of the water increases dramatically, such that the Reynolds number ends up being almost 5000, definitely in the turbulent regime. The diameter of the vessel was reduced to reach a minimum tempered water target of 55 L/min. So, any flow above 55 L/min will be turbulent. The normal tempered water flow to the first reactor stage is 90 L/min while the flow to the second stage is set at 63 L/min. Both flows are well above the minimum as a safety factor.

12. Conclusions and Recommendations

In conclusion, investing in the MFA plant designed for 5 million pounds of production per year is very risky. Ultimately, the capital investment will not be made back, nor will it even break even when MFA is sold at the price of \$1.17 per pound. If this plant is built, the IRR is will be negative, at -7%. This is not to say that the product cannot be profitable, but starting with a low production rate will ultimately result in failure. The breakeven point for the MFA plant is at four times the original production, 20 million pounds per year. For the plant to have an IRR above 12%, it must make at least 40 million pounds. The team finally decided that the most realistic, and potentially successful plant, would be at a production rate of 55 million pounds per year, resulting in an IRR of 22%.

However, the risks increase along with the production rate for a product that is not yet on the market. First, there is the risk of the confidence in lowering the GM price from Dow. A plant for GM was designed by the team in order to see how much it costs to make GM, and therefore how much Dow is marking up the price. While this data can be brought into business meetings with Dow when trying to barter a contract for GM, it does not ensure that Dow will lower the price for the MFA production plant. Even with the large amount of GM that is needed and the extra business it will bring their GM plant, it is only a hope that Dow will lower the price. Second, because of raw material costs, MFA will always cost more than styrene: \$1.17 to \$0.88 per pound, respectively.

Written By: CM
Checked: 

116

There are other ways to reduce styrene emissions, including buying equipment to treat the toxic emissions. This latter option is much more attractive to plant owners, rather than buying a whole new ingredient that must be put in the vinyl ester resin, especially since it's more expensive than styrene. Also, since MFA cannot replace all of the styrene and will need to be used continually, it is seen as a more inconvenient solution than a simple one-time purchase of process equipment.

Finally, there is the legislation that needs to be passed lowering the amount of acceptable styrene emissions. If this legislation is not passed, there will be no industry need whatsoever for MFA. Therefore, while the plant that produces 55 million pounds of MFA per year may be profitable on paper, is there a market to sell that much MFA? The reality is, with no legislation passed yet, there is no market for MFA.

Still, the benefits this product can bring to the environment should not be ignored. The positive impact it can have on the environment is sweeping. Since it can replace some of the styrene in the surfboard, boat and military industries – most importantly the latter since it is such a large industry - it has the ability to keep the environment safer and cleaner. Not only is this found in the lifetime of the product, but also, the process of making MFA is environmentally friendly. None of the materials are wasted, there are no toxic emissions and the release of greenhouse gases is very low. While styrene may not be legislated in the near future, a product like MFA that is so gracious to the environment should not be ignored, nor forgotten. Perhaps there may be some companies out there that want to be proactive and reduce their styrene emissions, no matter the verdict from the government. A market study

Written By: CM
Checked: JS

117

on small companies that put an emphasis on being environmentally friendly could find such a niche. Future focus on finding a small market, rather than mass-producing a product that may not be needed, could be something for the company to look into.

Ultimately, the recommendation is to not build the MFA plant. With the risks mentioned above, coupled with the negative numbers seen in the economic feasibility study at low production rates, this project should no longer be pursued by the company.

Written By: CM
Checked: 15

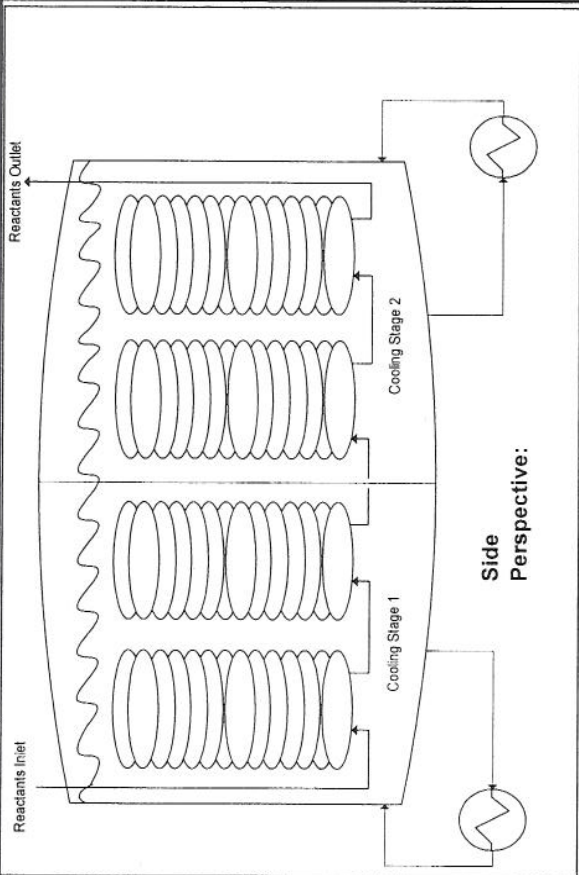
118

HEAT EXCHANGER SPECIFICATION SHEET									
Project Title: Methacrylated Fatty Acid Co-Monomer				Date: 4/27/2007		Compiled by: M. Matt			
						Checked by: N. Galante			
Item	E-202/E-203			E-120			E-220/E-230		
Flowsheet #	200			120			200		
Type:	Double Pipe			Double Pipe			Double Pipe		
	INSIDE	OUTSIDE		INSIDE	OUTSIDE		INSIDE	OUTSIDE	
Fluid Circulating	Tempered Water	Cooling Water		GM	Chilled Water		MFA	Cooling Water	
Temperature & Pressure									
Pressure, bar	7.7	4.0		2.0	4.0		1.98	4.0	
Temperature, °C in	117	33.3		20	10		110	33.3	
Temperature, °C out	107	40.6		19.997	15.6		97.3	40.6	
Liquid Flows									
Flow in, L/min	108	150		877	3.72		937	459	
Flow out, L/min	108	150		877	3.72		937	459	
Specific gravity	1	1		1.04	1		0.94	1	
Heat Capacity, kJ/molK	0.075312	0.075312		0.25	0.075312		0.3305	0.075312	
Viscosity, cP @ 20 C	1	1		2.5	1		48	1	
Performance									
Heat Duty, kJ/min	4519			268			10720		
Overall Coeff. W/m2K	850			850			850		
Fouling Factor	-			-			-		
Log Mean ΔT, °C	75.0			6.9			73.9		
Surface Area, m²	1.3			0.3			3.2		
Design									
Design Press., bar	8.4			4.4			4.4		
Design Temp., °C	142			45			135		
Elevation, m	Grade			Grade			Grade		
Materials of Construction	CS	CS		316L SS	CS		316L SS	CS	
Remarks:	Sized for 108 L/min Tempered Water, max TW side dT = 10°C								
	CP, SG assumed constant								

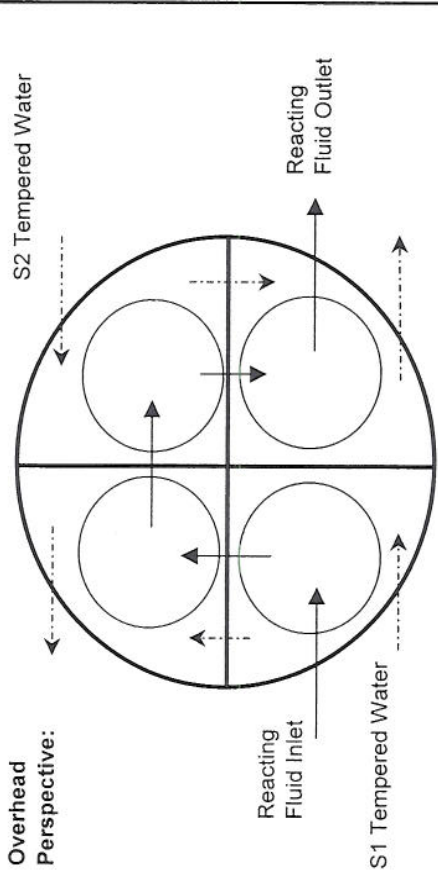
PUMP SPECIFICATION SHEET									
Project Title: Methacrylated Fatty Acid Co-Monomer				Date:	4/27/2007	Compiled by:	Checked by:	Compiled by:	Checked by:
Item				P-101	P-102	P-105	P-203, P-204	P-301	M. Matt
Flowsheet #				110	110	130	200	300	N. Galante
Fluid Circulating				Lauric Acid	Lauric Acid	AMC-2	MFA	MFA	P-201, P-202, P-301
Solids(%)				0	0	0	0	0	200
Temperature, °C				50	100	25	25	122	Tempered Water
Specific Gravity @ 20 C				0.87	0.87	1.01	0.935040474	1	0
Viscosity (cP)				2.5	7.3	N/A	48	1	122
Vapor Pressure (bara)				0.00133	0.00133	0	0.00133	2.1	1
Performance									2.1
NPSHa (m fluid)				7.60	7.60	7.60	7.60	7.60	7.60
Flow(L/min) Normal				876.92	1048.28	0.01	936.74	90.00	90.00
Flow(L/min) Design				964.62	1153.10	0.01	1030.41	1335.00	135.00
Suction Press. (barg)				0.05	0.04	0.05	0.04	4.00	4.00
Discharge Press. (barg)				1.97	1.43	23.46	1.98	7.66	7.66
TDH (m) Normal				17.18	14.78	214.78	19.27	33.92	33.89
TDH (m) Design				18.90	16.26	236.26	21.19	37.31	37.28
Hydraulic kW				5.17	4.44	0.002	5.68	1.37	1.37
Design									
Type of Pump				Centrifugal	PD - Metering	PD - Metering	Centrifugal	Centrifugal	Centrifugal
Position				Horizontal	Horizontal	Horizontal	Horizontal	Horizontal	Horizontal
Efficiency				60%	20%	20%	60%	60%	60%
Driver									
Motor kW				5.92	0.61	0.002	6.51	1.57	1.57
Phase				60 Hz	60 Hz	60 Hz	60 Hz	60 Hz	60 Hz
Efficiency				96%	96%	96%	96%	96%	96%
Motor Type				Fixed	Variable	Variable	Fixed	Fixed	Fixed
Remarks:				Viscosity @ 40 C	Viscosity @ 50 C	Viscosity @ 50 C	Viscosity @ 30 C	Viscosity @ 25 C	Viscosity @ 20 C Pvap
				Pvap @ 121 C	Pvap @ 121 C	Pvap @ 121 C			@ 122 C

VESSEL SPECIFICATION SHEET				
Project Title: Methacrylated Fatty Acid Co-Monomer		Date: 4/27/2007	Compiled by: M. Matt Checked by: N. Galante	
Item:	V-120	V-110	T-220/T-230	T-300
Description:	GM Feed Tank	LA Feed Tank	MFA Test Tanks	MFA Storage
Flowsheet #	120	110	200	300
PRESSURE:				
OPERATING, bara	1.013	1.013	1.013	1.013
DESIGN, bara	2.713	2.713	2.713	2.713
TEMPERATURE				
OPERATING, °C	20	100	110	25
DESIGN, °C	45	125	135	50
SHELL:				
Total Volume, L	11428	32068	10305	32423
I.D., m	2.13	3.01	2.06	3.02
Tan.-to-Tan., m	4.00	5.64	3.86	5.66
Wall Thick., mm	9.7	9.7	9.7	9.7
Corrosion Allow, mm	8.9	-	8.9	-
HEADS:				
TYPE	Fixed Cone Roof	Fixed Cone Roof	Fixed Cone Roof	Fixed Cone Roof
Min. Thick., mm.	5	5	5	5
CONNECTIONS				
Nozzles, size, in.	2	2	2	2
Manholes, diam., mm	609.6	609.6	609.6	609.6
Manhole, davit/hinge	Hinged	Hinged	Hinged	Hinged
MATERIALS				
Shell & Heads	316L SS	CS	316L SS	CS
Trays	-	-	-	-
Other Internals	-	-	-	-
Jacketing:				
Height (m)	-	4.51	-	-
OD, m	-	3.02	-	-
wall thickness, mm	-	6.35	-	-
Steam/Water	-	Steam - 2 bar	-	-
MISCELLANEOUS				
External Heat Exchanger	Yes - Refrigerant	-	Yes - Cooling Water	-
Insulation	85% Magnesita	85% Magnesita	85% Magnesita	-
Remarks:				

REACTOR SPECIFICATION SHEET			
Project Title: Methacrylated Fatty Acid Co-Monomer		Date: 4/27/07	Compiled by: M. Matt Checked by: N. Galante
Item	R-210		
Flowsheet #	200		
Reactor Coils:			
Pipe Diameter (Nom), mm	25.4		
Spacing between coils, mm	25.4		
Diameter of Coil, m	1.00		
Height of Coil Pack, m	4.57		
Length of Coil Pack, m	244		
# of Coil Packs	4		
Vessel:			
Height, m	5.7		
Diameter, m	3		
Total Volume, L	40397		
Wall thickness, mm	9.7		
Design Temperature, C	260		
Design Pressure, bar	9		
Reacting Fluid:			
Feed Temperature, C	60		
Feed Pressure, bar	20		
Exit Temperature, C	235.3		
Residence Time, min	94		
Flowrate, L/min	6.51		
Cooling Fluid Stage 1:			
Feed Temperature, C	Tempered Water		
Feed Pressure, bar	110		
Exit Temperature, C	6		
Flowrate, L/min	111		
Cooling Fluid Stage 2:			
Feed Temperature, C	Tempered Water		
Feed Pressure, bar	110.5		
Exit Temperature, C	6		
Flowrate, L/min	113		
Miscellaneous			
Materials of Construction	316L SS		
Coils	CS		
Vessel	CS		
Insulation of Vessel	85% Magnesia		
Remarks:			



Side Perspective:



Overhead Perspective:

13. Important Data and Properties Used

Process Water		
Amount Kmol/day	379073.218	
Molecular Weight	18	g/mole
Specific Gravity	1	
Viscosity	1	cp
Solubility in water		
Temperature	298	K
Pressure	1	atm
Heat Capacity	75.312	KJ/Kmole K
Heat of Formation	-285.83	kJ/mole

AMC-2 Catalyst		
Specific Gravity	1.01	
Viscosity	2.53	cP
Vapor Pressure	0	bara

Lauric Acid		
Molecular Weight		g/mole
Specific Gravity	0.87	
Viscosity	7.3	cP
Vapor Pressure	0.00133	bara
Heat Capacity	250	kJ/mol K

NaOH .50mol%		
Amount Kmol/day	3266.35135	
Molarity	0.5	mol per liter
Molecular Weight	40	g/mole
Specific Gravity	1.339	
Viscosity	1	cp
Solubility in water	complete	
Temperature	298	K
Pressure	1	atm
Heat Capacity	170.573312	KJ/Kmole K
Heat of Solution	-7.406	kg-cal/gmole
Heat of Formation	-416.88	kJ/mole

Written By: *NMG*
 Checked: *MFM*

Methacrylic Acid		
Amount Kmol/day	3266.35135	
Molecular Weight	86	g/mole
Specific Gravity	1.015	
Viscosity	1	cp
Solubility in water		
Temperature	298	K
Pressure	1	atm
Heat Capacity	123.1	KJ/Kmole K
Heat of Solution	negligible	kg-cal/gmole
Heat of Formation	-416.88	kJ/mole

Epichlorohydrin		
Molar Excess Ratio	3	
Amount Kmol/day	9799.05406	
Molecular Weight	92	g/mole
Specific Gravity	1.18	
Viscosity	1.03	cp
Solubility in water	6	wt %
Temperature	298	K
Pressure	1	atm
Heat Capacity	144.3468	KJ/Kmole K
Heat of Evaporation	38862.6	KJ/Kmole
Heat of Solution	negligible	kg-cal/gmole
Heat of Formation	-149	kJ/mole

Crude Glycidyl Methacrylate Storage Tanker		
Molecular Weight	142	
Specific Gravity	1.071	
Viscosity	2.53	cp
Solubility in water	2.04	wt %
Heat Capacity	250	KJ/Kmole K

Written By: *NMG*
 Checked: *MM*

Appendix

GM Section

1. Introduction

1.1 Background

The cost of Glycidyl Methacrylate, as currently quoted from Dow-Chemicals is \$4.43 per pound. With the existing stoichiometry in the plant requiring 41wt% of GM, and the remainder consisting of lauric acid (currently priced at \$.33 per pound according to ICIS), the total raw material outlay for MFA production would be \$1.94 per pound (ICIS). Considering that this analysis has neglected additional yearly operating expenses such as utility costs, labor costs and capital costs, this would be set as the bare minimum price per pound for the monomer. In turn, the ultimate breakeven price would then be considerably higher than this (roughly 30-40%).

For a plant that is contemplating producing a fatty acid monomer to replace styrene in VE resins, this cost calculation adjustment becomes a major issue in financial reports. Although this monomer's presence will significantly reduce the rate of VOC emissions from the resin and increase some of its mechanical properties (Palmese), it carries a significantly higher price than the monomer it wishes to replace, styrene. Current price data indicates that SM is purchased at a bulk price of \$.70/lb, which is \$1.24/lb cheaper than the material sought to replace it. As a result, the plants currently producing VE resin, which operate at emission levels higher than would be required with new legislation, would have a less pricey alternative. Instead of

purchasing the MFA monomer, the plants could install special equipment capable of reducing the emissions after they have been released.

It became apparent early in the research that in order to make this crude cost estimate financially feasible in the production of MFA monomers on an industrial scale the raw material costs would have to be lowered from their current status. The major focus for accomplishing this goal is to attempt to enter into a low cost/high volume contract with Dow for GM. Because GM is a specialty acrylate this allows Dow to factor in a high profit to the cost per pound without having the total bill become objectionable (Dow). For this reason, reducing the cost of GM by obtaining more information about its manufacturing process is a primary focal point for this project.

Without knowledge of the chemistry Dow uses in the production of GM, the team has performed a 'Study Estimate' basing the plant designs on an existing patent describing one route for the production of GM. (TBWS) This analysis revealed the most probable price for sale of GM on a large scale is \$1.38/lb. The work presented below, which details this calculation will be a bargaining chip when asking Dow for a guaranteed contract for GM.

1.2 *Process Overview*

Glycidyl Methacrylate is a specialty acrylate, which is produced by the combination of an alkali metal salt of methacrylic acid with epichlorohydrin

in the presence of a quaternary ammonia catalyst. The process contains three primary stages. Initially, methacrylic acid is neutralized with sodium hydroxide to produce the sodium salt of methacrylic acid. Subsequently, the second reaction involves the combination of epichlorohydrin with sodium methacrylate to produce glycidyl methacrylate. Finally, a purification step is required to ensure the GM obtained is of 98% purity, a value required by most processes using this material as a feed (Patent A).

2. GM Design Bases

2.1. Raw Materials

- Sodium Hydroxide
 - The GM plant requires the purchase of .50wt% sodium hydroxide. This was chosen as the nearest bulk concentration available to that used in patent A, .30wt%.
 - Price quotes from PQ Corporation shows this material can be purchased in bulk for \$.30/lb.
- Epichlorohydrin
 - Epichlorohydrin is made by Dow as an intermediate for several processes such as the production of propylene oxide. As such, it is available in a purity of 98wt% with very little standard deviation from this specification (Dow).

- Epichlorohydrin requires that materials used to transport and store such materials be made of stainless steel. Otherwise, over time, the free chlorine concentration may cause significant corrosion (MSDS).
 - Price quotes of ICIS show this material can be purchased in bulk for \$.89/lb
- Methacrylic Acid
 - The carboxylic acid group on methacrylic acid makes it mildly corrosive and all equipment in contact with this material must be of a stainless steel nature (MSDS).
 - Price Quotes from the Chemical Reporter show the price of bulk purchases to be around \$.95/lb

2.2. Purity Requirements

- Feed Quality Specifications
 - The purification process for obtaining GM is quite rigorous. First, the reactor's effluent passes through a batch decanter where most aqueous phase impurities will be removed. Then, the crude product is sent through a distillation tower where the bottoms temperature will vaporize most materials with a normal boiling point below 190°C. Thus, most impurities present in the feed will have negligible effect on product quality.

- However, impurities that have an affinity for GM or have high boiling points, such as Methacrylic Acid and Diglycidyl Ether, would cause the quality of GM to fail to meet specifications.
- Because present impurities are a risk, the GM plant will have quality control laboratories present to sample feed deliveries. However, since most impurities fall into the first category, this sampling will not require a significant amount of time nor money.
- Product Quality Specifications
 - The GM required for the production of MFA is 98% and the plant has been designed to obtain 99% purity to allow for small variations in feed quality.

2.3. Calculation Assumptions

- **Feed Delivery:**
 - It is assumed that deliveries of raw materials will be made once every two days. All storage tanks are sized to hold 2.2 times their daily capacity to allow for extra head space for vapor formation.
 - Pumps have been designed to complete transfer within two hours.
- **Pump Sizing**
 - Pump power was calculated from the following heuristic (TBWS) for centrifugal pumps

$$(2.1) \quad Power(kW) = \frac{1.67 * Flowrate \left(\frac{m^3}{hr} \right) * \Delta P(bar)}{Efficiency}$$

- Although pump efficiency varies with flowrate, an average efficiency of 70% provides a conservative assumption for the plant (Branan).
- The pressure increase provided by the pump was taken from estimates of average pressure loss between equipment (TBWS).
- Material property calculations such as specific gravity or heat capacity are based on weighted averages of the bulk materials present.

- **Heat Exchanger Sizing**

- Estimates for the heat required by the process stream, the heat exchanger area, and the flow of utility were calculated using heuristics from TBWS and the following equations

$$(2.2) \quad Q = \dot{m} C_p \Delta T$$

$$(2.3) \quad Q = U A F \Delta T_{lm}$$

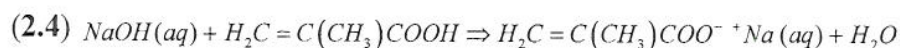
- The heat transfer coefficient used was $850 \frac{W}{m^2 K}$, an average for heat exchangers in plants (TBWS).
- Material property calculations such as specific gravity or heat capacity are based off weighted averages of only the bulk materials present.
- **Utility properties used**
 - Utility calculations are based off of the following heuristics (TBWS)

Utility	Temperature (°C)	Pressure (barg)
Cooling Water	25	2
Low Pressure Steam	135	2
Medium Pressure Steam	186	10
High Pressure Steam	231	27.6
Refridgerant (Chilled Brine)	-7	2

Table 2.1 – Heuristics used for GM plant

- **Reaction of Sodium Hydroxide and Methacrylic Acid**

- Reaction Chemistry



- Assuming analogous heats of reaction for carboxylic acid neutralization (Physics Forum), $\Delta H = -50.2 \text{ kJ / mole}$.
- Hess's law is used to calculate the heat of formation of sodium methacrylate to be -164.2 kJ / mole .
- Assuming the kinetics are similar to that for the reaction of ethyl acetate and sodium hydroxide, the rate constant is given by Fakultaelen to be

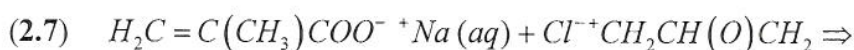
$$(2.5) \quad k = .3487 \exp \left[(5084.9) \left(\frac{1}{273 + 36.6} - \frac{1}{T} \right) \right]$$

- Assuming that the functional form of the rate law is consistent for carboxylic acid neutralizations with sodium hydroxide, the rate law is given by Yamasaki to be

$$(2.6) \quad \text{rate} = k [NaOH] [C_2H_4O_2]$$

- **Reaction of Sodium Methacrylate and Epichlorohydrin**

- Reaction Chemistry



- The heat of reaction, calculated through Hess's law is $\Delta H = -549.4 \text{ kJ / mole}$.

- Assuming the kinetic rate law is similar to the reaction between epichlorohydrin with alcohols and phenols (Chlebicki)

$$(2.8) \quad \text{rate} = k [C_3H_5ClO][C_2H_3O_2Na]$$

- Assuming the temperature dependence of this reaction is similar to the epoxy ring opening reaction of epichlorohydrin and methacrylic acid (Malshe), the rate constant formula is estimated to be

$$(2.9) \quad k = k_{T1} \exp \left[(5379) \left(\frac{1}{T1} - \frac{1}{T2} \right) \right]$$

- The rate constant at 90°C was found from experimental data in patent A, thus the rate law is given by

$$(2.10) \quad k = .061988 \exp \left[(5379) \left(\frac{1}{90 + 273} - \frac{1}{T2} \right) \right].$$

- **R-201: PFR for Production of Sodium Methacrylate**

- R-201 is designed to achieve 98.5% conversion of the materials. This is chosen because production of GM is limited by the concentration of sodium methacrylate and it is desirable to obtain as high a yield of GM as possible to reduce recycle costs.
- The pipe diameter was chosen to limit the length of the PFR to below 500 meters. In order to match one of the commonly available diameters of pipe sold, this diameter was then adjusted.
- Constructed of stainless steel to avoid corrosion caused by methacrylic acid.
- Heat generated by the reaction is cooled by heat exchange with cooling water along the pipe length.

- **R-202: PFR for Production of Glycidyl Methacrylate**

- R-202 is designed to achieve 99.8% conversion of sodium methacrylate. To avoid the costs of extra recycle needed to obtain a high overall yield, a high-single pass conversion was chosen.
- The reactor is fed with excess epichlorohydrin in a 3:1 ratio with sodium methacrylate to dilute the glycidyl methacrylate present while the catalyst remains in the system to avoid homopolymerization.
- The pipe diameter chosen to limit the length of the PFR to below 500 meters. This diameter was then adjusted to match one of the commonly available diameters of pipe sold.
- Constructed of stainless steel to avoid corrosion caused by epichlorohydrin and other corrosive impurities.
- Heat generated by the reaction is cooled by heat exchange with cooling water along the pipe length.
- The impurities created in this reaction are taken from patent A.

Crude GM Expansion	Wt%
GM	0.935
Glycerol Trimethacrylate	0.036
Dimethacrylate of Glycidol	0.024
Diglycidyl Ether	0.004

Table 2.2 – Impurity breakdown for reaction producing GM.

- It is conjectured that the presence of GM and the impurities recycle into the PFR does not hinder the conversion achieved.

- **Decanter**

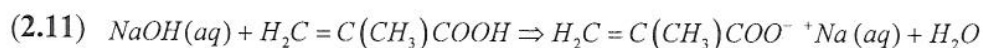
- Aspen assumes that the materials flowing into the vessel will separate from each other based on the fugacities of the materials.
- The size of the unit is based on a half hour residence time.
- Each phase is uniformly dispersed. This assumption is based on the writing of patent A when it discusses the affinity for the attraction of epichlorohydrin surrounding GM.
 - The specific gravity of the aqueous phase is about 1.
 - The specific gravity of the organic phase is about 1.15.
 - Organic phase is sufficiently denser than the aqueous phase to allow for simple discharge.
- For the aqueous salts present, sodium chloride and sodium methacrylate are assumed to reside only in the aqueous phase, since each has a relatively high solubility product in water (Chemicaland).
- The catalyst remains in the aqueous phase throughout the entire reaction and decanting stages (JTBaker).
- **Distillation Tower Assumptions**
 - Fractional recovery of GM in the bottoms is 99.6%.
 - Fractional recovery of epichlorohydrin in the distillate is 99.9%.
 - Column operates at .1bar to ensure maximum temperature is 125°C.
 - Column operates at 1.2 times the minimum reflux ratio.
 - Initial material balances are adjusted to come within 10 percent error with the associated rigorous calculations. The estimated material balances are used for the final stream compositions.

- Due to the high cooling requirements of the distillate, to avoid requiring two exchangers (total heat exchanger area required >1000 square meters) refrigerated water is used as the utility in the condenser.
- Due to the instability of GM, the tower uses forced circulation of GM with a temperature rise of 10°C to provide the heating.
 - The high pumping requirements for this design split the boil-up into two separate streams.
- Tray spacing is 24 inches.
- Vapor space at top and liquid holdup at bottom are set to 1.2 and 1.5 meters respectively, following heuristic data.
- **Recycle Loop**
 - A 5% purge is incorporated to allow the impurities created in R-202 to leave the system.
- **Capital Cost Estimation**
 - All equipment in the GM plant, except for the plug flow reactors, was estimated using CAPCOST. This program uses historical price data from vendors to correlate the cost of each piece of equipment based on a small number of inputs, which help estimate its size and capacity.

2.4. Chemistry Assumptions

Assumptions for the Reaction of Sodium Hydroxide and Methacrylic Acid:

The chemistry for this reaction is as shown below in equation 2.11.



While this is a simple neutralization reaction, common reaction practiced in many laboratories, it lacks both thermochemical and kinetic data.

Beginning with the former, heat of reaction data for this reaction is not located in any literature source the team has access to. The first attempt to approximate the heat of reaction for equations 2.11 was to use Hess's Law, which states the heat of reaction is equivalent to the sum of the heats of formation of the products less that of the reactants. However, the heat of formation of salts such as sodium methacrylate is not commonly published mainly due to the difficulty in measurement. Given that the reaction involves the breaking and forming of ionic bonds, the energy of which is not available in accessible literature, the heat of formation based on bond dissociation energies could not be predicted.

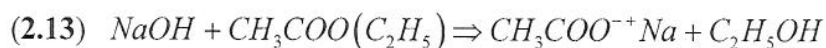
In view of the fact that all common analytical estimation techniques failed, the best estimate of the heat of reaction comes from comparison with similar reactions. To this effect, the reaction below, between acetic acid and sodium hydroxide was studied.



It is important to note the similarities between equations 2.11 and 2.12. Despite the differences in the species, the same molecular reactions are occurring. All species in equations 2.12 have tabulated heats of formation. However, the heat of formation of sodium acetate is available only in the solid form and this process has it present in the aqueous form. This problem is easily avoided by using a textbook estimate of the heat of reaction system, which is given as -50.2 kJ / mole (Physics Forum Library). This will be used as the estimated heat of reaction in equation 2.12.

For completion, the heat of formation for aqueous sodium methacrylate can be estimated through the use of Hess's Law. This value turns out to be -164.2 kJ / mole .

Turning to the kinetic relationship for this reaction, the team again found a lack of data in available literature sources. Neither equation 2.11 nor 2.12 were published in an accessible source. Exhausting all sources for data on the current reactions considered, similar reactions were then looked for, namely that between carboxylic esters and sodium hydroxide. This provided a paper from Fakultaelen, where ethyl acetate is reacted with sodium hydroxide. The chemistry for this reaction is shown in equation 2.13



While the species is changed again, it is kept close to the molecular reactions.

This reaction is different from that used in the process, yet due to lack of data on the current reaction, equation 2.13 will be used as an estimate for 2.14. From this paper, the second order rate constant in the process for the neutralization step is estimated to be

$$(2.14) \quad k = .3487 \exp \left[(5084.9) \left(\frac{1}{273 + 36.6} - \frac{1}{T} \right) \right]$$

The formulation of the values listed in the above equation is contained in separate Appendix.

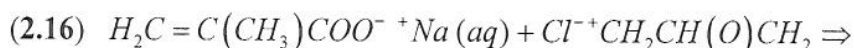
Finally, the functional form of the rate law was adapted from the discussion by Yamasaki, who showed the neutralization of lauric acid with sodium hydroxide was first order in each component. This suggests the rate law for methacrylic acid and sodium hydroxide is

$$(2.15) \quad \text{rate} = k [\text{NaOH}] [\text{C}_2\text{H}_4\text{O}_2]$$

This completes the approximations needed for the neutralization step of the process.

Assumptions for the Reaction of Sodium Methacrylate and Epichlorohydrin:

The chemistry for this reaction is



Once again, to start to analyze this reaction for industrial scale the first piece of data needed is the heat of reaction. This can be estimated using Hess's Law. The resulting estimate obtained is -528.12 kJ/mole . This value seems reasonable because the patent discusses both of the explained reactions in its write-up and suggests that cooling was needed for both.

The next step was to calculate the kinetic rate law for this reaction. From patent A, there is only one set of batch data given for the reaction with known amounts of feeds, products, temperature and time. However, this hints at nothing concerning the form of the rate law, including which species enter the rate law and to what order that species is for the reaction. It also does not address how this reaction might vary with temperature.

In order to estimate the functional form of the rate law, the team has found a kinetic paper for the reaction of epichlorohydrin with phenols and alcohols (Chlebicki and Novak). In these reactions, the epoxy ring of epichlorohydrin is

opened allowing the oxygen from the alcohol or phenol to attach to the end carbon of epichlorohydrin.

It is important to note that this chemistry does not match that operating in the reaction where the epoxy ring is left intact but, instead, simply remove the ionically bonded chlorine atom. However, this difference in chemistry will only affect the rate of the reaction and the heat of the reaction. This is a critical assumption the team has made because reactions of epichlorohydrin with sodium methacrylate, alcohols, and phenols are all bimolecular reactions over the same catalyst with an aqueous phase species. More concrete reasoning for this assumption will be a focus during the completion of this project.

Based on these papers, the rate law is first order in both epichlorohydrin and sodium methacrylate. Since the catalyst concentration remains constant throughout the reaction, it can be lumped into the rate constant (Chemical Land). The form of the rate law is now

$$(2.17) \quad \text{rate} = k [C_3H_5ClO][C_2H_3O_2Na]$$

The next step was to obtain how the rate constant for this reaction depends on temperature. The only temperature dependent kinetic data found involves the reaction of methacrylic acid with epichlorohydrin. However, the chemistry doesn't

match the chemistry of this process and, similar to the two kinetic papers mentioned above, the reaction operates to open the epoxide ring (Malshe).

The team observed that this reaction is similar to that done in the plant, but only in the reactant materials. In the actual chemistry, an ionic replacement varies considerably from a ring opening mechanism. The temperature dependent data may not be an accurate prediction for the reaction. However, since not much is known about this reaction because it is not a common reaction, the plant will operate very close to isothermal conditions leaving any error associated with this term to a minimum in its predicted values. Using the temperature data provided in the paper by Malshe and Vaidya, the reaction constants are estimated to be

$$(2.18) \quad k = k_{T1} \exp \left[(5379) \left(\frac{1}{T1} - \frac{1}{T2} \right) \right]$$

All that is left to finalize the kinetic analysis is to determine the value of the rate constant at some temperature. This can be accomplished from data given in the examples of patent A. At 90°C, 178 moles of epichlorohydrin combined with 32 moles of sodium methacrylate. The resultant mixture ran for five hours during which time 36 moles of Glycidyl Methacrylate was formed. This data was used to rewrite equations 2.19 as

$$(2.19) \quad k = .061988 \exp \left[(5379) \left(\frac{1}{90 + 273} - \frac{1}{T2} \right) \right].$$

This completes the assumptions posed for the reaction producing GM.

2.5. Justification of GM Stability

In reviewing the performance of the tower, a concern might be raised as to the high temperature at which GM is removed from the bottoms. Throughout the team's research of current literature, no probability statistics could be found relating the chances of homopolymerization of GM at different temperatures. However, the patent discusses sending GM through stage distillation sections where the temperature increases up to a reported 120°C. Thus, if laboratory data has shown the stability of GM at these temperatures, then allowing them to occur in the plant is a satisfactory assumption.

2.6. Justifications For Deviations From Patent A

The estimation techniques were based on procedures described in patent A, however some processes were changed to make the system more suitable for large-scale production of GM. It is the purpose of this section to give the rationalization used by the team in making these deviations.

First, the weight fraction of the sodium hydroxide used to produce sodium methacrylate was increased from .30 to .50. This change was made because purchase of sodium hydroxide is limited to only a few molarities, and .50 happens to be the closest one to the suggestion in the patent. Then, examining the process revealed that the weight fraction of sodium hydroxide has no effect on the process

except to add more volume to the setup and to reduce the corrosion potential of the caustic solution. In an effort to streamline the plant, it was decided that a purified water stream to reduce the concentration of NaOH was unnecessary since the aforementioned advantages of using .30wt% NaOH are quite minor.

Second, the patent's main finding was to calculate the ideal concentration of water present in the system during the reaction and purification stages to obtain the highest yield and highest purity of GM. However, the control equipment necessary to maintain the recommended levels of water content in a continuous process would be expensive. Furthermore, lowering the water content in the reactor would require installing a steam blower to evaporate the effluent water from R-201, and incorporating additional safety precautions in the plant to handle the solid sodium methacrylate. These costly additions made operation at low water content undesirable.

The patent also shows that raising the water content creates only those impurities that have relatively low boiling points. Thus, despite the decreased yield of glycidyl methacrylate, the purification of the resultant crude effluent from R-202 is made easier. This small reduction in yield was considered an acceptable risk by the team and the plant will operate with higher concentrations of water present.

The authors of patent A have shown that both obstacles can be handled by ensuring epichlorohydrin is fed to the reaction stage in an excess ratio of 3:1, with

sufficient water present. This will dilute the presence of GM while catalyst is present while simultaneously forming only low boiling impurities (Patent A).

3. *GM Process Description*

3.1. Preliminary Flow Diagram

The plant for producing GM encompasses five main sections

- Raw Material Delivery
- Neutralization Reaction forming Sodium Methacrylate
- Ionic Substitution Reaction forming Glycidyl Methacrylate
- Purification of Glycidyl Methacrylate
- Recycle of Epichlorohydrin

Below is a preliminary flow diagram for this process, showing the important pieces of equipment employed as well as the main-stream compositions, flowrates, and temperatures. To help guide the reader in the interpretation of the flow diagram, the team has added colors to indicate compositions of the major streams. The following legend explains the color, content distribution.

Color Legend for GM Flowsheets:

Violet: high purity NaOH
Brown: high purity Methacrylic Acid
Pink: high purity Epichlorohydrin
Orange (Diagram 1): high purity Sodium Methacrylate
Red: Wastewater
Blue: organic crude containing Epichlorohydrin and GM
Orange (Diagram 2): epichlorohydrin and water
Rose: Epichlorohydrin recycle stream
Green: high purity GM



3.2. Feed Delivery and Storage

The industrial complex requires the delivery of three raw materials: sodium hydroxide (.5wt%), methacrylic acid, and epichlorohydrin. Every two days, each of these materials would be transported to the plant by truck distribution. Thus, the storage tanks of these products are sized to hold 2.2 times the daily capacity of the plant that allowed for head-space in the tanks.

In order to ensure that methacrylic acid, which has a melting point of 16°C, remains in a liquid phase with no cold spots that could cause solidification in the tanks, the acid storage tank is jacketed with connection to low pressure steam, to maintain the vessel at 30°C. The remaining storage tanks require normal insulation.

3.3. Reaction #1: Formation of Sodium Methacrylate

The feed materials in the first reactor are sodium hydroxide and methacrylic acid. These materials are fed into the plug flow reactor (R-201) at 25°C. In this reactor, 14M sodium methacrylate is formed via the chemical reaction described in equation 3.1.



The heat of reaction for equation 3.2 is estimated to be -50.2 kJ/mole and is controlled through heat exchange with process cooling water. The kinetic

relationship for this reaction has been estimated based on data from the neutralization of acetic acid with NaOH, and takes the form,

$$(3.2) \quad rate = .3487 \exp \left[(5084.9) \left(\frac{1}{273 + 36.6} - \frac{1}{T} \right) \right] [NaOH][C_2H_4O_2]$$

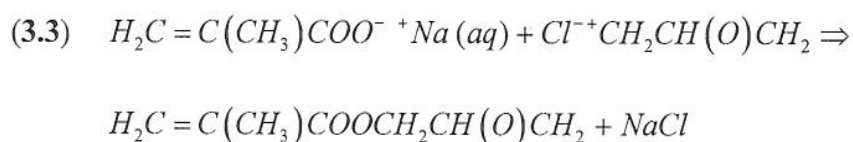
Based on equations 3.1 and 3.2, 98.5% conversion can be achieved with a 4-minute residence time. The effluent of the reactor is pumped into an insulated storage tank at the exit temperature of 69°C.

3.4. Reaction #2: Formation of GM

Stored aqueous sodium methacrylate is heated to 100°C and fed to a second PFR, (R-202). This inlet feed is combined with a recycle stream consisting mostly of epichlorohydrin (75mol%) and a fresh feed of epichlorohydrin where the ratio of recycle to fresh is 1.5:1. Both of the streams are also at 100°C

Excess epichlorohydrin is fed to this reactor in a 3:1 ratio to ensure GM remains in a dilute organic solution, thus reducing the possibility of GM homopolymerizing.

The reaction takes place according to the chemistry described by equation 3.3



This reaction between phases requires the presence of tetramethylammonium chloride. Though it is always fully dissolved only in the aqueous phase, this catalyst resides at the interface between the aqueous and organic phases. It has the ability to carry epichlorohydrin between the phases to react with sodium methacrylate and produce GM.

This reactor is kept approximately isothermal down its length by heat exchange with cooling water to handle the estimated heat release of 528 kJ/mole. Following reactions of epichlorohydrin with alcohols and phenols, and utilizing the experimental data from patent A, the following kinetic relationship is estimated,

$$(3.4) \quad rate = .061988 \exp \left[(5379) \left(\frac{1}{90 + 273} - \frac{1}{T2} \right) \right] [C_3H_5ClO][C_2H_3O_2Na]$$

Thus, the 32-minute residence time of the reactor allows for 99.8% conversion of the methacrylate salt.

The effluent is then cooled through heat exchange to reduce the exit temperature of 100°C to ambient temperature entering its storage tank.

3.5. Purification Preparation

The effluent from the second reactor contains excess epichlorohydrin and GM in the organic phase, with unreacted NaOH, methacrylic acid, sodium methacrylate, and tetramethylammonium chloride catalyst in the aqueous phase. This stream enters a continuous decanter unit with a residence time of .5 hours, at room temperature.

The average density of each phase is the weighted average density of the each component - 1.01 for the aqueous phase and 1.1 for the organic phase. Based on equilibrium fugacities, two phases form in this chamber.

During discharge, the heavy organic phase is loaded into the crude GM storage tank using gravity until a visible amount of aqueous phase has entered, roughly 3% of aqueous phase. The light aqueous phase is then pumped into storage where it will be sent out for wastewater treatment. Since the catalyst is dissolved in the water, a recovery system must be installed. However, the team could not find information on how to obtain this catalyst from an aqueous solution. For this level of estimation, it is assumed that recovery of 95% of the catalyst is possible.

3.6. Purification Section

The crude GM is fed into a distillation tower (T-201) operating at vacuum at storage (room) temperature. The high flow rate through this tower requires a large heat transfer area (>1000 square meters) for a reflux condenser operating with

process cooling water. To prevent the need for two exchangers, refrigerated water has been selected as the cooling utility to limit the number of exchangers required to one.

Because GM is heat sensitive, a high velocity forced circulation reboiler is used. Based on recommendations of the industrial advisor, the temperature rise through the circulation is set to 10°C.

At the bottoms of the tower is purified glycidyl methacrylate, 99.4mol%, at 125°C. The bottoms are immediately cooled via heat exchange to room temperature before being stored to await packaging. The distillate, consisting of 71.5mol% epichlorohydrin at 53°C is cooled to room temperature to prepare it for decanting.

3.7. Recycle Loop

The distillate taken off the column is fed to a continuous decanter with a .5 hour residence time. This operate similarly to those used on the reaction effluent, where the aqueous phase is again sent off for wastewater treatment. For the organic phase, consisting of 75mol% epichlorohydrin, 5% is sent to waste disposal as a purge for impurities, whereas the remainder is heated to 100°C and recycled to R-202.

It has been assumed that 95% of the waste epichlorohydrin is recovered by another separation train either on or off site.

4. GM Plant Stream Tables

Stream Number	1	2	3	4	5	6	7
Source	P-201	P-202	P-203	P-204	P-205	E-201	E-202
Destination	V-201	V-202	V-203	E-201	E-202	R-201	R-201
Temperature (°C)	25	25	25	25	25	25	25
Pressure (bar)	2.030612245	2.030612245	2.030612245	2.168027211	2.168027211	1.623809524	1.623809524
Vapor Fraction (molar)	0	0	0	0	0	0	0
Volumetric Flow (Liters / hr)	130654.1	138377.4	137842.9	32663.5	34594.4	32663.5	34594.4
Mass Flow (kg / hr)	147193.2	140453.1	162654.7	36798.3	35113.3	36798.3	35113.3
Mole Flow (kmole / hr)	6181.3	1633.2	1768.0	1545.3	408.3	1545.3	408.3
Component Mole Flow (kmole / hr)							
Diglycidyl Ether	0	0	0	0	0	0	0
Dimethacrylate of glycidol	0	0	0	0	0	0	0
Epichlorohydrin	0	0	1767.985484	0	0	0	0
Glycidyl Methacrylate	0	0	0	0	0	0	0
Glycidyl Trimethacrylate	0	0	0	0	0	0	0
Methacrylic Acid	0	1633.175677	0	0	408.2939194	0	408.2939194
Phenothiazine	0	0	0	0	0	0	0
Sodium Chloride (aq)	0	0	0	0	0	0	0
Sodium Hydroxide (aq)	1633.175677	0	0	408.2939194	0	408.2939194	0
Sodium Methacrylate (aq)	0	0	0	0	0	0	0
Tetramethyammonium Catalyst (aq)	0	0	0	0	0	0	0
Water	4548.118474	0	0	1137.029619	0	1137.029619	0

Stream Number	8	9	10	11	12	13	14
Source	R-201	P-206	P-207	E-203	P-208	E-204	R-202
Destination	P-206	V-204	E-203	R-202	E-204	R-202	P-209
Temperature (°C)	76.00252551	76.00252551	25	100	76.00252551	100	104.1196783
Pressure (bar)	1	2.168027211	2.168027211	1.623809524	2.168027211	1.623809524	1
Vapor Fraction (molar)	0	0	0	0	0	0	0
Volumetric Flow (Liters / hr)	28407.5	28407.5	34460.7	34460.7	28407.5	28407.5	142992.7
Mass Flow (kg / hr)	71911.6	71911.6	40663.7	40663.7	71911.6	71911.6	251806.5
Mole Flow (kmole / hr)	1953.6	1953.6	442.0	442.0	1953.6	1953.6	3433.6
Component Mole Flow (kmole / hr)							
Diglycidyl Ether	0	0	0	0	0	0	9.165250019
Dimethacrylate of glycidol	0	0	0	0	0	0	122.1820141
Epichlorohydrin	0	0	441.9963709	441.9963709	0	0	824.1860702
Glycidyl Methacrylate	0	0	0	0	0	0	376.2769575
Glycidyl Trimethacrylate	0	0	0	0	0	0	139.123821
Methacrylic Acid	6.124379359	6.124379359	0	0	6.124379359	6.124379359	10.94268778
Phenothiazine	0	0	0	0	0	0	0.60325431
Sodium Chloride (aq)	0	0	0	0	0	0	400.6956879
Sodium Hydroxide (aq)	6.124379359	6.124379359	0	0	6.124379359	6.124379359	6.124379359
Sodium Methacrylate (aq)	402.16954	402.16954	0	0	402.16954	402.16954	1.473852111
Tetramethyammonium Catalyst (aq)	0	0	0	0	0	0	2.0108477
Water	1539.199159	1539.199159	0	0	1539.199159	1539.199159	1540.823179

Stream Number	15	16	17	18	19	20	21
Source	P-209	E-205	P-211	R-203 to R-205	P-212	T-201	E-207
Destination	E-205	R-203 to R-205	Sec 300	V-205	T-201	E-207	V-206
Temperature (°C)	104.1196783	50	50	50	50	56.89373477	56.89373477
Pressure (bar)	2.168027211	1.623809524	2.030612245	1	2.168027211	0.098684211	0.098684211
Vapor Fraction (molar)	0	0	0	0	0	1	0
Volumetric Flow (Liters / hr)	142992.7	142992.7	27437.8	115554.9	115554.9	363406787.3	75682.8
Mass Flow (kg / hr)	251806.5	251806.5	50904.6	200901.9	200901.9	169581.3	169581.3
Mole Flow (kmole / hr)	3433.6	3433.6	1904.9	1528.7	1528.7	1324.1	1324.1
Component Mole Flow (kmole / hr)							
Diglycidyl Ether	9.165250019	9.165250019	7.65741E-05	9.165173445	9.165173445	9.064432267	9.064432267
Dimethacrylate of glycidol	122.1820141	122.1820141	0.00102081	122.1809933	122.1809933	140.5093294	140.5093294
Epichlorohydrin	824.1860702	824.1860702	0.006885936	824.1791843	824.1791843	947.7112813	947.7112813
Glycidyl Methacrylate	376.2769575	376.2769575	5.71596E-08	376.2769574	376.2769574	1.730874004	1.730874004
Glycidyl Trimethacrylate	139.123821	139.123821	0.001162356	139.1226587	139.1226587	159.9924092	159.9924092
Methacrylic Acid	10.94268778	10.94268778	5.307203573	5.635484206	5.635484206	5.832726153	5.832726153
Phenothiazine	0.60325431	0.60325431	0	0.60325431	0.60325431	0	0
Sodium Chloride (aq)	400.6956879	400.6956879	400.6956879	0	0	0	0
Sodium Hydroxide (aq)	6.124379359	6.124379359	5.910519036	0.213860323	0.213860323	0.245939371	0.245939371
Sodium Methacrylate (aq)	1.473852111	1.473852111	1.473852111	0	0	0	0
Tetramethyammonium Catalyst (aq)	2.0108477	2.0108477	2.0108477	0	0	0	0
Water	1540.823179	1540.823179	1489.500375	51.32280474	51.32280474	59.02122545	59.02122545
Stream Number	22	23	24	25	26	27	28
Source	V-206	P-212	P-213	T-201	P-214	E-208	T-201
Destination	P-213	T-201	R-204	P-214	E-208	T-201	R-206, R-207
Temperature (°C)	56.89373477	56.89373477	56.89373477	125.1895815	125.1895815	135.1895815	56.89373477
Pressure (bar)	0.098684211	2.168027211	2.168027211	0.098684211	2.168027211	1.623809524	2.168027211
Vapor Fraction (molar)	0	0	0	0	0	0	0
Volumetric Flow (Liters / hr)	65811.1	9871.7	65811.1	49129.5	4186631.2	4186631.2	65804.7
Mass Flow (kg / hr)	147462.0	22119.3	147462.0	53168.0	4530773.5	4530773.5	147453.5
Mole Flow (kmole / hr)	1151.4	172.7	1151.4	376.2	32055.6	32055.6	1151.2
Component Mole Flow (kmole / hr)							
Diglycidyl Ether	7.882115015	1.182317252	7.882115015	4.291361511	365.6933947	365.6933947	7.882115015
Dimethacrylate of glycidol	122.1820256	18.32730384	122.1820256	0.002883402	0.245712501	0.245712501	122.1820256
Epichlorohydrin	824.0967663	123.614515	824.0967663	0.032954778	2.808279975	2.808279975	824.0967663
Glycidyl Methacrylate	1.50510783	0.225766174	1.50510783	369.2765039	31468.32956	31468.32956	1.50510783
Glycidyl Trimethacrylate	139.1238341	20.86857511	139.1238341	0.002509642	0.213862094	0.213862094	139.1238341
Methacrylic Acid	5.071935785	0.760790368	5.071935785	1.958448686	166.8914974	166.8914974	5.071935785
Phenothiazine	0	0	0	0.60325431	51.40702221	51.40702221	0
Sodium Chloride (aq)	0	0	0	0	0	0	0
Sodium Hydroxide (aq)	0.213860323	0.032079048	0.213860323	0	0	0	0
Sodium Methacrylate (aq)	0	0	0	0	0	0	0
Tetramethyammonium Catalyst (aq)	0	0	0	0	0	0	0
Water	51.32280474	7.698420711	51.32280474	0.000140808	0.011999119	0.011999119	51.32280474
Stream Number	29	30	31	32	33	34	35
Source	R-206, R-207	P-216	P-217	E-209	R-206, R-207	P-218	P-219
Destination	P-216, P-217	Recycle Purge	E-209	R-202	P-218	Sec 300	TK-206
Temperature (°C)	56.89373477	56.89373477	56.89373477	100	56.89373477	56.89373477	25
Pressure (bar)	1	2.030612245	2.030612245	1.486394558	1	2.030612245	1
Vapor Fraction (molar)	0	0	0	0	0	0	0
Volumetric Flow (Liters / hr)	64911.1	3245.6	61665.6	61665.6	893.6	893.6	49743.8
Mass Flow (kg / hr)	146559.2	7328.0	139231.2	139231.2	894.3	894.3	53440.5
Mole Flow (kmole / hr)	1101.6	55.1	1046.5	1046.5	49.6	49.6	377.3
Component Mole Flow (kmole / hr)							
Diglycidyl Ether	7.882049161	0.394102458	7.487946703	7.487946703	6.58537E-05	6.58537E-05	1.283135002
Dimethacrylate of glycidol	122.1810048	6.109050238	116.0719545	116.0719545	0.00102081	0.00102081	0
Epichlorohydrin	824.0898811	41.20449406	782.8853871	782.8853871	0.006885189	0.006885189	0.082417918
Glycidyl Methacrylate	1.50510783	0.075255391	1.429852438	1.429852438	2.29E-10	2.28639E-10	374.7718496
Glycidyl Trimethacrylate	139.1226717	6.956133585	132.1665381	132.1665381	0.001162356	0.001162356	0
Methacrylic Acid	5.0719036	0.25359518	4.81830842	4.81830842	3.22E-05	3.21857E-05	0.563548421
Phenothiazine	0	0	0	0	0.00E+00	0	0.60325431
Sodium Chloride (aq)	0	0	0	0	0	0	0
Sodium Hydroxide (aq)	0	0	0	0	0	0	0
Sodium Methacrylate (aq)	0	0	0	0	0	0	0
Tetramethyammonium Catalyst (aq)	0	0	0	0	0	0	0
Water	1.709495497	0.085474775	1.624020722	1.624020722	49.61330924	49.61330924	0

Table 4.1 - GM Process Stream Table

5. GM Plant Lists

5.1. GM Plant Tower, Tank, Vessel and Reactor List

Equipment	T-201	TK-201	TK-202	TK-203	TK-204	TK-205	TK-206
Temperature at top (°C)	56.89373477	25	25	25	76.00252551	50	25
Temperature at bottom (°C)	125.1895815	25	25	25	76.00252551	50	25
Pressure (barg)	0.098684211	1	1	1	1	1	1
Diameter (m)	3.327536817	7.872840909	8.025010627	8.014664558	7.452459363	11.99609763	9.057816816
Height / Length (m)	8.797560976	11.80926136	12.03751594	12.02199684	11.17868904	17.99414644	13.58672522
Orientation	Vertical	Vertical	Vertical	Vertical	Vertical	Vertical	Vertical
Internals	10 SS Trays 24 inch spacing						
Capacity (cub m)		574.8778385	608.8607649	606.5089184	487.6182934	2033.766621	875.4911099

Equipment	V-201	V-202	V-203
Temperature at top (°C)	25	25	56.89373477
Temperature at bottom (°C)	25	25	56.89373477
Pressure (barg)	1	1	0.098684211
Diameter (m)	1.035904573	1.035904573	2.060250347
Height / Length (m)	4.14361829	4.14361829	10.30125173
Orientation	Vertical	Vertical	Horizontal
Capacity (cub m)	3.492280532	3.492280532	34.34154844

Equipment	R-201	R-202	R-203	R-204
Temperature (°C)	25	100	25	25
Pressure (barg)	1	1	1	1
Diameter (m)	0.152439024	0.508130081	2.7132582	2.504510241
Length (m)	203.2387228	374.0102107	18.9928074	10.01804097
Residence Time (min)	3.309	31.54	30	60
Amount of Catalyst (kmole/day)	0	16.0867816	0	0
Volume (cub m)			109.8149059	49.35353995

Table 5.1 – GM tank vessel and reactor list

5.2. GM Plant Pump List

Equipment	P-201 A/B	P-202 A/B	P-203 A/B	P-204 A/B	P-205 A/B	P-206 A/B	P-207 A/B
MOC	Carbon Steel	Stainless Steel	Stainless Steel	Carbon Steel	Stainless Steel	Stainless Steel	Stainless Steel
Power (kW)	5.354086327	5.670584041	5.648680276	1.516991126	1.606665478	1.319326898	1.600459412
Efficiency	0.7	0.7	0.7	0.7	0.7	0.7	0.7
Type	Centrifugal	Centrifugal	Centrifugal	Centrifugal	Centrifugal	Centrifugal	Centrifugal
Temperature (°C)	25	25	25	25	25	76.00252551	25
Pressure In (bar)	1	1	1	1	1	1	1
Pressure Out (bar)	2.030612245	2.030612245	2.030612245	2.168027211	2.168027211	2.168027211	2.168027211
Capacity (cub m/min)	2.17756757	2.306290776	2.297382267	0.544391892	0.576572694	0.473457527	0.574345567

Equipment	P-208 A/B	P-209 A/B	P-210 A/B	P-211 A/B	P-212 A/B	P-213 A/B	P-214 A/B
MOC	Stainless Steel	Stainless Steel	Stainless Steel	Stainless Steel	Stainless Steel	Stainless Steel	Stainless Steel
Power (kW)	1.319326898	6.800176288	0.140546978	5.503410951	0.416067151	2.773781006	197.668627
Efficiency	0.7	0.7	0.7	0.7	0.7	0.7	0.7
Type	Centrifugal	Centrifugal	Centrifugal	Centrifugal	Centrifugal	Centrifugal	Centrifugal
Temperature (°C)	76.00252551	104.1196783	25	-273	56.89373477	56.89373477	125.5725674
Pressure In (bar)	1	1	1	1	1	1	1
Pressure Out (bar)	2.168027211	2.168027211	2.030612245	2.168027211	2.168027211	2.168027211	2.168027211
Capacity (cub m/min)	0.473457527	2.440331242	0.057162048	1.974970223	0.14931108	0.995407201	70.93594423

Equipment	P-215 A/B	P-216 A/B	P-217 A/B	P-218 A/B
MOC	Stainless Steel	Stainless Steel	Stainless Steel	Stainless Steel
Power (kW)	0.289951757	0.175121678	3.781109336	0.036617961
Efficiency	0.7	0.7	0.7	0.7
Type	Centrifugal	Centrifugal	Centrifugal	Centrifugal
Temperature (°C)	125.5725674	56.89373477	56.89373477	56.89373477
Pressure In (bar)	1	1	1	1
Pressure Out (bar)	2.168027211	2.030612245	2.030612245	2.030612245
Capacity (cub m/min)	0.832423514	0.071223971	1.356900006	0.01489294

Table 5.2 – GM pump list

5.3. GM Heat Exchanger List

Equipment	E-201	E-202	E-203	E-204	E-205	E-206	E-207
Type	Floating Head	Floating Head	Floating Head	Floating Head	Floating Head	Floating Head	Floating Head
Duty (MJ / h)	9878.67561	3530.768531	18232.35282	51274.17891	80252.53128	9435.377653	4876.581984
Area (sq m)	61.59655285	14.57147685	174.8153103	503.1912198	579.2301669	36.14897431	38.84775441
Shell Side							
Max Temperature (°C)	135	186	40	25	186	186	135
Pressure (barg)	20	20	20	20	20	20	20
MOC	Carbon Steel	Carbon Steel	Carbon Steel	Carbon Steel	Carbon Steel	Carbon Steel	Carbon Steel
Phase	Cond. Steam	Cond. Steam	Liquid	Liquid	Cond. Steam	Cond. Steam	Cond. Steam
Tube Side							
Max Temperature (°C)	100	100	104.1196783	56.89373477	135.1895815	135.1895815	100
Pressure (barg)	4	4	4	4	4	4	4
MOC	Stainless Steel	Stainless Steel	Stainless Steel	Stainless Steel	Stainless Steel	Stainless Steel	Stainless Steel
Phase	Liquid	Liquid	Liquid	Cond. Vapor	Liquid	Liquid	Liquid

Table 5.3 – GM heat exchanger list

6. Operating Requirements

6.1 GM Plant Operating Requirements

6.1.1 Utility Requirements

The GM process requires four utilities: electricity, cooling water, steam (both low and medium pressure), and refrigerated water. To estimate the cost of each stream, it is assumed that each is provided outside of the battery limits of the GM plant. Prices originally derived from CAPCOST have been updated to current values by Professor Caincross. The following is a summary of the requirements and their cost per year.

Utility	lps	mps	cw	cw	mps
Equipment	E-201	E-202	E-203	E-204	E-205
Temperature In (°C)	135	186	20	5	186
Temperature Out (°C)	115	166	40	25	166
Heat Capacity (KJ / kmole K)	37	37	75.312	37	37
Flow (kmole/h)	13350	4770	12100	19500	10850

Utility	mps	lps	cw	cw
Equipment	E-206	E-207	R-201	R-202
Temperature In (°C)	186	135	20	20
Temperature Out (°C)	166	115	40	40
Heat Capacity (KJ / kmole K)	37	37	75.312	75.312
Flow (kmole/h)	12750	6590	3000	4000

Figure 6.1 - Utility usage summary for GM plant

Cost of Utilities	Type	Amount (GJ/day)	Cost (\$/GJ)	Yearly Cost (\$MM)
Electricity	110V-440V	6.958700079	16.89	0.038609408
Low Pressure Steam	lps	118.0420608	7.78	0.301683636
Medium Pressure Steam	mps	745.7494197	8.22	2.013724785
Cooling Water	cw	4629.688845	0.36	0.547507003
Refrigerated Water	cw	410.1934313	4.43	0.596936042
Total Cost of Utilities				3.498460874

Figure 6.2 - Utility cost summary for GM plant

6.1.2 Waste Streams

The GM process produces a total of three waste streams. Two of these are wastewater that contains small amounts of sodium hydroxide, sodium methacrylate, sodium chloride, methacrylic acid, epichlorohydrin, and tetramethylammonium chloride catalysts. The impurities present are in low concentrations, making their removal straightforward.

At this time, methods to treat wastewater has not been explored by the team. For the level of accuracy required for the GM plant design, it can be assumed this is performed outside of battery limits. Cost data has been obtained assuming the wastewater is of the 'tertiary' tier, which brings the highest cost of wastewater treatment, a conservative estimate of the cost will be performed.

The remaining waste stream is the purged epichlorohydrin. This material is hazardous to the environment. For the level of accuracy required, it is assumed that disposal of this material occurs outside of battery limits and the cost associated with hazardous waste will be used.

Cost of Wastewater Management	Type	Amount (L/day)	Amount (cub.m./day)	Cost (\$ / 1000 cub.m)	Yearly Cost (\$MM)
Wastewater Stream 17	Tertiary	219502	220	41	0.00296
Wastewater Stream 34	Tertiary	7149	7	41	0.00010
Cost of Waste Disposal	Type	Amount (kmole/day)	Amount (tonne/day)	Cost (\$ / tonne)	Yearly Cost (\$MM)
Epichlorohydrin Purge Stream 30	Hazardous	441	45	200	2.93
Reduced Waste from selling for credits (95%)				\$	(2.78)
Total Cost of Waste Management				\$	0.15

Figure 6.3 - Waste treatment cost summary for GM plant

6.1.3 Catalyst Requirements

Catalyst is only required for the reaction producing glycidyl methacrylate. For this reaction, it is necessary to have a phase transfer catalyst. In other words, it must be able to pull epichlorohydrin from the organic phase into the aqueous phase to react with sodium methacrylate and form glycidyl methacrylate. There are a number of catalysts that operate with these properties, however, since the team has data only for tetramethylammonium chloride catalyst, this will be used in the system.

The requirement is found from the example data given by patent A. The team has decided not to deviate from this value because the research has shown the catalyst concentration causes a nonlinear dependence on the rate equations, but the exact dependence is not published.

Besides the catalyst, a polymer inhibitor is also required to ensure the purified GM remains stable during production. The amount added is taken from the recommendations of patent A, which also purify GM via distillation. It has been understood by the group that this inhibitor stays entirely with GM through the process.

Cost of Catalyst and Inhibitor	Type	Amount (kmole/day)	Amount (lb/day)	Cost (\$/lb)	Yearly Cost (\$MM)
Phenothiazine	Inhibitor	4.792554275	517.5958617	49.9	8.484509004
Tetramethylammonia chloride	Catalyst	15.97518092	3303.667413	49.9	54.15421179
Total Cost					62.6387208

Figure 6.4 - Catalyst cost summary for GM plant

7. Environmental and Waste Minimizations

7.1. Wastewater

Two of the waste streams created in the GM plant serve to remove excess water from the process. The streams are described on an hourly basis in the figure below.

Stream Number	17	34	Raw Material Cost (\$/lb)	Cost (\$MM/yr)
Source	P-211	P-218	--	--
Destination	Sec 300	Sec 300	--	--
Temperature (°C)	50	56.89373477	--	--
Pressure (bar)	2.030612245	2.030612245	--	--
Vapor Fraction (molar)	0	0	--	--
Volumetric Flow (Liters / hr)	27437.8	893.6	--	--
Mass Flow (kg / hr)	50904.6	894.3	--	--
Mole Flow (kmole / hr)	1904.9	49.6	--	--
Component Mole Flow (kmole / hr)			--	--
Diglycidyl Ether	7.65741E-05	6.58537E-05	--	--
Dimethacrylate of glycidol	0.00102081	0.00102081	--	--
Epichlorohydrin	0.006885936	0.006885189	0.87	0.006372716
Glycidyl Methacrylate	5.71596E-08	2.28639E-10	--	--
Glycidyl Trimethacrylate	0.001162356	0.001162356	--	--
Methacrylic Acid	5.307203573	3.21857E-05	0.95	2.506908475
Phenothiazine	0	0	--	--
Sodium Chloride (aq)	400.6956879	0	--	--
Sodium Hydroxide (aq)	5.910519036	0	0.37	0.505749402
Sodium Methacrylate (aq)	1.473852111	0	--	--
Tetramethyammonium Catalyst (aq)	2.0108477	0	49.9	54.53252657
Water	1489.500375	49.61330924	--	--
Total				67.65465716

Figure 7.1 – Wastewater minimization in GM plant

Two waste minimization techniques have been employed on these streams.

First, the amount of wastewater generated was significantly reduced. From the process description, water has one unique purpose, to dissolve sodium methacrylate for reaction with epichlorohydrin. However, as can be seen from patent A, small amounts of water, above 1100 ppm, will complete the desired objective for reaction. Thus, a substantial amount of water present in the process is simply excessive.

Water enters the process at two areas. First, it is created in the reaction between methacrylic acid and sodium hydroxide. Water forms in the same

molar ratio as the formation of sodium methacrylate. This cannot be reduced without creating lower yields in the first reactor. Secondly, it enters the process as the solvent for sodium hydroxide. Here, the concentration of purchased sodium hydroxide was increased, thereby reducing the water levels in the system. The only drawback to this is the corrosive property of the feed is increased. However, in terms of cost, it was beneficial to upgrade the equipment handling this material to stainless steel to reduce the amount of wastewater released and the utility requirements to pump the excess water through the system. Also, by reducing the water present with sodium hydroxide in the feed, the concentration of the raw materials in R-201 and R-202 was increased allowing for shorter residence times.

The second recovery technique concerns the composition of this release. As can be seen from the truncated stream table above, raw material waste from this stream is relatively low and recovery of these materials will not be financially beneficial. However, all of the catalyst used in R-202, which brings a cost of \$58MM/yr, leaves the process dissolved in the wastewater streams. It has been assumed that recovery of 95% of this catalyst is possible through methods OSBL.

7.2. Epichlorohydrin Purge

This waste stream is necessary to prevent the buildup of impurities created in the glycidyl methacrylate reactor in the system. The composition of this waste stream is presented below.

Stream Number	30	Material Cost (\$	Cost (\$MM/yr)
Source	P-216	--	--
Destination	Recycle Purge	--	--
Temperature (°C)	56.89373477	--	--
Pressure (bar)	2.030612245	--	--
Vapor Fraction (molar)	0	--	--
Volumetric Flow (Liters / hr)	3245.6	--	--
Mass Flow (kg / hr)	7328.0	--	--
Mole Flow (kmole / hr)	55.1	--	--
Component Mole Flow (kmole / hr)		--	--
Diglycidyl Ether	0.394102458	--	--
Dimethacrylate of glycidol	6.109050238	--	--
Epichlorohydrin	41.20449406	0.87	19.06776134
Glycidyl Methacrylate	0.075255391	--	--
Glycidyl Trimethacrylate	6.956133585	--	--
Methacrylic Acid	0.25359518	0.95	0.119787387
Phenothiazine	0	--	--
Sodium Chloride (aq)	0	--	--
Sodium Hydroxide (aq)	0	0.37	0
Sodium Methacrylate (aq)	0	--	--
Tetramethyammonium Catalyst (aq)	0	--	--
Water	0.085474775	--	--
Total			19.18754873

Figure 7.2 – Epichlorohydrin minimization in GM plant

As can be seen from the above figure, two raw materials purchased by the plant are lost in this stream. Using each of their purchase prices, the yearly cost of this waste is significantly higher than the \$.2MM cost of disposal because of the \$20MM worth of raw material that is being lost. Due to this high value, the team assumed that OSBL methods can be installed or this stream can be sold to recover 95% of the cost.

8. Economic Feasibility

8.1. Capital Costs

The capital costs of the GM plant were calculated using CAPCOST. This program uses historical data and correlates the size, material, and pressure specification of the equipment to calculate an estimated cost of each unit. The following table shows the results of these calculations for the plant.

Heat Exchangers

Exchangers	Type of Exchanger	Shell Pressure (barg)	Tube Pressure (barg)	MOC	Area (square meters)	Purchased Equipment Cost	Bare Module Cost
E-201	Floating Head	20	4	Stainless Steel / Carbon Steel	61.6	\$ 21,300	\$ 103,000
E-202	Floating Head	20	4	Stainless Steel / Carbon Steel	18.1	\$ 18,400	\$ 89,300
E-203	Floating Head	20	4	Stainless Steel / Carbon Steel	175	\$ 33,500	\$ 163,000
E-204	Floating Head	20	4	Stainless Steel / Carbon Steel	504	\$ 72,200	\$ 351,000
E-205	Floating Head	20	4	Stainless Steel / Carbon Steel	579	\$ 81,700	\$ 397,000
E-206	Floating Head	20	4	Stainless Steel / Carbon Steel	36.2	\$ 19,000	\$ 92,200
E-207	Floating Head	20	4	Stainless Steel / Carbon Steel	38.8	\$ 19,200	\$ 93,200

Pumps

Pumps (with drives)	Pump Type	Power (kilowatts)	# Spares	MOC	Discharge Pressure (barg)	Purchased Equipment Cost	Bare Module Cost
P-201	Centrifugal	5.35	1	Carbon Steel	2.03	\$ 6,470	\$ 25,800
P-202	Centrifugal	5.67	1	Stainless Steel	2.03	\$ 6,580	\$ 32,700
P-203	Centrifugal	5.65	1	Stainless Steel	2.03	\$ 6,570	\$ 32,600
P-204	Centrifugal	1.52	1	Carbon Steel	2.17	\$ 5,070	\$ 20,200
P-205	Centrifugal	1.6	1	Stainless Steel	2.17	\$ 5,100	\$ 25,300
P-206	Centrifugal	1.32	1	Stainless Steel	2.17	\$ 5,000	\$ 24,800
P-207	Centrifugal	1.61	1	Stainless Steel	2.17	\$ 5,100	\$ 25,400
P-208	Centrifugal	1.32	1	Stainless Steel	2.17	\$ 5,000	\$ 24,800
P-209	Centrifugal	6.8	1	Stainless Steel	2.17	\$ 6,940	\$ 34,500
P-210	Centrifugal	1	1	Stainless Steel	2.03	\$ 4,900	\$ 24,300
P-211	Centrifugal	5.5	1	Stainless Steel	2.17	\$ 6,520	\$ 32,400
P-212	Centrifugal	1	1	Stainless Steel	2.17	\$ 4,900	\$ 24,300
P-213	Centrifugal	2.78	1	Stainless Steel	2.17	\$ 5,550	\$ 27,600
P-214	Centrifugal	198	1	Stainless Steel	2.17	\$ 42,100	\$ 209,000
P-215	Centrifugal	1	1	Stainless Steel	2.17	\$ 4,900	\$ 24,300
P-216	Centrifugal	1	1	Stainless Steel	2.03	\$ 4,900	\$ 24,300
P-217	Centrifugal	3.78	1	Stainless Steel	2.03	\$ 5,920	\$ 29,400
P-218	Centrifugal	1	1	Stainless Steel	2.03	\$ 4,900	\$ 24,300

Storage Tanks

Storage Tanks	Tank Type	Volume (cubic meters)	Type	Volume (gallons)	Purchased Equipment Cost	Bare Module Cost
Tk-201	Fixed Roof	574	Storage		\$ 71,600	\$ 78,700
Tk-202	Fixed Roof	608	Storage		\$ 73,200	\$ 80,600
Tk-203	Fixed Roof	606	Storage		\$ 73,100	\$ 80,500
Tk-204	Fixed Roof	488	Storage		\$ 67,200	\$ 73,900
Tk-205	Fixed Roof	2030	Storage		\$ 131,000	\$ 144,000
Tk-206	Fixed Roof	875	Storage		\$ 85,700	\$ 94,200
Tk-207	Fixed Roof	220	Decanter R-203		\$ 51,700	\$ 56,800
Tk-208	Fixed Roof	90	Decanter R-204		\$ 42,300	\$ 46,500

Towers

Towers	Tower Description	Height (meters)	Diameter (meters)	Tower MOC	Demister MOC	Pressure (barg)	Purchased Equipment Cost	Bare Module Cost
T-201	10 Stainless Steel Sieve Trays	10	3.3	Stainless Steel	Stainless Steel	1	\$ 125,000	\$ 613,000

Reactors

Reactors	Type	Residence Time (min)	Length (m)	MOC	Purchased Equipment Cost	Complete Installation Cost
R-201	Shell and Tube	3.3	203	Stainless Steel	\$ 35,447	\$ 177,233
R-202	Shell and Tube	31.5	374	Stainless Steel	\$ 171,777	\$ 858,886

Vessels

Vessels	Orientation	Length/Height (meters)	Diameter (meters)	MOC	Demister MOC	Pressure (barg)	Purchased Equipment Cost	Bare Module Cost
V-201	Vertical	4.12	1.03	Stainless Steel		1	\$ 5,870	\$ 46,400
V-202	Vertical	4.12	1.03	Stainless Steel		1	\$ 5,870	\$ 46,400
V-203	Vertical	10.3	2.1	Stainless Steel		1	\$ 28,300	\$ 224,000

Figure 8.1 - Equipment summary for GM plant

8.2. Manufacturing Costs

The manufacturing costs of the GM plant were calculated based off assumptions used by TBWS. The book presents a procedure for calculating the various costs required for running a chemical plant. The results of their analysis on the plant are presented below.

Cost of Raw Materials	Type	Amount (kmole/day)	Amount (lb/day)	Cost (\$/lb)	Yearly Cost (\$MM)	% of Raw Material Cost
Sodium Hydroxide	Feed	3266	287439	0.37	\$ 34.94	0.070520715
Methacrylic Acid	Feed	3266	617994	0.96	\$ 192.86	0.389293406
Epichlorohydrin	Feed	3536	715681	0.87	\$ 204.54	0.412864804
Phenothiazine	Inhibitor	5	521	49.9	\$ 8.54	0.017245831
Tetramethylammonia chloride	Catalyst	16	3327	49.9	\$ 54.53	0.110075244
Credits of Waste Streams (95%)						
Epichlorohydrin from Purge Stream 31	Feed				\$ 18.11	
Catalyst Recovery from Stream 17	Catalyst				\$ 51.81	
Total Raw Material Cost					\$ 425.49	0.858864211

Cost of Wastewater Management	Type	Amount (L/day)	Amount (cubic m/day)	Cost (\$/1000 cubic m)	Yearly Cost (\$MM)
Wastewater Stream 17	Tertiary	219502	220	41	0.00296
Wastewater Stream 34	Tertiary	7149	7	41	0.00010
Cost of Waste Disposal					
Type	Amount (kmole/day)	Amount (tonne/day)	Cost (\$/tonne)	Yearly Cost (\$MM)	
Epichlorohydrin Purge Stream 30	Hazardous	441	45	200	\$ 2.93
Reduced Waste from selling for credits (95%)				\$ (2.78)	
Total Cost of Waste Management					\$ 0.15

Cost of Utilities	Type	Amount (GJ/day)	Cost (\$/GJ)	Yearly Cost (\$MM)
Electricity	110V-440V	7	16.89	\$ 0.04
Low Pressure Steam	lps	118	7.78	\$ 0.30
Medium Pressure Steam	mps	746	8.22	\$ 2.01
Cooling Water	cw	4630	0.36	\$ 0.55
Refrigerated Water	cw	410	4.43	\$ 0.60
Total Cost of Utilities				\$ 3.50

Cost of Operating Labor	
Number of Heat Exchangers	17
Number of Reactors	4
Number of Towers	1
Number of Shifts	3.4
Number of Operators per Shift	4.5
Base Salary per Operator (\$/yr)	54000
Total Cost of Operating Labor (\$MM)	0.818661194

Estimate of Manufacturing Costs	
Fixed Capital Investment (\$MM)	\$ 6.43
Direct Manufacturing Costs (\$MM)	\$ 446.16
Fixed Manufacturing Costs (\$MM)	\$ 1.02
General Manufacturing Expense (\$MM)	\$ 85.20
COMd (\$MM)	\$ 531.23

Estimate of Unit Cost to Produce GM	
Total Costs of Production (\$MM/yr)	\$ 531.23
Total Production of GM (lb/yr)	309800000
Assumed Profit (%)	10
Total Unit Cost of GM (\$/lb)	\$ 1.89

Distribution of Unit Cost to Produce GM	
Raw Material Cost (\$ / GM lb)	\$ 1.37
Utility Cost (\$ / GM lb)	\$ 0.0113
Waste Treatment Cost (\$ / GM lb)	\$ 0.0006
Operating Labor Cost (\$ / GM lb)	\$ 0.0026
Administrative Cost of GM (\$ / GM lb)	\$ 0.33
Profit (\$ / GM lb)	\$ 0.17
Unit Cost of GM w/o Administrative (\$/lb)	\$ 1.38

Figure 8.2 - Manufacturing cost summary for GM plant

For the purposes of cost estimation, only the variable costs Dow produces GM for each year were taken into account, as the additional overhead costs will get rolled into each of their businesses and will have far less an effect as would be predicted for this plant.

8.3. Cost Per Pound of GM

A complete economic analysis reveals the price per pound to produce GM is \$1.38/lb. This value is the most likely price, the producers of MFA will be able to convince Dow to offer in a high volume low cost contract.

At first, this estimate may be considered high since the average price of raw material is under a dollar per pound. There are main two reasons for this higher price. First, the excess feed of epichlorohydrin to ensure stability adds cost of capital and utilities for the recycle loop as well as lost excess epichlorohydrin in the purge stream. Next, the number of raw materials needed to produce one product is three. Thus, this process requires the purchase of a large mass to only produce one salable product, GM, as well as other wasted products, water and sodium chloride.

The team has omitted two key parameters in determining this cost. First, overhead costs are ignored and profit in determining the price per pound for production of GM. As for the former, this value is probably going to be considerably low as these same costs will carry over many of Dow's products, not just GM. Profit must be present for Dow to remain in business, thus this would suggest the predicted value is lower than the actual. However, the other omitted parameter was optimization. Before constructing a GM plant, an optimization procedure will be conducted on the design, for example to take heat integration into account and waste minimization. This will allow the price to drop below its predicted value. Since these two omissions combat each other, it is a safe argument to suggest the calculated price of \$1.38/lb to be fairly accurate.

9. Calculations

9.1. *Centrifugal Pumps*

All pumps can be centrifugal since the GM process contains only liquid feeds and liquid products, as well as highly soluble salts and catalysts, which can be assumed completely dissociated in the liquid phase. The shaft power required of each pump is directly obtained from the following heuristic given by TBWS

$$(9.1) \quad Power(kW) = \frac{1.67 * Flowrate \left(\frac{m^3}{hr} \right) * \Delta P(bar)}{Efficiency}$$

This equation requires three pieces of information: the volumetric flow rate through the pump, the pressure rise given to the material, and the efficiency. For the latter, the efficiency will vary with flow rate; however, an average of 70% can be used as a conservative estimate. The volumetric flow rate is obtained from the material balance of the system. Finally, the pressure rise given to the material must be sufficient to flow the material through a piping network and into its destination vessel operating at some pressure.

To calculate this last number, heuristics from TBWS will be used. On average, pressure drop of a liquid flowing through a pipe is 2 psi / 100 feet. Also, preliminary estimates of line pressure drops in plants reveal an average equivalent length of 100 ft. If the pipe contains control valves, an additional 10 psi must be

added to obtain this control. In the plant, each pump must be able to overcome 12 psi of pressure drop before reaching its desired reactor.

In calculating the ultimate pressure rise, two more factors were considered. First, if the material must flow through a heat exchanger, an additional 2 psi must be overcome. Second, the pressure of the material must always be greater than the pressure of the discharge tank by at least 2 psi. Combining, the design pressure rise is equal to

$$(9.2) \quad \Delta P(\text{psi}) = 12 + 2 * (\# \text{ of heat exchangers}) + (2 + P_{\text{discharge unit}})$$


As an example, consider stream 4. From the flow diagram, it can be seen that the material must flow through one heat exchanger and discharge into R-201 operating at 1 bar pressure. The pressure rise is calculated as

$$\Delta P(\text{bar}) = \left(\frac{12 + 2 * (1) + (2 + 1)}{1.01} \right) = 16.8$$

From the stream table, it can be seen that the volumetric flow rate is 816587.8 L/hr. Assuming the efficiency is 70%, the power requirement is

$$\text{Power}(kW) = \frac{1.67 * 816.6 \left(\frac{m^3}{hr} \right) * 16.8(\text{bar})}{\text{Efficiency}} = 37.9$$

CAPCOST was used to estimate the capital costs of each pump. The required inputs are the type, material of construction, discharge pressure, and power requirement. This calculation is based off of recorded data for pumps and uses correlations to adjust the cost for size of the unit and inflation. A complete procedure of this can be found in TBWS.

Performed By: 

Checked By: 

9.2 Shell and Tube Heat Exchangers

Similar to centrifugal pumps, the design of the shell and tube heat exchangers for the GM and MFA plants was based off of heuristics. As mentioned previously, two equations for calculation of the heat required for the process streams are used - the area required for the heat exchanger and the flow rate required of the chosen utility.

$$(9.3) \quad Q = \dot{m} C_p \Delta T$$

$$(9.4) \quad Q = U A F \Delta T_{lm}$$

From this equation, the value for U has been estimated to be $850 \frac{W}{m^2 K}$ by TBWS

for shell and tube heat exchangers utilizing steam or cooling water. The value of F can be at a minimum .9 before replacement of the heat exchanger because of

fouling is necessary. Using this as a conservative estimate for the 1-1 shell and tube heat exchanger is satisfactory. Finally, estimation of the utility temperature for heating is done using the common temperatures of low-pressure steam of 250-275 F, or medium pressure steam of 285-300 F. For cooling requirements it uses the common temperature of cooling water at 80-90 F. For both operations, the rule of thumb that allows the utility to change by 10 F was used. This completes the necessary information for equation 9.4.

For an example of this, please consider Stream 5. The material balance of the plant shows that 408.3 kmole/hr of methacrylic acid must be heated from its storage temperature of 40°C to the reactor temperature of 70°C . The heat capacity of methacrylic acid is recorded as 123.1 kJ/kmole K . The heat required for this stream is

$$Q = \dot{m} C_p \Delta T = 408.3 \left(\frac{\text{kmole}}{\text{hr}} \right) * \left(\frac{\text{hr}}{3600 \text{ sec}} \right) * 123.1 \left(\frac{\text{kJ}}{\text{kmole K}} \right) * (343\text{K} - 303\text{K})$$

$$Q = 558.5 \text{ kJ/sec}$$


The heat exchanger area required is then,

$$\Delta T_{lm} = \frac{(T_{util,in} - T_{5,out}) - (T_{util,out} - T_{5,in})}{\ln \left(\frac{(T_{util,in} - T_{5,out})}{(T_{util,out} - T_{5,in})} \right)} = \frac{(408 - 343) - (398 - 303)}{\ln \left(\frac{(408 - 343)}{(398 - 303)} \right)} = 74.55 \text{ K}$$

$$A = \frac{Q}{U F \Delta T_{lm}} = \frac{558.5 \text{ kJ/sec}}{.85 \frac{\text{kJ}}{\text{m}^2 \text{ sec}} * .9 * 74.55 \text{ K}} = 9.8 \text{ m}^2$$

Finally, the required utility flow rate is

$$\dot{m} = \frac{Q}{C_p \Delta T} = \frac{558.5 \text{ kJ/sec} * \frac{3600 \text{ sec}}{\text{hr}}}{37.37 \frac{\text{kJ}}{\text{kmole K}} (408\text{K} - 398\text{K})} = 5433 \frac{\text{kmole}}{\text{hr}} \text{ lps}$$

Performed By: 

Checked By: 

9.3 Storage Tanks

From the assumption that deliveries will be made to the plant every two days, the size of the storage tanks must be large enough to hold this two-day capacity. In addition, a safety factor of 10% will be added to the design of the tank to allow for vapor space. The volume of each tank is calculated from

$$(9.5) \quad V(m^3) = 2.2 * (Daily \text{ Capacity } (m^3 / day))$$

It is assumed for each of these tanks that the L/D ratio is 1.5, a common value for process tanks. The diameter of the column can be calculated as

$$V = \frac{\pi}{4} D^2 * L = \frac{\pi}{4} D^2 * 1.5 * D = 1.5 \frac{\pi}{4} D^3$$

$$(9.6) \quad D(m) = \left(\frac{4 * V(m^3)}{1.5 * \pi} \right)^{1/3}$$

As an example, consider the storage tank for methacrylic acid TK-202. From Stream 5, the daily requirement of methacrylic acid is 34594 L/hr. Therefore, the volume of the tank must be


$$V(m^3) = 2.2 * \left(34594 (L/hr) * \frac{m^3}{1000L} * \frac{8hr}{day} \right)$$


$$V(m^3) = 608.86$$

And the diameter of the tank is

$$D(m) = \left(\frac{4 * 608.86(m^3)}{1.5 * \pi} \right)^{1/3} = 8.03$$

$$L(m) = 1.5 * D(m) = 1.5 * 8.03(m) = 12.04$$

Performed By: 

Checked By: 

9.4 Plug Flow Reactors with Heat Exchange

The designs of all plug flow reactors in the GM and MFA plants follow a numerical approach in solving the differential equations developed by Fogler. Since every reaction considered is exothermic, the models will be produced based from derivations made in the book where the heat is carried away via heat exchange with cooling water jackets around the pipe.

To illustrate the technique, consider R-201, where sodium hydroxide and methacrylic acid combine to form sodium methacrylate and water. The mole balances of each species, where F_i is the molar flow rate of species i,

$$\begin{aligned}
 (9.7) \quad & \frac{dF_{SH}}{dV} = -r_{SH} \quad SH = \text{sodium hydroxide} \\
 & \frac{dF_{MA}}{dV} = -r_{MA} \quad MA = \text{methacrylic acid} \\
 & \frac{dF_{SM}}{dV} = -r_{SM} \quad SM = \text{sodium methacrylate} \\
 & \frac{dF_W}{dV} = -r_W \quad W = \text{water}
 \end{aligned}$$

The rate of reaction was derived earlier and is

$$\begin{aligned}
 (9.8) \quad & \text{rate} = .3487 \exp \left[(5084.9) \left(\frac{1}{273 + 36.6} - \frac{1}{T} \right) \right] [SH][MA] \\
 & [SH] = \text{molar concentration of sodium hydroxide} \\
 & [MA] = \text{molar concentration of methacrylic acid}
 \end{aligned}$$

The molar concentration is related to the molar flow rate as

$$(9.9) \quad F_i = Q * [i] \quad \text{where } Q = \text{volumetric flow rate}$$

Combine equations 9.8 and 9.9 gives

$$(9.10) \quad r = .3487 \exp \left[(5084.9) \left(\frac{1}{273 + 36.6} - \frac{1}{T} \right) \right] \frac{F_{SH}}{Q} * \frac{F_{MA}}{Q}$$

$$\text{where } r = -\frac{dF_{SH}}{dV} = -\frac{dF_{MA}}{dV} = \frac{dF_{SM}}{dV} = \frac{dF_W}{dV}$$

Equation 9.10 is then rewritten in terms of residence time by applying

$$\theta = V / Q = \text{residence time}$$

$$(9.11) \quad \frac{dF_i}{dV} = \frac{dF_i}{dV \frac{Q}{Q}} = \frac{dF_i}{d\theta Q} = \frac{1}{Q} \frac{dF_i}{d\theta}$$

Thus, the mole balances on each species is

$$(9.12) \quad \frac{dF_i}{d\theta} = \frac{.3487}{Q} \exp \left[(5084.9) \left(\frac{1}{273 + 36.6} - \frac{1}{T} \right) \right] F_{SH} * F_{MA}$$

$$\frac{dF_i}{d\theta} = Q * r$$

Next, an energy balance is performed on this system to account for heat exchange with cooling water outside of the PFR and the heat produced by the reaction in the PFR. Fogler gives the result of this balance as

$$(9.13) \quad \begin{aligned} \frac{dT}{dV} &= \frac{Ua(T_w - T) + r^* \Delta H_{rxn}}{\Sigma F_i C_{p,i}} \\ \frac{dT_w}{dV} &= \frac{Ua(T - T_w)}{F_w C_{p,w}} \end{aligned}$$

$$\text{where } a = \text{Unit Heat Transfer Area} = \frac{4}{D}$$

Once again, this equation is rewritten in terms of residence time as

$$(9.14) \quad \begin{aligned} \frac{dT}{d\theta} &= Q \frac{Ua(T_w - T) + r^* \Delta H_{rxn}}{\Sigma F_i C_{p,i}} \\ \frac{dT_w}{d\theta} &= Q \frac{Ua(T - T_w)}{F_{CW} C_{p,w}} \end{aligned}$$

where F_{CW} = molar flow of cooling water

Utilizing Euler's method to solve these coupled differential equations, inlet conditions of the reactor are assessed first. The streams entering R-201 are streams 6 and 7. From these streams the inlet conditions are

$$\begin{aligned}
F_{MA} &= 6804 \text{ mol / min} \\
F_{SH} &= 6804 \text{ mol / min} \\
F_{SM} &= 0 \text{ mol / min} \\
F_W &= 744806 \text{ mol / min} \\
T_{in} &= 343 \text{ K} \\
T_W &= 323 \text{ K}
\end{aligned}$$

Choosing a residence time of .001 minutes, the conditions of the reactor are calculated as

$$\begin{aligned}
V &= \theta * Q = .001 \text{ min} * 14186 \text{ L / min} = 14.186 \text{ L} \\
\text{Length} &= V / A = \frac{14.186 \text{ L}}{\frac{\pi}{4} D^2} = \frac{.014186 \text{ m}^3}{\frac{\pi}{4} (.508 \text{ m})^2} \\
\text{Length} &= .07 \text{ meters down the PFR}
\end{aligned}$$

From equation 9.12

$$\begin{aligned}
F_{i,t+1} &= F_{i,t} + \Delta\theta * \left(\frac{.3487}{Q} \exp \left[(5084.9) \left(\frac{1}{273 + 36.6} - \frac{1}{T} \right) \right] F_{SH} * F_{MA} \right) \\
F_{i,t+1} &= F_{i,t} + .001 * \left(\frac{.3487}{14186} \exp \left[(5084.9) \left(\frac{1}{273 + 36.6} - \frac{1}{343} \right) \right] 6804 * 6804 \right) \\
F_{i,t+1} &= F_{i,t} + (4.812)
\end{aligned}$$

The flow rate of sodium hydroxide at this time step will be

$$F_{NaOH,1} = F_{NaOH,0} - (4.812)$$

$$F_{NaOH,1} = 6804.898 - (4.812) = 6800.086 \text{ mole/min}$$

Similarly, the temperature of the process stream and the cooling water stream are calculated using Euler's method,

$$T_{t+1} = T_t + \Delta\theta * Q \frac{Ua(T_{w,t} - T_t) + r_t * (\Delta H_{rxn})}{\Sigma F_i C_{p,i}}$$

$$T_1 = T_0 + .001 * 14186 \frac{(51) \frac{4}{.508} (298 - 343) + (.339) * (50.2)}{(6804 * .1706 + 6804 * .1231 + 744806 * .075312)}$$

$$T_1 = 343 - .0002534 = 342.99975 \text{ K}$$

$$T_{w,t+1} = T_{w,t} + \Delta\theta * Q \frac{Ua(T - T_w)}{F_{CW} C_{p,w}}$$

$$T_{w,1} = T_{w,0} + (.001) * 14186 \frac{(51) \frac{4}{.508} (343 - 298)}{5000 * .075312}$$

$$T_{w,1} = 298 + .009655 = 298.009655 \text{ K}$$

This procedure is continued down the length of the PFR until the desired conversion is met.

Performed By: 

Checked By: 

9.5 Riedel Equation

For most of the compounds present in the distillation section of the GM plant, it is not possible to find published data of their vapor pressure at various temperatures. To design the distillation column, the team has chosen to use the Riedel equation, which calculates the vapor pressure as a function of temperature for any liquid based on their critical properties.

$$\ln\left(\frac{P_{vp}}{P_c}\right) = A - \frac{B}{T_r} + C \ln(T_r) + D(T_r)^6$$

$$A = -35 * q, B = -36 * q, C = 42 * Q + \alpha, D = -q$$

$$q = .0838 * (3.758 - \alpha)$$

$$\alpha = \frac{.315 * \psi + \ln(P_c)}{.0838 * \psi + \ln(T_{br})}$$

(9.15)
$$\psi = -35 + \frac{36}{T_{br}} + 42 \ln(T_{br}) - T_{br}^6$$

T_c = critical temperature
 T_r = reduced temperature
 T_{br} = reduced normal boiling point
 P_c = critical pressure
 P_{vp} = vapor pressure

As an example, consider diethyl ether, a material for which critical properties are known as well as Antoine coefficients. This material, although not appearing in the plant, was chosen because of the availability of vapor pressure data as a function of temperature to show the accuracy of this equation.

The data for diethyl ether recorded from Felder is

Diethyl Ether Physical Properties	
Tb (°C)	34.6
Tc (°C)	194
Pc (atm)	35.6
Diethyl Ether Antoine Coefficients	
A1	6.92032
B1	1064.066
C1	228.799
Diethyl Ether Riedel Coefficients	
ψ	2.0375164
α	7.163619715
Q	-0.285390932
A	9.988682625
B	10.27407356
C	-4.822799435
D	0.285390932

Figure 9.1 – Diethyl ether data (Felder)

First, the vapor pressure at 10°C is calculated from the Antoine Equation,

$$P_{vp} (atm) = \left[A1 - \frac{B1}{T(^{\circ}C) + C1} \right] \left(\frac{1}{760} \right)$$

$$P_{vp} (atm) = \left[6.92 - \frac{1064.1}{T(^{\circ}C) + 228.8} \right] \left(\frac{1}{760} \right)$$

$$P_{vp} (atm) = .383$$

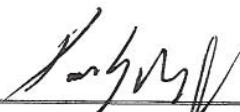
Using the Riedel equation, the vapor pressure is calculated as,

$$P_{vp} = P_c * \exp \left(A - \frac{B}{T_r} + C \ln(T_r) + D * T_r^6 \right)$$

$$P_{vp} = 35.6 atm * \exp \left(9.99 - \frac{10.27}{T_r} - 4.83 \ln(T_r) + .285 * T_r^6 \right)$$

$$P_{vp} = .381 atm$$

As can be seen, the Riedel equation gives numbers very close to the Antoine Equation. This example has shown the power of calculating vapor pressure using only critical properties of the material.

Performed By: 
 Checked By: 

9.6 Distillation Tower: Overall Balance

The first step in designing a distillation column is to perform an overall material balance around the column. The only known values are the inlet flowrate to the column and its composition. Stream 20 gives this data as

Stream Number	20
Source	E-206
Destination	T-201
Temperature (°C)	114.5580132
Pressure (bar)	1.623809524
Vapor Fraction (molar)	0
Volumetric Flow (Liters / hr)	145433.1
Mass Flow (kg / hr)	227222.5
Mole Flow (kmole / hr)	3023.6
Component Mole Flow (kmole / hr)	
Diglycidyl Ether	8.677056764
Dimethacrylate of glycidol	115.6736818
Epichlorohydrin	845.5191644
Glycidyl Methacrylate	356.2372861
Glycidyl Trimethacrylate	131.7130407
Methacrylic Acid	61.47360564
Phenothiazine	0.599069284
Sodium Chloride (aq)	0
Sodium Hydroxide (aq)	0.311286351
Sodium Methacrylate (aq)	0
Tetramethyammonium Catalyst (aq)	0
Water	1503.398905

Figure 9.2 – Stream 20 data

The following assumptions must be made to ensure the balance around the column can be completed. First, the main separation is between epichlorohydrin and GM where the latter is the heavy key and the former is the light key. Since a high purity of GM is required, it is a safe assumption that most of the light key is taken off of the top (99.9%). Furthermore, all components with boiling temperatures lower than that of the light key should be almost completely removed from the top (100%). The two components with vapor pressures between that of epichlorohydrin and GM, namely methacrylic acid and diglycidyl ether, are difficult to make a good first assumption. The team will arbitrarily set the percentage of each in the distillate of 90% and 86%, respectively, to ensure high purity of GM. Finally, since the process requires a 98% purity of GM, the recovery of GM in the distillate, by a trial and error procedure of the calculations presented below, will be set at .4%.

With these assumptions, the flow rate of each component can be calculated in the distillate, similar to the technique used below for epichlorohydrin.

$$F_{i,dist} = F_{i,feed} * (Assumed Fractional Recovery)$$

$$F_{epi,dist} = F_{epi,feed} * .999 = 845.5 * .999 = 844.7 \text{ kmole / hr}$$

After this has been done for each component, the total distillate flow rate can be calculated as

$$D = \sum_i F_{i,dist}$$

Then, the amount of each component the in the bottoms can be calculated by an overall column balance,

$$F_{i,bot} = F_{i,feed} - F_{i,dist}$$

$$F_{epi,bot} = F_{epi,feed} - F_{epi,dist} = 845.5 - 844.7 = .8$$

$$B = \sum_i F_{i,bot}$$

This completes the overall material balance of the column

Performed By: 

Checked By: 

9.7 Distillation Tower: Preliminary Analysis

To obtain an estimate of the size of the column and the minimum reflux ratio, the team has decided to use the Fenske and Underwood equations. In order to use this approach, the relative volatility of the materials must be known. This parameter can be estimated as

$$(9.16) \quad \alpha = \frac{P_{vp,epi}}{P_{vp,GM}}$$

Since, the vapor pressures of the substances vary with temperature, the temperature at which it will operate must be specified. It is known from the properties of glycidyl methacrylate that it has a boiling temperature of 196°C and that epichlorohydrin has a boiling temperature of 117°C. However, it will operate at less than 120°C to ensure the stability of purified GM, and would reduce the pressure of the column to achieve this temperature at the bottom. Thus, the average temperature of the column can be estimated to be 80°C.

The relative volatility of the materials at this temperature is

$$\alpha = \frac{3.05}{.116} = 26.4$$

Next, from the Fenske Equation, the minimum number of plates can be calculated as

$$N_{\min} = \frac{\ln \left[\frac{(x_{\text{epi}} / x_{\text{GM}})_{\text{distillate}}}{(x_{\text{epi}} / x_{\text{GM}})_{\text{bottoms}}} \right]}{\ln(\alpha)}$$

Where the mole fractions of epichlorohydrin and GM can be found from the overall material balance of the column. The result is

$$N_{\min} = \frac{\ln \left[\frac{(.317 / .0005)_{\text{distillate}}}{(.0002 / .98)_{\text{bottoms}}} \right]}{\ln(26.4)} = 4.5 \text{ trays}$$

Following a heuristic given by TBWS where the actual number of trays is usually twice the minimum, it is expected that the column will have nine trays.

Moving to the Underwood Equation, in order to calculate the minimum reflux ratio, the following equation needs to be solved for Φ ,

$$(9.17) \quad \Delta V_{\text{feed}} = F * (1 - q) = \sum \frac{\alpha_i * F_{\text{feed}} * x_{i,\text{feed}}}{\alpha_i - \phi}$$

Where q is the quality of the feed (1 for liquid). Using the Riedel equation to calculate the relative volatilities at 80°C, and obtaining the rest of the data from the material balance

$$0 = \frac{39.98_i * 1503}{39.98 - \phi} + \frac{26.53 * 131.7}{26.53 - \phi} + \frac{22.31 * 115.67}{22.31 - \phi} + \frac{26.414 * 845.5}{26.4 - \phi} + \frac{3.78 * 61.47}{3.78 - \phi} + \frac{3.85 * 8.677}{3.85 - \phi}$$

$$\phi = 1.12$$

The minimum vapor flow rate down the top of the column can then be calculated as

$$(9.18) \quad V_{\min} = \sum \frac{\alpha_i * D * x_{i,dist}}{\alpha_i - \phi} = 2767$$

The minimum liquid flow rate can be calculated from a material balance around the condenser

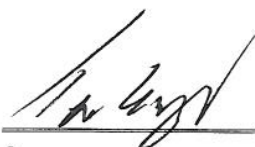
$$(9.19) \quad L_{\min} = V_{\min} - D = 2767 - 2660 = 107.33$$

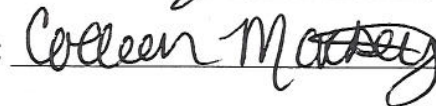
Thus, the minimum reflux ratio is found to be

$$(9.20) \quad R_{\min} = L_{\min} / V_{\min} = \frac{107.33}{2767} = .0388$$

However, for economic design of columns, Aspen recommends that the minimum reflux ratio be set at the lowest value of .1, their recommendation will be followed by the group. The actual reflux ratio of the column by using the heuristic

$$(9.21) \quad R_{act} = 1.5 * R_{\min} = 1.5 * .1 = .15$$

Performed By: 

Checked By: 

9.8 Distillation Tower: Stage by Stage Balances

To check the assumed component recoveries made in the overall material balance, it is necessary to perform a rigorous stage-by-stage balance on the column. Since, the column has LNK but no HNK, calculations will proceed from the top of the column and move down. This will give the most accurate assessment for the LNK because the concentration of LNK at the bottom is close to zero without actually being zero, but could not make a reasonable order of magnitude estimate to these values.

First, assume a temperature for the top of the column to be 40°C. Next, calculate the vapor pressure of each phase using the Riedel Equation. The K values can then be calculated by

$$(9.22) \quad K = \frac{P_{i,vp}}{P_{column}}$$

For epichlorohydrin at a column pressure of .1atm and the estimated stage temperature of 40°C, the K value becomes

$$K_{epi} = \frac{.056}{.1} = .573$$

The vapor composition on this stage is known from the overall material balance, the distillate composition. The liquid concentrations can be calculated from Raoult's Law,

$$(9.23) \quad x_{epi,1} = \frac{y_{epi,1}}{K_{epi,1}} = \frac{.3178}{.573} = .554$$


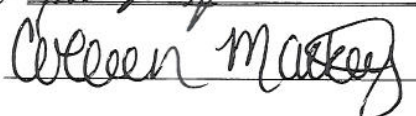
This procedure is followed for each component, and is tested by seeing if the liquid mole fractions sum to 1 to check the assumed temperatures. In this case, the sum is

$$\sum_i x_{i,1} = 2.26$$

Thus, a higher temperature must be guessed. The correct answer for stage one turns out to be 55°C.

Performed By:

Checked By:

9.9 Distillation Tower: Size

The diameter of the column should be sized along each stage, with designing based on the largest value achieved. As an example of the procedure consider the design around the top stage.

The first step in this procedure is to pick out tray spacing. Typical values can be from 6 to 36 inches. However, in an effort to keep the column diameter below 4 meters, a limit placed on towers in CAPCOST, the tray spacing for the GM column is 48 inches.

From correlations provided by Fair and Matthews, the capacity factor for 36 inch tray spacing can be estimated using

$$(9.24) \quad \log(C_{sb}) = -.85984 - .73980 \log(F_{lv}) - .23735 \log(F_{lv})^2$$

$$(9.25) \quad F_{lv} = \frac{L}{V} \sqrt{\frac{\rho_v}{\rho_L}}$$

From correlations of the capacity factor for tray spacings of 9, 12, 18, 24, and 36 inches, a linear equation can be fit to see the effect the tray spacing has on the capacity factor. This technique provides the following correlation, which calculates the multiplication factor for each tray spacing with a basis of .5 for 36 inch.

$$(9.26) \quad F_{c_{sp}} = .0119(\text{Tray Spacing}) + .0826$$

The flooding velocity can then be calculated from

$$(9.27) \quad u_{\text{flood}} \left(\frac{\text{ft}}{\text{sec}} \right) = C_{sb} \left(\frac{\sigma}{20} \right)^2 \sqrt{\frac{\rho_L - \rho_v}{\rho_l}}$$

Where the liquid and vapor densities are calculated as a weighted average of the properties of the dominating components at the top stage, epichlorohydrin and water, and σ is the surface tension in dynes per cm.

Finally the diameter can be estimated from

$$(9.28) \quad \text{Dia} = \sqrt{\frac{4 * V \left(\frac{\text{kmole}}{\text{hr}} \right) * R \left(\frac{\text{L atm}}{\text{mole K}} \right) * T(K)}{\pi * \eta * \text{fraction} * \frac{3600 \text{ sec}}{\text{hr}} * P(\text{atm}) * u_{\text{flood}} \left(\frac{\text{ft}}{\text{sec}} \right) \left(\frac{1000 \text{ mole}}{\text{kmole}} \right) \left(\frac{\text{m}^3}{1000 \text{ L}} \right) \left(\frac{3.28 \text{ ft}}{\text{m}} \right)^3}}$$

$\eta = .9$ is the fraction of area open for vapor flow
fraction = .9 is the fraction of flooding velocity operating at
from Jones and Mellborn

For the top of the column

Tray Spacing = 48 inches

$$\rho_L = \left(\frac{\rho_{epi} + \rho_w}{2} \right) = \left(\frac{73.6 + 62.4}{2} \right) = 68.16 \frac{lb}{ft^3}$$

$$\rho_v = \left(\frac{\rho_{epi} + \rho_w}{2} \right) = \left(\frac{.0209 + .0041}{2} \right) = .0125 \frac{lb}{ft^3}$$

$$F_{lv} = \frac{L}{V} \sqrt{\frac{\rho_v}{\rho_L}} = \frac{399.3 \text{ kmole/hr}}{3031 \text{ kmole/hr}} \sqrt{\frac{66.16}{.0125}} = .00177$$

$$C_{sp,36} = 10^{-.85984 - .73980 \log(.00177) - .23735 \log(.00177)^2} = .240$$

$$F_{C_{sp},48} = .0119(48 \text{ inch}) + .0826 = .6538$$

$$C_{sp,48} = \frac{F_{C_{sp},48}}{F_{C_{sp},36}} * C_{sp,36} = \frac{.6538}{.5} * .24 = .312$$

$$u_{flood} (ft/sec) = C_{sb} \left(\frac{\sigma}{20} \right)^2 \sqrt{\frac{\rho_L - \rho_v}{\rho_l}}$$

$$u_{flood} (ft/sec) = .312 \left(\frac{37}{20} \right)^2 \sqrt{\frac{68 - .0125}{68}}$$

$$u_{flood} (ft/sec) = 26.1$$

$$Dia = \sqrt{\frac{4 * V \left(\frac{kmole}{hr} \right) * R \left(\frac{L atm}{mole K} \right) * T(K)}{\pi * \eta * fraction * \frac{3600 \text{ sec}}{hr} * P(atm) * u_{flood} \left(\frac{ft}{sec} \right) \left(\frac{1000 mole}{kmole} \right) \left(\frac{m^3}{1000L} \right) \left(\frac{3.28 ft}{m} \right)^3}}$$

$$Dia = \sqrt{\frac{4 * 3060 * .0821 * 330}{\pi * .9 * .9 * 3600 * .11 * 26.1}} (3.28)^3$$

$$Dia = 12.8 ft = 3.9 \text{ meters}$$

The column height is calculated as

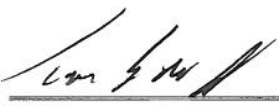
Number of Trays Theoretical = 8

Number of Trays Actual = 1.2 * 8 = 9.6 → 10

Height of Column = Vapor Space + Liquid Holdup + Tray Space

$$\text{Height of Column} = 1.2m + 1.5m + 1.219 \frac{m}{\text{tray space}} * 10 \text{ trays}$$

Height of Column = 14.9 meters

Performed By: 

Checked By: Celeen Mackey

9.10 *Decanter Size*

The phase separation section of the GM plant was designed using Aspen. The following is the input summary and results obtained.

Performed By: 

Checked By: Celeen Mackey

References

- 1) Branan. Rules of Thumb for Chemical Engineers. Gulf Professional Publishing. 2006.
- 2) CEH Marketing Research Reports. Chemical Economics Handbook. SRI Consulting. 2007
- 3) Chemical Land. Properties for Sodium Acetat. <http://www.chemicalant21.com>. (accessed 2007).
- 4) Chemical Land. Properties for Tetramethyl ammonium chloride. <http://www.chemicalant21.com>. (accessed 2007).
- 5) Chlebicki, Shiman, et all. The Kinetics and Mechanism of the Reaction between 1-Chloro-2,3-epoxypropane and p-Cresol. John Wiley and Sons. 1997.
- 6) Environmental Compliance and Risk Management Inc. Impact of Styrene Emission Reduction in Composite Manufacturing. American Composite Manufacturing Association. 2004.
- 7) EPA website. <http://www.epa.gov/ttn/atw/hlthef/styrene.html>.
- 8) Felder, Rousseau. Elementary Principles of Chemical Processes. John Wiley and Sons. 2000.
- 9) Fogler. Elements of Chemical Reaction Engineering. Prentice Hall. 2002.
- 10) Gomez-Nieto. Generalized Vapor Pressure Behavior of Substances between their Triple Points and Critical Points. AIChE Journal. 1977.
- 11) ICIS Chemical Business. <http://www.icispricing.com>. (accessed 2007).
- 12) Keusch. Kinetics of Alkaline Hydrolysis of Ethyl Acetate. Fakultæten. 2007.
- 13) Kosonen. Polystyrene/wood composites and hydrophobic wood coatings from water-based hydrophilic-hydrophobic block copolymers. Springerlink. 2004.
- 14) Knovel Database. <http://www.knovel.com>. (accessed 2007).
- 15) Malshe, Vaidya. Synthesis of 3-chloro-2-hydroxy propyl methacrylate and ion exchange resins therefrom. Science Direct. 1997
- 16) Nayyar, Mohinder L. *Piping Handbook*; 7th Edition. McGraw-Hill: New York, NY, 2000.
- 17) NIST Kinetics Database. <http://kinetics.nist.gov/kinetics/Detail?id=1994DEM/SAN:81>. (accessed 2007)
- 18) Novak. The Kinetics of 1-Chloro-2,3-epoxypropane with n-Butyl Alcohol. John Wiley and Sons. 1973
- 19) OECD SIDS. Glucidyl Methacrylate. Unep Publications. 2006.
- 20) Pipe Pressure Loss Calculator. http://www.efunda.com/formulae/fluids/calc_pipe_friction.cfm (accessed March 2007).
- 21) Riedel Equation. <http://www.pirika.com/chem/TCPEE/VP/Riedelcalc.htm>. (accessed 2007).
- 22) Rowell, George. Personal Interview. 07 Mar. 2007.
- 23) Sears, Avril. Texas. 01 March 2004. <
http://www.businessfacilities.com/bf_04_03_special2.asp>.
- 24) Sigma Aldrich. Product Details of Methacrylic Acid. 2007.
- 25) Solvay Electrochemistry and Derived Specialities. Epichlorohydrin. Solvay Chemicals. 2001.

- 26) Turton, Bailie, Whiting, Shaeiwitz (TBWS). Analysis, Synthesis, and Design of Chemical Processes. Prentice Hall. 2003.
- 27) The Dow Chemical Company. Glycidyl Methacrylate (GMA) Dual Functionality Monomer for Coatings and Resins.
http://www.dow.com/PublishedLiterature/dh_04ef/09002f13804efdce.pdf?filepath=epoxy/pdfs/noreg/296-01330.pdf&fromPage=GetDoc (accessed February 2007).
- 28) The Dow Chemical Company Website. <http://www.dow.com>. (accessed 2007)
- 29) Walas, S.M. *Chemical Process Equipment - Selection and Design*; Elsevier: New York, NY, 1990; Appendix Table E2.1.
- 30) Wankat. Equilibrium Staged Separations. Prentice Hall. 1944.
- 31) Yamasaki. A Kinetic and Thermodynamic Study on the Hydrolysis of Sodium Laurate in Aqueous Phase. Journal of Oleo Science. 2006.

INTENTIONALLY LEFT BLANK.

List of Symbols, Abbreviations, and Acronyms

3-D	three-dimensional
ACO	Advanced Composites Office at Hill Air Force Base
AF	U.S. Air Force
AFB	Air Force Base
API	Applied Poleramics, Inc.
ARL	U.S. Army Research Laboratory
ASTM	American Society for Testing and Materials
ATC	U.S. Army Aberdeen Test Center
BMVE	bimodal vinyl ester resin system
CCM	University of Delaware Center for Composite Materials
CEA	cost effective analysis
CoNap	cobalt naphthenate
CTC	Concurrent Technology Corporation
CTR	composite twisted rudder
DDG	current class of U.S. Navy destroyer
DDX	future class of U.S. Navy destroyer
DMA	dynamic mechanical analysis
DMMA	dimethylacetoacetamide
N,N-DMA	N,N-dimethyl analine
DOD	U.S. Department of Defense
ECAM	environmental cost analysis methodology
EIA	economic impact analysis
EF	emissions factor
EMI	electromagnetic interference

EPA	U.S. Environmental Protection Agency
ESTCP	Environmental Security Technology Certification Program
FA	fatty acid
FAVE	fatty acid vinyl ester resin system
FAVE-L	fatty acid vinyl ester resin system based on lauric acid
FAVE-O	fatty acid vinyl ester resin system based on octanoic acid
FTIR	Fourier transform infrared spectroscopy
GM	glycidyl methacrylate
GPC	gel permeation chromatography
HAP	hazardous air pollutants
HMMWV	high-mobility multipurpose wheeled vehicle
HQ	hydroquinone
JTP	joint testing protocol
kip	kilo-pound
ksi	kilo-pounds per square inch
LCA	life cycle analysis
MCM	mine countermeasure
MEK	methyl ethyl ketone
MEKP	methyl ethyl ketone peroxide
MFA	methacrylated fatty acid
MLau	methacrylated lauric acid
MOct	methacrylated octanoic acid
Msi	mega pounds per square inch
NSWCCD	Naval Surface Warfare Center Carderock
NESHAP	National Emissions Standard for Hazardous Air Pollutants
NMR	nuclear magnetic resonance spectroscopy
OO-ALC	U.S. Air Force Ogden Air Logistics Center

OEM	original equipment manufacturer
P2	pollution prevention
PMC	polymer matrix composite
RCO	Regenerative Catalytic Oxidizer
RPC	reinforced plastics composite
RRAD	Red River Army Depot
RT	room temperature
RTD	room temperature dry
RTO	regenerative thermal oxidizer
SBS	short beam shear
SCI	Structural Composites, Inc.
SEC	size exclusion chromatography
SERDP	Strategic Environmental Research and Development Program
SMC	Sioux Manufacturing Corporation
SENB	single-edge notch bend
SPO	Systems Project Office
TAC	total annual cost
T _g	glass transition temperature
THF	tetrahydrofuran
TGA	Thermogravimetric Analysis
TPY	tons per year
UPE	unsaturated polyester
VARTM	vacuum-assisted resin transfer molding
VE	vinyl ester
VOC	volatile organic compounds

NO. OF
COPIES ORGANIZATION

1 DEFENSE TECHNICAL
(PDF INFORMATION CTR
only) DTIC OCA
8725 JOHN J KINGMAN RD
STE 0944
FORT BELVOIR VA 22060-6218

1 DIRECTOR
US ARMY RESEARCH LAB
IMAL HRA
2800 POWDER MILL RD
ADELPHI MD 20783-1197

1 DIRECTOR
US ARMY RESEARCH LAB
RDRL CIO LL
2800 POWDER MILL RD
ADELPHI MD 20783-1197

NO. OF
COPIES ORGANIZATION

1 UNIV OF DELAWARE
(CD) COMP MANUFACTURING SCI LAB
N SHEVCHENKO
ACADEMY ST
NEWARK DE 19716

1 DREXEL UNIV
(CD) DEPT OF CHEMICAL AND
BIOLOGICAL ENG 3141
G PALMESE
CHESTNUT ST
PHILADELPHIA PA 19104

1 RRAD
(CD) US ARMY TACOM
RRAD AMSTA RR OM
M STARKS
TEXARKANA TX 75507-5000

1 NSWCCD
(CD) M FOLEY
9500 MACARTHUR BLVD
WEST BETHESDA MD 20817

2 AFRL/MLS OL
(CD) 5851 F AVE BLDG 849
L COULTER RM B-46
F BRUCE RM B-46
HILL AFB UT 84056

1 API
(CD) R MOULTON
6166 EGRET CT
BENICIA CA 94510-1269

1 CONCURRENT TECHNOLOGIES
(CD) CORP
H BRENT
425 6TH AVE STE 2850
REGIONAL ENTERPRISE TOWER
PITTSBURGH PA 15219

1 PROGRAM MANAGER
(CD) WEAPONS SYSTEMS & PLATFORMS
SERDP AND ESTCP PROGRAM OFC
B SARTWELL
901 N STUART ST STE 303
ARLINGTON VA 22203-1853

NO. OF
COPIES ORGANIZATION

ABERDEEN PROVING GROUND

6 DIR USARL
(2 HC RDRL WMM
4 CD) J ZABINSKI (HC)
RDRL WMM A
J SANDS (CD)
E WETZEL (CD)
RDRL WMM B
S BOYD (CD)
RDRL WMM C
J LA SCALA (1 HC & 1 CD)

INTENTIONALLY LEFT BLANK.